# The Proceedings of the 75th AESF Annual Technical Conference June, 1988 Los Angeles, CA

**Published by the**
**American Electroplaters**
**And Surface Finishers, Society, Inc.**
**12644 Research Parkway, Orlando, FL 32826-3298**

The American Electroplaters and Surface Finishers Society, Inc. (AESF) is an international, individual-membership, professional, technical and educational society for the advancement of electroplating and surface finishing. AESF fosters this advancement through a broad research program and comprehensive educational programs, which benefit its members and all persons involved in this widely diversified industry, as well as government agencies and the general public. AESF disseminates technical and practical information through its monthly journal, **Plating and Surface Finishing**, and through reports and other publications, meetings, symposia and conferences. Membership in AESF is open to all surface finishing professionals as well as to those who provide services, supplies, equipment, and support to the industry.




All rights reserved. Printed in the United States of America. This publication may not be reproduced, stored in a retrieval system, or transmitted in whole or in part, in any form or by any means—electronic, mechanical, photocopying, recording, or otherwise—without the prior written permission of AESF, 12644 Research Parkway, Orlando, FL 32826-3298.

Printed AESF Press

Copyright 1988

# Table of Contents

## Light Metals Finishing / Session A


**Color Measurement of Electrolytically Colored Anodized Aluminum** ..... **A-1**
A.W. Brace
Metal Information Services
Stonehouse, Glos., England

**Developments in the Coloring of Anodized Aluminum** .... **A-2**
Dr. G. Tscheulin
Sandoz Ltd.
Basle, Switzerland

**Coil Technology from Japanese Patent** ..... **A-3**
Teruo Mori
Mori Metalfinishing Consultant Office
871-3 Daitoh-Cho, Fujieda, Shizuokaken 426 Japan

**Meeting Military Specifications for Chromate Conversion Coatings on Aluminum** ..... **A-4**
Allan H. Reed
Electrochemicals
751 Elm Street
Youngstown, OH 44502

**Hard, Thick, Smooth and High Dielectric Strength Anodic Oxide Films** ..... **A-5**
Setsuo Tomita
Tomita Electrochemical Research Laboratories
Koda City 444-01

Sakae Tajima and Shigeyoshi Morisake
Electrochemistry Lab
Tokyo City University and
Environmental and Resources Research Institute (NRI)
Tokyo University of Agriculture
Tokyo

Yoshio Hirayama
Nikkei Giken Research Center
Kambara City 421-32

**An Electrochemical Method to Control the Anodizing Process** ..... **A-6**
S. Yousri
Pratt & Whitney Canada Inc.
1000 Marie Victorin
Lonqueuil, Quebec, J4G 1A1

**Designing an Automated Extrusion Anodizing Facility** .... **A-7**
Glenn C. Schoener
Walgren Company
Grand Rapids, MI


## Research / Session B


**Development of Chemical Sensors for Ions in Plating Solutions** ..... **B-1**
Robert F. Savinell, Chi-Jin Chen,
Sharon Reid and Chung-Chiun Liu
Department of Chemical Engineering
Case Western Reserve University
Cleveland, OH 44106

**Selective Pulse Plating of Gold and Tin-Lead Solder** ..... **B-2**
D-T. Chin and M.K. Sunkara
Department of Chemical Engineering
Clarkson University
Potsdam, NY 13676

**Thickness Effects on the Mechanical Properties of Electrodeposits** ..... **B-3**
Ingon Kim and Rolf Weil
Stevens Institute of Technology
Hoboken, NJ 07030

**Factors Affecting Low Temperature Interdiffusion** ..... **B-4**
L. Giannuzzi, H.W. Pickering and W.R. Bitler
The Pennsylvania State University
University Park, PA 16802

**Effects of Additives in Acid Chloride Zinc Deposition** ..... **B-5**
T.J. O'Keefe, J.S. Cuzmar
and Y.S. Park
Graduate Center for Materials Research
University of Missouri-Rolla
Rolla, MO 65401

S. Wagner
Missouri Electrochem Inc.
10958 Lin-Valle Drive
St. Louis, MO 63123

**Addition-Agent Effects in Functional Chromium Deposits** ..... **B-6**
N.M. Martyak
M&T Chemicals, Plating Division
Rahway, NJ 07065

R. Weil
Stevens Institute of Technology
Hoboken, NJ 07030


## Electronics I / Session C


**Nickel Phosphorus Alloy as a Low Cost Electrical Contact Material** ..... **C-1**
C.A. Holden, H.H. Law,
C.A. Mattoe and J. Sapjeta
AT&T Bell Laboratories
Murray Hill, NJ 07974

**Factors for Producing Low Contact Resistance of Nickel Phosphorus Alloys** ..... **C-2**
C.A. Holden, H.H. Law
and R.L. Opila
AT&T Bell Laboratories
Murray Hill , NJ 07974

**Effectiveness of Electrodeposited Coatings in Reducing Atmospheric Corrosion of Copper Substrates** ..... **C-3**
James E. Voytko and Terry R. Guilinger
Sandia National Laboratories
Albuquerque, NM

**To Be Sure of the Right Connections—You Must Have a Heart of Gold** ..... C-4
John Donaldson, Tech. Dir.
Mesa West, Inc.
Anaheim, CA

**An Overview of the Ductility Testing of Electrodeposits** ... C-5
Alan A. Halecky and Edward N. Balko
Engelhard Corp.
Electronic Products Group
One West Central Ave.
East Newark, NJ 07029

## Environmental I / Session D

**An Effective Approach to Regulatory Compliance—Program Development and Implementation** ..... D-1
Arthur N. Mabbett
Mabbett, Capaccio & Associates, Inc.
5 Alfred Circle
Bedford, MA 01730

**Plating Wastewater Discharge Compliance Using Integrated Microfiltration Technology** ..... D-2
David J. Gworek, P.E.
Cert Water Services, Inc.
25 Duval Lane
Plainville, CT 06062

**New Nickel/Chromium Plating Plant Goes to Total Recovery** ..... D-3
Jamie Maliszewski, CEF
Reliable Plating Works, Inc. **No Paper Available**
Milwaukee, WI 53219

**Advances in Removal of Copper From Printed Wire Board Effluents Using Sodium Borohydride** ..... D-4
Richard J. Colby and
Michael M. Cook
Morton Thiokol, Inc.
Ventron Products
150 Andover St.
Danvers, MA 01923

**A New Technology for Wastewater Treatment** ..... D-5
Dr. Ev Knight and
Dr. Jeffrey V. Dagdigian
Unocal 76 Corp.
Fullerton, CA

## Electronics II / Session E

**Innovative Control Systems for the Electronic Plating Process—Today and the Future** ..... E-1
Roger Herrscher
Jerry Tingwall
Robbins and Craig Manufacturing Corp.
2050 N. Durfee Ave.
South El Monte, CA 91733

**A Methodology for Laboratory Evaluation of Solder Electroplating Baths** ..... E-2
J.P. Melka, Jr. and D.L. Helder
AT&T
Richmond, VA

**Tin and Tin-Lead Alloy Electroplating in the Electronics Industry** ..... E-3
J.L. Martin and M.P. Toben
LeaRonal, Inc.
272 Buffalo Ave.
Freeport, NY

**A New Pure Palladium Electrodeposit for Electronic Applications** ..... E-4
A. Blair, G. Karustis,
and J. Wilcox
Engelhard Corp.
1 West Central Ave.
East Newark, NJ 07029

**Palladium Electroplating** ..... E-5
J.A. Abys
AT&T Bell Laboratories
600 Mountain Ave.
Murray Hill, NJ 07974

## Environmental II / Session F

**Acid Purification and Recovery Using Resin Sorption Technology—A Review** ..... F-1
Mike Dejak and Kevin Munns
Eco-Tec Limited
925 Brock Road, South
Pickering, Ontario L1W 2X9

**A Comparison of Vacuum and Atmospheric Evaporative Recovery Equipment** ..... F-2
Raymond A. Baker
Applications Engineer
Corning Process Systems
Big Flats, NY 14814

**Absolute Reclamation of Water and Bath Through Use of New Reverse-Osmosis-Based System** ..... F-3
Ronald R. Rich, CEF
Water Technologies Inc. **No Paper Available**
Minneapolis, MN

**Source Reduction of Chlorinated Solvents: Aerospace Applications** ..... F-4
Dr. Kathleen Wolf
Source Reduction Research Partnership
Los Angeles, CA

**Pickling Acid Recovery with Bipolar Membrane Technology** ..... F-5
Michael Prescott
Lancy International, Inc.
181 Thorn Hill Road
Warrendale, PA 15086-7527

**Some 'Unsolved' Problems in Closed Loop Nickel Recovery** ..... F-6
Lyle Kirman
Kinetico Inc.
10845 Kinsman Road
Newbury, OH 44065

**A New Technology for Wastewater Treatment Using Immobilized Algae** ..... F-7
Patrick M. Nelis and Dennis W. Darnall
Bio-Recovery Systems, Inc.
4200 S. Research Drive
P.O. Box 3982
Las Cruces, NM 88003

# Electronics III / Session G

**Cyclic Voltammetric Stripping Analysis for Use in the PCB Industry** ..... G-1
M. Kerman, Dr. P. Bratin
and R. Gluzman
ECI Technology
31 Cain Dr.
Plainview, NY 11803

**Multi-Layer Processing: Oxide Control** ..... G-2
Gary Marasovich
Electrochemicals
751 Elm Street
Youngstown, OH 44502

**Plating-Thru Holes in Printed Wiring Boards Which Are Restrained in the X/Y Direction During Thermal Excursions** ..... G-3
Phillip E. Hinton
Hinton "PWB" Engineering
Tucson, AZ

**Automation of Plating Rack Loading for Printed Circuit Panel Electroless Processing** ..... G-4
Donald P. Aupperle
Aupperle Associates, Inc.
6307 Seaview Ave., N.W.
Seattle, WA 98107

**Gold Processes for Plating Printed Circuit Boards Processed with Fully Aqueous Resist** ..... G-5
Dr. John Deuber
Degussa Corp.
South Plainfield

Dr. Hans-Joachim Luebke
Degussa AG
Schwaebisch Gmuend
West Germany

Dr. Franz Simon
Degussa AG
Schwaebisch Gmuend
West Germany

# General Interest / Session H

**Increasing the Crack Resistance of Porous Anodic Oxide Films on Aluminium** ..... H-1
Dr. Xavier Albert Ventura
Electroplating Consultant
Camprodón, 1-08012
Barcelona, Spain

**The Programmable Controller, A Powerful Tool Not Just for The Automotive Industry** ..... H-2
James J. Childs Jr.
AT&T Technologies

**The Interaction Between Electrogalvanized Zinc Deposit Structure and the Forming Properties of Sheet Steel** ..... H-3
James H. Lindsay, Robert F. Paluch
Physical Chemistry Department
General Motors Research Laboratories
Warren, MI 48090

Harmon D. Nine
Physics Department
General Motors Research Laboratories
Warren, MI 48090

Vernon R. Miller
United States Bureau of Mines
Rolla Research Center
Rolla, MO 65401

Thomas J. O'Keefe
University of Missouri-Rolla
Graduate Center for Materials Research
Rolla, MO 65401

**Effect of Additives on Performance of Acid Copper Plating Baths** ..... H-4
Morton Schwartz, Sunghee Yoon
and Ken Nobe
Department of Chemical Engineering
University of California
Los Angeles, CA 90024

**Corrosion Monitoring of Painted Autobody Test Panels By Electrochemical Impedance Spectroscopy (EIS) Measurement** ..... H-5
Yar-Ming Wang and Dusanka Radovic
Physical Chemistry Department
General Motors Research Laboratories
Warren, MI 48090

**Zinc Phosphating Films on Ferrous Metal Substrates** ..... H-6
C.C. Chang and H.K. Liu
Chung Shan Institute of Science & Technology
Taiwan, Republic of China

T.S. Lee
Scientific Resources, Inc.
Palatine, IL
**Paper Withdrawn**

**Adhesion of Platings on Substrates** ..... H-7
Martin Thoma
MTU Motoren- und Turbinen-Union Munchen GmbH
Munich, West Germany

# Electroless Deposition I / Session I

**Electroless Nickel Phosphorus Copper Study in Corrosive Atmospheric Chamber** ..... I-1
E. Yang, Saad K Doss
and P. Peterson

**Composite Coatings of Fluorinated Carbon (CFx) in Electroless Nickel Plating Bath** ..... I-2
Jung T. Kim
Allied-Signal Inc.
Buffalo Research Laboratory
20 Peabody Street
Buffalo, NY 14210
**Paper Withdrawn**

**Corrosion Characteristics of Electroless Nickel Coatings Developed Using Surface Analysis Techniques** ..... I-3
Lawrence Salvati, Jr.
Perkin-Elmer Corporation
Edison, NJ

Diane M. Tramontana
Occidental Chemical Corporation
Grand Island, NY

**Electric Properties of Electroless Copper Deposits** ..... I-4
Kuniaki Ohtsuka
Okuno Chemical Industries Co., Ltd.
10-25 1-chome Hanatenhigashi, Tsurumiku
Osaka Japan

**Some Physical Properties of Electroless Ni-P Alloy Deposited from Pyrophosphate Bath** ..... I-5
Masao Matsuoka, Shinji Imanishi
and Tadao Hayashi
Department of Applied Chemistry
University of Osaka Prefecture
4-804 Mozu-Umemachi, Sakai
Osaka, 591, Japan

**Advanced Process Control Methods for Electroless Plating Of Plastics** ..... I-6
Gary Shawhan, Edwin Bastenbeck
and Richard Bellemare
Enthone, Inc.
350 Frontage Rd.
West Haven, CT 06516

## Electroless Deposition II / Session J

**Electroless Nickel Waste Treatment** ..... J-1
W. Van Antwerp and T. Yamaguchi
Uyemura International
Los Angeles, CA

T. Otaka, K. Araki and K. Deguchi
C. Uyemura
Osaka, Japan

D. Bailey — **No Paper Available**
Baker Brothers/Systems
Stoughton, MA

**Factors Affecting Quality Electroless Nickel Plating of Thin Film Memory Disks** ..... J-2
Michael Aleksinas, Kashmira Parikh
and Phillip Hagberg
Fidelity Chemical Products Corp.
470 Frelinghuysen Avenue
Newark, NJ 07114

**Sublayer Processing for Rigid Memory Disks** ..... J-3
D. Leibman
Shipley Company Inc.
Newton, MA

**Mechanism of Electroless Nickel Deposition: A Review** ... J-4
Glenn O. Mallory
Electroless Technologies Corp.
Los Angeles, CA

**Electronic Applications of Electroless Nickel, New or Unusual** ..... J-5
Donald W. Baudrand
Allied-Kelite Div.
Witco Corp.
2701 Lake Street
Melrose Park, IL 60160

**Optimizing the Manufacturing Economics of Electroless Nickel Bath Operation** ..... J-6
Louis J. Kosarek
Technical Director
Precision Microelectronics
11550 Pellicano Dr.
El Paso, TX 79936

**Hope for the Best But be Prepared for the Worst** ..... J-7
David Kunces, CEF
MacDermid Inc.

## Analytical Methods / Session K

**CPVS Analysis of Acid Copper Plating Baths Used for Printed Circuit Boards** ..... K-1
G.L. Fisher and W. Sonnenberg
Shipley Co.
Newton, MA

**Plating and Micro-Etch Process Control for Printed Circuit Boards** ..... K-2
Dr. Trudy Lionel
Hewlett-Packard
Sunnyvale, CA

**In-Situ Composition and Rate Monitor for Tin-Lead Alloy Electrodeposition** ..... K-3
K. Keiji Kanazawa, Alison Sue
and Owen R. Melroy
IBM Research Division — **No Paper Available**
Almaden Research Center
San Jose, CA

**Data Forecasting and Warning Signal for the Control of The Plating Baths** ..... K-4
H.T. Morris, P.R. Scherer
and T.M. Tam
Lockheed Missiles & Space Co., Inc.
Sunnyvale, CA 94088

**A Study of Titanium and Aluminum Etching Solutions By Fluorine-19 Nuclear Magnetic Resonance Spectroscopy** ..... K-5
M.N. Cooper and T.W. Rodgers
Lockheed Missiles & Space Co.

**Measuring PTH Copper Ductility for Process Control** ..... K-6
Donald E. Storjohann
Shipley Company Inc. — **No Paper Available**
Newton, MA

**On-Line Electroplating Thickness Monitor** ..... K-7
C.G. Moore, P.E.
and J.P. Consentino
Rohrback Cosasco Systems
11841 East Smith Avenue
Santa Fe Springs, CA 90670

## Advances in Fundamentals And Applications / Session L

**Review and Update on Electrocomposites** ..... L-1
V.P. Greco
U.S. Army Armament Research,
Development, and Engineering Center
Close Combat Armaments Center
Benet Laboratories
Watervliet, NY 12189

**Electrodeposition of Amorphous Ni-Cr-P Alloys** ..... L-2
Terry R. Guilinger and James E. Voytko
Sandia National Laboratories
Albuquerque, NM 87185

**Pulsed Plating for Hard Chrome** ..... L-3
Lou Latham and Peter Cambria
Rapid Power Technologies
Brookfield, CT

**Comparison of Magnesium Acid Pickling Solutions By Electrochemical Impedance Spectroscopy** ..... **L-4**
Dr. Tim Rodgers, CEF
Lockheed Missiles & Space Co.
Sunnyvale, CA

**The Fundamentals of Zinc Brightener Design** ..... **L-5**
David E. Crotty, PhD
Allied-Kelite Div.,
Witco Corp.
29111 Milford Rd.
New Hudson, MI 48165

**Electroplating: Where it's Going and Why** ..... **L-6**
Earl C. Groshart
The Boeing Co.
P.O. Box 3999
M/S 2E-01
Seattle, WA 98124

**The Wear Characteristic of Ni-P-SiC Composited Coating** ..... **L-7**
Deng Zongang and Huang Xinmin
Department of Materials and Science
Hefei Polytechnic University
People's Republic of China

## Organic Coatings / Session M

**Measurement Systems Evaluaton for Organic Coatings Surface Finishers Using Statistical Methods** ..... **M-1**
Gordon G. Perrin Jr.
Ford Motor Co.
Livonia, MI
**No Paper Available**

**Advanced Solid Lubrication for Tribological Control At Elevated Temperatures** ..... **M-2**
Dr. Robert B. Gresham
E/M Corp.
P.O. Box 2400
West Lafayette, IN 47906

**From Plating to Powder: How to Get Started in Powder Coating** ..... **M-3**
Donald S. Tyler
Volstatic, Inc.
Florence, KY
**No Paper Available**

**The Power & Free Conveyor and Its Potential for Productivity Improvement** ..... **M-4**
Theodore A. Tylman
Unibilt Division
Jervis B. Webb Co.
Farmington Hills, MI

**Thermal Insulation and Related Properties of Organic Coatings** ..... **M-5**
J.S. Chen, C.C. Chang
and T.S. Lee
Chung-Shan Institute of Science & Technology
P.O. Box 1-2-26 Lung Tan, Taiwan 32526
Republic of China

**A Novel Alternative to Decorative Brass Electroplate** ..... **M-6**
Michael P. D'Angelo
Market Manager, Metal Finishing
MacDermid Inc.
245 Freight Street
Waterbury, CT 06702

A-1

# Light Metals Finishing
# Session A

## Color Measurement of Electrolytically Colored Anodized Aluminum

A.W. Brace
Metal Information Services
Stonehouse, Glos., England

# Color Measurement of Electrolytically Colored Bronze Anodized Aluminum

A W Brace

*Metal Information Services, Stonehouse, Glos., England.*

**Abstract**

*The paper initially discusses color theory and the response of the eye to color. Results are then given for color measurements made with three different instruments on specimens of electrolytically colored (2-step) bronze finishes on anodized aluminum, produced in industrial anodizing plants. Three proprietary processes were used - two based on tin electrolytes and the third employing cobalt salts. One of these instruments was considered superior to the others and was used to record color limits for standard shades, to investigate the effect of etching and to resolve color matching disputes.*

**Introduction**

The use of color in architectural anodizing first became commercially significant in the 1950's, which saw the introduction of integral coloring processes towards the end of the decade. During the next 20 years these processes were widely used, such that toward the end of that period they had largely replaced the adsorbtion dyeing which had previously dominated the market, particularly for the production of gold or bronze shades and black. For past seven years has seen integral coloring largely superseded by electrolytic coloring processes (often referred to as '2-step').

Some years ago Gardam published a paper [1] in which he posed the question "Why do we need to measure color ?" - to which he gave the following answers:

1. Standard colors arrived at visually are liable to show color drift, i.e. samples produced over a period to match original standards do not always reproduce the original shade and the color drifts away if the matching is purely visual.

2. Color measurement show up process factors which affect the color.

3. The need to resolve contractual disputes when work from an anodizer is rejected by a customer for not being within color limits.

Gardam used a reflectivity attachment on a spectrophotometer in conjunction with a 30-ordinate method [2] to obtain values which could be plotted on the color triangle using the C.I.E. method of measuring color [3]. This involves 30 separate measurements which have then to be integrated with the help of an electronic calculator or computer. Although the accuracy of the method is high, it is not a practical method for routine use in an anodizing shop.

Over subsequent years there has been a continuing need to find a technique of color measurement which could be used for routine color checking by anodizers to obtain good color matching, as well as to resolve dispute situations. The paper that follows represents work carried out by the author in an attempt to meet these objectives, as well as trying to keep the cost of such equipment below £2,500 (US$ 5,000).

## Factors affecting the Perception of Color

The response of the human eye to color depends upon the subjective response of any individual to the light reflected from the surface being viewed. An image is received by the retina of the eye, which transmits a signal to the brain. The interpretation of this signal is affected by the ability of each individual to perceive color, but the ability of the individual to perceive small differences in color varies widely. According to Wright [4], some 8.1% of the male population, but less than 0.5% of the female population, have inherent color vision deficiencies. These deficiencies are less in young men but become higher with age. Whilst color (like beauty) may be in the eye of the beholder, there is a high probability that no two beholders will see the same color.

## Color Theory

According to Maxwell's theory, any visible color is made up from three primary colors - red, green and blue, plus brightness this latter can be regarded as equivalent to adding various amounts of white to black. This also implies that white contains equal amounts of these three primary colors, whilst black is the absence of color. Any color can be expresses numerically in terms of the proportion of these primary colours present, plus what is known as the "Luminance factor". This can be considered as representing the level of brightness of the color, in that a theoretical black has no luminance and hence no color, whilst the maximum luminance theoretically possible for any primary color is 100%. If these primary colours are mixed in equal amounts the result is white.

On the basis of this theory it should be possible to define any color by the amount of the three primary primary colors present, plotted on an equilateral triangle whose vertices are R (red), G (green) and B (blue), which is known as the Color Triangle (Fig. 1). However, the colors seen by the human eye do not correspond to this theory, since only those colors bounded by the line BR and the curve RB can be seen by the human eye. In other words, an observed color has to be specified as if it lies within a triangle whose vertices are a red that is redder than the deepest red that can be seen by the human eye, and similarly for green and blue.

The most accurate way of measuring the color of a material is to obtain reflectance readings at 100 Å intervals over the range 4000 Å to 7000 Å. The procedure for converting these readings into the equivalent of the three primary colors, whose wavelengths are taken as 7000 Å for red (X), 5461 Å for green (Y) and 4358 Å for blue (Z), are given in reference. [3]. However, the color can only be fully specified if its brightness (luminance) is also measured, since this has a significant effect of the color perceived by the eye.

The values so obtained are converted to C.I.E. values, which are referred to as x, y, and z values, although once the x and y values have been obtained there is no need to calculate the z values. In fact, for the Color Triangle, any two values automatically defines the third. The conversion of the X, Y and Z values to $x$, $y$ and $z$ values is obtained as follows:

$$x = X/(X + Y + Z) \qquad y = Y/(X + Y + Z) \qquad z = Z/(X + Y + Z)$$

The values X, Y and Z are the reflectance values obtained either from the conversion of spectrophotometer readings to primary color values, as described above, or from reflectance values obtained using red (X), green (G) and blue (B) filters.

The luminance R = the reflectance value (%) obtained through the green filter.

## Low Cost Instruments for Color Measurement

After a survey of low cost instruments available in the United Kingdom for color measurement, it was decided to investigate the three instruments described below:

### *The Lovibond Flexible Optic Tintometer Mk 3* *

This instrument (Fig. 2) directs a beam of light via a flexible glass fibre optical leads on to the surface to be tested. Normally the transmitted light is directed on to the surface at 45° and the light reflected at 90° is received by a fibre optic receptor, whose end is parallel to the surface being measured. This feeds back the light received to the measuring system in the instrument. It is possible to reverse the leads so that the incident beam is at 90° and the reflected light is then received at 45°.

In the instrument itself a field is seen in the eyepiece which is split into two halves. The left hand portion consists of light reflected from the specimen into the eyepiece and the right hand portion consists of light which is transmitted through colored glass filters. The color can be matched by putting a succession of filters into place and adjusting the brightness until a match is obtained. This requires some experience and an operator with good color perception. The results obtained can remain as Lovibond units, as shown on the dials on the instrument, or they can be converted by a nomogram into C.I.E. values. However, where this instrument is in routine use this latter conversion requires the data to be handled using a micro-computer program which the manufacturers will supply.

### *Tri-Stimulus Reflectometers*

Basic these instruments employ color filters which allow a band of light to be transmitted whose peak value and spread are known. Normally, these will have peak transmission values near the wavelength which corresponds to the red, green and blue primary colors which are used to obtain C.I.E. values. Two instruments were investigated: (1) the Sheen Miniature Colorimeter ** and (2) Diffusion Systems Reflectance Spectrophotometer Mk.III - Model II ***. The peak values of the filters used in these instruments is as follows:

| *Instrument* | *X (Red)* | *Y (Green)* | *Z (Blue)* |
|---|---|---|---|
| Sheen Instruments Ltd | 6600Å | 5200Å | 4800Å |
| Diffusion Systems Ltd | 6300Å | 5300Å | 4300Å |

The two instruments differ in detail, since the filters of the Diffusion Systems instrument cover a greater span of wavelength and the Z (Blue) filter is closer to the specified wavelength of the C.I.E. system than that of the Sheen instrument. Further, the Sheen instrument uses a 45° reflectance head (Fig. 3), whilst that of Diffusion Systems is a 90° head (Fig. 4).

With both of these instruments there is a set-up procedure to standardize the instrument readings for each of the three filters. The results are initially recorded as reflectance values and then converted into C.I.E. values using the formulae given above. It must be appreciated that it is possible for tri-stimulus reflectometers to give identical C.I.E. values on specimens that may exhibit different spectrophotometric curves. This can happen with paint pigments, but is less likely to be found on electrolytically colored anodized surfaces. For a given material and process it was considered probable that the readings would reveal small but significant color differences where these exist.

* The Tintometer Limited, Salisbury, SP1 2JY, England. ** Sheen Instruments Limited, Richmond, TW9 2JL, England.
*** Diffusion Systems Limited, London, W7, England.

## Experimental

To evaluate these instruments, samples of flat 6063 extrusions were anodized to a thickness of 25μ (1 mil) in production plants which operated three commercial electrolytic coloring processes - 2 of which were based on tin salts but of different composition (identified as "AL" and "MX" respectively and the other ("AN") based on cobalt salts. In each of the plants the specimens were produced to cover the range of bronze shades regarded as standard by the plants concerned. Some black samples were also prepared. Although specific anodizing and coloring conditions were not disclosed, the sulphuric acid electrolyte concentration was understood to have been in the range of 160-190 g/l and the temperature within the range 15 - 20 °C (60 - 68°F, with a current density of 1.7 A/dm$^2$. The coloring processes were operated using suppliers recommendations.

### *Measurements using the Lovibond Flexible Optic Tintometer Mk.3*

A series of measurements were made on a set of panels produced to a set of internal color standards set by the anodizers operating the various proprietary processes. In the first of these measurements were made on the same series of panels, identified as panels P1 - P5, with the light source from the instrument directed at an angle of 45° to the surface of the specimen and the reflected light measured at 90° to the specimen surface. The results are shown in Table 1. The leads to and from the instrument were then reversed so that the light reaching the panel surface was at 90° and the reflected light was measured at 45°. The effect of these variants on the C.I.E. color values obtained are shown in Tables 1 and 2.

**Table 1: Lovibond Flexible Optic Tintometer readings on standard colours produced by the "AL" (tin) process - geometry 45°/90°.**

| Specimen | Instrument Readings | | | C.I.E. values | | |
|---|---|---|---|---|---|---|
| Identification | R | Y | Density | *x* | *y* | R% |
| P1 T* | 0 | 0.2 | 0.24 | 0.314 | 0.323 | 57.3 |
| L** | 0 | 0.3 | 0.31 | 0.315 | 0.326 | 48.7 |
| P3 T | 0.9 | 1.4 | 0.68 | 0.341 | 0.358 | 18.2 |
| L | 0.8 | 1.3 | 0.8 | 0.339 | 0.348 | 14.0 |
| P5 T | 2.1 | 1.3 | 0.80 | 0.373 | 0.371 | 9.5 |
| L | 1.9 | 2.8 | 0.89 | 0.368 | 0.368 | 7.9 |
| P7 T | 2.6 | 2.7 | 1.05 | 0.377 | 0.365 | 6.2 |
| L | 2.3 | 2.5 | 1.20 | 0.372 | 0.364 | 4.6 |
| P9 T | 1.3 | 0.7 | 1.54 | 0.334 | 0.328 | 2.4 |
| L | 1.2 | 0.6 | 1.70 | 0.331 | 0.325 | 1.7 |

* T = transverse direction ** L = longitudinal direction

It was found that the latter arrangement reduced the difference between the values obtained in the longitudinal (L) and transverse (T) directions. However, it was found that the principal limitation to the instrument was that it required an operator whose eyesight has good color discrimination, since the instrument requires the color in the two halves of the eyepiece of the instrument to be matched visually and then the values on the dials of the instrument read and converted to C.I.E. values. This was considered to be likely to limit the usefulness of the instrument as a routine color measuring device, so that further work was not carried out with this

instrument. However, the small size of the measuring head was an advantage when carrying out measurements on extrusions with only a limited flat surface.

**Table 2: Lovibond Flexible Optic Tintometer readings on standard colours produced by the "AL" (tin) process - geometry 90°/45°.**

| Specimen | Instrument Readings | | | C.I.E. values | | |
|---|---|---|---|---|---|---|
| Identification | R | Y | Brightness | *x* | *y* | R% |
| P1 T* | 0 | 0.4 | 71 | 0.317 | 0.329 | 55 |
| L** | 0 | 0.4 | 73 | 0.317 | 0.329 | 49 |
| P3 T | 1.1 | 1.7 | 86 | 0.348 | 0.356 | 17 |
| L | 1.1 | 1.7 | 88 | 0.348 | 0.356 | 15 |
| P5 T | 2.2 | 3.3 | 90 | 0.380 | 0.379 | 9.5 |
| L | 2.7 | 3.3 | 92 | 0.380 | 0.375 | 8.0 |
| P7 T | 2.7 | 3.3 | 94 | 0.386 | 0.375 | 6.0 |
| L | 2.4 | 1.3 | 99 | 0.375 | 0.367 | 5.3 |
| P9 T | 1.7 | 1.3 | 99 | 0.348 | 0.341 | 2.5 |
| L | 1.7 | 1.1 | 101 | 0.345 | 0.336 | 2.0 |

* T = transverse direction ** L = longitudinal direction

*Tests with the Sheen Miniature Colorimeter*

This instrument consists of a measuring head containing a photo-electric cell and a holder, within which filter wheels could be rotated. Light from a tungsten filament lamp is directed at 45° through the color filters on to the specimen surface. The reflected light is measured by a photocell in a measuring head also at 45° to the horizontal, so that the angle between the incident and reflected light was 90°. The aperture in contact with the specimen is approximately 35 x 25 mm. The light source used corresponds to C.I.E. Illuminant A, which approximates to a north light and is slightly yellower than Illuminant C, which is the normal illuminant for very precise measurement of C.I.E. values. Readings were taken in turn with the X, Y and X filters in position. In each case the instrument was standardized to give a 100 reading on the galvanometer, using a magnesium carbonate block as standard.

**Table 3: Reflectivity and C.I.E. color readings with the Sheen Colorimeter of panels electrolytically colored sheet specimens by the "MX" (tin) process**

| Color ref. | X% | *x* | Y% | *y* | Z% | *z* |
|---|---|---|---|---|---|---|
| MX1 | 32.1 | 0.349 | 31.2 | 0.339 | 28.7 | 0.312 |
| MX2 | 22.9 | 0.363 | 21.8 | 0.346 | 18.3 | 0.290 |
| MX3 | 15.6 | 0.374 | 14.7 | 0.352 | 11.4 | 0.274 |
| MX4 | 7.0 | 0.354 | 7.4 | 0.374 | 5.4 | 0.272 |
| MX5 | 2.4 | 0.276 | 3.9 | 0.448 | 2.4 | 0.276 |
| MX6* | 0.4 | 0.085 | 2.9 | 0.617 | 1.4 | 0.298 |

* Black

Measurements were made on extrusions colored two of the proprietary process and are reported in Tables 3 and 4. These results would appear to indicate that the specimens produced by "MX" process (Table 3) are broadly consistent with increasing depth of shade, but with a tendency for the MX5 sample to be slightly greener, whilst MX6 is effectively black.

It is useful to remember, when considering the values reported in Tables 3 and 4 that the value Y% is that obtained using the Y (green) filter and approximates to the average eye response, the value recorded being that of the "brightness" or "reflectivity" of the surface. It can be seen that these values are very low for the darker bronze and black shades.

The results obtained on the "AN" series (Table 4) show rather significant differences in the readings obtained in the longitudinal and transverse directions. The author considers that these are not surprising in view of the geometry of the measuring instrument, but are too great for the equipment to be considered satisfactory for routine use.

**Table 4: Reflectivity and C.I.E. color readings on extrusions with the Sheen Colorimeter on extruded sections electrolytically colored by the "AN" (cobalt) process.**

| | Longitudinal | | | | | | Transverse | | | | | |
|---|---|---|---|---|---|---|---|---|---|---|---|---|
| Color ref. | X% | *x* | Y% | *y* | Z% | *z* | X% | *x* | Y% | *y* | Z% | *z* |
| A541 | 55.5 | .414 | 44.5 | .332 | 34.1 | .254 | 46.7 | .371 | 37.7 | .300 | 41.4 | .329 |
| A543 | 40.1 | .453 | 28.6 | .323 | 19.8 | .223 | 33.1 | .407 | 24.4 | .300 | 23.9 | .294 |
| A545 | 18.6 | .522 | 10.9 | .306 | 6.1 | .171 | 14.5 | .457 | 10.0 | .315 | 7.2 | .227 |
| A547 | 4.0 | .526 | 3.2 | .421 | 0.4 | .053 | 3.0 | .454 | 2.8 | .424 | 0.8 | .121 |
| A549 | 1.8 | .375 | 2.7 | .562 | 0.3 | .062 | 1.3 | .382 | 1.4 | .412 | 0.7 | .206 |

A practical problem found when using this instrument was that the large measuring aperture of the instrument tended to let in light unless particular care was taken to exclude it, especially is the extruded surface was not quite flat. It also required a flat surface of greater than 25mm (1 inch) for a measurement to be made.

**Measurements made with Diffusion Systems Ltd. Reflectometer Mark II - Model 2**

This instrument is based on a reflectivity head developed for measuring the reflectivity of gloss paints, but this version has a color filter wheel inserted between the light source and the specimen being measured. However, the arrangement is such that the light from the tungsten bulb is directed to and reflected from the surface at an angle close to 90°. An annular photocell measures the light reflected from the specimen surface after it has passed through the required filter. A rotatable wheel contains three C.I.E. filters which are inserted between the beam of light from the lamp and the specimen. The output from the photocell is fed into a galvanometer, which is standardized against a magnesium carbonate block. To correct for equal energy response, the X filter should give a reading of 100, the Y filter 90.8 and the Z filter a value of 32.3.

Measurements were made initially on the "MX" series of specimens and as these seemed promising the "AL" and "AN" series were also measured. The results obtained are summarized as plots on the C.I.E. color triangle (Figs. 5, 6 and 7). These results are interesting, in that although the color range and hue observed seemed similar for the three processes, each had a different range of C.I.E. values. The "AL" series give the classic characteristic of lying on a straight line, thus showing a simple increase in depth of hue. The "MX" series show a much closer bunching of values, but again they lie on a straight line.

The results obtained from the "AN" series does not appear to conform to the expected relationship, in that the values for the 543, 545 and 547 specimens tend to increasing redness, but the 547 and 549 specimens have moved towards the blue-purple. This set of measurements has not been repeated on a second series of specimens similarly prepared, so it it not possible to state whether this behaviour is typical of the process.

Since the results from the Diffusion Systems instrument appeared to be the most promising, this was used exclusively for the measurements reported below.

**Effect of Etching**

It is well known that the luminance (reflectivity) of the specimen surface affects the color seen by an observer. Since etching is generally employed as a pretreatment prior to anodizing, it was decided to measure the effect of etching time on reflectivity and C.I.E. values. A set of small flat extrusions in 6063 alloy were etched in a proprietary caustic-gluconate etchant of 70 g/l concentration and operated at 60°C. for times up to 20 minutes. The effect of etching time on reflectivity for specimens anodized only is shown in Fig. 8, whilst its effect on C.I.E. values for specimens etched at the same time and electrolytically colored by the "MX" process to give a medium bronze shade (MX3) is shown in Table 5.

It can be seen that the effect of etching time is particularly critical for up to 12 minutes etching time, so that for good color matching long etching times seem essential.

**Table 5: Reflectivity and C.I.E. values for samples etched for varying times and anodized only using the same conditions as for the electrolytic (tin) MX2 colored extrusions measured with the Diffusion Systems Reflectometer**

| Etching time (mins) | X% | $x$ | Y% | $y$ | Z% | $z$ |
|---|---|---|---|---|---|---|
| 0 | 31.6 | 0.454 | 29.2 | 0.420 | 8.8 | 0.126 |
| 4 | 30.0 | 0.452 | 27.9 | 0.421 | 8.4 | 0.127 |
| 8 | 28.7 | 0.453 | 26.5 | 0.419 | 8.1 | 0.128 |
| 12 | 26.9 | 0.454 | 26.2 | 0.423 | 7.6 | 0.126 |
| 16 | 27.5 | 0.455 | 25.6 | 0.424 | 7.4 | 0.121 |
| 20 | 27.3 | 0.454 | 25.5 | 0.425 | 7.3 | 0.120 |

**Checking Color Drift on Standard Color Samples:**

Most architectural anodizers produce a set of color standards for customers to use as reference samples. These are usually matched against standard samples retained in the laboratory or quality manager's office. When a stock of samples is at an end, new ones are prepared by a visual match against the originals. Gardam[1] has previously demonstrated that 'color drift can occur from such a procedure, as a result of very small differences in match. This is often made worse by the fact that original samples can be lost and the match is not against the original standards.

To check the possibility that this was happening two sets of standard colors were checked, the first being ones prepared nearly two years after the original ones. The results are shown in Table 6. It can be seen that although the reflectivity values are reasonably close, there is a perceptible difference in instrumental values, particularly the $X$ values, so that color drift cannot be ignored in practice.

**Table 6: Reflectivity and C.I.E. values - measured by the Diffusion Systems Reflectometer for two sets of standard samples produced by the "AL" (tin) process after a time interval.**

| | First set | | | | | | Later set | | |
|---|---|---|---|---|---|---|---|---|---|
| Color ref. | X% | *x* | Y% | *y* | Z% | *z* | X% | Y% | Z% |
| AL1 | 63.9 | 0.451 | 57.4 | 0.405 | 20.3 | 0.143 | 64.4 | 58.2 | 19.5 |
| AL3 | 27.4 | 0.457 | 25.1 | 0.418 | 7.5 | 0.125 | 29.0 | 25.4 | 7.3 |
| AL5 | 11.5 | 0.422 | 11.2 | 0.431 | 3.3 | 0.127 | 12.8 | 11.7 | 3.2 |
| AL7 | 6.4 | 0.386 | 7.6 | 0.458 | 2.6 | 0.157 | 8.6 | 7.5 | 2.5 |
| AL9 | 2.3 | 0.237 | 5.1 | 0.526 | 2.3 | 0.237 | 4.1 | 4.4 | 2.3 |

**Establishing Color Limits:**

For practical purposes the C.I.E. values can be ignored once they have been recorded for the color range in use. For routine quality control purposes the *X, Y and Z* values are all that are needed for test purposes.

Samples were obtained of color samples offered showing the top and bottom limits within which the color would be produced for AN 547 and AN 549. The following were the results obtained:

**Table 7: Reflectivity and C.I.E. values - measured by the Diffusion Systems Reflectometer for top and bottom limits of AN 547 and AN 549 standard color.**

| Color reference | X % | *x* | Y% | *y* | Z% | *z* |
|---|---|---|---|---|---|---|
| AN 547 - top limit | 7.5 | 0.412 | 7.8 | 0.429 | 2.9 | 0.159 |
| AN 547 - bottom limit | 3.4 | 0.333 | 4.6 | 0.451 | 2.2 | 0.216 |
| AN 549 - top limit | 1.0 | 0.164 | 3.0 | 0.492 | 2.1 | 0.344 |
| AN 549 - bottom limit | 0.5 | 0.098 | 2.6 | 0.510 | 2.0 | 0.392 |

These colors are the two darkest bronze shades produced, so that the reflectivity readings are low and the most difficult to measure. However, it is considered that these values show that it can be used to carry out control tests on color matching.

**Color Measurements for Referee Purposes**

Having established these figures the author was called on to carry out referee testing in a dispute involving extrusions produced to the AN 547 color. Table 8 shows the results obtained:

It can be seen that the work rejected gave values which lie outside the reference sample limits. The instrument thus confirmed the inspector's visual inspection, although there were about 2% of the lengths tested which had been rejected that were just within limits. Since carrying out this initial work the author has used this instrument on a number of occasions to resolve disputes on color matching and has found it to be an acceptable instrument for this purpose.

**Table 8: Use of Diffusion Systems Reflectometer for resolving dispute on color limits on AN 547 (cobalt process) bronze color extrusions.**

| Color reference | Reflectance % | *x* | *y* | *z* |
|---|---|---|---|---|
| AN 547 - top limit | 7.8 | 0.412 | 0.429 | 0.159 |
| AN 547 - bottom limit | 4.6 | 0.333 | 0.451 | 0.216 |
| Work accepted (typical) | 6.6 | 0.389 | 0.443 | 0.168 |
| Work rejected (typical) | 9.0 | 0.438 | 0.448 | 0.114 |

The instrument has also been used to resolve disputes over color matching on electrolytically colored bronze anodized finishes obtained using tin electrolytes. Table 9 shows some typical results obtained:

**Table 9: Use of Diffusion Systems Reflectometer for resolving dispute on color limits on MX 3 (tin process) bronze color extrusions.**

| Color reference | Reflectance % | *x* | *y* | *z* |
|---|---|---|---|---|
| MX 3 - top limit | 14.1 | 0.490 | 0.370 | 0.130 |
| MX 3 - bottom limit | 12.8 | 0.517 | 0.380 | 0.120 |
| Work accepted (typical) | 13.8 | 0.490 | 0.370 | 0.130 |
| Work rejected (typical) | 12.1 | 0.480 | 0.360 | 0.140 |

Here it can be seen that the main reason for lack of color match is the heavier etch which has been given to some of the work produced. This confirms the results reported in the series shown in Table 5.

**Discussion**

To inspect color anodized aluminum parts for color matching it is useful to have an understanding of the basic theory of color. Apart from an appreciation that any color can be defined as a mixture of the three primary colors, it is also necessary to appreciate that the luminance (reflectivity) of the surface also affects color. In the course of using the Diffusion Systems Ltd. instrument over several years, it has been found that variations in the degree of etch can be a significant contributor to variability in color. This points to the need to institute a routine check on the degree of etch by reflectivity measurements after etching.

It is not intended that the above results should imply that the instrument used is the only one available that will be suitable for checking color match. It was the best available at the time within the price constraints which were imposed. It has proved to be quite a useful instrument for the purpose required. However, there is one inherent problem, in that careful setup and operation of the instrument is required because the reflectivity values which are recorded for the darker bronze shades are very low, so it is essential to recheck all reading to ensure they are repeatable. The author feels that the problem with some of the instruments currently available is not only their cost, but the fact that it requires a skill above and beyond that of the average quality inspector to use them.

It is also necessary to remember that the measurement can only be made on a flat surface, or nearly so. If steps are taken to exclude stray light entering the reflection head, it is not essential for the surface to be absolutely flat. It is also necessary with any instrument to check for directionality effects. The above work has shown that this is affected by the geometry of the measuring head. It would appear that one useful line of development would be to use fibre optic technology to replace the present conventional system.

**Acknowledgements**

Thanks are especially due to the Tintometer Co Ltd., Sheen Instruments Ltd. and Diffusion Systems Ltd. for their collaboration in this work. The specimens used in this work were provided as follows: "AN" specimens were produced by L.H.T. Anodising Ltd., Uxbridge, Middlesex, U.K. "AL" specimens were standard samples supplied by Penn Anodising Ltd., High Wycombe, Bucks., U.K. and the "MX" specimens came from Metoxal (U.K.) Ltd., Rugeley, Staffs., U.K. Thanks are due to these companies for their co-operation. The conclusions drawn from color measurements on these samples are those of the author of this paper and do not necessarily imply that they are accepted by the afore-mentioned companies.

**References**

1. G D Gardam: Trans. Inst. Met. Finishing 1964,41,(5),190.
2. P J Bouma: "Physical Aspects of color" Philips Technical Library. N.V. Philps, Gloeilampen Fabrieken, Eindhoven, Netherlands, 1947 p.105. Also H D Murray: "color in Theory and Practice" Chapman and Hall Ltd., London. 1952, p.263 and Appendix 2.
3. Commision Internationale de l'Eclairage, Publication No. 15 "Colorimetry" Committee 1.3.1., Bureau Central de la C.I.E., 4 ave de Recteur * Poincare, 75 Paris 16$^{e}$.
4. W D Wright: "The Measurement of color" (4th Edn.) Adam Hilger, London, 1969, p.44.

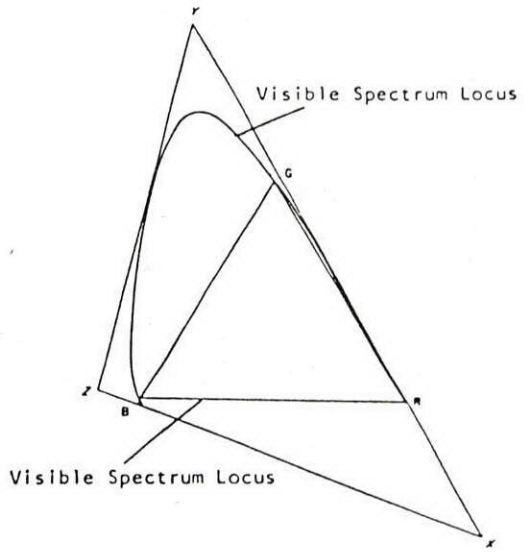


Fig. 1: The Color Triangle showing the Visible Spectrum Locus.

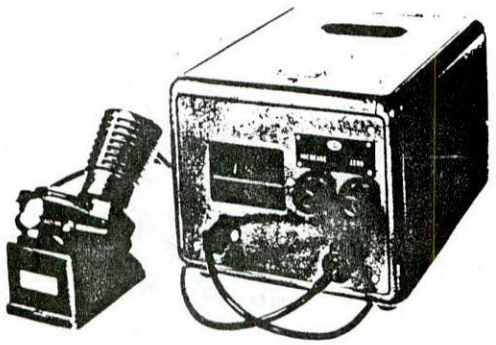

Fig. 2: The Lovibond Flexible Optic Tintometer Mk. 3.

Fig. 3: The Sheen Miniature Colorimeter.

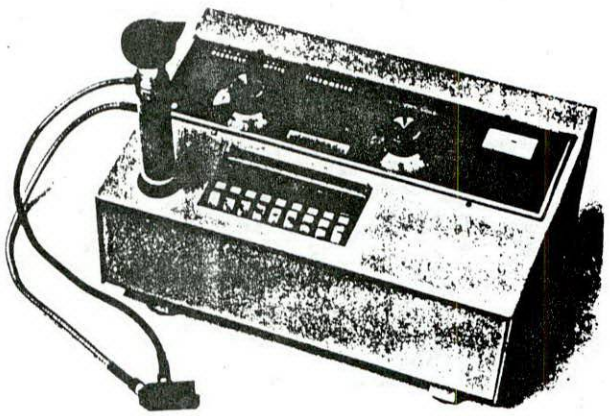

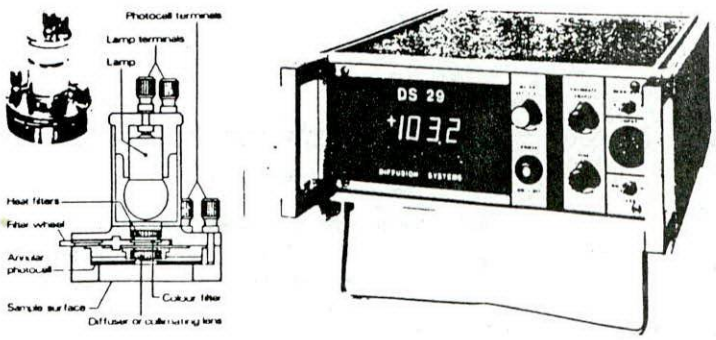


Fig. 4: Diffusion Systems Reflectance Spectrometer Mk. 3, Model II (left) used in conjunction with the DS29 Digital Galvanometer.

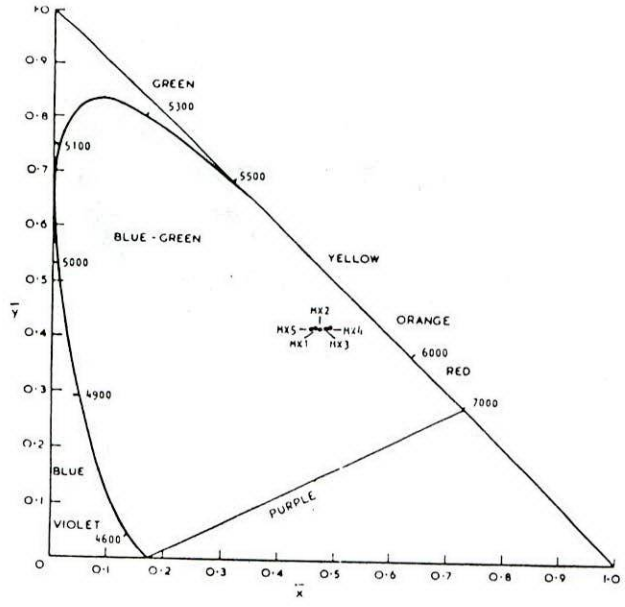


Fig. 5: C.I.E. values for the MX series of standard colors.

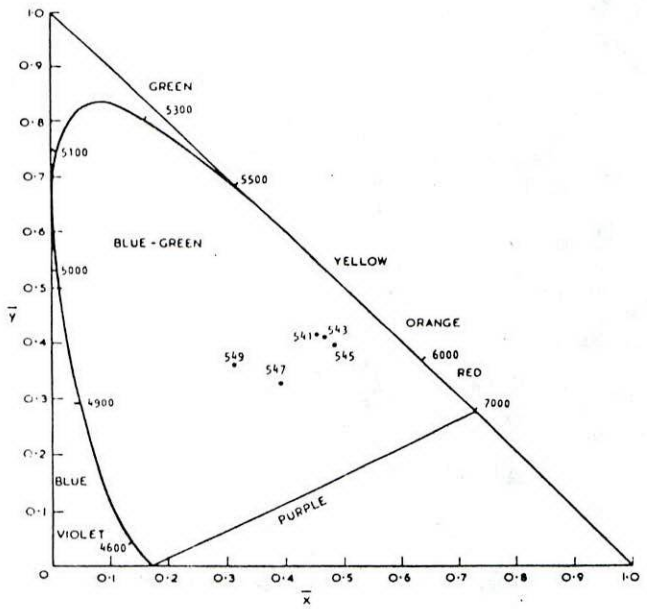


Fig. 6: C.I.E. values for AL series of standard colors.

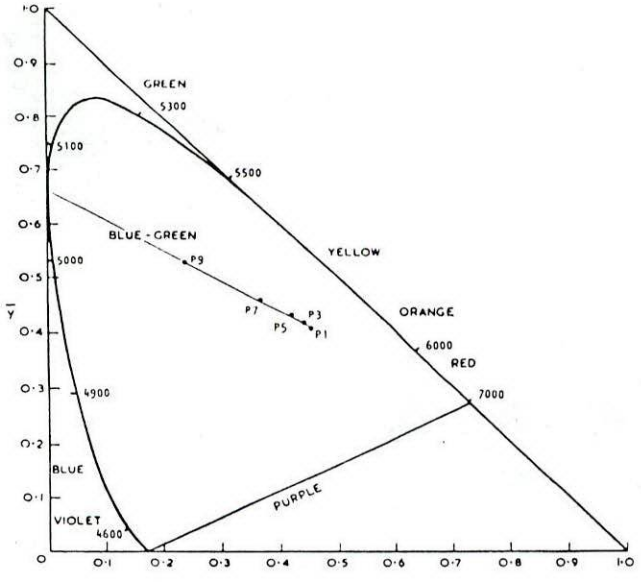


Fig. 7: C.I.E. values for the standard AN series of standard colors.

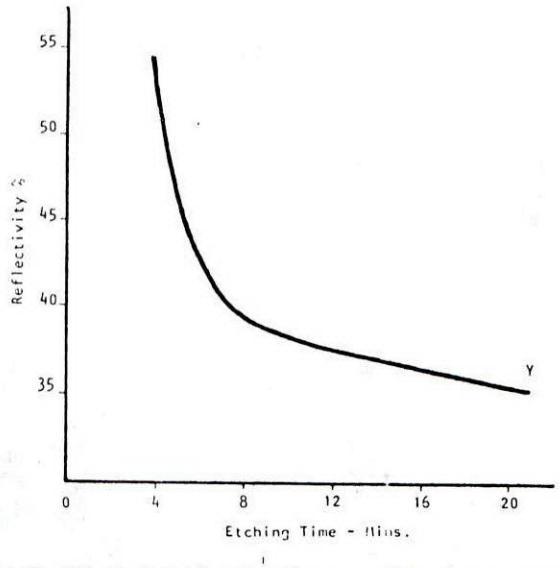


Fig. 8: Effect of etching time in a proprietary caustic gluconate etchant operated at 60°C, on reflectivity at anodized extrusions.

A-2

# Light Metals Finishing
# Session A

## Developments in the Coloring of Anodized Aluminum

Dr. G. Tscheulin
Sandoz Ltd.
Basle, Switzerland

# DEVELOPMENTS IN THE COLORING OF ANODIZED ALUMINUM

(Dr. G. Tscheulin, Sandoz Ltd., Basle, Switzerland)

In recent years various systems have been developed for the production of colored anodic coatings on aluminum. The coloring processes now available include the following:

- Inorganic chemical coloring
- Integral or one-step coloring
- Electrolytic or two-step coloring
- Adsorption coloring with organic dyes
- Combination coloring (electrolytic coloring followed by overcoloring with dyes)

The common feature of all five processes is that:

- The coloring system, whether based on organic dye molecules, organic sulfo derivatives or inorganic substances, is either directly bonded to the metal or deposited in the pores of the anodic coating.

- The hard, anodic colored coating is inseparably bonded to the aluminum. This is quite different from other coloring methods such as color coating.

- The colored anodic coatings are characterized by very good resistance to fading and corrosion.

- The metallic character of the aluminum is retained after the coloring process.

In my talk today, I will concentrate on two processes, adsorption coloring with organic dyes[1] and combination coloring[2].

Anodizing

In the electrolytic oxidizing process, it is known that:

- First a very thin (< 1 um), nonconductive coating (barrier layer) is formed consisting of amorphous or microcrystalline aluminum oxide.

- After the barrier layer has been formed, the anodic coating continues to grow. The coating always grows from the metal outwards,

(1) SANODAL®: Trademark of Sandoz Ltd., Basle Switzerland

(2) SANDALOR®: Trademark of Interoxyd AG, Altenrhein, Switzerland

i.e., at the aluminum-aluminum oxide interface. The first layer formed constitutes the outer surface.

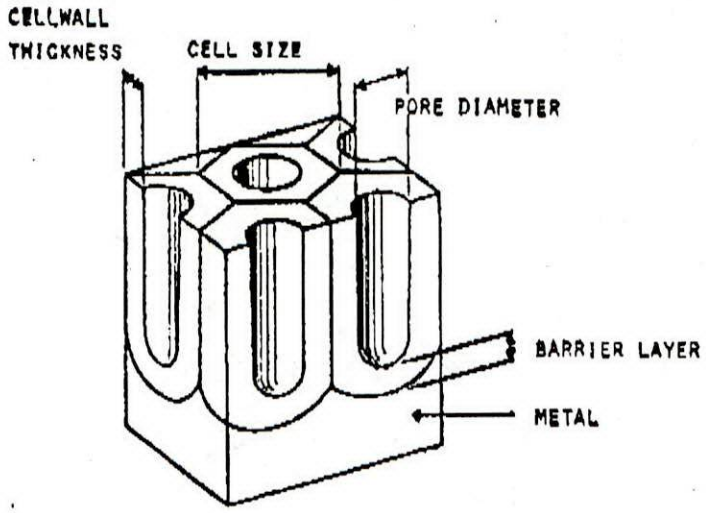


The anodic coating consists of a multitude of hexagonal cells, aligned perpendicular to the metal surface. Each cell contains a pore in it's center. There are about $10^{10}$ pores per square centimeter of surface, each having a diameter of about 100 Å and a length of several hundred thousand Å.

The pores of these films:

- exhibit large adsorption capacity
- improve hardness and abrasion resistance
- make it possible to color the aluminum with organic and inorganic dyestuffs.

Adsorptive Dyeing Process

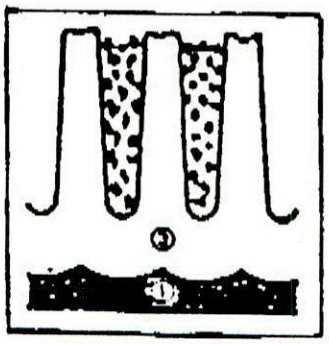

Adsorption of organic dyestuff by the pore system by immersion.

When anodized in $H_2SO_4$, the metal surface becomes positively charged with the bisulfate anion ($HSO_4^-$) acting as a counter ion. Anionic dyes are mostly used in this dyeing process. Their adsorption is mainly based on the exchange of the bisulfate counter ion with dye anions (e.g. $-SO_3^-$. $-PO_3^{2-}$, $-CO_2^-$ ) which are covalently bonded to dye molecules.

$$Al\ \ HSO_4^- + Na^- O_3S\text{——}F \rightleftharpoons Al^- O_3S\ \ F + NaHSO_4$$

Where F represents the dyestuff molecule.

By increasing the concentration of hydrogen ions in the dyebath, the positive charge of the metal surface is increased, thus improving the capacity for adsorbing acid dyes. The bonding of the ions can be supplemented by additional bonding forces such as Van der Waals and hydrogen bridging. However, these forces

are much less in evidence here than in textile dyeing, probably due to the fact that the surface is very rigid as compared with cellulose and protein substrates.

The dye molecule can be bonded either covalently or ionically by either ion exchange with dye anions or with anionic micelles of dye.

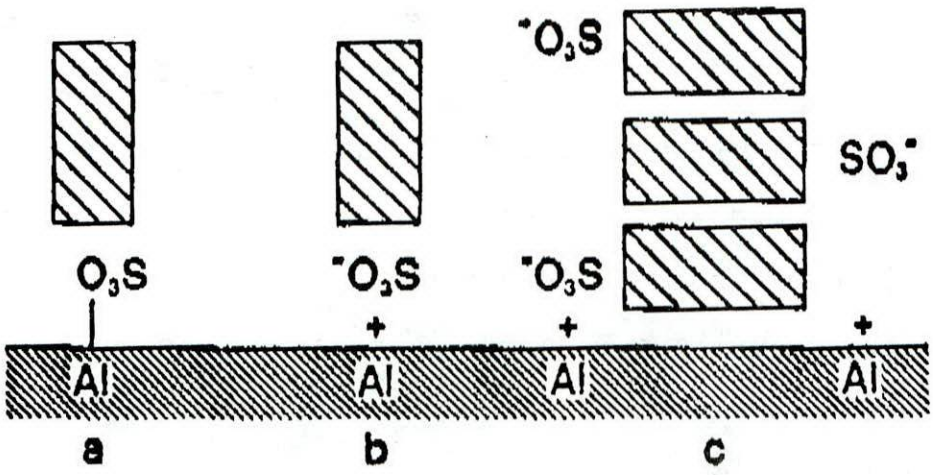


- Diagram of probable nature of dye-alumina bonds with sulphonated dyes on the anodic film: (a) Covalent bond; (b) ion exchange with individual dye anions; (c) ion exchange with anionic micelles of dye.

Combination Process (Overdyeing)

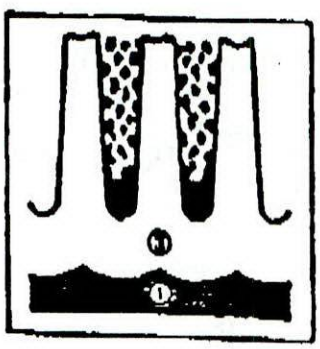

Electrolytic coloring combined with adsorptive dyeing.
This method is a successful, more recent development for the production of weather-fast colorations in spectral colors on anodized aluminum. The method consists in first coloring the anodic coating electrolytically in a light to dark bronze tone and then overdyeing directly with the highly lightfast, organic dyes in the second bath. Two different coloring substances - precipitated metal and the dye molecule - are layered in the anodic coating and do not affect one another. the coatings are as hard as those of electrolytic colorations alone.

With the combination process, the color palette is considerably richer than with any of the other coloring methods listed at the beginning of this talk. With this combined coloring technique, any desired muted shade and depth - from curry yellow to black can be produced.

This combined coloring technique offers a real alternative to color coating since in the combination process there is:

- No chalking of the surface, and
- No separation of the color coat since the hard colored coating is inseparably bonded with the aluminum.

Moreover, the metallic character of the aluminum is retained even after the coloring treatment.

Analytical Methods

To investigate the dyeing kinetics and equilibrium, methods must be available for determining the amount of dye adsorbed on the coating. One possibility is by means of desorption of the dyes from the unsealed anodic coating using tartaric acid + sodium hydroxide solution and then determining the dye content spectrophotometrically.

With an electron microprobe it is possible to determine not only the amount of the dye but also its distribution in the coating. Here heavy metals of metal complexes contained in the dye are determined. The following diagrams show very clearly that the dyes diffuse down into pores.

Electron micro-probe

electrolytic bronze (tin)

dyed (copper)

nickel seal (nickel)

metal traces

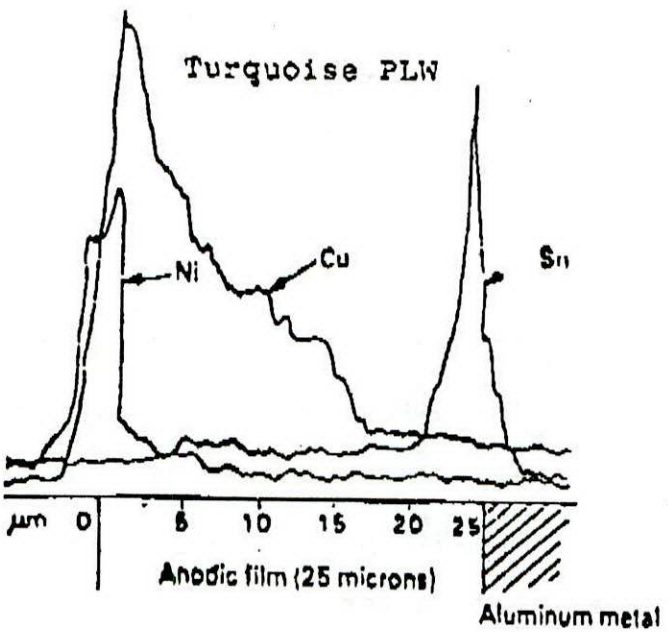


I would now like to mention a number of test results, which should make clear the quality level of aluminum colorations produced by this process.

Light and Weather Fastnesses

A number of long-term weathering tests were carried out in the

- Xenotest 450
- Weather-Ometer (Atlas 600 WRC)
- Open-air weathering stations in different countries.

The results show that only gold colorations in heavy shades suffered a 30% loss in intensity.

In all the other shades the loss of color intensity is much lower, 10% on average, which can hardly be detected by the eye. The results also make it clear that combination colorations are at least as weatherfast as corresponding organic dyeings.

Sealing Quality and Corrosion

Parallel tests with uncolored aluminum, electrolytically colored aluminum, organic dyeings and combination colorations have shown that all these processes produce practically the same results with respect to corrosion.

## CORRELATION OF SEALING QUALITY TEST METHODS

In principle, three different sealing mechanisms are distinguished: Water sealing , sealing with nickel salts and cold sealing . When dyeing with aluminum dyes however, only nickel salt sealing is used since only this type of sealing will prevent bleeding of the dyestuff.

On testing the quality of sealing, three ISO norm tests are now generally employed in industrial practice.

- Weight loss
- Impedance
- Dye stain

The question thus arises whether these 3 tests lead to results which can be correlated, or under what conditions would a different picture of the quality of the seal be obtained. Investigations were carried out with oxide films produced by various methods and sealed:

- with demineralized water

. with the addition of so-called sealing inhibitors (phosphates, silicates, fluorides)
. with the addition of a sealing smut suppressant
. in a typical Ni sealing bath

The results provide the following picture:

1. The three sealing quality tests correlate only in the case of demineralized water. In the presence of a sealing inhibitor however, the three methods lead to quite different assessments of the quality of the sealed test samples.

2. Hot water sealing with and without a suppressant is very heavily influenced by $PO_4^{3-}$ ions.

3. Weight loss values become distinctly poorer in the presence of even small amounts of $PO_4^{3-}$ ions.

4. Impedance tests, on the other hand, still show excellent results even with higher concentrations of $PO_4^{3-}$ ions.

5. The dye stain test correlates with the weight loss test and provides comparable values.

6. Ni sealing reacts much less sensitively to the presence of $PO_4^{3-}$ ions. Even at relatively high phosphate concentrations, good results are still obtained.

These statements apply both to oxide films produced by different processes and to dyed and undyed samples.

A Possible Reaction Pattern

How then can these differences in results be explained?

Sealing inhibitors such as phosphates, e.g. due to their complex-building properties, may accumulate at reactive sites on the aluminum oxide particles on the pore walls, and thus impair hydration. The sealing process is then delayed or even rendered impossible. The depth of penetration however remains limited, since during the pore-filling phase the sealing proceeds rapidly from the metal toward the outside. The pore-filling mass should still be penetrable by water but not inhibitor ions. For this reason, the hydration process is only hindered at the outermost region of the anodic coating, whereas the reaction process in the pore itself can proceed undisturbed.

Based on these statements, the following conclusions can be drawn:

1. In the weight loss test only the state of the outermost region of the oxide film (0.5 um) is assessed, while the layers below it are not affected. Assessment is therefore made of the outer layer only, which explains why $PO_4^{3-}$ ions can cause the values to go so much lower.

2. In the case of the impedance test, the quality of the entire oxide coating is assessed.

   This value depends on the

   - sealing time
   - sealing temperature
   - pH value
   - film thickness,

   which clearly shows that "weak spots" in the outermost layer of the film do not weigh so heavily in the values obtained.

3. In the case of the dye stain test, the quality of the outermost layer is assessed, in a similar manner to that of the weight loss test. In the dye stain test, the sealed oxide film is pretreated with an acid, after which a drop of dye solution is place on the surface, and in this manner the adsorptivity of the coating is determined. Depending

on the quality of the sealing, greater or lesser staining of the surface occurs. It is therefore understandable that the results of the dye stain and weight loss test are roughly parallel.

When sealing is carried out with nickel acetate, nickel hydroxide precipitates in the outermost region of the pores of the coating immediately after the sealing process begins and this seals the pores very rapidly. In this manner the diffusion of dissolved substances such as $PO_4^{3-}$ ions into the coatings is suppressed. Trials have shown that at boiling temperature, the nickel hydroxide deposit into the pores is already complete after 1 minute. With longer sealing there is no further uptake of nickel hydroxide.

## Conclusion

If the results of only one test are considered, the sealing quality of a production sample may not always be correctly assessed. A much more realistic picture of the actual sealing quality is given by the combined results of the three methods discussed.

## COLD SEALING

Cold sealing or impregnation processes are all based on solutions of nickel salts, most commonly nickel fluorides, and in some cases using alcohol solutions to facilitate the deposition of the nickel as its hydroxide. The treatment temperatures are from 25 - 35°C and the treatment times range up to 20 min. Investigations permit the supposition that nickel hydroxide is the principal pore-filler and the aluminum fluoride complexes are formed.

### Cold Sealing Quality

Various cold sealing products were compared with conventional nickel hot water sealing in terms of the aforementioned three ISO norm tests. Light fastness and corrosion (Cass and Kesternich) tests were also performed.

Both natural-coloured aluminum as well as coatings electrolytically bronze-coloured and dyed with organic dyes were investigated.

The conclusions to be drawn from these comparative tests on cold-sealed products are as follows:

1. Accelerated laboratory tests indicate that impregnation processes made shortly after treatment lead to high, unacceptable apparent impedance measurements. These values, however, are found to become acceptable with time.

2. The weight loss values are for the most part already acceptable at the beginning, but improve appreciably with time.

3. The stain test shows no difference between impregnation and conventional sealing.

4. The Kesternich test leads in certain cases to corrosion.

5. In the salt spray tests, the impregnated specimens show more traces of corrosion than with conventionally sealed ones. The differences are not great.

6. After heat treatment (70°C for 3 h), very clear evidence of crazing of the oxide occurs. Test specimens treated in this manner also corrode.

7. A hot water dip at 70°C for 5-10 minutes improves the results decisively.

8. After 3 years outdoor exposure in an industrial atmosphere there is not much difference between hot-sealed and cold-sealed samples.

When the sealing treatment has been carried out to full effectiveness, the aluminum coating or dyeing attains optimum corrosion, light and weather resistance, because the dyes absorbed by the film are sealed into the correct sealing procedure. This is of decisive importance for the quality of the finished aluminum particularly for dyeings on aluminum.

However, here as with all anodized aluminum, smut formation on sealing and on exposure to weather are problems not yet fully solved.

Sealing and Weather Smut

In water sealing, we now know that sealing smut differs from weathering smut, and that the former may play a role in the formation of the latter.

Although the sealing smut problem has been partially resolved with a number of proprietary products, the weathering smut problem has not yet been solved - but is currently undergoing intensive investigation.

May I conclude my talk by showing you some of the colored buildings. Today worldwide, about 700 buildings using organic or combination colored aluminum have been constructed. The oldest among them are now over 17 years old and are in Australia. Their condition is described as very good.

A-3

# Light Metals Finishing
# Session A

## Coil Technology from Japanese Patent

Teruo Mori
Mori Metalfinishing Consultant Office
871-3 Daitoh-Cho, Fujieda, Shizuokaken 426 Japan

# COIL TECHNOLOGY FROM JAPANESE PATENT

MORI METALFINISHING CONSULTANT OFFICE
TERUO MORI
871-3 DAITOH-CHO FUJIEDA SHIZUOKAKEN 426 JAPAN

(1) SUMMARY

Plate mass-production is better coil than batch treatment. Coi treatment gives us high productivity and high constant quality. It uses for producing color anodizing plate, presensitized plate, electro plating. Thire proccess usually has three main processes. They are chemical, mechanical and electro chemical process. Most important process is electro chemical process .

This report describes a lot of device points for electro chemical equipment from Japanese patent between 1910 and 1985.

In electro treatmet , there are six type treatment structures.

## (2) COIL-TECHNOLOGY FROM JAPANESE PATENT

Electorolyte solution is put through between coil and electrde, and it is started to turn on electorotritic current coil and electrode. In this world, we must study high-speed electroplating for mass production and saving energy for cost down.

If we want much more mass production, we must run coil faster, so we usually face the following subjects.

1) Big current introducing
2) Uniformity of coating weight of width direction

There are strecture and film producing efficiency investigation in the big current introducing, it includes current distribution, electrode structure, pumping system supplement equipment. We have to get uniformed coating film, and saving energy including one-side, local electroplating subject. Fig 1 shows those deatiled subjects.

## (3) HISTORY OF CONTINUOUS ELECTORO PLATING TREATMENT ON PATENT

In Germany, it was written on patent 1942 DLS 71895. Fig 2 showed this patent. It is possible to treat coil face to electrode in Fig 2. This structure is very simple water rising room devide into feeding tank and plating tank. And it is useful for them.

UK's first patent about coil treatment is 1936 and Japanese patent is also 1936. Continuous coil treatment become popular in the ninety-forties.

## (4) TYPICAL STRUCTURE OF ELEMENT ON PATENT

### 4, 1) CLASSIFACATION OF TYPICAL STRUCTURE

Fig 3 shows typical coil plating structure. First classificatiuon was devided with typical or suportsystem for coil, Secound classifacation is devided with path pattern.
Third classification is devided with others.

### 4. 2) (DRUM +CONTACT ) STYLE

This structure makes coil run along ronnd of big drum surface. The most bnifit point of this point is that this style can take very easy simple structure. This structure has a good another point to be able to set bearing upper electrolyte solution. So this structure is independent techniqu and corrosion of bearing.

If gas stays under bottom surface long time, it induces rainbow pattern, because plating film is not uniformly produced by gas. So it get bad visual appearance and get no good quality.

Engineer has another reason to select this structure, it is able to get perfect one side plating. This structure is able to reduce 25-30% current compared with flat bed type bath.

Fig 4 shows typical drum-contact structure. Coil(1) comes and dips electrolyte bath along the drum-style roller(2). Electrode(5) is set up against coil(1) after filling electrolyte in the bath. It is turnned on coil(1) and electrode(5).

This Fig 4-1 is standard style process. Round-electrode style Fig4-2, 4-3 has a bigger round electrode square compared with standard style(1).

Electrode has also a function to be bath wall. It is able to move electrolyte quickly. And flow rate is easily controlled with pump-through out. This structure has some quality defect to induce ununiform flow rate and temparature distribution.

Spray style Fig4-3 has a strong point flow rate compared with round electrode style. This structure get good qualities, because coil surface is refreshed with spray. It is not suitable to turn on big current, because it has a small electrode-square.

Fig4-1~4-3 has a common point which is defect feeding system. Direct feeding method (Metal contact) is that Metal/Metal contact resistance is big, so it seem to induce coil-strain, stain, and spark with heat and contact defect. In order to improve those points some time liquid contact(Indirect feeding method) is adapted for coil treatment.

Liquid contact type Fig4-4 has a liquid contact and electrode. It is possible to feed big current but automatically voltage is bigger. This structure has better points not to be defect of metal-metal contact. Fig 4-4 liquid contact decide on bath into 2 room , first room is liquid contact , and last room is plating section. If liquid contact is too small sommtime it is possible to arrenge liquid contact cell serially.

4. 3) (DRUM NON-CONTACT ) STYLE

Fig 4 group has a significance to ccontact roller and coil. Fig 5 shows drum-noncontact style. In this structure , coil doesn't contact roller. There is a big fixed roller with a lot of holes on surface. Electoryte is sprayed out from the hole and this spray pressure makes narrow distance between roller and coil, this disdance indicates electorolysis distance.

This equipment has non contact system between coil and drum, so there is no scrach. This system has one side perfect plating and high speed flow rate, so it is possible top get bigger current density plating. This equipment is the best methode to get maxium current density compared to other methods. This method has a defect that coil condition on running is vibrated for vertical direction, so hole number, pattern, distribution is studied for coil runing ballance. This method is thought the best plating system, because it's higher flowrate make to get rid of reaction gas easy and get nice surface finishing. Electoro -coil distance is short , so this is useful for saving energy.

4. 4) (HPRIZONAL+DIP) STYLE

There is a diffect point to keep electorolyte solution on plating the previous system. We can keep it in a tank with roller for running. This is very useful for plating system. Fig 6 shows those plating equipment.

Fig 6-1 indicates standard style . Help roller makes a coil dip in the tank. There is 2 room deviding by isolated plate , those each has independent electorode and cathode.

Standard style has some defects for plating and otrhefers. There a small leak current anode and cathode , because this srtructure has not enough to isolate. Multi type Fig 6-2 has plural isolate plates, but it is still perfect. This leak is called as short cut current or bipath current.

Fig6-3 perfectly cut off it. Air feeding style is not suitable for bigger current electo plating because coil will get warp with jule heat . Separate type Fig 6-4 cut off leak current perfectly, it auto matically increase voltage. This style eventualy must dip coil surface and back face in electrolyte, so it is very difficult to plate only one side about 30~50% current will reach unexpectedface.

(4. 5) (HORIZON+SPRAY) STYLE

Fig 7 (HORIZON+SPRAY) style has some defect.

1) It is impossible to make a perfect one side plating .
2) It is beggerIRdrop between coil and spray
3) It is diffcult to get quality for wide direction

To get rid of those deffect, coil surface put reaction side, and coilback face put feeding side. This is call verticalcurrent electrolysis This method the most current effective plating method theoritically.

But there are some difficultpoint for adapting plating electolyte and feeding electorolyte. It is leak current causing to contact reaction electrolyte and feeding electorite,

Now we can not get success to separate their electorolyte solution .

We can supply electoro with spray for surface it has a problem spray electorode is has only several metal, so it is not so long life even if it is so expensive.

(4, 6) (HORIZON+FLOW) STYLE

If we dip coil surface and back face, automatically coil both side fase is treated. If we treat only one side fase we only supply electoryte one side face.

Fig 8 show (horizonal + flow) type. Surface electolyte is isolated with in the tank. It always needs to get red of reaction gas immedately, if it appearance becomes rainbow color and get stain.

Bottom electorolyte coil must suport the all wight of electolyte , so it needs to set hight tension handling or back up rolle.

(4, 7) VERTICAL STYLE

Fig 3~8 shows reveal or horizonal but fig 9 show verticalline plating , spray type and dipping type.

Spray type Fig 9-1 is that coil line set vertical direction and put multi spray power sorce contact spray and rolle spraied solution drop for down direction, so it is very easy to change surface solution and it's very effiency to exchange coil, it is possible to operate a small amounts

Fig 9-2 shows vertical line style and it is narrow style, it is easy to plate both side because each sidee has some condition about gas temperature.

We can adapt metal contact or liquid contact for the system in any case. If coil is explored on air, it's easy to appear stain on coil surfase.

## 5) CONCLUSION

I studied fundimental structure of continuous coil treatment with Japanese patent and others.
Mane subjects of those patent are

1) High current density plating

2) Saving energy plating

They are six type of fundimental structure of continuous coil treatment to get mass production and cost down.

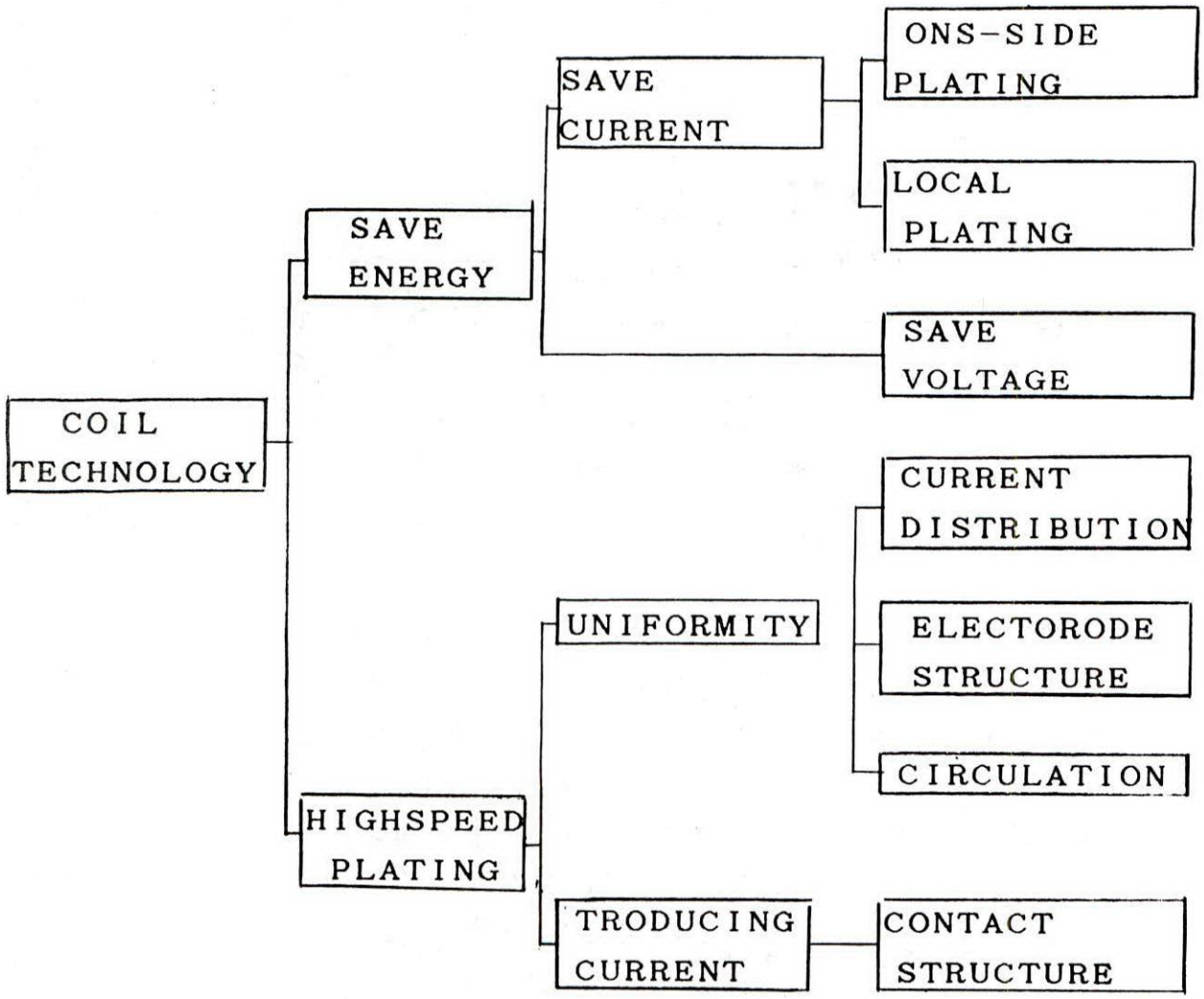


FIG 1 COIL PLATING SUBJECT FROM PATENTS

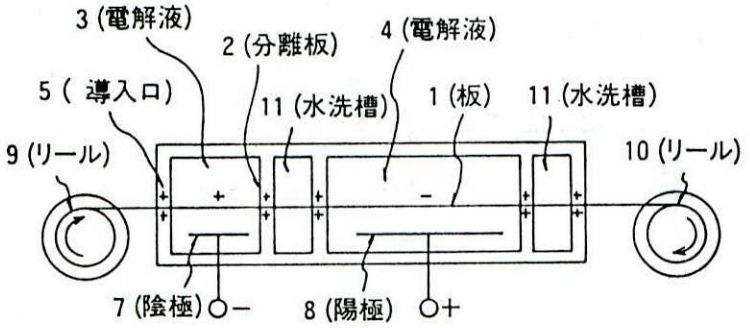


| | |
|---|---|
| 1 | COIL |
| 2 | SERARATER |
| 3, 4 | ELECTOLYTE |
| 5 | INPUT |
| 7 | CATHODE |
| 8 | ANODE |
| 9, 10 | COILER |
| 11 | WASHING TANK |

FIG 2 DLS 718975 (1942)

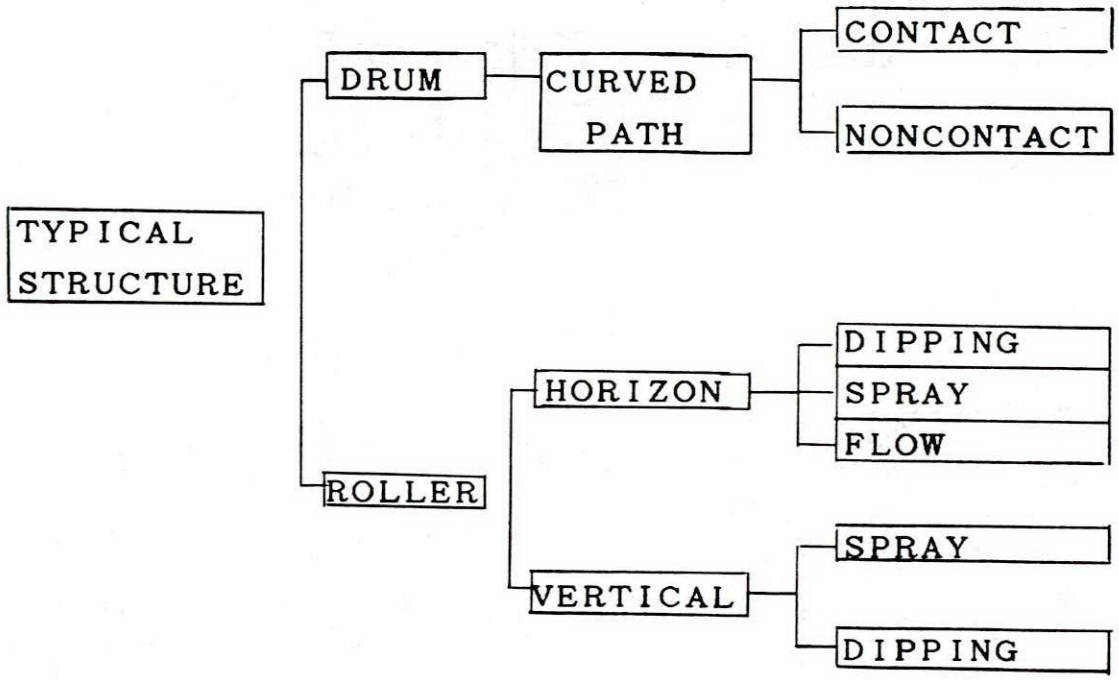


FIG 3 TYPICAL COIL PLATING STRUCTURE

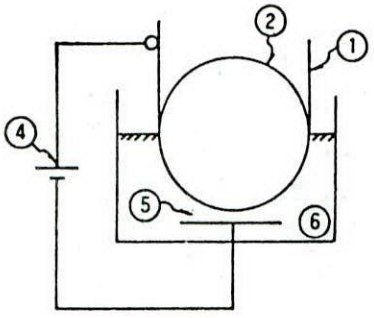


(1) STANDARD

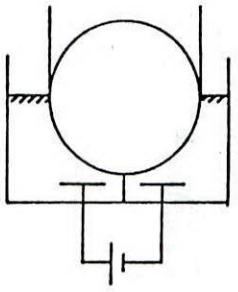

(4) LIQUID

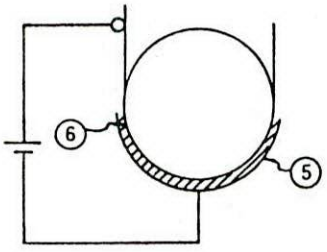


(2) ROUND ELECTORODE

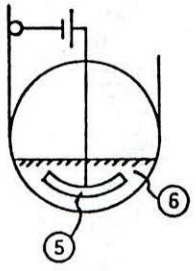


(5) INSIDE REACTION

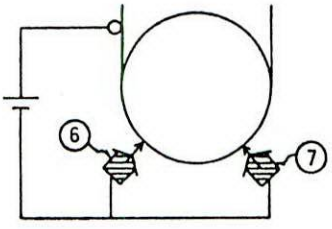


(3) SPRAY

FIG 4 (DRUM+CONTACT) STYLE

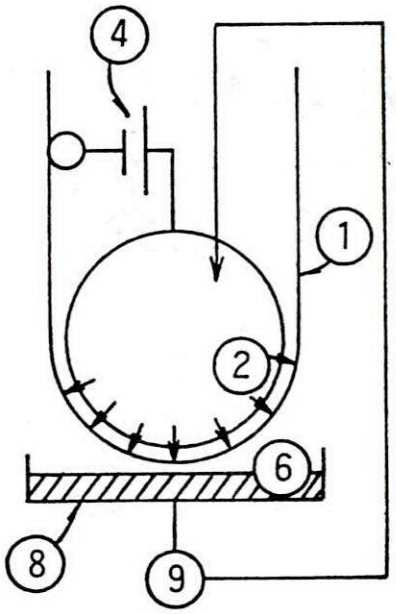


FIG 5 (DRUM+NONCONTACT) STYLE

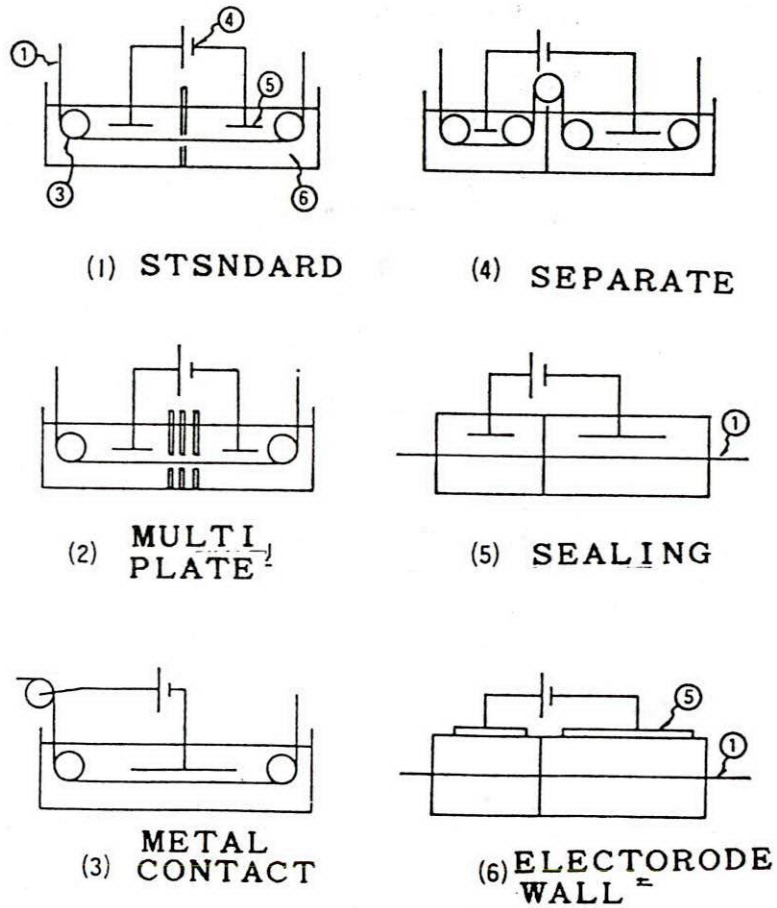


FIG 6 (HORIZON+NONCONTACT) STYLE

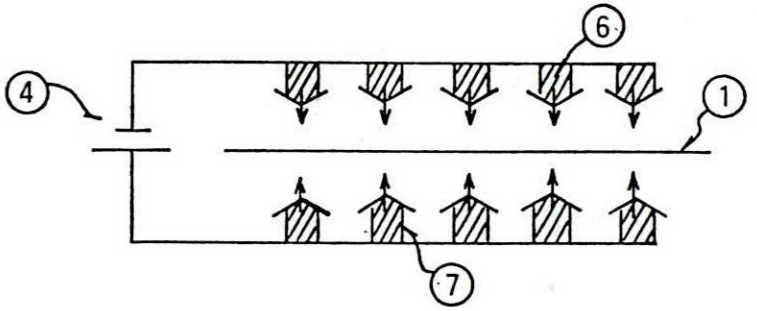


FIG 7 (DIP+SPRAY) STYLE

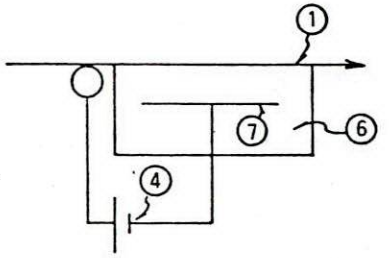


(1) SURFACE

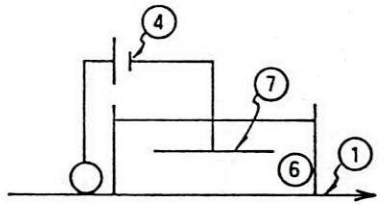


(2) BOTTOM

FIG 8 (HORIZON+FLOW) STYLE

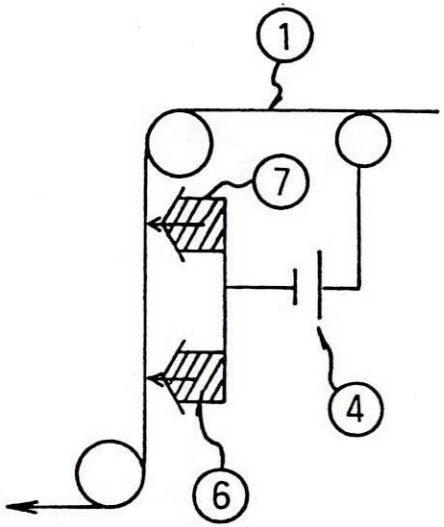


SPRAY STYLE

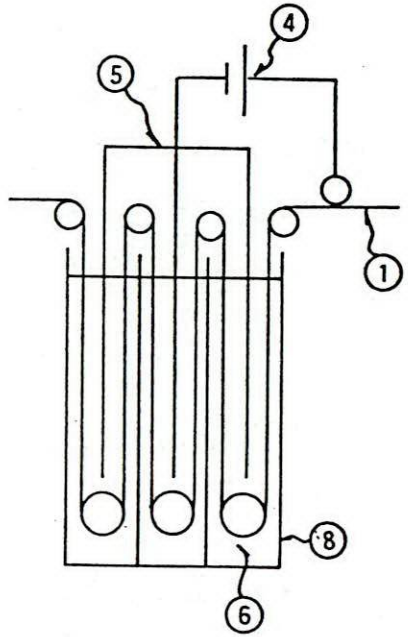


DIPPING STYLE

FIG 9 VERTICAL STYLE

A-4

# Light Metals Finishing
# Session A

## Meeting Military Specifications for Chromate Conversion Coatings on Aluminum

Allan H. Reed
Electrochemicals
751 Elm Street
Youngstown, OH 44502

# Meeting Military Specifications For Chromate Conversion Coatings on Aluminum

by
Allan H. Reed
Electrochemicals
751 Elm Street
Youngstown, Ohio 44502

Aluminum and aluminum alloys are widely used in today's diverse economy because of their desirable characteristics of light weight, high strength, low cost, and ease of fabrication. However, since aluminum is attacked by many substances in the environment, some type of corrosion-resistant surface finish is generally required to protect it from corrosion and pitting. In many cases, paint is the most obvious and economical choice of finishes. Paint, however, will not adhere directly to an aluminum surface, even when a primer is used, because of the thin, naturally-occuring oxide which is always present on aluminum.

In order to obtain an adherent coating of paint on aluminum, a chromate conversion coating must first be applied to the surface of the aluminum prior to the application of paint or primer. These conversion coating are the subject of two Military Specifications:

MIL-C-5541C (14 April 1981) gives the requirements for conversion coatings on aluminum alloys and MIL-C-81706 (30 June 1970) covers the chemical materials used to produce the coatings. Both of these specifications describe the performance requirements that the conversion coatings must meet.

For most metal finishers, MIL-C-5541C is the pertinent specification. It describes two classes of coatings.

Class 1A - For maximum protection against corrosion for surfaces to be painted or left unpainted.
Class 3 - For protection against corrosion where low electrical resistance is required.

The only requirement in MIL-C-5541C for the chemical coating is that it be produced from a solution conforming to MIL-C-81706. These requirements are directed specifically toward military applications; however, chromate converstion coatings have many commercial applications and any coating that meets military requirements will certainly provide adequate commercial performance.

The government maintains a Qualified Products List (QPL) for MIL-C-81706 as well as for many other specifications. A QPL lists products that have been tested by the government and have been shown to meet specification requirements. By maintaining such lists, the need for much duplicative testing by government agencies and contractors is eliminated. Thus, the proprietary chemical processes for producing chromate conversion coatings listed on the QPL for MIL-C-81706 have all been shown to produce coatings that meet the requirements of MIL-C-5541C. Therefore, a user can be assured, without further testing, that any product on this list, when properly applied, will produce coatings that meet the requirements of the specification.

Considerable testing is required to qualify a product for inclusion on a QPL. First, a manufacturer must determine by actual tests that the product meets all the requirements of the specification. Second, a report of the test data must be submitted to the government agency responsbile for the specification. (In this case, the Navy Department). Third, the manufacturer provides two samples of material, each sufficient to prepare a 10-gallon bath. Fourth, the government agency uses one sample to prepare panels for testing according to the specification. If the panels pass all tests, the product is placed on the QPL. The second sample of material is used to prepare another set of panels for testing after the material has been stored for a specified period of time to determine its storage stability. All testing is done using 3 inch by 10 inch by 0.032 inch thick aluminum alloy panels.

## Description of Coatings

Chromate films on aluminum are generally thought to be a hydrated gel containing aluminum, hexavalent chromium, water, and other film-forming ions from the chromating solution. Chromating solutions, while usually proprietary in nature, contain chromic acid, other compounds whose ions contribute to the structure of the film, and ions to increase the rate of film formation. The chromate film, when first formed, is soft and easily damaged. However, it "cures" in about twenty-four hours. It is important not to heat the coatings to accelerate this "cure" since the structure and corrosion-resistant nature of the film will be destroyed if water is driven off from the gel structure of the film.

The color of chromate conversion coatings on aluminum varies from almost clear to an iridescent yellow or brown depending on the specific chemical nature of the chromating solution and the composition of the particular aluminum alloy. In

general, colored coatings are preferred since their color makes visual inspection for defects easier. Since the films are very thin and somewhat soft, they have only limited abrasion resistance. Normally, they will withstand moderate handling and careful cold-forming operations without significant damage to the films. In some instances, minor scratches in the coating are self-healing because the ions in the gel-like film can react with the exposed aluminum in the presence of moisture to reform the chromate film.

Performance Requirements

The performance requirements to be discussed are those of MIL-C-81706 which all chromating materials must meet in order to be placed on the QPL for this specification.

Materials used to produce Class 1A coatings are evaluated on aluminum alloys 2024-T3 and 7075-T6, while materials used to produce Class 3 coatings are evaluated on aluminum alloy 6061-T6.

The Class 1A coatings produced by these materials must meet the following requirements:

1. **Corrosion Resistance.** Chromated aluminum test panels must show no evidence of corrosion after 336 hours of 5-percent salt spray testing.
2. **Paint Adhesion (knife).** Paint applied over a primer to chromated aluminum test panels must not flake or separate when scored in a cross-hatch pattern.
3. **Paint Adhesion (tape).** Peeling of tape applied to the scored areas of the panels from the previous test must not cause a separation between the primer and the chromate coating or between the chromate coating and the aluminum substrate.
4. **Coating Weight.** The coating weight must be at least 40 milligrams per square foot as determined by weight difference when the coating is stripped in nitric acid.

Class 3 coatings produced by these materials must meet the following requirements:

1. **Corrosion Resistance.** Test panels must show no evidence of corrosion after 168 hours of 5-percent salt spray testing.
2. **Paint Adhesion (knife).** Same as for Class 1A panels.
3. **Paint Adhesion (tape).** Same as for Class 1A panels.
4. **Contact Electrical Resistance.** The contact electrical resistance of the coatings must not be greater than 5,000 microhms per square inch after application nor greater than 10,000 microhms per square inch after exposure to the 168-hour salt spray test.

## Evaluation of Test Panels

1. **Corrosion Resistance.** After salt spray, the test panels are examined visually with a naked eye. Bleaching or other changes of the iridescent color of the panels is not cause for rejection as long as there is no evidence of corrosion pits.
2. **Paint Adhesion.** Painted panels are evaluated visually after knife cross-hatching and again after tape is peeled from the scored area. No evidence of flaking or separation beyond the scored areas should be seen.
3. **Coating Weight.** After weighing, the panels are immersed in a freshly-prepared solution of nitric acid at room temperature for 60 seconds. The nitric acid solution is made up of equal parts by volume of concentrated nitric acid and water. The panels are then rinsed, blown dry with clean, oil-free air, and reweighed. The weight of the chromate conversion coating is calculated in milligrams per square foot as

$$\Delta W \times 2.4$$

   where $\Delta W$ is the difference between initial and final weights of the panels in milligrams. Table I shows the weight of chromate conversion coatings applied to the three different aluminum alloy test panels. These weights are averages of triplicate determinations. All of the coating weights significantly exceed the minimum of 40 milligrams per square foot specified for Class 1A coatings on 2024-T3 and 7075-T6 alloys. There is no specified minimum weight for Class 3 coatings.
4. **Contact Electrical Resistance.** The electrical resistance of Class 3 panels is measured before and after salt spray testing. Ten measurements are made on each of five panels. The panels are clamped between flat copper electrodes under a pressure of 200 psi. The average contact resistance must not exceed 5,000 microhms per square inch before and 10,000 microhms per square inch after salt spray testing. Individual readings not greater than 20 percent in excess of these maximum values are acceptable as long as the average of all ten measurements does not exceed the maximum values.

Table II shows the averages of ten contact resistance measurements on each of five chromated Class 3 panels before and after salt spray testing for 168 hours. The averages (as well as all of the individual measurements) are well below the specified limits.

## Process Description

The key to obtaining an acceptable chromate conversion coating on aluminum is the same as that for obtaining any other satisfactory surface finish: namely, proper surface preparation. The following sequence of steps has been demonstrated to

produce chromate conversion coatings that meet the requirements of both Class 1A and Class 3 coatings. Thorough rinsing must follow each step.

1. **Solvent Clean (Optional).** This step removes loose grease and marking inks.
2. **Soak Clean.** Use a mild alkaline cleaner especially formulated for cleaning aluminum. Such cleaners contain no caustic soda and therefore do not etch aluminum. A typical cleaner is operated at a concentration of 4 to 6 ounces per gallon and a temperature of 140 to 160°F.
3. **Etch (Optional).** An etch prior to chromating is often used to increase paint adhesion. A solution containing 6 ounces per gallon of caustic soda at 160°F can be used to produce a suitable etch. The time required to produce the etch depends on the particular alloy and the degree of etching desired.
4. **Desmut.** Etching of aluminum alloys, particulary those containing high copper concentrations, leaves a loosely-adherent smut on the surface. This smut can be removed in a solution of 50 percent nitric acid or a mixture of 2 to 3 parts concentrated nitric acid to one part 70 percent hydrofluoric acid. These desmutting solutions dissolve the smut and activate the surface by removing any aluminum oxide left on the surface. The best choice of desmutting solution will depend on the particular aluminum alloy being treated.
5. **Chromate.** Most chromating solutions are run at 75 to 85°F and require an immersion time of one to two minutes to produce a satisfactory conversion coating. Specific operating instructions for particular proprietary solutions should be followed carefully. Following chromating, parts should be thoroughly rinsed to remove all traces of the chromating solution. Final rinsing in warm (120- 140°F) water facilitates drying. When air is used to blow the parts dry, only cool (120-125°F) air should be used so that the coating will not be damaged by excess heat.

A bright aluminum pickle process can be used as an alternate to the etch and desmut steps described above. This process, based on sulfuric acid and hydrogen peroxide, will lightly etch, deoxidize, and desmut in one step. This process is usually operated at about 120°F. In addition to shortening the process sequence, it also has the advantage of eliminating the use of the hot caustic solution and the nitric or nitric- hydrofluoric acid solution, all of which are hazardous and expensive to operate.

Chromate conversion coatings offer many advantages in preparing aluminum surfaces for painting. They provide the best known method for obtaining paint adhesion as well as ease and speed of application, a fairly wide range of process parameters, and a coating that can be readily stripped and reapplied if a mistake is made.

TABLE I
WEIGHTS OF CHROMATE CONVERSION COATINGS ON ALUMINUM

| ALLOY | WEIGHT, mg/sq.ft. |
|---|---|
| 2024-T3 | 98.5 |
| 7075-T6 | 118.7 |
| 6061-T6 | 51.7 |

TABLE II
AVERAGE CONTACT RESISTANCE OF CHROMATED ALUMINUM

| | Resistance, Microhms/sq. inch | |
|---|---|---|
| Panel Number | Before Salt Spray | After Salt Spray |
| 1 | 1831 | 1955 |
| 2 | 2140 | 2403 |
| 3 | 702 | 2704 |
| 4 | 988 | 1915 |
| 5 | 1071 | 2332 |
| Grand Average | 1346 | 2262 |

# A-5

# Light Metals Finishing
# Session A

## Hard, Thick, Smooth and High Dielectric Strength Anodic Oxide Films

Setsuo Tomita
Tomita Electrochemical Research Laboratories
Koda City 444-01

Sakae Tajima and Shigeyoshi Morisake
Electrochemistry Lab
Tokyo City University and
Environmental and Resources Research Institute (NRI)
Tokyo University of Agriculture
Tokyo

Yoshio Hirayama
Nikkei Giken Research Center
Kambara City 421-32

# HARD,THICK,SMOOTH AND HIGH DIELECTRIC STRENGTH ANODIC OXIDE FILMS

Setsuo Tomita(Tomita Electrochemical Research Laboratories,Koda City 444-01)
Sakae Tajima and Shigeyoshi Morisaki(Electrochemistry Lab, Tokyo City Univ. and Environmental and Resorces Research Inst.(NRI), Tokyo University of Agriculture,Tokyo) and
Yoshio Hirayama(Nikkei Giken Research Center, Kambara City 421-32)

## Abstract

Hard,thick,lustrous,high dielectric strength and high thermal resistance anodic films on aluminum have been developed from organic acid based electrolytes in rather short time.. Dielectric strength 3000-4000 V(50 micron thick), 5000 V up (100 micron thick), DC (AC gives lower value), Hv 450 up, were attained at 20 ± 1°C , C.D. 2-5 A/dm$^2$ in 40- 80 min. for nearly all wrought alloys except some cast alloys, 2024 and 7075. Al-Mg(5052) and 3 N Al give excellent results. The films are smooth and crack-free with naked eyes and lustrous. Fewer corner effects are noted by not so strong shocking. Abrasion resistance is generally superior . Further ca. 500 micron(0.5 mm) thick films,still lustrous, reddish brown to brown colored, will be shown together with SEM picture. Detailed data will be given particularly for breakdown voltage. These data are the results from the comparison with the conventional sulfuric acid hard anodizing. The quality may be still improved by further efforts.. For presentation,slides,OHP(SEM and thermal analysis) and real samples will be used.

## Introduction

Early in 1904, F.Fischer(5) reported that 300 micron thick anodic oxide film could be formed on Al-tube in 24% sulfuric acid by passing cold water through the tube. A.Miyata(1,2), Th.Rummel(1,2,3,4) ,G.Elssner(1,2,3,4),during 1930-1940, obtained thick films in oxalic or sulfuric acid. However,N.D.Tomashov(7) seems the first who applied these thick films as hard and abrasion resistant films for engineering purposes. Thereafter, practical hard anodizing became popular. The process proposed by Tomashov is briefly outlined as follows:

Electrolyte 200 g/l, 1-3°C.
Voltage 23-100 V, 240 min.
Film thickness 130-170 micron
Porosity 20 % for 1010 Al, 35 % for 2018.

M.M.Lerner of the Sanford Process Corp. in US seems the successor of this tradition. However, as to the high dielectric strength and accordingly high thermal resistant films, the research interest had not been so intensive,it seems. At one time, the breakdown voltage measurement was used as a measure of anodized film thickness. A.Miyata(2) who pioneered in "sealing"(by steam ,5-6 kg/cm$^2$ in an autoclave) and also first proposed the"barrier + porous" duplex structure, was originally an electric engineer who, of course , had an interest in "breakdown"voltage both in wet and dried states. But it seems,he had more interest in the former,i.e. pure barrier utilization for electrolytic capacitors. The barrier layer grows in,e.g., borate solutions by 10-14 Å/V and the maximum breakdown voltage is ca.700 V(equivalent to ca. 1 micron thick).
For oxalic acid duplex type film, 30 micron, Miyata obtained 10.3 kV/mm(10.3 V/micron), 14,5 kV(14.5 V/micron) for steam-sealed film,by applying AC(50 cycles). Miyata stated that the electric resistance of as-anodized film is nearly equal to the value of the same thickness of "air" and concluded that barrier layer is only playing a rôle of "separator". Since the pure barrier film is so thin that the engineering and mechanical use can not be expected.

Measurement of Breakdown Voltage in Dried States(1,2,3)

In order to determine the electric breakdown voltage,particularly of anodic aluminum oxide films,,there exist the two typical test methods. The one is the "Probe test" which uses graphite or stainless steel rod as counter electrode and the other electrode is,of course, basis aluminum plate. The other method is "Mercury pool" or "Evaporated silver" as counter electrode. However,there exist numerous complex factors such as degree of humidity, and vacuum,the rate of voltage rise,use of DC or AC and the cyles, the permissible leakage current,roughness of the surface and existence of cracks,, impressed presure of the counter electrode etc and no general definite methods seem exist.. The reports in this field seem to use the method of their own choice. Usually DC gives higher values than AC. At any rate, the hitherto reported data : 10-20 V/micron seems the average value.

The maximum dielectric strength hitherto attained (4) seems ca. 2000 V.

| | | |
|---|---|---|
| ASTM B-110(Probe test) | 100-125 micron | 1800 V for 2024-T3 |
| | | 6061-T6 |
| Mercury pool method | " | below 600V for 2024-T3 |

by R.F.Hafer quoted by J.Machlin et al(7).

From these not a big amount of data, it is known that the values of dielectric strength is rather fluctuating.

For comparison, the data for some synthetic plastics are shown:

| | |
|---|---|
| PVC | 1000-1200 V/100 micron |
| Polyethylene | 1200-1400 V/100 micron |
| Vinyl carbasol | 3000-4000 V/100 micron |

From these data,the value of dielectric strength , apart from the original properties,is dependent how thick, compact and smooth the mamaterial is.

Classification of Hard Coatings

As seen in the last Paragraph, the high dielectric films must be thick and smooth in order to secure good contact between dielectrics and the counter-electrode, while thicker films mean hard coatings in the case of anodic aluminum oxides. One of the authors,Tajima(3,8,9) defined hard coating(except corrundum coating(3,4,10) as the "semi-barrier" type coating,i.e.,the intermediate between "pure barrier film" and "barrier + porous-layered film(duplex type). The duplex film usually after reaching maximum thickness(ca.25-35) finally disappears (3) by temperature rise and induced strong solvent action of the electrolyte.

The semi-barrier type films can be classified into 3 types as shown in Table 1. It is to be noted that the anodic oxide and the anion content in the electrolyte and in the film is ,so to say, in a dynamic balanced state,i.e.,the concentrations are nearly the same. Sulfuric acid coating contains nearly similar amount of sulfate. The high potential gradient produced by low temperature leads to the "coloring potential" or "excited state potential" causing excess $Al^{\circ}$ in the film(18,11,8) or "excited carboxylate ions" in the case of oxalic acid films etc, causing EL(electroluminescence) in the dark ,finally ends in the tarry products(yellow through reddish brown to brown). Excess $Al^{\circ}$ in sulfuric acid film causes light brown through brown to black color(so to say, dirty gem).

Formation of Hard,Smooth,High Corrosion Resistance and High Dielectric Strength Films

Table 1. Classification of Hard Coatings

| | So-called Hard Coating | Integral Color(A) | (B) |
|---|---|---|---|
| Electrolyte | Sulfuric acid 1-30 % (basic acid) | Sulfonated aliphatic or aromatic acid + sulfuric acid | Oxalic acid or other mixtures |
| Temperature | -5-20 C | 20-30 C | 5-40 C |
| C.D. $A/dm^2$ | ≒ 3 | 1-2 | 1-5 |
| Thickness, μm | below 200 | normally up to 40 for architectural | 500 or more |
| Type | Semi-barrier | Semi-barrier | Semi-barrier |
| Composition | $Al_2O_3$ + sulfate + $Al^\circ$ + some sulfur | $Al_2O_3$ + sulfate + $Al^\circ$ | $Al_2O_3$ + organic polymerized tarry products |
| Color | light brown, grey to black | light, deep brown to black | light yellow, gold, reddish brown |
| Origin of color | excess $Al^\circ$ + some S in the film | excess $Al^\circ$ in the film | excited carboxyl radicals(and polymerized tarry products) |
| Smell | deposited S, $H_2S$ at low temp. or when too thick | -- | -- |
| Coloring potential | above 20 V | above 15 V | 7V especially AC |
| Luminescence | -- | -- | EL, PL by UV |
| Roughness | becoming rough with thickness | rather smooth | smooth and lustrous |
| Cracks and corner effect | many and brittle | many micro-cracks | apparently few long streaks above 250 micron |
| Hv | ≒350 | ≒400 | above 450 |
| Dielectric strength | not good (detailed in other Tables) | permissible | excellent |

As shown in Table 1, we presumed that the most promising coatings may come from the Integral color(B). Incidentally the electrolyte composition is similar to that proposed by P.Lelong, R.S.Segond and J.Herenguel(12), followed by E.Lichtenberger and co-workers(13,14) as rapid anodizing. According to Lichtenberger and Hollo, at the formation voltage up to 50 V, the barrier thickness may be up to 540 Å(by the Hunter method) and the coatings are substantially less porous, e.g. 1-2 x $10^8$ pores/$cm^2$. The cell diameter is correspondingly larger, which will be shown later by our SEM picture. In this connection, Lichtenberger and G.J.V.Raja(13) reported the breakdown voltage as 1000-1200 V at anodizing voltage at 55 V DC for 10-12 micron film. Oil uptake 0.002-o.0006 g/$dm^2$ is described. But no mention is made on the method of breakdown voltage and as-anodized or after oil-uptake. It seems they examined no thicker films than about 50 micron due to excessive heating of the bath.

Now we shall describe our proposed conditions. As mentioned before, the electrolyte is similar to those of Lelong et al. and Lichtenberger et al. However, we made a unique and creative designing in the bath construction, electrode materials and improvement of anode throw and way of cooling, and cleared at least 5000V per 100 micron or more and Hv above 450.

| | | | |
|---|---|---|---|
| Electrolyte | Oxalic acid | 80 g/L | Initial voltage is 60 V as compared with 20-30 V of Lichtenberger, perhaps due to our strong cold jet stream. |
| | Formic acid | 50 g/L | |
| Temperature | 5-40 C | | |
| Counter cathode | graphite sheet, C.D. 2-6A/$dm^2$ | | |

Very smooth, lustrous, hard, hard, thick, lustrous, reddish-brown films are obatained with less crack up to 300 micron and up to 500 or more with few but long stretched streaks. We think that the reason of the difference in appearance, feature of cracking and smoothness from those of sulfuric acid hard coating is due mostly to the tarry products in the film as mentioned in Table 1. Al-oxalate complex had been extracted and final cyclization are confirmed by M.Shimura and S.Tajima 15,16).

For the present purpose,,an important bath construction was designed by S.Tomita (17) which was registered as US and Japanese Patent(1980 and 1985) and further improved. The appearance of the bath in operation is shown in Fig.1. The anode works assembly is racked with all titanium frame. The counter cathodes are of graphite plates which are located below the electrolyte level in order to enhance cooling efficiency(cooled electrolyte circulation is not disturbed). One series of anode works are located between the two series of cathodes only. Works are not hanged but tightly fixed to the anode racks. No anode rocking is adopted. Instead, the anode works are subjected to anolyte jet stream(1.5 m/s). which is overflown to the outer jackets where the electrolyte is cooled by heat-exchanger and pumped up again into the anodes as jet stream. Thus the cooling-throw is uniform and the efficiency becomes excellent to avoid overheating from the desired temperature and to permit film thickening., In this way, anodizing can be performed at 2-6 A/$dm^2$ and at 5-30 C. in spite of great amount of heat evolved. Fig.2 and 3 show the rackings and finished products.

Measurement of Breakdown Voltage(Typical Examples)

The measurement is based on Probe tests as described before. Stainless steel rod (6 mm diameter) was pressed on the anodized specimen under the load of 100 g. By impressing DC or AC voltage, the breakdown voltage, is judged from the initiation of 40 mA flow . The apparatus used was the dielectric strength measuring apparatus made by the Toyo Seiko Co. and the maximum value is 5000 V

Table 2. Breakdown Voltage of Anodic Films on 5052(Al-Mg), mill-cut (V)$_{DC}$

| Sample | 0 unsealed | 1 boiling water 30 min | 2 boiling water and paraffin | 3 steam-sealed 5 kg/cm$^2$ |
|---|---|---|---|---|
| | 1400 | 3000 | 3100 | 1500 |
| 1 | 1400 | 2800 | 3000 | 1400 |
| | 1600 | 3000 | 2500 | 1600 |
| (20 $\mu$) | 1800 | 3000 | 3100 | 2200 |
| | 1300 | 2900 | 3100 | 2400 |
| ave | 1500 | 2940 | 2960 | 1820 |
| | 3900 | > 5000 | 4500 | 4600 |
| 2 | 4300 | 4700 | 4400 | > 5000 |
| | 5000 | 4800 | 4500 | > 5000 |
| (50 $\mu$) | 4400 | 4200 | 4300 | > 5000 |
| | 4400 | > 5000 | 4500 | > 5000 |
| ave | 4400 | – | 4440 | – |
| | > 5000 | > 5000 | > 5000 | > 5000 |
| 3 | > 5000 | > 5000 | > 5000 | > 5000 |
| | > 5000 | > 5000 | > 5000 | > 5000 |
| (100 $\mu$) | > 5000 | > 5000 | > 5000 | > 5000 |
| | > 5000 | > 5000 | > 5000 | > 5000 |
| ave | > 5000 | > 5000 | > 5000 | > 5000 |
| | > 5000 | > 5000 | > 5000 | > 5000 |
| 4 | > 5000 | > 5000 | > 5000 | 3200 |
| | > 5000 | > 5000 | > 5000 | 4200 |
| (150 $\mu$) | > 5000 | > 5000 | > 5000 | 3900 |
| | > 5000 | > 5000 | > 5000 | > 5000 |
| ave | > 5000 | > 5000 | > 5000 | – |

Table 3. Breakdown Voltage of Anodic Films on 5052(Al-Mg), mill-cut (V) AC

| Sample | 0 unsealed | 1 boiling water 30 min | 2 boiling water and paraffin | 3 steam-sealed 5kg/cm$^2$ |
|---|---|---|---|---|
| | 900 | 2450 | 2150 | 1800 |
| 1 | 850 | 2500 | 2650 | 1050 |
| | 450 | 2450 | 1950 | 1450 |
| (20 $\mu$) | 850 | 1450 | 2550 | 1450 |
| | 650 | 2050 | 2550 | 1500 |
| ave | 740 | 2180 | 2370 | 1450 |
| | 1500 | 3800 | 3450 | 3100 |
| 2 | 1450 | 3800 | 3450 | 3300 |
| | 1500 | 3600 | 3800 | 2900 |
| (50 $\mu$) | 1550 | 3550 | 3650 | 2600 |
| | 1400 | 3850 | 3850 | 2700 |
| ave | 1480 | 3720 | 3640 | 2920 |
| | 1950 | 4100 | 3700 | 3400 |
| 3 | 2050 | 4300 | 3800 | 3350 |
| | 2250 | 4300 | 4100 | 3800 |
| (100 $\mu$) | 2300 | 4200 | 3850 | 3450 |
| | 2300 | 4500 | 3300 | 4000 |
| ave | 2170 | 4280 | 3750 | 3600 |
| | 2950 | 4100 | 2850 | 3350 |
| 4 | 3300 | 4600 | 3500 | 2900 |
| | 3450 | 4750 | 4150 | 3700 |
| (150 $\mu$) | 3500 | 4450 | 4600 | 3300 |
| | 3550 | 4350 | 4000 | 2500 |
| ave | 3350 | 4450 | 3820 | 3100 |

Table 4. Breakdown Voltage of Anodic Films on 5052(Al-Mg) as-rolled (V) DC

| Sample | 0 unsealed | 1 boiling water 30 min | 2 boiling water and paraffin | 3 steame-sealed 5 kg/cm$^2$ |
|---|---|---|---|---|
| 1 | 1000 | 2000 | 2800 | 2350 |
| (20 $\mu$) | 1200 | 1850 | 2500 | 1700 |
| | 1050 | 2700 | 1900 | 2600 |
| ave | 1080 | 2180 | 2400 | 2220 |
| 2 | 1300[1] | 4700 | >5000 | 3100[2] |
| (50 $\mu$) | 3000 | 4700 | >5000 | >5000 |
| | 2800 | 4350 | >5000 | 4300[2] |
| ave | 2900 | 4580 | >5000 | – |
| 3 | 4900 | >5000 | >5000 | 4500 |
| (100 $\mu$) | >5000 | >5000 | >5000 | 4500 |
| | >5000 | >5000 | >5000 | 4300 |
| ave | – | >5000 | >5000 | 4430 |
| 4 | >5000 | 3800 | 3900[4] | 3350 |
| (150 $\mu$) | >5000 | 4800 | >5000 | 2800[3] |
| | 4250[3] | 5000 | 4100[4] | 3150 |
| ave | – | 4530 | – | 3100 |

Note 1) material defects ?
2) cracked parts
3) fault
4) white spot

which is regretably low in the present experiment. By considering the effect of surface condition before anodizing, 5052(Al-Mg) plates were mill-cut or used as-rolled and finally alkaline-degreased. The reason for taking up 5052 is that it gives best and reproducible results,together with 3N or 4N Al.
The detailed data are shown in Table 5,6,7.
From the Tables,it is understood that mill-cut surfaces(DC) give best and stable results,clearing up 5000 V already at 100 microns(50 V up per micron).
It is already known that DC gives higher values than AC.
In any case , unsealed and steamed-sealed (6 kg/cm$^2$) gave lower and fluctuated values. Meanwhile, it is generally believed in Japan that the steam-sealed surface gives stable and higher values. The reasons in our case are not yet well clarified.A.Miyata(2) states that steam-sealing is best fitted for oxalic films.
During the research,we examined the limit of available thickness and obtained ca. 500 micron . The surface is deep reddish brown and still lustrous,but a few long streaks were noted instead of micro-cracks. Fig.4 shows 206-208, 303-306 and 494-497 micron (left to right) thick disks.

Tests for other Al-alloys

Here we show the brief summaries of Hardness, abrasion resistance,corrosion resistance(CASS R.N.) etc for typical Al, wrought and cast alloys as compared with the conventional sulfuric hard coatings.

(A) Wrought alloys ca. 50 micron thick
1. Excellent hardness Hv + 450 especially for pure Al and 5052. against 350 doe sulfuric acid coatings.
2. Abrasion resistance(ISO-1,400 g load,1500 cycles), excellent except 2024 and 7075
3. Corrosion resistance is all excellent. CASS R.n. 9.5-9.8 against 7-9.8 (Nickel acetate sealing)
4. Dielectric strength is also superior, ca. 2000 V/50 micron
5. Specific resistance is excellent especially for Al and 5083,10.0-123x10$^{10}$ ohm cm.

(B) Cast alloys, ca.50 micron.
1. Hardness is superior in sulfuric acid coating except AC4A and AC7A.
2. Abrasion resistance is superior in the present process for AC,4A,7A and ADC. For others the conventional process is better.
3. Corrosion resistance is nearly the same.
4. Dielectric strength is not good in both processes.
5. Specific resistance is only superior by AC7A only and sulfuric acid coatings are usually superior.

SEM and Thermal Analysis

Fig.5 shows the 426 micron thick Al disk formed at 2.5 A/dm$^2$, 20 ± 1 C and its fractured surface and a SEM analysis sample on the right.
Fig.6 shows the fractured surface taken by scanning electronmicro scope(SEM, x10,000. Parallel pore structure is quite distinct. Cellsize ca 2000,pore dia,ca800 Å.
Fig.7 shows the SEM picture at Al and Oxide boundary cut by microtome x3000. Scratch on basis Al by microtome is distince but the pore just above is a little ambiguous.

Further,we have examined the same film(426 micron) with DTA and TG analysis. The experiments were made from 50 to 600 C(25 C/min). At 300 C, 0.9 wt. % water was lost and at 500 C, further 0.9 wt.%(organic substance).Thus totao 1.8wt% has been lost,which is surprisingly a small amount. It explains that the film, 425 micron thick is very compact, smooth and lustrous and hard--semi-barrier type.

References

(1-4) General references
1. Max Schenk, Werkstoffe Aluminium und seine Anodische Oxydation, pp.1042 (A/Francke Verlag, Bern 1948)
2. Akira Miyata, Anodic Oxidation(in Japanese), pp.232(Nikkan Kogyo Shimbunsha Tokyo 1954)
3. Sakae Tajima, Anodic Oxidation of Aluminum,pp.229-362 with 424 references together with authors and titles, in "Advances in Corrosion Science and Technology" Vol.1(M.G.Fontana and R.W.Staehle,editors, Plenum Press, New York (1970)
4. S.Wernick and R.Pinner, The Surface Treatment of Aluminium and its Alloys, Vo..I and II, pp.1274. Robert Draper Ltd.,Teddington 1972. Revised edition (P.G.Sheasby cooperating, Finishing Publications,1987)
5. F.Fischer, Z.Elektrochem., 10, Nr.46, 860-877(1904)
6. N.D.Tomashov, Vestnik Inzenvori i Teknishov 59(1946); Light Metals 9,429(1946)
7. I.Machlin and N.J.Whitney, Metal Finishing 59, No.2, 55-57(1961)
8. S..Tajima, Sur/Fin '87, Intern. Technical Conf. Proc.,Chicago 1987,Session H, H-7(Light Metals Finishing III)
9. S.Tajima,M.Soda,N.Baba and T.Mori,Electrochim. Acta 1,205(1959)
10. S.Tajima, Y.Tanabe ,M.Shimura and T.Mori, ibid.,6 127(1961)
11. K.Wefers and E.T.Evans, Plating and Surface Finish. 63 951(1975)
    K.Wefers and P.F.Wallace, Aluminium 52 485(1976)
12. P.Lalong, D.R.Segond and J.Herenguel, Rev.de l'Aluminium, 37 67-76(1960)
13. E.Lichtenberger and G.J.Jagandha Raju, Electroplating and Metal Finishing 15 No.1o, 342-348(1962)
14. E.Lichtenberger and M.Hollo , Metaux-Corrosion-Industrie, No.449, 1-13(1963)
15. M.Shimura and S.Tajima, Chemistry Letters(Chem. Soc.,Japan) 1435(1974)
16. M.Shimura,Farad. Trans.I, 72 2248(1976)
17. S.Tomita et al. USP 4,225,339(Sept. 30, 1980)
18. S.Tajima, Electrochim. Acta 22,No.9, 995-1011(1977)
    S.Tajima, N.Baba, K.Shimizu and I.Mizuki, Electrocomponent Sci. and Techn., 3. 91-95(1976); S.Tajima, K.Shimizu, N.Baba and H.Sakai, ibid. 3,127-130(1976)
    Y.Yamamoto,N.Baba and S.Tajima,Nature , 289, No.5798, 572-524(Feb. 12,1981)
    S.Tajima, N.Baba and I.Mizuki, Extended Abstracts Vol.73-1,The Electrochemical Society, Spring Meeting pp.52-53,Chicago.May (1973)

Fig. Captions

Fig.1 A newly designed anodizing tank at work. All the anode works and cathodes are located below the electrolyte level. Apparent eddy motion of the electrolyte is due to cooled jet stream. Details in the text(Tomita Electrochemical Research Laboratories)

Fig.2 Racking and the finished air-cylinders(Tomita Electrochemical Research Laboratories)

Fig.3 Racking of demonstration works. and the finished gifts(205 micron thick, reddish brown and lustrous(Tomita Denka Research Laboratories)

Fig.4 From left to right, 206-208, 303-306 and494-497 micron thick disks. These films are smooth and lustrous and reddish brown.

Fig.5 Disk,426 micron,,fractured and the specimenfor SEM examination near the right side

Fig.6 Fractured section of the sample,Fig.5. 10000 x. Details in the text. Cell size ca. 2000 Å and pore diameter ca.800 Å

Fig.7 The boundary of basis Al and the oxide(microtomed) 3000 x. Details in the text.

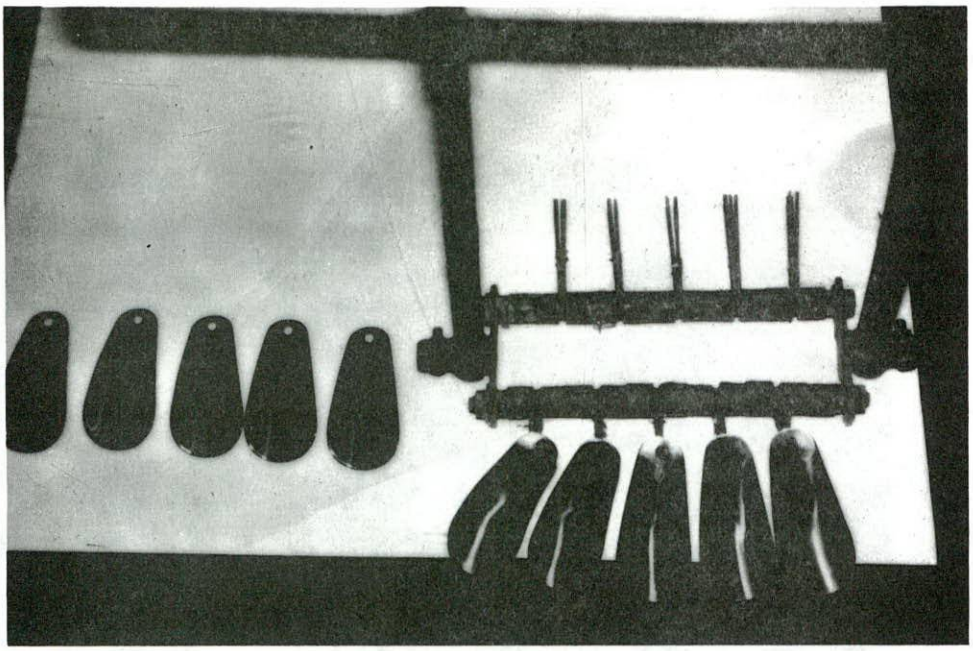

Fig.1

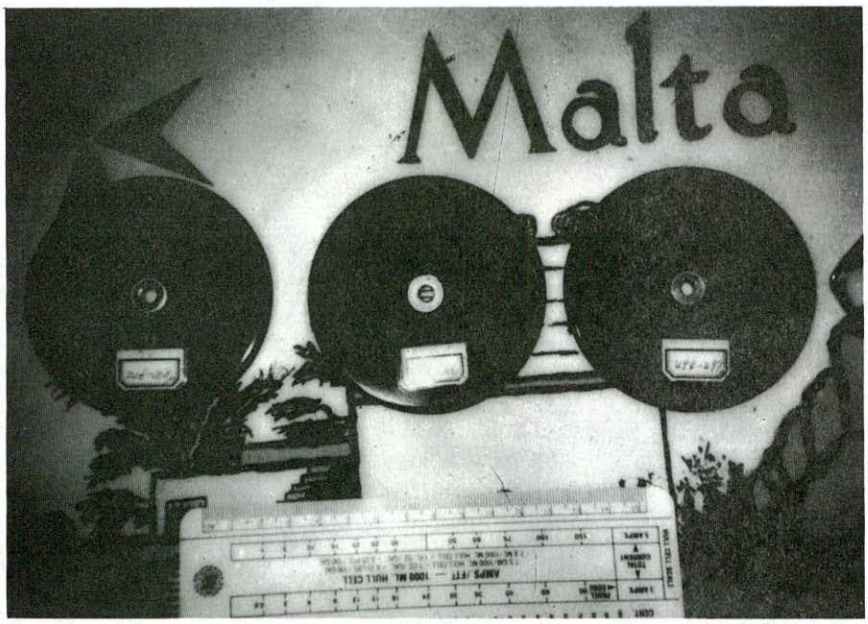


Fig 2

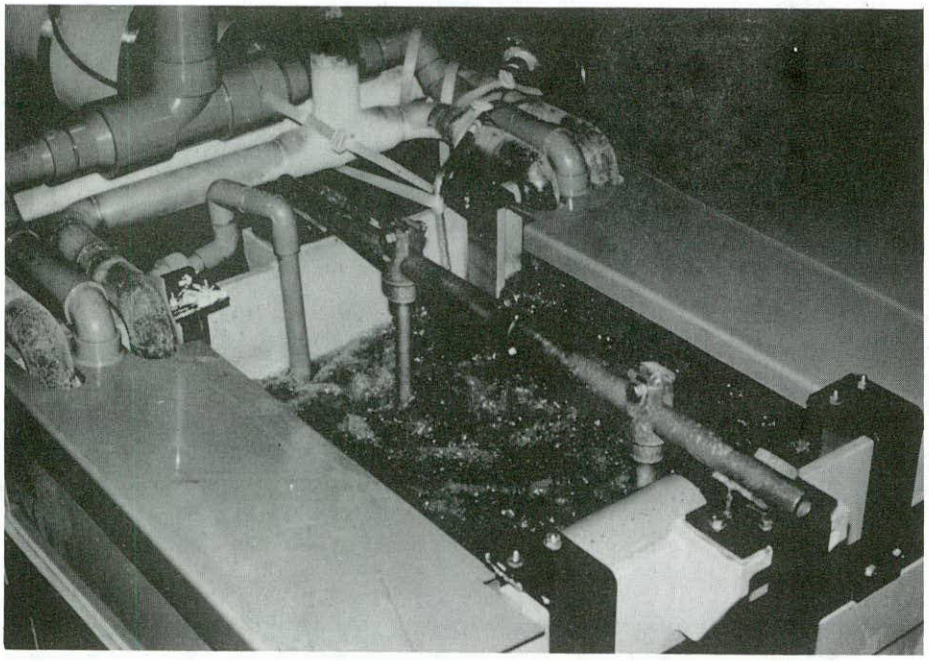

Fig.3

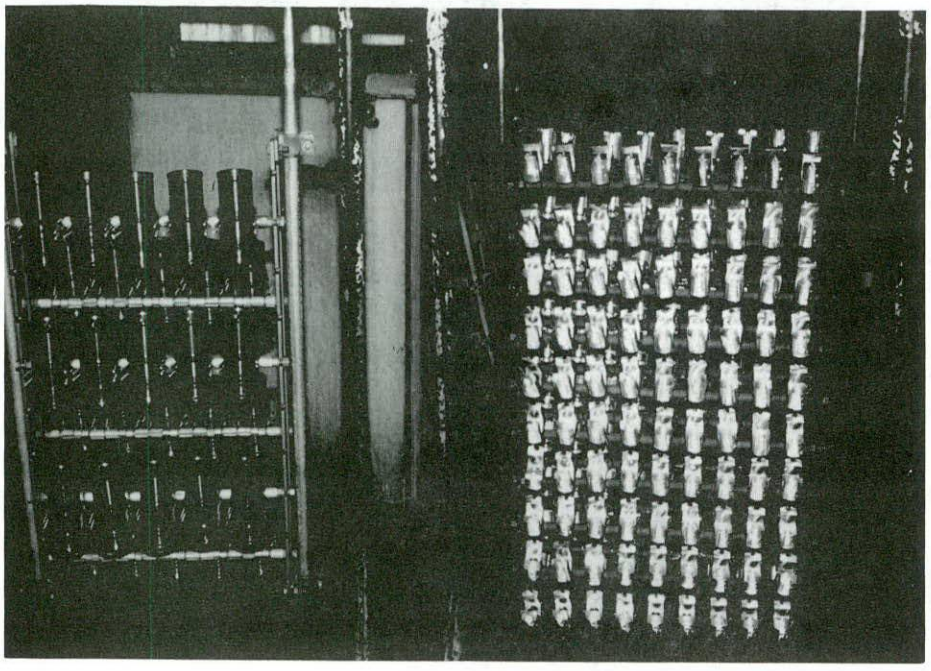

Fig.4




Fig.5

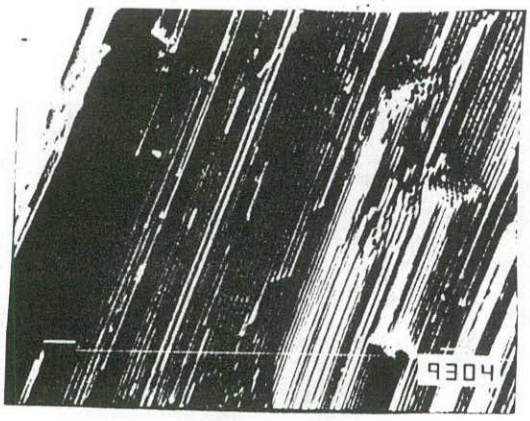


Fig.6

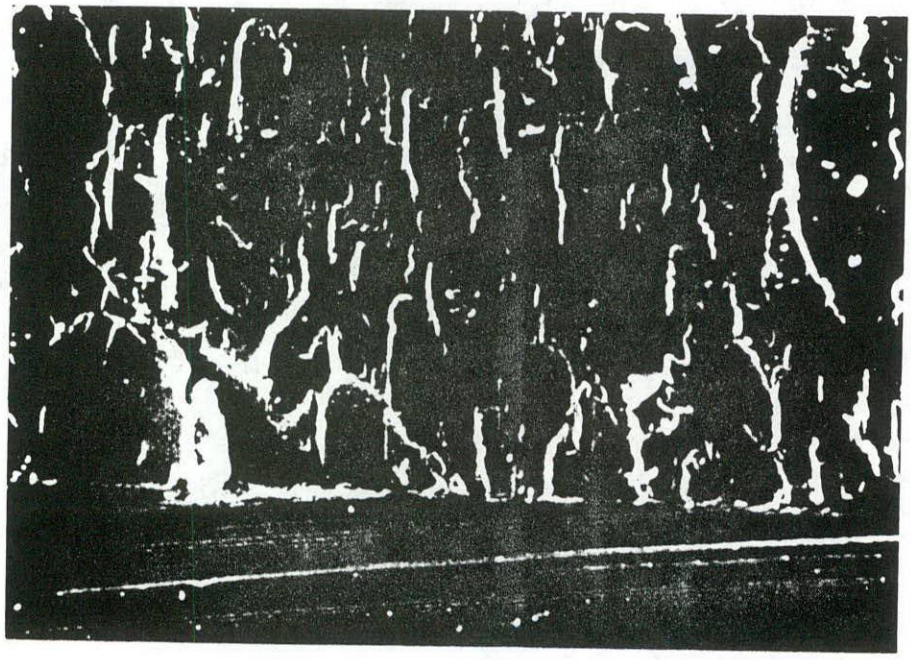

Fig.7

A-6

# Light Metals Finishing
# Session A

## An Electrochemical Method to Control The Anodizing Process

S. Yousri
Pratt & Whitney Canada Inc.
1000 Marie Victorin
Lonqueuil, Quebec, J4G 1A1

# AN ELECTROCHEMICAL METHOD TO CONTROL THE ANODIZING PROCESS

By
S. Yousri
Pratt & Whitney Canada Inc.
1000 Marie Victorin, Lonqueuil, Quebec, J4G 1A1

## Abstract

An electrochemical method has been developed to rapidly evaluate the quality of anodized aluminum coupons. (1) The test has been optimized for quality control applications via a sample test fixture which allows standard sample coupons to be conveniently interchanged.

## Introduction

The aluminum anodizer has to make decisions on a daily basis regarding the performance of his operations.

For example one part processed 10 days ago is showing corrosion in the Salt Spray (ASTM B-117)

Do I change the sealant tank?

Do I run a complete analysis of the anodizing tank?

Do I change or verify the cleaning process or the rinsing process?

Do I change everything and start fresh?

The answer could be one of the above or a combination thereof. Once action is taken you wait again for the salt spray test to be completed. You still face the distinct possibility that sooner or later the problem will return and you have to start all over again. At Pratt & Whitney Canada the use of the Electrochemical test method has removed all the doubts from the anodizing process control, with the following results:

- No salt spray failure of a part processed in 3 years
- The chromic acid anodizing tank was not changed in 3 years
- Sealant tank performance is monitored on a daily basis and the sealant solution cleaned or changed to maintain maximum performance.

## Theory

The electrochemical techniques for corrosion rate measurements employ a potentiostatic circuit to simultaneously apply a potential to the specimen in solution while measuring the current that flows due to the electrochemical reaction induced by the applied potential. It has been shown (2,3) that if the applied potential is systematically scanned in a region close to the specimen's open-circuit potential (Ecorr), a plot of applied potential versus the Log current can be used to calculate the corrosion rate. This type of plot is called the Tafel plot.

Figure 1 shows an idealized Tafel plot. It can be seen in this figure, that for a simple metal-solution system, linear regions of the scan can be extrapolated back to the open-circuit potential to yield a quantity called the corrosion current (Icorr). Icorr is the current which will flow to support a corrosion reaction under naturally occurring conditions, i.e., at the open-circuit potential.

The physical interpretation of the plot is as follows: At the open-circuit potential a net current of zero is flowing at the electrode, because both oxidation and reduction reactions are simultaneously occurring at equal rates. As the potentiostat is used to remove the specimen potential from Ecorr, one or the other electrochemical reaction is accelerated. If the applied potential is positive of Ecorr, then the oxidation reaction will be enhanced and a net positive (anodic) current will be observed. If the applied potential is negative of Ecorr, then the reduction reaction will be enhanced and a net negative (cathodic) current will be observed.

Icorr is directly related to the corrosion rate by the equation:

$$\text{Corr. Rate} = \frac{0.13 \times \text{Icorr} \times \text{E.W.}}{d}$$

Where: E.W. = equivalent weight of the oxidized element in grams

Icorr = corrosion current density in microamps per square centimeter

d = specimen density in grams per cubic centimeter

The acquisition and analysis of Tafel plots can be automated via microprocessor-controlled or PC-based instrumentation.

## Experimental

The electrochemical instrumentation consisted of an EG&G Princeton Applied Research Model 350-1 Corrosion Measurement System. This system was used to automate the acquisition of Tafel plots, identify linear trends in the plots, and calculate the corrosion rate estimates.

The specialized electrochemical cell shown in Figure 2 was used in place of the standard corrosion measurement cell which is normally supplied with the system. This cell consisted of a hollow Teflon cylinder (A) with a 5.00 cm outside diameter and 11.5 cm height. The walls of this cylinder were 1.5 cm thick at the top and widened to 6.0 cm at the bottom to facilitate clamping to the base (B). The base was a solid Teflon cylinder with a 7.5 cm diameter and 2.5 cm height.

The cell was assembled with the test coupon (C) inserted between the hollow cylinder and the solid base. A rubber o-ring was used along with a clamp to create a water-tight seal. In this way, the test coupon surface acually served as the bottom of the cell.
The test coupons were the same standard AMS 4037 test panels (3 inch x 10 inch) that are used in the salt spray testing. To facilitate electrical contact, one corner of the anodized panel was ground to expose bare metal.

The Teflon lid (D) for the cell had three holes bored into it to allow the platinum wire counter electrode (E), saturated calomel reference electrode (F), and an air agitation device (G) to be introduced into the test solution.

The resulting test cell, allowed a solution volume of 200 milliliters to be be used with a moderate air-stirring rate. This volume of solution was found to be sufficient to negate the effects of metal dissolution which occurred during the course of a typical test.

Prior to testing, each specimen panel was solvent degreased, rinsed with deionized water, and activated at a potential of +1.0 Volts vs. SCE for 30 seconds. Following this pre-conditioning potential, the open-circuit potential was monitored and the scan was initiated once the system had equilibrated (as evidenced by a stable open-circuit potential). This generally required between 20 seconds and 5 minutes.

The instrumentation automatically recorded Ecorr and executed the applied potential scan from Ecorr +400 mV to Ecorr -400 mV. A scan rate of 0.5 mV per second was used, which resulted in a scan time of 26 minutes.

## Results

Figures 3a and 3b show actual instrument outputs for the tests of two anodized specimens. Figure 3a shows the Tafel plot report for a specimen with a relatively good anodic coating. Note the reported corrosion rate (designated MPY in the figure) of 0.013 milli-inches-per-year. It should be noted that the implied precision of the reported value is a function of how precisely the constants (equivalent weight and density) were input to the instrument by the operator. The real precision of this value is probably only good to the second decimal place. The high corrosion rate of 0.68 MPY is calculated in Figure 3b for a specimen with a poor anodic coating.

Four years of studies comparing different panels processed under different conditions and testing duplicates in the salt spray cabinets helped us establish the following process control parameters.

1. Panels showing corrosion rates under 0.1 MPY will not fail the salt spray.

2. When panels display a corrosion rate of over 0.1 MPY but under 0.5 MPY, the Laboratory warns Production that the anodizing process is deteriorating and corrective action is taken immediately.

   Panels processed under those conditions will pass the salt spray 9 times out of 10.

3. Panels with corrosion rates over 0.5 MPY: The Laboratory requests immediate corrective action. Parts are reprocessed if the corrosion rate is over 1 MPY. Between 0.5 and 1.0 MPY, the judgement is dependent on the parts application.

4. Optimized the sealant times: It was found that with very fresh deionized water the optimum seal time was 8 minutes. On the other hand a month old seal solution will require 15 minutes to seal properly.

5. Optimized the sealant temperature: Due to a failure in a steam heating coil, the temperature in the sealant tank dropped to 85°C (within our previous specs.). Panels tested that day showed corrosion rates higher than 0.5 MPY. The line was stopped until an auxiliary coil was added and the corrosion rate dropped to 0.01 when the temperature reached 95°C. The problem was corrected in a few hours. (95°C ± 5°C is our present spec).

## Conclusions

Electrochemical techniques are quickly emerging as a tool for rapid control of any surface finishing process. We are presently working to extend our findings on the aluminum anodizing process to other finishes. We have tested the effects of different solutions on Titanium and Magnesium alloys and the results are encouraging.

The main advantage of the technique is that it answers a basic question: Since a coating or a finish is applied to prevent corrosion, how can we find out if it works without waiting several days.

## References


1. S. Yousri and P. Tempel, Plating & Surfacing Finishing Vol 74, No 11 (1987).

2. M. Stern and A.L. Geary, J. Electrochem. Soc., 104, 56 (1957).

3. EG&G Princeton Applied Research Application Note Corr-4. Available from EG&G Princeton Applied Research, Electrochemical Instruments Division, upon request.

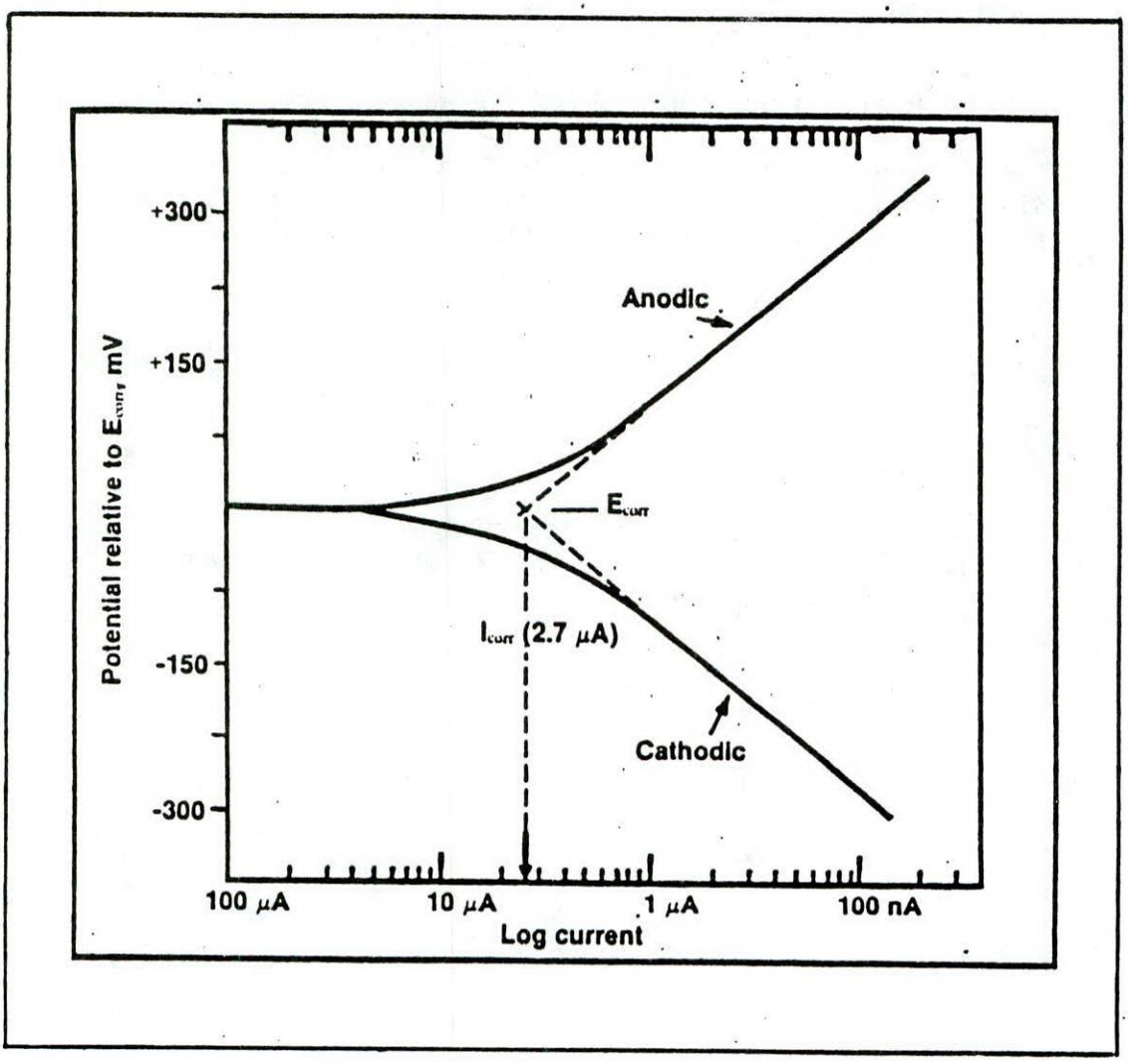


Fig. 1– Tafel plot for ideal electrochemical system

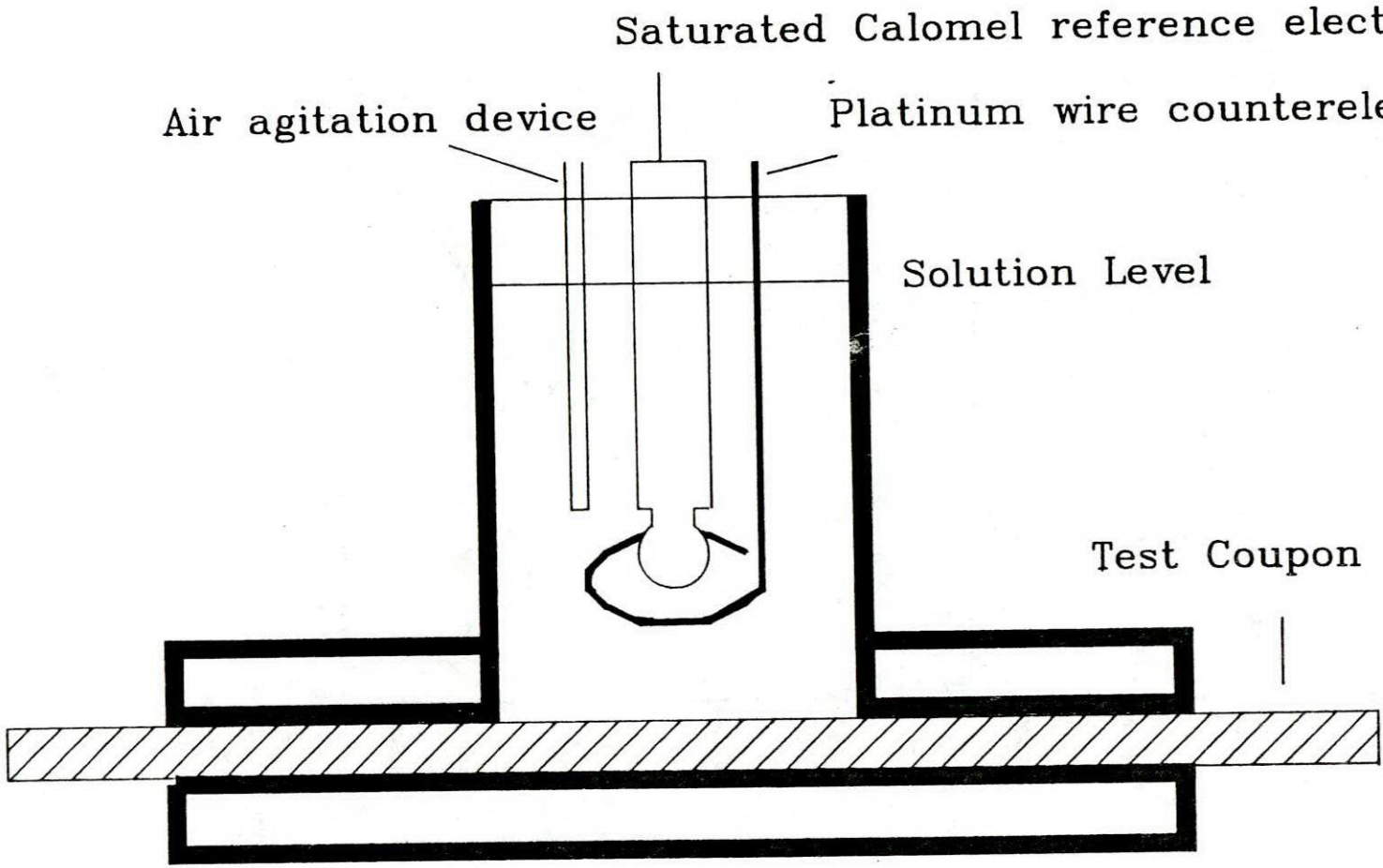


Fig. 2 – Cell for testing anodized coupons.

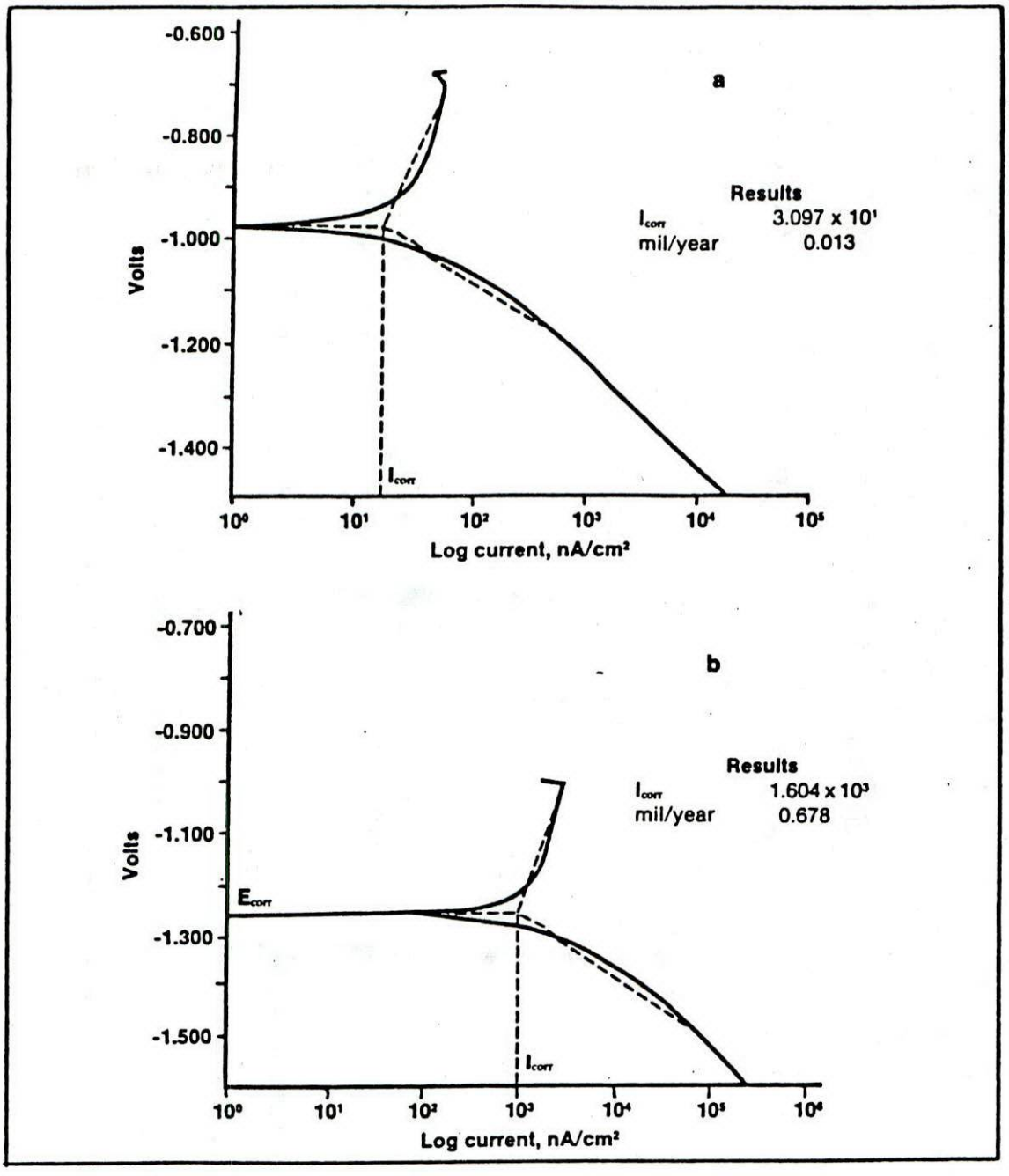


Fig. 3– System printouts for two typical tests (a) good and (b) poor coating

A-7

# Light Metals Finishing
# Session A

## Designing an Automated Extrusion Anodizing Facility

Glenn C. Schoener
Walgren Company
Grand Rapids, MI

# DESIGNING AN AUTOMATED EXTRUSION ANODIZING FACILITY

Glenn C. Schoener

Walgren Company
Grand Rapids, Michigan

Fully automated extrusion anodizing facilities represent the current state-of-the-art in anodizing technology. Five such facilities have been or are being built today. Several more are currently in the design stages. Automating an anodizing plant results in the realization of several significant benefits such as:

1. INCREASED PRODUCTIVITY
2. LOWER REJECT RATES
3. LOWER OPERATING COSTS
4. IMPROVED QUALITY

The installation of a fully automated extrusion anodizing facility requires the engineering and integration of seven major component sub-systems. These are:

1. TANK SYSTEM
2. HEATING SYSTEM
3. COOLING SYSTEM
4. POWER SUPPLIES
5. VENTILATION SYSTEM
6. MATERIAL HANDLING SYSTEM
7. COMPUTER CONTROL SYSTEM

Each of these component sub-systems must be engineered in terms of the available design options such that the sub-systems can be integrated into the total facility. The available design options for each sub-system must therefore be discussed in greater detail.

## Tank System

The tanks employed in an extrusion anodizing facility can be constructed of five possible materials. These are:

1. MILD STEEL
2. STAINLESS STEEL
3. POLYPROPYLENE
4. FIBERGLASS
5. CONCRETE

Mild steel tanks are constructed of 1/4" thick material and can be built to almost any size, provided they are braced

properly. Tanks up to 115 feet long and 14 feet deep are currently being used in production facilities. Mild steel tanks are typically only used for alkaline solutions due to its lack of corrosion resistance. Mild steel tanks are fairly easy to repair and represent the lowest cost of installation.

Stainless steel tanks are usually constructed of 10-ga material and can also be built to almost any desired size. They exhibit excellent corrosion resistance to most of the chemical solutions employed in the anodizing process. Although stainless steel tanks can be easily repaired, they do require a significantly higher initial capital expenditure.

Polypropylene tanks are constructed of 1/4" to 1" thick material properly braced with an encapsulated steel structure. They can be built economically up to 10 feet long and 6 feet deep. They provide excellent corrosion resistance and good dielectric properties for use in electrified tanks. Polypropylene tanks have proven themselves suitable for most solutions encountered in an anodizing plant. Unfortunately, polypropylene is difficult to repair in the field.

Fiberglass tanks are usually fabricated of 1/4" to 1/2" thick material and can be constructed up to 10 feet long and 6 feet deep economically. They provide good corrosion protection to most solutions in an anodizing facility. They are easy to repair in the field but do exhibit a tendency to crack with age.

Concrete tanks are only economical for large tank systems in excess of 30 feet in length. Concrete tanks can reduce overall line length by utilizing 6" to 8" thick common walls between tanks. These systems must be lined inside and outside with a sprayed on coating of chopped fiberglass for corrosion and electrical resistance. Concrete tanks are difficult to repair and costly to maintain.

Corrosion resistant, non-conductive tank lining materials are required to electrically insulate anodizing or electrolytic coloring tanks that have been fabricated from conductive materials. Lining materials such as P.V.C., rubber and fiberglass are most commonly employed. Tank linings can be easily damaged and are very difficult to repair. It is therefore best to construct the tanks of suitable materials inside and outside and to utilize tank liners only where absolutely necessary.

## Heating System

The second major sub-system that requires engineering expertise is the heating system employed to reach and maintain

the required processing temperatures. There are two main approaches to process heating.

1. IMMERSION BURNER TUBES
2. STEAM COILS

Gas fired, immersion burner tubes can be mounted in tanks from 6 feet to 40 feet long. The width or the depth of the process tanks must be increased as a result of the diameter of the tubes. Although burner tubes are less efficient than steam coils, they are less expensive to install and maintain than a steam coil-boiler system.

Steam coils can be used in any size tank down to two feet long. Coils are the most widely used heating system in anodizing process tanks today. Coils can be fabricated of the proper corrosion resistant material to withstand any solution found in anodizing lines. They are the easiest to remove, repair or replace.

Standard engineering calculations are used to determine the BTU heat input needed to reach and maintain the desired operating temperatures regardless of the type of heating system employed.

## Cooling System

The third major sub-system requiring engineering is the cooling system. Cooling of the anodizing electrolyte is mandatory if acceptable quality anodic coatings are to be produced.

Small anodizing tanks less than four feet long employing no more than 1000 amps DC can be cooled by pumping a cooling solution directly through coils in the anodizing tank. The coils can be constructed of stainless steel, lead or teflon.

In most cases, larger anodizing tanks are cooled more efficiently with the use of an external heat exchanger. The anodizing electrolyte is pumped through one side of the exchanger and chilled water through the other side. The exchangers must be constructed of stainless steel and the electrolyte pumps must be Carpenter 20 stainless or F.R.P. (fiberglass reinforced plastic).

The primary component of the cooling system is the chiller. It is also the most expensive. The chiller must be sized to remove the total amount of heat generated by the application of electrical energy in the process tanks. The exact size of the chiller for any particular installation can be easily calculated. The total BTU/hr generated in the anodizing and elec-

trolytic coloring tanks can be found by multiplying the applied voltage by the amperage current flow and the factor 3.412. The BTU/hr heat generated divided by 12,000 equals the tons of refrigeration required by the chiller. If water cooled rectifiers are employed, the heat generated by the power supplies must also be added to the total chiller requirements.

Either water-cooled or air-cooled chillers can be utilized in the cooling system. Water-cooled units are more efficient than air-cooled units, especially on very hot summer days. Water-cooled units must be connected to a cooling tower located outside the building. Water is then pumped from the chiller condenser to the remote cooling tower. Air-cooled chillers located out of doors eliminate the cost of buying and maintaining a cooling tower and cooling tower pump.

The last major components of the cooling system are the external heat exchangers. The only practical choice for this type of heat exchanger is the plate type due to its very high heat exchange efficiency. The corrosive nature of the anodizing and electrolytic coloring solutions necessitate the use of 316 stainless steel. Other types of heat exchangers, such as the shell and tube, and other materials of construction, such as graphite, glass and teflon are also being employed. However, the 316 stainless steel plate heat exchanger is the most commonly recommended type due to it's relative cost, high efficiency and lack of required maintenance.

In addition to the chiller and external heat exchangers, the cooling system requires chilled water pumps, a cooling tower (only required if a water-cooled chiller is employed) and acid pumps to circulate the electrolytes. The solution flow rates required by each of these components are readily calculated from available engineering equations. Typical flow rates and materials of construction are shown below:

| PUMP | FLOW RATE | MATERIAL |
|---|---|---|
| 1. CHILLED WATER | 2.4 GPM/TON | CAST IRON |
| 2. COOLING TOWER | 3.0 GPM/TON | CAST IRON |
| 3. ELECTROLYTE | BTU/3000 | CARP. 20 |

## Power Supplies

The next major component sub-system to be considered in the design of a new extrusion anodizing facility is the power supply requirement. This would include both the DC rectifiers for the anodizing tanks and the AC power supply for the electrolytic coloring tank, if included in the facility. Care must

be taken to insure that the power supplies have been properly sized to provide the required output voltage and amperage based on the designed load size. Typical voltage and amperage requirements are shown below:

| POWER SUPPLY | VOLTAGE | AMPERAGE |
|---|---|---|
| DC RECTIFIER | 24 V | 12 ASF |
| AC POWER | 30 V | 5 ASF (AVG.) |

Multiplying the appropriate current densities, from the table above, by the maximum design load size in square feet of surface yields the current output which must be provided by the power supplies.

Most DC rectifiers in use today employ SCR's (silicon controlled rectifiers) for current output regulation and either SCR's or diodes for rectification of incoming AC to DC output.

AC power supplies utilize step-down transformers to convert high voltage/low amperage input to low voltage/high amperage output. Regulation of the applied output voltage can be controlled using either motor driven powerstats or SCR circuitry.

Both AC and DC power supplies are available in either air-cooled or water-cooled units. Water-cooled units are preferred because they are completely sealed thus protecting the internal components from humidity, dust and fumes.

The power supplies used in a fully automated anodizing facility must be more sophisticated than those normally used in the industry. They must be capable of receiving operating commands from and sending response signals to the automated control system.

## Ventilation

Ventilation of the process tanks represents another major sub-system that requires engineering design for a new extrusion anodizing facility. The tanks that require ventilation are the soak cleaner, caustic etch, anodize and seal tanks. Chemical brite dip tanks, if installed, would also require ventilation equipment. In order to properly size the ventilation system, the amount of air to be vented per unit time per open tank surface area (CFM/SQ.FT.) must be known. Guidelines for CFM/SQ.FT. have been published in the Handbook of Industrial Ventilation.

There are two basic ventilation designs which may be utilized. They are referred to as "pull-pull" and "push-pull". Pull-pull systems require higher exhaust rates than push-pull systems and also require two exhaust hoods instead of one. Since considerably less air is exhausted with the push-pull ventilation system, it is less expensive to install and operate. The table below compares air exhaust rates typically required for each type system for the various process tanks.

| TANK | PULL-PULL | PUSH-PULL |
|---|---|---|
| CLEANER | 150 CFM/FT$^2$ | 75 CFM/FT$^2$ |
| ETCH | 200 CFM/FT$^2$ | 85 CFM/FT$^2$ |
| BRITE-DIP | 250 CFM/FT$^2$ | 95 CFM/FT$^2$ |
| ANODIZE | 250 CFM/FT$^2$ | 95 CFM/FT$^2$ |
| SEAL | 175 CFM/FT$^2$ | 80 CFM/FT$^2$ |

Ventilation hoods are of two different designs; either updraft or downdraft. The type best suited to the particular facility being designed is dependent upon the size of the process tanks and the design of the material handling system that will be employed.

The exhaust hoods can be constructed of mild steel, stainless steel, P.V.C. or F.R.P. The hood material must withstand the attack of the particular chemicals within the tank as well as the physical abuse from dropped parts and racks. Therefore, the main points to be considered when choosing a material of construction are the corrosion and mechanical damage resistance. Hoods should be designed with cross-sectional areas large enough to reduce excessive air velocity noise. Cross-sectional area based on 2,000 FPM air flow rate are usually adequate.

Both round and rectangular ventilation ductwork is used in the industry. Round is preferred since it is generally easier to install and requires no internal bracing. Ducts should be sized such that the velocity inside the duct does not exceed 2,500 FPM for maintaining low noise levels. Mild steel, stainless steel, FRP and PVC are all used for duct material. PVC is usually the preferred material due to its light weight, corrosion resistance and ease of installation.

In addition to the ventilation hoods and associated ductwork, anodizing ventilation systems must include a fume scrubber to remove chemical mists from the exhausted air. There are at least ten different scrubber designs available today. All of them are capable of adequately removing the very soluble fumes which are generated by the etch and anodize tanks.

Scrubbers are usually fabricated of PVC or fiberglass. The design of the scrubber most provide adequate cross-sectional area to allow the vapors to condense on the packing material. The proper packing thickness and density are critical to ensure adequate scrubber efficiency.

Tank ventilation systems on large extrusion anodizing facilities may exhaust several hundred thousand cubic feet of air per minute. The exhausted air must be replaced and this is usually accomplished using gas fired air make-up units. Typically, only 80% of the exhausted air is replaced so that a constant negative pressure is maintained in the building.

Material Handling System

The sixth major sub-system of an automated extrusion anodizing facility which requires engineering expertise is the material handling system. This is the most important sub-system of the facility since it directly effects the production output of the anodizing line as well as the overall quality of the parts produced. Since only automated facilities are being discussed, the choice of material handling system must be restricted to those systems which allow control of material movement through the use of a PLC (programmable logic controller). Therefore, only two types of material handling systems, shown below, need be discussed.

1. SIDE ARM HOIST
2. OVERHEAD HOIST

The side arm hoist system is a fully programmable material transport system which will process loads up to 500 pounds in weight and can work over tanks up to six feet long. It is the least expensive automatic material handling system to purchase and install. The side arm hoist system is easy to build and install due to the construction design. The side arm hoist provides a lot of cycle flexibility at minimal cost when operated over an anodizing line with numerous process cycles.

The overhead hoist systems offers the same flexibility in process cycles that the side arm hoist provides. Overhead hoist systems typically operate with loads from 1,000 to 12,000 pounds over tanks from 4 feet to 40 feet long. They can be equipped with variable speed drive motors to insure smooth starts and stops, thus eliminating rack sway. The overhead hoist system is the most widely used automatic material handling system in use in extrusion anodizing plants today.

Either of these material transport systems can be readily automated through the use of programmable logic controllers (PLC). The programmable controller can be programmed in "CATWALK LANGUAGE" such as; up, down, forward and reverse. The process cycle instructions can be entered into the programmable controller through an operator keyboard on the face of the control panel. The keyboard also permits easy program modification should alteration of the cycle sequence become necessary.

The hoist controllers can also be programmed to set the voltage or current output of the rectifiers and AC power supplies for each load entered into the system.

## Computer Control System

The total automation of the extrusion anodizing facility can only be achieved by integrating all of the component sub-systems. This is achieved by utilizing industrial computers to oversee the operation of all of the component sub-systems. The computer can be programmed to contain all of the various load cycle date that would be necessary for random loading of different process cycles. The operator would only be required to key in the part number and quantity on each load. The computer would then select the proper load cycle recipe and calculate the proper current or voltage settings. This information would then be passed down to the programmable logic controller which would direct the operation of the hoist throughout the process sequence. The computer would control and record the current, voltage and temperature of appropriate process tanks for each load processed.

The chemical concentrations of the individual process baths can be determined and recorded by a computer controlled automatic chemical analyzer. This unit could be programmed to withdraw a sample of each process bath and perform the required analysis on a schedule basis. The chemical analyzer could be programmed to add the required amount of chemicals to the individual process baths when the concentrations are found to be below their set points. The chemical concentration data is recorded and can be displayed in either tabular or graphic formats.

Data communication between the PLC hoist controller, chemical analyzer and industrial computer would complete the automated control system. The inter-communication capabilities would facilitate the gathering and recording of important production information such as:

1. PART STATUS REPORTS

2. PROCESS LINE STATUS REPORTS
3. WORK SCHEDULES
4. PART PROCESSING SEQUENCES
5. PART HISTORY
6. CHEMICAL USAGE
7. MAINTENANCE SCHEDULES
8. CHEMICAL INVENTORIES
9. SPARE PARTS INVENTORIES
10. STATISTICAL PROCESS CONTROL DATA

All of this information could be displayed, stored, printed or passed along to a central factory computer.

In conclusion, there are many equipment options which must be considered when designing a new extrusion anodizing plant. All of them need be seriously reviewed in order to provide a new facility that is cost effective to operate and maintain. The use of programmable controllers and industrial computers to fully automate every aspect of the extrusion anodizing process are becoming more common in the industry. This is primarily a result of the significant production costs savings and increase in quality which result from the utilization of this technology.

B-1

# Research Session B

## Development of Chemical Sensors For Ions in Plating Solutions

Robert F. Savinell, Chi-Jin Chen,
Sharon Reid and Chung-Chiun Liu
Department of Chemical Engineering
Case Western Reserve University
Cleveland, OH 44106

# DEVELOPMENT OF CHEMICAL SENSORS FOR IONS IN PLATING SOLUTIONS

Robert F. Savinell, Chi–Jin Chen, Sharon Reid, Chung–Chiun Liu
Department of Chemical Engineering
Case Western Reserve University
Cleveland, OH 44106

## Summary

Electrochemical sensors fabricated by microelectronic thick and thin film metallization techniques are being developed for detecting ions in plating solutions. The advantage of this approach is that small, reliable and fast responding sensors can be fabricated on a relatively small single substrate. The design of this sensor uses interconnected square element working electrode and band electrode arrays in order to enhance the sensor response time and sensitivity. However, possible interaction and interference of the reactions occuring at electrode surfaces in this design must be considered. This study analyzes the potential interactions and provides a mathematical model of the sensor design. The validity of this mathematical model is verified by experimental investigation for sensing ferric ion in a simulated Zn–Fe plating bath solution. Over the ferric ion concentration range of 1 to 6 gpl, a good linear relation exists between the current output of the sensor and the ferric ion concentration. Both the mathematical model established and the fabrication approach used in this study are potentially important for the development of practical sensors for the plating industry.

## Introduction and Background

The plating and surface finishing industry has a need for simple chemical sensors to detect specific ion concentrations. In this research program sponsored by the American Electroplaters and Surface Finishing Society (AESF), we are developing sensor devices for possible applications in the plating industry. In this paper, we will discuss our results to date on developing a sensor for detecting and quantifying ferric ion in Zn–Fe (and Ni–Fe) alloy plating baths. The accumulation of ferric ion in these baths is known to be detrimental to the performance of the bath [1].

Our approach employs electrochemical techniques. Namely, we apply controlled potential amperometry and linear sweep voltammetry using arrays of microelectrodes. Electrochemical techniques are selective in that only certain electrochemical reactions can occur within a properly chosen potential window. In the case of the ferric/ferrous couple, the standard electrode potential of the reaction

$$Fe^{3+} + e \rightleftharpoons Fe^{2+}$$

occurs at 0.55 volts positive of a silver/silver chloride reference electrode. Ignoring concentration effects and using an appropriate electrode material (e.g. platinum), an overpotential of several hundred millivolts negative of the standard electrode potential of the reaction will produce a net cathodic reaction resulting in a current which is proportional to the ferric ion concentration. Interference from zinc, sulfate or chloride ions and dissolved oxygen are expected to be minimal under this condition.

The uniqueness of our approach is that the sensor is fabricated by using microelectronic techniques. In this way an array of microsensors can be placed on a single small size substrate, i.e. a chip. Also with the sensing electrode, the reference and counter electrode can be fabricated onto the same chip. This approach permits the fabrication of a small sensor which will be practical for installation in industrial processes.

There are other advantages using microelectronic techniques to fabricate the sensor. One advantage is that very reproducible electrode surfaces can be produced using photolithographic reduction, and thick or thin film metallization. Therefore, since the current is directly related to the electrode surface area, the calibration of these electrodes will be simplified. Also, small dimensional sensing electrodes are fast responding with enhanced current densities [2,3]. The advantage of having an array of electrodes with proper signal processing is that redundancy of electrodes leads to more reliable measurements.

The geometrical configurations of the sensing electrodes developed are arrays of square electrode elements and band–type electrodes (see Figure 1). In this figure, three electrodes are shown on a single chip. The bottom electrode, counter electrode, represents three band electrodes in parallel. The center electrode is a Ag/AgCl reference electrode. The top electrode, the sensing electrode, is the same as the bottom but strips of insulating epoxy are overlayed perpendicularly to them. This gives an array of square electrode elements which are interconnected in parallel. The width of the band electrode or the size of the square electrode element is the characteristic dimension. The smallness of this dimension is responsible for the microelectrode type performance. The length of the band electrode or the number of elements in an array can be increased to yield larger currents, therefore enhancing the sensitivity of the electrode.

In this paper the testing results of an array of square sensing electrode elements for dectecting ferric ion in Zn–Fe plating baths are reported. Interactions between adjacent electrodes are examined by mathematical simulation of a band electrode configuration. These simulations result can be applied to arrays of square electrode elements. The comparison of simulation results with experimental data is reported.

## Modeling the Band Electrode

For a single electrode with micro dimensions, the current density is enhanced significantly due to the effect of radial diffusion. However, different behaviors arise for electrode arrays. At very short time, each electrode acts like an isolated single electrode. However, at a longer time, the electrode arrays will react like an apparent electrode of much larger dimensions (about $1/r$ times a single element, where r is the fraction of conducting area) at which the mass transfer approaches to semi–infinite linear diffusion.

A model which simulates the limiting current response of both single and multiple electrode cases to a step change in potential is developed. This model examines the interactions between the band electrodes and will be useful for designing sensor devices with optimum performance.

According to Fick's law, the corresponding partial differential equation which describes the unsteady, semi–infinite diffusion of uncharged species (or dilute charged species in a supporting electrolyte) to band–shaped multiple electrodes as shown in Fig. 2 is given by:

$$\frac{\partial C}{\partial t} = D \left( \frac{\partial^2 C}{\partial x^2} + \frac{\partial^2 C}{\partial y^2} \right) \tag{1}$$

where C is the concentration of ferric ion and D is the diffusion coefficient.
The initial and boundary conditions are as follows:

$$t = 0, \qquad C = C^o \tag{1.1}$$

$$t > 0,\ x = a/2, \qquad \frac{\partial C}{\partial x} = 0 \tag{1.2}$$

$$t > 0,\ x = 0, \qquad \frac{\partial C}{\partial x} = 0 \tag{1.3}$$

$$t > 0,\ y = 0,\ 0 \le x \le w/2, \qquad C = 0 \tag{1.4}$$

$$t > 0,\ y = 0,\ w/2 < x < (w+a)/2 \qquad \frac{\partial C}{\partial y} = 0 \tag{1.5}$$

$$t > 0,\ y \to \infty, \qquad C = C^o \tag{1.6}$$

The third boundary condition (1.4) states that under the conditions of experiment the concentration of the active species is reduced to zero immediately upon application of the potential step, i.e., the reaction is purely diffusion controlled. Thus the local diffusion limited current density to the system is written as:

$$i(x) = nFD \left( \frac{\partial C(x)}{\partial y} \right) \Big|_{y=0} \tag{2}$$

where n is the number of electrons being transferred and F is Faraday's constant. While the average dimensionless limiting current density, $\bar{i}_{avg}$, is :

$$\bar{i}_{avg} = \int_0^{w/2} \frac{\partial \bar{C}(x)}{\partial y} \Big|_{y=0} dx \tag{3}$$

where $\bar{C}$ is the dimensionless concentration, $\bar{C} = C/C^o$.

Similarly, the diffusion equations for single band–shaped electrode are the same as for multiple ones (Eqns. (1)–(3)); however one boundary condition (Eqn. (1.2)) is substituted by :

$$t > 0,\ x \to \infty, \qquad C = C^o \tag{1.7}$$

The diffusion equation (Eqn. (1)) associated with initial and boundary conditions (Eqns. (1.1)–(1.7)) for both multiple and single electrode cases are solved

by numerical method. The Hopscotch finite difference algorithm proposed and analyzed by Gourlay [4,5] was chosen to accomplish the simulation. This technique is more accurate and faster than conventional explicit methods; yet requires less storage space than implicit methods.

The results of the model predictions and comparison with experimental data are given later in this paper.

## Experimental

Fabrication of Electrode Array: The experimental electrode used was a band–type electrode type fabricated by conventional photographic reduction, photolithographic and thick film metallization techniques [6,7]. One inch square alumina substrate having a thickness of 0.025 inch (Coors Industries) was used, and platinum ink(#A4731, Engelhard) was employed for the thick film metallization.

The actual arrangement of the electrodes on the substrate is shown in Figure 1. This arrangement has two sets of electrodes separated by a reference electrode. All three of these electrodes could be used in a self–contained sensor device. In this research, the set of band electrodes and the array of square electrode elements were tested independently against an external counter and reference electrode.

Testing Procedure: A three compartment cell was used to test the array and band electrodes. An external platinum counter electrode and a calomel reference electrode (SCE) were used in this work. A potentiostat (model 273, Princeton Applied Research) was used to apply potential steps and linear potential sweeps and the resulting current/time transients were recorded on an X–Y recorder. In later experiments oxygen was suppressed by sparging the solution with nitrogen prior to measurements and blanketing the solution with nitrogen during the experiment.

Experiments performed to evaluate the array of electrode elements in simulated plating solutions were with the following composition [1]: 55 gpl $Na_2SO_4$, 153.8 gpl $ZnSO_4$, 3 gpl citric acid, 347.5 gpl $FeSO_4$ and 0–6 gpl ferric ion. The testing of band electrodes to corroborate the modeling simulation was done in a solution of 1M $ZnSO_4$ and 0–6 gpl ferric ion.

## Results and Discussion

### Evaluation of Electrode Arrays in Simulated Zn–Fe Plating Solutions

A series of tests on the array electrode configuration was performed with varying ferric ion concentration in a simulated plating solution. In these tests the solutions were not deoxygenated. The potential of the working electrode was scanned (10–100mV/s) from +200 mV to –200 mV vs SCE. This represents a potential range where ferric ion should be reduced without interference from other reactions. Two characteristics of the data are noted. First, the hysteresis during the scan appears to increase as the ferric ion concentration increases. Secondly, this hysteresis becomes less at the slower scan rates. The scans with simulated solutions without ferric ion were near the zero current baseline. This indicates that dissolved oxygen does not interfere with sensor sensitivity to ferric ion. The linear response of the sensor is shown in Figure 3.

Model Simulation Results and Experimental Verification

Interactions between elements in band–shaped electrode arrays and their effects on the transient current response to a potential step were investigated using ferric ion reduction. The experimental data from deoxygenated electrolytes are compared with the model predictions. In comparison, the total current from simulation takes into account both contributions of single–electrode and multiple electrodes :

$$I = nFDC^{o}l\left(4(\bar{i}_{avg})_{int} + 2(\bar{i}_{avg})_{ext}\right) \qquad (4)$$

where, $(i_{avg})_{int}$ and $(i_{avg})_{ext}$ represent the dimensionless current density predicted from multiple electrode and single electrode models respectively. Fig. 4 shows excellent agreement between the experimental results at band electrode arrays and those predicted from Eqn. (4). In these comparisons, a diffusion coefficient of $D = 6 \times 10^{-6}$ $cm^2/s$ from literature [8] was used in the calculations.

Two characteristic limiting bounds for electrode arrays are predicted from simulations and found from experimental results with platinum electrodes as shown in Fig. 4. At very short times, when diffusion layer thickness is smaller than the width of each single electrode, the lower bound is formed since the current behaves like semi–infinite linear diffusion to each electrode. The lower bound is given by the Cottrell equation [9] and rewritten in dimensionless form :

$$(\bar{i}_{avg})_{low} = \frac{Nw}{\sqrt{\pi Dt}} \qquad (5)$$

where N is the number of electrodes having width ,w.

As time increases, the diffusion layer thickness of each electrode increases gradually, and finally the diffusion layer overlaps adjacent electrodes. The array of single electrodes now form an apparent planar electrode which is large enough such that the edge effect is negligible. Therefore, the current behavior approaches an upper bound as semi–infinite diffusion to an apparent planar electrode, namely:

$$(\bar{i}_{avg})_{up} = \frac{Nw(2/r+1)}{\sqrt{\pi Dt}} \qquad (6)$$

The current–time relationship of experimental data is well confined within two limiting bounds (Eqn. (5) and Eqn. (6)) as shown in Fig. 5. Again, as shown, the model predictions are confirmed with experimental data.

## Conclusions

Based on the results to date, the following conclusions can be formulated:

1. An array of miniature electrodes were tested in a simulated Zn–Fe plating solution. The electrodes responded to a linear potential sweep with limiting currents directly proportional to the concentration of ferric ion. Oxygen reduction did not interfere in the test.

2. The current transient to a potential step predicted by a mathematical model was shown to be bounded by semi–infinite linear diffusion models (at the low end by the single electrode result, and at the high end by an apparent electrode dimension).

3. Experimental data was in excellent agreement with the model predictions.

4. The research indicates that this approach will yield reliable and fast responding sensors for detecting ferric ions in plating solutions.

## Acknowledgement

This research is supported by an AESF Fellowship (Project #73 of the Research Board) and by the National Science Foundation (CBT–869073).

## References

1. AES Fourth Continuous Strip Plating Symposium, Proceedings of the Symposium held at the Continental Hotel, Chicago, IL, May 1–3, 1984 (American Electroplaters society, Florida), 1984.

2. P.M. Kovach, W.L. Caudill, D.G. Peters and R.M. Wightman, J. Electroanal. Chem., 185, 285(1985).

3. C.A. Amator, M.R. Deakin and R.M. Wightman, J. Electroanal. Chem., 206, 23(1986).

4. D. Shoup and A. Szabo, J. Electroanal. Chem., 160 (1984) 1.

5. A.R. Gourlay, J. Inst. Math. Appl., 6 (1970) 375.

6. C.C. Liu, M.R. Neuman, K.L. Montana, and M.C. Oberdoerster, Marine Technol., 16 (1980) 468–472.

7. C.C. Liu and M.R. Neuman, Diabetes Care, 5 (1982)275–279.

8. D.J. Pickett, "Electrochemical Reactor Design," Elsevier, (1979) p.99

9. F.G. Cottrell, Z. Phys. Chem., 42 (1902) 385.

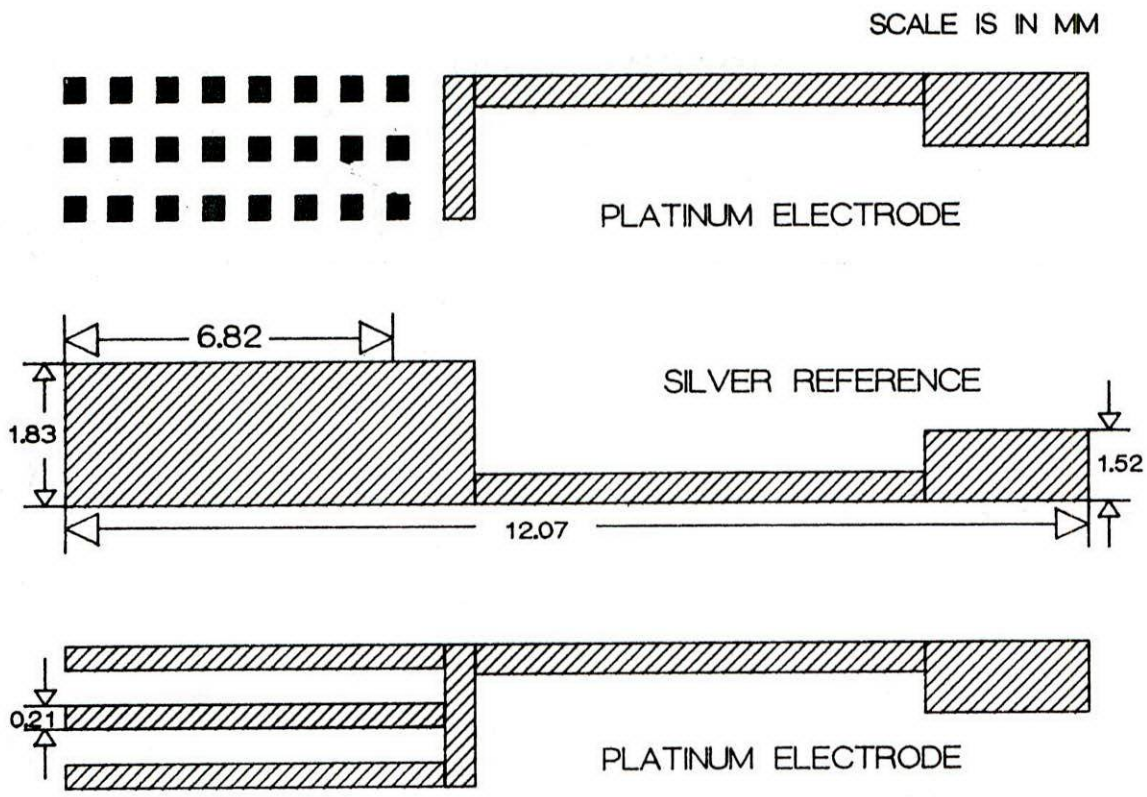


Fig. 1 Schematic of Three-Electrode Micro-Sensor Fabricated at CWRU

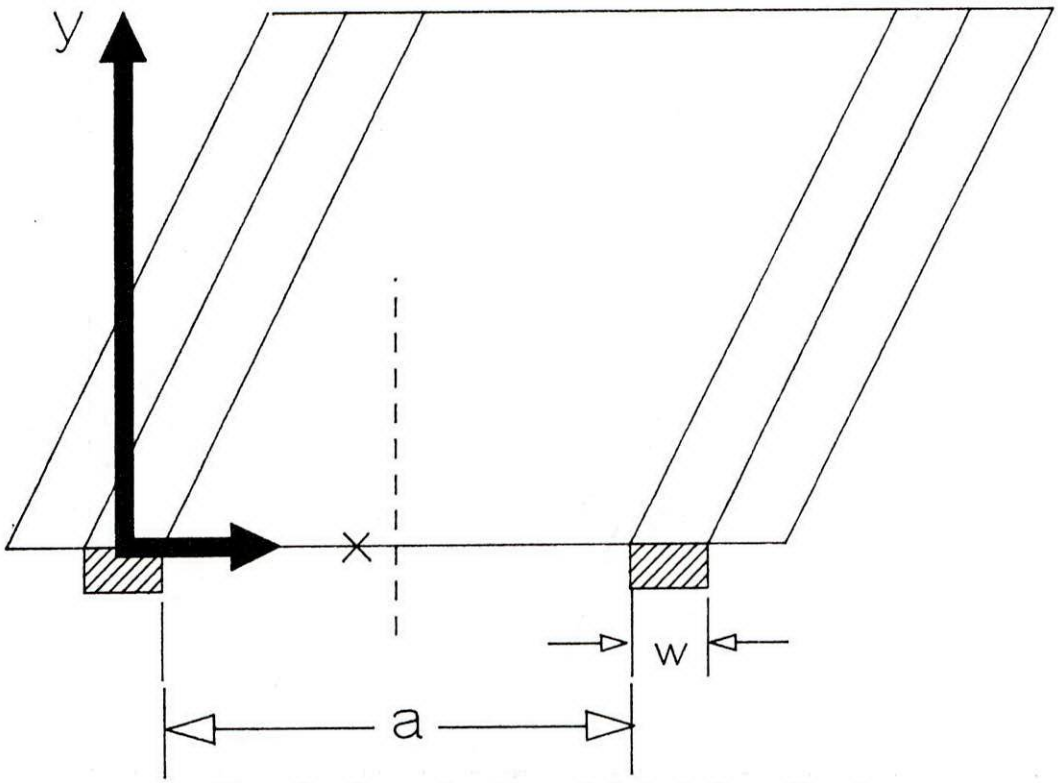


Fig. 2 Coordinate of Modeling System

W:electrode width ; a:the distance between two electrodes

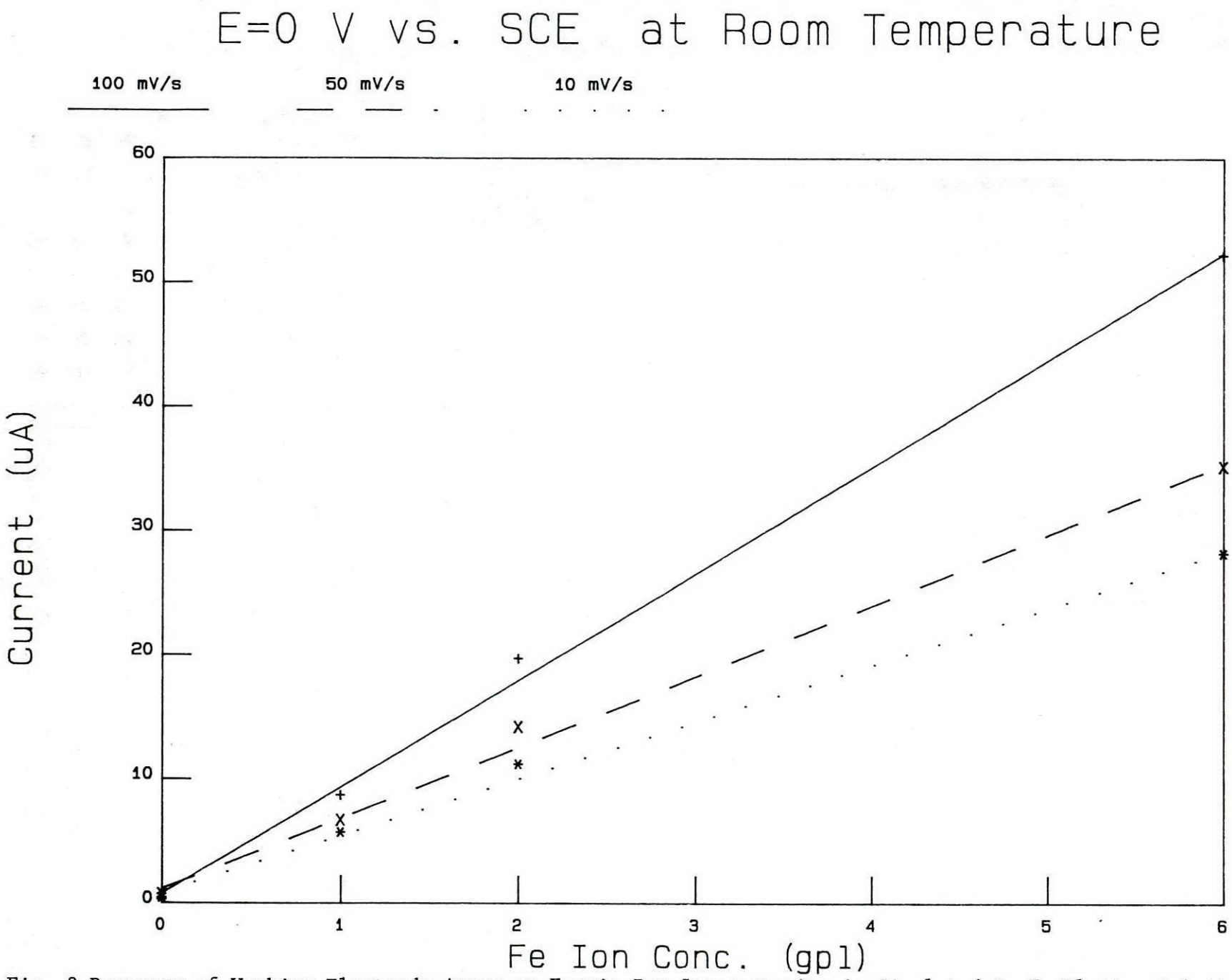


Fig. 3 Response of Working Electrode Array to Ferric Ion Concentration in Simulated Zn-Fe Plating Solution.

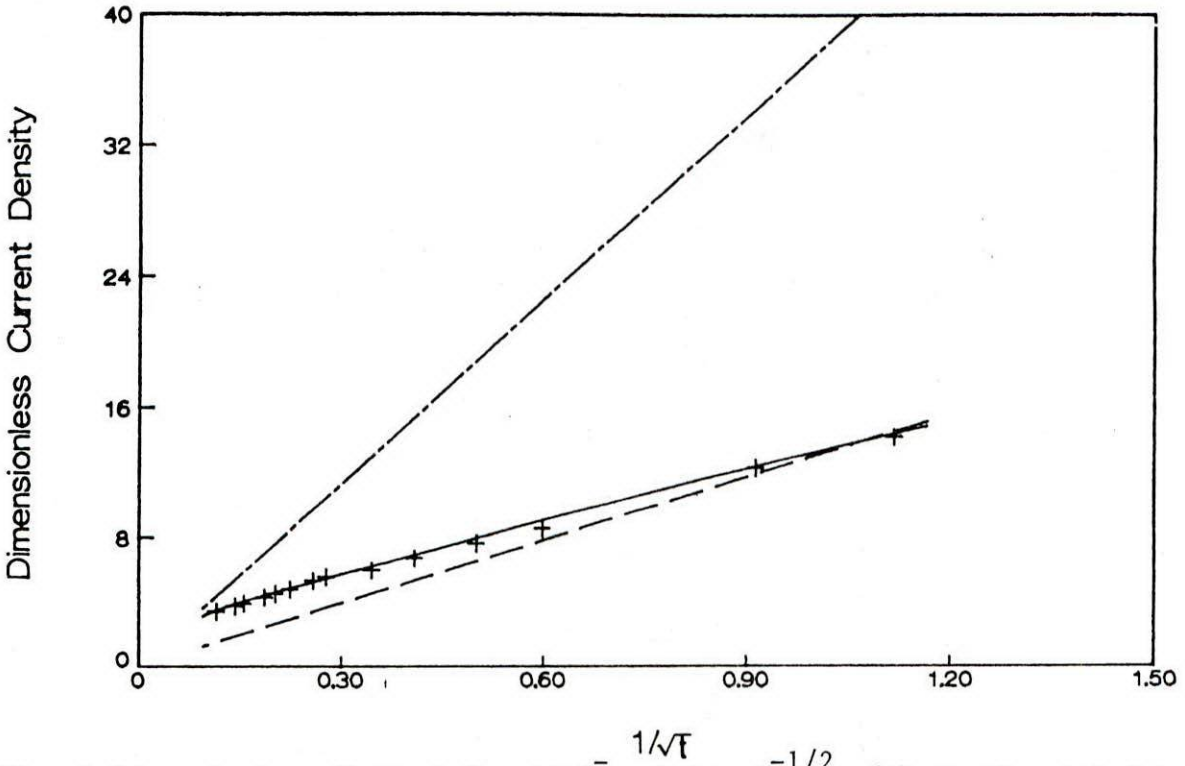


Fig. 4 Dimensionless Current Density($\bar{i}_{avg}$) vs. $t^{-1/2}$. (+)experimental data; (——)model prediction; (---)lower bound(from eqn.(5)); (----)upper bound(from eqn.(6)). Experimental condition : $Fe_2(SO_4)_3$ 36mM; $ZnSO_4$ 1M. Applied potential -0.25V.

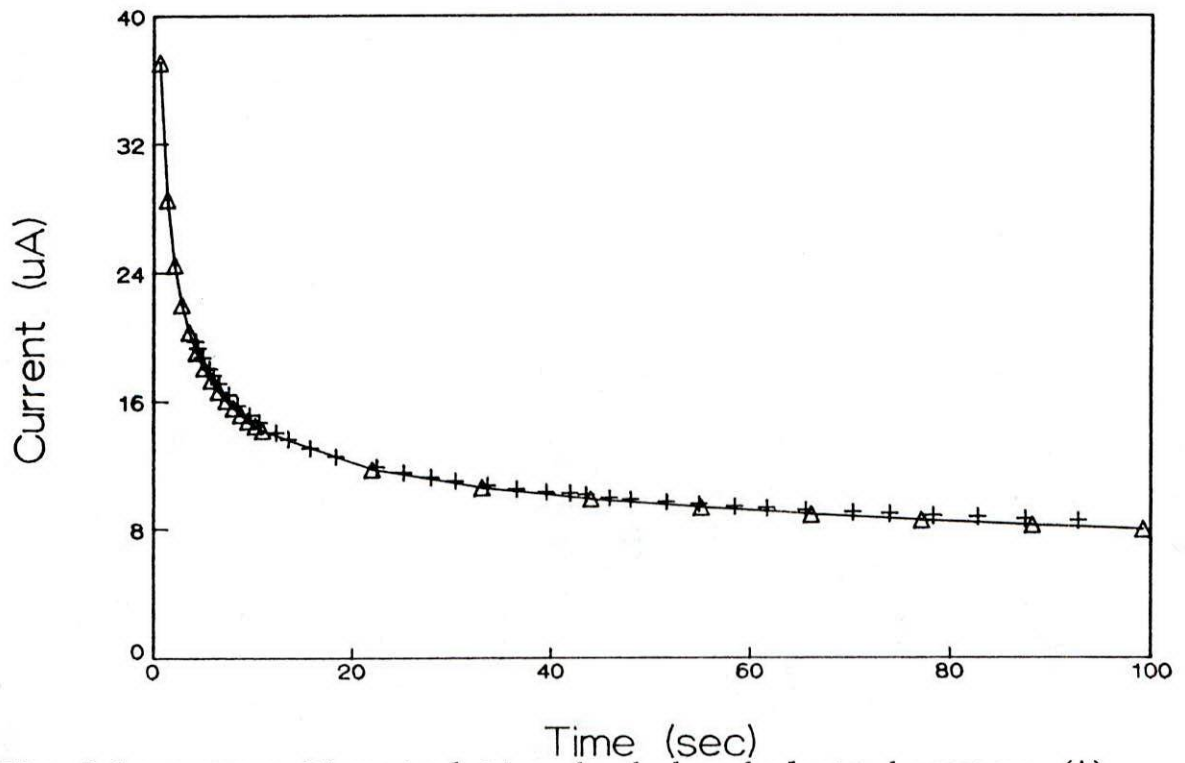


Fig. 5 Current vs. Time at platinum band-shaped electrode arrays. (+) experimental data; (—△—)model prediction(from eqn.(4)). Experimental condition : $Fe_2(SO_4)_3$ 5mM; $ZnSO_4$ 1M. Applied potential -0.25V.

# B-2

# Research Session B

## Selective Pulse Plating of Gold and Tin-Lead Solder

D-T. Chin and M.K. Sunkara
Department of Chemical Engineering
Clarkson University
Potsdam, NY 13676

# SELECTIVE PULSE PLATING OF GOLD AND TIN-LEAD SOLDER

D-T. Chin and M.K. Sunkara
Department of Chemical Engineering
Clarkson University
Potsdam, New York 13676

## ABSTRACT

This study is concerned with the use of pulse current to selectively deposit metal on a localized area of an unmasked cathode. The localization of electrodeposition is achieved by directing a small anode toward a large maskless cathode at the desired location, and by applying high peak pulse current density of 1-20 $A/cm^2$. In this paper, the experimental results obtained with a 24 Kt hard acid bright gold bath and a 60% tin - 40% lead solder bath are presented. The effect of current pulse on the metal distribution and morphology of electrodeposits is discussed.

## INTRODUCTION

Selective plating (also called spot plating) has received increasing attention in the metal finishing industry because of the high cost of noble metals and the need to localize metal deposition in the manufacture of electronic contacts and printed circuit boards. The localization of metal deposits is generally achieved by the application of cathode masks, photo-resist coatings, and brush platings. These techniques require a series of pre-plating and post-plating treatment procedures, rendering high production cost in the overall finishing process.

The purpose of this work is to study the feasibility of using pulse plating to localize the electrodeposition process on a maskless cathode. Several theoretical inveatigations (1,2) have shown that in pulse plating with short pulse durations and high pulse frequencies, very high instantaneous pulse current densities on the order of 10-100 $A/cm^2$ can be used without depleting the concentration of metal ions at the cathode surface. At high plating current densities, the primary current distribution prevails, and the throwing power is worse than that of the secondary current distributions. This suggests that spot plating can be achieved by: i) directing a small insoluble anode toward a large unmasked cathode; ii) keeping the anode-cathode spacing at a small value; and iii) applying a high peak pulse current density to localize the electrodeposition at the selected area facing the anode.

This paper describes an experimental study of the effect of pulse current density, duty cycle, pulse period, and anode-cathode spacing on the metal distribution and morphology of gold, and 60% tin - 40% lead solder deposits on a maskless cathode. The results of pulse plating are compared to those of DC plating at the same average current density. The current distribution on the maskless cathode was calculated with a two dimensional mathematical model.

## EXPERIMENTAL

The details of experimental setup and instrumentation have been described in previous publications (3,4). The electroplating cell consisted of a large unmasked cathode and a small insoluble circular anode. The cathode was supported vertically in the cell, and the circular anode having its exposed plane parallel to that of the cathode was introduced from one side of the cell. The anode-cathode spacing could be adjusted by sliding the anode support rod through a water-tight fitting on the cell wall. A saturated calomel electrode located in a Luggin capillary was used as the reference electrode, and a thermometer inserted through the cell cover was used to measure the electrolyte temperature.

The pulse plating experiments were carried out under the galvanostatic controlled conditions. A function generator (Hewlett-Packard 3311A) connected to a mini-pulsir (LWD Scientific) and a variable resistor was used to generate a rectangular pulsating voltage signal of desired magnitude, duty cycle, and frequency. The pulsating voltage signal was fed to a high power potentiostat (Wenking HP72) and was converted to pulsating current by operating the potentiostat on the galvanostatic mode. A Commodore PET 4032 computer was used to interface with a Hewlett-Packard 3421A digital data acquisition unit to monitor the time-averaged DC plating current, average potential drop between the cathode and reference electrode, and average anode-cathode cell voltage. Suitable software using IEEE 488 interfaces was developed to process the plating data.

The pulse plating of gold was carried out with a 24-Kt acid hard bright gold bath (Orosene 999, Technic Inc.) containing 0.029 M potassium gold cyanide, 0.37 M mono-potassium phosphate, and 0.84 M citrate in the form of citric acid and potassium citrate (pH 4.5). The minor additives in the bath included cobalt chelates and wetting agents. A copper plate, 5 cm long by 5 cm wide by 0.038 cm thick was used as the cathode. A stainless steel disk of 6 mm in diameter flush-mounted on a Teflon sleeve was used as the anode. For each run, the copper cathode was polished with 0.3 micron alumina polishing compound, degreased with methanol, and rinsed in water. It was plated with 0.75 micron bright nickel and then pre-coated with 0.025 micron gold from an alkaline gold strike bath. Pulse plating experiments were carried out over a range of peak pulse current densities 0.025-20 $A/cm^2$, duty cycles 1-100%, and pulse periods 1-100 ms. Each experiment was terminated after 25 coulombs of charge (based on the time-averaged DC current) had passed through the cell. The metal distribution of gold deposit at the cathode was measured with a coulometric thickness gage (UPA Technology, Inc., Model CM-100), and the morphology of gold deposits was examined under a scanning electron microscope.

The pulse plating of 60% tin - 40% lead solder was carried out using a nonfluoborate bath (Techni-Solder NF acid, Technic Inc.) and a fluoborate bath (Techni-Solder 60/40 Plating Solution, Technic Inc.). The nonfluoborate bath was composed of 0.17 M stannous methyl sulfonate, 0.048 M lead methyl sulfonate, and 15% by volume of methyl sulfonic acid. The

fluoborate bath contained 0.13 M stannous fluoborate, 0.048 M lead fluoborate, and 40% by volume of fluoboric acid. A circular stainless steel disk of 6 mm in diameter was used as the anode, and a large uncoated brass sheet was used as the cathode. For each run, the brass cathode was polished to 0.3 micron smoothness; degreased in methanol; dipped in dilute HCl; and rinsed in water prior to transferring to the cell. The plating experiments were carried out for a range of peak pulse current densities 0.025-10 $A/cm^2$, duty cycles 1-100%, and pulse periods of 1-1000 ms. The deposit thickness was measured with a coulometric thickness gage (Couloderm CM100, UPA Technology, Inc.), which had been calibrated with a standard coating of 60% tin - 40% lead alloy. It was assumed that the deposit composition did not vary with the plating conditions and with the locations on the cathode substrate.

## RESULTS AND DISCUSSION

With the present cell geometry, the active area on the cathode where the electrodeposition took place varied with experimental conditions. Unless otherwise noted, the current density values reported in this section will be all based on the constant anode area. An anode-cathode spacing of 3 mm was used in the plating experiments. All measurements were made at a constant room temperature of 21°C.

### (1) Gold Plating

Figure 1 shows the results of metal distribution for DC plating of gold over a range of current densities from 0.025 to 0.2 $A/cm^2$. The local metal thickness is plotted as a function of radial distance from the center of gold deposit. The gold deposit was thickest at the center and became thinner with increasing radial position. With increasing DC current densities, the thickness at the center decreased, and the metal distribution became less uniform.

The effect of pulse current on the metal distribution of gold is shown in Figure 2. In these runs, the average current density and pulse period were kept at 0.05 $A/cm^2$ and 10 ms, respectively; whereas the duty cycle varied from 100% (DC) to 1%, corresponding to a range of peak pulse current densities of 0.05-5 $A/cm^2$. Pulse current increased the thickness of gold deposit at the central area facing the anode, and made the metal distribution more localized than that of DC plating. At 1% duty cycle, the gold deposit at the center was 6 times thicker than that of DC plating.

Figure 3 shows the effect of average current density in pulse plating on the metal distribution of gold deposit. These data were obtained at 10 ms pulse period and 10% duty cycle; the average current density varied from 0.025 to 0.2 $A/cm^2$, corresponding to a range of peak pulse current density of 0.25-2 $A/cm^2$. The results were similar to those of DC plating that

increasing average current density increased the localization of gold deposit. The metal thickness at the center with 0.2 $A/cm^2$ average current density was 3.5 times greater than that obtained with 0.025 $A/cm^2$.

The effect of pulse period (or frequency) on the metal distribution of gold deposit is shown in Fig. 4; these data were obtained by keeping the average current density at 0.05 $A/cm^2$ and duty cycle at 10%. A uniform metal distribution was obtained with the pulse plating at 1 ms pulse period (corresponding to 1000 Hz pulse frequency). The metal distribution became less uniform with increasing pulse period (or decreasing pulse frequency). The most localized gold deposit was obtained at 200 ms pulse period (or 5 Hz pulse frequency) as shown in the figure.

The morphology of gold deposit at the central area facing the anode was examined with a scanning electron microscope (SEM). Figure 5 shows a set of photomicrographs obtained with DC plating (Fig. 5a) and pulse plating at 10% duty cycle and 10 ms pulse period (Fig. 5b); the deposits were obtained at the same average current density of 0.05 $A/cm^2$. The gold deposits exhibited hemispherical nodular growth. The grain size obtained with DC plating was 1-2 microns in diameter. With pulse plating at the same average current density, the grain size increased to 10-15 microns in diameter as shown in Fig. 5. Figure 6 shows the effect of average current density on the morphology of gold deposits with pulse plating at 10% duty cycle and 50 ms pulse period. Increasing the average current density from 0.05 $A/cm^2$ to 0.2 $A/cm^2$ caused a decrease in the grain size from more than 10 microns in diameter to 1-2 microns.

(2) 60% Tin - 40% Lead Solder Plating

Figure 7 shows the typical pulse plating results obtained with the nonfluoborate bath at an anode-cathode spacing of 3 mm. In these runs, the average current density and pulse period was kept at 0.1 $A/cm^2$ and 10 ms, respectively, while the duty cycle changed from 100% (DC) to 1%. This covered a range of peak pulse current densities of 0.1-10 $A/cm^2$. The pulse current improved the localization of the tin-lead deposition. The thickness of the tin-lead deposit at the center with pulse plating of 1% duty cycle was 6.5 times greater than that of DC plating. The effect of average current density on the tin-lead solder plating was similar to that of copper and gold plating that the metal distribution became more localized with increasing average current densities for a given duty cycle and pulse period.

The metal distributions of tin-lead solder from the fluoborate bath are plotted in Fig. 8 for pulse plating at 0.025 $mA/cm^2$ average current density and 10 ms pulse period. Uniform metal distribution was obtained with DC plating as shown by the 100% duty cycle curve. Decreasing the duty cycle resulted in increasing localization of the tin-lead solder deposit.

With 1% duty cycle pulse plating, the metal thickness at the center facing the anode was 13 times greater than that of DC plating. Figure 9 shows the effect of pulse periods (or pulse frequencies) on the metal distribution of tin-lead solder from the fluoborate bath. The data in the figure were taken by varying the pulse period from 1 to 1000 ms while keeping the average current density at 0.025 $A/cm^2$ and duty cycle at 10%. The metal distribution of the tin-lead solder deposits became more localized with increasing pulse period (or decreasing pulse frequency). With 1000 ms pulse period, the deposit at the center was nearly 4 times thicker than that with 1 ms pulse period.

(3) Mathematical Modeling of Current Distribution

The present experimental results may be interpreted with a two dimensional mathematical model for the current distribution on an unmasked cathode. Figure 10 shows the schematic representation of an electrochemical cell used for the theoretical analysis. The cell consists of an infinitely long cathode and a parallel finite anode. The anode has a width of $2L_a$; its exposed surface is flush with a semi-infinte insulation surface as shown in the figure. The center of the cathode is taken as the origin of a pair of rectangular coordinates, x and y, with x being the surface distance on the cathode and y being the vertical distance from the cathode surface. The anode-cathode spacing is H. To simplify the analysis, the following assumptions are incorporated into the model: i) the anode polarization is negligible; ii) the solution is well stirred and the concentration polarization is negligible; iii) the pulse period is sufficiently large (or the pulse frequency is sufficiently low) such that the effect of electric double layer on the current distribution is negligible; and iv) the solution properties, such as conductivity and density, are constant. The anode surface is taken as the reference plane where the solution potential is set to be zero. Accordingly, the governing equations describing the current distribution in the cell may be given by the following equations:

i) Voltage Balance

$$E = E_o + \eta_c + \eta_{ohm} \tag{1}$$

where E is the cell voltage during the plating; $E_o$ is the open-circuit cell voltage; $\eta_c$ is the local activation overpotential at the cathode; and $\eta_{ohm}$ is the local ohmic potential drop across the electrolyte between the anode and cathode.

ii) Charge Balance

$$\int_{-\infty}^{\infty} i_c(x)dx + \int_{-L_a}^{L_a} i_a(x)dx = 0 \tag{2}$$

where $i_a$ and $i_c$ are the local current density at the anode and cathode surfaces, respectively. Using the present convention, the cathode current is taken to be negative. Equation (2) states that the total current flowing across the cathode/electrolyte interface must be equal to the total current flowing across the anode/electrolyte interface.

iii) Ohmic Drop in the Cell - The ohmic potential drop, $\eta_{ohm}$, in the cell is obtained by solving the two dimensional Laplace equation for the potential distribution in the electrolyte.

$$\frac{\partial^2\phi}{\partial x^2} + \frac{\partial^2\phi}{\partial y^2} = 0 \tag{3}$$

where $\phi$ is the electric potential in the solution phase. The associated boundary conditions are:

$$\text{at the cathode } (y = 0),\ \partial\phi/\partial y = -i_c(x)/k \tag{3a}$$

$$\text{at the anode } (y = H,\ -L_a \leq x \leq L_a),\ \phi = 0 \tag{3b}$$

$$\text{at the anode insulation plane } (y = H,\ |x| > L_a),\ \partial\phi/\partial y = 0 \tag{3c}$$

$$\text{at the center line } (x = 0),\ \partial\phi/\partial x = 0 \tag{3d}$$

$$\text{at the edge of the cell } (|x| = \infty),\ \partial\phi/\partial x = 0 \tag{3e}$$

where k is the conductivity of the electrolyte.

iv) Activation Overpotential at the Cathode - For a given average current density, the activation overpotential during the pulse plating is different from that of DC plating (1). To simplify the analysis, we choose a semi-empirical approach, i.e., the current density vs. activation overpotential relation will be supplied from a set of empirical polarization data in the form:

$$i_c = f[\eta_c,\ T,\ \theta] \tag{4}$$

where $i_c$ and $\eta_c$ denote the time-averaged current density and activation overpotential at the cathode; T is the pulse period; and $\theta$ is the duty cycle. For a given electrolyte system and pulse current of fixed duty cycle and pulse period, the function 'f' is determined from the experimental polarization measurements (3,4).

Equations (1) - (4) must be simultaneously solved to determine the cathodic and anodic current distributions in the cell. A computer code using Fortran 77 and a finite element technique has been developed to perform the numerical calculations. Figures 11 and 12 show the cathodic and

using Fortran 77 and a finite element technique has been developed to perform the numerical calculations. Figures 11 and 12 show the cathodic and anodic primary current distributions for gold plating from the acid hard gold 0bath. A measured conductivity value of 0.0065 $ohm^{-1}cm^{-1}$ was used for the calculation. The horizontal axis in the figures is a dimensionless distance defined as the ratio of cathode surface distance to half-anode width, $x/L_a$. The dimensionless anode-cathode spacing, $H^*=H/L_a$, was equal to one. The theoretical current distribution curves at the cathode (Fig. 11) exhibited the same trend as those of experimental metal distribution curves shown in Figs. 1-3. Increasing the average current densities at the anode improved the localization of metal deposition at the cathode. The agreement between the theory and experiments was reasonably good for both the DC and pulse platings. The theory also reveals that the current distribution at the anode is not uniform. The local anodic current density is high near the edge of the anode, and decreases toward the center. The anodic current distribution becomes less uniform with increasing average anode current densities as shown in Fig. 12.

## CONCLUSIONS

A study has been made of the selective pulse plating of gold and 60% tin - 40% lead solder on localized areas of an unmasked cathode. The localized deposition was achieved by directing a small anode toward the unmasked cathode at a small anode-cathode spacing, and by applying a high pulse current density. The results indicate that the metal distribution at the cathode became more localized with increasing peak pulse current density, with decreasing duty cycle, and with increasing pulse period (or decreasing pulse frequency). Highly localized gold and tin-lead solder deposits were obtained by operating the pulse plating at: i) the anode-cathode spacing less than half anode diameter (or width); ii) small duty cycles less than 1-10%; iii) high instantaneous pulse current densities greater than 1-10 $A/cm^2$; and iv) high pulse period of 0.05-1 s (or 1-20 Hz). Pulse current also changed the morphology of gold deposit. At the same average current densities, the individual grains of gold deposits obtained with pulse plating were much larger than those obtained with DC plating. For a given pulse period and duty cycle, the size of gold grains decreased with increasing average current densities. The experimental results were interpreted with a two dimensional mathematical model for current distribution in the plating cell. The calculated cathodic current distribution for gold plating agree qualitatively with experimental metal distribution curves.

## ACKNOWLEDGEMENT

The authors gratefully acknowledge the financial support of AESF. Thanks are also due to James Voytko of Sandia National Laboratories for his encouragement and many helpful discussions.

REFERENCES

1. D-T. Chin, J. Electrochem. Soc., 130 1657 (1983).

2. N. Ibl, Proc. AESF 2nd Int'l Pulse Plating Symp. (1981).

3. D-T. Chin and N.R.K. Vilambi, 73rd AESF Annual Technical Conference Proceedings, paper G5 (1986).

4. N.R.K. Vilambi and D-T. Chin, Plating and Surface Finishing, 75, No. 1, 67 (1988).

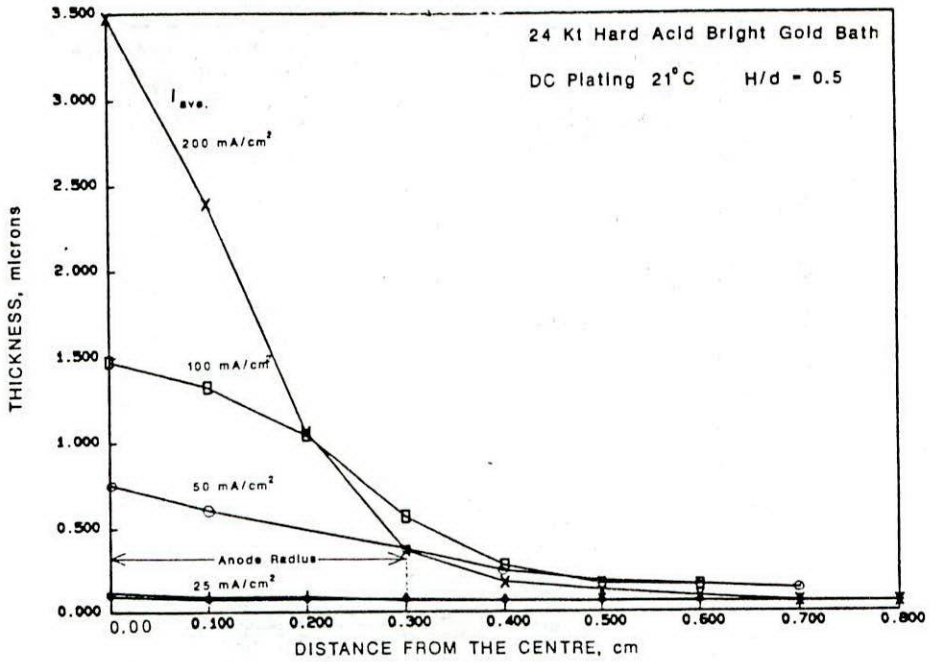


Figure 1. Thickness distribution of gold deposits with DC plating.

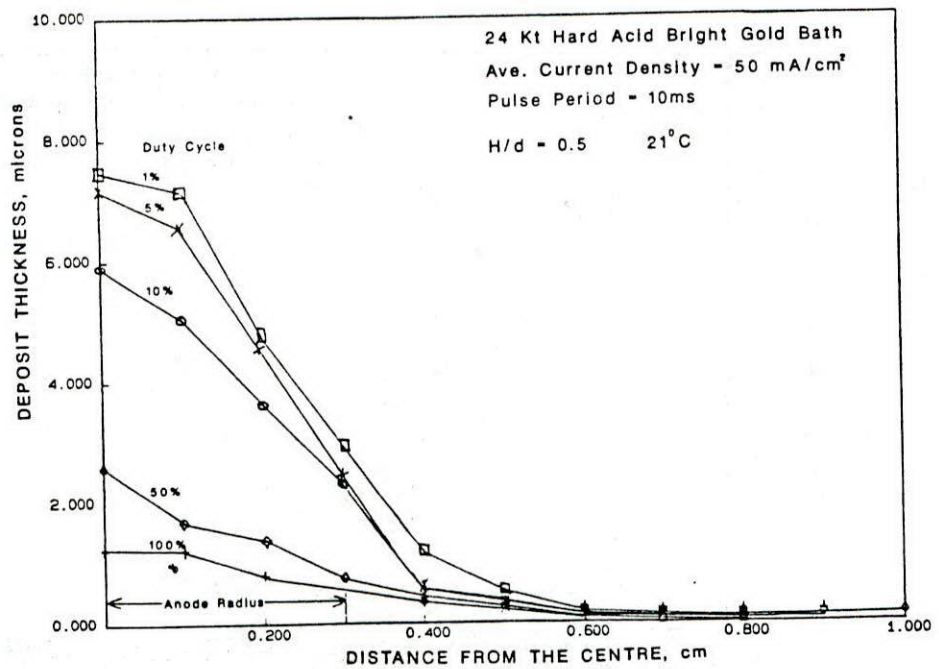


Figure 2. Thickness distribution of gold deposits with pulse plating.

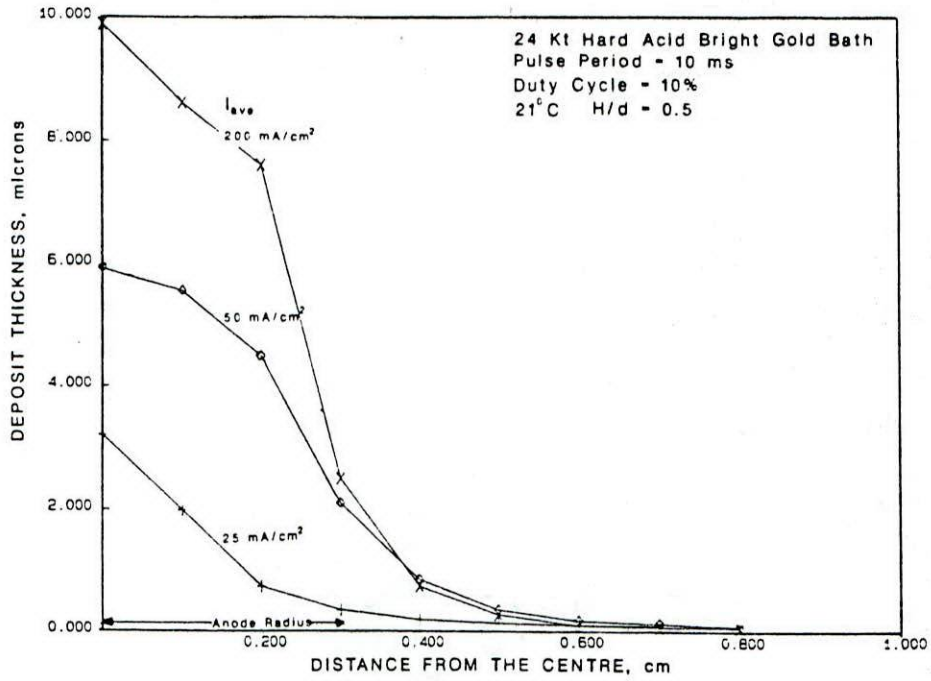


Figure 3. Effect of average current density on the metal distribution of gold deposits in pulse plating.

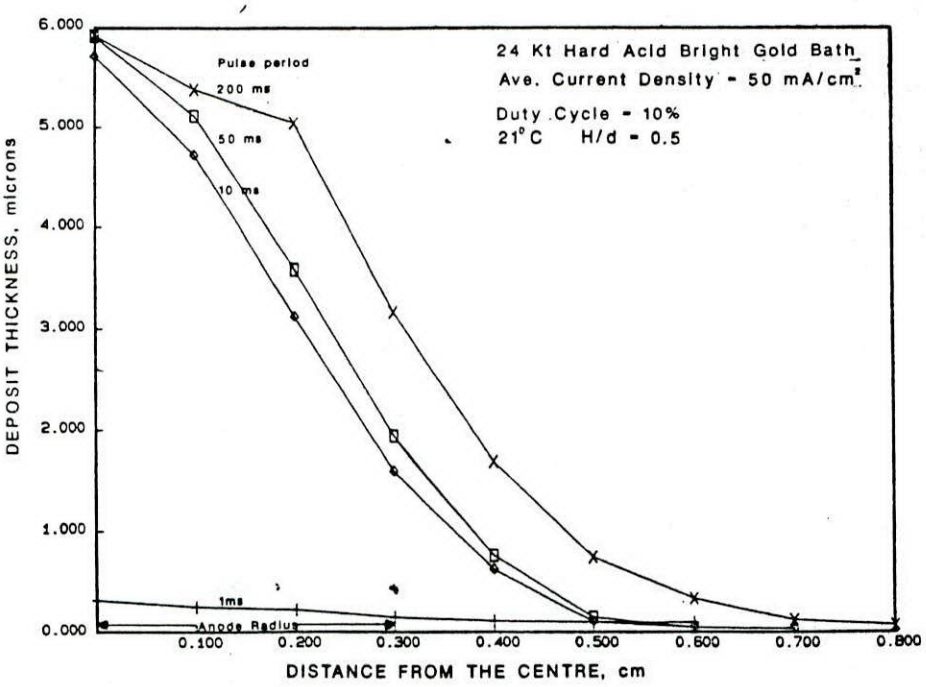


Figure 4. Effect of pulse period on the metal distribution of gold deposits in pulse plating.

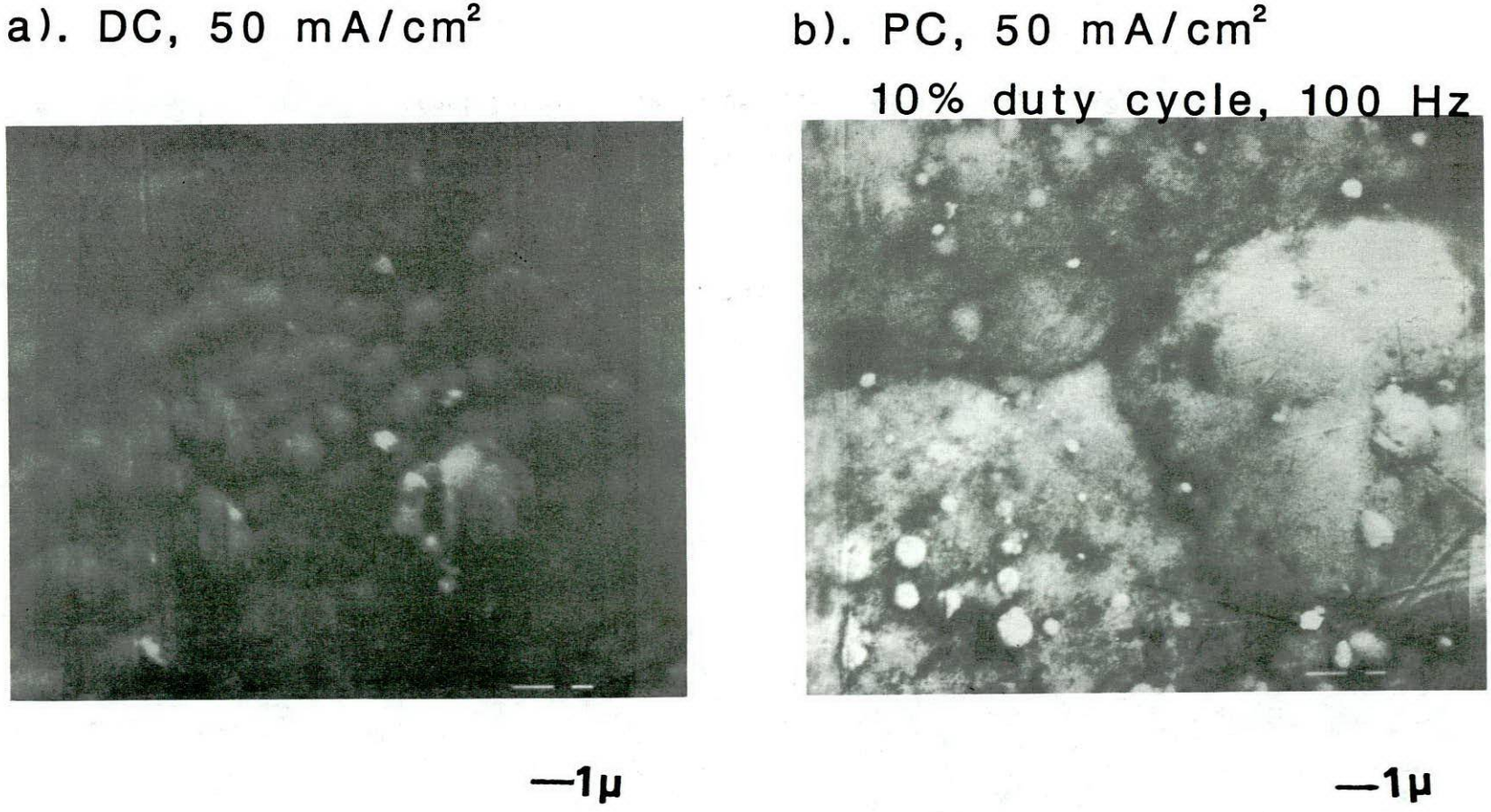


Figure 5. SEM photomicrographs of gold deposits obtained with: (a) DC plating; and (b) pulse plating at 10% duty cycle and 10 ms pulse period. The average plating current density for the both deposits was 0.05 $A/cm^2$.

a). PC, 50 mA/cm$^2$
10% duty cycle, 20Hz

b). PC, 200 mA/cm$^2$
10% duty cycle, 20 Hz

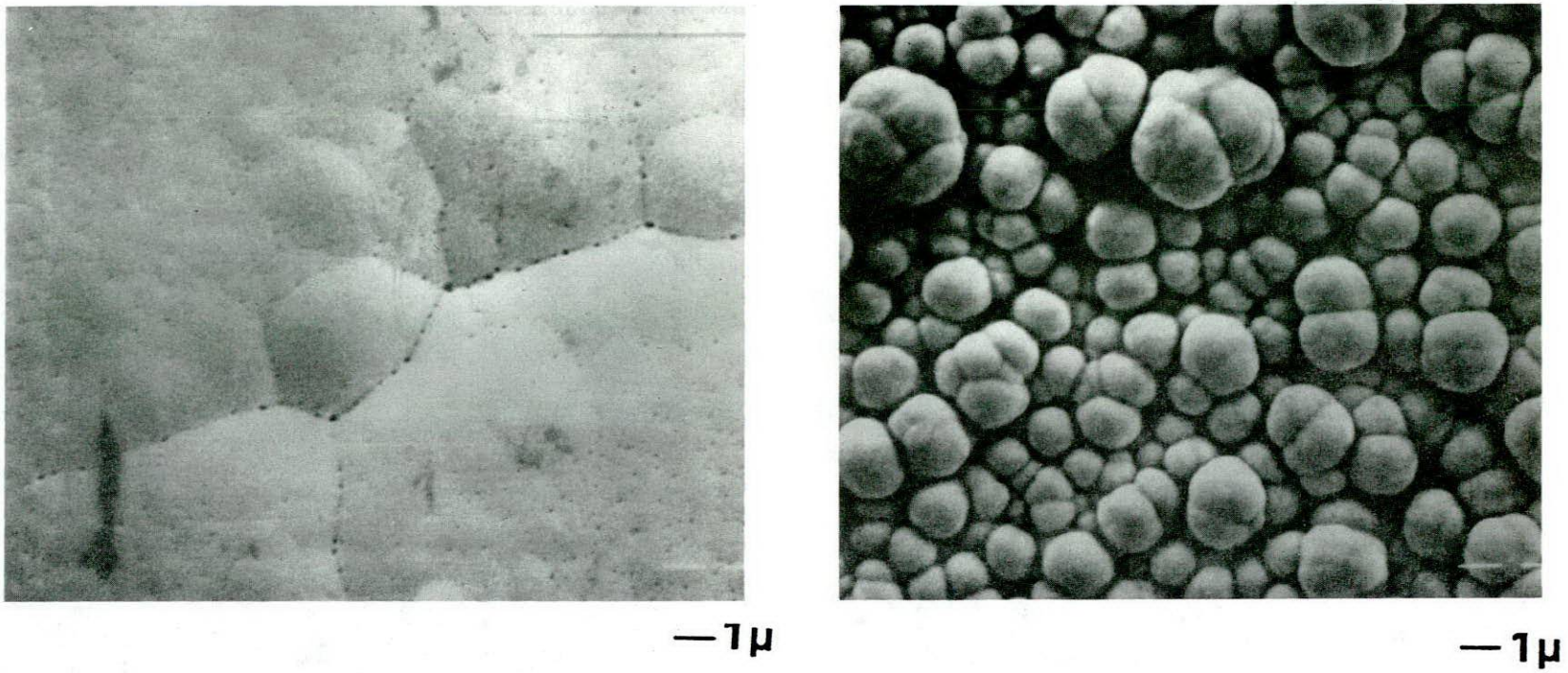


Figure 6. SEM photomicrographs of gold deposits obtained with pulse plating at 10% duty cycle and 50 ms pulse period. The average current densities were: (a) 0.05 A/cm$^2$; and (b) 0.2 A/cm$^2$.

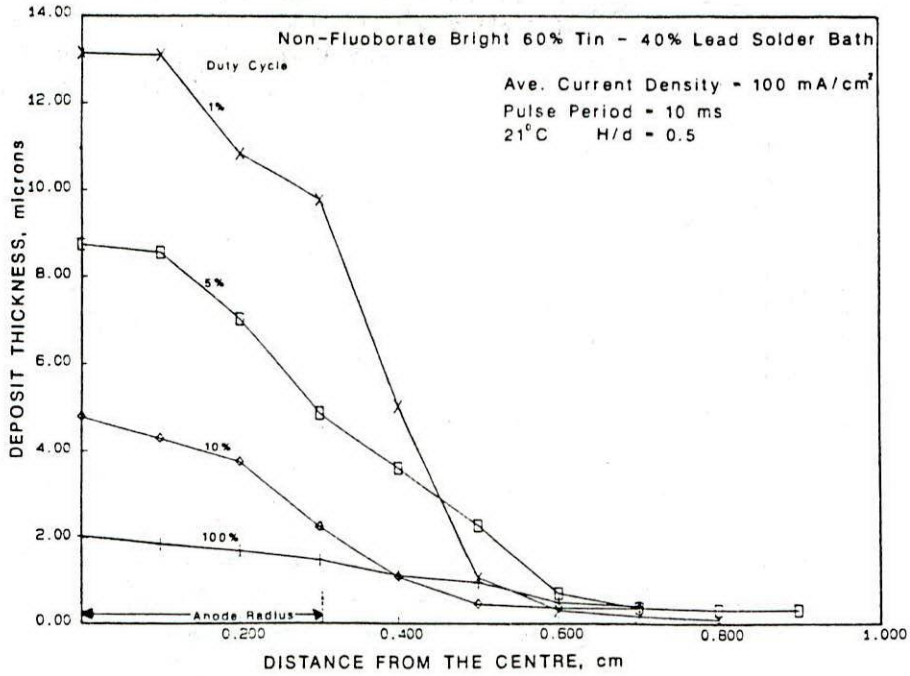


Figure 7. Thickness distribution of tin-lead solder deposits obtained with pulse plating from the nonfluoborate bath.

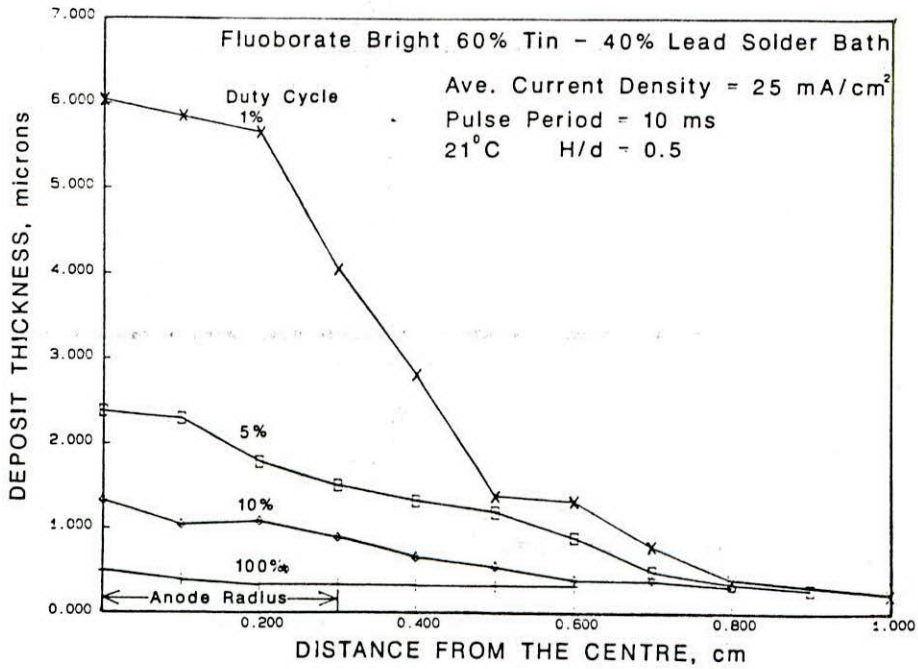


Figure 8. Thickness distribution of tin-lead solder deposits obtained with pulse plating from the fluoborate bath.

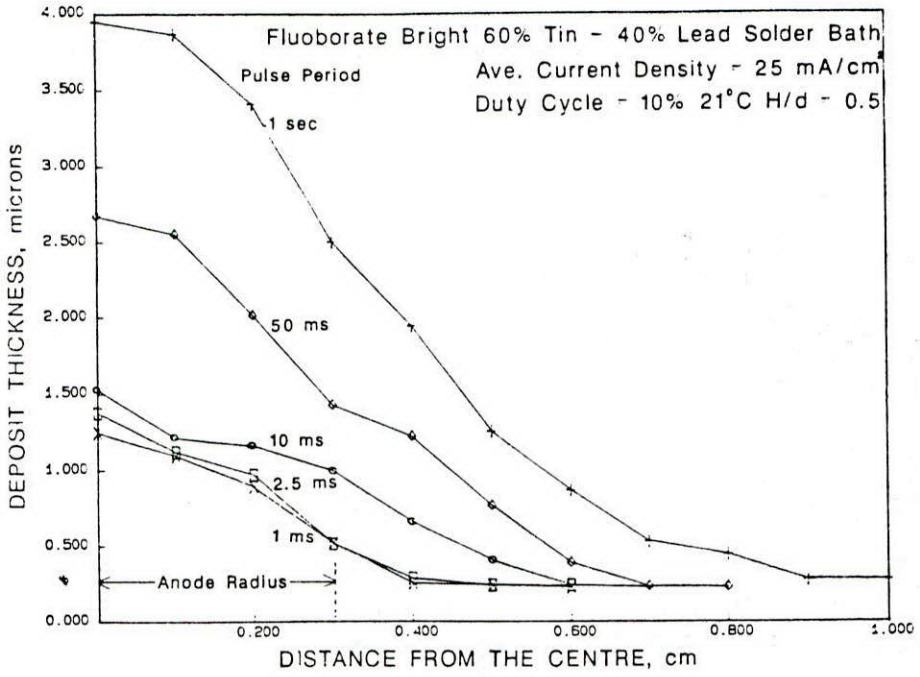


Figure 9. Effect of pulse period on the metal distribution of tin-lead solder deposits from the fluoborate bath.

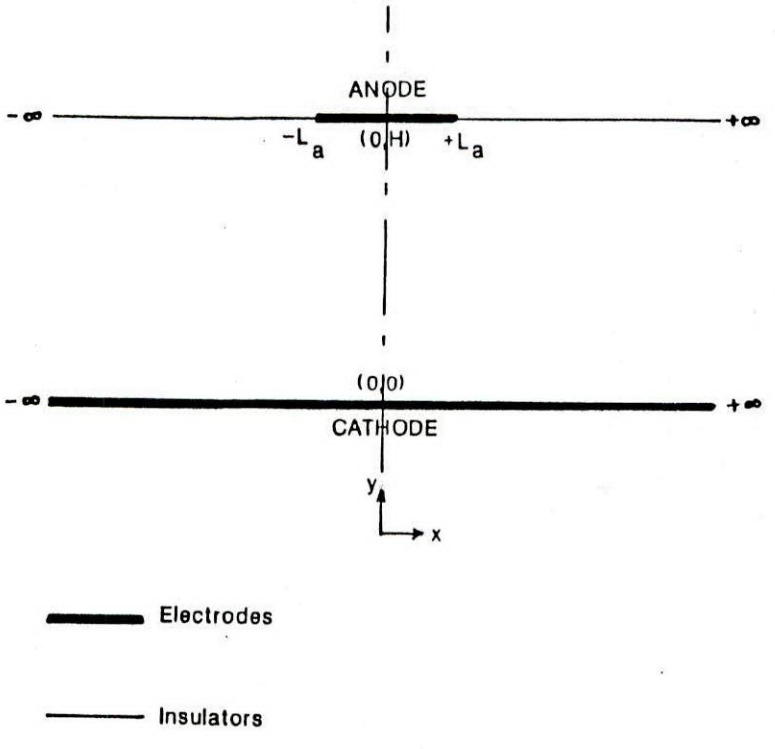


Figure 10. Schematic diagram of electrode geometry used in mathematical modeling.

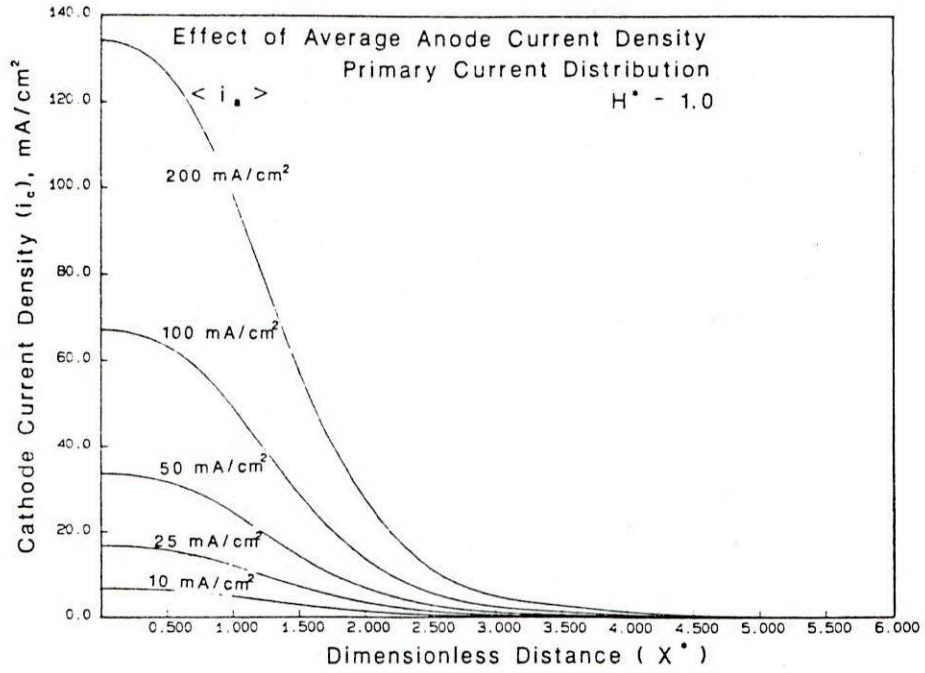


Figure 11. Calculated primary current distribution on a maskless cathode for gold plating from the acid hard gold bath.

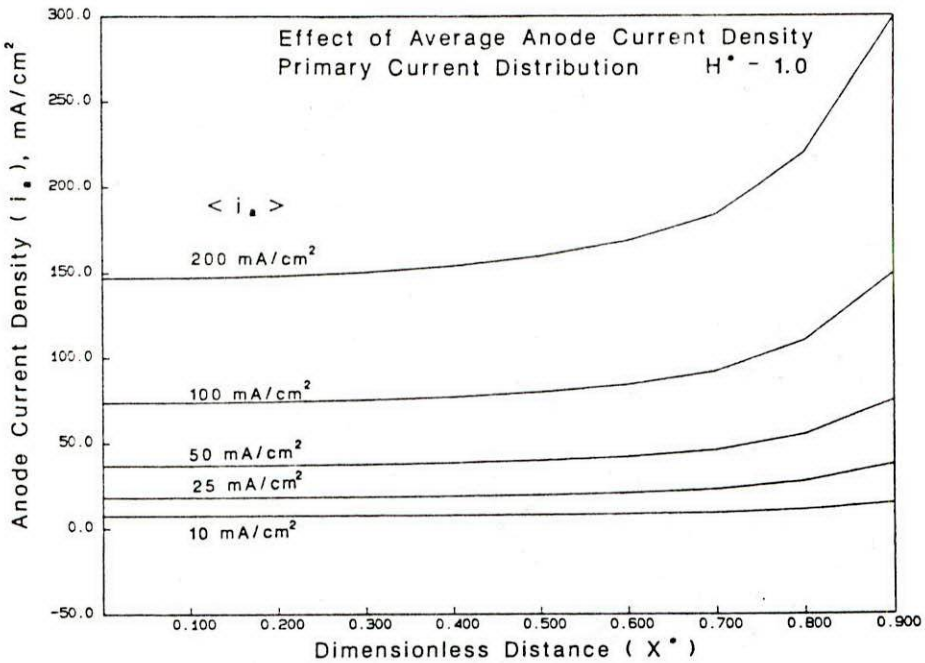


Figure 12. Calculated anodic primary current distribution for gold plating from the acid hard gold bath.

B-3

# Research Session B

## Thickness Effects on the Mechanical Properties of Electrodeposits

Ingon Kim and Rolf Weil
Stevens Institute of Technology
Hoboken, NJ 07030

# THICKNESS EFFECTS ON THE MECHANICAL PROPERTIES OF ELECTRODEPOSITS

Ingon Kim and Rolf Weil

Stevens Institute of Technology, Hoboken, NJ 07030

## INTRODUCTION

The mechanical properties of thin foils have been of interest to investigators since 1933 when Orowan (1) observed that thin mica sheets exhibited exceptionally high strengths. Since then most of the studies of the mechanical properties of thin foils have involved vapor deposits. Investigators of the properties of electrodeposits have generally only measured the hardness. No systematic study of the mechanical properties of electrodeposits which included those with thicknesses in the submicron range, where the greatest strength increase occurs in vapor deposits, has been performed. As part of the investigation of the mechanical properties of electrodeposits under AESF Research Project 69, the effects of deposit thickness were studied. Because of the initial design of a minitensile machine and a specimen for it carried out under AESF Project 38 (2), it was possible to test electrodeposits in simple tension which were as thin as 200 nm which is only about 1000 atom layers . The results of this study are reported here.

## EXPERIMENTAL PROCEDURE

The substrates were pieces of cube-textured copper sheet i.e., most of the grains had a {100} crystal plane parallel to the surface. Photolithography was used to plate the tensile specimens directly to the desired shape. The surfaces of the substrates were coated with photoresist prior to plating. The mask having four cutouts in the shape of the tensile specimen shown in Figure 1 was then placed on the photoresist-coated substrate. The masks were placed on the substrate so that the prospective tensile direction was parallel to <012> in most grains. The mask also did not cover a 2 cm wide boarder. After exposure to ultra-violet light, the photoresist was developed so that it was dissolved in the areas exposed to the ultra-violet light. In this way, only areas having the shapes of the four tensile specimens were not insulated and thus could be nickel plated. The boarder was also not insulated so that when it was plated, the current density in the central region would be uniform. The uninsulated areas were electropolished in a 67% aqueous phosphoric-acid solution. After rinsing, they were plated in a solution containing 112 g/l $NiSO_4 \times 6H_2O$ and 30 g/l $H_3BO_3$ . The current density was 2.5 $mA/cm^2$ ; the pH was 4

and the temperature of the solution was 20C. The deposit thickness varied from 200 nm to 9.5 μm.

The specimen design shown in Figure 1 made it posssible to test deposits as thin as 200 nm. Specimens so thin would have been too weak to be handled after dissolving the substrates without additional support. Therefore while the deposits were still attached to the substrates, the gage-length portion was coated with an insulating laquer and the remaining area was futher nickel plated. This heavier plated area was painted black for illustrative purposes on the photograph which is Figure 1. The thicker deposit on the ends and on the segment parallel to the gage length acted as a supporting frame to prevent the thin portion from deforming.

After dissolving the copper substrate in a chromic-sulfuric acid solution, the specimens were mounted on the grips of the minitensile machine. The functioning of the minitensile machine was described previously (3). The segment parallel to the gage length of the tensile specimen was severed after mounting on the grips. After testing, the fractures were examined by transmission and scanning electron microscopy. Scanning electron microscopy and weighing were used to determine the specimen thicknesses.

## RESULTS AND DISCUSSION

The mechanical properties of the nickel deposits are listed in Table 1. Each value is the average of at least three measurements. The values in parentheses are the variations in the individual measurements.

It is seen that Young's modulus is not significantly affected by the deposit thickness. The variations with deposit thickness are probably due to small thickness nonuniformities. The yield strength is seen to decrease with increasing thickness and that of the 200 nm-thick deposits is significantly larger than the other values. The high yield strength of the thinnest deposit is probably due to surface pinning of dislocations. Figure 2 shows no evidence of any dislocation motion even in the areas near the fracture. The decrease in the yield strength as the thickness increased was probably due to greater dislocation mobility and the activation of sources for their generation. The tensile strengths are seen to be relatively unaffected by the thickness of the deposits. The values remained constant probably because the increased activation of sources for dislocation generation in the thicker deposits resulted in greater rates of work hardening. The degree of dislocation immobility thus became essentially the same in all deposits.

Table 1

Mechanical Properties of Nickel Electrodeposits

| Thickness (μm) | Young's Modulus (GPa)* | Yield Strength (MPa)# | Tensile Strength (MPa) | Percent Elongation |
|---|---|---|---|---|
| 0.2 | 80 (3) | 220 (5) | 220 (5) | 0 |
| 2.0 | 92 (1) | 154 (3) | 200 (5) | 2.2 (0.2) |
| 4.2 | 92 (0) | 137 (7) | 190 (6) | 3.7 (0.2) |
| 5.7 | 87 (1) | 130 (11) | 200 (7) | 6.2 (0.2) |
| 7.5 | 86 (3) | 122 (8) | 210 (13) | 7.0 (0.1) |
| 8.3 | 84 (2) | 130 (8) | 204 (4) | 7.0 (0.3) |
| 9.5 | 85 (2) | 123 (7) | 205 (5) | 7.0 (0.2) |

* 7 GPA = approx. 1 million psi. # 7 MPa = approx 1000 psi

The reason why the 200 nm-thick deposit had no ductility as manifested by the percent elongation can be seen in Figure 2. As already mentioned, there is no evidence of any dislocation motion, i.e., plastic deformation having taken place. The fracture occurred in the boundaries of the grains which had a {100} plane parallel to their surface. Fracture also occurred within a grain which had a {111} plane parallel to its surface. This grain was thinner than the others. The probable reason the <100>-oriented grain were thicker is that the fiber axis of nickel plated in an all-sulfate solution is <100>. A fiber texture developes because grains with its orientation grow faster than the others (4). Thus the <100>-oriented grains grew to a greater thickness than the ones with the <111> orientation. The smaller thickness led to a higher stress and fracture within the grain while the others failed in the grain boundaries which were also probably a little thinner.

After the maximum load from which the tensile strength was calculated, had been applied, the thickness was substantially reduced over a portion of the gage length. This phenomenon is called necking. The portion of the gage length over which necking occurred increased with increasing thickness. Most of the platic deformation occurred in the

necked portion. Therefore the increase in the gage length at fracture from which the elongation was calculated, depended on how long a portion underwent necking. The greater the portion of the gage length which plastically deformed and necked, the greater was the elongation.

All deposits, regardless of initial thickness, were about 200 nm thick just prior to fracture. This result is evident in Figure 3, which shows the fracture of the thickest deposit which was tested. Evidently, it was thin enough adjacent to the fracture to be transparent to the electron beam which means that there it was less than 200 nm thick. The fracture shown in Figure 3 occurred in a grain with a {100} plane parallel to it surface. It fractured along two mutually perpendicular <110> directions and therefore probably on {111} planes. The final thinning before fracture took place by mechanical twinning. The twins can be seen at the fracture edge in Figure 3.

If the reduction in area is taken as an indication of ductility, the thick deposits are extremely ductile. The apparent thickness prior to fracture of about 200 nm seen in Figure 3 yields a calculated reduction in area of 99%. Also the true stress at fracture, which is the load divided by the actual area, is very high. There was little change in the gage length between the application of the maximum load and when fracture occured. Therefore, it was not possible to determine the fracture load. If the load which caused fracture is assumed to be half the maximum one, the true fracture stress would be about 1000 MPa, i.e., five times the tensile strength. On the other hand, the true fracture stress of the very thin deposits which showed no necking, was the same as the tensile strength.

It can be concluded that very thin electrodeposits exhibit high yield strengths. While the tensile strength was essentially the same for all deposits, the true fracture stength increased with increasing thickness because of necking. The elongation increased with increasing thickness because a larger portion of the gage length deformed plastically. Because all deposits necked down to essentially the same thickness prio to fracture, the reduction in area increased with increasing thickness.

## REFERENCES

1. E. Orowan, Z. Physik, 82 , 234 (1933).

2. M. Parente and R. Weil, Plating and Surf. Finish, 71 , 114 (5/1984).

3. I. Kim and R. Weil, Testing of Metallic and Inorganic Coatings, W. B. Harding and G. A. DiBari, Eds., ASTM STP 947, 11, American Society for Testing and Materials, Phila. PA.

4. R. Weil, Proc. Interfinish '84, 28 (1984)

## ACKNOWLEDGEMENTS

The support of the Research Board of the American Electroplaters and Metal Finishers Society and its supporting members is gratefully acknowledged as is the advice of the members of the Project Committee consisting of Messrs. A. Damjanovic, G. Fisher, D. Hardesty, J. Horner, F. Koch, S. Nakahara, Y. Okinaka, T. Palumbo and M. Paunovic.

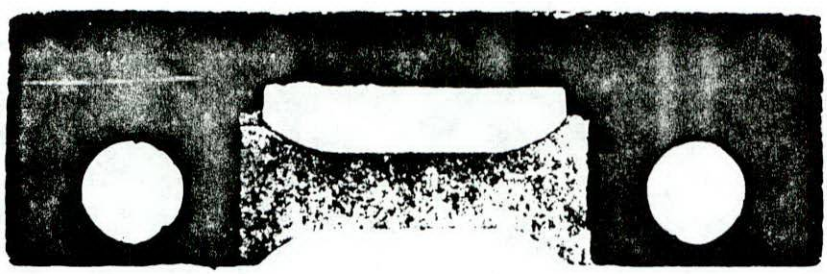

Figure 1. Tensile Spcimen. Blackened Areas were Plated Heavier When Deposits were thin.

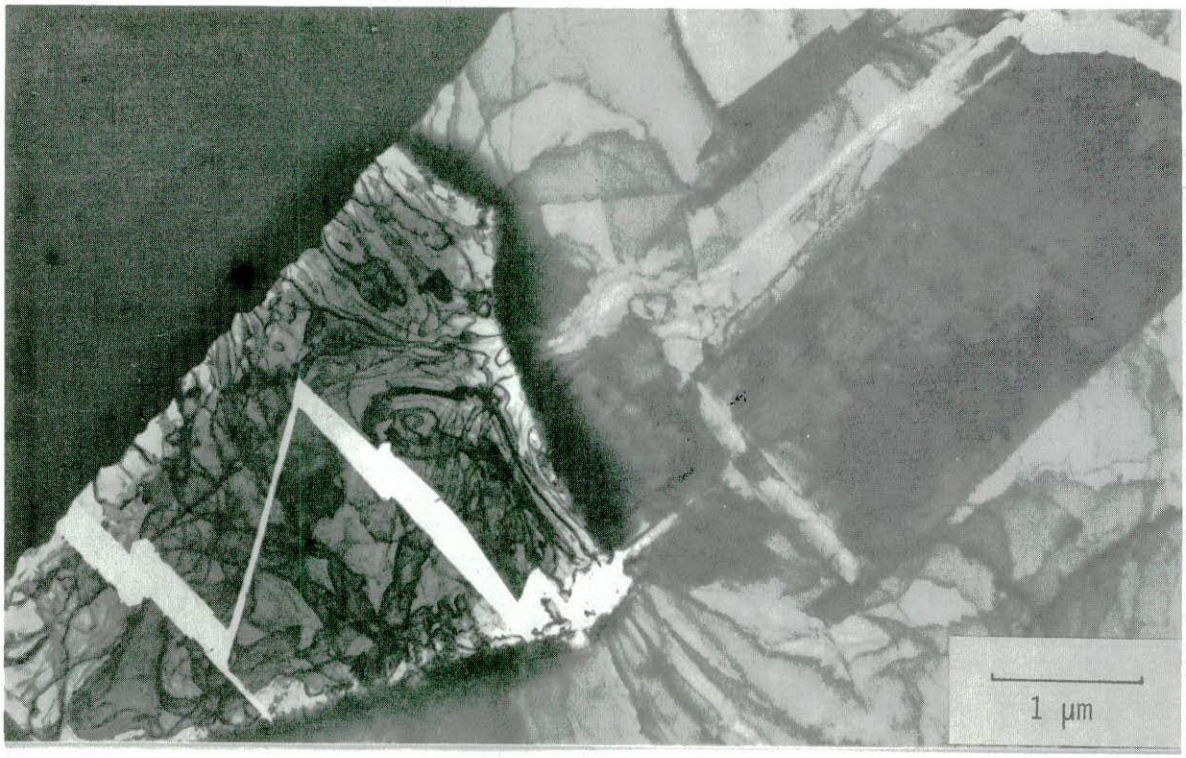


Figure 2. Fracture Region in 200 nm Thick Deposit.

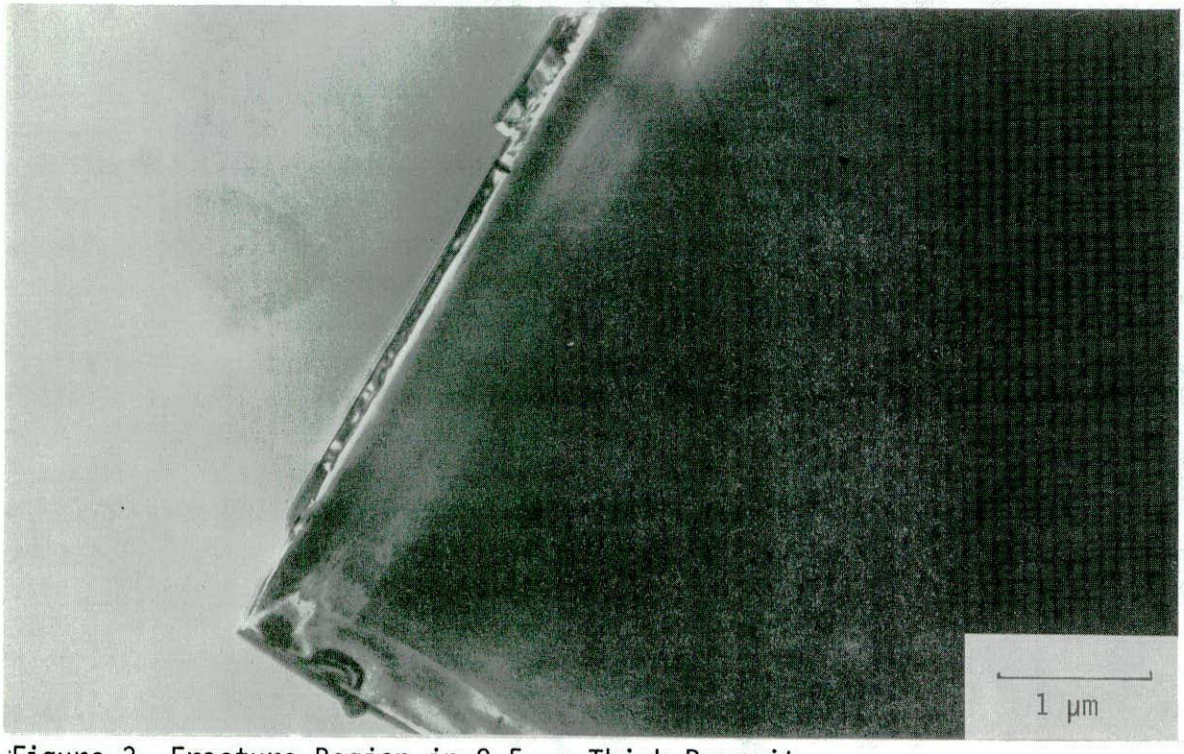


Figure 3. Fracture Region in 9.5 μm Thick Deposit.

B-4

# Research Session B

## Factors Affecting Low Temperature Interdiffusion

L. Giannuzzi, H.W. Pickering and W.R. Bitler
The Pennsylvania State University
University Park, PA 16802

# Factors Effecting Low Temperature Interdiffusion

L. Giannuzzi, H. W Pickering, and W. R. Bitler
The Pennsylvania State University
University Park, PA 16802

Diffusion in crystalline solids can take place through the lattice and through the grain boundaries. It is believed that in most metals the mechanism of this diffusion is motion by interchange of atoms and vacancies. Because vacancies are present in higher concentration in the vicinity of grain boundaries and because these vacancies are more mobile than those in the lattice away from the grain boundaries, diffusion can take place at a faster rate in grain boundaries than in the lattice. There are two different aspects of grain boundary diffusion. First in a diffusion couple between two different chemical species, say for example between nickel and gold, the nickel can diffuse into the gold through the lattice and also through the grain boundaries and then into the lattice. If the time for diffusion is long enough for the diffusion from the grain boundaries into the lattice to completely penetrate the individual grains then the overall effect is the same as if there were only lattice diffusion but at a much higher rate than the diffusion rate would be in the absence of grain boundaries. Such an effect is indicated in Fig.1. This is a plot of the log of the diffusivity verses 1/T where T is the temperature in kelvins. The steep line to the left of the diagram which is continued as a dotted line is the diffusivity one would observe in a single crystal, i.e. in the absence of grain boundaries. The lines with lower slopes represent the contribution to the volume diffusivity arising from the presence of grain boundaries and as one would expect the effect increases with the number of grain boundaries, i.e. as the grain size decreases. Note that because this is a logarithm plot, this means that at low temperatures (the right side of the graph) the effective D determined for polycrystalline samples can be orders of magnitude larger than for a sample without grain boundaries. This project has examined a number of systems for this effect in the past and reported on them. To secure such data at low temperatures requires long diffusion anneals at low temperatures, sufficiently long such that the diffusion from the grain boundaries

into the grains effectively completely penetrates the grains.

It is apparent that the grain size plays an important role with the effect getting larger as the grain size decreases. In prior reports the effect of pH of the plating bath on the grain size of palladium deposits was reported for Pd electrodeposited from ammonia containing baths. As the pH was increased the grain size increased, but not uniformly. Instead a bimodal grain size distribution developed with increasing pH although the average grain size increased. The maximum pH realizable with this bath was a pH of 9. At higher pH the bath becomes unstable with the evolution of ammonia. Additional grain size data will be reported for Pd deposited from a bath not containing ammonia in which the pH can be extended up to a pH of 12.

A second effect is that at shorter diffusion times and/or at lower temperatures such that the diffusion into the grains from the grain boundaries may be negligible, there still may be significant diffusion along the grain boundaries over comparatively large distances. Thus at distances large compared to the grain size and large compared to the diffusion distance in the lattice from the original interface between two chemical species, again for example in a gold- nickel diffusion couple, the Ni penetration into the Au grain boundaries may be significant. Because the thickness of the grain boundaries is so small, of the order of Ångstroms, the amount of the diffusing species within the grain boundary is so small that it can not be detected by a microprobe. This does not mean however that the transport through the grain boundaries can be ignored. For example in a thin film, e.g. an electrodeposit, one may find that in terms of data obtained by a microprobe that the diffusion of the substrate into the electrodeposit has advanced only a small fraction of the way through the electrodeposit. However an examination of the free surface by techniques such as Auger spectroscopy may indicate that there has been penetration of the electrodeposit by grain boundary diffusion and a significant build up of the substrate material on the free surface. This surface build up of the substrate material can influence the surface properties such as the wettability of the surface and in turn effect such technologically important properties as solderability. It is the current goal of this project to

explore means to reduce the permeation of thin films by grain boundary diffusion. A promising avenue for such control is to introduce impurities in low concentrations that are segregated to the grain boundaries and effect the grain boundary diffusivity. Preliminary data on the effect of Bi on the grain boundary diffusivity of Au and Ni into copper will be presented.

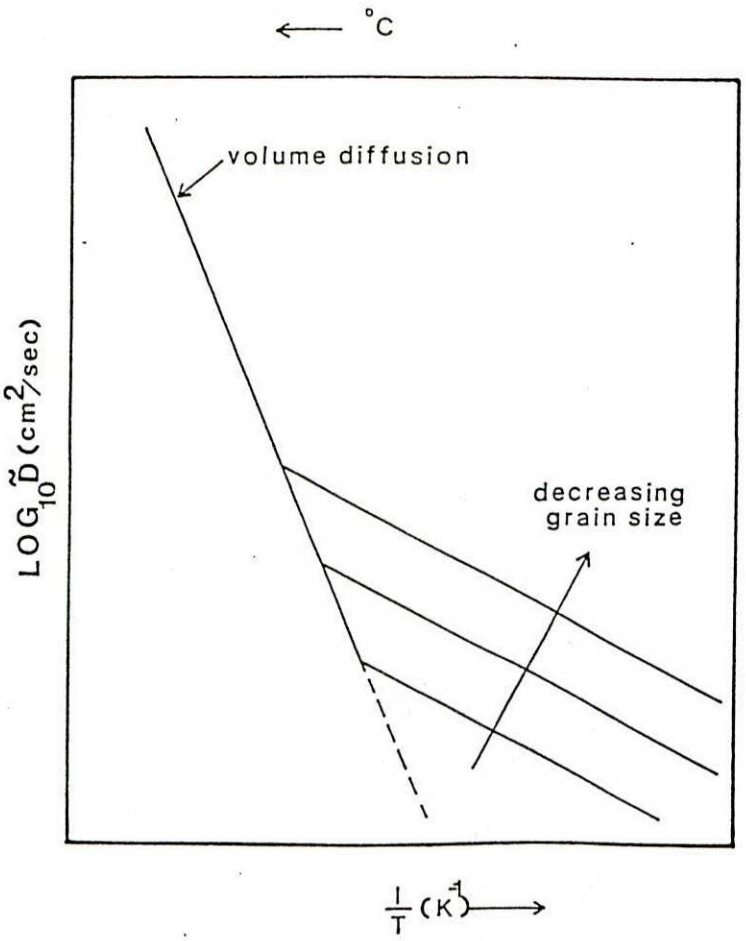

B-5

# Research Session B

## Effects of Additives in Acid Chloride Zinc Deposition

T.J. O'Keefe, J.S. Cuzmar
and Y.S. Park
Graduate Center for Materials Research
University of Missouri-Rolla
Rolla, MO 65401

S. Wagner
Missouri Electrochem Inc.
10958 Lin-Valle Drive
St. Louis, MO 63123

# EFFECTS OF ADDITIVES IN ACID CHLORIDE ZINC DEPOSITION

T. J. O'Keefe, J. S. Cuzmar, Y. S. Park
Graduate Center For Materials Research,
University of Missouri-Rolla, Rolla, MO 65401

S. Wagner
Missouri Electrochem Inc.,
10958 Lin-Valle Drive, St. Louis, MO 63123

Abstract

The effect of additives on morphology, crystal orientation, and polarization behavior for zinc deposition onto steel substrates from chloride solutions was investigated. Cyclic voltammetric techniques showed the polarization to be strongly dependent on both the wetting and brightening agents. The influence of agitation on the deposit was also studied.

## 1. Introduction

Electrodeposited zinc coatings are used extensively to provide improved corrosion resistance for steel. In addition to providing cathodic protection to the underlying metal, the plated pieces are attractive in appearance as a result of the variety of bright zinc systems developed by the metal finishing industry. Any number of zinc plating technologies are available and include cyanide, alkaline, and acid chloride based electrolytes [1,2]. Each process offers different advantages in performance, ease of operation, effluent treatment, and overall economics and efficiency. The final selection must then be made by choosing a process which most closely meets the criteria as they relate to the final end use [3]. Some excellent descriptions of the zinc plating processes have been given and further elaboration will not be made in this paper. However, an area that seems to have received little attention is the polarization characterization of the zinc deposition process.

One major objective of this work, which was sponsored in part by the AES, was to initiate studies on determining various electrochemical aspects of the process. In particular, the behavior of two prominent additives in the zinc chloride process [4], a surfactant and a brightener were evaluated. Cyclic voltammetry techniques were used to generate polarization curves on the system. Galvanostatic deposits at a fixed current density and Hull cell tests were also made. In addition to providing fundamental information about the process, the research was directed toward determining the possibility of using electrochemical tests for electrolyte and additive analysis and plating bath characterization [5,6]. Deposits were made using synthetic electrolytes and beaker cells at the University of Missouri-Rolla (UMR) laboratories, while commercial electrolytes were used for zinc deposition for the industrial tests. Duplicate deposition tests and exchange of materials was employed to insure that any results obtained might more likely be correlated with industrial practice.

## 2. Experimental

### 2.1. Electrodeposition System

Synthetic solution was prepared by dissolving 44.94 g/l zinc chloride, 112.34 g/l potassium chloride, and 25 g/l boric acid in deionized water. All solutions were filtered to remove suspended impurities prior to use. The pH was about 5.2, and the temperature was maintained at 27°C during the tests by immersing the cell in a water bath.

AISI 1008 low carbon steel strips, 19 mm x 76 mm, were used as the starting cathode substrate. The strip was first cleaned ultrasonically in laboratory grade detergent, rinsed with deionized water, dried with absorbent paper, and degreased in trichloroethylene. The electrodes were covered with plater's tape to give a circular 1 $cm^2$ area to be plated. The exposed area was then anodically cleaned at 100 $mA/cm^2$ at 60°C in 15 g/l proprietary alkaline cleaner for 30 seconds, dipped into the 1 M hydrochloric acid for 30 seconds, rinsed with deionized water, and dried in a stream of nitrogen.

For the cyclic voltammetry experiments, AISI 1008 low carbon steel rod with 1 $cm^2$ cross sectional area was mounted in an epoxy resin, polished with 600 grit silicon carbide paper, rinsed, and dried in a stream of nitrogen before immersing into the electrolyte. The pure zinc anodes, 26 mm x 110 mm, were cleaned ultrasonically in 0.5 M hydrochloric acid for 30 seconds, rinsed, and dried prior to use. The cell for the plating and cyclic voltammetry tests consisted of a 250 ml beaker, with a plexiglass lid with provisions for mounting the cathode, the anode, and the reference electrode. The anode to cathode spacing was 25 mm for deposition tests and 30 mm for the cyclic voltammetry tests; 200 ml of electrolyte was used. The steel substrate was held in the electrolyte for 15 seconds prior to plating to provide time for an equilibrium condition to be established. Most of the galvanostatic deposits were made at a current density of 35 $mA/cm^2$. After 10 minutes deposition, the cathode was removed from the cell, rinsed, and dried with nitrogen for further study by SEM and x-ray diffraction for morphology and orientation.

### 2.2. Hull Cell Test

For the Hull cell deposition tests, both carbon filtered and unfiltered electrolyte were used, but initial results showed no difference between them. A standard low carbon steel panel (10 x 6.6 cm) was used for the cathode.

The amount of electrolyte was 267 ml, which contained 45 g/l zinc chloride, 123.57 g/l potassium chloride, and 24.34 g/l boric acid. The pH was about 5.2 and the plating tests were made at room temperature for 5 minutes using a current of one ampere. The electrolyte was agitated in some tests, as well.

To examine the zinc deposits from the Hull cell tests, the steel panels were cut into sections representing the various current densities. Samples

at a current density of 35 mA/cm$^2$ were used most often for SEM and x-ray diffractometer examination.

### 2.3. Potentiodynamic Test

The polarization curves were generated using a low carbon steel working electrode which was allowed to stay at open circuit potential for 15 seconds prior to initiating the scan. The cyclic voltammetry scans started at -0.85 V vs. SCE at a rate of 5 mV/sec, and the direction was reversed at -1.35 V vs. SCE.

### 2.4. Additives

Various additives were used in the study. Included were an anhydrous, liquid non-ionic surface agent produced by the reaction of nonylphenol with 10.5 moles of ethylene oxide (Surfactant I), a 70% active solution made from a non-ionic surface active agent produced by the reaction of nonylphenol with 30 moles of ethylene oxide (Surfactant II), and a commercial non-ionic Surfactant III were used as the wetting agents. Ortho-chlorobenzaldehyde, and commercial brightener were used in combination with the surfactants.

## 3. Results and Discussion

### 3.1. Deposit Morphology

The synthetic solution without additives gave a light grey, level deposit at 35 mA/cm$^2$ current density, 27°C for 10 minutes plating time. The morphology of the deposit is shown in Figure 1. A sample was taken at the 35 mA/cm$^2$ position from a deposit made in a Hull cell using industrial solution, and the morphology is shown in Figure 2. Additional tests are planned to see if there are any subtle changes that might emerge due to the difference in purity of the various chemicals used or if the finer grain size on the Hull cell deposit is more a function of the deposition method employed.

Upon the addition of various non-ionic wetting agents, a finer grained structure was obtained, compared to the structure from addition-free electrolyte. Generally, as the amount of wetting agents increased, the deposit become a darker grey to brown color, and a nodular finely dendritic structure was obtained. Figures 3, 4, and 5 show the structures obtained for the three surfactants used. The deposits for Surfactant I and III were similar, both showing a uniform dense deposit, but probably with a microscopic surface roughness. Both appeared to be a brownish color in reflected light. Surfactant II gave a needle-like, dendritic growth with a very open and non-continuous growth and was dark grey in color.

The concentrations for the wetting agents were in the range of 0.3% in volume for Surfactant I and II, and 1.5% in volume for Surfactant III. Commercial brightener and ortho-chlorobenzaldehyde were added in the concentration range of 0 to 0.3% for commercial brightener and 0 to 50 ppm for ortho-chlorobenzaldehyde to electrolyte containing the surfactants. These concentrations were suggested by the suppliers and users of the chemicals.

As the amount of brightener increased, more hydrogen evolved at the cathode surface, particularly with Surfactant I, but smooth bright deposits were obtained, once sufficient brightener was present. In some cases, a striated appearance occurred, probably due to the hydrogen gas streaming across the cathode surface. Figure 6 shows that 1.5% Surfactant III with 0.15% commercial brightener gave a smooth, dense deposit, and with agitation a similar and even brighter, smoother deposit was obtained (Figure 7). When the brightener content was increased to 0.3%, a nodular deposit was produced and extensive gas evolution was evident during plating (Figure 8). When the electrolyte was agitated, the deposit remained bright, even at the higher brightener concentration, but some sub-micron pitting was noticed, as shown in Figure 9. Figure 10 shows that 0.3% Surfactant I with 15 ppm ortho-chlorobenzaldehyde also gave a reasonably good deposit but a slight discoloration was noticed with time.

It is well known that the wetting agent and brightener concentrations are important to obtaining quality deposits [7,8]. The morphology results reveal not only the need to maintain a proper balance of surfactant to brightener, but that this ratio is then influenced by the relative degree of agitation, and must be considered when establishing the operating parameters used for the process.

### 3.2. Deposit Orientation

Table 1 shows the crystal orientations of the zinc deposited from the solutions of addition-free, surfactant, and surfactant plus brightener. Without additives, the deposit made from synthetic electrolyte was strongly (110) and (101) oriented. The Hull cell deposit gave a dominant (101) orientation. The orientation of deposits made with only surfactants present gave stronger (100) peaks in addition to the (101), and a noticeable increase in the (002) as well. When the deposits made with surfactant and brightener were smooth and bright, the intensity of the (002) was noticeably low (0-12%), but in the case of the dark grey deposit, the (002) intensity was higher than about 17%. Agitation did not change the preferred orientation of the deposits.

### 3.3. Polarization Behavior

Representative polarization curves for addition-free, synthetic and industrial electrolytes, with and without agitation, are given in Figure 11. Very roughly, the curves are similar up to about 10 $mA/cm^2$, indicating there is little mass transport dependency at a current density lower than this value. Without agitation, a limiting current density of 45 $mA/cm^2$ is noted. A limiting current density of 100 $mA/cm^2$ was obtained with 500 rpm stirring speed. The curves indicate that additional fundamental information on the mass transport characteristics on this system might prove valuable in gaining better insight into the acid zinc chloride system. The anodic portion of the curves shows little or no diffusional control involved during zinc dissolution.

The presence of the three surfactants in the synthetic electrolytes caused an increase in the polarization, as indicated in Figure 12. A

characteristic current plateau was obtained for each in the forward scan, probably due to the strong influence of the initial absorption of the organic on the working electrode. The apparent limiting current density was also significantly decreased, but less for Surfactant III than the other two. The front sweep portion of the curve is indicative of the nucleation overpotential needed to initiate zinc deposition on the steel substrate. The curve is less polarized on the reverse sweep and is more of an equilibrium condition, since zinc is now depositing on a zinc surface. The degree of hysteresis observed is an indication of the relative differences between the overpotentials for zinc nucleation and growth. The relative overpotentials at 10 $mA/cm^2$ resulting from increasing amounts of each of the surfactants are given in Figure 13. The polarization is highest for Surfactant III, with increases noted up to concentrations of 1.5%. Those for the other two are much less and reach a constant value of 0.3%. The exact significance of these values is not known, but it is interesting to observe that the concentrations suggested for use, correspond to the approximate values at which no further increase in polarization is observed. From the curves in Figure 14, the polarizing effect of Surfactant III is seen to be a function of the concentration added.

When a combination of 0.3% Surfactant III and varying amounts of commercial brightener were added to the solution, considerable nucleation overpotential occurred (Figure 15). The magnitude of the initial polarization was related to the brightener content, with larger values occurring as the concentration increased from 0.03% to 0.2%. Some increase in polarization was observed on the reverse scan, and again was dependent on the brightener concentration, but to a lesser degree. The anodic curve also showed a polarizing effect which appeared to be a function of the brightener concentration.

When the surfactant is increased from 0.3% to 1.5% on even greater increase in nucleation overpotential occurs and is proportional to the amount of brightener present (Figure 16), change also is noted in the reverse sweep portion, with considerably more and approximately linear polarization behavior observed. The amount of overpotential is also related to the brightener concentration in this portion of the curve.

Polarization behavior with and without agitation for solutions containing 1.5% Surfactant III plus various amounts of commercial brightener is shown in Figure 17. All the curves are for the reverse scan direction. An interesting combined effect of the polarizing effect of the additives with the depolarization due to the enhanced mass transport caused by agitation is observed. The data indicate that the relative amount of active additive present at the deposition surface is strongly dependent on degree of agitation. The change in overpotential with stirring, at the various concentrations of brightener, is also much greater than when the electrolyte is quiescent.

When ortho-chlorobenzaldehyde was used with the commercial surfactant, a polarization behavior similar to that for the commercial brightener was obtained in the back sweep direction. The magnitude of the polarization was also increased as the amount added increased. However, the curve was

substantially different from the one generated when only surfactant was present.

## 4. Summary and Conclusion

Hull cell and beaker cell deposition tests have been conducted in an attempt to more clearly identify parameters of electrochemical importance in acid zinc chloride plating. The various surfactants used were found to be fairly strong polarizers, and then concentrations, in turn, determined the effectiveness of the brightener. The system was strongly mass transport dependent with an interesting relationship being observed between concentration and activation polarization with increasing current density.

In general, both additives exhibited strong polarizing effects, the degree observed being a function of the concentration. Although considerably more research is needed to more clearly elucidate the role of the various parameters, preliminary results on the use of polarization techniques for analyzing and characterizing the zinc chloride system are encouraging.

## 5. References


[1] H. G. Creutz and S. Martin, "Zinc Plating-Present Technology and Future Trends", Plating And Surface Finishing (1975).

[2] H. Geduld, "Zinc Plating", Metal Finishing (1986).

[3] V. K. Kansupada, "Zinc Plating Technology-Which Option Is Best For You ?", Finisher's Management (1985).

[4] M. P. D'angelo, "Chloride Zinc Plating", Products Finishing Directory (1987).

[5] B. A. Lamping and T. J. O'Keefe, "Evaluation of Zinc Sulfate Electrolytes by Cyclic Voltammetry and Electro Microscopy", Metallurgical Transactions B (1976).

[6] T. J. O'Keefe, "Techniques for Evaluating Electrolytes for Metal Recovery", J. Electroanal. Chem., 168 (1984).

[7] S. Martin, A. Z. Cutler and R. H. Bauer, "Recent Applications Of Acid Zinc Technology On A Commercial Scale", AES Paper (1985).

[8] R. Sard, "Advances in Functional Zinc And Zinc Alloy Coatings", Plating and Surface Finishing (1987).

Table 1. The Preferred Orientation and Appearance of the Deposits from the Synthetic Electrolyte without Agitation.

| | (002) | (100) | (101) | (110) | (201) | (Appearance) |
|---|---|---|---|---|---|---|
| Random | 53 | 40 | 100 | 21 | 17 | |
| Addition-free | 17 | 21 | 91 | 100 | 19 | light grey |
| Surfactant I[2] | 21 | 48 | 100 | 28 | | brown |
| Surfactant II[2] | 42 | 37 | 100 | 41 | | brown |
| Surfactant III[2] | 19 | 100 | 96 | | 24 | brown |
| Surfactant I[2] & co. brightener[1] | 22 | 47 | 100 | 48 | | striated, gas evolution |
| Surfactant II[2] & co. brightener[1] | | 64 | 100 | 27 | 14 | bright |
| Surfactant III[2] & co. brightener[1] | | 55 | 100 | 14 | 16 | bright |
| Surfactant III[3] & co. brightener[1] | 12 | 71 | 100 | 95 | 29 | bright |
| Surfactant I[2] & o-CB[4] | 17 | 59 | 100 | 43 | | brown |
| Surfactant I[2] & o-CB[5] | 7 | 56 | 100 | 49 | 17 | bright |
| Surfactant II[2] & o-CB[4] | 45 | 41 | 100 | 49 | | dark grey |
| Surfactant II[2] & o-CB[5] | 4 | 62 | 84 | 100 | 21 | bright |

1 : 0.15% 2 : 0.3% 3 : 1.5% 4 : 1 ppm 5 : 15 ppm

Surfactant I : nonylphenol with 10.5 moles of ethylene oxide
Surfactant II : 70% active solution of non-ionic surface active agent of nonylphenol with 30 moles of ethylene oxide
Surfactant III : commercial non-ionic surface active agent
Co. brightener : commercial brightener
o-CB : ortho-chlorobenzaldehyde

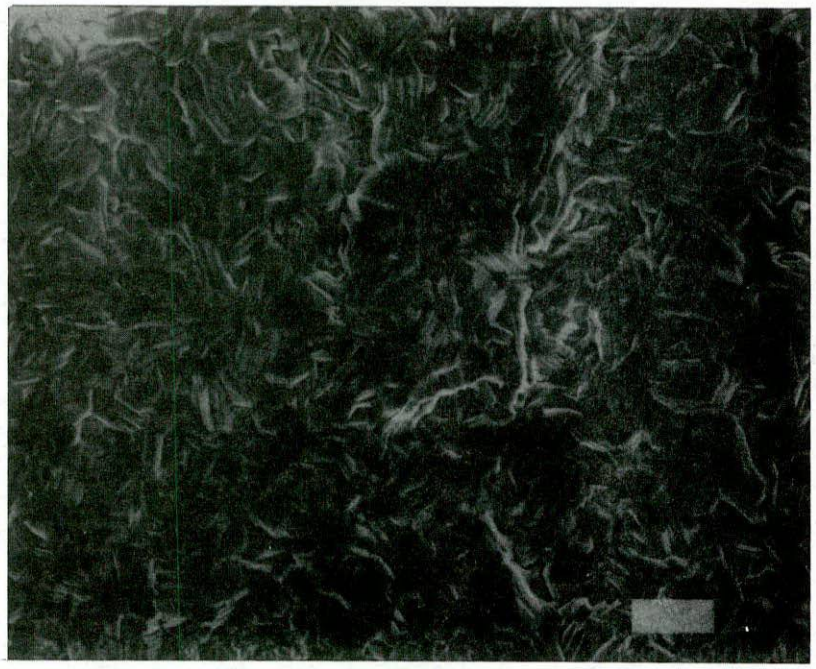

Figure 1. Zinc deposit from addition-free synthetic electrolyte, 1000x.

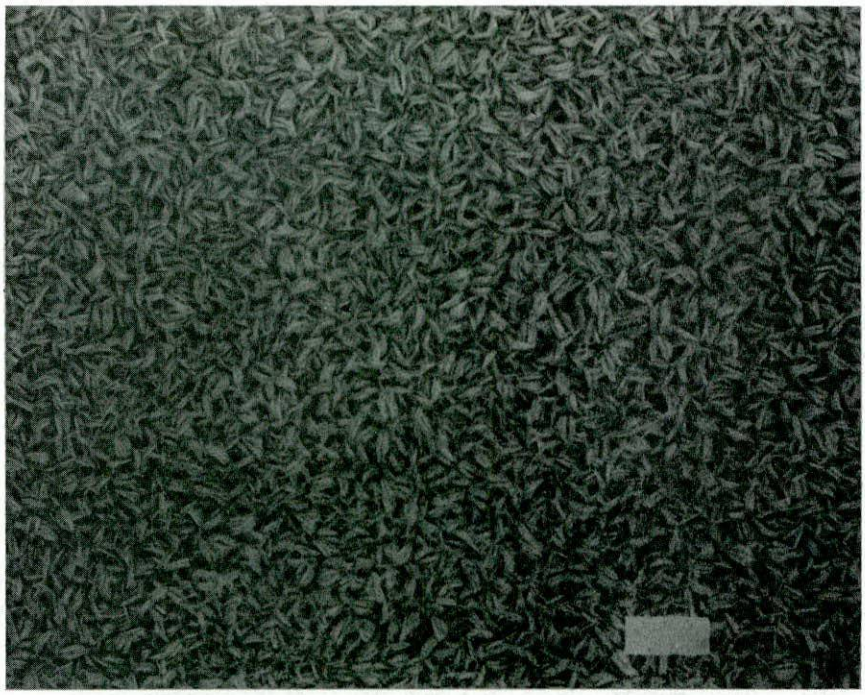

Figure 2. Zinc deposit from addition-free industrial electrolyte, 1000x.

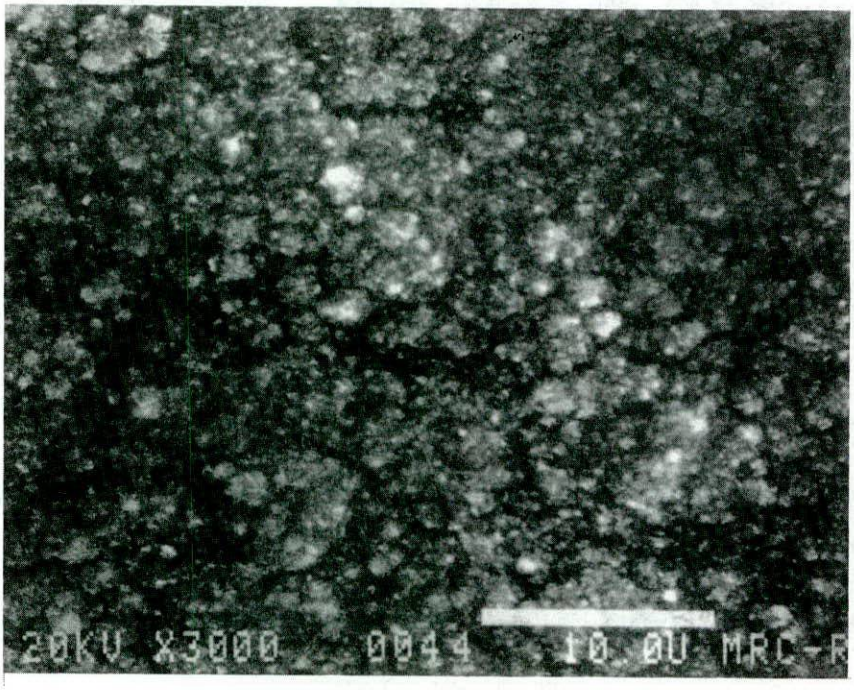


Figure 3. Zinc deposit from synthetic electrolyte containing 0.3% Surfactant I, 3000x.

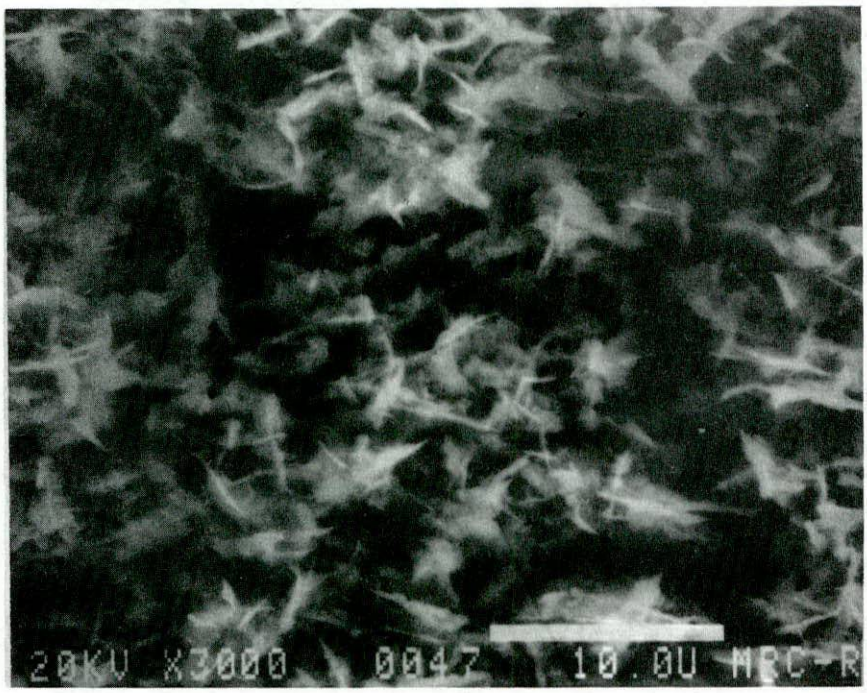


Figure 4. Zinc deposit from synthetic electrolyte containing 0.3% Surfactant II, 3000x.

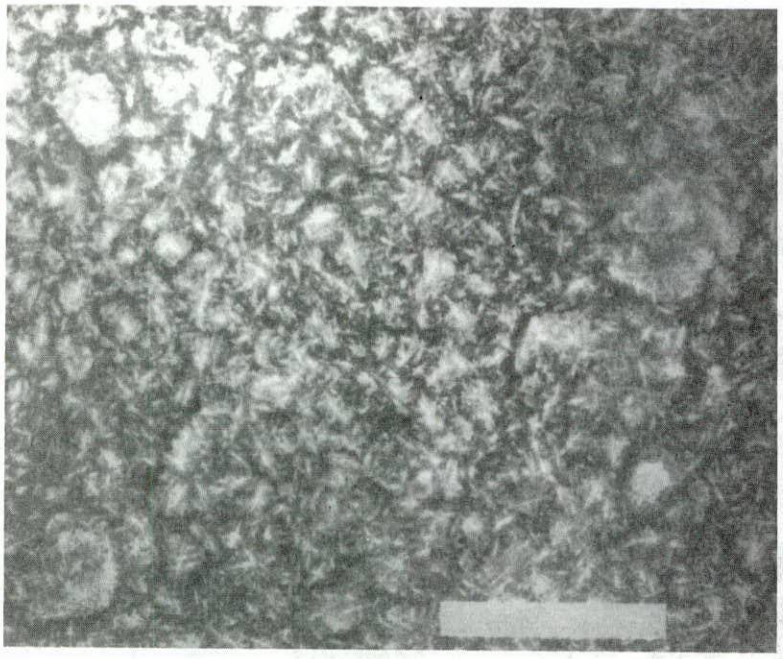

Figure 5. Zinc deposit from synthetic electrolyte containing 0.3% Surfactant III, 2000x.

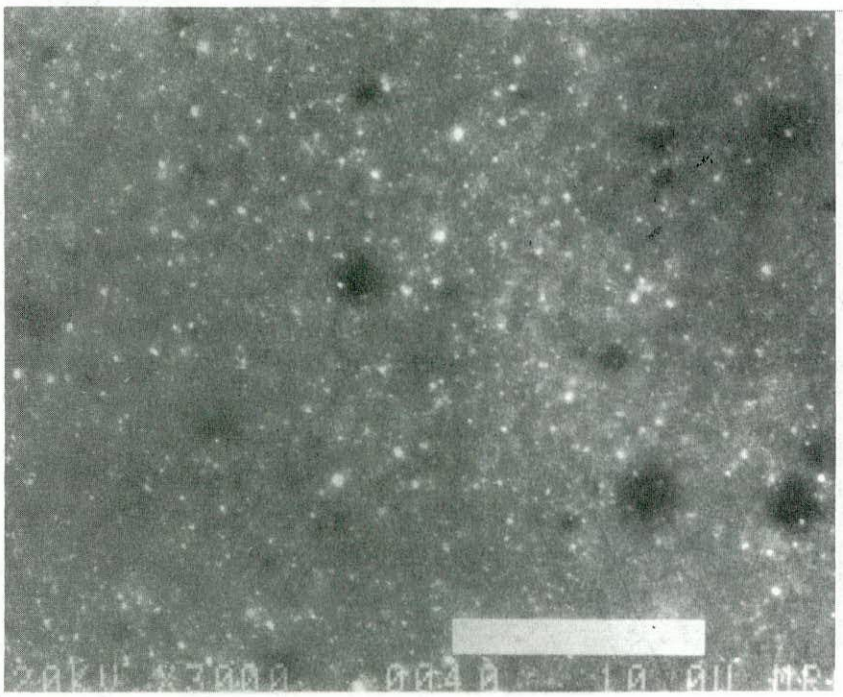

Figure 6. Zinc deposit from synthetic electrolyte containing 1.5% Surfactant III and 0.15% commercial brightener, 3000x.

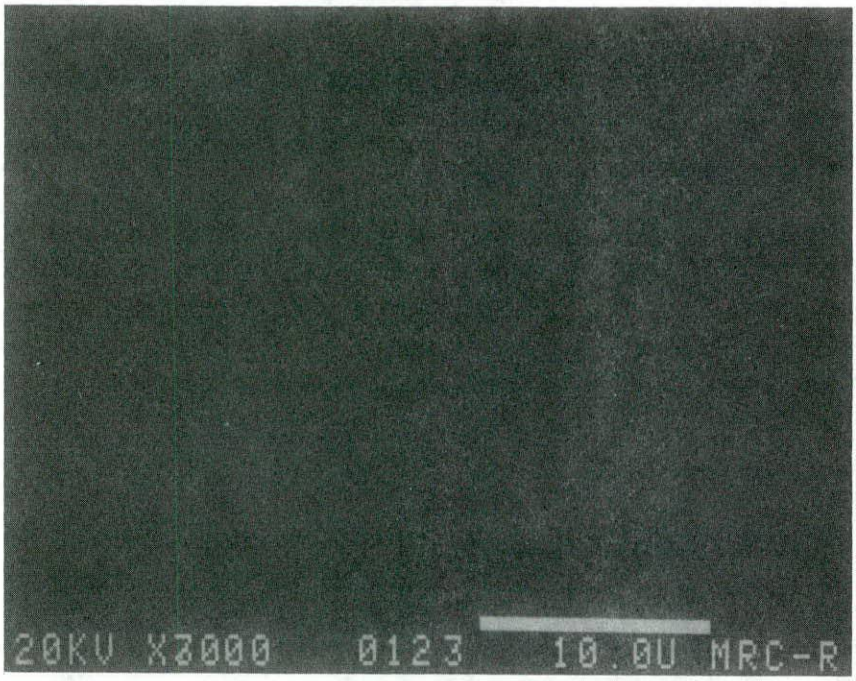


Figure 7. Zinc deposit from synthetic electrolyte containing 1.5% Surfactant III and 0.15% commercial brightener at 500 rpm stirring, 3000x.

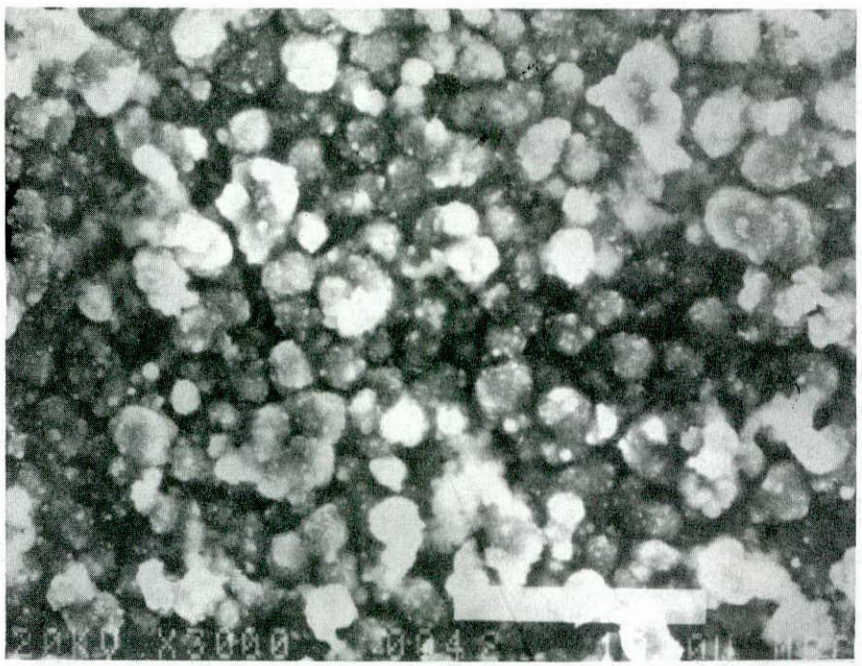

Figure 8. Zinc deposit from synthetic electrolyte containing 0.3% Surfactant III and 0.3% commercial brightener, 3000x.

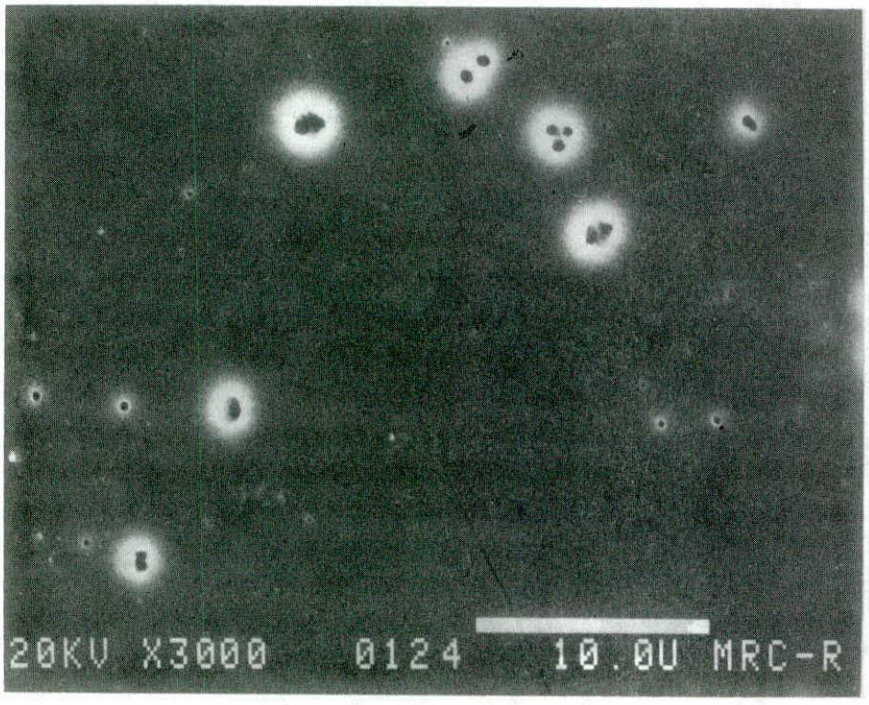


Figure 9. Zinc deposit from synthetic electrolyte containing 1.5% Surfactant III and 0.15% commercial electrolyte at 500 rpm stirring, 3000x.

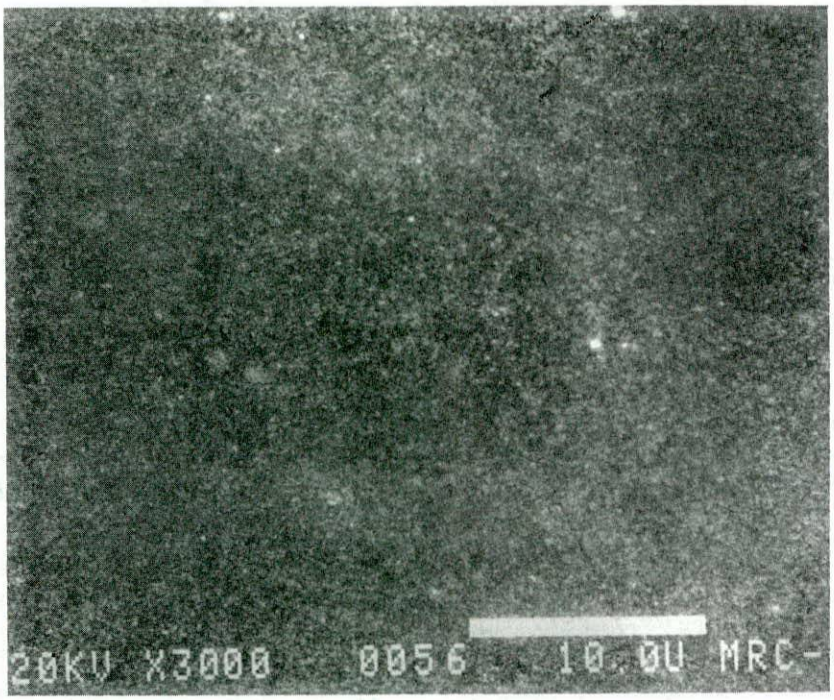


Figure 10. Zinc deposit from synthetic electrolyte containing 0.3% Surfactant I and 15 ppm ortho-chlorobenzaldehyde, 3000x.

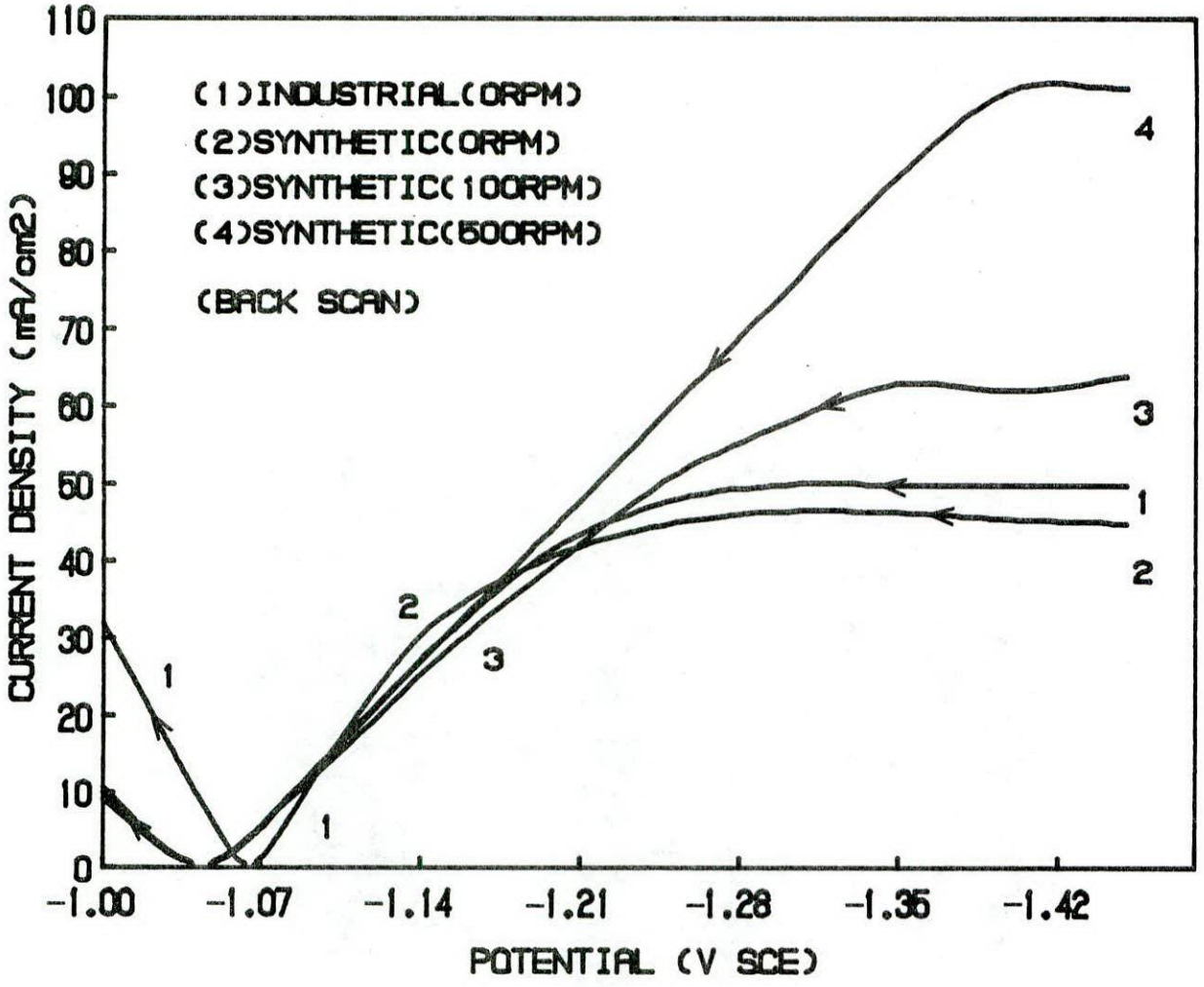


Figure 11. Polarization curves (back scan) of addition-free industrial and synthetic electrolytes with and without agitation.

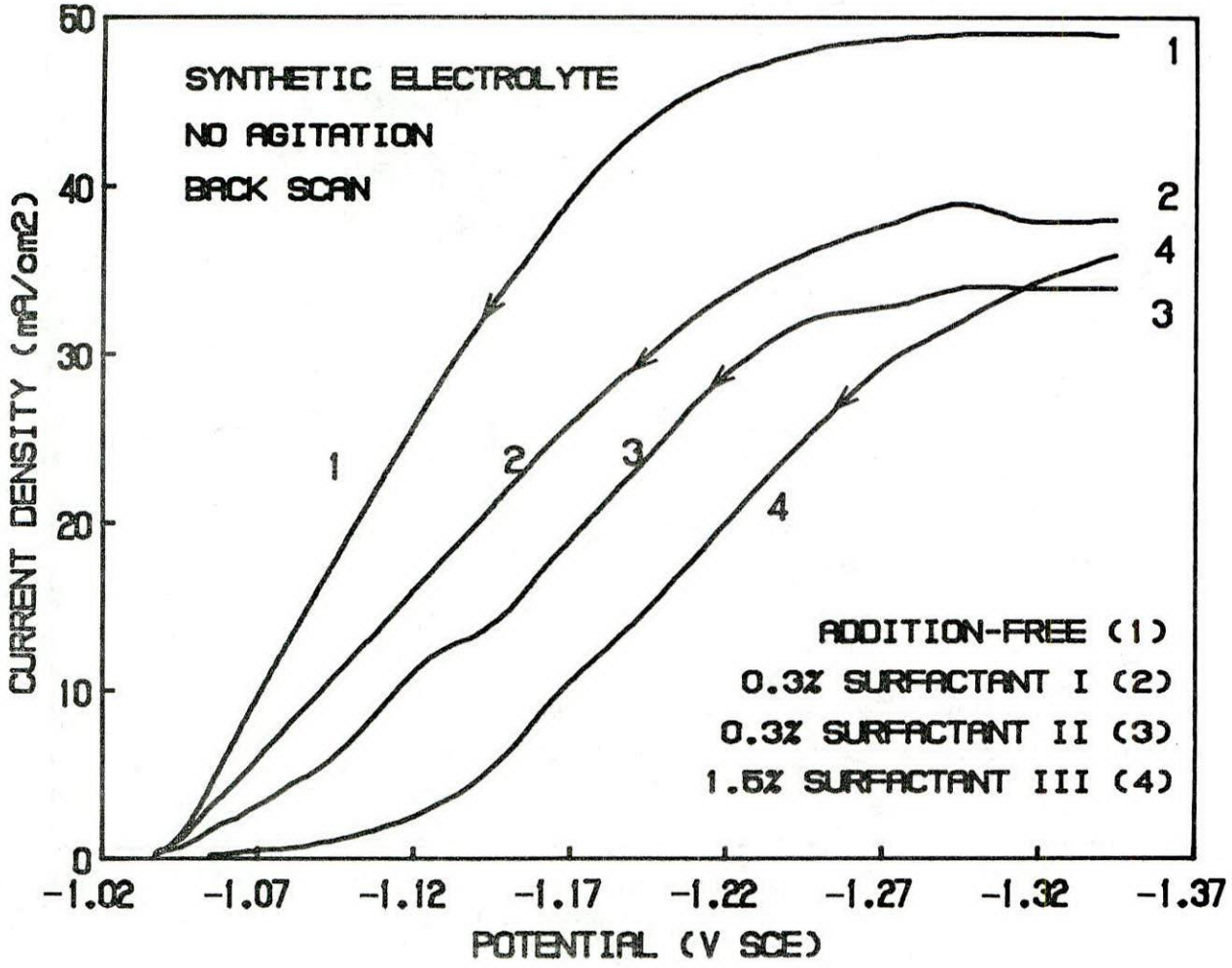


Figure 12. Polarization curves (back scan) for synthetic electrolyte containing different surfactants.

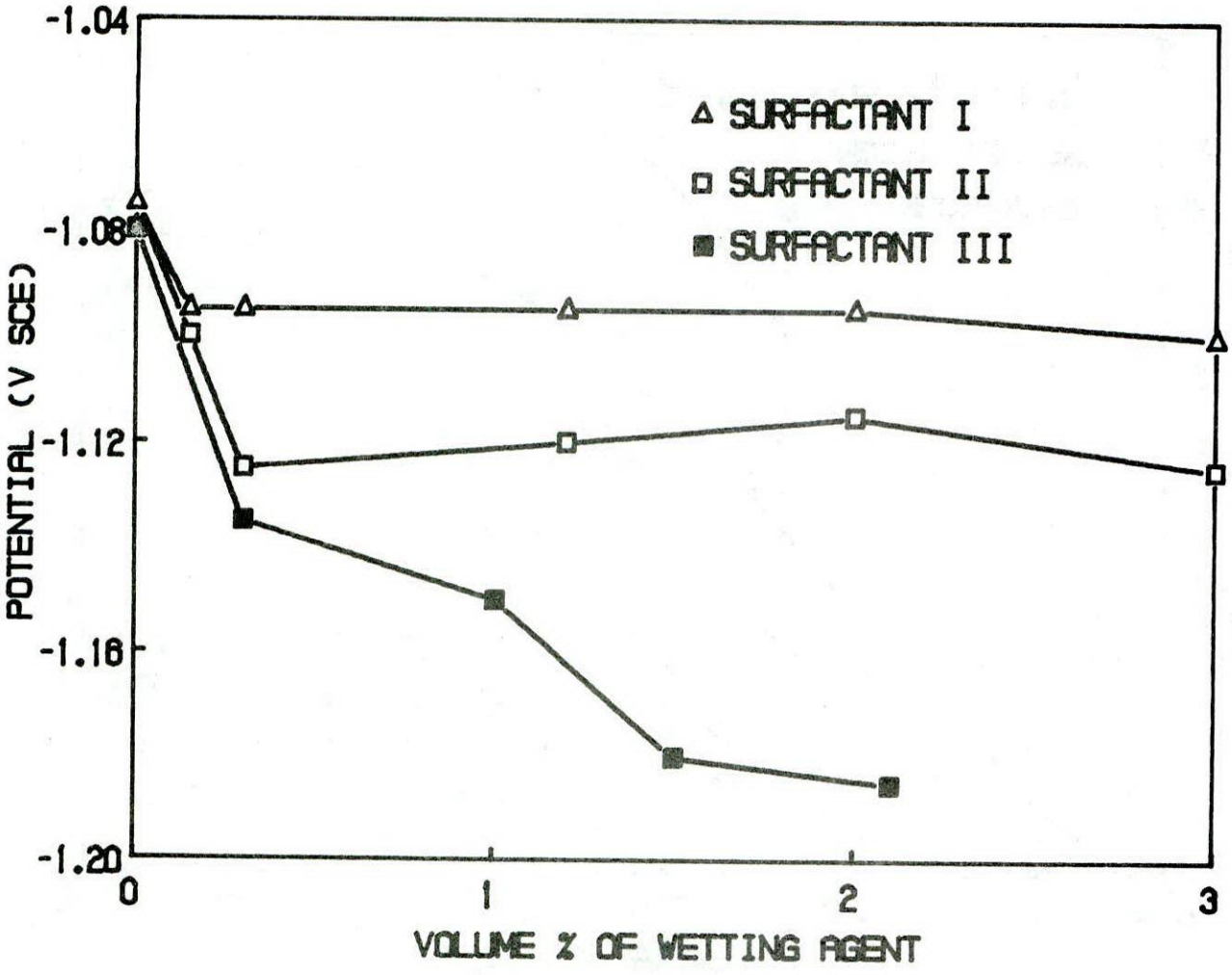


Figure 13. Overpotentials at 10 mA/cm$^2$ resulting from various concentrations of surfactants in synthetic electrolyte.

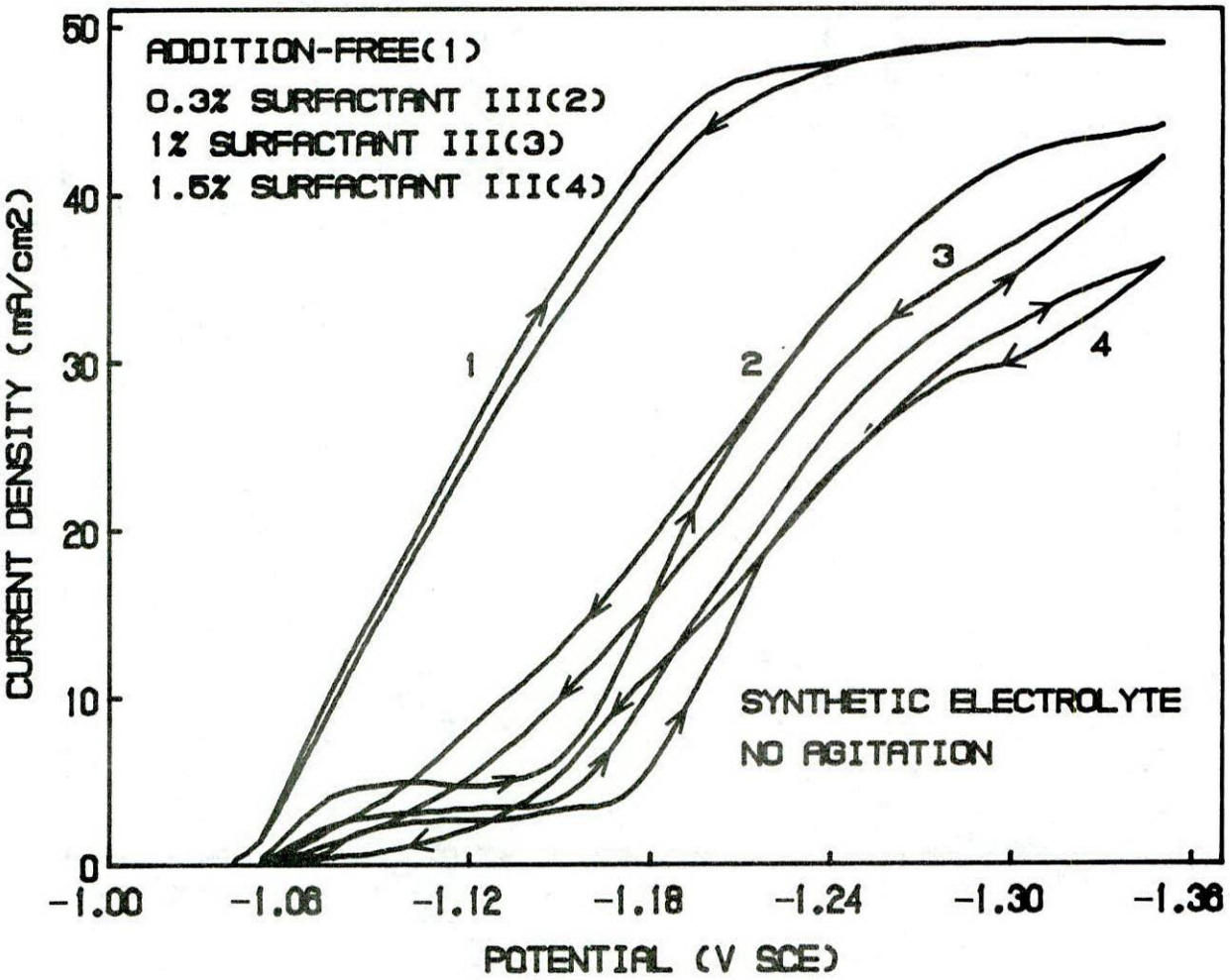


Figure 14. Polarization effects of different concentrations of Surfactant III in synthetic electrolyte.

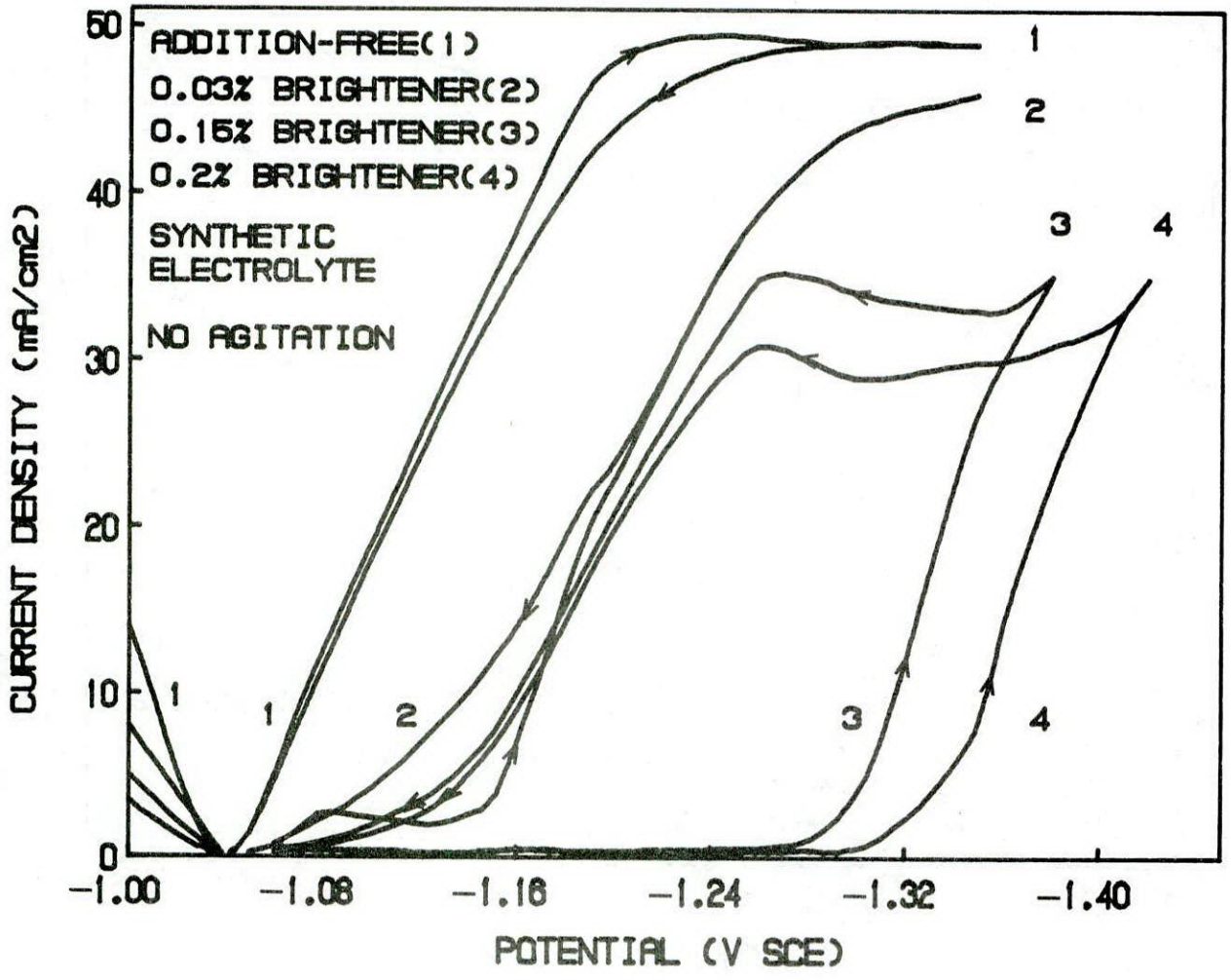


Figure 15. Polarization effects of 0.3% Surfactant III with varying concentrations of commercial brightener in synthetic electrolyte.

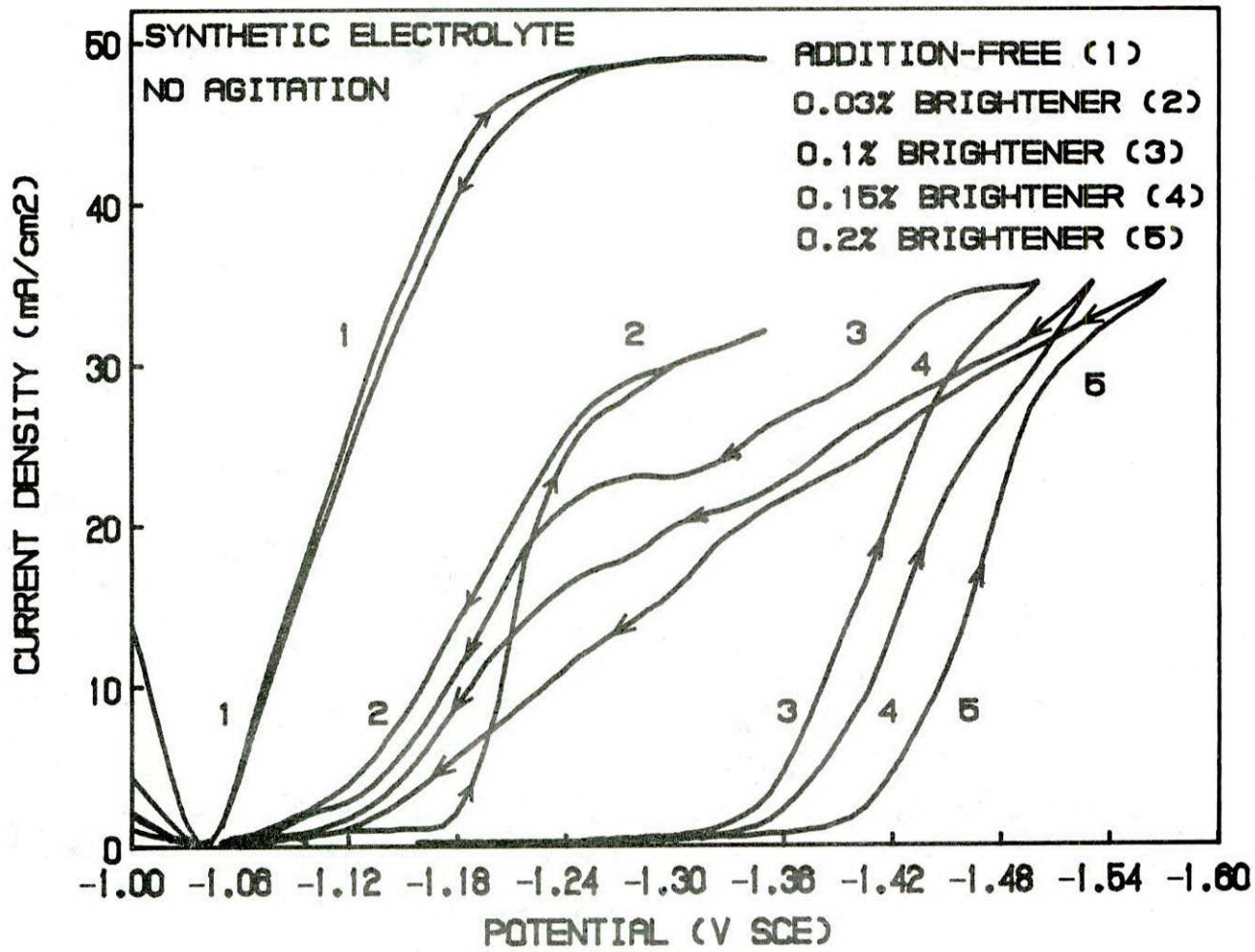


Figure 16. Polarization effects of 1.5% Surfactant III with varying concentrations of commercial brightener in synthetic electrolyte.

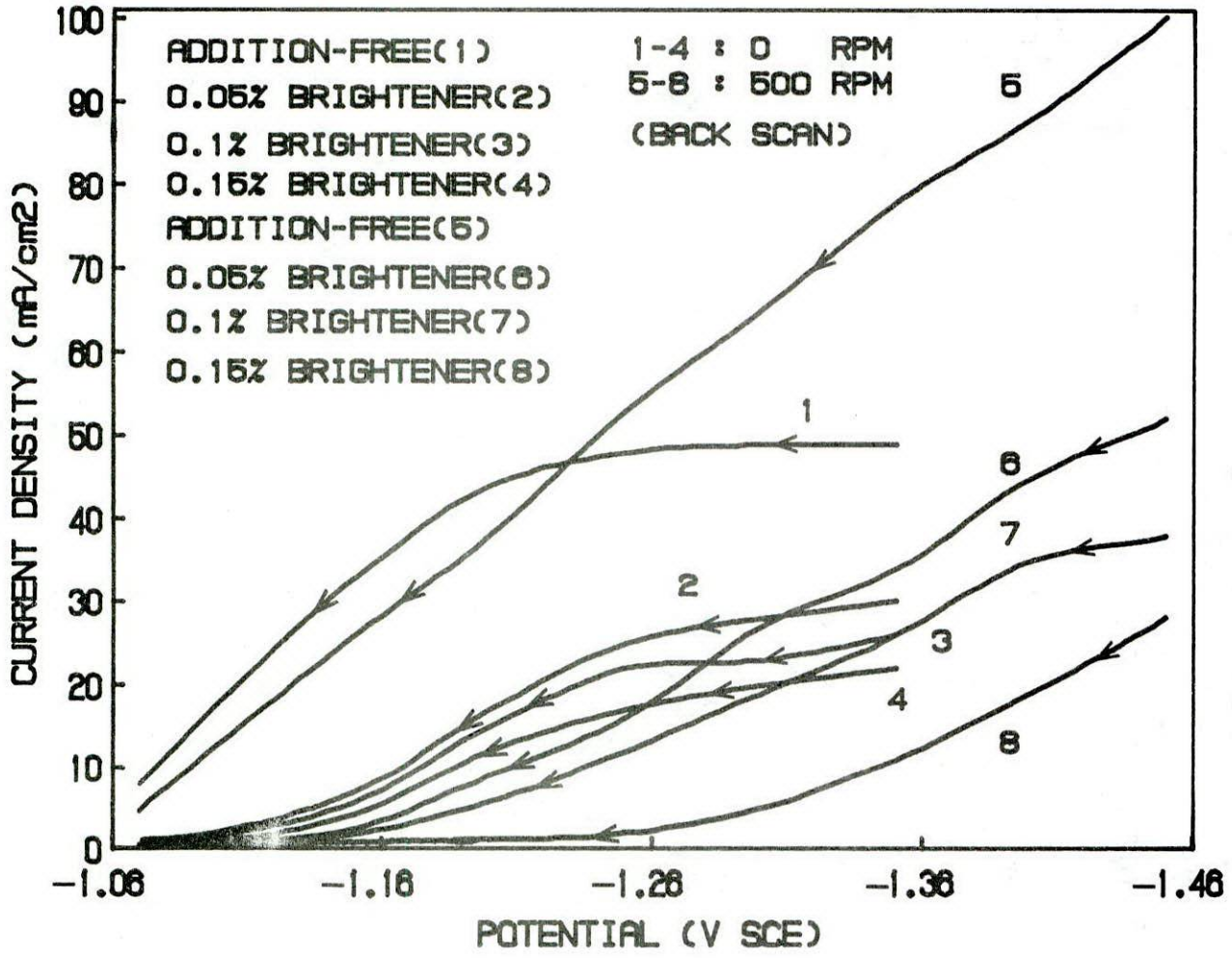


Figure 17. Comparison of polarization effects in the back scan region by 1.5% Surfactant III with varying concentrations of commercial brightener in synthetic electrolyte with and without agitation.

B-6

# Research Session B

## Addition-Agent Effects in Functional Chromium Deposits

N.M. Martyak
M&T Chemicals, Plating Division
Rahway, NJ 07065

R. Weil
Stevens Institute of Technology
Hoboken, NJ 07030

# ADDITION-AGENT EFFECTS IN FUNCTIONAL CHROMIUM DEPOSITS

N. M. Martyak
M&T Chemicals, Plating Division, Rahway, NJ 07065

R. Weil
Stevens Institute of Technology, Hoboken, NJ 07030

## INTRODUCTION

Additives are intentionally included in plating solutions for a variety of purposes. They can reduce the grain size by impeding growth. A small grain size is a necessary condition for brightness. A fine grain size is also associated with greater hardness and higher strength. Other additives can result in a better distribution of the grain-refining additive so that growth is inhibited uniformly over the entire deposit surface. Non-uniform growth inhibition leads to crevices which causes loss of brightness, decreased strength and ductility. Addition agents can affect the internal stresses. Exfoliation or cracking of the deposit may be prevented if tensile stresses are decreased or changed to compressive ones. Also, increasing tensile stresses can result in a greater density of the cracks which are characteristic of functional chromium electrodeposits. If additives result in the formation of compounds which are stable at elevated temperatures, they can impede grain-boundary movement and thereby better retain the hardness after annealing.

Brightness, hardness and its retention after heating and the crack patterns which result from internal stress are important properties of chromium electrodeposits. Therefore the effects of certain additives in the plating solution on these properties is of interest and is the topic of this paper.

## EXPERIMENTAL PROCEDURES

The compositions of the four plating solutions used in this investigation are listed in Table 1. Chromium from the four plating solutions was deposited at a current density of 0.5A/cm$^2$ at 55° C on non-hardened steel drill rods. The preplating procedure consisted of degreasing, anodic cleaning in a strong alkaline medium, and anodic etching in the plating solution for 15 sec. The thickness of the deposits from the three additive-containing solutions (i.e., Plating Solutions 2, 3 and 4) was about 100 $\mu$m. The thickness obtained from Solution 1 was about 50 $\mu$m. Chromium was also deposited on flat steel coupons which were subjected to the same preplating procedure as the drill rods.

Table 1

Composition of Plating Solutions

| | Plating Solution 1 | Plating Solution 2 | Plating Solution 3 | Plating Solution 4 |
|---|---|---|---|---|
| $CrO_3$ | 2.5M | 2.5M | 2.5M | 2.5M |
| $SO_4^{--}$ | 0.025M | 0.014M | 0.023M | 0.023M |
| $SiF_6^{--}$ | ---- | 0.025M | ---- | ---- |
| Catalyst A * | ---- | ---- | 0.543M | 0.543M |
| Additive B(1) | ---- | ---- | ---- | 0.001M |
| Additive C(2) | ---- | ---- | ---- | 0.133M |

* organo-sulfur compound

Chromium films about 100 nm thick were deposited on electropolished copper foils. The preplating procedure was the same as in a previous investigation(3).

Plated drill rods and flat coupons were annealed in air at 350°, 500° and 850°C for 2 hours. Slices were cut from the as-plated and annealed drill rods and metallographically polished. The hardness of the cross sections of the chromium electrodeposits were measured using a Knoop indenter in a Tukon Hardness Tester and a 100g load. The surfaces of the drill rods were anodically etched in a 2.5M sodium hydroxide solution at 1 A/cm$^2$ for 1 minute at room temperature in order to develop the crack pattern. The number of cracks per linear cm was determined with an optical microscope. The surfaces of the flat coupons were examined by scanning electron microscopy. The thin chromium films were examined by transmission electron microscopy as previously described(3).

## Results and Discussion

The structure of the surfaces of the deposits on the steel coupons, except for the one from the Solution 3 in Table 1, was too fine to resolve by scanning electron microscopy. The sur-

face of the deposit from Solution 3 is shown in Figure 1. Regions surrounded by relatively deep crevices are seen. The surface structure of the deposit from Solution 3 resulted in a matte appearance while that of the other three caused them to be bright. A non-uniform outgrowth from Solution 3 was already apparent in the 100 nm-thick film. Figure 2, which represents the structure of this film, shows some regions which are darker than the rest. Some of these are designated by arrows. The darker regions grew to a greater thickness. It is likely that these faster growing regions also spread laterally. The slower growth between them then resulted in the crevices seen in Figure 1. The thin films from the other three plating solutions exhibited a more uniform outgrowth as can be seen in Figures 3-5. In Figure 3, slightly taller particles can be seen to have grown on a grain boundary in the copper substrate. These particles are also indicated by an arrow. The same phenomenon was observed in the other films, but is not shown in Figues 4 and 5. The extremely fine grain size of all the chromium deposits was resolved by transmission electron microscopy. The smallest, individual black dots, which can be best seen in Figure 5, are the grains. Their size is less than 10 nm.

The likely cause of the crevices seen in Figure 1 is a non-uniform distribution of co-deposited sulfur from Catalyst A. A similar phenomenon was observed by Weil and Jacobus(4) in nickel deposits. When only the sulfur-containing, so-called control agent(5), was present in the plating solution, crevices formed where it was concentrated and preferentially inhibited growth. When the brightener(5) was also present in Solution 4, the deposit was specularly bright as no crevices had formed. Edwards and Levett(6) found that the brightener provides sites where the control agent can adsorb and thus lead to a uniform distribution of the control agent over the surface of the deposit. Apparently, the other additives in Solution 4 acted in a similar manner to cause a uniform inhibition of outgrowth.

The crack densities of the as-plated deposits from the four solutions are listed in Table 2. It is clear that the additives increased the number of cracks compared to the number in the deposit from Solution 1. It is probable that the additives increased the internal tensile stresses. These stresses will be measured and the results should be available when this paper is presented. The larger crack density in the deposit plated from Solution 3 was probably a result of the crevices, which would act as stress raisers.

The hardness values are also listed in Table 2. It is again apparent that the additives increased the hardness. The mechanism of the hardness increase remains to be elucidated.

Table 2

| Solution No. | Cracks/cm | Hardness ($KHN_{100}$) as-plated | 350° C | 500° C | 850° C |
|---|---|---|---|---|---|
| 1 | 315 | 950 | 700 | 675 | 325 |
| 2 | 475 | 1150 | 950 | 875 | 450 |
| 3 | 700 | 1300 | 1450 | 1500 | 600 |
| 4 | 475 | 1400 | 1450 | 1525 | 650 |

The decrease in hardness on annealing at the temperatures specified can also be seen in Table 2. It appears that the organo-sulfur additive resulted in better hardness retention. A possible cause could be that compounds formed during annealing inhibited the growth of grains. Grain growth typically results in a lower hardness. This phenomenon will also be investigated further.

In summary, it is seen that addition agents can significantly affect the brightness, hardness, retained hardness, and stress in chromium deposits.

REFERENCES


1. M. Perakh, H. Ginsburg, E. Salomon, V. Shargorodsky, and L. Rubinstein, US Patent No. 4,234,396 (1980).

2. N. M. Martyak, US Patent Pending (1988).

3. K. Raghunathan and R. Weil, Surface Technology, 10, 331 (1980).

4. R. Weil and W. N. Jacobus, Jr., Plating, 53, 102 (1966).

5. A. H. DuRose, Trans. Inst. Metal Finish., 38, 27 (1961).

6. J. Edwards and M. J. Levett, ibid, 44, 27 (1966).

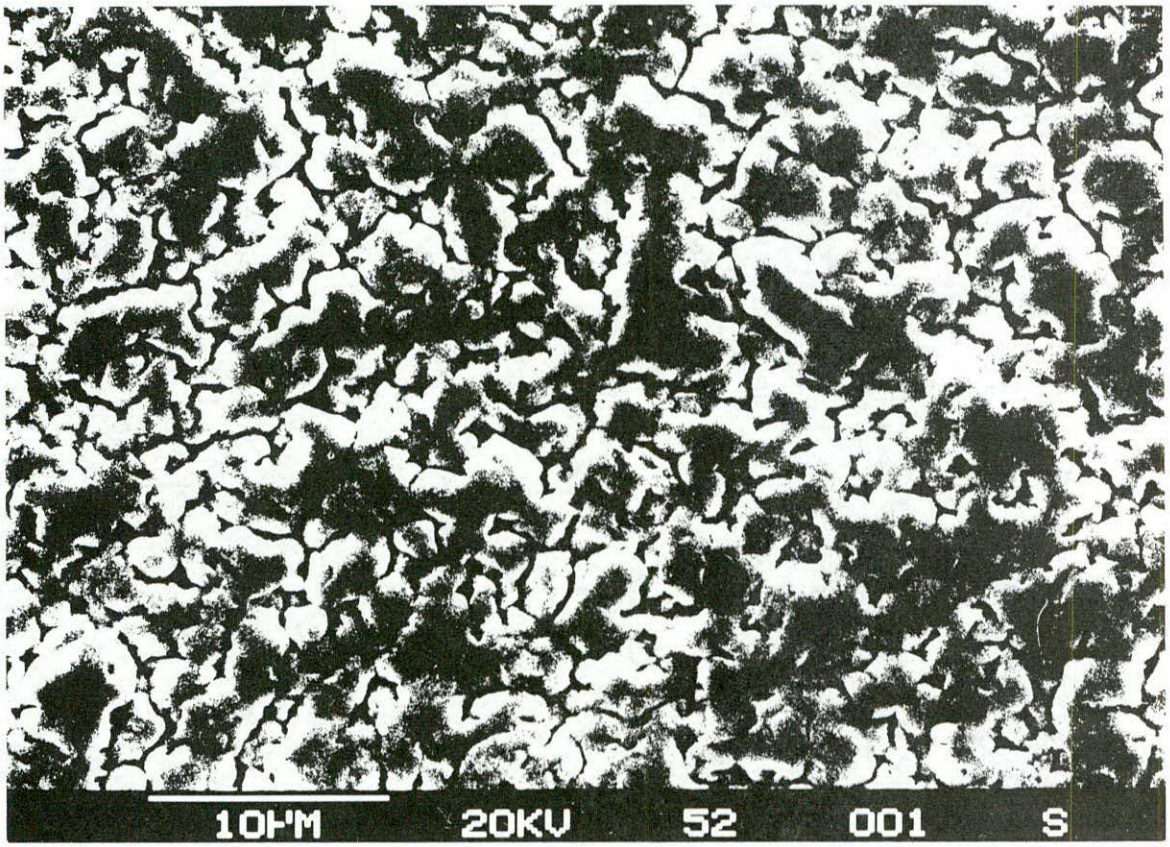


Figure 1. Scanning Electron Micrograph of Deposit from Solution 3

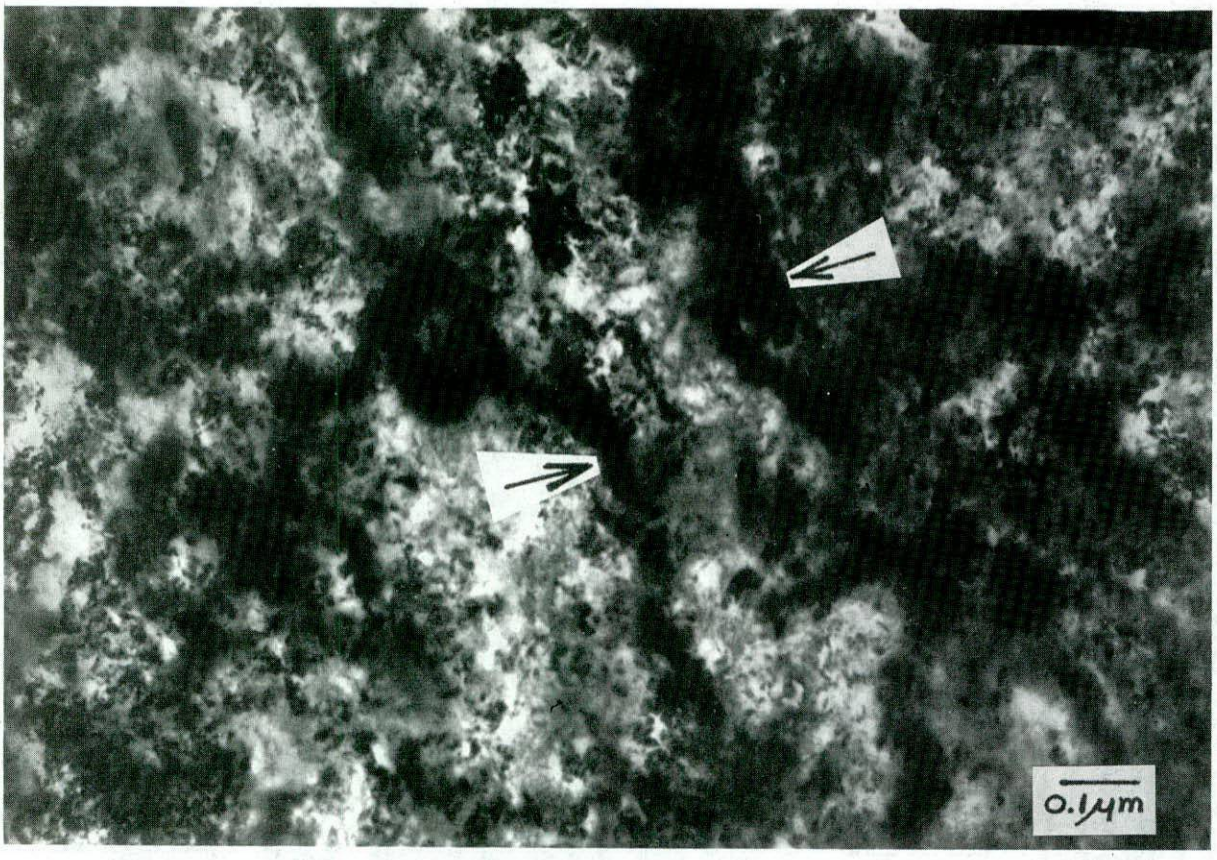


Figure 2. Transmission Electron Micrograph (TEM)
of Deposit from Solution 3.
Arrows indicate faster-growing regions.

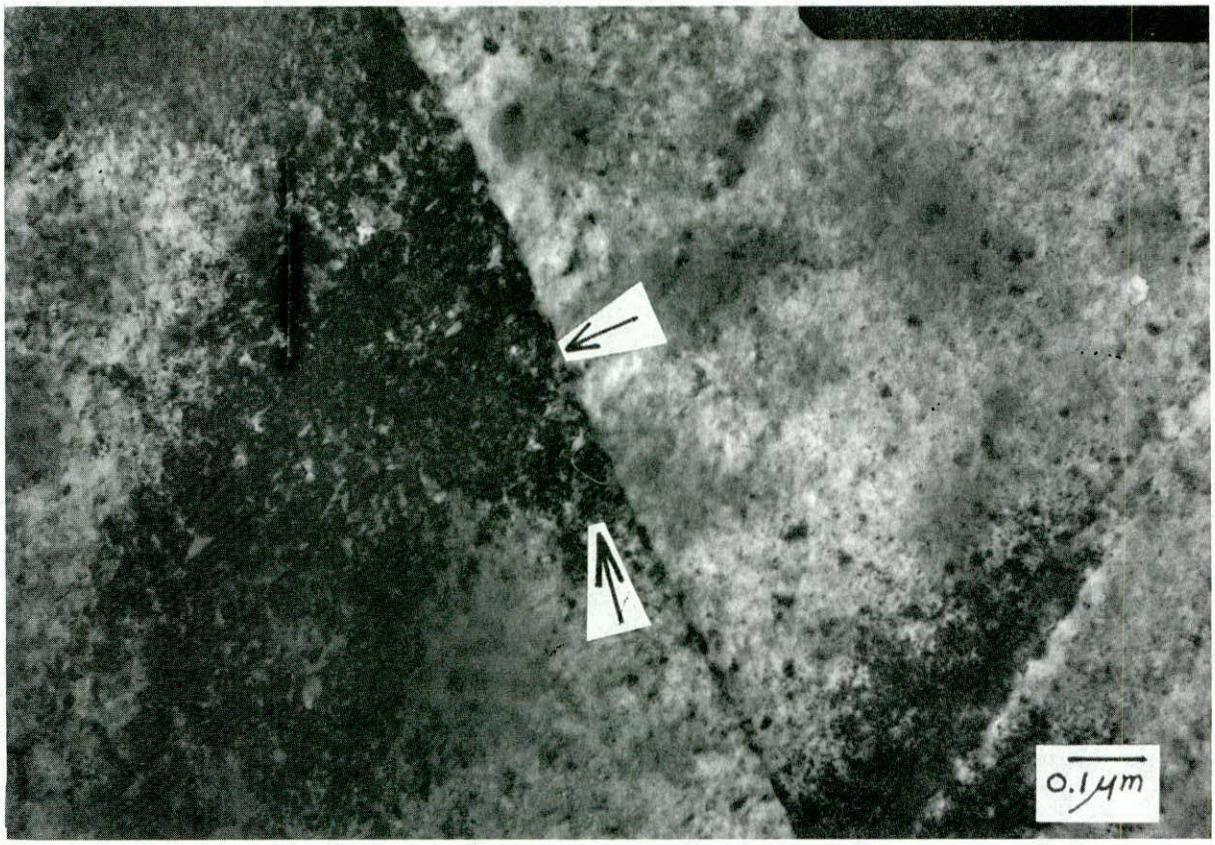


Figure 3. TEM of Deposit from Solution 1. Arrows shows larger particles at substrate grain boundary.

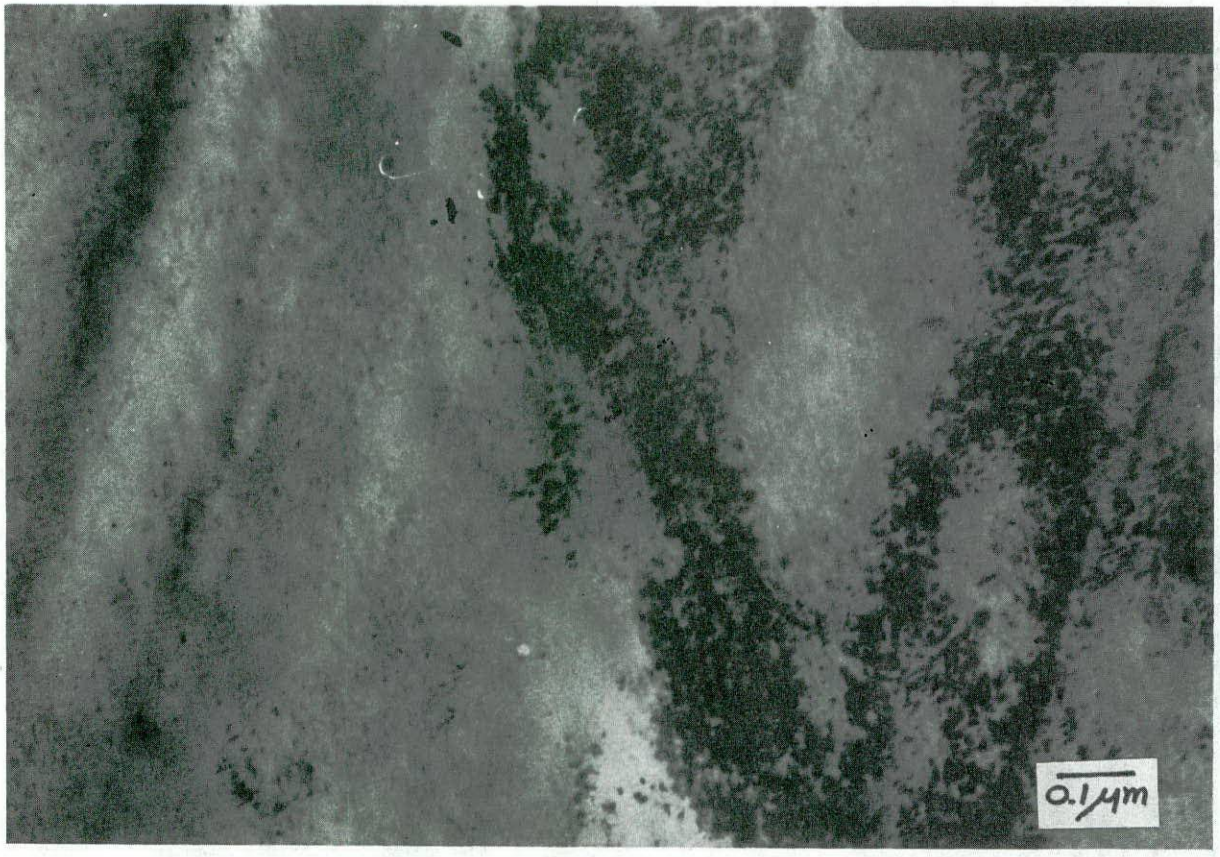


Figure 4. TEM of Deposit from Solution 2.

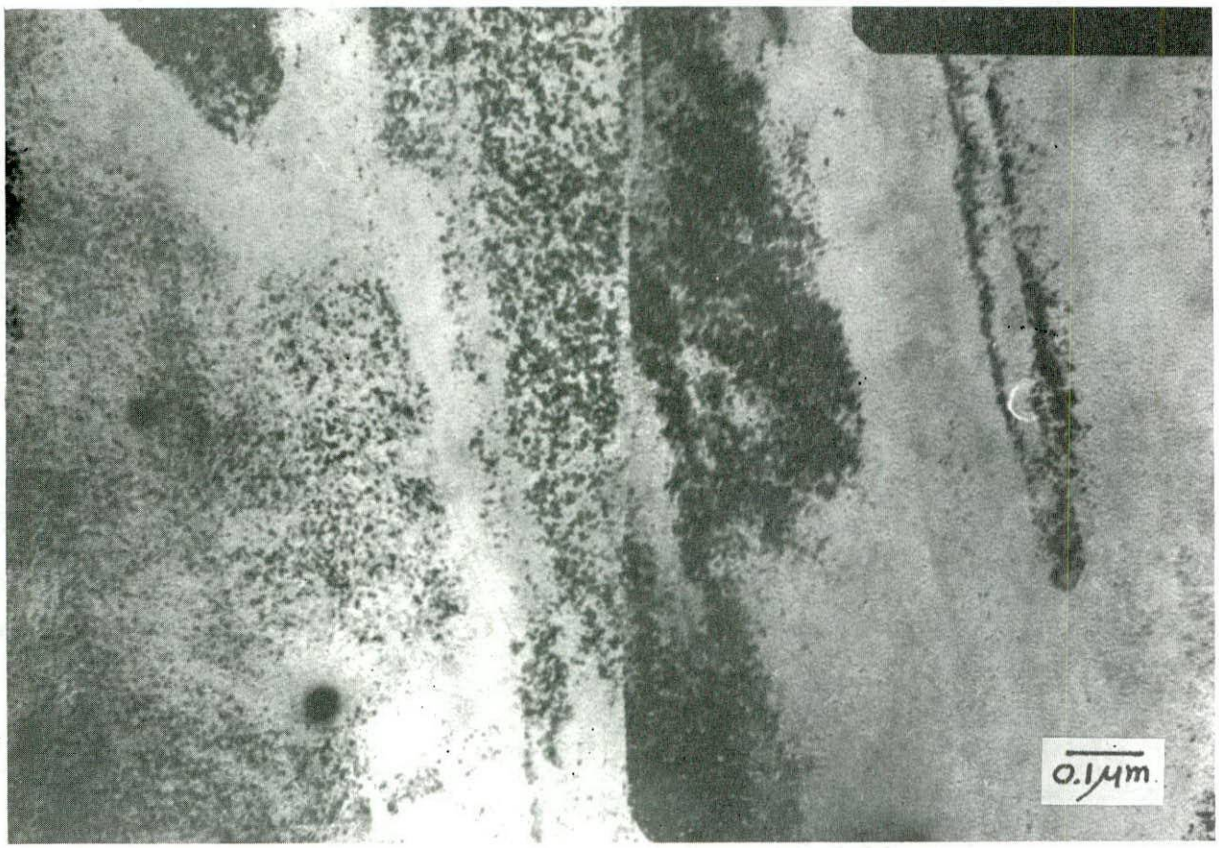


Figure 5. TEM of Deposit from Solution 4.

C-1

# Electronics I
# Session C

## Nickel Phosphorus Alloy as a Low Cost Electrical Contact Material

C.A. Holden, H.H. Law,
C.A. Mattoe and J. Sapjeta
AT&T Bell Laboratories
Murray Hill, NJ 07974

# Nickel Phosphorus Alloy as a Low Cost Electrical Contact Material

*C. A. Holden*
*H. H. Law*
*C. A. Mattoe*
*J. Sapjeta*

AT&T Bell Laboratories
Murray Hill, New Jersey 07974

*ABSTRACT*

Since a 40 year life is no longer an overall criterion for all electrical contacts, there has been a relaxation in electrical requirements in some project designs which allows contact resistance ($R_c$) values up to 50 mΩ. This is a range over which non-precious metal deposits may be effective as replacement coatings. One promising candidate is the nickel phosphorus alloy (Ni/P).

A neutral pH ammoniacal plating bath has been developed that produces low phosphorus content gray colored Ni/P deposits that have favorably low $R_c$ (2-7 mΩ) after exposure to several accelerated tests. The internal stress of the Ni/P deposit is comparable to that of the typical hard gold plate used on plug-in type electrical connectors. The ductility of the Ni/P deposit is less than either pure nickel or hard gold. Preliminary wear results show that lubricated Ni/P deposits appear to perform well for nearly 100 wear cycles. A flash of gold (≤5 μin) improves its wear resistance by at least an order of magnitude.

Although this low $R_c$ gray Ni/P alloy has been successfully plated in the laboratory, it is necessary to demonstrate conclusively that this Ni/P bath can withstand the rigors of everyday use that an industrial bath incurs. With appropriate nickel anodes, the neutral pH ammoniacal Ni/P plating bath can be operated continuously to deposit the Ni/P alloy at >95% cathode efficiency. With only minimal maintenance, the bath continues to function effectively for at least 35 bath turnovers. The current investigation also indicates that the bath chemistry is rather complex and that all of the constitutents are required for proper operation. Based on its adaptability to a flow cell operation, this Ni/P plating bath is a good candidate for use in a production strip-plating machine.

## *1. Introduction*

Precious metals, such as gold and palladium, have been and will continue to be the premier electrical contact materials for low voltage operations in critical areas where interruptions of service cannot be tolerated or where access to initiate repair of faulty connectors is impractical. However, there are many non-critical areas where a 40 year life is no longer an overall design criterion. Thus in some project designs, there has been a relaxation in electrical requirements which allows contact resistance ($R_c$) values up to 50 mΩ. This is an area where non-precious metal deposits may be able to replace gold.

One candidate is the nickel phosphorus alloy (Ni/P). A survey of the literature pertaining to the electrodeposition of Ni/P alloys shows that most of the work has been with low pH acid systems. There exists little information pertaining to ammoniacal systems. This is perhaps due

to the fact that the low pH baths produced electroplated deposits having a broad range of P contents, while the ammoniacal baths yielded only deposits with the low P content.

Robbins et al. [1] reported that the Ni/P deposits with a P content of 3-8 a/o, plated from a low pH bath, have favorable $R_c$ values. This finding supports the present approach of considering low P content Ni/P deposits as contact materials. The Ni/P deposits from the low pH bath and from the neutral bath are likely to be very different.

The purpose of this work is to report that low P content Ni/P deposits plated from a neutral pH ammoniacal bath are a promising contact material for replacing gold in some applications. This is demonstrated by the $R_c$ data obtained after accelerated environmental tests and the stress, ductility, and wear resistance properties of the Ni/P deposits. Although this low $R_c$ gray Ni/P alloy has been successfully plated in the laboratory, it is necessary to demonstrate conclusively that this Ni/P bath can withstand the rigors of everyday use that an industrial bath incurs. Since the bath chemistry of this neutral ammoniacal Ni/P solution is not simple, to obtain optimum performance it is necessary to determine the operating parameters such as solution flow rate, type of nickel anode, and pH range and to monitor the concentrations of bath constituents, which include nickel, chloride and phosphite ions. It was decided that a flow cell operation would be the best choice for generating high bath turnover, and a flow cell arrangement that simulates a strip plating machine operation was employed.

## 2. *Experimental*

Contact resistance was measured at a 50 gram load, which was applied using a converted microhardness tester [2]. A pure gold wire (0.02 inch diameter) makes contact at the prescribed load with the test sample, and the $R_c$ is measured using a four wire instrument whose open circuit voltages were low enough (<20 millivolts) to prevent electrical breakdown of any film that might be present on the test sample.

Internal stress was obtained with a modified SEL-REX IS meter based on the principle of measuring the deformation of a thin plane specimen plated on both sides. The detail is described

elsewhere [3]. Ductility was measured with a method of Nakahara et al. [4]. The thickness of all deposits was 2.5 microns. The annealed copper foil substrate was 50 microns thick and has a ductility of about 8% elongation.

In the wear testing, the Ni/P plated wires (80 mil diameter) were mounted on the apparatus with their axes at right angles. The setup has been described elsewhere [5]. The top wire is held rigid while the bottom wire moves back and forth at a 45° angle so that the wear products are pushed to the sides of the wear track instead of piling up at the ends. The load (0-1500 g) can be varied by applying pressure to the lower wire through a balanced beam arrangement and a load of 200 g was used in the present study.

The bath composition during operation of the flow cell (Fig. 1) that simulates a strip plating machine operation was monitored extensively. Plating bath samples were prepared by taking one ml of bath, adding one ml of ammonium hydroxide to prevent precipitation on standing, and diluting to a final volume of 50 ml. These samples were then analyzed for nickel, chloride, and phosphite. The concentration of nickel was determined by atomic absorption spectrophotometry using a calibration curve. The concentrations of chloride and phosphite were determined by ion chromatography using Dionex HPIC-AG3 and HPIC-AS3 columns with an anion suppressor and conductivity detection. Plating bath samples were diluted 1:10 before injection. With 1 mM sodium carbonate as eluent and a flow rate of 1.8 ml/min, chloride and phosphite showed retention times of approximately 5 and 20 minutes, respectively. Concentrations were determined by running a daily calibration curve for each ion, with an error of about 5%.

## *3. Results and Discussion*

### *3.1 Contact Resistance*

A typical Hull cell panel from the Ni/P bath is shown in Fig. 2A. The good deposit is the light gray deposit at the lower current density (C.D.) region. The $R_c$ is much lower than that of the bright area (higher C.D.). The Hull cell pattern is opposite to that obtained from a typical Watts nickel plating bath without any $H_3PO_3$. Figure 2B shows the latter pattern, which is

common in electrodeposition: matte and bright deposits in the lower C.D. region (0-80 mA/cm$^2$) and gray deposits in higher C.D.(>80 mA/cm$^2$). However, the gray deposits are not the same. After an exposure to 50°C and 95% relative humidity (R.H.) for 86 hours, the $R_c$ of the gray-colored Watts nickel deposit at 100 mA/cm$^2$ (Fig. 2B) was 100 mΩ, compared to the $R_c$ of 5 mΩ for the gray Ni/P deposit at 60 mA/cm$^2$ (Fig. 2A). This clearly established the difference in $R_c$ between the pure nickel deposit and the Ni/P alloy.

A longer exposure period to the warm humid environment showed similar $R_c$ values. After 26 days the Ni/P deposit plated at a lower C.D. of 35 mA/cm$^2$ (gray area) has a $R_c$ of 2-2.4 mΩ, while the $R_c$ in the the high C.D. region (200 mA/cm$^2$) Ni/P deposit has a very high $R_c$ (20-4000 mΩ) similar to bare nickel (700-3800) after 9 days exposure to the same environment.

The $R_c$ of the gray Ni/P deposit also remained low when the deposit was exposed to other accelerated tests. After 90 days exposure to a dry heat of 205°C, the $R_c$ values of Ni/P deposits plated at C.D. of 25-50 mA/cm$^2$ were 3-7 mΩ. In another test the Ni/P deposits, bare nickel, and copper were subjected to moist sulfur vapor, generated from flowers of sulfur, at 50°C and 75% R.H. for 72 hours. As expected, the $R_c$ of the copper was that of an insulator, while the $R_c$ of three Ni/P deposits were 1.0-2.8 mΩ and the $R_c$ of bare nickel was of 60-2000 mΩ.

*3.2 Stress and Ductility*

The change of the internal stress with the deposit thickness of Ni/P plated at 35 mA/cm$^2$ is shown in Figure 3. When the deposit is more than 0.05 mil thick, the stress reaches a constant value of 25 kg/mm$^2$. The current density does not affect the stress. The stress of Ni/P deposits obtained at both 25 and 35 mA/cm$^2$ is 25 kg/mm$^2$. This is lower than the stress of 35 kg/mm$^2$ found with Ni deposited from a $NiCl_2$ bath (pH 4.8). The stress of the Ni/P is in the range of the reported values for nickel from a chloride bath (21-60 kg/mm$^2$) and for cobalt hardened gold (22-29 kg/mm$^2$) [6]. Thus the internal stress of the Ni/P should not cause any problem if the alloy is used as a contact material.

The ductility of Ni/P plated at different current densities is compared to that of the cobalt

hardened gold and to nickel plated from a $NiCl_2$ bath in Table I. Within the experimental accuracy, the ductility of Ni/P deposited at 25 and 35 $mA/cm^2$ is the same. The value is less than that found for both hard gold and nickel. This is expected because Brenner et al. [7] reported that Ni/P alloy with less than 2% P is strong and slightly ductile. Although no specific data were given, the deposits become more brittle as the phosphorus content was increased. It is clear that the Ni/P prepared with the present method is not appropriate for applications requiring ductile material. For such applications and the ones where lower stress is desirable, the use of an alternating current to plate the Ni/P should be considered. Kendrick [8] reported that nickel deposits obtained from an all-chloride solution have higher ductility and lower stress when the plating is performed at frequencies of 500 c/s with relatively large amounts of deplating during each cycle. The use of AC plating for depositing Ni/P is being explored.

*3.3 Wear Resistance*

The wear resistance of the gray Ni/P deposit was evaluated using a crossed wire wear test method [5] that simulates the wear that develops on plug-in type printed wiring boards. This wear testing method has been used since 1963 to evaluate gold plating from proprietary hard gold baths prior to their acceptance for connector use in by AT&T Technologies. After 100 cycles, the wear resistance of the lubricated Ni/P deposit was comparable to that of a typical hard gold plate. However, some type of organic lubrication, which is necessary for the initial wear-in of any material, including hard gold, appears to be limited in its effectiveness in preventing appreciable wear of the Ni/P deposit after 150-200 cycles with this wear apparatus. One method that is likely to provide excellent wear resistance (similar to hard gold) is to put a flash of gold ($\leq$5 μin) on the deposit. The gold will also act as a lubricant in the initial "break-in" during wear. A flash of gold over rhodium has been used as a lubricant since at least 1967 [5].

*3.4 Operation of Flow Cell*

In the first run, nickel sheet anodes (200 series Ni) were used and the desirable gray Ni/P deposit was obtained. However, the depletion of nickel from the solution was rapid, and within 1.5 bath turnovers the nickel concentration was about 80% of the initial value (Fig. 4). An

addition of nickel chloride brought the nickel concentration to the initial value and increased the chloride concentration by 4 g/L. The rate of nickel depletion remained the same. Thus, the anodic current efficiency is about 87% of the cathodic current efficiency (~92%). Over a longer period, it can be expected that an excessive amount of chloride will accumulate and subsequently imbalance the complex chemistry of the Ni/P bath. If the anodic current efficiency were not improved, the life of the plating bath would not be long enough for practical operation.

The reason for this nickel depletion was the passivation of the nickel anodes that initiated the formation of a heavy slimy green precipitate of nickel hydroxide. Although an increase in pH from 7.8 to 8.0-8.3 considerably reduced the precipitation on the anodes, the nickel concentration in the solution continued to be depleted, though at a slower rate. It appears that the anodic reaction consists of not only nickel dissolution but also oxygen evolution. Since hydronium ions are produced with oxygen, the pH at the anode surface would be in the range of 5-7, where the precipitation of nickel hydroxide would occur. Once the surface is coated with the nickel hydroxide, the anode, for all practical purposes, ceases to dissolve and the oxygen reaction dominates, resulting in a heavy precipitate. By increasing the pH to the range of 8-8.3, the oxygen evolution was slowed down, but not sufficiently to maintain constant nickel concentration. Thus it was reasonable to try the depolarized nickel anodes.

After confirming that the depletion of nickel still occurred in a new bath, the nickel concentration was brought to the initial value by adding nickel chloride, and sulfur-bearing depolarized anodes were substituted. It was found that the passivation that occurred on the original nickel anodes was prevented. However, when the pH was allowed to drift below pH 8 for an extended period of time, nickel hydroxide did appear, though to a lesser degree. Hence, the anodic efficiency of nickel dissolution using sulfur depolarized anodes was about the same as the cathodic current efficiency, i.e., the amount of nickel dissolved into the solution was the same as the amount plated out.

Over four months the same Ni/P bath was used with only minor additions of ammonium citrate, phosphorous acid, and ammonium chloride being made as necessary to compensate for the

normal dragout and to maintain bath chemistry. No further addition of nickel salts was made since the depolarized nickel anodes were dissolving sufficiently to maintain an adequate nickel concentration. The concentrations of nickel and phosphite were maintained to within 20% of the initial values, whereas the concentration of chloride was within 10%.

When the cathodic efficiency fell below 90%, analysis by ion chromatography showed that the chloride and phosphite ions were low, indicating a slight imbalance in bath chemistry. Although the citrate ion was, unfortunately, not clearly detected by our ion chromatography set-up, its concentration was assumed to be proportionately lower than its initial value. Small additions of phosphorous acid, ammonium citrate, and ammonium chloride were made with subsequent improvement in cathode efficiency. Of course, with these additions ammonium hydroxide was added to insure that the optimum complex chemistry existed and to maintain the pH at 8-8.3. Thus the cathodic current efficiency is a good indicator of whether the bath components are within the desirable range.

During these four months, there were approximately 35 bath turnovers with an average cathode efficiency >95%. The desirable gray colored Ni/P deposit, as determined by SEM micrographs and Auger electron spectroscopy, was consistently obtained.

*4. Conclusions*

A neutral pH ammoniacal plating bath has been developed that produces low phosphorus content gray nickel deposits that have favorably low $R_c$ (2-7 m$\Omega$) after exposure to several accelerated environmental conditions: a temperature of 50°C and 95% R.H. for one month, a dry temperature of 205°C for three months, and sulfur vapor at 50°C and 75% R.H. for 72 hours.

Stress, ductility and wear resistance of the Ni/P deposit have been evaluated. The stress of the Ni/P deposit is comparable to nickel from a chloride bath and to cobalt-hardened gold (used for wear). The ductility of the Ni/P deposit is less than that of nickel or hard gold. For applications where high ductility is desired, the use of an alternating current to plate the Ni/P should be considered.

Preliminary wear results show that lubricated Ni/P deposits appear to be limited to <100 wear cycles with this wear apparatus. A flash of gold (≤5 μin) appears to improve its wear resistance by at least an order of magnitude.

It has been demonstrated that, with sulfur bearing depolarized nickel anodes, the neutral pH ammoniacal Ni/P plating bath can be operated continuously to deposit a gray colored Ni/P alloy at >95% cathode efficiency. With only minimal maintenance, the bath still works perfectly after 35 bath turnovers, which is considered to be a good lifetime for a commercial bath. The current investigation also indicates that the bath chemistry is rather complex and that all of the constituents are required for proper operation. Based on its adaptability to a flow cell operation, this Ni/P plating bath is a good candidate for use in a production strip-plating machine.

## *5. Acknowledgment*

We wish to acknowledge our appreciation for the help from our colleagues: J. A. Abys and V. Lambrecht for the ductility measurements, and R. Opila for his analysis of the phosphorus content of the Ni/P deposits. We are also grateful to Mr. P. C. Milner for stimulating discussions.

*References*

[1] Robbins, M., and Plewes, J. T., Hauser, J. J., Haynes, R. and Ng, S.-L., *Plating and Surface Finishing, 74(3)*, 56 (1987).

[2] Baker, R. G. and Palumbo, T. A., *Plating and Surface Finishing, 69 (11)*, 66 (1982).

[3] Mattoe, C. A. and Palumbo, T. A., private communication, 1986.

[4] Nakahara, S., Okinaka, Y., and Turner, D. R. *Journal of Testing and Evaluation, 5*, 178, (1977).

[5] Holden, C. A., "Wear Study of Electroplated Coatings for Contacts", *Proceedings of the Engineering Seminar on Electrical Contact Phenomena*, November 6-9, 1967.

[6] Safranek, W. H., *The Properties of Electrodeposited Metals and Alloys*, American Elsevier Publishing Company, 1974.

[7] Brenner, A., *Electrodeposition of Alloys*, Vol. II, Academic Press, 1963, pp. 457-482.

[8] Kendrick, R. J. *Transactions of the Institute of Metal Finishing, 44*, 78 (1966).

Table I. Ductility of Electrodeposits

| Deposit | % Elongation |
|---|---|
| Ni (Ni Chloride bath) | 1.4 |
| Au (Co hardened) | 2.4 |
| Ni/P (25 $mA/cm^2$) | 0.3 |
| Ni/P (35 $mA/cm^2$) | 0.5 |

# FLOW CELL DESIGN

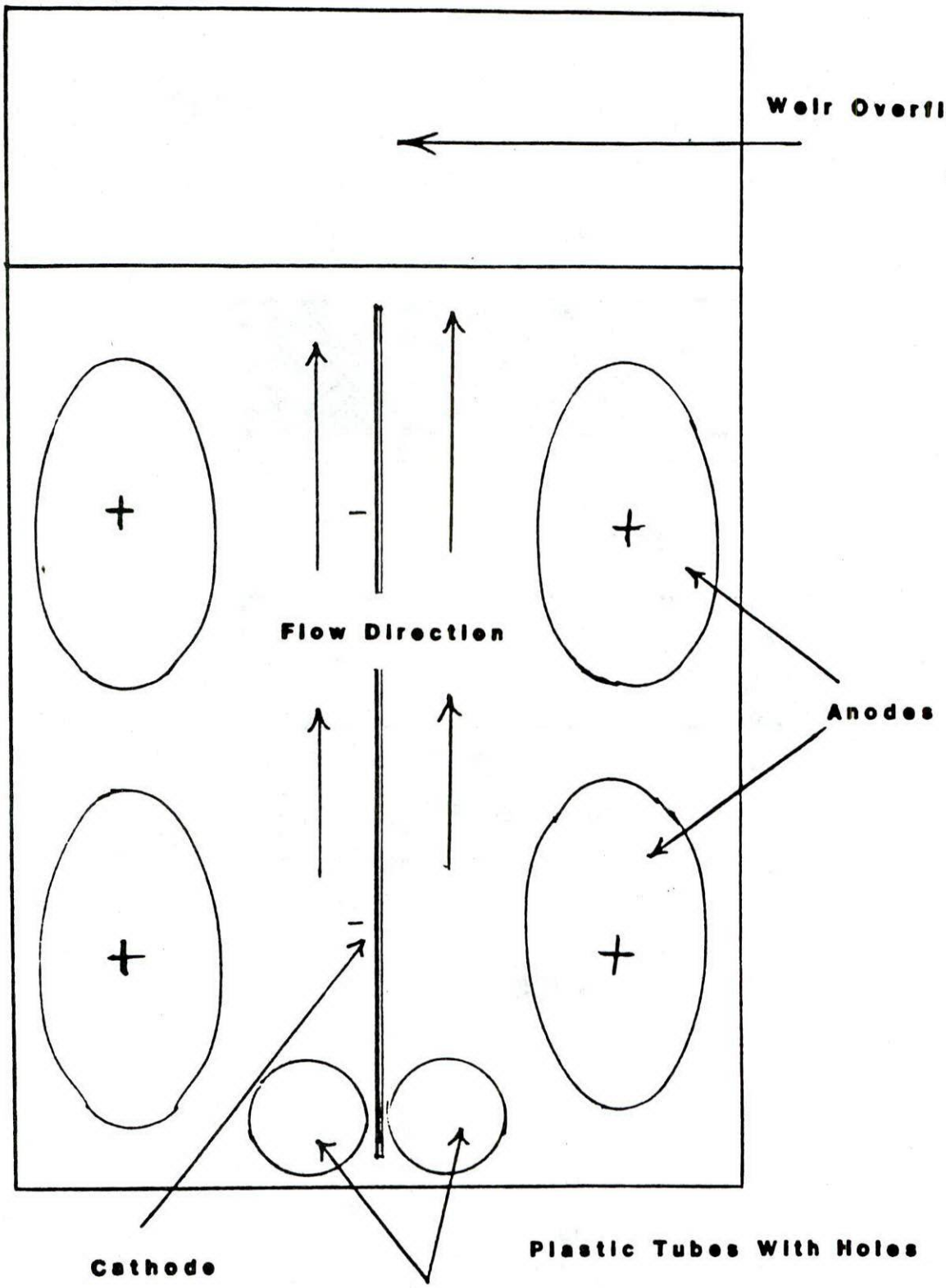


TOP VIEW OF THE PLATING FLOW CELL.

**FIGURE 1**

HULL CELL PANELS

Gray

Bright

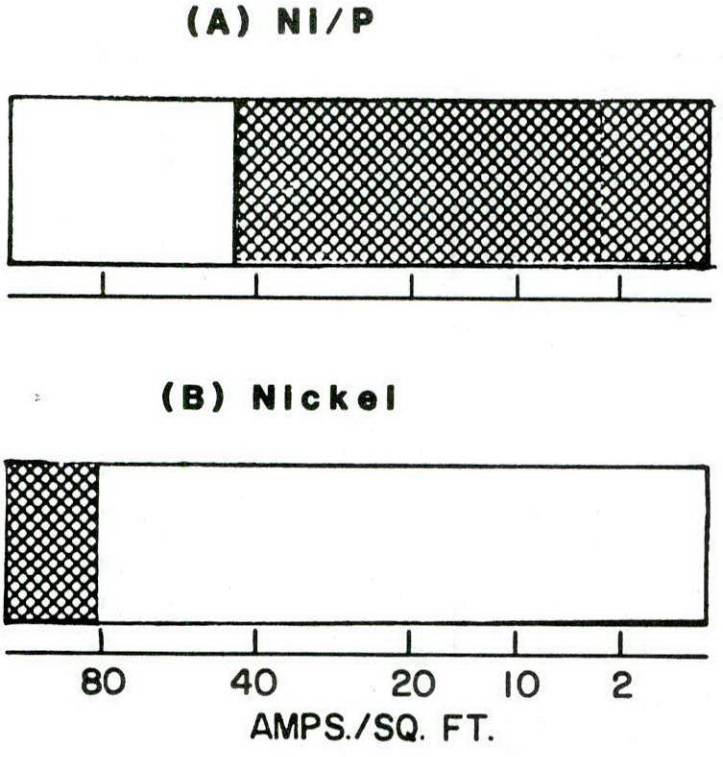


HULL CELL PANELS OF NI/P AND NICKEL DEPOSIT.

**Figure 2**

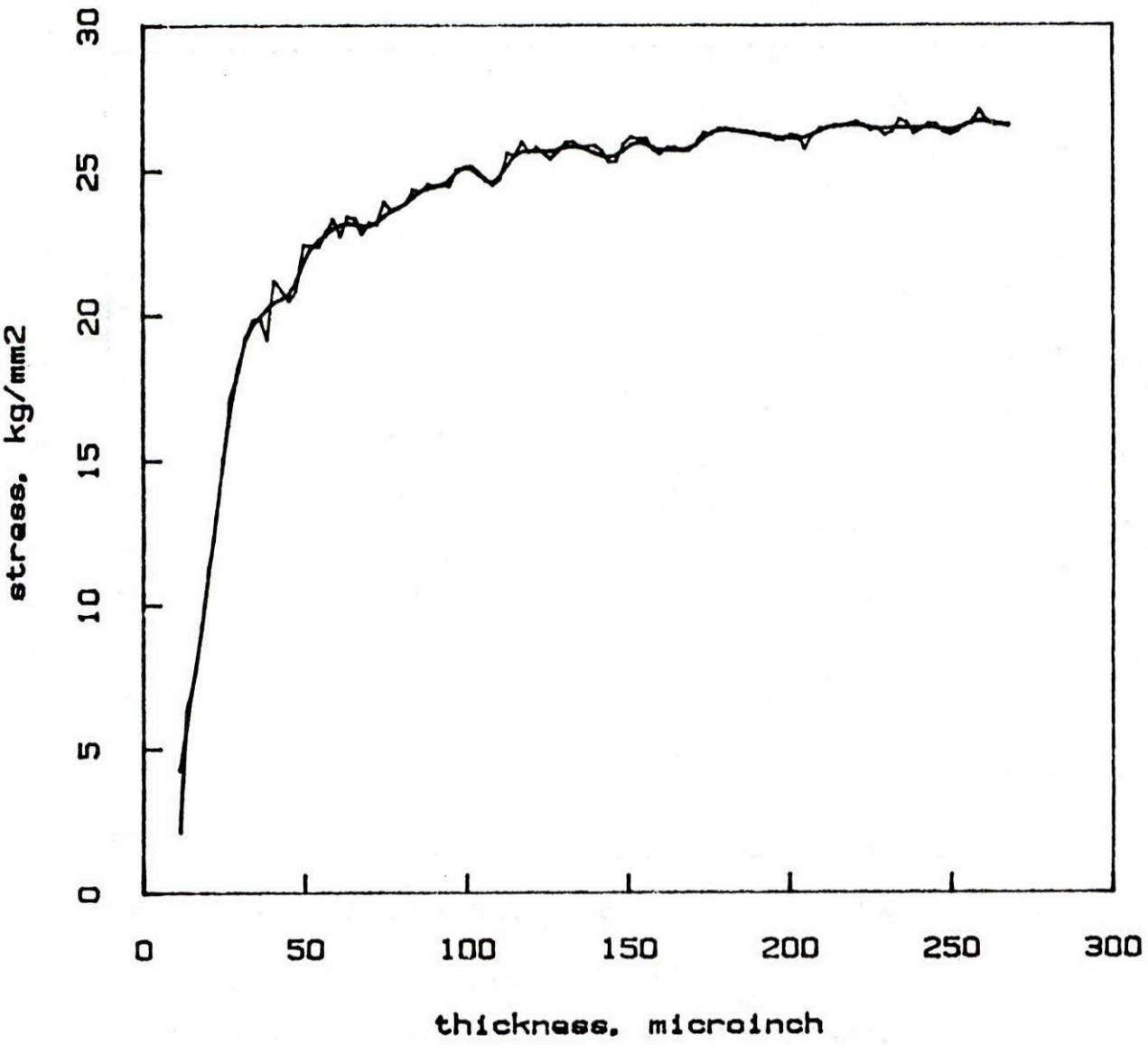


INTERNAL STRESS OF NI/P DEPOSIT VS. THICKNESS.

**Figure 3**

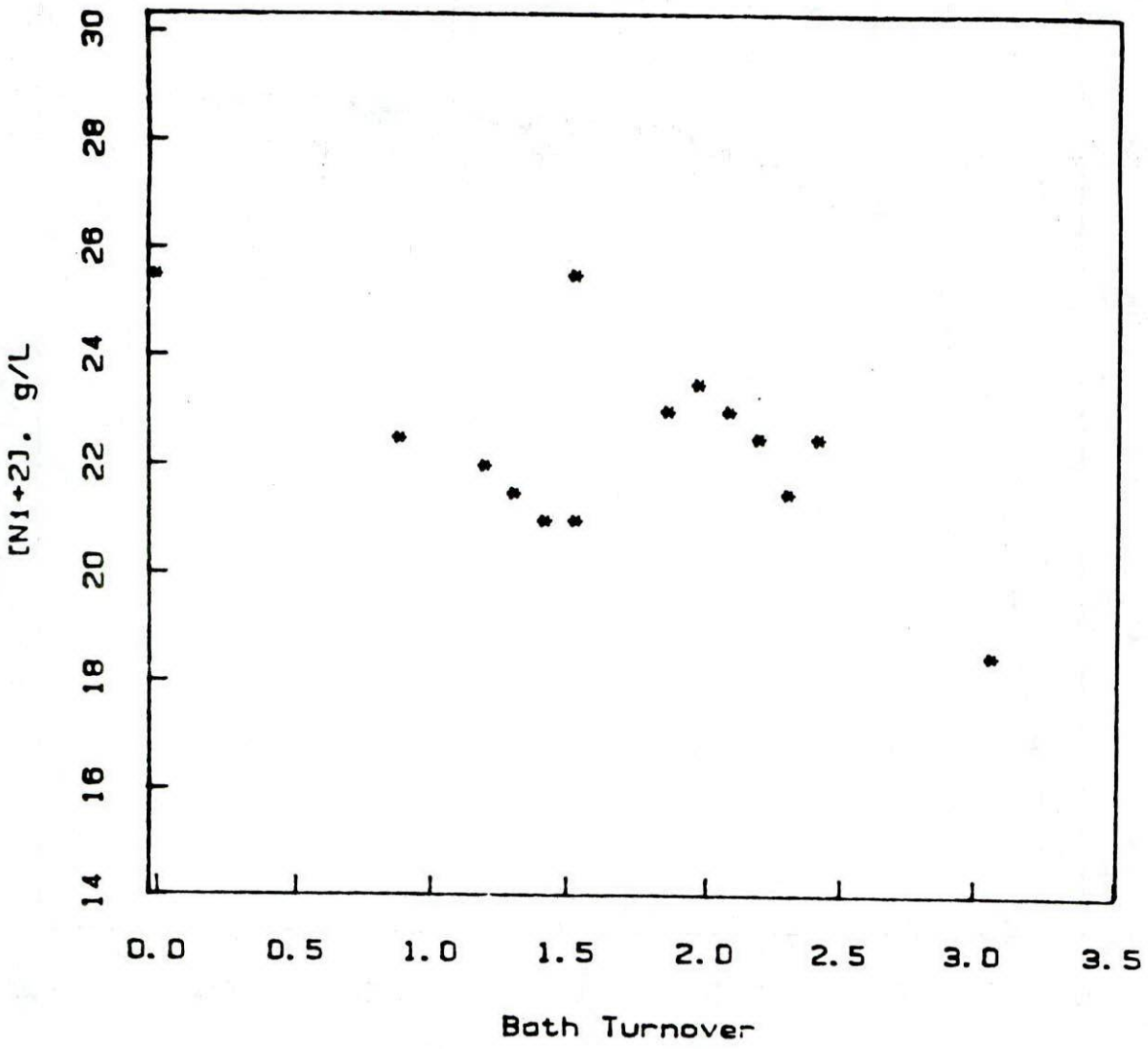


CONCENTRATION OF NICKEL VS. BATH TURNOVER SHOWING THE DEPLETION OF NICKEL FROM THE SOLUTION DUE TO ANODE PASSIVATION.

**Figure 4**

C-2

# Electronics I
# Session C

## Factors for Producing Low Contact Resistance Of Nickel Phosphorus Alloys

C.A. Holden, H.H. Law
and R.L. Opila
AT&T Bell Laboratories
Murray Hill, NJ 07974

# Factors for Producing Low Contact Resistance of Nickel Phosphorus Alloys

*C. A. Holden*
*H. H. Law*
*R. L. Opila*

AT&T Bell Laboratories
Murray Hill, New Jersey 07974

*ABSTRACT*

As more electronic products become disposable because it is cheaper to replace than to repair, the product life cycle becomes shorter and shorter and the need for a low cost electrical contact material for use in separable connectors in these products becomes greater. One promising candidate is a nickel phosphorus alloy (Ni/P) plated from a neutral ammoniacal bath. The objective of the present investigation was to determine the factors that produce the low contact resistance ($R_c$) because an understanding of these factors should define the reliability of this Ni/P coating.

The surface morphology of the gray colored Ni/P deposits appears to be the predominant factor in producing low $R_c$. The gray deposit consists of a multitudinous number of tightly spaced microscopic star-like asperities of relatively uniform height when viewed at a magnification of 2000X. This structure may assist in breaking through any oxide or other insulating film on the base metal deposit and in inhibiting the subsequent ingress of oxygen or other contaminants that would affect the intimate a-spot contacts provided by the protrusions. The presence of the phosphorus in the Ni/P deposit also seems to retard the oxidation rate to a level appreciably less than that typical of pure nickel.

## *1. Introduction*

As more electronic products become disposable because it is cheaper to replace than to repair, the product life cycle becomes shorter and shorter and the need for a low cost electrical contact material for use in separable connectors in these products becomes greater. Table I shows the current cost of three of the electroplated metals commonly used for separable connectors and the cost of nickel, which is relevant to this discussion. Gold is about four times more expensive than gold flashed palladium and about three hundred times more expensive than base metal finishes such as tin-lead. Although the cost of the noble metal may be only a small fraction of the total cost of a connector, these figures give a clear idea of the magnitude of the savings possible when a much lower cost contact material is substituted in high volume production.

Tin-lead solder plate, a common base metal finish, is recommended[1] for usage in benign environments and at moderate ambient temperature, when the number of insertions required is small, when life requirements are relatively short, and when reliability requirements are modest. In the case of connectors that mate with wiping contacts, the number of contacts per connector is

restricted to about 20-30 due to the high friction forces. Tin-lead solder plate is therefore quite limited in application, and a better base metal finish is desirable.

One candidate is a nickel phosphorus alloy (Ni/P) plated from a neutral ammoniacal bath[2]. Low (<2 atomic %) phosphorus content gray colored Ni/P deposits have favorably low contact resistance ($R_c$) (less than 10 mΩ) after exposure to several accelerated environmental tests. This $R_c$ is well below the relaxed electrical requirements in some project designs which allow $R_c$ values up to 50 mΩ. The engineering properties of the Ni/P coating further support its study as a promising low cost contact material.

The objective of the present investigation was to determine the factors that produce the low $R_c$ because an understanding of these factors should also define the reliability of this Ni/P coating. In order to understand the mechanism for low $R_c$, it is useful to review briefly electrical contact phenomena and the attributes that lead to low contact resistance.

## 2. *Electrical Contact Phenomenon*

When two stationary contacts come together, the ideal "welded" condition will give the lowest $R_c$. Since contact surfaces are microscopically rough, the ideal condition does not exist. The actual contact is provided by the asperities (a-spots) on both surfaces (Fig. 1). If a film is present, the contact resistance consists of the constriction resistances $R_1$ and $R_2$ in the two members, respectively, as well as the film resistance $R_f$. Thus

$$R_c = R_1 + R_2 + R_f$$

According to this definition,[3] the $R_c$ is a surplus resistance in the body of the contact members, caused by the narrowness of the paths through the a-spots, to which may be added the resistance of a film on the a-spots. For two identical metals, the total constriction resistance is $\rho/2\alpha$ where $\rho$ is the resistivity of the metal and $\alpha$ is the radius of the equivalent circular contact area. These a-spots that touch and deform to support the applied load are the only places through which electrons can flow. The observed resistance is then the parallel sum of the resistances associated with these a-spot contact areas, which typically are on the order of $10^{-3}$ to $10^{-4}$ of the apparent

contact area.

On gold or freshly cleaned base metal surfaces such as copper or nickel, only a few elastically or plastically deformed a-spots are necessary to provide low $R_c$. However, once a resistive tarnish film forms on a base metal, even heavy plastic deformation of a typical contact surface may not create sufficient metal-to-metal a-spot contacts to carry the current through the film. The $R_c$ is increased because of the higher film resistivity. If the thickness of the film remains at a level where electron tunneling can occur, the $R_c$ would, on the other hand, not be high. Thus, a reasonable strategy to achieve low $R_c$ with base metals is: (1) increase the number of a-spots on the surface, and (2) use a contact material that has an oxide layer or tarnish film with low resistivity and that is resistant to further oxidation or tarnishing so that the film remains thin.

*3. Experimental*

Contact resistance was measured at a load of 50 grams with a modified Kentron microhardness tester. The set-up has been described elsewhere.[4] The $R_c$ is obtained using a Hewlett Packard micro-ohmmeter, Model 4328A, a four wire instrument with a low open circuit voltage (<20 mV) to minimize electrical breakdown of any film that might be present on the test sample. All the $R_c$ measurements were made with a pure gold wire (0.02 inch diameter) except where a gray Ni/P alloy plated copper wire (0.018 in dia.) was specified.

For the humidity testing, the samples were placed in a quart size mason jar and suspended above a saturated salt solution of potassium sulfate. The jar was then placed in an oven where the temperature was controlled at 50°C for various time periods. The salt, potassium sulfate, was chosen because it can maintain a constant relative humidity of about 95 % within a wide temperature range of 40°C to 100°C.

*4. Results and Discussion*

It appears that the surface morphology of the gray colored Ni/P deposits is the predominant factor in producing low $R_c$. The gray deposit consists of a multitudinous number of tightly spaced microscopic asperities of relatively uniform height when viewed at a magnification of

2000X. Fig. 2 shows clearly the surface morphology of the gray deposit and a bright Ni/P deposit after an exposure for 26 days to a warm humid environment.

The upper left SEM micrograph (Fig. 2A) shows a bright Ni/P deposit ($R_c$>400 mΩ). It has a "rolling hills" structure with some scattered relatively large protrusions. This is typical of bright deposits obtained from most plating baths. The lower left micrograph (Fig. 2B) shows a matte-white to very light gray Ni/P deposit ($R_c$>200 mΩ). It shows considerable smoothing of the "rolling hills" seen in the bright deposit (2A). Also, there is a hint of the surface morphology of the full gray colored Ni/P deposit ($R_c$ <10 mΩ) shown in the lower right micrograph (2C). In this Ni/P deposit the "rolling hills" are no longer evident and only the tightly spaced microscopic asperities that are suggested to be the predominant factor in providing low $R_c$ are observed. It may also be pertinent that the tips of these protrusions are star-like in structure. However, this tip structure is not as clear-cut in the upper right micrograph (2D) of a dark gray Ni/P deposit ($R_c$ <10 mΩ). Here, the microscopic asperities are even more closely packed, which may account for the lack of clarity in determining the structure at the tips.

This star-like structure, which is clearly visible in the micrograph (2C) of the gray Ni/P deposit, may assist in breaking through any oxide or other insulating film on the base metal deposit and in inhibiting the subsequent ingress of oxygen or other contaminants that would affect the intimate a-spot contacts provided by the protrusions. As a consequence, the constriction resistance of the mating contact surfaces should be very low, with only the bulk resistance (resistivity) of the Ni/P deposit affecting the observed $R_c$.

Further evidence substantiating the influence of the a-spot asperities in the gray Ni/P deposit on reducing the constriction resistance between two mating surfaces is the data obtained from studies in which a gray colored Ni/P plated copper wire was substituted for the gold wire used in the probe of the apparatus for making $R_c$ measurements. Initially, whether a gold or a Ni/P panel was tested with the Ni/P wire at a 50 gram load, the $R_c$ values were low (1-2 mΩ). However, after approximately 150 $R_c$ measurements, the $R_c$ between the gray Ni/P wire and a clean gold panel was considerably higher (40-45 mΩ). When a Ni/P panel was substituted for the gold

panel, the $R_c$ decreased to 2-3 mΩ. This alternation of Ni/P and gold panels in contact with the Ni/P wire was repeated several times with the same result: high $R_c$ with gold and low $R_c$ with Ni/P.

A plausible explanation for this unexpected result is that after the ~150 $R_c$ measurements, the asperities on the Ni/P plated wire had been flattened considerably, thereby reducing the number of points capable of intimate (a-spot) contact with the gold substrate. This flattened Ni/P wire had become a typical oxidized base metal which no longer had an atypical surface that could make pin point intimate contact. As a consequence, high $R_c$ between the Ni/P wire and the gold panel would be predicted.

When the Ni/P panel was substituted for the gold panel, the multitudinous number of microscopic protrusions, each with a high unit load, were able to penetrate the oxidized layer on the Ni/P wire, thus making intimate contact and reducing the constriction resistance between the mating surfaces. In this respect, the unique surface morphology of the gray colored Ni/P deposit is better than that of gold.

If the surface morphology is the predominant factor, then smoothing the top layer of a Ni/P deposit should result in higher $R_c$ Table II shows that after 20 cycles of abrasion with a Taber Abraser at a 200 gram load, the $R_c$ of the gray Ni/P deposit had increased approximately eightfold to 33-35 mΩ. This $R_c$ change occurred after exposure to 50°C and 95% R.H. for 17 days. A view of the abraded surface at a magnification of 2000X showed that the tips of the closely packed protrusions were flattened considerably. Many of the protrusions had been completely worn away. However, these were only a small fraction of the area of the abraded surface. In all likelihood, the flattened asperities account for the increase in $R_c$ as in the case of the Ni/P wire in contact with the gold panel.

After 50 cycles of abrasion at a 200 gram load, the $R_c$ increased to >1000 mΩ after exposure to 50°C and 95% R.H. for 17 days. This increase in $R_c$ is similar to that of bare nickel after a similar exposure to a warm humid environment. A view of the 50 cycle abraded surface at 2000X shows that only a small percentage of asperities remain. Most of the microscopic

protrusions are completely worn away. Since the surface morphology of the Ni/P has been, for all practical purposes, obliterated, the large increase in $R_c$ after exposure to high temperature and humidity is predictable.

The results of these abrasion tests appear to substantiate the theory that the surface morphology of tightly spaced asperities with star-like tips is the predominant factor in achieving low $R_c$ with the gray colored Ni/P deposit. This leads to the important question of whether the surface morphology is the only factor.

It has been known since 1950 that at least some Ni/P deposits have higher corrosion resistance than nickel[5]. Electroless Ni/P deposits with 14% P were considerably more resistant than nickel to attack by acids, being corroded only about 1/100 as much in hydrochloric acid. Marton and Chan[6] reported that, at temperatures below 280°C, electroless Ni/P deposits containing 16 atomic % (a/o) P are "practically inoxidizable, at least in terms of a surface oxide film." In studying the catalytic activity of electroless deposited Ni/P substrates (2-3 wt % P) in electroless nickel plating, Fils and Duquette[7] attributed the observed higher activity to thinner, less stable, or discontinuous oxides on the surface. From these studies, it appears that Ni/P would have the desirable properties of a good contact material, and yet no work has been reported on these materials until recently at AT&T Bell Laboratories. A low pH bath was developed[8] and it was found that the resulting bright Ni/P deposits with a P content of 4-7 a/o also have favorable $R_c$ values. Hauser, Robbins, and Plewes[9] investigated the mechanisms for improving the $R_c$ of nickel and found that an exposure test at 75 °C and 95% R.H. for 65 hours produces a top layer of oxide only 25 Angstroms thick on selected nickel alloys.

To distinguish the effect of surface morphology and the intrinsic properties of the Ni/P alloy with low P content, different nickel coatings with similar surface structures were prepared. Gray colored nickel deposits produced by constant current and pulse plating at high current density from low pH acid nickel chloride solutions were compared with gray Ni/P deposits produced at low current density from neutral pH ammoniacal baths where low $R_c$ gray deposits have been consistently obtained. Table III shows that after 14 days of exposure to 50°C and 95% R.H., the

$R_c$ of gray deposits pulsed-plated from the low pH NiCl bath is significantly higher than that of Ni/P deposits. SEM micrographs show that the pulse-plated deposit also has a similar star-like structure (Fig. 3b) to the gray Ni/P deposits. Thus, alloying with phosphorus does influence the $R_c$ behavior.

As also shown in Table III, the $R_c$ of high current density plated deposits from the low pH nickel chloride bath is high, being about 40 mΩ after only 7 days of exposure. An SEM micrograph (Fig. 3c) shows that, even though it is gray, the microstructure is nodular rather than the star-like structure as found with the Ni/P deposits from the neutral ammoniacal bath (Fig. 3A). Not all gray deposits yield low $R_c$.

In the relatively long time period (9 weeks) of the tests reported in Table III, the $R_c$ of the gray Ni/P deposit was not greater than seven mΩ. The results of this exposure test continue to substantiate previous data indicating that the gray colored Ni/P deposit is unique in its consistently low $R_c$ values, since the pulsed-plated acid NiCl gray deposit appears to have a similar surface structure. It seems likely that the phosphorus content of the Ni/P deposit retards the oxidation rate to a level appreciably less than that typical of pure nickel. However, further testing of gray deposits produced by pulse plating from NiCl baths (with and without P) appears to be necessary to provide a clearer insight into the effect of P content on the low $R_c$ of the gray colored Ni/P deposit.

One important observation from these long term and previous short and long term temperature and humidity tests (50°C and 95% R.H.) is that a one week exposure is not sufficient for definitive results (see Table III). It appears that at least a minimum of three weeks is necessary before definitive $R_c$ data are obtained under these test conditions that sharply differentiate the various coatings. A cumulative percentile plot (Fig. 4) strongly suppports this observation. The $R_c$ of the Ni/P deposit is <10 mΩ after 9 months.

## 5. *Conclusions*

The surface morphology of the gray colored Ni/P deposits appears to be the predominant

factor in producing low $R_c$. The gray deposit consists of a multitudinous number of tightly spaced microscopic asperities of relatively uniform height. This star-like structure may assist in breaking through any oxide or other insulating film on the base metal deposit and in inhibiting the subsequent ingress of oxygen or other contaminants that would affect the intimate a-spot contacts provided by the protrusions.

The phosphorus content of the Ni/P deposit also seems to retard the oxidation rate to a level appreciably less than that typical of pure nickel. Gray deposits pulsed-plated from the low pH NiCl bath without P also have the star-like structure, but the $R_c$ is significantly higher than that of Ni/P deposits after 14 days of exposure to 50°C and 95% R.H. Thus, alloying with phosphorus does influence the $R_c$ behavior.

## *6. Acknowledgment*

We are grateful to Mr. T. A. Palumbo and Mr. P. C. Milner for stimulating discussions and Mr. G. R. Crane for interpreting SEM micrographs.

*References*

[1] Antler, M., AT&T Bell Laboratories, private communication, Sept. 30, 1985.

[2] Holden, C. A., Law, H. H., Mattoe, C. A., and Sapjeta, J., *Proceedings of the American Electroplaters and Surface Finishers Society Technical Meeting*, Los Angeles, June 27-30, 1988.

[3] Holm, R., *Electric Contacts Handbook*, Springer-Verlag, 1958.

[4] Baker, R. G. and Palumbo, T. A., *Plating and Surface Finishing, 69 (11)*, 66 (1982).

[5] Couch, D. E., and Brenner, A., unpublished work, National Bureau of Standards, 1950, quoted from A. Brenner, *Electrodeposition of Alloys*, Vol. II, Academic Press, 1963, p. 479.

[6] Marton, J. P. and Chan, E. C., *J. Appl. Phys., vol. 43*, 1681 (1972).

[7] Fils, J. and Duquette, D. J., *J. Electrochem Soc., 131*, 34 (1984).

[8] Robbins, M., Plewes, J. T., Hauser, J. J., Haynes, R., and Ng, S.-L., *Plating and Surface Finishing, 74 (3)*, 56 (1987).

[9] Hauser, J. J., Robbins, M. and Plewes, J. T., "Influence of Disorder on the Contact Resistance of Ni", submitted to be published in *J. Appl. Phys.*

Table I. Cost of Metals

| Metal | Cost ($/cm$^2$) | Thickness (μinch) |
|---|---|---|
| Au | 1.3E-2 | 25 |
| Pd | 3.1E-3 | 25 + 2 (Au) |
| Sn/Pb | 4.5E-5 | 300 |
| Ni | 2.5E-5 | 200 |

Table II. Contact Resistance of Abraded Ni/P Panels (mΩ)

| Abrasion Number of revolutions | 0.1 mil Coating | 0.2 mil Coating |
|---|---|---|
| 0 | 5 | 4 |
| 10 | 11 | 19 |
| 20 | 33 | 36 |
| 50 | >1000 | >1000 |

Taber Abraser at 200 gram load.
Contact Resistance (mΩ) measured after exposure at 50°C and 95% RH for 17 days.

Table III. Contact Resistance of Gray Ni and Ni/P Coatings (mΩ)

| Days Exposure** | 7 | 14 | 21 | 42 | 63 |
|---|---|---|---|---|---|
| Ni/P | 5 | 6 | 4 | 6 | 7 |
| Ni, Pulse* | 5 | 23 | 29 | 24 | 56 |
| Ni, High I* | 42 | 43 | 57 | 88 | >1000 |

** 50°C and 95% RH
* Ni Chloride bath; low pH.

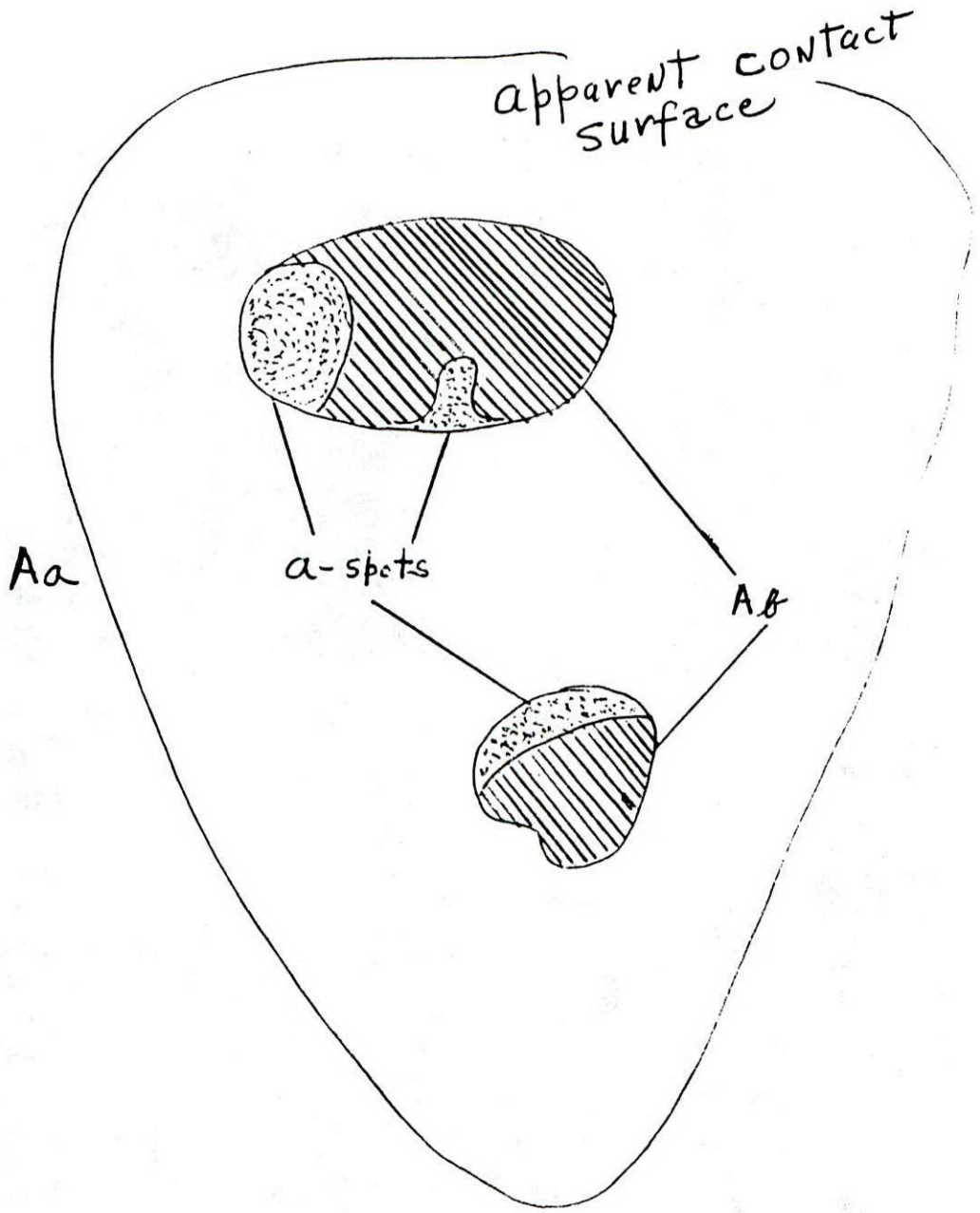


**Figure 1**

Apparent contact surface, $A_a$, load bearing contact area, $A_b$, containing insulating spots, shaded, and conducting a-spots, dotted.

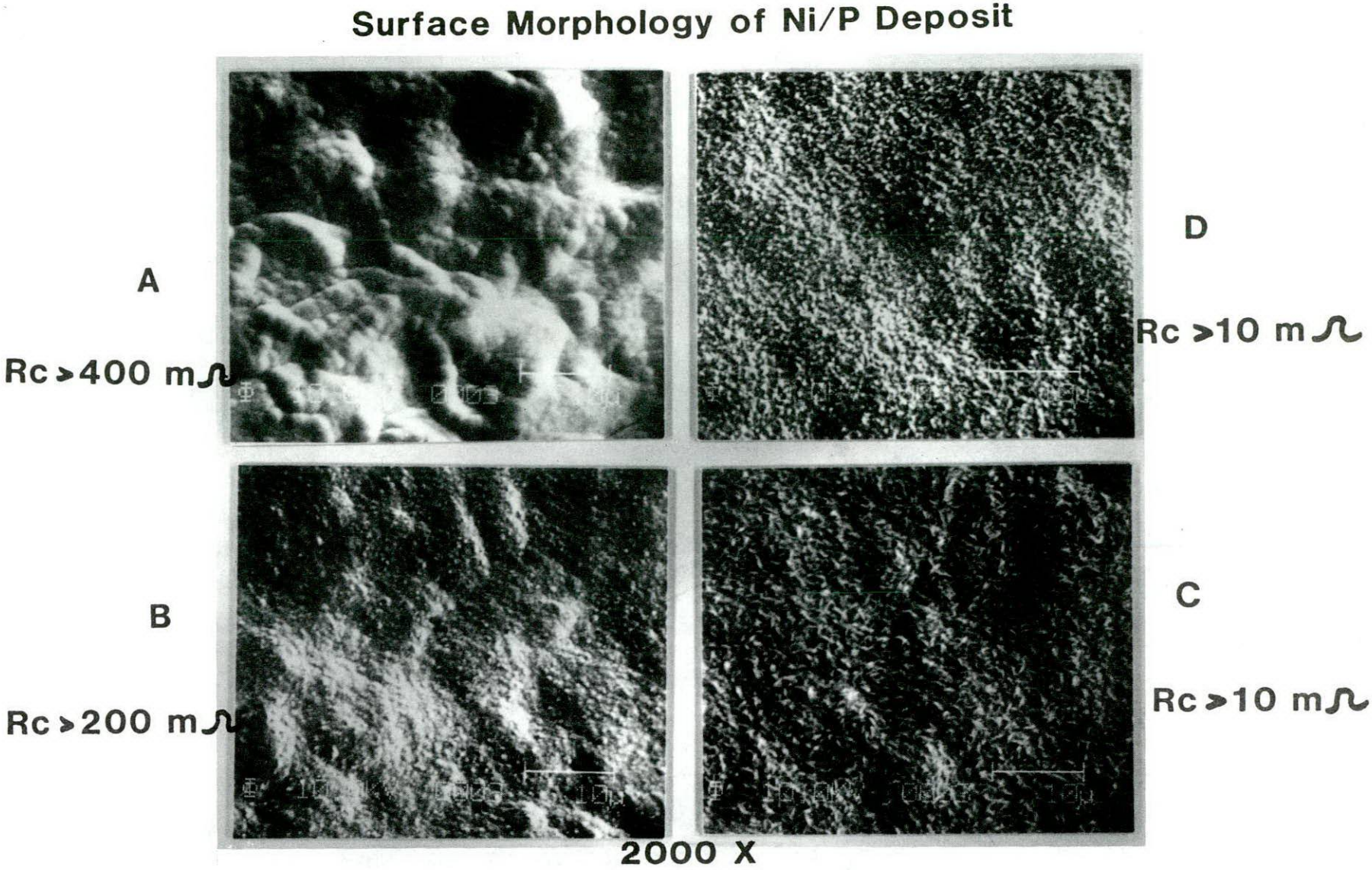


SEM micrographs of gray and bright Ni/P deposits with corresponding $R_c$ values.

# Surface Morphology of Gray Colored Deposits

5000 X

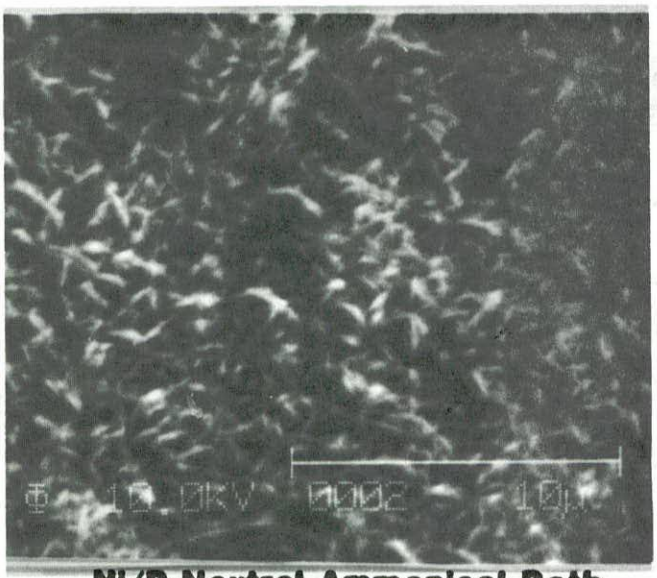

Ni/P Neutral Ammonical Bath

A

5000 X

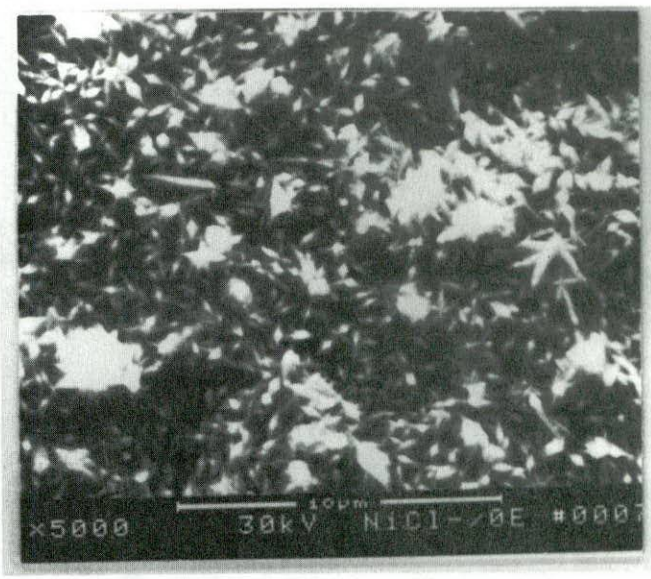


Acid NiCl Bath - Pulse-Plated

B

5000 X

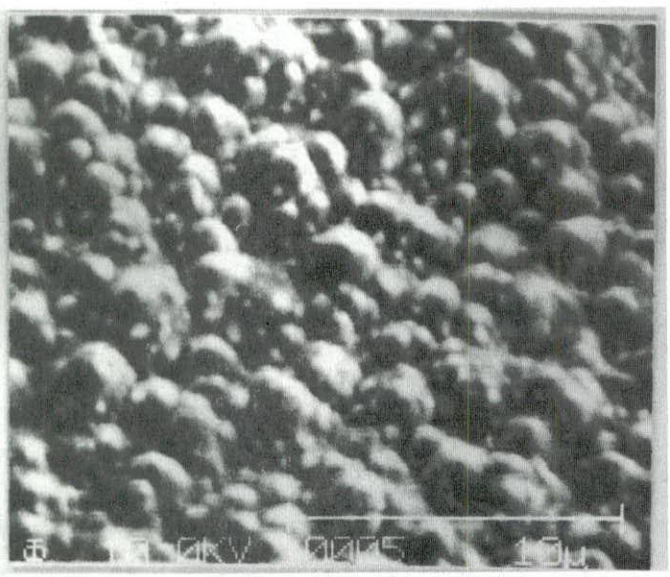

Acid NiCl Bath - Constant Current

C

SEM micrographs of gray Ni and Ni/P deposits.

Figure 3

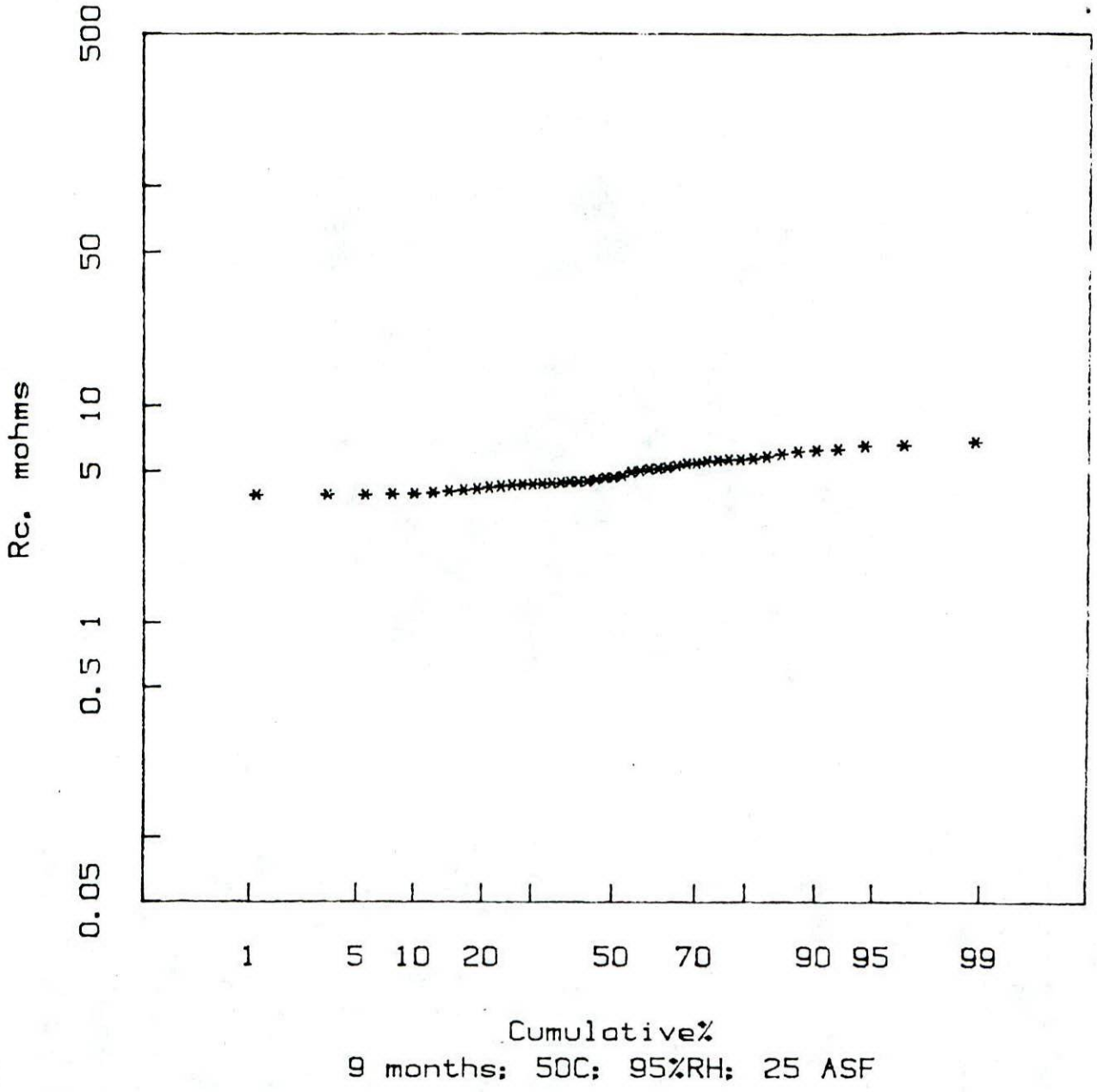


Cumulative plot of $R_c$ of Ni/P deposits.

**Figure 4**

C-3

# Electronics I
# Session C

## Effectiveness of Electrodeposited Coatings in Reducing Atmospheric Corrosion of Copper Substrates

James E. Voytko and Terry R. Guilinger
Sandia National Laboratories
Albuquerque, NM

# EFFECTIVENESS OF ELECTRODEPOSITED COATINGS IN REDUCING ATMOSPHERIC CORROSION OF COPPER SUBSTRATES

James E. Voytko and Terry R. Guilinger
Sandia National Laboratories
Albuquerque, New Mexico

## Abstract

Coatings of gold, nickel, palladium, and nickel with 20 at% phosphorus were electrodeposited on copper substrates at thicknesses of 50 and 150 microinches. These coated samples were exposed in an atmosphere of 100 ppb nitrogen dioxide, 100 ppb hydrogen sulfide, and 10 ppb chlorine, with a relative humidity of 60% and a temperature of 38°C for 332 hours. Weight gain of the samples was monitored to determine corrosion rate. Pore densities and sizes were measured after exposure to compare the performance of each deposit. Although the number of pores in the nickel coatings were fewer than in the other samples, pore sizes were significantly greater. Gold over nickel exhibited smaller pores but a higher density. Palladium at 50 and 150 microinches showed low pore densities. Surface analyses on the pores of the various coatings showed Cu and S as the principal species. The presence of these corrosion products affected the solderability of the samples. Gold plated on nickel over a copper substrate retained its solderability better than the other coating combinations.

## Introduction

Electrodeposited coatings are used to provide corrosion protection and to enhance the physical and electrical properties of copper-based high reliability electronic contacts and interconnections. Typically, these coatings are chosen to be various thicknesses of gold over nickel[1]. The nickel provides a diffusion barrier between the gold and the underlying copper or copper alloy substrate. Also, the nickel improves the hardness and wear resistance of the contact. The gold layer provides good electrical conductivity with long term stability in corrosive atmospheres.

Recently, palladium[2] and palladium alloy[3,4] electrodeposits have found increased use as a replacement for the nickel/gold combination. The impetus for such substitutions has been the increased cost of gold. Studies of palladium and palladium alloys, such as palladium-silver and palladium-nickel, indicate that these materials exhibit low contact resistance, particularly when a gold flash (2 to 5 microinches) is used over the palladium layer.

Besides low and stable contact resistance, the coating layer must also exhibit good solderability. When soldering gold contacts, it is necessary to limit the thickness of the gold layer to control the amount of gold/tin intermetallic formed. Typically, gold layer thicknesses are limited to approximately 50 microinches in these soldered contacts. The porosity of gold

layers at these thicknesses allows access to the underlying nickel and/or copper substrate. Corrosion products from the nickel and copper layers may then form in the pores and creep over the surface of the gold. The existence of corrosion products in, or on, the gold surface impedes solder wettability and may require the use of activated solder fluxes. In critical applications, the use of active fluxes is discouraged since inadequate removal of the flux leads to further corrosion problems.

The requirements of providing good solderability and quality solder joints led to a study aimed at evaluating the effectiveness of alternate materials to coat copper and copper alloy substrates. Such materials must have good electrical conductivity, low porosity, high corrosion resistance, and good solderability. We identified several possible contact materials for comparison with the standard gold over nickel combination including palladium and palladium alloys, nickel with 20 at% phosphorus and duplex gold over nickel. This preliminary report discusses the corrosion behavior of gold, nickel, palladium, gold over nickel, and nickel-phosphorus electrodeposits on copper substrates. The full scope of this study will include other contact materials.

## Experimental

OFE grade copper panels were prepared by photo-imaging and etching to provide test coupons. A matrix of 30 samples, measuring approximately 3/4 inch by 1 inch, was plated as a panel to ensure uniformity in plating thickness. No special polishing of the copper substrates was performed since it was our intent to examine surfaces which are representative of those found in actual contacts.

The panels were degreased in 1,1,1 trichloroethane, soak cleaned in an alkaline cleaner, and immersed in 10% (volume) $H_2SO_4$ prior to electroplating. With the exception of the Ni-P deposit, all plating was done in commercial plating solutions as prescribed by the operating conditions provided by the manufacturer. Gold was deposited from a high purity acid gold solution, nickel was deposited from a sulfamate solution, and palladium was deposited from a non-ammonia alkaline phosphate solution. Make-up and operating conditions for the Ni-P deposits are listed in Table 1. The Ni-P deposits were plated on individual coupons after degreasing in acetone and immersing in concentrated $HNO_3$ followed by concentrated HCl.

During panel plating, a rack located the panels equidistant from the two platinized titanium parallel anodes, thus allowing plating to occur on each side of the panel. After plating, all samples were thoroughly rinsed in deionized water, dried, and stored in dry nitrogen until use. Thickness measurements were taken on each side of the panel-plated coupons by X-ray fluorescence. Composition of the Ni-20P deposits was verified by X-ray fluorescence. Thicknesses of the Ni-20P deposits were determined by weight gain during deposition. Table 2 shows the plating conditions and resulting thicknesses of each deposit.

Samples were also examined metallographically and by scanning electron microscope (SEM) to verify deposit quality prior to exposure to a corrosive atmosphere.

The plated samples were exposed in a chamber to an atmosphere which accelerates aging in a carefully controlled environment[5]. Atmospheric conditions in the chamber, shown in Table 3, were selected to accelerate both nickel and copper corrosion[6,7]. Each coupon was weighed prior to, during, and after exposure. Additional characterization was done microscopically to determine pore density and pore size by examining corrosion spots on the surface of the deposits. Some corrosion spots were analyzed by Auger electron spectroscopy and SEM. Solderability tests were performed on coupons not used for surface analysis using a mildly activated flux followed by a 60-40 tin-lead solder. Solderability analysis followed the procedure described by Jellison et al. [8].

## Results

Table 4 contains the weight gain and pore density and size data. Although weight gain measures corrosion rate accurately in uniform samples, the highly localized corrosion behavior of the test coupons lessens the significance of the weight gain measurements. For electronic contact performance, pore density and pore size are more important indicators of corrosion behavior.

Data in Table 4 show that the gold over nickel combinations performed better than gold or nickel alone since they have both small pore densities and pore sizes. Palladium at a thickness of 150 microinches combined very small pore densities with among the smallest pore sizes of any deposit. The thinner palladium deposit exhibited larger pores at a density about the same as the thicker palladium.

Table 5 summarizes the solderability results on the various coating combinations. Following the procedure of Jellison et al. [8], we report several solderability parameters: $t_{90}$, wetting rate, and contact angle from meniscograph tests as well as meniscus height. The $t_{90}$ and wetting rate parameters are best understood by examining Fig. 1 which shows a typical meniscograph for a 50 $\mu$in Ni coating which was not exposed to the corrosive atmosphere. The $t_{90}$, or time to 90° turnaround, describes the time for the solder meniscus to become perpendicular to the sample. The wetting rate is a function of the slope of the force-time meniscograph and, as recommended by Jellison et al., was the parameter we used to compare the solderabilities of the electrodeposited coatings.

Not shown in Table 5 are the solderability results for Ni and Cu substrates. In both cases, when these samples were exposed to the corrosive atmosphere, the solderability tests yielded a negative wetting rate.

The solderability parameters in Table 5 should be used to compare exposed with unexposed samples within a particular coating combination. Thus, the 150 $\mu$in Au coating soldered better than its 50 $\mu$in counterpart when comparing the wetting rates of

the exposed versus unexposed samples. We look first for high wetting rates since this is the most significant soldering parameter [8]. Samples with good solderability should also have a low $t_{90}$ and contact angle with a large meniscus height. Using these criteria, Table 5 shows little change in solderability for all the Au and Au/Ni samples in response to corrosion testing. NiP and Ni alone both showed decreased solderability due to corrosion product formation. The data for Pd are somewhat inconclusive as the solderability data were not reproducible. We are currently examining a 2-5 $\mu$in Au flash over the Pd to determine if this flash aids in obtaining consistent solderability data.

We attribute the decrease in solderability to the formation of copper sulfides on the surface of the test coupons as determined by surface analyses. Figure 2 shows a representative SEM-EDS analysis of a Au/Ni 50/150 $\mu$in sample. No evidence of Ni was found in the corrosion products of this or any of the Au/Ni samples. In areas of corrosion, Cu and S were always identified with a few occurrences of K, Na, and Cl which could have come from plating bath residue.

## Summary

Atmospheric corrosion testing of palladium, nickel, gold, and nickel-phosphorus electrodeposits on copper substrates indicated that palladium and gold over nickel deposits exhibited the smallest pore densities. Analyses of the pores by Auger and SEM-EDS showed Cu and S as the predominant species indicating sulfidation of the underlying Cu substrate through nearly all of the coating combinations tested. Solderability testing of the various coating combinations both before and after atmospheric corrosion testing showed gold over nickel over a copper substrate best retained its solderability. We attributed the decreases in solderability for the various coating combinations to the presence of Cu and S on the surfaces of the exposed samples. We are in the process of expanding the scope of this investigation to include other coating combinations such as Pd-Ni alloys, Au flash over Pd and its alloys, Au over amorphous Ni-P, and Au over Ni-Cr-P amorphous alloys.

## Acknowledgments

Thanks are due to J. O. Stevenson and W. G. Yelton for experimental assistance, to G. C. Nelson for Auger analyses, and to F. A. Greulich for SEM results. This work was performed at Sandia National Laboratories, supported by the United States Department of Energy under contract number DE-AC04-76DP00789.

## References

1. R. Sard and R. G. Baker, Plating Surf. Finish., 67, 42-47, (1980).

2. J. A. Abys, Proc. AESF 2nd Symposium on Economic Use of and Substitution for Gold, Oct. 5-6, Danvers, Mass., (1982).

3. P. Wilkinson, Trans. Inst. Met. Finish., 65, 33-37, (1987).

4. F. I. Nobel, Electronic Contacts-1984, Proc. 12th Int'l. Conf. Electrical Contact Phenomena, Sept. 17-21, Chicago, Ill., 137-54, (1984).

5. N. R. Sorensen, C. H. Greenholt, and T. R. Guilinger, Development and Performance of a Facility for Atmospheric Corrosion Testing, Sandia National Laboratories Internal Report, in preparation.

6. W. H. Abbott, Electronic Contacts-1984, Proc. 12th Int'l. Conf. Electrical Contact Phenomena, Sept. 17-21, Chicago, Ill., 47-52, (1984).

7. D. W. Rice, P. B. P. Phillips, and R. Tremoureux, J. Electrochem. Soc., 127(3), 563-8, (1980).

8. J. L. Jellison, D. R. Johnson, and F. M. Hosking, IEEE Trans. Parts, Hybrids, Packaging, PHP-12(2), 126-33, (1976).

Table 1. Composition and Operating Conditions for Ni-P Plating

| Component | Concentration(gpl) |
|---|---|
| $NiCl_2 6H_2O$ | 200 |
| $H_3PO_4$ | 50 |
| $H_3PO_3$ | 45 |

Plated at 163 ASF at room temperature with Pt mesh anode

Table 2. Plating Data for Samples Exposed to Atmospheric Corrosion Testing

| Sample No. | Deposit | Current Density (ASF) | Thickness ($\mu$in) | Std. Dev.* ($\mu$in) |
|---|---|---|---|---|
| 2-1 | Ni | 20 | 47.4 | 1.9 |
| 2-2 | Ni | 20 | 49.7 | 1.9 |
| 4-1 | Ni | 20 | 147.6 | 5.3 |
| 4-2 | Ni | 20 | 148.9 | 7.5 |
| 9-1 | Au | 2 | 49.5 | 1.1 |
| 9-2 | Au | 2 | 49.9 | 0.9 |
| 10-1 | Au | 2 | 151.3 | 3.5 |
| 10-2 | Au | 2 | 151.2 | 5.0 |
| 11-1 | Au/Ni | 2/20 | 50.3/49.5 | 1.1/5.1 |
| 11-2 | Au/Ni | 2/20 | 51.3/54.6 | 1.2/5.1 |
| 12-1 | Au/Ni | 2/20 | 55.3/155.0 | 2.2/8.3 |
| 12-2 | Au/Ni | 2/20 | 56.1/147.4 | 2.0/9.9 |
| 14-1 | Au/Ni | 2/20 | 155.4/46.1 | 6.1/1.3 |
| 14-2 | Au/Ni | 2/20 | 158.3/43.0 | 5.4/2.2 |
| 15-1 | Au/Ni | 2/20 | 148.7/145.0 | 5.9/6.1 |
| 15-2 | Au/Ni | 2/20 | 150.1/148.7 | 5.5/5.4 |
| 16-1 | Pd | 10 | 51.2 | 1.9 |
| 16-2 | Pd | 10 | 53.2 | 5.8 |
| 18-1 | Pd | 10 | 162.3 | 10.9 |
| 18-2 | Pd | 10 | 134.2 | 4.3 |
| ---- | Ni-P | 163 | 50.0** | --- |
| ---- | Ni-P | 163 | 150.0** | --- |

* Based on 36 measurements per sample.
**Calculated thickness from weight gain on plating.

Table 3. Atmospheric Corrosion Testing Conditions

| Component | Test Condition |
|---|---|
| $NO_2$ | 100 ppb |
| $H_2S$ | 100 ppb |
| $Cl_2$ | 10 ppb |
| Rel. Hum. | 60 % |
| Temperature | 38°C |
| Duration | 332 hours |

Table 4. Weight Gain, Pore Density, and Approximate Pore Size for Plated Samples after 332 Hours Exposure

| Plate | Thickness ($\mu$in) | Weight Gain ($\mu g/cm^2$) | Pore Density ($cm^{-2}$) | Approx. Size ($\mu$m) |
|---|---|---|---|---|
| Ni | bulk | nd* | -- | -- |
| Pd | 150 | nd | 13 | 10 |
| Pd | 50 | 13 | 13 | 50 |
| Au/Ni | 150/150 | nd | 21 | 10 |
| Au/Ni | 150/50 | nd | 25 | 10 |
| Au/Ni | 50/150 | nd | 26 | 10 |
| Au/Ni | 50/50 | 5 | 33 | 10 |
| Au | 150 | 6 | 141 | 10 |
| Au | 50 | 8 | 87 | 25 |
| Ni-P | 150 | 25 | 14 | 50 |
| Ni-P | 50 | 30 | 39 | 75 |
| Ni | 150 | 40 | 4 | 30 |
| Ni | 50 | 40 | 6 | 100 |

*none detected

Table 5. Solderability Results for the Electrodeposited Coatings

| Sample & Thickness | Exposed* | $t_{90}$(sec) | Wetting Rate (dyne/cm/sec) | Contact Angle(°) | Meniscus Height(cm) |
|---|---|---|---|---|---|
| Ni 50** | N | 1.13 | 163 | 8.8 | 0.258 |
| Ni 50 | Y | 2.44 | 50 | 11.6 | 0.214 |
| Ni 50 | Y | 3.18 | 84 | 12.8 | 0.234 |
| Ni 150 | N | 1.68 | 160 | 10.8 | 0.243 |
| Ni 150 | Y | 3.26 | 95 | 15.2 | 0.214 |
| Ni 150 | Y | 2.75 | 63 | 17.4 | 0.196 |
| Ni 150 | Y | 3.03 | 80 | 18.7 | 0.218 |
| Au 50 | N | 1.03 | 130 | 34.6 | 0.202 |
| Au 50 | Y | 1.12 | 105 | 55.3 | 0.148 |
| Au 50 | Y | 1.33 | 121 | 52.9 | 0.164 |
| Au 150 | N | 1.05 | 143 | 10.2 | 0.259 |
| Au 150 | Y | 1.18 | 138 | 17.7 | 0.244 |
| Au 150 | Y | 1.05 | 138 | 19.6 | 0.238 |
| Pd 50 | N | 1.33 | 121 | 67.9 | 0.128 |
| Pd 50 | Y | 0.86 | 47 | 82.9 | 0.055 |
| Pd 50 | Y | N.A. | 11 | 102. | 0.100 |
| Pd 150 | N | 1.92 | 145 | 67.5 | 0.134 |
| Pd 150 | Y | 3.86 | 19 | 76.0 | 0.056 |
| Pd 150 | Y | 2.22 | 144 | 81.6 | 0.079 |
| NiP 50 | N | 1.55 | 144 | 23.2 | 0.220 |
| NiP 50 | Y | N.A. | 1 | 100. | 0.100 |
| NiP 50 | Y | N.A. | 26 | 125. | 0.155 |
| NiP 150 | N | 0.63 | 204 | 38.0 | 0.211 |
| NiP 150 | Y | N.A. | 59 | 121. | 0.113 |
| NiP 150 | Y | 1.22 | 22 | 62.9 | 0.075 |
| Au/Ni 50/50 | N | 0.92 | 166 | 33.0 | 0.220 |
| Au/Ni 50/50 | Y | 1.06 | 130 | 43.3 | 0.186 |
| Au/Ni 50/50 | Y | 0.92 | 148 | 49.4 | 0.171 |
| Au/Ni 50/150 | N | N.A. | 162 | 26.2 | 0.227 |
| Au/Ni 50/150 | Y | 1.19 | 134 | 46.6 | 0.173 |
| Au/Ni 50/150 | Y | 0.97 | 156 | 49.3 | 0.178 |

Table 5. Solderability Results (cont.)

| Sample & Thickness | Exposed* | $t_{90}$(sec) | Wetting Rate (dyne/cm/sec) | Contact Angle(°) | Meniscus Height(cm) |
|---|---|---|---|---|---|
| Au/Ni 150/50 | N | 0.83 | 165 | 34.0 | 0.205 |
| Au/Ni 150/50 | Y | N.A. | 129 | 37.0 | 0.187 |
| Au/Ni 150/50 | Y | 1.33 | 122 | 37.3 | 0.193 |
| Au/Ni 150/150 | N | 0.85 | 160 | 33.8 | 0.217 |
| Au/Ni 150/150 | Y | 1.09 | 132 | 34.0 | 0.189 |
| Au/Ni 150/150 | Y | N.A. | 124 | 33.6 | 0.197 |

* Exposed indicates if the sample was exposed to accelerated atmospheric corrosion testing.

** Thickness reported in microinches.

N.A. Not available because of the shape of the meniscograph.

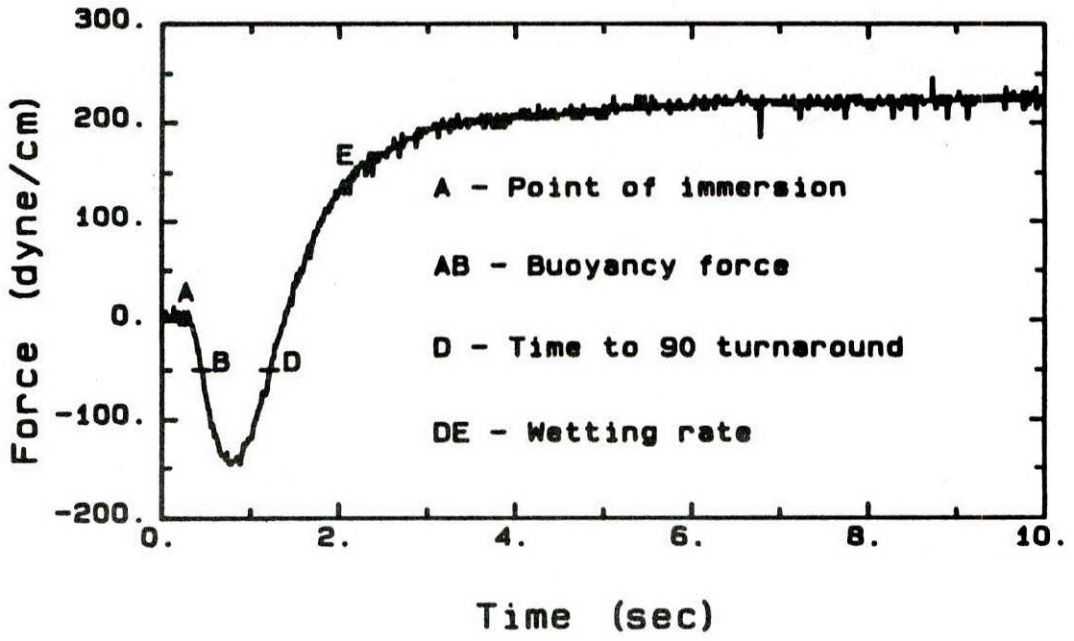


Figure 1. Solderability meniscograph for a 50 $\mu$in Ni coating on Cu substrate not exposed to atmospheric corrosion.

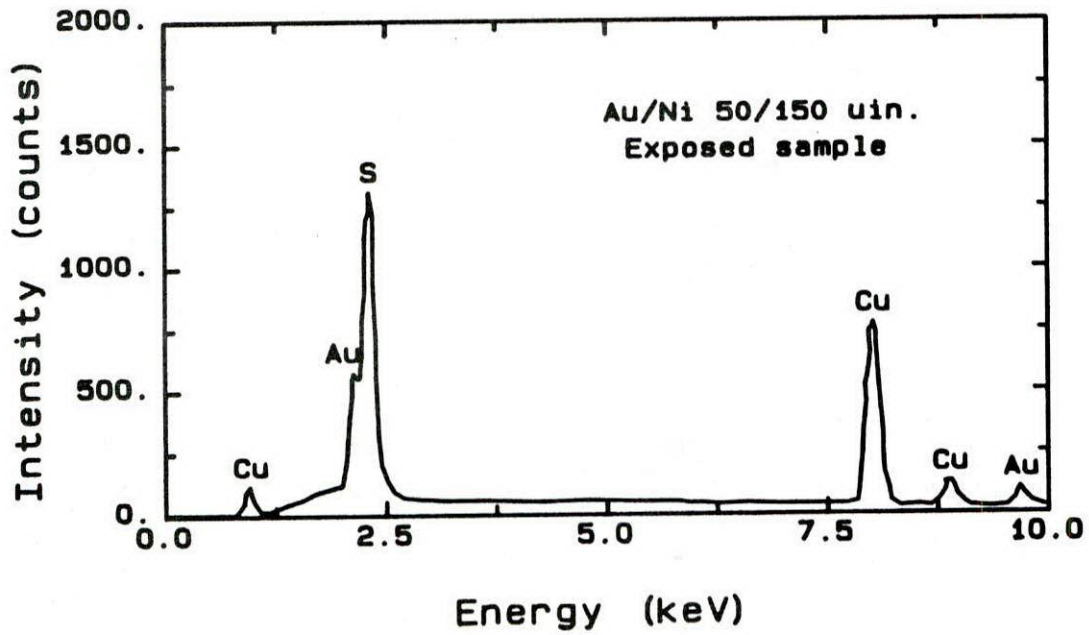


Figure 2. SEM-EDS of sample exposed to atmospheric corrosion showing presence of Cu and S on surface.

C-4

# Electronics I
# Session C

## To Be Sure of the Right Connections—
## You Must Have a Heart of Gold

John Donaldson, Tech. Dir.
Mesa West, Inc.
Anaheim, CA

# TO BE SURE OF THE RIGHT CONNECTIONS
## (You Must Have a Heart of Gold)

John Donaldson, Tech. Dir.
Mesa West, Inc
Anaheim, CA

A few years ago the AESF sponsored a special symposium having the well structured and publicised objective of advising electronics engineers and component designers how to make their products work better, last longer, and cost less by utilizing the knowledge and the unique and proven capabilities of electroplaters and the surface finishing industry. A grand total of two, equalling about 5% of those attending, qualified as the target audience, thus underscoring what have long been two major concerns of many "Platers for Electronics".

The first of these concerns is that it seems too many specifiers and users of plated electronic components and devices do not understand that designing appropriately for electroplating, and selecting the correct metal coatings, can significantly improve the quality, reliability and performance of their products, while usually reduce processing costs. The second, and perhaps even more bothersome one is that a number of them don't seem to care. Far too many AESF technical offerings are ignored by those who could really benefit from them, and the events become simply forums for platers and plating suppliers to tell each other what we pretty well already know.

For whatever reason, our "customers", those who require the products of our tanks and bubbling cauldrons, seem strangely hesitant to mingle with, or even be seen with platers. And yet we are that very segment of industry that produces the coatings which actually provide electrical components with the ability to function, and function reliably for as long as the system is needed.

Admittedly this hesitancy to rub shoulders with electroplaters could be due to the peculiar aroma sometimes noted in their immediate vicinity. A more probable and acceptable cause of the poor showing of "non-platers" at our tech sessions is a woeful lack of understanding of the technical importance of plated for electronics coatings.

Carrying that supposition just a bit further - the problem might be even deeper than that! It's conceivable that more than a few of the aforesaid designers and specifiers pay but little heed to the vital role of certain of the components of which electrical devices and equipment are fabricated!

For instance it's a good bet that at least half of the electronics engineers asked to name the principle components of a typical electronic system will fail to mention the one that can with some justification claimed to be the most important of all! Not present in their lists of such exotics as semi-conductors, resistors, integrated circuits and printed circuits will be that 'anything but' exotic device with the mundane pseudonym of "plug" - the electrical connector.

The fact is that no matter how exotic or technically unique they might be, none of the other devices of an electronic system can perform it's electronic miracle if not appropriately "plugged" into a power source and/or suitably interconnected with the other components of the system. And whatever their assignment, commercial, industrial and/or military, connectors must transmit electrical impulses from the terminal end of one conductor to that of another, instantly, repeatedly, and reliably for many, many years. Failure to perform satisfactorily, even when the interval of interrupted function is measured in nano seconds, can result in anything from disruptive irritant to another Chernobyl type disaster to international warfare!

The electrical connector was invented about sixty years ago to permit quick, easy and simultaneous connections of a couple to maybe half a dozen wires. There's no denying that in those days it was truly but little more than what it was officially named, - a plug! But now in this dynamic age of electronics the number of simultaneous connections typically run from fifteen to several hundred. In today's electronics devices and systems the amount of current transmitted is usually so small that a half century ago they'd have had a tough time accurately measuring it. And the connectors used today are required to work in once unimaginable adverse conditions of heat, cold, pressure, humidity and corrosive environments.

The simple "plug" has most certainly evolved into a very sophisticated and complex electronic device. No longer a substitute for a few twisted or soldered wires, connectors are now produced in a seemingly limitless number of sizes, shapes and styles which each year cost U.S. electronics industries about five billion dollars.

Of course there are those who neither ignore, nor are ignorant of, the critical role that electrical connectors play. In a fairly recent publication one went so far as to deem them the "heart" of electronics systems. It was that very statement that inspired the observations and conclusions set forth in this presentation.

Naming connectors the heart of an electronics system, while certainly a well meant designation, is from a technical view, just a bit off target, and the record needs to be set right. The actual transmission of electrical impulses between connectors is accomplished by the connector's contacts, the pins and sockets. It is the touching or "mating" of the *surfaces* of these contacts that enables the passage of electrons, and therefore the true heart of electrical systems is really the surface of the contacts in connectors. It follows that this is why electroplaters - and their steaming vats and cauldrons - are of such critical importance to the electronics trade. Most of the several billions of contacts that each year are assembled into connectors are fabricated from copper and copper alloys. Many are made of nickel and its alloys, and some applications may require or allow the use of contacts formed from such metals as molybdenum, tungsten, aluminum, titanium, stainless steel, and even plain steel. None of these metals have all, or even most of the necessary functional and performance characteristics required of an electrical contact. Thus the need to electroplate them with metals that do.

Many types connectors must repeatedly perform their plebeian task satisfactorily and with absolute reliability in whatever type of service in whatever type of environment for whatever length of time. It is particularly on the contacts of these that gold plating is specified, the total amount accounting for close to ten percent of the worth of the connectors annually purchased.

This is about the 25th year of an era that could be named "The ***Golden Age of Electronics.***" Such a designation is due partly to the tremendous proliferation of electronic inventions and innovations during those years; and partly due to the tons and tons and tons of gold used to plate them.

The following gold usage history, often repeated at seminars like this one, is here restated to support a subsequent claim that through scientific endeavor, technical skills, and common

sense the plating industry has done an extremely admirable job conserving gold and improving its utilization. So admirable that it can be claimed that it has been the platers for electronics have been the financiers of the Golden Age.

Between 1960 and 1970 the amount of gold used each year for plating electronics components in the United States increased eight times, from two hundred and fifty thousand to almost two million Troy Ounces. During the 1970's, despite a tremendous increase in the numbers of lead frames, contacts, headers, semiconductors, PC's and other electronics devices being produced, the amount of gold used for electronics plating declined by almost 50% to about one million ounces, dropping even further since 1980 to a level of approximately 850,000.

Several factors contributed to this phenomenal reduction in gold usage that each year saves the electronics trade about Four Hundred Million Dollars (with gold at $ 400.00 per Ounce). The top three, in the probable order of impact, are:

(1) Selective Plating; (2) Reduced Minimum Thicknesses; and (3) Gold Substitutes (replacements)

With respect to factors one and two, it is important to know that even with far less gold being used to plate a far greater quantity of electrical parts, neither function nor reliability have been sacrificed, or even compromised. Actually, quite the opposite is true, with invention and modification of gold plating processes, equipment, and plating techniques having considerably upgraded the quality and performance features of the coatings even at considerably reduced thicknesses. The stressed and brittle deposits, excessive porosity, poor wear, unreliable bondability and solderability and poor heat resistance, once too common defects of gold electrodeposits, no longer "plague the platers. (Or, at least they shouldn't)

As for reason number three, substitutes, or more aptly termed "replacements," this note of caution for those responsible for specifying contact finishes: "Take care!" .... Keep firmly in mind that what you're messing with is the "heart" of electrical systems, and a weak or defective heart is as undesirable in electronic equipment as it is unfortunate in the human body. As in humans, when the heart isn't working too well it weakens the whole system (body); and should it fail all of the other components and devices (organs) are brought to an untimely end.

Just as we don't want our own "tickers" to give out, we are not too enthused about defective or failing hearts in the systems that keep our electronic world 'turned on and tuned in.' This is especially so when it comes to things like fighting wars -or better yet - not fighting them; conquering space, ocean or super highway; and particularly when being transported through the air from city a to city b, an event which most of us fervently hope occurs without serious mishap or undue aggravation.

The best things in life may be free, but the best thing on connector contacts is definitely not. Gold is not called a precious metal just because it looks nice, and when specified it adds much to the cost of manufacturing and using connectors featuring gold plated contacts. In these days of rampant competition from both within and without the United States pressures remain high to minimize processing and material costs. Predictably, gold is a favorite target for cost reductions efforts. The big question, as it has been, continues to be how to use less without sacrificing any of gold's needed attributes and capabilities?

The question will be again answered for the most part by two of the three techniques already identified; reduced minimum thickness specifications and selective plating. There is every reason to believe that these answers have the potential to save even more gold in the coming years than they have here-to-fore!

Consider thickness. About a decade ago connector and semiconductor producers determined that gold thicknesses of 0.0001", 0.000060, and particularly for bonding, even 0.000030 could be halved and more without losing the desired functional capabilities of the deposit. Since then, continued investigation of the effectiveness of barrier layers and post-gold plating processes, along with years of "real time" experience, have resulted in an accumulation of data that should be the basis for a new round of gold thickness reduction efforts.

For instance, increasing the thickness of a nickel barrier coating greatly reduces potential problems of surface films and corrosion by minimizing the effects of porosity, thereby allowing for very thin deposits of gold when wear is not an important consideration. And when it is, wearability can be greatly enhanced by the simple expedient of utilizing a post-plating lubricant or coating graphite type coating.

Another technique that allows a significant reduction in gold thickness by negating the effects of innate porosity, is to employ copper passivation treatments after gold plating. Fairly good and long term corrosion resistance results from chemical conversion of the copper that is present at the base of pores in the plating.

There's been another consequential advancement in plating during recent years that should make the use of thinner deposits even more palatable for electronics engineers. This is the accumulation of a wealth of knowledge pertaining to the equipment and solution parameters that effect plating distribution in batch gold plating processes. Modifications in equipment and some minor adjustments to, and close control over such variables as pH, solution conductivity and metal content, will greatly limit the plating thickness range in any lot plated. Coupled with much more accurate and reliable measurement systems now available at an affordable price, accurate and reliable measurement now possible, this factor helps assure the user that all of the contacts of any plated lot will have more than the specified minimums. Therefore th-ere should be little reason to over specify plating thickness minimums in order to "play it safe."

So reduced gold plating thickness is definitely a viable way for connector users to effect further gold savings without losing gold's valuable properties. And Selective Plating, already described as having been "super effective." is another, especially since "super selective" plating systems can now place extremely small gold spots in once virtually inaccessible locations.

As new methods for obtaining selective deposits have been developed and refined to produce "super selective" deposits, the design of many styles of contacts have been revised (despite previous inferences that this has not generally happened) to take advantage of them. A classic example is the use of a slightly raised area, or bump, on the mating surface of a spring or blade contacts that when selectively plated assures steady and intimate connections at every insertion. Another example is the use of pre-plated gold striped strip which when formed becomes the ID surface of the mating end of female or socket contacts.

Naturally, most of the above statements about selective plating relate to the continuous pre-plating of strip before forming and plating pre-stamped and formed contacts affixed to a carrying strip. However the greatest area for future exploitation of selective gold plating techniques to produce very, very substantial savings actually is in another arena, on "loose piece" or machined contacts.

A minimum thickness of .000050" is typically specified on connector contacts for military applications. Usually formed by cold heading, screw machining, or rolling equipment the contacts are produced "loose" and in large quantities, and have always been plated in bulk processing operations. However the functional areas of these contacts, that is the sites that in service become the "heart" of electronics systems, are but a short segment of the outer surface of the pin and the inner diameter of the socket. Gold is not needed on the rest of the contact.

During the past two years the military has been conducting an in-depth test of contacts that were selectively plated. Approval can revolutionize the manner in how contacts plated to Mil Specs are processed. Connector manufacturers will be allowed the options of continuing to supply over all plated contacts, or ones which have been selectively plated. Competition will most certainly force them to adapt the latter system.

Naturally the heat will be on both in-house engineers and equipment suppliers to develop selective loose piece parts plating capabilities. And this will most certainly cause many platers, plating engineers, department managers and all of the others involved a lot of consternation, bafflement, and sleepless nights.

Several equipment manufacturers and at least two or three major connector houses did invent and develop such equipment a couple years ago anticipating a fairly rapid move into this technology. But two things happened: (1) the very conservative attitude of the government agency(s) charged with evaluating selective plated contacts and the ensuing very extended testing period; and (2) the equipment built either didn't work very well, or if it did, was seriously lacking in versatility and proved too difficult and cumbersome to operate successfully for extended periods of time. (Contacts are made in a whole bunch of shapes and sizes and are not always "perfectly" dimensioned.)

It is predictable that approval of selectively plated machined contacts, if and when it actually happens, will precipitate a flurry of activity - with the dust being blown off a number of existing plating lines and from the plans for several more. Necessity truly being the Mother of Invention, its likely that some firms will be successful in designing equipment that will work and even be at least marginally cost effective.

But its also probable that a couple other techniques will ultimately be utilized for selectively plating most volumes of machined connector contacts. Both are already in use, however both must be improved and refined to handle the large numbers of contacts that will have to be processed.

The most likely candidate is "bandoliering" of the contacts, not a particularly easy thing to do because of their round shape and wide variety of diameters and lengths. But indications are that what was once impossible is now being accomplished, pointing the way for the best technique for loose piece parts platng. Since contacts affixed to a bandolier are plated on conventional continuous strip plating lines, the plating equipment itself is in place, ready and waiting.

The second potentially effective technique is to automatically feed a controlled number of contacts into a magazine, or clip which is then continuously conveyed through a plating lines suspended from a small chain fixture; or is combined with several more clips in a special fixture for "rack" plating. While the potential production rate is a bit slower than bandolier plating, it is a good (and proven) system, particularly because of its versatility, ability to processes small volumes, availability of equipment and the relative low cost of that equipment.

Now to briefly summarizing the essential points of this unabashedly circumlocutory presentation. The primary goal is to explain the need to continue specifying gold plating on electrical contacts used in critical applications requiring highly reliable components. However, recognizing the need for further reductions in production costs in manufacturing connectors, a second purpose is to offer some advice for reducing gold consumption while losing none of its needed characteristics.

It should be pretty clear that the message is directed at those who direct and control product design and specifications, thus the mandate expressed in the title, ***"HAVE A HEART OF GOLD -AND YOU'RE SURE TO HAVE THE RIGHT CONNECTIONS."*** However it will be the Platers for Electronics who must provide gold deposits that will assure the Right Connections at the least possible cost, so it's important that they too appreciate what it is that is the "true heart" of electronics systems.

References:


1. FLECK REPORT, Vol 3, No. 2 (1984)
2. Milling-Stanley, et al GOLD 1986, Consd Gold Fields PLC
3. C. Michalopolous, GOLD 1986 - THE US MARKET, Consd Gold Fields PLC
4. M. Antler, GOLD BULLETIN, Vol 16, No 1 (1983)
5. R. Baker and T. Palumbo, P&SF Dec. 1985
6. D. Hinderman, et al THE WESTERN ELECTRIC ENGINEER April 1983
7. Takehito Sate, et al P&SF August 1983.

C-5

# Electronics I
# Session C

## An Overview of the Ductility Testing of Electrodeposits

Alan A. Halecky and Edward N. Balko
Engelhard Corp.
Electronic Products Group
One West Central Ave.
East Newark, NJ 07029

# AN OVERVIEW OF THE DUCTILITY TESTING OF ELECTRODEPOSITS

Alan A. Halecky and Edward N. Balko
Engelhard Corporation
Electronic Products Group
One West Central Avenue
East Newark, New Jersey 07029

## ABSTRACT

A review of ductility testing methods is presented with a discussion of the advantages and disadvantages of each method. Special attention is given to the measurement of the ductility of electrodeposits attached to a substrate (composite specimens).

## INTRODUCTION

In developing a new palladium electroplating bath in our laboratory, our objective was to have the deposit meet a set of physical properties that our marketing people deemed necessary. One of these target properties was to have the deposit exhibit a ductility of six percent or greater. During our initial screening phase of various electrolytes, we tried to make foils from our palladium deposits for tensile testing. The deposit was plated on a stainless steel coupon and an attempt was made to peel the foil from the substrate. This invariably resulted in broken foils. Furthermore, it is not possible to obtain palladium foils by dissolving away the substrate metal in acid, as it is with gold electrodeposits. This leads to uptake by the palladium of hydrogen formed during the metal dissolution, which, in turn results in embrittlement of the deposit. Therefore the palladium was plated on copper followed by an attempt to remove the copper by dissolution in cyanide with a mild

oxidizing agent. The slow rate of attack on the copper by cyanide rendered this approach impractical. At this point we decided to do our ductility testing on deposits attached to a substrate material of greater ductility than that of the palladium film. At the time we thought that this was a novel approach to the ductility testing of electrodeposits and therefore a discussion of this technique was to have been the focus of this paper. A search of the older literature, however, revealed that tensile testing of electrodeposits attached to the substrate had been performed as early as 1962[1]. Since many knowledgeable people in the electroplating field are unaware of this useful ductility testing method, we decided that it would be useful to transform this paper into a review of ductility testing with emphasis on the testing of composite specimens. The intent of this paper is not to provide a complete review of ductility testing procedures, as there are many fine review articles written on the subject, but rather to provide the electroplater with a brief introduction to the methods available to him in the selection of an appropriate method.

## DISCUSSION

The need for the determination of the ductility of electrodeposits arises in a number of instances: 1) when a part is subjected to forming operations after electroplating such as connectors formed from stripe-on-strip; 2) when a plated piece will be subjected to stresses arising from thermal loading, as happens to printed wiring boards during soldering operations; 3) in the fabrication of flexible circuitry or, 4) when a deposit is overplated by a deposit having a large tensile stress, such as chromium plated on nickel. If the deposit is not sufficiently ductile to withstand the applied forces, the deposit will crack and may exfoliate from the piece.

On the surface of things, the definition of ductility as "the ability of a material to deform plasticly without fracturing[2]" seems relatively straightforward. However, the relationship between the means devised for the measurement of ductility and the above definition is anything but straightforward. The technique by which the specimen is

deformed in the test procedure gives rise to the questions of interpretation and accounts for the profusion of methods for the measurement of ductility. Currently, no standard test for the measurement of film ductility exists, although attempts to devise a standard method continue[3]. Further complications arise when it is attempted to transfer bulk ductility measurement techniques to the measurement of the ductility of electrodeposits. Below a thickness of about five microns the mechanical properties of films begin to deviate substantially from that of bulk specimens. Effects due to inhomogeneities and defects that are averaged out in thick specimens become important determinants of material behavior in thin specimens[4]. To collect accurate mechanical performance data, it is therefore prudent to conduct ductility testing on deposits of thickness comparable to that of the application coating thickness.

The four general classes of ductility test methods are categorized by how the specimen is deformed: uniaxial tensile test, bulge tests, bend tests, and fatigue tests[4].

Tension Test

In the uniaxial tensile test, also known as a tension test (**Figure One**), a sample is clamped between two jaws and a force is applied along one axis of the specimen (hence, the name "uniaxial") and it elongates in the direction of the applied force. The internal force that resist this elongation is known as the stress. The change in the specimen length divided by the original length of the specimen is known as the strain. The data obtained from the tensile test is presented as a plot of stress vs. strain as is illustrated in **Figure Two.** The straight line portion of the curve represents the elastic region; over this region, if the stress is removed from the test piece, the specimen would be restored to its original length: No permanent strain results from stresses applied in the elastic portion of the curve. By contrast, if a sufficiently large stress is applied to the material under test to cause an increase in the length of the specimen, which is not reversed when the stress is removed, the piece is said to be plastically deformed. The region of plastic deformation exists on the curve in **Figure Two** from point A to point B. The strain at which fracture occurs multiplied by 100 is called the

percent elongation. It is this value which is most often taken as a measure of the ductility of the material being tested. It should be noted that the percent elongation is easily and directly determined from the graph in the tensile test. In all of the other test methods to be described in this paper, the percent elongation must be derived from an indirect measurement and it is the accuracy of the mechanical model employed that will determine value of the ductility data obtained.

Bulge Tests

Bulge tests are biaxial tensile tests: The forces applied to a specimen to cause it to deform in this type of test are applied along the two axes of a plane (**Figure Three**). The result, as the name implies is the formation of a bulge in an originally flat sample. Many variations on the bulge test exist, depending on what is used to cause the bulge[5]. The hydraulic bulge test[6] is used for testing very thin specimens. In this technique, the sample is tightly clamped over the mouth of a chamber and oil is pumped into the chamber through a small hole as can be seen from **Figure Four.** The force that induces the sample to bulge is transmitted to the specimen by the pressure that the oil exerts on the side of the sample clamped to the chamber. The oil pressure is increased until the bulge ruptures. The elongation is derived, using a great many assumptions, from the measured height of the bulge and the oil pressure at fracture. By far the most common technique used to apply the force that gives rise to bulging is to anchor the flat specimen and to drive a spherical ball into the specimen until a crack appears in the surface (**Figure Five**). This approach is the basis of a very convenient and simple to construct bulge testing apparatus shown in **Figure Six**[7]. Though some investigators in the past have reported problems with accuracy and reproducibility with bulge tests, we have found the apparatus pictured in **Figure Six** to give good results. From the geometrical arrangement depicted in **Figure Five,** one can derive equations which allow one to calculate the percent elongation which the piece suffers at fracture. The bulge tests may be used either on foils or composite samples, though if composite specimens are to be used with this apparatus, our experience has shown that the substrate must be sufficiently thin to transmit the force applied to the attached film. Another disadvantage of the bulge test,

albeit a minor one, is that the strain at fracture is not given directly, as it is in the tension test, but rather must be calculated.

Bend Tests

There are are numerous types of bend test[3], many of which provide only qualitative results, while others provide quantitative data of questionable value. All of the procedures rely on detecting the first appearance of cracks in a specimen which is subjected to bending. The test methods can be differentiated in to two broad groups: 1) the specimen is bent without a support, or 2) the specimen is bent against a mandrel (a supporting structure of well defined geometry) [see **Figure Seven**]. Testing can be performed on either a foil or on composite test pieces in both of these categories. In one of the more frequently used unsupported bend tests[9], a foil is bent into a "U"-shape and placed between the jaws of a micrometer. The jaws are then slowly closed on the piece until the specimen fractures. From the deposit thickness and the size of the opening between the micrometer jaws at fracture, the percent elongation is calculated.

The supported bend test procedures can be further subdivided by the shape of the mandrel employed (cylinder, triangle, etc.) and the number of mandrels used (three-point and four-point bend tests); the cylindrical mandrel is the most comonly employed geometry. In a common supported bend test, a composite specimen is bent around mandrels of progressively smaller diameters until fracturing of the deposit is observed. The percent elongation is then calculated from the diameter of the mandrel which first gave rise to deposit fracture and the specimen thickness. This test suffers from poor reproducibility; further, the relationship of the calculated measure of ductility obtained from this test to that of the corresponding percent elongation at fracture measured by a tension test is highly questionable. In fact, in a side-by-side comparison of a the tension test and a popular bend test carried out on nickel deposits, it was demonstrated that a difference of as much as one hundred percent existed between the ductility values obtained from each test[1]. The problem lies in the inability of the test to discriminate fully between the elastic and

plastic deformation experienced by the test piece. A variation of the successive mandrel test uses a conical mandrel so that a continuum of mandrel diameters can be achieved with one bend over one mandrel. An end of the test piece is anchored to the mandrel and the deposit is wrapped in a spiral over the length of the mandrel. The radius of curvature of the support at which a crack is first observed on the deposit is used in conjunction with the film thickness to derive a value for the percent elongation. This test provides better ductility values than the former but also shares the flaws inherent in the simpler bend test.

Fatigue Tests

The final category of ductility tests to be discussed is the fatigue test. This type of test provides the least quantitative value for ductility and exhibits poor reproducibility. At best, they offer only a ballpark estimate of ductility. Invaribly, in fatigue tests, the specimen, either foil or composite piece, is bent, straightened out, and then bent in the opposite direction. This cycle of operations is carried out until fracture is detected. The number of bends to fracture is taken as a measure of the ductility. To ensure a uniform angle of bending from cycle-to-cycle as well as from specimen-to-specimen, one fatigue test procedure uses a vice to bend the specimen[10].

Most ductility determinations on electrodeposited films reported in the literature are performed on foils made either by dissolving the substrate metal away from the film or to a lesser extent by mechanically stripping away the deposit from a substrate to which the deposit has poor adhesion. The reason that testing is so often performed on foils is to obtain ductility measurements that are free from substrate-film interactions. These interactions arise from stresses at the interface between the two metals. For highly ductile metals such as copper or low-stress nickel, the preparation and handling of foils is manageable. The inherent disadvantages in using foils are the time-consuming sample preparation and the tendency of foils to wrinkle. This wrinkling effect gives rise to a value for the ductility which is larger than the true value since some of

the "elongation" recorded is the result of unwrinkling of the foil. Further,the substrate used to generate the foil can influence the mechanical properties of the foil. In one study[12], the percent elongation of a copper electrodeposit over electroless copper was found to be more than double that of the copper plated over stainless steel.

Since the "true" ductility of an electrodeposit is not measured using composite test pieces, owing to the substrate-deposit interactions, it may be asked what is to be gained by the testing of composites. One obvious answer is that no measure of the ductility of brittle films could be obtained if they had to be measured as foils. An even better answer is the fact that if the test substrate material is chosen so that it has mechanical properties closely matched to that of the application material, then realistic conclusions can be drawn about the deposit performance in its intended actual use. Such a test then takes into account the real world fact that the performance of a deposit is intimately linked to the substrate to which it is attached. It also avoids problems caused by artifacts which may appear in the preparation of foils.

The tension testing of composite specimens in our development of a new palladium plating bath proved to be both convenient and well suited to the application. Our test pieces were prepared by plating palladium deposits onto ten mil thickness dog bone-shaped coupons (**Figure Eight**). Copper was chosen because its ductility far exceeds that of the palladium deposit as well as the fact that stripe-on-strip connectors are often made of copper. The requirement that the substrate exhibit greater ductility than the deposit is necessitated by the fact that the deposit must fracture before the substrate does in order to derive any meaningful data.

The specimens were clamped in the jaws of our tension tester and elongated in 0.1 percent increments followed by examination at 50X magnification until lateral cracks extending the width of the panel were first detected. The resolution of the technique could, of course, be improved by conducting the elongations in smaller increments. The

reproducibility of the percent elongation at fracture values is from specimen-to-specimen is about five percent and no significant variation of ductility was observed over the thickness range from fourty to eighty microinches. Test results on the new palladium plating bath are reported elsewhere[13].

The conclusion we draw from our survey of ductility testing methods is that the choice of a testing method should be guided by the end use for the data. If the data are to be used to advance the the scientific understanding of materials behavior, then careful quantitative tests based on accurate physical models are essential. On the other hand, if a practical understanding of how a deposit will perform in an actual application is required, then a test procedure which most nearly models the application environment is what is called for. The tradeoff in simulating the complex physical reality is a loss in exact physical relationships that can only be understood in simplified models. Therefore, all of the tests described above have their place in the spectrum of testing needs.

## REFERENCES


1. S.D. Cashmore and R.V. Fellows "A New Method of Ductility Testing of Nickel Electrodeposits," Trans. Inst. Met. Finishing, 39, 70 (1962).

2. Ductility: Papers Presented at a Seminar of the American Society for Metals, October 14 and 15, 1967, American Society for Metals, 1968.

3. R. Rolff, "Survey of Ductility Testing," ISO?TC107/SC2, Document N341, November, 1982.

4. C.N. Neuberger, J. Appl. Physics, 31, 1096 (1960).

5. Metals Handbook, Volume 8: Mechanical Testing. American Society for Metals, 1985.

6. G.C. Van Tilburg, "The Measurement of Ductility," Proc. Amer Electroplaters Soc., 50 (1963).

7. S. Nakahara, Y. Okinaka, and D.R. Turner, "A Simple Ductility Tester for Metal Films," J.Testing and Evaluation, 5, 178 (1977).

8. T.A. Prater and H.J. Read, Plating, 36, 1221 (1949).

9. Anton F. Mohrnheim, "The Bend Test for Measuring the Strain Limit of Surfaces," Plating 50, 1094 (1963).

10. C. Durban, Proc. Amer. Electroplater's Soc., 38, 119 (1951).

11. P.F. Foster, The Mechanical Testing of Mterials and Alloys, p.218, I. Pitman and Son, Ltd., London (1936).

12. T.D. Dudderar and F.B. Koch "Mechanical Property Measurements on Electrodeposited Metal Foils," p.187, in Properties of Electrodeposits: Their Measurement and Significance, eds. R. Sard, H. Leidheiser, Jr., and F. Ogburn, The Electrochemical Society (1975)

13. A. Blair, G. Karustis, and J. Wilcox, "A New Pure Palladium Electrodeposit for Electronic Applications" Paper presented at this conference.

FIGURE ONE

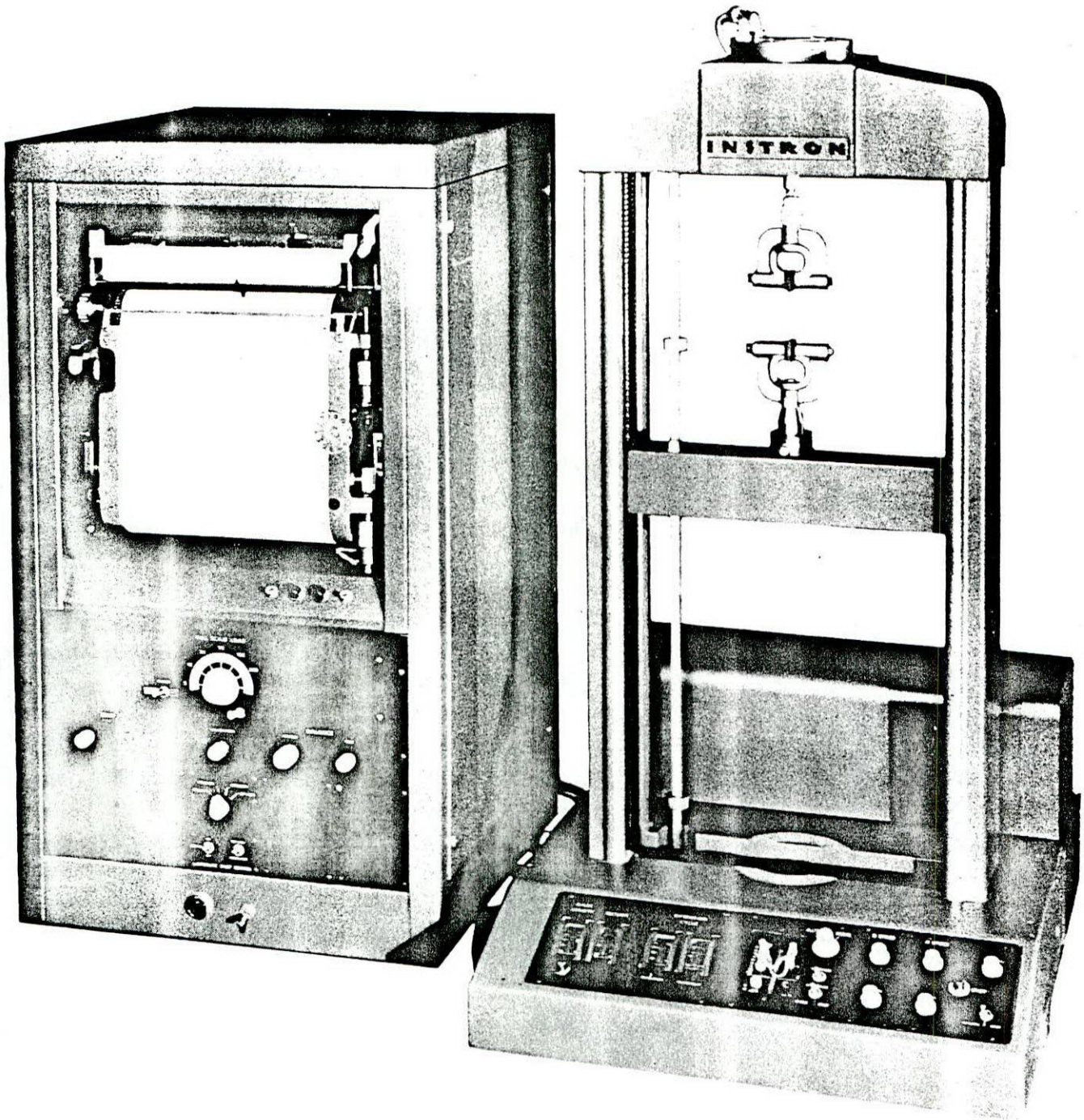


APPARATUS FOR PERFORMING UNIAXIAL TENSILE TESTING

FIGURE TWO

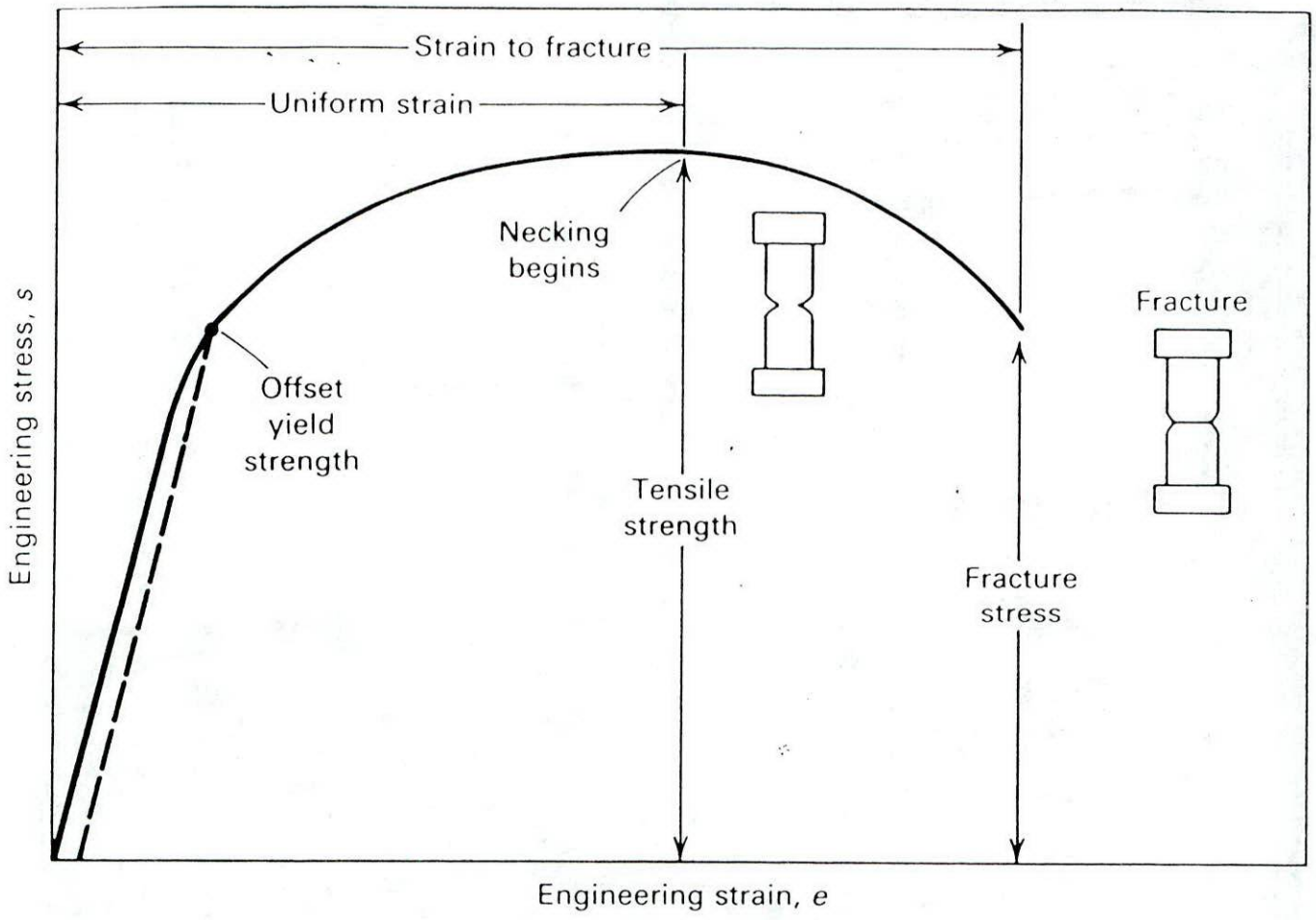


PLOT OF STRESS VERSES STRAIN OBTAINED FROM THE UNIAXIAL TENSILE TEST

FIGURE THREE

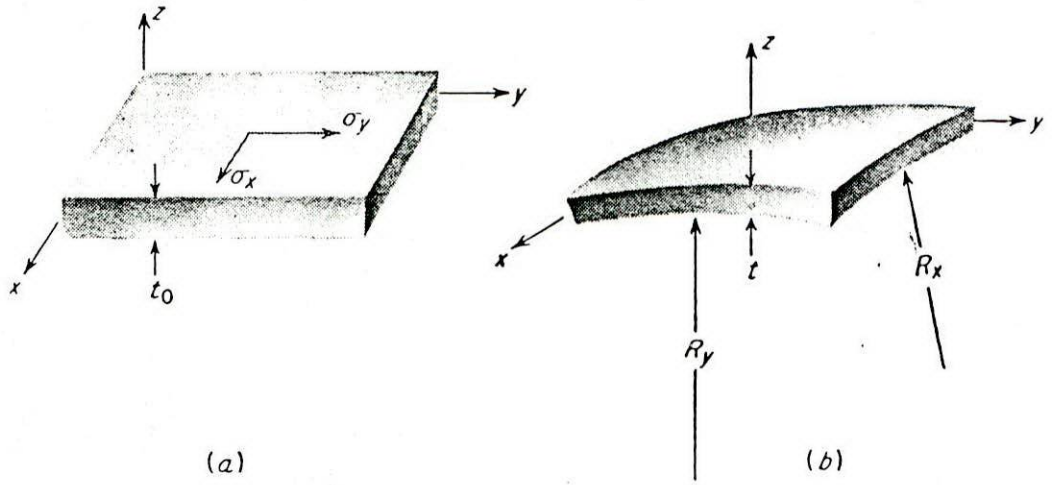


(a) Coordinate system for measuring biaxial stress in thin sheet; (b) curvature produced by removing material from top surface.

FIGURE FOUR

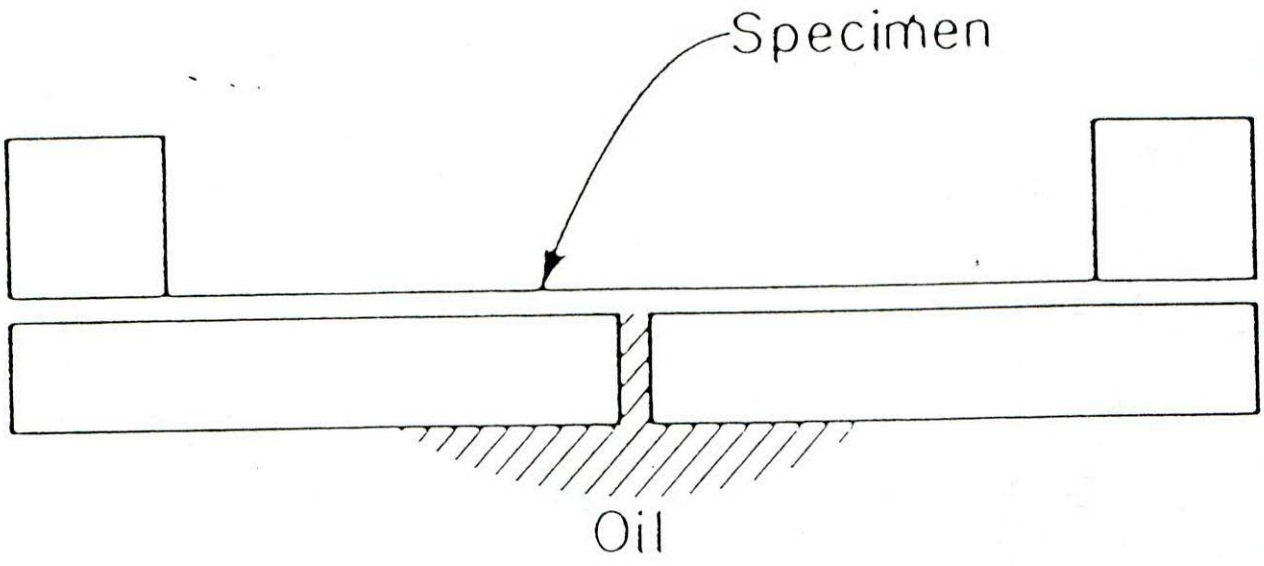


(a)

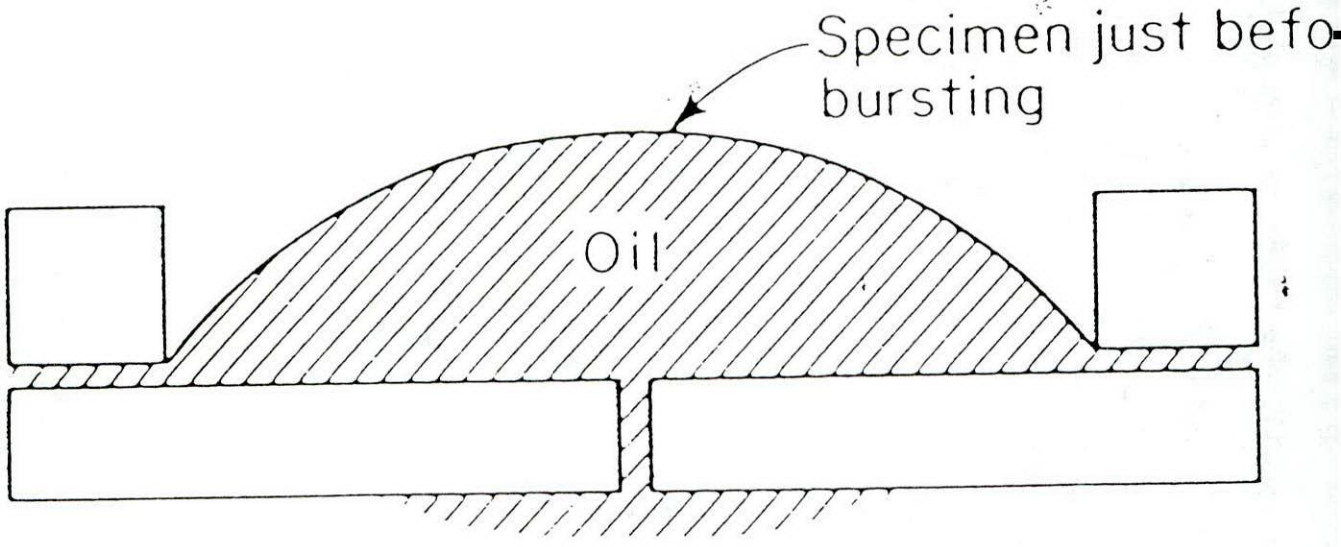


(b)

THE HYDRAULIC BULGE TEST

FIGURE FIVE

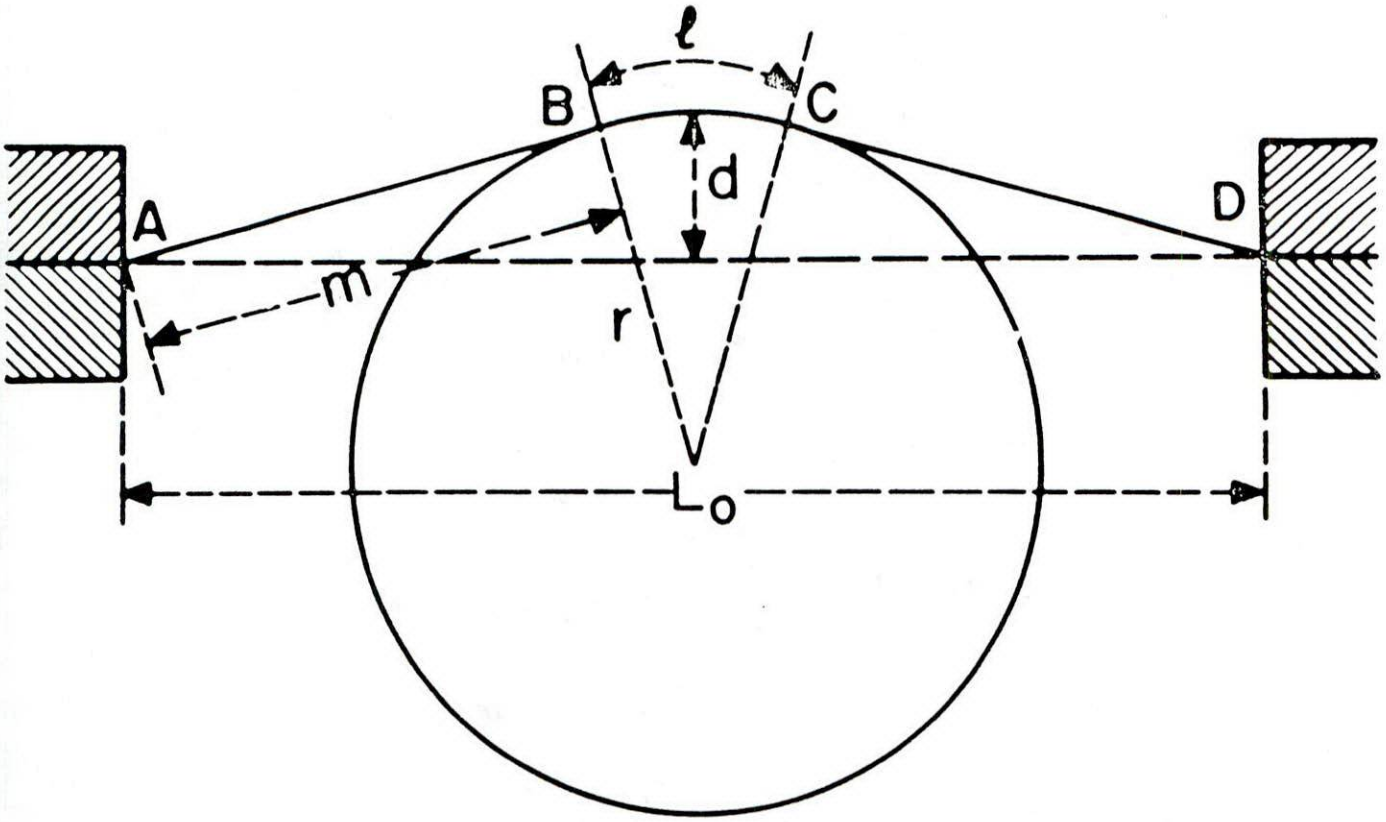


GEOMETRICAL RELATIONS FOR DETERMINING THE PERCENT ELONGATION AT FRACTURE USING THE BULGE TEST APPARATUS ILLUSTRATED IN FIGURE SIX.

FIGURE SIX

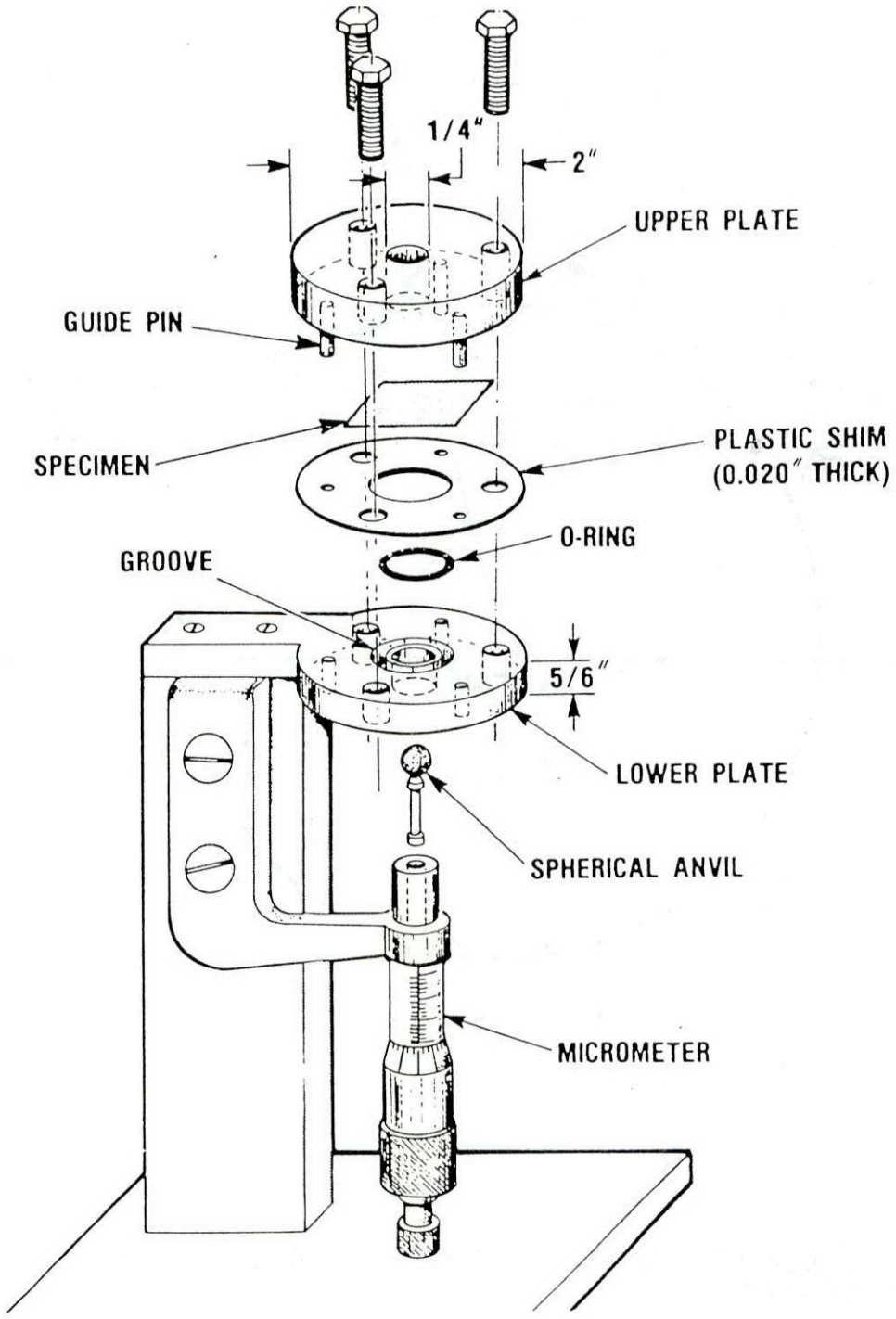


LABORATORY APPARATUS FOR PERFORMING ROUTINE BULGE TEST ON THIN FILM SPECIMENS (FROM REFERENCE 7)

FIGURE SEVEN

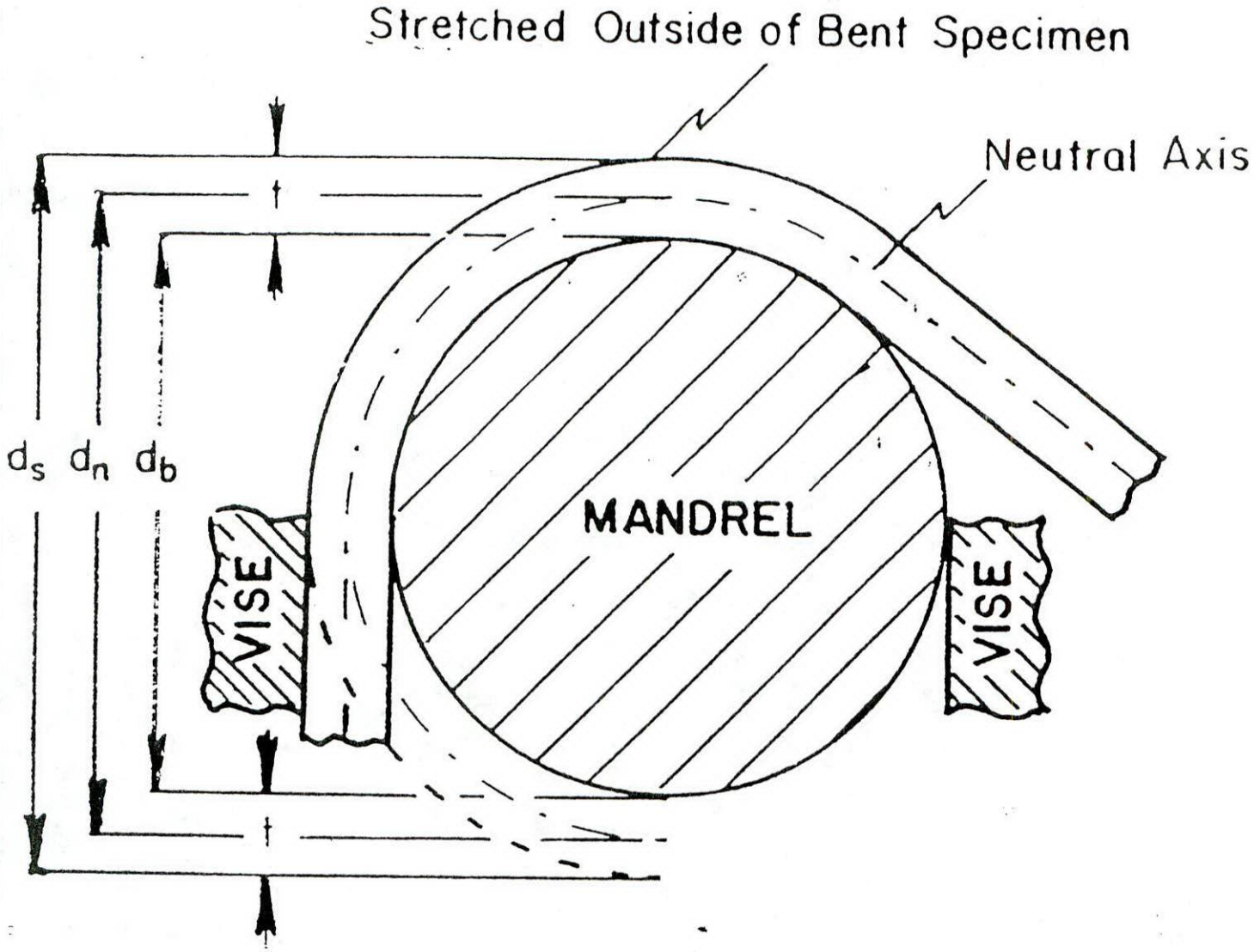


ILLUSTRATION OF THE BASIC SETUP OF ALL SUPPORTED BEND TESTS.

FIGURE EIGHT

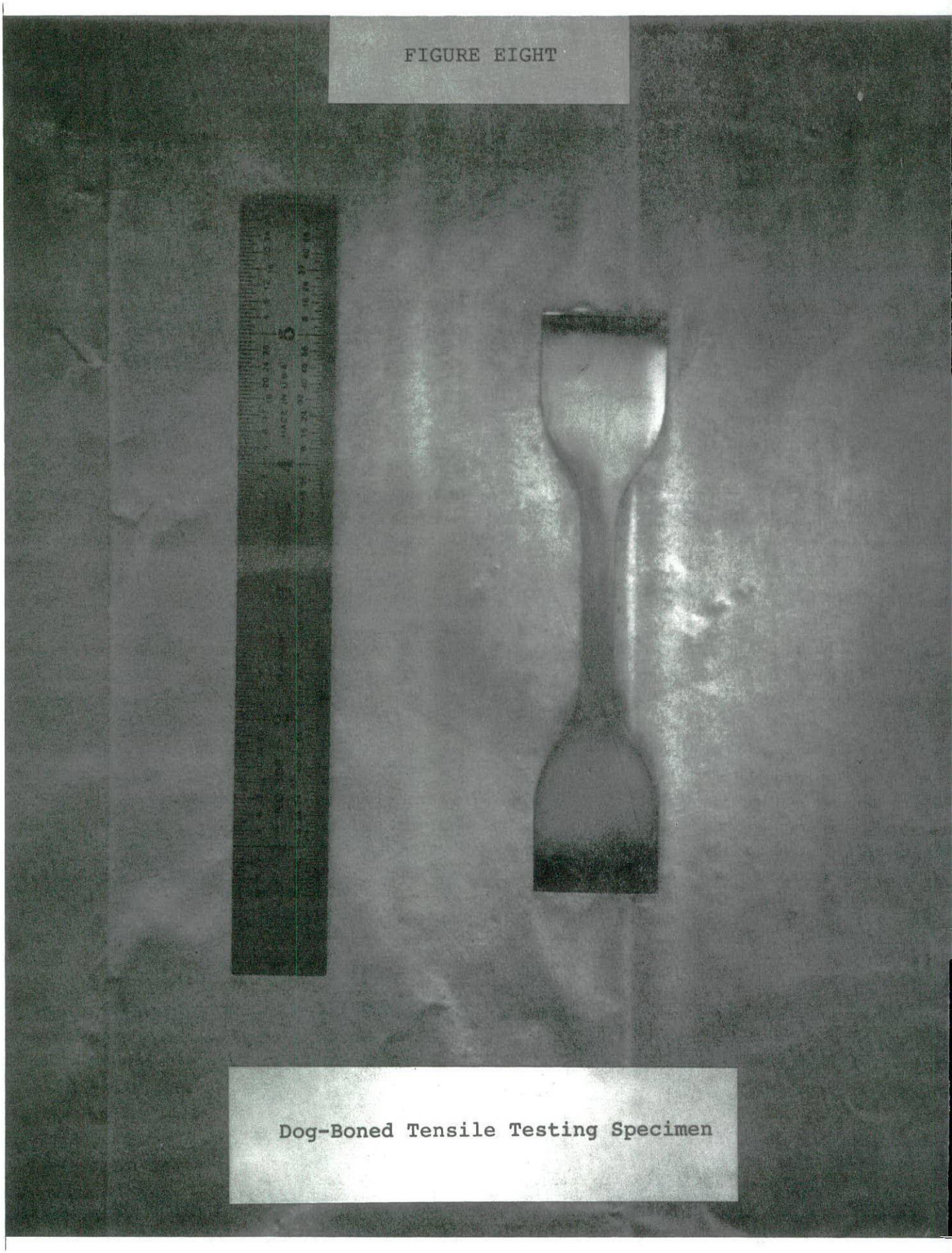

Dog-Boned Tensile Testing Specimen

D-1

# Environmental I
# Session D

## An Effective Approach to Regulatory Compliance—Program Development and Implementation

Arthur N. Mabbett
Mabbett, Capaccio & Associates, Inc.
5 Alfred Circle
Bedford, MA 01730

# AN EFFECTIVE APPROACH TO REGULATORY COMPLIANCE-PROGRAM DEVELOPMENT AND IMPLEMENTATION

By
Arthur N. Mabbett
Mabbett, Capaccio & Associates, Inc.
5 Alfred Circle, Bedford, MA 01730

## Introduction

Manufacturing industry must ensure its continued compliance with existing environmental pollution control and occupational safety and health statutes, as well as future regulations as they are promulgated. Failure to do so can have potentially catastrophic impact on the natural environment, employee health, local area populations, corporate and personal/individual liability.

Increased regulatory enforcement at the local, state, and Federal levels necessitates that each manufacturer carefully assess its current operations, policies, and procedures to help ensure a facility's continued compliance, reduction and/or elimination of risk and potential liability. Both civil administrative as well as criminal penalties provide further incentive to establish a formal regulatory compliance program.

This paper presents an overall approach to effective regulatory compliance based on our extensive experience in serving the needs of manufacturing industry.

Compliance activities should be cost effective and have a positive impact on the day-to-day operations of a manufacturer. Programs must be tailored to meet each individual facility's needs. The primary objective of any such program is to help ensure continued regulatory compliance in the most cost effective manner using existing and available resources without having an adverse impact on the company's manufacturing operations. The program must be formally established and implemented by management on a consistent basis to help ensure that it becomes part of the company's routine activities. Individual department managers and supervisors must realize that they have primary responsibility to ensure continued and effective implementation of the company's regulatory compliance program. Such individuals must be held accountable by senior management or else the program will not succeed.

The following activities are essential elements to develop and implement an effective regulatory compliance program.

## Know Your Regulatory Requirements

The first step in the development of a regulatory compliance program must be the definition of applicable environmental pollution control (i.e. air, water, and hazardous waste), and occupational safety and health laws and regulations. Every manufacturer must determine which local, state, and Federal statutes apply to the process operations completed at its facility.

Upon definition of applicable regulations, the manufacturer should obtain a copy of the regulation for internal use and reference. Keeping up-to-date can be a continuing dilemma, however, there are solutions! Subscribe to selected periodicals and technical journals to include the subscription service offered by the National Technical Information Service, 5285 Port Royal Road, Springfield, VA 22161, for OSHA's Standards Relating to Labor, 29 CFR Parts 1900 to 1910; and such commercial sources as the Bureau of National Affairs, Environment Reporter and OSH Reporter. Most state regulatory agencies publish newsletters to keep industry informed of regulatory requirements and proposed statutes. Each manufacturer should contact the Public Affairs Office of its state agency and be sure it is placed on the mailing list for newsletters and other technical publications.

Manufacturers should also establish a basic library applicable to its process operations and regulatory requirements. Reference texts, if utilized by a facility's staff, can help ensure process completion in such a manner that environmental pollution control, and health and safety impacts are minimized. Technical publications can also assist responsible personnel to efficiently operate installed pollution control systems, particularly industrial wastewater and air pollution control.

## Itemize Your Permits

It is not uncommon for many manufacturers to approach environmental permitting and/or permit requirements in a somewhat haphazard manner. In order to eliminate the possibility of missing a specific permit submittal and/or renewal date, a manufacturer should prepare a master list of all environmental permits issued to its facility. The list should identify the issuing agency; date issued; permit number(s); the effective period; renewal and expiration dates. The master permit list should also detail specific permit requirements. Permit conditions, periodic monitoring, and reporting requirements should be clearly identified. Preparation of this list and updates as existing permits are renewed or modified, and new permits issued, will allow management to monitor compliance status in an efficient manner.

## Develop An Effective Relationship With Control Authorities

A primary activity in the development and implementation of a successful regulatory compliance program must be the establishment of effective relationships with local, state, and regional control authorities. Our experience indicates that there are eight essential elements to develop such relationships. These elements are:

1. Establish good communications;
2. Develop an honest relationship;
3. Communicate on a periodic basis;
4. Negotiate from a position of strength;
5. Educate yourself and your staff;
6. Educate environmental authorities;

7. Participate in the standard development process; and
8. Obtain professional assistance, if necessary.

Understanding and accepting the fact that communications on a continuing basis with regulatory agencies are essential, will help to mitigate misunderstandings and the adversarial relationship that can often exist between a manufacturer and regulatory authorities. Developing and maintaining a positive relationship with environmental control authorities is a critical element of any regulatory compliance program. Failure to communicate can have significant adverse impact!

Recognize And Evaluate Deficiencies

All manufacturers should consider the completion of an initial Baseline and periodic Environmental Audits. The purpose of such audits are to:

1. Identify environmental pollution control, occupational safety and health areas of concern, and potential liabilities;
2. Assess current compliance status with applicable permitting requirements and appropriate local, state, and Federal laws and regulations; and
3. Develop recommendations to help reduce or eliminate potential/actual hazards, deficiencies, risk, and liabilities to the corporation, employees, and third parties.

The scope of an environmental audit should include an evaluation of such areas as:

1. General facility siting/location approvals;
2. Hazardous materials/waste management;
3. Water pollution control;
4. Air pollution control;
5. Occupational safety and health; and
6. Environmental/occupational safety and health program management.

An Environmental Operating Permit Audit is the most basic audit that all manufacturers should complete. The Operating Permit Audit identifies required environmental operating permits, and assesses compliance status with Orders of Condition, issued permits, and routine monitoring and/or reporting requirements. No new data is generated i.e., no sampling or laboratory analyses are performed. The Operating Permit Audit is primarily a review of regulatory requirements applicable to a facility and documents which have been issued.

Comprehensive Baseline Audits on the other hand, assess specific regulatory requirements as related to pollution control systems design and operation; operating policies and procedures related to basic facility work activities; training, recordkeeping, and reporting requirements; and selected aspects of facility design. The comprehensive Baseline Audit often includes completion of qualitative and/or quantitative sampling and laboratory analyses in order to help determine current compliance status.

Management Assessment

Another area for periodic auditing concerns the assessment of a facility's and/or a Corporation's management policies and procedures related to applicable environmental pollution control and occupational safety and health requirements. Management's awareness, sensitivity, development, and implementation of the regulatory compliance program is actually assessed. Interviews are conducted with selected management and supervisory personnel to gather required data. Findings are evaluated and the results discussed with senior management personnel at the local facility and/or Corporate level.

Any company contemplating the implementation of an Environmental Audit program should be committed to the correction of any noted deficiencies identified during the audit. Failure to implement follow-up actions can be considered by some regulatory agencies as willful and/or criminal intent. In addition, under certain circumstances, an Environmental Audit may be conducted through a corporation's legal counsel, if it is deemed necessary in the counsel's opinion, to establish a client-lawyer privilege. It is therefore recommended that companies contemplating the implementation of Environmental Audit programs, discuss the program in advance with their legal counsel.

Companies possessing experienced environmental and safety and health professionals can complete both initial Baseline and follow-up Audits. Professional consultants can be utilized for those companies who do not have adequate internal resources, who desire an objective third party to initially determine Baseline Compliance status, and/or to train internal personnel. Companies should carefully screen any third party consultant to be sure the consultant has direct experience and a proven track record serving a company's particular industry.

Audit follow-up can include the completion of special studies, surveys, design, and/or the development of administrative control programs. Implementation timetables should be established and management should periodically review progress to ensure the timely correction of noted deficiencies. Environmental Audits can serve as the basis for a plan to bring a facility into compliance over a defined period of time.

Compliance Strategies

Based on the results of either an internally or externally completed Environmental Baseline Audit, a company can define its compliance strategy. Three primary areas should be considered:

1. Administrative and management control procedures;
2. Waste minimization; and
3. Design of pollution control or hazard reduction-elimination systems.

Administrative and management control procedures can include the development of personal protective equipment-use programs to include vision,

hearing conservation, and respiratory protective equipment; Hazard Communication; hazardous waste management contingency plan; and wastewater pretreatment system operation and maintenance manual, etc.

Waste minimization techniques generally focus on the reduction of pollutant quantities via chemical and/or process substitution and modification, recycling, reuse and recovery, and alternative treatment techniques.

The design of any pollution control or hazard reduction-elimination system should involve the technical evaluation of various options. Cost analyses should be conducted to include initial capital, installation, operation and maintenance, and liability-risk potential. Based on these factors, a decision is made and final design engineering and construction can occur. The completion of an engineering evaluation or the final design of a pollution control system should only be completed by an experienced professional who has a proven track record.

Training Programs

The only way a company can ensure that both its production and management personnel are aware of specific regulatory requirements and internal policies and procedures is to develop and implement an on-going training program. Training is conducted for a number of reasons to include:

1. Preparing an individual for their specific job/position requirements;
2. Keep up-to-date regarding changing technology, new regulations, and/or company policies and procedures;
3. As a requirement of specific regulations (e.g., hazardous waste management, hazard communication, etc.); and
4. Attitude development.

Training influences human behavior and can encourage safe job performance by helping individuals to develop proper work procedures, teach the procedures effectively, assure that the procedures are followed and maintained, and as such can foster a positive work attitude.

Training programs must be consistently implemented and should occur when:

1. New employees are hired;
2. New processes or equipment is introduced into the facility;
3. Procedures have been revised or developed;
4. Employee performance requires improvement; or
5. New information must be made available to personnel.

In order to develop an effective training program, four primary areas should be considered: definition of training needs; program objectives; course materials; and training methods. Training programs should include a balance between external seminars and conferences as well as in-house continuing education programs.

Checks and Balances

Management should establish a system of checks and balances to help ensure successful implementation of the regulatory compliance program. Routine coordination and approvals should be required where necessary. Examples include: centralized chemical procurement; approval to modify an existing process operation or to purchase a new chemical not already on an approved chemical list; and authorization to dump a concentrated and/or new process bath to the wastewater treatment system.

Management reviews should also be conducted at various levels within the organization. Environmental and occupational safety and health (OSH) justification(s) should be a part of a company's equipment procurement program. Periodic status reports of actions taken to correct noted deficiencies should be provided to management. Environmental pollution control and OSH considerations should be included as part of the employee/ personnel review process.

Unannounced inspections, evaluations, and audits of production areas should be routinely completed. Such activities can be conducted on a daily or weekly basis by the immediate area supervisor or periodically i.e., quarterly by a department representative. Annual Audits can be completed by Corporate management or by an outside third party professional consultant.

Case Studies

A company with facilities in over fifteen different states, implemented a comprehensive Environmental Operating Permit and a Baseline Hazardous Waste Management Audit program over a two year period. The results of the audit identified specific deficiencies at each of the local facilities. The audit also noted areas where the establishment of Corporate policies and procedures could alleviate unnecessary duplication and help to ensure regulatory compliance at the local level. Facility managers are responsible to inform Area Vice Presidents of actions completed to correct deficiencies identified during the audit. The Corporate Office has begun to develop specific written program documents and guidance for local facility use. An example of such a Corporate program has been the establishment of a "Spill Prevention Control and Counter Measures Plan" as required by the Federal Clean Water Act.

In another case, a Corporation desired to obtain an independent third party professional appraisal of its metal finishing/electroplating process operations at one of its out-of-state facilities. Local management had reported to the Corporate Office that the facility was in substantial regulatory compliance. The Corporate Office however, wanted to verify actual compliance status and as such, commissioned a comprehensive Environmental Operating Permit and Baseline Audit in the areas of water and air pollution control, hazardous waste management, and occupational safety and health. Upon completion of the audit, a comprehensive report was provided which indicated that significant permitting, operation, and

pollution control system design deficiencies existed at the local facility. The Corporate Office and local facility are currently utilizing the Audit to develop both short and long-term plans, goals, and objectives to bring the facility into compliance.

## Conclusion

The development and effective implementation of a regulatory compliance program should be an integral basic management function. Such programs can help to identify and correct internal deficiencies before they adversely affect regulatory compliance status. Implementation of a regulatory compliance program can also help to eliminate the "crisis-fire-fighting" mode of operation common to many companies. Management's endorsement of the approach outlined herein makes good business sense. Failure to recognize the value of this approach can have serious financial and liability impacts for both the corporation, individual employees, and third parties.

D-2

# Environmental I
# Session D

## Plating Wastewater Discharge Compliance Using Integrated Microfiltration Technology

David J. Gworek, P.E.
Cert Water Services, Inc.
25 Duval Lane
Plainville, CT 06062

# PLATING WASTEWATER DISCHARGE COMPLIANCE USING INTEGRATED MICROFILTRATION TECHNOLOGY

By: David J. Gworek, P.E.
Cert Water Services, Inc.
25 Duval Lane
Plainville, CT 06062

The National Pollutant Discharge Elimination System (NPDES) permit limits for metals and suspended solids that all direct dischargers are required to meet was an ongoing challenge for Litton-Winchester Electronics, located in Oakville, Connecticut. The company is one of the largest electronic connector manufacturers in the country and a division of Litton Systems, Inc. They take pride in their efforts to comply with all environmental regulations, especially the very visible wastewater treatment discharge permit limits.

The latest permit issued in 1985 by the Connecticut Department of Environmental Protection (DEP) required stricter limits for the metals being discharged. These metals included nickel, copper, gold, and lead. (See Table #1). The limits included a Maximum Instantaneous Concentration which is the highest allowable concentration for any grab sample, a Maximum Daily Concentration (MDC) which is the highest allowable concentration for a daily composite sample, and an Average Monthly Concentration (AMC) which is the highest allowable concentration determined by the arithmetic average of all daily composite samples.

Litton-Winchester made a commitment in mid 1986 to investigate all possible filtration options. The objectives were to assure compliance 100 per cent of the time, assure metal was low enough to achieve compliance with the upcoming biotoxicity requirements and limits and initiate a first step toward rinsewater recycling and "closed loop" operation for the future.

TABLE #1
(NPDES Permit Limits)

| Parameter | Average Monthly Concentration (mg/1) | Max. Daily Concentration (mg/1 | Max. Instantaneous Concentration (by grab sample) (mg/1) |
|---|---|---|---|
| Copper | 1.0 | 2.0 | 3.0 |
| Nickel | 1.0 | 2.0 | 3.0 |
| Gold | 0.1 | 0.5 | 0.75 |
| Lead | 0.1 | 0.5 | 0.75 |
| Total Suspended Solids | 20.0 | 30.0 | 45.0 |
| Cyanide Amenable | 0.1 | 0.2 | 0.3 |
| pH | | 6.50-9.50 | |

The existing plating process and waste treatment operations were reviewed in full to determine what might be done to eliminate pollutants or improve the operation of the treatment system. The conventional treatment system utilized sodium hydroxide for metal hydroxide precipitation, along with a calcium chloride and aluminum chloride mixture to assist in the precipitation/coagulation process, and finally, an anionic polymer for flocculation and aid in settling. Chemical treatment alternatives were evaluated for more effective removal. As results from lab tests were not encouraging it was decided that a chemical treatment change was not going to be made as part of the evaluation and system upgrading proposal.

We concluded that the most straight forward and effective method for metals and suspended solids removal from our treated wastewater would be any one of various advanced filtration technologies. Three filtration systems were evaluated; a Diatomaceous Earth (DE)/Magnesium Silicate precoat filter, a DE/Sulfide precoat filtration system and a membrane microfiltration system manufactured by Ionics, Inc.

The DE/Magnesium Silicate filter was evaluated by lab tests and pilot tests at Litton-Winchester Electronics. The initial lab tests showed promise in the suspended solids and metals removal. Suspended solids were reduced from approximately 20 to 30 ppm down to 2 to 5 ppm. The metals, including nickel, copper, and lead, were reduced by 30 to 50 percent. The subsequent pilot test that included one weeks operation on the actual treated wastewater just prior to discharge showed similar, but not quite as effective removal.

The DE/Sulfide filter was evaluated by lab tests performed at the manufacturer's facility. The tests, along with previous tests and operation data, showed that the suspended solids could be reduced by 80 to 90 percent and the metals by 40 to 90 percent. The suspended solids removal capabilities of this filter was identical to the DE/Magnesium Silicate filter. This was due to the fact that the filtration system equipment was virtually identical in technology. The difference in the metals removal capabilities was due to the controlled addition of sulfide to further precipitate excess metals, which would be removed as suspended solids. This sulfide technology was much more effective than the magnesium silicate technology in metals removal.

The final filtration system that was tested was the Ionics Enviromat$^{R}$ Integrated Membrane Microfiltration System with Aqua-Pore$^{R}$ membranes. This relatively new technology incorporates membrane cross flow filtration under relatively low pressure similar to ultrafiltration (UF) systems. Tests were made in Ionics lab and, also, with a pilot unit at Litton-Winchester Electronic's facility for a month. The results of both the lab and pilot tests were equivalent. The suspended solids removal was 90 to 100 percent, while the metals removal (nickel, copper, lead, and gold) was 80 to 100 percent.

A small quantity of activated carbon is added to the wastewater stream as it enters the microfiltration system to adsorb unwanted and chelating organics. This carbon effectively breaks down any chelating agents that may hold some metals in solution so the metals can be removed by the filtration. Data accumulated from the pilot testing provided the information required for proper sizing of a full scale filter system.

The first two DE filtration systems tested were end of the pipe technologies. That is, these systems would filter the water as it discharged from the settling tanks after complete treatment and settling of precipitate. This is a conventional approach to suspended solids filtration. The microfiltration system filters the water as it flows out of the neutralization tank prior to the polymer addition for flocculation. The metals are precipitated by the sodium hydroxide and calcium chloride/aluminum chloride and the particulate matter is large enough to be removed by the microfiltration. The polymer addition is not required and, in fact, would have a detrimental effect on the membrane filter tubes. The membrane microfiltration system eliminates the need for a flocculation tank and settling tanks.

In the Litton-Winchester conventional treatment system, the neutralization tank upstream of the flocculation and precipitation steps was used to control pH for the effluent water being discharged. All three systems that were evaluated would include a final pH adjustment tank after the filter to assure the pH is within the permitted limits. This final pH adjustment tank facilitates much greater control and ease of permit compliance for pH.

A final comprehensive evaluation was made based on projected costs and the testing results for all three filtration type systems. The results of this evaluation favored Ionics' Integrated Membrane Filtration System. During testing of the Ionics' pilot filter system measurements of metal concentrations for copper nickel gold and lead were made in our conventional system neutralization tank (feed to the microfiltration system) microfiltration system effluent discharge, and the conventional waste treatment system effluent discharge (WED). The average concentrations of metals in the neutralization tank during the testing period were nickel - 2.67 ppm, copper- 1.56 ppm, lead - 0.25 ppm, and gold - 0.12 ppm. The average concentrations for the microfiltration system effluent were nickel - 0.02 ppm, copper - 0.04 ppm, lead - non-detectable, and gold - 0.01 ppm, while at the same time the average concentrations for the conventional treatment system effluent were nickel - 1.23 ppm, copper - 0.77 ppm, lead - 0.04 ppm, and gold 0.14 ppm.

The advantages provided by the microfiltration system were as follows:

- Removal of organic materials that may be complexed with heavy metals.

- Prevention of temporary upset conditions in the settling tank which result in inadequate treatment.

- Provide an absolute particle barrier to ensure no periodic upsets resulting from the inherent ineffectiveness of gravitational settling.

- Provide a large safety margin in environmental pollution control, not only for the current discharge limits, but also for possibly more stringent limits should they be imposed in the future.

Following analysis of the options Litton-Winchester decided to incorporate the Enviromat equipment into their existing wastewater treatment system.

The installation of the Enviromat membrane filtration system required some modification of the conventional wastewater treatment system. This included the elimination of the need for the flocculation tank and the two settling tanks. Flow diagrams (Figures 1 & 2) illustrate the old conventional system and the changes made for the new system. The Ionics system was installed into the physical space made available by removal of one settling tank. The floc tank and other settling tank were retained in place to be used for flocculation and settling/solids removal in the event of an emergency situation. These provisions allowed for continuous operation and discharge of a properly treated effluent.

The original treatment system was designed to treat cyanide and acid/alkali bearing wastewaters from the electroplating of copper, nickel, gold, and tin-lead on electronic contacts and components. It consisted of a pH adjustment step followed by chlorination with sodium hypochlorite to destroy cyanide. Treated cyanide wastewater was then combined with all acid/alkali rinsewaters in a neutralization tank where pH was controlled in the 8.5 to 9.5 range by the addition of sulfuric acid or sodium hydroxide. A calcium chloride/aluminum chloride mixture was also metered into the neutralization tank to aid in precipitation of metals for removal.

The total flow from the neutralization tank, about 43 gallons per minute, flowed to a 500 gallon flocculation tank where an anionic polymer was added at a concentration of approximately 3 ppm.

The flocculated wastewater then flowed through two 3900 gallon rectangular settling tanks in series. Prior to discharge, the water was filtered through 25 micron cartridge filters to remove any suspended solids that had not settled.

This treatment system was adequate most of the time to comply with the permit limits, but the system was labor and cost intensive and not able to compensate well for upsets or flow surges and lulls. The filter cartridges were changed two times per day to allow for the best suspended solids removal. The use of the anionic polymer was expensive and finicky depending on the level and types of contaminants in the water. The sludge that was removed from the bottom of the settling tanks and dewatered in a filter press was very gelatinous and difficult to dewater with a typical solids content of 20 percent.

Integrating the Enviromat membrane microfiltration system did not require any change to our basic treatment system chemistry or equipment prior to the flocculation tank. In other words, the cyanide pH adjustment cyanide chlorination, cyanide reaction, and neutralization tanks, their equipment and treatment chemicals remained the same. The changes came into play starting with the flocculation tank where the anionic polymer was no longer used (except for emergency backup). A secondary pH controller with an acid and caustic pump was added to polish the pH and keep it at the desired level prior to introduction into the microfiltration system.

The wastewater then flowed to the microfiltration system recirculation tank. Activated carbon is added into this tank on a daily basis to remove excess organic materials that may affect the precipitation of metals and to assist in the cleaning process of the microfiltration membranes. The carbon provides a mechanical scrubbing action on the membrane surface. Approximately 200 gallons of 3 to 5 percent solids are pumped on a daily basis from the microfiltration system recirculation tank into a sludge holding tank for dewatering.

The wastewater in the recirculation tank is pumped through the microfilter itself which contains 16 modules with 37, 0.5 inch diameter, by 3 foot long Aqua-Pore membrane tubes. These tubes are the key to the system. They provide a positive barrier against all particles while delivering a clean effluent that is guaranteed by the vendor to meet the NPDES permit limits. (See Figure #3). The microfiltration membranes are made of an inert porous substructure on the outside with a thin teflon based film on the inside. The thin film provides the 0.1 micron filtration and allows the tubes to withstand a wide pH range (1-14), oxidative, corrosive environment, and the harsh condition of industrial wastewater.

The system is capable of handling flows of 40 to 60 gpm. The influent feed water from the recirculation tank is pumped through the membrane modules at a rate of 350 to 400 gpm and 35 to 40 psi.

The pressure drop through the membrane modules is approximately 10 psi. The tubular configuration of the membrane is used to minimize fouling by maintaining a turbulent cross flow pattern that scrubs the solids from the membrane surface. This allows for effective filtration and concentration of the precipitated metals and contaminants to 5 percent solids or more.

Gradual membrane fouling does occur during the operation of the membrane microfilters. This fouling reduces the flux rate, thus requiring cleaning. The system at Litton-Winchester Electronics is cleaned once per week or when the effluent flow falls below 40 gpm. A solution of weak nitric acid is pumped through the membrane modules for 30 to 60 minutes after first flushing the modules with tap water. The nitric acid cleaning solution is recirculated in the same flow pattern as the wastewater. After the cleaning acid is used several times, it is pumped to the sludge holding tank after batch neutralization with sodium hydroxide.

The effluent from the microfilter goes into a final neutralization tank in which pH is adjusted to within the NPDES permit limits of 6.5 to 9.5. The water from this tank is then discharged directly to a brook.

The total suspended solids in the effluent has averaged 1.6 mg/l since the installation of the Enviromat Integrated Membrane Filtration System. Metals concentrations have averaged as follows: Copper - 0.03 mg/l; Nickel - 0.06 mg/l; Gold - 0.01 mg/l; Lead - less than 0.01 mg/l. These average concentrations are from the period of 8/3/87 to 1/18/88 with samples taken three times a day during the first shift. The same parameters were analyzed from 3/20/87 to 7/17/87 prior to the installation of the microfilter with the following average results: Total Suspended Solids - 13.4 mg/l; Copper - 0.61 mg/l; Nickel - 0.94 mg/l; Gold - 0.12 mg/l; Lead - 0.02 mg/l. Table #3 shows the comparison of these results, along with the range of concentrations and the average percent reduction with conventional treatment and with the integrated microfiltration system.

TABLE #3

Comparison of actual sample data with conventional treatment and with the Enviromat integrated microfiltration approach.

| Parameter / Dates- | Feed Concentration 3/20/87-1/18/88 | | Conventional Treatment (mg/l) 3/20/87-7/17/87 | | |
|---|---|---|---|---|---|
| | mean | range | mean | range | percent reduction |
| Copper (mg/l) | 1.50 | 0.06-7.58 | 0.61 | 0.03-5.34 | 59.3 |
| Nickel (mg/l) | 7.85 | 0.90-16.75 | 0.94 | 0.00-5.14 | 88.0 |
| Gold (mg/l) | 0.15 | 0.00-1.89 | 0.12 | 0.00-0.70 | 20.0 |
| Lead (mg/l) | 0.04 | 0.00-1.10 | 0.02 | 0.00-0.87 | 50.0 |
| Total suspended solids (mg/l) | - | - | 13.4 | 1.4-37.1 | - |

| | Microfiltration (mg/l) 8/3/87-1/18/88 | | |
|---|---|---|---|
| | mean | range | Percent reduction |
| Copper (mg/l) | 0.03 | 0.00-0.50 | 98.0 |
| Nickel (mg/l) | 0.06 | 0.00-0.84 | 99.2 |
| Gold (mg/l) | 0.01 | 0.00-0.20 | 93.3 |
| Lead (mg/l) | 0.00 | 0.00-0.11 | 97.5 |
| Total suspended solids (mg/l) | 1.6 | 0.4-6.6 | - |

The sludge that is generated from the solids removed from the microfiltration system is higher in solids content than the conventional treatment sludge due to the concentrating effect of the membrane filtration system. Typically, prior to dewatering in the filter press, the conventional treatment sludge had a solids content of 0.5 to 1.5 percent, while the sludge from the microfilter's recirculation tank is 3 to 5 percent solids. A typical sludge sample from each process was analyzed for solids and metals concentration after dewatering. The results, Table #4, show a two fold increase in concentration for these parameters. The increased solids contents, 41.5 percent, is more desirable, easier to handle, and less costly to dispose of. The substantial decrease

in the copper and lead concentrations in the microfilter sludge may be due to several factors at the time the sludge samples were taken. The plating production of these metals could have been reduced, better dragout control of these plating solutions, or possibly, adsorption onto the activated carbon portion of the sludge which was not dissolved or digested in the analysis.

TABLE #4

Dewatered sludge analysis comparison

| Parameter | Sludge by Conventional Treatment | Sludge by Microfiltration |
|---|---|---|
| Total solids (wt %) | 16.7 | 41.5 |
| Nickel (lb/ton) | 12.7 | 25.7 |
| Copper (lb/ton) | 18.0 | 4.3 |
| Gold (T.O./ton) | 0.78 | 1.69 |
| Lead (lb/ton) | 1.5 | 0.7 |

The sludge volume that was shipped for disposal was reduced with the microfiltration system. The first half of 1987 saw 8-1/2 tons of sludge sent for disposal while utilizing conventional treatment. The second half of the year, utilizing the microfiltration system, saw 6 tons of sludge being generated. This reduction can be attributed mainly to the increased solids content of the dewatered microfiltration sludge.

Installation of the Enviromat Integrated Membrane Microfiltration System enabled Litton-Winchester Electronics to meet all their goals that had been set. Permit compliance was attainable 100 percent of the time, the metal limits were sufficiently low so that compliance with biotoxicity requirements and limits was also attainable, and finally, the microfiltration system provided the initial step for water recycle and reuse. This last step can be achieved in the future by the installation of electrodialysis, ion exchange or reverse osmosis technology.

The key to both conventional wastewater treatment systems and those incorporating membrane microfiltration is correct pretreatment chemistry to ensure complete cyanide destruction and total precipitation of metal contaminants. The advantage of the microfiltration system is that it is not prone to the problems associated with the conventional system such as the need for consistency of wastewater loading, hydraulic loading and flocculation. In addition it results in a significant improvement in the quality of treated wastewater effluent while at the same time reducing the volume of sludge resulting from the pretreatment chemistry.

| DAY & TIME | PARAMETER | LITTON-WINCHESTER ELECTRONICS NEUTRALIZATION TANK/IONICS FILTER FEED | IONICS FILTER PRODUCT | PERCENT REDUCTION FROM FEED | ACTUAL WED DISCHARGE | PERCENT REDUCTION FROM NEUTRALIZATION TANK |
|---|---|---|---|---|---|---|
| | | (ppm) | (ppm) | | (ppm) | |
| 2:00 P.M. | Ni | 3.06 | ND | 100.00 | 0.96 | 68.60 |
| | Cu | 1.92 | 0.01 | 99.50 | 0.85 | 55.70 |
| | Pb | 0.03 | ND | 100.00 | 0.02 | 33.30 |
| | Au. | 0.26 | ND | 100.00 | 0.14 | 46.20 |
| Day 27 2:00 P.M. | Ni | 1.31 | ND | 100.00 | 0.89 | 53.40 |
| | Cu | 1.11 | ND | 100.00 | 0.49 | 55.90 |
| | Pb | 0.02 | ND | 100.00 | 0.06 | NR |
| | Au. | 0.06 | ND | 100.00 | 0.26 | NR |
| Day 28 11:00 A.M. | Ni | 1.65 | 0.16 | 90.3 | 0.97 | 41.20 |
| | Cu | 1.73 | ND | 100.00 | 0.94 | 45.70 |
| | Pb | 0.22 | ND | 100.00 | 0.09 | 59.10 |
| | Au. | 0.08 | 0.01 | 87.50 | 0.12 | NR |
| 2:20 P.M. | Ni | 1.73 | 0.09 | 94.80 | 0.77 | 55.50 |
| | Cu | 1.75 | 0.05 | 97.10 | 0.69 | 60.60 |
| | Pb | 0.09 | ND | 100.00 | 0.04 | 55.60 |
| | Au. | 0.60 | 0.01 | 98.30 | 0.08 | 86.70 |
| Day 30 10:00 A.M. | Ni | 1.70 | 0.02 | 98.80 | 0.82 | 51.80 |
| | Cu | 1.28 | 0.04 | 96.90 | 0.47 | 63.30 |
| | Pb | 0.24 | ND | 100.00 | 0.03 | 87.50 |
| | Au. | 0.08 | 0.05 | 37.50 | 0.09 | NR |

OVERALL AVERAGES

| | | Min. | Avg. | Max. | Min. | Avg. | Max. | | Min. | Avg. | Max. | |
|---|---|---|---|---|---|---|---|---|---|---|---|---|
| DEC-23-86 THRU JAN-23-87 | Ni | 0.68 | 2.67 | 6.08 | ND | 0.02 | 0.17 | 99.30 | 0.56 | 1.23 | 2.87 | 53.90 |
| | Cu | 0.30 | 1.56 | 5.65 | ND | 0.04 | 0.15 | 97.40 | 0.12 | 0.77 | 1.92 | 58.60 |
| | Pb | ND | 0.25 | 2.94 | ND | ND | 0.02 | 100.00 | ND | 0.04 | 0.09 | 84.00 |
| | Au | ND | 0.12 | 0.66 | ND | 0.01 | 0.06 | 91.70 | ND | 0.14 | 0.52 | NR |

TABLE #2

IONICS PILOT FILTER EVALUATION

| DAY & TIME | PARAMETER | LITTON-WINCHESTER ELECTRONICS NEUTRALIZATION TANK/IONICS FILTER FEED | IONICS FILTER PRODUCT | PERCENT REDUCTION FROM FEED | ACTUAL WED DISCHARGE | PERCENT REDUCTION FROM NEUTRALIZATION TANK |
|---|---|---|---|---|---|---|
| | | (ppm) | (ppm) | | (ppm) | |
| Day 1 8:15 A.M. | Ni | 0.65 | ND | 100.00 | 1.53 | NR |
| | Cu | 0.55 | 0.12 | 78.20 | 0.85 | NR |
| | Pb | 0.19 | 0.02 | 89.50 | 0.09 | 52.60 |
| | Au. | 0.03 | -- | -- | 0.23 | NR |
| 9:30 A.M. | Ni | 3.42 | ND | 100.00 | -- | -- |
| | Cu | 3.36 | 0.09 | 95.60 | -- | -- |
| | Pb | 0.38 | ND | 100.00 | -- | -- |
| | Au. | 0.58 | 0.06 | 89.70 | -- | -- |
| 1:20 P.M. | Ni | 2.58 | ND | 100.00 | 0.67 | 74.00 |
| | Cu | 1.52 | 0.15 | 90.10 | 0.59 | 67.10 |
| | Pb | 0.14 | ND | 100.00 | 0.04 | 71.40 |
| | Au. | 0.14 | ND | 100.00 | 0.10 | 28.60 |
| | | Started w/Carbon Treatment | | | | |
| Day 14 2:30 P.M. | Ni | 1.32 | ND | 100.00 | 0.05 | 20.50 |
| | Cu | 1.30 | 0.04 | 96.90 | 1.10 | 15.40 |
| | Pb | 0.34 | ND | 100.00 | 0.06 | 82.40 |
| | Au. | 0.05 | ND | 100.00 | 0.09 | NR |
| Day 15 8:45 A.M. | Ni | 2.40 | ND | 100.00 | 0.56 | 76.70 |
| | Cu | 0.52 | 0.01 | 98.01 | 0.12 | 76.90 |
| | Pb | 0.44 | ND | 100.00 | ND | 100.00 |
| | Au. | 0.06 | ND | 100.00 | 0.07 | NR |

KEY: NR = NO REDUCTION SEEN
ND = NON DETECTABLE BY FLAME ATOMIC ABSORPTION(AA) (VARIAN 1475)
LOWEST DETECTION LIMITS ARE AS FOLLOWS --

NICKEL (Ni) = 0.01 ppm COPPER (Cu) = 0.003 ppm
LEAD (Pb) = 0.01 ppm GOLD (Au) = 0.01 ppm

| DAY & TIME | PARAMETER | LITTON-WINCHESTER ELECTRONICS NEUTRALIZATION TANK/IONICS FILTER FEED | IONICS FILTER PRODUCT | PERCENT REDUCTION FROM FEED | ACTUAL WED DISCHARGE | PERCENT REDUCTION FROM NEUTRALIZATION TANK |
|---|---|---|---|---|---|---|
| | | (ppm) | (ppm) | | (ppm) | |
| 2:30 P.M. | Ni | 3.20 | ND | 100.00 | 1.17 | 63.40 |
| | Cu | 0.61 | 0.02 | 96.70 | 0.72 | NR |
| | Pb | 0.03 | ND | 100.00 | 0.02 | 33.30 |
| | Au. | 0.08 | 0.03 | 62.50 | 0.09 | NR |
| Day 20 9:30 A.M. | Ni | 2.78 | ND | 100.00 | 0.69 | 9.70 |
| | Cu | 0.41 | 0.01 | 97.60 | 0.37 | 5.90 |
| | Pb | ND | ND | NR | 0.04 | 61.90 |
| | Au. | 0.26 | ND | 100.00 | 0.15 | 43.30 |
| 1:00 P.M. | Ni | 6.08 | ND | 100.00 | 0.91 | 85.00 |
| | Cu | 5.65 | 0.03 | 99.50 | 0.63 | 88.80 |
| | Pb | 2.94 | ND | 100.00 | 0.03 | 99.00 |
| | Au. | 0.22 | ND | 100.00 | 0.08 | 63.00 |
| Day 22 10:30 A.M. | Ni | 3.08 | ND | 100.00 | 1.41 | 53.90 |
| | Cu | 0.86 | ND | 100.00 | 0.61 | 29.10 |
| | Pb | ND | ND | 100.00 | 0.05 | NR |
| | Au. | 0.16 | 0.01 | 93.80 | 0.22 | NR |
| 12:30 P.M. | Ni | 3.39 | ND | 100.00 | 1.42 | 58.10 |
| | Cu | 1.80 | 0.04 | 97.80 | 0.61 | 66.10 |
| | Pb | 0.02 | ND | 100.00 | 0.05 | NR |
| | Au. | 0.26 | ND | 100.00 | 0.22 | 15.40 |
| 2:30 P.M. | Ni | 3.70 | ND | 100.00 | 0.84 | 77.30 |
| | Cu | 1.33 | 0.02 | 98.50 | 0.56 | 57.90 |
| | Pb | 0.06 | ND | 100.00 | 0.02 | 66.70 |
| | Au. | 0.41 | 0.03 | 92.70 | 0.14 | 65.90 |
| Day 23 9:00 A.M. | Ni | 3.46 | ND | 100.00 | 2.63 | 24.00 |
| | Cu | 1.65 | 0.02 | 98.80 | 1.51 | 8.50 |
| | Pb | 0.03 | ND | 100.00 | ND | 100.00 |
| | Au. | 0.26 | ND | 100.00 | 0.52 | NR |
| 11:00 A.M. | Ni | 2.96 | ND | 100.00 | 1.98 | 33.10 |
| | Cu | 1.85 | 0.02 | 98.90 | 1.22 | 34.10 |
| | Pb | 0.09 | ND | 100.00 | 0.04 | 55.60 |
| | Au | 0.32 | ND | 100.00 | 0.21 | 34.40 |

| DAY & TIME | PARAMETER | LITTON-WINCHESTER ELECTRONICS NEUTRALIZATION TANK/IONICS FILTER FEED | IONICS FILTER PRODUCT | PERCENT REDUCTION FROM FEED | ACTUAL WED DISCHARGE | PERCENT REDUCTION FROM NEUTRALIZATION TANK |
|---|---|---|---|---|---|---|
| | | (ppm) | (ppm) | | (ppm) | |
| 10:00 A.M. | Ni | 2.31 | ND | 100.00 | 0.71 | 69.30 |
| | Cu | 0.30 | ND | 100.00 | 0.47 | NR |
| | Pb | 0.24 | ND | 100.00 | 0.02 | 91.70 |
| | Au. | 0.02 | ND | 100.00 | 0.04 | NR |
| 1:30 A.M. | Ni | 3.18 | ND | 100.00 | 2.87 | 9.70 |
| | Cu | 2.04 | 0.02 | 99.00 | 1.92 | 5.90 |
| | Pb | 0.21 | ND | 100.00 | 0.08 | 61.90 |
| | Au. | 0.30 | 0.03 | 90.00 | 0.17 | 43.30 |
| Day 16 10:30 A.M. | Ni | 3.50 | ND | 100.00 | 0.92 | 73.70 |
| | Cu | 0.87 | ND | 100.00 | 0.56 | 35.60 |
| | Pb | 0.13 | ND | 100.00 | 0.05 | 61.50 |
| | Au. | 0.05 | ND | 100.00 | 0.09 | NR |
| Day 17 10:20 A.M. | Ni | 1.86 | ND | 100.00 | 1.47 | 30.00 |
| | Cu | 0.54 | 0.02 | 96.30 | 1.09 | NR |
| | Pb | ND | ND | NR | 0.02 | NR |
| | Au. | ND | ND | NR | 0.12 | NR |
| 11:30 A.M. | Ni | 1.24 | ND | 100.00 | 0.86 | 30.60 |
| | Cu | 0.43 | 0.01 | 97.70 | 0.42 | 2.30 |
| | Pb | 0.04 | ND | 100.00 | ND | 100.00 |
| | Au. | 0.03 | ND | 100.00 | 0.09 | NR |
| 2:10 P.M. | Ni | 2.98 | 0.17 | 94.30 | 1.60 | 46.30 |
| | Cu | 2.94 | 0.09 | 96.90 | 0.91 | 69.00 |
| | Pb | 0.33 | ND | 100.00 | ND | 100.00 |
| | Au. | 0.04 | 0.06 | NR | ND | 100.00 |
| Day 19 1:00 P.M. | Ni | 2.63 | ND | 100.00 | 1.98 | 24.70 |
| | Cu | 0.76 | 0.02 | 97.40 | 0.67 | 11.80 |
| | Pb | 0.04 | ND | 100.00 | 0.03 | 25.00 |
| | Au. | 0.11 | ND | 100.00 | 0.17 | NR |

KEY: NR = NO REDUCTION SEEN
ND = NON DETECTABLE BY FLAME ATOMIC ABSORPTION(AA) (VARIAN 1475)
LOWEST DETECTION LIMITS ARE AS FOLLOWS --

NICKEL (Ni) = 0.01 ppm COPPER (Cu) = 0.003 ppm
LEAD (Pb) = 0.01 ppm GOLD (Au) = 0.01 ppm

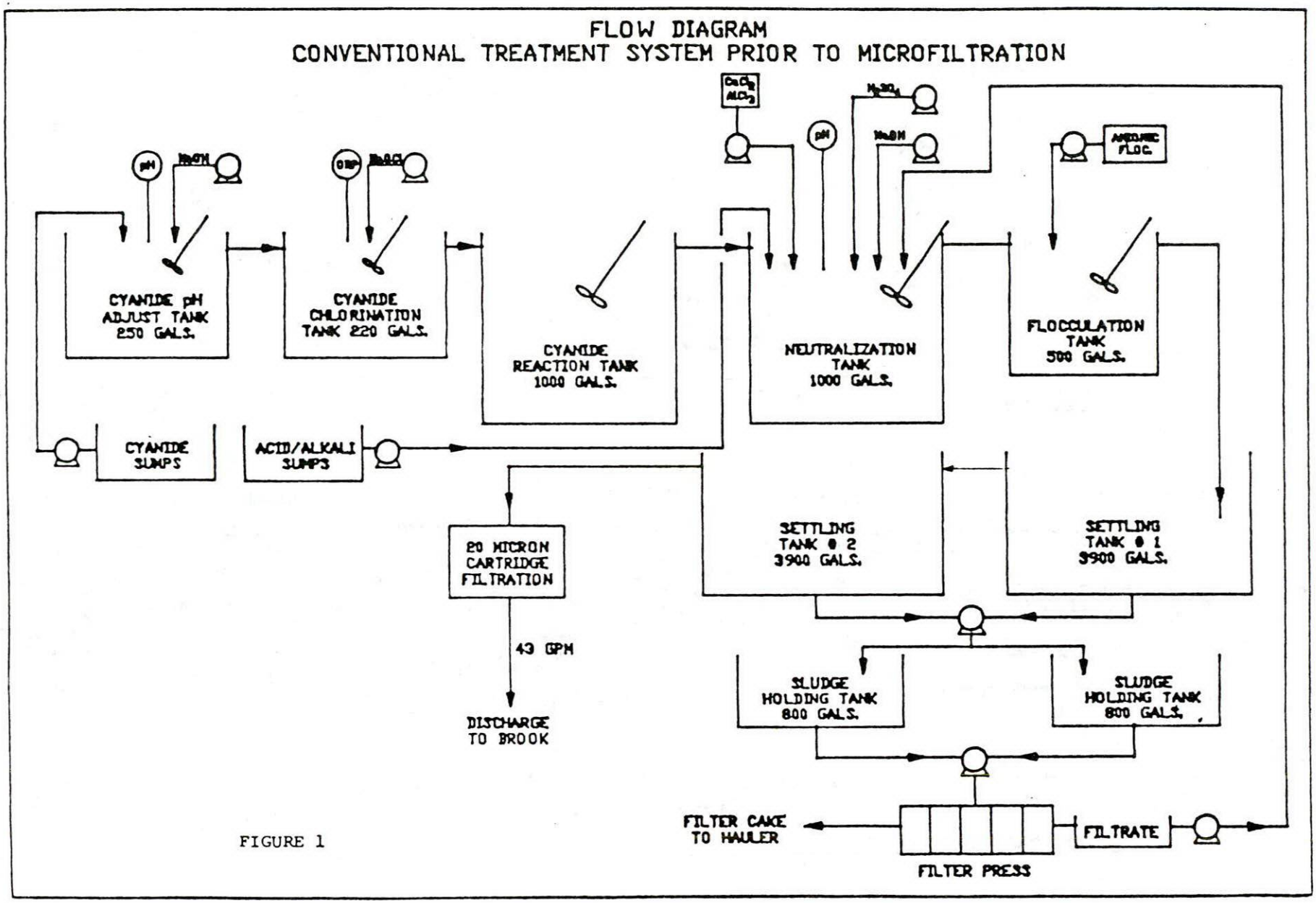
FLOW DIAGRAM
CONVENTIONAL TREATMENT SYSTEM PRIOR TO MICROFILTRATION
pH
NaOH
ORP
NaOCl
CYANIDE pH ADJUST TANK 250 GALS.
CYANIDE CHLORINATION TANK 220 GALS.
CYANIDE REACTION TANK 1000 GALS.
NEUTRALIZATION TANK 1000 GALS.
FLOCCULATION TANK 500 GALS.
ANIONIC FLOC.
CYANIDE SUMPS
ACID/ALKALI SUMPS
20 MICRON CARTRIDGE FILTRATION
43 GPM
DISCHARGE TO BROOK
SETTLING TANK # 2 3900 GALS.
SETTLING TANK # 1 3900 GALS.
SLUDGE HOLDING TANK 800 GALS.
SLUDGE HOLDING TANK 800 GALS.
FILTER CAKE TO HAULER
FILTER PRESS
FILTRATE

FIGURE 1

# FLOW DIAGRAM
## ENVIROMAT® INTEGRATED MEMBRANE FILTRATION SYSTEM

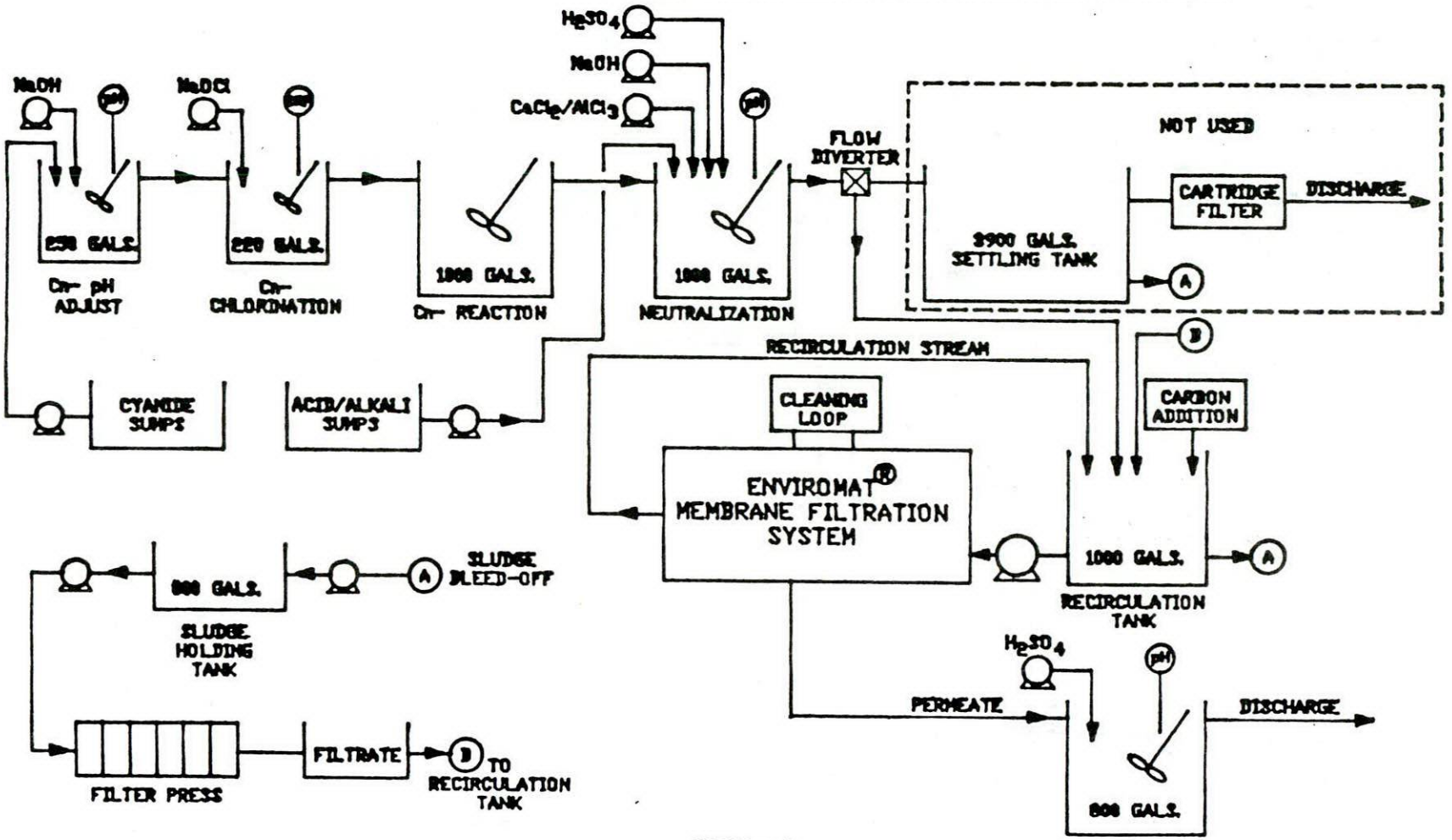


FIGURE 2

FIGURE 3

# CROSSFLOW MICROFILTRATION

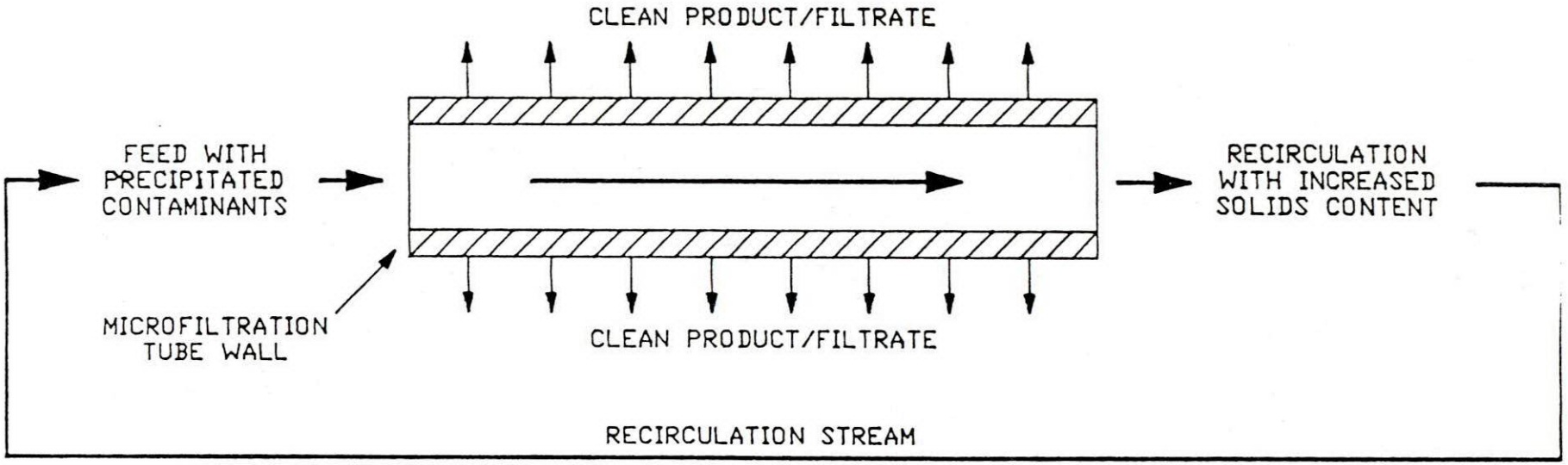

# D-3

# Environmental I
# Session D

## New Nickel/Chromium Plating Plant Goes to Total Recovery

Jamie Maliszewski, CEF
Reliable Plating Works, Inc.
Milwaukee, WI 53219

**PAPER NOT RECEIVED IN TIME FOR PUBLICATION***

New Nickel/Chromium Plating Plant Goes to Total Recovery

Jamie Maliszewski, CEF, Reliable Plating Works, Inc., Milwaukee, WI

In 1983, Reliable Plating Works decided to build a nickel/chromium plant to plate steel tubing for the exercise industry. The new line was designed with both rinses and sprayers operating in the counterflow mode. Every rinse (except those for acid) sprays back over the previous process tank. Acid rinses counterflow back to the cleaner rinses and the water from the tanks is sprayed on parts exiting the cleaners. Evaporative recovery is used with nickel and chromium plating. The end result is a savings of 40 percent on cleaners and nickel and 90 percent on chromium. Compliance with pretreatment standards is also achieved.

* For copies of this paper, please contact the author directly

Mr. Jamie Maliszewski, CEF
Reliable Plating Works, Inc.
5634 W. Oklahoma Avenue, #211
Milwaukee, WI 53219
(414) 271-5731

# D-4

# Environmental I
# Session D

## Advances in Removal of Copper From Printed Wire Board Effluents Using Sodium Borohydride

Richard J. Colby and
Michael M. Cook
Morton Thiokol, Inc.
Ventron Products
150 Andover St.
Danvers, MA 01923

# ADVANCES IN REMOVAL OF COPPER FROM PRINTED WIRE BOARD EFFLUENTS USING SODIUM BOROHYDRIDE

Richard J. Colby and Michael M. Cook
Morton Thiokol, Incorporated
Ventron Products
150 Andover St.
Danvers, MA 01923

## Abstract

This presentation reviews recent advances in the use of sodium borohydride for the chemical reduction and subsequent removal of copper from printed wire board manufacturing effluents. Improvements, particularly in the associated engineering aspects of using this technology, result in greater efficiencies and lower chemical costs. Use of a motionless pipe mixer in place of a stirred tank reactor results in improved utilization of sodium borohydride. Crossflow membrane filtration following the chemical reduction step affords improved solid/liquid separation and eliminates the need for coagulant and flocculent additions.

## Introduction

Over the past five years we have developed and advanced the technology for the chemical reduction/removal of copper from printed wire board (PWB) effluents based on the use of sodium borohydride.[1-5] This technology has demonstrated advantages over other precipitation methods and reducing agents. Specifically these advantages include:

A. Ability to achieve increasingly stringent federal, state, and local copper discharge limits;
B. Major reduction in amount of sludge produced;[6]
C. Significantly higher metal content in sludge;
D. Smelting/reuse of copper-rich sludge;[6]
E. Use of stable aqueous based reducing agent(s);
F. ORP control of reducing agent feed.

Pollution control/metal recovery technology based on sodium borohydride reduction has also been developed for related applications[7-8] (eg. spent electroless nickel baths[9-13] and precious metal recovery[14-20]).

This presentation will concentrate on the following engineering aspects of using sodium borohydride solution for removing copper from PWB effluents:

A. Review a typical PWB waste treatment system presently using borohydride solution;

B. Discuss the results of laboratory studies on impeller type and impeller diameter/tank diameter ratio variables in a stirred tank reactor with respect to solid/liquid separation;

C. Review the results of laboratory scale motionless pipe mixer/reactor studies;

D. Review the results of pilot scale crossflow membrane microfiltration studies.

Present Method of Employing Sodium Borohydride Solution for PWB Waste

Typically, PWB facilities operating with borohydride technology have adapted this chemistry to a system designed and engineered for a metal precipitation/removal technology. This approach minimizes additional capital equipment costs, allows the facility to meet discharge requirements, and reduces sludge generation with only minor modifications to the present waste system. Figure 1 shows a typical PWB waste treatment system using borohydride for copper reduction. It consists of a stirred reaction tank where the pH is adjusted to 4.5-5.0, and a solution of bisulfite is fed on ratio control to the incoming flow to maintain a level of 50-200 mg $Na_2S_2O_5$/L flow. Bisulfite is used to reduce any oxidizers and serves as an electron transfer agent for subsequent copper reduction. A coagulant (alum or a cationic polymer) is also added at low levels to the reaction tank to aid in intial particle formation. Sodium borohydride solution is added to a second stirred reaction tank. The copper reduction begins immediately and proceeds stepwise through a brown intermediate (presumably a cuprous species[21-23]) and then to a black copper/copper oxide precipitate. The borohydride solution feed rate is maintained at optimal levels by ORP control (approximately a -500 to -600 mV ORP reading signals a slight excess of the reducing agent). The retention time in each reaction tank is typically 15-20 minutes. A flocculent (e.g. an anionic polymer) is generally added at low levels to facilitate particle agglomeration prior to gravity settling (usually with an inclined plate clarifier). A final polishing filter ensures removal of potential clarifier solids carry-over before final discharge.

Although this arrangement was adequate, several engineering modifications were envisioned which could improve the system performance and optimize chemical usage. Conceptually, these modifications centered on improved solid/liquid separation and better reaction kinetics through improved mixing.

Effects of Tank Agitation on Particle Size Formation [24-26]

The inherent nature of the borohydride reduction chemistry is that of low solids generation. Although providing benefits in terms of reduced hazardous waste disposal costs, the low solids generation can present problems in terms of solid/liquid separation. For this reason it is necessary to employ a dual cationic-anionic polymer system as well as provide optimum mixing for coagulation and agglomeration of the generated particles. The focus of this presentation is to define the importance of proper tank agitation and its effect on particle size formation. The

size and nature of the flocculated particles formed will significantly affect the subsequent solid/liquid separation steps and ultimately the effluent quality.

These studies demonstrated the effects of agitator speed and the ratio of impeller diameter to tank diameter (the D/T ratio) on particle size formation. There is an optimum agitation level that can be found for a given tank and impeller such that the shear rate or velocity gradient is large enough to allow the particles to agglomerate but not so great as to shear the resultant flocculated particles. Laboratory studies with a Chemineer agitator kit helped define these optimum agitation parameters which can then be incorporated in the design of a larger scale system.[27,28]

A chelated copper solution was chosen for this evaluation to represent a "typical" PWB copper waste stream. This solution was prepared by dissolving 100 mg copper (as $CuSO_4$) and 900 mg EDTA $Na_4$ per liter of tap water (giving a 1.5 molar ratio of EDTA/$Cu^{2+}$). For these experiments, the reaction, coagulation and flocculation steps were all accomplished in the same tank. To simulate conditions in the first reaction tank, sodium bisulfite (350 mg $Na_2S_2O_5$/L) and alum (100 mg $Al^{3+}$/L) were added to the chelated copper sulfate solution prior to treatment. In the reduction step, sodium borohydride solution (0.45 mg $NaBH_4$/mg Cu) was added to chemically reduce the metal and form particles. The coagulation of the particles was effected by the alum already in solution. The flocculation of the particles was achieved with the subsequent addition of an anionic polymer.

In waste treatment reactors where particle agglomeration and complete solid/liquid separation are desired, axial mixing is preferred over radial mixing. The axial mixing provides top to bottom blending. A high-efficiency axial flow impeller (Chemineer HE-3) was used in these studies to provide this type of mixing while minimizing the shear applied to the agglomerated particles. In addition, the HE-3 impeller provided comparable axial flow mixing at lower power requirements than that achieved with marine type turbine impellers.[29]

Our experiments were conducted using the agitator kit with both a 20 and 4 liter flat bottom tank. This equipment provides D/T ratios of 0.3 (20 liter scale) and 0.8 (4 liter scale).

The impeller is set concentrically in the tank at a distance of 0.17 times the tank diameter from the bottom of the tank (or about 1 to 2 inches). In these studies aggitation was maintained at a constant 175 rpm for 10 minutes during and following the addition of sodium borohydride solution. An agitator speed of 60, 175 or 350 rpm was maintained for 3 minutes during and after the anionic polymer flocculent addition. The agglomerated particles were then allowed to settle for 60 minutes before sampling. The copper level in a unfiltered sample, taken 1 inch below the liquid surface, was determined in each run. In all

cases the soluble copper level of a filtered sample (through a 0.8 μm membrane syringe filter) was ≤ 0.05 mg Cu/L; indicating the reduction was complete in every instance. In all the experimental runs the chemical aspects of these reductions (i.e. the change in ORP and pH with reaction time, and the observed color changes) were parallel. The same chemical ratios for all reagents were used in each experiment.

The results suggest that much better particle formation can be achieved by increasing the D/T ratio and/or rotational speed (Table 1).

Table 1. Effects of Stirring Speed and D/T Ratio on Final Copper Levels

D/T Ratio = 0.8

| RPM | Total Copper[a] |
|---|---|
| 60 | 3.7 mg/L |
| 175 | 1.5 mg/L |
| 350 | 0.5 mg/L |

Agitation Speed = 175 rpm

| D/T Ratio | Total Copper[a] |
|---|---|
| 0.3 | 7.9 mg/L |
| 0.8 | 1.5 mg/L |

[a] unfiltered sample taken 60 minutes following polymer addition

These data illustrate the beneficial trend of a higher D/T ratio with good axial mixing. A similar trend was evident in a field study undertaken at a PWB facility. This facility had a 5.0 ft diameter/1200 gallon flocculation tank. This tank had a dual 12 inch axial flow impeller arrangement (D/T = 0.2) with a variable speed control. In order to maintain adequate mixing in the tank for both uniform solids distribution and flocculation, an agitator speed of 250-300 rpm was required. However, the effluent from the clarifier and samples from settling cones consistently contained unacceptable amounts of nonsettling particles, resulting in unsatisfactory effluent copper concentrations. All attempts to adjust mixing speed and/or polymer dosage in the facility did not resolve the problem. In all cases an additional few minutes of mixing on a magnetic stirrer produced a clear supernatant. As the result of this study the dual 12 inch impellers were replaced with a single 21' inch axial flow impeller (D/T ratio = 0.35). Agitator speeds were reduced to 75-120 rpm which provided adequate mixing in the tank. With this new arrangement, significant improvements in effluent quality were realized in terms of reduced solids carryover from the clarifier, which resulted in total copper concentrations being below discharge limits.

## Motionless Pipe Mixer Studies

It was anticipated that the kinetics of the reduction reaction and particle formation could be enhanced with the use of a motionless pipe mixer. These motionless mixers provide complete blending of any given cross section of fluid in a minimum amount of space.

A laboratory motionless mixer system was built to continuously treat a 100 mg Cu/L chelated waste stream analogous to that described in the previous section. The system configuration, as illustrated in Figure 2 shows that the waste stream is pumped from the reservoir, and then through a rotameter before entering the motionless mixer. Since these mixers do not blend one cross section of fluid with another, it was necessary to add the borohydride solution at a constant (nonpulsed) flow rate. This was accomplished by a pressurized reservoir and calibrated needle valve delivery system. This delivery system ensured that the borohydride was continuously introduced into the waste stream just ahead of the motionless mixer. The mixer, a 15 element (LUWA) 0.5 inch tube, provided rapid blending of the reactants. The kinetics of the borohydride-copper reduction was so rapid that under optimum conditions (pH 4-5) the reaction was virtually complete by the time the flow exited the mixer (as indicated by the black color and the ORP of the exiting solution). A coagulant (alum) was needed to ensure that the chemically reduced particles agglomerated sufficiently to be removed by a 0.8 um pore filter (see Table 2).

Table 2. Results of Motionless Pipe Mixer Studies [a,b]

| pH Intial | pH After RXN | Alum[c] | ORP mV | Copper Level in Effluent[d] (0.8 μm Filter) |
|---|---|---|---|---|
| 4.0 | 4.5 | No | -640 | 38 mg Cu/L |
| 4.0 | 4.9 | Yes | -550 | 0.04 mg Cu/L |
| 4.0 | 4.9 | Yes | -550 | 0.04 mg Cu/L |
| 4.0 | 4.9 | Yes | -550 | 0.06 mg Cu/L |

Notes

a. Sodium borohydride was added at a rate of 0.42 mg $NaBH_4$/mg $Cu^{2+}$ in the feed.

b. Sodium bisulfite (350 mg $Na_2S_2O_5$/L) was preadded in all cases.

c. When alum was used, 100 mg $Al^{3+}$ per liter was preadded.

d. Sample taken from a stirred collection tank after the motionless mixer.

Improved efficiencies have been observed with the use of the motionless mixer over the stirred tank. In the laboratory studies with a stirred tank reactor, designed to depict typical field conditions, borohydride usage rates were approximately 40% greater than those required by the motionless pipe reactor (see Table 3).

Table 3. Comparison of Sodium Borohydride Usage Rates[a]

| | mg $NaBH_4$/100 mg $Cu^{2+}$ |
|---|---|
| Motionless Pipe Reactor | 42 |
| Chemineer Agitator Kit Study | 45 |
| Magnetically Stirred Tank | 57 |

a On an EDTA chelated copper solution where initial copper levels were 100 mg $Cu^{2+}$/L and the final copper level was reduced to < 0.8 mg $Cu^{2+}$/L

Microfiltration Studies [30-32]

In traditional treatment systems which rely on gravity settling to achieve solid/liquid separation, the size of the agglomerated particles formed in the flocculation step is critical to proper system operation. If the particles are too small, solids carryover in the clarifier can result. A final polishing filter may be required to remove the carryover. Because of this potential problem, care must be taken to provide optimum conditions for proper flocculation. In some situations however, changes in the waste itself suddenly create havoc with the flocculation chemistry and produce a system upset resulting in unsatisfactory effluent. Crossflow filtration eliminates the need to build particle size with complex polymer systems, eliminates the need for a large clarifier and produces better more consistent effluent quality.

For these reasons, crossflow microfiltration systems are now used in PWB waste treatment applications. These systems, based on separation of a metal hydroxide, or other insoluble metal salts, are designed to provide 200 GFD (gal/$ft^2$ membrane/day) of permeate.

Because of the low volumes of high density sludge produced in the borohydride based technology, crossflow membrane filtration should have particular advantages in these applications. In addition to the general advantages noted above, improved flux rates and reduced cleaning schedules might be expected with the borohydride reduced metals.

Two pilot scale field tests conducted on a side stream of actual PWB effluent using tubular and spiral wound crossflow microfiltration units have shown excellent results. Each of these studies ran ca. 8 hours/day

for 1-2 weeks using borohydride based chemistry. Very good permeate quality was achieved in these studies without the need for coagulants or flocculents. Typical results of the incoming and exiting metal concentrations are shown in Table 4.

Table 4. Results of Effluent Quality Before and After Treatment and Membrane Filtration

| Experimental Date | Type of Unit | Starting Copper Level in Waste Stream (mg/L) | Copper Level in Membrane Filtered Permeate (mg/L) |
|---|---|---|---|
| 3/31 | spiral wound | 34.5 | 0.03 |
| 4/1 | spiral wound | 28.8 | 0.01 |
| 4/2 | spiral wound | 30.0 | ND |
| 7/31 | tubular | 50.0 | 0.03 |
| 8/17 | tubular | 39.8 | 0.03 |
| 8/18 | tubular | 45.3 | 0.05 |

In one study a 0.5 inch i.d., 0.5 μm pore size tubular membrane system was used. The systems was operated continuously using fresh PWB effluent. The pH was adjusted to 4.5 and the bisulfite was added on ratio control (at 360 mg $Na_2S_2O_5$/L). The sodium borohydride solution was then added on ORP control (to a set point of -550 mV) to reduce the copper. A linear velocity of 12 ft/sec was achieved and a transmembrane pressure of 40-50 psi was maintained in the filter tubes. The continuously operating system maintained a permeate flux rate of 279 GFD at 29°C. Operation of the system with a linear velocity of ca. 5 ft/sec did not result in a stable flux rate (see Figure 3).

Pilot scale tests on a corrigated spaced spiral wound membrane system were completed with 0.8 μm, 0.2 μm pore size and a 50,000 molecular weight cut off membranes at 29°C. The 0.8 μm sized membrane, as expected, gave the best permeate flux rates (230 GFD); the small size membranes gave much lower flux rates (74 GFD with the 0.2 μm and 60 GFD with the 50000 mw cutoff). Although no problems were noted, the potential for plugging the corrigated spacing (ca 0.125 inch) of the spriral wound membrane with solid contamination in the waste was a concern. The chemical treatment was similar to that described in the previous study except that batches of waste were treated and then filtered due to the configuration of this pilot scale equipment.

Currently several PWB facilities are successfully using borohydride based copper reduction with crossflow membrane filtration for solid/liquid separation. The chemical aspects of these treatments parallel that described in the pilot scale work. All of the facilities are consistently seeing high quality effluent at permeate rates of > 200 GFD.

## Future Developments

A pilot scale unit incorporating a motionless pipe mixer/reactor has been designed and is being constructed based on the developments reviewed in this presentation. In this unit, solid/liquid separation can be done by crossflow microfiltration. Gravity settling parameters can also be determined through settling cone studies.

As noted, several facilities with membrane filtration equipment have successfully implemented a borohydride based technology and have significantly reduced their sludge volumes. In addition, where feasible, full scale systems have been modified to incorporate the other engineering advances described in this paper.

It is anticipated that data from these studies will provide more information for the optimum design of full scale systems based on borohydride reduction technology.

## References


1. J. A. Ulman, Spec. Chem. 1985, 5(2), 27.

2. J. A. Ulman, "Control of Heavy Metal Discharge with Sodium Borohydride", Spec. Publ.-R. Soc. Chem. 1986, 61, 173; Chem. Abstr. 106 72317p.

3. M. J. Lindsay and M. E. Hackman, "Sodium Borohydride Reduces Hazardous Waste", presented at the Purdue Industrial Wastewater Conference (May 1985).

4. J. A. Ulman, "Control of Heavy Metal Discharge in the Printed Circuit Industry with Sodium Borohydride," presented at the 1984 AESF SUR/FIN Annual Technical Conference and Exhibit, New York City (July 1984).

5. S. F. Heleba, "EPA Effluent Compliance and Hazardous Sludge Control with Sodium Borohydride," presented at the Massachusetts Hazardous Waste Source Reduction Conference and Exhibition, Boxboro, MA (October 1983).

6. M. J. Lindsay and R. S. Stennick "Pollution Control Using VenMet Solution", Annu. Tech. Conf. Proc. - AM. Electroplat. Soc. 1986, 73rd, Paper C-1; Chem. Abstr. 105 84548h.

7. M. M. Cook, et al., Proc. Ind. Waste Conf. 1979 (pub. 1980), 34th, 514; Chem. Abstr. 93 12566x.

8. T. F. Jula, Process Eng. 1975 (Feb.), 123; Chem. Abstr. 83 151770r.

9. M. E. Fleming and J. A. Ulman, "Sodium Borohydride Environmental Control Application: Reduction of Nickel(II) Complexes in Spent Electroless Plating Bath," presented at Electroless Nickel Conference IV, Chicago, April, 1985.

10. W.-C. Ying, R. R. Bonk and M. E. Tucker, "Precipitation Treatment of Spent Electroless Nickel Plating Baths", 42nd Purdue Industrial Wastes Conf., 1987; submitted for publication in J. Hazardous Materials.

11. K. Parker, "The Waste Treatment of Spent Electroless Nickel Baths," presented at the First AES Electroless Plating Symposium, St. Louis (March 1982).

12. R. N. Duncan and J. R. Zickgraf, Products Finishing, 1982, 55.

13. F. S. Tuznik and A. A. Lis, Proc. World Congr. Met. Finish, 11th, 1984, 197.

14. H. Iga, Jitsumu Hyomen Gijutso 1979, 26(5), 202; Chem. Abstr. 91 143874c.

15. H. Iga, Jitsumu Hyomen Gijutso 1979, 26(8), 360; Chem. Abstr. 91 16088u.

16. H. U. Galgon; et al. Ger.(East) 204,169 (1983); Chem. Abstr. 100:112186e.

17. G. Dietz and R. Skomoroski, U.S. 4092154 (1978); Chem. Abstr. 89 133136h.

18. L. F. Hohnstedt et al., Anal. Chem., 1965, 37(9), 1163 (1965); Chem. Abstr. 63 10641c.

19. M. M. Cook and J. A. Lander J. Appl. Photogr. Eng. 1979, 5(3), 144; Chem. Abstr. 92 85858h.

20. G. F. Medding and J. A. Lander Precious Met. [Proc. Int. Precious Met. Inst. Conf.] 5th 1981 (Publ. 1982), 3; Chem. Abstr. 97 220285q.

21. M. Dasgupta and M. K. Mahanti, Trans. Met. Chem. 1986, 11, 286.

22. R. J. Spokas and B. D. James, Inorg. Chim. Acta 1986, 118, 99.

23. Private Communications and Discussions with Professor R. D. Archer, University of Massachusetts (1985).

24. J. Y. Oldshue, O. B. Mady, Chemical Engineering Progress, 1979, 75(5), 72-75.

25. T. R. Camp., Transaction ASCE 120; 1-16 (1955).

26. J. Y. Oldshue. Fluid Mixing Technology, McGraw Hill Publications Co., New York, New York, 1983.

27. R. R. Corpstein, et al., Chemical Engineering Progress, 1979 75(2), 66-74.

28. R. R. Rautzen, et al., Chemical Engineering, October 25, 1976, 119-126.

29. Product Data Sheet on Chemineer HE-3 High-Efficiency Impeller, Chemineer, Inc., Dayton, Ohio.

30. R. H. Perry and D. Green (Ed.), Chemical Engineers Handbook, McGraw Hill, New York, 1984, (17)27 to (17)34.

31. P. A. Schweitzee (Ed.), Handbook of Separation Techniques for Chemical Engineers, McGraw Hill, New York, 1979, (2)3 to (2)103.

32. T. V. Tran, "Advanced Membrane Filtration Process: Treats Industrial Wastewater Efficiently", Chemical Engineering Progress 1985, 81, (3),29.

# Figure 1. Typical Waste Treatment System using Borohydride for Copper Reduction

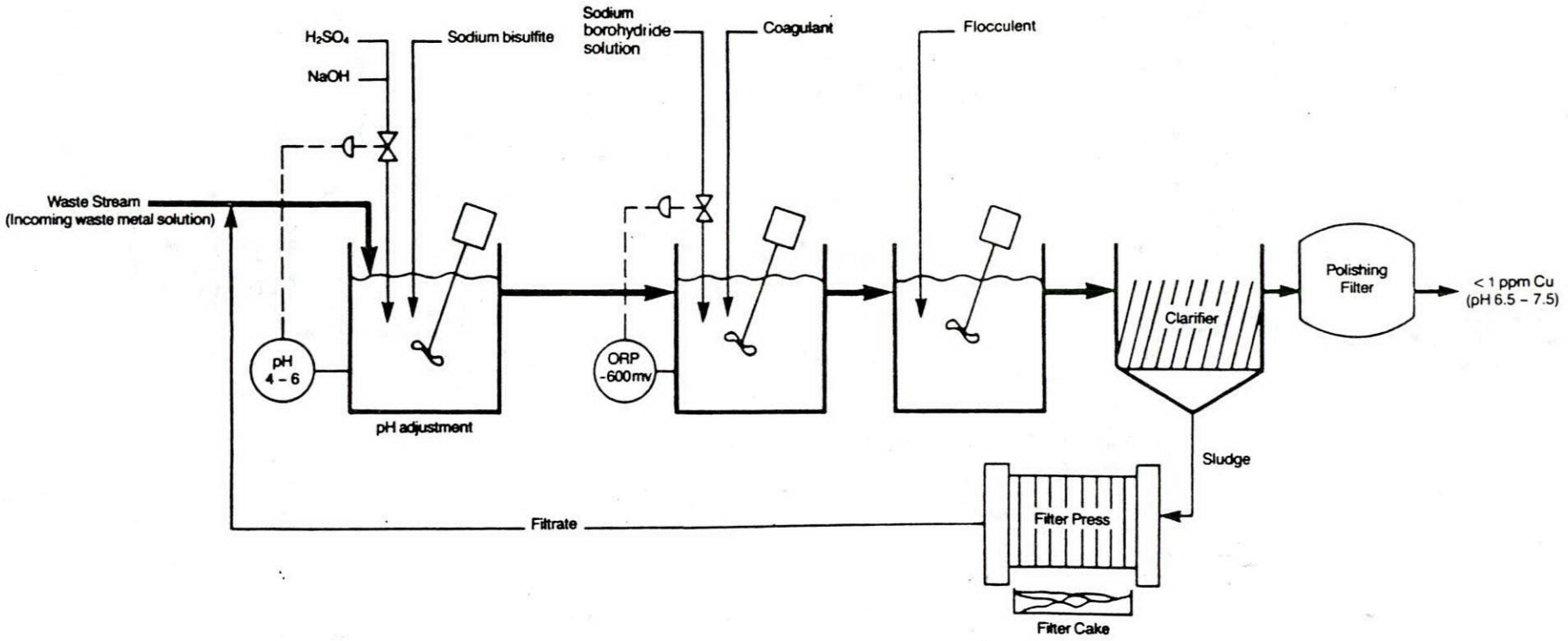

Figure 2. General Motionless Pipe Mixer System Schematic

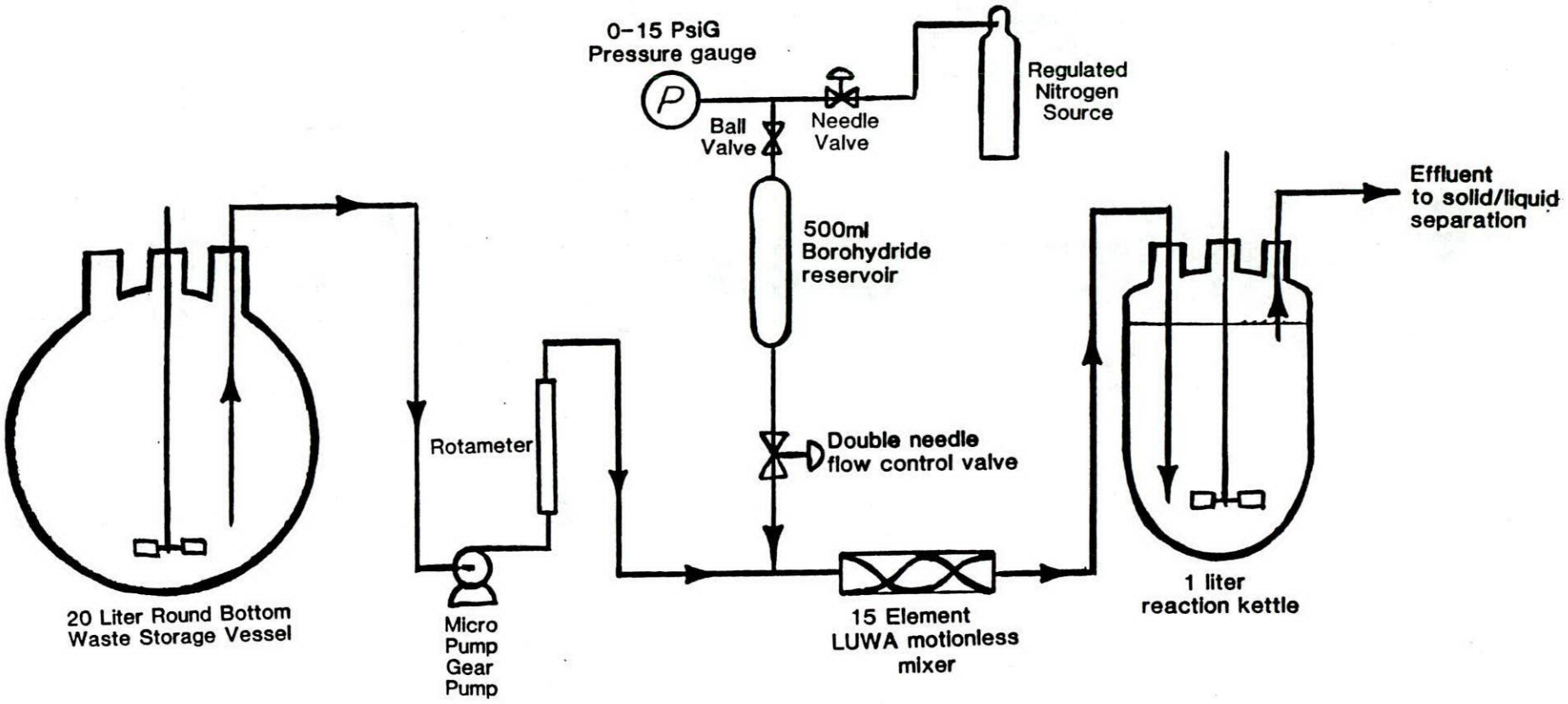

Figure 3. Permeate Flux Rate versus Operating Time for a Tubular Crossflow Microfiltration Unit

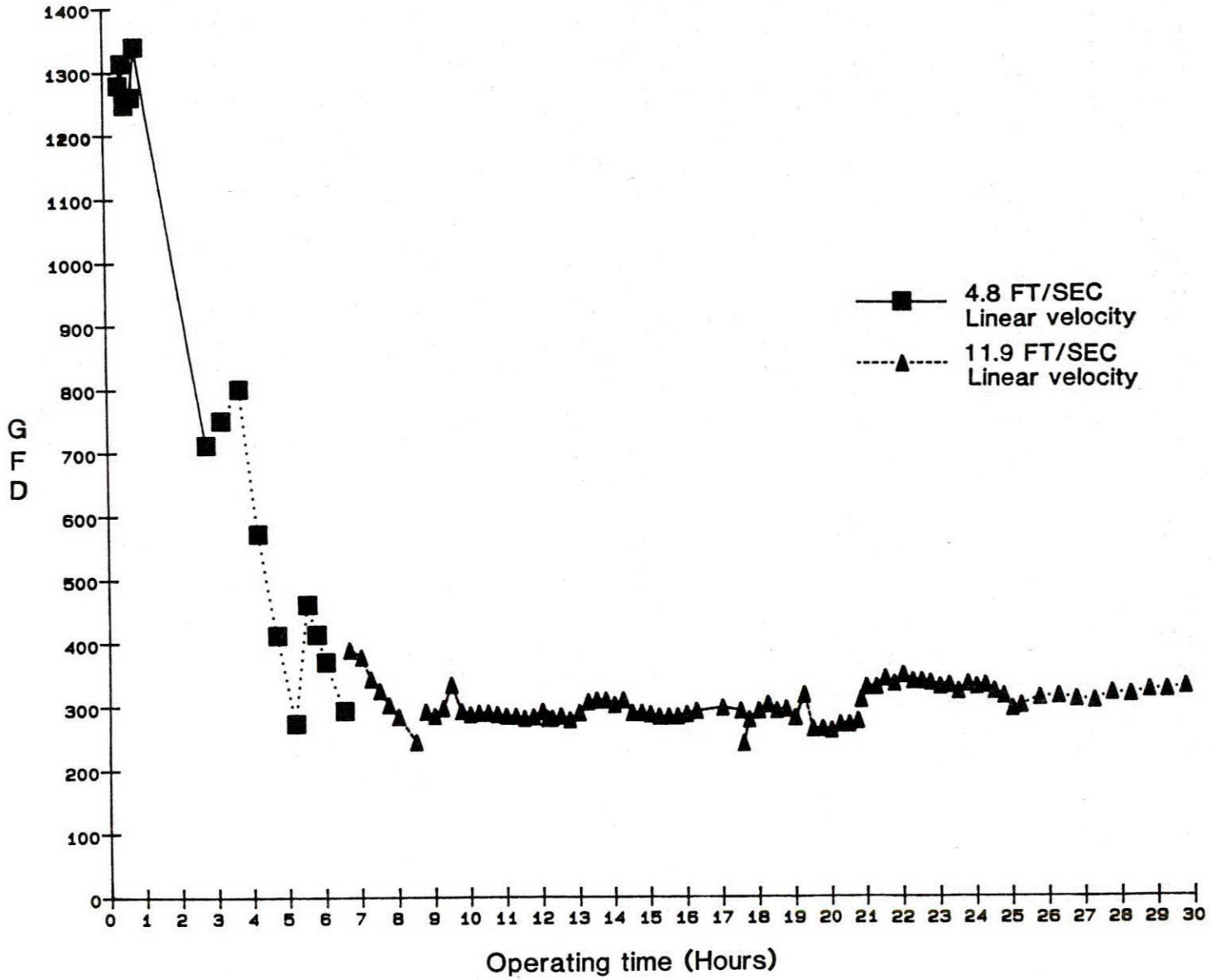

# D-5

# Environmental I
# Session D

## A New Technology for Wastewater Treatment

Dr. Ev Knight and
Dr. Jeffrey V. Dagdigian
Unocal 76 Corp.
Fullterton, CA

# A NEW TECHNOLOGY FOR WASTEWATER TREATMENT

Dr. Ev Knight and Dr. Jeffrey V. Dagdigian
Unocal 76 Corporation, Fullerton, CA

Wastewater treatment has been a consideration of manufacturing engineers ever since the industrial revolution. At first, these pioneers were interested in simple neutralization; the goal being the preservation of their plant sewer system or even their manufacturing equipment. Later, as their needs became more sophisticated and competition became more keen, simple recovery of metals in waste materials became important. In the beginning, wastewater treatment was implemented for purely economic reasons; government regulation and enforcement was simply not a consideration.

With the advent of the Clean Water Act in 1972, its later amendments, the conception of the EPA, and insuring wastewater discharge Categorical Regulations the emphasis on wastewater treatment has shifted from economics to compliance. The role of the manufacturing engineer has expanded and environmental specialists in the fields of the government regulations, engineering, and analytical chemistry have been added to company's staffs. Today, designing, engineering, installing, operating, and maintaining a wastewater treatment facility is costly and serious business. Even evaluating the myraid of technologies and their appropriateness in your wastewater environment is difficult and expensive. Becoming compliant and staying compliant can save your company from further expenditure of its resources in an area that generates no profits. Picking the right technology for your needs can save you time and expense but most importantly it can mean difference between being consistently compliant and not.

Early in 1983, Unocal Corporation developed a new chemistry for precipitating heavy metals from wastewaters. This process is unique because it relies on the chemistry of a single element and it is based on chemical kinetics versus chemical thermodynamics (or the solubility properties of individual metals). For these reasons, the process can be readily optimized and treatment can be repetitive. In fact, this treatment process can treat the effluent from wastewater that has been previously treated via conventional alkaline precipitation.

As mentioned above, UNIPURE Process Technology centers around the solubility of a single element rather than on the individual solubilities of various toxic heavy metals. That element is common, inexpensive iron. The secret to this technology lies in associating the heavy metals with the soluble iron and rapid precipitation of the resulting complex.

Unocal scientists discovered that when properly activated, iron is capable of binding toxic heavy metals. When the iron in this complex is precipitated, the associated heavy metals are removed via a mechanism similar to classical coprecipitation but at efficiencies orders of magnitude greater.

Heavy metals are attracted to the iron in solution via an occlusion and adsorption type binding. This creates a concentration or entropy effect which greatly enhances the efficiency of metals removal while also minimizing sludge formation.

As a result, the heavy metals are trapped in an insoluble iron matrix. The coprecipitation of heavy metals is so effective that thermodynamic equilibrium laws are actually superceded. This process is a substantial improvement over classical ferrous or ferric based coagulation or coprecipitation.

Exploiting the chemistry of iron to remove heavy metals achieves results that are impossible with pH adjustment alone. Typical results are listed in the table below.

Aerospace Products, Div
SPS Technology
Santa Ana, California

| Major Contaminants | Average Influent Composite | UNIPURE Actual 30-Day Composite | EPA Metal Finishing Regulations 1 Day Max. | EPA Metal Finishing Regulations 30-Day Max. |
|---|---|---|---|---|
| Cd | 15.7 | 0.1 | 0.69 | 0.26 |
| Cr | 3.4 | 0.05 | 2.77 | 1.71 |
| Cu | 5.7 | 0.1 | 3.38 | 2.07 |
| Ni | 6.5 | 0.2 | 3.98 | 2.38 |

Flow Rate: 100 gpm Avg.

Because UNIPURE Process Technology relies on a kinetic process, the reaction never reaches equilibrium. The process becomes more effective the faster the chemistry run. The treated water can be treated repeatedly with additional heavy metals removal after each pass-through. That means it is now possible to design wastewater treatment systems for any level of metals removal.

Due to UNIPURE Process Technology's unique metals removal mechanism both cations and anions are removed. This means that segregation and pretreatment of chromate is not necessary. Recent experimentation suggests significant efficiencies at removing ionizable hydrocarbons.

This chemical process is extremely robust. It can operate effectively at pH's between 7 and 10. This makes process control simple and thus more effective.

Operating the process at near neutrality can reduce your chemical costs and also reduces sludge production by producing a more dry sludge material. At neutral pH's, the surface charge of precipitated particles is well diffused and little water (which has a dipole) can bind. At higher pH's (those that conventional alkaline precipitation operate at), the surface of the precipitated particles is highly negatively charged. Water is chemically bound to help disperse the charge on the particles This results in a wetter sludge and eventually in increased sludge hauling and disposal costs. With UNIPURE Process Technology drier sludges are formed and this helps reduce expenses associated with sludge formation.

UNIPURE Process Technology can be easily installed in new or existing systems. In the Metal Finishing Industry, best results are obtained using the process as a polish to existing systems. This engineering configuration reduces sludge formation and produces a system which is difficult to defeat (see attached flow diagram). UNIPURE Process Technology can help you achieve compliance 100 percent of the time.

E-1

# Electronics II
# Session E

## Innovative Control Systems for the Electronic Plating Process—Today and the Future

Roger Herrscher
Jerry Tingwall
Robbins and Craig Manufacturing Corp.
2050 N. Durfee Ave.
South El Monte, CA 91733

# INNOVATIVE CONTROL SYSTEMS FOR THE ELECTRONIC PLATING PROCESS - TODAY AND THE FUTURE -

Roger Herrscher
Jerry Tingwall
Robbins and Craig Manufacturing Corporation
2050 N. Durfee Ave.
South El Monte, CA 91733

## 1.0 General

The control system for the electronic plating process must be sophisticated enough to handle many complex processes simultaneously, while still having a simple and easy to use operator interface.
Among the tasks to be performed are the closed loop control of process parameters, chemical handling, data collection capabilities, the analysis of collected data, the control and tracking of parts through the process, as well as several other tasks.
All of these will be discussed in this paper.

### 1.1 Abstract

- As an important part of an automated plating facility, the control system for an automated plating line must have certain characteristics that allow it to be easily integrated into the overall facility control system.

- It is designed to automatically route parts to and from the plating line, automatically monitor and control the flow of chemicals to and from the plating line, and automatically monitor and control the process through which the parts pass.

- To accomplish this the plating line will need a closed loop control of process parameters, chemical handling (flow monitoring and control) capabilities, data collection capabilities, and the ability to communicate with a host computer or network.

- It is the intention of this document to describe a control system that accomplishes the above.

## 2.0 Control System Description

The plating line control system will have the following capabilities and utilities available.

### 2.1 **Dynamic Processing**

- The "Dynamic Scheduler" uses tank sequence, desired dwell times, and some ancillary data about the tanks, (i.e. tolerance for dwell times), to interactively create new hoist programs for any series of processes to be run.

- The system computer accepts requests for new processes from the line operator, and using the data files, design a new program for the hoist. This allows programming of new process recipes without interrupting the regular operation of the line.

### 2.2 **Closed Loop Control**

- The plating line will have closed loop control of important process parameters and variables. The control loops will be configurable to provide the necessary sensors and signal conditioning. The control parameters will be user alterable. Examples of control parameters include set points, alarm points, dead bands, etc.

- In addition, the control system will monitor variations or deviations of the controlled parameters from the desired values. Thus closed loop control also provides the capability for data collection.

## 3.0 Master Controller

The master controller controls programmable line parameters such as temperature, conductivity, pH, bath replenishment, rectifiers, and other ancillary equipment. It monitors the operation of the other controllers and coordinates their actions to operate rectifiers and bath replenishment systems. It also logs system activity by filing and/or printing collected data. Multiple hoist can be controlled by the system.

### 3.1 **Control**

- All line setpoints can be programmed 'offline' without changing setpoints in use.
- Process engineers can define new processes while the line is being used.
- All line setpoints can be changed through the master console.
- Inputs to the line computer may be provided as 0-5V, 0-10V, or 4-20 mA signals.

### 3.2 **Temperature Control**

- Values specified and displayed in deg C or deg F.
- ON/OFF control of heaters and coolers with dead band programmable by user, or PROPORTIONAL control using PID control algorithm.
- Warning levels programmable by user. Alarm inputs may be used to shut off outputs.

### 3.3 **Conductivity Control (Rinse Water)**

- Selective full scale range (50, 2000, 5000,...)
- ON/OFF solenoid control with dead band programmable by user.
- Proportional control with user alterable gains.
- Warning levels programmable by user. One discrete alarm input per conductivity input, may be used to disable controlled output.

3.4 **pH Control**

- ON/OFF solenoid control with dead band programmable by user.
- Proportional control with user alterable gains.
- Warning levels programmable by user. One discrete alarm input per conductivity input, may be used to disable controlled output.

3.5 **Bath Replenishment**

- Replenishment based on continuous analysis via interaction with instrumentation, i.e., Ion Chromatography Colorimeter, Polarograph, etc.
- Setpoints for all replenishment modes are programmable by the user.
- Replenishment 'on time' is programmable by the user in 1 second increments to 255 seconds.

Optional

- Replenishment on accumulated surface area which has passed through tank.
- Replenishment on accumulated amp-seconds in electrolytic tanks.
- Replenishment on accumulated time since last replenishment.
- Replenishment on accumulated immersion time since last replenishment.

3.6 **Ancillary Control**

- Programmed ON/OFF control for pumps, filtration systems, main water inlets, blowers, bubblers, mechanical and air agitators and the like.
- One discrete alarm input per ancillary, may disable controlled output.

3.7 **Flow**

- Flow rates are only monitored and displayed, (not controlled).
- Warning levels programmable by user. One discrete alarm input per flow input.

3.8 **Pressure**

- Pressures are only monitored and displayed, (not controlled).
- Pressures may be either single ended or differential.
- Warning levels programmable by user. One discrete alarm input per pressure input.

3.9 **Spray Rinse**

- Sprays can be actuated when work is entering a station, leaving a station, while in a station, or any combination of those options.
- Sprays for entry, exit and while in a station, may be from different solutions.
- One discrete alarm input per controlled spray, may be used to disable controlled output.

3.10 **Rectifier Control**

- Up to 72 unique power supplies may be controlled and monitored
- Up to 8 independently controlled rectifiers per station.
- Current range dependent on power supply used.
- Measured voltage displayed.
- Measured current may be displayed.
- User programmable delay-time and on-time for each rectifier.
- User programmable warning levels for measured voltage.
- One discrete alarm input per rectifier, may be used to disable controlled output.

## 4.0 Data Collection

The control system will collect data about events which pertain to the effective and efficient operation of the plating line. There are two kinds of events, process data events and process control events. One example of a data event of interest is the deviation of a controlled variable outside some defined limits.

4.1 An example of a control event would be the creation of a new bath.

- Another example of a control event would be the completed plating of a set of parts.

- The following is a list of the required events and status information to be available (perhaps as records in a file on the hard disk).

- a) Deviation of any controlled variable outside defined limits. This implies the capability to download these limits as well as the control parameters

- b) Current physical status of the plating line, hoist system, and automatic load and unload systems.

- c) Creation of new chemical baths or changing of tank chemicals with the chemical lot information.

- d) Location of parts within plating line.

## 5.0 Data Trending

Software includes the data trending feature which saves all sampled data for a period of approximately two weeks in a series of disc files. These files can be copied onto floppy discs, sent to a host computer, printed and/or displayed on the color graphics monitor.

The user may select sample points between 1 and 60 minute intervals. This sample record will contain the minimum, maximum and mean values for the previous sample periods. Should a load enter or leave a station during the sampling period, the sample record will be produced that covers from the start of the sample period until the time that the load entered or left the station.

5.1 **The file structure is:** TRymmddp.dat where

a) y is last digit of the year, 6 for 1986
b) mm is the month from 1-12
c) dd is the day of the month
d) p is the part of the day (A-Z)

Note: The files will be less than 300k bytes each so that they will fit onto a floppy disk.

5.2 **The general record format will be:**
<record type>;<data>....<date>;CR LF

Note: All the data will be in metric units

5.3 **Specific Record Formats**

a) Workbar lot information records. Recorded when a bar is loaded:

bar;<in|out>;<number>;<hours>;<minutes>;<seconds>;
<qty>;<lot>;<qty>;<lot>;<qty>; CR LF

i.e., bar;in;14;22;54;13;13542;
100;11432;10;13425;10;CR LF

b) Data record. Recorded at sample period or when a bar leaves a tank:

data;<station>;<parameter>;<hours>;<minutes>;<seconds>;
<min>;<mean>;<max>;<status>;<bar>;CR LF

i.e., data;N34;temp.,tank;12;10;15;
120.1;134.2;144.3;green;14;CR LF

5.4 **Hoist Interface** - optional

The control system can be connected to a host computer via an RS232 line. The host will send a message, "Send ymmdd Nongreen", this will start transmission of all nongreen parameters for the specified (ymmdd) date. The record will be sent and the system will wait for an acknowledgment of receipt prior to sending the next record.

5.5 **Reports** - optional

A report will be produced wit either all the data, all non-green data or all red (out of limit) data. This report can be directed to the local printer or to the host computer.

a) By lot number:
Data for lot 1234567:
Time in MM DD, YYY:
Workbar 34 first 32 boards
Workbar 45 second 54 boards
Workbar 15 third 20 boards

| | | GROUP 1 WORKBAR 34 | | | | GROUP 2 WORKBAR 45 | | | | GROUP 3 WORKBAR 15 | | | |
|---|---|---|---|---|---|---|---|---|---|---|---|---|---|
| STA | PARAMETER | MIN | MEAN | MAX | STAT | MIN | MEAN | MAX | STAT | MIN | MEAN | MAX | STAT |
| 13 | Temp..tank | 34 | 38 | 45 | RED | 39 | 40 | 41 | GRN | 39 | 40 | 41 | GRN |

b) All data:
From MM DD,YYYY HH:MM,YYYY HH:MM

| STA | PARAMETER | TIME | MIN | MEAN | MAX | STAT | BAR |
|---|---|---|---|---|---|---|---|
| 13 | Temp..tank | 23:15 | 34 | 38 | 45 | RED | 3 |

The actual format will be ##,###,## for all parameters. This report will be 132 columns.

5.6 **Color Graphics Display of Trended Data**

Up to three parameters may be plotted with the total period for the display from 1 to 14 days. For each parameter there will be three curves: the upper curve defining max values, center curve for the mean values and the bottom curve for the minimum values. The plating line will be displayed at the bottom of the screen while the trended curves are displayed.

Real time trending of parameters is optional. This option allows the user to see data points plotted as they are collected. A moving bar erase will be used to maintain current data on the screen.

6.0 The control system will accomplish the data collection, and provide overall facility control and incorporate the plating line controller into a communications network. An additional computer will be used to implement the line control.

## 7.0 PARAMETERS CONTROLLED

The following chart indicates which functions will be controlled by the control system and whether they will be controlled by value or on/off.

| Parameter | On/off | Value |
|---|---|---|
| A. Temperature | | $^{o}F$ or $^{o}C$ |
| B. Conductivity or Resistivity | | mhos |
| C. Flow | X | |
| 1. GPM may be recorded | | Optional |
| D. Level Controls | X | |
| 1. Level status | X | Optional |
| E. Mechanical Agitation | X | |
| F. Rectifiers | | |
| 1. Current or voltage (both are recorded and limited) | | |
| 2. Ramp rate | | |
| 3. Amp-minutes | | |
| G. pH | | pH units |
| H. Ancillary Controls or Off-Line Devices (i.e., automatic analytical instrumentation, chemical feeds, automatic loading/unloading, etc.) | X | X |

The values for your system will be input in a spreadsheet format and are alterable by the user with the correct password access.

SYSTEM MANAGER

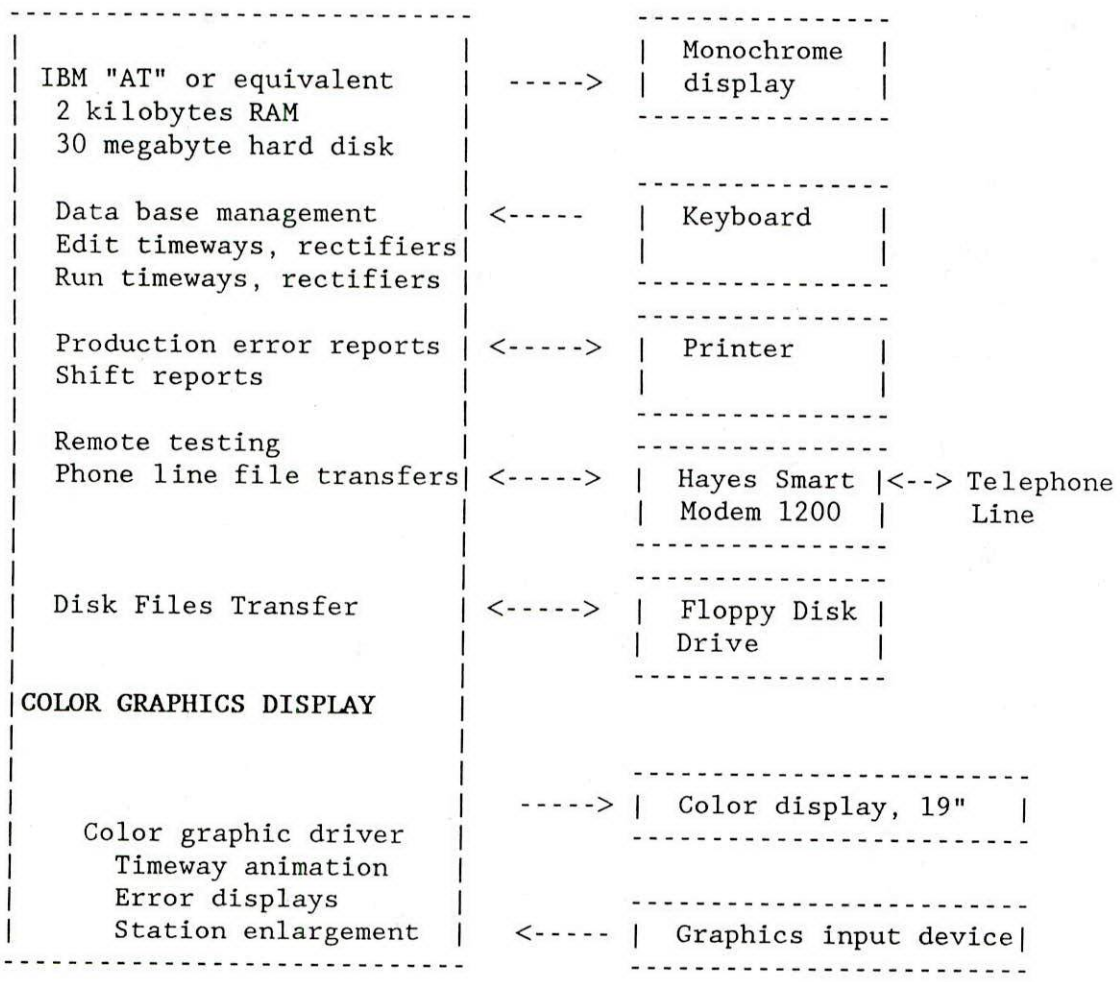


HARDWARE

Licensed Software Included
Battery Backed Clock
Also Provides for RAM Expansion
Modem
Monochrome Graphics
16 Channel Digital I/O
Require Clock Board

I/O SYSTEM

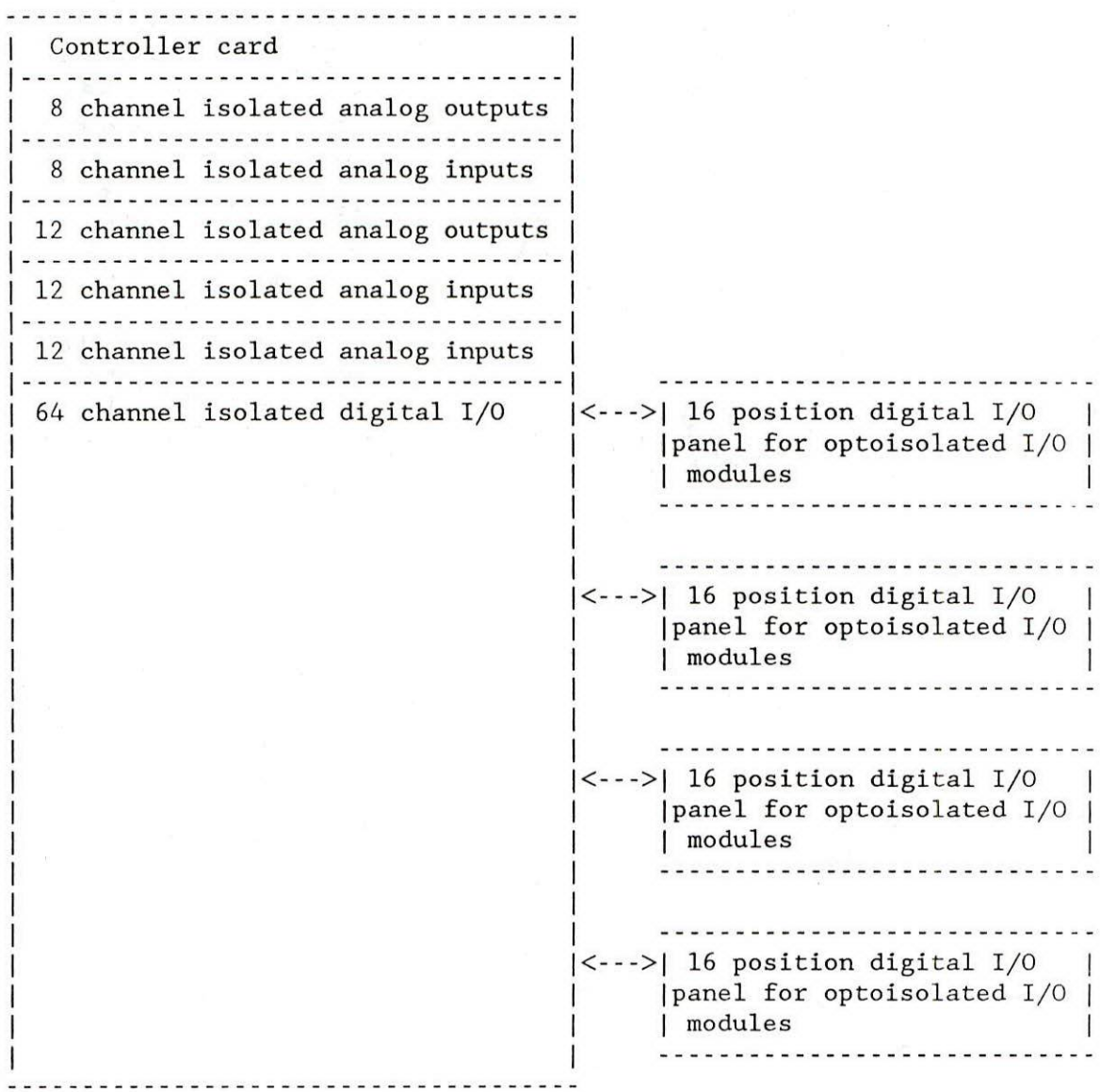


Control Card and Card Cage
8 channel isolated analog output (temperature control)
8 channel isolated analog input (flow counting)
12 channel isolated analog input (RTD temperature, pH, conductivity)
64 channel isolated digital input/output

Some features of the system are:

* All analog inputs are isolated to 1000 volts
  This is very important on the 60 mVolt current shunt input

* All analog inputs are filtered to 1 Hz
  This is very important in an industrial environment

* All analog outputs are isolated to 1000 volts
  This is very important on the control outputs to the rectifiers

* All the computer and analog I/O hardware is off the shelf.
  The computer hardware has local service in most cities.
  The analog I/O hardware has local service some cities

* The system is easily expandable to several computers for larger installations. The computers are all connected together with a local area network which is a high speed serial communications network using a coaxial cable

SPECIFICATIONS:

Analog Inputs ----------

Isolation 1,500 volts channel to channel and input to output
Maximum differential voltage 130 V rms without damage
CMRR with 10 ohm unbalance, 60 Hz is 120 db.
Inputs filtered to be down 3 db at 3 Hz and 160 db at 60 Hz
Accuracy better than 0.1% of full scale

| Signal |
| --- |
| + - 50 mV for current sensing |
| + - 10 V for voltage sensing. Larger signals may be divided down. |

Analog Outputs ----------

Isolation 1000V channel to channel and input to output
Maximum differential voltage 130 V rms without damage
CMRR with 10 ohm unbalance, 60 Hz is 120 db.
Inputs filtered to be down 3db at 3 Hz and 160 db at 60 Hz

| Signal |
| --- |
| 0 to 5 V with an output impedance of 250 ohms to control rectifier voltage |

Digital Inputs ----------

Isolation 2500V channel to channel and input to output

| Signal |
| --- |
| 90V to 140V AC |
| 180V to 280V AC |
| 10V to 32V DC |

Digital Outputs ----------

Isolation 2500V channel to channel and input to output

| Signal |
| --- |
| 12V to 140V AC |
| 24V to 280V AC |
| 0V to 60V DC |

E-2

# Electronics II
# Session E

## A Methodology for Laboratory Evaluation of Solder Electroplating Baths

J.P. Melka, Jr. and D.L. Helder
AT&T
Richmond, VA

# A METHODOLOGY FOR LABORATORY EVALUATION OF SOLDER ELECTROPLATING BATHS

by
J. P. Melka, Jr.
D. L. Helder

AT&T

Richmond, VA

ABSTRACT

A low-cost, but effective methodology was designed to examine those aspects necessary to a comprehensive evaluation of solder electroplating baths for printed wiring boards. The evaluation included examining electrodeposits on test panels and selected circuit patterns by traditional and specifically developed techniques. Systematic examination of data, image analysis, and carefully chosen statistical analysis yielded a strong indication for a best first choice production plating bath. Moreover, this investigation precipitated the development of a comparative plating bath evaluation methodology which has capability for more general application.

## I. INTRODUCTION

Selection of an electroplating process for high volume routine manufacturing use is always a risky and tenuous endeavor. The usual practice is to perform laboratory experiments as a preliminary step in the selection process. Unfortunately, a laboratory scale examination can often yield results that are not truly representative of what occurs in production size facilities. Hence, orderly comparative studies are typically necessary.

While engineers in the PWB industry periodically examine alternative or "improved" electroplating baths, there appeared to be a definite lack of a formalized general methodology which could be readily applied to facilitate the formation of a plan of comparative evaluation to address the specific needs at hand. When this investigation was initiated, it was approached with the idea that the experimental design should be of such a nature that a general investigative methodology might be abstracted from the design and formally documented.

The purpose of this paper is to present that methodology to help define the details of laboratory investigations which may enhance the probability of successful scale-up to manufacturing levels. Solder plating was the vehicle chosen to exemplify the methodology since the field of alloy plating is more complex than single metal deposition.

## II. EXPERIMENTAL

### A. Formation of List of Attributes

The first step was to compile all of the attributes of solder electroplating performance which must be included in order to make a sound decision on the relative performance of the baths under study. Collective engineering judgement, product requirements, and manufacturing experience were the prime tools employed in this phase. In general, the attributes which are selected will, of course, depend on the particular requirements on the product being manufactured, any manufacturing problem areas which need to be specifically addressed, and the manufacturing and environmental considerations prevalent at the plant location.

Some of the attributes chosen will most probably be those of typical concern such as throwing power and variation in alloy. Gathering of data in the established attribute areas can usually be accomplished by established methods, e.g., metallographic cross-sections, atomic absorption, etc. However, in

addressing the more sophisticated requirements of advanced product designs or eliminating weaknesses in a manufacturing sequence, it can become necessary for the investigators to develop specific additional attributes as well as associated methods of testing in order to obtain the proper data to meet the needs at hand. This was true of the evaluation discussed in this paper.

It must be emphasized that a list of attributes can become unnecessarily long if all possible items which might conceivably receive consideration are included. Therefore, any investigative team would find it profitable to reconsider selected items for deletion if their outcome is deemed predictable with an adequate degree of certainty or if their expected impact on the results is deemed minor. Usually available time, prior experience, or economic considerations will govern the extent of judicious experimental "trimming."

Using the techniques described above, the attributes specific to this comparative solder electroplating bath investigation were developed. The more traditional concerns included:

a. alloy composition
b. surface electrodeposit thickness
c. through-hole electrodeposit thickness
d. resultant throwing power
e. the distributions of the values of the above four items

The other concerns which were directed toward specific product requirements and which may have required specific development of analytical procedures as well as development of the attributes themselves included:

a. surface morphology
b. chemical nature of the surface
c. organic coating adhesion

B. Test Panels

Three different panel configurations were used during the plating experiments. The first was a three-inch wide strip of copper clad epoxy glass substrate. Once the designated solder plating runs were completed, these strips were used for three different tests. Firstly, they were subjected to an examination of the surface topography by scanning electron microscopy to determine the nature of the surface morphology and to observe the consistency of that morphology throughout the

plating tests. Secondly, portions of these panels were subjected to a surface analysis for a particular attribute associated with a specific requirement on a portion of the PWB product. This analysis was specifically developed for this investigation. The values achieved in this analysis allowed the test baths to be rank ordered according desirability of performance. Finally, the remaining portions of these panels were subjected to organic coating adhesion tests according to ASTM Test Designation D3359-83. This designation is essentially an assessment of adhesion by a tape test.

The second test vehicle was a quarter of a production panel of a circuit pack code which had gone through production copper plating but was removed from production processing immediately after the rinse following copper electrodeposition. The code that was chosen had a circuit configuration which was typical of a significant part of normal production. It had a relatively homogeneous circuitry distribution, but also an area of nonuniformity in order to create a skewed electrical field on a portion of the circuit pattern within the plating cell.

The third test vehicle was a quarter of a production panel of a thick backplane code where greater than 80 percent of the panel was exposed area (i.e., not covered by photoresist). This test vehicle was also intercepted immediately after the rinse following copper electrodeposition. This code was also chosen because it is typical of a significant portion of normal production.

Both sets of quarter panels were used for the same types of examinations:

1. alloy composition and the distribution thereof by differential thermal analysis, [1]

2. plating thickness on path and land surfaces and the distribution thereof by light section microscopy,

3. through-hole plating thickness and the distribution thereof by metallographic cross-sectioning,

4. throwing power by the ratios of the surface and through-hole plating thickness measurements.

A number of measurements (typically eight) were made for each of the above categories for each quarter-panel plated. Moreover, the sites where the samples were taken or measurements were made on the quarter-panels were carefully chosen to

include areas which represented extremes of current density for the specific circuit configurations chosen as the test vehicles.

C. Experimental Electroplating Cell

The experimental plating cell was designed and constructed specifically for this investigation. The cell was designed around the concept of plating the lower half of a quarter-panel on both sides with anode arrays symmetrical to a centerline lying within the plane of the cathode and perpendicular to the surface of the electrolyte. The tank itself was constructed of polypropylene. Teflon guides were fitted relatively snugly along both longer dimensional sides of the tank so that when the quarter-panel was inserted into the guides all the way to the floor of the tank, the plating cell was essentially divided into two separate mirror-image sub-cells. Agitation was provided for each sub-cell by medium-duty, variable-speed lab stirrers with polypropylene shafts and impellers. Short length tin/lead anodes, cut from regular shop anodes, reaching to approximately three-quarters of an inch from the tank floor were hung from anode bars which were parallel to and close to the short dimensional ends of the tank. Electrical contact from the rectifier was made with appropriate wires and alligator clamps which were kept meticulously clean throughout the entirety of the laboratory experimentation. The working volume of plating solution in the tank was 12 liters. The experimental cell is illustrated in Figure 1 and Figure 2.

Figure 1 shows the electroplating setup for the three-inch wide test strips. During this portion of the experimentation an unclad epoxy quarter-panel was inserted into the Teflon guides to divide the cell into the aforementioned two sub-cells. Two strips were clamped onto both sides of the insulating quarter-panel (one in each sub-cell) and plated simultaneously during a single experimental run. One anode was hung from each anode bar directly in line with the corresponding strip in its sub-cell.

Figure 2 shows the plating setup for plating the imaged and copper-plated quarter-panels. Here the quarter-panel itself divides the cell as mentioned before. In this case two anodes were hung from each anode bar, evenly spaced across the width of the tank.

As with all plating tests, various ancillaries were required in conjunction with the cell itself. In this case, one acidic cleaning tank, one deionized water pre-plate rinse tank, and

one city water post-plate rinse tank were employed. The polypropylene rinse tanks were placed on a large tray in which a corner drain had been fabricated so that the rinses could be operated in an overflow fashion. The acidic clean tank was placed in between the rinse tanks for convenience. When it was required, electric heaters were used for heating of the city water rinse and warming the plating bath. The entire setup is illustrated in Figure 3.

It can be readily observed from Figure 3 that the equipment was merely set up on the top of a standard laboratory bench. It required no "installation" as such. Most of the equipment employed was typical of small laboratory electroplating apparatus found in a testing or process control laboratory for general applications. The only specialized portion of the entire testing facility was the teflon (PVC or polypropylene would have been equally suitable) guides which held the panels in position during electrolysis. The construction of the guides was accomplished with the most basic of tools: hand drill, hacksaw, etc. The economies of the test apparatus employed should be obvious.

D. Electroplating Baths Studied

The data sheets of commercially available solder baths were examined for their suitability and advisability for this laboratory investigation.

The data sheets were examined for the recommended current density range, operating temperature range, chemical basis of the brightener system, and bath acid basis. Three were chosen on the basis of overall apparent suitability.

The vendors were then solicited to submit five-gallon samples of their baths for our evaluation. The intention was that the baths were to be formulated, mixed, and purified by the vendors prior to submission for our testing. The rationale for doing this was to allow the vendors to maximize their advantage by providing an optimum bath formulation.

The solder plating bath which is currently in use in the solder plating operation at the Richmond Works was used as the control bath in the comparative study. In the case of this bath, the sample for experimental plating was obtained by drawing an adequate amount from the shop production bath which was deemed to be functioning properly by the functional process engineer.

All baths, hereinafter, shall be referred to by their letter designation: A, B, C or D.

E. Experimental Electroplating and Rinsing Sequence

For each solder electroplating bath tested, a total of 24 test panels were plated. To start, four pairs of the three-inch wide unimaged panels were plated. The first pair and fourth pair plated received a high flow rate, approximately 80 to 85°, city water final rinse for two minutes. The second and third pairs of three-inch wide panels in this first segment of electroplating tests were rinsed in city water heated to approximately 150° Fahrenheit. [2]

The second segment of electroplating tests consisted of plating four circuit pack quarter-panels and four backplane quarter-panels. In order to offset any possible effects of bath aging as the test plating proceeded, plating of the circuit pack and backplane quarter-panels was alternated so that the circuit pack quarter-panels were plated in the first and consecutive odd numbered positions in the order of plating. During this second segment, the rinse water was maintained at approximately 90° Fahrenheit with a high flow rate.

The third segment of the plating test again involved four sets of three-inch wide unimaged panels. The third segment was essentially a repeat of the first segment. The rationale for running the three-inch wide unmasked panels in this fashion, bracketing the quarter-panel electroplating tests, was based on the fact that all surface characterization studies were to be run on the three-inch wide panels. Therefore, it was deemed necessary that these panels should be representative of the minimum and maximum aging of the test baths as the plating trials were performed.

The suppliers of all the baths claimed that the amount of proprietary additive contained in their respective baths would be adequate for the entire experimental sequence. Consequently, no brightener replenishments were made to the baths once the above discussed pattern of plating trials had commenced.

## III. RESULTS

A. General Appearance

Upon completion of the electroplating tests and final rinsing, all of the three-inch wide strips possessed staining along the

edges and corners of the solder plated portion of said test strips when dry. This was attributed to the fact that they were all simply air dried in a plastic rack. The balance of the surfaces on the test strips displayed an even coloration and were not at all blotchy. Bath C samples presented the most desirable appearance, being light and even. The Bath B samples were still even but somewhat darker in coloration. The Bath A panels were lighter in appearance than the Bath B panels, but displayed some nodularity at the edges of these panels on those samples run near the end of the experiment. The Bath D panels were decidedly darker in general coloration than all the rest. However, they still were even in coloration and possessed no nodularity along the edges.

B. Latitude of Brightener Behavior

The observations discussed in this section concern the consistency of surface appearance resulting from an extended experimental run without brightener replenishment of the bath under test. The appearances of all samples from three of the baths were consistent throughout the entirety of their respective experimental runs. The exception was the Bath A which exhibited need for replenishment (the edge nodularity discussed above) during the last two runs of the total experiment.

C. Surface Character by Scanning Electron Microscopy (SEM)

This particular phase of the investigation yielded results which were relatively unambiguous in regard to interpretation for the characteristics under study. The baths are discussed in this section in the order of desirability of their surface character for the adhesion of an organic coating to the electrodeposited solder surface. The results are based exclusively on judgements made on the character of the topography as derived from experimental results on other projects which involved a study of an organic applied to a metallic surface. [3]

Within each group of scanning electron micrographs of the electrodeposit surfaces from the three-inch wide strips from a given electroplating bath, image analysis techniques were used to rank order all of the micrographs according to surface roughness. A simplified version for obtaining agglomerate and general particle size distribution by measurement of the intercept cord-length was employed. [4] These measurements were applied only where appropriate to the nature of the surface.

1. Bath D

Figure 4 shows the median micro-surface. The surface is composed mainly of ridges of sharper edged granules (as seen at the 5000X magnification) which form a harsh textured surface (as seen at the 1000X magnification). These sharper edged granules would be expected to form a good "tooth" to penetrate an organic coating, so as to maximize solder to organic coating contact while requiring a minimum amount of flow of said organic.

2. Bath B

Figure 5 shows the median micro-surface. Here the surface is composed of somewhat rounded granules which are 40 to 60 microinches in size (as seen at the 5000X magnification) with tendencies to become agglomerated along linear laterally oriented patterns which possibly correspond to the vendor generated brush marks in the copper substrate (as seen at the 1000X magnification). Such a surface would be expected to require a low amount of flow of an organic to maximize contact between the organic coating and the solder in order to achieve good adhesion. However, the rounder granules would limit the amount of penetration of solder into the organic coating.

3. Bath A

Figure 6 shows the median micro-surface as determined by image analysis. The surface is composed of granules, 20-40 microinches in size, which are intimately agglomerated to form generally rounded nodules (as seen at the 5000X magnification) which are, in turn, positioned in a random, but even close-packed array across the surface (as seen at the 1000X magnification). This type of surface morphology would require a greater flow of organic to maximize the organic coating and solder contact. However, the nature of the nodules provides ready sites for the organic coating to physically lock onto, hence, providing a surface whose organic coating adhesion properties would probably be comparable to the Bath B structure discussed above.

4. Bath C

Figure 7 shows the median micro-surface. This surface tends to exhibit a transition between nodular and rounded

granular surfaces which has the potential to bring out the detrimental characteristics of both. The larger irregular nodular agglomerates are generally rounded, being 60 to 160 microinches in size and composed of smaller intimately packed granules of such varying sizes to prevent a meaningful measurement (as seen at the 5000X magnification). These agglomerates, while generally positioned in a random close-packed array, are also seen to occasionally take on a somewhat linear alignment which may correspond to the vendor generated brush marks on the copper substrate (as seen at 1000X magnification).

D. Surface Analysis

Table I provides the results for the surface analysis performed on the solder plated surfaces of the three-inch wide copper strips.

The results achieved were totally unambiguous and the baths were readily rank ordered. This was first done qualitatively and then proportionally, based on the values of the data obtained. The nature of this portion of the investigation did not appear to require statistical evaluation to achieve a practical conclusion at the end of the study.

E. Organic Coating Adhesion Testing

The means of the results of the organic coating adhesion testing are also included in Table I. The results of the tests are expressed numerically on a scale of 1 to 5 (with a value of 5 indicating the highest adhesion). The results of the adhesion testing appear essentially to track one-to-one with the surface analysis ranking. However, it can just as easily be claimed that the organic coating adhesion testing results track one-to-one with the analysis of the results of the surface character regarding the desirability for adhesion as judged from the scanning electron microscope topography examinations.

Whatever the case, the more darkly colored deposits from Bath D produced the highest level of adhesion. The Baths A and B results were approximately comparable when all the values from which the means were calculated were examined. Bath C unquestionably produced the electrodeposit which was the poorest performer, having not only the lowest composite average adhesion values, but also generating the lowest single values for any individual tests (i.e., a value of 1).

F. Alloy Variation

When the tin/lead composition means and standard deviations for each of the two different types of quarter-panels (circuit pack and backplane) were calculated for the four baths under examination, the relative capabilities for consistency of performance of the individual baths were not readily evident. These values were then subjected to further examination by appropriate statistical analysis. Initially, a form of a box plot of the distribution of the data was made. This is illustrated in Figure 8. This type of plot shows the range of values for each of the two types of quarter-panels plated in each of the four baths under study. The asterisks within each of the thin bar plots is not indicative of the number of measurements made. The broken line connects the arithmetic means of the individual groups of data.

Upon initial examination of this plot, it would appear that Bath C and Bath D performed more consistently since the length of the bars covering their data points are obviously the shortest. One would also be tempted to award the Bath D a slight edge in performance. However, it was deemed most advisable to apply appropriate statistical analysis to the numerical values of the data to provide a means for a firmer judgment on the experimental results.

The object of good bath performance is consistency across the workpiece. In other words the less variation in the values of the attribute under observation (be it alloy composition, plating thicknesses, etc.) the better. Hence, a statistical test for differences in variance was applied. The specific method chosen was the Siegel-Tukey non-parametric test. [5] In this test, statistical significance was acknowledged when the confidence level exceeded 90 percent in rejecting a two-sided equivalency hypothesis.

The results indicated that for both backplane and circuit pack quarter-panels the variation of the Bath D was indeed less than the Bath A or Bath B. However, no statistical difference in variation could be demonstrated between the performance of Bath C and Bath D.

G. Surface Thickness Variation

The distribution plot of the data for each of the two types of quarter-panels plated in each of the four baths is illustrated in Figure 9. While a definite difference is seen in the data distribution between the backplane and circuit pack quarter-

panels, it is not really possible to make a judgment on the performance of the individual baths by simple observation. The Siegel-Tukey non-parametric test was applied for the same reasons as discussed in the above section. No statistical difference between baths was indicated for the experimental runs using the circuit pack quarter-panels. However, for the backplane quarter-panels, the variation in Bath D was again lower than either Bath A or Bath B.

H. Hole Thickness Variation

The distribution plot of the data for each of the two types of quarter-panels plated in each of the four baths is illustrated in Figure 10. There is a temptation to make a judgment in favor of Bath D based upon a simple observation of the distributions. However, the Siegel-Tukey non-parametric test still provided the best means for making a judgment on the results. Once again, no statistical differences in variation were obtained among the four baths for the circuit pack quarter-panels. However, the data for the backplane quarter-panels indeed indicated in favor of Bath D as having less variation than Baths A, B, or C.

I. Throwing Power

Figure 11 illustrates the composite deposit distribution plots of the data for both surface and hole thicknesses for each of the two types of panels plated in each of the four baths. On this plot the upper and lower broken lines connect the surface thickness and hole thickness means, respectively. The ratio of the value of the upper broken line to the value of the lower broken line would give an "average" throwing power. However, the variation for the data as well as the values of the means preclude any observational judgment on the graphically presented results. Moreover, because of the observed differences in variance, the means do not provide adequate information for a meaningful statistical evaluation.

## IV. DISCUSSION

While the general appearance of the plated specimens varied in hue, all had approximately the same degree of evenness in surface appearance. However, this cannot be viewed as strongly indicative of relative shop performance since typically the evenness (or lack of blotchiness) upon drying is closely related to the drying system for any given production plater. Judgments made on the operational latitude of any of the baths, especially regarding the nodularity along the edges of the latter Bath A samples must also be viewed

with reservation since routine operating replenishment could offset the observed nodularity. This cautionary commentary appears justified since the SEM study of the plated surfaces generally indicated an acceptable latitude in operation for all of the baths. This can be said for two reasons. Firstly, the surface character observed for all experimental groups was reasonably constant from the first three-inch wide panel plated at the beginning of the experiment to the last three-inch wide panel plated at the end of the total experiment for any given bath. Moreover, those scanning electron micrographs illustrated in this report as the median samples were generally not associated with their position in the sequence of electroplating trials. This was also true of samples judged roughest and smoothest from each of the four bath groups.

Initially, the generally dark coloration observed on the samples plated in Bath D was suspected of being due to a lead rich electrodeposit. The data used to plot the Bath D distribution in Figure 8, however, shows that indeed this is not the case. In fact, the Bath D yielded the second highest average tin content of all the alloys examined. Thus, it would be logical to say that the surface configuration observed in the scanning electron microscope studies (Figure 4) is apparently the main contributor to the darker coloration. The relatively jagged surface topography would be expected to be the least reflective of all of the surfaces produced during the experimentation.

The statistical analyses for alloy and deposit thickness variations fortunately followed a pattern which was generally noncontradictory to the surface characterization results. In this particular case, it proved fortunate that the results indicated the same bath as the most likely candidate for continued production use or as an alternative for production trials (whichever the case may be for any given investigation). This is so since surface characteristics and minimal deposit characteristic variations are both important attributes to be considered in the choice of a solder plating bath. Had the results been otherwise; that is, different baths exhibited prime surface characteristics and minimal deposit characteristic variations, the decision methodology for suggesting a course of action would have become far more complex. It would then become the task of appropriate engineers to perform a typical weighted rank ordering of all of the attributes studied. In order to perform this properly, the engineers would first give "best judgement" weightings to each attribute. These weightings would then be subjected to an established scaling routine in order to give the weightings more meaningful relative values in the decision making process. Then each of the baths under study would be ranked ordered within each attribute category (according to the outcome of the experimental results and analysis of data). Finally, multiplying each rank for a

given bath in each category by the weighting of that category and summing the products of said multiplications would generate a figure of merit for that bath. The resultant figures of merit for the individual baths examined could then be used in making the decision regarding shop testing of an alternative or continuation of the current bath.

Prior to the initiation of this investigation an accepted formal methodology for comparative testing for evaluation of electroplating baths for printed wiring board applications did not truly exist. More often than not, electroplating engineers have had a tendency to resort to a short series of beaker-scale trials with a procedure derived for the needs at hand each time such needs arose. The beaker trials would then be followed by shop trials, ofttimes initiated with inadequate preliminary characterization of the bath "selected" for testing. Too often a program to test a group of plating baths smacked more of improvisation than investigation.

Beside performing a periodic reassessment of an electroplating bath vital to printed wiring board production, the basic methodology of testing, setup of equipment, and the scope of attributes examined, described herein, also constituted a simultaneous attempt to fill the chronic void described above. The authors submit that the design of this investigative technique has accomplished that end. It would appear from the nature of the results achieved, that such a submission is reasonable and proper.

The apparent lack of ambiguity of the results, while not a necessary outcome of even the most well-designed experimental procedure, are possibly attributable to the careful screening and choice of the baths tested. Technical judgment and prior experience which involved an assessment of the published technical vendor data played a major role in the selection of the baths to be tested. The balance of the screening was done according to the suitability of their advertised operating conditions to fit into the Richmond Works production shop.

While, all in all, it would appear that the methodology of this investigation forms a thorough and valid screening procedure with accompanying applicable statistical tests, it must still be emphasized that the ultimate value of such an undertaking to the overall engineering effort can only be proven out by the performance of the indicated "best choice" bath during actual shop operation. The scaling up of an electrolytic process from laboratory to production has always been one more of experienced engineering judgment as opposed to a mathematical transformation. It does, however, seem totally reasonable to expect that if a given bath from a group of baths performed the best when subjected to a carefully

followed experimental procedure performed in a properly designed test vessel, it would retain its relative performance in a larger system designed for overall balance.

## V. CONCLUSIONS

A comprehensive comparative solder plating testing program has been developed which appears to be capable of providing enough information to select the most likely candidate(s) for production trials. By conducting a series of carefully coordinated experiments involving both small panel and selected product electrodeposition followed by examination of results using SEM topography, surface analyses, chemical analyses of the baths, organic coating adhesion testing, surface and hole plating thickness variation by cross-section and light-section microscopy, alloy variation by differential thermal analysis, and finally subjecting all appropriate data to statistical analysis by Siegel-Tukey non-parametric testing, the original objective was accomplished. From a carefully screened group of baths, one bath emerged as the most likely candidate.

## VI. ACKNOWLEDGEMENTS

The authors wish to recognize those individuals whose associated work, assistance, or appropriate input contributed to the material contained in this document:

Mike Grindle - for his collaboration on the choice of baths for examination.

Dick Sands and his Process Control Laboratory Staff - for their work on the metallographic cross-sections, differential thermal analysis, and light-section microscopy.

Dave Henderson - for the scanning electron microscopy work.

Jim Walker - for the performance of all of the ASTM adhesion tests.

Toni Bonner - for the photographs of the apparatus used in the experimentation.

Iris Artaki and Bob Woods of the Engineering Research Center - for their work on the surface analysis.

Linda Mayer of the Sel-Rex Company - for her consultation regarding need for a general test methodology.

## REFERENCES


1. Kuck, V. J.; "Analysis of Tin-Lead Solders Using Differential Thermal Analysis;" AES Analytical Methods Symposium; March 20, 1985.

2. Jacky, G. F.; "Immersion Tin - An Effective, Low-Cost Printed Circuit Board Coating;" Proceedings of the First Printed Circuit World Convention; June 5, 1978.

3. Melka, J. P.; "Chemical Scrubbing of Printed Circuits Prior to Photoresist Lamination;" AES 8th Symposium on Plating in the Electronics Industry; January 21, 1981.

4. Underwood, E. A.; Quantitative Stereology; Addison-Wesley; 1970; pp. 126-133.

5. Gibbons, J. D.; Nonparametric Methods for Quantitative Analysis; Holt, Rinehart, and Winston; 1976; pp. 207-218.

TABLE I

Surface Analyses and Organic Coating Adhesion Tests

| Bath Designation | Surface Analysis Rating | | Average Organic Coating Adhesion Values |
|---|---|---|---|
| | Qualitative | Weighted | |
| A | 3 | 3.13 | 4.0- |
| B | 2 | 2.05 | 4.0 |
| C | 4 | 4.0 | 3.5- |
| D | 1 | 1.0 | 5.0 |

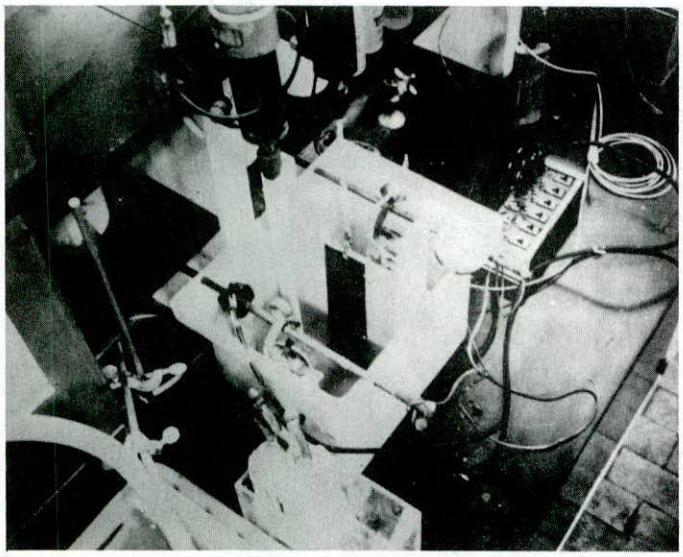

FIGURE 1

Electroplating Test Cell Set Up For 3-Inch Wide Panel

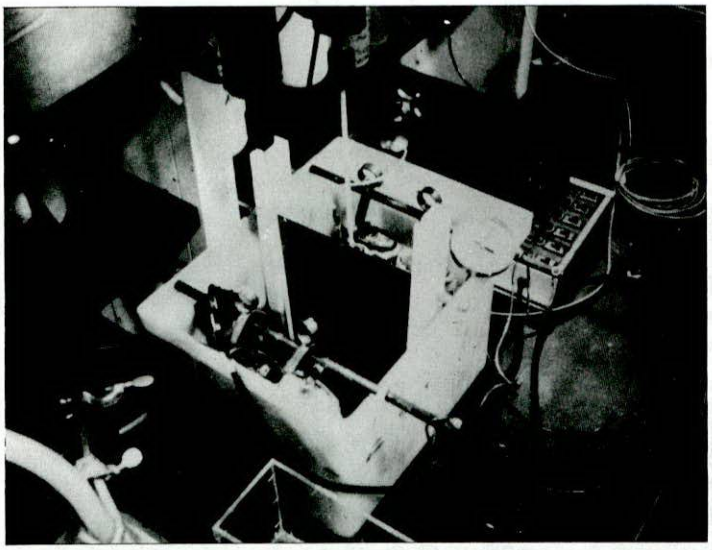

FIGURE 2

Electroplating Test Cell Set Up for Q-Panels

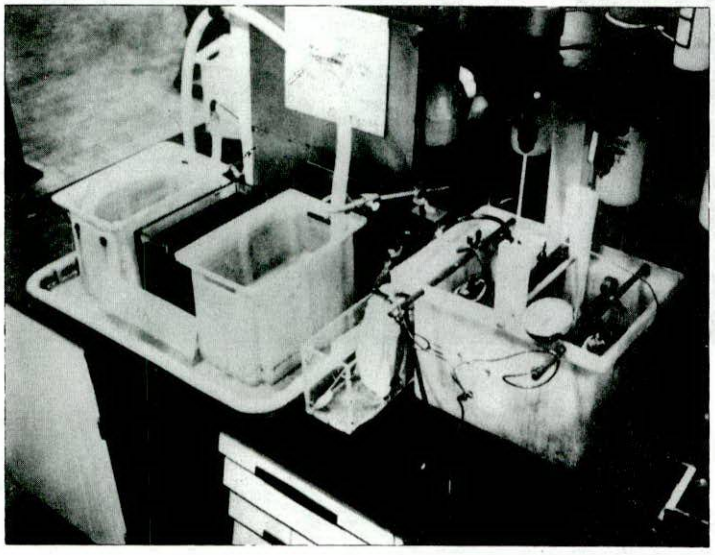

FIGURE 3

Entire Experimental Electroplating Apparatus
(Test Cell and Ancillaries)

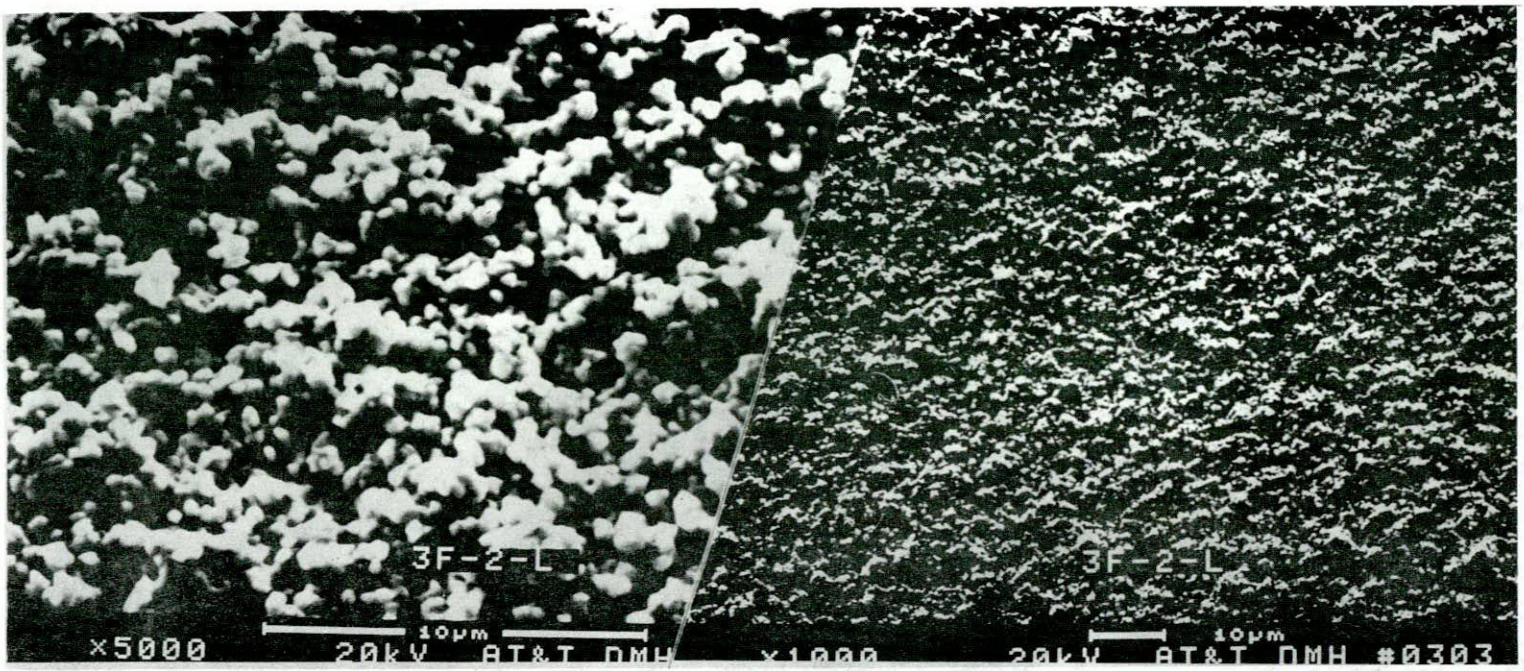


FIGURE 4

SEM Topograph of Bath D Electrodeposit Surface
Ranked Median (5000X/1000X)

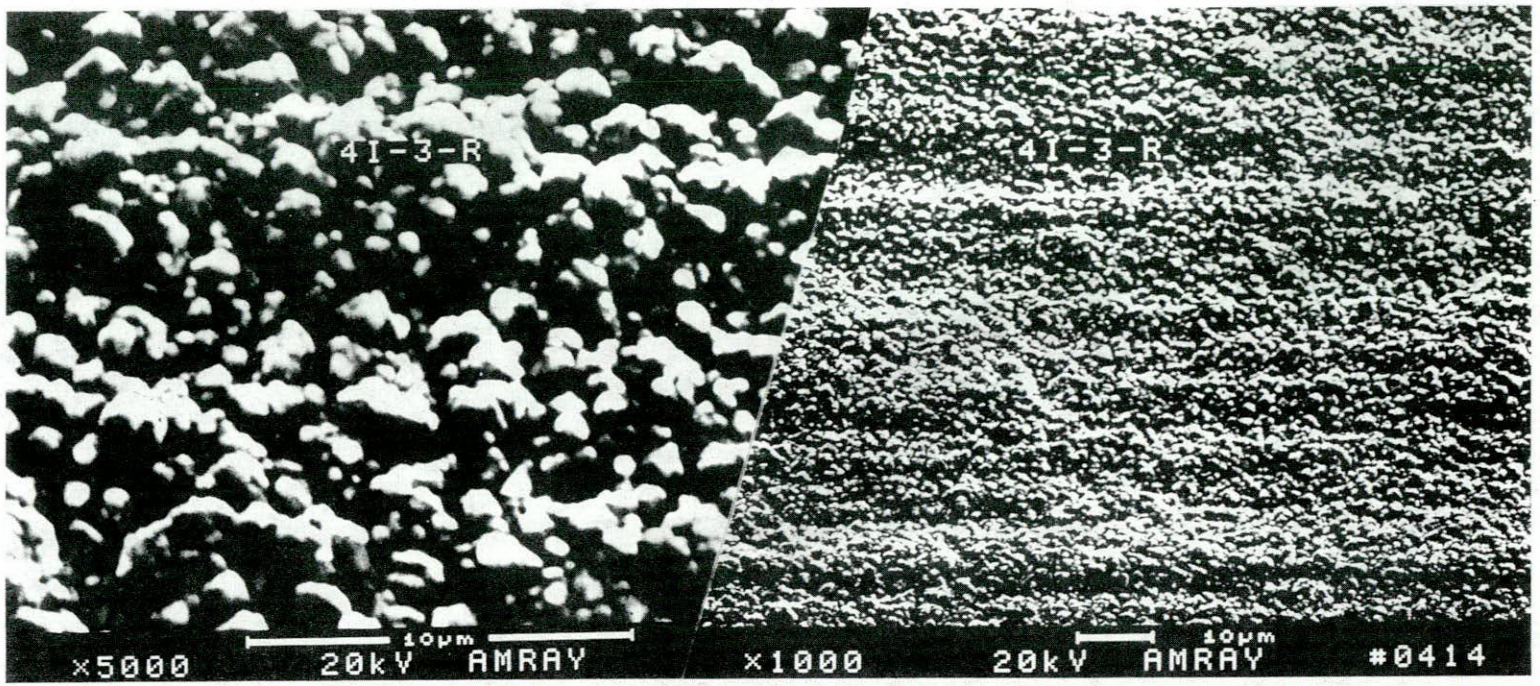


FIGURE 5

SEM Topograph of Bath B Electrodeposit Surface
Ranked Median (5000X/1000X)

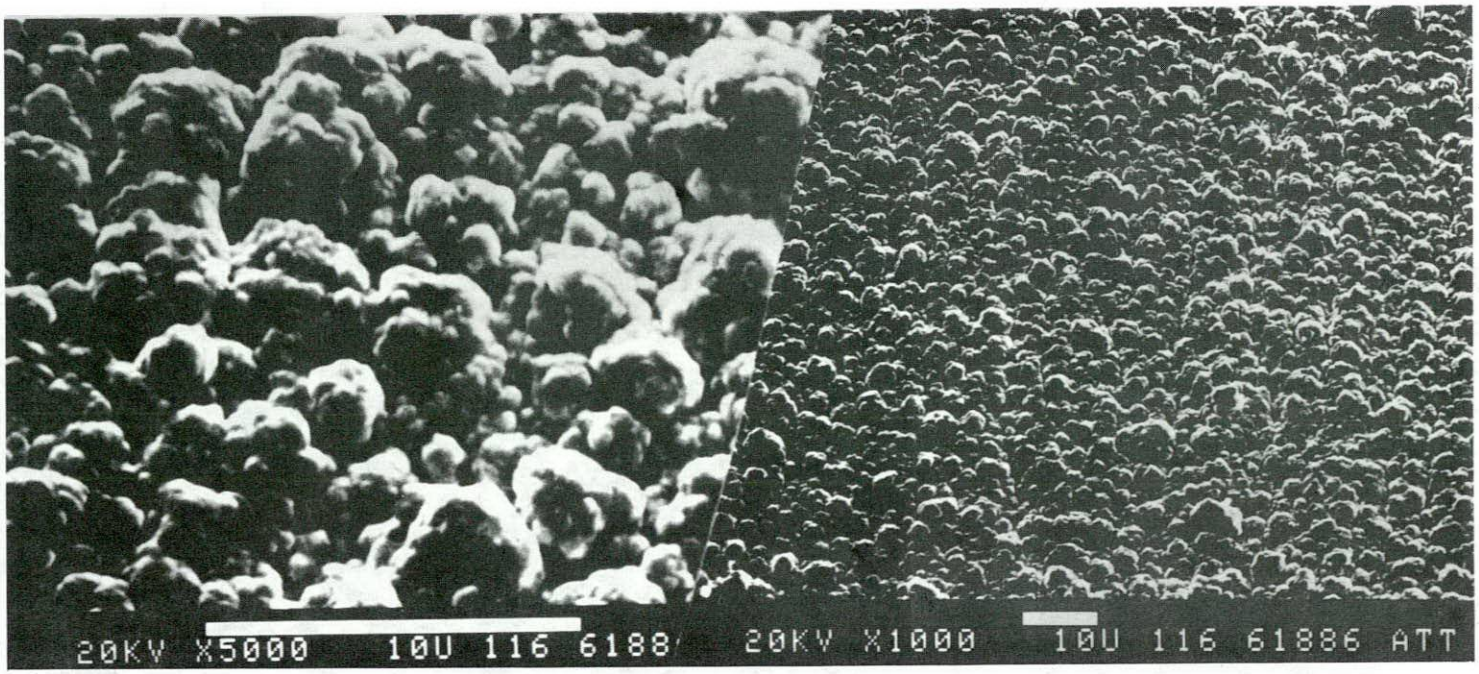


FIGURE 6

SEM Topograph of Bath A Electrodeposit Surface
Ranked Median (5000X/1000X)

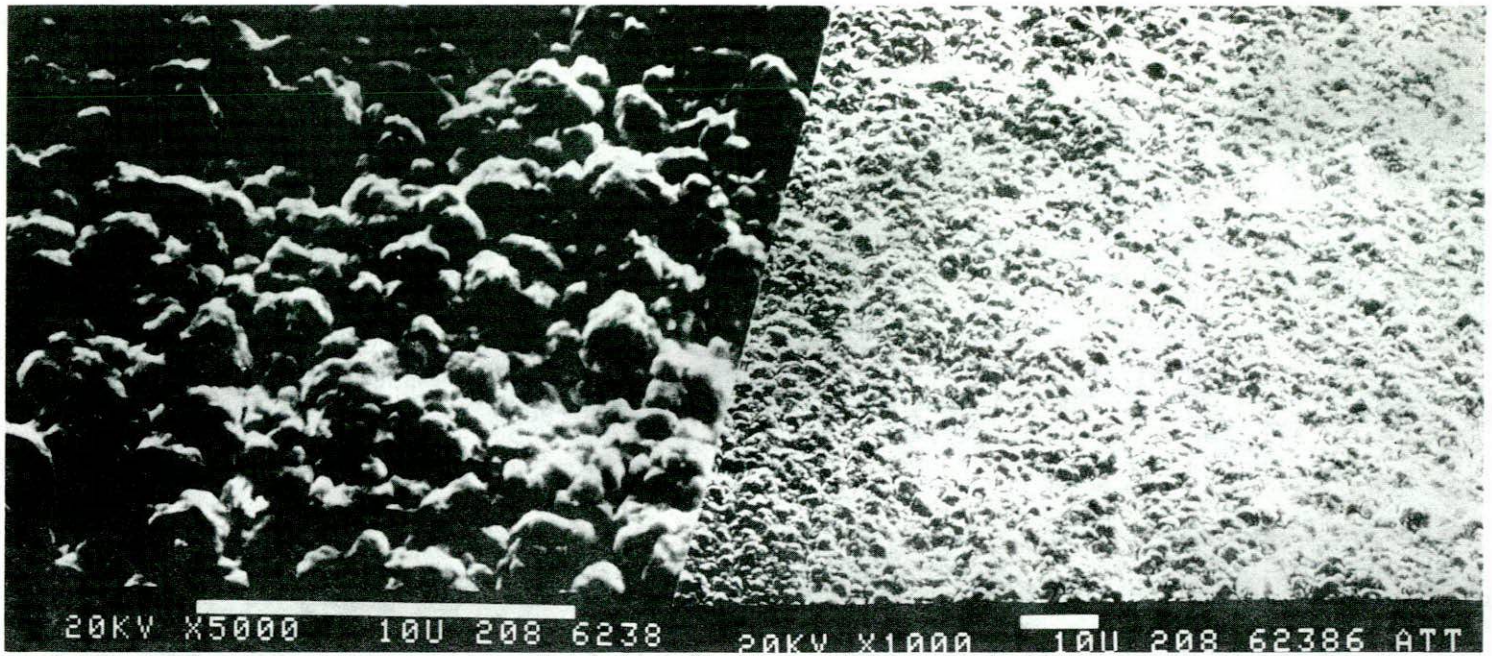


FIGURE 7

SEM Topograph of Bath C Electrodeposit Surface
Ranked Median (5000X/1000X)

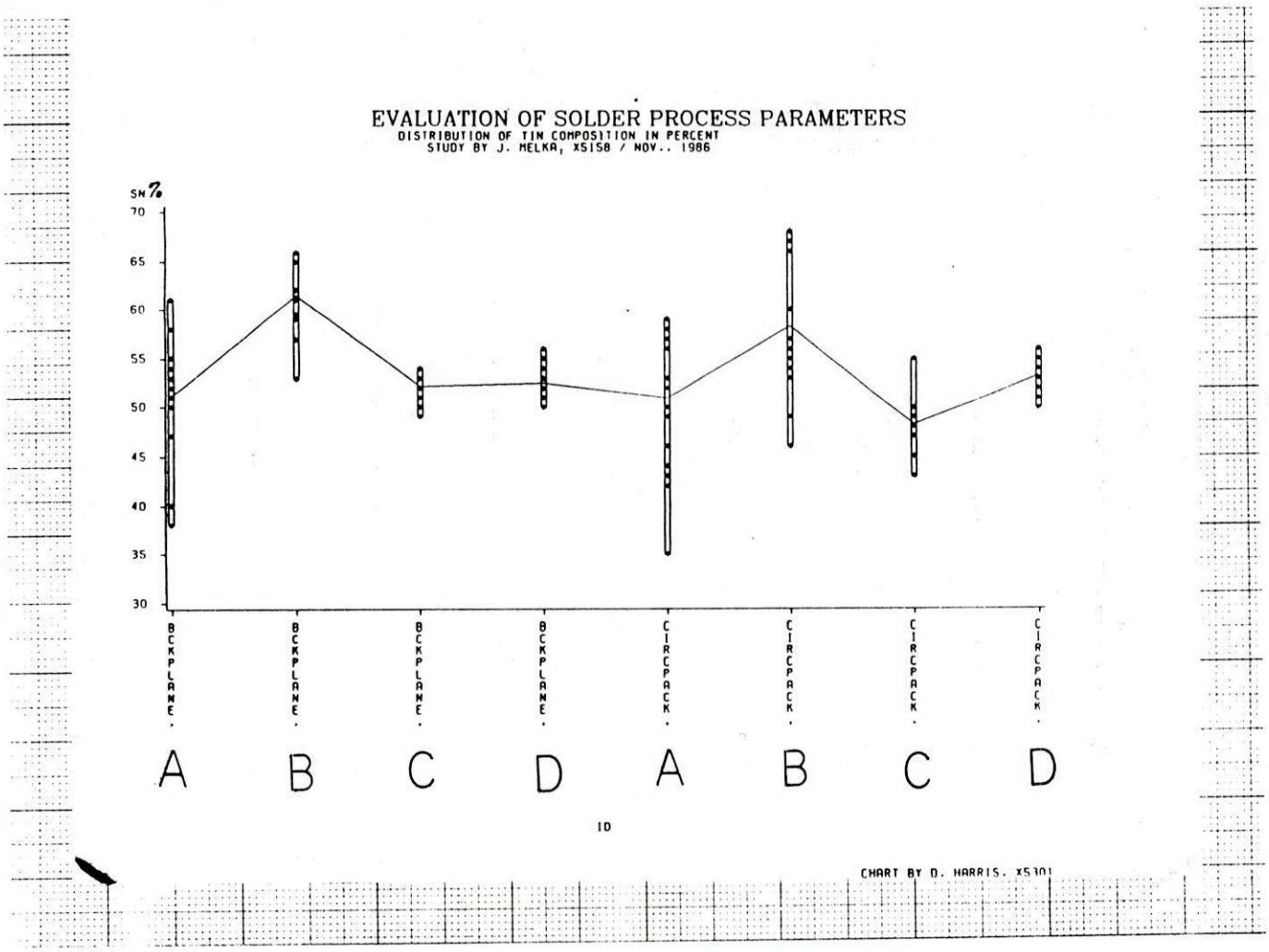


FIGURE 8

Distribution Plot of Tin Content for the Two Types of Test Q-Panels from the Four Baths

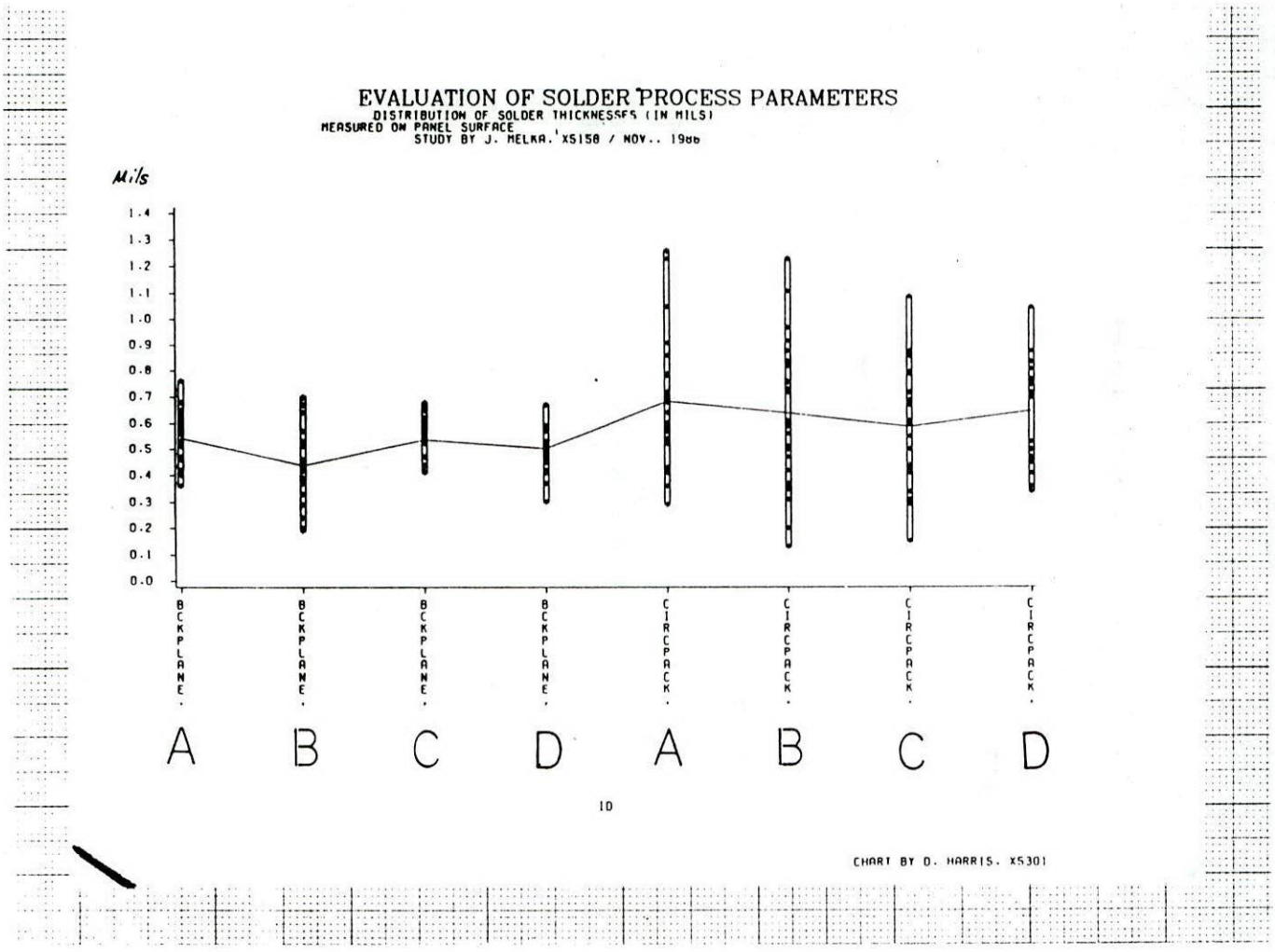


FIGURE 9

Distribution Plot of Surface Electrodeposit
Thickness for the Two Types of Test
Q-Panels from the Four Baths

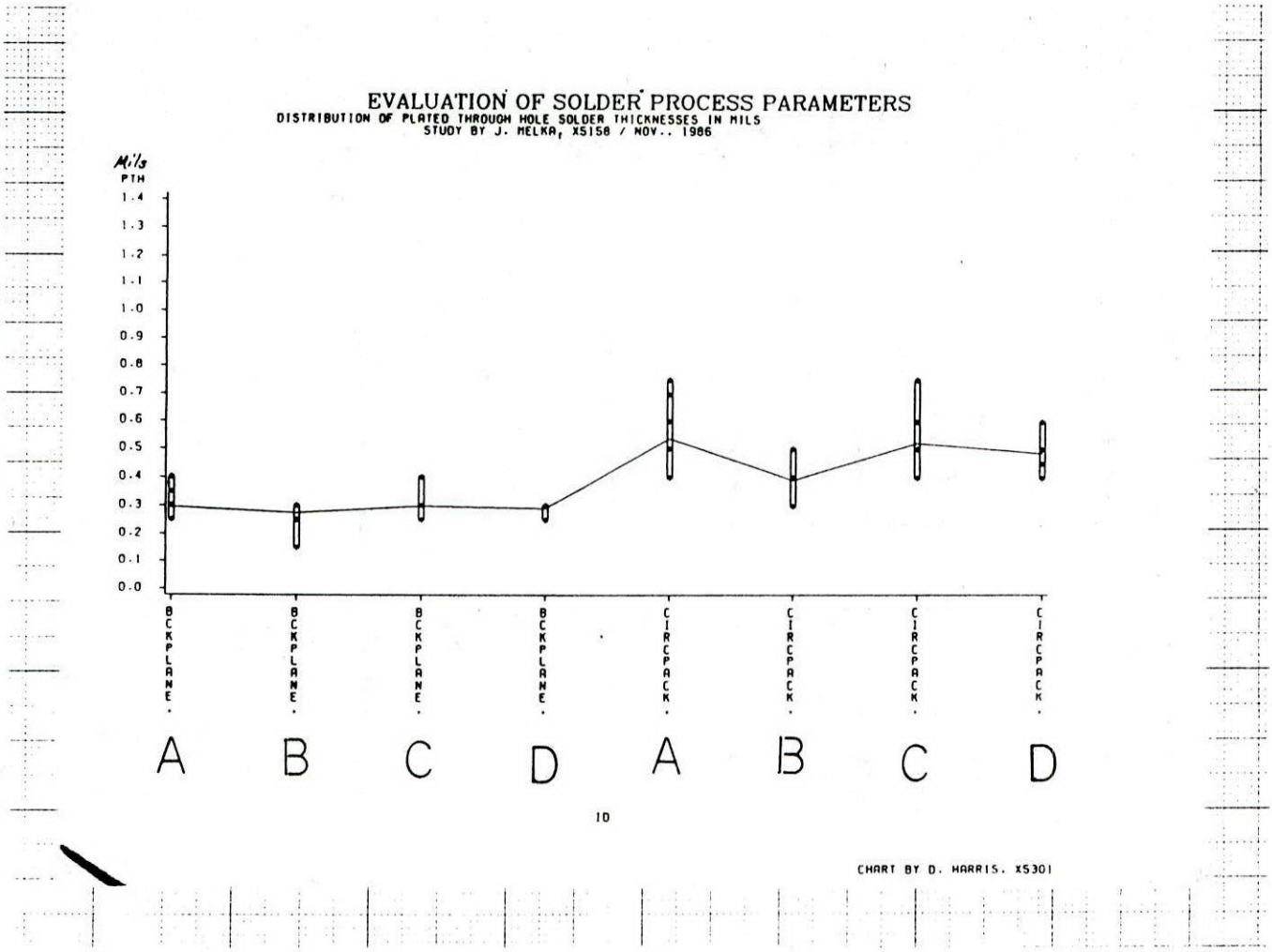


FIGURE 10

Distribution Plot of Hole Electrodeposit Thickness for the Two Types of Test Q-Panels from the Four Baths

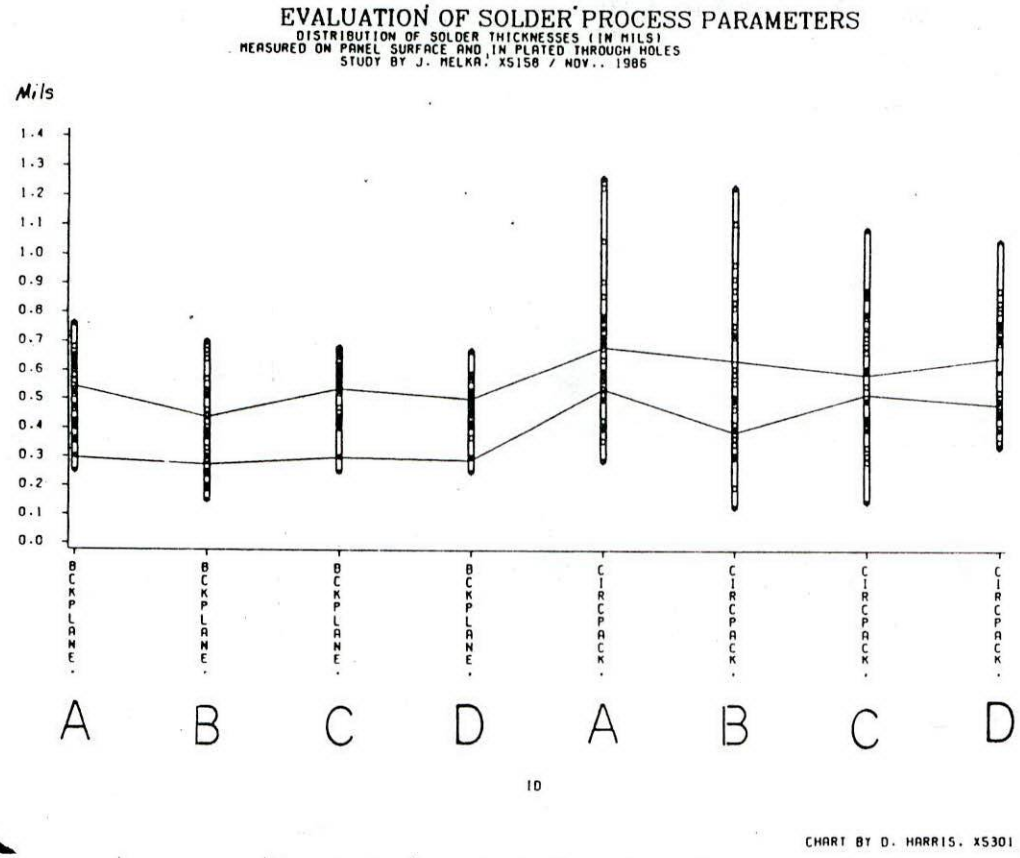


FIGURE 11

Combined Distribution Plot of All Electro-deposit Thickness for the Two Types of Test Q-Panels from the Four Baths

E-3

# Electronics II
# Session E

## Tin and Tin-Lead Alloy Electroplating in the Electronics Industry

J.L. Martin and M.P. Toben
LeaRonal, Inc.
272 Buffalo Ave.
Freeport, NY

# TIN AND TIN-LEAD ALLOY ELECTROPLATING IN THE ELECTRONICS INDUSTRY

By J. L. Martin and M.P. Toben

LeaRonal, Inc.
272 Buffalo Ave.
Freeport, NY

Tin and tin-lead alloy electrodeposits are an integral part of a majority of electronic components and subassemblies such as connector blocks and printed circuit boards.

The fundamental properties of tin and tin-lead alloys, low melting point, low cost corrosion resistance and ductility, make them the natural choice of the design engineer to effect a permanent soldered interconnection during component assembly and to allow for ease of component replacement when necessary.

The increased demand for and complexity of electronic components make process selection a crucial step in establishing an operation which is both cost effective and capable of producing a tin or tin-lead alloy finish to meet the quality requirements of the final product.

## Quality Requirements and End Use Specifications

In today's production environment the importance of quality control in predicting reliability of performance is a major factor in a company's ability to remain competitive.

Tin and tin-lead alloy electrodeposits are subject to some of the most stringent quality checks to substantiate reliability. These include solderability testing, both before and after accelerated aging, porosity and corrosion tests, and naturally, thickness and alloy checks. Many of the tests are the subject of both national and military specifications.[1-6] In the United States the most commonly applied specification is the Military Standard Mil-Std-202F.

Since the final assembly of a component may take place following prolonged periods of storage, accelerated aging tests designed to simulate storage in various climatic conditions have been studied extensively, in order to predict the useful life of tin and tin-lead alloy finishes.

As of April 1, 1987, Mil.-Std. 202F Method 208F has been updated in this regard, the duration of the steam aging test being increased to 4 - 8 hours from the 1 hour previously required. Ackroyd[7] reports that although resistance to 8 hours steam age correlates well with 6 months shelf life, a 24 hour steam age is required in order to distinguish the variation in solderability performance between deposit thicknesses in the range of 2 - 8 microns (80 - 320 microinches). Other accelerated aging tests used in the industry include dry heating at 155°C for 16 hours,[8,9] claimed to be equivalent to the effect of 12 months' normal storage.

Many of the findings of the accelerated aging studies are incorporated by individual manufacturers to take account of their customer's requirements and improve reliability of performance after storage.

The ultimate requirement for any tin or tin-lead finish is solderability either by fusing or by dipping in molten solder. The components are evaluated by the uniformity of coverage or "wetting" of the solidified solder coating. The temperature at which the molten solder test is conducted also varies from specification to specification. Currently the Mil-Std. 202F Method 208F requires a temperature of 245°C, recently increased from 232°C, whereas other specifications call for a temperature of up to 260°C.

In order to meet minimum specifications, the electrodeposits must have the following basic properties:

**Uniformity of thickness and alloy composition**

**Fine grained crystal structure**

**Low or zero porosity.**

## Process Selection

The processes used to achieve these deposit characteristics are evaluated on the basis of:

**Finish required**

- matte or bright
- alloy composition
- deposit thickness

**Ease of operation**

- control requirements
- availability of analytical control methods
- consistency
- ease of handling
- ease of treatment and disposal of effluent

**Economy of use**

- cost of raw materials
- cost of maintenance and equipment
- yield versus cost

**Productivity**

- yield versus time

The vast majority of electrolytes currently used for the high volume tin and tin-lead alloy electroplating of electronic components are based on acid solutions of soluble stannous tin Sn II and lead Pb salts.

Acid solutions have become the choice of the electronics industry despite their inherent corrosive nature because of the high rates of deposition achievable from these systems. The high solubility of the divalent metal salts in these matrices allows the formulation of electrolytes to achieve the high current densities required for efficient production in modern high speed reel to reel electroplating equipment.

There are three electrolytes commonly in use:

1. **Sulfuric acid based**
2. **Fluoboric acid based**
3. **Organic sulfonic acid based.**

The specific formulation of the electrolyte in terms of metal ion and acid concentrations will vary, dependent on the process, the particular application and the production equipment. However, since the electrolyte type will impact all subsequent decisions related to process selection, thorough consideration should be given to the relative merits of the alternative electrolytes available before proceeding.

## Sulfuric Acid Based Electrolytes

Due to the insolubility of lead sulfate, $PbSO_4$, the sulfuric acid based electrolytes are restricted to the electrodeposition of pure tin. However, because of the low initial cost of sulfate based chemicals, the system is still used despite its limitations.

## Fluoboric Acid Based Electrolytes

Fluoborate based systems came into prominence due to their ability to electrodeposit both pure tin and a wide range of tin-lead alloys at extremely high current densities.

Both tin and lead are added as liquid concentrates of tin fluoborate $Sn(BF_4)_2$ and lead fluoborate $Pb(BF_4)_2$.

## Organic Sulfonic Acid Based Electrolytes

Electrolytes based on organic sulfonic acids are relative newcomers to the electroplating industry. Introduced commercially in the early 1980's, the systems were well received due to their inherent advantages with respect to ease and flexibility of operation and have successfully established themselves as the preferred process for the high speed reel to reel tin and tin-lead alloy electroplating of electronic components.

The tin and lead are added as liquid concentrates of tin organic sulfonate and lead organic sulfonate.

Since all the sytems are acidic and contain stannous tin Sn II salts, there are inherent and common problems associated with their use. These are the corrosive nature of the electrolytes and the tendency for the divalent stannous tin to oxidize to tetravalent stannic tin Sn IV.

## Corrosive Nature of the Electrolytes

By far, the most corrosive electrolyte is the fluoborate based system. The corrosive nature of fluoboric acid itself is compounded by the formation of the fluoride ion during electrolysis which mandates the use of the most acid resistant materials of construction to avoid premature degradation of plant and equipment. It also precludes the use of silica based materials such as silica sheathed heaters, glass electrodes and silica based filter aids.

Another unique negative feature of the fluoborate system in this regard is the tendency for the electrolyte to "creep" over hardware, leaving highly corrosive films on surfaces, even in areas remote from the electroplating equipment.

The sulfuric acid and organic sulfonic acid based electrolytes, although corrosive by definition, are much less severe on plant and equipment and are generally easier to handle than the fluoborates.

The organic sulfonate electrolytes are the least corrosive of the electrolytes under comparison which not only allows a wide choice in hardware but also minimizes attack on plant, decreasing both maintenance and capital equipment costs.

## Oxidation of Divalent Tin

The oxidation of divalent stannous tin to tetravalent stannic tin caused by atmospheric and anodic oxidation leads to various problems in process control. The loss of stannous tin, if uncorrected, will ultimately affect both the high current density range and cathode efficiency of the process, the net effect of which is a loss in depositon rate and productivity.

In tin-lead alloy electrolytes, the loss of stannous tin will decrease the ratio of divalent tin to lead in solution and hence alter the electrodeposited alloy composition. In practice, the stannous tin can be replenished according to analysis before the above problems compromise process control and product quality. However, the frequency with which the analysis must be performed and the subsequent amounts of stannous tin replenished have a direct effect on the overall cost of the process and final product.

A more visual effect of the oxidation is the build-up of sludge produced from the precipitation of stannic tin compounds. The precipitates can cause rough deposits which compromise product quality, producing rough deposits, and ultimately the accumulated sludge must be removed, a costly and time consuming procedure. The sulfate electrolyte is the most prone to sludge build-up.

Although most proprietary processes contain anti-oxidants to minimize the oxidation of the divalent tin, only the organic sulfonates have an inherent ability in this regard. In fact, the organic sulfonic acid based processes are sufficiently resistant to oxidation to allow the use of insoluble anodes, a classic source of highly oxidative nascent oxygen.

Based on a comparison of the corrosive nature and stability of stannous tin alone, the organic sulfonic acid based electrolytes show clear advantages over either the sulfuric or fluoboric acid based systems.

The organic sulfonates' resistance to oxidation is particularly beneficial in high speed operations where the necessary use of vigorous solution agitation in combination with high current densities of operation produce highly oxidative conditions.

The systems are the least prone to sludge build-up and generally give longer service than either the fluoborate or sulfate systems.

The properties of the organic sulfonic acid based electrolyte allow flexibility in material selection for equipment design which improves process control and product quality. The use of anode pieces in titanium baskets makes for ease of anode maintenance and therefore helps ensure a consistent anode area and cell efficiency. The use of insoluble anodes allows the use of specific cell designs with very short anode to cathode distances where the ultimate in speed and profile are required.

Finally, the effluent from the organic sulfonate system can be rendered innocuous by simple neutralization and filtration procedures.

**Proprietary Processes and Additive Packages**

Regardless of the type of electrolyte selected, some form of organic additive is usually required to produce electrodeposits with the necessary properties to meet the quality requirements of the final product. It is at this stage that specialty suppliers of proprietary chemicals are normally consulted and the choice of process package made. The decision making process should take into account not only the initial requirements but also the quality and continuity of ongoing support available from the supplier.

Different additive packages are used, dependent on the cosmetic finish required, matte, semibright or full-bright. However, common to all applications and particularly important for high speed electroplating conditions is the need for a primary grain refiner and an anti-oxidant. The anti-oxidant, as previously discussed, is designed to inhibit the oxidation of divalent tin.

The primary grain refiner inhibits the tendency for dendritic or outward deposit growth, which produces rough, powdery and poorly adherent deposits of little practical value. This effect is often referred to as "treeing" when observed at high current densities.

Although the detailed mechanism of grain refinement has never been fully elucidated, surface adsorption of the organic additives certainly plays a role in the modification of the electrogrowth process.

In systems designed to produce full-bright deposits, secondary organic additives which further modify the growth process to produce finishes with specular reflectance are incorporated.

The effect of proprietary additives, often wrongly classified simply as brighteners, on the solderability of tin and tin-lead alloy electrodeposits has been and continues to be the subject of considerable debate and discussion. An area of primary focus is the amount of organic matter from the additives and their breakdown products occluded in the electrodeposit. As a general rule, it is believed that the higher the occluded organic content of the deposit, the more solderability and fusing problems will be encountered. This has led to a greater emphasis being placed on the control of organic

additive in the process in order to maximize their beneficial effects without compromising the solderability properties of the deposit. Analytical methods such as Ultra Violet Spectroscopy and High Pressure Liquid Chromatography, coupled with various detection techniques for the separated organic species, are being utilized to effect this improvement in process control. Cyclic voltammetry is also being applied to process control. This technique is based on electrokinetic measurements and has the advantage of detecting materials having a dynamic effect on the electrodeposition process. This makes it a powerful tool, not only for process control but also in additive development.

## Research Work

A great deal of previous work has been reported on factors which influence solderability.[7, 10-13]

The research work presented in this paper was initiated to compare the influence on solderability, both before and after accelerated aging of different proprietary additives designed to produce bright electrodeposits from an organic sulfonic acid based system.

Included in the study was the influence of underplate type and finish, as well as thickness of the tin-lead electrodeposits.

One premise of the comparison was that the generalization of higher occluded organics being detrimental to solderability may not always apply, since it does not take account of either the type of organic material occluded or the nature of its dispersion through the electrodeposit.

## Experimental

### Substrates and Underplates

Previous solderability experiments conducted using polished brass Hull cell panels cut into strips as test coupons had been shown to be unsuitable for an evaluation of solderability of tin-lead alloy electrodeposits. Variations in tin-lead alloy thickness between the center and edge of the panels, coupled with the observation that dewetting tended to be associated with the sheared edge of the panels ruled out this configuration as nonreproducible.

It could, of course, be argued that these are the real variables experienced in stamped and formed components. However, it was felt that a standard reproducible configuration was a prerequisite in order to ensure that the solderability performance of the tin-lead finishes were compared rather than component effects.

It was for this reason that 1/4 inch diameter copper rods of the type shown in Fig. 1 were chosen as the standard test coupons. This configuration has three distinct advantages:

1. There are no edge effects.
2. The test coupons can be electroplated in a rotating cathode fixture[14] Fig. 2, which allows the researcher to duplicate the flow characteristics of a high speed electroplating cell and ensures a uniform thickness profile over the entire surface.
3. The experimental technique is easily reproducible.

The 1 x 3 inch flat brass coupons were, however, used for the electrographic porosity testing of the tin-lead finishes.

In many cases, an initial nickel coating of between 1.25 and 5 microns (50 - 200 microinches) is electrodeposited to improve long term corrosion resistance and prevent copper diffusion into the functional final finishes. For tin and tin-lead coatings, copper diffusion is a particular problem since the copper-tin intermetallics are brittle compounds and can lead to failure of a solder joint through fracture. The intermetallics are also more difficult to wet with solder and are therefore undesirable in the electroplated components.

The introduction of an underplate introduces a new variable for solderability testing. Electrodeposited nickel can be produced in a range of cosmetic appearances from dull/matte to full-bright, and again organic additives are used in many of the processes.

In this work, three undercoats were studied, dull nickel, bright nickel and bright acid copper. The electrolytes used and thicknesses of deposits produced are listed in Table 1.

Table 1

**Electrolyte Formulations for Each Underplate Finish Studied**

| Dull Nickel | | Bright Nickel | | Bright Acid Copper | |
|---|---|---|---|---|---|
| Nickel Sulfamate | 320 g/l | Nickel Sulfate | 270 g/l | Copper Sulfate | 75 g/l |
| Nickel Chloride | 40 g/l | Nickel Chloride | 20 g/l | Copper Metal | 20 g/l |
| Nickel Metal | 85 g/l | Nickel Metal | 80 g/l | | |
| Boric Acid | 45 g/l | Boric Acid | 50 g/l | Sulfuric Acid | 100 ml/l |
| Additives | None | Additives | Primary & Secondary | Additives | Yes |
| Temperature | 57°C | Temperature | 57°C | Temperature | 24°C |
| Thickness | 4.0 µm | Thickness | 4.0 µm | Thickness | 12.5 µm |

**Solderability**

90% tin 10% lead electrodeposits were chosen for this study due to the prevelant use of this alloy composition in the connector industry. Full bright finishes, Fig. 1, were used in order to exaggerate the effects of occluded organics. However, as previously discussed, the type of organic may be as important as the quantity occluded. Therefore, in the present study, electrodeposits produced using primary grain refiners of different chemical types were compared.

One set of matte, 6 µm thick deposits, Fig. 1, produced using the primary grain refiners only, was included for control and comparison. Only bright nickel substrates were used for the matte deposits.

The electrolytes used were of the organic sulfonic acid type. The specific formulations are given in Table 2.

Table 2

Tin-Lead Electrolytes

| Electrodeposit Type | A | B | C | D |
|---|---|---|---|---|
| Tin Concentration | 40 g/l | 40 g/l | 40 g/l | 40 g/l |
| Lead Concentration | 5 g/l | 5 g/l | 5 g/l | 5 g/l |
| Organic Sulfonic Acid | 50 ml/l | 50 ml/l | 50 ml/l | 50 ml/l |
| Primary Grain Refiner | "A" | "B" | "A" | "B" |
| Secondary Grain Refiner | 40 ml/l | 40 ml/l | | |

In order to evaluate the influence of tin-lead deposit thickness, samples were plated at thicknesses of 3.0, 6.0 and 12.0 microns.

**Electroplating Cycle**

The following cycle was used for all samples:

Cathodic Alkaline Electroclean
Double Rinse
10% Sulfuric Acid
Double Rinse
Underplate
Double Rinse
20% Organic Sulfonic Acid
Tin-Lead Finish
Double Rinse
Deionized Water Rinse
Hot Air Dry

Rods to be tested for solderability were electroplated at a current density of 100 ASF using an AFASR rotator[14], Fig. 2, at a rotation speed of 2000 rpm.

The 1 x 3 inch brass coupons used for porosity testing were electroplated at a current density of 100 ASF using stir bar agitation and reciprocal movement of the part.

## Testing of Deposits

The deposits were evaluated as follows:

1. Thickness and alloy check
2. Percent Occluded Organic
3. Percent Occluded Carbon
4. Porosity
5. Solderability

## Test Procedures

Thickness and alloy composition of all tin-lead electrodeposits were determined by X-ray fluorescence.

The percent occluded organic was determined by measuring the weight loss after fusing of electrodeposited tin-lead foils.[11]

The carbon content of the electrodeposited foils was measured by a pyrolitic technique[15], the carbonaceous materials being converted to and measured as carbon dioxide.

Electrographic porosity testing[16] was performed on a selection of samples, which exhibited poor solderability after steam aging, in an attempt to correlate poor performance with the degree of porosity. 1 x 3 inch flat brass test coupons with 12.5 µm of a bright acid copper undercoat were used for the test.

### Conditions of Test

| | |
|---|---|
| Electrolyte: | 100 g/l Sodium Bicarbonate Solution |
| Detection Method: | Cadmium Sulfide Papers |
| Current: | 650 mA |
| Time: | 60 sec |

Solderability testing was carried out in accordance with Mil-Std 202F Method 208F both before and after the following accelerated aging tests:

1. Eight hours exposure to steam according to Mil-Std 202F.
2. Sixteen hours exposure to dry heat at 155°C.

All systems were prepared and tested in triplicate to improve statistical confidence.

Solderability performance was evaluated by examination of each soldered sample under 10X magnification. Defects such as dewetting, nonwetting and pinholing were assigned an index value corresponding to the degree of defect:

| | Index Value |
|---|---|
| Less than 1% of surface area exhibited defects. | 0 |
| 1 - 3 % of surface area exhibited defects. | 1 |
| 4 - 6% of surface area exhibited defects. | 2 |
| Greater than 6% of surface area exhibited defects. | 3 |

Examples of the soldered rods showing good solderability and typical defects are shown in Fig. 3.

## Results

### Codeposited Organic Matter

| Electrodeposit Type | Occluded Organic Content | Occluded Carbon Content |
|---|---|---|
| A | 0.41% | 0.156% |
| B | 0.42% | 0.280% |

### Porosity

No porosity was detected in any of the samples tested.

### Solderability

The solderability performance of the two full-bright tin-lead electrodeposits A and B are presented in Tables 3 and 4, respectively. The tables are compiled using the measured index values and compare the influence of tin-lead thickness, accelerated aging and underplate.

The individual effects of tin-lead thickness, aging and underplate on solderability performance are presented graphically in Figs. 4, 5 and 6.

The results of the matte electrodeposits C and D are presented in Fig. 7.

Fig. 8 compares the effects of aging on the solderability performance of electrodeposits A, B, C and D.

Table 3

**Electrodeposit A**

| | As Plated | | | Steam Aged | | | Heat Aged | | |
|---|---|---|---|---|---|---|---|---|---|
| Underplate | 3 μm | 6 μm | 12 μm | 3 μm | 6 μm | 12 μm | 3 μm | 6 μm | 12 μm |
| Dull Nickel | 0 | 1 | 1 | 0 | 2 | 1 | 1 | 1 | 0 |
| Bright Nickel | 0 | 0 | 1 | 3 | 2 | 2 | 2 | 3 | 1 |
| Bright Acid Copper | 0 | 0 | 1 | 2 | 2 | 2 | 2 | 3 | 1 |

Table 4

**Electrodeposit B**

| | As Plated | | | Steam Aged | | | Heat Aged | | |
|---|---|---|---|---|---|---|---|---|---|
| Underplate | 3 μm | 6 μm | 12 μm | 3 μm | 6 μm | 12 μm | 3 μm | 6 μm | 12 μm |
| Dull Nickel | 0 | 0 | 0 | 1 | 1 | 0 | 1 | 1 | 0 |
| Bright Nickel | 0 | 0 | 0 | 0 | 1 | 1 | 1 | 0 | 1 |
| Bright Acid Copper | 0 | 0 | 0 | 1 | 1 | 0 | 0 | 0 | 1 |

## Conclusions

1. The total occluded carbon of the Type B electrodeposit is higher than that of Type A. This difference is not apparent from the organic content of the deposits.

2. The influence of the underplates is most evident with the Type A electrodeposit, (Fig. 6). The beneficial effect of a dull nickel underplate is highlighted by these results.

3. Thickness of the tin-lead electrodeposits, in the range 3 - 12 μm tested, has little influence on the solderability performance, (Fig. 4). This is supported by the porosity test results.

4. Although the use of primary grain refiner "B" resulted in tin-lead electrodeposits with higher occluded carbon content, their solderability performance is superior overall to tin-lead electrodeposits produced with primary grain refiner "A".

   This result is confirmed by the solderability performance of the matte tin-lead electrodeposits, Type C and D, (Fig. 7).

   The difference is particularly evident following accelerated aging of the electrodeposits, (Figs. 5 and 8).

## Summary

A review of the major problems encountered by the process engineer and materials scientist in meeting production demands and end use specifications for electronic components with tin-lead finishes has been presented.

The importance of the composite finish and electroplating processes used, to achieve these requirements has been demonstrated.

## REFERENCES


1. U.S. Military Standard Mil-Std-202F.
2. American Society for the Testing of Materials, ASTM Standard B678-86.
3. Institute of Printed Circuits, IPC Test Method S-801.
4. British Standards Institution.
5. International Electrotechnical Commission.
6. Electronic Engineering Association.
7. Ackroyd, M.L., "A Survey of Accelerated Ageing Techniques for Solderable Substrates." Tin Research Institute, Perivale, Greenford, Middlesex, England.
8. British Standard BS 2011 : Part 2T : 1966.
9. International Electrotechnical Commission IEC 68-2-20 (1968).
10. 10th Annual Soldering/Manufacturing Seminar Proceedings, Naval Weapons Center, China Lake, California, February 1986.
11. Luke, D. L., PC Fab, May 1981, pgs 46 - 56.
12. Carano, Michael, Plating and Surface Finishing, July 1983, pgs 58-59.
13. Davis, P.E., Warwick, M.E., Muckett, S.J., Plating and Surface Finishing, August 1983, pgs 49-53.
14. Apparatus manufactured by Pine Instruments, Grove City, PA, Rotator Model AFASR.
15. Apparatus manufactured by LECO Corporation, St. Joseph, MI.
16. British Standard BS9760 Clause 1.2.6.7 Method B.

Figure 1

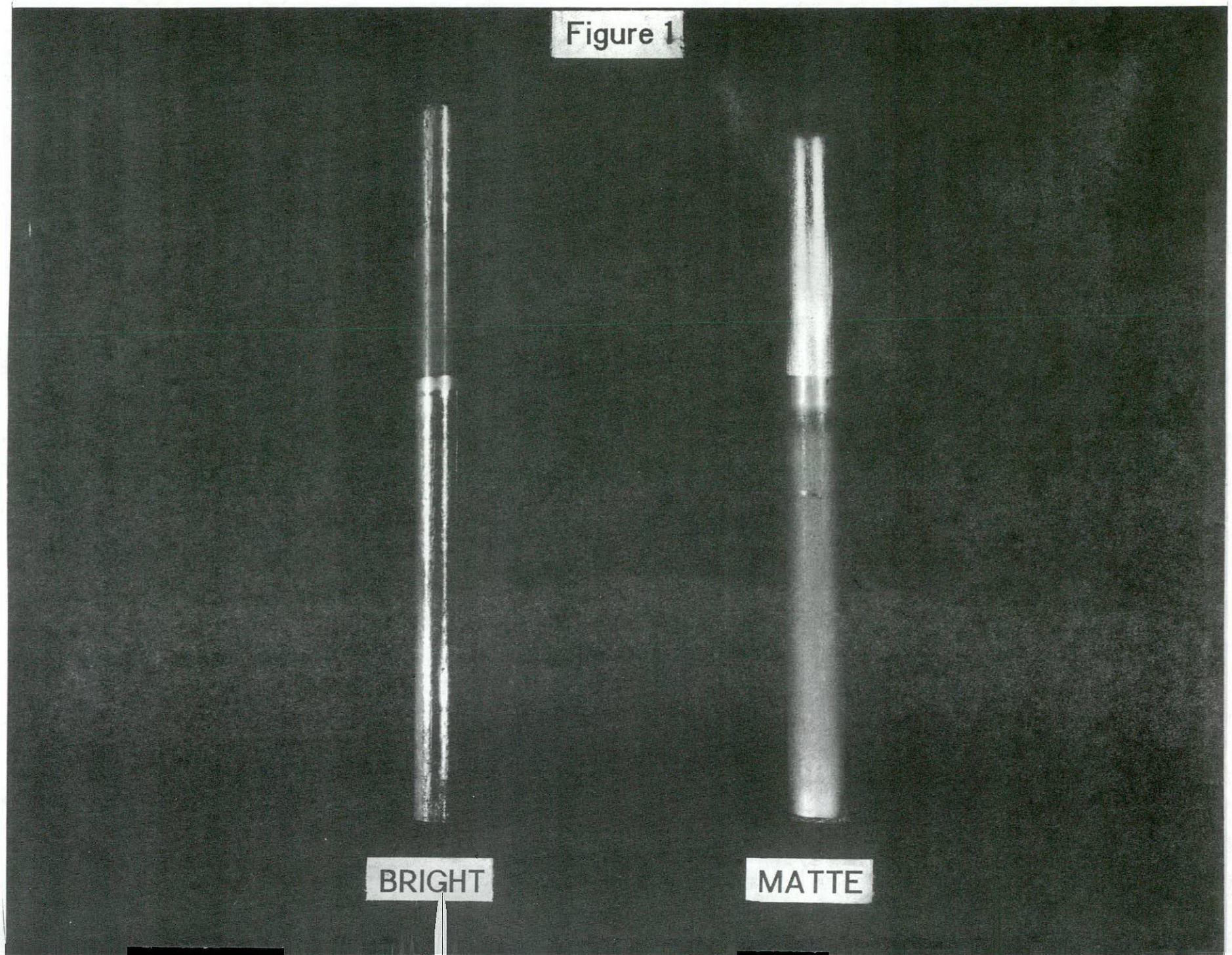

FIGURE 2

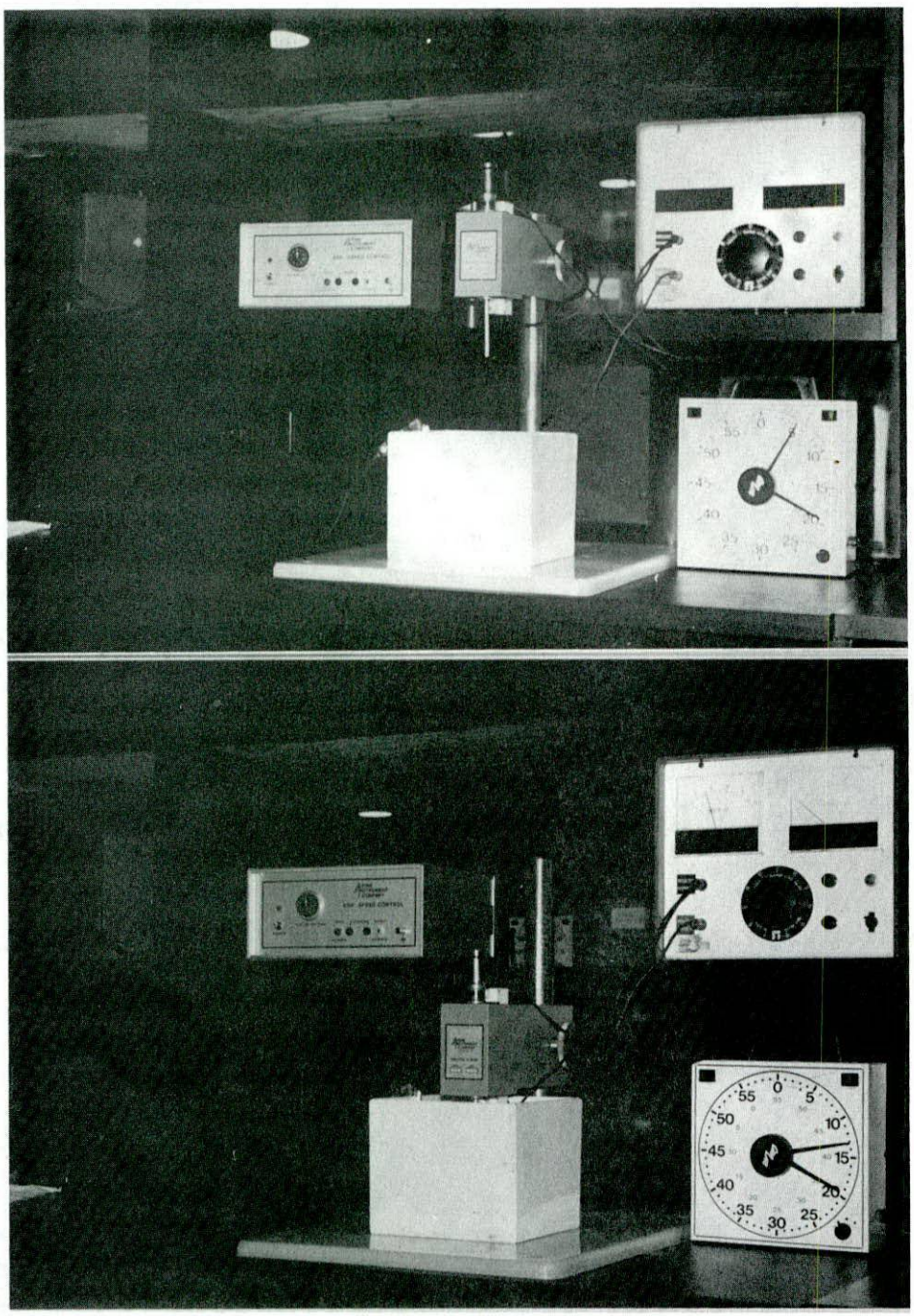

Figure 3

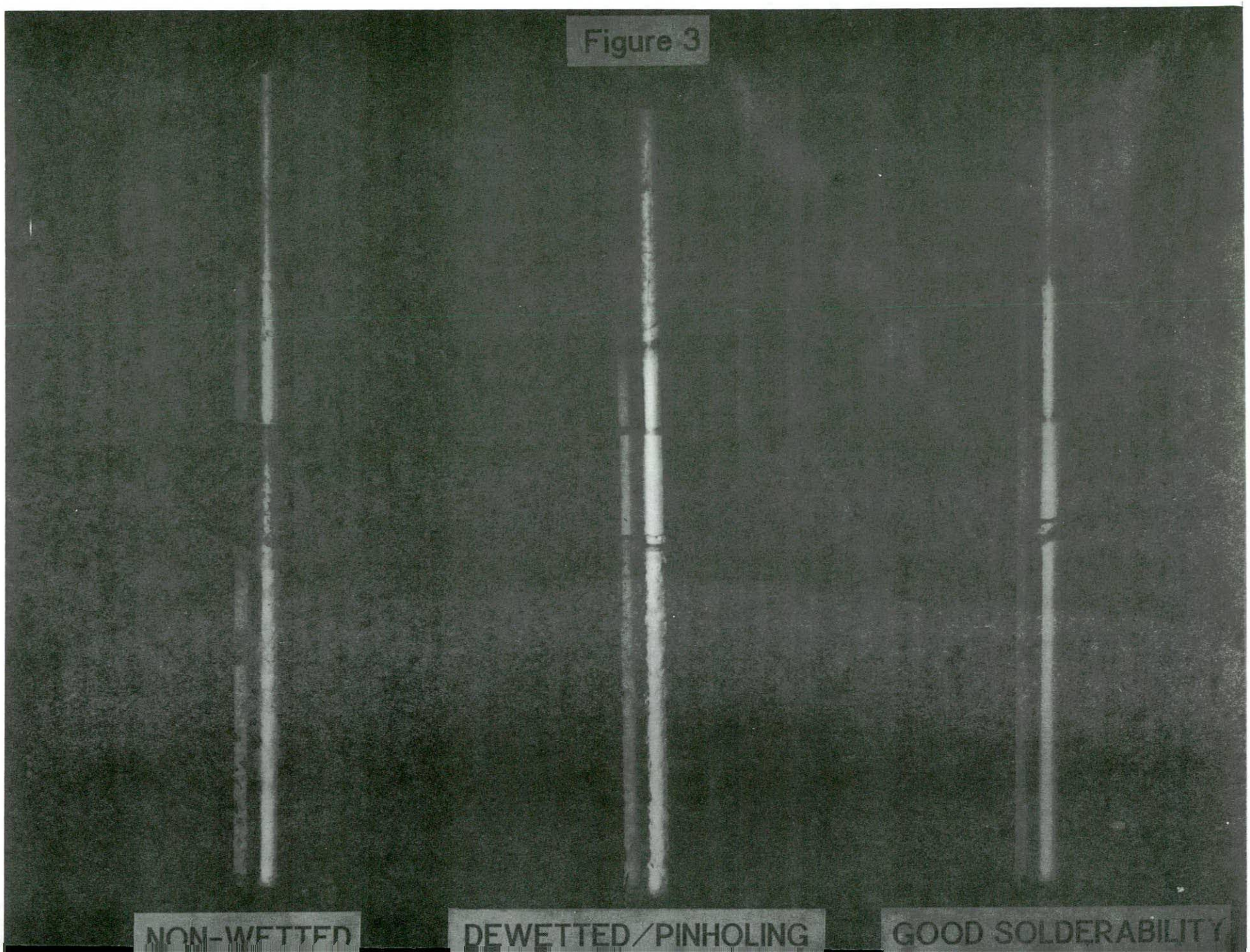

**FIGURE 4**

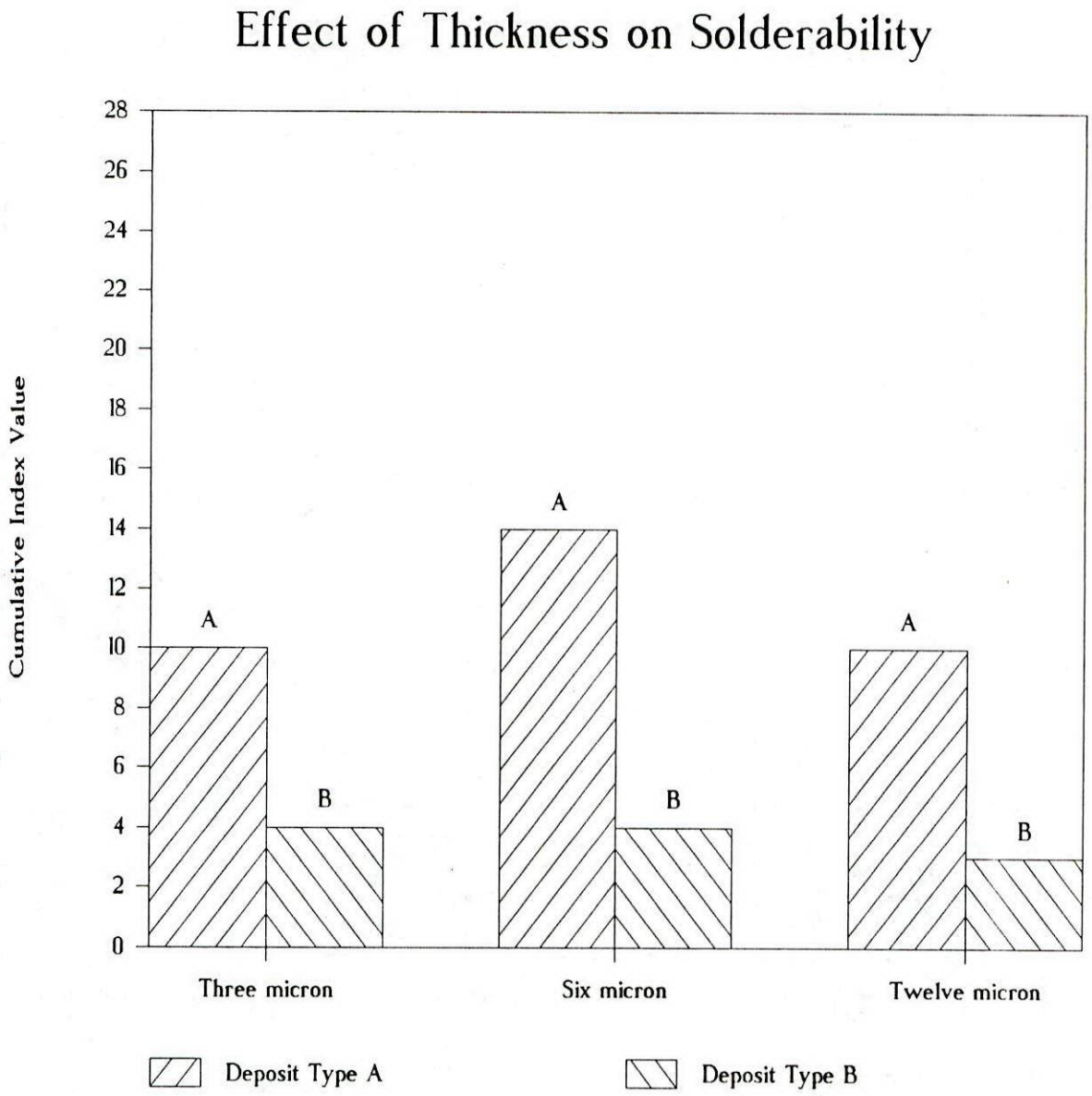
Effect of Thickness on Solderability
Cumulative Index Value
28
26
24
22
20
18
16
14
12
10
8
6
4
2
0
A
B
A
B
A
B
Three micron
Six micron
Twelve micron
Deposit Type A
Deposit Type B

**FIGURE 6**

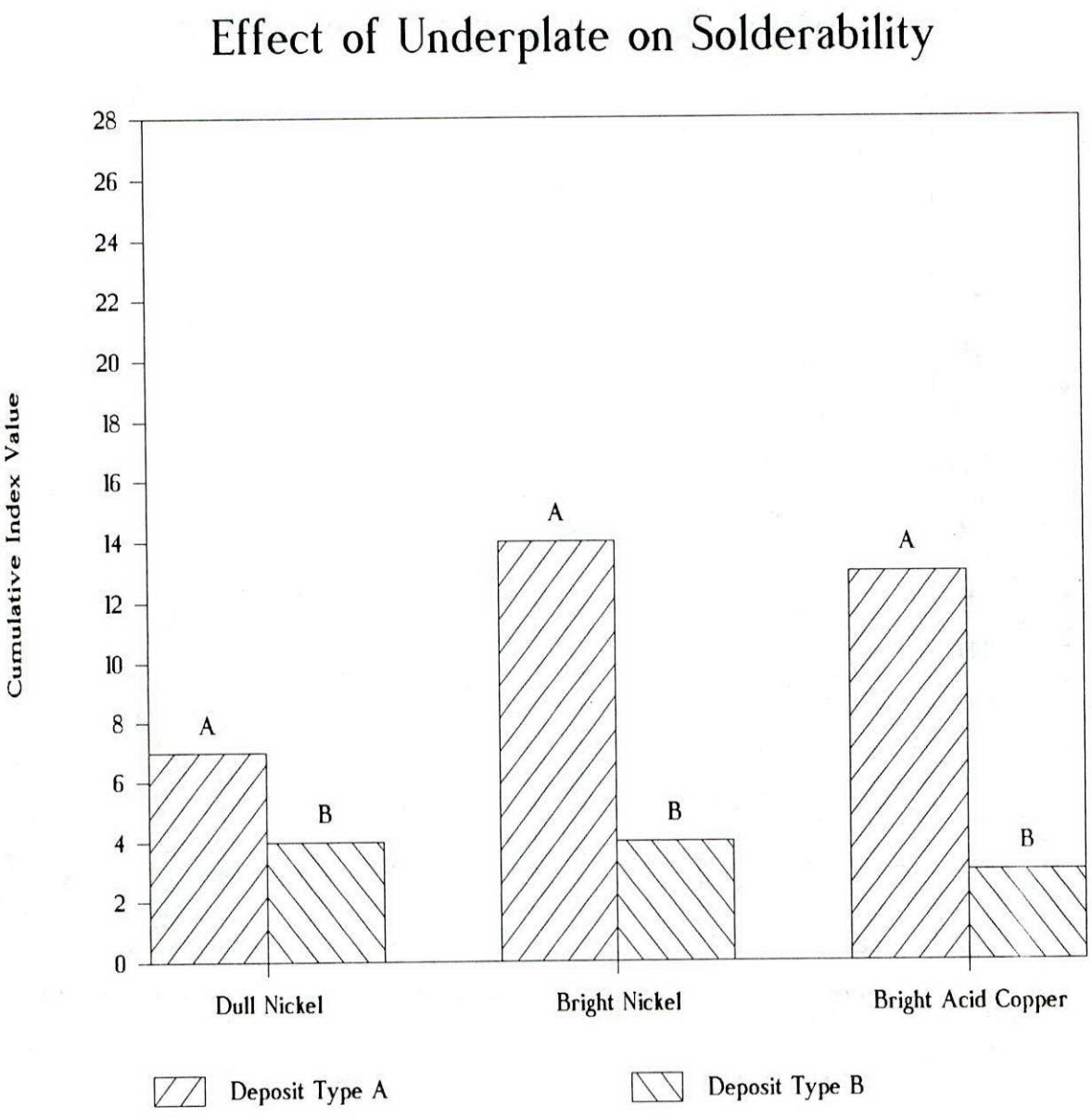
Effect of Underplate on Solderability
Cumulative Index Value
28
26
24
22
20
18
16
14
12
10
8
6
4
2
0
A
B
A
B
A
B
Dull Nickel
Bright Nickel
Bright Acid Copper
Deposit Type A
Deposit Type B

**FIGURE 7**

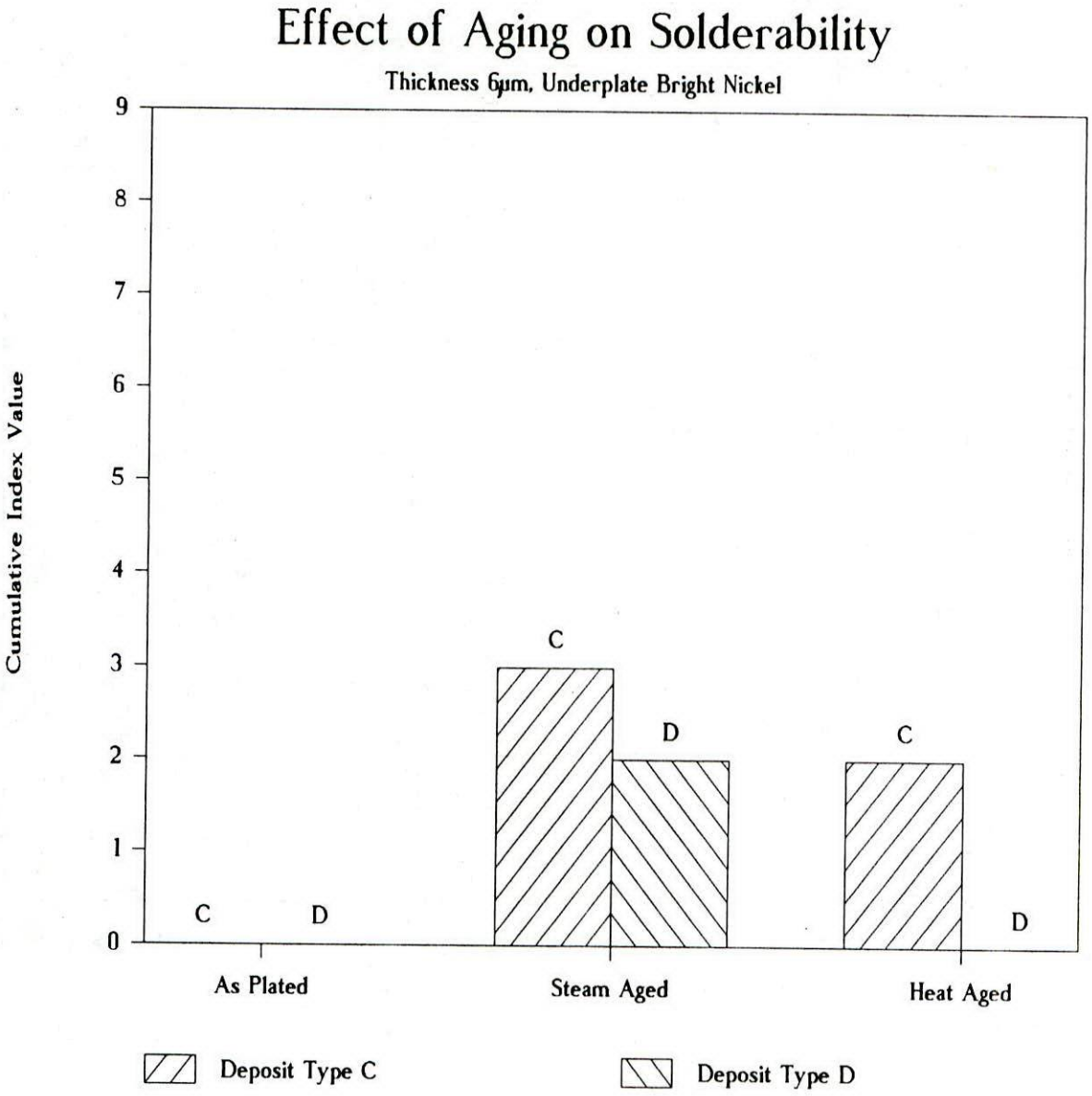
Effect of Aging on Solderability
Thickness 6µm, Underplate Bright Nickel
Cumulative Index Value
9
8
7
6
5
4
3
2
1
0
C
D
C
D
C
D
As Plated
Steam Aged
Heat Aged
Deposit Type C
Deposit Type D

**FIGURE 8**

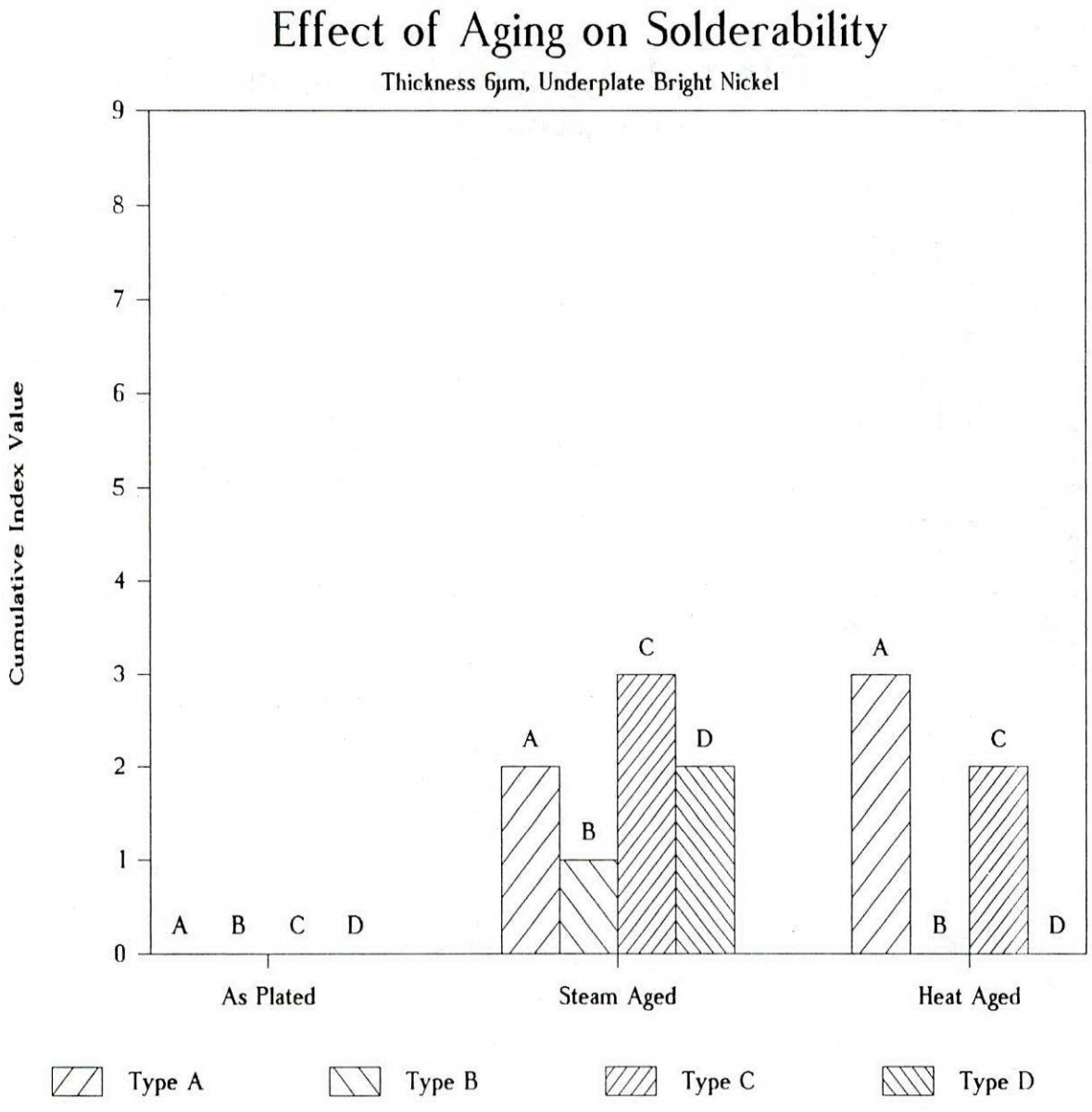
Effect of Aging on Solderability
Thickness 6µm, Underplate Bright Nickel
Cumulative Index Value
0
1
2
3
4
5
6
7
8
9
A
B
C
D
A
B
C
D
A
B
C
D
As Plated
Steam Aged
Heat Aged
Type A
Type B
Type C
Type D

E-4

# Electronics II
# Session E

## A New Pure Palladium Electrodeposit for Electronic Applications

A. Blair, G. Karustis,
and J. Wilcox
Engelhard Corp.
1 West Central Ave.
East Newark, NJ 07029

# A NEW PURE PALLADIUM ELECTRODEPOSIT FOR ELECTRONIC APPLICATIONS

A. Blair, G. Karustis, and J. Wilcox

Engelhard Corp.
1 West Central Ave.
East Newark, N.J. 07029

## Abstract

The physical properties of deposits obtained from a new palladium electroplating bath are discussed. Data on ductility, contact resistance, corrosion resistance, hydrogen uptake, and preferred orientation of the deposits are presented and compared to those obtained using a traditional palladium plating formulation.

## Introduction

Electrodeposited palladium, both pure and alloyed, over-plated with a thin layer of gold has proved to be a suitable contact finish for many electronic applications (1, 2, 3, 4).

Its acceptance by design and production engineers, however, has been slow because of several factors. Hard gold electrodeposits work well; they have been an industry standard for many years and, although expensive to produce, their costs have been acceptable even though gold has been valued at $300 - $400 per troy ounce. These factors combined with poor traditional palladium plating processes, deposits that have been stressed, and palladium's reputation for catalytic activity have worked against the acceptance of this metal as a contact material.

As reliable electrolytes are formulated and data on the properties of these electrodeposits are accumulated, palladium will increasingly be recognized as a viable connector material. The object of this paper is to describe an electrolyte which has been formulated specifically for high speed electroplating of connectors or stripstock, and to add to the information base on Palladium as a deposit.

## The Plating Process

Throughout the paper we will compare the electrolyte operation and deposit properties of this novel palladium process (5) with a traditional formulation based on palladium diammine dinitrite (6).

A comparison of operating parameters is given in Table 1. The traditional electrolyte is composed of a solution of ammonium sulfamate and depends upon the $NH_3/NH_4^+$ buffer for pH stability. The excess ammonium ions also stabilize the palladium tetraammine complex, particularly at the anode. Under rack plating conditions the process is adequate provided that frequent additions of ammonium hydroxide solution are made. At higher deposition speeds and the high-aeration conditions of most reel to reel plating lines ammonia is driven off at a rapid rate. This causes pH instability, palladium salt precipitation on the anodes and operator discomfort.

In designing a high speed palladium plating solution this shortcoming was overcome by eliminating the offending buffer system and replacing it with a combination of a stable palladium complex, a simple conducting salt which does not hydrolyze and a salt buffer which is especially effect at inert anode surfaces where local pH tends to fall dramatically due to destruction of hydroxide ions. The end result is a solution which can be operated over a wide pH and temperature range without instability or offence to the operator's sense of smell.

Deposition speed is important if a plating process is to be applied in a selective deposition mode in, for example, the connector industry. Typical hard gold plating solutions deposit at rates of up to 10 microinches per second (15 micrometers/minute) in suitable equipment. Although even higher speeds are in use, it is usual to operate at approximately 3 microinches/second (4.5 micrometers/minute).

Traditional pure palladium electrolytes cannot even approach these speeds. However, the new formulation under discussion here can comfortably match 3 microinches/second at 180 to 200 $A/ft^2$ ( 19.4 to 21.6 $A/dm^2$) with reasonable agitation in order to provide good mass transfer. This result indicates a cathode efficiency of about 85% or 28 mg/Amp. min. Efficiency remains largely constant over a wide range of pH values and current densities.

## The Deposit Properties

### Hydrogen Content, Ductility and Stress

One of the major factors limiting use of palladium deposits has been their tendency to crack after plating is completed. This is caused by codeposited hydrogen leaving the deposit. This phenomenon has been well documented and measurement of the hydrogen content of deposits has been established and reported (7, 8) for both pure and nickel alloyed palladium deposits. Reasonable ductility is a requirement for any contact finish that might be subjected to mechanical or thermal deformation during subsequent manufacturing operations or in its service life. Deposit cracks might expose the substrate materials to corrosive environments and lead to high contact resistance in the connector assembly.

The measured hydrogen content of these deposits are reported in table 2, and the ductility, internal stress and microhardness are compared with those for a typical hard gold deposit in table 3.

Ductility has been measured by elongating deposits of 50 microinch (1.25 micrometer) thickness on a soft copper foil substrate. The integer percentage elongation prior to the appearance of cracks in the deposit is the figure quoted. Under no test condition was the elongation of the high speed formulation deposit less than 4% and most results fall into the range of 6-8%. The traditional formula and the typical hard gold gave at best 2% and 3.5% respectively. An observation made during testing was that the P -salt deposits cracked abruptly at a given elongation, indicative of a brittle material. Deposits from the new palladium formulation developed small cracks which slowly expanded on further elongation. (figures 1, 2 and 3).

In the light of these results it might be expected that internal stress of the deposits would be ranked inversely. There was evidence during testing that the deposits produced in the traditional palladium solution were stress relieving themselves during plating (figure 4). Hard gold is well-known for its relatively poor ductility which often necessitates the use of soft gold pre-plate layers as a hard gold foundation.

## Porosity And Contact Resistance

The porosity of these deposits (a property often referred to as corrosion resistance) was evaluated using copper substrates and a moist sulfur dioxide atmosphere. It is noteworthy that the traditional nitric acid vapor test is not appropriate for testing palladium since this metal is soluble in nitric acid. The method employed was similar to that of Leeds and Clark (10).

Panels 3 inches by 1 inch (7.5 cm x 2.5 cm) were plated with 40 microinch (1 micrometer) and 80 microinch (2 micrometer) thick deposits of palladium or gold. Pores and cracks through to the substrate copper were rendered visible by the copper salts of the corrosion product on the precious metal surface. A summary of the results is given in table 4.

The test conditions are quite severe as shown by the porosity in the hard gold standard. The traditional palladium corroded badly, probably due to cracking more than classical porosity. The excellent result for the new palladium agrees well with Updegraff's (11).

Contact resistance was measured on flat test panels using a modification of ASTM B539-80 which has been reported previously (12). A minimum of 25 readings per square centimeter were taken automatically at a load of 100 grams. Results are expressed in table 5 and show no anomolies.

## Crystal Orientation

X-ray diffraction patterns were obtained for both types of palladium deposit and compared to that from finely divided palladium powder which can be considered to have random crystal orientation. The peaks chosen for analysis were (200) at 46.6 degrees, (220) at 68.2 degrees and (222) at 86.6 degrees. Diffraction intensities are reported in table 6. From these figures it is possible to calculate relative intensities; relative to the powder sample, that is. Also by expressing the relative intensity of each peak as a fraction of the total intensity for each sample we can more clearly see any preferred orientation that might exist. A normalized intensity, arrived at this way, which exceeds 0.33 indicates a preferred orientation.

It is clearly illustrated by these results that the traditional P-salt electrolyte produces a deposit with virtually random orientation. Also the new formulation produces deposits the crystals of which are strongly oriented in the (220) plane (edge-up), at the expense of the (200) plane (face-up). The (222) plane (corner-up) is not present at all.

## Conclusions

An electroplating solution has been developed which will operate at high deposition speeds without excessive maintenance or operator discomfort.

The deposit produced by this process shows a definitive crystal orientation and low hydrogen content leading to excellent ductility, freedom from porosity and good contact resistance properties.

## Acknowledgement

The authors wish to recognize Dr. W. O. Mc Sharry and Dr. J. E. Phillips of the Materials Characterization Laboratory, Electronic Products Group, Engelhard Corporation for their work in producing the x-ray data and analysis.

## References


1. J. A. Abys, 2nd AES Symposium on Economic Use of and Substitution for P.M. in Electronics. Danvers, Oct. 1982.

2. A. Graham et al, Ibid.

3. A. Blair, Proceedings 6th IPMI Conference. Newport Beach, June 1982.

4. H. D. Hedrich and Ch. J. Raub, Surfaces Technology, 8 (1979).

5. G. Karustis and J. J. Wilcox. Patent applied for.

6. R. J. Morrissey, Metal Finishing Guidebook Directory 1987, 85, 265.

7. Ch. J. Raub, Plat. Met. Rev., 26(4), 158.

8. P. Wilkinson, et al, AESF Sur/Fin´85, Detroit, 1987

9. A. Dvorak and L. Vrobel, Trans. Inst. Met. Finish. 46, 1971.

10. M. Leeds and J. M. Clark, Trans. Inst. Met. Finish. 46, 1968.

11. S. W. Updegraff, Connection Technology. 1986, 41.

12. M. J. Pike - Biegunski and R. F. Bazzone, AES 1st Symposium on Economic Use of and Substitution for P.M. in Electronics. Danvers, Sept. 1980.

Table 1. Comparison of operating conditions the Palladium plating processes.

| | High Speed | P-Salt |
|---|---|---|
| Pd. metal , g/L | 25 | 15 |
| Conducting and buffering salts, g/L | 50 | 100 |
| pH | 8.5 | 8.0 |
| Temp. , °C | 50 | 35 |
| Test C.D., $A/ft^2$ ($A/dm^2$) | 60 (6.5) | 10 - 20 (1.1 - 2.2) |
| Production C.D., $A/ft^2$ ($A/dm^2$) | $< 350$ ($< 37.8$) | 10 - 20 (1.1 - 2.2) |

Table 2. Comparison of the hydrogen content of Palladium deposits.

| | High Speed | P-Salt |
|---|---|---|
| H/Pd atomic ratio | 0.004 | 0.02 |
| Weight percent | 0.0038 | 0.019 |
| NmL $H_2$/g Pd | 0.42 | 2.1 |

Table 3. Ductility, internal stress and microhardness of two types of pure palladium deposits and a typical hard gold deposit.

| | High Speed Pd | P-Salt Pd | Hard Au |
|---|---|---|---|
| Ductility (elongation, %) | 4 - 8 | $<2$ | $<3.5$ |
| Internal Stress ($N/mm^2$) (all tensile) * | 255 | 225 | 190 |
| Microhardness (Knoop, 25g) | 200 | 275 | 175 |

* Dvorak and Vrobel method (9).

Table 4. Summary of porosity counts for palladium and gold. Substrate was pure copper foil, the atmosphere was moist $SO_2$ for 24 hours at 25°C.

| Deposit thickness (average) | Average pore count/in$^2$ | | |
|---|---|---|---|
| | High Speed Pd | P-Salt Pd | Hard Au |
| 40 microinches | 3 | * | >100 |
| 80 " | 3 | * | >100 |

* Too corroded to count pores accurately.

Table 5. Contact resistance of palladium and hard gold deposits.

All deposits were 40 microinches (1 micrometer) average thickness and were tested on the "as plated" condition. Load 100g.

| | High Speed Pd | P-Salt Pd | Hard Au |
|---|---|---|---|
| Contact resistance, mΩ | 2.0 - 4.5 | 2.0 - 3.7 | 1.8 - 2.5 |

Table 6. X-ray Diffraction Data for palladium powder and the two deposits.

| | Crystal Plans | High Speed Pd | P-Salt Pd | Pd Powder |
|---|---|---|---|---|
| Relative Intensities (%) | (200) | 23.8 | 54.3 | 63.2 |
| | (220) | 76.2 | 34.2 | 29.4 |
| | (222) | -0- | 11.4 | 7.3 |
| Relative Orientation | (200) | 0.36 | 0.81 | 1.00 |
| | (220) | 2.71 | 1.32 | 1.00 |
| | (222) | -0- | 1.38 | 1.00 |
| Normalized Preferred Orientation | (200) | 0.12 | 0.23 | 0.33 |
| | (220) | 0.88 | 0.37 | 0.33 |
| | (222) | -0- | 0.39 | 0.33 |

E-5

# Electronics II
# Session E

## Palladium Electroplating

J.A. Abys
AT&T Bell Laboratories
600 Mountain Ave.
Murray Hill, NJ 07974

# PALLADIUM ELECTROPLATING

*J. A. Abys*

AT&T Bell Laboratories
600 Mountain Avenue
Murray Hill, N.J. 07974

## Introduction

All electronic devices contain interconnects that enable an electrical signal—and hence a message—to be transmitted from one component system to another, and any such component must provide a stable pathway for such transmission. This is true for hardware as simple as a wall socket or printed wiring board fingers in a complex system such as a circuit pack in an electronic switching system. In the case of electronic switching systems, computer hardware and most telecommunication equipment, high reliability and low-noise requirements are the determining factors in designing interconnects and selecting electrical contact materials.

Several criteria are used to determine the suitability of contact materials. Contacts and the associated contact materials must be conductive and withstand a wide variety of environmental conditions while maintaining stable contact resistance. In addition, contacts must withstand being connected to and disconnected from other contacts without appreciable physical deterioration, which could lead to unstable electrical resistance. The contact material must therefore be corrosion and wear resistant. Additional functional requirements are imposed on specific connector systems taking into consideration the design and geometry of the connector, the particular contact pressure, the cycles of operation, the ambient conditions to which it is exposed and the expected lifetime.

Thus, while copper and silver are the most conductive metals available, they are not acceptable contact materials in most electronic applications because they corrode easily and show poor wear performance.

On the other hand, gold, while not as conductive as silver or copper, is still a good electrical conductor and is extremely resistant to corrosion. In addition, high-percentage gold alloys exhibit excellent bondability, solderability, low contact resistance and wear properties, and are easily electroplated to form high-quality, stable contact surfaces. Thus, the use of thick electroplated Au films for contact surfaces has been the standard in the electronics industry.[1–3]

Reliance on gold-based contact technology is not without a price, however. In 1972, gold sold for $59 a troy ounce. By 1980, it hit a high point of about $800 a troy ounce and averaged roughly $500. Also in 1980, the United States used about 22.5 metric tons—724,000 troy ounces worth $362 million—of gold in electronic devices. The estimated gold usage in the entire western world was roughly 60 metric tons worth approximately one billion dollars. About 56 per cent of this gold was used in connector contacts and 23 per cent went into printed wiring board fingers.

The highly competitive nature of the electronics market demanded a less-costly, reliable contact finish as a substitute for gold, and research in this area became extremely active.[3–6] Non-precious metals were an area of interest.[7–12] For example, plain solder contacts were acceptable in some consumer electronic applications with design lives of only five years. However, for high-reliability applications and the bulk of telecommunications component systems, platinum-group metals were considered as the most likely alternatives. Of the pure, non-alloyed metals examined, only ruthenium and palladium were serious contenders because they cost much less than gold. For example, recently the price of gold was $460 per troy ounce whereas palladium cost $130 per troy ounce.

Ruthenium was examined for use in relay switches,[13–15] but for separable connectors its use was precluded because of poor wear resistance and insurmountable problems with high-speed electrodeposition processes.

Palladium (Pd), a platinum group metal, has been viewed as a suitable alternative. The lower price of Pd metal (Figure 1) coupled with its lower electroplated density (Pd ~ 10 g/cm$^3$ vs. Au ~ 17.3 g/cm$^3$) implies considerable cost savings on utilizing Pd as a contact material (Figure 2). However, despite these economic advantages there has not been an appreciable demand for Pd electrodeposition. This is due to the relative difficulty of electrodepositing Pd with satisfactory physical properties, paucity of contact reliability data and little impetus to develop such a process due to dependence on the well established and reliable Au electroplating technologies.

The recent acceptance of palladium and gold flashed palladium (GFPd) as contact materials reflects the resolution of these technical problems[16–24] and the availability of cost effective reliable electrodeposition processes.

## Palladium Electrodeposition

The electrochemical deposition of Pd has many difficulties. The most prominent is the evolution and incorporation of $H_2$ which is a reaction that can occur simultaneously with Pd deposition and leads to $H_2$ embrittlement (Figure 3 and 4). This codeposition of $H_2$ and Pd leads to the formation of palladium hydride alloys ($PdH_2$).[25]

Palladium and palladium hydrides have what is known as a face centered cubic, or "FCC" structure, and in palladium hydrides that FCC structure occurs in an alpha and a beta phase. Pure palladium, at 3.889 angstroms, and alpha palladium hydride, at 3.893 angstroms, have similar lattice constants and are both mechanically stable.[26–27, 29]

However, the beta-palladium hydride, which contains significantly higher levels of hydrogen, has an FCC structure whose lattice, at 4.04 angstroms, is greater than pure palladium.[28, 29] The hydrogen embrittlement problem, then, stems from the thermodynamic instability of the beta-palladium hydride alloy—which spontaneously evolves hydrogen and decomposes to the alpha-palladium hydride alloy. This phenomenon is accompanied by corresponding lattice contractions and changes in the mechanical properties of the palladium films, resulting in highly-stressed and cracked deposits.[25] The extent of hydrogen incorporation and embrittlement, therefore, depends on the extent of codeposition during palladium electroplating.

Codeposition is determined by the relative reduction potential of palladium and hydrogen—a function of the thermodynamic stability of the palladium-complex, the kinetics of reduction, the overpotential of hydrogen on palladium and the operating conditions of the system.[30]

Many palladium electroplating chemistries are highly susceptible to hydrogen embrittlement, and this severely limits their effectiveness. In addition, many have a tendency to dissolve the base metal used as a substrate for the contact, and in the worst cases the contact disintegrates and contaminats the plating solution with other metals. Some chemistries are also plagued by the presence of volatile components, the formation of precipitates, and chemical or electrochemical degradation of solution constituents[30] (Figure 5).

Overall, these difficulties cannot be easily controlled in a large-scale manufacturing environment. Thus, there was a need to develop a palladium electroplating chemistry for mass production. By 1980 a systematic investigation of palladium electrochemistry at AT&T Bell Laboratories led to the development of a palladium electrodeposition process.[30–36]

This process produces palladium electrodeposits with the desired physical characteristics under a wide range of conditions. It is a simple chemistry employing only three chemical constituents: the palladium complex, a phosphate buffer, and a palladium replenishing compound to replace the metal removed by the deposition process (Figure 6).

## Materials Properties

An important aspect of any electrodeposition technology is understanding the relationship between the operating parameters of the electrodeposition process and the material properties of the deposited films. Extensive studies have shown that while palladium electroplated with this process is harder than gold, it is slightly more ductile. Palladium electroplated with this chemistry — which is also less dense than

electroplated hard gold — is slightly purer in composition and thermally more stable (Figure 7). In short, this process provides palladium deposits whose physical properties are comparable to gold.[30, 31, 36]

## Gold Flashed Palladium

Palladiumm is a catalyst for many organic reactions, and early research showed that in ambients of organic gases, frictional polymerization on the surfaces of vibrating contacts could form polymers, which act as non-conducting films.[37, 38] Palladium is also more susceptible to corrosion than gold,[18, 19] especially in high-chloride environments,[22, 23] such as chemical manufacturing and seashore areas.

To overcome these potential problems, a thin gold layer of 1 to 2 microinches is deposited over the palladium surface, resulting in what is known as "gold-flashed" palladium.[24] This very thin gold film (Figure 8) on one or both mating contacts eliminates polymerization, improves corrosion resistance and acts as a lubricant which reduces friction and improves wear.[16, 17, 24] Finally, the gold-plated palladium looks very much like gold, making the finished product more appealing to the customer.

## Contact Reliability

An extensive series of environmental and wear tests has been performed on AT&T connector hardware with gold-flashed, palladium-plated contacts. These contacts have been exposed to a variety of tests designed to simulate a 20- to 40-year service life span. In all cases, gold-flashed palladium performs as well as or slightly better than comparable gold contact finishes (Figure 9).[24] As a result of this testing, gold-flashed palladium is now being used as a contact material for numerous AT&T products.

## Technology Transfer

The ultimate test of any process, no matter how successful it is in the laboratory, is its performance in a manufacturing environment. The manufacturing potential of this particular technology has been demonstrated by numerous successful engineering trials, and its subsequent incorporation into the manufacturing process at several AT&T Technologies plants (Figures 10-13), and non AT&T Manufacturting locations.[36, 39] This palladium electrodeposition process requires no special facilities, and no extraordinary plating techniques are used: the gold bath in an existing plating line is simply replaced by palladium. This facilitates the transition from gold to palladium, since capital plant expenditures required for the conversion are minimal.

Since its introduction to commercial use in 1981, system designers have begun to specify gold-flashed palladium in their products. Printed wiring board fingers, loop plant transmission equipment, backplane interconnections hardware, and telephone handset parts such as modular cord jack spring contacts are among the products now made with gold-flashed palladium.

# PALLADIUM vs GOLD
## YEARLY AVERAGES

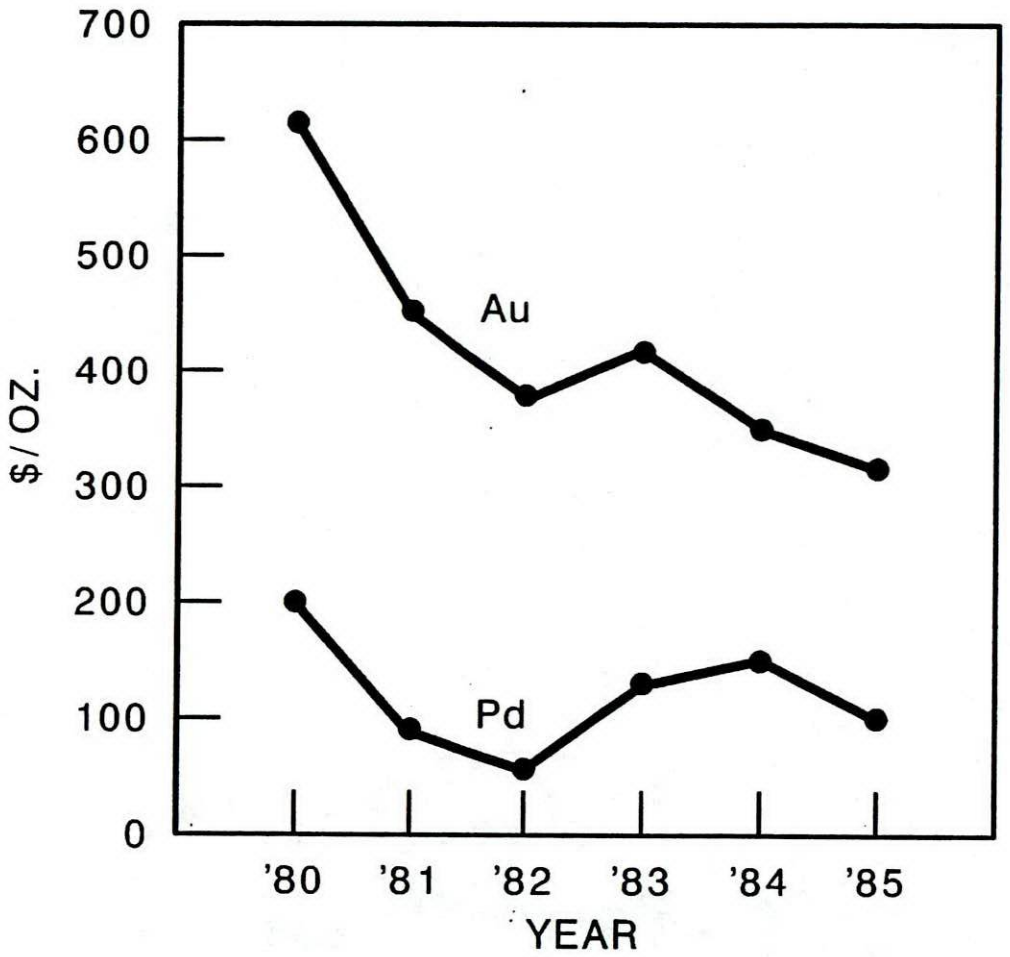


MH6531B.33

FIGURE 1. PALLADIUM vs GOLD YEARLY AVERAGES (1980-1985) DOLLARS PER TROY OUNCES.

# SOURCES OF COST SAVINGS

- THE COST OF PALADIUM IS SUBSTANTIALLY LESS THAN THAT OF GOLD
- THE DENSITY OF PALLADIUM IS 60% THAT OF GOLD; THEREFORE, IT TAKES FEWER TROY OUNCES TO PLATE TO A GIVEN THICKNESS WITH PALLADIUM THAN GOLD
- THE DENSITY OF THE AT&T PALLADIUM PLATE IS APPROXIMATELY 85% OF THE THEORETICAL, WHICH IS AN ADDITIONAL MATERIAL SAVINGS

MH6531B.25

FIGURE 2. SOURCES OF COST SAVINGS ON REPLACING Au WITH Pd.

# HYDROGEN EMBRITTLEMENT PROBLEM

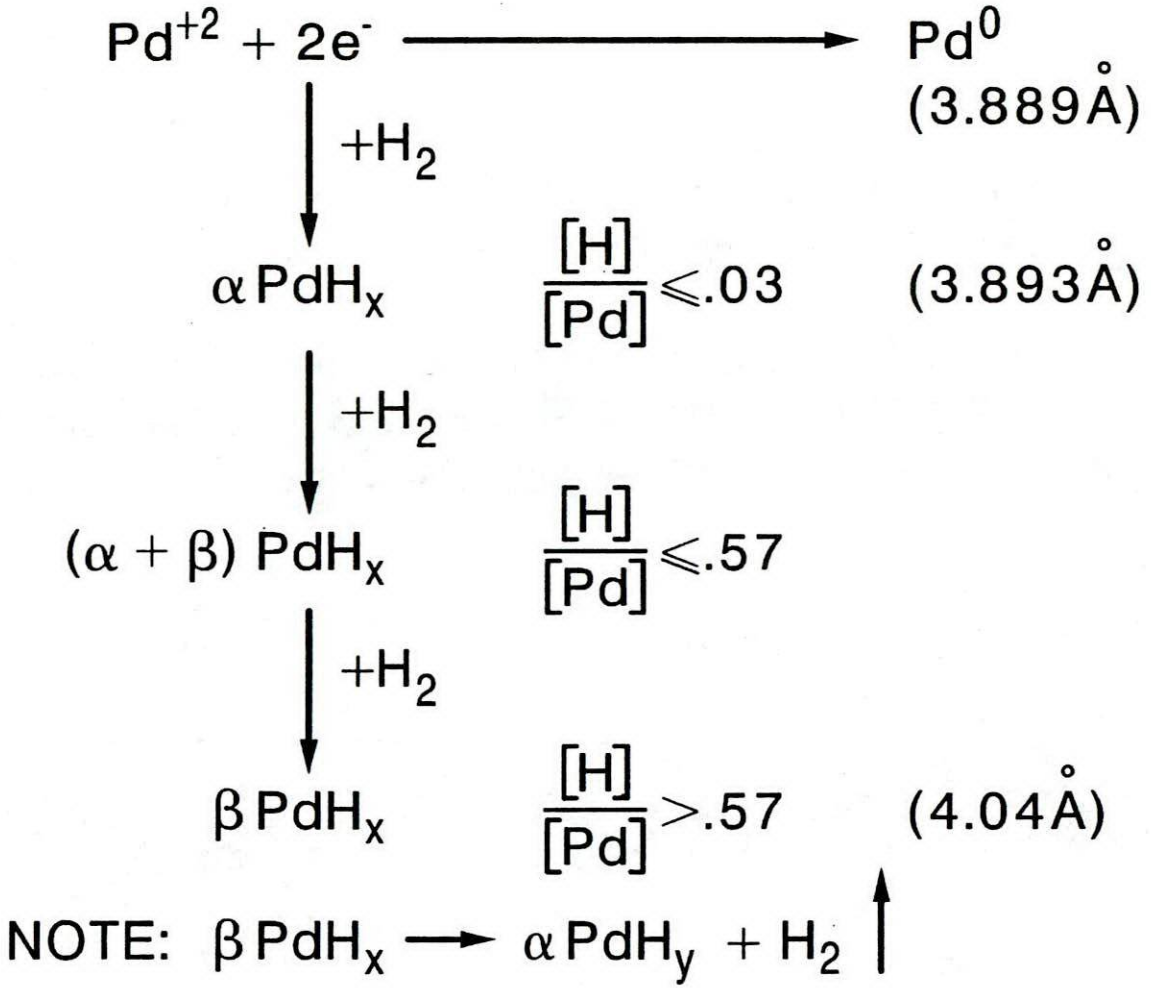


MH6531B.31

FIGURE 3. THE HYDROGEN EMBRITTLEMENT PROBLEM.

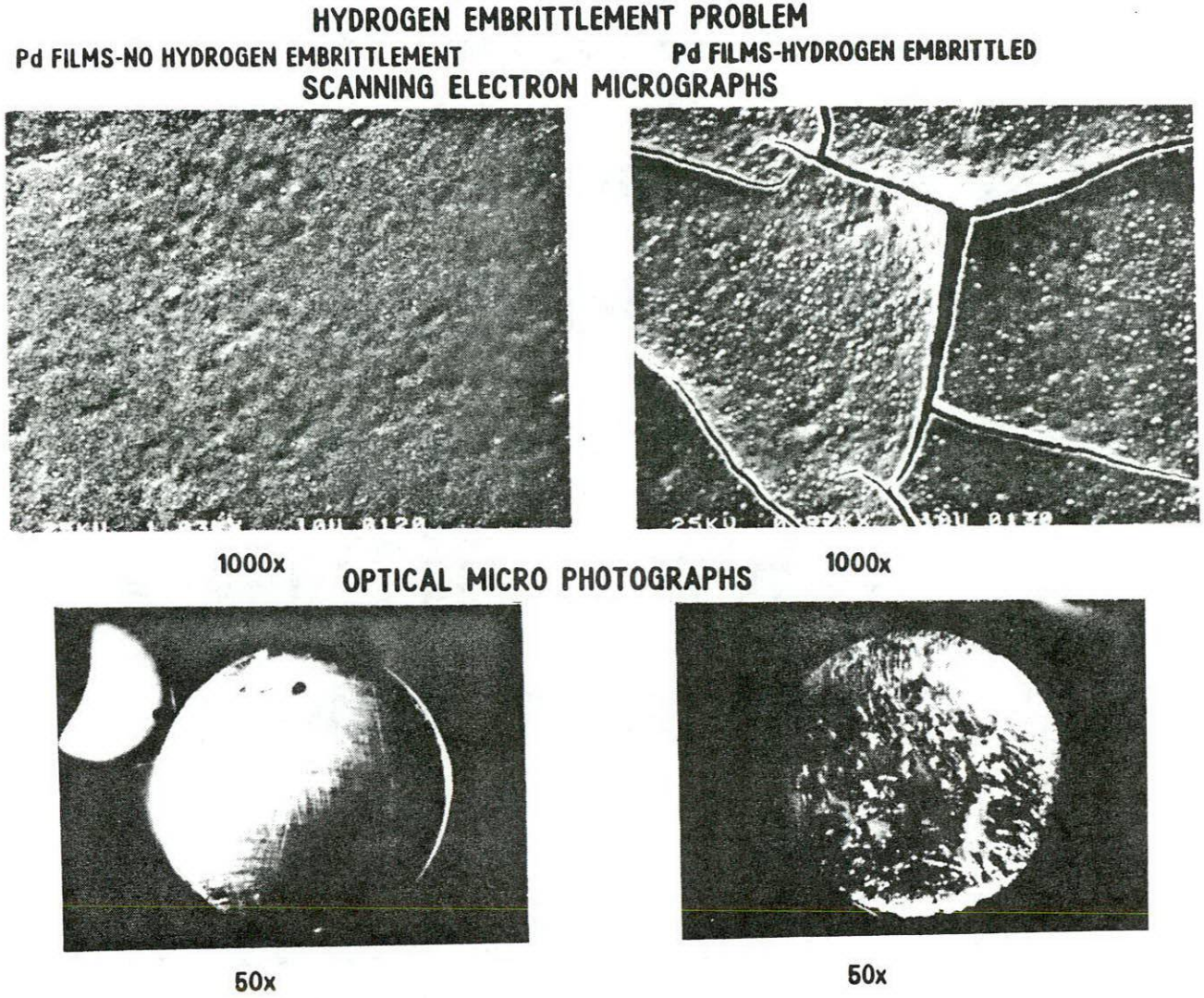


FIGURE 4. SCANNING ELECTRON MICROGRAPHS OF Pd DEPOSITS WITH AND WITHOUT HYDROGEN EMBRITTLEMENT.

# PROBLEMS ENCOUNTERED WITH PALLADIUM ELECTROPLATING

- HYDROGEN EMBRITTLEMENT
- LIMITED DEPOSITION RATES
- UNSTABLE CHEMICAL SYSTEMS
- UNSTABLE BUFFER SYSTEMS
- CHEMICAL ATTACK OF BASE METAL
- LIMITED PROCESSING WINDOWS

FIGURE 5. LIMITATIONS OF PALLADIUM PLATING CHEMISTRIES.

# PALLADIUM ELECTRODEPOSITION CHEMISTRY

- PALLADIUM CHELATE COMPLEX
- ALKALINE PHOSPHATE BUFFER
- SIMPLE REPLENISHMENT SYSTEM

MH6531B.16A

FIGURE 6. CONSTITUENTS IN THE AT&T Pd PLATING CHEMISTRY.

# COMPARISON OF FILM PROPERTIES

## PALLADIUM VERSUS HARD GOLD

| | PALLADIUM | HARD GOLD |
|---|---|---|
| HARDNESS ($KHN_{25}$) | 250-350 | 140-200 |
| HARDENING AGENTS | NONE | Co,Ni |
| GRAIN SIZE (Å) | 30-100 | 200-250 |
| DENSITY | 9.5-10.5 | ~17.3 |
| DUCTILITY (% ELONGATION AT 50 μin) | 3.5-5.0 | 2.5-3.5 |
| VOLATILE IMPURITIES (WT%) | $<0.5$ | $\leqslant 1.5$ |
| METALLIC IMPURITIES (WT%) | $<<1.0$ | $\leqslant 1.0$ |
| THERMAL STABILITY ($^0C$) | $\geqslant 360$ | $\leqslant 150$ |

MH6531B.21

FIGURE 7. COMPARISON OF FILM PROPERTIES OF PALLADIUM VERSUS HARD GOLD

# WHAT IS THE FUNCTION OF THE GOLD CAP?

- LUBRICANT
- REDUCES POTENTIAL FOR FRICTIONAL POLYMER FORMATION
- MINIMIZES PALLADIUM CHLORIDE FORMATION
- GIVES APPEARANCE OF GOLD

MH6531B.18



FIGURE 8. REASON FOR PLATING Au CAP ON Pd.

# PALLADIUM CONTACT FINISH EVALUATION

## RESULTS

- IN ALL TESTS, FOR ALL PRODUCTS EVALUATED, 25 µin PALLADIUM OVERPLATED WITH 1 µin GOLD FINISHES PERFORMED EQUAL TO OR BETTER THAN STANDARD GOLD FINISH
- NO DATA EVEN SUGGESTS ANY CONCERN THAT WOULD PRECLUDE IMMEDIATE IMPLEMENTATION

MH6531B.24



FIGURE 9. SUMMARY OF CONTACT RELIABILITY STUDIES PERFORMED ON GFPd.

# LOW SPEED BARREL PLATING PARAMETERS AND CONTROLS

PHYSICAL & CHEMICAL PARAMETERS

| | |
|---|---|
| • [Pd] | 0.75 - 1.5g/l |
| • [pH] | 11.5 - 12.2 |
| • T (°C) | 47 - 53°C |
| • [LIGAND] | 0.1 - 0.5M |
| • SPECIFIC GRAVITY | 1.15 - 1.30 |
| • [PHOSPHATE] | ~ 0.5M |

DAILY CONTROLS

- [Pd]
- [Cu]
- pH
- T (°C)
- [LIGAND]
- SPECIFIC GRAVITY
- PLATING EFFICIENCY - WEIGHT GAIN ANALYSIS
  THICKNESS MEASUREMENTS

MH7662A.25A



FIGURE 10. OPERATING CHARACTERISTICS AND DAILY PROCESS CONTROLL PARAMETERS FOR BARREL PLATING OPERATION.

# LOW SPEED BARREL PLATING
## Summary

- PLATED CONTINUOUSLY > 2 YEARS
- PLATED ~190 MILLION PARTS/ BATH
- PLATED > 200 BATH TURNOVERS
  LITTLE MAINTENANCE
  NO CARBON TREATMENT

MH7662A.27A

FIGURE 11. SUMMARY OF BARREL PLATING OPERATIONS.

# REEL TO REEL HIGH SPEED PLATING PARAMETERS AND CONTROLS

PLATING PARAMETERS

- CONTROLLED DEPTH PLATING CELL
- CELL LENGTH ~ 6 FT.
- LINE SPEED 20 FT/ MIN
- PLATING SPEED 80 - 120 ASF
- PALLADIUM THICKNESS ~ 25 μ"; X-RAY FLUORESCENCE

DAILY PROCESS CONTROLS

- CONCENTRATION - Pd, Cu, Ni, LIGAND
  pH, SG, T(°C), CD (ASF)
- MICROCRACKING - SEM 3000X
- THICKNESS
- ADHERENCE
- ELECTROGRAPHIC POROSITY

MH7662A.20A

FIGURE 12. OPERATING CHARACTERISTICS AND DAILY PROCESS CONTROL PARAMETERS FOR HIGH SPEED REEL TO REEL PLATING.

# SUMMARY OF PRODUCTION DATA
## High Speed Reel to Reel Plating



- PLATED CONTINUOUSLY FOR 7 MONTHS
- PLATED 3659 REELS/ 182,950,000 PINS
- PLATED 8.5 - 9.0 BATH TURNOVERS
  WITH LITTLE MAINTENANCE
  WITH NO CARBON TREATMENT

MH7662A.13A

FIGURE 13. SUMMARY OF HIGH SPEED REEL TO REEL OPERATIONS.

## REFERENCES


1. W. A. Fairweather, Trans. Inst. Met. Finish. 64, 3 (1986).
2. J. M. Deuber, Met. Finish 81, 11 (1983); Met. Finish 81, 10 (1983).
3. R. G. Baker and R. Duva, Plat. and Surf. Fin., 70, 63 (June 86).
4. AES Symposium on Substitution for Gold, 1980 Milwaukee, WI.
5. AES Symposium on economic use of and substitution for precious metals in the electronics industry, Sept. 16-17, 1980 Danvers, Ma.
6. AES second Symposium on economic use of and substitution for precious metals in the electronics industry, 1982, Danvers, Ma.
7. E. M. Bock and J. M. Whitley, *Proc. Holm Seminar on Electric Contacts,* p. 130 (1974).
8. M. U. Rao, Proc. 1976 *Electronics Components Conf.,* p. 406 (1976).
9. R. J. Buchan and M. W. Ohman, *Proc. Nat'l. Electronic Packaging and Production Conf.,* p. 334 (1967).
10. W. O. Freitag, *Proc. Holm Seminar on Electric Contacts,* p. 17 (1975).
11. S. M. Arnold, *Proc. Electronics Components Conf.,* p. 75 (1959).
12. S. C. Britton, *Trans. Inst. Met. Fin.,* **52**, 95 (1974).
13. R. G. Baker and R. Sard, ibid., **66**, 36 (Aug. 1979).
14. T. A. Palumbo, ibid., **66**, 42 (Aug. 1979).
15. T. Sekiya, T. Umemoto and T. Takeuchi, *Proc.. 3rd Int'l and 22nd An. Nat'l. Relay Conf.* (1974).
16. M. Antler and E. S. Sproles, *IEEE Trans. Components, Hybrids, Mfg. Technology,* CHMT-5, 1, 158 (1982).
17. T. Sato et al., ibid., CHMT-5, 1, 10 (1981).
18. G. Herklotz and D. Poss, *Proc. 2nd AES Symp. on Econ. Use of and Substitution for Precious Metals,* Danvers, MA (1982).
19. S. P. Sharma, *Proc. Holm Seminar on Electric Contacts,* 191 (1981).
20. C. A. Hague and M. Antler,ibid. 183 (1981).
21. R. J. Russell, *Electronic Packaging and Production,* p. 182 (1980).
22. P. O. Papp and R. J. Russell, *Proc. Technical PGM,* NEPCON, Anaheim, CA (Mar. 1983).
23. F. E. Bader, *Proc. 11th Int'l. Conf. on Electrical Contact Phenomena,* Berlin, W. Germany, p. 133 (1982).
24. G. J. Russ, *IEEE Trans. Components, Hybrids and Mfg. Technology,* CHMT-6, 4, 389 (1983).
25. H. D. Hedricks and C. J. Raub, Metaloberflache, 31 (11): 512-20 (1977).
26. J. R. Lacher, Proc. Roy. Soc. A, 161, 525 (1937).
27. L. J. Gillespie and L. S. Dolstown, J. Am. Chem. Soc., 58, 2565 (1935).
28. L. J. Gillespie and W. R. Runs, J. Am. Clem. Soc., 62 2496 (1939).
29. J. W. Simmons and T. B. Flanagan, J. Phys. Chem., 69, 3581, 3773 (1965).

30. J. A. Abys, "2nd AES Symposium on Economic use of and Substitution for precious metals in the electronics industry," 1982, Danvers Mass.

31. J. A. Abys, Y. Okinaka, H. S. Trop and B. T. Kerns, 35th Meeting of the International Society of Electrochemistry, August 1984, Berkeley, CA.

32. J. A. Abys and H. S. Trop, U.S. Patent 4, 486, 274.

33. J. A. Abys and Y. Okinaka, U.S. Patent 4, 468, 296.

34. J. A. Abys and Y. Okinaka, U. S. Patent 4, 512, 963.

35. J. A. Abys, U.S. Patent 4, 427, 502.

36. J. A. Abys, IMF 'Connectors 87'.

37. H. W. Hermace and T. F. Egan J. Bell System Tech., 37, 739 (1958).

38. E. S. Sproles, Proc. 14th An. Connector Symp., Philadelphia, Pa (Nov 11-12, 1981).

39. H. S. Trop and A. V. Siaweleski, "2nd Symposium on Economic use of and substitution for precious metals in the electronics industry," Danvers, Ma.

F-1

# Environmental II
# Session F

## Acid Purification and Recovery Using Resin Sorption Technology—A Review

Mike Dejak and Kevin Munns
Eco-Tec Limited
925 Brock Road, South
Pickering, Ontario L1W 2X9

# Acid Purification and Recovery using Resin Sorption Technology - A Review

by: Mike Dejak and Kevin Munns
ECO-TEC LIMITED
925 Brock Road, South
Pickering, Ontario
L1W 2X9

In the metal finishing industries solutions of strong mineral acids (sulfuric, nitric, hydrochloric) are used to remove surface oxides that impair subsequent manufacturing operations. To a large degree these oxides are dissolved by the acids and as the concentration of dissolved metals increases there is a corresponding decrease in free acid concentrations. Although fresh acid can be added to the solution to make up for this, the oxide removal (pickling) rate generally decreases[1] when the metals concentration increases. The bath must be dumped when the oxide scale is no longer being adequately removed.

This method of operation can cause productivity related problems. Freshly formulated pickling baths containing very low levels of dissolved iron are very aggressive and can cause overpickling. Material of substandard quality can also be produced as the bath approaches the spent condition. Rework may be necessary to prevent problems with subsequent surface treatment processes.

In addition, spent pickle liquors can contain large amounts of unused or "free" acid. Free acid in a spent pickle bath represents a loss of valuable chemicals and a waste treatment liability. Continuous purification of pickle liquors can, therefore, offer several benefits to steelmakers:

- uniform product quality with reduced rework
- increased average pickling speed
- reduced chemical consumption
- reduced waste handling requirements

## 2.0 The APU Process

Certain ion exchange (IX) resins, similar to those used in water softeners and water deionizers, have the ability to absorb strong acids while excluding metal salts of these acids. The acids can readily be desorbed from the resin beads with a water wash. While this phenomena, known as "acid retardation", was observed by researchers in the early sixties[2] it was not successfully commercialized at that time. This was likely due to the limitations of conventional IX equipment design.

While the acid retardation work was underway, a novel ion exchange[3] process was being developed at the University of Toronto. This totally new approach to ion exchange embodied several unique design features:

- Fine mesh resin beads ..... to increase the surface area per cubic foot and improve reaction kinetics.
- Short resin beds .... reducing pressure drop and equipment size
- Fixed resin beds .... to minimize intermixing and dilution of feed and regenerant phases.
- Countercurrent flows .... of feed and regenerant steps to maximize chemical efficiency.

In 1975 a program was initiated to apply the process to acid retardation. The program was a success and the first acid retardation system using this technology was installed in 1977 for the purification of sulphuric acid anodizing solutions[4]. Since that time over 150 similar systems have been installed.

## 3.0 Basic System Design

In many pickling operations, the bath is formulated, worked, adjusted for free acid content as required until the dissolved metals reach a critical level, and dumped. An Acid Purification System is normally designed to hold the dissolved metal levels at a preferred operating level, typically 50 - 60% of normal dump concentration. Free acid concentration can be maintained at whatever level is required to provide the necessary pickling rate.

An Acid Purification System process is shown in Figure 1. There are three basic steps in the System including:

- Bath cooling (if required)
- Bath filtration
- Acid Absorption

a) Bath cooling

Bath cooling is necessary where oxidizers such as nitric acid or hydrogen peroxide are present. While sulphuric and hydrochloric acids can be treated at temperatures up to 80°C, the presence of oxidizers necessitates that the feed be cooled to about 32°C.

City water is normally used for cooling. A variety of cooler designs are available depending on the particular requirements of the system. The water may be used for regeneration of the absorption resin and rinsing on the pickle line.

# GENERAL APU® PROCESS

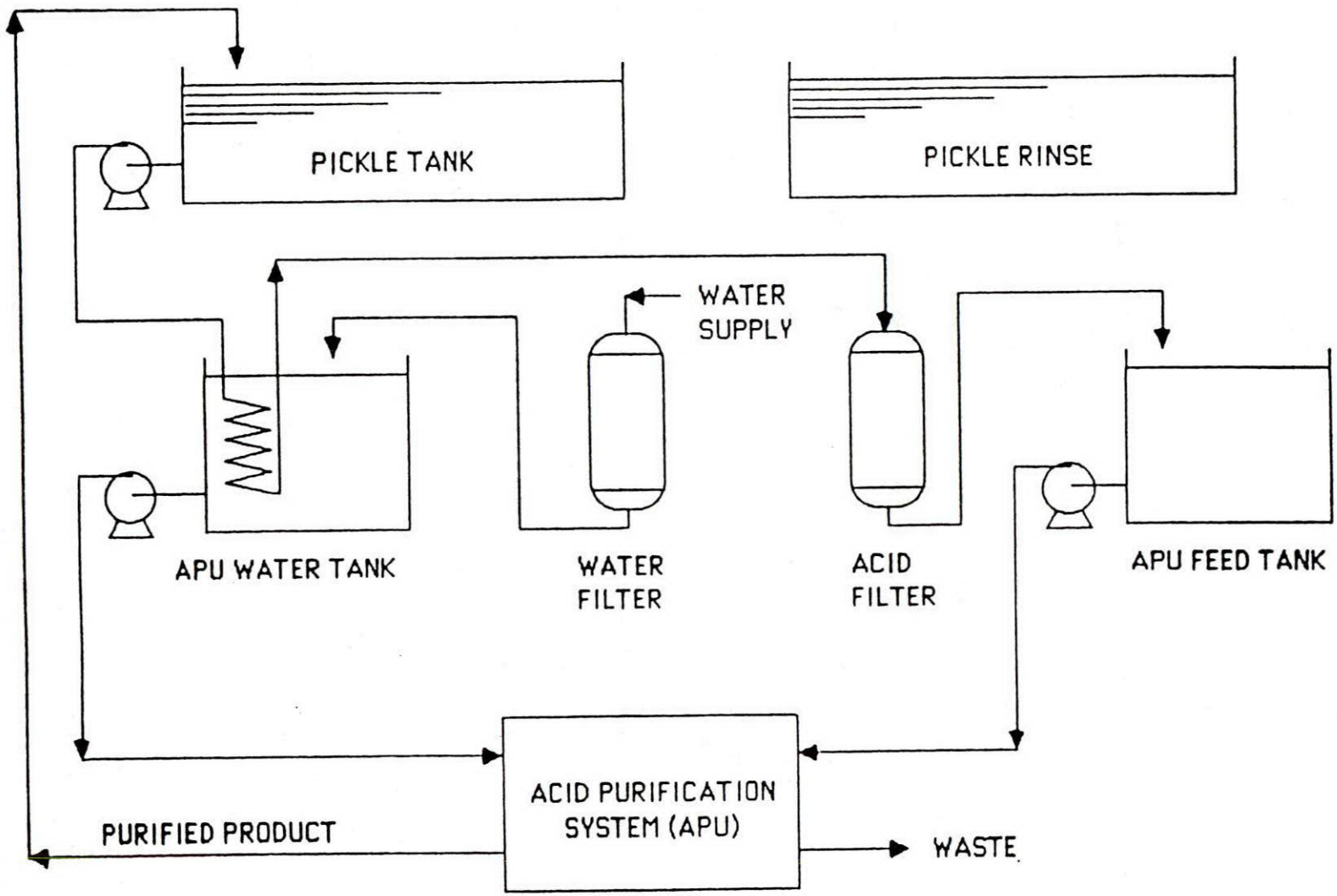


FIGURE 1: TYPICAL ACID PURIFICATION (APU) SYSTEM PROCESS

b) Bath filtration

Proper filtration of the pickling acid and the regeneration water is necessary to minimize pressure drop across the absorption resin bed.

Pickling acid solution is filtered in a multimedia pressure filter. A backup cartridge filter is also used. The amount of solids to be removed will depend on what alloy has been pickled and how much scale has been removed, however it should be noted that the solids load is usually much lower with the purification system in operation. This is because dissolved metal concentrations are kept below their solubility limit and crystallization of metal salts does not take place.

A monitor on the filter checks the differential pressure between the inlet and the outlet and indicates when a backwash is required. A combination of water and compressed air is used to backwash and scour the media. The backwash sequence begins with an air blowdown to exhaust the entrained pickle liquor to the surge tank. The media is then fluidized with a combination of air and water to remove trapped solids. The waste water from the backwash may contain small amounts of acid and should be treated with rinse waters from the pickle line.

Water for regeneration of the absorption resin is filtered in a multi-media filter similar to the one used for the feed acid. With this filter no special air blowdown or scouring is required.

c) Acid Absorption

Acid absorption takes place in a skid mounted device called an Acid Purification Unit or APU$^{R}$. The APU consists of a container or "bed" of absorption resin, process valves and controllers. It is the heart of the System. Figure 3 is a photograph of an Acid Purification System for sulphuric acid service.

The resin bed is a cylindrical vessel 30 - 60 cm (12" - 24") in height. Bed diameter is dependent upon the feed flow and typically varies between 15 - 180 cm (6" and 72").

The APU works on a very simple two - step cycle. During the first part of the cycle, the upstroke, filtered acid is pumped up through the resin bed and free acid is absorbed by the resin beads. Dissolved metals pass through the unit unhindered. This step continues until the resin bed has been fully loaded with acid.

Byproduct solution flowing from the unit will contain dissolved metals and a small amount of dissolved acid. In some cases the byproduct may contain recoverable chemicals, however, in most cases it must be neutralized and clarified prior to discharge. The suitability of the plant's effluent treatment system should be checked to ensure adequate capacity is available in neutralization tanks and filters.

After the resin bed has been loaded with acid, filtered water is pumped down through the bed during the "downstroke" part of the cycle. The water desorbs the acid from the resin at a concentration suitable for recycle back to the pickle tank. This step continues until the bed has been fully regenerated.

At the beginning of each of these steps a void solution can be recycled. In the case of the upstroke step this void is essentially just the water that was left in the bed from the preceeding cycle. The void during the downstroke is feed acid that can either be mixed with the purified acid or returned to the feed tank.

The unit's operation is regulated by a flow totalizer that is coupled to a programmable controller. It is worthy to note that in all applications, acid is pumped up through the bed and water is pumped down through the bed. This utilizes the density differences of the two solutions to maintain a stable interface between the acid and water, approaching plug flow through the resin bed. Solution intermixing and dilution is minimized.

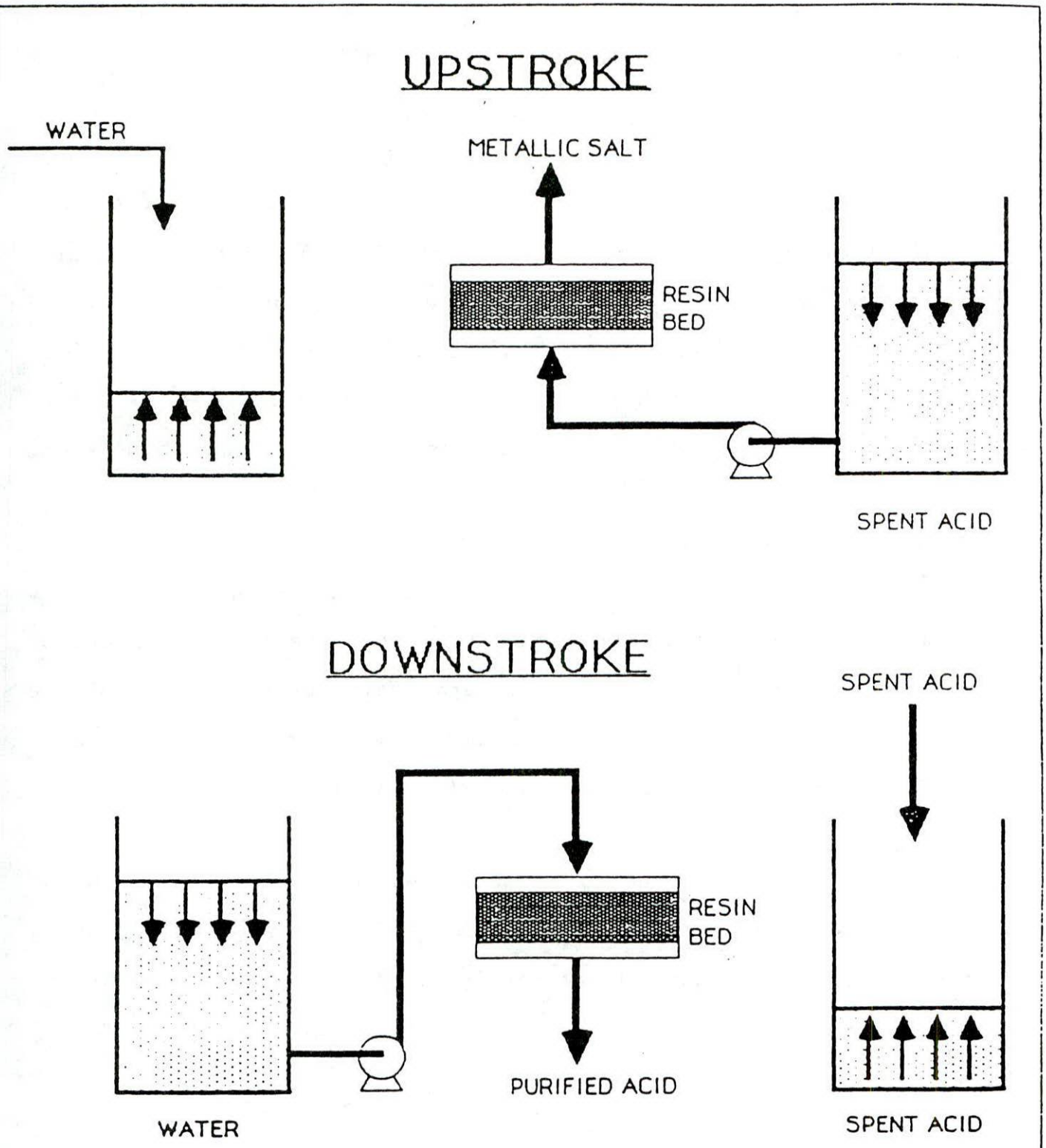


FIGURE 3: STEPS IN THE APU® PROCESS

## 4.0 Applications in the Steel Industry

The three pickling solutions used most frequently in the steel industry are based on sulphuric, hydrochloric or nitric acids.

### 4.1 Stainless Steel (Mixed Acid) Pickling

Mixtures of nitric and hydrofluoric acids are used to remove scale from most grades of stainless steel. Generally, these baths are formulated with 10 - 15 percent by weight nitric acid and 1 - 4 percent by weight hydrofluoric acid, depending on the alloy to be treated. Bath temperatures are maintained at 55 - 65 degrees C. During the pickling process iron, chromium and nickel are dissolved into the acid.

Concentrated nitric and hydrofluoric acid must be added regularly to maintain free acid levels, however, when the metals content of the solution exceeds 5 - 6% w/w, metal salts begin to crystallize out of solution and the bath must be dumped. Frequently, manual labour must be used to remove the sediment from the tank.

With the APU System, the total dissolved metals concentration can be continuously maintained in the range of 2-4% w/w. This enables the solution to be used indefinitely. Typical results using the APU on mixed acid service are given in Table 1.

Table 1: APU Results - Nitric / Hydrofluoric Service

| Component | Feed | Product | Waste | % Loss |
|---|---|---|---|---|
| Nitric acid (g/L) | 120 | 114 | 5 | 5 |
| Hydrofluoric acid (g/L) | 30 | 24 | 5 | 20 |
| Iron (g/L) | 30 | 9 | 18 | 70 |
| Chromium + Nickel (g/L) | 10 | 3 | 6 | 70 |
| Relative Flow | 1 | 1 | 1.2 | |

The concentrations of nitric and hydrofluoric acid shown above are free acid concentrations. The absorption process has been observed to be more efficient with highly dissociated (strong) acids. As the hydrofluoric acid is a weaker acid than the nitric, the recovery efficiency is lower.

The installed cost of the APU System is dependant upon the amount of dissolved metals that must be removed from the pickle liquor and can vary between $75,000 and $500,000. These capital costs can be recovered very quickly due to value of the acids involved.

An Economic Evaluation is presented for the APU System on mixed acid service in Table 2. The evaluation is based on the following conditions:

Spent bath flowrate: 1500 L/hour (400 USGPH)

Spent bath composition: 100 g/L $HNO_3$ (9% w/w)
20 g/L HF (1.8% w/w)
40 g/L Fe (3.6% w/w)

Plant operation: 6000 hours per year

Table 2: Economic Evaluation on Mixed Acid Service

| Cost Component | Annual Cost ($/year) | |
|---|---|---|
| | Simple Neutralization | APU System |
| 70% HNO3 $150 per tonne | $192,900 | $13,800 |
| 70% HF $950 per tonne | $769,500 | $592,800 |
| Lime $50 per tonne | $86,700 | $46,500 |
| 45% Cake Haulage $40 per tonne | $173,500 | $144,400 |
| Labor $15 per hour | | $30,000 |
| Replacement parts | | $12,000 |
| Utilities | | $3,000 |
| Total Operating Costs | $1,222,600 | $842,500 |
| Savings compared to Simple Neutralization | | $380,100 |
| **Estimated Capital Costs** | | $300,000 |
| **Payback Period (years)** | | 0.79 |

Notes:

a) All costs are expressed in 1987 U.S. dollars. All weights are expressed in metric tonnes (2200 lbs).

b) Chemical costs based on prevailing rates as reported in Chemical Marketing Reporter (7/87).

There is a lesser reduction in hydrofluoric acid purchases than might be expected from the operating data presented in Table 1. It has been assumed for the sake of the analysis that both iron and chromium metals are tri-valent and present in solution as complex fluoride salts. Despite this, the chemical and treatment cost savings can readily justify the capital expense. The evaluation does not attempt to quantify benefits associated with uniform pickling rates (reduced rework) and composition (prevention of salt crystallization and tank cleaning) although these can be very significant.

## 4.2 Hydrochloric Acid Pickling

Hydrochloric acid is commonly used for pickling of mild steel on batch and continuous lines. Baths are made up with a free acid concentration of 10 - 15 percent by weight and can be operated between 20 and 80 degrees celcius. The baths are dumped when the dissolved iron level reaches 8 - 10% by weight. It is possible to reduce free acid levels to less than 5% as the bath reaches a spent condition. Spent acid can be contract hauled, neutralized with lime or, in some cases, used to produce ferric chloride.

Continuous strip lines frequently operate three or four pickle tanks in series with the flow of acid running continuously between tanks. This design allows spent pickle liquor to be continuously withdrawn at very low free acid levels. In order to achieve the high pickling rates required in these lines, elevated temperatures must be used. This can lead to problems with acid vapour losses. With the APU System it is possible to reduce the solution temperature by operating the pickle liquor at higher free acid concentrations. This can be done economically since the APU System recovers virtually all of the free acid.

In batch pickling operations the level of free acid in the spent liquor can be substantial. The APU can be used to continuously remove iron from the bath thus eliminating bath dumps. This reduces the loss of free acid and the attendant treatment requirements. In addition, by allowing the economical use of higher free acid concentrations and lower dissolved iron

concentrations, pickling speeds can be increased. The elimination of lost production time due to bath dumping and re-formulation is another benefit of continuous purification.

Typical results for the APU System on hydrochloric acid service are given in Table 3.

Table 3: APU Results - Hydrochloric Acid Service

| Component | Feed | Product | Waste | % Loss |
|---|---|---|---|---|
| Hydrochloric acid (g/L) | 150 | 153 | 8.6 | 4 |
| Iron (g/L) | 50 | 32 | 29 | 40 |
| Relative Flow | 1 | 0.94 | 0.7 | |

The product is returned from the APU in a slightly concentrated state. Consideration must still be paid to the water balance in the pickle tank, particularly since commercial grade hydrochloric acid is a relatively weak (32% w/w) solution. If steam spargers are used for bath heating, difficulties may be encountered with the dilution caused by the condensed steam. Out-of-line heating systems using shell and tube heat exchangers are preferred to maximize the acid recovery.

An Economic Evaluation is presented for the following conditions:

Spent bath flowrate: 1500 L/hour (400 USGPH)

Spent bath composition : 100 g/L HCL (9%)

70 g/L Fe (6.5%)

Plant operation: 6000 hours per year

Table 4: Economic Evaluation on Hydrochloric Acid Service

| Cost Component | Annual Cost ($/year) | |
|---|---|---|
| | Simple Neutralization | APU System |
| 32% HCL<br>$70 per tonne | $371,600 | $199,500 |
| Lime<br>$50 per tonne | $94,700 | $50,800 |
| 45% Cake Haulage<br>$40 per tonne | $105,300 | $98,100 |
| Labor<br>$15 per hour | | $30,000 |
| Replacement parts | | $6,400 |
| Utilities | | $1,600 |
| Total Operating Costs | $571,600 | $386,400 |
| **Savings compared to Simple Neutralization** | | **$185,200** |
| **Estimated Capital Cost** | | **$160,000** |
| **Payback Period (years)** | | **0.86** |

Notes:

a) All costs are expressed in 1987 U.S. dollars. All weights are expressed in metric tonnes (2200 lbs).

b) Chemical costs based on prevailing rates as reported in the Chemical Marketing Reporter (7/87).

This comparison shows the APU System to be a very cost effective option for treatment of hydrochloric acid pickling solutions. As previously discussed, other productivity related benefits have not been considered. In addition to quality related benefits, the APU System can allow higher free acid concentrations to be used economically. This may permit lower bath temperatures to be used. In addition to energy savings, lower temperatures lead to a reduction in HCl vapor losses and the attendant treatment requirements.

## 4.3 Sulphuric Acid Pickling

Sulphuric acid is most commonly used in batch pickling operations although, there are still some continuous sulphuric pickling lines in use. Generally, at least 10% w/w sulphuric acid must be maintained in the pickling acid to ensure minimum pickling rates. The acid becomes spent when the dissolved iron level reaches 6 - 8% by weight. At higher levels the iron will crystallize out of solution. Care must be taken not to allow either the free acid level, or the bath temperature, to get too high as this will depress the solubility of the ferrous sulphate. In addition to the control considerations required with sulphuric acid, the spent bath can be difficult to treat. Dosing with lime generates large amounts of calcium sulphate (gypsum) sludge.

Use of the APU on sulphuric acid pickling solutions can overcome these disadvantages. Continuous bath purification ensures that dissolved iron concentrations don't exceed solubility levels.

Since the APU recovers free ( or unused ) acid in solution, higher sulphuric acid concentrations can be used economically. This can lead to signifigantly increased productivity levels. Typical results are given below.

Table 5: APU Results - Sulphuric Acid Service

| Component | Feed | Product | Waste | % Loss |
|---|---|---|---|---|
| Sulphuric acid (g/L) | 150 | 138 | 10 | 8 |
| Iron (g/L) | 70 | 26 | 40 | 65 |
| Temperature ($^{o}$C) | 80 | 76 | 19 | 5 |
| Relative Flow | 1 | 1 | 1.15 | |

It is worth noting that the APU System recovers most of the heat in the feedstock. An Economic Evaluation for the APU System on Sulphuric acid service is presented in Table 5. The comparison is based on the following conditions:

Spent bath flowrate: 1500 L/hour (400 USGPH)

Spent bath composition : 150 g/L H2SO4 (13%)

70 g/L Fe (6.5%)

Plant operation: 6000 hours per year

The APU process does not remove the ferrous sulphate in a recoverable form and magnesium hydroxide treatment is recommended. While this results in the generation of a considerable amount of ferrous hydroxide sludge, the filter cake is generally considered to be non-hazardous and can be used as a landfill.

Table 6: Economic Evaluation for the APU System

| Cost Component | Annual Cost ($/year) | |
|---|---|---|
| | Simple Neutralization | APU System |
| 93% H2SO4 $82 per tonne | $216,300 | $111,800 |
| Magnesium Hydroxide $215 per tonne | $312,100 | $161,400 |
| 45% Cake Haulage $40 per tonne | $90,100 | $90,100 |
| Labor $15 per hour | | $30,000 |
| Replacement parts | | $7,200 |
| Utilities | | $1,800 |
| Total Operating Costs | $618,500 | $402,300 |
| **Savings compared to Simple Neutralization** | | **$216,200** |
| **Estimated Capital Costs** | | **$200,000** |
| **Payback Period (years)** | | **0.93** |

Notes:

a) All costs are expressed in 1987 U.S. dollars. All weights are expressed in metric tonnes (2200 lbs).

b) Chemical costs are based on prevailing rates as reported in the Chemical Marketing Reporter (7/87).

## 5.0 Summary

A proven low-cost purification system based on absorption resin technology is now available for a variety of pickling acids including the nitric / hydrofluoric mixtures used for stainless steels. In addition to reducing acid purchases and disposal requirements, the continuous system allows pickling baths to be economically operated at higher free acid and lower dissolved metal levels than would normally be considered practical. This can lead to significant increases in productivity.

## 6.0 References

1. Metals Handbook, 9th Edition, Volume 5, pp 73-74, American Society for Metals, Metals Park, Ohio
2. M.J. Hatch, J.A. Dillon, Industrial and Engineering Process Design and Development, 2, 4, 253 (1963)
3. I.H. Spinner, R.F. Hunter, Canadian Journal of Chemical Engineering, 42, 28, (1964)
4. C.J. Brown, D. Davy, P.J. Simmons, Plating and Surface Finishing, 66, 54 (January 1979)

F-2

# Environmental II
# Session F

## A Comparison of Vacuum and Atmospheric Evaporative Recovery Equipment

Raymond A. Baker
Applications Engineer
Corning Process Systems
Big Flats, NY 14814

# A COMPARISON OF VACUUM AND ATMOSPHERIC EVAPORATIVE RECOVERY EQUIPMENT

by
Raymond A. Baker
Applications Engineer
Corning Process Systems
Big Flats, NY 14814

## Introduction

Evaporative recovery is a proven technology to recover plating chemicals from rinsewater. It reduces expenditures for chemicals as well as minimizes waste generation, thus reducing waste treatment and disposal costs.

This paper will discuss all aspects of evaporative recovery so that this technology can be used successfully. The various types of evaporators will be discussed, along with their operation, design, sizing, installation, and maintenance. The features of atmospheric evaporation and vacuum evaporation will be compared.

## Evaporative Recovery

Evaporative recovery is the physical separation of one group of chemical components from another by evaporation in order to reuse the chemicals. Evaporation is a single stage distillation, using heat energy to drive the separation.

For example, heat is applied to a mixture of water and metallic salts. The water boils and water vapor separates from the salt solution. The water vapor is driven to condenser where it is condensed back to pure water. This leaves a concentrated bath of metallic salts which can be reused or recovered back to a process; and a pure water stream which can also be reused. If the mixture of salts and water is a waste stream, then evaporative recovery recovers two streams of previously unusable chemicals to two usable products. This will save chemical and water costs, as well as eliminates the need for waste treatment and disposal.

Evaporation can also be used to consolidate a waste stream by removing water, thus reducing the volume to be treated.

There are many types of evaporation equipment including batch stills, thermosyphon evaporators, climbing or thin-film evaporators, vapor recompression evaporators and atmospheric evaporators. The evaporators used in the metal finishing industry for plating chemical recovery can be classified as vacuum evaporators, which use steam heat to evaporate water within a closed system at a vacuum; and atmospheric evaporators, which use process heat and warm air to evaporate water in an open system.

Plating Chemical Recovery with Vacuum Evaporators

In plating operations, plating chemicals are dragged out with the plated parts to the rinse baths where excess plating solution is removed from the parts as well as the racks. Thus, the rinse water contains the plating bath chemicals and is considered a hazardous waste stream. The metal finishing industry has developed many techniques to treat rinse water, eventually separating the plating chemicals from the water into a sludge which is landfilled as a hazardous waste. Current regulations head towards banning the land disposal of this material in the near future, so waste minimization and recovery of the plating chemicals is of utmost importance.

Evaporative recovery of plating chemicals from rinse water has been very successful in the metal finishing industry, where vacuum evaporators have been widely used for greater than 10 years. An example vacuum evaporator used for plating chemical recovery is the climbing-film evaporator.

The climbing-film evaporator consists of a climbing-film boiler, vapor-liquid separator, vapor condenser, and the associated piping, valving and automatic controls. The boiler consists of a metal shell with vertical metal tubes sealed into ceramic or teflon tubesheets. The separator, condenser, and piping are fabricated from materials compatible with the plating solution.

Plating rinse water is continuously fed to the climbing film boiler. Low-pressure steam provides the energy by which the rinse water vaporizes and drives a climbing film of concentrated liquid up the tubes and into the vapor-liquid separator. In the separator, the liquid phase with the plating chemicals settles out, while the water vapor continues through a demister to the condenser. When the recovered plating chemical solution reaches the desired concentration, it is drained into a storage tank and held for reuse. The recovered distilled water returns as rinse water.

Other types of vacuum evaporators include the flash evaporator, submerged tube evaporator, double effect evaporator and mechanical vapor recompression evaporator.

Vacuum evaporators are recovering plating chemicals from acid solutions in decorative chrome plating; chrome etch for plating on plastics; nickel plating; acid zinc, copper, tin, and gold plating; nickel sulfamate and tin-lead fluoborate plating. Evaporative recovery is also used on alkaline baths such as alkaline zinc and all of the metal cyanide complexes. Other solutions used in metal finishing operations are also candidates for evaporative recovery. Many case histories have been published on the use of vacuum evaporators for plating chemical recovery.[1,2,3,4,5,6,7,8]

Evaporative recovery has been found to be very economical for plating chemical recovery.[9] The installed cost for a 75 gal./hr. evaporator on

a chrome plating line is $60,000. The major operating cost is energy, or typically the cost of steam to operate the evaporator. Normal maintenance consists of periodically cleaning the boiler, and replacement of some parts after several years of use.

Annual savings are realized by reduced purchases of plating chemicals, lower water and sewage charges, and elimination of waste treatment and disposal costs. The evaporator can recover about 90% of the chrome used in the plating process, because this amount of chrome is usually dragged-out with the plated parts and lost through the rinse water. Thus 90% of the chrome plating chemical costs can be saved. Disposal of a barrel of sludge is variable but can range between $60. and $300. Disposal costs are increasing, therefore elimination of disposal costs is seen as a major economic factor in evaporative recovery.

When designing an evaporative recovery system, the available utilities, materials of construction, flowrate of rinse water, temperature sensitivity of the recovered chemical, and control of contaminants should all be evaluated.

The climbing-film evaporator requires low pressure steam for the evaporation, cooling water for the condenser, and electric power for the pumps and controls. Most evaporators are prefabricated, complete with controls, capable of fully automatic fail-safe operation. The evaporator can be set in the plant and simply piped up to the utilities and feed and product lines. The materials of construction should be evaluated to be compatible to the plating solution.

The flowrate of rinse water to the evaporator is critical because the major operating cost is energy to evaporate the rinse water. The entire plating operation and evaporative recovery system should be set up to minimize the use of rinse water. Techniques such as multiple rinse tanks, countercurrent rinsing, spray rinses, air agitation or other methods can be used to improve the rinsing of the plated product with lower rinse water flowrates.

The evaporative recovery system can be set-up for total recovery or partial recovery. Total recovery (Figure 1) cycles the total volume of water used by the rinse tanks through the evaporator. The purified water is returned to the rinse tanks and all plating chemicals are recovered and returned to the plating bath.

Partial recovery (Figure 2) capitalizes on the fact that 90% of dragged out chemicals remain in the first two rinse tanks. The evaporator processes only the water from the first two tanks, and in so doing recovers 90% or more of the dragged out chemicals. Fresh rinse water supplies a third rinse tank to complete the final rinsing; this rinse water would need to go to waste treatment. Partial recovery results in a low concentration of chemicals going to treatment, and minimized evaporator size and operating cost.

A liquid ring vacuum pump or other vacuum apparatus is usually supplied with the evaporator to generate the vacuum. Vacuum reduces the need for a feed pump, and will control the temperature of the evaporation. Many plating chemicals are temperature sensitive. High temperature may degrade the organic additives in the recovered plating solution making it unable to be reused. Operating the evaporator under vacuum will reduce the boiling point of the water, so evaporation will be at a lower temperature and not harm the chemicals. For example, chrome can tolerate higher temperatures, so a chrome evaporator operates at 12" Hg vacuum, and 185°F. Nickel plating solution contains brighteners which degrade at high temperature, so a nickel evaporator should run at 19" Hg vacuum or 165°F. Acid zinc plating solution may contain organic additives which degrade at temperatures over 110°F, so the acid zinc evaporator should operate at a very high vacuum, 27.7" Hg and 105°F.

Note that the size of the evaporator is affected by vacuum. At higher vacuums the vapor densities are very low, so that the same weight of vapor will have a much higher vapor velocity through the boiler tubes and separator. Therefore, the evaporator tube and separator diameters have to be larger at high vacuum; this increases the cost of the evaporator.

Evaporative recovery systems also concentrate any plating bath contaminants, which are usually dragged out of the bath. These contaminants need to be removed before the recovered plating chemicals can be properly returned to the bath. Recovery systems commonly have a purification operation to remove contaminants. Chrome plating recovery utilizes cation resin bed exchangers to purify the recovered solution. The cation exchanger is hooked to the first rinse tank so that cationic impurities such as nickel, zinc, etc. are removed before the rinse water goes to the evaporator. Nickel plating recovery utilizes carbon filters for purification. Also deionized water should be used for make-up.

Figure 3 shows the total layout of an evaporative recovery system on a plating line. Vendor literature goes into much greater detail on evaporator sizing, installation and control of contaminants. One excellent resource is 'Evaporative Recovery', an AESF Illustrated Lecture prepared by William McLay for the society's Environmental Compliance & Control Course (1980).

Atmospheric Evaporation

The atmospheric evaporator consists of a container where process solution is pumped and sprayed over packing to maximize the contact between solution and air, which is blown into the evaporator through the packing. Water from the solution is evaporated into the air, which is ducted outside or through an existing ventilation system. The unit is typically located at a higher elevation than the process tank it is servicing to allow for gravity flow return of the concentrated liquid. The entire system is chemically compatible with the process solution; materials of construction such as PVC, polyethylene, and polypropylene are commonly used in the plating industry.[10]

Evaporation rate for atmospheric evaporators depends on volume of air, its' original humidity, the surface area of the packing and the temperature of the solution.

The atmospheric evaporator is commonly used in plating systems where rinse water counterflows through several rinse tanks to the plating tank. This technique also recovers the dragged-out plating chemicals in the rinses back to the plating tanks, which reduces the need for waste treatment and disposal. The atmospheric evaporator is used to remove the excess water from the plating tank to accomodate the flow of rinse water with the return of the dragged-out chemicals. In this manner, the evaporator works directly on the plating tank and evaporates water from a concentrated solution.

For low temperatue processes, heated tanks are added to collect the rinse water and dragout. These tanks feed the atmospheric evaporator. Concentrated solution is returned to the process as needed. Also, the evaporator can work off individual rinse tanks to decrease volume for additional rinse water.

Partial recovery can also be set up with atmospheric evaporation.

Other uses of atmospheric evaporation include stopping growth of zinc or trivalent chrome solutions; and providing cooling for low temperature processes.

Comparison of Vacuum and Atmospheric Evaporation

Perhaps the best way to show the features of vacuum and atmospheric evaporative recovery is to compare. Table 1 provides a listing of the relative features. Follows is a brief description of the relative features:

Equipment Cost: Atmospheric evaporators are considered a low cost option for plating chemical recovery. An entire system on a plating line with low drag-out may have a capital cost less than $10,000. Vacuum evaporators are considered to have high capital cost. As the plating line size increases, the difference in equipment capital cost becomes smaller.

Reduced Waste Treatment and Disposal: Both types of evaporators, if operated properly, can reduce waste treatment costs by substantially reducing the quanity of sludge which is generated and disposed as a hazardous waste.

Heat Transfer: Atmospheric evaporators use direct heat transfer where the energy for evaporation is transfered directly from the process solution, in direct contact with an air stream to the evaporating liquid/vapor. Vacuum evaporators utilize indirect heat transfer where the heat for evaporation passes through a medium such as the boiler tube walls from an energy source such as steam.

Energy: Vacuum evaporation uses energy sources such as condensing steam, hot water or hot oil contained within boiler tubes. Atmospheric evaporation uses energy from the process within the heated plating solution, energy from the environment within the heated room air, and occasionally supplemental energy from steam coils. Calculating energy costs for atmospheric evaporation is complex because, in some cases, energy is wasted by excess warm air going out a stack, and in other cases, energy is less costly because heat is used from a process which needs to be cooled, or from a hot room which needs to be ventilated. Note, that in both atmospheric and vacuum evaporation, the energy used to evaporate a pound of water is approximately the same (1,000 BTU/lb).

Purification: Both atmospheric and vacuum evaporation require purication of the recovered plating chemicals to maintain proper bath chemistry. The purification method should remove any unwanted chemicals that can build-up in the bath during the plating process and are normally removed by drag-out. Also, chemicals introduced by evaporation may need to be removed. Atmospheric evaporation may introduce contamination from the air (dust, etc.) because of the high contact between the solution and the air. Purification equipment typically works on a dilute stream such as a rinse tank which also feeds the evaporator.

Open/Closed System: Vacuum evaporation can be considered a closed system. All process streams stay within the tanks, equipment and piping of the system. All plating chemicals are returned to the baths; all evaporated water is returned to the rinses. No stream contacts the environment. Atmospheric evaporation can be considered an open system, where the process streams contact the environment. The plating solution contacts air in the evaporator; the evaporated water is exhausted to the outside. The atmospheric evaporator cannot be used with baths which may release toxic compounds to the atmosphere.

Currently, exhaust from atmospheric evaporators may have to be identified as point sources with environmental agencies. Often the exhaust is sent to scrubbing systems. The U.S. Environmental Protection Agency is currently evaluating air discharges from the metal finishing industry. Chrome mist in the exhaust from chrome plating line ventilation is considered carcinogenic, and regulatory guidelines on chrome exhausts are scheduled to go into effect midyear-1990. Atmospheric evaporators currently have not been reviewed for regulation, yet I would predict atmospheric evaporators on chrome to have some regulation in the mid-1990's.

Evaporator Feed: Atmospheric evaporators are set-up to take feed directly from the plating tank, where water is evaporated from the plating solution to make room for the return of dragout. The concentrated plating solution returns directly to the bath. Also, atmospheric evaporators are set-up on individual rinse tanks or side tanks of rinse water to make room for the fresh rinse water. Vacuum evaporators usually take feed from the first rinse tank in a counter-current rinse system and evaporates water from the dilute rinse while concentrating plating chemicals to the bath strength.

Evaporation Rate: Vacuum evaporators usually have a constant evaporation rate. Evaporation rate is controlled by steam pressure, vacuum and boiling point of the concentrated liquid. These parameters stay within a close range, so the evaporation rate as well as the rinse water flowrate can be expected to stay close to a preset constant.

The evaporation rate for atmospheric evaporators is controlled by volume of air and it's humidity and process temperature. Air humidity can change according to the weather, so evaporation rate can vary from day to day dependent on the weather.

Concentration: Vacuum evaporators concentrate plating chemicals to a preset level. The concentration of the returned solution from atmospheric evaporators is dependent on the evaporation rate. As the rate varies, the concentration of the returned solution can vary; however bath concentration should be balanced by the return of the dragout.

Foaming: Foaming can affect all evaporators. Some plating baths will foam, some will not, depending on the chemistry. Plating bath chemistry can be adjusted to reduce foaming. Vacuum evaporators have special vapor/liquid separator designs to reduce the effects of foaming. Atmospheric evaporators have special nozzle designs to reduce foaming.

Plugging: Plugging is another operation concern with all evaporators. Salts from over-concentrated solutions could precipitate within the evaporator. This results in plugged tubes and deposits with vacuum evaporators, and plugged packing with atmospheric evaporators. In both cases, the evaporator should be maintained with periodic chemical cleaning.

Pumps: Atmospheric evaporators have feed pumps and fans which have to be maintained. Vacuum evaporators have vacuum pumps to be maintained. It is critical that the vacuum pump receive sufficient sealant water for proper operation.

## REFERENCES


1. "Closed-loop unit recovers electroplating wastes", IRON AGE, August 9, 1976.

2. Bhatia, S., Jump, J., "Metal recovery makes good sense!", ENVIRONMENTAL SCIENCE & TECHNOLOGY, Vol. 11, P. 752, August 1977.

3. "Recovers 80 Pct of Chromium Solution", PRODUCTS FINISHING, August 1977.

4. "The quest for optimum plating water treatment", INDUSTRIAL FINISHING, July 1978.

5. "99 Pct Recovery, Effluent Below One PPM", PRODUCTS FINISHING, August 1978.

6. Rose, B., "Design for recovery", INDUSTRIAL FINISHING, May 1979.

7. Blout, E., "How Guide Recovers Nickel and Chromium", PRODUCTS FINISHING, December 1980.

8. "Passing the test of time", POLLUTION ENGINEERING, April 1987, p. 44.

9. U.S. Environmental Protection Agency, "Environmental Regulations and Technology - The Electroplating Industry", EPA/625/10-85/001, September 1985, p. 18-19.

10. Singelyn, D., Singelyn, P., "Low Cost Recovery", AESF 73rd Annual Technical Conference Proceedings - Philadelphia, PA Environmental II, Session E-4, June 23-26, 1986.

TABLE 1
Comparison of Evaporative Recovery Equipment

| Atmospheric Evaporation | Vacuum Evaporation |
|---|---|
| Low Capital Cost | Higher Capital Cost |
| Reduced Waste Treatment and Disposal | Reduced Waste Treatment and Disposal |
| Direct Heat Transfer | Indirect Heat Transfer |
| Process, Room and Steam Heat | Steam Heat |
| Purification Required | Purification Required |
| Open to Environment Discharge to Outside | Closed System |
| Evaporates from Plating Tank and Rinse Tank | Evaporates from Rinse Tank |
| Evaporation Rate can Vary | Good Control of Evaporation Rate |
| Concentration of Returned Bath can Vary | Good Control of Concentration |
| Foaming | Foaming |
| Plugging of Packing | Plugging of Tubes |
| Fan and Feed Pump | Vacuum Pump |

## Total Recovery

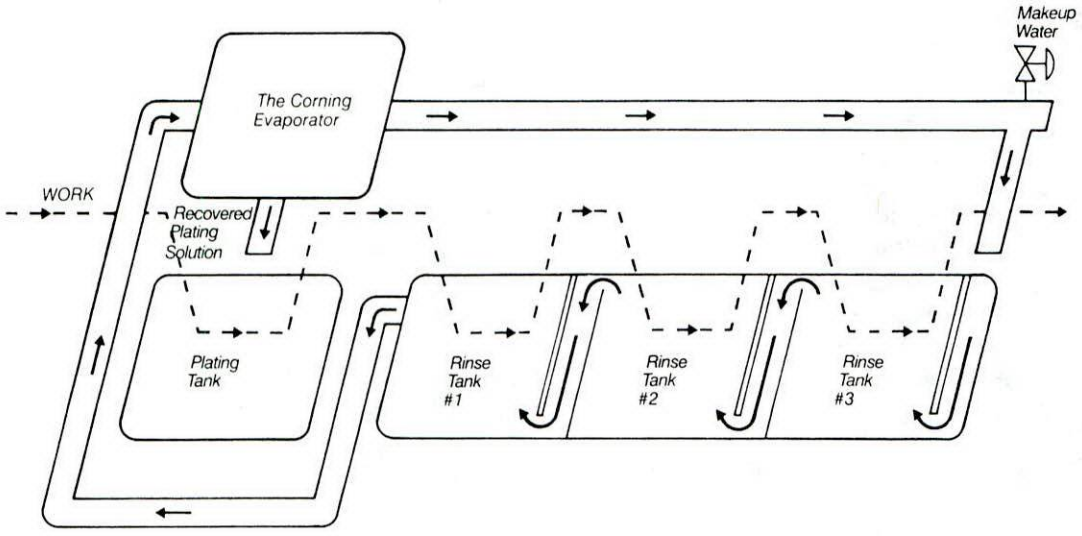


Figure 1

## Partial Recovery

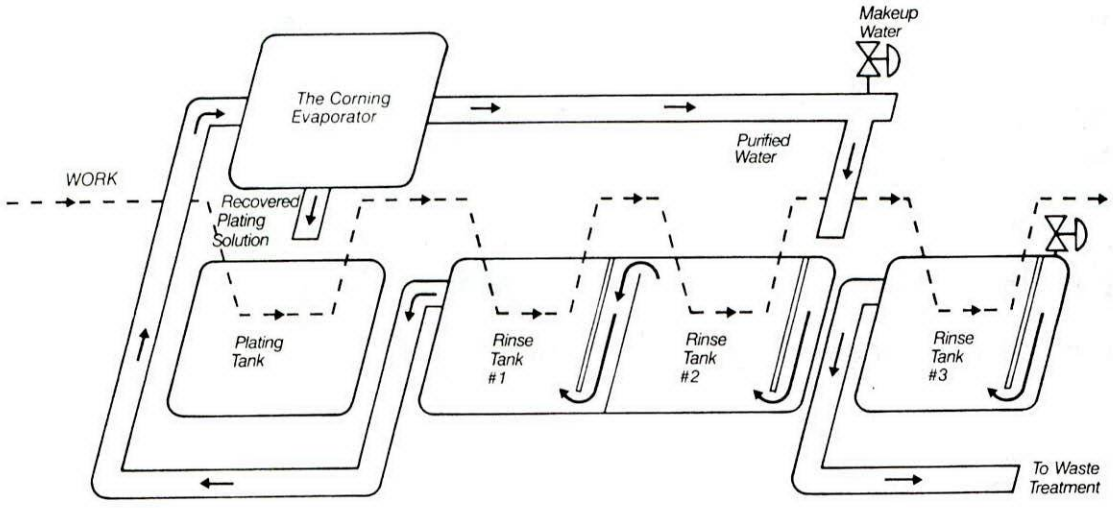


Figure 2

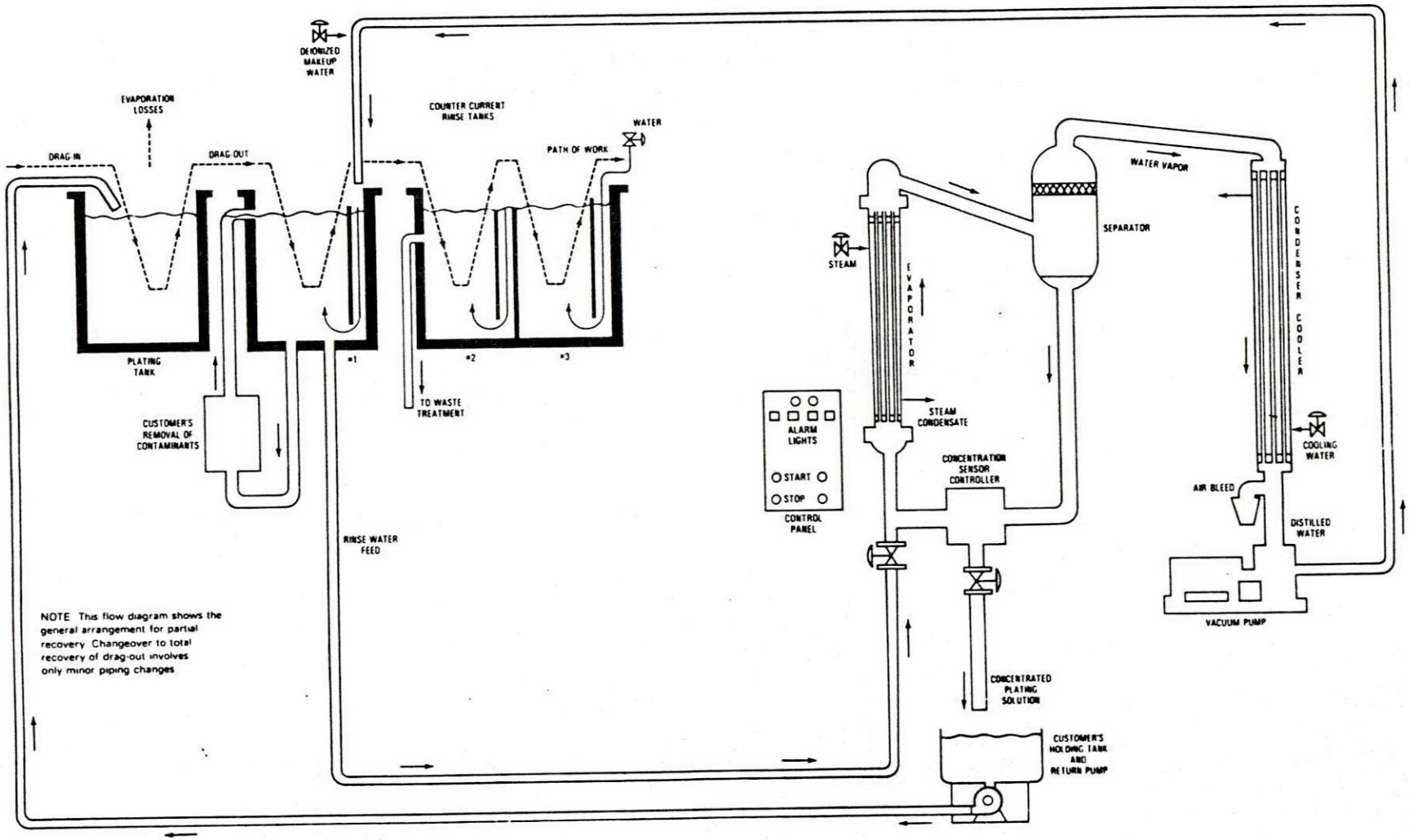


CORNING PROCESS SYSTEMS
Corning Glass Works

Corning Plating Chemical Recovery Unit

Figure 3

F-3

# Environmental II
# Session F

## Absolute Reclamation of Water and Bath Through Use of New Reverse-Osmosis-Based System

Ronald R. Rich, CEF
Water Technologies Inc.
Minneapolis, MN

**PAPER NOT RECEIVED IN TIME FOR PUBLICATION***

# Absolute Reclamation of Water and Bath Through Use of New Reverse-Osmosis-Based System

Ronald R. Rich, CEF, Water Technologies Inc., Minneapolis, MN

A self-contained, completely automated system has been developed for total reclamation of plating and etching rinsewaters. The system is based primarily on pH-tolerant reverse osmosis using proprietary technology. The purified water is reused and the separated materials are concentrated for direct reintroduction to the process bath without special evaporation or additional processing. Labor requirements are minimal and no cleaning or chemical additions are required for operation. Case studies of performance and economics of the system at three U.S. plating and printed circuit board facilities will be presented.

* For copies of this paper, please contact the author directly

Mr. Ronald R. Rich, CEF
President
Water Technologies, Inc.
7180 Shady Oak Road
Minneapolis, MN 55344
(612) 941-6031

F-4

# Environmental II
# Session F

## Source Reduction of Chlorinated Solvents: Aerospace Applications

Dr. Kathleen Wolf
Source Reduction Research Partnership
Los Angeles, CA

# Source Reduction of Chlorinated Solvents:

## Aerospace Applications

Dr. Kathleen Wolf, Source reduction Research Partnership
Los Angeles, CA

The Source Reduction Research Partnership (SRRP) is a joint venture of The Metropolitan Water District of Southern California and the Environmental Defense Fund. The partnership is sponsoring a study to estimate the potential for source reduction of chlorinated solvents in the southern California area served by Metropolitan. The project is analyzing source reduction measures in the major solvent using industries including metal cleaning, dry cleaning, electronics, paint stripping, aerosols, pharmaceuticals, pesticides, adhesives and coatings.

The aerospace community in southern California uses large quantities of chlorinated solvents for various purposes. This paper discusses available and emerging source reduction options in two of the most important solvent applications--electronics and paint stripping. The chlorinated solvents involved in these processes are methylene chloride in paint stripping and CFC-113, 1,1,1-trichloroethane and methylene chloride in electronics.

The source reduction options that will be discussed for paint stripping include substitution of alternative chemical strippers, substitution of mechanical stripping techniques, and reformulation of methylene chloride based strippers to encourage off-site recycling. The source reduction options in electronics include substitution of aqueous cleaning systems, substitution of terpenes, and use of flux-removal filters.

F-5

# Environmental II
# Session F

## Pickling Acid Recovery with Bipolar Membrane Technology

Michael Prescott
Lancy International, Inc.
181 Thorn Hill Road
Warrendale, PA 15086-7527

**Mr. Michael Prescott**
Lancy International, Incorporated
181 Thorn Hill Road
Warrendale, PA 15086-7527
Telephone: (412) 772-0044

# Title: Pickling Acid Recovery with Bipolar Membrane Technology

## ABSTRACT

Bipolar membrance technology offers an efficient and economical approach for the recycle of spent industrial acids. The recovery system nucleus is a patented membrane stack which provides virtually complete regeneration of spent acids.

This waste acid recovery system is particularly applicable in specialty steel manufacturing for recovering spent pickle liquor acids (such as hydrofluoric/nitric acid mixtures) for reuse; providing an environmentally sound alternative to waste treatment and/or disposal of spent acids, resulting in the reduction of long-term liability.

*This paper is an Edited Version of "Aquatech Systems: An Economic and Environmentally Sound Commercial Process to Recycle Spent Pickle Liquor", By Carolyn Hutter-Byszewski, Andrew Bogeatzes of Allied Signal Corporation and Harold Moore of Washington Steel Corporation

## INTRODUCTION

An electrodialytic membrane process has been developed which economically separates salt solutions into their constituent acids and bases. This technology when applied to waste pickling acid regeneration offers an economic, environmentally sould alternative to dumping. The steel industry is keenly aware of the soaring costs of disposal and the ever growing contraints being imposed on dumping.

Resource recovery and waste minimization technology is the practical solution. It transforms the once-thru pickling process into an essentially closed loop process with minimal chemical makeup requirements and potentially no disposal costs.

The technology has been successfully piloted at the Washington Steel facility in Washington, Pennsylvania, for over two years, resulting in the design and construction of the first commercial plant. This plant will regenerate over 1.5 million gallons of spent pickle acid per year into reuseable $HF/HNO_3$ acid as well as eliminate the threat of the ever increasing disposal cost - now estimated at $0.55/gal. ($0.86 million dollars annually).

We will provide a brief background on the Bipolar Membrane technology as it applies to waste acid recovery, as well as review pickling

chemistry to more clearly reveal the benefits of bipolar membranes over competitive diffusion dialysis or ion exchange adsorption technologies. We will touch on highlights of the pilot plant performance and finally, a complete review of the Commercial Plant design and process flow capabilities concluding with an economic analysis will be presented.

## TECHNOLOGY BACKGROUND

The bipolar membrane technology is an electrically driven membrane process, similar to electrodialysis in that it employs conventional ion exchange membranes to separate ionically charged species in solution, but distinguished by the unique water splitting capabilities of the bipolar membrane.

Under an electrical potential, conventional monopolar ion exchange membranes are capable of selectively transporting charged species across their boundary, thus effecting separation. Cation membranes have fixed negative charges which allow the transport of positively charged ions (cations) such as $K^+$ to pass across them, while rejecting negative ions (Figure 1). Conversely, anion membranes have fixed positive charges which allow the transport of negative ions (anions) such as $F^-$ or $NO_3$ to pass across them, while rejecting positively charged ions.

## Electrodialysis For Concentrating KF

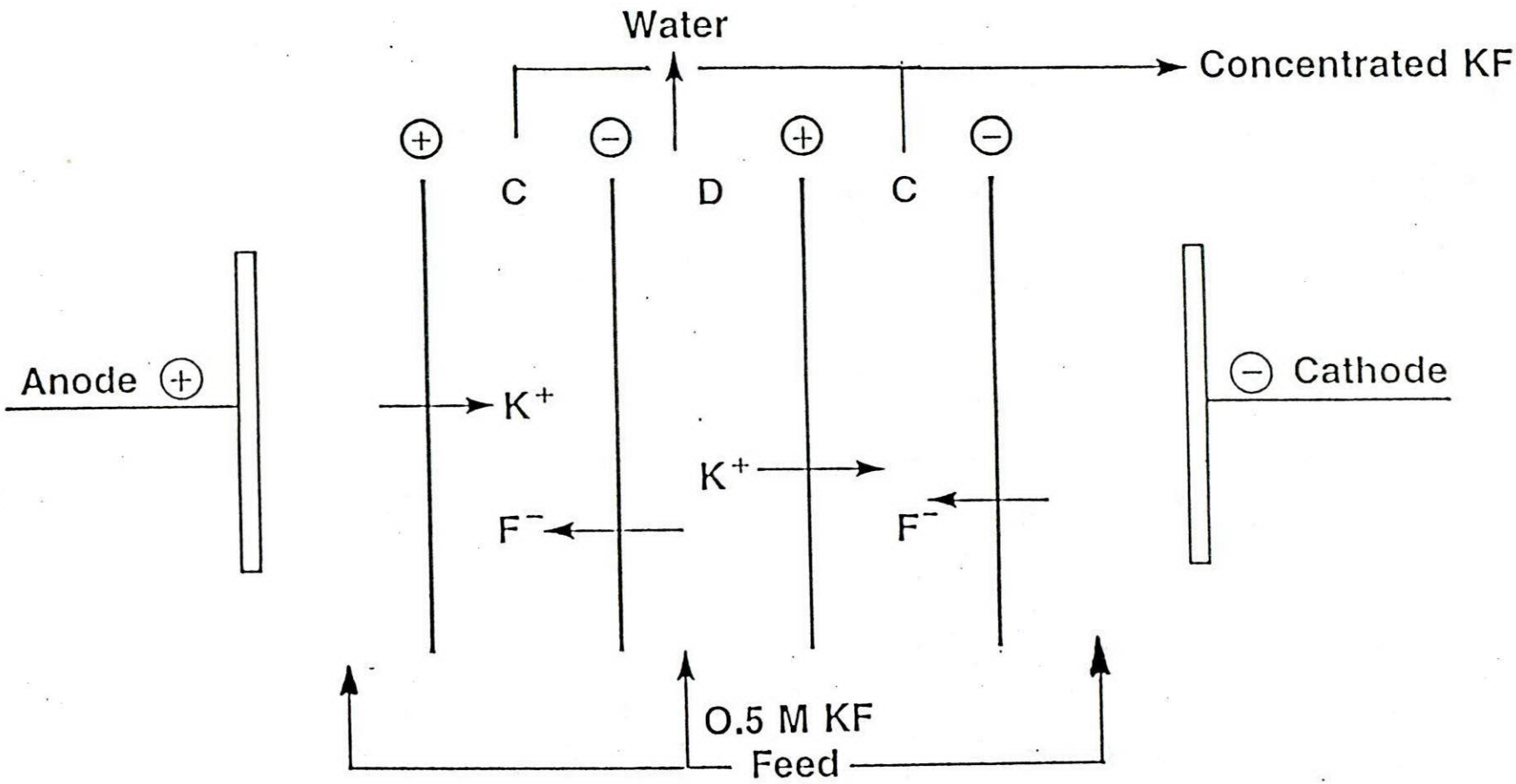


⊕ Allied Cation Membrane

⊖ AMV Anion Membrane

Figure 1

The bipolar membrane is a unique ion exchange membrane in that it is composed of two distinct layers of oppositely charged ion exchange material (Figure 2).

Unlike conventional monopolar membranes, this novel membrane is capable of dissociating water into hydrogen ($H^+$) and hydroxyl ($OH^-$) ions under the influence of an electrial potential. Combining the capabilities of both monopolar and bipolar ion exchange membranes gives the system unique advantages (Figure 3). Supplying salt solution to the stack along with DC current to the electrodes results in the conversion of an aqueous salt solution such as $KF/KNO_3$ into the base KOH and the mixed acid $HF/HNO_3$.

RECYCLING SPENT PICKLING ACID

Conventional disposal of spent acids generally includes neutralizing the waste acid with lime ($Ca(OH_2)$, precipitating and filtering out an insoluble $CaF_2$ salt complexed with $Fe(OH)_3$ cake for landfill and discharging a $Ca(NO_3)_2$ salt solution to the waterways. Here steel producers must pay high costs to dispose of valuable resources like $F^-$ and $NO_3^-$ as well as burden themselves with the liabilities of transporting and disposing of liquid hazardous wastes - a triple cost situation.

## Bipolar Membrane Construction and Operation

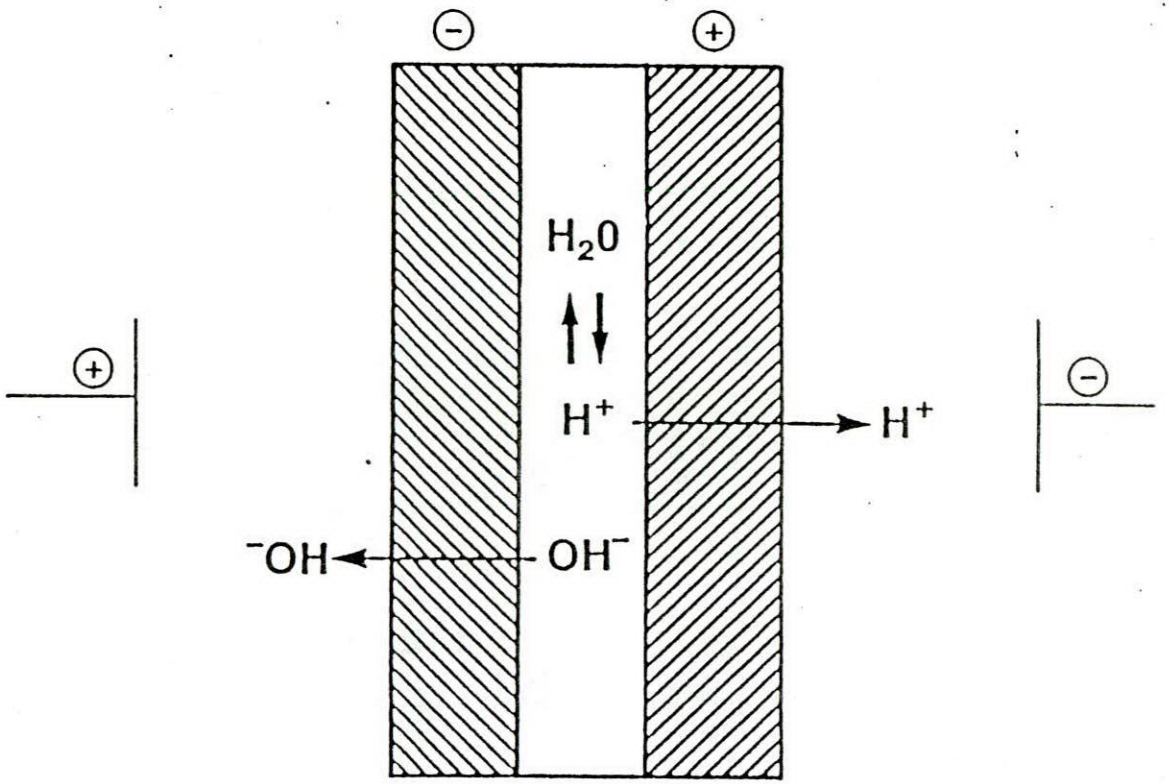


Figure 2

# Waste Pickling Acid Application
# Three Compartment Cell

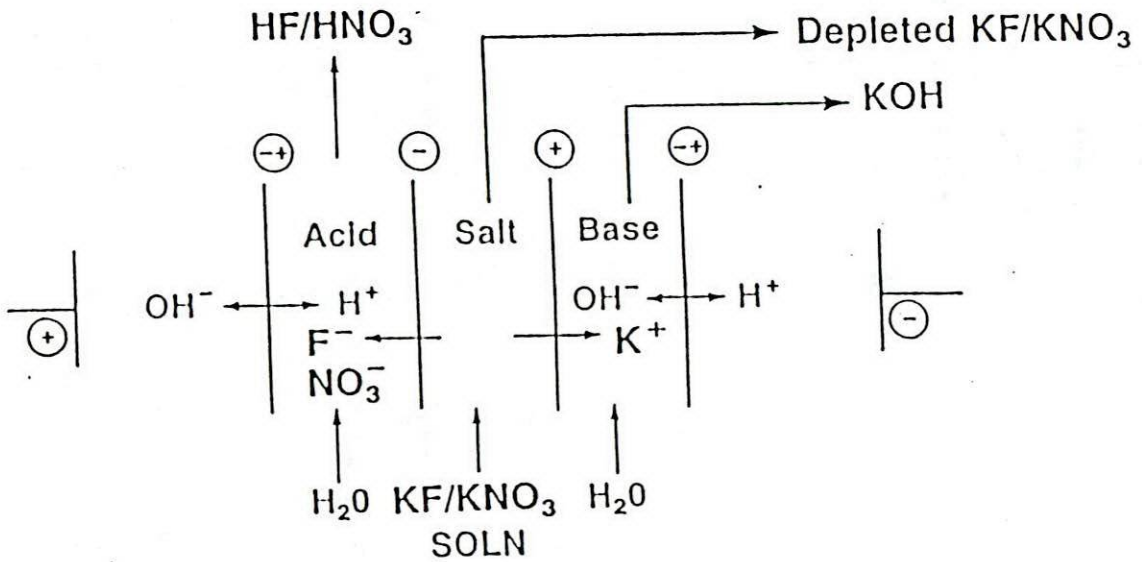


Legend

- ⊖⊕ Bipolar Membrane
- ⊕ Cation Membrane
- ⊖ Anion Membrane

Figure 3

Alternatively, incorporating the bipolar membrane process with a potassium hydroxide (KOH) neutralization results in a virtually closed loop resource recovery scheme as illustrated in Figure 4. The KOH neutralization to pH 10 differs from $Ca(OH)_2$ neutralization in that it results in a metal hydroxide precipitate free of fluoride complexes, while the fluoride and nitrate values are retained in solution as the soluble salts KF and $KNO_3$. Conventional plate and frame filtration yields a metal hydroxide cake of Fe, Ni, Cr hydroxides which with further drying and processing is suitable for recycle to the smelter. The filtrate is suitable for feed to the bipolar membrane. Here through the driving force of a direct current, the $KF/KNO_3$ salt is converted to 8-10 wt. % (1.5N) KOH and a mixed acid $HF/HNO_3$ of similar composition as the waste acid (typically 2.5 - 4N) (Figure 5). The KOH base in recycled to the neutralization step while the fresh product acid is sent to the pickling tubs.

## PILOT PLANT PERFORMANCE

In October 1984, Washington Steel Corporation piloted this technology for waste acid reclamation. The pilot plant has been in operation intermittently since March 1985, for over two years testing various facets of the process including: resource recovery efficiency, operating conditions, membrane life expectancy, system performance, filtrate and product quality and energy consumption.

# STAINLESS STEEL PICKLE LIQUOR REGENERATION

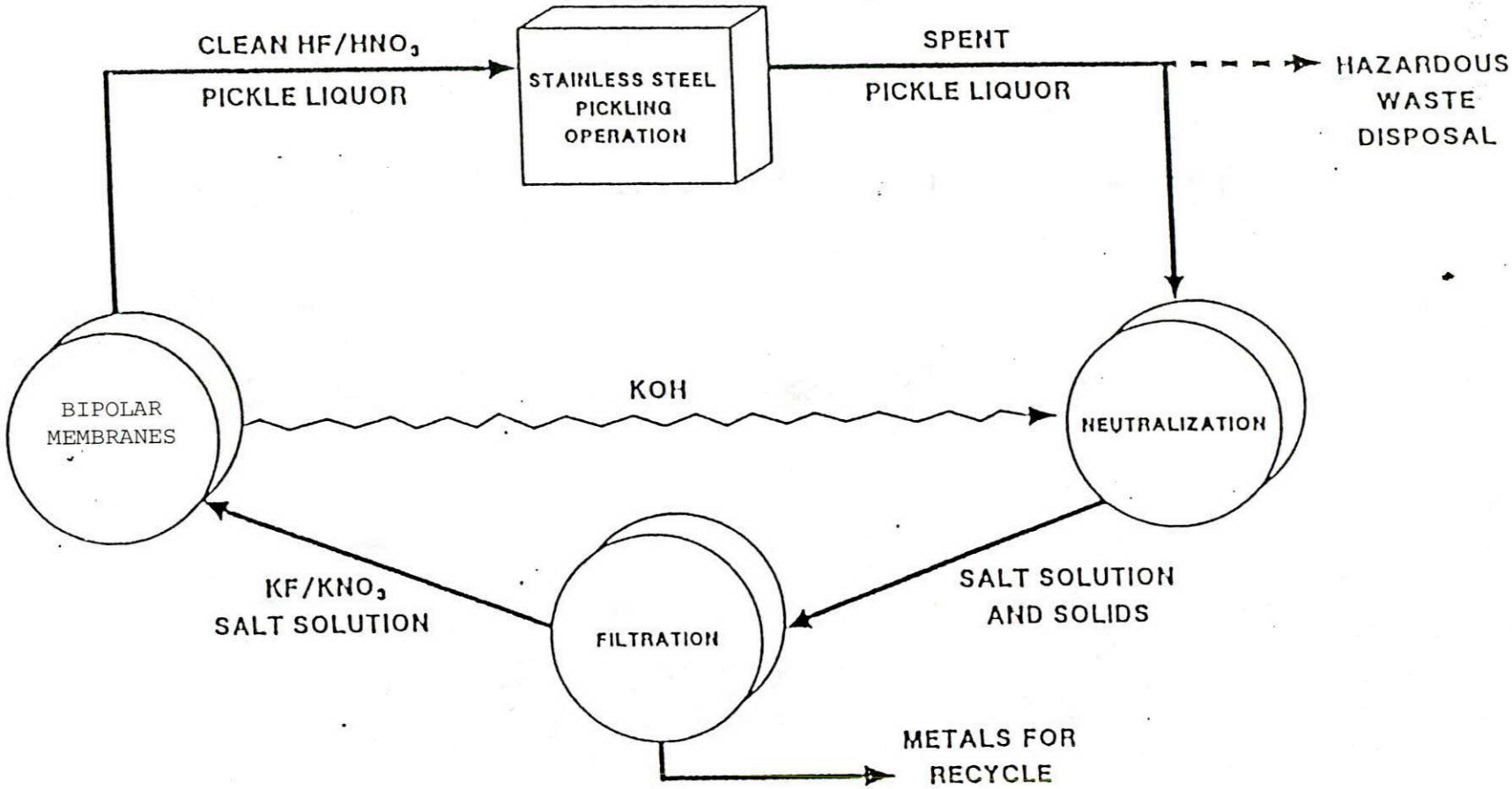


FIGURE 4

BIPOLAR MEMBRANE CHEMISTRY

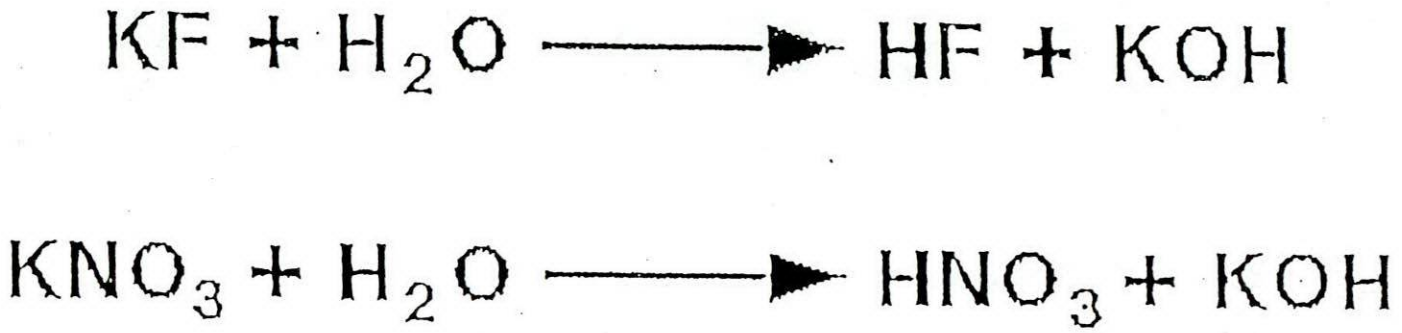


FIGURE 5

To verify the recovery rates of fluorides, nitrates and potassium by our process, a material balance was performed around the pilot plant. As shown in Figure 6, the streams entering the battery limits are waste acid, makeup water and KOH, while those exiting include product acid and filter cake. The results of the overall material balance show that the system consistently recovered:

93% of all fluoride values both complexed and free
99+% of all nitrate values
96+% of all potassium values

The material balance in Table 1 also illustrates the very substantial reduction in waste mass. One thousand gallons of pickle liquor is approximately 10,000 lbs. of hazardous liquid waste. With the bipolar membrane system, the cake byproduct reduced to a 2640 lbs. cake initially at 40 wt.% solids. Further drying to 90 wt.% solids results in a recyclable iron hydroxide cake of 660 lbs. This represents a 94% reduction in waste mass or a 15 fold volumetric reduction, as well as transformation of waste into a more easily managed form suitable for recycling.

Optimal operating conditions are listed in Table 2 along with normal operating ranges for each critical parameter. Varying process parameters such as current density, temperature, and voltage provide extensive system flexibility and 25% turndown capabilities, with little effect on current efficiency.

# Pickle Liquor Recovery Process

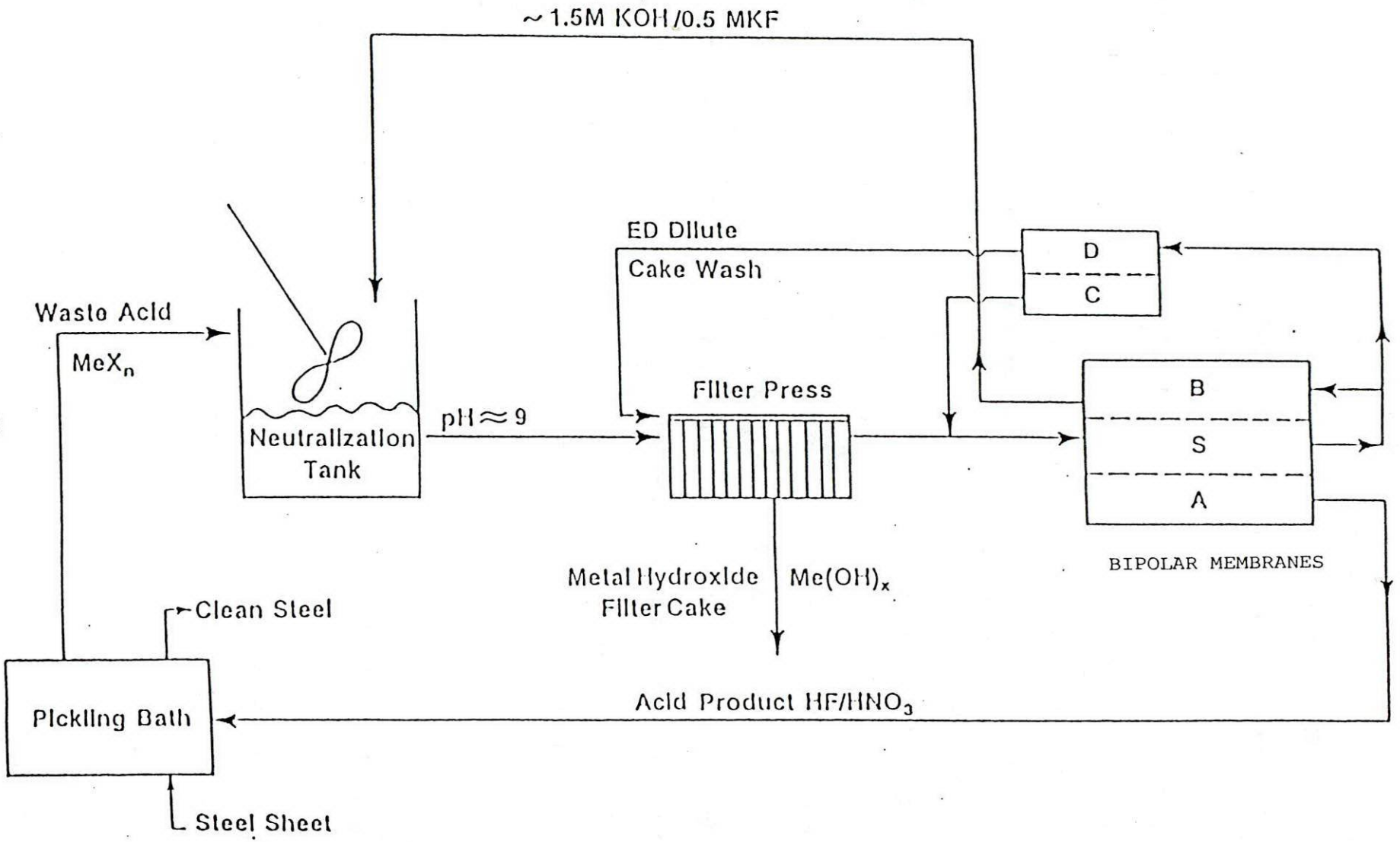


Figure 6

The pilot plant operated continuously for a 170 day period to allow a comparative study of membrane performance. Quality control performance tests were performed on the membrane samples at zero, 90 and 170 days. The results of the tests tabulated in Table 3 show an expected predictable rise in membrane voltage over time with no significant effect on membrane permselectivity or efficiency. Based on this 0.3 volt/6 month rise in membrane voltage, a one year life was projected.

Plate and frame filtration consistently produced a feed quality acceptable to the cell stack with Cr, Fe and Ni ions less than 3 wppm. Product acid composition and strength were maintained in ratios proportionate to the waste acid provided. Finally the power required to produce one ton $HF/HNO_3$ (4/8 wt.%) plus corresponding co-product 1.5 ton KOH was measured at 2000 KWH/Ton $HF/HNO_3$

## BIPOLAR MEMBRANE ADVANTAGES

To fully appreciate bipolar membrane's advantage over the alternatives, such as diffusion dialysis, acid retardation techniques and ion exchange adsorption methods, a review of pickling bath chemistry is required. The pickle bath is a complex chemical environment with solubility limits, concentration swings and phase changes. It is widely agreed that while both $F^-$ and $NO_3^-$ values aid in pickling, it is the $F^-$ ion that is the aggressive pickling agent

TABLE 1

## Washington Steel Corporation
## 100 Day Pilot Run – Overall Material Balance

| # | Stream | Gallons | Lbs. | Material Handled, Lbs. | | |
|---|---|---|---|---|---|---|
| | | | | $F^-$ | $NO_3^-$ | $K^+$ |
| 1 | Waste Acid | 1000 | | 520 | 800 | |
| 2 | Recycle Base | 2450 | | 190 | | 1750 |
| 3 | Acid Product | 1800 | | 486 | 800 | |
| 4 | Cake | | 2640 | 34 | 0 | 70 |

| | | |
|---|---|---|
| Overall Recovery | $F^-$ | 93% |
| | $NO_3^-$ | 99+% |
| | $K^+$ | 96% |

TABLE 2

Operating Parameters

| | Optimal | Range |
|---|---|---|
| Current, AMPS/FT$^2$ | 80 | 60-90 |
| Volts/Cell | | |
| Initial | 2.0 | 2.0-3.0 |
| Final | | <3.0 |
| Products | | |
| Acid, Normality | 3.0 | 2.5-3.5 |
| Base, Normality | 1.5 | 1.0-2.0 |
| Salt, Normality | 0.1 | 0.01-0.2 |
| Average Efficiency, % | 80 | 70-90 |
| Temperature, DEG F | 90 | 75-110 |

TABLE 3

# Washington Steel Corporation
# Pilot Test Review
# Membrane Analysis

| Type | Manu-facturer | Units | Nominal (When New) | 100 Days | 170 Days |
|---|---|---|---|---|---|
| Bipolars | Allied | Volts @110mA/cm$^2$ | 1.1 | 1.29 | 1.4 |
| Cation | Allied | ohm-cm$^2$ | 6.0 | 6.9 | 6.8 |
| Anion | RAI 4035 | ohm-cm$^2$ | 2.3 | 2.7 | 2.2 |

which removes oxide films and converts them to complexed metal fluorides. The nitric acid functions primarily as a facilitating moderating agent which retards pitting of metal under layers. The nitrate salts remain in solution as dissolved salts. The spent bath then has three key ingredients; the dissociated nitrates whether salts or acids, the dissociated free acidic fluorides and the complexed metal fluorides. Depending on the bath composition and the extent of depletion, the complexed metal fluorides can represent 50 up to 90+% of the fluoride values.

Diffusion Dialysis, ion exchange adsorption or acid retardation techniques recover only the free nitrates and fluorides and are unable to recover the majority of the fluorides which are tied up as complexed metal salts. With the bipolar membrane process, through its neutralizing reaction step breaks the complex fluoride salts to form soluble salts. Fluoride and nitrate anions and metal cation balance analysis of waste acid using ICP methods confirm this. Since fluoride is 6-7 times more valuable than the nitrates, this recovery process realizes proportionally higher savings.

Finally, Figure 7, research published by Dr. Albert Krepler show the increased metals solubility attainable at lower excess HF concentration. Figure 7 further illustrates how increases in acid concentration via acid spiking midway through the pickling process

FIGURE 7

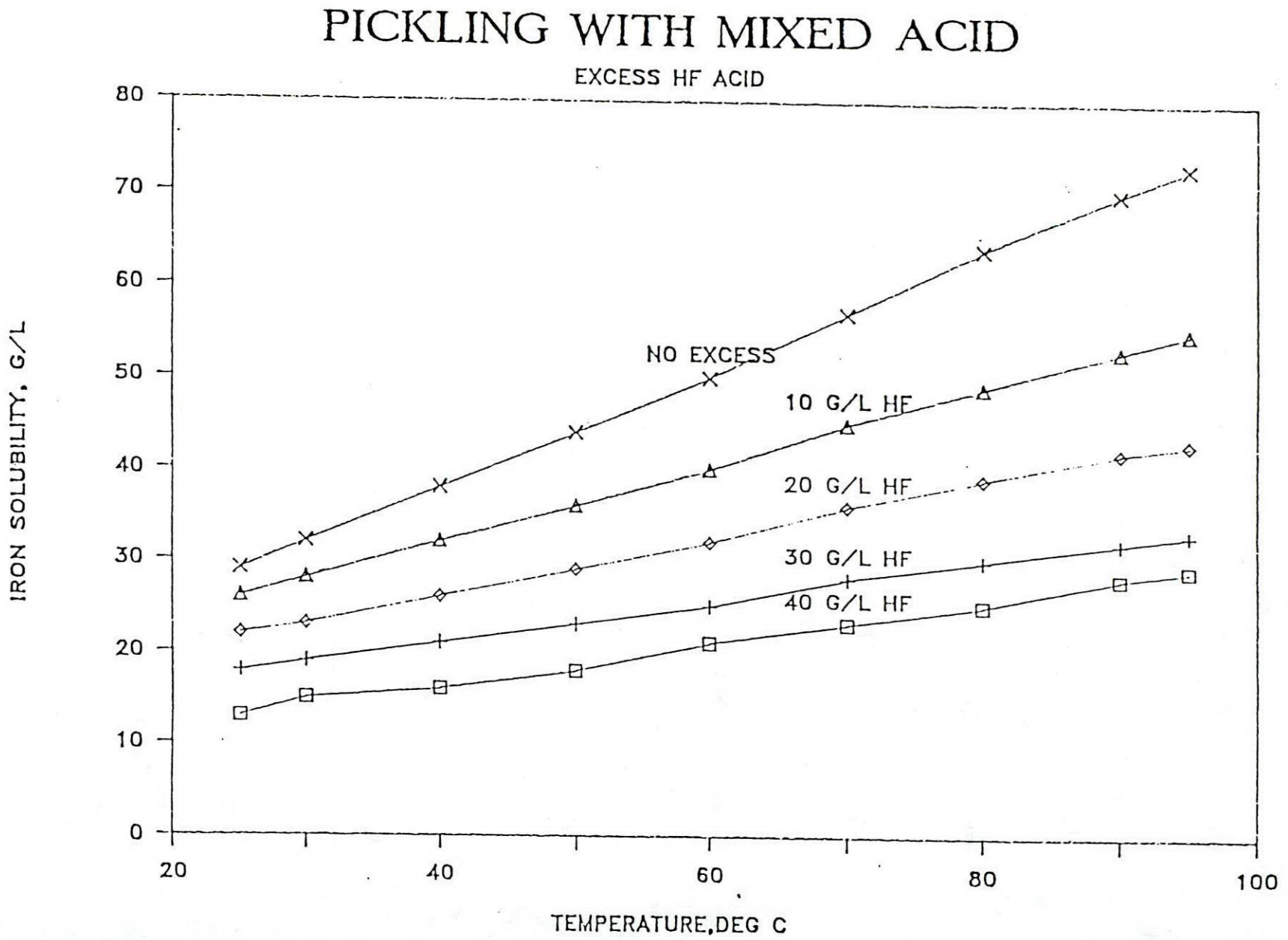
PICKLING WITH MIXED ACID
EXCESS HF ACID
IRON SOLUBILITY, G/L
TEMPERATURE,DEG C
NO EXCESS
10 G/L HF
20 G/L HF
30 G/L HF
40 G/L HF
0
10
20
30
40
50
60
70
80
20
40
60
80
100

results in sludge formation. Sudden increase in excess acid concentration lowers solubility limits resulting in ion fluoride complexes precipitating. The ability of the bipolar membrane system to deliver a dilute mixed acid product to the pickling tubs should substantially reduce sludge formation.

Minor bath concentration adjustments can be accomplished with additions of HF and $HNO_3$ still required due to drag out and vapor losses.

COMMERCIAL PLANT PROCESS FLOW

Figure 8 is a block diagram showing the commercial process for the recovery of spent pickle acid. Step 1 consists of treating the used acid (metal salts plus small amount of free nitric/hydrofluoric acid) with potassium hydroxide to form the potassium nitrate/fluoride salts. At this point the metals (iron, chrome, nickel, etc.) present in the spent pickle acid are precipitated out as metal hydroxide solids. The solids (stream 3) are removed from the salt solution using a filter press (step 2) before treatment of the salt solution in the bipolar membrane cell stack system.

In the bipolar membrane system (step 4) the potassium nitrate/fluoride salts are converted back to their respective acid and base components - $HF/HNO_3$ (5) and KOH (6).

FIGURE 8

BIPOLAR MEMBRANE PROCESS
FOR THE RECOVERY OF SPENT PICKLE ACID

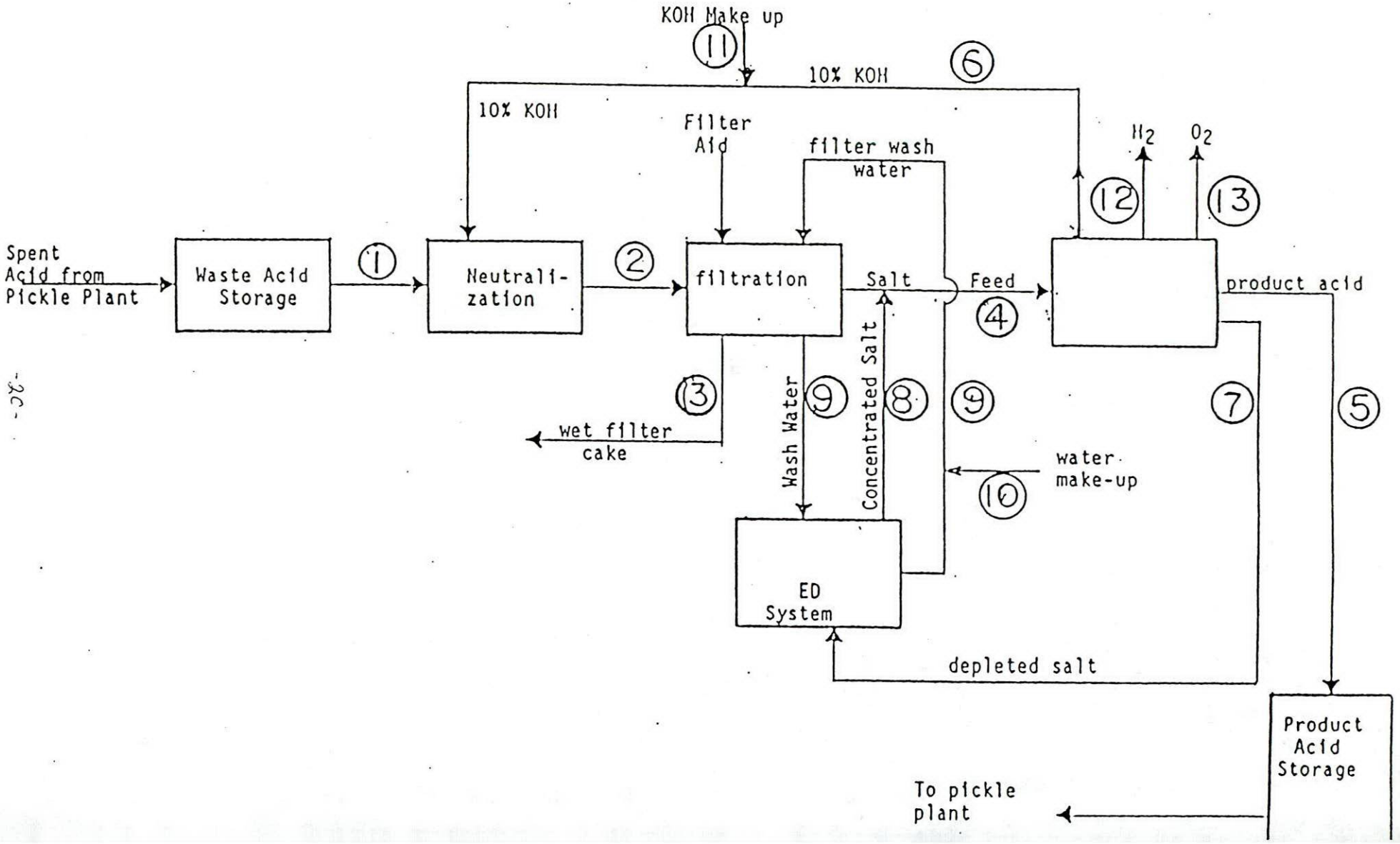

The bipolar membrane process is essentially a closed loop system. The depleted salt solution from the bipolar membrane (stream 7) is treated in an electrodialysis (ED) system containing monopolar membranes to upgrade its concentration. The concentrated salt is returned to the bipolar membrane cell stacks for further acid and base recovery. The water recovered in the ED system is used to wash the filter press cake (stream 9). The metal hydroxide cake, with further drying to 90 wt.% solids and briquetting, is suitable for recycle.

Small amounts of water (stream 10) and KOH (stream 11) are added as make-up for the KOH and water lost in the wet filter cake.

Small amounts of hydrogen (12) and oxygen (13) gases form at the cathodes and anodes as a result of the electrolytic reactions taking place. An electrode rinse solution is pumped through the electrodes to sweep up the gases which are vented off.

## EQUIPMENT DESIGN BASIS

The basis used for the plant design is shown as Table 4. Over 1.6 million gallons of waste acid will be recycled, recovering 90 - 95% of the fluoride values while consuming less than 428 kw of energy.

The major equipment for the process is listed on Table 5. The three large storage tanks and neutralization tank are located outside.

TABLE 4

- PLANT CAPACITY - 1.65 MILLION GALLONS OF SPENT PICKLE ACID PER YEAR
- POWER REQUIREMENT - MAXIMUM OF 428KW FOR MEMBRANE CELL STACKS
- ACID RECOVERY - 90 - 95%
- FILTER CAKE - 70 CU. FT. PER SHIFT
- WATER MAKEUP - 1 GAL./MIN
- BASE MAKEUP - 200 LBS./DAY (45% KOH)

TABLE 5

Commercial Plant

Major Equipment

| | |
|---|---|
| • THREE STORAGE TANKS | - 10,000 TO 15,000 GAL. |
| • TWO STORAGE TANKS | - 3,000 GAL. EACH |
| • NINE PROCESS TANKS | - 200 TO 600 GALLONS |
| • NEUTRALIZATION TANK/AGITATOR | - 8,000 GALLONS |
| • HEAT EXCHANGER | - 500 $FT^2$ |
| • CHILLER | - 1,000,000 BTU/HR. |
| • FILTER PRESS | - 82 CU. FT. |
| • TWO MEMBRANE STACK PRESS FRAMES | - 3' X 13' EACH |
| • ONE MEMBRANE STACK PRESS FRAME | - 3' X 10' |
| • TWO POWER SUPPLIES | - 227 KW EACH |
| • POWER SUPPLY | - 26 KW |
| • SIXTEEN PUMPS | - 1 GPM TO 120 GPM |

The smaller storage tanks and the other remaining equipment are housed in a 70 ft. x 32 ft. building. The total plant area is approximately 3500 $ft^2$.

With the exception of the filtration step, the process is highly automated. The neutralization step is a batch process and includes a batch-volume of spent acid feed and a pH controller for the addition of the base.

The bipolar membrane and ED systems and associated equipment are semi-continuous and are computer process controlled. An automatic titrator is used to control the concentration of the product acid. A conductivity controller is used in the ED system, which upgrades the concentration of the depleted salt from the bipolar membrane cell stack system.

It is expected that the present operators from the exisitng adjacent water treatment plant plus one additional operator will be used to operate the plant which will normally be operated six days per week.

BENEFITS SUMMARY

Bipolar Membranes offers many advantages in waste acid regeneration. Table 6 itemizes plant economics specified for the Washington Steel Project. Key benefits include 93% fluoride recovery including both

TABLE 6

## Pickle Liquor Recovery
## Capital and Operating Costs

Basis:

$1.6 \times 10^6$ Gals/ Yr. of Spent Pickle Liquor Containing
5 wt% F , 10 wt% $NO_3$
8000 Hrs./Yr.
One Year Life for Cell Assembly
Acids Recovered (Net): 350 T/Yr. of HF
740 T/Yr. of $HNO_3$

Total Battery Limits Capital for Plant $2.2 \times 10^6$
Aug. '87 Costs
All Costs in US Dollars

### Operating Cost Summary

| | |
|---|---|
| **Raw Materials** | |
| Makeup KOH @ $540/Ton | 36,000 |
| Filter Aid @ $300/Ton | 14,000 |
| Cell Maintenance | 300,000 |
| Electricity @ 5 /KWH | 128,000 |
| Cake Processing @ $110/Ton | 229,000 |
| Other Maintenance | 78,000 |
| Labor & Supervision | 40,000 |
| Depreciation @ 10% | 220,000 |
| Taxes & Insurance @ 2% | 44,000 |
| Total Operating Costs | 1,089,000 |
| **Product Credits** | |
| HF @ $1,365/Ton | 480,000 |
| $HNO_3$ @ 205/Ton | 152,000 |
| Waste Material @ $0.55/Gal. | 880,000 |
| Total Credits | 1,512,000 |
| Savings | 432,000 |
| ROI | 19% |
| Payback | 3.2 Yrs. |

free and complexed fluorides, 99+% recovery of nitrates, a 94% reduction in waste mass which is transformed into a solid hydroxide cake suitable for recycle and the elimination of liquid waste handling. On a basis of 1000 gallons of pickle liquor, the process can potentially save about $650 per 1000 gal/P.L. above operating costs by taking credit for only disposal cost savings and recovered resource values.

Some of the more subtle benefits such as increased plant safety by minimizing concentrated acid handling and eliminating liquid waste disposal must also be considered.

F-6

# Environmental II
# Session F

## Some 'Unsolved' Problems in Closed Loop Nickel Recovery

Lyle Kirman
Kinetico Inc.
10845 Kinsman Road
Newbury, OH 44065

# "SOME 'UNSOLVED' PROBLEMS IN CLOSED LOOP NICKEL RECOVERY"

Lyle Kirman
Kinetico Incorporated
10845 Kinsman Road
Newbury, Ohio 44065

In some ways it seems strange to talk about problems in closed-loop nickel recovery, when there are so many recovery systems operating today and there are so many platers who add virtually no nickel chemicals to their baths.

Has the loop truly been closed by the recovery technologies available today or are substantial quantities of nickel still ending up as hazardous waste? As the EPA moves to restrict or possibly even to ban land disposal of this type of waste, what problems do nickel platers face and what alternatives do they have? This paper attempts to address these issues, to discuss possible ways to further close the loop, and the potential problems raised by them. Various papers (1,2,3) show that most systems which are designed as closed-loop recovery systems actually recover only 80-95% of the nickel dragged out of the bath. Even when no nickel salts need to be added to the bath, this often represents substantially less than 90-95% recovery of dragout, due to the 3 - 5% difference between anode and cathode efficiencies.

Most studies on this subject also fail to take into account significant nickel losses from bath treatments, routine filter cleanings and the cleaning of the recovery equipment itself. If frequent carbon treatments or high pH treatments are required, losses from these can be almost as large a source of waste as the dragout itself, and it is doubtful that the operation can be accurately described by the term "closed-loop".

If most nickel recovery systems recover less than 95% of the influent to a waste treatment system, how then can a nickel plater further close the loop without risking reduced quality, re-work or scrap? The essential problems are revealed by completing a materials balance for all bath constituents, including water and impurities. Selecting a recovery technology or technologies which best completes this balance, while avoiding problems due to bath contamination, is no simple task.

Since most efforts for nickel recovery have involved only one technology and were designed primarily to reduce purchases of nickel salts, little or no thought was given to the impurity problems they might create. Therefore, some discussion of impurity problems is appropriate.

Table 1 lists technologies which have been used for open and closed-loop nickel recovery and some of the characteristics of each. This table highlights the impurity and materials balance problems which are the most formidable barriers to a truly closed-loop recovery system. Table 2 highlights just the impurity problems which occur in nickel plating baths and lists possible solutions. Each of these is amplified below.

Calcium is known to cause problems when it reaches a concentration of about 500 mg/l. Even a simple dragout rinse can cause calcium to rise to this level when hard water is used for evaporative make-up. Fortunately, calcium problems can be virtually eliminated simply by using purified water for all make-up to the bath. While using softened water for this purpose would avoid calcium problems, at high levels of recovery the eventual increase in bath salinity would also be deleterious. Therefore, only highly purified water is suitable for make-up to a nickel bath with a recovery system.

Sodium was virtually never a problem in nickel plating baths until the advent nickel recovery systems. Plating problems begin to occur when sodium exceeds 20,000 mg/l and become progressively worse above this point. Our experience has been that until recovery exceeds about 75%, the sodium concentration in a bright nickel bath usually stays below 20-30,000 mg/l and is manageable. There are platers today, however, who are struggling with 40,000 mg/l. Even this high level of contamination usually represents only 85-90% recovery of the salts dragged out of the bath, or lost due to bath treatments.

At this time, only two recovery approaches can control sodium build-up problems at high levels of recovery. Precipitation and re-dissolution, an old technique which may see a revival, can effectively remove excess sodium from nickel values. Another technique, developed by my colleagues and I, is a modification to conventional ion exchange recovery. Figure 1 illustrates how this system works to remove sodium. The modification is simply to exploit the much greater affinity of ion exchange resins for nickel over sodium. By placing two cation resin beds in series, sodium can be "bled" out of the first bed while nickel is still concentrating there. The second cation vessel catches the sodium and thereby allows the water to be completely deionized by passing it through an anion resin. Fig. 2 is a picture of a system of this type which in operation has recovered over 95% of the nickel in rinse water while simultaneously removing over 80% of the influent sodium.

TABLE 1

COMPARISON OF NICKEL RECOVERY TECHNOLOGIES

| TECHNOLOGY | CAPABLE OF CLOSING LOOP? | INITAL COST | OPERATING COST | POTENTIAL IMPURITY PROBLEMS | | | | | | | POTENTIAL MATERIALS BALANCE PROBLEMS | |
|---|---|---|---|---|---|---|---|---|---|---|---|---|
| | | | | PLATING BATH | | | | | RINSE WATER | | | |
| | | | | SODIUM | CALCIUM | HEAVY METALS | ORGANIC | EXCESS ACID | NICKEL | CHLORIDES | BORATES | ORGANIC | ANODE VS. CATHODE % EFF. | NICKEL VS. EVAPORATION | VOLUME OF RECOVERED |
| 1. Precipitation | Y | Moderate To High | Low | N | N | Y | N | Y | | | | | Y | ? | |
| 2. Evaporation | | | | | | | | | | | | | | | |
| A. Dragout Rinse | N | V. Low | V. Low | N | Y | Y | N | N | | | | | Y | N | |
| B. Atmospheric Evaporator | Y | Moderate To High | High | Y | Y | Y | Y | N | Y | Y | Y | Y (If rinse flow is limited) | Y | N | |
| C. Vacuum Evaporator | Y | High | High | Y | Y | Y | Y | N | Same as above. | | | | Y | N | |
| 3. R.O. | Y | Moderate To High | Low to Moderate | Y | Y | Y | Y | N | N | N | Y | Y | Y | Y | |
| 4. Ion Exchange | Y | Moderate To High | Low to Moderate | ? | ? | Y | N | Y | N | N | N | N | Y | Y | |
| 5. ED/EDR | Y | High | Low to Moderate | Y | Y | Y | Y | N | Y | Y | Y | ? | Y | Y | |

Y = Yes
N = No

TABLE 2

NICKEL BATH IMPURITY PROBLEMS MADE WORSE BY RECOVERY

| IMPURITY | PRIMARY SOURCE(S) | EFFECT(S) | POSSIBLE SOLUTION(S)* |
|---|---|---|---|
| 1. Calcium | Water Used | - Rough Plate<br>- Extra Filter Cleanings | - Use only purified water for make-up and additions. |
| 2. Sodium | Addition Agents & Brighteners | - Dull Plate<br>- Loss of Efficiency | - Modified ion exchange recovery.<br>- Precipitation and recovery. |
| 3. Heavy Metals | Parts Being Plated | - Dull Plate<br>- Roughness<br>- Loss of Ductility | - Improved rinsing before nickel and improved housekeeping.<br>- Continuous dummying.<br>- Selective ion exchange. |
| 4. Excess Acid | Ion Exchange or Precipitation Recovery | - Lower Cathode Efficiency<br>- Dull Plate | - Ion exchange to remove excess acid. |
| 5. Organic | Brightener Breakdown | - Dull Plate<br>- Excess Brightener Additions<br>- Decrease Corrosion Resistance (Duplex Nickel) | - Possible use of regenerable. Polymeric adsorbents.<br>- Ion exchange recovery.<br>- Precipitation recovery. |



* Batch bath treatments are not included on this list and due to the large quantities of sludge they produce, are considered to be a last resort.

FIGURE 1.

## ION EXCHANGE NICKEL RECOVERY SYSTEM WHICH ELIMINATES SODIUM AND ORGANIC BUILD-UPS

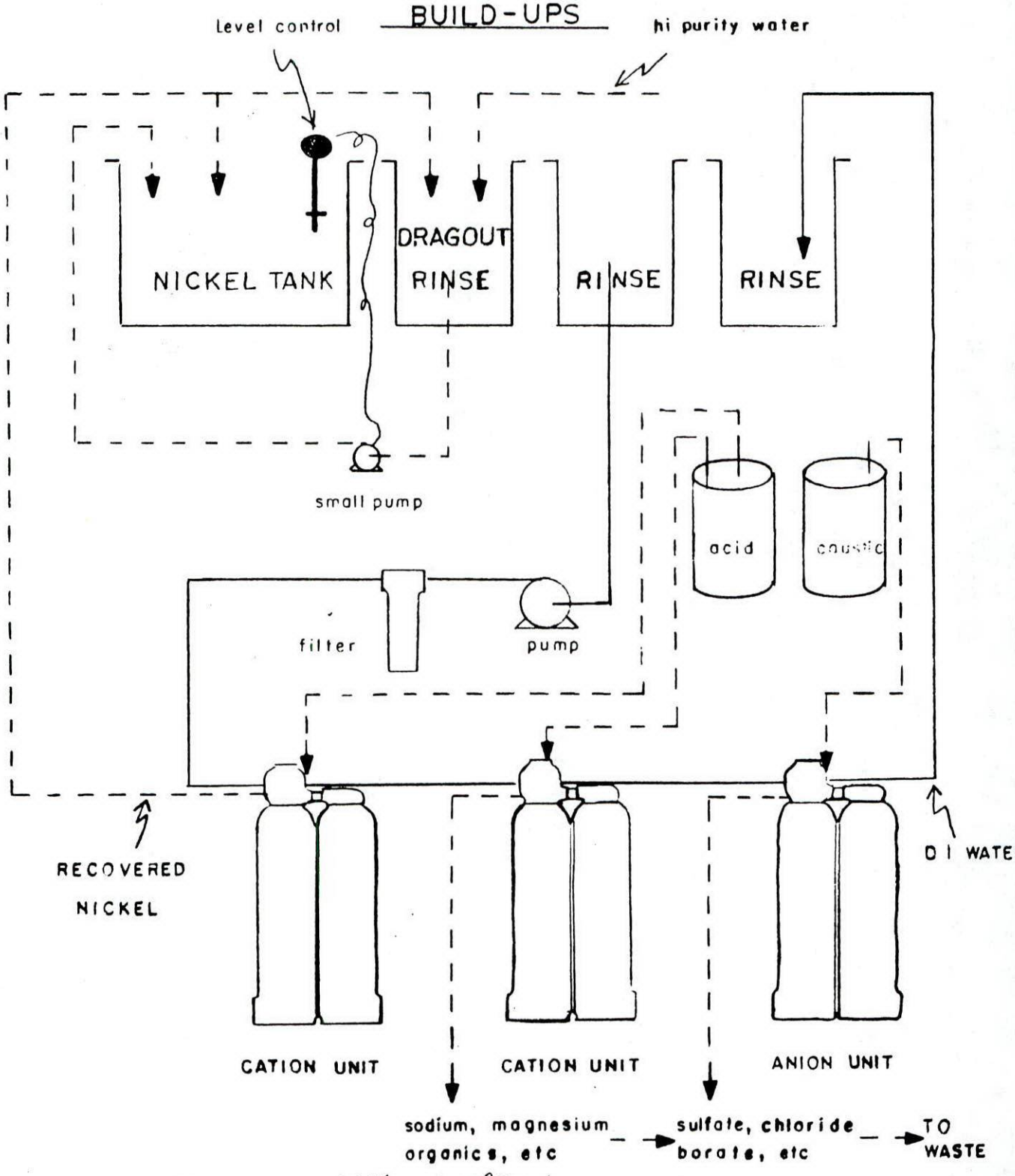

Heavy metal contaminants are returned with recovered nickel by all of the recovery technologies listed. Therefore, better housekeeping and good rinsing before the nickel bath are essential to any successful system. If these are not sufficient, then continuous dummying is the most desirable remedial action since it produces no sludge. Because of the large volume of hazardous waste produced, batch treatments should be done only as a last resort; selective ion exchange and solvent extraction may provide alternatives to batch treatment to remove heavy metals in the future.

Excess acid is a problem which only occurs in precipitation/re-dissolution or ion exchange recovery systems. In most cases it is removed by a subsequent ion exchange step which removes most of the excess acid, leaving the nickel solution at or near the desired pH range.

Organic impurities represent one of the greatest barriers to high levels of nickel recovery. This is especially true for duplex nickel plating systems where even minute amounts of a Class I brightener render the recovered nickel unsuitable for use in a semi-bright bath. Even in simplex bright nickel baths, however, breakdown products accumulate very rapidly with recovery and are not well removed by either continuous activated carbon filtration or even the slude-generating, batch oxidation and carbon treatments.[4] The quick and dirty solution to this problem is to add ever-increasing amounts of brightener, but eventually this only further aggravates the problem.

Our lab has had some encouraging results using regenerable adsorbents rather than carbon to strip organic contaminants from nickel plating baths. It is too soon to tell, however, if this approach will be practical or economical.

There are only two approaches to recovery which do not contribute to the organic contamination problem. Precipitation and redissolution has been demonstrated [5] to be an effective technique in this regard, and published reports [6,7] as well as work done with systems of our own show that ion exchange can separate nickel from the troublesome organics present in nickel plating baths. Even duplex nickel plating systems can use and have successfully used ion exchange to convert bright nickel dragout into nickel solution suitable for semi-bright baths. Membrane recovery techniques are capable of slowing the buildup of organic breakdown products, but only if all or part of the "clean water " is discarded. Unfortunately, this approach

results in nickel sludge and can also cause calcium problems if pure water is not used for make-up.

In addition to problems in the nickel plating bath which are caused and/or aggravated by nickel recovery systems, there are also potential rinse purity problems. Each type of recovery system has the potential for insufficient or contaminated rinsing as compared to no recovery at all, but some problems are associated with a particular technology. Some of these are summarized in Table 3.

Evaporation, due to its high operating cost, seeks to minimize rinse flows to the greatest extent possible. As a result, problems with subsequent chrome plating due to insufficient rinsing are likely unless good design is built into the system and regular maintenance is practiced. Atmospheric evaporators are particularly vulnerable to rinse-related problems, since their performance varies somewhat with seasonal variations in humidity. It is doubtful that a closed-loop evaporative recovery system can recover nickel economically and also provide adequate rinsing with fewer than 4 rinse tanks. Membrane systems like R.O. and E.D. have very poor rejection for borates and some organics.[8, 9, 10] These systems require one or more rinses not in the recirculation loop, as shown in Fig 3, or partial opening of the loop. Unfortunately, partially opening the loop invariably creates some added volume of nickel wastes.

Many membrane-based systems do not recycle part or all of the water; this can avoid rinse purity problems, but risks adding unwanted ions to the bath from the water used for make-up.

Likewise, precipitation does not usually create rinse purity problems, since the water is either not recycled, or the recovery rinse(s) is followed by one or more rinses flowing to a waste treatment system. Ion exchange systems rarely causes rinse problems because they usually recirculate water at much higher rates than are necessary for adequate rinsing, because they work best on relatively dilute solutions.

One way to solve rinse purity problems is by combining two technologies into a hybrid system. An example of this would be to use evaporation for recovery from 1 or 2 rinses and then ion exchange for the remaining rinses. While technically feasible, this approach is probably only economical for large

TABLE 3

## RINSE IMPURITY PROBLEMS MADE WORSE BY NICKEL RECOVERY

| IMPURITY | PRIMARY CAUSE(S) | EFFECT(S) ON CHROME | POSSIBLE SOLUTION(S) | DRAW BACK(S) |
|---|---|---|---|---|
| 1. Organics | - Insufficient Rinsing<br>- Poor Rejection | - Poor Coverage | - Add additional rinse tank(s). | - Physical space.<br>- Lost productivity. |
| 2. Chlorides | - Insufficient Rinsing | - Disrupts catalyst balance. | - Add make-up water to un-recirculated tank(s) (RO or ED). | - Same as above. |
| 3. Borates | - Insufficient Rinsing or poor rejection. (RO, ED) | - Hazy Appearance<br>- Disrupts catalyst balance. | - Increase rinse flow. | - Equipment limitation. (RO,ED,E,IX)<br>- High cost. (E) |
| 4. Nickel | - Insufficient Rinsing | - Loss of efficiency. | - Open the loop, 1 or more rinses to waste treatment. (Last resort.) | - Some nickel sludge produced. |
| | | | - Hybrid systems, e.g. E/IX, or E/ED. | - Cost of added equipment.<br>- Complexity |

RO = Reverse Osmosis, ED = Electrodialysis, E = Evaporation, IX = Ion Exchange

FIG 3 SOLUTIONS TO RINSE IMPURITY PROBLEMS WITH NICKEL RECOVERY SYSTEMS

A. RINSES NOT IN THE RECIRCULATION LOOP

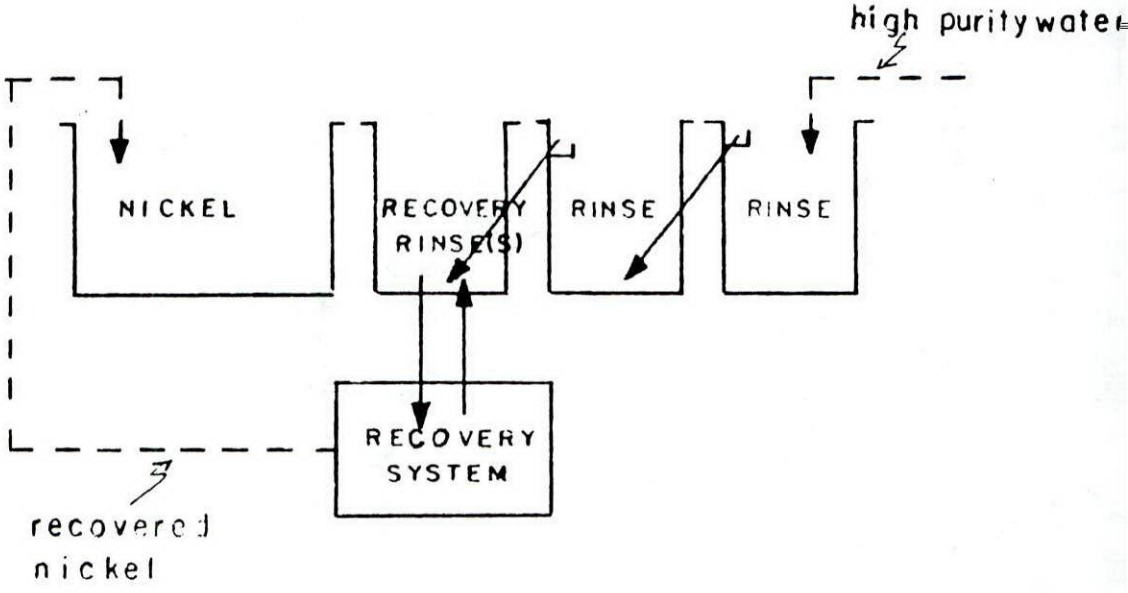


B. OPEN LOOP RECOVERY

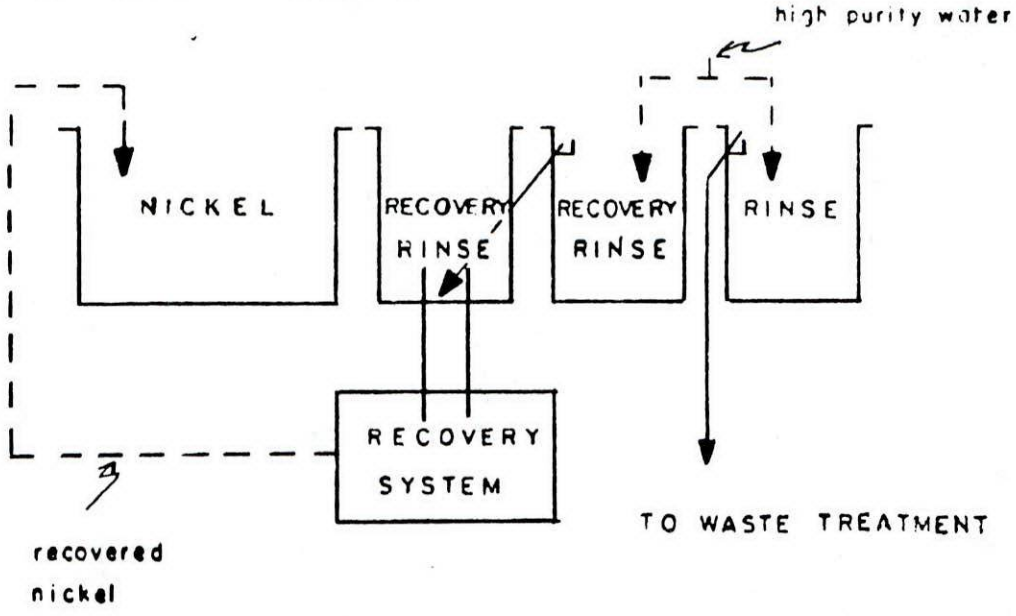

plating installations due to the additional equipment costs.

Another frequently encountered situation which causes rinse purity problems is an undersized recovery system. Since all recovery systems are designed with a specific capacity, they are not always able to accommodate increases in productivity or changes in product mix which increase the dragout volume. Unless an oversized system is purchased initially, any expansion may force the unpleasant prospect of adding additional tanks to the line, opening the loop, or buying additional equipment.

Materials balance problems in nickel recovery range from the trivial to the very difficult. Excess acid, heavy metal and organic build-ups, etc. which could also be considered as materials balance problems were treated as impurities instead because they directly interfere with the plating process. Likewise, insufficient rinse flow was considered separately.

Table 4 depicts one non-serious and one very serious materials balance problems to closing the loop on nickel: The volume of recovered nickel solution vs. bath evaporation and the excess of nickel which results from differences in anode and cathode efficiencies.

Ion exchange, reverse osmosis and some other technologies do not produce product solutions with high nickel concentrations. Operations with a high ratio of dragout to evaporation (typically 1:6) usually require supplemental evaporation in order to close the loop.

The most formidable barrier to true, closed-loop nickel recovery, however, is the difference between anodic and cathodic efficiencies in the nickel tank. Simply stated, nickel dissolves 3 - 5% faster than it is plated out in most bright nickel plating operations, resulting in an excess of dissolved nickel. Normally, dragout more than compensates for this, however, a high level of recovery will inevitably cause nickel concentrations to rise to undesirable concentrations in the bath.

What this means to the nickel materials balance is illustrated in Fig 4. A plater who plates 20,000 $FT^2$/day with a thickness of 0.25 mils, will generate the equivalent of over 40 pounds of nickel sulfate per day additions in the

TABLE 4

MATERIALS BALANCE BARRIERS TO CLOSED-LOOP NICKEL RECOVERY

| | BARRIER | POTENTIAL SOLUTION(S) | DRAWBACK(S) |
|---|---|---|---|
| 1. | Volume of Recovered Nickel Bath Evaporation | 1. Add supplemental evaporation. | 1. Cost. |
| 2. | Anodic vs. Cathodic Efficiency | 2. A. Plate at lower CD (partial solution). | 2. A. Impractical, lower productivity. |
| | | B. Combination of soluble and insoluble anodes. | B. Oxidizes organics rapidly causes plating problems. |
| | | C. Same as B., but with cation membrane isolating insoluble anode. | C. Not demonstrated. |
| | | D. Electrowin nickel for re-use as anode. | D. Cost of additional equipment.<br>-Requires no chlorides in solution; only precip. or IX are suitable.<br>-Possible economies of scale. |
| | | E. Re-use spent nickel to make other commercial chemicals. | E. Must have sufficient market. |

Fig. 3

POUNDS OF EXCESS NICKEL SULFATE
GENERATED PER 1000 $FT^2$ OF PLATED AREA*

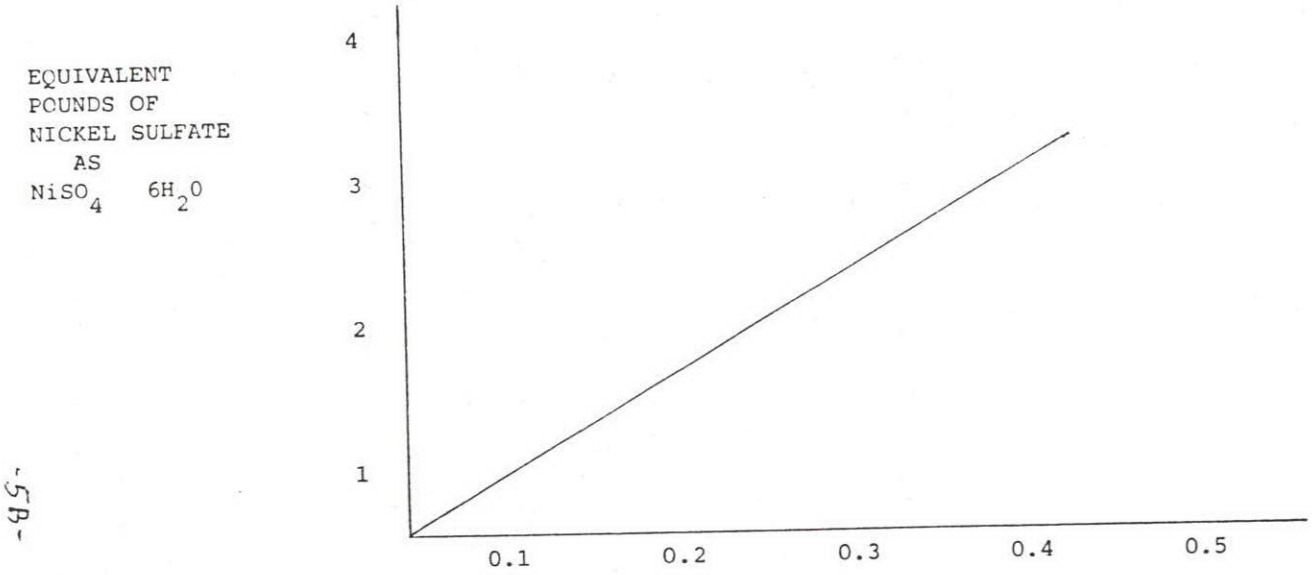


*Based on 40 ASF cathodic current density and 4% difference between anodic and cathodic efficiency.

nickel tank! Obviously, simply tabulating chemical additions will give only part of the materials balance for nickel. Similarly, the elimination of nickel chemical purchases is not actually an indication of a truly closed-loop system, since large quantities of nickel may still end up as hazardous waste.

Table 4 shows some potential solutions to the nickel balance problem, but no one solution is pre-eminent at this time. Lancy [11] proposed a combination of precipitation and electrowinning nickel for re-use as anode as a solution to organic contamination problems. This approach would solve the nickel balance problem as well.

Until now, most recovery systems have been designed with the idea of reducing or eliminating nickel chemical purchases, and not specifically to eliminate the generation of nickel hydroxide sludges. Now that the emphasis is changing, many platers are tightening up their operations to reduce the amount of nickel and other metals going to waste treatment. In many cases, they find that these efforts cause the concentration of bath constituents and impurities to rise to such high levels that plating quality is affected and/or the bath may actually crystallize at room temperature. At present, the only solution to this problem is to periodically dump a portion of the bath.

While most platers would like someone to buy this type of solution and recycle it, thereby relieving themselves of disposal costs and liabilities, there are very few people willing to accept this material now. Whether or not viable markets will develop for spent nickel solutions or sludges of this type is not yet certain.

On the other hand, electrowinning nickel for re-use as anodes can allow a plater to be in complete control of the nickel balance, without being dependent upon others. Since electrowinning requires an all sulfate solution, however, and of all the recovery technologies discussed only precipitation/re-dissolution or ion exchange can provide a suitable nickel concentrate, these are the only technologies suitable for this approach.

Since these two are the only demonstrated technologies which also solve sodium and organic contamination problems, any plater who wants to truly close the loop on nickel would do well to investigate them. More importantly, anyone

with a nickel recovery system, or anyone considering the purchase of one, should carefully consider what problems may be associated with them and take steps to avoid or minimize them.

FOOTNOTES

1. Cadotte, Monteith, and Golomb, "Contaminant Build-Up in the Plating Bath Resulting from Closed Loop Operation", Plating And Surface Finishing, (January 1979); pp. 42-48.

2. Tran, T.V., & P.B. Clemens, "Recovery of Nickel Salts by Electrodialysis Reversal Process", Proceedings of the 73rd Annual AESF Technical Conference, June 1986; TP 334-ST.

3. Steward, F.A., "Conservation and Recovery of Materials and Treatment of Wastes", in Metal Finishing Guidebook and Directory, mid January 1981; p. 820.

4. Lancy, L.E., "Accumulation of Organic Impurities from Recovery of Nickel Plating Drag-Out", Metal Finishing, (April 1983); pp. 27-32.

5. Ibid.

6. Nadeau, T. and M. Dejak, "Copper, Nickel and Chromium Recovery In a Jobshop", Plating And Surface Finishing, (April 1986); pp. 48-54.

7. Cadotte et. al., Op. cit.

8. Ibid.

9. Mattair, R. and J. Keller, "Closed Loop Recovery of Nickel Plating Rinse", Proceedings 75th National Meeting American Institute of Chemical Engineers, June 4, 1973.

10. McNulty, J., R. Goldsmith & A. Gollan, "Reverse Osmosis Field Test: Treatment of Watts Nickel Rinse Waters", EPA Report No. EPA-600/2-77-039, (February 1977).

11. Lancy, Op. cit.

OTHER REFERENCES

12. Gianelos, L., "Troubleshooting of Nickel Plating Solutions", Plating and Surface Finishing, (October 1977); pp. 32-35.

F-7

# Environmental II
# Session F

## A New Technology for Wastewater Treatment Using Immobilized Algae

Patrick M. Nelis and Dennis W. Darnall
Bio-Recovery Systems, Inc.
4200 S. Research Drive
P.O. Box 3982
Las Cruces, NM 88003

# A NEW TECHNOLOGY FOR WASTEWATER TREATMENT USING IMMOBILIZED ALGAE

Patrick M. Nelis and Dennis W. Darnall

Bio-recovery Systems, Inc.
4200 S. Research Drive
P. O. Box 3982
Las Cruces, NM 88003

## ABSTRACT

Scientists at Bio-recovery Systems have developed a new sorption process for removing heavy metal ions from water which is based upon the natural, very strong affinity of the biological materials such as cell walls of plants and microorganisms for heavy metal ions. Biological materials have been immobilized in a polymer to produce a "biological" ion exchange resin. The material has a remarkable affinity for heavy metal ions and is capable of concentrating heavy metal ions by a factor of many thousand-fold. Comparison of this new process to other metal recovery processes for wastewater treatment is made.

## INTRODUCTION

With the passage of federal legislation which prohibits the land disposal of metal-containing sludges as early as August 1988, many electroplaters, metal finishers and circuit board manufacturers are examining wastewater treatment alternatives which eliminate or minimize the production of hazardous sludge. Several recovery technologies such as reverse osmosis, electrodialysis, evaporation, electrodeposition and ion exchange, are currently available. These recovery technologies either produce a metal salt, which in some instances can be returned to the process stream or a metallic product which can be sold.

Each recovery technology has certain advantages and disadvantages. For example, reverse osmosis is most cost effective when metal contaminants are relatively high in concentration rather than at the lower concentrations which are often maintained in order to provide effective rinsing. Likewise electrodialysis and electrodeposition are most cost effective for solutions which contain 100 ppm or higher of metal ion. An advantage of both electrodeposition and electrodialysis is that the recovered product is at very high concentration and thus occupies a small

volume. Evaporation, while producing a product of high concentration is relatively energy intensive, and any ions or dissolved substances in the rinse waters are concentrated to the same extent as the metal ions. In addition, the effectiveness of evaporation is highly dependent on ambient temperature and humidity. Ion exchange technologies work best on waters containing low concentrations of metal ions, are very energy efficient and can be made in certain instances, specific for metal recovery.

While ion exchange has been used for many years by metal finishers and printed circuit board manufacturers for producing deionized water, it is only recently that this technology has been adapted to remove and recover metal ions from industrial rinse streams. This has led to the development of specialty ion exchange resins which have properties which are beneficial in specific areas of wastewater treatment. This paper describes technology developed by Bio-recovery Systems for the treatment of heavy metal-containing wastewaters or groundwaters. The technology is based upon the use of immobilized algae* which has demonstrated high affinity for metal ions (1) and which behaves as a "biological" ion exchange resin.

## Immobilized Algae for Heavy Metal Recovery

It has long been known that microorganisms have chemical groups on their cell walls which have a high affinity for metal ions. The reaction of metal ions with algal cells is depicted schematically in Figure 1.

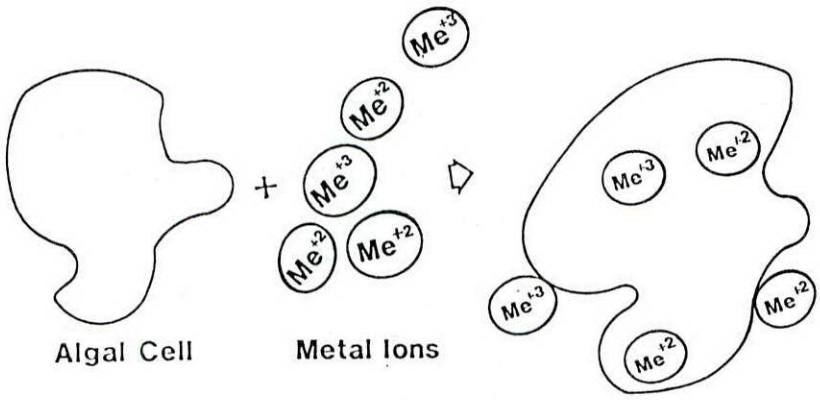


Figure 1. The Reaction of Divalent and Trivalent Metal Ions with an Algal Cell.

For a number of years we have been working with this new sorption process for removing heavy metal ions from water (1-5). We have immobilized algal cells in a polymer and have used this preparation much

* The immobilized algae is a proprietary material patented and owned by Bio-recovery Systems, Inc. and is marketed under the trade name AlgaSORB™.

as ion-exchange resins are used today. This material has a remarkable affinity for heavy metal ions; in some cases the metal-binding capacity is as much as 10 percent of the dry weight of the cells. The algae matrix is capable of concentrating heavy metal ions by a factor of many thousand-fold. The algae are killed in the immobilization process indicating that sorption does not require a living organism, and hence the alga matrix can be exposed, with little or no ill effects, to solution conditions which would normally kill living cells. The pores of the polymer are large enough to allow free diffusion of ions to the algal cells, since similar quantities of metal ions are bound by free and immobilized cells. The immobilization process serves two purposes: (1) It protects the alga cells from decomposition by other microorganisms. We have observed no decrease in metal binding efficiency of immobilized algal cells immersed in aqueous solution for over a year. (2) It produces a hard material which can be nicely packed into chromatographic column which can be pressurized and which have excellent flow characteristics.

Not only does immobilized algae appear to be useful for the removal of the "traditional" heavy metals from solution, but it also seems to be particularly useful for near quantitative removal and recovery of very low concentrations (in the parts per billion range) of precious metals such as gold, silver, platinum and palladium. In addition, conditions have been developed for removing metallic oxoanions such as chromate from aqueous solutions using immobilized algae. The potential of immobilized algae has been verified for removing copper, iron, aluminum, cobalt, nickel, chromium, cadmium, lead, zinc, vanadium, uranium, beryllium, manganese, molybdenum, mercury, silver, gold and platinum from aqueous solutions. In most instances the metal ions are removed leaving effluents containing less than 0.1 ppm of metal.

The immobilized-algae matrix functions as a "biological" ion exchange resin. Like ion-exchange resins, the algae-silica system can be recycled. We have sorbed and stripped metal ions over many cycles with no noticeable loss in efficiency. In contrast to current ion exchange technology, however, a real advantage of the algal matrix is that the components of hard water ($Ca^{+2}$, $Mg^{+2}$) or monovalent cations ($Na^{+}$, $K^{+}$) do not significantly interfere with the binding of toxic, heavy metal ions. The binding of $Ca^{+2}$ and $Mg^{+2}$ to ion-exchange resins often limits ion exchange usefulness since these ions are frequently present in high concentrations and compete for heavy metal ion binding. This means that frequent regeneration of ion-exchange resins is necessary in order to remove heavy metal ions from solutions. Thus, the immobilized algae system has the potential to be particularly useful for removing metal ions from operations which use "hard" tap water or as a polishing treatment for waters resulting from a lime or caustic treatment system.

Figure 2 shows that calcium ion at concentrations as high as 10,000 ppm have little effect on copper binding to algae cells. These data show that the algae-matrix would be particularly adept at removing copper ion from lime-treated effluents.

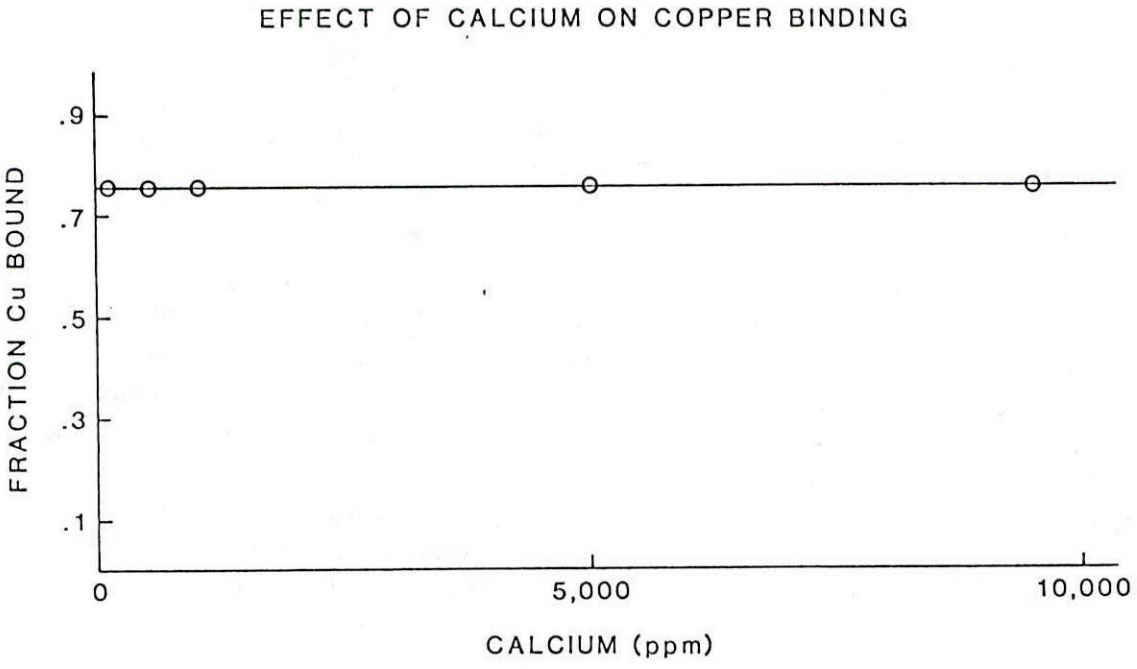


Figure 2. The Effect of Calcium Ion on The Binding of Copper to Immobilized Alga. Copper was initially present at a concentration of 6.4 ppm.

Figure 3 shows that immobilized algae is more effective than commercial, specialty chelating ion exchange reins for "polishing" a lime-treated effluent from a printed circuit board manufacturer.

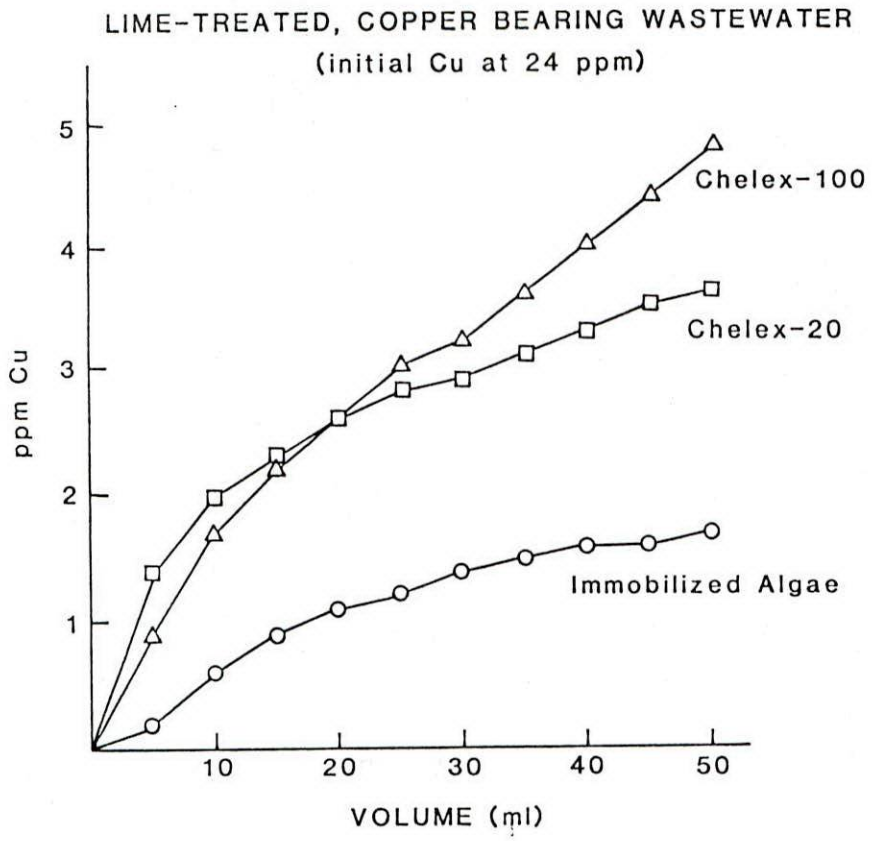


Figure 3. Comparison of Immobilized Algae to Chelating Ion Exchange Resins for Copper Removal From Lime-Treated Copper Bearing Wastewater.

Immobilized algae is also particularly effective for treatment of waters containing organic residues. Organics often foul synthetic ion exchange resins which limits their utility in many wastewater treatment applications. Figure 4 illustrates the effectiveness of immobilized algae in treating fume scrubber wastewaters from a large printed circuit board manufacturer. The scrubber solutions contained high concentrations of

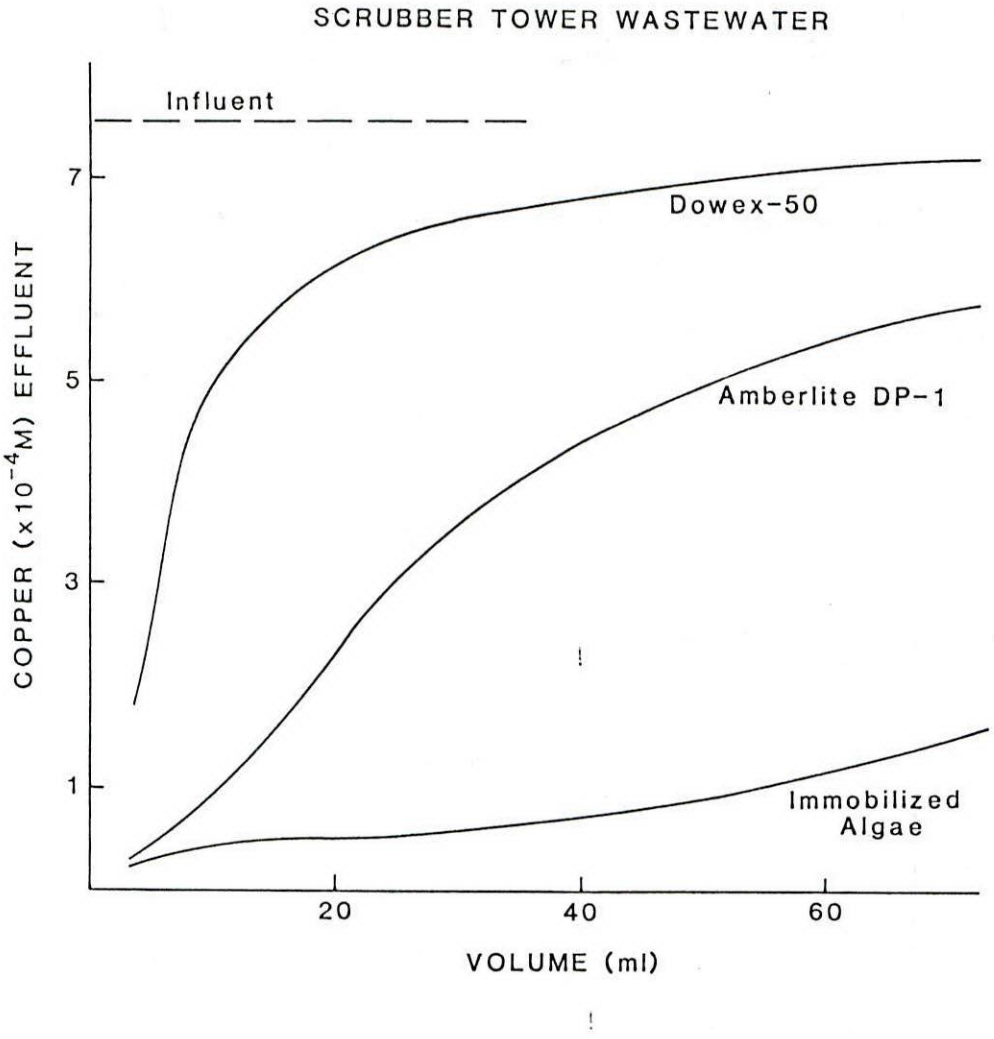


Figure 4: Comparison of Immobiized Algae to a Strong Acid Cation Exchange Resin (Amberlite) and a Weak Acid Cation (Dowex) Ion Exchange Resin for Removal of Copper from Fume Scrubber Tower Wastewaters.

organics as well as ammonia. Figure 4 clearly shows immobilized algae is more effective than other synthetic ion exchange resins for these applications.

Once immobilized algae becomes saturated with metal ions, the metal ions are conveniently stripped with caustic or acids. Figure 5 shows

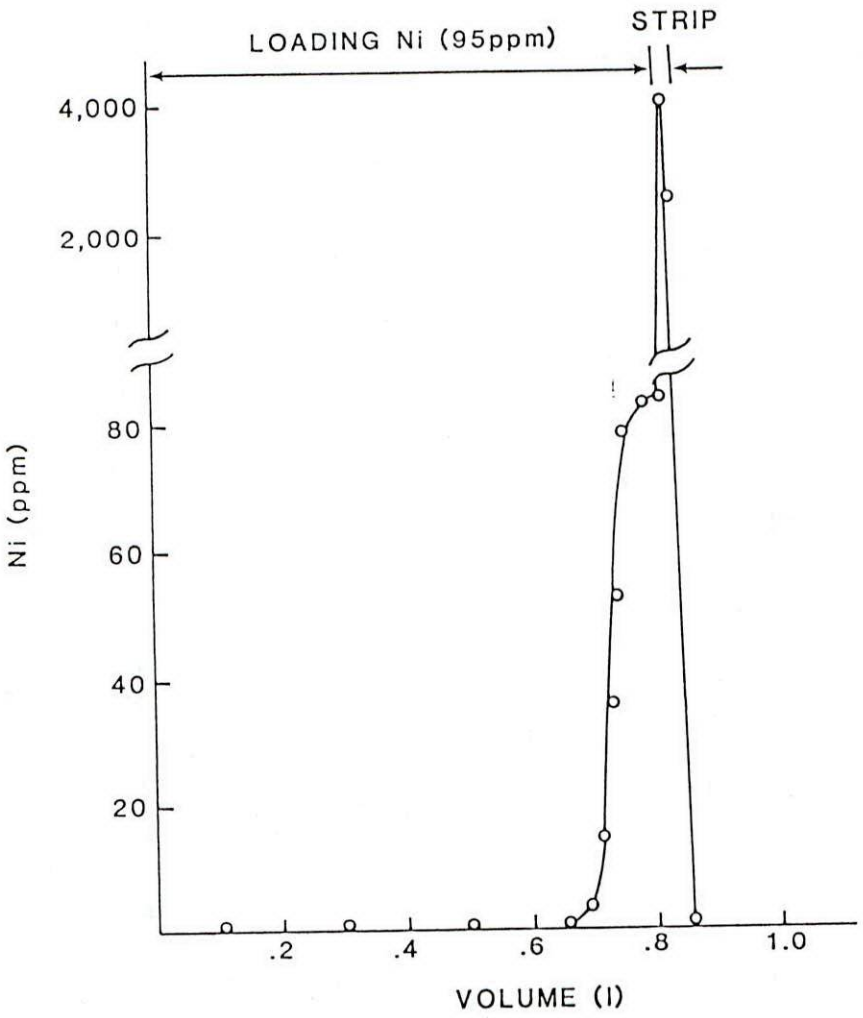


Figure 5. Removal and Recovery of Nickel from Electroplating Rinse Water. Dragout waste containing 95 ppm nickel was passed through a small column containing immobilized algae. After breakthrough of nickel, the bound nickel was stripped in a small volume with acid.

the loading and stripping of nickel originally in a nickel-containing waste rinse. The immobilized algae, once stripped of metal ion, is then ready for reuse.

Effluents from alkaline etchers in the printed circuit board industry are often particularly difficult to treat with traditional precipitation technology because the copper-ammonia complex is particularly stable in caustic or lime treated waters. Figure 6 shows the results of passing alkaline etcher effluents through a small column of immobilized algae. In these experiments copper was loaded on the immobilized algae until, at

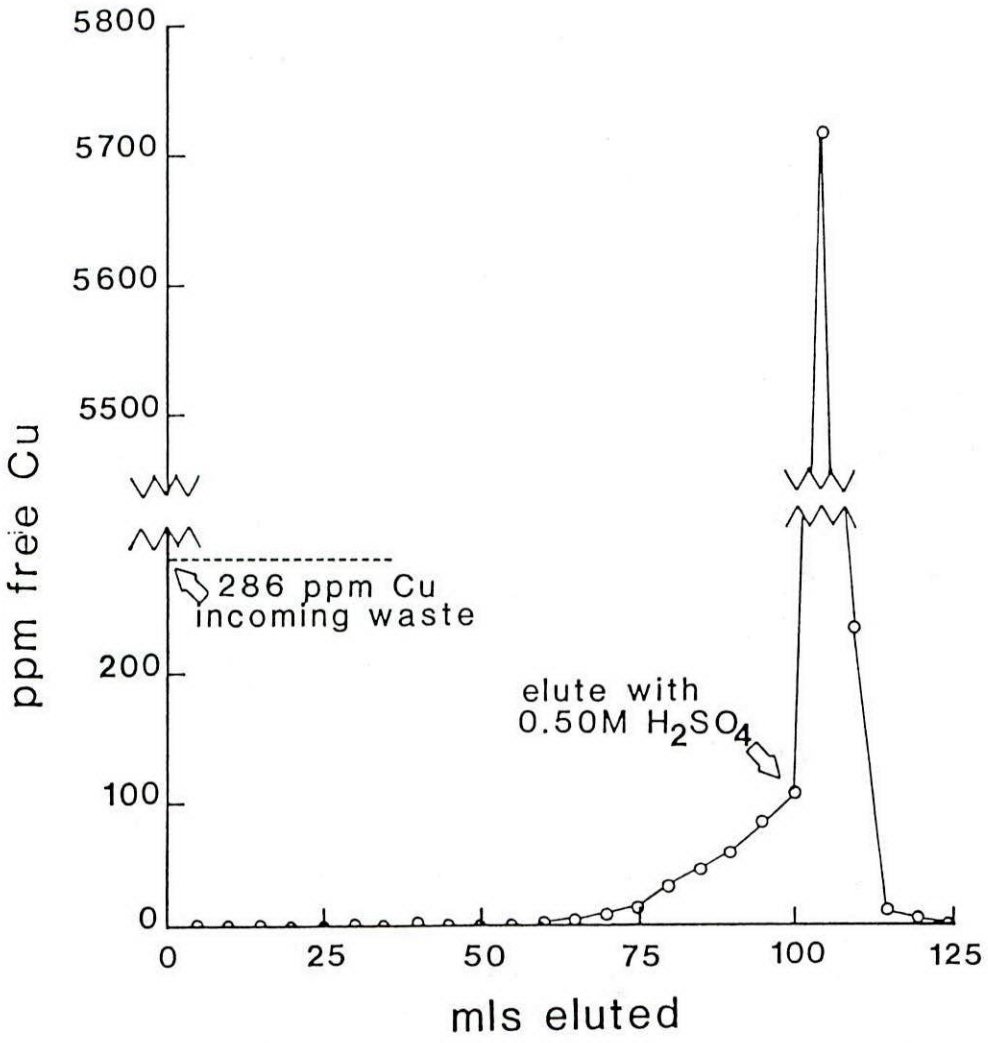


Figure 6. Removal and Recovery of Copper from an Alkaline Etcher Efluent from a Printed Circuit Board Manufacturer. The effluent was passed through a small column of immobilized algae. Once breakthrough of copper occurred, the copper was stripped with sulfuric acid.

breakthrough, copper loading was nearly eight percent of the dry weight of the immobilized algae. Once the copper was bound, it was easily stripped with acid thereby rendering the material ready for reuse.

## Conclusions

Bio-recovery Systems' immobilized algae technology clearly has attributes which make it superior to commercial ion exchange resins for certain applications. While immobilized algae will not replace commercial ion exchange reins for some applications (e.g. production of deionized water), it never-the-less is particularly useful for treating waters with high concentrations of calcium or magnesium, for waters that contain organics and for particularly troublesome metal-ammonia complexes. The special ion-exchange properties of immobilized algae are particularly useful for treatment of metal-contaminated ground waters or for polishing effluents from present treatment systems. It is also particularly useful for treating segregated, metal-containing rinse waters directly at the source.

## References


1. Krambeer, C. "Bigger Profits Through Improved Wastewater Treatment," Finishers Management, November-December 1987.

2. Darnall, D. W., Greene, B., Henzl, M.T., Hosea, J.M., McPherson, R.A., Sneddon, J., and Alexander, M.D., "Selective Recovery of Gold and other Metal Ions from an Algal Biomass", Environ. Sci. Tecnol., 20, 206 (1986).

3. Greene, B. Darnall, D.W., Alexander, M.D., Henzl, M.T., Hosea, J.M., and McPherson, R.A., "The Interaction of Gold(I) and Gold(III) Complexes with Algal Biomass", Environ. Sci., Technol., 20, 627 (1986).

4. D. W. Darnall, B. Greene, M. Hosea, R.A. McPherson, M. Henzl, and M.D. Alexander, "Recovery of Heavy Metals by Immobilized Algae, " in Trace Metal Removal from Aqueous Solution, Edited by R. Thompson, The Royal Society of Chemistry, London (1986), p. 1-24.

5. Benjamin Greene, Robert McPherson, and Dennis W. Darnall, "Algal Sorbents for Selective metal Ion Recovery," in Proceedings of the International Symposium on Metal Speciation, Separation and Recovery," Lewis Publishers, Chicago (1986), pp III, 53-70.

G-1

# Electronics III
# Session G

## Cyclic Voltammetric Stripping Analysis For Use in the PCB Industry

M. Kerman, Dr. P. Bratin
and R. Gluzman
ECI Technology
31 Cain Dr.
Plainview, NY 11803

# CYCLIC VOLTAMMETRIC STRIPPING ANALYSIS FOR USE IN THE PCB INDUSTRY

M. Kerman, Dr. P. Bratin and R. Gluzman
ECI Technology, 31 Cain Dr., Plainview, N.Y. 11803

## Abstract

The Cyclic Voltammetric Stripping (CVS) analysis technique has become an important analytical tool for the control of various plating baths used in the PCB industry. This paper presents procedures and concrete examples along with some DO's and DON'Ts for the control of copper, solder and nickel baths. An emphasis will be placed on the role which CVS can play as an effective method for the early detection and prevention of potential problems and a useful troubleshooting tool.

## Introduction

The plating of quality PCB's requires that many distinct yet interrelated factors be closely monitored. The Cyclic Voltammetric Stripping (CVS) technique [1] has emerged as an accurate and efficient method for the control of the effective additive concentration, degree of organic contamination and overall bath performance, in various stages of the plating process. The plating of acid copper will be used as an example with additional references to solder and nickel baths.

## Principles of CVS Technique

The analysis of an organic species is accomplished by examining their effect on the deposition rate of the metal (Cu, Ni,....) onto a platinum rotating electrode. The potential of the electrode is cycled so that the metal in solution is alternately plated onto the platinum surface and then stripped back into solution. The charge required to strip the metal off the platinum surface is measured, and called the Area Rotating ($A_R$) value. It is this parameter which is then related to the effective additive concentration and the performance of the bath. The relationship between the $A_R$ value and additive concentration can be seen by analyzing several graphs shown in Figures 1-3.

The calibration curve, Fig. 1 is generated by plotting the $A_R$ values as a function of additive concentration. This yields an overall qualitative description of the behavior of the additive. This curve, generated for SAS-type additives shows two distinct regions - one at a low additive concentration where the $A_R$ values are sharply decreasing, and a second portion where

the $A_R$ values are gradually increasing. The first region is due to the small concentration of wetting agents which cause a polarization of the copper plating. The $A_R$ values decrease as the "suppressors" are added until saturation has occurred. The second region is caused by the brightener component of the additive. Since the suppressors and brighteners are active at distinctly different concentrations, they can be analyzed independently.

A technique called Dilution Titration [2] is used for wetter analysis and the Linear Approximation Technique (LAT) [3] for brightener analysis. These techniques have been reviewed in earlier papers [4-5].

Let us now discuss a few stages in the plating process where CVS is used with great success. These processes are the analysis of incoming batches of additives, control of additives during the plating process and the monitoring of contamination and carbon treatment process.

1. Using CVS to analyze incoming additives

One of the first important factors to be considered is the activity of the additive. Earlier studies have shown large discrepancies in the Cyclic Voltammetric Stripping behavior of various additive batches (Fig.4). In addition, organic additives deteriorate at various rates while on the shelf and thus lose their effectiveness. Furthermore, entire batches of additives may become contaminated during manufacturing, testing or packaging. Therefore, in order to avoid possible problems, it is a good practice to verify the quality and integrity of the additive prior to its use in the plating bath. This can be accomplished quickly and accurately using the CVS technique. Manufacturers, in an effort to reduce batch-to-batch variations have been using the CVS technique as their quality control tool and the results have been promising.

A calibration curve (Fig. 1-2) is a graphic representation the relationship between the active additive concentration and the rate of metal deposition on the platinum surface. The curve generated is dependent on the ratio of components of the additive and their relative activities. The additive sample can be analyzed as the shape of this curve should be predictable and reproducible, both from run to run and from one additive batch to another. In their strive for perfection, manufacturers are, from time to time, changing and improving their additives or their components, thus creating a "family" of additives, each with different composition and behavior. The CVS calibration curve can be used to distinguish between the activities of modified additives, and help the user to maintain a properly functioning bath.

As mentioned earlier, the dilution titration method (Fig. 3) is used to determine the activity of the wetting agent component of the additive. Diluted additive is added to pure stock solution and its concentration corresponding to a 50% decrease in the initial $A_R$ value is measured. This concentration, called a 'z' value, is a function of the wetting agent activity and should again be reproducible both from run to run and one batch to another. The lower the 'z' value, the more active are the wetting agents in this batch of additive.

From the above descriptions, it is clear that the notion of an additive standard deserves some mention. For analytical purposes, a single, synthetic compound generating a highly reproducible CVS response would be ideal. However, a more realistic alternative would be a proprietary standard supplied by each manufacturer. Cooperation among major additive manufacturers, instrumentation manufacturers and users is needed in order to establish the practice of supplying either synthetic or proprietary additive standards. Currently, several manufacturers supply standards to select customers and this procedure should be adopted by all. For the analysis of wetting agents, one plausible standard which has been used with success in the past [4] is Polyethylene Glycol (PEG) polymer of a specified molecular weight. Without standards for additive components, it is pointless to compare CVS results obtained using different additives. To perform such a comparison, one needs a standard for the analysis and another standards as far as the quality criteria are concerned.

It is a good laboratory practice to store for future reference a few additive batches for which CVS and quality responses are known. These samples should be used whenever questions about the performance of the instrument or bath arise.

Furthermore, an accurate record-keeping system of batch numbers, z-values and subsequent quality performance will aid in the detection of unacceptable additive lots and will eliminate the deteriorated or contaminated incoming additive as a possible source of plating problems.

## 2. Control of additive during actual plating process

Before the effect of the additive on the actual plating process can be examined, it is essential that the concentrations of metal, acid and chloride be determined and held constant. It seems rather senseless to be concerned about monitoring the additive use when more fundamental variables are not controlled.

The most fundamental point in the control of plating baths is the correlation between the quality of plating and additive

activity. The actual idea of 'quality' must be defined by the user and varies greatly from user to user. Is visual inspection enough of a quality check or does quality imply passing such tests as solder flow, cross section and tensile strength or elongation? As the demands on the plating quality increase, the acceptable additive activity range becomes much narrower and thus more attention must be paid to the selection of the additive, its concentration and its control.

The achievement of an optimum additive range and its subsequent maintenance requires the cooperation of the user, the additive manufacturer and the manufacturer of the analytical instrumentation. In the past, this cooperation has resulted in modifications to both the additive manufacturer's recommendations as far as bath maintenance is concerned as well as to the CVS technique. Through this cooperation, the user is able to obtain more accurate and reproducible results on a particular type of additive chemistry, leading to better quality and lower down-time.

It is advisable to build a bath history by keeping record of the volume of additive consumed, CVS results, manufacturer's recommendation and plating quality. Using the manufacturer's recommended additive concentration range as a starting point, the addition rate of the additive should be modified as needed to achieve the desired plating quality. Once this is obtained, the activity can be maintained using CVS analysis. The actual addition rate arrived upon can be higher or lower than the recommended start-up amount.

One such case is a facility in New Jersey (Fig. 5-7) [6] which was experiencing plating quality problems. CVS results indicated severe additive overdosing of the plating bath. By working with the additive manufacturer, the brightener addition rate was decreased by a factor of 4 from the recommended starting amount. This resulted in a decrease in the rejection rate from 3% to less than .25% while achieving optimum plating quality. The actual additive concentration needed is facility-dependent and depends on such factors as agitation, current-density, type of boards and anodes, temperature and anode/cathode ratio. It is therefore necessary to experiment with addition rates (starting with the recommended values) and optimize them for given conditions.

Brightener concentration is usually mentioned as the major cause of plating problems. The CVS technique can eliminate incorrect additive use as a source of problems and thus takes away the guess work out of maintaining a proper level of additive in the bath at all times. This enables the plater to concentrate on eliminating other sources of problems.

## 3. CVS and the Carbon Treatment process

The last step in assuring plating quality is bath maintenance and carbon treatment. Since the CVS technique is sensitive to oxidizable contamination, the CVS readings correlated to a bath history provide an accurate measure on which to base the frequency of carbon treatment. The ability to efficiently schedule the carbon treatment process minimizes bath downtime and reduces loss. Previous work [8] has shown that the use of CVS in determining proper carbon treatment intervals resulted in a three-fold decrease in the contaminant levels. Besides serving as a scheduling aid, the CVS technique can evaluate the success or failure of the treatment. A properly treated bath should yield similar CVS results to those of a virgin stock solution. If these readings do not agree, the process was not effective and the source of the problem should be investigated.

A question can be asked at this point: Why should I worry about removing every single drop of additive if I have to put it right back in?

The answer is simple. Since CVS is so highly sensitive to additives, we can use them as an indicator of complete carbon treatment. If all of the additives were not removed, what else was left in the solution? Field experiences have shown that contaminants decrease the activity of brighteners, thus requiring increased addition rates of additive. This results in increased manufacturing costs as well as further increasing the contamination level while decreasing the overall plating quality.

Several cases outlining problems which can be detected by CVS were previously described in literature [7]. In one case, high contamination levels were detected in a bath after treatment. Re-filtering using a fresh cartridge produced the same, or worse, CVS results. The source of the problem turned out to be that the filter supplier had switched manufacturers and contaminants were leaching from the new filters into the solution during the filtration process. In another case [8], contamination has been traced to carbon, which was not of sufficiently high quality, causing leach-out of contaminants. Anodes of different grain sizes, photoresists, inefficient rinsing process and other problems can also cause contamination of plating baths.

In all cases, CVS results were instrumental in detecting the problem and locating the source.

## 4. Further Applications of CVS technology

Although CVS was originally used to analyze copper pyrophosphate baths, procedures have been developed for applications to other plating baths, such as acid copper, tin, solder and nickel. Several manufacturers have made available CVS procedures for additives in fluoroborate and non-fluoroborate solder baths [9], and an increasing number of CVS users are presently adding the solder bath monitoring to required procedures. CVS procedures have also been published for determination of Class 1 brighteners (e.g. Saccharin) in Nickel baths (Fig. 8) [10], and for additives in Tin plating baths (Fig. 9) [5].

So extensive has been the progress in CVS application to plating bath control that work has started at some facilities to include CVS in closed-loop, "hands-off" manufacturing processes. For laboratory applications, a semi-automated system is now available to increase the through-put of the lab and decrease guesswork.

## Conclusion

The CVS technique has become a important method for plating bath control due to its wide range of analytical applications and direct correlation of results to additive activity in solution. The ability of CVS to detect plating problems early on and help prevent their reoccurrence make it a valuable tool for the PCB industry where tight control is essential, resulting in monetary savings and increased quality.

## Bibliography


1. D. Tench and C. Ogden, "A New Voltammetric Stripping Method Applied to the Determination of the Brightener Concentration in Copper Pyrophosphate Plating Baths", J. Electrochem., Soc., 125, 194 (1978).

2. W.O. Freitag and M.R. Manning, "Analysis of Additives in Acid Copper Baths by Cyclic Voltammetry", Proceedings of 70th AES Technical Conference, Sur/Fin, June 1983, Indianapolis, IN.

3. R. Gluzman, "The Use of Cyclic Voltammetric Stripping for Determination of Additive Concentration in Copper Plating Baths", Proceedings of 70th AES Technical Conference, Sur/Fin, June 1983, Indianapolis,IN.

4. P. Bratin, "New Developments in the Use of Cyclic Voltammetric Stripping for Analysis of Plating Solutions," Proceedings of AES Analytical Methods Symposium, March 1985, Chicago IL.

5. P. Bratin, "Recent Developments in CBS Analysis of Plating Solutions", Proceedings of 74th AESF Technical Conference, Sur/Fin, July 1987, Chicago.

6. M. Bacchetta, "Reduction of Acid Copper Burning Rejects Using Statistical Methods", Proceedings of AES Analytical Methods Symposium, March 1985, Chicago, IL.

7. B. Lowry, C. Ogden, D. Tench and R. Young, "Production Implementation of Cyclic Voltammetric Stripping Analysis for Control of Copper Pyrophosphate CIrcuit Board Plating Baths", Plating & Surface Fin, 70(9), 70 (1983).

8. D. Anderson, M. Hanna, C. Ogden and D. Tench, "Purification of Acid Copper Plating Baths", Plating & Surface Fin., (70)12, 70(1983).

9. J. McCaskie, "Electroanalytical Methods for Process Control of Printed Circuit Plating: Copper and Solder", Proceedings of 74th AESF Technical Conference, Sur/Fin, July 1987, Chicago, IL.

10. P. Bratin, D. Cupolo and W. Ward, "Application of CVS to the Analysis of Organic Additives in Nickel Plating Baths", Proceedings of the 72nd AES Technical Conference, Sur/Fin, June 1985, Detroit, MI.

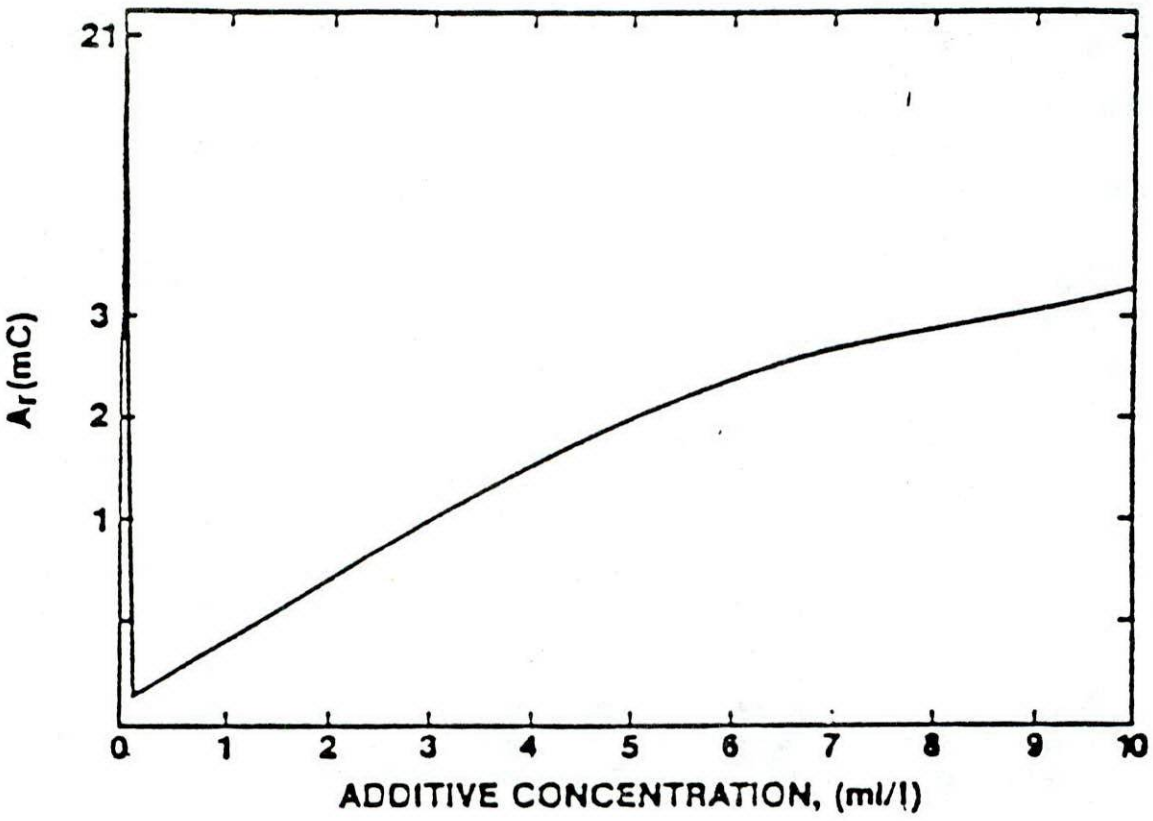


Fig. 1 Typical CVS calibration curve for SAS-type additives in acid copper plating bath (scan rate = 100mV/S, rotation rate = 500RPM, scan limits = -0.2 to 1.6V).

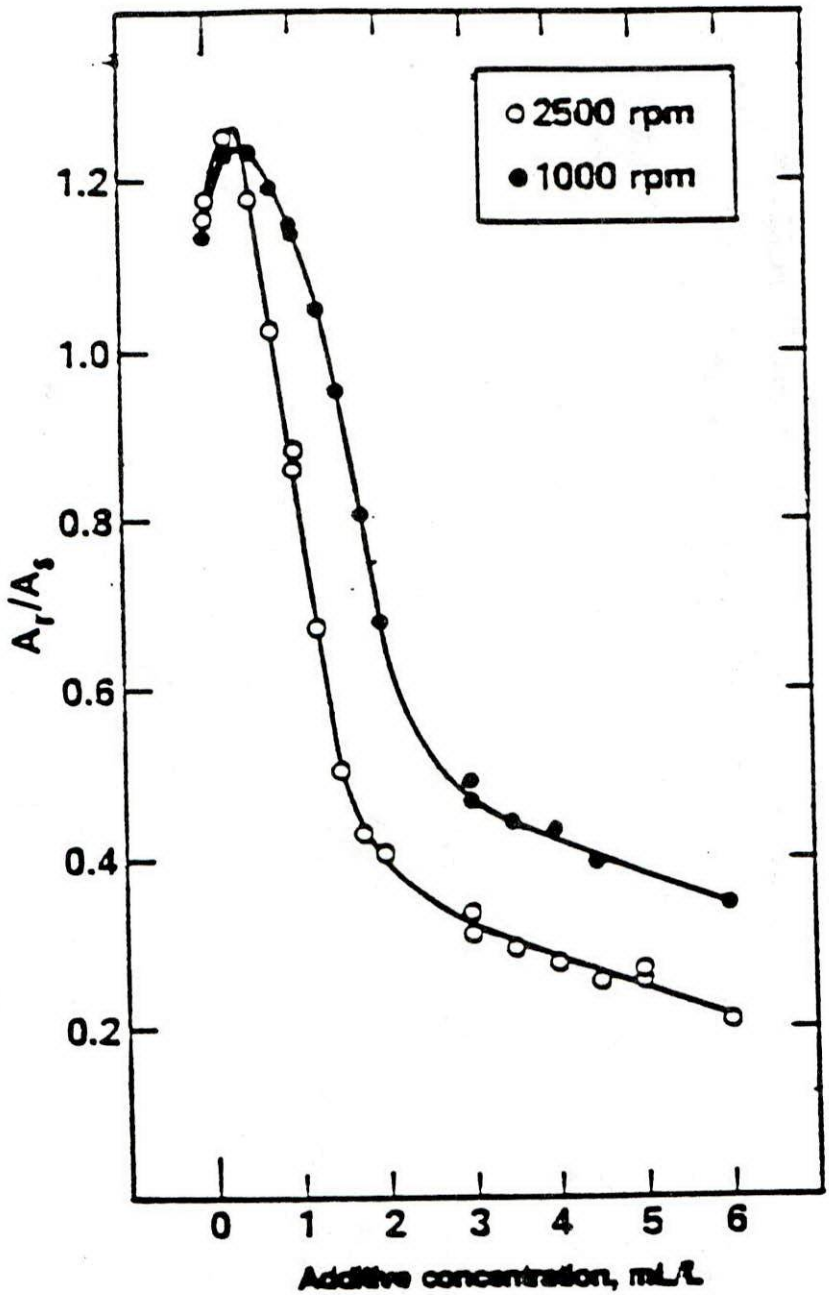


Fig. 2 Typical calibration curve for PES-type additives in acid copper sulfate plating bath (scan rate = 100mV/S, scan limits = -0.15 to 1.9V).

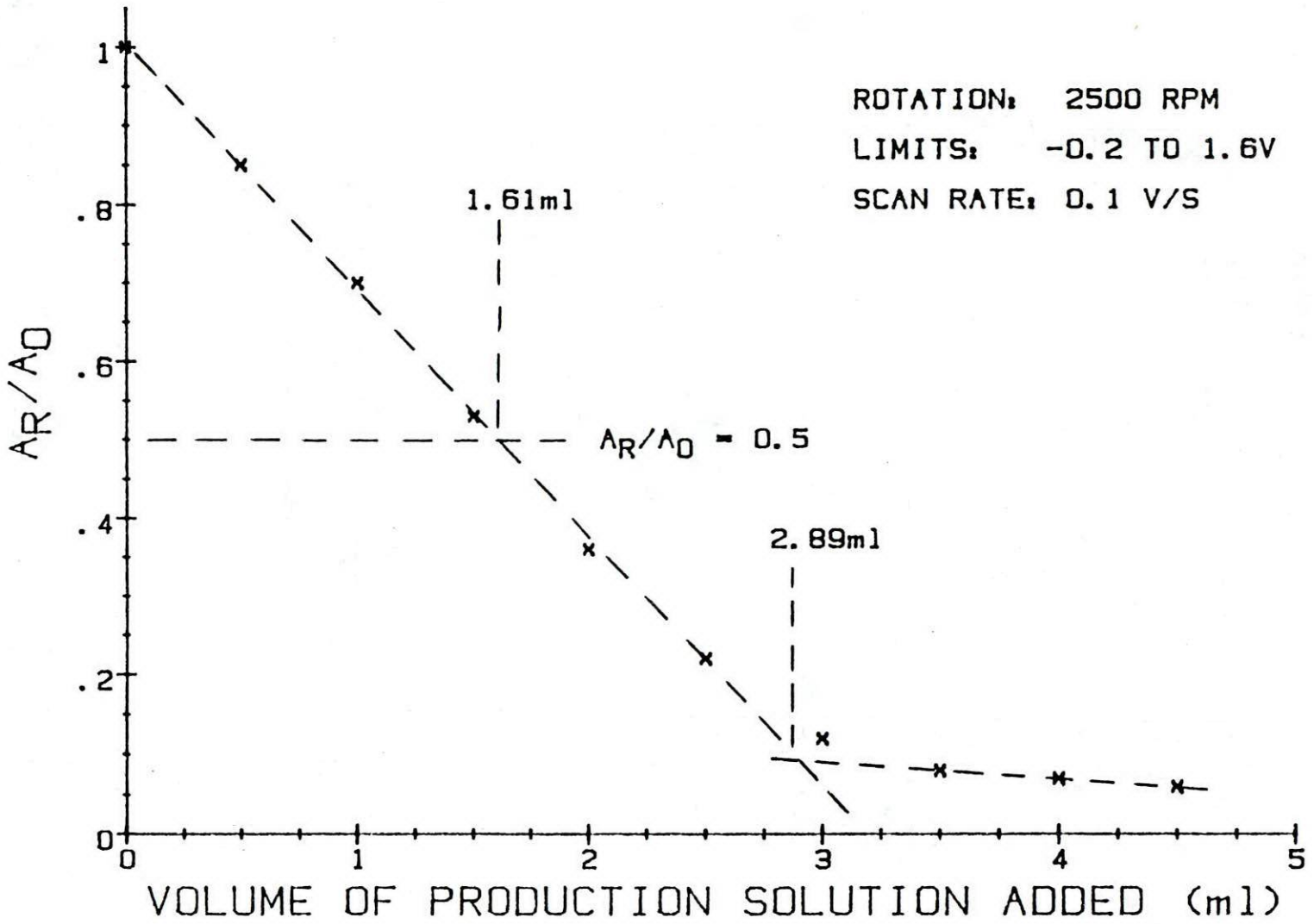
DILUTION TITRATION CURVE
ROTATION: 2500 RPM
LIMITS: -0.2 TO 1.6V
SCAN RATE: 0.1 V/S
1.61ml
2.89ml
$A_R/A_O = 0.5$
$A_R/A_O$
VOLUME OF PRODUCTION SOLUTION ADDED (ml)
0
.2
.4
.6
.8
1
0
1
2
3
4
5

Fig. 3

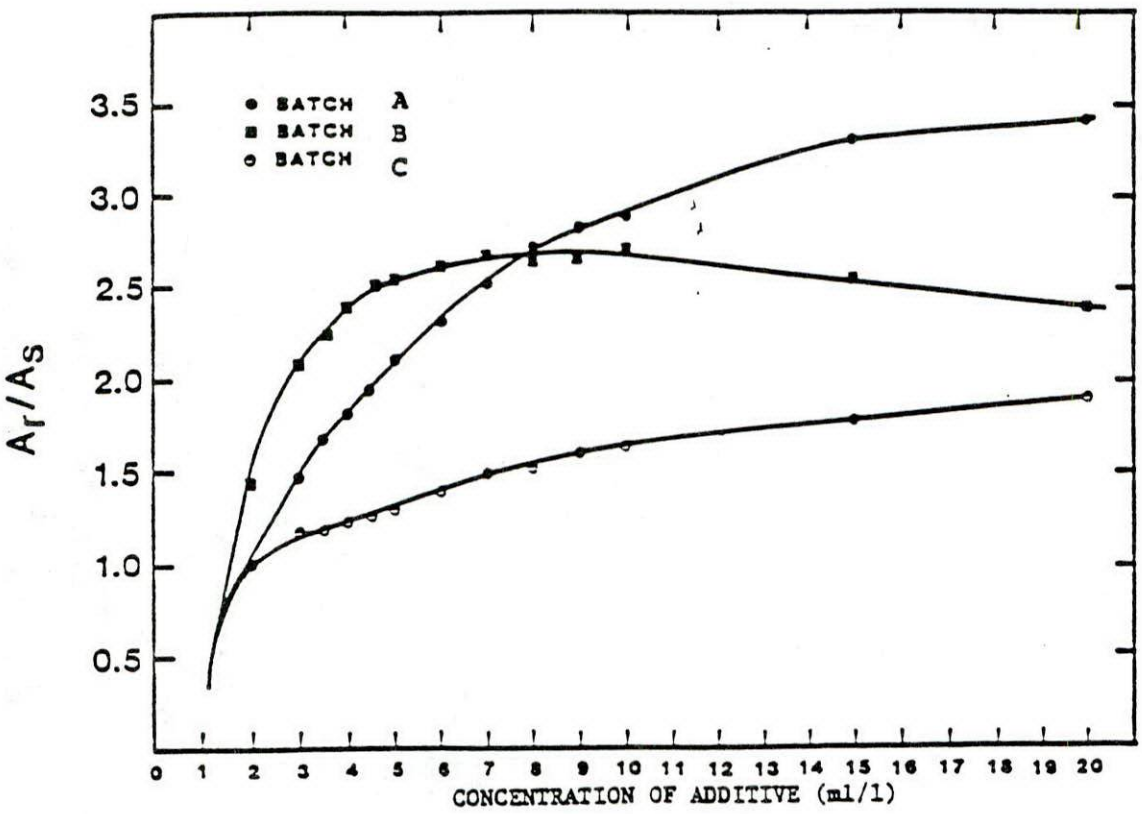


Fig. 4 Voltammetric comparison of three batches of acid copper sulfate proprietary additive, showing large variations in activity.

# Brightener Concentration

February ,1984 to May ,1984

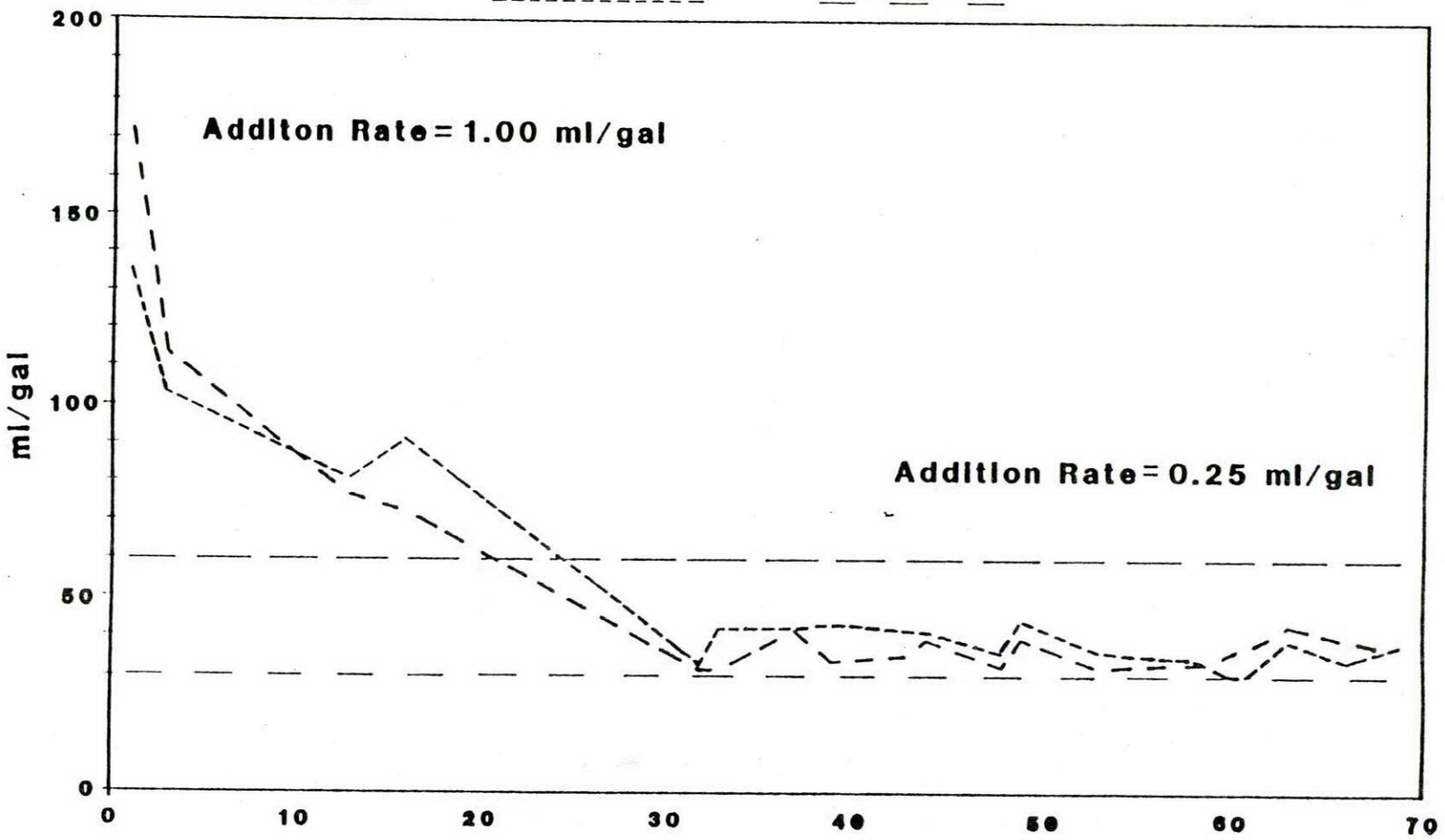


Courtesy of M. Bacchetta ,HP

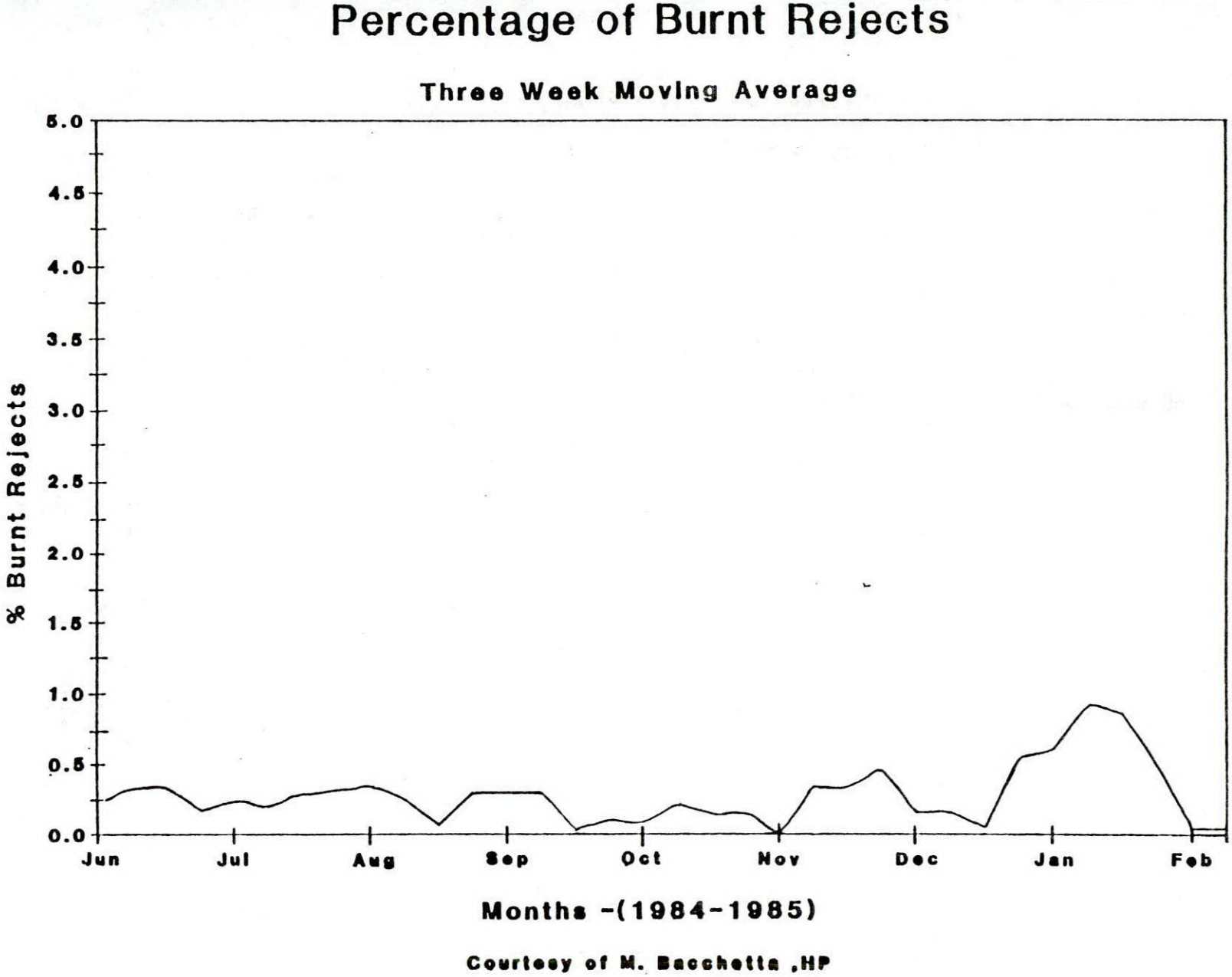
Percentage of Burnt Rejects
Three Week Moving Average
% Burnt Rejects
5.0
4.5
4.0
3.5
3.0
2.5
2.0
1.5
1.0
0.5
0.0
Jun
Jul
Aug
Sep
Oct
Nov
Dec
Jan
Feb
Months -(1984-1985)
Courtesy of M. Bacchetta ,HP

Fig. 6

# Percentage of Burnt Rejects

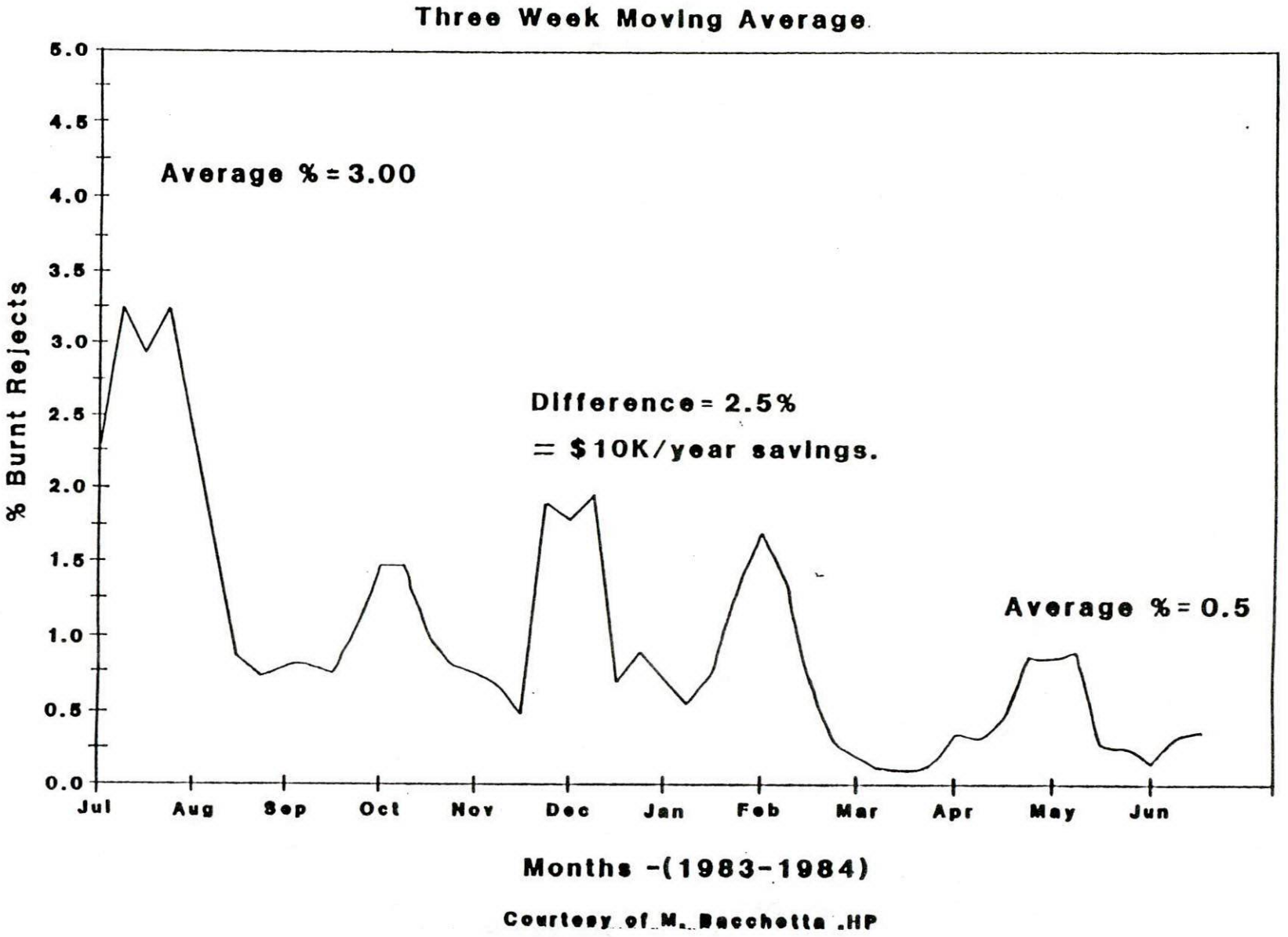


Fig. 7

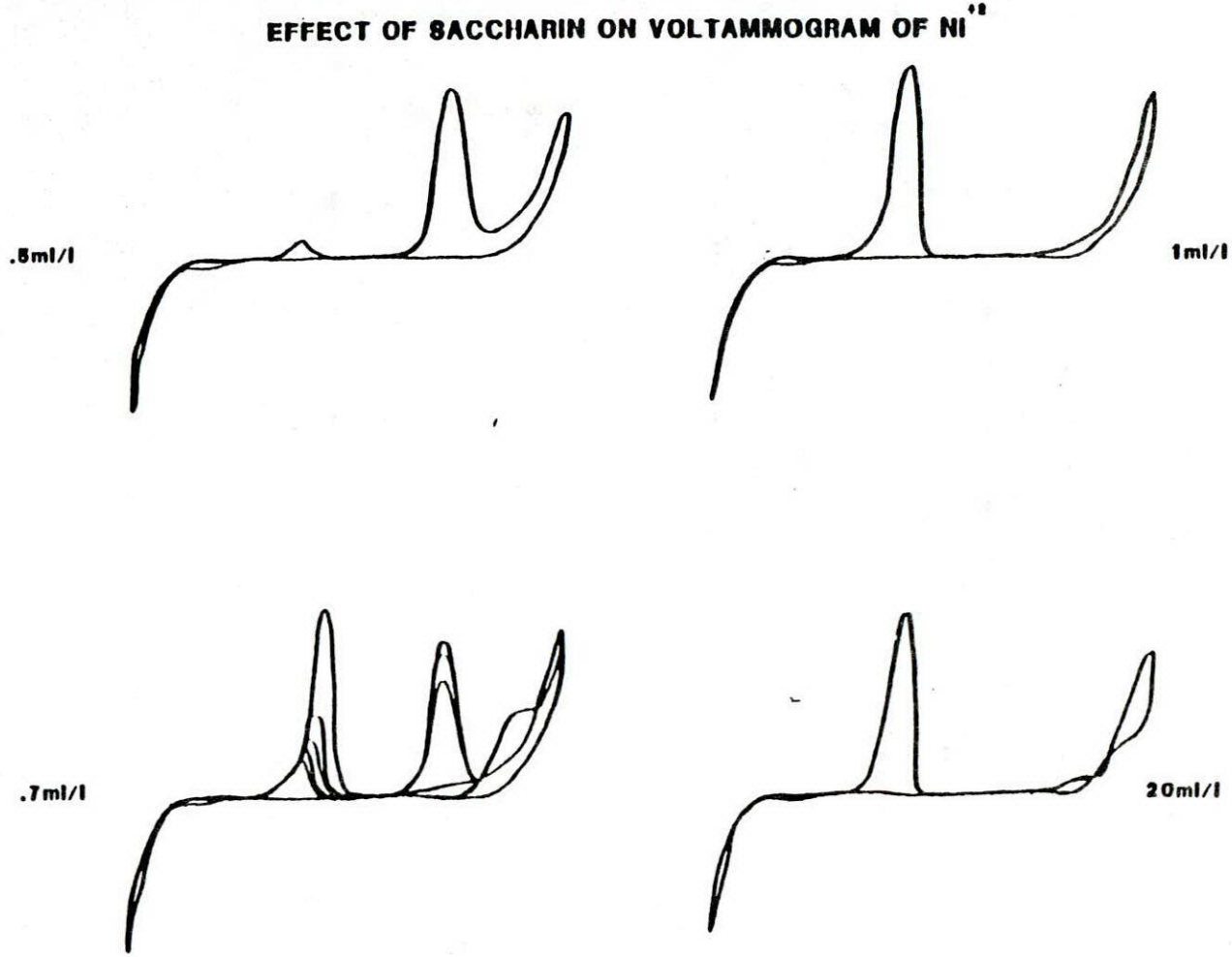


Fig. 8 Effect of saccharin-containing additive on the voltammogram of Watt's nickel plating bath (Pt rotating electrode, scan limits = -1.20 to 1.75V vs SCE, scan rate = 100mV/S, rotation rate = 2500RPM).

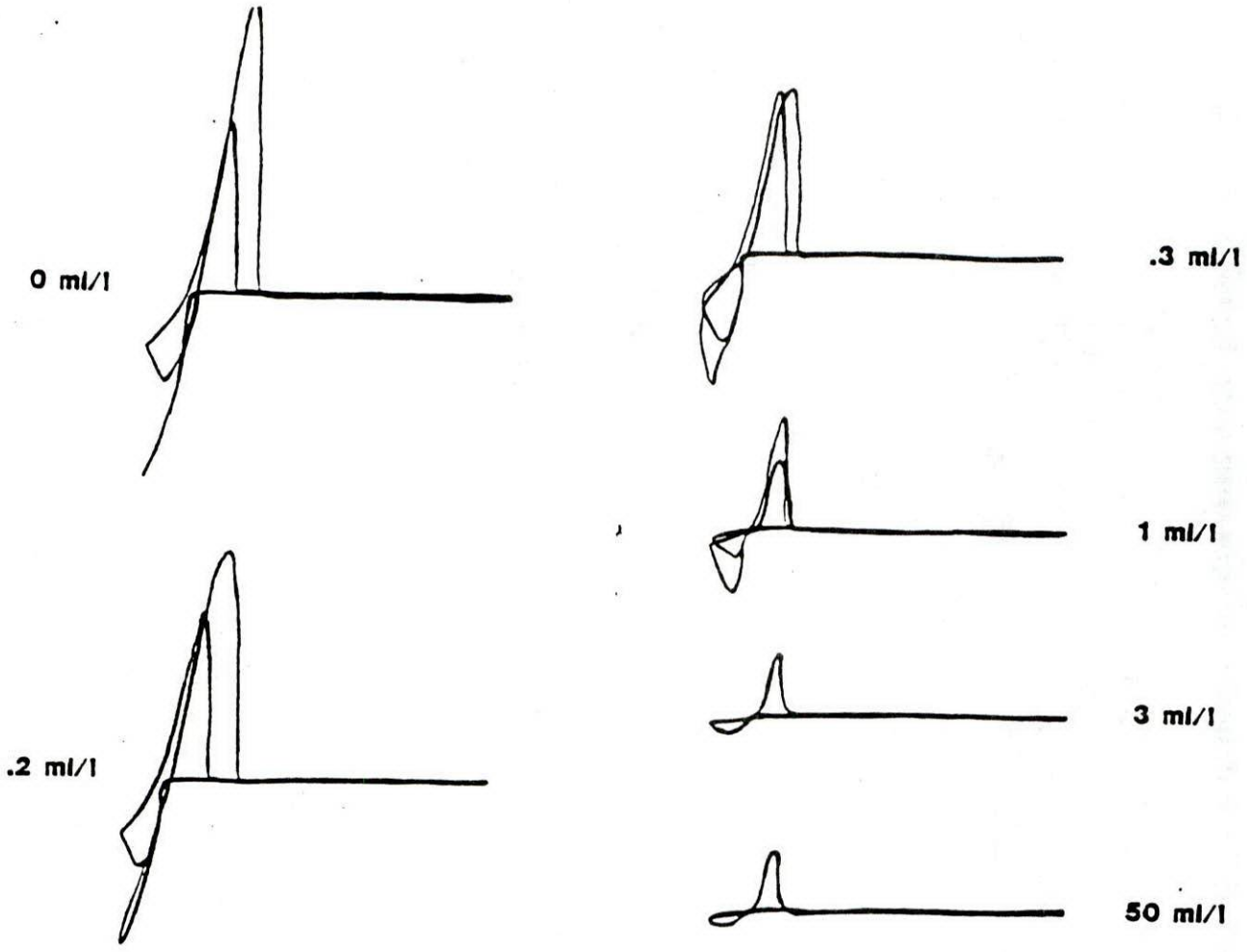


Fig. 9 Effect of the make-up component of the proprietary additive on the voltammogram of the acid tin sulfate bath (Pt electrode) scan limits = -0.55 to 0.2V vs SCE, scan rate = 100mV/S, rotation rate = 2500RPM

G-2

# Electronics III
# Session G

## Multi-Layer Processing: Oxide Control

Gary Marasovich
Electrochemicals
751 Elm Street
Youngstown, OH 44502

# MULTI-LAYER PROCESSING: OXIDE CONTROL

By
Gary Marasovich
Electrochemicals
751 Elm Street
Youngstown, Ohio 44502

## Introduction:

During the infancy of multi-layer technology, the engineers attempted to laminate bare copper to a glass weave material that is impregnated with a partially cured resin. The adhesion of bare copper to "B-STAGE PREPREG" was extremely poor, yielding peel strength tests less than 2# per inch.

Subsequently, the engineers felt that by changing the surface topography of the smooth copper surface to a mechanically or chemically roughened surface that peel strength test results would increase. As expected, peel strengths did increase, but only slightly. The copper surface was roughened, but still not ideal for copper-prepreg adhesion.

What was needed was a unique approach to roughening the copper surface. Rather than just mechanically and/or chemically roughening the copper surface, chemically changing the copper surface to a form that would have better adhesive qualities toward prepreg was attempted.

The technology for this first attempt to chemically change the topography of the copper surface was borrowed from the Metal Finishing industry. For many years the Metal Finishing industry employed an oxidizing process to produce a functional/ decorative finish for copper and brass. This black oxidizing process was applied to the innerlayers of the multilayer booklet. The results were quite favorable, hence, the surface topography was better suited for copper-prepreg adhesion. After years of modifications, present day black oxide processes produce peel strengths upwards of 6# per inch.

As the multilayer segment of the PC industry developed, the black oxide process became the center of attention. Two new requirements were placed upon the oxidizing process. First, the black oxide process needed to be modified to obtain higher peel strengths for FR-4 material. Secondly, and more importantly, the oxidizing process needed to have the ability to bond successfully to dielectric materials other than epoxy.

Research and development chemists and engineers discovered that by refining the black oxide formula, both of these requirements could be met. This chemical re-formulation produced an oxide coating different than the velvety black coating that was characteristic of the black oxide bath. This new oxide was bronze

to dark brown in color, and is referred to as "BROWN" oxide. This brown oxide coating produced peel strengths in the range of 9# to 12# per inch for epoxy dielectric materials and 2# to 4# per inch for polyimide dielectric materials. Refer to Table #1 for a comparison between bonding techniques and peel strengths for FR-4 and polyimide dielectric materials. Therefore, due to the ingenuity of the early multilayer engineers and the increased requirements placed upon the oxide process, the trend towards miniaturization via multilayer printed wiring boards has become feasible. The multilayer manufacturers have obtained their goal to produce a strong, heat-resistant bond between copper circuitry and B-STAGE prepreg.

Oxide coatings also have other advantages besides producing a strong, heat resistant bond between copper circuitry and B-STAGE prepreg.[1] A second advantage is the passivation of the copper surface.[1] The oxide process produces a fully oxidized surface of cupric oxide (CuO). Therefore, during the lamination process the copper is not available to react under the heat and pressure cycling to produce disadvantageous gases. Trapped gases, including water vapor, would deter adhesion of the copper circuitry to the prepreg resulting in delamination. Finally, the other advantage is that the oxide coating is easily applied. Although the oxide line may be lengthy, it does not require expensive, specialized equipment nor specialized personnel to produce properly coated innerlayers.

Basic Oxide Process:

A typical oxide line appears as Figure #1. The requirements for this line are as follows:

1. Alkaline Cleaner

This step is designed to remove heavy soils and dirt from the innerlayers. It should also remove residual resist debris that may still be present on the innerlayers after resist stripping.

2. Acid Cleaner/Neutralizer

This step is designed to remove light soils and dirt while neutralizing any residual alkaline cleaner still present on the innerlayers by the previous rinse step. This step should leave the innerlayers very clean so that the following micro-etch step will uniformly etch the copper surface.

3. Micro-Etch

This step is critical for producing a perfectly clean copper surface. It is recommended to micro-etch 50 - 75 microinches from the copper surface to insure residue-free surfaces (no residues from cleaners, adhesion promoters from photoresists, etc.). The

type of etchant is not important, but the innerlayer must be perfectly clean and oxidation-free. Refer to Table #2 for a comparison between micro-etch type and peel strength test results.

4. Pre-Dip

This step is the final preparatory step prior to the oxide bath. It is designed to permit optimal performance of the oxide coating. Presently, the industry uses either an acid or alkaline pre-dip.

A. A 10% by volume HCl solution is used to produce an oxidation-free surface, since pre-oxidation deters uniform oxide coatings. If an acid pre-dip is used, then a subsequent rinse must be employed to minimize neutralization of the alkaline oxide bath by acidic $H^+$ ions from this type of pre-dip.

B. An alkaline pre-dip (a dilute amount of the alkaline component of the oxide bath or dilute NaOH) is preferred. This pre-dip prevents neutralization of the oxide bath, allows direct immersion into the oxide bath, and increases the speed of the formation of the crystalline oxide coating. The temperature of this bath should be approximately $70^{\circ}F$ and the immersion time should be relatively short to prevent pre-oxidation before entering the oxide bath.

5. Oxide Bath

This bath is formulated as an alkaline oxidizing solution. Upon bath make-up the source of alkalinity normally comes from two sources NaOH (sodium hydroxide) and a buffering agent for highly alkaline solutions. Following use, a third source of alkalinity becomes evident by the reaction of NaOH and $CO_2$ (carbon dioxide) from the air, i.e. $Na_2CO_3$ (sodium carbonate).

The basic chemical reaction when an oxide coating is formed on a copper surface is as follows:

$$Cu + NaClO_2 + H_2O \rightarrow 2\ Cu(OH)_2 + NaCl$$

$$2Cu(OH)_2 \rightarrow 2CuO + H_2O$$

$$2\ NaOH + CO_2 \rightarrow Na_2CO_3 + H_2O$$

6. Dry

The final drying step is mandatory to prevent moisture entrapped in the oxide crystal lattice from being introduced into the multilayer booklet.[2] This drying step can be accomplished by a one hour bake at $110^{\circ}C$.

Oxide Processing Considerations:

Although the quality of rinsing in many chemical processes may not be considered critical, proper rinsing between all major process steps in the oxide line is essential to obtain optimum performance of the process. For example, the quality of rinsing between the cleaners, micro-etch, and oxide bath can determine the uniformity of the oxide coating. The quality of rinsing after the oxide bath can influence the adhesive nature of the oxide surface. Failure to remove the alkaline oxide solution from the innerlayers increases the possibility of ionic contamination and subsequent delamination. The final rinse is recommended to be between pH 5 and pH 7 with a temperature of 120° - 130°F. This hot, slightly acidic final rinse neutralizes any alkaline surface condition that may still remain on the innerlayers along with aiding in the drying step.

The control of the oxide bath is similar to other chemical processes. The critical parameter for oxide control are immersion time, bath temperature, and chemical concentration. These three parameters are strongly related to oxide performance and must be scrutinized when optimizing the oxide bath. By varying these parameters, the spectrum of oxide colors and crystalline topography can be generated. Some of the relationships between these parameters and oxide performance will be discussed in the following paragraphs.

A visual comparison of brown and black oxide crystalline topography appears as Figure #2. Brown oxide appears as a short, fine-grained crystal with a larger surface area in comparison to the long, needle-like crystal of black oxide. The brown oxide crystal structure produces superior peel strengths in comparison to the fragile and less thermally-stable black oxide crystal structure. This fact is attributed to the fact that the bonding mechanism of oxide to pre-preg is primarily mechanical in nature, not chemical.[3] Thus, brown oxide is better suited for polyimide dielectrics which receive higher thermal and mechanical (pressure) stresses in lamination and in final board operation.

Brown oxide baths are formulated to operate between 140° to 200°F. Black oxide baths generally operate at approximately 200° F, although low temperature black oxide baths are being developed. For oxide baths, temperature directly influences the rate of crystal formation. The higher the temperature, the less time required to generate a certain weight of cupric oxide.

The relationship between chemical concentration, temperature, and oxide color can be determined from Figures #3 through Figure #6.[4] From these figures, one can also notice that black oxide baths are more alkaline than brown oxide baths.

To optimize the amount of the oxide coating present, a weight

gain experiment is generally performed. Here, a dry oxide coated panel of known dimensions is weighed, the oxide is removed in $H^+$ (acid), dried, and then reweighed. The weight difference is generally tabulated in grams per $ft^2$, refer to Table #3. These weight gain values are optimized with respect to prepreg material, exact oxide process employed, lamination cycle, and post-bake cycle. If this procedure is followed, the adhesion of copper oxide to prepreg is maximized (optimized). The effect of the method of oxide application, oxide color, and post-bake cycle versus peel strength tests are tabulated as Tables #4, #5 and #6 respectively. From Table #4 one can notice that the oxide formed from either spray or immersion systems are identical within experimental limitations. Table #5 shows that a brown to dark brown oxide color produces the highest peel strength values. Table #6 shows the importance of optimizing post-bake cycles for FR-4 and polyimide dielectric multilayer booklets.

Conclusions:

Production of good-quality multilayer printed wiring boards can be achieved by:

-producing a fine-grained, non-porous oxide coating that is thermally stable

-employing a proper innerlayer treatment process prior to lamination

-having careful quality control on incoming raw materials (chemicals, pre-preg, etc.)

-determining the optimum lamination and post-bake cycles for the dielectric material used for the booklet

Optimization of the oxidizing process is required to enhance the reliability and performance of multilayer printed wiring boards.

References:

1. Nargi, K., "Red and Black Oxide Coatings for Improved Multilayer Bonding," P.C. Fab, June 1985.

2. Scarlett, J. A., The Multilayer Printed Circuit Board Handbook, Electrochemical Publications Ltd., Scotland, P. 180-204.

3. Reed, A. H., "Treating Copper with Brown Oxide for Improving Multilayer Board Adhesion," Electri-Onics, November 1983.

4. Barringer, T., Electrochemicals Internal Data.

TABLE #1

COMPARISON OF BONDING TECHNIQUES TO PEEL STRENGTH TESTS

| BONDING TECHNIQUE | INNER LAYER DIELECTRIC MATERIAL | |
|---|---|---|
| | FR-4 | POLYIMIDE |
| | PEEL STRENGTH (#/INCH) | PEEL STRENGTH (#/INCH) |
| SMOOTH COPPER | LESS THAN 2 | 0 |
| CHEMICALLY/MECHANICALLY ROUGHENED COPPER | LESS THAN 3 | 0 |
| BLACK OXIDE | 4 - 6 | LESS THAN 1 |
| BROWN OXIDE | 9 - 12 | 2 - 4 |

TABLE #2

PEEL STRENGTH
EFFECT OF PRECLEANING

| TYPE OF MICRO-ETCH | PEEL STRENGTH (#/INCH) | |
|---|---|---|
| | FR-4 | POLYIMIDE |
| SULFURIC-PEROXIDE | 8.7 | 4.8 |
| CUPRIC CHLORIDE | 8.8 | 4.6 |
| SODIUM PERSULFATE | 8.7 | 4.8 |

TABLE #3

| IMMERSION TIME (MINUTE) | BROWN OXIDE WEIGHT IN GRAMS/$FT^2$ OF AREA | BLACK OXIDE WEIGHT IN GRAMS/$FT^2$ OF AREA |
|---|---|---|
| 2 | 0.058 | 0.44 |
| 4 | 0.08 | 0.95 |
| 8 | 0.16 | 1.17 |
| 16 | 0.16 | 1.35 |
| 32 | 0.16 | 1.35 |

TABLE #4

EFFECT OF APPLICATION METHOD ON PEEL STRENGTH

| METHOD OF APPLICATION | BROWN OXIDE PEEL STRENGTHS (#/INCH) FR-4 | POLYIMIDE |
|---|---|---|
| SPRAY | 8.7 | 4.9 |
| IMMERSION | 8.8 | 4.8 |

TABLE #5

EFFECT OF COLOR ON PEEL STRENGTHS

| | PEEL STRENGTH (#/INCH) | |
|---|---|---|
| OXIDE COLOR | FR-4 | POLYIMIDE |
| BRONZE | 7.1 | 3.4 |
| BROWN | 8.7 | 4.9 |
| DARK BROWN | 8.8 | 4.8 |
| BLACK | 3.2 | 0.3 |

TABLE #6

POST BAKE EFFECT ON PEEL STRENGTHS

| POST BAKE TIME (MINUTES) | BROWN OXIDE PEEL STRENGTHS (#/INCH) FR-4 300°F | FR-4 350°F | POLYIMIDE 425°F |
|---|---|---|---|
| 0 | 6.0 | 6.0 | 0.6 |
| 1 | 6.3 | 6.5 | 1.0 |
| 2 | 7.0 | 6.5 | 4.0 |
| 3 | 6.6 | 6.3 | 4.4 |
| 4 | 6.0 | 4.8 | 3.6 |
| 5 | 5.7 | 5.2 | 2.4 |
| 6 | 5.0 | 5.0 | 2.6 |

FIGURE #1

TYPICAL OXIDE LINE

ALKALINE CLEAN

RINSE

ACID NEUTRALIZE/CLEAN

RINSE

MICRO-ETCH

RINSE

PREDIP

RINSE (OPTIONAL)

OXIDE

RINSE

RINSE

DRY

FIGURE #2

CRYSTAL STRUCTURE COMPARISON BETWEEN
BROWN AND BLACK OXIDE



BROWN OXIDE
CRYSTAL STRUCTURE



BLACK OXIDE
CRYSTAL STRUCTURE

*SCANNING ELECTRON MICROGRAPHS
AT 10,000 MAGNIFICATION

# OXIDE COLOR

TEMPERATURE= 140 F  TIME= 3 MINUTES

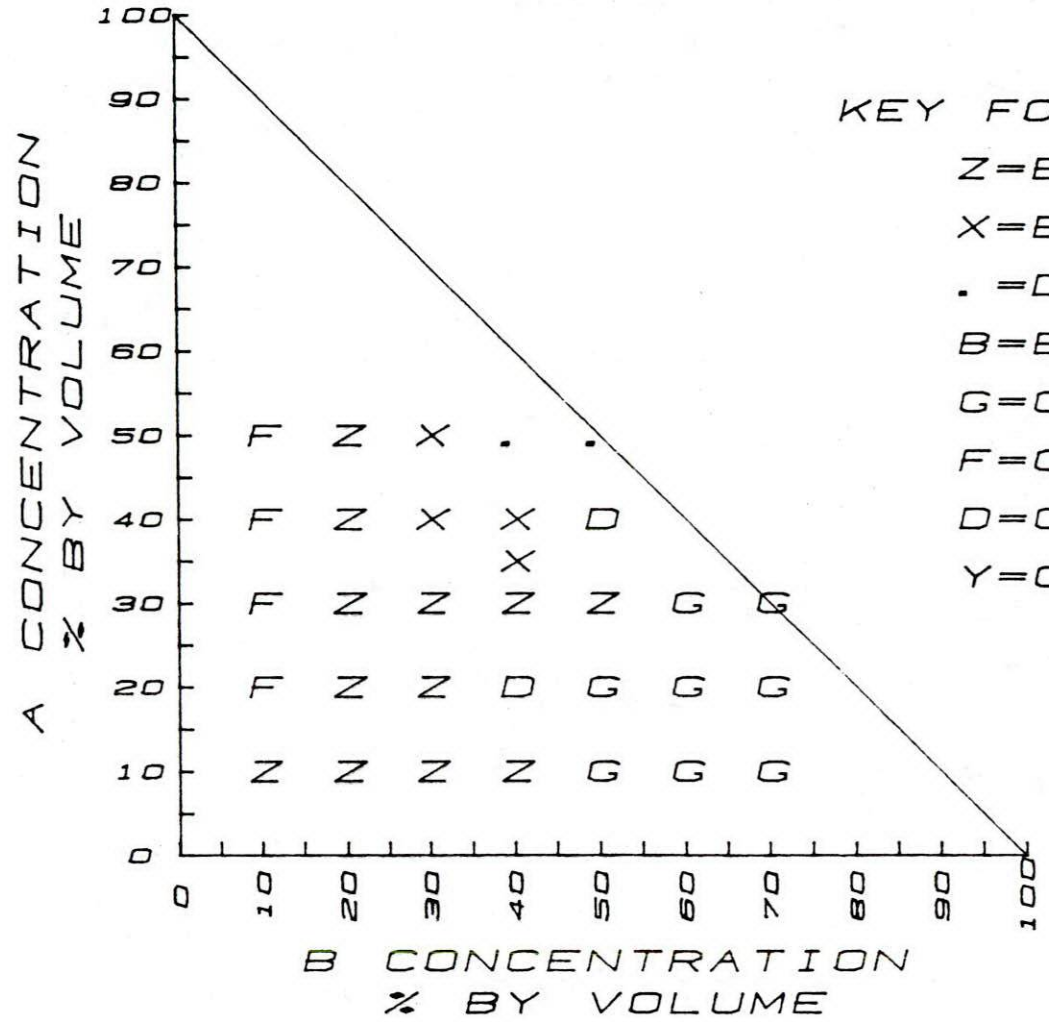


KEY FOR COATING COLOR

Z=BRONZE

X=BROWN

. =DARK BROWN

B=BLACK

G=GREY

F=GREY/BRONZE

D=GREY/BROWN

Y=GREY/BLACK

A=OXIDIZER

B=ALKALINE

FIGURE #3

# OXIDE COLOR

TEMPERATURE= 160 F  TIME= 3 MINUTES

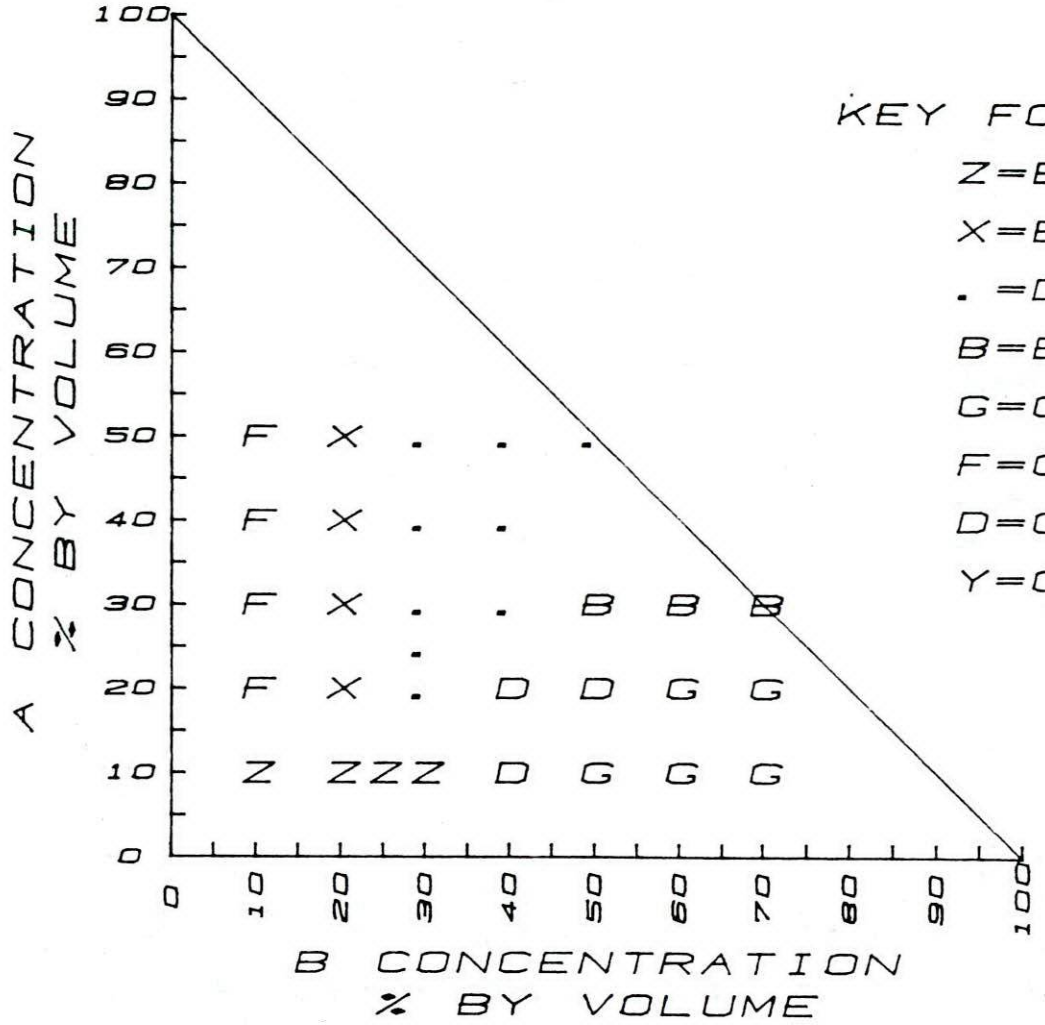


KEY FOR COATING COLOR

Z=BRONZE

X=BROWN

. =DARK BROWN

B=BLACK

G=GREY

F=GREY/BRONZE

D=GREY/BROWN

Y=GREY/BLACK

A=OXIDIZER

B=ALKALINE

FIGURE #4

# OXIDE COLOR

TEMPERATURE= 180 F  TIME= 3 MINUTES

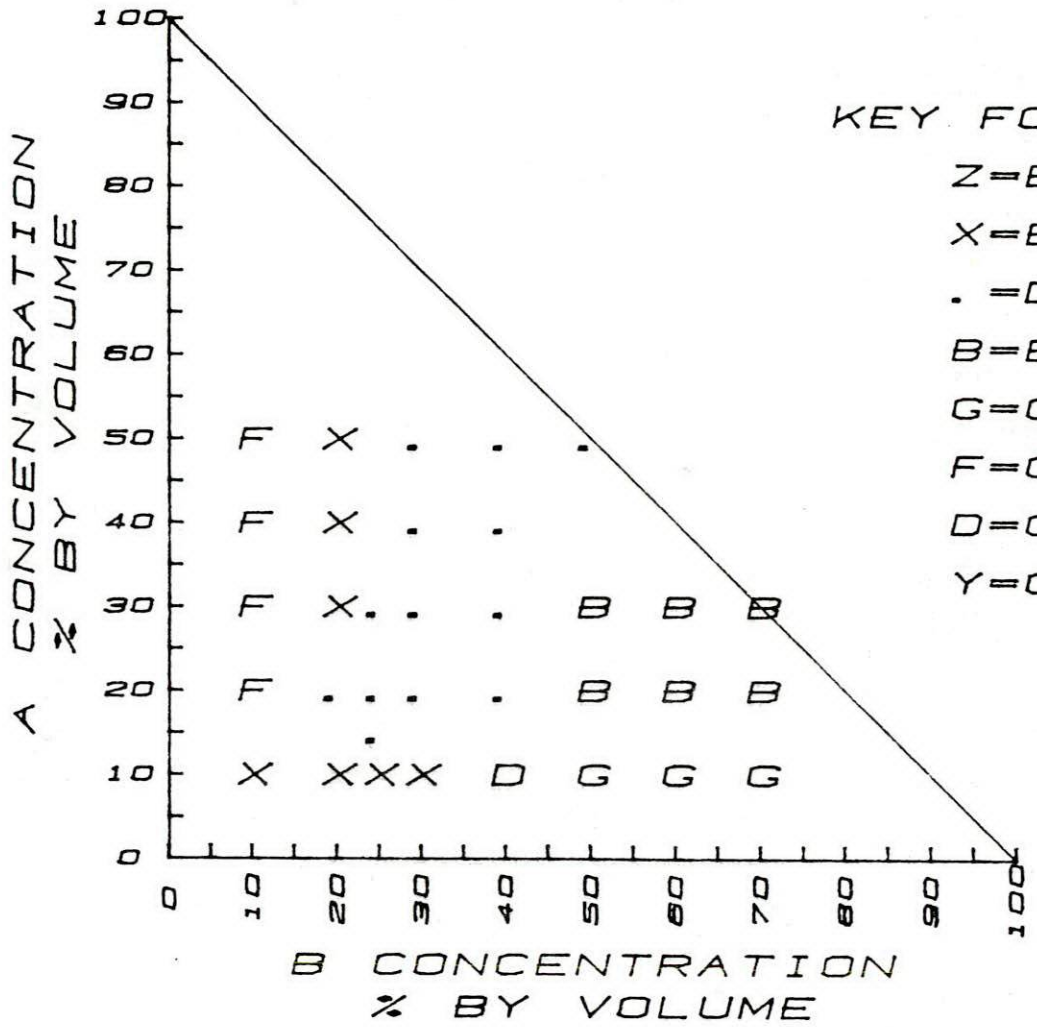


KEY FOR COATING COLOR

Z=BRONZE
X=BROWN
. =DARK BROWN
B=BLACK
G=GREY
F=GREY/BRONZE
D=GREY/BROWN
Y=GREY/BLACK

A=OXIDIZER
B=ALKALINE

FIGURE #5

# OXIDE COLOR

TEMPERATURE= 200 F  TIME= 3 MINUTES

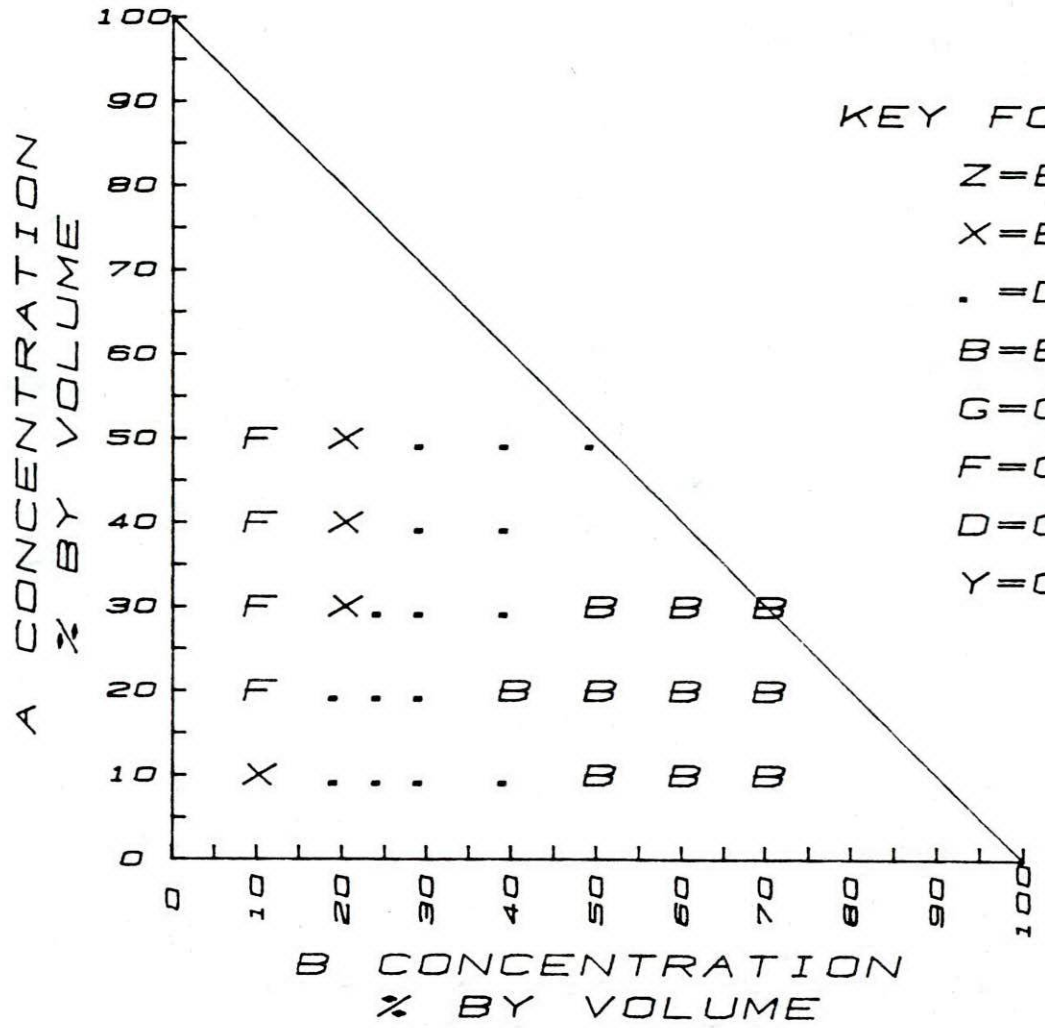


KEY FOR COATING COLOR

Z=BRONZE

X=BROWN

. =DARK BROWN

B=BLACK

G=GREY

F=GREY/BRONZE

D=GREY/BROWN

Y=GREY/BLACK

A=OXIDIZER

B=ALKALINE

FIGURE #6

G-3

# Electronics III
# Session G

## Plating-Thru Holes in Printed Wiring Boards Which are Restrained in the X/Y Direction During Thermal Excursions

Phillip E. Hinton
Hinton "PWB" Engineering
Tucson, AZ

# PLATING-THRU HOLES IN PRINTED WIRING BOARDS WHICH ARE RESTRAINED IN THE X/Y DIRECTION DURING THERMAL EXCURSIONS

Phillip E. Hinton
Hinton "PWB" Engineering
Tucson, AZ

Abstract: Printed wiring boards which contain materials which restrain the planar expansion or shrinkage during deviations from ambient temperature create some unique processing requirements. The restraining material which include Invar planes or quartz and aramid fibers produce construction requirements and a hole-wall structure which make necessary a different set of parameters for processing internal layers and preplate hole preparation for the electroless and electrolytic plating systems. Despite these difficulties, the process systems can be modified so that acceptable registration, interconnects and hole-wall plating can be effected.

## INTRODUCTION

Multilayer printed circuit boards which are designed so that their planar coefficient of thermal expansion (CTE) closely matches the coefficient of thermal expansion of surface mounted devices require some different processing techniques than are used in the conventional lead-in-hole printed boards. The most common of the materials employed in the industry to achieve a controlled thermal expansion are; quartz fibers, aramid fibers and copper-clad Invar planes. These materials are used in combination with epoxy resins, polyimide resins and resin impregnated glass cloths. The current methods of; (1) imaging, (2) laminating, (3) drilling, (4) hole prep and desmear, and (5) plating-thru must be modified in order to fabricate acceptable products when these non-conventional materials become a functional part of the board or circuitry. The conditions noted in the following paper were experienced during the manufacture of 6 and 8 layer multilayer boards using 0.013 to 0.020 inch dia. plated-thru via holes and represent several constructions. Figures shown are of Invar type boards only; photomicrographs of sections containing quartz and aramid are usually indistinquishable from the common epoxy glass sections.

## IMAGING and ETCHING

The materials from which the cured laminate is made must be the first consideration when implementing the imaging and etching plan. The multilayer construction is determined by the position and pattern density of the copper layers on the panel.

Quartz and Aramid: Both of these fiber composite materials have a lower CTE in their planar direction than the copper foil which is applied to both sides at the laminate supplier. When

the supplied clad laminate is at to room ambient conditions, the double clad laminate is relatively flat and amenable to imaging. However, if the imaging and etching process removes the surface copper so that the remainimg cladding is unbalanced from side to side then the nicely imaged and etched interal layer detail will emerge from the etcher in a tightly rolled tube; if it emerges at all and does not entangle in the etcher. Additionally, even if the copper image is balanced on both sides the residual stress relief when the copper is removed causes the internal layers to shrink in the planar direction. Usually more in the warp direction than in the fill direction dependent upon thickness of the dielectric layer.

A solution to the rolled-up interal layer is to make it with balanced metal layers. This can be partially accomplished by adding more copper to the lowest circuit pattern side of the internal layer. More difficult to balance is the externals and the first buried layers; therefore, it is more desirable to make the first buried layer a part of one of the internal layer details and apply the externals as cap-foil.

Pattern shrinkage of the interal layers after etching is a less easily solved problem since it is not predictable for each construction and is controlled by the amount of retained copper. However, if a similar border copper pattern is used for each interal layer, an artwork compensation is usually acceptable. The use of a thinner copper layer (1/2 ounce) imparts less residual stress and final dimensional change in the etched internal layer. A post bake at as high a temperature possible after making the laminate or prior to starting fabrication will decrease some of the post etch shrinkage.

Invar: Copper-clad Invar is a relatively stable material during imaging and etching and the conventional methods are utilized with either ferric or cupric chloride etchants. The galvanic differences between Invar and copper do cause undercutting of one or the other; use of the higher metal concentrations in the etchants reduce this effect but will slow etching time. The thickness of the material (0.005 to 0.010 inch) makes the relative time to etch the pattern in the Invar planes quite long. A dimensional change is experienced in the planar directions after laminating and requires artwork compensation as is discussed in the next section.

## LAMINATING

The three types of materials act quite differently during multilayer lamination and usually must have some compensation programmed into the artwork for boards with high density and small tolerance to pattern shift.

Quartz: The quartz fiber materials are most stable with some

shrinkage seen in the multilayer boards after laminating; the initial change after etching is of a larger magnitude. Boards made from quartz fibers systems usually require little or no artwork compensation if all internal layers are balanced and external copper is applied by the cap-foil method. Quartz fiber multilayer boards also will have less shift during laminating if a kiss cycle of about 25 PSI is applied and the temperature rate of rise is near 15 degrees F. per minute.

Aramid: The aramid fiber materials when used in the printed boards also exhibit shrinkage after laminating which often approaches 0.001 of an inch per inch. The shrinkage is increased by a large amount of retained copper pattern which seems to produce the destabilizing effect. The high amount of dimensional change seen during lamination of aramid boards almost always requires an artwork compensation in the initial patterning if hole pattern and registration limits are tight.

Invar: The laminated epoxy-glass boards with restraining Invar planes indicate that there is a pattern shrinkage in the Invar layers and a growth of the images previously generated on the epoxy-glass internal layers. For polyimide resin systems the difference in the growth and shrinkage is slightly greater than for epoxy-glass systems. The mismatch between the internal copper layers and the Invar layers after lamination is found to be from 0.0007 to 0.0012 inch per inch. This high mismatch condition is determined to be caused by the wide CTE difference between the copper/resin-glass laminate and the Invar material; at laminating temperatures the expanded planar images are quite divergent. At the temperature at which the Invar and glass-resin material are laminated together the image/pattern relative positions are frozen-in, when the panel is returned to room temperature the Invar layers are in compression and the copper/resin-glass layers are in tension. The stronger material will cause the other material to conform and cause a drill pattern misfit. Higher initial clamping pressures, 300 PSI, proposed to cause the resin-glass material to move with the Invar layers only caused an asymmetric pattern shift which seemed to start at one corner of the panel instead of being the perferred equidistant from the center; the B-stage when it melts seemed to act as a lubricant which allows nearly free expansion of the internal layer up to the Tg or softening point temperature of the resin binder. A lower laminating temperatures at 290 degrees F. for and initial resin hardening helps to decrease the mismatch for polyimide materials. After determining initial pattern shifts in the Invar and the resin-glass internals, a compensated artwork for one or the other of the materials is necessary.

## DRILLING

The drilling is again uniquely different for the three types of materials. Quartz systems with its harder reinforcement exhibits the greater difficulty and is the least manageable while the

other two offer problems, but conventional solutions are more available.

Quartz: The quartz reinforcement wears out carbide drills at a very rapid rate; about fifty hits between drill changes being about the best achieved with conventional feeds, speeds and drills. Drill wear is improved by using the lower speeds (35000 rpm) and lower feeds (0.001 inch per rpm) than are normally used with the glass reinforcements. Some improvement of drill life is seen with the diamond impregnated drills, 1000 to 2000 hits with quite good hole quality. Drill cost with the diamond drill is between 10 and 20 cents a hole or about 100 times the cost per hole with carbide drills and epoxy-glass multilayers.

Aramid: The aramid fiber reinforcement does not drill so that the hole quality is as acceptable as with the glass reinforced materials. Among the problems are high amount of fiberous residue in the hole; a tendancy for the drill to drift and a loading of the drill with the laminate materials. A method of drilling the hole in two steps will generally aid in all of these conditions if a good vacuum scavenging around the drill is maintained. The high fibrous residue remaining in the holes must be cleared at a later desmearing step, namely plasma.

Invar: Copper-clad Invar in the panel drills like a heavy layer of 3 to 7 ounces of copper foil. The drills load and the Invar extrudes and spreads at the hole-wall interface. A good vacuum vacuum scavenging and sharp drills are very important. Drill feeds should be 0.001 inch per rpm chip load with a speed of 50,000 rpm. Two step drilling shows some improvement in decreasing drill loading. Nail heading as measured will often be a high number but is very seldom a problem if a percentage of foil thickness is used for acceptablity criteria.

## HOLE WALL PREPARATION AND DESMEAR

At least one of the methods of hole-wall preparation is acceptable for each of the restained boards.

Quartz: The quartz fiber/resin systems are very similar to their equivalents in the glass system. Etch-back of the quartz fiber with the acid-fluorides compounds is somewhat slower than on the E-glass, perhaps due to a normally larger fiber size. Plasma, sulfuric acid, chromic acid and alkaline permanganates are used on epoxies while the polyimide systems are best desmeared with plasma and alkaline permangnates. Grit blasting the holes with one of the several machines on the market also decreases residual debris.

Aramid: Some reactions are seen with all of the desmearing agents on the aramid fibers but to reduce the high fiber residue in the holes and prevent the resulting roughness the plasma method is by far the most satisfactory. An oxygen burn out cycle

at the end of the regular plasma cycle aids in coverage by the electroless copper.

Invar: Copper-clad Invar due to high galvanic activty between the dissimilar metals creates several conditions which must be avoided or considered in the overall hole-wall preparation. Plasma being non-aqueous is very sucessesful for both epoxy and polimide systems when combined with Invar. A commonly used post-plasma clean with an alkaline permanganate may cause deep etchback in the Invar layers if chlorite compounds are used for permanganate regeneration (See figure 1); additionally, sulfuric acid or sulfuric acid and hydroxyl-amine sulfate solutions used to neutralize the permanganate will quickly pick up copper ions and deposit copper on the Invar layers as an immersion coating which must be removed prior to electroless coating. Concentrated sulfuric acid will also perform satisfactorly as an epoxy smear removal if kept fresh with very little water or copper ion contamination. Chromic acid also may be used on epoxy systems. The alkaline permanganates if used following plasma must be handled with care and any permanganate regenerative compound must not be reduced to a chloride or a large amount of Invar erosion will result.

## ELECTROLESS COPPER

The quartz and aramid systems can be electrolessly copper coated by the conventional methods, but the Invar system exhibits a more troublesome operation due to the dissimilar metal couple of the copper and Invar.

Invar: A micro-etch in the form of sulfuric-peroxide or acidified persulfate may be used to prepare the surface copper cladding and the copper foil interface for electroless copper; however, the dwell time must be short since a reaction occurs at the copper-Invar diffusion layer in less than thirty seconds and a "V" shaped etchout appears at this place. The micro-etch also deposits immersion copper on the Invar which must be removed or the hole-wall to Invar bond is weak and may show pullaway at microsection examination. (See figure 2).

A second microetch is necesssary to slightly etch the Invar and strip any immersion copper which may have be deposited on the Invar at the desmear neutralization step or the at the first microetch. For this second microetch either a cupric or a ferric chloride solution is used. Again a short dwell is necessary because both of these solutions will more quickly etch the copper cladding on the Invar faster than the Invar itself. An etchout of the copper cladding on the Invar 0.001 to 0.003 inch deep will result. The larger the the ratio of Invar to copper the faster the etchout. (See figure 3).

When using the conventional tin-palladium catalyst systems, the

catalyst predip and the palladium-tin catalytic system should not be a very low acid solution or poor Invar to electroless bond will result. Additionally, with the tin-palladium catalyst the accelerator should be the fluoroboric type in order to avoid a poor adhesion to the Invar. An electroless system which uses an alkaline catalyst and does not contain tin has been found to work very well with the Invar systems; however, the ferric or cupric pre-etch must also be used.

Electroless coppers plate onto the activated hole wall at a different rate on the Invar surfaces than on the copper surfaces or on the polymer. The higher deposition rate is often noted on the Invar when a bath is is on the high side of its activity. Copper whiskers up to 0.015 inch long by 0.0001 inch in diameter will sometime grow from the Invar; the whiskers plate up in the electrolytic bath and cause nodules which will almost clog the hole. (See figure 4).

## ELECTROLYTIC PLATING

With quartz and aramid fiber the plating process after the electroless may follow the conventional practices used for the glass fiber materials. With the Invar the extreme activity of the two dissimilar metals create some odd conditions which are not experienced with the single-metal board. If an electrolessly coated board is immersed in the acid-copper electrolytic solution without a voltage exceeding the couple voltage (about 0.55 volts) for as little as 30 seconds, a rapid undercutting of the Invar layers result. The undercutting can be up to 0.010 inch within about 5 minutes. (See figure 5). No such undercutting was found when the same conditions were presented to a panel in pyrophosphate-copper elelectrolyte.

Several reports have been circulated in the industry for the past few years in which boards with restrained growth/shrinkage in the x/y planes have had a reduced ability to withstand long term thermal cycling from -55 to +125 degrees celcius. Additional testing has confirmed these reports, but it is also been found that electrodeposits from acid-copper with low codeposited additive and pyrophosphate-copper from a non-additive bath will withstand may thousands of thermal cycles without barrel cracking or interconnect failure.

## SUMMARY

The processing of plated-thru hole multilayer boards which contain materials to restrain the thermal expansion or shrinkage in the planar directions is more difficult and costly than the FR-4 multilayer boards. However, within the present printed wiring board industry the methods, tools and chemistry are used and available to all fabricators and they can produce excellent results. (See figure 6).

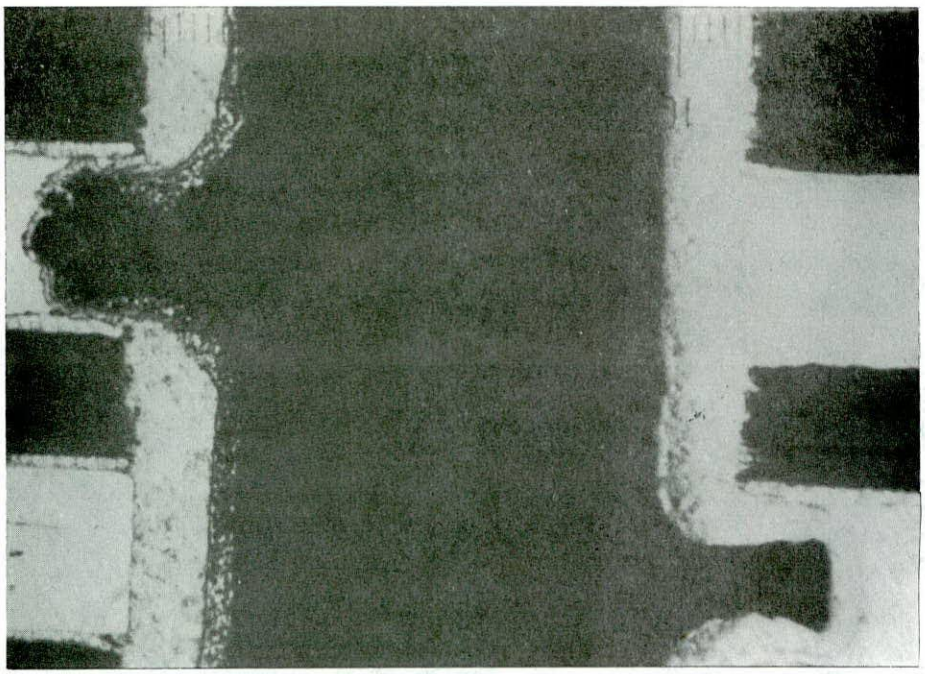

FIG. 1. HOLES ETCHED IN THE INVAR IN THE PERMANGANATE DESMEAR

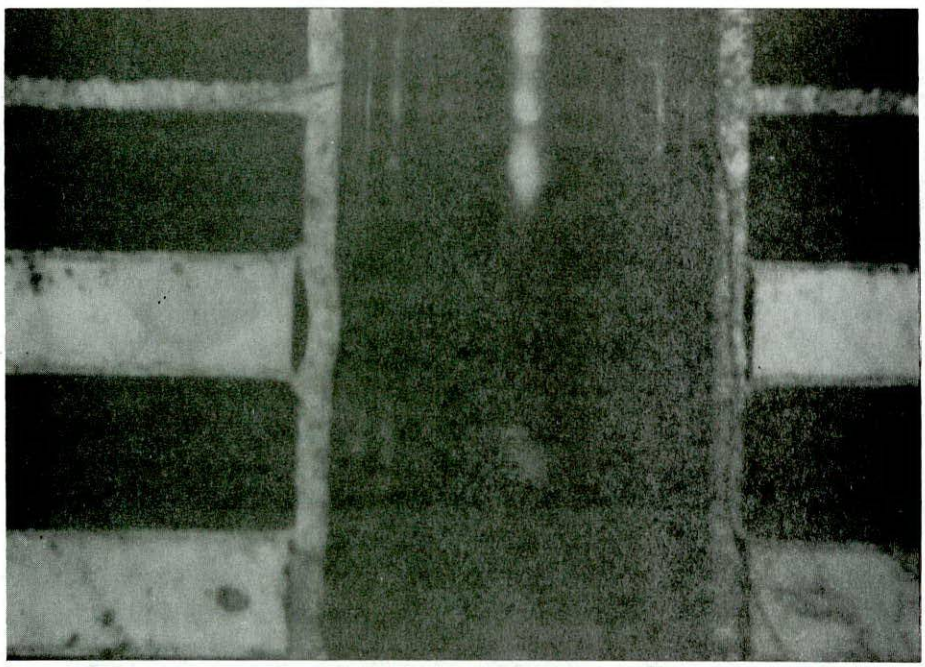

FIG. 2. SEPARATION OF THE COPPER PLATING FROM THE INVAR

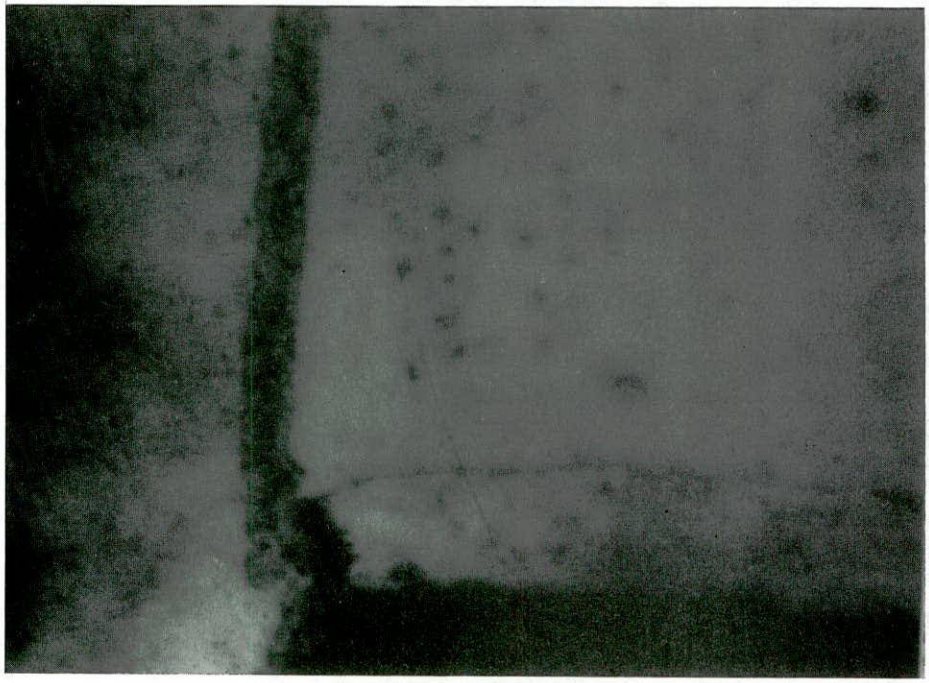

FIG. 3. ETCHBACK OF THE COPPER CLADDING ON THE INVAR IN CUPRIC CHLORIDE



FIG. 4. PLATED-UP WHISKERS THAT GREW OUT OF THE INVAR

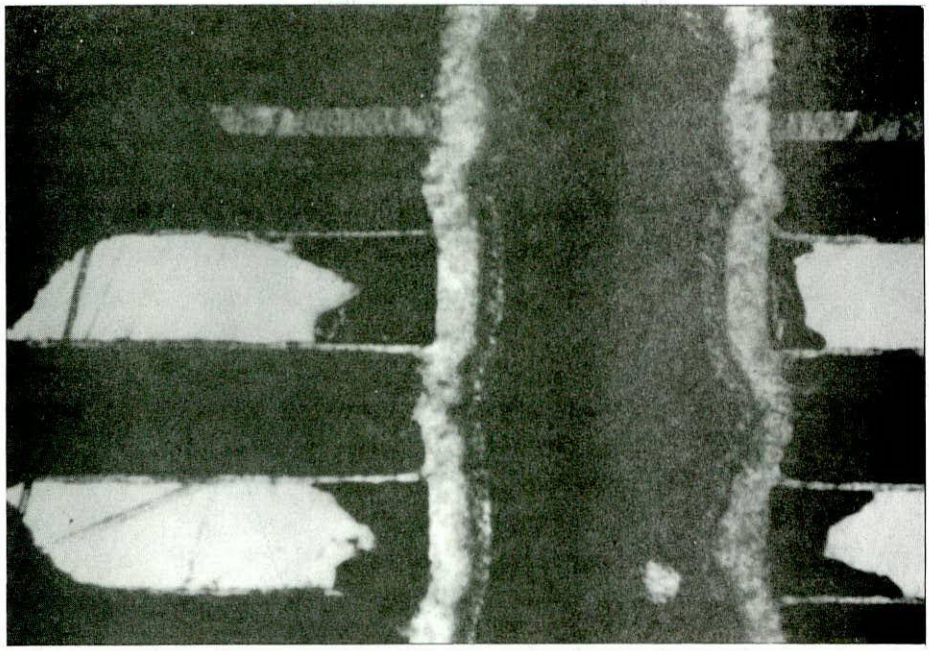

FIG. 5. ETCHOUT OF INVAR BY THE ELECTROLYTIC COPPER PLATING SOLUTION

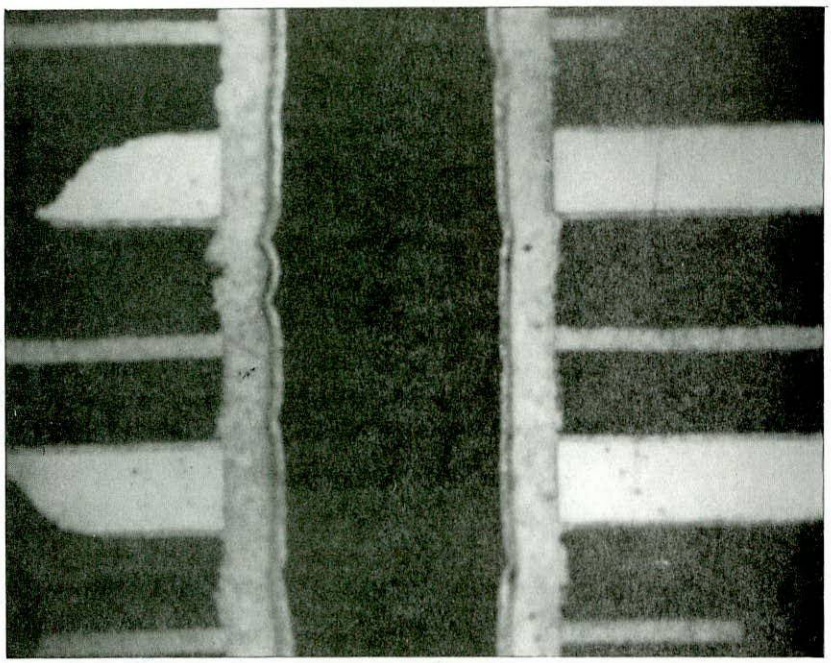

FIG. 6. PROPER HOLE PREP. AND ELECTROLESS COPPER TECHNIQUES PRODUCE ACCEPTABLE INTERNAL CONNECTIONS

G-4

# Electronics III
# Session G

## Automation of Plating Rack Loading for Printed Circuit Panel Electroless Processing

Donald P. Aupperle
Aupperle Associates, Inc.
6307 Seaview Ave., N.W.
Seattle, WA 98107

# AUTOMATION OF PLATING RACK LOADING FOR PRINTED CIRCUIT PANEL ELECTROLESS PROCESSING

Donald P. Aupperle
Aupperle Associates, Inc.
6307 Seaview Avenue N. W.
Seattle, WA 98107

*ABSTRACT*

Automated panel loading into and out of electroless plating racks is an integral part of a fully automated plating operation. Discussed here are a number of considerations that need to be addressed in integrating such automation into a plating facility. Emphasis is on planning for product flow, automatic process record keeping, control system requirements, rack handling options, and rack design. Photographs of scale models of systems being developed and installed are used to illustrate the points discussed. A brief look is also taken at loading of electrolytic processes.

## *Product Flow*

A fully automated plating line can be treated as a long conveyor with work orders flowing one after another through the line and on to the next process in a continuous first in, first out stream. Commonly, an incoming stack of panels will represent all or part of a work order. It is mandatory that this grouping remain the same after plating even though a given work order may be distributed over several plating racks, or a rack may contain panels from more than one work order. To accomplish this we need to look both upstream and downstream from the plating operation.

Upstream the panels need to be stacked on pallets, the panels always in the same orientation. In a fully automated facility a loaded pallet is brought to the plating line load station by conveyor or automatic guided vehicle. The panels are then removed from the top of the stack one at a time and fed to the loader. After plating, the panels are unloaded one at a time and restacked, but with the top panel now on the bottom. The pallets of plated panels are moved to the next operation by conveyor or AGV.

Layout planning of a facility must include space for moving loaded pallets to the load station, transferring empty pallets to the unload station, and moving plated product pallets away from the line. It is particularly critical to have space at the unload station for both empty and full pallets so there is a place to put panels exiting the plating line. Queue space at the load end is less critical but desirable. A plating line starved for parts is under-productive. A plating line stalled because of a downstream bottleneck will create scrap.

## *Automatic Code Reading*

Automatic reading of a hole pattern drilled near the edge of each panel to identify its part number, or work order number, is an integral requirement for a fully automatic load/unload system. As each panel approaches the load station, an on-the-fly reader provides this coded information to the loader control system.

The control system then compares this input with data provided by the facility host system to determine if the panel arriving is expected, and is a process match for the other panels being loaded. If all is in agreement, a data base is created representing the panels as they are loaded in each rack. This data base is then used by the plating line control system to tag any out-of-limit process information to a specific rack load of parts. At the unload station, a second panel reader confirms that the panels being re-stacked are as anticipated and that none have been inadvertently swapped at inspection stations or during manual backup loading.

Automatic panel reading makes it possible to generate accurate quality control and production records for each unit. This, combined with labor savings, can be the major justification for an automated loading system.

*Control System*

The controller used consists of a personal computer running a true multitasking operating system and communicating with the facility host system and other plating line controllers over an RS-232 network. Residing in a fresh-air pressurized cabinet at the load station, the PC provides a complete display and keyboard for communication with the operator. An optional printer provides hard copy records, reports, or listings as desired.

Because of the computing power available in the PC, it is used for decision making regarding the operation of the load system. Fault display, corrective actions required, re-routing of panels received out of sequence, and count and data base record keeping are all tasks assigned to the PC.

Security passwords allow access to the equipment programs by appropriate level personnel. Within the program all devices and steps are labeled with English names and descriptions. No external programming equipment is required, although the programs can be remotely generated and downloaded if desired. In contrast to programmable logic controllers operating with ladder logic, the personal computer based system is much more tolerant of interruptions in its cycle, can provide an interlock checking routine to prevent machine crashes during manual interaction, and can automatically sequence the machine to a safe starting condition after interruption.

*Rack Handling Options*

Two options exist for load/unload stations relative to a plating line. The first is for the plating line hoist to service the load station directly. The second is for the racks to be transported a short distance away from the line for loading.

Photos 4-6 represent the former arrangement. The major advantage of this configuration is that no intermediate rack handling equipment is required. The disadvantages are constricted space for product flow to and from the load station, and proximity to the corrosive chemistry environment. For longevity, sensitive components must be isolated from the corrosive atmosphere and the rest of the equipment built of corrosion resistant materials.

Photos 1-3 are of a remote system. Although the rack handling equipment is more complex, if it is combined with rack storage the additional equipment required is minimal. Careful attention must be paid to the rack exchange time as the load station becomes more remote. Because the rack loading time is typically paced by maximum panel delivery rates, delays in exchanging racks will decrease throughput.

Regardless of the arrangement chosen, precise rack positioning is required for automatic loading. A system working from coarse to fine provides the required precision in a series of steps. The large, heavy racks illustrated in photos 1-4 are, for instance, first placed on a platform with a resolution of $\pm$ 1/2". The platform can then be moved $\pm$ 1" to locate the rack against physical stops. The panel loading head or magazine has a limited amount of float so that it can take its final alignment directly from the rack. This third level of positioning accommodates for slight variations between racks and some inevitable distortion of the racks in production.

*Electroless Rack Design*

The throughput requirements for a line determine the rack capacity and configuration. Solution flow through the loaded rack determines the preferred panel edge guide orientation. The system in photos 1-5 all assume a solution flow of front to back (walkway toward hoist) and so are guided top and bottom, leaving the front and rear as open to solution flow as possible.

Edge guiding should be continuous. PC panel material bears an uncanny resemblance to an abrasive cut-off saw and its effect on a stainless steel rack is similar. Therefore it is recommended that the weight carrying surface on which the panels slide be of large area and easily replaced. A rack design has evolved where the functions of panel support and panel guiding are separated. Panel supports are heavier, intermittent, and anchored in machined details within the rack structure for dimensional control. The guides are light and open to reduce surface area and promote drainage.

The rack frame requires open sides so that the unload mechanism can reach in to push the panels out. Frame structure must be sufficient to withstand production handling both on and off the line, yet minimized for low thermal mass and surface area. Automatic loading demands close dimensional control between individual racks. Hand loaded racks can vary by several inches but automatically loaded racks must be alike. Critical dimensions need to be determined by machining operations and not by welding alone.

The electroless racks illustrated are for constant panel sizes, of self supporting panel thicknesses (1/16" and greater). Varying panel sizes and thinner, inner layers can be accommodated with more complex racks. As rack complexity increases so does the ratio of incidental plate-out relative to the product plating. As panels decrease in size this ratio also increases. The cost of stripping and recycling this material is another factor in determining optimum panel sizes.

*Rack Loading Systems*

Two options for loading racks are illustrated in the accompanying photos. The first system, shown in photos 1, 2, and 4 uses an intermediate magazine that is pre-loaded at the maximum panel delivery rate. While this is occurring the rack is being positioned for loading. The magazine is then brought into contact with the rack and an entire section of

the rack is filled at one time as the panels are pushed from the magazine into the rack. As the rack is moved to load the next section the magazine is refilled. This "parallel processing" saves a considerable amount of time in a load cycle, and has been found necessary to meet throughput requirements where the rack has more than one section. To supply this parallel system, the feed of panels to the loader must be continuous. The system illustrated utilizes a semi-standard panel "unstacker" with two pallet handling sections to provide this continuous flow of panels while exchanging pallets.

Unloading is done in essentially the reverse order. Panels are pushed from the rack into a magazine, and then fed singly to a dual panel stacker.

The second system, illustrated in photo 5, directly loads one panel at a time into a single section rack. This system is simpler and is recommended when throughput requirements are low enough to permit its use. Unloading this rack must be done from the opposite side to preserve the first in, first out order.

*Automatic Loading For Electrolytic Process*

Photo 6 shows an adaptation of a single panel, direct loading mechanism to an electrolytic rack. Although it illustrates a single panel rack, any production system that could justify automatic handling would require a 2x2, 2x3 or larger matrix. Ideally the product flow would be normal to the axis of the line with two tiers of panels moving through the rack at a combined load/unload station. This arrangement permits minimum cycle time while preserving the first in first out sequence.

*Conclusions*

As panel plating facilities become more automated, automatic loading and unloading of racks will take its place along side automatic hoist control and automatic process control as a cost effective system. Planning for automation of the load and unload operations must take into account the product flow both upstream and downstream of the plating line.

Prerequisites for a successful installation are: a well defined panel coding and reading system; a host computer system to manage flow through the facility; a loader control system smart enough to do record keeping, decision making, and communicate with both the host and other equipment controllers; and racks designed for automatic handling.

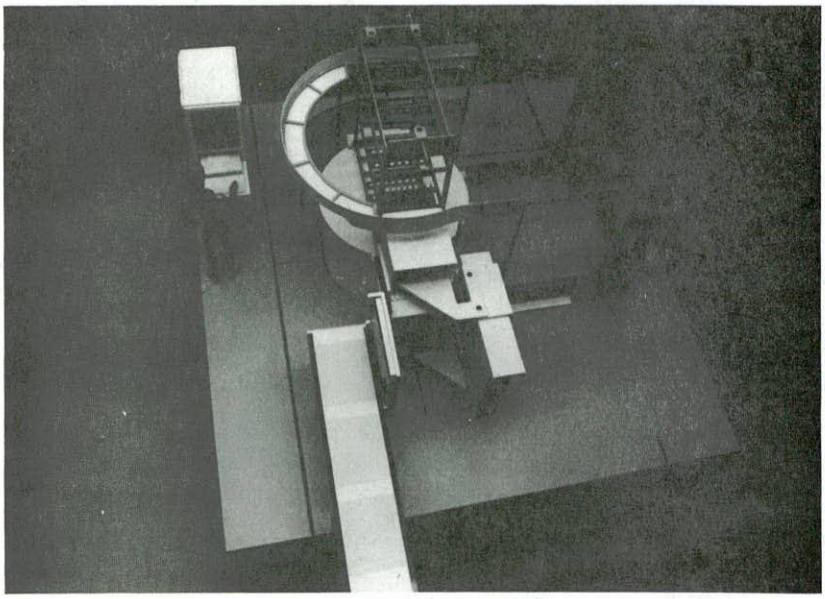

Photo 1

Birds eye view of remote load station - Rack has been raised off rack cart and the cart withdrawn to the right. The first quadrant is being loaded from the accumulating magazine as the pusher transfers the panels into the rack.

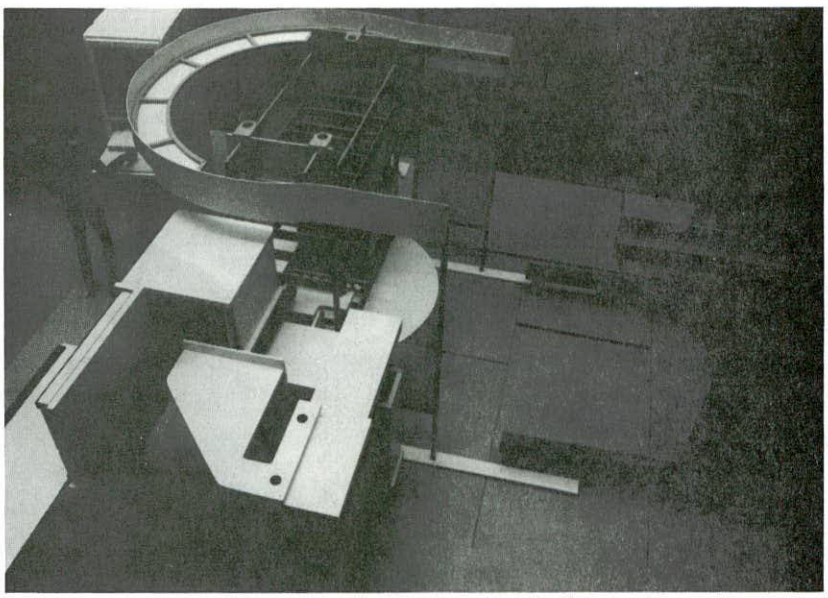

Photo 2

Rack positioned for loading third quadrant - The magazine is nearly filled with panels arriving on the conveyor at the lower left.

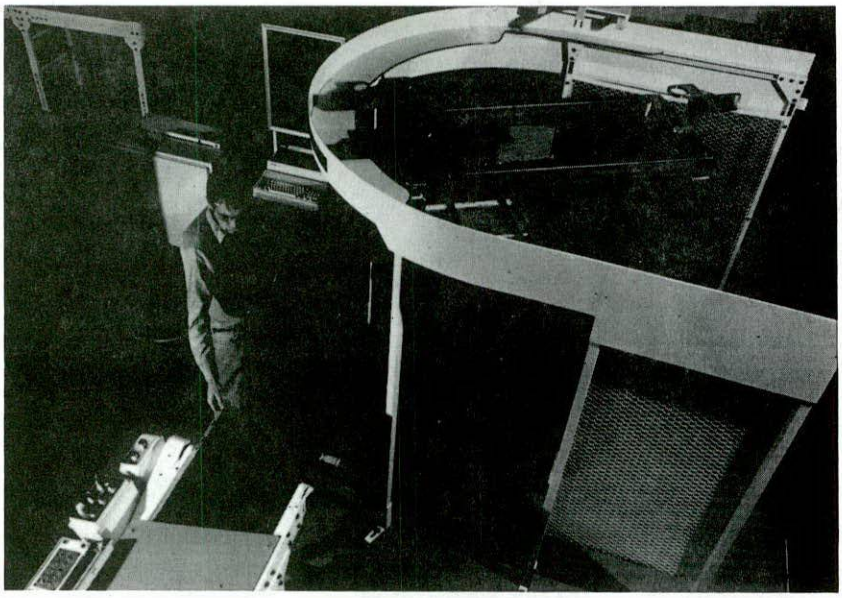

Photo 3

Similar viewpoint to photo 2 - This is the actual machine prior to installation of the loading magazine. Note that the rack is positioned for manual loading of panels. This feature is retained in the automatic system as a backup.

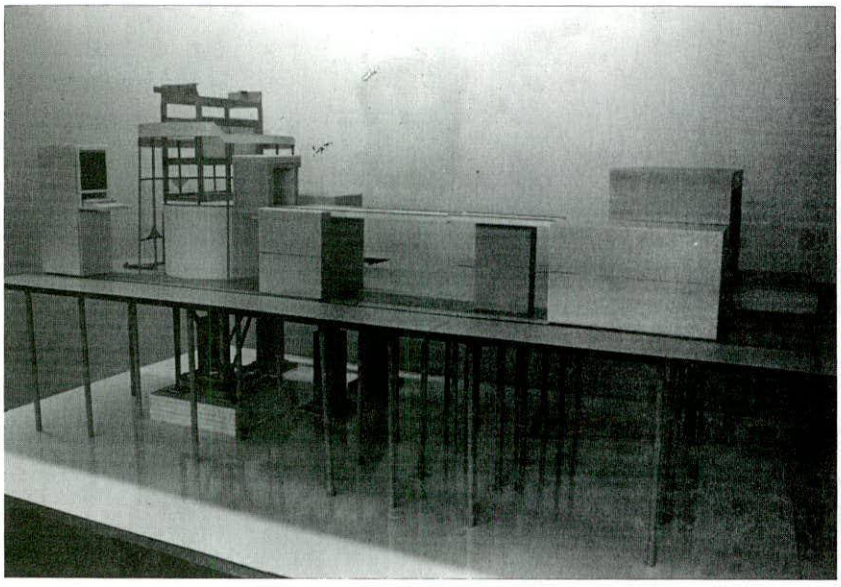

Photo 4

Unload station served by plating line hoist directly - Lift is in the up position. Rack is oriented as it would be left by the plating line hoist running left and right . Structures below the chemical grating are part of the lift mechanism and piers that support the plating line framework. Unit to the right is a dual panel stacker served by an AGV.

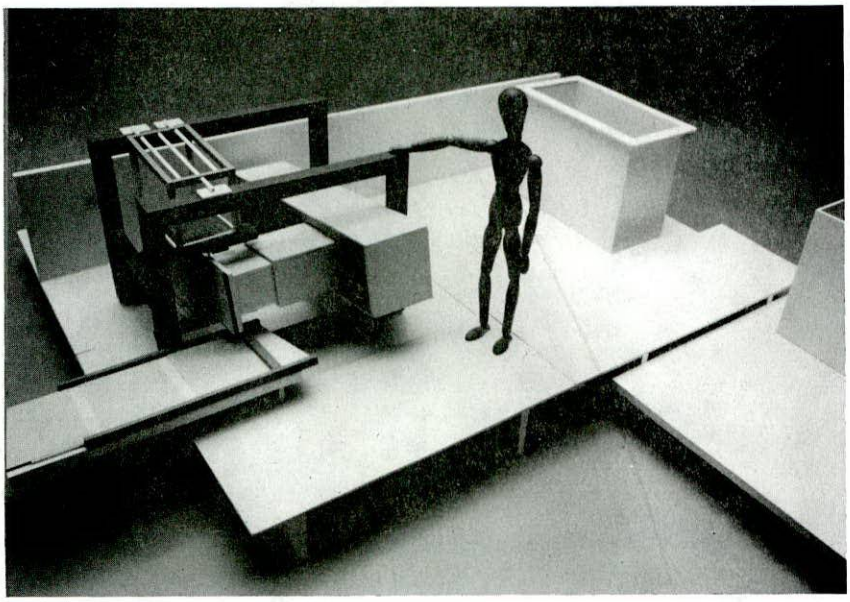

Photo 5

Direct loading machine for smaller electroless system - Rack is delivered to the load station by the plating line hoist. Panels arrive on the conveyor at the left. Space between the load machine and the first tank behind the figure is queue space for racks. Model is of a "U" shaped plating line. A similar mirror image machine will be placed across the walkway in the foreground as an unload machine.

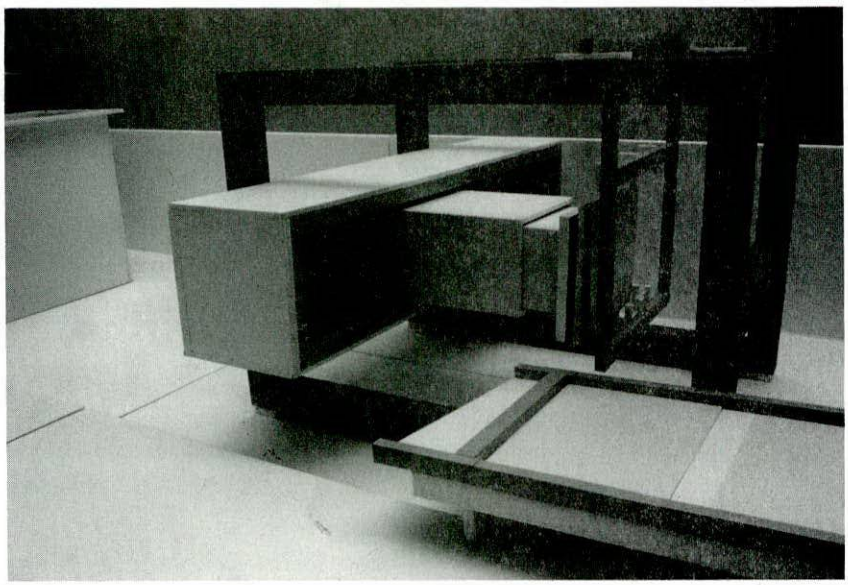

Photo 6

Conceptual arrangement for an electrolytic rack loader - Equipment developed for electroless panel handling can also be used for loading an electrolytic line. The model shown illustrates a single panel rack. Production racks would be multiple panel.

G-5

# Electronics III
# Session G

## Gold Processes for Plating Printed Circuit Boards Processed with Fully Aqueous Resist

Dr. John Deuber
Degussa Corp.
South Plainfield

Dr. Hans-Joachim Luebke
Degussa AG
Schwaebisch Gmuend
West Germany

Dr. Franz Simon
Degussa AG
Schwaebisch Gmuend
West Germany

# GOLD PROCESSES FOR PLATING PRINTED CIRCUIT BOARDS PROCESSED WITH FULLY AQUEOUS RESIST

by

Dr. John Deuber
Degussa Corporation
South Plainfield

Dr. Hans-Joachim Luebke
Degussa AG
Schwaebisch Gmuend
West Germany

Dr. Franz Simon
Degussa AG
Schwaebisch Gmuend
West Germany

## Abstract

Plating printed circuit boards processed with fully aqueous resists with the traditional acid gold electrolytes is problematic due to hydrogen lifting of the resist. This paper describes three novel gold electrolytes that plate at high efficiencies thereby avoiding the hydrogen lifting problem. Discussed are electrolyte operation and deposit properties. Special attention will also be paid to the influences of normally encountered impurities on the operation of the electrolytes.

## Introduction

Ever since gold has been plated on circuit boards, changes in technology have impacted the type of gold processes used. Years ago the hot cyanide gold electrolytes, common in the jewelry industry for heavy plating, were found to be totally useless by the printed circuit board manufacturers. These systems yielded deposits with inadequate wear resistance and the alkaline nature of the electrolytes attacked not only the laminate, but also the plating resists themselves. The first silver gold electrolyte introduced in the late 1950's was a step in the right direction. The deposits plated with this system, even though they represented an improvement, still gave insufficient wear protection. Again, in the late 1950's a major breakthrough took place

when it was discovered that potassium gold cyanide is stable in acidic systems down to pH values approaching three. It was also found that the addition of small amounts of salts of cobalt, nickel, and/or indium to a gold electrolyte buffered with an organic acid/salt matrix, capable of complexing the base metal, would result in bright hard deposits when electroplating was accomplished at pH 4, room temperature and 10 amps per square foot. Deposits from these systems gave the printed circuit board manufacturers the wear resistance and constant, low contact resistance that they required. Also, the electrolyte did not attack the plating resists or laminates that were used to manufacture printed circuit boards.

With the rapid growth of the printed circuit board industry, it soon became obvious that these electrolytes were much to slow to satisfy the throughput requirements of that industry. At 10 amps per square foot, it took more than ten minutes to plate the then specified 100 microinch thickness. In order to achieve faster plating rates, some users in the industry resorted to increasing gold concentrations to levels sometimes in excess of four troy ounces per gallon and working at elevated temperatures and higher current densities. It therefore became possible to reduce the plating time from more than ten minutes to less than three minutes for the required 100 microinches. However, working at these high concentrations was costly, especially when the gold price escalated in the late 1970's and problems with solubility were encountered.

These efforts were complimented by the introduction of the bottom anode tab plater, which made it possible to process the tabs on many boards simultaneously in one apparatus. These bottom anode tab platers gave the printed circuit board manufacturers the throughput requirements that were necessary to maintain their elevated production levels. However, they were pigs as far as gold consumption was concerned. This equipment plated the maximum gold thicknesses on the bus bar, which was later sheared from the board and the lower end of the tabs rather than the middle of the tab where the thickness was measured. Due to this waste, printed circuit board manufacturers looked to other types of equipment to plate their tabs. What they found was the first automatic tab plater which was introduced into this industry almost ten years ago. When the first automatic tab platers were introduced, they still required elevated gold concentrations sometimes in excess of three troy ounces per gallon to achieve the then required plating rate of 100 microinches of hard gold in 30 seconds. Shortly after the introduction of this type of equipment, the first truly high speed cobalt

and iron gold plating processes were introduced into that industry. It was now possible to plate the required 100 microinches of hard gold in 30 seconds with a gold concentration of only 1.5 troy ounces per gallon.

Further developments in the printed circuit board industry led to circuit board designs that did not lend themselves to being processed on tab platers. The tabs had to be plated on the full panel with the other areas masked off. Adaptation of the new high speed gold electrolytes to this type of plating, yielded a system that would plate at twenty amps per square foot, but require only 0.5 troy ounces per gallon of gold. Not only was the gold concentration reduced here decreasing drag out losses and investment costs, but these electrolytes yielded better plate distribution then their forerunners. These systems worked well until the introduction of fully aqueous resists. The hydrogen gassing action of these systems, which had proven beneficial working with solvent resists, resulted in undercutting of the fully aqueous resists and the subsequent scrubbing action cleaned these resists right off the circuit board. A new type of gold electrolyte had to be developed to accomodate fully aqueous resists.

The fully aqueous resists were introduced because of problems that the chlorinated solvents, used to strip solvent resists, had on the environment. The desire of the printed circuit board industry was the elimination of these solvents. The way this was accomplished was the development of first semi- and finally fully aqueous resists which are strippable with alkaline aqueous solutions. Unfortunately, advances in an industry are many times accompanied by unwanted disadvantages. In the case of the fully aqueous resists, the disadvantage was that the acid gold electrolytes used to plate tabs on boards stripped these resists. The stripping phenomenon is based on two factors. First, the higher the pH of the solution, the weaker is the bond to the substrate. The second factor, which appears to be the more predominant one, is the undercutting of the resist by the hydrogen gassing. In the case of boards processed with solvent resist, the hydrogen gassing was beneficial in that the scrubbing action enhanced the adhesion of gold to the nickel underplate eliminating the need for a gold preplate; but in the case of boards processed with fully aqueous resists the hydrogen gassing must be drastically reduced or if possible totally eliminated. There are essentially two methods of accomplishing this. The first is to modify the chemistry of existing gold baths which utilize either cobalt or nickel hardening agents so the plating efficiency is increased and the hydrogen gassing reduced. The second method would involve developing a

totally new electrolyte which plates at close to the theoretical 100% cathode efficiency, eliminating hydrogen gassing. This would be possible because these electrolytes would not contain the traditional hardening agents such as cobalt or nickel which generally reduce plating efficiencies. The rest of this paper dedicated to these two types of systems.

## Modified Cobalt and Nickel Gold Electrolytes

Increasing the operating pH of cobalt and nickel gold electrolytes will also increase the cathodic plating efficiency. Unfortunately, an increase in pH will also result in the dulling of the deposit appearance, usually before that point at which the efficiency is sufficiently high to eliminate hydrogen lifting. What is needed here is a bright range extender to prevent the dulling of the deposit appearance and an accelerator to further increase the cathodic efficiency thereby reducing the hydrogen gassing effect. Inclusion of these two additives in cobalt and nickel gold electrolytes will result in systems that are operable under conditions and yielding the plating rates indicated in Table 1.

Deposits from these electrolytes exhibit a hardness in the 130-200 KHN range and a gold purity in excess of 99.7% which allows them to meet the requirements of Mil G 45204B Type I, Grade C and Type II, Grade C. Because these deposits also possess excellent wear resistance and a low, constant contact resistivity, they are ideally suited for the plating of printed circuit board edge contacts (tabs). The deposits from these modified electrolytes exhibit less stress cracking than is encountered with many of the traditional nickel and cobalt golds. This is evidenced by the fact that hardness coupons can be plated in these electrolytes to thickness in excess of 1 mil without the formation of stress cracks visible to the naked eye. Because these systems plate at cathodic efficiencies approaching 70%, they can be utilized to plate most printed circuit boards processed with fully aqueous resists. Obviously the type of resist utilized and the manner in which it has been processed is a prominent factor in the successful gold plating of boards using these resists. In general, the thicker resists, in excess of 2 microns, can be processed with these electrolytes with little or no problems. Other meaningful factors are the age of the resist, the preplate operations, as well as the thicknesses of copper and nickel that have been deposited prior to plating the gold. The one disadvantage of these modified gold electrolytes is, because of their high cathodic efficiency, one can encounter

adhesion problems to the nickel undercoat. To avoid this the nickel deposit must be activated non-electrolytically and sometimes a gold preplate must be included prior to depositing the hard gold. Unfortunately, the use of the preplate will enhance the lifting of the resist; so its usage must be limited to providing the absolute minimum thickness needed for adhesion purposes.

## High Efficiency Gold Electrolyte Without Nickel or Cobalt Hardening Agents

As indicated previously, cobalt and nickel tend to decrease the cathodic efficiency of gold electrolytes. Therefore, the driving force here is to develop a new system utilizing a brightener which hardens the deposit, but does not decrease the plating efficiency. A system giving these characteristics was developed and operates under the conditions yielding the plating rates indicated in Table 2.

Deposits from this electrolyte exhibit a hardness of 250 KHN and a gold purity in excess of 99.9% enabling them to meet the requirements of Mil G 45204B Type I Grade D and Type II Grade D. Inspite of this relatively high hardness, these deposits possess excellent ductility which eliminates the fear of stress cracking when tabs are routed. The deposits also possess an extremely low contact resistance, however, their wear is inferior to those of deposits plated in the traditional cobalt and nickel gold electrolytes. The wear resistance can be enhanced by top coating these deposits with either the cobalt or nickel gold previously mentioned in this paper.

Because the plating efficiency of 110 mg/amp minute is 90% of theoretical value, these electrolytes operate with almost no hydrogen gassing. Because the hydrogen gassing effect is the main factor that causes lifting of resists, this electrolyte is the most ideally suited one for plating boards processed with fully aqueous resists, in spite of the pH value of the bath being 6.

In general, prior to using a new electrolyte in production, the effects of commonly encountered impurities must be determined. In the event that these impurities are harmful, their removal potential should also be investigated. Impurities that one would anticipate to contaminate a gold bath utilized to plate printed circuit boards are lead, iron, copper, nickel and possibly zinc. The effects of critical concentrations of these impurities on the gold electrolyte and removal potential are listed in Table 3.

Deposits from the high efficiency electrolyte exhibit other interesting properties. Due to the ductility of the deposit and the fact that those deposits possess low internal stress, it is possible, many times, to plate with this electrolyte directly over nickel without the use of a gold preplate. Nevertheless, the preplate is advantageous in case passive nickel is encountered.

## Conclusion

Throughout the development years of printed circuit boards, gold electrolytes have been successfully modified to satisfy the end point requirements of the printed circuit board manufacturers, and to operate with a minimum waste of gold. The lastest innovation in the printed circuit board industry, which specifies the use of fully aqueous resists, has rendered the more traditional gold electrolytes totally unsatisfactory. This is due to the fact that the hydrogen scrubbing action, which accompanies gold deposition, will undercut and lift these resists. Once again, novel gold electrolytes have been developed which resolve this problem and also meet the end point requirements of the printed circuit board industry.

## TABLE I

## OPERATING PARAMETERS AND PLATING RATES

## FOR MODIFIED COBALT AND NICKEL GOLD ELECTROLYTES

| | Recommended | Range |
|---|---|---|
| Metallic Gold Content | 1.0 tr. oz./gal (8.2 g/L) | 0.75 - 1.5 tr. oz./gal (6.1 - 12.3 g/L) |
| pH | 4.7 | 4.5 - 4.9 |
| Specific Gravity | 14°Be (1.11 g/cc) | 12° - 19°Be (1.09 - 1.15g/cc) |
| Bath Temperature | 90°F (35°C) | 86° - 104°F (30°-40°C) |
| Current Density | 10 ASF | Up to 20 ASF |
| Anodes | Platinized titanium | |
| Agitation | Vigorous solution flow is required | |
| Filtration | Continuous through Dynel or polypropylene cartridges | |
| Plating Rate | 80 mg/amp-min at 10 ASF pH 4.7 and 1.0 tr. oz./gal gold concentration | Up to 85 mg/amp-min |
| Gold Consumption | Approx. 1 tr. oz. gold per 400 amp-min at 10 ASF, ph 4.7 and 1.0 tr. oz./gal gold concentration | 1 tr. oz. gold for every 350 to 600 amp-min |
| Time to deposit 40 microinches (1 micron) | 2.5 min at 10 ASF pH 4.7 and 1.0 tr. oz./gal gold concentration | As low as 1.3 min |

## TABLE II

## OPERATING PARAMETERS AND PLATING RATES FOR HIGH EFFICIENCY GOLD ELECTROLYTE

| | Recommended | Range |
|---|---|---|
| Metallic Gold Content | 1.0 tr. oz./gal (8.2 g/L) | 0.8 - 1.25 tr. oz./gal (6.5 - 12.3 g/L) |
| pH | 6.0 | 5.8 - 6.2 |
| Specific Gravity | 10°Be (1.074 g/cc) | 8° - 14°Be (1.058 - 1.106 g/cc) |
| Bath Temperature | 125°F (52°C) | 120° - 130°F (49°-54°C) |
| Current Density | 8 amp/sq. ft. | |
| Anodes | Platinized titanium | |
| Agitation | Vigorous solution flow is required | |
| Filtration | Continuous through Dynel or polypropylene cartridges | |
| Plating Rate | 110 mg/amp min | |
| Gold Consumption | Approx. 1 tr. oz. gold per 285 amp-min | |
| Time to deposit 40 Microinches (1 Micron) | 2.2 min at 8 amp/sq. ft. | |

TABLE III

EFFECTS OF IMPURITIES ON HIGH EFFICIENCY GOLD BATH

| Impurity | Critical Conc. mg/L | Effect | Percent Removable |
|---|---|---|---|
| Lead | 2 | Brown Deposits | 50% |
| Iron | 200 | Drop in Efficiency | No Method |
| Copper | 30 | Red/Brown Deposits Drop in Efficiency | 55% |
| Nickel | 350 | Drop in Efficiency | 60% |
| Zinc | 50 | Green Deposits in High CD | 80% |

H-1

# General Interest
# Session H

## Increasing the Crack Resistance of Porous Anodic Oxide Films on Aluminium

Dr. Xavier Albert Ventura
Electroplating Consultant
Camprodón, 1 - 08012
Barcelona, Spain

# INCREASING THE CRACK RESISTANCE OF POROUS ANODIC OXIDE FILMS ON ALUMINIUM

Dr. Xavier Albert Ventura
Electroplating Consultant
Camprodón, 1 - 08012 Barcelona, Spain

## Abstract

The feasibility of strengthening anodic oxide films by limiting or preventing the growth of films cracks was investigated. Oxide films were subject to internal stresses caused by a variety of factors, including the presence of metallic impurities in the aluminium, conditions of anodization and film thickness.It is thought that these internal stresses influence the growth of cracks resulting from stretching of the film.

The appearance of cracks in the anodic oxide film is accompanied by an increase in stick-slipping, peeling of the film and adhesion wear on the exposed metal. This paper consists of an examination of internal stresses in optimization process of anodic oxide films. It is followed by a discussion of how internal stresses may be reduced and crack resistance increassed.

## Internal Stresses in Anodic Oxide Films

Based on existing literature on the measurement of internal stress in anodic oxide film (1), (2), (3), measurements were made in a similar manner using the curvature produced in Al foil specimens with anodic oxide films grown on one side.

## Parameters for Anodizing

1. Energy per micra of thickness

$$E_1 = \frac{V\ I\ t}{-S_1\ 3600} \quad wh/m^2$$

2. Energy per gram of anodic coating

$$E_2 = \frac{V\ I\ t}{3600\ P} \quad wh/gr\ Al_2\ O_3)$$

3. Anodic efficiency

$$R = \frac{60\ e}{0.4\ D\ t} \times 100\ \%$$

4. Apparent density

$$D = \frac{P}{eS} \text{ gr/cm}^3$$

5. Coating ration CR'

$$CR = \frac{P}{P_1}$$

6. Current efficiency

$$R_e = \frac{P_1}{96500\ I\ t} \times 100\ \%$$

V = Mean anodizing voltage
I = Mean anodizing current
t = Anodizing time, in seconds
$S_1$ = Anodized surface is expressed in $m^2$
e = Mean thickness is expressed in mm.
D = Current density, in $A/dm^2$
P = Anodic coating weight is expressed in grams
$P_1$ = Dissolved aluminium weight for anodic coating formation is expressed in grams

Experimental

Using fully annealed 95.5 % pure aluminium foil 50 in thickness, anodic oxide films 2 µm to 32 µm in thickness were grown on one side.

Anodization was carried out in a 180 gr/l solution of $H_2SO_4$ at a temperature of $18^{\pm}$ and an anodic current density of 1.5 to 3.5 $A/dm^2$.

Anodic Oxidation

Unlike the electrocoating processes in which the layer increasses toward the electrode outer part of the metal and there in anodic oxidization the layer growth is toward the inner part of the metal and therefore consuming it.

If we concentrate on the faradic conversion of Al to oxide we observe that for each gram of metal consumed, 1.889 grams of oxide is obtained. The coating relation is defined as the oxide amount formed per gram of reacted aluminium which experimental value double weighting measurement show us the efficiency of the anodic process

The classification of the anodized layer during the formation process can be made in accordance with the dissolvent amount of

the electrolyte in that layer.

A -Non-porous layer. B -Porous layer

Non- Porous Layer

The non-porous layers are those wich do not retain dissolvent in the formed oxide layer and therefore are compact, dielectric and thinner. The layer tickness initially depends on the applied potential and temperature. In a dielectric enviroment, if the potential applied is high enough a strong discharge is produced,thus perforating the layer. We call this effect layer's breakage. The electrolytes causing this type of breakage are aqueous dissolutions of borates, tartres, succionates, citrates, phosphates and carbonates. The breakage potential for the non-porous layers oscilates between 500 and 700 V. and refers to thickness between 7,000 to 10,000 Å. If the applied potentials are lower, the current's density becomes almost zero and the layer's growth is gradually slowed down until becoming non existening.

The velocity formation in the initial layer increases lineally in relation to the current density and the coating relation value is near to the theoretical value of 1.889 as for process that has not secundary reactions.

Porous Layer

Porous layers are those which do not hold dissolvent in the formed oxide layer. They are gelatinous and therefore thick and soft.In the porous layer the coating relation has a value of 1.35 to 1.46 due to the existing competitive effect of dissolution against that of oxide formation. The porous layer because of its physical characteristics cannot serve the purpose of being a protective layer. The insolubility if the porous layers is achieved through sealing. This seems to transform the superficial layer in small crystallines nuclei of hydratated oxide which several authors believe to be boehmite. However, most probably what happens is the formation of a defective variety of pseudoboehmite $Al_2O3$ x $H_2O$. (x between 1.8 to 2.5).

Dissolving Electroliytes of the Aluminium Oxide Layer

In this case, the growing layer is competing with the dissolution of the superficial layer. In coatings achieved in this way, two layers can be differentiated:

The first -in touch with the metal- presents the sames characteristics as a non-porous layer of thickness 100-700 Å.

The second, belongs to the type of porous layers and its thickness varies between 100-700 Å.

The second, belongs to the type of porous layers and its thickness varies between 1 $\mu$ and 30 $\mu$ for a thin, porous film and 100 $\mu$ for a thick, porous film.

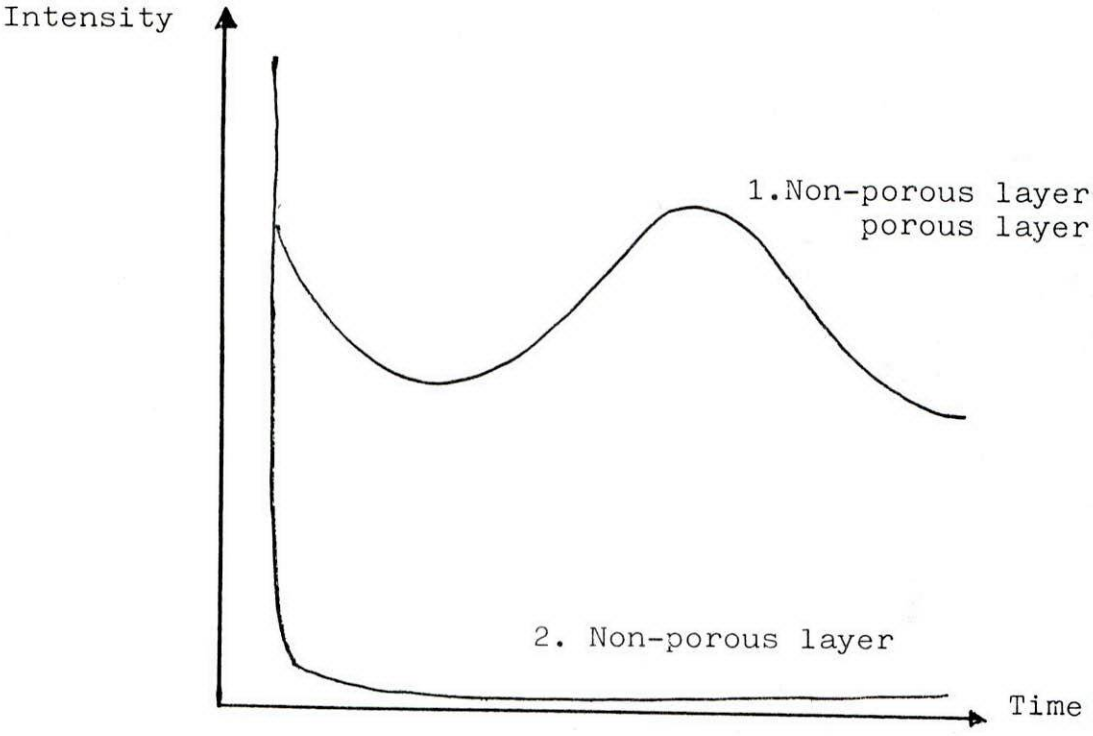


Process 1, is that of forming a non-poroues layer and as its thickness increases, so does its resistance, because it is dielectric and therefore intensity decreases until practically becoming nule.

In process 2, both layers are formed. Initially the formed layer is non-porous and because of it, the obtained curve is similar to the previous one but goes inmediately through a maximum due to the formation process of the porous layer and both in competition with their dissolution reach a point in which become equally even and from then on their intensity remain constant.

## The Electric Double Layer

Between two phases in contact, an electrode dipping into an electrolyte, there will normally be a difference in potential and an accumulation of net charges on each side of the interface.

The two charges are equal but of opposite sign, and it is usually called the electric double layer.

The system will act as a capacitor with a certain double layer capacitance $C_d$, 1, which can be measured.

The double layer capacitance is directly related to the charge q of the double layer, and to the interfacial tension $\gamma$

$$C_{d,1} = \frac{\delta q}{\delta E} = - \left(\delta^2 \gamma / \delta E^2\right)$$

The relationship between double layer capacitance and interfacial tension is valid as long as there is no charge transfer across the double layer.

Such transfer may give rise to an extra accumulation of charge and a corresponding pseudo-capacitance. Information on double layer phenomena is thus obtained from double layer capacitance as well as interfacial tension data.

Double layer capacitance can be determined by ac impedance measurements, from the capacitative part of the impedance at high frequencies.

An alternative method is the galvanostatic pulse method, where the slope of the initial rise of potential is directly related to the double layer capacitance.

$$C_{d,1} = i/dE/\ dt$$

Interfacial tension is measured as a function of potential by the electrocapillary method. For solid electrode materials the wetting angle at solid-liquid-gas interface can be determined.

The double layer capacitance of new anodes was about 20-40 $\mu F/cm^2$. There was considerable scatter with results ranging from 15 to 70 $\mu F/cm^2$. By lenghty electrolysis, it was found that the double layer capacity increased tenfold, although it rarely was higher than 350 $F/cm^2$. When the current was interrupted, a 50 % increase of the double layer capacitance was observed.

Drossbach and Hashno reported that the double layer capacitance varied with the anodic with a maximum at $1mA/cm^2$.

Determined the double layer capacitance in the potential range from 0.3 V to 1.4 V positive to the aluminium electrode a more cathodic potentials appreciable current would flow, giving rise to high and irreproducible capacity values. On the anodic side, current oscillations caused by gas evolution rendered accurate measurements difficult.

The alumina film has a significant strength when detached from the metal. It has been used for pressure discs by dissolving the backing metal over a circular area in the middle of a plate. For barrier layer films the breaking pressure $P_{max}$ in mmHg has been empirically determined as

$$P_{max} = \frac{400}{d} \log 10 \frac{V}{24}$$

where V = anodizing voltage (between 5 and 50 V)
d = diameter of circle mm.

Calculation Proccedure

Foil curvature was measured and internal stress in $Kg/mm^2$ was calculated in accordance with the equation

$$\sigma = \frac{h^2 E}{6rd\ (i-d/h)}$$

where h = foil thickness in mm
E = Young's modulus for the aluminium foil 7.000 $Kg/mm^2$
r = radius of curvature in mm
d = film thickness in mm

Magnitude of the Internal Stress

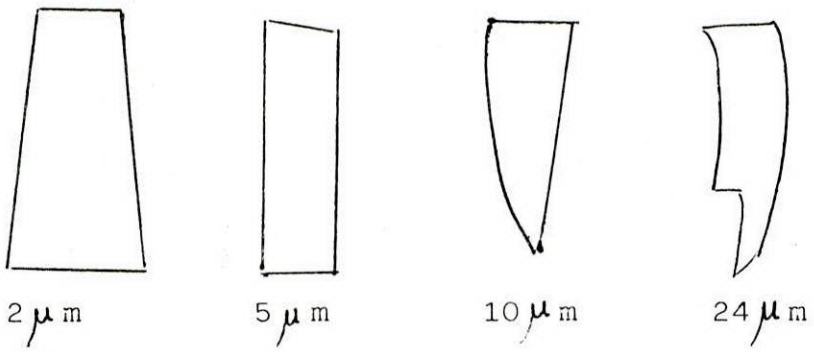


Fig. 1 Foil curvatures for varying thickness of anodized oxide film.

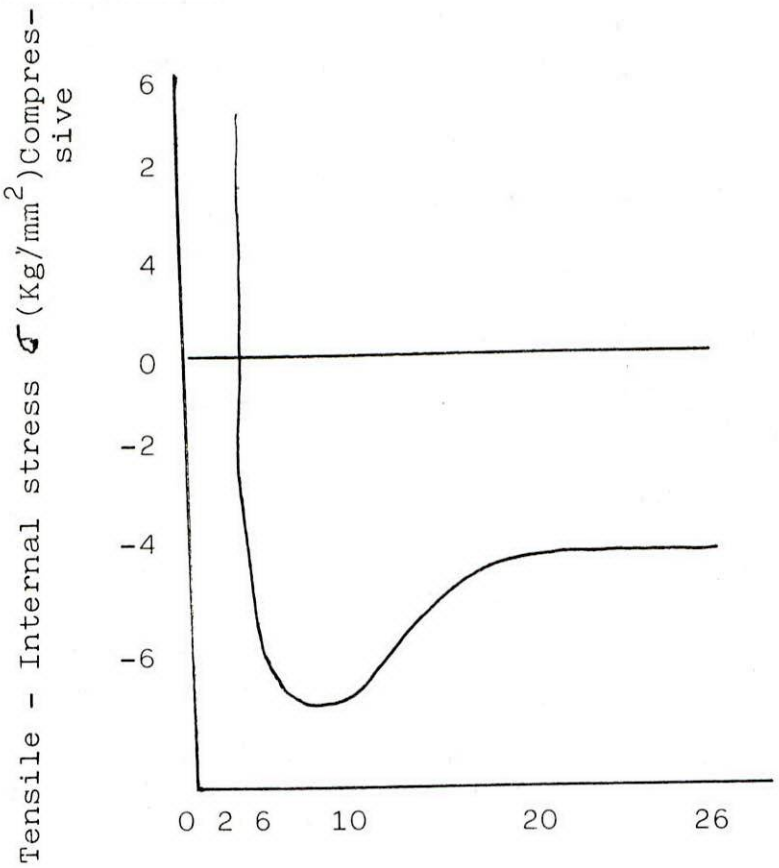


Fig. 2 Internal stresses in anodic oxide film.

Plots internal stresses, as calculated by eq. 1. Concavities indicate tensile stress, while convexities show the presence of compressive stress. Stress was compressive in the thinner films, but became tensile as film thickness increased, reaching a max-

imum at about 8 µm fig. 2.

Reduction of Internal Stress

It is suggested that internal stress increases in accordance with two factors:

.In the case of compressive stress, the existence of a barrier layer.
.In the case of tensile stress, due to increased porosity resulting from growth of the anodic oxide film and chemical dissolution at the surface.

Actual internal stress does result from a combination of these two factors. It is well known that when the combination of internal stress factors is tensile, cracks appear readily. The importance of reducing tensile stress is therefore obvious.

Two methods of doing so are suggested:Increasing the thickness of the barrier layer;

controlling the chemical dissolution and impregnating or sealing using a suitable material.

Investigacions were conducted on a number of methods for doing this, under specified experimental conditions. First to be investigated were two practical methods:

1. Sealing by hydration, using boiling water or steam 30 minutes at 100°C.
2. Impregnation by a secondary process in an electolytic solution of metal salts.

10 minutes at 16°C to 25.5°C solution of 2.2 wt % Ni $F_2$, 1,5 wt% $(NH_4)$ F, 3.0 wt % $H_3BO_3$ and 10-20 V optimun to 50 V pH 4.8.

Effectiveness of Stress Reduction in Preventing Crack Growth

A scratch test using a sapphire pin was used to simulate the mechanics of crack growth on abrasive wear and investigate the effectiveness of preventing the growth of cracks on original specimens -anodic oxide film only- and on specimens treated by methods 1 through 2.

Scratch force was measured and the coefficient of friction was calculated. As can be seen en fig. 5, there is much less crack growth in the specimens treated by method 2 than in the original or untreated films.

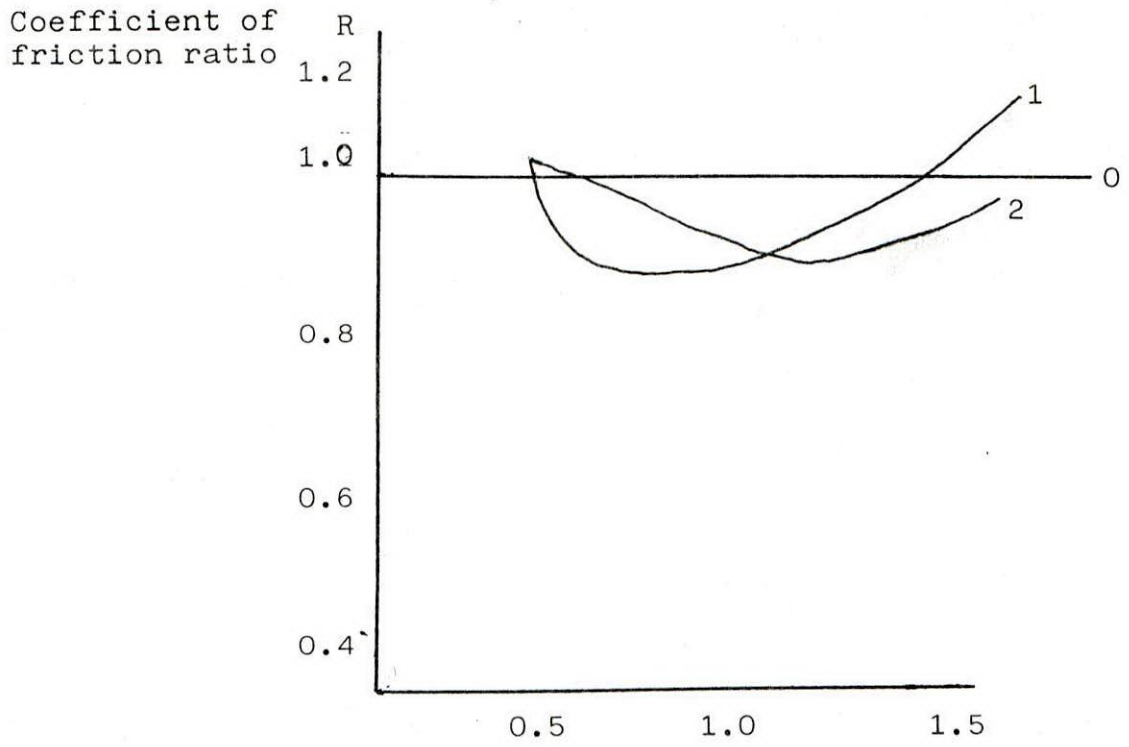


Fig. 6 Relationship between a ratio formed by dividing the coefficient of friction of specimens treated by methods 1 through 2 by that of untreated anodic oxide film the load on the pin used in scratching.

## CONCLUSIONS

Two methods were investigated for optimization process for reducing tensile stress and thereby decreasing crack formation in anodic oxide films. It was found that a method involving secondary anodic electrolysis.

Increasing the thickness of the barrier layer and impregnating the pores of the anodic oxide film with metallic oxide or sulfide was found to reduce tensile stress and thereby strengthen the anodic oxide film.

## References

-T.W.Diggles,'Oxide and Oxides Film', I.Marcelo Dekker Inc.,N.Y.
-H.Gonbitch, W.Geymeyer & E.Buvik, 'Aluminium 37'.

-Shimura M.,Arsumyutin Hyoden,Shari Kenkyu,Chara Hukurku,'Japan 86', 49 Ref. C.A. 87,59867 n 1877; 60-1,Ref.C.A. 87,75443 b
-'Analytical chemistry', Vol 45m number 3, March 1973.
-W.Harmon Ray & Julian Szekely, 'Process Optimization'.
-D.A.Vermilyea,'Journal of the Electrochemical Society'345,April 1963.
-R.Weil 'Plating', 57 (12) 1231 (1970)
-I.Lalved Newell, 'Metal Finishing 58', 1960, No. 10.

Experimental Test Results

| Simplex Vertrex Number | Previous Vertrex Number | Anode | Cathode | pH=cte=4.8 Temperature |
|---|---|---|---|---|
| 11 | | 0.023 | 0.012 | 17 |
| 12 | | 0.040 | 0.022 | 17.5 |
| 13 | | 0.082 | 0.049 | 16.5 |
| 14 | | 0.092 | 0.082 | 16 |

| Simplex | Factor | Anode | Cathode | pH=cte=4.8 Temperature |
|---|---|---|---|---|
| 15a | -0.5 | 0.018 | 0.014 | 17 |
| 15b | 0.5 | 0.032 | 0.021 | 17.5 |
| 15c | 1 | 0.048 | 0.039 | 16.5 |
| 15d | 2 | 0.069 | 0.078 | 16 |

| Simplex Vertrex Number | Previous Vertrex Number | Anode | Cathode | pH=cte=4.8 Temperature |
|---|---|---|---|---|
| 21 | 1 | 0.018 | 0.014 | 18 |
| 22 | | 0.029 | 0.019 | 18.5 |
| 23 | | 0.047 | 0.036 | 17.5 |
| 24 | | 0.065 | 0.074 | 17 |

| Simplex | Factor | Anode | Cathode | pH=cte=4.8 Temperature |
|---|---|---|---|---|
| 25a | -0.5 | 0.016 | 0.013 | 18 |
| 25b | 0.5 | 0.026 | 0.017 | 18.5 |
| 25c | 1 | 0.044 | 0.038 | 17.5 |
| 25d | 2 | 0.062 | 0.079 | 17 |

| Simplex Vertrex Number | Previous Vertrex Number | Anode | Cathode | pH=cte=4.8 Temperature |
|---|---|---|---|---|
| 31 | | 0.014 | 0.011 | 19 |
| 32 | | 0.023 | 0.021 | 19.5 |
| 33 | | 0.049 | 0.037 | 18.5 |
| 34 | | 0.059 | 0.081 | 18 |

| Simplex | Factor | Anode | Cathode | pH=cte=4.8 Temperature |
|---|---|---|---|---|
| 35a | -0.5 | 0.012 | 0.010 | 19 |
| 35b | 0.5 | 0.021 | 0.021 | 19.5 |
| 35c | 1 | 0.044 | 0.036 | 18.5 |
| 35d | 2 | 0.055 | 0.076 | 18 |

| Simplex Vertrex Number | Previous Vertrex Number | Anode | Cathode | pH=cte=4.8 Temperature |
|---|---|---|---|---|
| 41 | 1 | 0.014 | 0.011 | 20 |
| 42 | | 0.019 | 0.020 | 20.5 |
| 43 | | 0.042 | 0.035 | 21 |
| 44 | | 0.056 | 0.071 | 21.5 |

| Simplex | Factor | Anode | Cathode | pH=cte=4.8 Temperature |
|---|---|---|---|---|
| 45a | -0.5 | 0.013 | 0.009 | 20 |
| 45b | 0.5 | 0.015 | 0.014 | 20.5 |
| 45c | 1 | 0.039 | 0.o32 | 21 |
| 45d | 2 | 0.052 | 0.074 | 21.5 |

| Simplex Vertrex Number | Previous Vertrex Number | Anode | Cathode | pH=cte=4.8 Temperature |
|---|---|---|---|---|
| 51 | | 0.011 | 0.010 | 21 |
| 52 | | 0.018 | 0.012 | 21.5 |
| 53 | | 0.037 | 0.036 | 22 |
| 54 | | 0.099 | 0.092 | 22.5 |

| Simplex | Factor | Anode | Cathode | pH=cte=4.8 Temperature |
|---|---|---|---|---|
| 55a | -0.5 | 0.008 | 0.009 | 21 |
| 55b | 0.5 | 0.016 | 0.011 | 21.5 |
| 55c | 1 | 0.031 | 0.033 | 22 |
| 55d | 2 | 0.084 | 0.082 | 22.5 |

| Simplex Vertrex Number | Previous Vertrex Number | Anode | Cathode | pH=cte=4.8 Temperature |
|---|---|---|---|---|
| 61 | | 0.007 | 0.009 | 22 |
| 62 | | 0.018 | 0.014 | 22.5 |
| 63 | | 0.030 | 0.031 | 23 |
| 64 | | 0.082 | 0.079 | 23.5 |

| Simplex | Factor | Anode | Cathode | pH=cte=4.8 Temperature |
|---|---|---|---|---|
| 66a | -0.5 | 0.016 | 0.008 | 22 |
| 66b | 0.5 | 0.016 | 0.015 | 22.5 |
| 66c | 1 | 0.029 | 0.024 | 23 |
| 66d | 2 | 0.076 | 0.078 | 23.5 |

| Simplex Vertrex Number | Previous Vertrex Number | Anode | Cathode | pH=cte=4.8 Temperature |
|---|---|---|---|---|
| 71 | 1 | 0.006 | 0.007 | 24 |
| 72 | 2 | 0.014 | 0.011 | 24.5 |
| 73 | | 0.022 | 0.016 | 25 |
| 74 | | 0.075 | 0.072 | 25.5 |

| Simplex | Factor | Anode | Cathode | pH=cte=4.8 Temperature |
|---|---|---|---|---|
| 77a | -0.5 | 0.006 | 0.008 | 24 |
| 77b | 0.5 | 0.014 | 0.011 | 24.5 |
| 77c | 1 | 0.018 | 0.013 | 25 |
| 77d | 2 | 0.072 | 0.069 | 25.5 |

| Simplex Vertrex Number | Previous Vertrex Number | Anode | Cathode | pH=cte=4.8 Temperature |
|---|---|---|---|---|
| 81 | 3 | 0.006 | 0.008 | |
| 82 | 4 | 0.014 | 0.011 | |
| 83 | | 0.015 | 0.011 | |
| 84 | | 0.068 | 0.064 | |

The last value is discarded to reach an experimented optimum. In both anode and cathode the same anodic layer is obtained, using a bath of flouride of nickel, flouride of ammonia and boric acide.

# H-2

## General Interest
## Session H

### The Programmable Controller, A Powerful Tool Not Just for the Automotive Industry

James J. Childs Jr.
AT&T Technologies

# THE PROGRAMMABLE CONTROLLER, A POWERFUL TOOL NOT JUST FOR THE AUTOMOTIVE INDUSTRY

James J. Childs Jr.

AT&T Technologies

## ABSTRACT

Programmable Controllers (PCs) have been in existence for almost twenty years. Their origin dates back to the late 1960's when the Hydramatic division of General Motors Corporation wrote a specification for a solid state relay replacement system. This system needed both the flexibility of a computer and the ability to withstand harsh industrial environments.[1]

Initial PCs were what General Motors had asked for, on/off relay replacement devices. They ran assembly lines, go no go inspection machines and other relay type devices that needed to be changed quickly. In the last 10-15 years however; PCs have emerged as a powerful automation and control tool capable of far more than just relay replacement. When combined with analog input/output devices they can monitor temperatures, pressures and other variable information and respond in a logical manner. Of late, some PC manufactures even support proportionate-integral-derivative control techniques, such as pH and high speed motor control.[3]

The automotive industry uses the lion's share of the PCs and for the most part PC manufactures design their product around the requirements of the automotive industry. Out of this has trickled a control system very suitable for a wide range of other industrial applications.

This paper will discuss what programmable controllers are and how they operate. In addition, an example of how PCs can be utilized in an integrated plating system (PWB manufacture) will be presented.

## INTRODUCTION

Since it's conception two decades ago for the automotive industry, as a replacement for relays, the programmable controller has become the basic building block of the automated factory. The reasons for its success are simple to see. The programmable controller is unsurpassed in its function to monitor and control a large number of Input and Output devices in real time. They are rugged devices capable of dealing with substantial amounts of electrical noise, electro-magnetic interference, extreme temperature gradients and high humidity.

The hardware and software is easily maintained by electricians or technicians. Virtually all components are modular and plug in, alleviating wiring changes for replacement. Error diagnostic circuits allow for quick failure analysis. They can be programmed in Ladder Logic which is familiar to at least three generations of factory workers. This familiarity makes trouble shooting easy. With expanded memory and mathematical abilities the original relay replacement device has become a universal automation tool kit.The benefits from their use are substantial and far greater than the few suggested.

## BASIC ELEMENTS

According to (NEMA) The National Electrical Manufacturers Association Programmable Controllers (PCs) are "digital electronic apparatus with a programmable memory for storing instructions to implement specific functions, such as logic, sequencing, timing,counting and arithmetic, to control machines an processes"[2]. The function of a PC is to examine a set of input conditions from the field and based on their status, regulate a set of output devices. The combinations of the input and output data reflect the logic in the system. The arrangement of input and related output responses reflect the control plan or program resident in the PC's Central Processing Unit (CPU) or brain [1].

A PC is composed of four basic elements. These elements are the Central Processing Unit, Input/Output (I/O)devices, Memory and Power Supply see Figure 1.

### CPU

The CPU scans the status of input devices and correlates these inputs to the logic in memory, and articulates the appropriate output. The logic in the CPU can usually be embellished to include: flow control, data manipulation, timing counting, data transfer and arithmetic functions.

The intelligence of the CPU is usually microprocessor based.

These integrated circuits perform the control function and system duties of the PC. The control function assures that the correct output devices on manipulated by the logic program according to system inputs devices. System duties include error checking of communication links and system checks such as battery level, power supply, execution time limit alarms.

There are different types of CPU arrangements. Some PC manufactures use a a hardwired processor in conjunction with a microprocessor to execute system duties. In this configuration the hardwired processor would perform ladder logic control while the microprocessor performed computational and data manipulation functions. Other manufactures allow microprocessors to perform all tasks. A derivative from the micro computer industry has been to have the CPU made up of several microprocessors. In this processor-coprocessor arrangement control duties are segmented over several microprocessors. This is analogous to using a math coprocessor chip on a Personal Computer. By using several microprocessors, program execution time is greatly decreased and high level control algorithms are able to be implemented. Another factor that effects program execution time is the word size used by the CPU. The word size in modern controllers can range from 8 bits to 32 bits (one to four bytes). Since word length is a direct function of processor speed a 32 bit microprocessor in the CPU can handle data at least three times faster than an 8 bit microprocessor.

When the PC is running the CPU reads all field input devices, compares these values against the control logic, and energizes de-energizes the appropriate outputs. The process of reading inputs, solving logic, and driving outputs is known in the PC industry as program scan. The time it takes to accomplish this task is known as scan time. Figure 2 depicts a program scan.

INPUTS/OUTPUTS

Inputs to a PC are either discrete or continuous. Discrete inputs may come from micro switches, limit switches, push buttons, proximity switches or pressure switches. Continuous inputs may come from sources such as thermocouples, potentiometers or voltmeters. Discrete outputs from a PC are directed to actuating hardware such as solenoids, solenoid valves, and motor starters. Continuous output devices can include analog valves and actuators, chart recorders, motor drives and analog meters.

Input/output devices (I/O) for a PC are usually modular plug in devices. These modules are the physical connection between field devices and the CPU. The I/O modules connect the field devices to the CPU by first converting the external voltage (115Vac, 230Vac, 24Vdc, etc.) to a TTL level signal of 0 or 5Vdc (ie.in case of two state devices). The CPU then compares the signals

against the logic program to determine the appropriate output response. A 0 or 5 Vdc signal is then transmitted to the appropriate output module, which then converts the signal to the response domain (115 Vac, 230Vac, 24Vdc,0V, etc.). Figure 3. depicts a block diagram of an AC/DC input circuit.

The bridge rectifier, noise filter and threshold detection blocks are signal validators. The bridge rectifier converts the signal AC or DC to the TTL level. The filter block protects against signal bounce and noise on the input power line. The threshold detection block determines whether the signal has reached the specific rating for the input device. If the signal remains at the specified rating for longer than the delay caused by the filter block (4-45msec), a valid signal will be passed to the optical isolator and into the CPU. By using an optical isolator separation of input power and control logic power is accomplished. This prevents voltage spikes or power non conformities from damaging the CPU.Figure 4 is the simplified electrical schematic of the AC/DC input circuit in Figure 3. This figure is courtesy of the Gould Electronics Industrial Automation Division.With the exception of level detection, output circuits are for the most part the reversal of an input circuit. Figure 5 depicts a block diagram for an output circuit.

The CPU sends a signal that a particular output is to be energized. This signal is passed through the optical isolator to a switching device. These switching devices vary with manufacture and for AC circuits are usually Triacs or Silicon Controlled Rectifiers (SCR). DC output devices use power transitors to switch loads. Both AC and DC circuits are both protected from electrical noise that could hinder or damage the circuit. AC devices commonly use RC snubbers with Metal Oxide Varistors (MOV) to protect the system from electrical noise and spikes. DC devices use a free wheeling diode. Figure 6 and 7 are the electrical schematic for AC and DC output devices respectively. They are both courtesy of the Gould Electronics Industrial Automation Division.

MEMORY

Control logic and sensor input signals are stored in memory. The most fundamental unit is a bit. A bit is a two state entity which can be related to a switch either on or off. Most data in a PC consists of 8 bit groupings or bytes. The word size in modern PC's range from 8 to 32 bits (one to four bytes), depending on processor size.

Memory size in a PC is measured in either bits, bytes or words. PC memory can be classified in two categories: volatile and non-volatile. Volatile memory loses stored information when the power is removed. Non-volatile memory retains its memory even when power is removed. Of the six common types of memory, random

access memory (RAM) is the only volatile memory and the most common because of the ease with which it can be programmed and edited. Roughly 90% of the microprocessor based PCs are of the RAM type. A battery back up system must be used with to retain RAM memory. PC manufactures state battery life as from one to five years. Experience warrants changing batteries each year regardless of manufacturers statements.

The five non-volatile memory types are: Core, ROM (Read Only Memory), EARPROM (Electronically Alterable Read Only Memory), PROM (Programmable Read Only Memory), and EEPROM (Electronically Erasable Programmable Read Only Memory). EEPROM is fast becoming very popular because of its non-volatile characteristic and programming ease.

Power Supply

The Power Supply's function is two fold; first it must supply the needed DC power for the CPU,Memory and I/O devices, secondly it must regulate supplied voltages. PC power supplies will accept (when specified) either AC or DC voltages. Control systems must then be configured with these two criteria in mind. Manufacturers give the power requirements of the CPU and I/O devices. These requirements must be summed together to find the intended load on the Power Supply. This number is than used to specify the ( depending on the manufacturer) power supply or power supplies required.

Good voltage regulation, the second duty of a power supply, is often taken for granted as having been incorporated by the manufacturer. Industrial complexes often experience line voltage fluctuations of between 10 and 20 percent. Power supplies must be able to tolerate this fluctuation. When input line voltages do go out of bounds most power supplies will issue a sleep or shutdown command to the CPU. This sleep command protects the Control system and the physical equipment not to mention operators.

Well designed power supplies will compensate for line fluctuations. If line fluctuations exceed the upper or lower bounds of the power supply or the power supply is not well designed, PC sleeping will occur. A remedy for this is through the use of a constant voltage transformer (CVT). A CVT will compensate for line disturbances. Some CVT manufacturers state that at full load their units can maintain within one percent of the intended input line voltage.

PC-TYPES

PCs may be divided into to five groups according to the number of I/O they can accommodate. These sizes are Mini (less than 32 I/O), Micro (32-64 I/O), Small (64-128 I/O), Medium (128-512 I/O) and Large (512 I/O and above). They can further be broken down by

memory size and functional capabilities. These three criteria homogenize well because PCs with a small number of I/O have limited memory and functional capabilities. PCs that can accommodate large numbers of I/O size have increased memory size and functional capabilities.

Mini-Micro PCs are little more than relay replacements. Larger units however may have the capabilities to generate reports,maintain high level communications and conduct close loop PID control.

Programmimng

Instructions that are put into a PC are called programs. There are four main programmimng languages. These are Ladder Logic, Boolean mnemonics, Functional blocks, and English statements. Some PC systems even support high level programmimng languages such as BASIC and PASCAL. English statements and Functional Blocks are considered high level languages. Ladder Logic and Boolean mnemonics are considered low level programmimng languages. Ladder Logic is a derivative of the ladder diagrams used with electrical relay systems. Ladder logic is probably the most popular programmimng language.

A Ladder Logic program consist of ladder elements. These elements represent contacts, switches, coils timers counters and other control elements. Simply put, the Ladder Logic represents the actions required as a series of switches which are on or off. Figure 8 lists some common relay logic and ladder diagram characters. When integrated these characters form the control program used by the PC.

Ladder Logic Example

Figure 9 shows a simple chemical mixing system. Here chemical A and chemical B are to be added into a tank. After they are added they are mixed for two minutes. At the end of the mixing cycle the tank is drained and the process is ready to start again. Figure 10 shows a Ladder Logic program which could control such a system.

Referring to line one and two of this figure, when the start PB is depressed contact 10001 is energized , if normally-closed contact 00006 is de-energized the MCR coil 00001 will latch on. In line three, with the MCR on and the tank level limit switch 10002 de-energized solenoid coil 00002 and 00003 will activate allowing the tank to fill. When the tank level limit switch 10002 is energized the filling will stop. In line five, with the tank full, (denoted by contact 10002 being energized), the mixer coil 00004 will energized and run for two minutes. At the end of this two minute period the mixer stops and drain solenoid 00005 is activated. Line seven shows with the MCR, solenoid 00005 and

limit switch 10003 energized the tank empty light 0006 will come on and the system will reset.

Programmimng Hardware

In order to establish the logic sequence of control for a process the control program must be entered into the CPU. Depending on the size of the controller this can be done by using one of the following devices.

1) A CRT Industrial Program loader
2) A Personal Computer
3) A Hand held Program loader

Though these devices may look different, they pass the same information to the CPU. All PC vendors manufacture some sort of programmimng device. Of late, vendor and third party software has allowed personal computers (PCs)to be used as programmimng devices.

PWB Plating system example

Figure 11 shows a control architecture and line layout for a copper/tin automated (PWB) plating system. The main control approach is to integrate a small computer with a Programmable Controller. The small computer function is to allow the operator to:

1) Enter the bath sequence and bath set points for various codes.
2) Display line animation.
3) Display alarms.
4) Down load bath sequence and bath setpoints to Programmable Controller.
5) Optimize hoist sequencing.
6) Generate reports.
7) Track codes in system.

The PC control functions include:

1) Maintaining tank levels.
2) Starting pump motors.
3) Adding chemicals.
4) Temperature control.
5) Humidity control.
6) pH control.
7) Rectifier voltage/current control.
8) System interlocks
9) Hoist movement horizontal

10) Hoist movement vertical

By merging a small computer with a programmable controller a powerful control system can be developed. This allows for the best of both devices to be utilized. Small Computers are excellent for report generation, data trending,lot tracking, data base management, number crunching etc. They are however not real-time controllers. Most depend on a single processor,thus they can only handle one function at a time. Most PCs use bit/slice processors each designed to make a rapid decision required by the control task. This allows real-time control of discrete and continuous devices. PCs can accommodate report generation,data trending, lot tracking etc. The costs; however, are significantly reduced scantime, increased program development/implementation and reduced system flexibility.

LINK

In past, the major gray area of such a control system has been the link between the small computer and the PC. Previously a custom interface had to be created for a specific project or a modification of an interface used on a different project. Often a third computer would have to be used as the processor for the interface. The implications here are a complex operating system, multiple programmimng languages and unfamiliar hardware. Interface development is unique in nature and therefore requires specialized personnel for development and maintenance. The cost for the interface for this type of control system often makes financial justification impossible.

The need for building a standard or standard type interface is apparent. Hardware has to withstand industrial environments and be easily understood . The software has to be clear other than to a PHD in computer science. To this end, personal computers have become the processor for the interface. For easily modifiable programs simple languages such as BASIC, FORTRAN, PASCAL and C can be used [4].

All these languages can run on personal computers. They are easy to learn and simple to debug. BASIC,FORTRAN, AND PASCAL are however very slow for real time machine control. If assembly language subroutines utilities are implemented with these languages real time control can be accomplished [5,6]. Many software houses offer assembly language subroutines to interface personal computers with PCs. The majority of these subroutines are communication drivers. They let the user concentrate on using the data rather than communicating the data. These drivers format user information into the protocol necessary to communicate with the PCs. They are called by the user application programs and are easily implemented.

## PROGRAM ARCHITECTURE

Figure 12 shows the control architecture spun from the merging of the personal computer and the PC. The personal computer runs the application programs for setting tank control setpoints, hoist sequence, line animation, alarm conditions and lot tracking. The PC is responsible for implementing these setpoints and sequences. The PC Ladder Logic is broken down by tanks and hoists. The logic for each tank or hoist is written as a separate subprogram. Changing the logic in one tank would not than greatly effect the logic controlling another. The setpoints for the PC to run from are down loaded from the personal computer through the assembler utility programs. If the personal computer were to shutdown, the line could continue to run. The PC only needs the setpoint data from the personal computer once it has this data it runs until stopped or the setpoints are changed again. Of course lot tracking, line animation and other applications programs which need constant updating from the personal computer would be lost. If the personal computer were down for and extended period, and setpoint changes had to be made, they could be done by a PC programming preipheral device.

## CONCLUSION

The author has tried to give insight into what programmable controllers are and how they operate. In conjunction with this, a control format for an integrated plating system was reviewed.

Programmable controllers are no longer just a tool of the automotive industry. PCs are also to be found in applications as diverse as combustion chamber control, printing press operation, coal mining,chemical processes and printed circuit board manufacturing. A programmable controller seems secure in its role as a control device. It combines the best features of the microcomputer industry with proven technology. The programmable controller is ready to be what the PC was to the modern office an inexpensive reliable device which can accomplish a wide range of task [7].

References


[1] Wysk, R.A; "Technical Draft for PCs", Penn State University, 1982.

[2] Jones, C.T. and Bryan, L.A.; Programmable Controllers",International Programmable Controls, Inc. 1983.

[3] Childs Jr, J.J.;"Programmable Controllers What Are They and How Are They Used., Commline magazene, Summer 1987.

[4] Arnold, J.N.;"Practical Techniques for Linking Foreign Devices to a Distributed System",Programmble Controls, November-December 1987.

[5] Battista, F. F.;"A Toolkit Approacah to Operator Interface Systems," Proceedings for the North Cost Conference and Exhi Instrument Society of America, Cleveland Oh, May 20-22 1986.

[6] Marsh, C.E. and Tucker, T. W.;"Local Workstation Concepts in a Small distributed System," Intech, Vol 33, No 5; May 1986, pp. 41.

[7] Miller, R;"Prices Have Plunged, Features Proliferated for Programmable Logic Controllers", Managing Automation, Septe 1987,pp. 38.

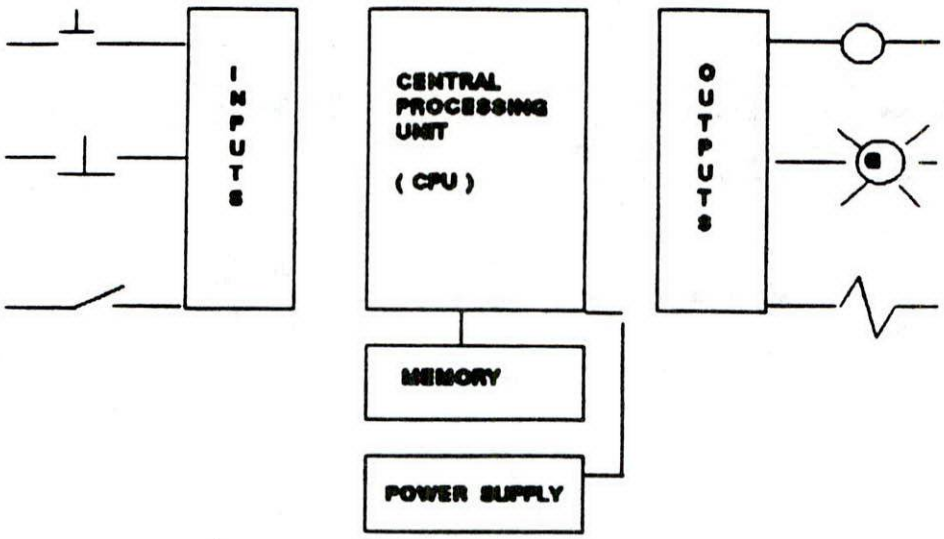


FIG 1. THE ELEMENTS OF A PROGRAMMABLE CONTROLLER

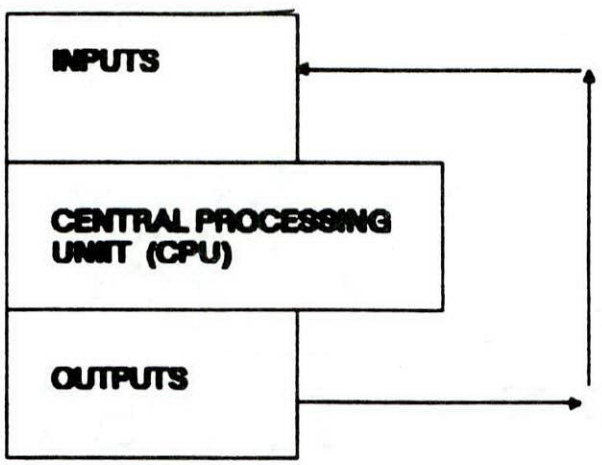


FIG. 2 PROGRAM SCAN




FIG 3. BLOCK DIAGRAM OF INPUT CIRCUIT

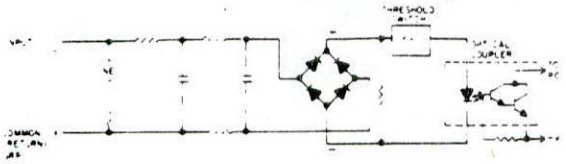

FIG 4. SCHEMATIC OF SIMPLE AC/DC INPUT CIRCUIT




FIG 5. BLOCK DIAGRAM OF OUTPUT CIRCUIT

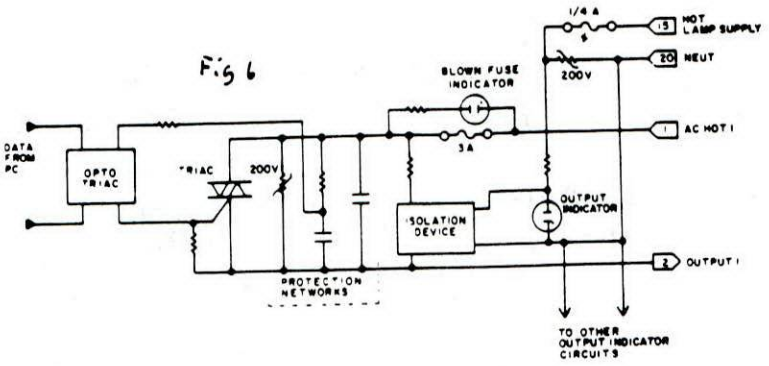


FIG 6. SCHEMATIC OF SIMPLE AC OUTPUT CIRCUIT

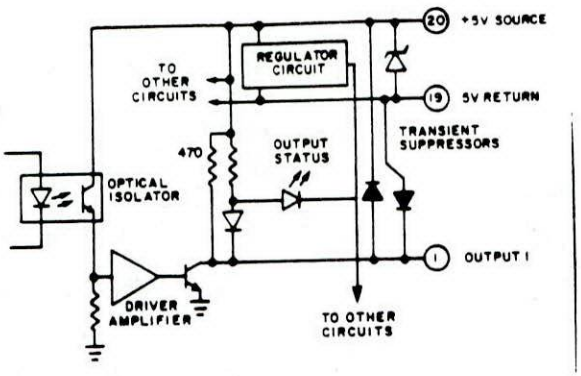


FIG 7. SCHEMATIC OF SIMPLE DC OUTPUT CIRCUIT

FIG 8. LOGIC REPRESENTATION

| DEVICE | GRAPHIC LOGIC | LADDER LOGIC | CURRENT AT SITE |
|---|---|---|---|
| TOGGLE SCISSOR OPEN |  | 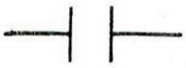 | NO |
| TOGGLE SCISSOR CLOSED |  |  | YES |
| PUSH BUTTON OPEN |  | 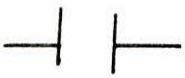 | NO |
| PUSH BUTTON CLOSED | 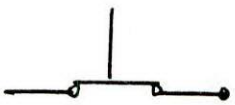 | 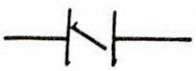 | YES |
| COIL RELAY | 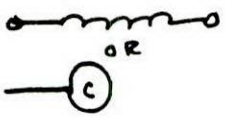  |  | NO |
| PROXIMITY SWITCH | | 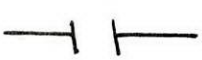 | NO |
| TIMER |  | 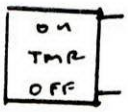  | NO |
| COUNTER | | 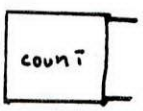  | NO |

## FIG 10. LADDER LOGIC FOR CHEMICAL MIXING EXAMPLE

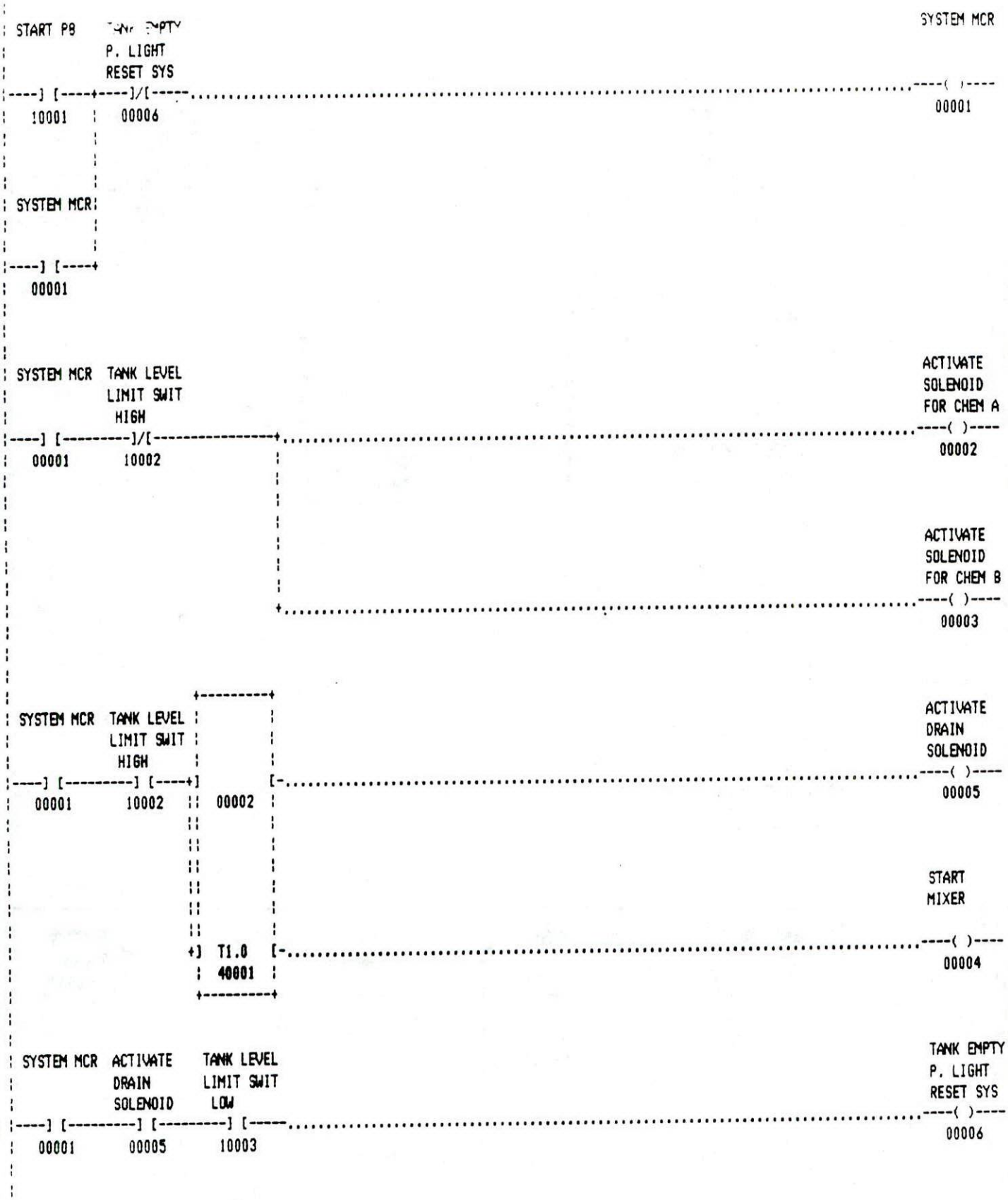

FIG 9. CHEMICAL MIXING SYSTEM

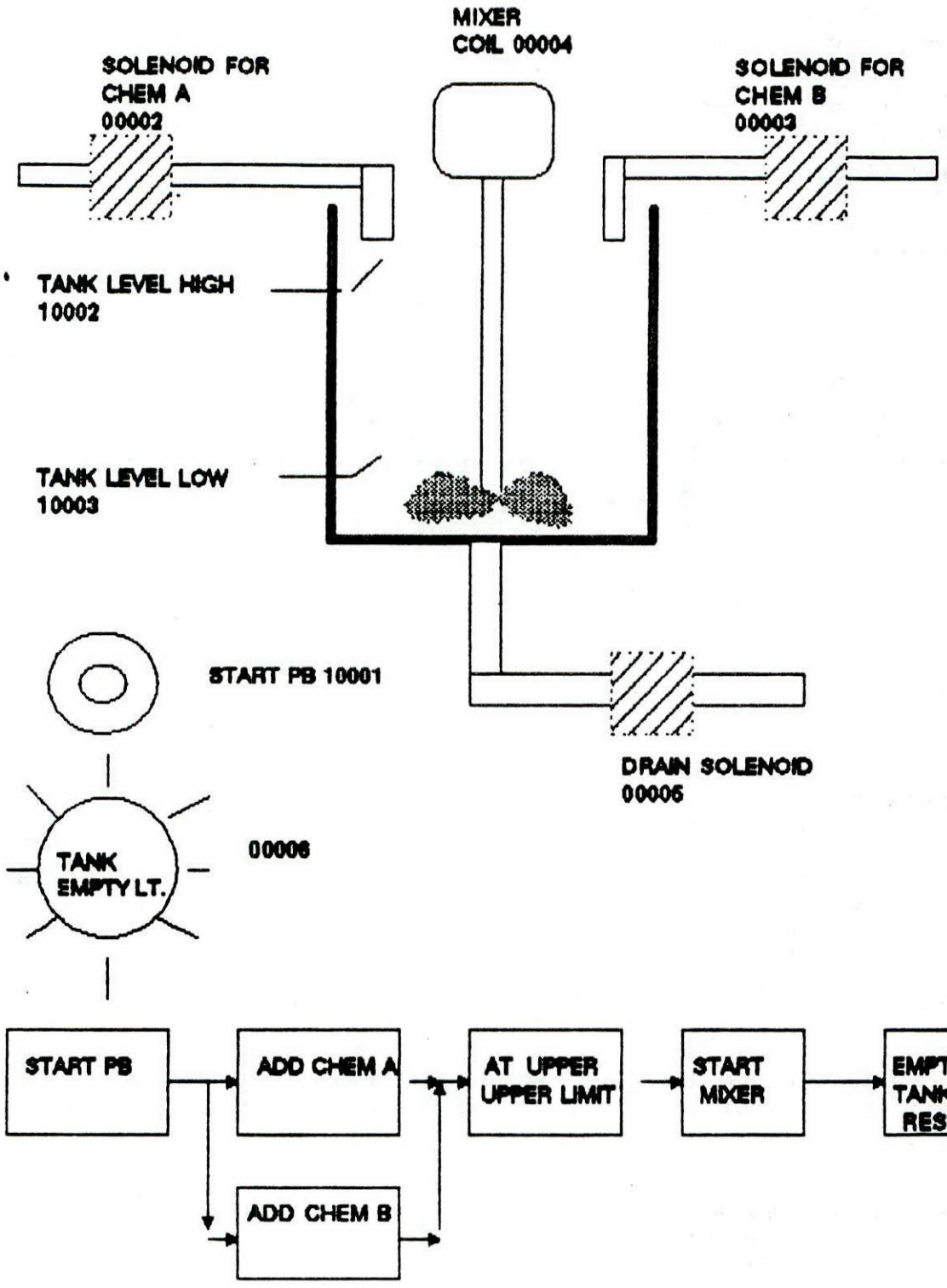


PROCESS EVENT FLOW

## FIG 10. LADDER LOGIC FOR CHEMICAL MIXING EXAMPLE

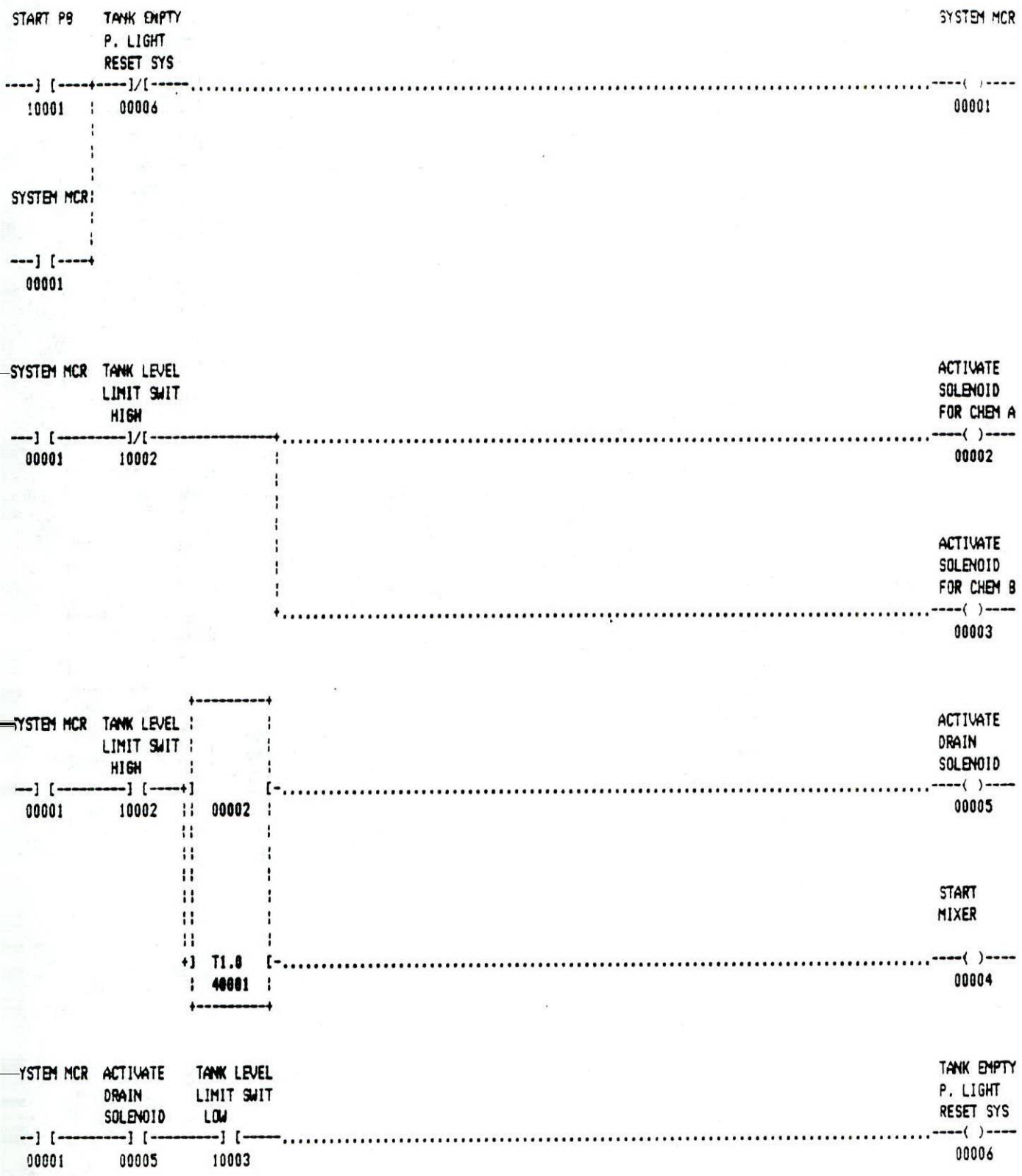

FIG 11. COPPER / T IN PLATING LINE EXAMPLE

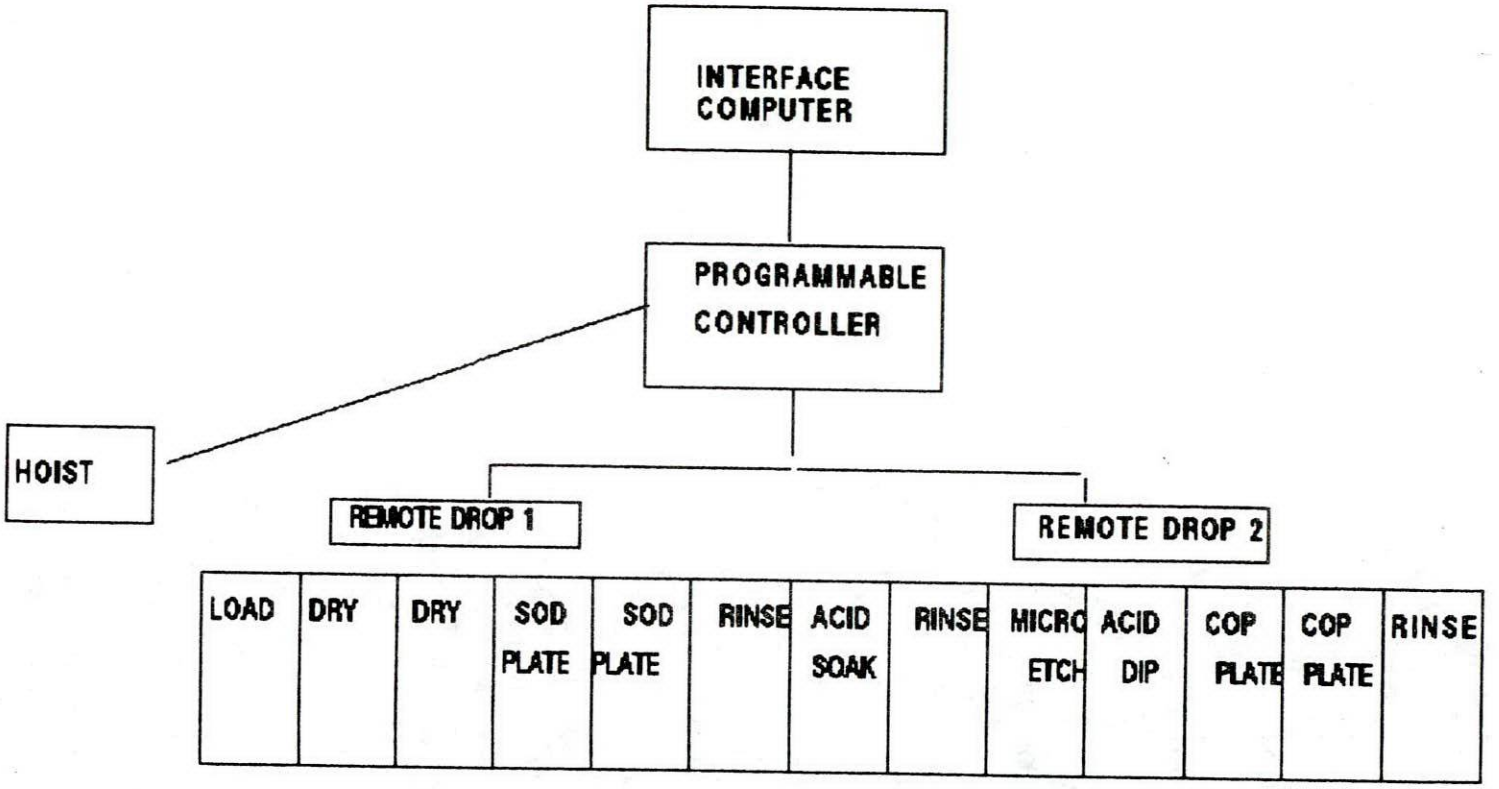

FIG 12. CONTROL ARCHITECTURE FOR COPPER/TIN PLATING LINE

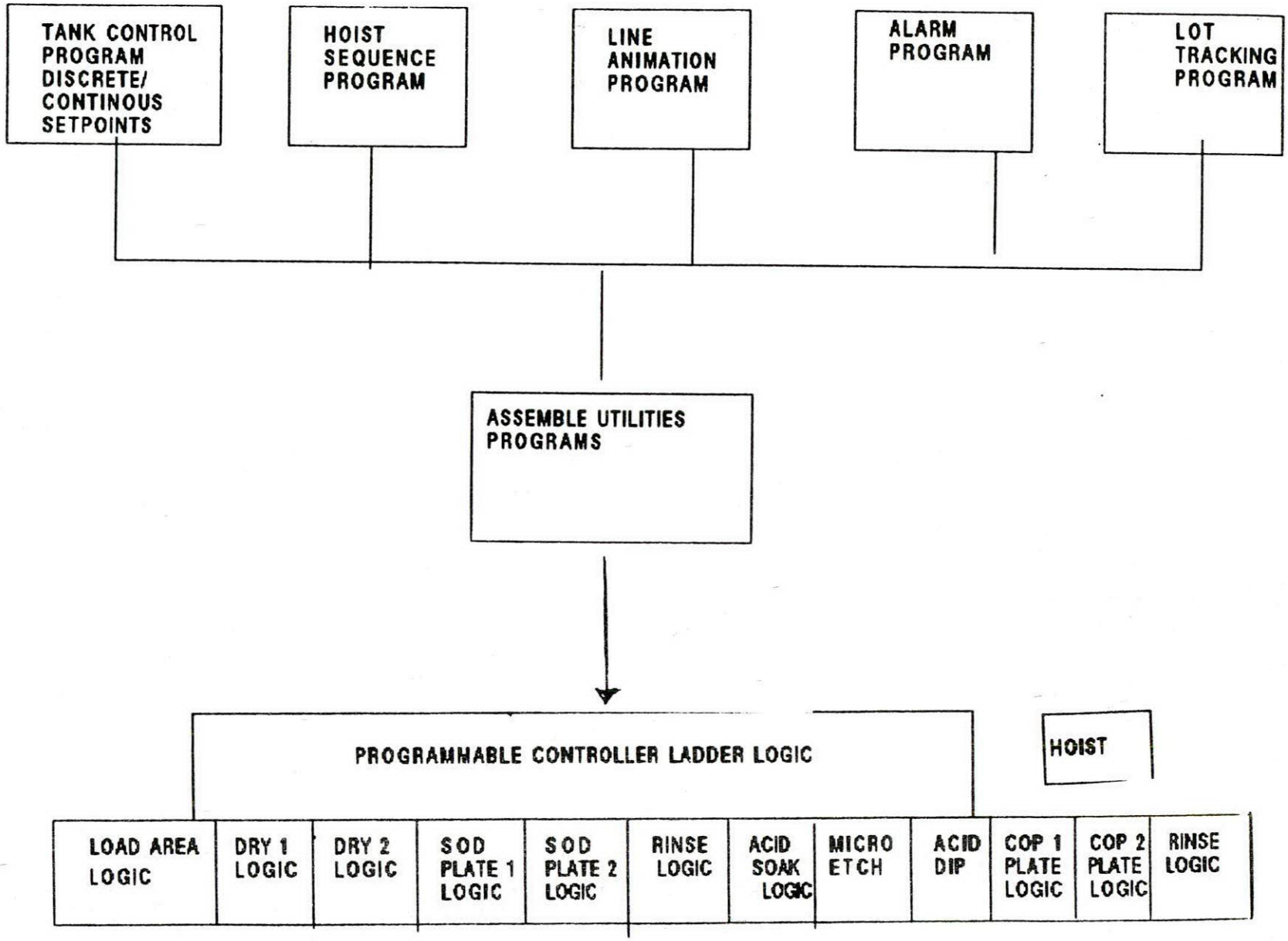

# H-3

# General Interest
# Session H

## The Interaction Between Electrogalvanized Zinc Deposit Structure and the Forming Properties Of Sheet Steel

James H. Lindsay, Robert F. Paluch
Physical Chemistry Department
General Motors Research Laboratories
Warren, MI 48090

Harmon D. Nine
Physics Department
General Motors Research Laboratories
Warren, MI 48090

Vernon R. Miller
United States Bureau of Mines
Rolla Research Center
Rolla, MO 65401

Thomas J. O'Keefe
University of Missouri-Rolla
Graduate Center for Materials Research
Rolla, MO 65401

# THE INTERACTION BETWEEN ELECTROGALVANIZED ZINC DEPOSIT STRUCTURE AND THE FORMING PROPERTIES OF SHEET STEEL

James H. Lindsay, Robert F. Paluch
Physical Chemistry Department
General Motors Research Laboratories
Warren, Michigan 48090

Harmon D. Nine
Physics Department
General Motors Research Laboratories
Warren, Michigan 48090

Vernon R. Miller
United States Bureau of Mines
Rolla Research Center
Rolla, Missouri 65401

Thomas J. O'Keefe
University of Missouri - Rolla
Graduate Center for Materials Research
Rolla, Missouri 65401

## ABSTRACT

The use of electrogalvanized steel to enhance the corrosion resistance of automobile body panels is of consequence in the forming of sheet steel. The zinc coating structure and morphology, as influenced by electrolytic and hydrodynamic conditions during electrodeposition, can influence the drawing character of electrogalvanized sheet. Sheet steel samples plated with zinc deposits exhibiting 1) strong basal (0001) plane and 2) strong pyramidal plane ($10\bar{1}X$) orientation were prepared. Sheet metal forming properties, including cup deformation and drawbead performance, were related to deposit morphology and structure. The results were compared to those for commercial electrogalvanized product.

## INTRODUCTION

The continuing quest for improved quality and product durability in the automotive industry has led to the extensive use of electrogalvanized sheet steel to increase the corrosion performance of automotive body panels. Such material is found to meet performance standards which typically involve 5-years' resistance to "cosmetic" deterioration and 10-years' resistance to basis metal perforation.

While the primary purpose of the zinc coating is to enhance corrosion resistance via sacrificial protection, the presence of that coating must not hamper subsequent operations. These deposits must be considered in the larger context of a "system". During manufacture of an automotive body panel, the coated sheet steel undergoes blanking, forming, spot welding, phosphating and painting. The success of industrial electrogalvanizing is thus heavily dependent on obtaining a zinc deposit structure compatible with the various treat-

ments and environments to which the coated substrate is subjected. The work reported here deals with the interaction between the zinc electrodeposit structure and formability.

Sheet Metal Forming. In metal stamping operations, a double-action press is commonly used. As shown schematically in Fig. 1, the upper die half contains two elements: 1) the upper binder and 2) the punch. These are complemented in the lower half by the lower binder and die cavity, respectively. As the die is closed, the upper binder first descends on the outer rim of the sheet metal blank to hold it in place (Fig. 1A). The punch then moves downward to form the metal into the desired shape (Fig. 1B).

During forming, sheet metal is drawn from the binder area into the cavity. The binder surface acts to control the rate of metal flow. The binder restraining force must lie in a range that is high enough to prevent excessive metal flow, which would cause wrinkling, and yet low enough so as not to tear the metal. On the right side of Fig. 1A, a simple flat binder is shown. Here, frictional forces are the primary means of restraint. In many cases, friction alone is inadequate to sufficiently retard the metal flow. Accordingly, a drawbead geometry, shown on the left side of Fig. 1A, is used to provide added restraint, through the addition of a deformation force component (1). With drawbeads, deformation nominally provides 75% of the restraining force, with friction accounting for the remainder (1,2). Drawbead configurations are commonly used in die design to optimize control of the metal.

In addition to their functional application in stamping dies, drawbeads have become a useful tool in metal forming research, with the development of drawbead simulation equipment. Analysis of the drawbead restraining force into its friction and deformation components has been used to aid in modeling the forming process (2). Drawbead simulation studies have provided information on the effects of sheet metal material, lubricant and surface morphology on system drawing characteristics (1-5).

The use of coatings, such as zinc, on sheet metals has presented another variable to the system. Studies of commercial hot-dipped and electrogalvanized products have indicated that the coating can alter forming characteristics (3-5). Correlation between zinc surface morphology and the coefficient of friction is suggested (4).

Zinc Structure and Surface Morphology. Electrogalvanized zinc coatings are relatively fine-grained and typically exhibit a surface appearance like the commercial deposit shown in Fig. 2. The primary characteristic is a predominance of hexagonal crystal platelets (about 5-10 $\mu$m in size), whose hexagonal faces are tilted with respect to the plane of the substrate. This morphology is significantly different from that of bare cold-rolled sheet steel, where the primary characteristic would be a directional pattern of rolling marks.

In reference to the hexagonal close-packed (HCP) lattice planes in Fig. 3, the hexagonal faces correspond to the basal (0001) planes (Fig. 3A). Deposits with complete basal plane orientation parallel to the substrate are not normally obtained in commercial practice. The same is true for basal plane orientation perpendicular to the substrate. Such would be the case where a prism

plane (e.g., $(10\bar{1}0)$, Fig. 3B) is aligned with the substrate surface. Rather, commercial deposits are oriented between these two limits, although they may have a portion of the crystals oriented in such a manner. The commercial deposit shown in Fig. 2 suggests that the pyramidal planes ($10\bar{1}1$, $10\bar{1}2$,...$10\bar{1}$ X) (Figs. 3c,d) are oriented parallel to the substrate. Indeed, our X-ray diffraction studies show the predominant orientation to be pyramidal. A preponderance of high index planes ($10\bar{1}3^{+}$) would result in the basal planes being tilted at a more shallow angle. With the low index ($10\bar{1}1$ and $10\bar{1}2$) planes dominant, the platelets would be tilted at steeper angles.

Prior work (6-8) has shown that the surface morphology and deposit structure are strongly influenced by electrolytic and hydrodynamic conditions during electrodeposition. A degree of control of the preferred crystallographic orientation of the zinc deposit is possible with specific values of temperature, pH, flow rate and current density (6). A large proportion of basal (0001) orientation was obtained under conditions of low pH (1.5) in an acidified zinc sulfate electrolyte (150 g/L Zn). While no deposits were obtained with strong prism plane $(10\bar{1}0)$ orientation, those with strong low-indexed pyramidal plane ($(10\bar{1}1)$, $(10\bar{1}2)$) and minimal basal plane alignment were obtained under several sets of conditions.

Zinc Coating Deformation. The most common manifestation of plastic deformation in crystalline solids is slip, the successive displacement of one plane of atoms over another (slip planes) by dislocation movement (9). The slip plane is that with the highest density of atoms within it; in the case of HCP metal, the basal (0001) plane is the major slip plane. The direction of easy slip is that in which the atoms are most closely spaced, $\langle\bar{1}2\bar{1}0\rangle$ in this case.

Considering the hypothetical cases of total basal or total prism plane orientation, one would expect that the deformation of each of these might produce different results, as shown schematically in Fig. 4 for simple bending. For the basal plane case, plastic deformation would result in an elongation of the individual grains and a sliding of one layer of grains over the other (Fig. 4A). This mode of deformation would tend to preserve the continuity of the coating, which, in terms of corrosion resistance, is essential. For the prism plane orientation, the stress acts normal to the slip plane, and fracture would be likely (Fig. 4B). Such results would not be unexpected for deposits dominated by low-index pyramid plane orientation.

In practice, the deformation results are not as simple. The section of a typical automotive sheet metal stamping, shown in Fig. 5, indicates evidence of deformation through convex bending, concave bending and stretching. Certain areas are subject to more of one kind of deformation than others. Effects of drawing friction have manifested themselves in large areas of surface galling, where the original zinc structure is smoothed over. This is seen in the large concave bend on the lower part of this section, shown in Fig. 6. In any event, the net result is to rearrange or alter the grain structure of the deposit.

With these considerations in mind, we undertook to prepare deposits exhibiting structures which approached the extremes of total basal and total prism

plane orientation. In the former case, deposits with strong basal orientation were successfully produced. In the latter case, deposits exhibiting strong low-index pyramidal plane ($10\bar{1}X$) orientation, with steeply tilted basal planes, were as close to the ideal as could be prepared. In addition, three lots of commercial samples, produced from sulfate electrolytes, were obtained for study. With this material in hand, the deposit structure and surface morphology were examined and evaluated with respect to forming properties, including deep draw cup deformation and drawbead performance tests.

## EXPERIMENTAL

Electrogalvanizing Flow Cell. The electrogalvanized zinc deposits were produced in a polypropylene flow cell, using a pump to move the electrolyte past the stationary electrodes, simulating a moving strip line. The cell, designed to produce a deposit on one side of the cathode, is illustrated in Fig. 7. The anode used was composed of lead containing 1.0 wt% silver. Both the anode and the steel cathodes were 10 by 20 cm in size. The electrode spacing was 9 mm. The electrolyte flow rate through the cell was measured using a paddle-wheel type sensor and meter. It was regulated using a combination of valves and a bypass loop. The flow rates obtained correspond to flow velocities of 1.0 to 5.0 m/s at the electrode surface.

The electrolyte temperature was measured with an iron/constantan thermocouple and held at the desired level with a 5-kW immersion heater in the reservoir tank. Operation in the 25-30°C range required auxiliary cooling, supplied by a refrigerant cooling coil in the reservoir.

Current was supplied to the cell from a 50 V, 1800 A DC power supply using constant current operation. Time and current were adjusted for different current densities to produce coatings 14 $\mu$m in thickness (100 g/m$^2$). A preset coulometer was used to turn off the current when the desired coating thickness was obtained.

Processing Sequence. Drawing quality, aluminum-killed (DQAK) sheet steel, similar to the material used commercially, was used as substrate material. Residual oil was wiped from the substrate, after which the specimens were degreased in trichlorethylene (TCE) as follows:

| | |
|---|---|
| a) Immerse in boiling TCE | 60 s |
| b) Ultrasonic clean in TCE | 60 s |
| c) Hold in TCE vapor zone | 120 s |
| d) Cool and air dry. | |

The cleaning and activation sequence, prior to zinc electrodeposition, was as follows:

| | |
|---|---|
| a) Acid pickle (25% HCl) | 10 s |
| b) Water rinse | |
| c) Anodic alkaline electroclean | 30 s, 85-90°C, 7.5 A/dm$^2$ |
| d) Water rinse | |
| e) Acid activation (10% $H_2SO_4$) | 15 s |
| f) Water rinse | |
| g) Install in electrogalvanizing flow cell | |

After the specimen was properly mounted, solution flow was started. When stable circulation was established, the sample was electrogalvanized as desired. After removal of the plated sample, it was rinsed twice in water, once in alcohol and air-dried.

Plating Conditions. Earlier studies (6) had indicated that a degree of control of the preferred crystallographic orientation of the zinc deposit was possible by using specific values for the temperature, pH, flow rate and, to a lesser extent, current density. With the exception of pH, all were hydrodynamic factors. By changing these variables, it was possible to produce zinc coatings that were predominantly oriented with the basal (0001) planes parallel to the substrate, or with the pyramidal ($10\bar{1}X$) planes aligned with the substrate.

In order to obtain the optimum conditions necessary to produce the two groups of deposit samples, a series of screening tests was run. X-ray diffractometer traces were run to determine deposit orientation. The percentage of a specific orientation was determined by dividing the total count in the peak for that plane (corrected for the standard pattern intensities) by the total corrected count for all planes and dividing by 100. Selected results are shown in Table I.

**TABLE I. Zinc Orientations under Selected Deposition Conditions.**

| Process Variable | | | | Estimated Percent Orientation | | |
|---|---|---|---|---|---|---|
| C.D. ($A/dm^2$) | Flow (m/s) | Temp. °C | pH | Basal (0001,0002) | Prism ($10\bar{1}0$) | Pyramidal ($10\bar{1}X$) |
| 50 | 2.2 | 33 | 3.5 | >56 | 0 | 35[1] |
| 50 | 4.2 | 26 | 3.5 | >60 | 0 | 32[1] |
| 150 | 4.2 | 26 | 3.5 | >55 | 0 | 40[3] |
| 150 | 2.2 | 50 | 3.0 | 80-95 | 0 | 5-20[1,4] |
| 50 | 2.2 | 26 | 4.5 | 20 | 0 | >75[1] |
| 150 | 2.2 | 26 | 4.5 | 6 | 2 | 80[3] |
| 150 | 4.2 | 26 | 4.5 | 2 | 0 | 80[2,4] |
| 50 | 2.2 | 50 | 4.2 | >40 | 0 | >50[1] |
| 150 | 2.2 | 50 | 4.2 | >45 | 0 | >45[1] |
| 50 | 4.2 | 50 | 4.2 | >40 | 0 | >50[1] |
| 150 | 4.2 | 50 | 4.2 | >45 | 0 | 45[1] |

[1]High index planes ($10\bar{1}3$,$10\bar{1}4$) predominant.
[2]Low index planes ($10\bar{1}1$,$10\bar{1}2$) predominant.
[3]Pyramidal planes evenly distributed.
[4]Condition selected for study.

Of the variables studied, the pH was found to most strongly influence the orientation. Electrolyte temperature altered the orientation to a lesser extent. The effect of flow rate in this flow cell was small.

It was desirable to obtain these deposits by changing a minimum number of electrodeposition variables. The optimum plating conditions for the sulfate plating bath are summarized in Table II.

**TABLE II. Optimum Plating Conditions for Oriented Deposits.**

| Orientation: | Basal | Low-Index Pyramidal |
|---|---|---|
| Zinc Metal (g/l) | 100 | 100 |
| Current Density ($A/dm^2$) | 150 | 150 |
| Temperature | 50 | 30 |
| Flow Velocity (m/s) | 2.2 | 4.2 |
| pH | 3.0 | 4.5 |

As the deposits were produced, X-ray diffractometer traces were run periodically to assure reproducibility. With experience, the two orientations could be differentiated visually. The basal plane oriented deposits exhibited smooth texture, with minimal facets. The pyramidal plane deposits appeared grainy and faceted. However, the visual technique was only a qualitative indicator.

Morphology and Structural Analysis. The surface morphology of the deposits was determined by scanning electron microscopy (SEM). Panel uniformity was checked by examining samples for each orientation group in several locations over the entire panel. We found the surface uniformity to be excellent over the 10 x 20 cm sample area. The SEM was used for as-plated and deformed deposits for the basal, low-index pyramidal and commercial samples.

Crystallographic orientation was determined by X-ray diffractometry (10), scanning from $\theta = 35$ to $90^{\circ}$. As noted earlier, the percent orientation was determined by dividing the total corrected count in the peak for a given plane by the total corrected count for all planes and dividing by 100. Pole figure techniques were not used; analysis of the diffractometer trace was deemed sufficient for these studies.

Draw Cup Formability. One phase of the forming study consisted of a deep draw cup formability test. The electrogalvanized samples were deep drawn into cups on an Olsen sheet metal tester. First, 92-mm diameter disks were punched from the electrogalvanized sheets. The uncoated side was lubricated with a thin layer of silicone grease and placed on the ram of the tester. The zinc-coated side was covered with a thin sheet of polyethylene, which served as a lubricant and a means of retaining any zinc powder that might form during drawing. The disk was clamped with a force of 4.448 kN (1000 lb) and drawn into a cup 33 mm deep and 42 mm in diameter. The maximum load required to form the cup was recorded. The draw cup was examined under the SEM in several areas representing different modes of deformation.

Drawbead Simulation. Drawbead simulation studies were performed to determine the frictional characteristics of the electrogalvanized steel. The apparatus, as shown in Fig. 8, is designed for use in a universal testing machine. A 5-cm wide x 20-cm long strip specimen is drawn through a set of three fixed drawbeads which duplicate the geometry of the drawbead illustrated in the simplified die drawing of Fig. 1. A hydraulic ram is used to maintain the binder hold-down

force, while the strip is drawn through the fixture (Inset). Load cells measure the clamping and drawing loads. The strip pull rate was 508 cm/min.

It was noted earlier that the drawbead force consists of frictional and deformation components. When pulling through the fixed beads, the combined force is measured. In order to determine the component forces, a special roller bead fixture is used in which the fixed beads are replaced by free-rolling cylinders. Any rolling friction is considered to be negligible. The force required to pull a strip through this arrangement is then solely due to deformation.

The coefficient of friction is expressed as the ratio of friction stress, $\tau$, to normal stress, P, or

$$\mu = \frac{\tau}{P} = \frac{\frac{D_{d+f}}{A} - \frac{D_d}{A}}{2 \cdot \frac{\pi}{2} \cdot \frac{C_{d+f}}{A}} = \frac{D_{d+f} - D_d}{\pi C_{d+f}} \qquad (1)$$

where $D_{d+f}$ = measured drawing force for fixed drawbeads,
$D_d$ = measured drawing force for "frictionless" drawbeads
and $C_{d+f}$ = measured clamping force for fixed drawbeads.

The remaining terms represent an area factor based on passage of the strip around two half-circumferences of a drawbead surface. Comprehensive discussion of the development and application of drawbead simulation methods is given elsewhere (1,2).

The development of drawbead simulation methods was based on friction forces acting on both sides of the strip. In an evaluation of coated steel, it would follow that the coating should be applied on both sides of the specimen. However, the design of the electrogalvanizing flow cell allowed deposition of zinc on only one side of the panel. A fixed drawbead test of a sample with electrodeposited zinc on one side and bare steel on the other would give a composite coefficient of friction with vague physical meaning.

In order to obtain a value representing the friction on only the electrogalvanized surface, a single fixed drawbead was bracketed by two roller drawbeads (i.e., the right-side of the fixed bead fixture shown in the inset of Fig. 8 was replaced with the corresponding side of the roller bead fixture). Thus, the frictional component arose only from contact with the zinc surface. Since the strip would contact the drawbead over one half-circumference, the coefficient of friction would be:

$$\mu = \frac{\tau}{P} = \frac{\frac{D_{d+f}}{A} - \frac{D_d}{A}}{\frac{\pi}{2} \cdot \frac{C_{d+f}}{A}} = 2 \cdot \frac{D_{d+f} - D_d}{\pi C_{d+f}} \qquad (2)$$

The above analysis does not consider any perturbation of the deformation force arising from the roller beads on the other side of the specimen. Nevertheless, the results are valid on a relative basis. Although the commercial samples were coated on two-sides, the same one-side friction test was used for these materials to examine the results with the same frame of reference.

Drawbead studies were carried out with two degrees of lubrication. A split-phase prelube oil, formulated for metal stamping operations, was used to simulate actual lubrication conditions during drawing. A thinner mil oil, not designed for drawing applications, was used to test the steel under adverse drawing conditions. Preferred orientation samples were run without lubricant, but concerns over potential damage to the drawbead fixture made it expedient to limit testing to one sample each.

In order to examine the effect of severe deformation on the various zinc-coated samples, the surface morphology of the drawbead-tested specimens was examined with the SEM.

## RESULTS & DISCUSSION

As-Plated Deposit Structure and Surface Morphology. The surface morphologies of the as-plated zinc electrodeposits are shown in the SEM photographs in Fig. 9. The corresponding X-ray diffraction results are presented in Table III. The basal plane deposits are seen to differ markedly from the pyramidal plane deposits. The pyramidal plane deposits more closely resemble the general surface character found in commercial deposits. The three commercial deposits, while exhibiting the same general surface character, show some variation in basal plane tilt and grain size.

TABLE III. X-Ray Diffractometer Results - Orientations

| Crystal Plane | Estimated Percent Orientation: Basal Group | Pyramidal Group | Commercial "A" | Commercial "B" | Commercial "C" |
|---|---|---|---|---|---|
| BASAL PLANES: | | | | | |
| (0001) | 99.2 | 5.8 | 3.9 | 59.6 | 5.8 |
| (0002) | 0.2 | | | 0.1 | |
| Σ = | 99.4 | 5.8 | 3.9 | 59.7 | 5.8 |
| PYRAMIDAL PLANES: | | | | | |
| (10$\bar{1}$1) | | 62.9 | 21.6 | 12.8 | 69.1 |
| (10$\bar{1}$2) | | 11.3 | 24.0 | 4.9 | 11.3 |
| (10$\bar{1}$3) | 0.6 | 13.5 | 45.5 | 21.4 | 8.8 |
| (1$\bar{1}$02) | | 3.2 | 3.9 | 0.1 | 4.0 |
| Σ = | 0.6 | 90.9 | 95.0 | 39.2 | 93.2 |
| PRISM PLANE: | | | | | |
| (10$\bar{1}$0) | | 3.0 | 1.1 | | 0.5 |
| Σ = | 0.0 | 3.0 | 1.1 | 0.0 | 0.5 |

When the deposition conditions favor the alignment of basal planes parallel with the substrate surface, the surface morphology takes on an entirely different character (Fig. 9a). There is no overlapping of grains as observed in deposits exhibiting pyramidal plane alignment. The vertical stacking appears to allow a more open structure, as noted between grains. X-ray diffractometry shows the strong dominance of the basal plane reflections. Virtually all other planes are absent from the spectrum.

The pyramidal plane surface (Fig. 9b) more closely resembles those found in the commercial specimens (Figs. 9c-e). In fact, X-ray results indicate that samples from commercial group "C" have similar high proportions of low-index pyramidal plane orientation. Both "A" and "C" groups show similar total fractions of basal and pyramidal orientation. The pyramidal plane deposit from the flow cell exhibits more variable grain size.

The X-ray diffraction data correlates well with the surface morphology. The differences between the basal and pyramidal groups are very clear. More significant is the ability to discern between the commercial deposits. The X-ray data show that the "B" commercial group has a smaller portion of low-index pyramid planes and a significant amount of basal plane alignment. The surface in Fig. 9d exhibits basal planes positioned at shallower angles than what is observed in groups "A" and "C". However, the differences in relative portions of the various pyramidal planes of the "A" and "C" samples cannot be reliably discerned.

The electrogalvanizing flow cell tests confirm that electrolytic and hydrodynamic conditions influence the structure and surface morphology of the zinc electrodeposits. Electrolyte pH was dominant in influencing the orientation of the basal planes, while temperature played a lesser role. Under the conditions studied, the effect of flow rate on morphology was minimal.

Deep Draw Cup Deformation. Analysis of the surfaces of the basal and pyramidal plane specimens after draw cup formation showed significant differences in deformation behavior. The SEM results are shown in Figs. 10 and 11 for the basal and pyramidal deposits, respectively.

The draw cup surface is subject to several modes of deformation, depending on location, as shown in Fig. 10. The vertical side of the cup (a) primarily undergoes draw deformation as the punch pushes the center of the blank toward the top of the cup and the flat binder restricts the metal flow from the bottom. Metal flow at the top of the cup is minimal and the deformation at the upper edge (b) is mainly due to tensile bending. In the binder area (c), frictional forces serve to control metal flow into the cup and thus act on the metal surface. Beyond the binder, where the material flows into the die cavity (d), compression bending is added to the frictional deformation produced when that particular metal area was in the binder.

The primary deformation characteristic of the basal plane oriented deposit is elongation. The slip characteristic hypothesized in Fig. 4 is evident in Fig. 10. In the area of draw deformation (a), the zinc grains are elongated but no fracture is evident in the coating. In the tensile bend (b), the surface morphology is relatively undisturbed, with no apparent elongation. There is a suggestion of a widening of the space between grains, but no indication of fracture is

noted. Slight elongation is seen in the binder area (c) and there is no evidence of galling. The main characteristic in the concave bend (d) is a major realignment of the individual grains brought about by the compressive stress which formed the concave surface. There is no evidence of surface galling such as was noted in the stamping shown in Fig. 6; the use of the polyethylene sheet during drawing prevented direct metal-to-metal surface contact.

Fracture is the dominant characteristic of the deformation produced in the pyramidal plane oriented deposits, as seen in Fig. 11. This was also in line with the cracking suggested in the diagram of Fig. 4. Cracking is the dominant characteristic in the draw deformation (a) and tensile bending (b) areas. The zinc deposit in the binder area (c) was subject to draw deformation; grain elongation and reorientation is noted. Cracking is also seen in the concave radius area (d). The relatively wide variation in grain size noted in the as-plated deposits is evident in these photographs. No surface galling was noted in any of the areas studied.

Drawbead Simulation - Surface Effects. The SEM results for the flow cell and commercial deposits subjected to the drawbead simulator with and without prelubricant are presented in Figs. 12 and 13, respectively.

The basal plane and low-index pyramidal plane deposits generally exhibited the same deformation characteristics observed in the deep draw cup deformation study (Fig. 12). The basal plane oriented deposits underwent little notable change while the low-index pyramid plane deposits were subject to fracture. A pattern of parallel cracks normal to the direction of the draw can be clearly seen in the low magnification (200X) photos (Fig. 12b,d).

All deposits, including the commercial specimens, exhibited galling in the drawbead study. This was observed with all specimens and is related to the test procedure, rather than to the nature of the deposits. This was not observed in the deep draw cup study, owing to the use of polyethylene sheet as a lubricant. Severe surface deformation in drawbead areas is not uncommon in practice. Such areas are designed to be trimmed off the final part in the later stages of the stamping sequence.

The use of the prelube tended to reduce the amount of galling for both types of deposits. The total area subject to galling was reduced when compared to the corresponding SEM photo for the drawbead test specimen run without lubricant. In general, there was little difference in surface change between the specimens run with the poor lubricant (mil oil) and those run dry.

The effect of drawbead deformation on the surface of the commercial electrogalvanized specimens was primarily one of surface galling, as shown in Fig. 13. Although not apparent at the magnification shown (1000X), the previous trend of decreased area of galling with the use of the prelubricant was observed, at lower magnification. Surprisingly, no cracking was observed in the commercial "C" deposits, whose crystallographic orientation was found to be virtually identical to that of the low-index pyramidal plane deposits prepared in the flow cell. This behavior difference may in part be attributed to grain size, which in turn is determined by the conditions of electrolysis (including temperature, pH, current density, etc.). The grain size of the "C" deposits was smaller and more uniform than that of the flow cell pyramidal deposits.

Drawbead Simulation - Coefficients of Friction. Coefficient of friction measurements for all deposits are summarized in Table IV. With the use of the prelubricant, the coefficients of friction vary little from one group to another, indicating that the lubricant is doing what it is supposed to do. Under poor lubrication conditions, differences become apparent.

**TABLE IV. Drawbead Test Results - Coefficient of Friction**

| Oil Type | Coefficient of Friction (Mean ± Std. Dev.) Basal Group | Pyramidal Group | Commercial "A" | Commercial "B" | Commercial "C" |
|---|---|---|---|---|---|
| Prelube | 0.11±0.01 | 0.11±0.01 | 0.09±0.02 | 0.11±0.01 | 0.10±0.01 |
| Mil Oil | 0.19±0.03 | 0.13±0.01 | 0.14±0.01 | 0.16±0.02 | 0.16±0.03 |
| Dry | 0.20 | 0.15 | --- | --- | --- |

Considering the results for the mil oil drawbead runs, the basal plane deposits exhibit higher friction than the pyramidal plane deposits. The same result holds for the tests without lubricant. On first analysis, one might expect the opposite, owing to the favorable slip plane orientation in the basal deposits. However, this alignment, in aggregate, actually gives rise to an increase in area of contact with the die surface, as shown in Fig. 14a. The pyramidal deposits, along with the commercial deposits, would exhibit reduced direct contact area, since point- or line-type contact would be established with the corners or edges of the deposit grains, as in Fig. 14b. These effects were also observed qualitatively. Galling effects resulted in an accumulation of zinc on the surface of the drawbead. The amount of the buildup was higher for the basal deposits, where the friction was higher. The larger standard deviation for the basal plane deposits may be attributed to the fact that a slight misalignment of planes will result in a disproportionately large decrease in true contact area.

The coefficient of friction for the pyramidal plane specimens was lower than the values measured for the commercial samples. Since these samples had virtually identical orientation, the reason for this difference is not clear. One reason may be that the commercial samples were electrogalvanized on both sides. The standard deviations for these results are larger than what has been experienced in past drawbead work on coated or uncoated sheet steel (1,2). This may be related to several factors. The use of the combination roller bead/fixed bead fixture arrangement could have subtly changed the pull characteristics during the test. Because of surface galling, zinc tended to accumulate on the surface of the fixed bead after two or three tests, requiring cleaning. The zinc buildup may have contributed to some of this variation.

Electrogalvanized Coating Performance Considerations. The results of this work indicate that the forming characteristics of electrogalvanized sheet steel can be altered by variations in the structure and surface character of the zinc electrodeposit. The low-index pyramid structures produced in this work were subject to cracking under conditions of draw deformation. Fortunately, the

cracking behavior observed for deposits created in the electrogalvanizing flow cell was not found in the commercial products tested. However, because of the profound effect of pH on the crystallographic structure, the prudence of monitoring process variables is readily apparent.

Consideration of the phenomena observed in this work would lead one to expect that the interactions between orientation and forming properties would carry over to other performance properties, including phosphatability, paintability and corrosion performance. Wang (11), in a study of the corrosion of zinc single crystals has found that various crystallographic planes will corrode at different rates. The basal plane exhibits the slowest rate. It may be that the alignment of the basal plane can influence corrosion and, because of surface reactivity, the phosphating process. Future work will address these issues.

## CONCLUSIONS

1. Zinc electrodeposits, prepared in the laboratory from a sulfate electrolyte, whose basal (0001) planes are oriented parallel to the plane of the substrate undergo elongation under draw deformation conditions. Surface galling is encountered under conditions of drawbead simulation. The deformation conditions were not detrimental to the continuity and integrity of the coating.

2. Zinc electrodeposits, prepared in the laboratory from a sulfate electrolyte, whose pyramidal ($10\bar{1}X$) planes are oriented parallel to the plane of the substrate can undergo inter- and intra-granular fracture under conditions of draw deformation and bending. Surface galling and cracking was encountered under conditions of drawbead simulation.

3. Commercial zinc electrogalvanized deposits, from sulfate electrolytes, whose pyramidal ($10\bar{1}X$) planes are oriented parallel to the plane of the substrate retained deposit integrity under conditions of draw deformation and bending. Surface galling was encountered under conditions of drawbead simulation. The difference in performance with 2) above may be related to grain size distribution.

4. In sulfate electrogalvanizing electrolytes, variations in electrolyte pH have a significant influence on the crystallographic orientation and surface morphology of the zinc electrodeposits. Electrolyte temperature alters the orientation to a lesser extent. The effect of flow rate is negligible under the conditions studied.

5. The coefficient of friction of basal plane oriented deposits is higher than that for pyramidal plane oriented deposits, owing to geometric surface area factors. This difference is erased with the presence of an efficient lubricant.

## ACKNOWLEDGEMENTS

We are most appreciative of the dedicated teamwork and efforts of Ray Prater, Jr., Thomas Stachowski, Jody Mawhorter and Jean Laverty, of the Resource Processing Group, Rolla Research Center (U.S. Bureau of Mines). They were instrumental in obtaining reproducible deposits from the flow cell in a timely manner.

The authors gratefully acknowledge the skillful efforts of Robert S. Conell, Physical Chemistry Department and H. M. Wang, University of Missouri - Rolla, in performing the X-ray diffraction work. The assistance and helpful comments of Mr. J. J. Moleski, Physics Department, in the drawbead work are also appreciated.

Finally, we are indebted to Messrs. Joseph Bronson and Abhay Vadhavkar, Chevrolet-Pontiac-Cadillac Group Engineering, for supplying us with the commercial samples for comparative evaluation.

REFERENCES

1. Nine, Harmon D., "Drawbead Forces in Sheet Metal Forming", Mechanics of Sheet Metal Forming, (Koistinen, D. P. and Wang, N.-M., Editors) 179-211, Plenum Publishing Co., New York, NY (1978).

2. Nine, H. D., "The Applicability of Coulomb's Friction Law to Drawbeads in Sheet Metal Forming", J. Applied Metalworking, 2, (3), 200-210 (1982).

3. Meuleman, D. J. and Zoldak, J. J., "The Interactions of Coated Steels, Die Materials and Forming Lubricants", SAE Technical Paper Series No. 860432, Society of Automotive Engineers, Warrendale, PA (1986).

4. Keeler, S. P. and Dwyer, T. E., "Frictional Characteristics of Galvanized Steels Evaluated with a Draw Bead Simulator", SAE Technical Paper Series No. 860433, Society of Automotive Engineers, Warrendale, PA (1986).

5. Brazier, W. G. and Thompson, R. W., "The Effects of Zinc Coatings, Die Materials and Lubricants on Sheet Metal Formability", SAE Technical Paper Series No. 860434, Society of Automotive Engineers, Warrendale, PA (1986).

6. Chen, S. F., Cuzmar, J. S., O'Keefe, T. J., Cole, E. R., Miller, V. R. and Lindsay, J. H., "Measurement of Mass Transfer Effects in Sulfate Electrogalvanizing Electrolyte", Proc. AESF 5th Continuous Plating Symposium (May 5-7, 1987), Amer. Electroplaters' and Surf. Finishers' Soc., Orlando, FL (1987).

7. Roberts, T. R. and Guzzetta, F. H., "Effect of Processing Temperature on the Microroughness of Electroplated Zinc Coatings on Steel", Proc. AESF 5th Continuous Plating Symposium (May 5-7, 1987), Amer. Electroplaters' and Surface Finishers' Soc., Orlando, FL (1987).

8. Jiricny, V., Choi, H., and Evans, J. W., "Zinc Electrodeposit Morphology Under Conditions of Fluctuating Current Density", J. Applied Electrochem., 17, 91-103 (1987).

9. Hull, D., Introduction to Dislocations, Pergamon Press, New York, NY (1965).

10. Cullity, B. D., Elements of X-ray Diffraction, Addison-Wesley, Reading, MA (1959).

11. Wang, Y-M., Private Communication (1987).

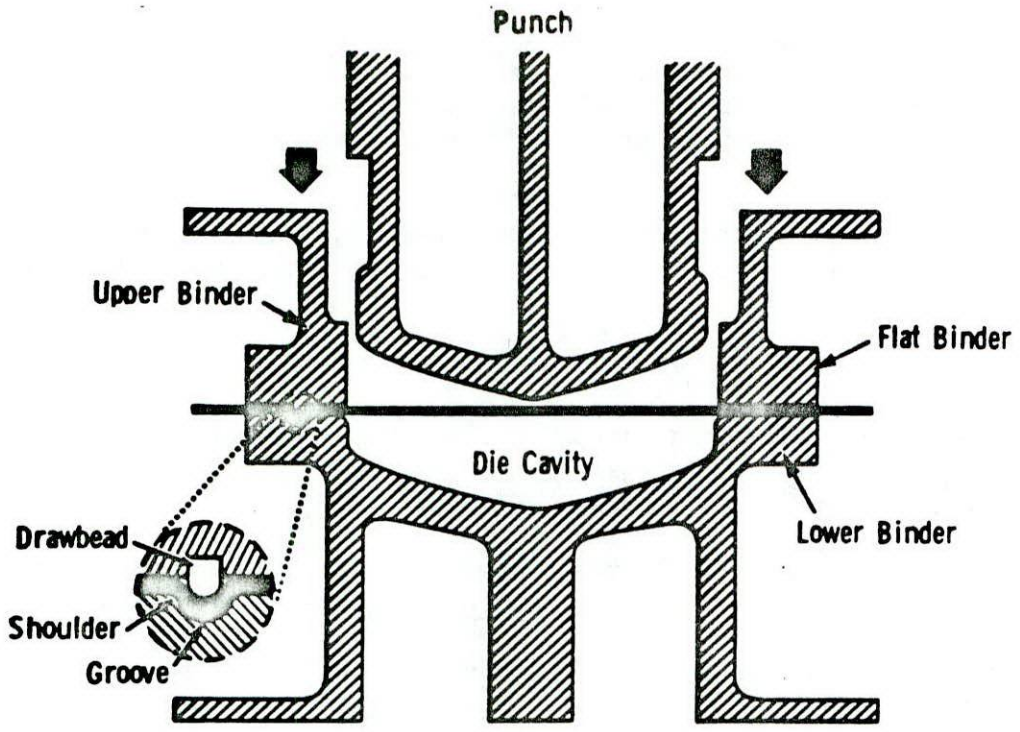


a) Upper binder moves down to hold the sheet metal in position for forming.

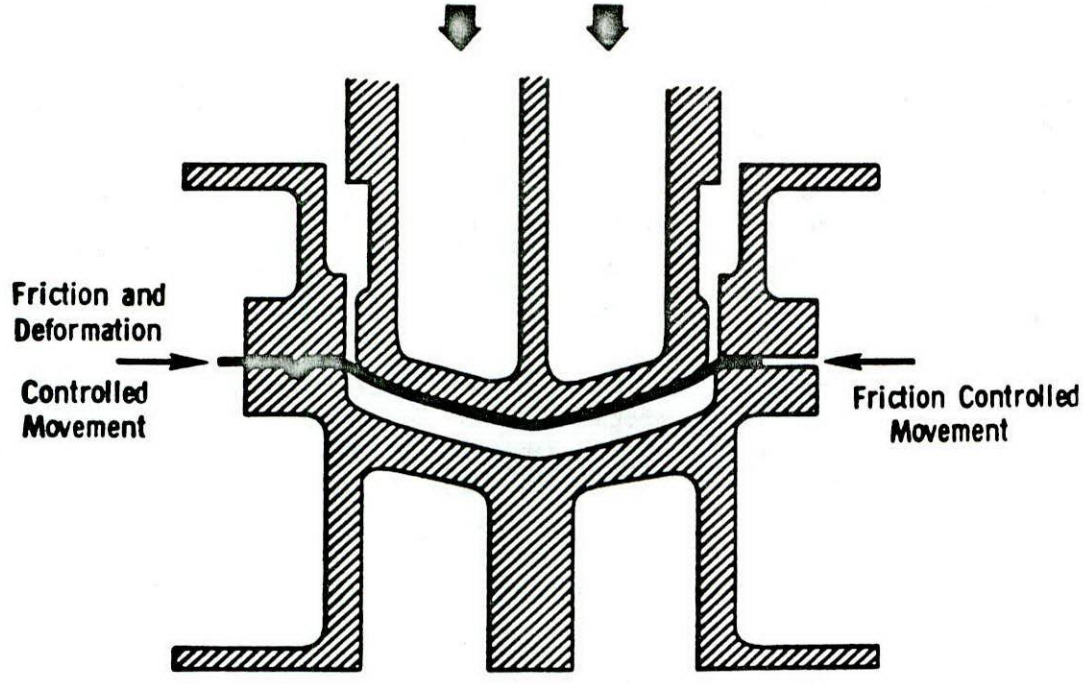


b) Punch moves down into lower die cavity, drawing sheet metal into the die through the binders.

Fig. 1 - Double Action Press

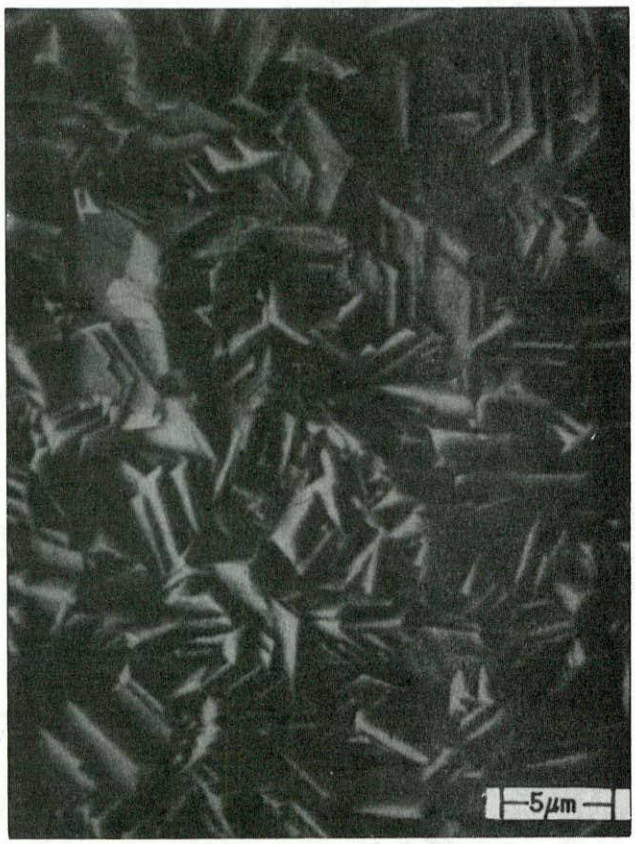


Fig. 2 - Typical surface appearance of a commercial electrogalvanized zinc coating. (SEM: 3000X)

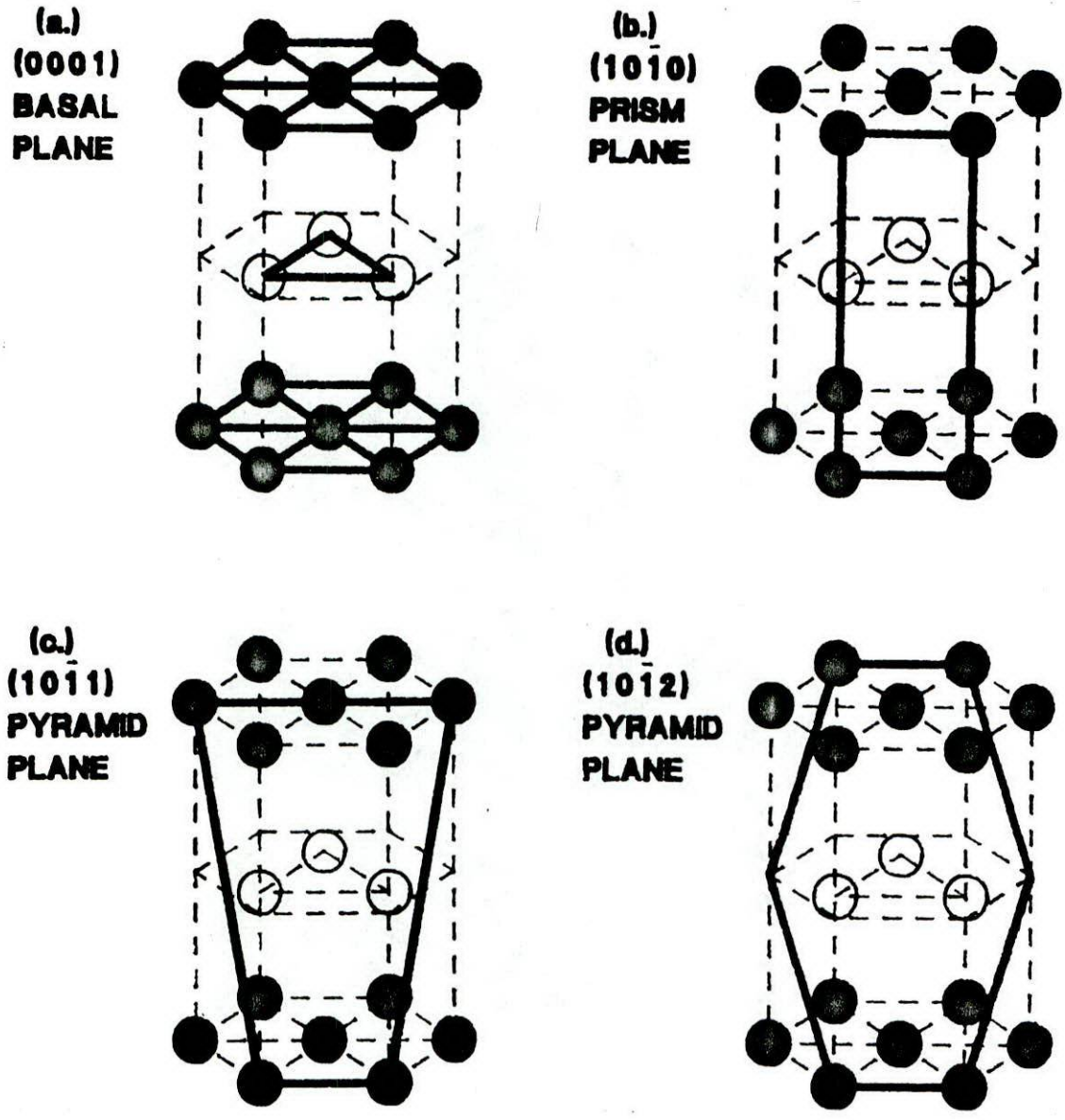


Fig. 3 - Principal orientation planes for zinc HCP crystals.

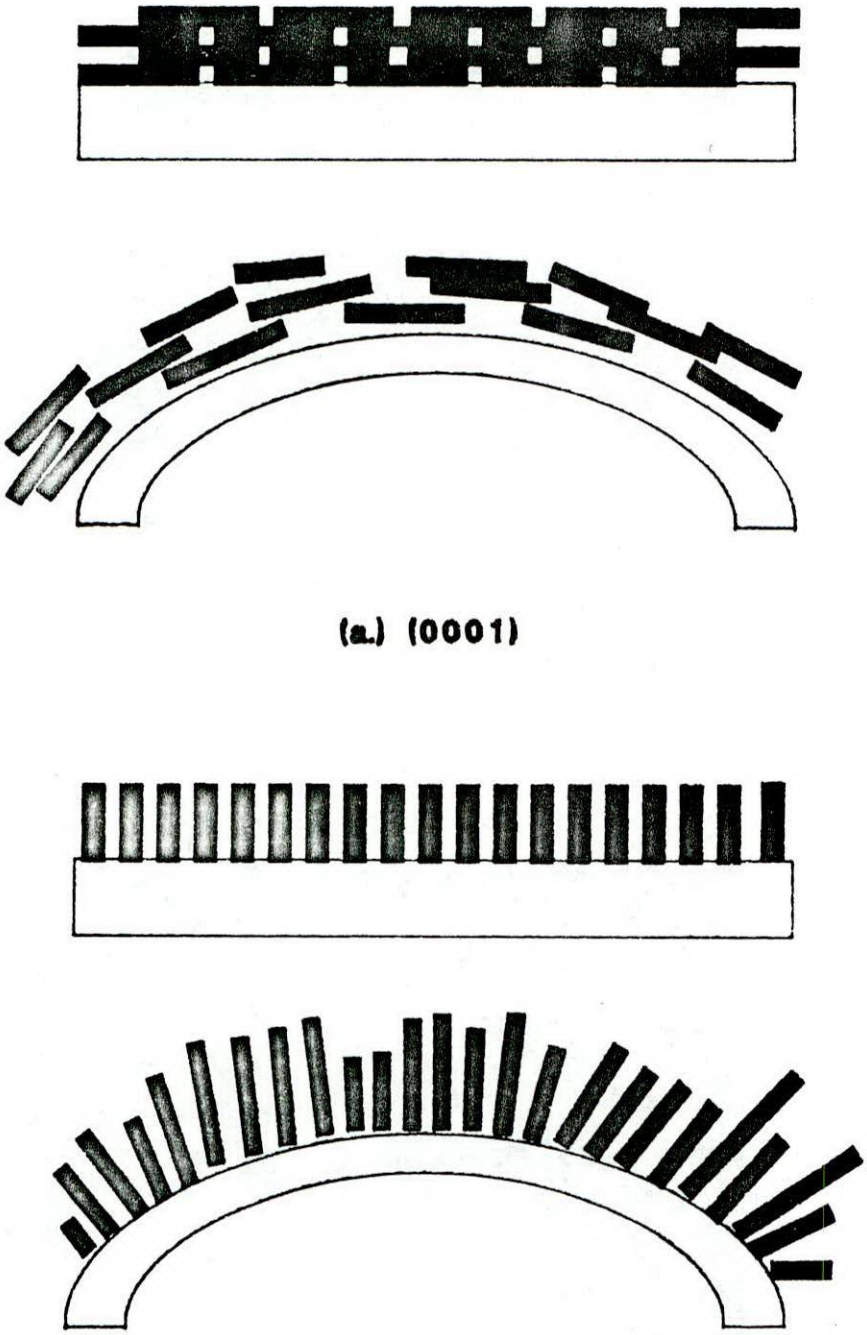


Fig. 4 - Consequences of simple tensile bending on deposits of complete basal and prism plane orientation.

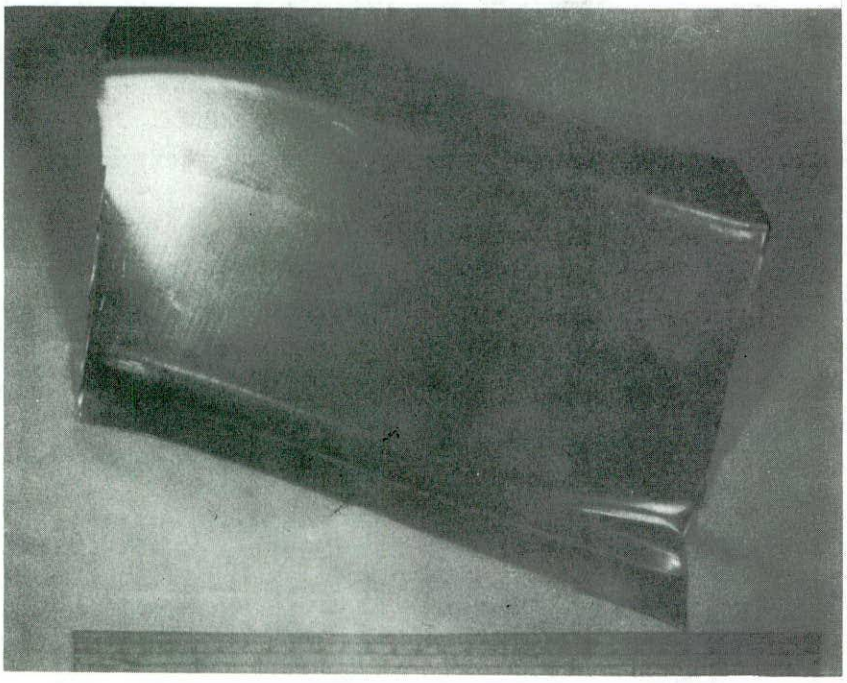

Fig. 5 - Section of a typical EG sheet stamping.

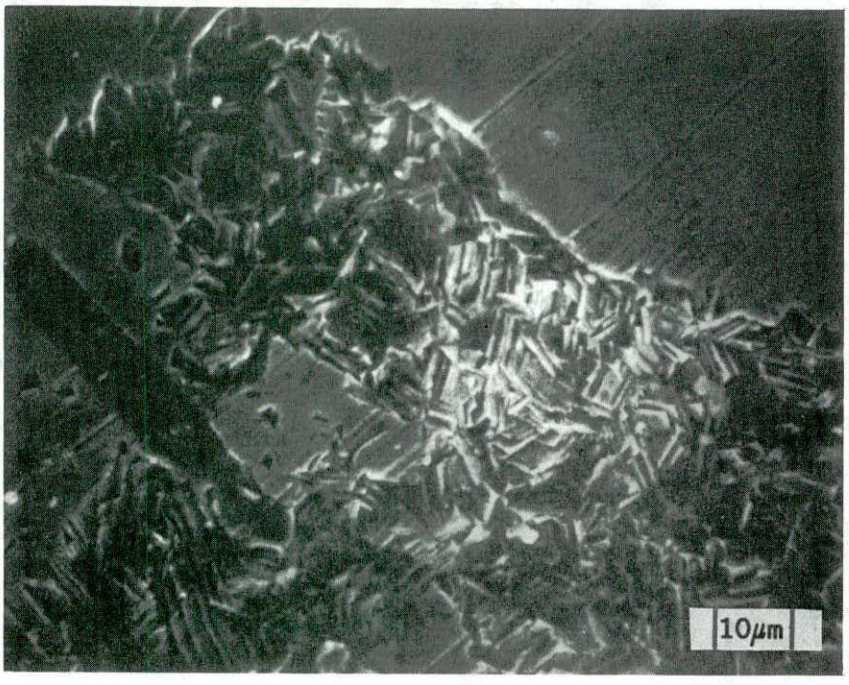


Fig. 6 - Galling of electrogalvanized surface of sheet metal stamping. (SEM: 1000X)

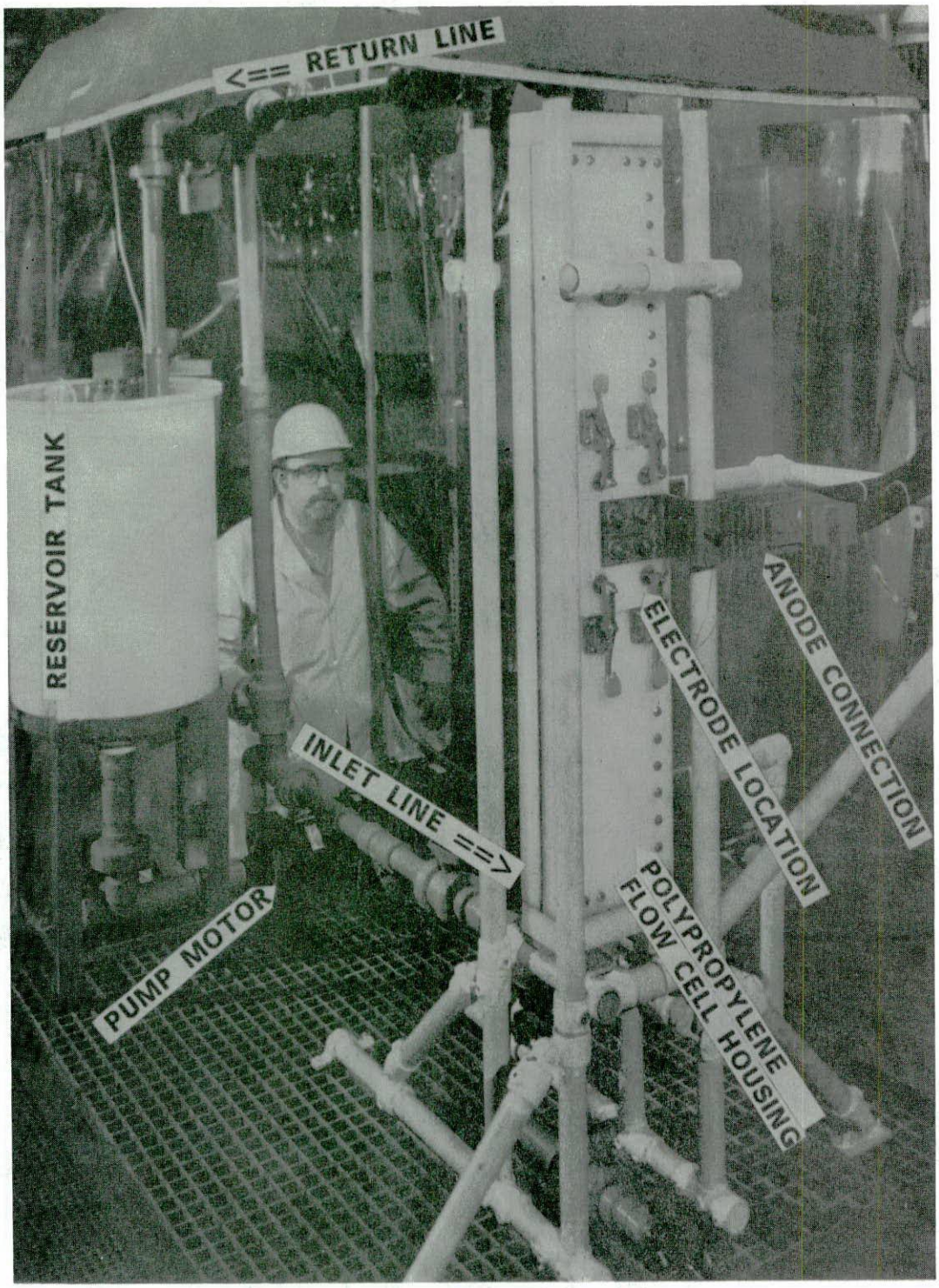


Fig. 7 - Layout of electrogalvanizing flow cell.

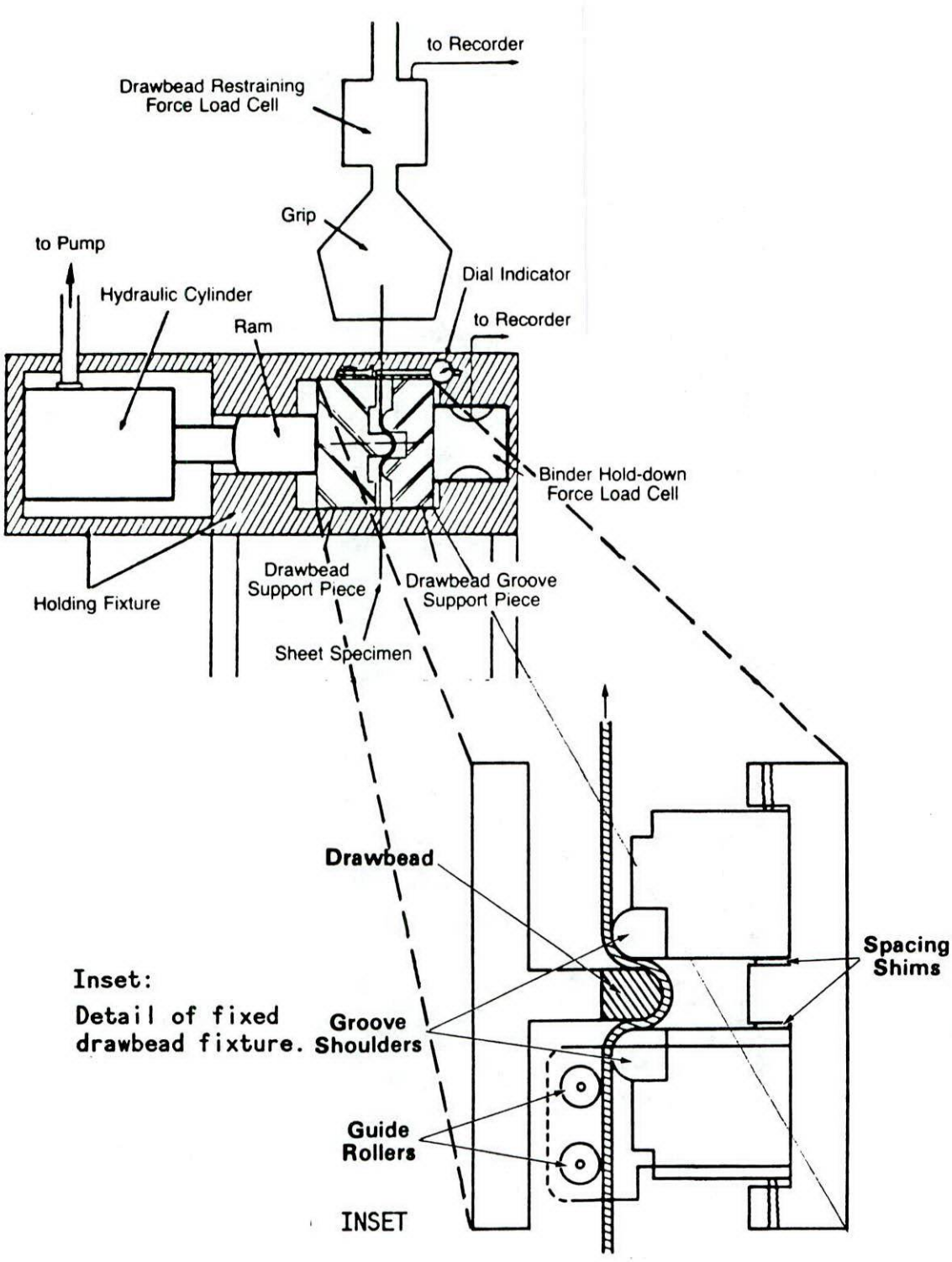


Fig. 8 - Schematic diagram of drawbead simulator apparatus.

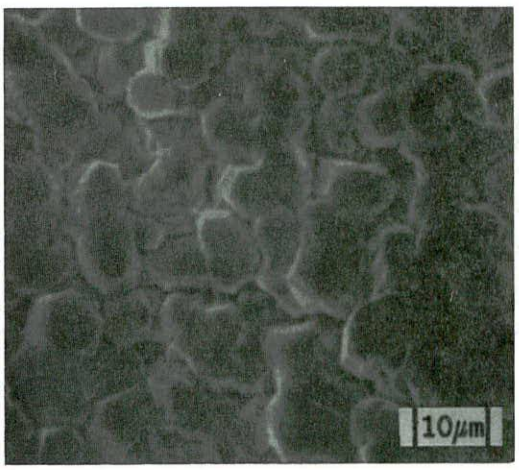


a) Basal plane deposit

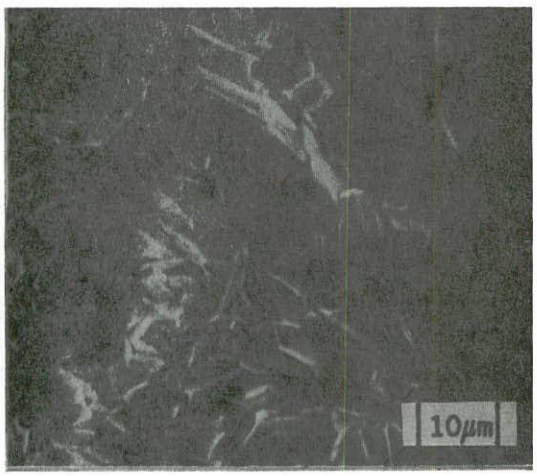


b) Pyramidal plane deposit

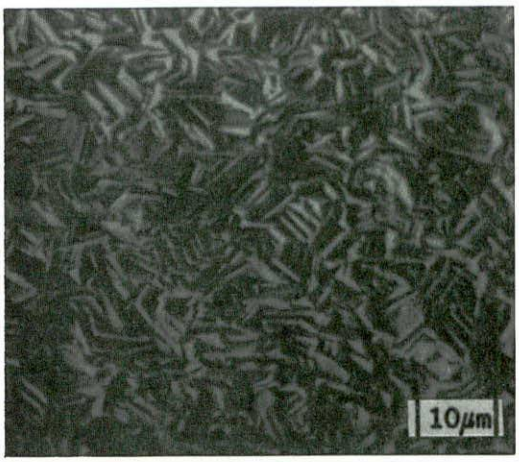


c) Commercial deposit "A"

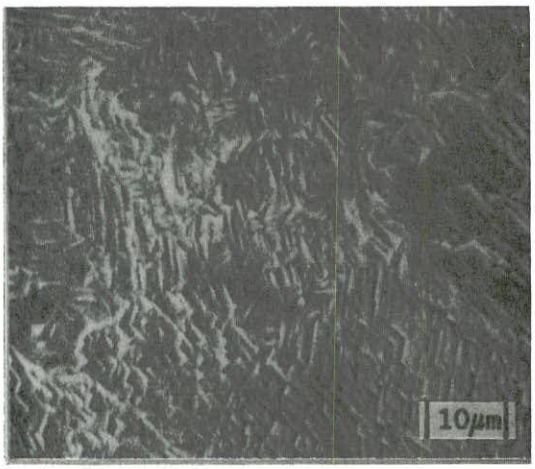


d) Commercial deposit "B"

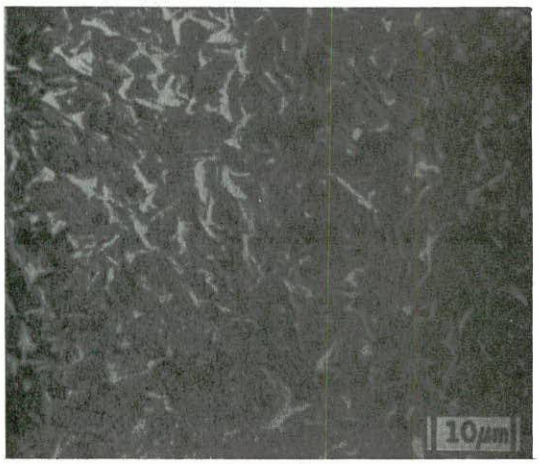


e) Commercial deposit "C"

Fig. 9 -
Electrogalvanized zinc in the as-deposited condition. (SEM: 1000X)

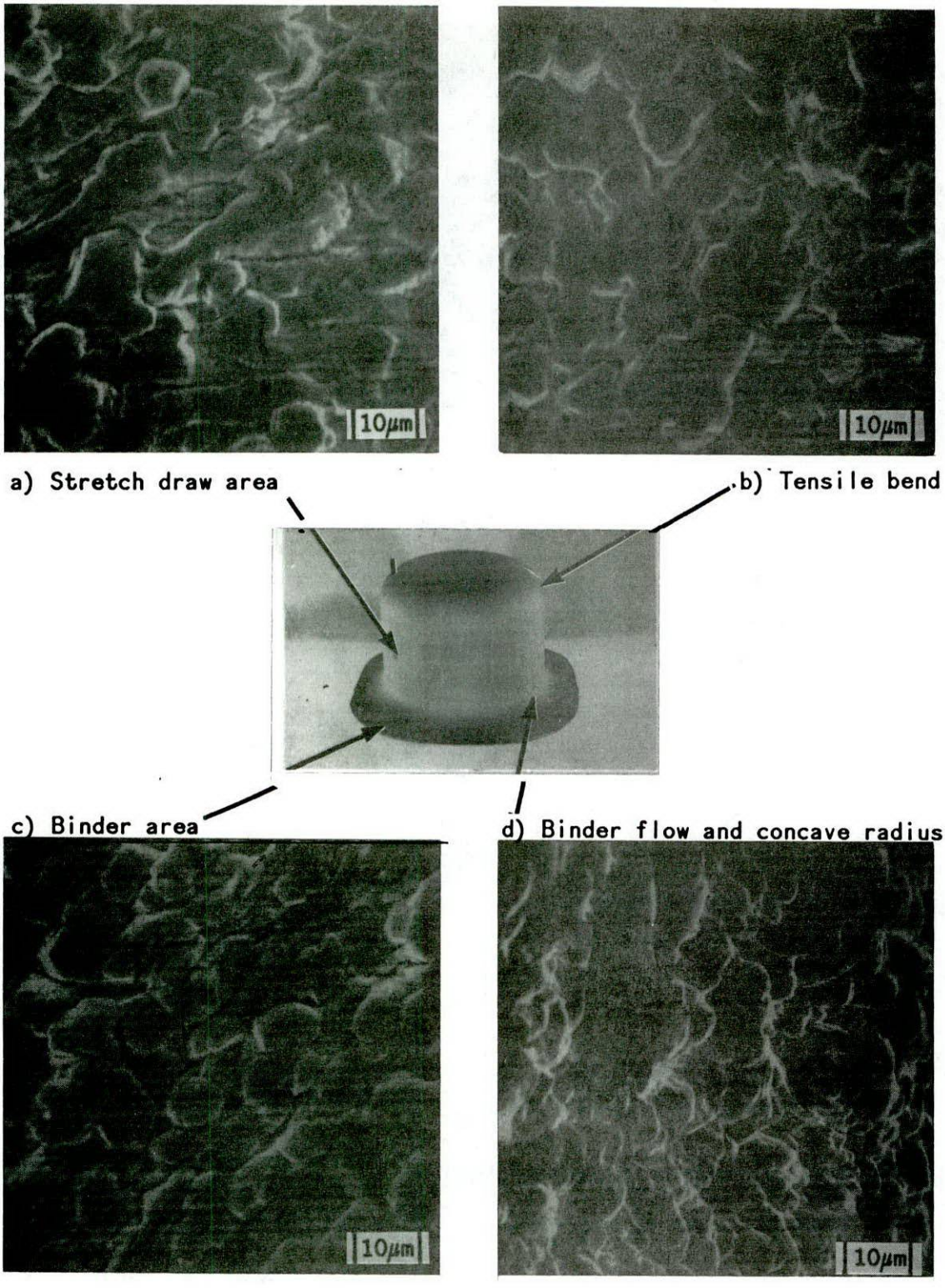


Fig.10 - Draw cup results - basal plane samples. (SEM: 1000X)

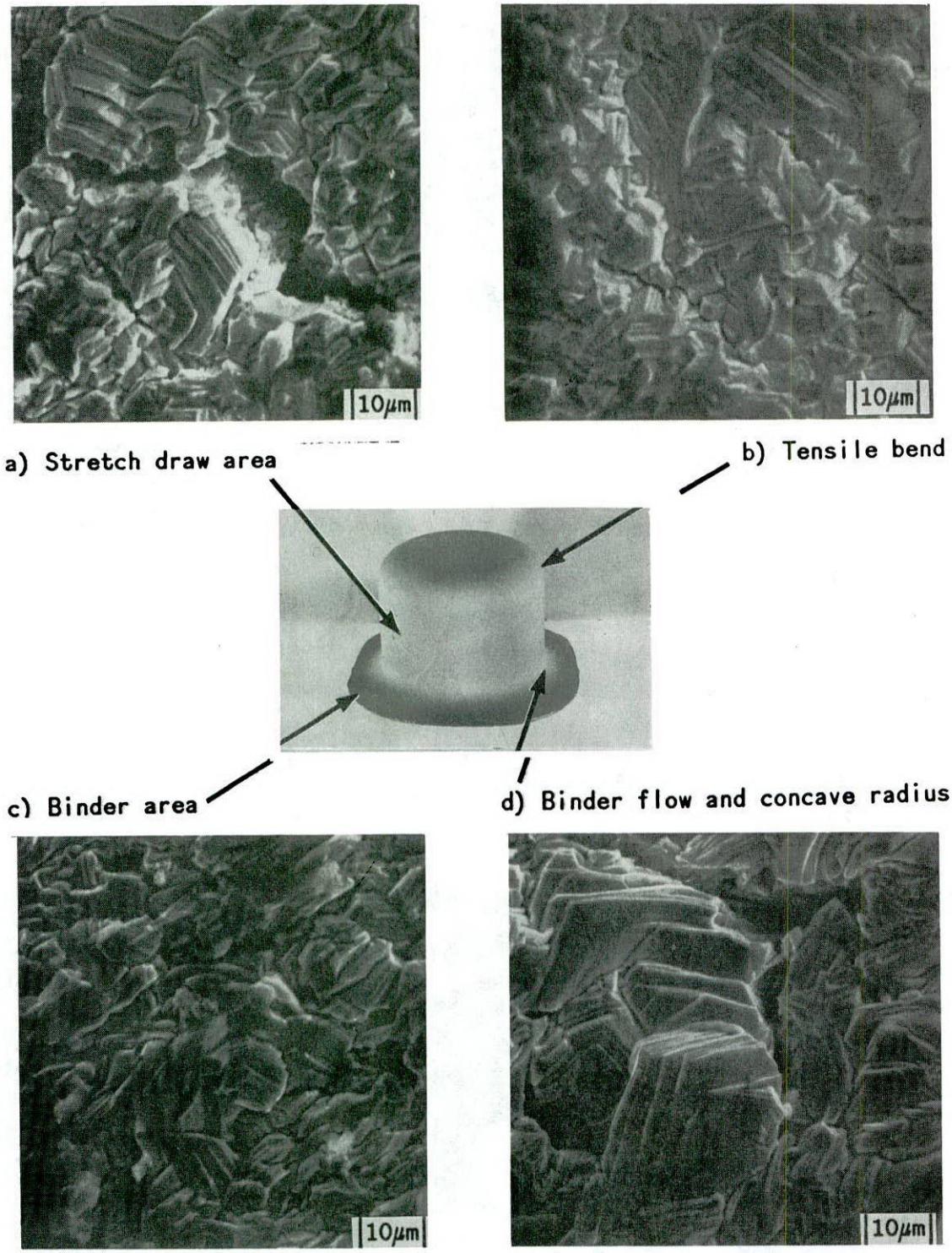


Fig.11 - Draw cup results - pyramidal plane samples. (SEM: 1000X)

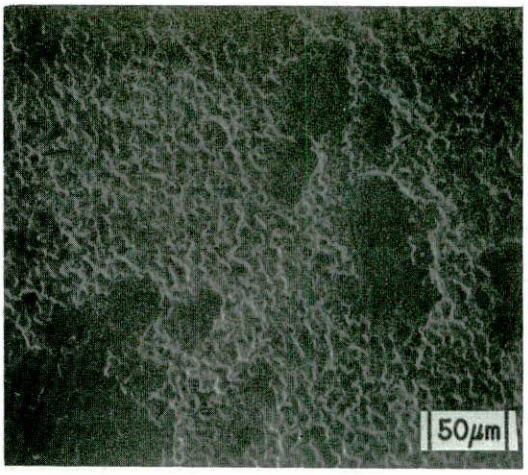


a) Basal - Prelube (200X)

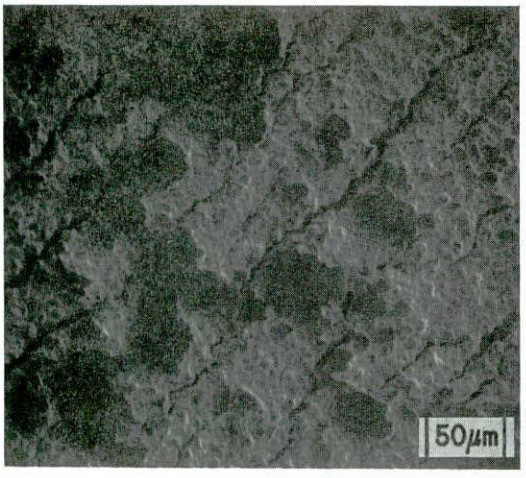


b) Pyramidal - Prelube (200X)

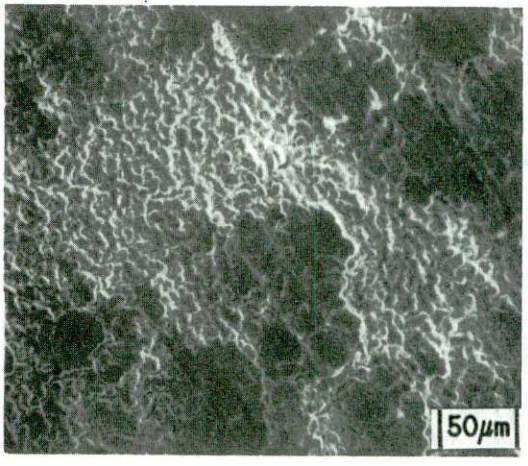


c) Basal - Dry (200X)

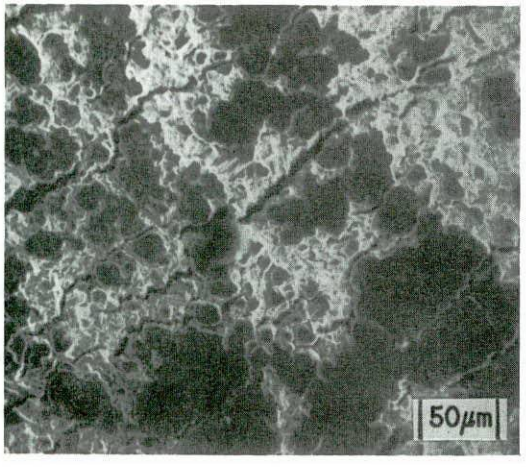


d) Pyramidal - Dry (200X)

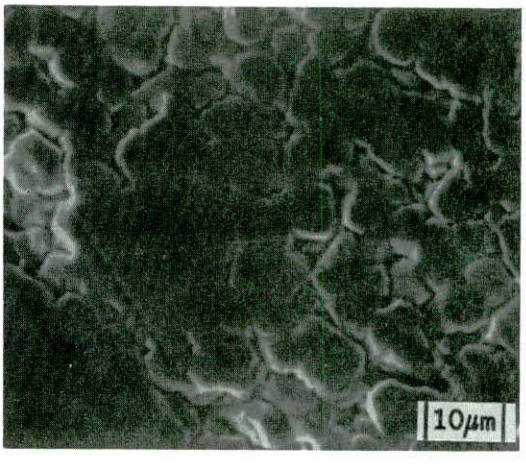


e) Basal (1000X)

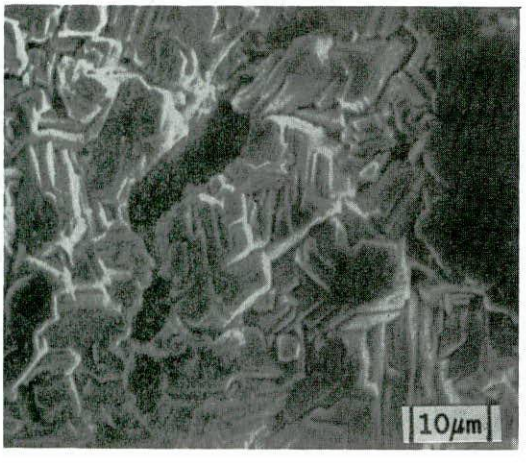


f) Pyramidal (1000X)

Fig.12 - Electrogalvanized zinc surfaces after drawbead tests - Orientation groups. (SEM)

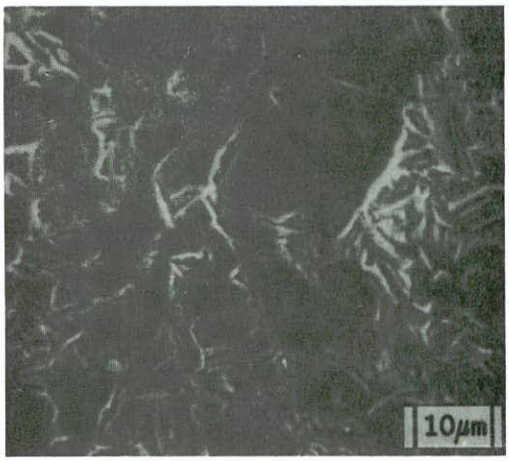


a) Commercial "A" - Prelube

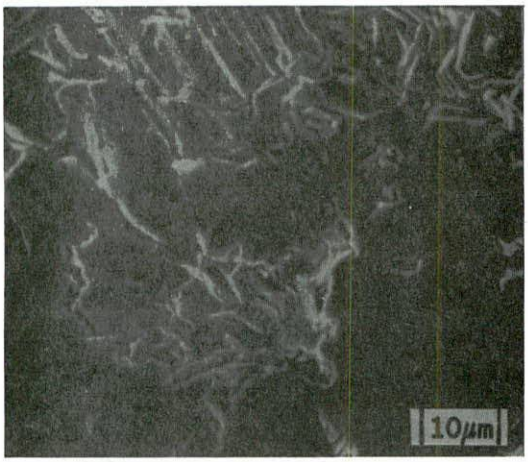


b) Commercial "A" - Mil Oil

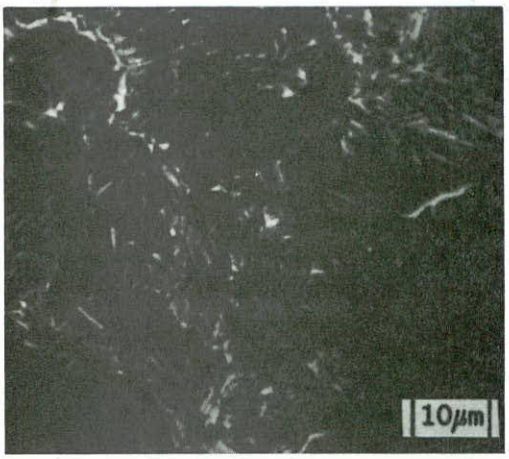


c) Commercial "B" - Prelube

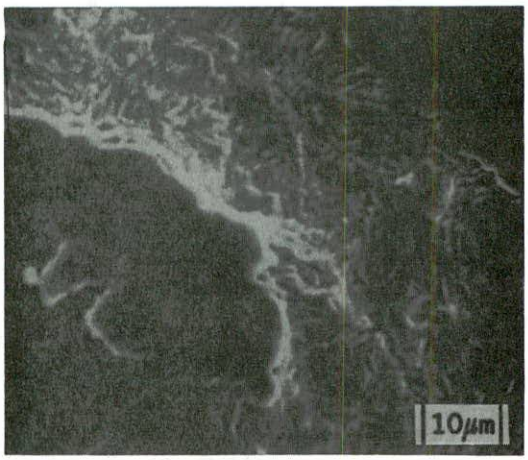


d) Commercial "B" - Mil Oil

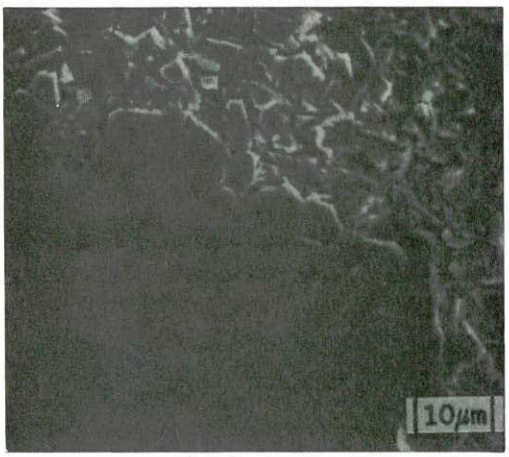


e) Commercial "C" - Prelube

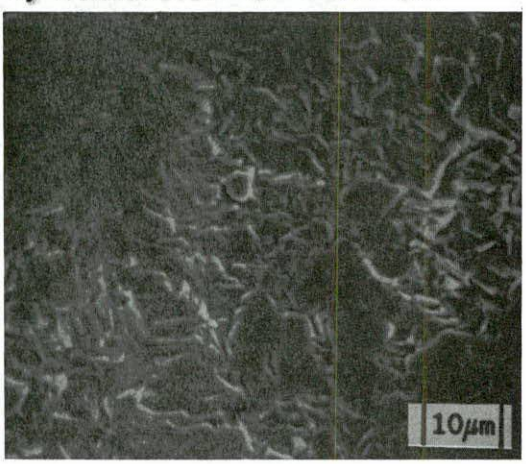


f) Commercial "C" - Mil Oil

Fig. 13 - Electrogalvanized zinc surfaces after drawbead tests - Commercial samples. (SEM: 1000X)

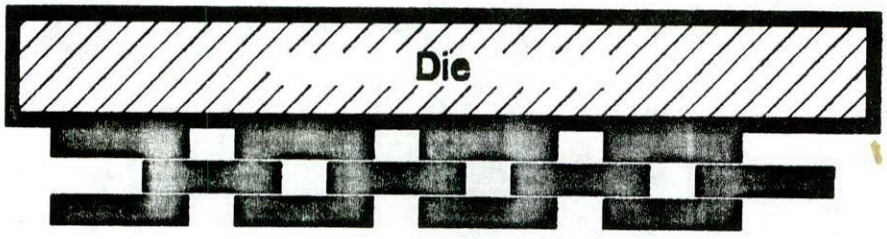


a) Basal plane - large contact area

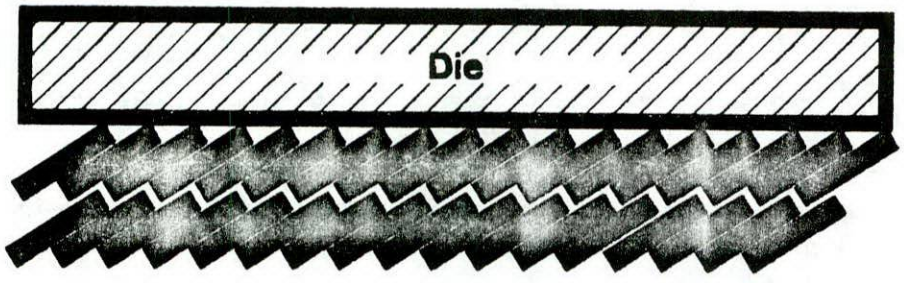


b) Pyramid plane - reduced line and point contact area

Fig. 14 - Die / deposit contact geometry.

H-4

# General Interest
# Session H

## Effect of Additives on Performance of Acid Copper Plating Baths

Morton Schwartz, Sunghee Yoon
and Ken Nobe
Department of Chemical Engineering
University of California
Los Angeles, CA 90024

# Effect of Additives on Performance of Acid Copper Plating Baths

Morton Schwartz, Sunghee Yoon and Ken Nobe
Department of Chemical Engineering
University of California
Los Angeles, CA 90024

## Abstract

The dependence of bright copper electrodeposits on $Cl^-$, organic additives and mass transfer in acid copper sulfate baths was investigated with rotating ring disk electrodes. The surface appearance of copper deposits was examined either visually or with an optical microscope after potentiostating the disk electrode. Thiourea and a proprietary brightener (PB) were selected as organic additives. Bright copper deposits were obtained in the presence of thiourea or PB only with the addition of small optimum amounts of $Cl^-$. Minimum hydrodynamic flow conditions (Reynolds no. ~200) for bright copper deposits are estimated for both thiourea and PB baths.

## Introduction

It has been found that the addition of small amounts of additives to copper sulfate baths has a significant effect on copper deposit characteristics such as brighteners, grain size, hardness, ductility and internal stress. Unsaturated organic compounds containing sulfur, nitrogen or oxygen are known to brighten copper deposits [1]; 10 to 100 mg/L chloride ions are usually necessary with proprietary brighteners for bright copper plating [2,3]. In industrial acid copper sulfate baths, anodes are usually oxygen-free copper or phosphorized copper containing 0.02 to 0.08% phosphorous [4].

The electrodeposition and electrodissolution kinetics of copper in copper sulfate baths was studied by Mattsson and Bockris [5]. They proposed that a two-step mechanism for electrodeposition and electrodissolution with $Cu^+$ as an intermediate. Their model which included the $Cu^{2+}/Cu^+$ reaction step as rate-determining showed good agreement between theory and experiment.

The role of chloride ions in copper-refining electrolyte was investigated by Yao [6]. The grain size decreased and the hardness of copper deposits increased by addition of up to 15 mg/L $Cl^-$. However, further addition above 15 mg/L $Cl^-$ increased grain size and decreased hardness.

Even though there have been numerous studies of brightening by addition of small amounts of organic additives and/or chloride ions to copper sulfate baths [7-20], the synergistic effect of $Cl^-$ and organic additives is still not understood. Deposit characteristics are influenced by such variables as additives, chemical composition of the electrolyte, temperature, impurities, cathode current density and agitation [2,21]. Mass transfer is increased by agitation of the solution by air sparging and/or mechanical movement of the cathode. There have been few fundamental studies to ascertain the effect of mass transfer on producing bright copper deposits.

This study is directed to investigate the dependence of bright copper deposits on $Cl^-$, organic additives and mass transfer in acid copper sulfate baths with rotating ring disk electrodes (RRDE).

## Experimental

The rotating risk disk electrode (RRDE) consisted of a copper disk (disk diameter = 0.594 cm, disk area = 0.277 $cm^2$) and a gold ring (inner ring diameter = 0.703 cm, outer ring diameter = 1.23 cm, theoretical collection efficiency = 0.56). Teflon was used as an insulating material and epoxy glue was used to minimize the leakage between electrodes and Teflon insulator. Details of the RRDE assembly are given elsewhere [22,23]. A Princeton Applied Research (PAR) model 173 potentiostat was used to control the disk potential, and a Tacussel potentiostat type PRT 10-0.5L was used to control the ring

potential. The linear potential sweeps were performed with a PAR Universal Programmer (model 175) and the PAR potentiostat. Disk potential-disk current curves were obtained by a PAR x-y recorder (model RE 0074). Ring currents were measured with a Keithley electrometer (model 602) whose output was recorded by a Hewlett Packard x-y recorder (model 7035B).

Annealed, oxygen-free pure (99.99%) copper was used as the working disk electrode and a platinum foil served as the auxiliary electrode. The gold ring was made by soldering a 3 mm thick pure wrought gold sheet to a copper holder using gold solder and machining to a ring shape. The reference electrode was a saturated calomel electrode (SCE). To minimize the diffusion of $Cl^-$ from the SCE, and SCE was placed in a small Pyrex reservoir with a closed Teflon stopcock located between the Pyrex reservoir and the Luggin capillary; these were connected with small diameter (1.59 mm) Teflon tubing. Figures 1 and 2 illustrate the RRDE and instrumental assemblies. Before each run, the Cu disk was prepared by metallographic polishing. The Au ring was also slightly polished for reproducible results. The RRDE was then degreased with acetone and rinsed in distilled water.

The acid copper sulfate baths in this study consisted of 0.3 M $CuSO_4 \cdot 5H_2O$ and 2 M $H_2SO_4$. This composition is commonly used in the electronics industry for through-hole plating because of its high throwing power.

The electrolyte was maintained at room temperature (~23 C) and deoxygenated with prepurified nitrogen gas for at least 12 hours before each experiment. The nitrogen gas was passed over the electrolyte during an experimental run. Deionized-distilled water is used to prepare the electrolyte. All chemicals were reagent grade. Thiourea (5 mg/L) and a proprietary brightener (1% by vol.) were selected as organic additives.

The linear potential sweeps (10 mV/s) were started at the rest potential of the Cu disk. A stable disk rest potential and ring current were obtained after the RRDE had been immersed in the electrolyte for 3 minutes. The ring potential was set at +0.6 V (vs. SCE) to detect cuprous species, which oxidize to cupric ions since a diffusion limiting ring current was observed at this ring potential [22]. To determine any oxidation effects due to the organic additives at the ring, comparisons of the background ring current were made on electrolytes with and without these additives. The surface appearance of Cu deposits was examined either visually or with an optical microscope after potentiostating the disk electrode for a total cathodic charge density of about 20 $C/cm^2$. All potentials are reported relative to the SCE.

Typical cathodic polarization behavior of Cu electrodeposition and the corresponding ring currents are shown in Figure 3. In the potential range examined (rest potential to -0.9 V) there are four distinct regions: (i) the Tafel region, (ii) the transition region, (iii) the limiting current region, and (iv) the post-limiting current region. The ring current corresponds to the concentration of intermediate species (Cu(I)) formed at the disk electrode during electrodeposition. (The ring currents are not corrected for the background ring current and the collection efficiency.)

## Results and Discussion

### I. Additive-free copper sulfate baths

A measurable ring current for rotating electrodes is obtained at the open circuit potential in additive-free copper sulfate baths and increases with increasing rotating rates, while only the background ring current is obtained for stationary electrodes. The ring open circuit current is attributed to the formation of Cu(I) at the Cu disk.

The electrodeposition of Cu in additive-free copper sulfate baths is independent of rotating rate in the Tafel region. However, the ring current increased with increased rotation, reached a maximum at about +0.03 V and then decreased to a minimum. This maximum ring current, which was reported by Nekrasov and Berezina [24], may be due to the superposition of the reaction rates in the following two consecutive steps.

$$Cu^{2+} + e = Cu^{+} \qquad (1)$$

$$Cu^+ + e = Cu \quad (2)$$

That is, reaction (1) is predominant as the potential decreases whereas reaction (2) is the faster reaction at about +0.03 V.

The electrodeposition of Cu in the transition region is dependent on bath potential and rotation rate. The limiting current region becomes narrower and less well-defined as the rotating rate increases. In both the transition and limiting current regions no significant amount of Cu(I) is detected. A log-log plot of limiting current density and rotation rate produces a straight line with a slope of 0.5 indicating that electrodeposition of Cu in this region is under mass transfer control. The diffusion coefficient of $Cu^{2+}$ in our copper sulfate baths (obtained from our experimental limiting current data) is $4.18 \pm 0.21 \times 10^{-6}$ $cm^2/s$. This value is in fairly good agreement with the other results (range: $4.89–5.9 \times 10^{-6}$ $cm^2/s$) obtained in similar electrolyte compositions [25-28].

In the post-limiting current region, the hydrogen evolution reaction is dominant. The onset of the post-limiting current region occurs at higher potentials at higher rotation rates. Only the background ring current was obtained in $H_2$-saturated sulfuric acid and copper sulfate baths, indicating that the ring current observed in the post-limiting current region is not due to electrooxidation of molecular hydrogen.

## II. Effect of organic additives

It was reported by Szymaszek et al. [29] that $Cu^{2+}$ is chemically reduced to $Cu^+$ with the formation of formamidine disulfide in the presence of thiourea

$$2Cu^{2+} + 2(NH_2)_2CS = 2Cu^+ + (NH_2)_2(NH)_2C_2S_2 + 2H^+ \quad (3)$$

and that thiourea and formamidine disulfide form a redox couple, that is,

$$2(NH_2)_2CS = (NH_2)_2(NH)_2C_2S_2 + 2H^+ + 2e \quad (4)$$

They concluded from polarographic studies that $Cu^+$ forms a complex with formamidine disulfide $[Cu(FD)]^+$ at low concentrations of thiourea and complexes of thiourea at high concentrations of thiourea. The formation of $Cu^+$ complex with excess thiourea has also been reported by others [30,31].

The addition of thiourea (5 mg/L) to copper sulfate baths significantly suppressed Cu electrodeposition at potentials above -0.3 V for rotating electrodes, while no significant effect was observed for stationary electrodes. The cathodic polarization of Cu electrodeposition for rotating electrodes in the presence of thiourea showed a limiting current plateau, which was barely affected by the rotating rate, followed by the potential plateau where the disk current increased very rapidly with a small decrease of potential. The limiting diffusion current and post-limiting current regions were not affected by the addition of thiourea. The suppressed electrodeposition of Cu observed at the potentials above -0.3 V may be due to inhibition of the adsorbed $[Cu(FD)]^+$ complex.

Significantly increased ring currents were observed with the addition of thiourea to copper sulfate baths, the ring currents increasing with increasing rotation rates. The increased background ring currents in the presence of thiourea are attributed to the electrooxidation of thiourea on the ring at +0.6 V.

The proprietary brightener (PB) used in copper sulfate baths did not undergo electrooxidation at the ring in the absence of the copper disk, that is, the background ring current was not affected by addition of PB. The PB (1% by vol.) significantly inhibited Cu electrodeposition at potentials above -0.1 V on rotating electrodes, but not on stationary electrodes. In the presence of PB, there is a potential plateau around -0.1 V. Disk currents in the limiting diffusion and post-limiting regions were not affected by the addition of PB.

## III. Effect of chloride ions

The addition of up to 50 mg/L $Cl^-$ had little or no effect on Cu electrodeposition in the Tafel and transition regions. At 100 mg/L $Cl^-$ and above a small disk current peak and a minimum are observed between -0.1 to -0.18 V.

The ring currents increased with increasing $Cl^-$ concentrations and rotating rates. At higher $Cl^-$ concentrations, the increased ring currents with increasing $Cl^-$ concentrations are attributed to increased formation of $CuCl_2^-$ which electrooxidizes at the ring, that is,

$$Cu^{2+} + e = Cu^+ \quad (1)$$

$$Cu^+ + Cl^- = CuCl \quad (5)$$

$$CuCl + Cl^- = CuCl_2^- \quad (6)$$

Increased mass transfer of $CuCl_2^-$ from the Cu disk as the rotating rate is increased results in higher ring currents. Ring current maxima appear between -0.12 to -0.15 at 100 mg/L $Cl^-$ and above. The ring current maximum and the disk current peak observed at the $Cl^-$ concentrations of 100 mg/L and above occur at the same disk potential.

The limiting diffusion current region becomes narrower and less well defined as the $Cl^-$ concentration increases; the onset of the post-limiting current region occurs at higher potentials as $Cl^-$ concentration increases.

With the addition of thiourea (5 mg/L) to chloride-containing electrolytes, a "limiting current" region was observed in the potential range of 0.0 V to -0.2 V. This region progressively diminished as the $Cl^-$ concentration increased. The corresponding ring currents exhibited a minimum around -0.1 V and a large maximum between -0.12 V and -0.22 V at chloride concentrations ≥50 mg/L.

The addition of chloride to the 1% PB containing baths did not result in such a "limiting current" region, nor were any minimum/maximum ring currents observed.

## IV. Additive and mass transfer effects on brightening Cu deposits

The appearance of Cu deposits was examined either visually or with an optical microscope after potentiostating the disk electrode for a total cathodic charge density of about 20 $C/cm^2$. Bright Cu deposits were obtained in the presence of thiourea or PB only with the addition of $Cl^-$. Potentiostatic experiments at -0.2 V were chosen to assess mass transfer effects on brightening Cu deposits. Minimum hydrodynamic flow conditions for bright Cu deposits are estimated by a Reynolds number (Re) of about 200 for both thiourea and Pb baths.


### Acknowledgment

This work was supported by a grant from the UC Water Resources Center (Project No. W-674). Mr. Yoon was a recipient of a scholarship from the Scholarship Committee of AESF.


### References


1. W. C. Freitag, C. Ogden, D. Tench and J. White, *Plat. & Surf. Fin., 70(10),* 55 (1983).
2. W. H. Safranek, in *Modern Electroplating,* (Ed.: F. A. Lowenheim), John Wiley & Sons, NY (1974).
3. R. Walker and S. D. Cook, *Surf. Tech., 11,* 189 (1980).
4. E. W. Thompson, *Trans. Inst. Met. Fin., 59,* 30 (1981).
5. E. Mattsson and J. O'M. Bockris, *Trans. Faraday Soc., 55,* 1586 (1959).
6. Y. L. Yao, *Trans. Electrochem. Soc., 86,* 371 (1944).
7. W. H. Gauvin and C. A. Winkler, *J. Electrochem. Soc., 99,* 71 (1952).
8. B. Ke, J. J. Hoestra, B. C. Sison and D. Trivich, *J. Electrochem. Soc., 106,* 382 (1959).
9. L. Mandelcorn, W. B. McConnell, W. Gauvin and C. A. Winkler, *J. Electrochem. Soc., 99,* 84 (1952).
10. D. R. Turner and G. R. Johnson, *J. Electrochem. Soc., 109,* 798 (1962).
11. G. R. Johnson and D. R. Turner, *J. Electrochem. Soc., 109,* 918 (1962).
12. D. R. Gabe and D. J. Robinson, *Trans. Inst. Met. Fin., 49,* 17 (1972).
13. A. Szymaszek, J. Biernat and L. Pajdowski, *Electrochim. Acta, 22,* 359 (1977).
14. M. R. H. Hill and G. T. Rogers, *J. Electroanal. Chem., 86,* 179 (1978).
15. C. O. Kang and J. S. Lee, *Kumsok Pyomyon Choli, 16(4),* 190 (1983).

16. M. Yokoi, S. Konishi and T. Hayashi, *Denki Kagaku, 51,* 456 (1983).
17. M. Yokoi, S. Konishi and T. Hayashi, *Denki Kagaku, 51,* 310 (1983).
18. M. Yokoi, S. Konishi and T. Hayashi, *Kinzoku Hyomen Gijutsu, 34,* 434 (1983).
19. J. D. Reid and A. P. David, *J. Electrochem. Soc., 134,* 1389 (1987).
20. J. D. White, *J. Appl. Electrochem., 17,* 977 (1987).
21. J. Jackson and D. A. Swalheim, *Plat. & Surf. Fin., 65(5),* 38 (1978).
22. H. P. Lee, Ph.D. Dissertation, University of California, Los Angeles, CA (1983).
23. H. P. Lee and K. Nobe, *J. Electrochem. Soc., 133,* 2035 (1986).
24. L. N. Nekrasov and N. P. Berezina, *Dokl. Akad. Nauk SSSR, 142,* 855 (1962).
25. A. F. W. Cole and A. R. Gordon, *J. Phys. Chem., 40,* 633 (1963).
26. C. J. Milora, J. F. Henrickson and W. C. Hahn, *J. Electrochem. Soc., 120,* 488 (1973).
27. T. Kessler and R. Alkire, *J. Electrochem. Soc., 123,* 990 (1976).
28. C. R. Wilke, M. Eisenberg and C. W. Tobias, *J. Electrochem. Soc., 100,* 513 (1953).
29. A. Szymaszek, J. Biernat and L. Pajdowski, *Electrochim. Acta, 22,* 359 (1977).
30. T. J. Lane, J. V. Quagliano and E. Bertin, *Anal. Chem., 29,* 481 (1957).
31. L. E. Onstott and H. A. Laitinen, *J. Am. Chem. Soc., 72,* 4724 (1950).

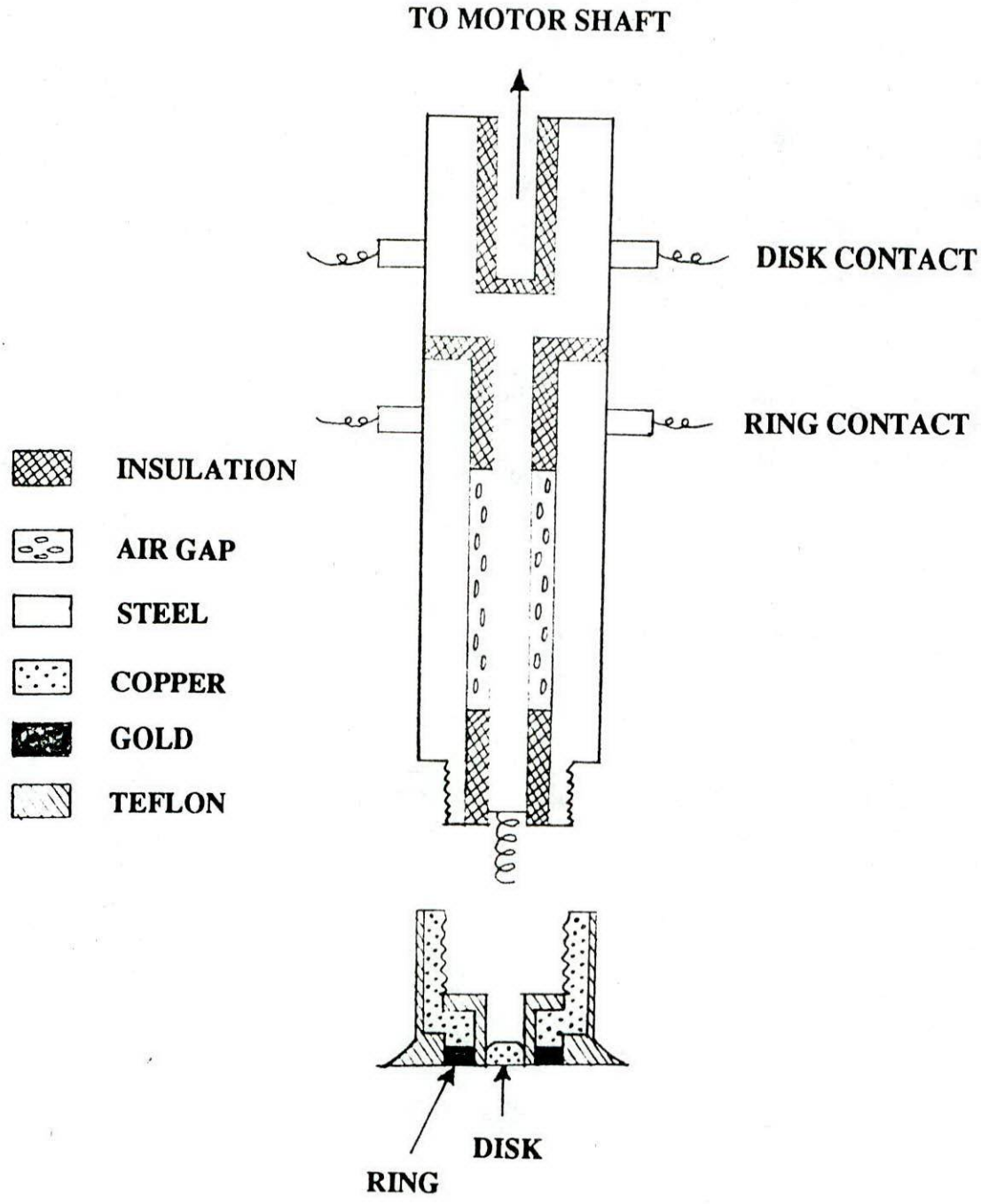


Fig. 1. Rotating Ring Disk Electrode (RRDE) Assembly.

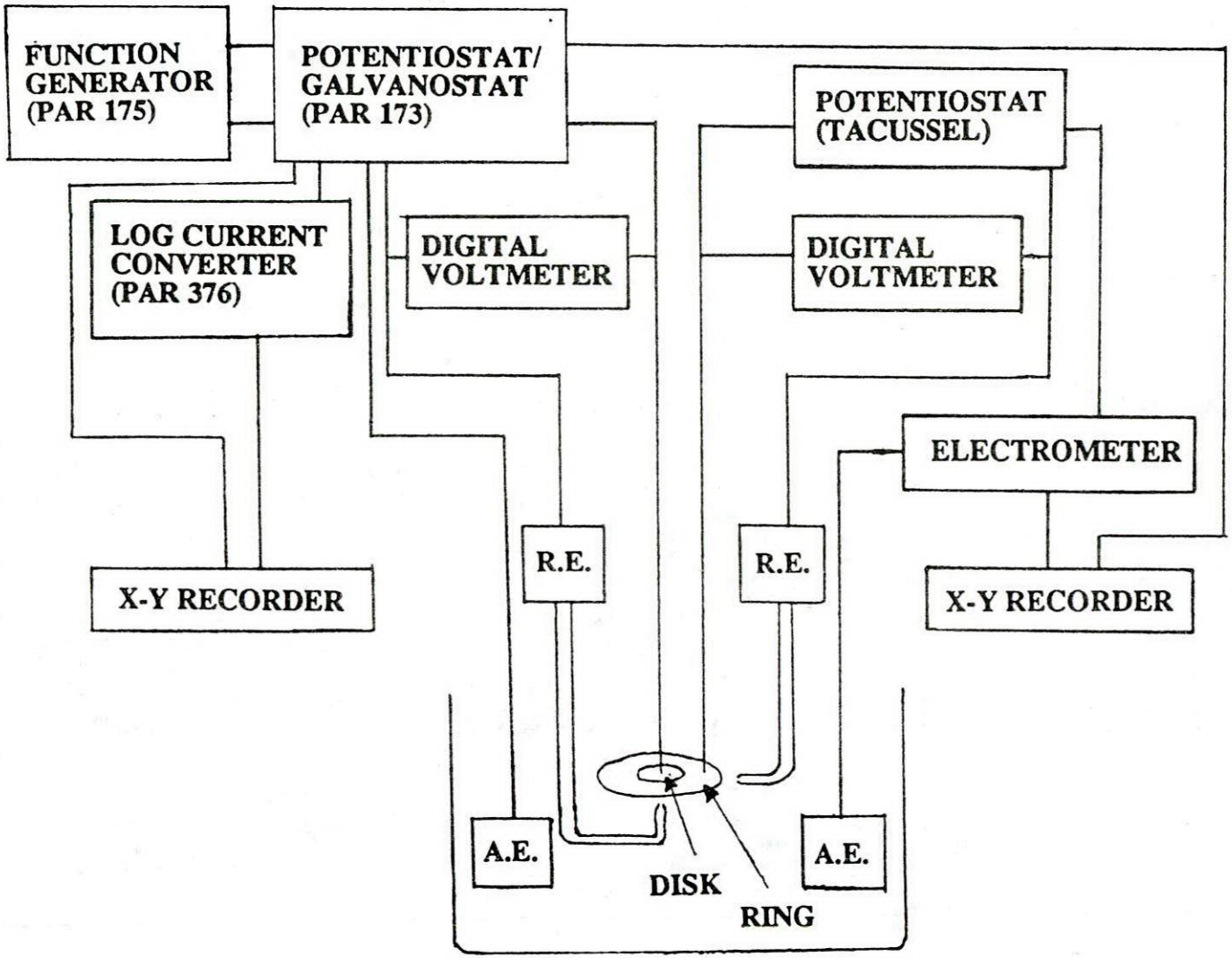


Fig. 2. Experimental Set-up.

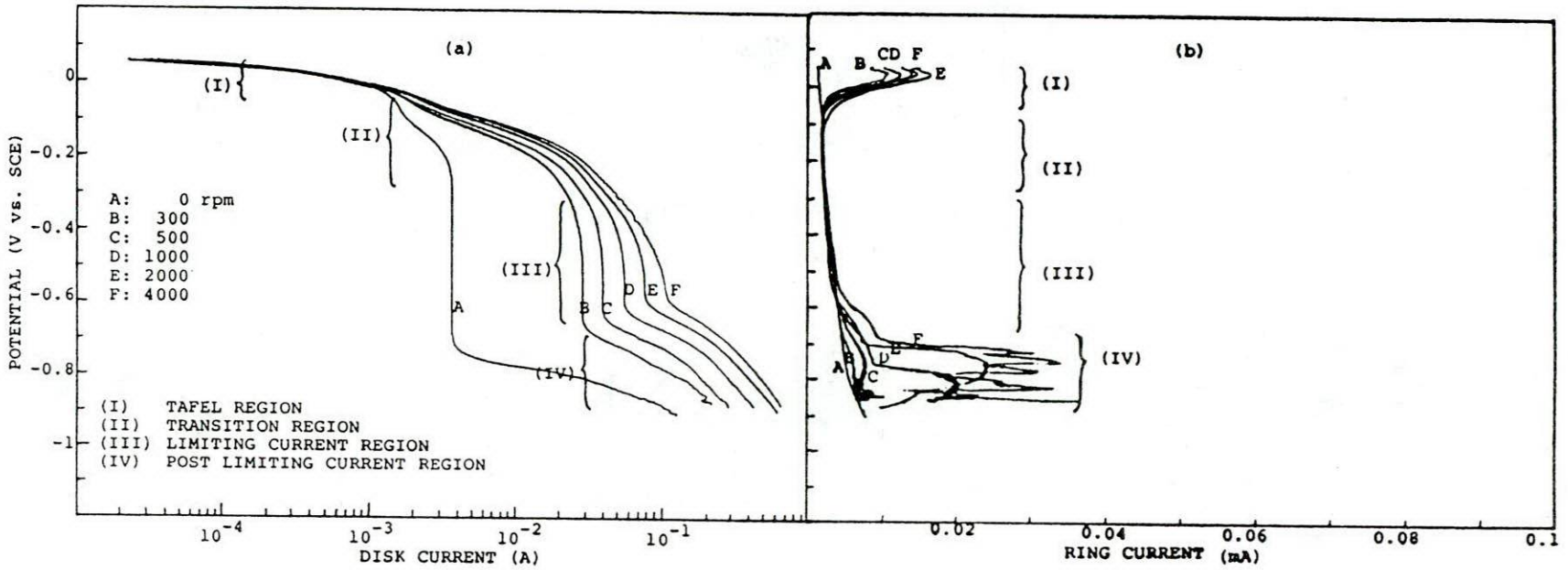


Fig. 3. Typical Polarization Curves.
a) disk current,
b) corresponding ring currents.

H-5

# General Interest
# Session H

## Corrosion Monitoring of Painted Autobody Test Panels By Electrochemical Impedance Spectroscopy (EIS) Measurement

Yar-Ming Wang and Dusanka Radovic
Physical Chemistry Department
General Motors Research Laboratories
Warren, MI 48090

# CORROSION MONITORING OF PAINTED AUTOBODY TEST PANELS BY ELECTROCHEMICAL IMPEDANCE SPECTROSCOPY (EIS) MEASUREMENT

Yar-Ming Wang and Dusanka Radovic
Physical Chemistry Department
General Motors Research Laboratories
Warren, Michigan 48090-9055

## ABSTRACT

Electrochemical impedance spectroscopy (EIS) method has been used to monitor the corrosion processes of painted autobody test panels in 3.5 wt% NaCl, under total immersion condition. EIS data were analyzed with the aid of a simplified, yet physically significant equivalent circuit model. Cross-sectional micrographs of the corroded panels and corrosion potential data were also examined to gain additional insight into the corrosion processes. The EIS technique has been shown to have a high information content, and with further refinement it possibly may be used as a routine diagnostic tool for monitoring corrosion of metals under paint films.

## INTRODUCTION

Various accelerated tests have been devised to predict the service life of painted metals. Some involve exposing samples to a severe testing environment to accelerate the paint failure. Others measure the physical properties of coatings, such as oxygen, water, and ion permeabilities, and use these quantities as indicators of corrosion resistance. The shortcoming of these accelerated tests is that they are not based on a sound understanding of the corrosion mechanisms for painted metals, so it is understandable that results from such tests do not always correlate well with field test data.

The corrosion processes under organic coatings are electrochemical in nature (1). Electrochemical techniques such as corrosion potential measurement, dc polarization, and more recently EIS measurement have been used extensively to provide information on the thermodynamics and kinetics of the painted metal corrosion processes (2-3). In terms of offering a basic understanding of the corrosion mechanisms for the coating/metal system, EIS is the most promising and is considered as a high-information technique. The application of EIS measurement allows one to follow the penetration of electrolyte into the coating and detect the initiation of corrosion at the coating/metal interface. Measurements over a wide range of frequencies allow separation of the various processes relating to the coatings and the substrate. It is possible, in principle, to measure diffusion of electrolyte through the coating layers, the porosity of the coating layers, and the extent of corrosion occurring at the coating/metal interface.

In this investigation, we carried out corrosion potential and EIS measurements on three types of coated autobody test panels. EIS data were analyzed with the aid of a simplified, yet physically significant equivalent circuit representation of a painted metal system. Cross- sectional micrographs of the corroded panels were also examined to gain additional insight into the corrosion process.

## EXPERIMENTAL

Panel samples with the coatings given in Table I were fabricated by the Advanced Coating Technologies, Inc. The corrosion test cell (Figure 1) consists of a Pyrex O-ring joint sealed to the test panel with a commercial screw-applied clamp. The electrolyte consisted of 3.5 w/o NaCl solution made up from distilled water and the reagent grade salt. A perforated platinum cylinder served as the counterelectrode, and a $Ag/AgCl_2$ electrode was used as the reference electrode. The exposed area was 15.9 $cm^2$ (diameter 4.5 cm). In some tests, a small hole (diameter 0.16 cm, area 0.02 $cm^2$) was drilled to the bare metal surface to simulate damaged paint systems. The immersion tests were conducted at 25°C with the electrolyte at equilibrium with atmospheric oxygen. EIS measurements were conducted daily and each measurement took about 12 minutes.

The EIS measuring system is shown in Figure 2. It consists of a Solartron 1250 Frequency Response Analyzer (FRA), a Stonehart BC1200 potentiostat, and a Commodore CBM 8096 Microcomputer. The FRA can be programmed to produce a series of sinewave output signals of known voltage amplitudes (0 to 10V rms) and frequencies (65KHz to 1$\mu$Hz), which are applied to the input of the potentiostat which in turn controls the test cell. At each frequency, the fundamental response of the test cell to the applied voltage signal is measured in terms of the impedance modulus Z and the phase angle $\theta$. All the data are stored in the computer and plotted as Bode Plots (log Z and $\theta$ vs. log f).

After the immersion tests, test panels were rinsed with distilled water and methanol to remove any adhering corrosion product. The samples were then cut by a diamond saw and mounted in cold-cured epoxy to expose the cross-section of the corroded area. The mounted samples were hand-polished with No. 600 grit emery paper, followed by wheel-polishing with diamond pastes of 5 and 0.3 $\mu$m sizes. The samples were then examined by an optical microscope.

## RESULTS AND DISCUSSION

### Corrosion potentials of painted panels - paint films punctured with a hole

When a metal sample is in contact with an electrolyte, a steady-state potential (corrosion potential, $E_{corr}$) can be measured against a reference electrode. According to the mixed-potential theory (4), $E_{corr}$ is related to the equilibrium potentials and the kinetics of the anodic and cathodic reactions. In the case of CRS immersed in NaCl solution (pH=4), the equilibrium potentials (5) for the following simple reactions are calculated to be:

Anodic reaction

$$Fe + 2(OH)^- \rightarrow Fe(OH)_2 + 2e^- \quad E^\circ = -0.882 \text{ V (SCE)} \qquad \langle 1 \rangle$$

Cathodic reaction

$$1/2\ O_2 + H_2O + 2e^- \rightarrow 2(OH)^- \qquad E^\circ = -0.452\ V \qquad \langle 2 \rangle$$

Since the corrosion of iron is under cathodic control, $E_{corr}$ is close to $E^\circ(Fe)$. In the case of galvanized steel corrosion, the anodic reaction is dominated by the zinc dissolution reaction,

$$Zn + 2(OH)^- \rightarrow Zn(OH)_2 + 2e^- \qquad E^\circ = -1.235\ V \qquad \langle 3 \rangle$$

and the $E_{corr}$ is expected to be close to $E^\circ(Zn)$.

The corrosion potential data are summarized in Table II. For the CRS panels, potential values are indicative of iron corrosion. For the galvanized steel panel (Panel G), the hole was drilled to the steel surface, and the exposed steel surface was initially cathodically protected by the thin zinc ring. The initial potential measured was the corrosion potential of zinc (-1.1 V). However with the unfavorable anode to cathode ratio (1:22) the zinc lost its effectiveness in protecting the exposed steel surface after about 200 hours immersion, and the potential shifted towards the corrosion potential of iron (-0.7 V).

Optical microscopy results

Cross-sectional micrographs of the corroded samples are shown in Figures 3-5. Before the immersion test a hole was drilled through the coating layers to expose the bare metal. The starting exposed metal surface is highlighted by a dotted white line. For Panels C and A, corrosion of the substrate (CRS) proceeded inward, no paint lifting at the zinc phosphate/CRS (Panel C) or electrodeposited paint/CRS (Panel A) interface was observed. The corrosion behavior of these two panels, once the bare metal surface was exposed, was very similar.

The cross-sectional micrograph of Panel G with paint layers intact is shown in Figure 6. Three distinct coating layers are clearly discernable in the picture; these are spray paint, electrodeposited paint, and zinc phosphate on zinc layers. There is no clear demarcation between zinc and zinc

phosphate layers. After 384 hours immersion, zinc layers surrounding the exposed CRS substrate preferentially dissolved away. The CRS substrate also corroded indicating that the recessing zinc ring could not effectively protect an increasingly exposed CRS substrate. As the zinc corroded laterally along the thin zinc film, the diffusion path (a narrow path between CRS and the paint film) for the zincate ion was increasing in length; this led to the precipitation of zinc oxide. The 200 mV shift in corrosion potential at the end of the immersion test indicated that the initial cathodically-controlled corrosion process was shifting to a resistance-controlled process (IR losses due to precipitated anode corrosion product). The loss of the underlying zinc layer adjacent to the hole, the release of the internal stresses of the paint film, in conjunction with the formation of the zinc oxide near the zinc dissolution sites, forced the paint films to curl away from the hole as shown in Figure 5.

## Equivalent circuit model for painted metal

From the measurements of impedance parameters as a function of frequency, it is possible by standard A/C theory to model the test cell behavior with resistors and capacitors in various series and parallel combinations. A basic four-element model is used to describe the impedance response of a painted metal system as shown in Figure 7. $C_p$ represents the capacitance of the intact coating layers, $R_h$ represents the hole resistance due to the electrolyte penetration at the damaged area of the paint, $C_d$ and $R_t$ are respectively the double layer capacitance and the charge transfer resistance at the metal/electrolyte interface at the base of the hole. The Bode plot of the equivalent circuit shown in Figure 7 is given in Figure 8. Values of the elements were chosen to be representative of a painted metal system. In actual tests, the impedance spectra similar to that shown in Figure 8 have been observed. Values of the individual circuit element are determined through a series of decoupling steps as outlined in a previous publication (6).

EIS data of painted panels - paint films intact

Panels (A, C & G) with paint films intact all showed purely capacitive behavior as indicated by the -1 slope of the log Z vs. log f line and a close to -90° phase angle (Figure 9). The coatings act as a dielectric barrier, and the $C_p$ values as a function of immersion time are tabulated in Table III. Variation of the $C_p$ values among various panels was less than 10% indicating that the uniformity of the paint application is satisfactory. $C_p$ values showed very little changes even after 500 hours immersion in NaCl solution reflecting that an undamaged paint film is an effective corrosion barrier. We observed no rust spots on the exposed paint surface after immersion tests. The constancy of $C_p$ indicates that the paint was not permeated by water. If water had entered the paint, one would expect to observe a significant change in $C_p$ (dielectric constant, $\epsilon$, for water is 80, and for organic materials is less than 10). Also, by knowing thickness of the paint system, one can calculate $\epsilon$ from $C_p$.

EIS data of painted panels - paint films punctured

Bode plots of test panels after 10 minutes immersion are shown in Figures 10-12. EIS measurements were carried out by potentiostatically holding the electrode potential at the corrosion potential and by superimposing a 3 mV (RMS) ac sinewave probing signal. Impedance values were much lower than that of the undamaged panels, suggesting the occurrence of corrosion at the bottom of the hole. $R_h$ was determined from the impedance arrest at the high frequency end, $C_d$ was determined from the mid-frequency region of the impedance, and $R_t$ was calculated by substrating $R_h$ from the low frequency impedance arrest ($R_t + R_h$). If the low frequency arrest was not present (Figure 11), then the $R_h+R_t$ value was estimated from $Z\cos\theta$ measured at the lowest frequency data point. $R_h$ is related to the size of the hole, thickness of the coatings, and the resistivity of the electrolyte; $C_d$ relates to the electrolyte composition as well as the actual area of the corrosion sites; $R_t$ also relates to the corrosion area and is inversely proportional to the corrosion current ($I_{corr}$). Bode plots of successive EIS measurements at various immersion time for three test panels are shown in

Figures 13-15 . Phase angle curves were omitted to avoid overcrowding of the plots. The evolution of the corrosion processes can be clearly monitored by tracing these time-dependent spectra.

Table IV summarizes the EIS data of test panels as a function of immersion time. For Panel C, values of $R_h$ remained the same, while $R_t$ decreased with time. The decrease of $R_t$, signifying an increase in the corrosion current, reflects an increase in the area of active corrosion. This is consistent with an increase in $C_d$ which is proportional to the electrochemically active area. Cross-sectional micrograph results discussed earlier confirmed the increase in the corrosion area. A similar behavior was observed for Panel A, this implies that once the zinc phosphate coating is damaged, the exposed metal will be corroded. For Panel G, the situation was much more complicated; there was a 30% decrease in $R_h$ values, indicating a significant increase in the corrosion area. The initial corrosion rate of zinc from the pinholed electrogalvanized (EG) panel was quite high as judging by the relatively low $R_t$ values for the first 60 hours of immersion. As the zincate (corrosion product of zinc) ion concentration in the hole reached the saturation level, it deposited on the zinc dissolution sites as zinc hydroxide (white rust). The blocking of zinc corrosion sites shifted the mixed potential toward that of the iron corrosion potential. The $R_t$ value of Panel G after 384 hours immersion was estimated to be greater than 10 KΩ, an indication that at the later stage of the immersion test, the CRS surface started to dissolve as well. The $C_d$ values of the EG panel increased dramatically with increasing immersion time indicating a drastic increase in the exposed surface area.

More work on the effects of zinc coating weight, types of paint defect, and test environments on the EG panel corrosion should be carried out in order to accurately correlate laboratory test results with actual field performance. Our preliminary results showed that EIS technique can be a very useful tool toward developing a valid accelerated corrosion test for predicating coating performance.

## CONCLUSIONS

- Painted panels with paint layers intact showed no sign of corrosion after 500 hours immersion test indicating that the undamaged coating layer is an effective corrosion barrier. EIS measurements can be used to determine the physical properties of the paint films.

- For a damaged painted panel, the high frequency response (1-60 KHz) of the impedance spectrum is related to the electrolyte paths (pores) to the metal surface. The lower frequency response (< 1 KHz) is associated with the corrosion processes occurring at the metal/coating interface. The parameters calculated from the lower frequency response, the charge transfer resistance and the double layer capacitance, can be used to monitor the progress of corrosion at the metal/coating interface.

- Among the parameters determined by the EIS measurements, the charge transfer resistance gives a direct measurement of the corrosion rate of the coated metal. The other parameters (pore resistance, double layer capacitance, and diffusion impedance) are qualitatively related to the protective efficiency of the coatings.

## ACKNOWLEDGEMENTS

We would like to thank M. J. Kutcher of the Durability Test and Development Group, GM Milford Proving Ground, for providing test panels and background information of these panels. Thanks also are due to R. F. Reising and D. W. Hardesty of the GMR Physical Chemistry Department for their many helpful discussions.

## REFERENCES

1. J.E.O. Mayne, Journal of the Oil and Colour Chemists Association, 40, 183, (1957).

2. J.D. Scantlebury, K.N. Ho, and D.A. Eden, ASTM STP 727, "Electrochemical Corrosion Testing," 187, (1981).

3. F. Mansfeld, M. Kendig, and S. Tsai, International Congress on Metallic Corrosion, 8th Proc., Mainz, Germany, 1014, (1981).

4. M.G. Fontana and N.D. Greene, Corrosion Engineering, McGraw-Hill, (1967).

5. M. Pourbaix, Atlas of Electrochemical Equilibria in Aqueous Solutions, Pergamon Press, (1966).

6. Y-M. Wang, S.W. Liu, and R. Huo, "AC Impedance Analysis of a Liquid Crystal Display", the Transactions of SAE (1986), Paper No. 860352.

**Table I. Description of Test Panels**

(Panels prepared by Advanced Coating Technologies, Inc.)

Panel C

Coating system

Cold-Rolled Steel/Zinc Phosphate/Electrodeposited Paint/Spray Paint

Cold-rolled steel: GM 6-9 Audit CRS

Zinc phosphate: Chemfil C168 zinc phosphate, 134 mg/sq. ft

Electrodeposited paint: PPG ED3150A, 1.20 to 1.38 mils thickness

Spray paint: Glasurit 872W 012 White HSE, 2.30 mils

Panel A: same as C excluding zinc phosphate layer

Panel G: same as C except the substrate was electrogalvanized steel, GM 16-90e (EG 70/70)

**Table II. Corrosion Potential Measurements of Test Panels**

| Immersion time | $E_{corr}$ (V vs. SCE) | | |
|---|---|---|---|
| (hours) | Panel C | Panel A | Panel G |
| 1 | -0.693 | -0.753 | -1.103 |
| 67 | -0.787 | -0.790 | -1.116 |
| 384 | -0.737 | -0.748 | -0.937 |

**Table III. EIS Data of Test Panels with Coating Layers Intact**

| Immersion time (hours) | $C_p$ (nF) Panel C | Panel A | Panel G |
|---|---|---|---|
| 40 | 1.20 | 1.06 | 1.10 |
| 500 | 1.22 | 1.09 | 1.22 |

**Table IV. EIS Data of Test Panels with Coating Layers Punctured**

| | Panel C | | | Panel A | | | Panel G | | |
|---|---|---|---|---|---|---|---|---|---|
| Immersion Time (hrs) | $R_h$ (Ω) | $R_t$ (KΩ) | $C_d$ (μF) | $R_h$ (Ω) | $R_t$ (KΩ) | $C_d$ (μF) | $R_h$ (Ω) | $R_t$ (KΩ) | $C_d$ (μF) |
| 1 | 68 | 22.9 | 2.5 | 63 | 16.6 | 2.6 | 60 | 2.6 | 2.6 |
| 67 | 62 | 16.5 | 3.2 | 70 | 8.1 | 4.1 | 40 | 0.6 | 300 |
| 384 | 65 | 10.5 | 5.9 | 64 | 9.3 | 4.8 | 43 | >10.0 | 1400 |

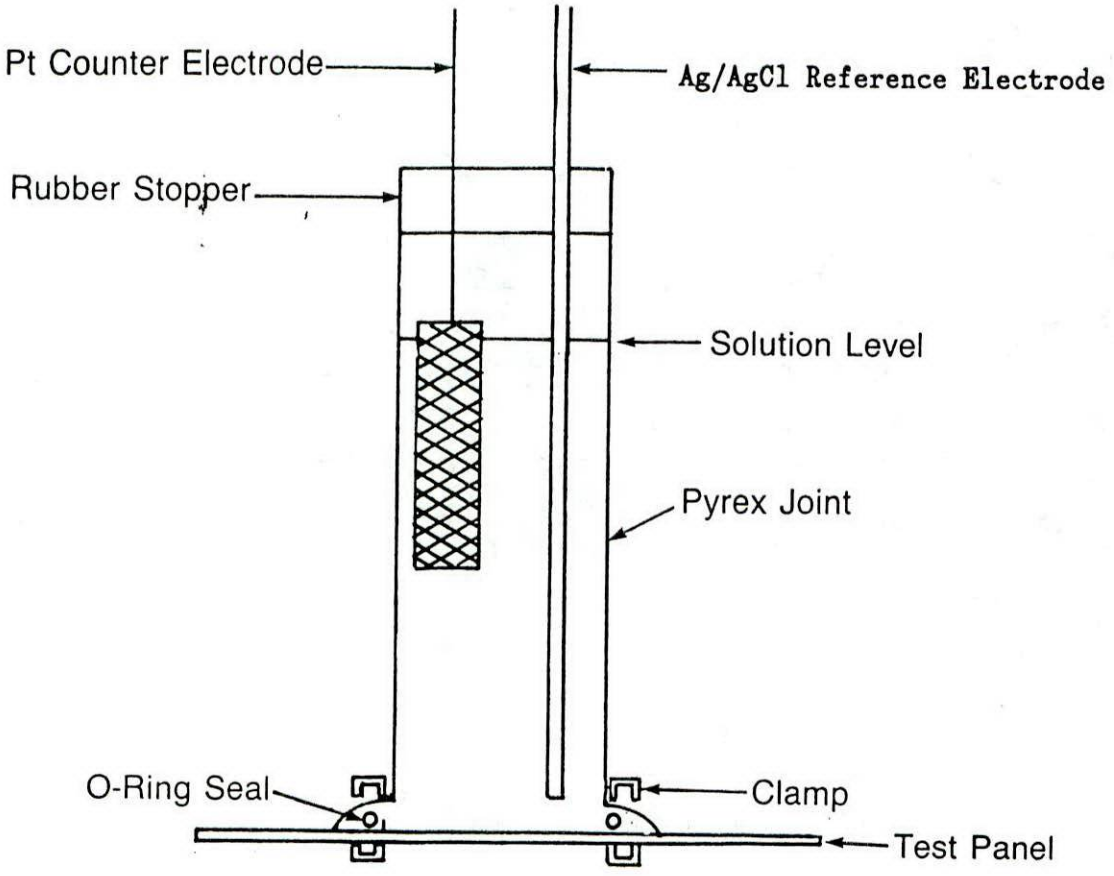


Figure 1. Cell assembly for corrosion testing of painted panels.

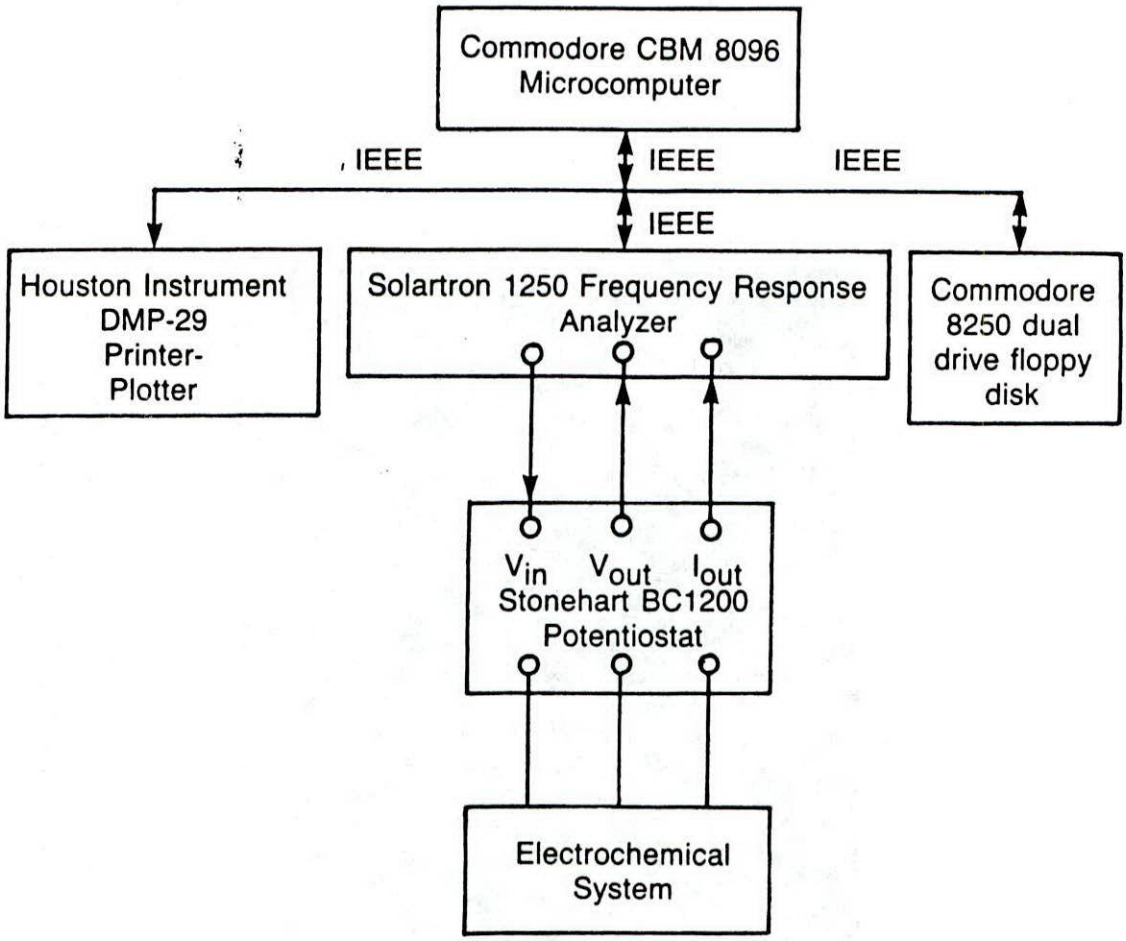


Figure 2. Schematic diagram of the system used for EIS measurements.

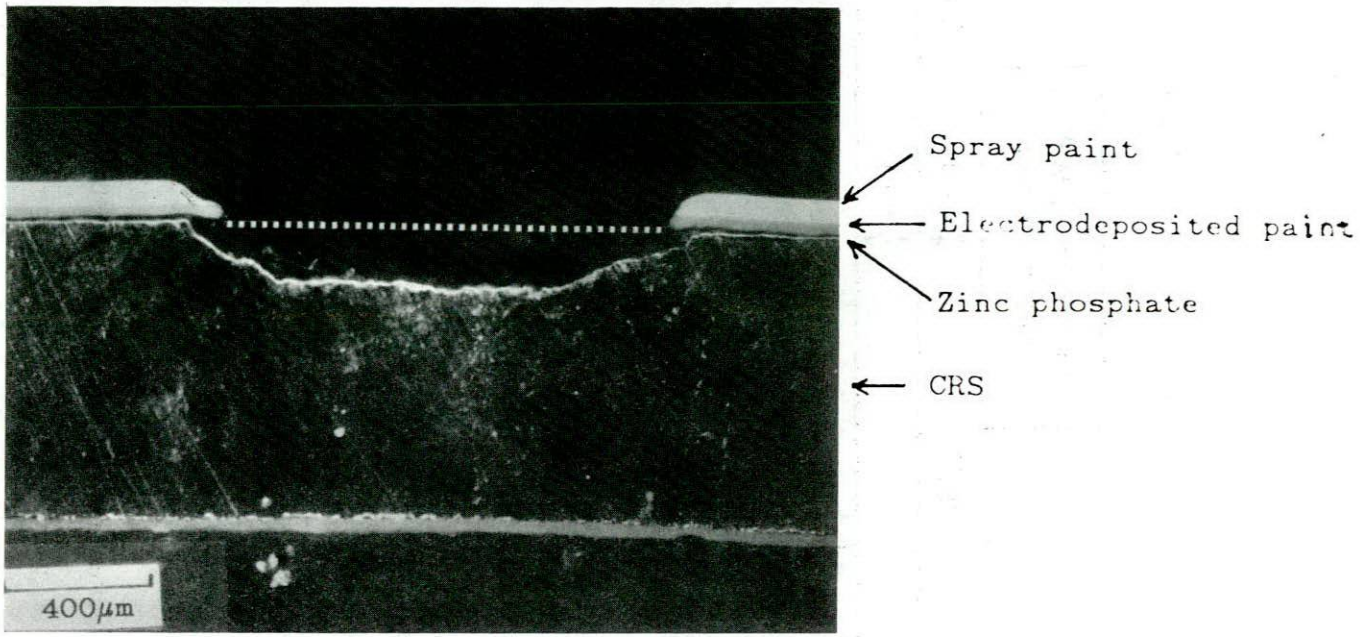


Figure 3. Cross-sectional micrograph of Panel C after 384 hours immersion in stagnant 3.5 w/o NaCl, air-saturated, and at 25°C.

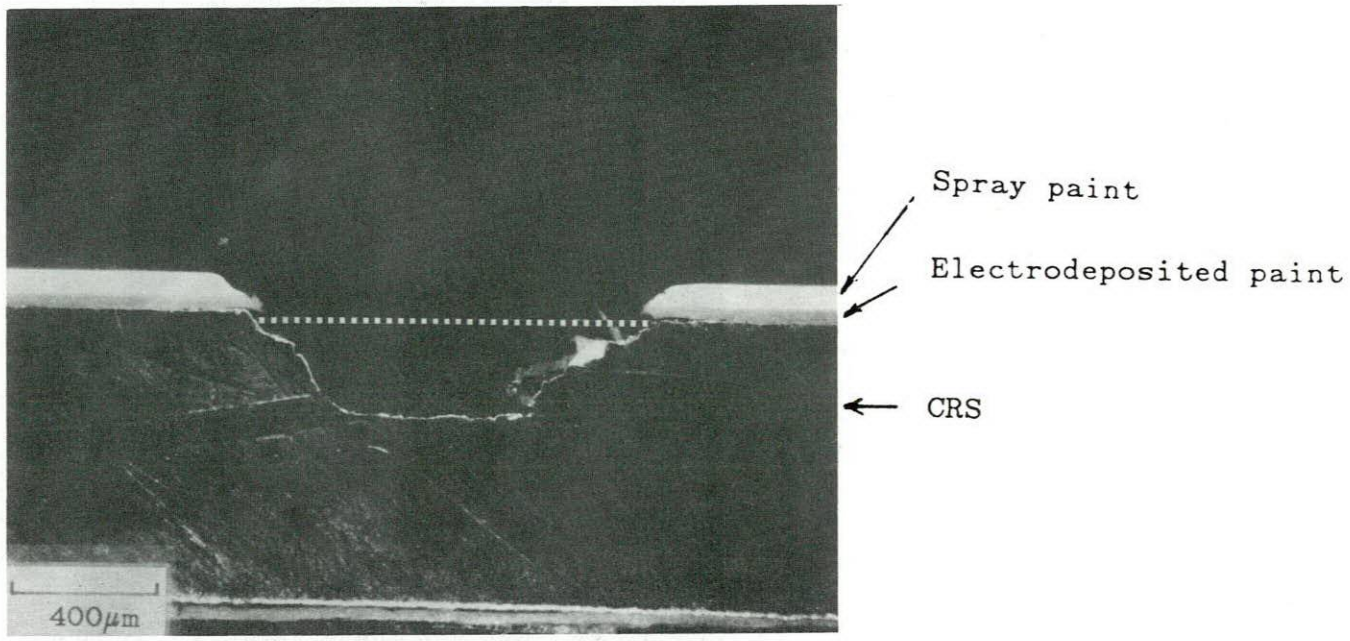


Figure 4. Cross-sectional micrograph of Panel A after 384 hours immersion in stagnant 3.5 w/o NaCl, air-saturated, and at 25°C.

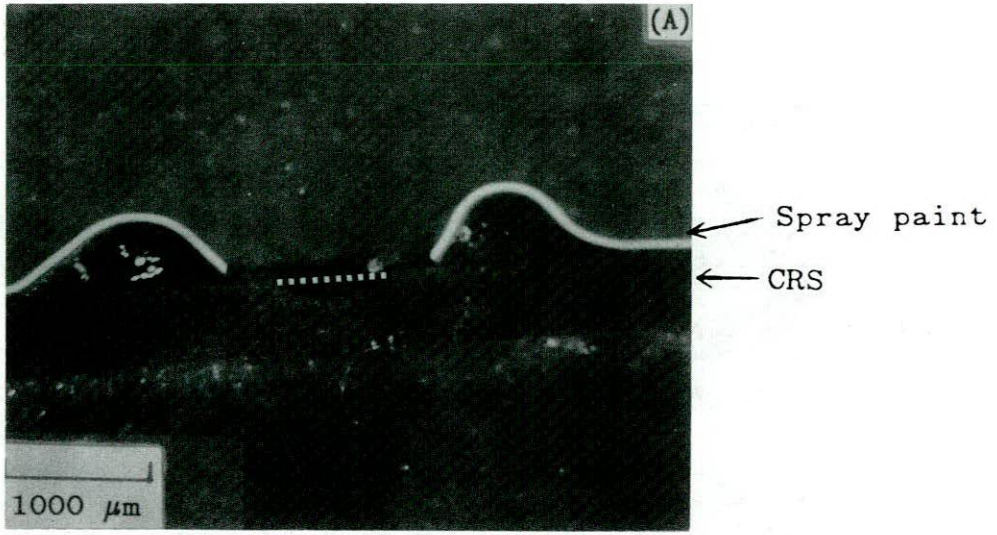


Figure 5A. Cross-sectional micrographs of Panel G after 384 hours immersion in stagnant 3.5 w/o NaCl, air-saturated, and at 25°C. Lower magnification.

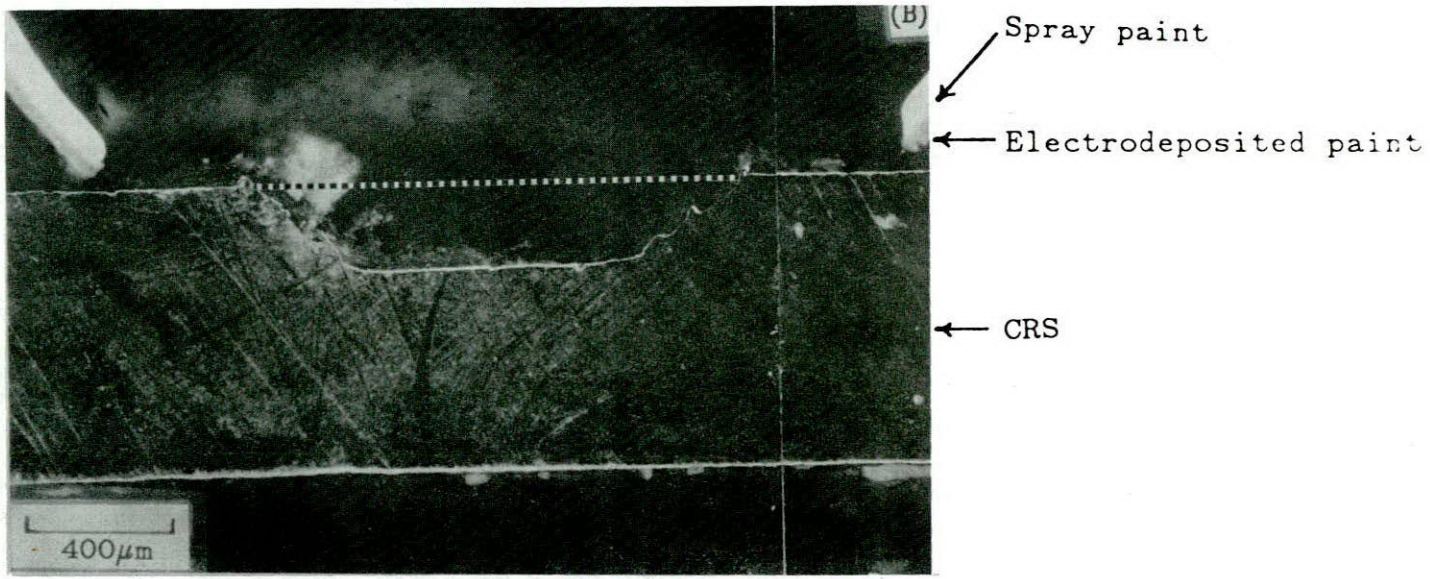


Figure 5B. Cross-sectional micrographs of Panel G after 384 hours immersion in stagnant 3.5 w/o NaCl, air-saturated, and at 25°C. Higher magnification.

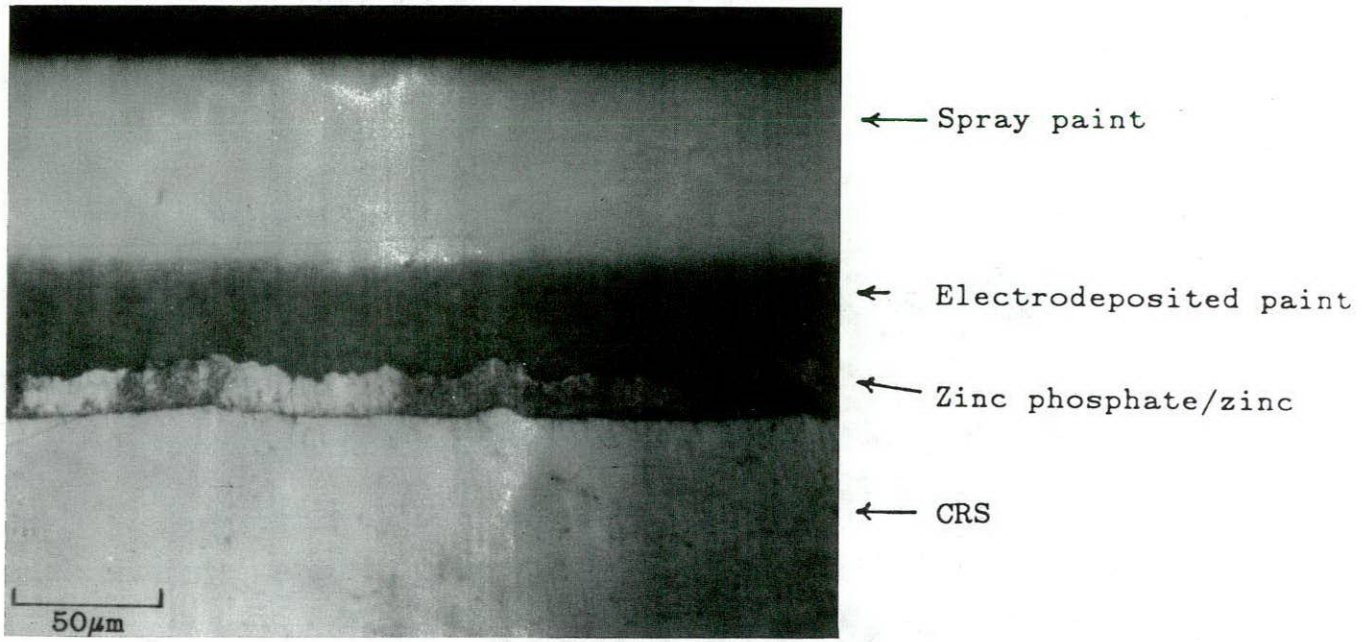


Figure 6. Cross-sectional micrograph of Panel G with paint layers intact.

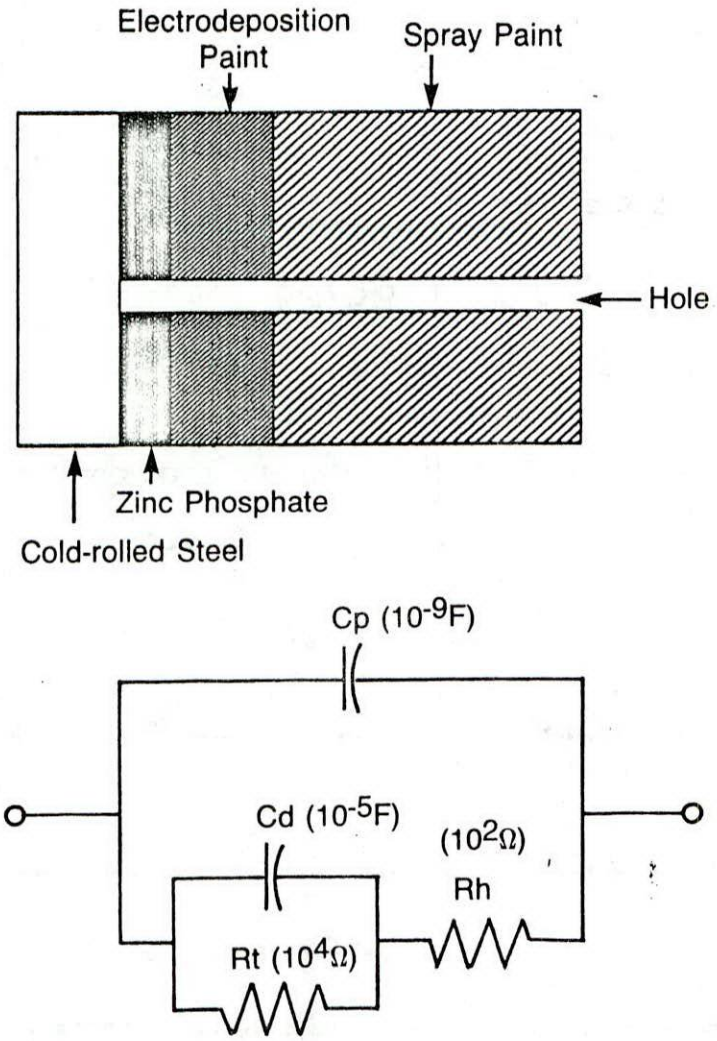


Figure 7. Painted metal/solution interface equivalent circuit model.

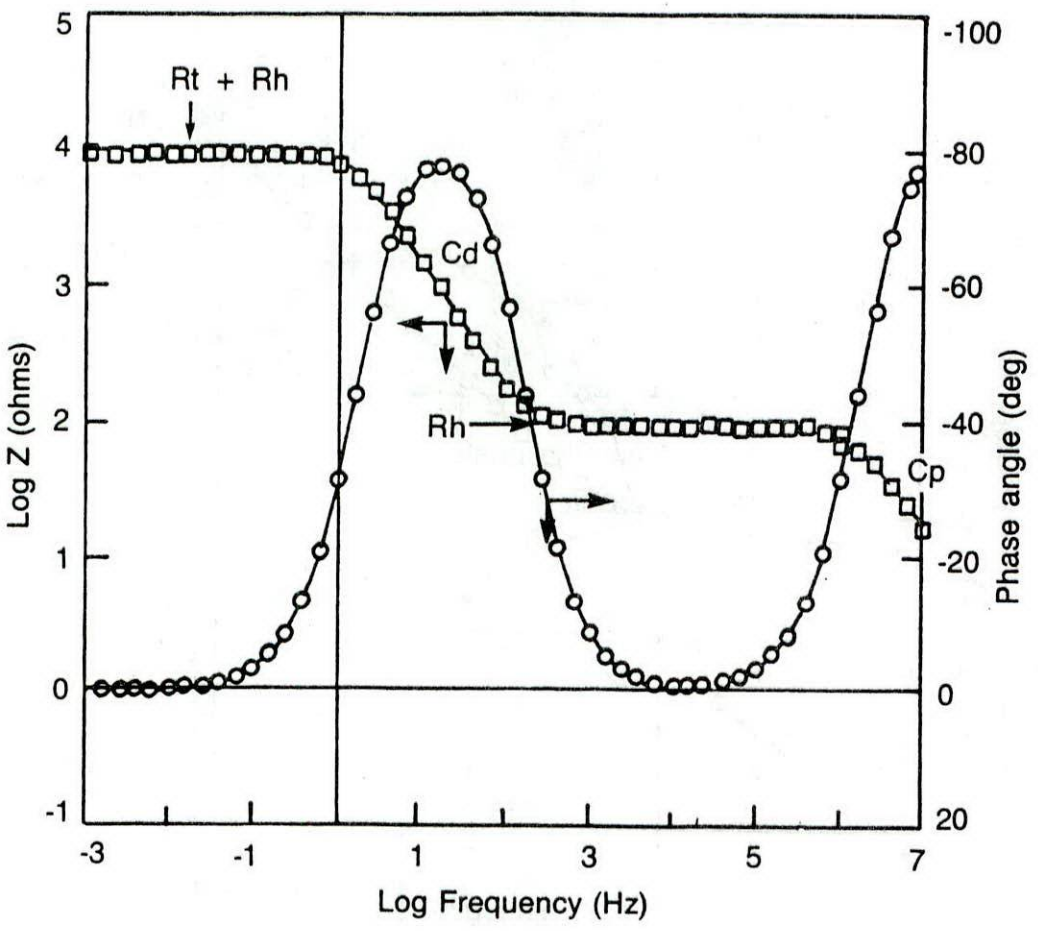


Figure 8. Bode plot for painted metal/solution interface model shown in Fig. 7.

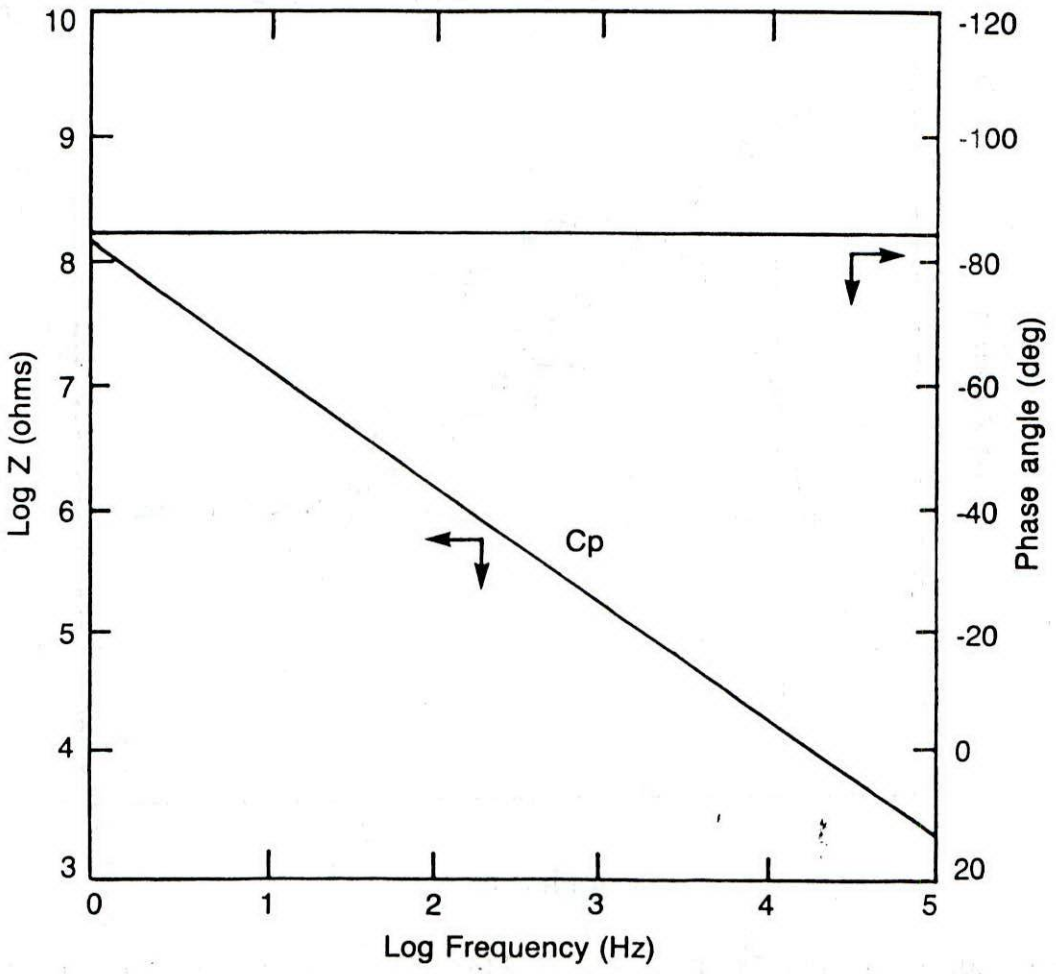


Figure 9. Bode plot for Panel A, coatings intact, after 500 hours immersion in 3.5 w/o NaCl.

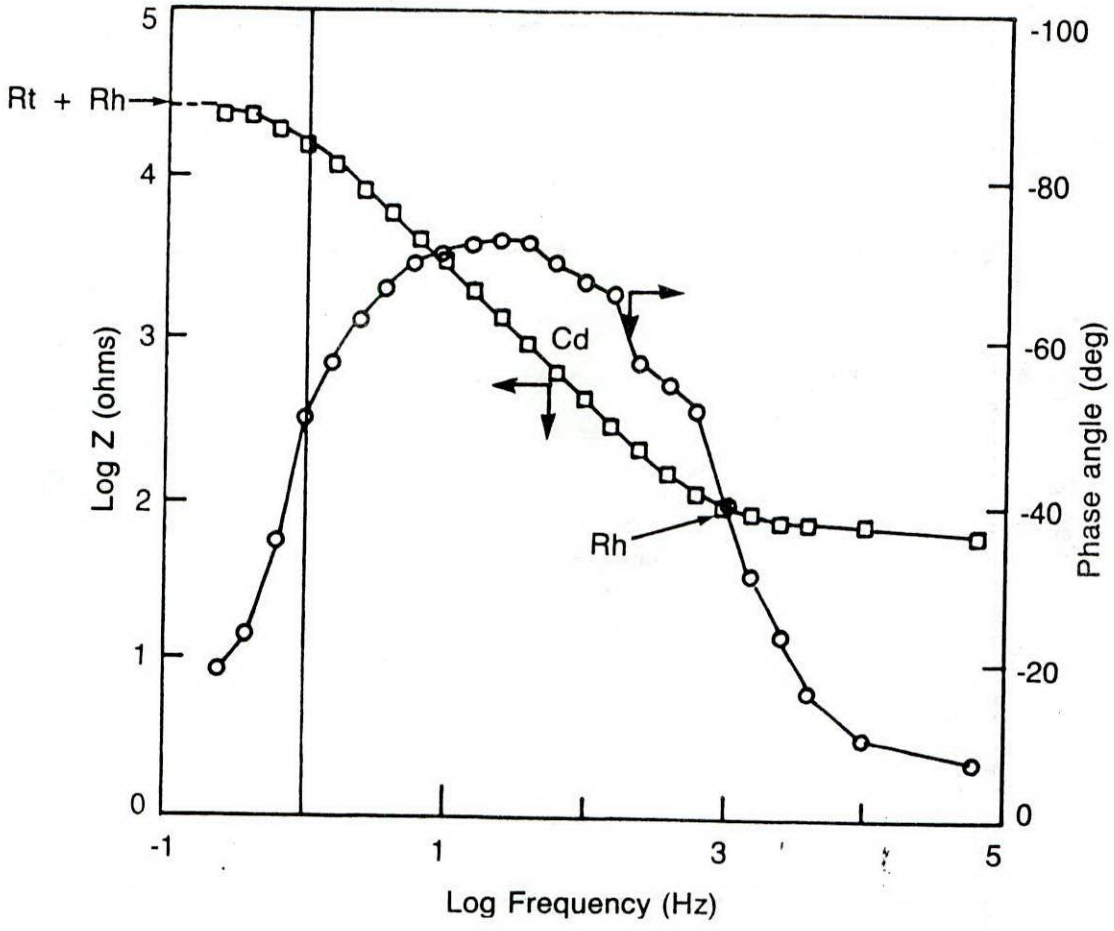


Figure 10. Bode plot for Panel C, drilled with a hole and after 10 minutes immersion in 3.5 w/o NaCl.

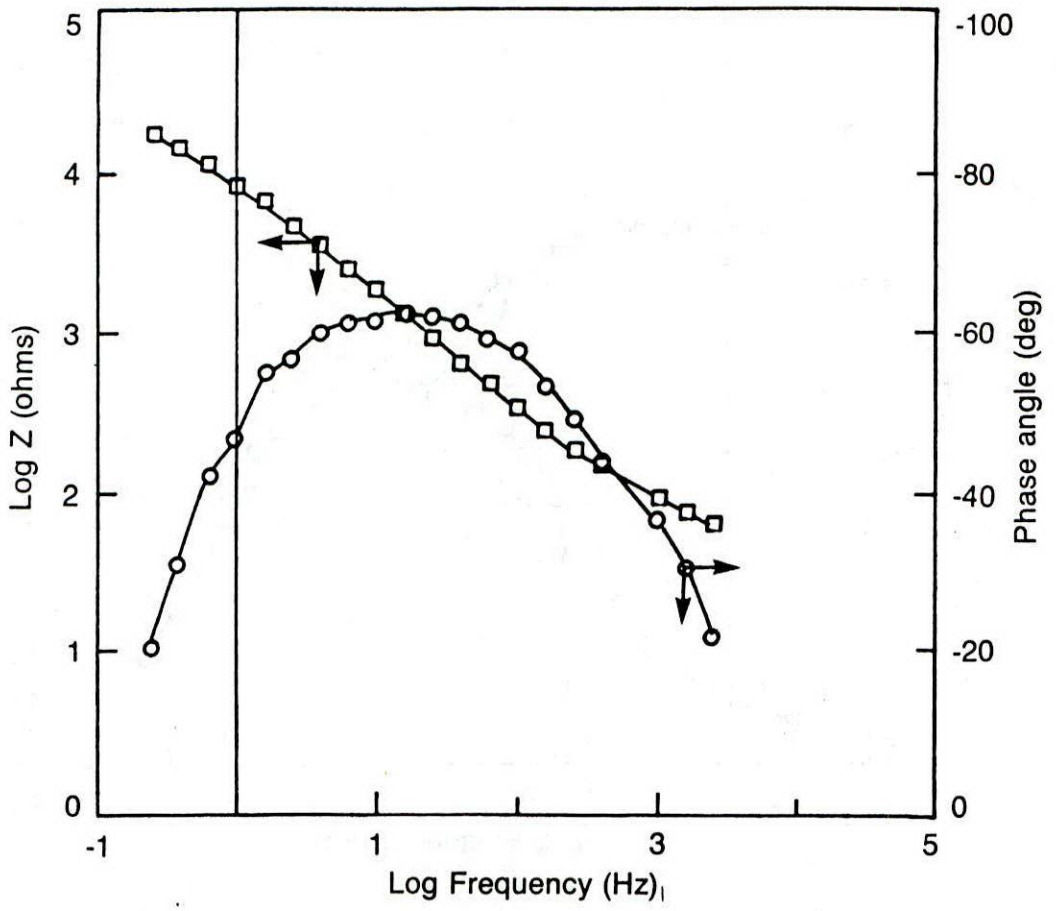


Figure 11. Bode plot for Panel A, drilled with a hole and after 10 minutes immersion in 3.5 w/o NaCl.

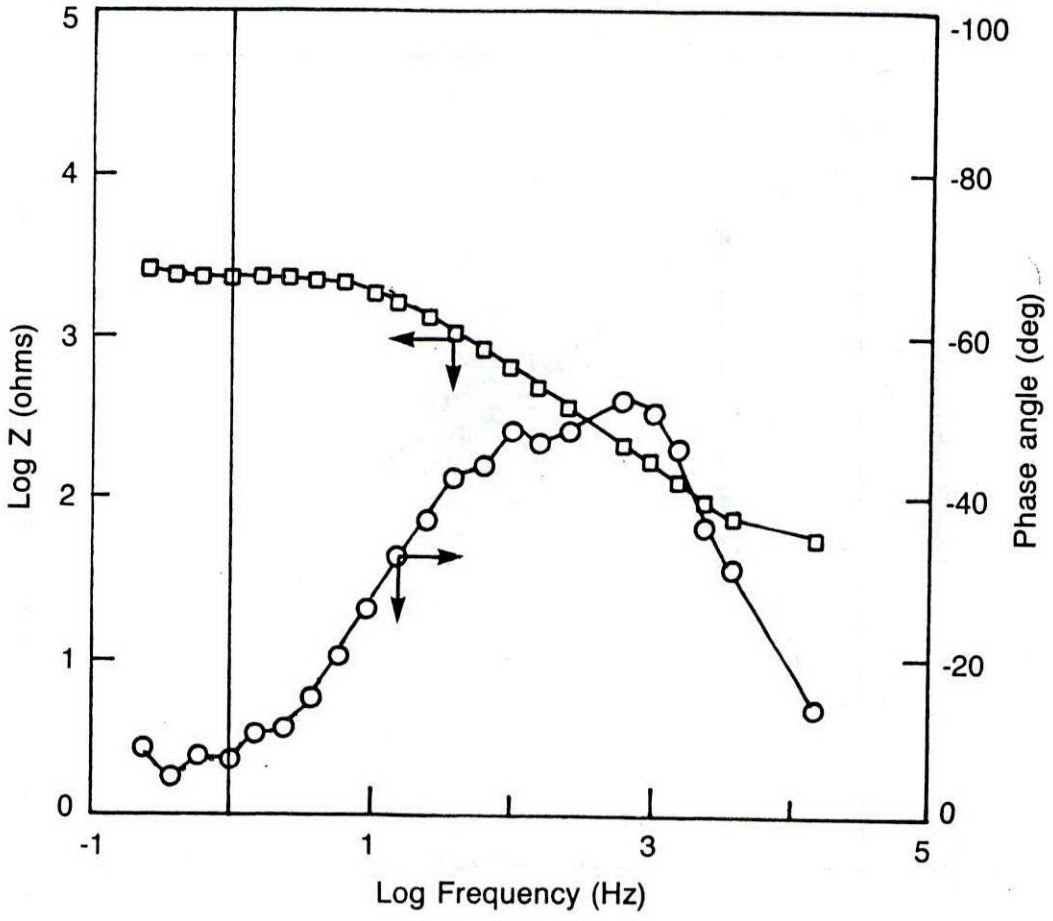


Figure 12. Bode plot for Panel G, drilled with a hole and after 10 minutes immersion in 3.5 w/o NaCl.

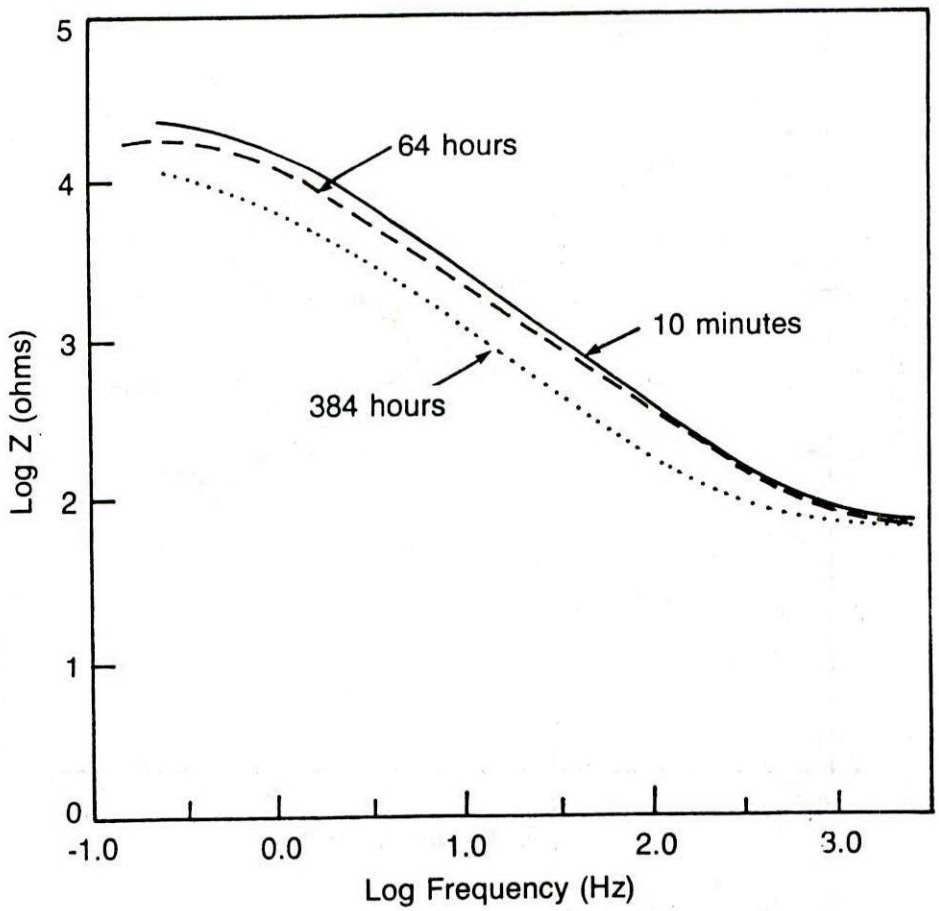


Figure 13. Bode plots of successive measurements at different immersion time in 3.5 w/o NaCl for Panel C drilled with a hole.

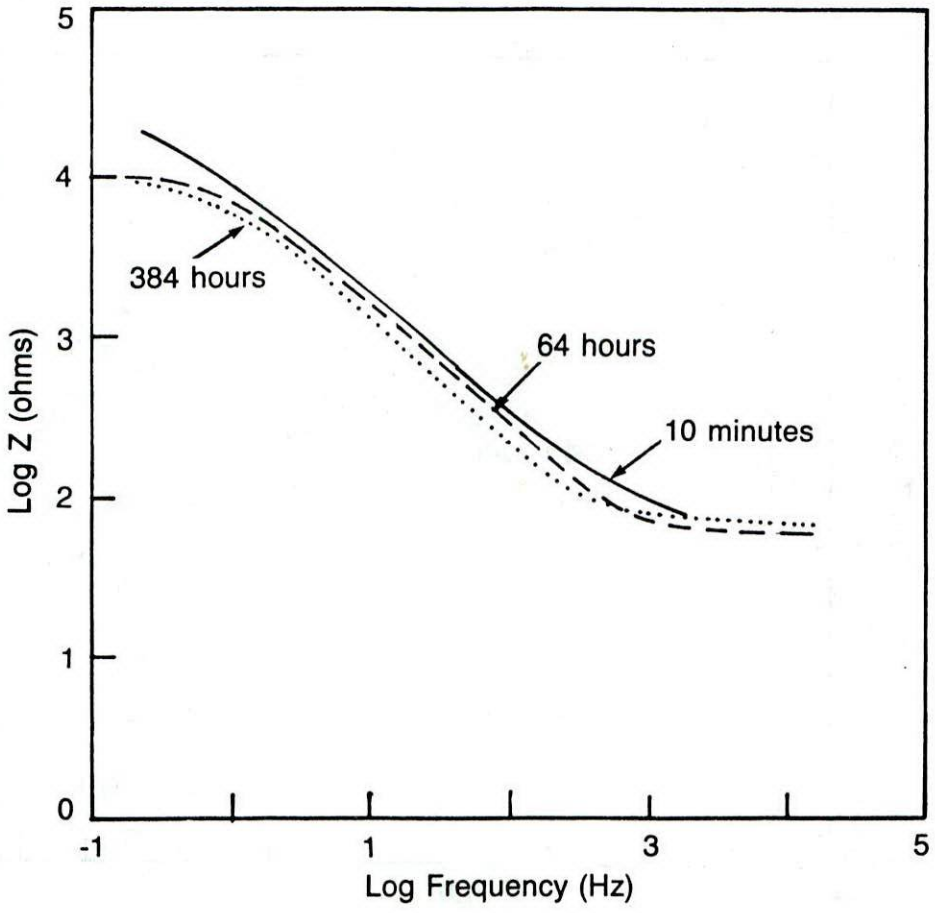


**Figure 14.** Bode plots of successive measurements at different immersion times in 3.5 w/o NaCl for Panel A drilled with a hole.

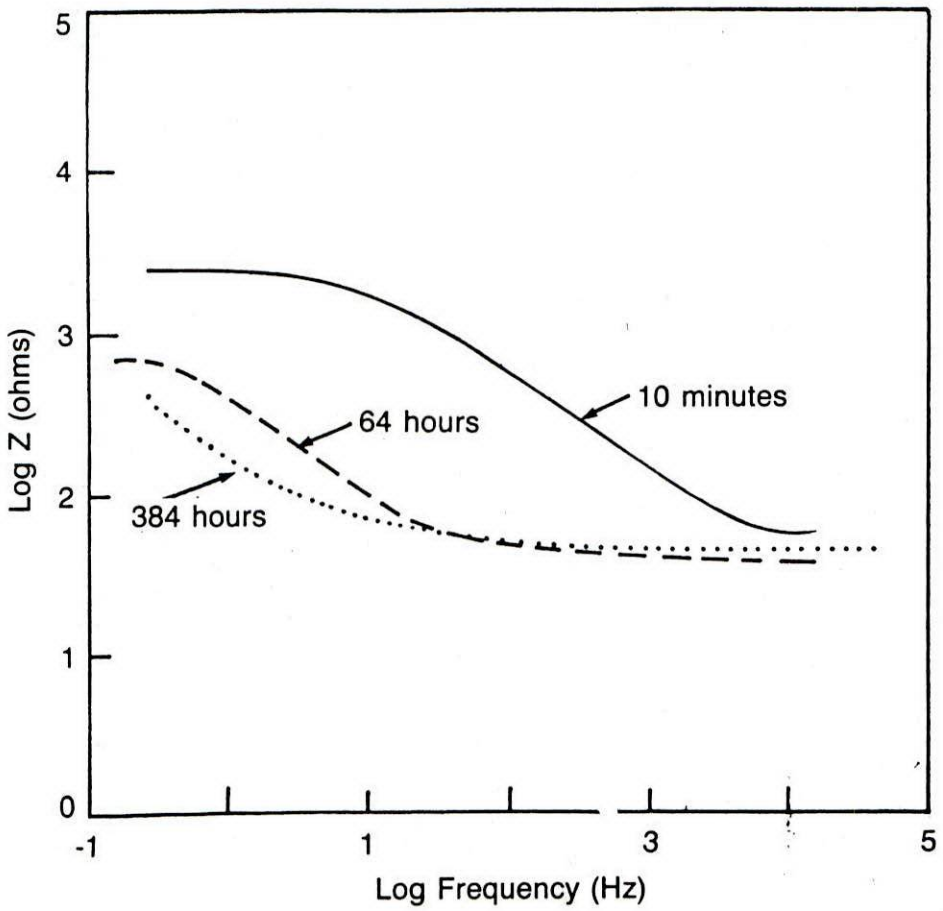


**Figure 15.** Bode plots of successive measurements at different immersion times in 3.5 w/o NaCl for Panel G drilled with a hole.

H-6

# General Interest Session H

## Zinc Phosphating Films on Ferrous Metal Substrates

C.C. Chang and H. K. Liu
Chung Shan Institute of Science & Technology
Taiwan, Republic of China

T.S. Lee
Scientific Resources, Inc.
Palatine, IL

**PAPER NOT RECEIVED IN TIME FOR PUBLICATION***

Zinc Phosphating Films on Ferrous Metal Substrates

C.C. Chang and H.K. Liu, Chung Shan Institute of Science & Technology, Taiwan, Republic of China, and T.S. Lee, Scientific Resources, Inc., Palatine, IL

Zinc phosphating is frequently applied to provide corrosion protection to ferrous metal substrates. This study correlates zinc phosphate corrosion resistance, as measured by salt spray, with other variables such as film thickness, coating formation temperature, contact resistance, and the ratio of $Zn_2Fe(PO_4)_3{:}4H_2O$ to $Zn_3(PO_4)_2{:}4H_2O$ (Hopeite). Results will be discussed and compared with published data.

* For copies of this paper, please contact the author directly

Mr. T. S. Lee
Scientific Resources, Inc.
1058 Whytecliff
Palatine, IL 60067

H-7

# General Interest Session H

## Adhesion of Platings on Substrates

Martin Thoma
MTU Motoren- und Turbinen-Union München GmbH
Munich, West Germany

# ADHESION OF PLATINGS ON SUBSTRATES

**Martin Thoma**

**MTU Motoren- und Turbinen-Union München GmbH**
**Munich, West Germany**

## ABSTRACT

In order to obtain optimum adhesive strength results, a number of different substrates - carbon fibre reinforced plastics (CFRP), aluminium and titanium alloys, stainless steels and high-temperature superalloys - were subjected to various pretreatments before plating. Adhesion was then tested by a variety of methods. The results of the various qualitative and quantitative adhesion test methods are discussed with respect to the substrate pretreatments.

## INTRODUCTION

Carbon fibre reinforced plastics (CFRP), aluminium and titanium alloys, stainless steels and high-temperature superalloys are finding increasing use in aerospace applications. Although these materials already possess good thermal strength and corrosion resistance characteristics, electroplating can be necessary in repairing components that are dimensionally out of tolerance, or for improving resistance to wear. The best possible adhesion of the plating on these highly-stressed components is imperative. Knowledge of the bond strength of platings on the various substrates is the primary consideration for a decision in favour of an electroplating.

## ELECTROPLATING

Direct plating of CFRP is essentially possible because of the electrical conductivity of the carbon fibres [1], although the plating-carbon adhesion is too low under stress. Therefore, an additional, suitable preparation of the matrix (epoxy or polyimide) is necessary.
Plating of aluminium alloys is a well-known and well-established process [2]. The zinc immersion technique combined with copper striking gives good adhesion with an electroless nickel plating [3]. The experiments involved an investigation of the adhesion of an electroless nickel plating applied directly to a difficult-to-plate aluminium alloy (6061-T6).
Titanium alloys, stainless steels and superalloys are all normally resistant to a wide variety of corrosives. This property is due to the presence of a thin, transparent oxide film on the surface, which re-forms on removal. This film does not just protect the metal, it also prevents or impairs the adhesion of electroplatings.

However, if the film is removed and its re-formation prevented until the surface is covered with a metal plating, practically any of the usual metals can be electrodeposited onto it with good adhesion.
Titanium and its alloys cannot be electroplated by conventional methods. This is because titanium materials have a greater tendency to passivate: a thin, natural oxide film forms immediately when an oxide-free surface is exposed to air or water [4].
There is a whole range of familiar activation treatments [5] for steels and superalloys.
The currently most common treatment is Wood's nickel strike treatment [6].

## EXPERIMENTAL PROCEDURE

### Materials

*CFRP*
The composite materials used in aircraft contain up to 70% carbon fibre, giving a correspondingly heterogeneous structure. Epoxy resins are used almost exclusively as the matrix in modern, high-performance composites. Polyimides are used only for higher-temperature applications.

*Aluminium alloy*
The aluminium alloy AlMgSil (1% Mg, 1% Si, 0.1% Cr, 0.7% Mn), which is comparable to 6061-T6, was used.

*Titanium alloys*
Examples of titanium materials used in aero-engine construction are Ti6Al4V, Ti2Cu, IMI 685 and Ti6Al2Sn4Zr2Mo. Their precise chemical compositions are shown in table 1. Like pure titanium, titanium alloys can form a hexagonal $\alpha$ phase or cubic, body-centred $\beta$ phase. Ti6Al4V, Ti6Al0.8Mo5Zr (=IMI 685) and Ti6Al2Sn4Zr2Mo are alloys of the $\alpha$ and $\beta$ type. Ti2Cu is an $\alpha$alloy with precipitation hardening via $Ti_2Cu$.

*Stainless steels and superalloys*
The chromium-nickel steel X10CrNiTi189 and the three superalloys Nimonic 75, Inconel 718 and Waspaloy were used. Their chemical compositions are shown in table 2. Alongside the nickel base, the following alloying constituents are included in particular: chromium, to increase oxidation resistance; aluminium, titanium and columbium for precipitation hardening via the $\gamma'$ phase $Ni_3$ (Al, Ti, Cb); or molybdenum for solid-solution hardening [7].
Nimonic 75 has a high scaling resistance due to its 15-20% chromium content and is used, for example, in combustion chamber linings, casings and afterburner components for gas turbines. Inconel 718 is a "classic" high-temperature alloy with medium $\gamma'$ hardening. In addition to its high scaling resistance, this alloy also has good creep strength. It is used in gas turbines and aero-engines for discs, rings, shafts and afterburners. Waspaloy is a high $\gamma'$ hardened nickel alloy, which also has good scaling resistance and creep strength.

Pretreatments

*CFRP*
The CFRPs were subjected to the following principal process steps:
- cleaning of the surface with organic solvents
- blasting
- chemical etching
- Pd coating
- electroless Cu
- (Cu) plating.

*Aluminium alloys*
Of the methods available for preparing aluminium for plating, the zinc immersion technique is the most practical and gives the most satisfactory results. This procedure, referred to as zincating, consists in immersing the aluminium part in a solution containing zinc oxide and sodium hydroxide. The sodium hydroxide dissolves the surface layer of oxide from the aluminium, and zinc is deposited onto this fresh surface by chemical displacement. The thin layer of zinc prevents the oxide layer from re-forming and acts as an adherent base onto which other metals can be deposited.

*Titanium alloys*
The plating procedure [4] involves the following steps:
- vapour degreasing
- blasting
- etching
- activation
- plating.

The technique has the advantage that the parts do not have to be plated immediately after activation, as would otherwise be the case. The activation allows deposition with good adhesion, without the need for an intermediate layer.
The etching and activating stages are material-removing operations. The etching process involves material removal of approximately 3.5 /um per unit area, and activation some 3 /um, i.e. the total material removal is approximately 6 /um per unit area. Surface roughness was measured after blasting, etching and activation. The roughness of the initial condition remains practically unchanged by the process.

*Stainless steels and superalloys*
Electrolytic and chemical preparation techniques were tested to determine their effectiveness [8]. The bath compositions can be seen in table 3.
Both the chemical and the electrolytic treatments are material-removing processes. The amount of material removal depends on the material and technique. For example; the material removal rate in the $FeCl_3/HCl/HNO_3$ solution is 0.2 /um/min for Waspaloy and 0.6 /um/min for Nimonic 75.

## Bond strength testing

*Qualitative tests*
Different types of stressing can be simulated by qualitative tests:
- sheet bending test - deformation
- cutting machining - shearing stress
- blasting - deformation and compressive stress
- thermal shock - temperature cycle.

*Quantitative tests*

- *Peel test*
In this test, the plating at one end of a plated test strip is raised along a length of approximately 10 mm to allow a traction fixture to be attached. The detached end of the plating is subjected to a tensile force until it can be pulled off the strip at a 90° angle (figure 1).
A prerequisite of this test is that the tensile strength of the plating is greater than its bond strength, otherwise the plating will tear. Platings which are too thin can be reinforced with an additional copper coating, for example.

- *Tensile bond strength test*
For this test method (figure 2) a disc (dia. 25.4 mm) of an appropriate material is plated on one side only. This plated disc is the finished tensile test body for determining bond strength in tension. The plated test body is cemented on both faces and bonded into an appropriate tensile test rig, which is then subjected to tensile stress, so that the bond strength of the plating can be determined.

- *Bond strength test by pressing*
This test method is an inversion of the Ollard test (figure 3). A cylindrical test body with a hole drilled from one end is plated to a thickness of several millimeters at the other end. The hole is extended into the plating. The plating is turned off, down to the base metal, so that a ring of defined area is left adhering to the plating. The plating is then pressed off with a punch.

- *Ring shear test*
A ring is generated on a pin by plating and turning/grinding. The plating is then sheared off against a fixed sleeve (figure 4). The advantage of this technique is that very little technical effort is involved, since no auxiliary equipment is required apart from the turning fixture and test machine. The disadvantage of this shear test method is that, due to the necessary clearance between the pin and sleeve, the shearing plane is preset and located inside the plating.

## RESULTS

### CFRP

The adhesion of platings on CFRP depends on the matrix. Adhesive strengths of up to 470 N/cm are possible with epoxy-based CFRP, whilst the adhesive strength of a copper plating on polyimide-based CFRP is only 150 N/cm.

### Aluminium alloy

The adhesion of an electroless nickel plating applied directly onto AlMgSi1 is relatively low. Depending on the zincate treatment, bond strengths in the range 30-50 MPa can be achieved.

### Titanium alloys

*Qualitative tests*

Figure 5 shows a sheet bending test on nickel plated Ti2Cu. The adhesion of the nickel plating is very good. Nickel platings can be machined off, even down to the base metal, without difficulty and without any signs of separation at the plating/substrate boundary. For a thermal shock test, a braced ring of Ti2Cu was manufactured and sulphamate nickel plated to a thickness of 1.5 mm. Segments were cut from the ring and subjected to the various temperature cycles shown in table 4. The nickel plating showed good adhesion after all four thermal shock cycles.

*Quantitative tests*

The bond strengths of all the tested platings on Ti6Al4V and Ti2Cu are shown in table 5. Under both tensile and shear stresses, the bond strengths are between approximately 70 and 110 MPa.

### High-alloy steels and superalloys

The achievable bond strengths of electrodeposited platings on the various materials are shown according to preparation technique (table 6).
If the characteristics of the materials and the electrodeposited nickel plating are considered, the following statements can be made:

- *X10CrNiTi189*
  Separation occurs at the boundary between base metal and plating. Better bond strengths (>600 MPa) are achieved with the electrolytic preparation technique than with the chemical one.
- *Nimonic 75*
  Bond strengths of around "only" 350 MPa are achieved with all preparation techniques, so the nickel plating is detached at the boundary. Electrolytic and chemical preparation techniques are equivalent.
- *Inconel 718*
  Such good adhesion can be achieved with electrolytic preparation techniques that the separation occurs in the nickel plating, i.e. the bond strength is greater than the tensile strength of the nickel (>600 MPa). The bond strengths achieved with chemical preparation techniques are not so high.
- *Waspaloy*
  With electrolytic preparation, the separation occurs in the nickel plating in this case as well, i.e. the bond strength is greater than 600 MPa. The chemical preparation techniques give bond strengths of 150 MPa ($FeCl_3$/HCl) and 350 MPa ($FeCl_3$/HCl/$HNO_3$) respectively.

## REFERENCES


1. O. Tuscher and R. Suchentrunk, *Metalloberfläche*, 38, (1984) 243

2. W.G. Zelley, in *Modern Electroplating*, F.A. Lowenheim, Editor, John Wiley & Sons (1974) 591-600

3. J.W. Dini, *Electroless Nickel Conference III*, (1983)

4. M. Thoma, *Plating and Surf. Finish.*, 70, (1983) 96-98

5. "Preparation of and Plating on Stainless Steel", ASTM B 254-70, American Society for Testing and Materials, Philadelphia, PA

6. D. Wood, *Metal Industry*, 36, 330 (1938)

7. W. Dienst, *Hochtemperaturwerkstoffe* (1978), Werkstofftechnische Verlagsgesellschaft mbH, Karlsruhe

8. M. Thoma, *Galvanotechnik*, 75, (1984) 1124-1130

| Alloy | Alloying Constituents | | | | | |
|---|---|---|---|---|---|---|
| | Al | Cu | Sn | Mo | V | Zr |
| Ti2Cu | - | 2 | - | - | - | - |
| Ti6Al4V | 6 | - | - | - | 4 | - |
| Ti6Al2Sn4Zr2Mo | 6 | - | 2 | 2 | - | 4 |
| IMI 685 | 6 | - | - | 0.8 | - | 5 |

Table 1: Titanium alloys

| Alloy | Alloying Constituents | | | | | | | | | |
|---|---|---|---|---|---|---|---|---|---|---|
| | C | Ni | Cr | Co | Fe | Al | Ti | Mo | Cb | others |
| AMS 5510 | 0.06 | 9 | 18 | | | | 0.6 | | | |
| Nimonic 75 | 0.12 | 75 | 20 | | <5 | | 0.4 | | | |
| Inconel 718 | 0.06 | 53 | 19 | | 18 | 0.6 | 0.9 | 3 | 5.3 | |
| Waspaloy | 0.06 | 55 | 20 | 14 | <2 | 1.3 | 3 | 4.3 | | 0.1 Zr |

Table 2: Stainless steel and nickel base alloys

| | | |
|---|---|---|
| 1 | 900 g/L | $H_2SO_4$ |
| 2 | 50 Vol%<br>10 Vol% | $H_2SO_4$<br>HF |
| 3 | 65 Vol%<br>5 Vol% | $H_2SO_4$<br>HF |
| 4 | 125 g/L<br>280 g/L<br>20 g/L | $FeCl_3$<br>HCl<br>$HNO_3$ |
| 5 | 290 g/L<br>68 g/L | $FeCl_3$<br>HCl |

Table 3: Etching solutions for stainless steels and nickel base alloys

| Cycle | Heating/Air | Cooling/Water | Number of Cycles |
|---|---|---|---|
| 1 | 350°C | 20°C | 100 |
| 2 | 350°C<br>450°C | 20°C<br>20°C | 70<br>30 |
| 3 | 450°C | 20°C | 50 |
| 4 | 450°C/40 h<br>450°C | -<br>20°C | 1<br>50 |

Table 4: Thermocycles

| Deposit | Face tensile | Adhesion MPa Pressure | Ring shear |
|---|---|---|---|
| Co | >*70 | n.d. | n.d. |
| Cu | n.d. | 50-60 | 55-70 |
| Ni | >70 | 70-110 | 90-120 |
| Ni/P | >70 | n.d. | n.d. |

* Strength of the adhesive ~ 70 MPa

Table 5 : Adhesion of platings on Ti6Al4V

| Substrate | Solution* | | | | |
|---|---|---|---|---|---|
| | 1 | 2 | 3 | 4 | 5 |
| X10CrNiTi189 | 550-620 | 230-250 | 410-430 | 340-370 | 330-380 |
| Nimonic 75 | 350-370 | 370-400 | --- | 320-380 | 340-400 |
| Inconel 718 | 650-750 | 100-120 | 600-650 | 210-250 | 280-340 |
| Waspaloy | 800-850 | 370-420 | --- | 320-350 | 120-150 |

* see table 3

Table 6: Adhesion (MPa) of nickel on stainless steel and nickel base alloy

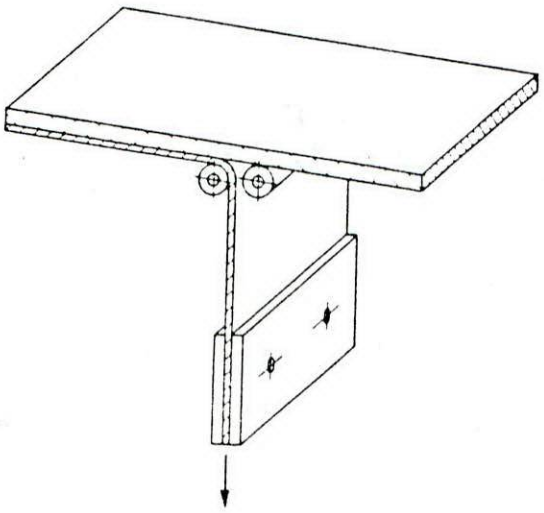

Fig. 1: Peel test

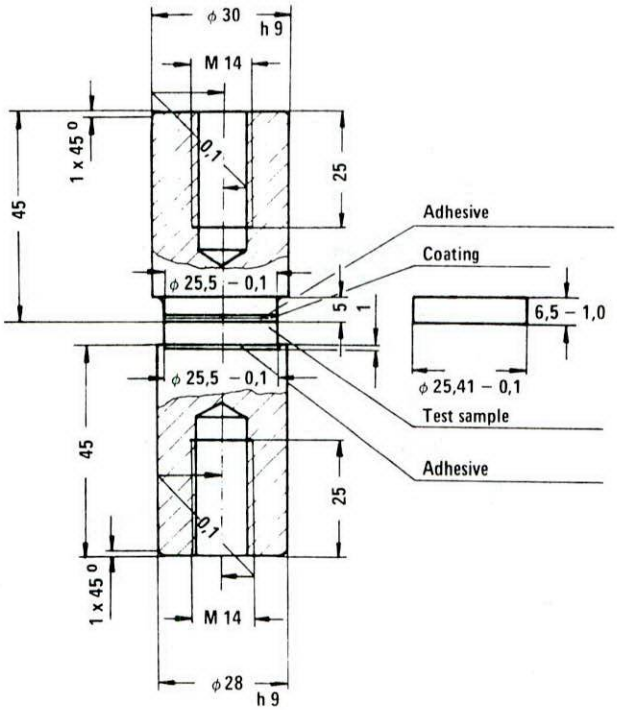


Fig. 2: Face tensile adhesion test




Fig. 3: Adhesion test by pressing

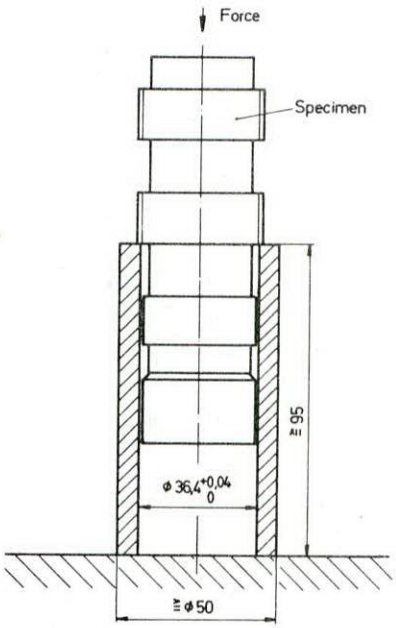


Fig. 4: Ring shear test

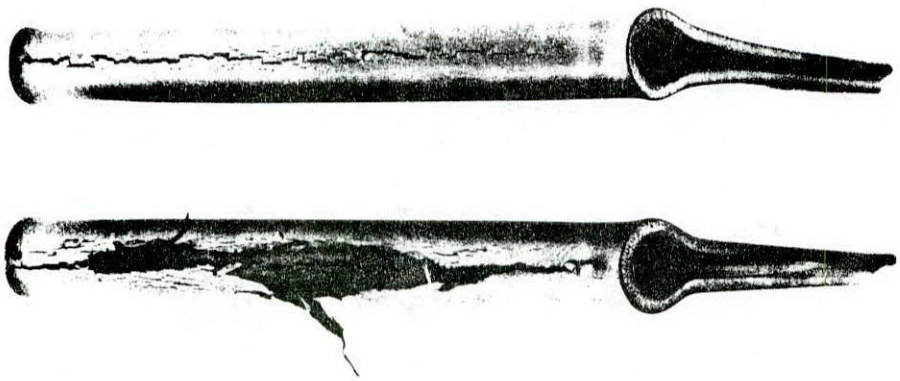

Fig. 5: Bending test
Nickel on Ti2Cu: top - activated
bottom - not activated

I-1

# Electroless Deposition I
# Session I

## Electroless Nickel Phosphorus Copper Study in Corrosive Atmospheric Chamber

E. Yang, Saad K. Doss
and P. Peterson

# ELECTROLESS NICKEL PHOSPHOROUS COPPER

Study in Corrosive Atmospheric Chamber

by
E. Yang, Saad K. Doss, and P. Peterson

## Abstract

AlMg substrates with an electroless deposited layer of a NiPCu alloy from various plating runs were exposed to a corrosive atmosphere for ten days. The corrosion was monitored by weight gain and optical inspection. Surface roughness, corrosion rates, and film compositions were correlated with plating bath age. The first run has the smoothest surface and the last (30) run has the roughest surface. The roughness has a tendency to increase with the age of the bath. The root mean square roughness of the surface varies from 86 to 276 $A^{o}$. The arithmetic average roughness varies from 67 to 220 $A^{o}$; and the peak to valley values run from 475 to 1436 $A^{o}$. The corrosion rate correlates closely with roughness of the surface. If the effect of the roughness is eliminated, the corrosion rate is almost constant independent of the plating sequence. The corrosion rates in term of weight gain range from 0.23 ug/cm2/hr to 0.28 ug/cm2/hr, which is slightly lower than that of permalloy in the same enviornment.

From the analysis of the corrosion product it was determined that the NiPCu films collect hydrogen chloride most efficiently, sulfur dioxide second, and nitrogen dioxide least.

## Introduction

In this study a propriety bath is used to electroless deposit the NiPCu alloy on ground AlMg substrate. The average compositions of electroless plated NiPCu layers are 88% of Ni, 11.3% of P and 0.7% of Cu with no effect from the plating run number. This deposit is amorphous, and hard (with a Knoop hardness of 600 $Kg/mm^2$ (with a 25g load)) (1), with a highly bright, smooth finish, and defect free. NiPCu films from different runs within the same bath solutions were evaluated for surface roughness, susceptibility to corrosive atmosphere, and composition.

The experiment includes four sections. The first section is surface characterization of NiPCu films, including optical microscopy and roughness measurement. The second section studies accelerating corrosion in atmospheric gas chamber. The third section deals with the analysis of the corrosion products on the substrates. The last part of the experiment contains the composition analysis of the film. The analysis of corrosion products were compared with the composition of the corrosive atmosphere to which they were exposed.

## Experimental

The preplating process required the AlMg (AA 5086) ground substrates to be cleaned in an alkaline cleaner, conditioned in an acid deoxidizer, and then double zincated in acid

zincate immersion bath. The plating bath is a proprietary one which operates at 93°C and at a plating rate of 12 um/hr. This experiment used a 400 liter bath. The plating bath was used for a total of 30 runs. Each run consisted of 2.3 square meters surface area. The plating time was 75 minutes per run. There were seven samples selected for this experiment. These samples were taken from runs 1, 5, 10, 16, 20, 25, and 30.

1. Surface Characterization

   Optical microscope was used at magnifications of 100, 200, 500, and 1,000 for visual inspection of the substrates. The roughness of the surface is measured by (Wyko Topo-3D) interferometer for root-mean-square (RMS), average roughness (RA), and peak-to-valley (P-V) in both X and Y directions.

2. Corrosion in the Atmospheric Chamber

   The atmospheric chamber is an accelerating test chamber that controls the desired temperature, relative humidity, various gas concentrations, and air flow (2). The chamber conditions are listed in Table 1.

   Table 1. Conditions of the Environmental Chamber

| | | |
|---|---|---|
| TEMPERATURE: | 25°C | |
| RELATIVE HUMILITY | : 70% RH | |
| GASES | : NO2 | 500 ppb |
| | SO2 | 300 ppb |
| | H2S | 40 ppb |
| | HCl | 3 ppb |
| CARRIER | : AIR | with face velocity 0.5 m/sec |

   Seven substrates, one from every fifth plating run, were placed in the chamber. The weights of the substrates were monitored each day and optical micrograph was taken for one substrate to observe the corrosion progress. The substrates were removed from the chamber after ten days.

3. Analysis of Corrosion Products

   The corroded substrates were first extracted with 100 ml of DI water to remove any water soluble corrosion products. The extractant from each substrate was analyzed with a liquid ion chromotographer (Dionex 2020i) (for qualitative and quantitative analysis of inorganic anions). In addition, EDX (energy dispersive x-ray) was employed to identify elements on one substrate after water extraction.

4. Chemical Composition of the Nickel Phosphorous Copper Deposit

   A substrate representative from each run (total of 30 substrates) was cut into small pieces. These pieces were etched in hot 3M NaOH to separate the NiPCu films from the substrates, then weighed (40 to 60 mg), dissolved in 2 ml concentrated $HNO_3$ acid and volumetrically diluted to 100 ml. A Plasma Spectrometer (Beckman/SMI Spectraspan 5

D.C.) was used to evaluate the Ni, P, and Cu. The analysis indicates that the deposit composition is very consistent throughout the cycle life of the bath.

## Results/Discussion

1. Surface Characterization

Optical microscope photographs of the substrate surfaces from magnification of 500 are shown in Figures 1 through 7.

From the photographs, the surface finish varies with plating run. The substrate from run 1 has the smoothest surface and the surface from the last run, 30, seems the roughest with large sizes of semispherical NiPCu deposit. In addition, the grinding marks from the substrates are observed on surfaces of as-plated NiPCu deposits.

The observation on roughness is confirmed by interferometer. The average values of RMS, RA and P-V according to the plating runs are plotted in Figure 8.

The roughness measurements show a slight increase of roughness with run number. However the last run (30) has double the roughness of the first run.

2. Corrosion in the Atmospheric Chamber

The photographs of the substrates from run 1 in the corrosion chamber are shown in Figures 9 through 11. These figures show the corrosion progress after 2, 5, and 10 days exposure respectively.

At the end of first day in the chamber, the corrosion product appeared as submicron droplets on the surface. The droplets grow in size and in number with time in the chamber. The increased number of fringes seen within each drop shows that these drops were increasing in thickness as well as diameter. By the eighth day, solid corrosion products became appearent within these drops.

Blisters at the edges of the substrate were also seen after 8 days. The mechanism of blistering is due to loss of adhesion between the NiPCu film and the AlMg interface, as the result of corrosion through pin holes in the NiPCu layer (3).

The weight gains are calculated and plotted as a function of days in the chamber for each substrate in Figure 12. After an initiation period of 2 days, the weight gains increased linearly with exposure in the chamber.

In general, the amount of corrosion increases with run number. The weight gains per unit area per hour after 10 days in the chamber plotted according to run number are shown in Figure 13. The amount of corrosion correlated better with surface roughness than run number as shown in Figure 8 and Figure 13. For example, run 16 is smoother than run 10, consequently the weight gain of run 16 is less

than run 10. The same applies to runs 20 and 25.

The correlation between corrosion weight gain in the atmospheric chamber and roughness is presented in Figure 14, as weight gain versus roughness. Using a first order approximation to relate corrosion to roughness and factoring the roughness variable out of the data, no corrosion rate dependence on plating run sequence was shown. If the effect of roughness is eliminated, the corrosion rate of NiPCu layers in the chamber is independent of plating run sequence, as shown in Figure 15.

The roughness of the surface contributes to the corrosion rate of the substrate, this can be explained by the microscopic surface area. The rougher the surface, the more surface area is available for corrosion. Therefore, the corrosion rate in term of weight gain is higher for rougher surface. However, the corrosion rate does not depend on the sequence of plating run and the age of the bath if the effect of roughness is removed.

3. Analysis of Corrosion Products

From liquid chromotography, $Cl^-$, $NO_3^{-2}$, and $SO_4^{-2}$ were the only anions detected in the water extractions. Figure 16 shows bar charts on molar concentrations of ions. The sulfate products are the highest in concentration, and the percentages of ions in the extracted solutions are presented in Figure 17. The percentages of ions of each substrate are approximately constant, as shown in Table 2 for average ionic percentages and their standard deviations. The sulfate is almost four times of chloride. However, the chamber gas concentration ratio of $(SO_2)$ to $(Cl^-)$ is 100. That is, although the chloride ion has far less concentration in the corrosion chamber, it reacts more aggressively with NiPCu than the Sulfur dioxide. The sticking efficiency of hydrogen chloride on NiPCu is the greatest; sulfur dioxide is more than an order of magnitude lower than chloride and nitrogen dioxide is two orders of magnitude lower than the chloride.

Table 2. Average Ionic Percentage in Extracted Solutions from Corroded Substrates in Mole

| ION | AVERAGE% | STANDARD DEV. | % NORMALIZED WITH Cl |
|---|---|---|---|
| Cl | 18.04 % | 1.98 % | 1.00 |
| N03 | 15.27 % | 1.79 % | 0.85 |
| S04 | 66.69 % | 3.68 % | 3.75 |

In addition, optical micrographs of substrate surfaces after DI water extraction are shown in Figures 18 and 19. The photographs are also taken from SEM and EDX for the substrate from run 20 after extraction, shown in Figures 20 and 21. Other than Ni and P, only S (sulfur) is detected in EDX analysis. This remaining sulfur is present as water insoluble nickel sulfur com-

pounds. All of the chloride has been removed by the water extraction.

4. Composition Analysis

The chemical composition of runs 1, 5, 10, 16, 20, 25, and 30 are summarized in Figure 22. The anlysis shows a consistent chemical composition of the NiPCu deposit throughout the bath cycle. The average chemical composition is in Table 3.

Table 3. Average Chemical Composition from 30 NiP Runs

| ELEMENT | AVERAGE COMP. (WEIGHT %) | STD DEV. |
|---|---|---|
| Ni | 88.0 % | 0.8 % |
| P | 11.3 % | 0.7 % |
| Cu | 0.7 % | 0.3 % |


Summary

The surface roughness of as-plated substrates vary with plating runs. The roughness increases slightly with run number. The roughness of surface can contribute to the rate of corrosion in the corrosion chamber since the rougher surface provides more microscopic area for corrosion. However, the corrosion rate of NiPCu layers in the corrosion chamber does not increase with the age of the plating bath without the effect of roughness. The variation found between the highest and lowest corrosion rates is not enough to be of any concern. The average corrosion rate in terms of weight gain of these NiPCu deposits is 0.26 ug/cm2/hr comparing to that of permalloy, 0.33 ug/cm2/hr.

The analysis of corrosion products indicates that chloride ions, sulfate ions, nitrate ions and $H_2O$ are the critical pollutants. In addition, the chloride is reacting most efficiently with NiPCu since the concentration of $Cl^-$ to $SO_2$ is only 1 to 100 and the mole composition ratio of corrosion product is 1 to 4. The compositions of NiPCu layers are almost constant through out the lifetime of the bath. The NiPCu layer contains 88% of Ni, 11.3% of P and 0.7% of Cu.



Acknowledge

The authors would like to thank Cheryl White for her assistant on roughness measurement. Leland Chen for his assistant on SEM/EDX, Kay Sommers for her assistant in obtaining the ion chromotergraphy data, and Jerry Sherrad for maintaining the corrosion chamber.


Reference


1. Electroless NiPCu Plating Bath Performance and its Relation to Deposition Parameters, Saad K. Doss, The 172 nd Meeting of the Electrochemical Society, Inc., Honolulu, Hawaii, October 18-23, 1987.

2. Corrosion Mechanism of Thin Film Disk Magnetic Recording Structures, S. K. Doss and G. A. Condas, ASM ISTFA 1986 Int. Symp. for Testing and Failure Analysis, 8618-003, Oct. 1986.

3. Atmospheric Corrosion of Magnetic Film Structures, S. K. Doss and G. A. Condas, Metal. Trans. 18A, 158, Jan. 1987.



Figure 1. Micrograph of as plated NiPCu on AlMg substrate. Run #1, 500X



Figure 2. Micrograph of as plated NiPCu on AlMg substrate. Run #5, 500X



Figure 3. Micrograph of as plated NiPCu on AlMg substrate. Run #10, 500X

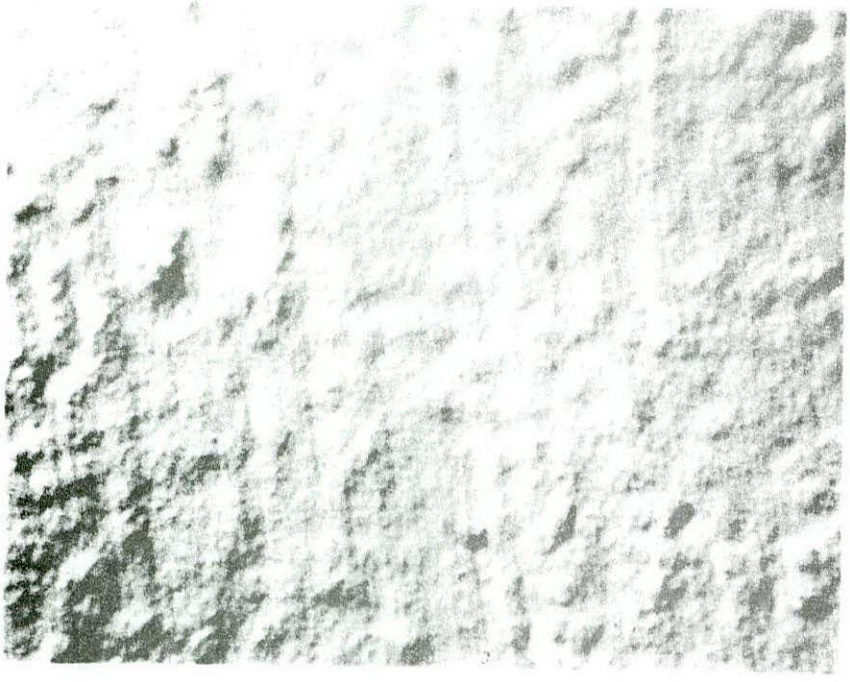

Figure 4. Micrograph of as plated NiPCu on AlMg substrate. Run #15, 500X

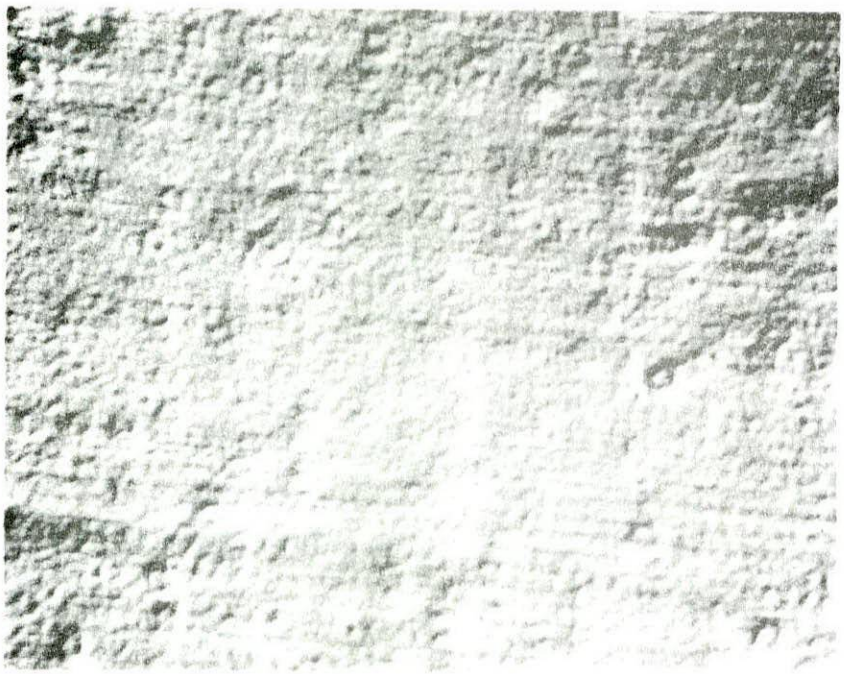

Figure 5. Micrograph of as plated NiPCu on AlMg substrate. Run #20, 500X

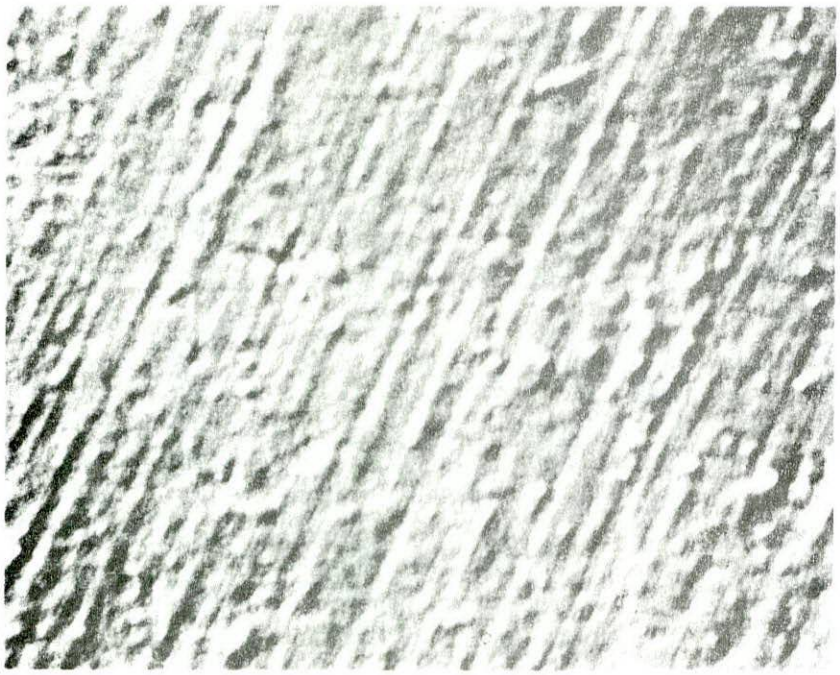

Figure 6. Micrograph of as plated NiPCu on AlMg substrate. Run #25, 500X



Figure 7. Micrograph of as plated NiPCu on AlMg substrate. Run #30, 500X

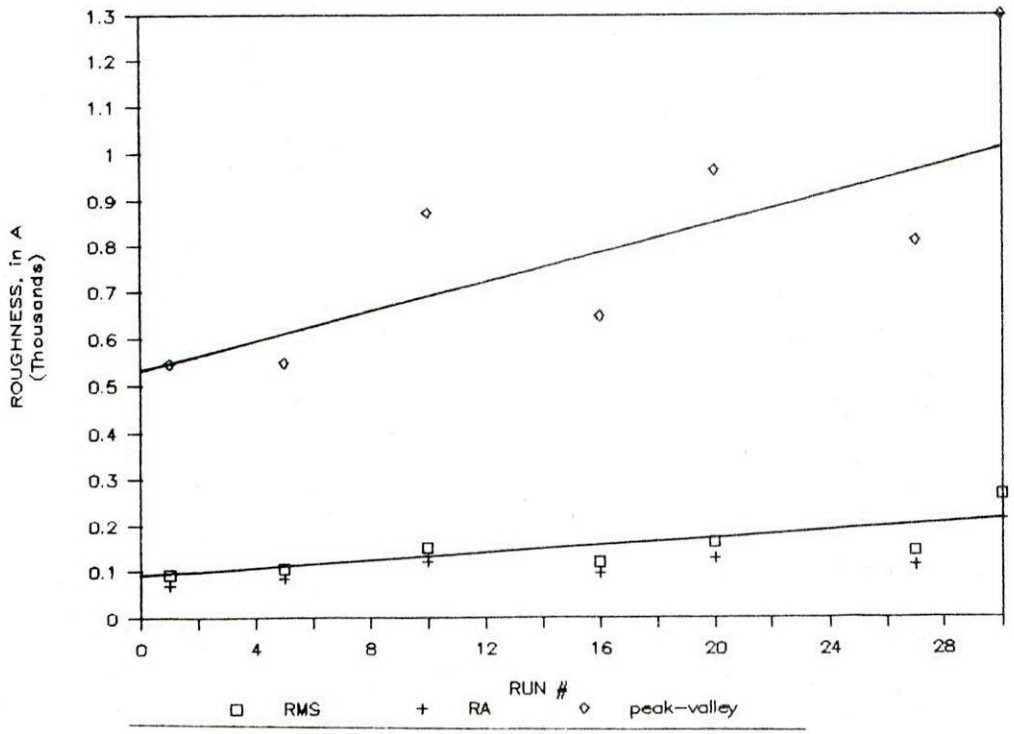


**Figure 8. WYKO roughness measurement of NiPCu deposits.**



Figure 9. Corrosion progress of NiPCu film after 2 days in the corrosion chamber Run #1, (100X)

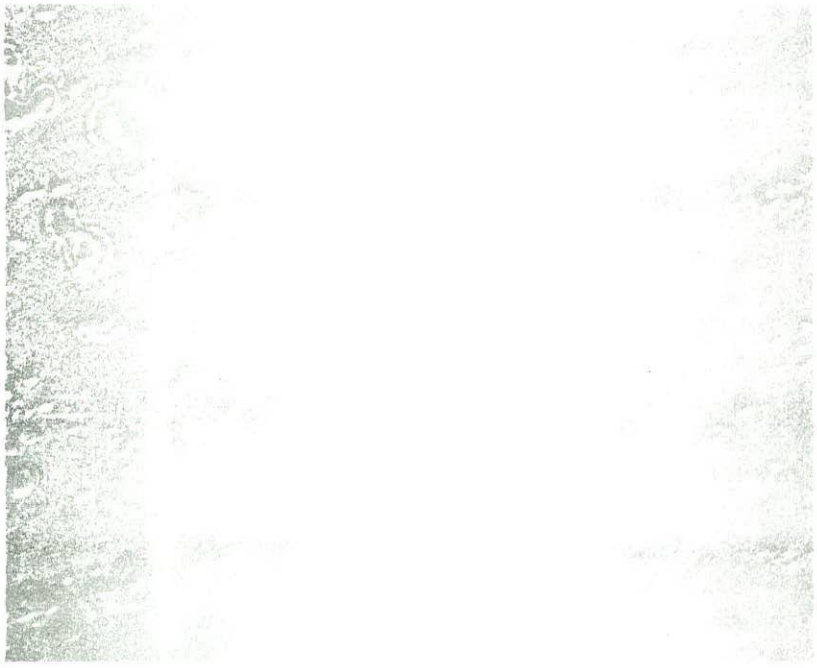

Figure 10. Corrosion progress of NiPCu film after 5 days in the corrosion chamber Run #1, (100X)

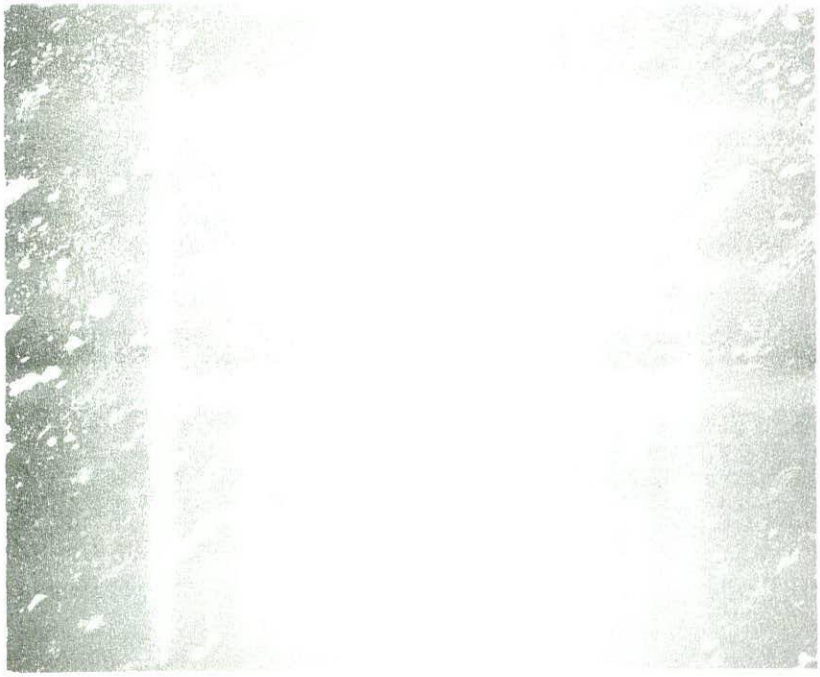

Figure 11. Corrosion progress of NiPCu film after 10 days in the corrosion chamber Run #1, (100X)

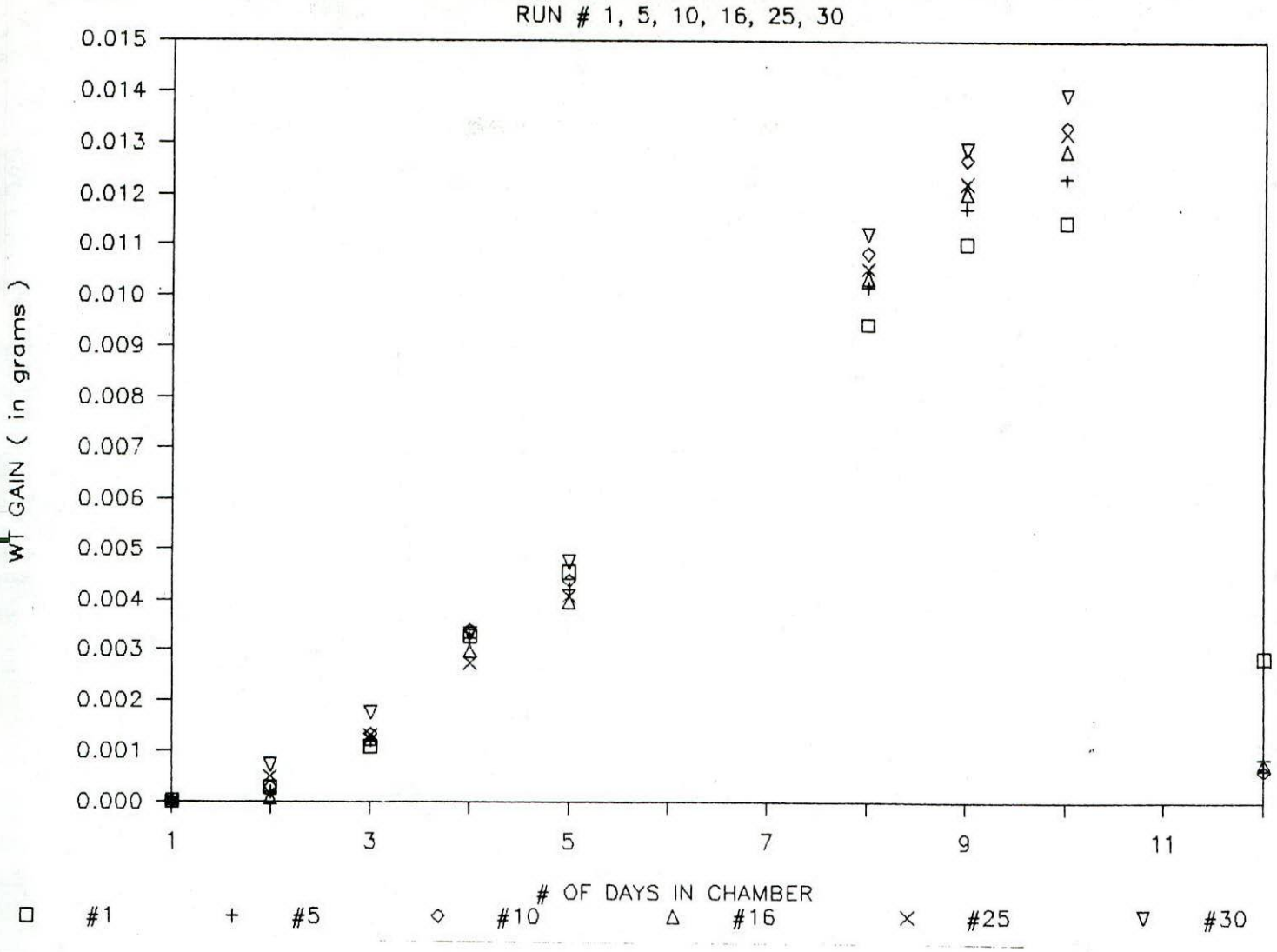


**Figure 12. Weight gain in the corrosion chamber.**

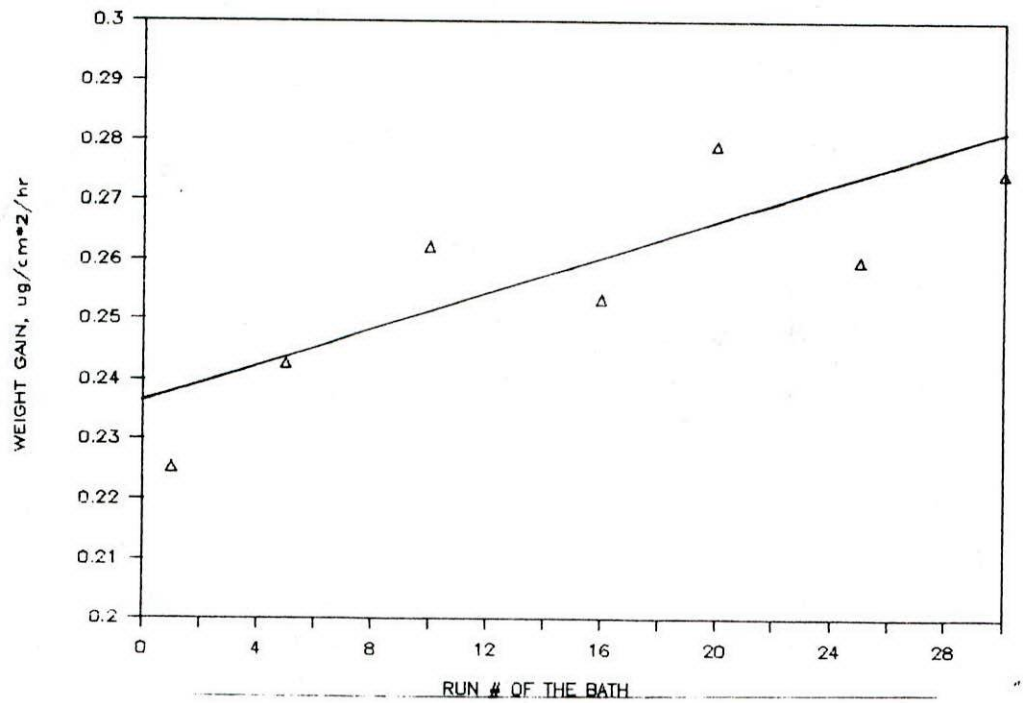


**Figure 13. Weight gain measurement (nine days in corrosion chamber).**

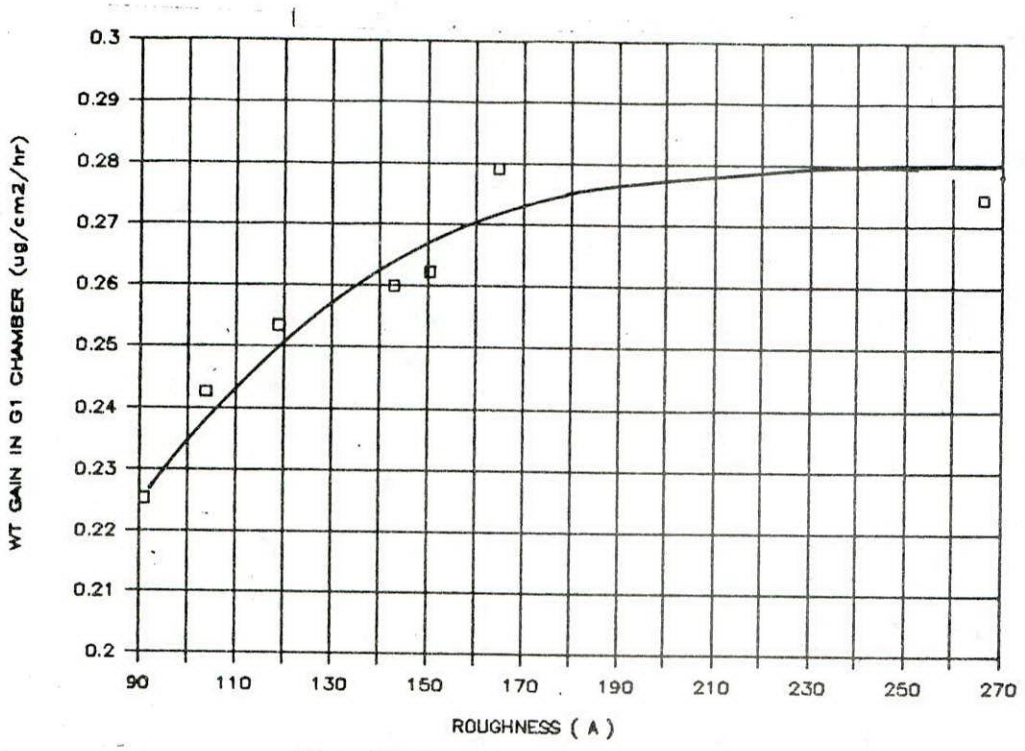


**Figure 14. Corrosion rate vs. roughness.**

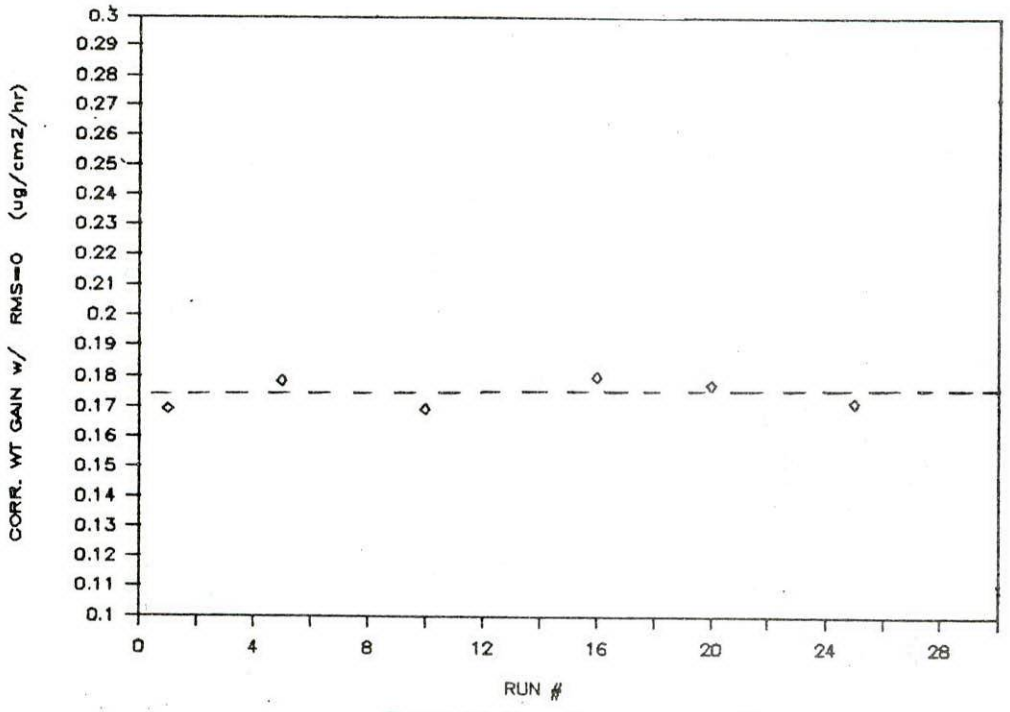


**Figure 15. Corrosion rate vs. run No.**

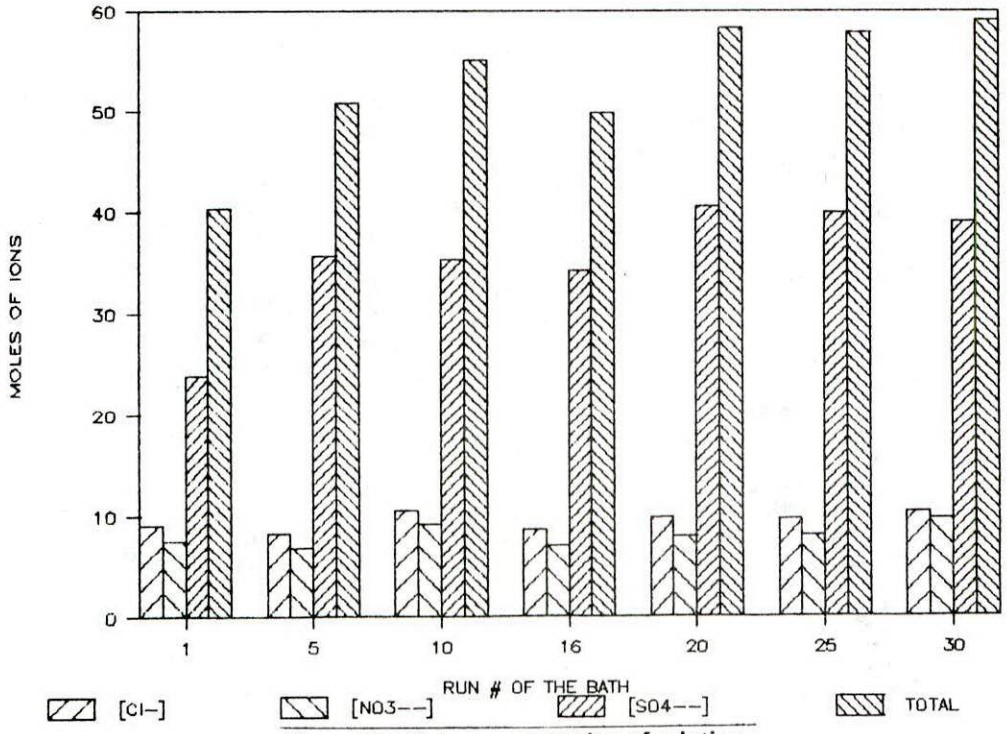


**Figure 16. Molar concentration of solution.**

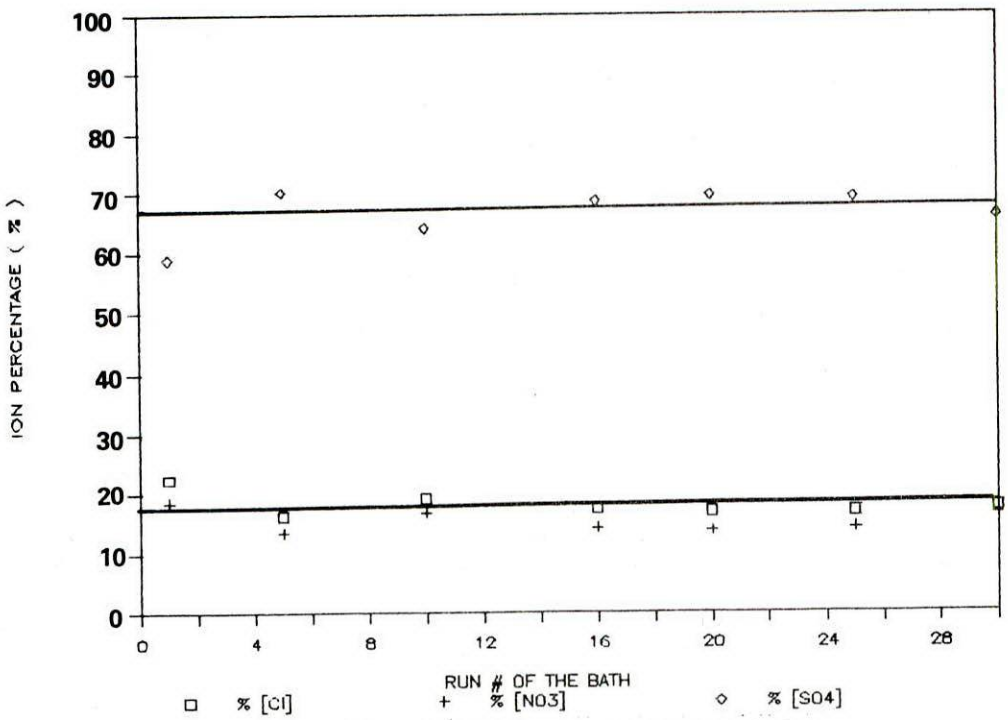


**Figure 17. Molar percent of ions in solution.**



Figure 18. NiPCu film after water extraction (100X)



Figure 19. NiPCu film after water extraction (1000X)

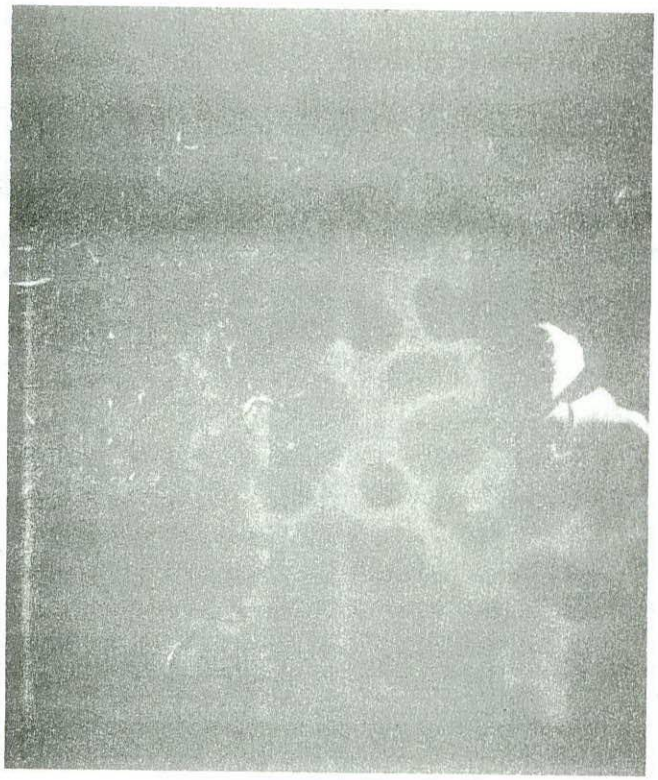

Figure 20. SEM of NiPCu film after water extraction (2000X)

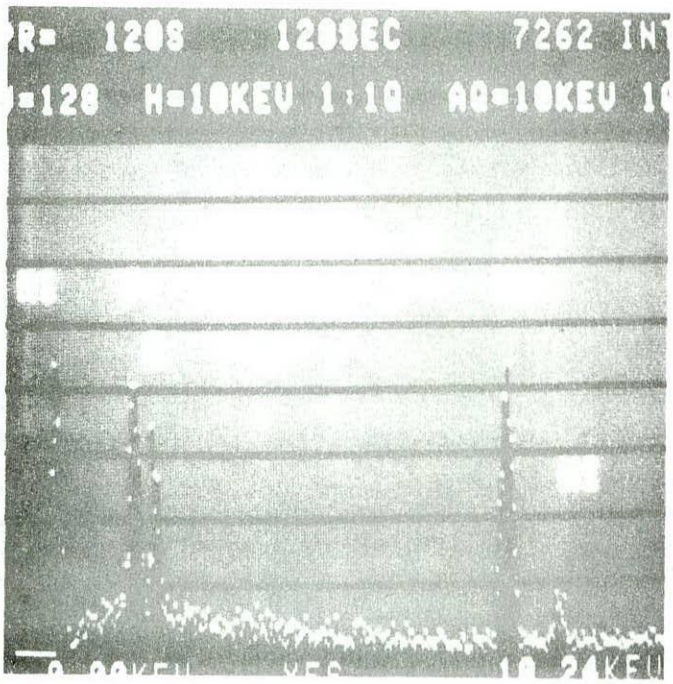


Figure 21. EDX of NiPCu film after water extraction

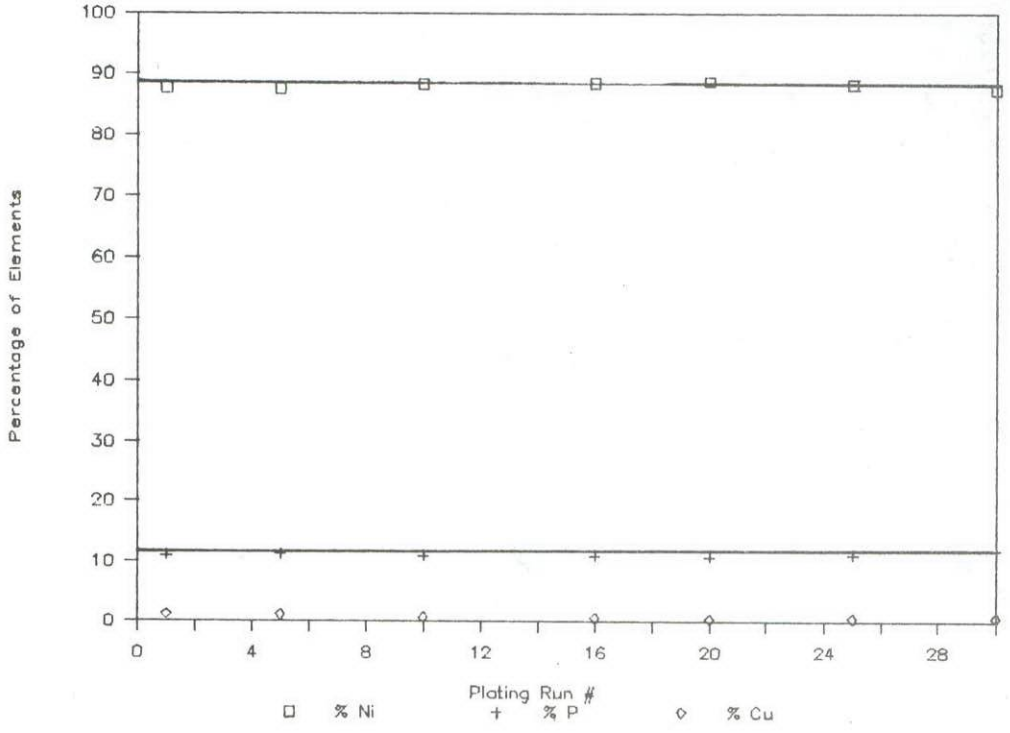


**Figure 22** Chemical compositions of NiPCu deposites.

I-2

# Electroless Deposition I
# Session I

## Composite Coatings of Fluorinated Carbon (CFx) In Electroless Nickel Plating Bath

Jung T. Kim
Allied-Signal Inc.
Buffalo Research Laboratory
20 Peabody Street
Buffalo, NY 14210

# Composite Coatings of Fluorinated Carbon ($CF_x$) in Electroless Nickel Plating Bath

Jung T. Kim

Allied-Signal Inc.
Buffalo Research Laboratory
20 Peabody Street
Buffalo,New York 14210

## ABSTRACT

Fluorinated carbon ($CF_x$) and nickel are co[illegible]om an electroless nickel plating bath onto a suitable so[illegible]g a thin surface layer having low surface energy and good [illegible]$CF_x$ particles with various particle size (from 0.2$\mu$m [illegible]e dispersed in aqueous solution containing a nonionic s[illegible]aving HLB number of 10 to 20, optionally including up [illegible]m 20% of cationic surfactant based on the amount of no[illegible]ctant used. The amount of $CF_x$ codeposited in nickel ma[illegible]es with the $CF_x$ concentration in the bath. The process [illegible]ion of Ni/$CF_x$ bath are discussed.

PAPER WITHDRAWN

I-3

# Electroless Deposition I
# Session I

## Corrosion Characteristics of Electroless Nickel Coatings Developed Using Surface Analysis Techniques

Lawrence Salvati, Jr.
Perkin-Elmer Corporation
Edison, NJ

Diane M. Tramontana
Occidental Chemical Corporation
Grand Island, NY

# CORROSION CHARACTERISTICS OF ELECTROLESS NICKEL COATINGS DEVELOPED USING SURFACE ANALYSIS TECHNIQUES

Lawrence Salvati, Jr., Perkin-Elmer Corporation, Edison, New Jersey

Diane M. Tramontana, Occidental Chemical Corporation, Grand Island, New York

## INTRODUCTION

The effect of phosphorus content on the corrosion behavior of metals and alloys has been studied in various forms.[1-5] Detrimental effects of alloys with phosphorus segregated to grain boundaries include increased susceptibility to intergranular corrosion and stress corrosion cracking. The beneficial effects of phosphorus are mainly observed in amorphous alloys and electroless nickel coatings. The ability of the phosphorus to influence in a positive and negative manner suggests that it can also influence the corrosion performance of the surface layers. J. Flis and D.J. Duquette[1] have shown that increased anodic dissolution and catalytic activity for electroless plating is apparently associated with the deterioration of a passivating oxide film. Electron Spectroscopy for Chemical Analysis (ESCA) studies [6,7,8] have shown evidence of $P^5$ species (as phosphates) in the surface layers of phosphorus containing alloys. It has been further suggested, that the appearance of these phosphates significantly contributes to the corrosion protection of the surface layer [1,6,7,8].

Recent corrosion studies [9,10] in chemical process environments have questioned the theory that higher phosphorus contents always enhance the corrosion protection of electroless nickel (EN) alloys. R.P. Tracy et al.[9] demonstrated that lower phosphorus containing alloys (1-2% phosphorus) have superior resistance to corrosion in several chemical process environments (Table 1). The corrosion performance of low phosphorus electroless nickel alloys is especially superior to high phosphorus alloys in sodium hydroxide environments (Table 1). This corrosion behavior of the low phosphorus electroless nickel coating indicates differences in surface film structure and components.

In the present study, Electron Spectroscopy for Chemical Analysis (ESCA or XPS) and Auger Electron Spectroscopy (AES or SAM) were used to characterize a series of Electroless Nickel (EN) coatings. The EN samples investigated included

as-plated, after heat treatment and after corrosion testing in several industrial process environments. In all of these cases, the EN coatings were prepared with varying amounts of phosphorus. The corrosion tested EN materials were the same samples reported on by Tracy et al.

The primary emphasis of this investigation was directed at characterizing the surface composition of as-plated EN coatings. The principle goal of this study was to determine the effects of phosphorus content on the surface chemistry and ultimately the corrosion properties of these materials. Based on the ESCA and angle dependent ESCA (ADESCA) results presented in this report, a correlation between the surface chemistry and phosphorus concentration of the plating bath was clearly indicated. Preliminary ESCA results collected for the corrosion tested samples further suggested that the as-plated surface composition influenced the corrosion properties of the EN coating. In addition, this report will also present data obtained for heat treated EN materials. This data showed that the surface chemistry and composition of the heat treated EN coatings was significantly different from that of the corresponding as-plated material.

## EXPERIMENTAL PROCEDURES:

Three electroless nickel coatings were evaluated: low phosphorus (1-2%), medium phosphorus (6-8%), and high phosphorus (10-11%) as expressed in weight percent. In the text, these materials will be referred to by the designations LP, MP, and HP. All three coatings were deposited at a thickness of 50-65 microns. ASTM G-31, "Laboratory Immersion Corrosion Testing of Metals" was used to test the panels. Mild steel (AISI 1010) panels were cleaned using the following cycle: vapor degrease, hot alkaline soak ($85^{0}$C), water (DI) rinse, electroactivation with periodic reverse, water rinse, plated, water rinse, and air dried. Only those panels with a negative ferroxyl test were used in the testing program. The surface area was measured, using a digital caliper (=0.01 cm), and recorded. The details of the actual immersion data including the particulars of each chemical environment are presented by R.P. Tracy et al. in reference 9.

The ESCA and ADESCA measurements were obtained using a Perkin Elmer Model 5000 LS Spectrometer. A Mg anode (Mg$k\alpha$ =1253.6eV) run at 400 watts (15kV and 27mA) was employed as the primary x-ray source. The vacuum inside the main analytical chamber was typically better than $5x10^{-9}$ Torr. The binding energy positions of the photoelectron lines were determined by referencing to the C1s line at 284.6eV. All

instrument operations, data acquisitions and data massage routines were accomplished using a Perkin Elmer Version 2.0 ESCA software package.

The AES results were obtained on a Perkin Elmer Model 660 SAM system. This system utilizes a $LaB_6$ filament with a minimum beam diameter of 250Å. The beam voltage was variable between 1 and 30keV. The results presented here were obtained at a beam voltage of 5keV and beam current of approximately 1 μA. The base vacuum inside the main analytical chamber was < $1x10^{-9}$ Torr. Sputter depth profiling was accomplished using a Model 06-650 duoplasmatron ion gun. The primary beam voltage in the ion gun was 4 keV with $^{40}Ar$ as the sputtering gas. The sputter rate at these conditions was calculated to be 65Å/min for $SiO_2/Si$.

## RESULTS AND DISCUSSION

### As Plated EN Coatings

The initial section of this discussion presents the ESCA and ADESCA results obtained for the as-plated LP, MP, and HP EN materials. ESCA survey spectra collected for the as-plated EN materials indicated the presence of Ni, O, C, and P. The Ni and P peaks were expected, since the EN process involves the co-deposition of both of these elements. The presence of oxygen was most likely due to surface oxidation and adsorption of $H_2O$, while atmospheric contamination was the probable source of the C peak. High resolution spectra were obtained for each of these elements. This data was used to more closely evaluate the chemical and quantitative composition of the EN surfaces.

High resolution spectra acquired for the Ni2p region were similar for all of the as-plated EN materials investigated. An example of the Ni2p spectrum obtained for the as-plated surfaces is illustrated in Figure 1. The spectra consisted of six peaks (labeled I-IV and S). The spectra appeared complex, but the interpretation was straightforward. Due to the inherent energy separation of the $2p_{3/2}$ - $2p_{1/2}$ atomic levels in the nickel atom, the Ni2p photoelectron spectrum characteristically exhibits two peaks. The peak separation exhibited by the nickel spin orbit doublet ($Ni2p_{3/2,1/2}$) is a direct reflection of the atomic energy level difference and typically falls within the range of 17-18eV. The exact energy difference is characteristic of the particular nickel species present. Based on this information, it was concluded that the Ni2p spectra (Figure 1) reflected the presence of two distinct nickel species resulting in two sets of Ni2p

doublets. The two low energy peaks (I and III) were identified as $Ni2p_{3/2}$ lines, while the peaks centered around 872 eV (II and IV) were the corresponding $Ni2p_{1/2}$ lines. The additional lines designated S represented shake up satellite lines.

Identification of the nickel species was based on the measured binding energy positions of the $Ni2p_{3/2}$ lines (peaks I and III). The binding energy of peak I (Figure 1) was determined to be approximately 852eV which compared with the literature value for metallic nickel [15]. The position of line III was approximately 856.5eV which matched the reference value for $Ni(OH)_2$ [15-16]. It is beyond the scope of this report to discuss the origin of the shake up lines in any detail. For the purposes of this discussion, it is sufficient to state that the peak shape and position of the shake up lines (S) correlated closely with published reference spectra for $Ni(OH)_2$ [16]. This confirmed the presence of $Ni(OH)_2$ on the as-plated EN surfaces.

High resolution ESCA spectra obtained for the P2p region also supplied valuable information concerning the chemistry and composition of the as-plated EN materials. The phosphorus spectra exhibited two peaks for all of the as-plated EN samples. The binding energies of these peaks were measured at approximately 129eV and 133eV. Unlike the Ni2p region, the spin orbit splitting for the $P2p_{3/2,1/2}$ lines is approximately 1.0eV [18] and is not easily resolved by ESCA. Based on this data, it was concluded that two distinct phosphorus species were present. The binding energy values measured for these peaks suggested the presence of free phosphorus plus a $PO_4^{-3}$ type species. The peak at 129eV was characteristic of free phosphorus. The peak at a binding energy position of ~133eV was characteristic of a $PO_4^{-3}$ species [15].

The Ni2p and P2p data discussed above indicated the presence of a thin (<100Å) "passive" oxide layer comprised of $Ni(OH)_2$ and $PO_4^{-3}$ on the as-plated EN surfaces. In the region below this oxide layer, the data suggested that the coating consisted of nickel metal and free phosphorus. To formulate a better understanding of the surface composition, a series of ADESCA measurements were obtained which provided a non-destructive depth profile of the coating surface. Figures 2 and 3 illustrate representative ADESCA spectra collected for the as-plated EN coatings, while the corresponding atomic concentration (AC) results are listed in Tables 2 and 3.

Figure 2 illustrates the $Ni2p_{3/2,1/2}$ spectra collected for the as-plated a) LP, b) MP, and c) HP coatings at a $90^0$ take off angle. These results implied that the depth of the

oxide overlayer was dependent on the phosphorus content of the coating. This observation was based on the fact that the relative nickel metal/$Ni(OH)_2$ peak heights varied significantly for the different EN materials. In the LP spectrum (Figure 2a), the nickel metal peak was most intense, while for the HP sample (Figure 2c), the predominant nickel species was $Ni(OH)_2$. It was apparent from these spectra that the relative Ni/$Ni(OH)_2$ peak height ratio decreased systematically as the phosphorus content of the coating was incremented. This trend indicated that the oxide ($Ni(OH)_2$) overlayer thickness was dependent on the phosphorus content of the coating and/or plating bath.

The P2p ESCA spectra for as-plated a) LP, b) MP, and c) HP coatings at $90^0$ are presented in Figure 3. As with the nickel results (Figure 2), the phosphorus spectra also demonstrated differences in chemical composition as a function of the phosphorus content in the deposit. In this case, the spectra showed an increase in the $P/PO_4$ peak height ratio as the phosphorus content was incremented. This behavior was opposed to that demonstrated by the nickel spectra (Figure 2). Whereas the HP EN deposit was characterized to have the thickest oxide, the $P/PO_4$ ratio for this sample was significantly greater than that determined for the LP sample.

The ADESCA spectra shown in Figures 4 and 5 further supported the presence of a thin $Ni(OH)_2$ overlayer. The Ni2p spectra illustrated in Figure 4 demonstrated the classic behavior characteristic of a uniform overlayer. In other words, the oxide peak dominates the surface ($15^0$) spectrum, but as the sampling depth is increased (higher $\theta$), the peak due to nickel metal grows relative to the oxide peak. The explanation for the phosphorus ADESCA data was not as straightforward. In this case, the spectra did exhibit the expected behavior with the relative contribution of the free phosphorus peak increasing as the take off angle was incremented from $15^0$ to $90^0$. It was also evident from the spectra that the phosphorus concentration detected by ESCA was greater as the sampling depth was increased.

Atomic concentration values calculated from the ADESCA spectra provided a semi-quantitative depth profile of the surface composition. These values are listed in Tables 2 and 3. In addition, P/Ni ratios have also been tabulated to facilitate direct sample to sample comparisons. The figures in Table 2 represent the AC values obtained for as-plated LP, MP, and HP coatings at angles of $30^0$ and $90^0$. Table 3 includes a comprehensive AC data set for LP and HP coatings at angles of $15^0$, $30^0$, $45^0$, and $90^0$.

It was obvious from the data (Table 2), that the distribution of phosphorus within the surface region varied as a function of the bulk phosphorus concentration. In addition, the data further indicated a non-uniform distribution of phosphorus within each individual material. For example, Table 2 shows that the P/Ni ratios declined in the order LP > MP > HP at a take off angle of $30^0$, while at $90^0$ the opposite behavior was observed (i.e. LP < MP < HP). The ADESCA results presented in Table 3 show that the P/Ni ratio drops steadily as a function of take off angle for the LP coating. Conversely, the HP results showed an increase in the ratio as the sampling depth was expanded.

The combined results obtained for the as-plated EN coatings provided a comprehensive picture of the surface composition. The data clearly showed the existence of a thin oxide overlayer composed of predominantly $Ni(OH)_2$. It was further demonstrated that the thickness of this oxide layer varied as a function of the phosphorus content in the deposit. The LP material was determined to have the thinnest oxide and the HP material the thickest. In all cases, the thickness of the oxide was less than the sampling depth of the ESCA technique (20-100Å).

It was also apparent from this investigation that phosphorus was depleted in the oxide region. This conclusion was based on the observed behavior of the P/Ni ratios presented in Tables 2 and 3. The LP material was characterized to have the thinnest oxide, yet this same material exhibited the highest surface ($15^0$) P/Ni ratio. At the same time, the P/Ni ratio calculated for the $90^0$ data yielded the lowest value. These results suggested that the phosphorus was predominantly associated with the metallic nickel. The $PO_4^{-3}$ species detected was most likely located at the metal/oxide interface.

## Heat Treated EN Coatings

ESCA and AES data was obtained for LP and HP EN coatings before and after heat treatment. The Ni $2p_{3/2,1/2}$ data for a HP sample a) as-plated and b) after heat treatment is pictured in Figure 6. The heat treated material produced a spectrum that differed significantly from the as-plated coatings. Only one form of nickel was evident in this spectrum, which based on the peak position and peak shape was identified as NiO [15]. The fact that a nickel metal peak was not observed suggested that the oxide overlayer was thicker than the sampling depth of ESCA (~ 100Å). This was confirmed by AES sputter depth profiling. Similar results were also obtained for the heat treated LP material.

Figure 7 illustrates the corresponding P2p spectra obtained for the a) as-plated and b) heat treated HP sample. The P2p spectrum of the as-plated sample compared closely with the spectra previously presented in Figure 3. For the heat treated HP EN coating, the spectrum (Figure 7b) exhibited two peaks at a binding energy of approximately 139eV and 144eV. The measured binding energy positions of these peaks were too high to be representative of a phosphorus species. After careful consideration, it was concluded that this spectrum was characteristic of the $Pb4f_{7/2,5/2}$ spin orbit doublet. The source of lead was not definitely known, but lead ions are often used as stabilizers in EN plating baths [14]. The P2p spectra acquired for the LP sample were similar to those shown in Figure 7.

Auger sputter depth profiling was employed to determine the oxide thickness and phosphorus distribution of both the as-plated and heat treated coatings. The resultant profiles obtained for the HP EN sample a) as-plated and b) after heat treatment are presented in Figure 8. This data showed that the depth of the oxide layer was much greater for the heat treated coating than for the as-plated sample. In the profile for the as-plated sample, the oxygen level dropped to near 0 atomic percent within the first minute of sputtering which indicated that the oxide layer was less than 100Å. This agreed with the conclusions determined from the ADESCA data. The profile showed the phosphorus level increasing from ~10% to a steady state value of ~30% in the bulk. As a comparison, the results collected for the LP sample indicated an initial phosphorus concentration of ~12% and a steady state value near 18 atom percent. In both instances, the concentration values quoted were based on the standard Auger sensitivity values.

The corresponding sputter depth profile of the heat treated coating is shown in Figure 8b. Based on this data, the oxide thickness was estimated to be 150-200Å. The oxygen level remained equal to the nickel concentration of ~45% for the first 2-3 minutes of the profile. In this same region, no appreciable concentration of phosphorus was detected. At approximately 3.5 minutes, the oxygen level dropped sharply and the phosphorus level rose rapidly above 37% before declining to an equilibrium value of approximately 30%. This bulk phosphorus concentration compared closely with the results of the as-plated coating (Figure 8a).

These results clearly demonstrated that the heat treatment process significantly affects the surface chemistry and composition of EN coatings. The data showed that heat treatment produces a relatively thick NiO layer which was depleted of phosphorus. The oxide layer was estimated to be

150-200Å, relative to the as-plated samples which were found to have much thinner (20-100Å) oxides. The data further indicated that the growth of the oxide occurred through a diffusion process. This process formed the NiO layer, while the phosphorus remained in the "bulk". This growth process was suggested based on the enhanced phosphorus levels apparent in the profile at the oxide/metal interface.

## Corrosion Tested EN Coatings

The final segment of this investigation involved the characterization of the LP, MP, and HP EN coatings after 60 days of exposure to one of the industrial process environments listed in Table 1. The samples analyzed were the same materials used by Tracy [9] to measure corrosion rates. ESCA spectra were recorded for all of the samples listed (Table 1). At this point, only the preliminary results of the surface characterization study will be discussed. Data for EN coatings exposed to orthochlorobenzyl chloride (OCBC), benzotrichloride (BOC), phosphoric acid ($H_3PO_4$), and 73% caustic soda (NaOH/NaCl) will be presented. The results obtained for the corrosion tested samples were difficult to interpret due to the complexity of the test environments employed.

Table 4 lists typical ESCA AC results obtained for the EN coatings listed above. The results presented show that some corroaents had a significant effect on the surface composition of the EN coatings, while for other environments the surface composition was relatively unchanged. The changes in surface composition were most evident from the P/Ni ratios. The samples tested in an OCBC environment exhibited P/Ni ratios very similar to those measured for the as-plated materials. Materials exposed to $H_3PO_4$ and NaOH/NaCl environments showed a significant depletion in the surface phosphorus concentration.

Changes resulting from the corrosion testing were also evident in the high resolution Ni2p and P2p ESCA spectra recorded. Figures 9 and 10 illustrate several examples of the Ni2p spectra obtained for the tested EN coatings. Figure 9 includes the spectra acquired for HP coatings exposed to a)OCBC, b)BOC and c)$H_3PO_4$ environments. The spectrum of the sample tested in OCBC (Figure 9a) indicated the presence of nickel metal and $Ni(OH)_2$. This compared closely with the composition of the as-plated surface. Conversely, only $Ni(OH)_2$ was detected on the sample tested in $H_3PO_4$ suggesting the presence of an enhanced oxide overlayer.

The results recorded for the LP materials shown in Figure 10 appeared similar to the HP results (Figure 9). There were, however, some notable differences. For example, the spectrum of the OCBC exposed sample indicated the presence of a thicker oxide layer than that for the corrosion tested HP sample (Figure 9a). In comparison, the oxide layer was determined to be thinner for the LP coating as-plated. Differences were also observed for the EN coatings tested in $H_3PO_4$. Comparing the corrosion tested LP and HP materials suggested that oxide layer was greater for the HP coating.

The ESCA results collected for the corrosion tested samples implied that the surface composition of the as-plated coating has a direct affect on the corrosion properties of the EN surface. More importantly, the results indicate that the as-plated surface interacts differently for each type of corrodent tested. For some corrodents, the LP coating yielded the best results, while for other environments it was the HP or MP coatings that exhibited the superior corrosion protection.

## SUMMARY

The results of this investigation clearly demonstrated that the surface composition of EN deposits were dependent on the phosphorus content of the coating. This study involved EN deposits with three different phosphorus levels. For each of these coatings, the surface composition was shown to be similar in some respects and different in others. All three of the EN materials characterized were found to have a thin (<100Å) overlayer of $Ni(OH)_2$. The bulk species was nickel metal. Phosphorus was determined to be present in two forms; phosphate and free phosphorus. However, the distribution of these phosphorus species within the surface region was found to vary with the phosphorus content of the coating.

These differences were most readily apparent from the ADESCA results presented in Figures 4-5 and Tables 2-3. It was determined that the depth of the oxide ($Ni(OH)_2$) overlayer varied in the order LP < MP < HP. These results also suggested that phosphorus was depleted in the oxide layer. The $PO_4^{-3}$ species detected was most likely located at the metal/oxide interface. The free phosphorus was associated with the nickel metal in the bulk of the coating. These conclusions were based on the observed differences in the P/Ni ratios (Table 3). For the surface ($15^0$ and $30^0$) measurements, the P/Ni ratio was highest for LP and lowest for HP. At a take off angle of $90^0$, the P/Ni ratios fell in the expected order; HP > MP > LP.

Heat treatment was shown to produce a thick oxide on the EN surface. This oxide was identified as NiO and the thickness was estimated to be approximately 200Å. As with the oxide present on the as-plated samples, no phosphorus was detected in the oxide formed during the heat treatment process. Two types of EN, low phosphorus and high phosphorus, produced similar results with the exception of the bulk phosphorus level measured. The AES sputter depth profile results indicated that the oxide was formed by nickel diffusion, which resulted in a pile up of phosphorus at the metal/oxide interface.

The final segment of this investigation involved the surface characterization of LP, MP, and HP EN coatings in a series of industrial process environments. The results obtained for these materials indicated a strong correlation between the composition of the as-plated surface and the resultant corrosion protection of the coating. The interpretation of the data, however, was unclear due to the complexity of the chemicals used in the corrosion testing experiments. It seems evident that a more controlled set of corrosion experiments could provide a better understanding of the affect of surface composition on corrosion properties of EN materials.

**REFERENCES:**


1. J. Flis and D.J. Duquette, Corrosion, Vol. 41, No. 12, p. 700-706, Dec. 1985.

2. J.S. Armijo, Corrosion, Vol. 24, No. 1, p. 24, 1968.

3. A. Joshi, D.F. Stein, Corrosion, Vol. 28, No. 9, p. 321, 1972.

4. C.L. Briant, Corrosion, Vol. 36, No. 9, p. 497, 1980.

5. C.L. Briant, Corrosion, Vol. 38, No. 4, p. 230, 1982.

6. K. Hashimoto, T.J. Masumoto, Non-Cryst. Solids, Vol. 28, p. 403, 1978.

7. K. Hashimoto, Passivity of Metals and Semiconductors, M. Fremont, Ed., Elsevier, Amsterdam, p. 235, 1983.

8. P. Cadet, M. Keddam, H. Takenouti, 4th Int. Conf Rapidly Quenched Metals, Sendai, p. 1447, 1981.

9. R.P. Tracy, J.F. Colaruotolo, A. Misercola, B.R. Chuba, Materials Performance, p. 21-29, August 1986.

10. R.P. Tracy and B.R. Chuba, Corrosion 87, Paper No. 462, March 9-13, 1987.

11. C.J. Powell, Amer. Lab., Vol. 10, No. 4, p. 17, 1978.

12. D.M. Hercules and S.H. Hercules, J. Chem. Ed., Vol. 61, No. 6, p. 483, 1987.

13. C.J. Powell, Scanning Electron Microscopy, 1984 IV, p. 1649, 1984.

14. K. Parker, Plating and Surface Finishing, p. 60-65, February, 1987.

15. W.M. Riggs, L.E. Davis, J.F. Moulder, and G.E. Muilenberg (ed.), Handbook of X-ray Photoelectron Spectroscopy, Perkin Elmer Corp., MN, 1979.

16. N.S. M$^{c}$Intyre and M.G. Cook, Anal. Chem., Vol. 47, No. 13, p. 2208, 1975.

17. N.S. M$^{c}$Intyre, T.E. Rummy, M.G. Cook, and D. Owen, J. Electrchem. Soc., Vol 123, p. 1165, 1976.

18. T.A. Carlson, Photoelectron and Auger Spectroscopy, Plenum Press, New York, 1975.

# VS. OTHER COMMONLY USED MATERIAL IN CHEMICAL PROCESS ENVIRONMENTS

**All Corrosion Rate in μm/yr., 60 Days Exposure at 40°C ∓2°C**

| Corrodent* | Nickel 200 | EN Coatings: Low Phosphorus (1-2%) | EN Coatings: Medium Phosphorus (6-8%) | EN Coatings: High Phosphorus (10-12%) | Mild Steel | AISI 316 S. |
|---|---|---|---|---|---|---|
| Thionyl Chloride | 7.0 | 900.0 | 1.8 | 2.5 | 200.0 | 5. |
| Orthochlorobenzyl Chloride (Crude) | 12.7 | 3.8 | 7.4 | 7.1 | NA | 25. |
| Orthochlorobenzyl Chloride | 12.7 | 5.3 | 13.5 | 9.4 | NA | 25. |
| Phosphoric Acid | 10.0 | 900.0 | 193.0 | 19.3 | 1270.0 | 2. |
| 73% Caustic Soda** | 5.1 | 2.3 | 7.4 | F | 1448.0 | 332. |
| Phosphorus Oxychloride | 10.0 | 28.4 | 1.5 | 2.5 | 100.0 | 18. |
| Benzotrichloride | 5.1 | 2.5 | 5.6 | 6.1 | 9.0 | 5. |
| Benzoyl chloride | 5.1 | 1.0 | 0.8 | 0.5 | 8.6 | 5. |

*Corrodents used in this study were of final product grade except where noted

NA = No data available

** = 100 Day Exposure

F = Failed

TABLE 2

# ADESCA RESULTS FOR AS PLATED EN COATINGS

| | Ni | O | C | P | P/Ni |
|---|---|---|---|---|---|
| $\Theta = 30^\circ$ | | | | | |
| LP | 1.44 | 27.59 | 68.64 | 2.32 | 1.61 |
| MP | 1.92 | 23.89 | 71.79 | 2.40 | 1.25 |
| HP | 1.66 | 20.93 | 75.63 | 1.78 | 1.07 |
| $\Theta = 90^\circ$ | | | | | |
| LP | 5.92 | 37.01 | 53.23 | 3.84 | 0.65 |
| MP | 5.84 | 31.24 | 54.06 | 8.87 | 1.52 |
| HP | 4.06 | 29.26 | 59.65 | 7.03 | 1.73 |

TABLE 3

# ADESCA RESULTS FOR LP & HP EN COATINGS

| | Ni | O | C | P | P/Ni |
|---|---|---|---|---|---|
| **Low Phosphorus** | | | | | |
| 15° | 0.89 | 19.14 | 78.51 | 1.46 | 1.64 |
| 30° | 1.44 | 27.59 | 68.64 | 2.32 | 1.61 |
| 45° | 2.15 | 32.27 | 62.83 | 2.75 | 1.28 |
| 90° | 5.92 | 37.01 | 53.23 | 3.84 | 0.65 |
| **High Phosphorus** | | | | | |
| 15° | 0.96 | 15.07 | 83.13 | 0.83 | 0.86 |
| 30° | 1.66 | 20.93 | 75.63 | 1.78 | 1.07 |
| 45° | 2.25 | 25.39 | 68.99 | 3.37 | 1.50 |
| 90° | 4.06 | 29.26 | 59.65 | 7.03 | 1.73 |

TABLE 4

# ESCA RESULTS FOR CORROSION TESTED EN COATINGS

| Corrodent | | Ni | O | C | P | P/Ni |
|---|---|---|---|---|---|---|
| OCBC-F.P. | HP | 11.3 | 38.4 | 42.7 | 7.4 | 0.66 |
| | MP | 12.0 | 39.6 | 40.9 | 7.6 | 0.63 |
| | LP | 6.8 | 30.1 | 58.4 | 4.7 | 0.69 |
| OCBC-C | HP | 8.1 | 31.9 | 51.1 | 8.5 | 1.1 |
| | MP | 3.6 | 27.8 | 61.4 | 6.1 | 1.7 |
| | LP | 8.5 | 27.6 | 56.6 | 5.1 | 0.6 |
| $H_3PO_4$ | HP | 7.2 | 44.6 | 36.0 | 2.9 | 0.40 |
| | MP | 7.1 | 65.3 | – | 4.8 | 0.68 |
| | LP | 10.2 | 43.8 | 40.6 | 2.0 | 0.20 |
| NaOH/NaCl | HP | 3.4 | 23.3 | 70.8 | 0.8 | 0.24 |
| | MP | 4.0 | 26.6 | 64.9 | 0.4 | 0.10 |
| | LP | 4.8 | 29.7 | 62.0 | 0.9 | 0.19 |

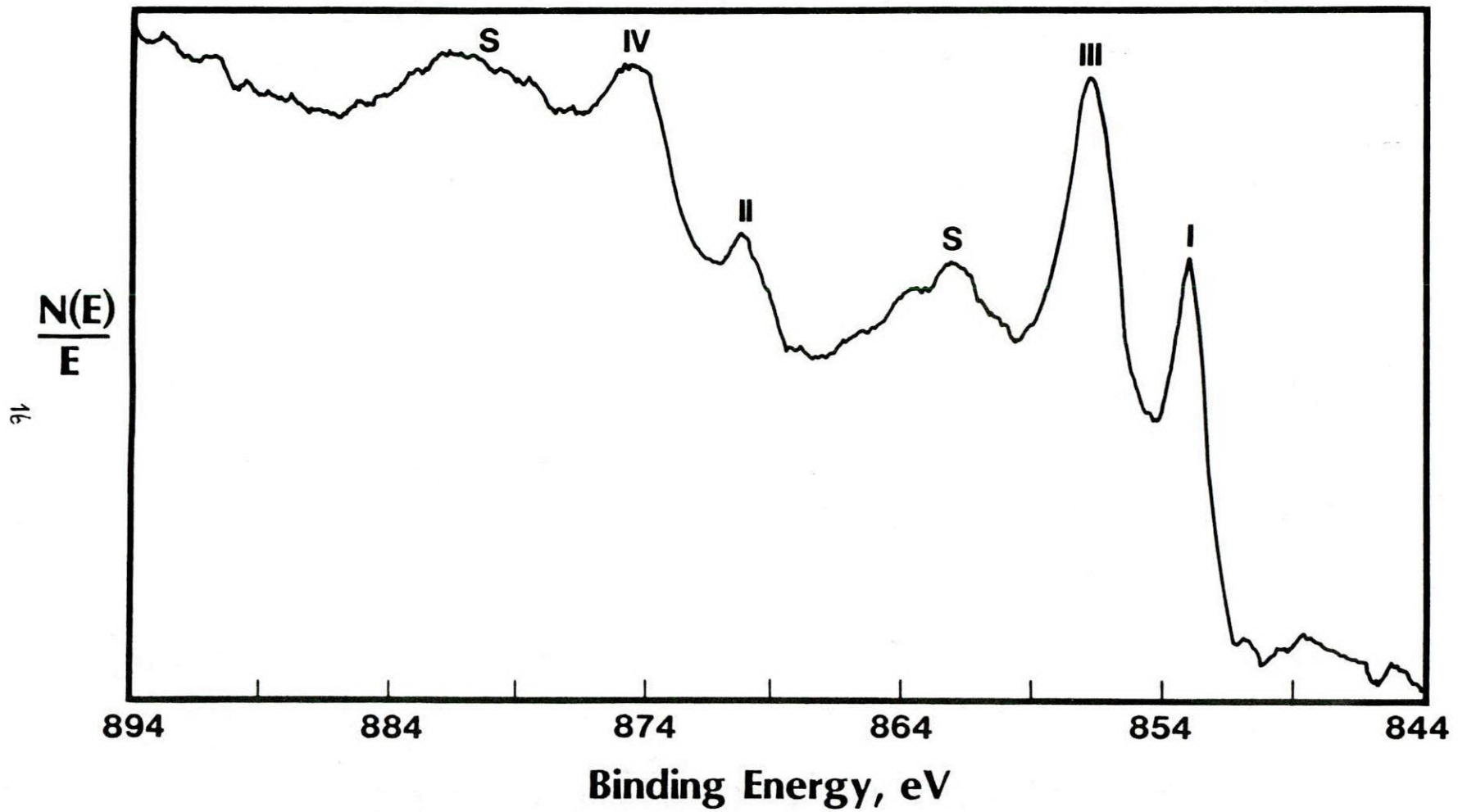


Figure 1. Representative Ni2p ESCA spectrum for the as-plated EN surface. The spectrum shown was obtained for a MP coating at a take off angle of 45°. The peak notations are explained in the text.

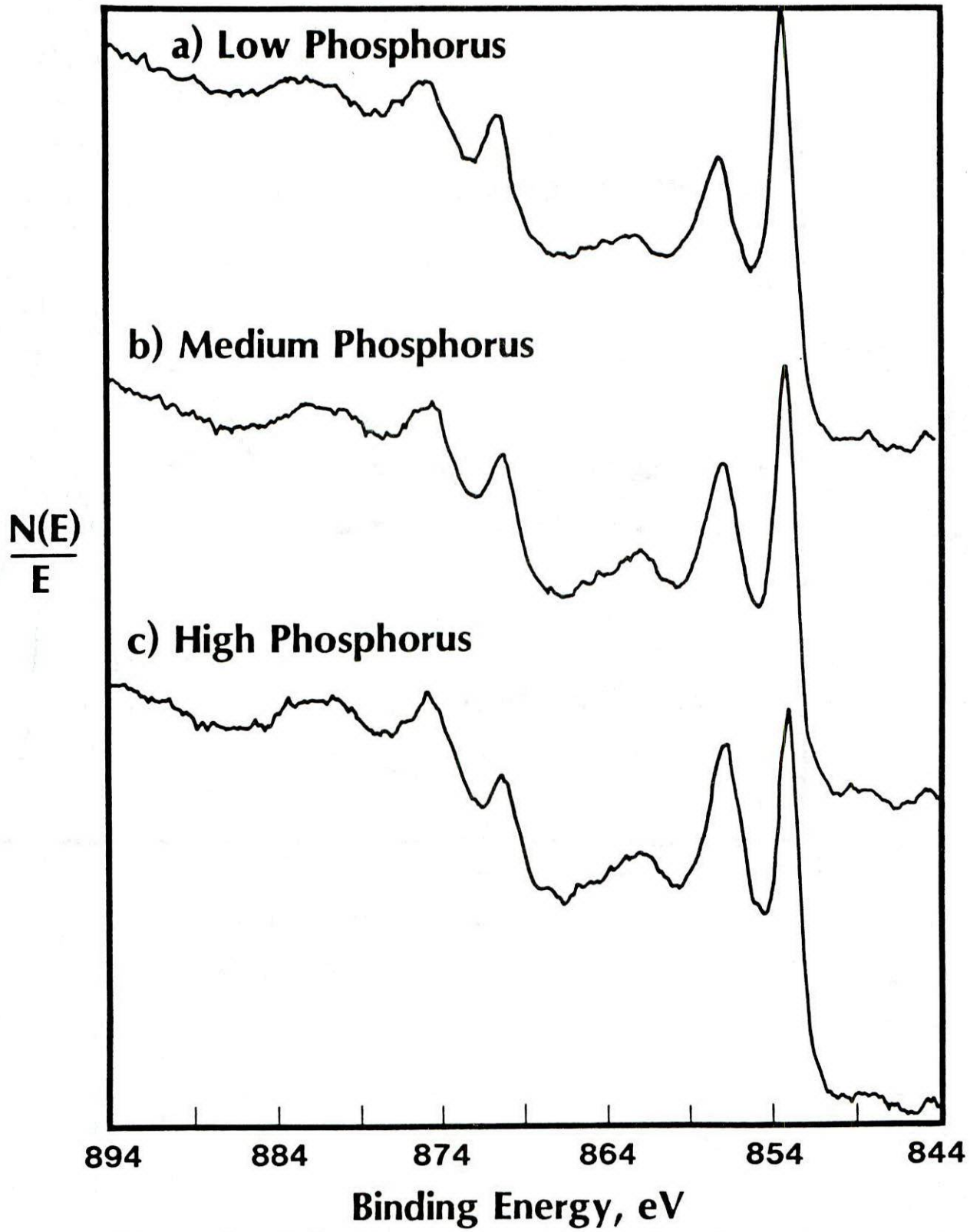


Figure 2. Ni2p ESCA spectra of as-plated a) LP b) MP and c) HP EN coatings at a 90° take off angle.

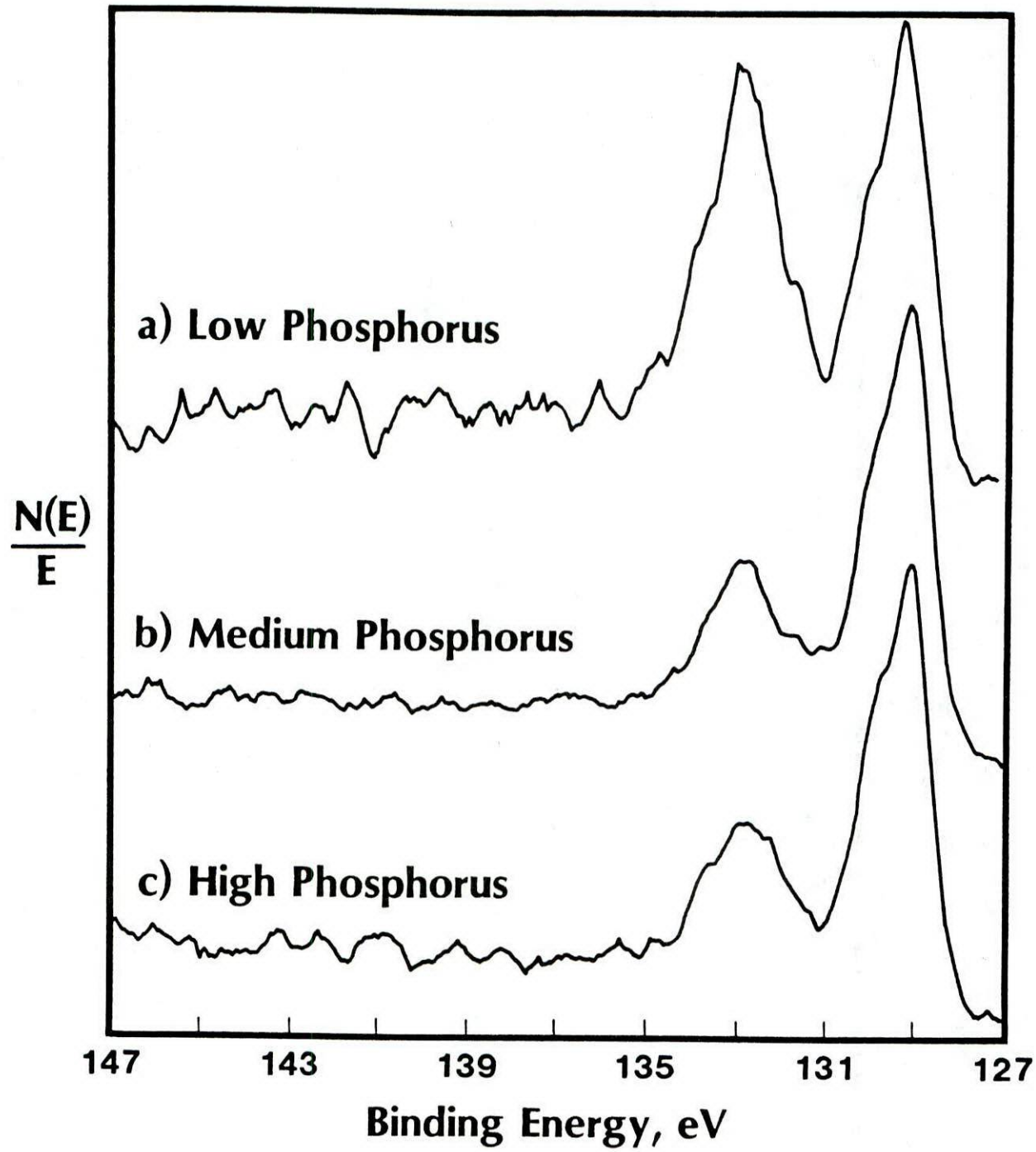


Figure 3. P2p ESCA spectra of as-plated a) LP b) MP and c) HP EN coatings at a 90° take off angle.

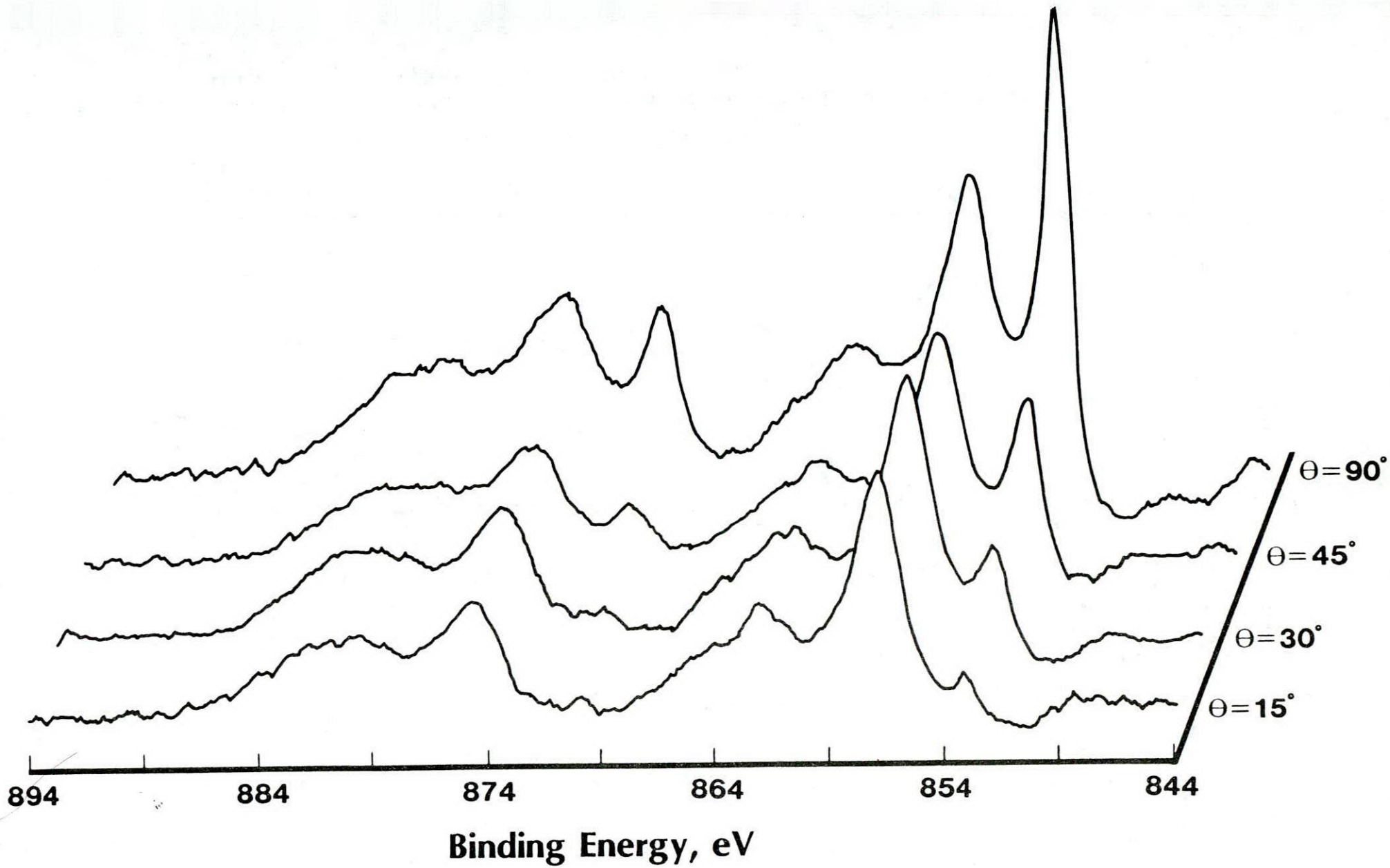


Figure 4. ADESCA Ni2p spectra collected for the as-plated MP EN coating. Spectra are shown at angles of 15°, 30°, 45° and 90°.

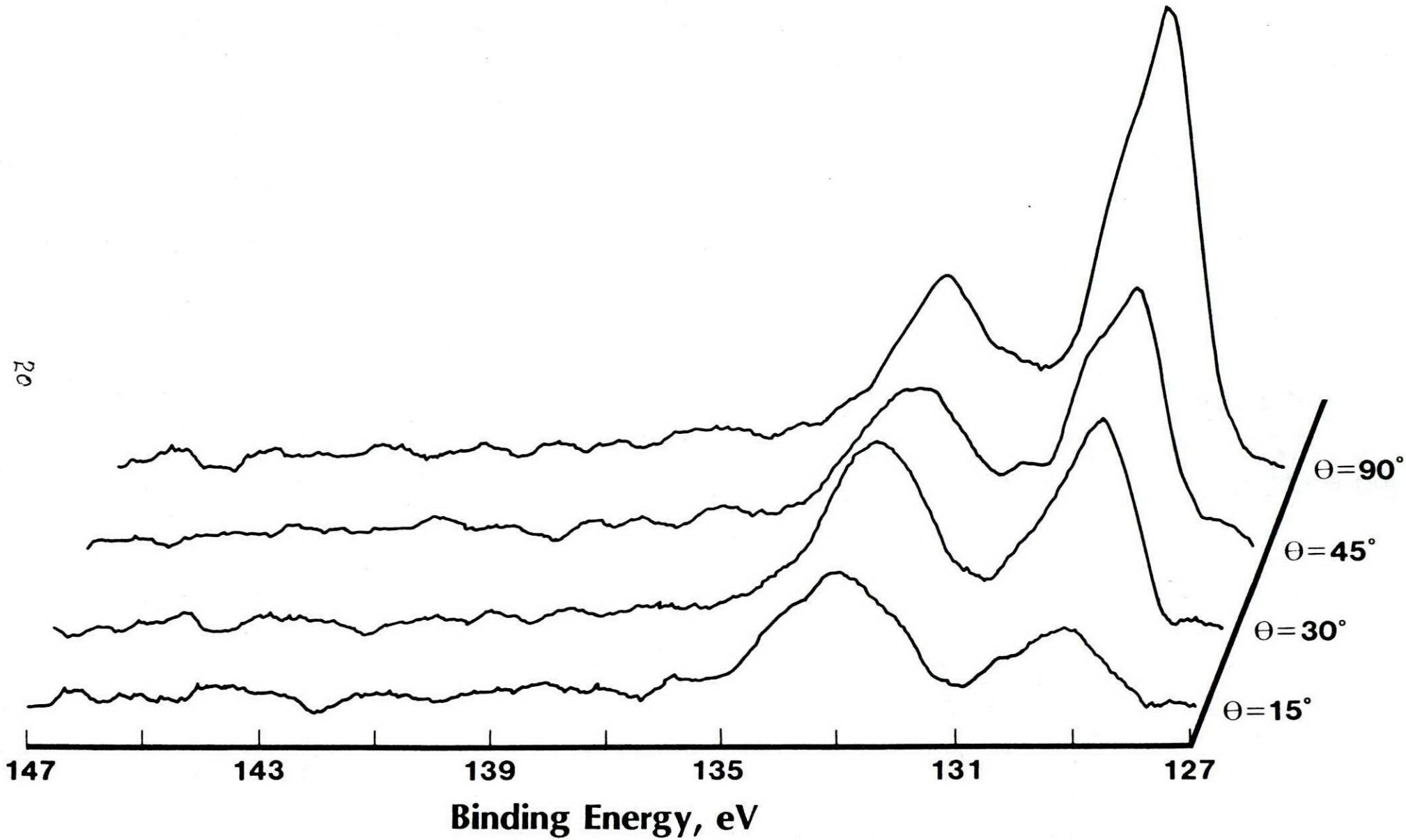


Figure 5. ADESCA P2p spectra for the as-plated MP material. Spectra are shown for take off angles of 15°, 30°, 45° and 90°.

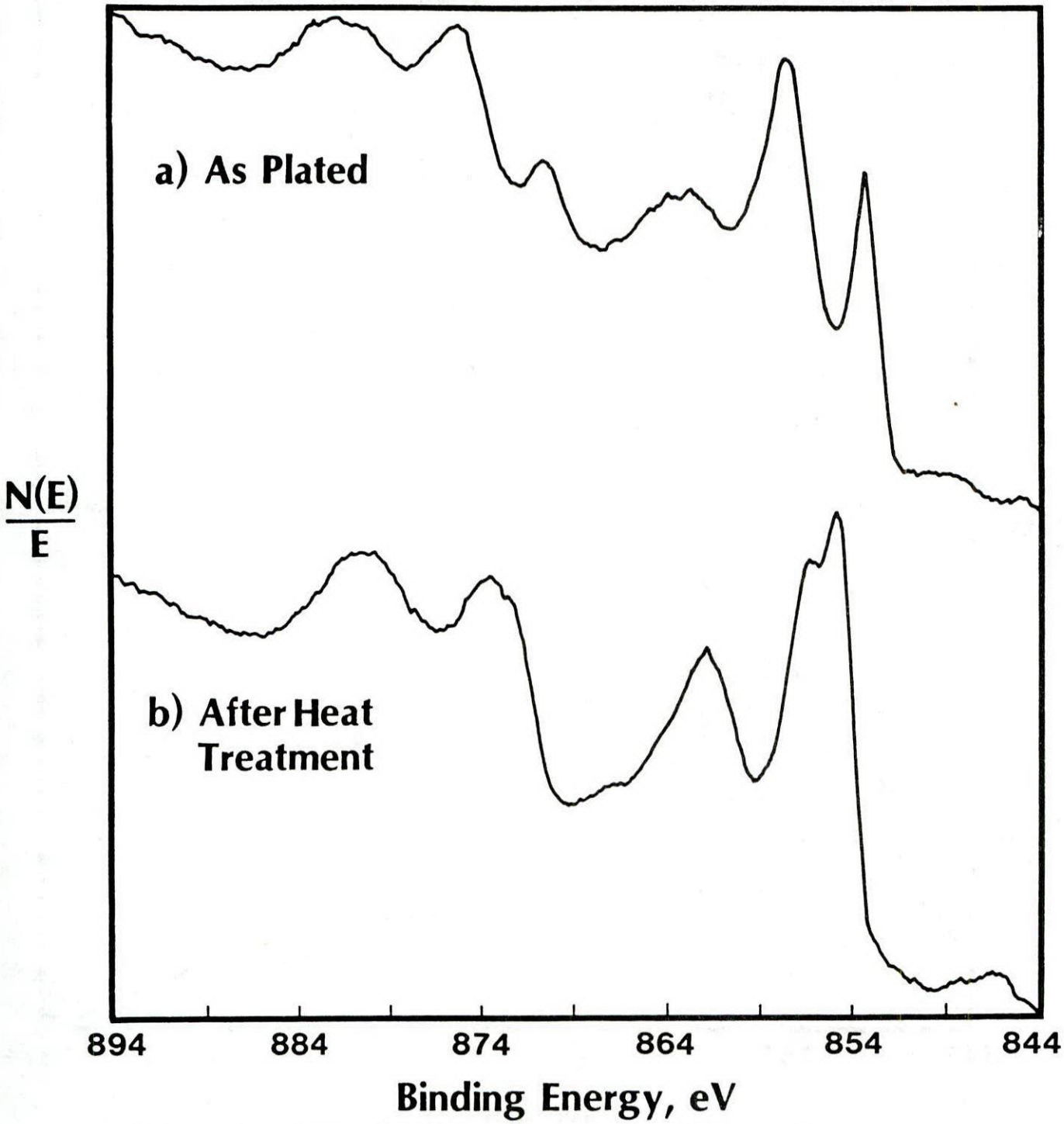


Figure 6. Ni2p ESCA spectra of a HP EN coating a) as-plated and b) after heat treatment.

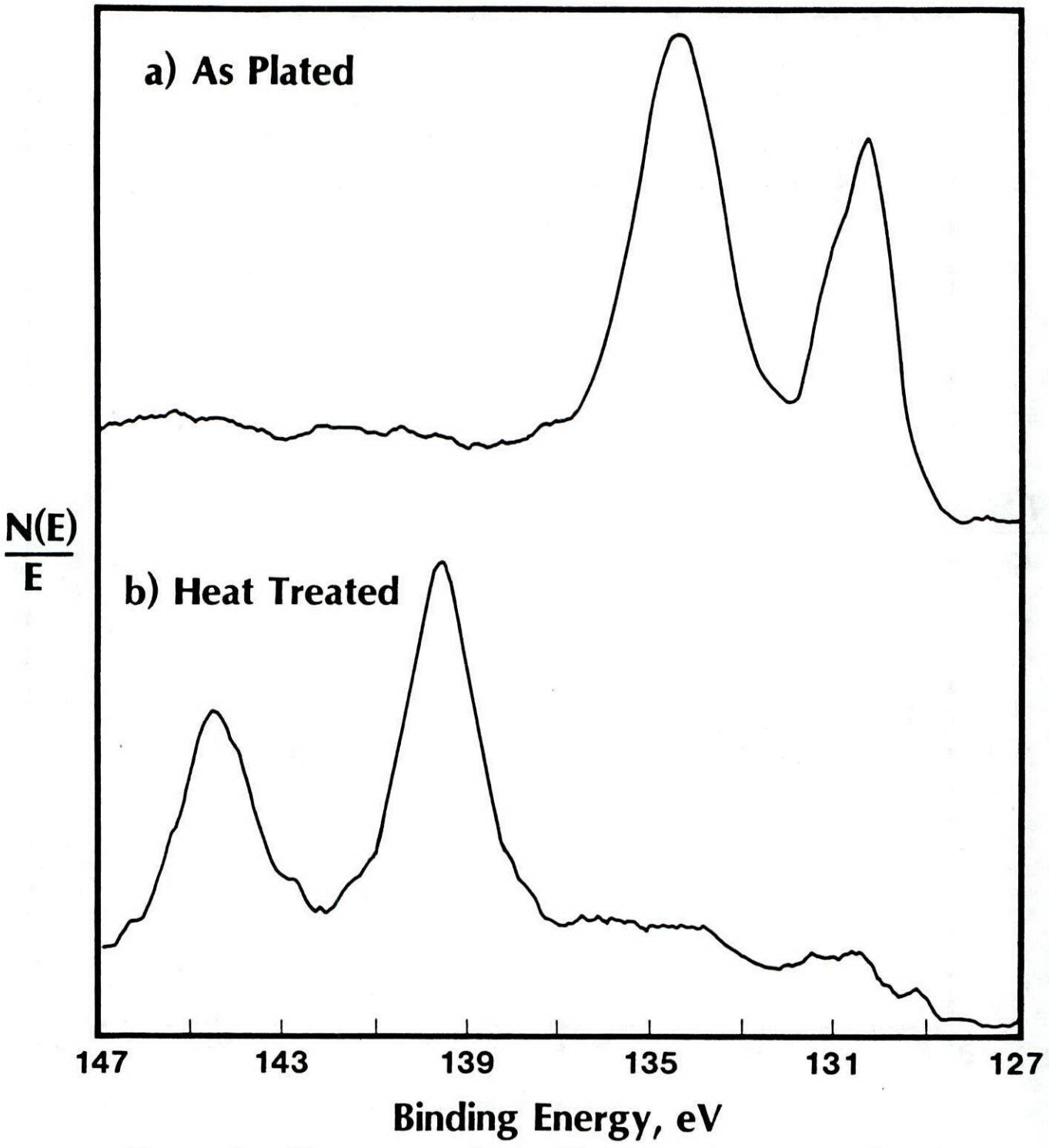


Figure 7. P2p spectra for a HP EN coating a) as-plated and b) after heat treatment.

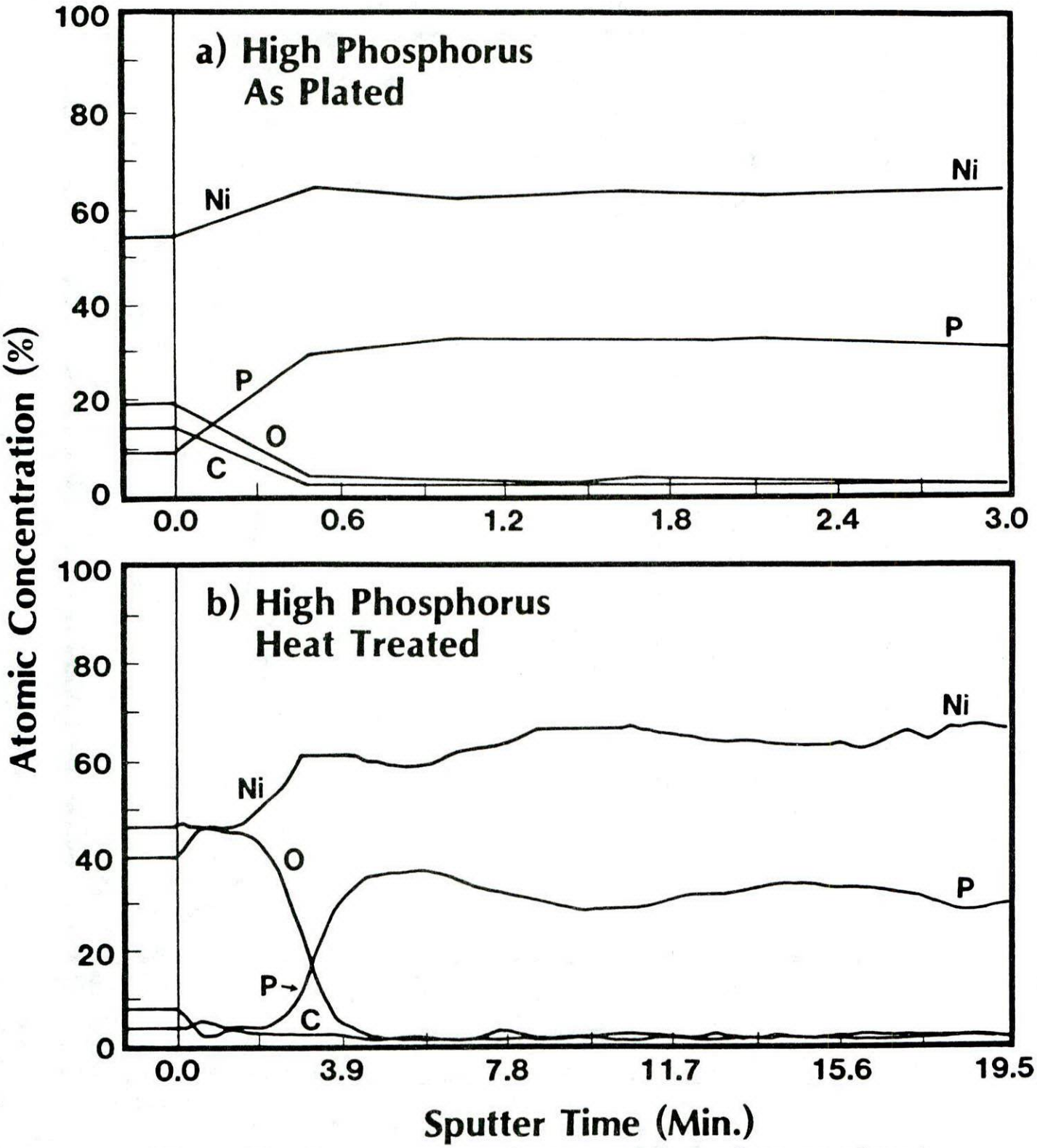


Figure 8. Auger sputter depth profiles of a) as-plated and b) heat treated HP EN. The sputter rate was 65A/min. measured relative to a $SiO_2$ standard.

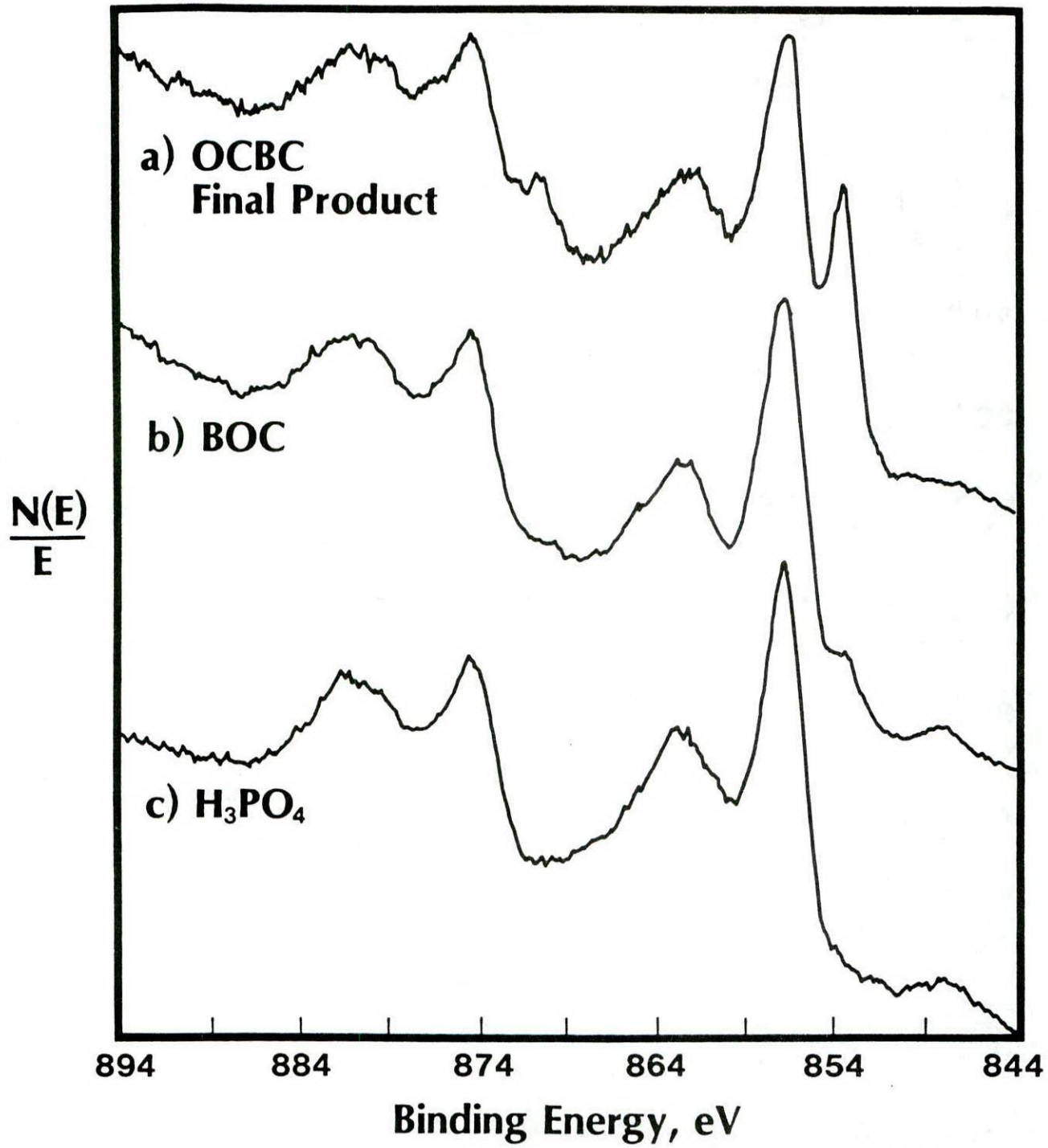


Figure 9. Examples of Ni2p ESCA spectra obtained for corrosion tested HP coatings. Spectrum a) was tested in OCBC, spectrum b) BOC and spectrum c) $H_3PO_4$. All of the data was collected at a take off angle of 45°.

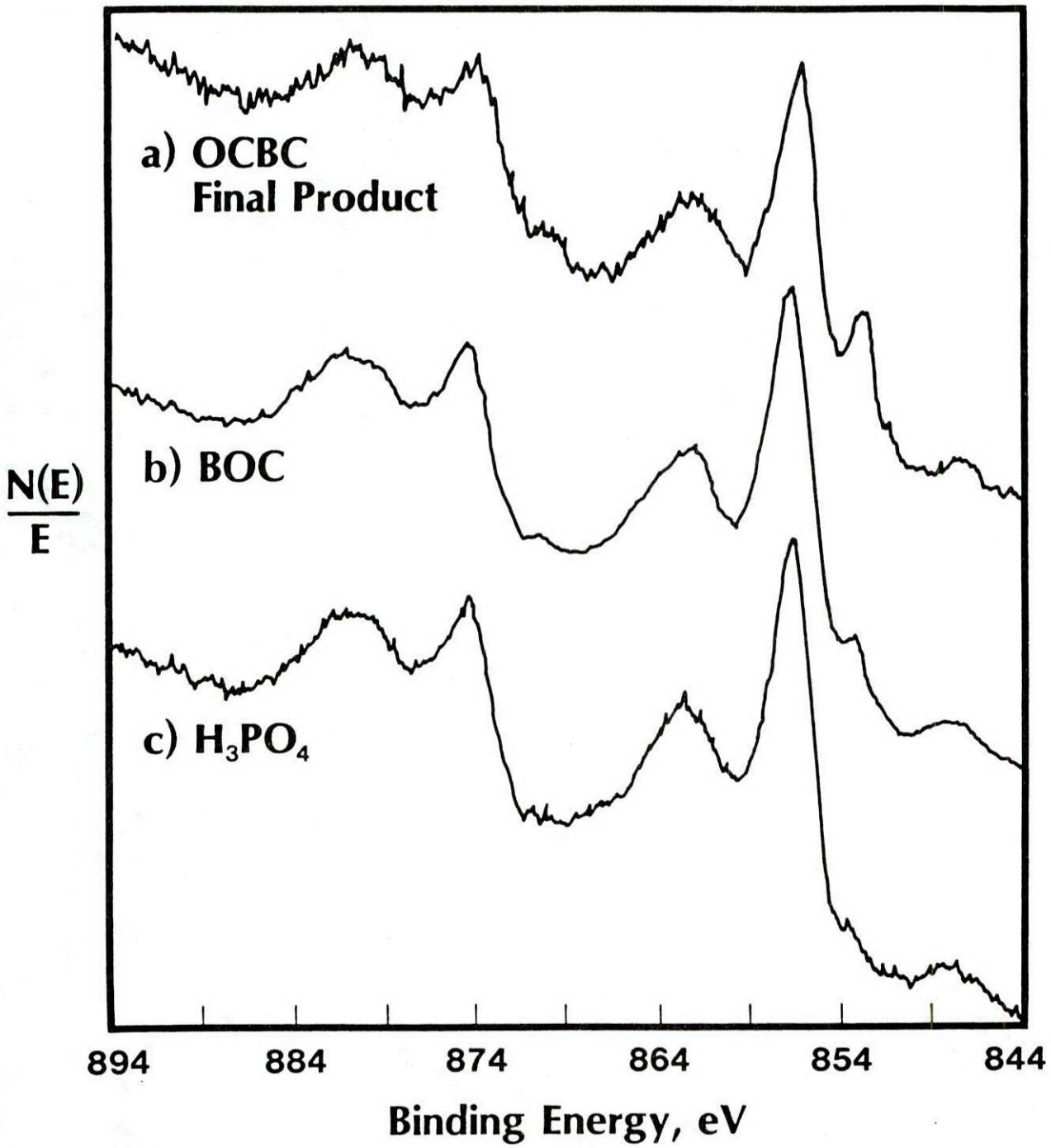


Figure 10. Typical Ni2p ESCA spectra obtained for corrosion tested LP coatings. The spectra represent coatings tested in a) OCBC b) BOC and c) $H_3PO_4$. All of the spectra shown were obtained at a 45° take off angle.

I-4

# Electroless Deposition I
# Session I

## Electric Properties of Electroless Copper Deposits

Kuniaki Ohtsuka
Okuno Chemical Industries Co., Ltd.
10-25 1-chome Hanatenhigashi, Tsurumiku
Osaka Japan

# Electric Properties of Electroless Copper Deposits

Kuniaki Ohtsuka
Okuno Chemical Industries Co., Ltd.
10-25 1-chome Hanatenhigashi Tsurumiku Osaka Japan

## 1. Introduction

Electroless copper plating is used in circuit preparation for printed wiring boards and plating for non-conductors such as plastics. Many research reports have been presented on plating bath compositions and deposit's physical properties.

Electroless copper plating has recently been applied to the preparation of high-frequency circuits, dielectric filters, etc., and is now drawing much attention.

With the increase in the quantity of information in parallel with the recent remarkable progress in the information field, electric waves and communication apparatuses have been subjected to high-frequency implementation, along with the further compactization of radiotelegraph apparatuses. Accordingly, the high-frequency filters required for such advancements also need to be compact in size and sophisticated in performance when associated with a high dielectric constant and other factors.

Such high-frequency filters have conventionally been prepared by thermally coating silver paste over dielectric ceramics with a high dielectric constant, thereby obtaining electodes.

We found that the characteristics of dielectric filters prepared by electroless copper plating are greatly affected by the bath composition, in particular by trace additives ratio. We conducted further investigations in relation to various physical properties of the deposits.

## 2. Experiments[1)2)]

### 2-1 Preparation of test pieces

#### 2-1-1 Barium titanate ceramics

For determining high-frequency characteristic values $\eta(\%)$ of dielectric filters, electroless copper plating to 20 μm thickness was carried out for barium titanate ceramics (Fig. 2) in accordance with the process shown in Fig. 1-(a).

#### 2-1-2 Stainless steel plates

For measuring mechanical characteristic of deposits obtained by electroless copper plating, electroless copper plating to 30 μm thickness was carried out using stainless steel plates (50 × 100 mm) in accordance with the process shown in Fig. 1-(b).

### 2-2 Plating baths and bath conditions

As shown in Table 1, various additives were added to the basic bath containing EDTA as a chelating agent, and the ex-

perimental baths thus obtained were used for plating experiments at 65°C.

2-3 Determination of high frequency characteristic values η(%)

Barium titanate after being subjected to 20 μm copper plating in accordance with the plating of Fig. 1-(a) was used as a band elimination filter for the high-frequency range. Frequency characteristics were measured, as shown in Fig. 3. This was followed by calculation of the value η(%) from equation (1).

$$\eta(\%) = \frac{Qu}{Qcu} \times 100 \quad \cdots\cdots\cdots\cdots\cdots\cdots \quad (1)$$

where Qu and Qcu are values representing filter fineness, Qcu being a theoretical value approximately expressed by equation (2) and Qu being calculated value by equation (3).

$$Qcu = 42 \sqrt{f_0} \times 1.8 \quad \cdots\cdots\cdots\cdots\cdots\cdots \quad (2)$$

$$Qu = 10^{\frac{L_0}{20}} \left(\frac{f_0}{f_2 - f_1}\right) \quad \cdots\cdots\cdots\cdots\cdots\cdots \quad (3)$$

where $f_0$ represents center frequency; $(f_2 - f_1)$ represents bandwidth at 3 dB; $L_0$ represents maximum attenuation quantity.

2-4 Determination of mechanical properties of deposits[3)]

Deposit film (30 μm) obtained by electroless copper plating in accordance with the plating process of Fig. 1-(b) was stripped and cut into pieces 1 cm in width and 5 cm in length. The breaking elongation and breaking tension of the test pieces were determined by means of a tensile tester (made by Shimadzu Corporation, Autograph SD-100-C).

2-5 Observation of crystal form of deposits

Using a scanning electron microscope (made by Hitachi Ltd., S-510), observations were made of the crystal form of deposits

2-6 Determination of film thickness

A copper plate 20 × 20 mm in size was plated simultaneously with each subject materrial and the film thickness was calculated by gravimetry.

3. Results and Discussion

3-1 Effects of additives on η value

Different η values were obtained depending upon type and concentration of trace additives. (Fig. 4 (a)∿(d))

When 2,2'-dipyridyl or sodium cyanide was added, η value decreased with the increase in additive concentration; value reached the maximum when 10 to 20 mg/l of 2,2'-dipyridyl was added.

The effects of various compounds used in combination with 10 mg/l of 2,2'-dipyridyl were next examined. As shown in Fig. 4-(c), the addition of thiodiglycolic acid raised η value to a high degree with the maximum being obtained at 5 mg/l concentration. When PEG #1540 (polyethylene oxide) was added, η value showed gradual decreases in proportion to the increased concentration. In the case of potassium nickel cyandide, its addition greatly reduced η values.

3-2 Effects of additives on deposition rate

When 2,2,'-dipyridyl or sodium cyanide was added, deposition rate decreased with the increase in additive concentration. In particular, 2,2'-dipyridyl had a great effect. (Fig. 5 (a) and (b))

The effects of various compounds when used in combination with 10 mg/l of 2,2,'-dipyridyl on deposition rate were then examined. As a result, PEG #1540 was found to have no considerable effect on deposition rate. However, in the case of addition of potassium nickel cyanide or thiodiglycolic acid, deposition rate showed noticeable decreases with the increase in additive concentration. In particular, when thiodiglycolic acid was added in a ratio of 30 mg/l or more, deposition rate decreased to almost zero. (Fig. 5 (c) and (d))

Comparing Fig. 5 with Fig. 4, it was conjectured that there is no correlation between deposition rate and high-frequency characteristic.

3-3 Effects of additives on mechanical properties of deposit film

When 2,2'-dipyridyl was added alone, the breaking elongation and breaking tension of deposit film both exhibited the maximum value at 20 mg/l concentration. When used in combination with 1 g/l ethylenediamine (EDA), however, breaking elongation increased while breaking tension decreased, with the increase in 2,2'-dipyridyl concentration. (Fig. 6 (a))

Fig. 6 (b), (c) and (d) present the results obtained in cases where various compounds were used in combination with 10 mg/l of 2,2'-dipyridyl. When potassium nickel cyanide or PEG #1540 was added, breaking elongation increased while breaking tension decreased, with the increase in additive concentration. When thiodiglycolic acid was added, breaking elongation and breaking tension both decreased with the increase in additive concentration.

Comparing Fig. 6 with Fig. 4, it was conjectured that there is no correlation between the mechanical properties of deposit film and the high-frequency characteristic of the obtained filter.

3-4 Relationship between additives and crystal form of deposits

When 2,2'-dipyridyl or sodium cyanide was added, deposit grain size tended to decrease with the increase in additive concentration. (Fig. 7 (a)∿(d))

EDA and thiodiglycolic acid both tended to reduce deposit grain size. In particular, EDA was noticeable in relation to such effect. (Fig. 7 (e) and (f))

Potassium nickel cyanide and PEG #1540 both tended to upgrade deposit grain size, and PEG #1540 also made deposit crystal form sharply angled. (Fig. 7 (g) and (h))

Comparing Fig. 7 with Fig. 4, it was conjectured that there is no correlation between the crystal form of deposits and the high-frequency characteristic of the obtained filter.

## 4. Conclusion

(1) In preparing barium titanate ceramic band elimination filters for high-frequency waves by electroless copper plating, filter characteristics are greatly affected by the trace additives in plating bath; it has become possible to obtain highly reliable dielectric filters by selecting a suitable bath composition.

(2) It was found that there is no correlation between the high-frequency characteristic of ceramic filters prepared by electroless copper plating and the mechanical properties or crystal form of the deposit film.

## Reference

1. L. G. Bhatgadde and S. Mahapatra, Metal Finishing, 85, 55

2. Donald W. Bardrand, Metal Finishing, 85, 115

3. S. Yamato and M. Tadakoshi, Metal Finishing, 85, 67

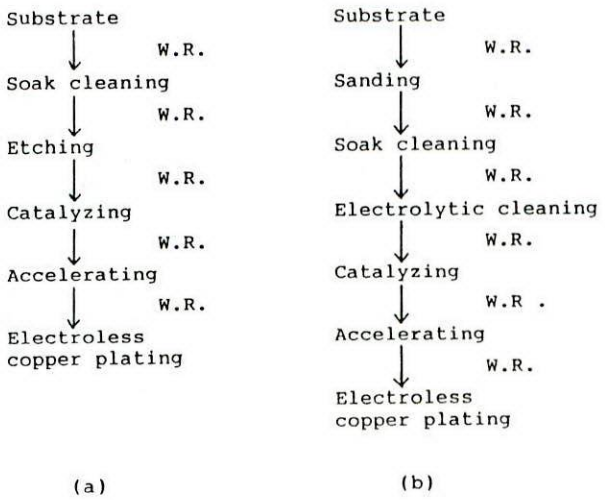


Fig. 1 Plating processes

(a) is the plating process for barium titanate ceramics and (b) is the plating process for the stainless steel.

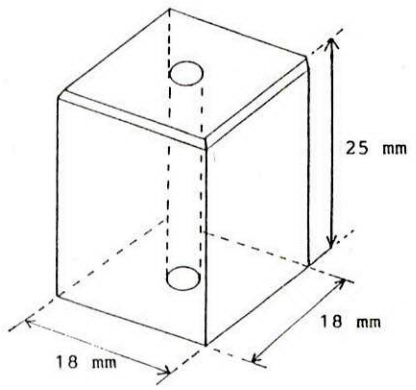


Fig. 2 Test piece

Barium titanate ceramics for measurements of the high frequency characteristic

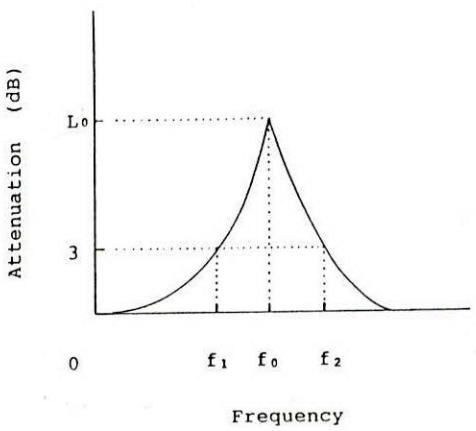


Fig. 3 A rough sketch of frequency characteristic curve.

| | | |
|---|---|---|
| The base of plating bath compositions | NaOH | 10 g/l |
| | $CuSO_4 \cdot 5H_2O$ | 10 g/l |
| | EDTA · 2Na · $2H_2O$ | 30 g/l |
| | HCHO | 4 g/l |
| Aditives | NaCN | 0 - 100 mg/l |
| | $K_2Ni(CN)_4$ | 0 - 100 mg/l |
| | 2,2'-dipyridyl | 0 - 100 mg/l |
| | Tiodiglycolic acid | 0 - 100 mg/l |
| | PEG #1540 | 0 - 3 g/l |
| | Ethylenediamine | 0 - 1 g/l |

Table 1. Plating bath compositions

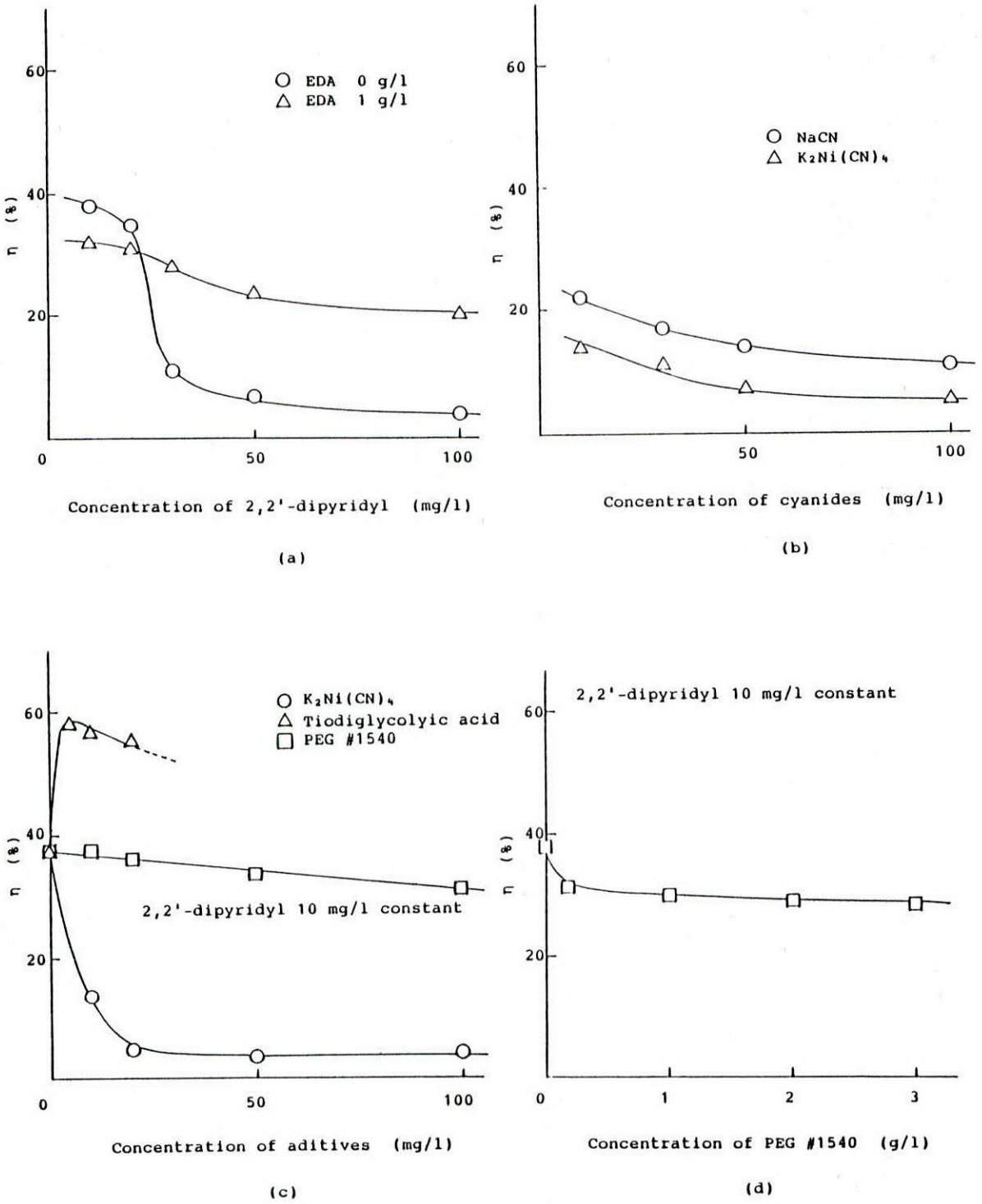


Fig. 4 The relation between the aditives and the high frequency characteristic.

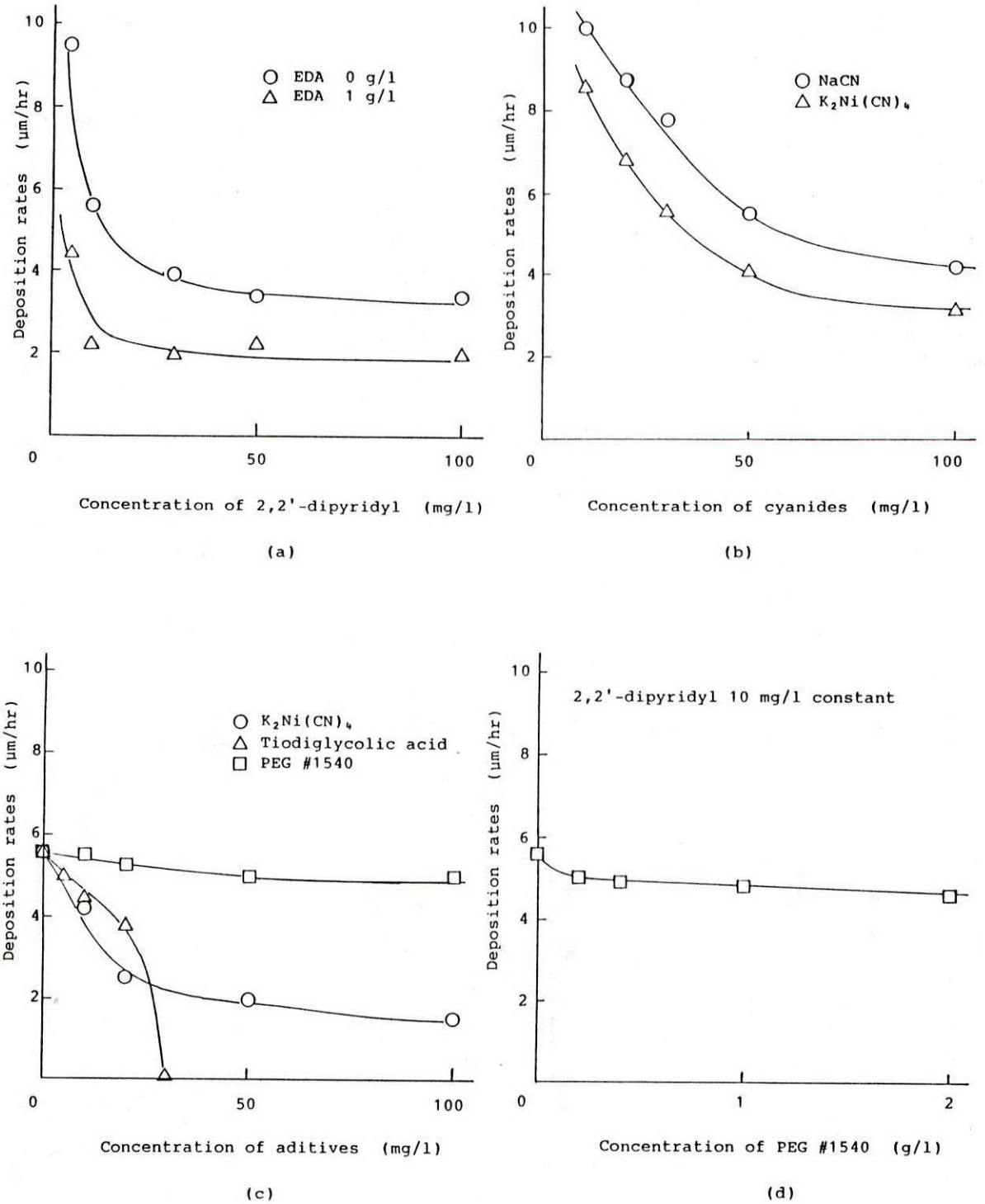


Fig. 5 The relation between the aditives and the deposition rates.

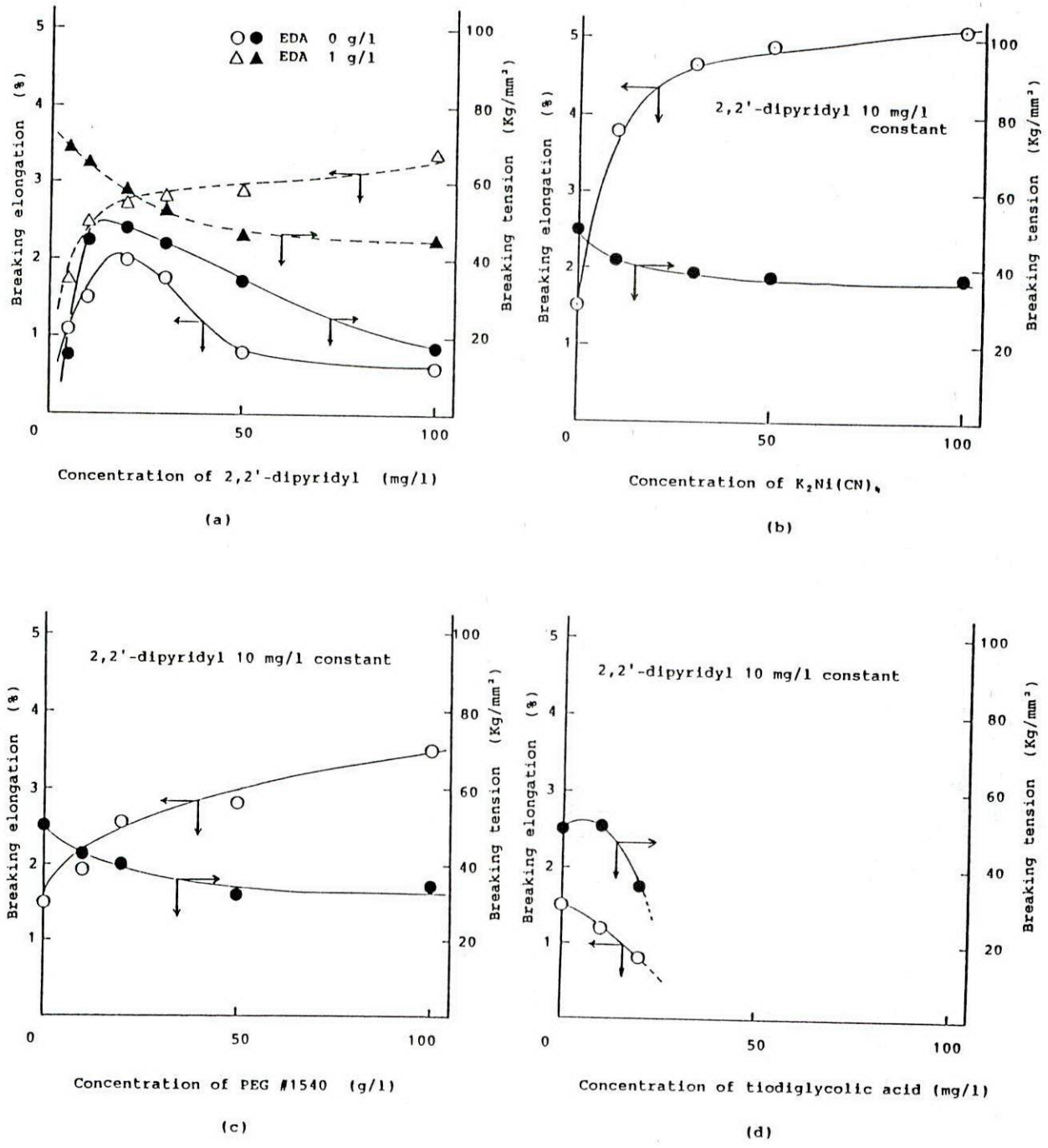


Fig. 6 The relation between the aditives and the mechanical property of deposits.

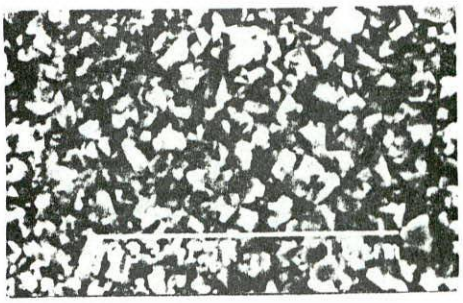

(a) 2,2'-dipyridyl 10 mg/l

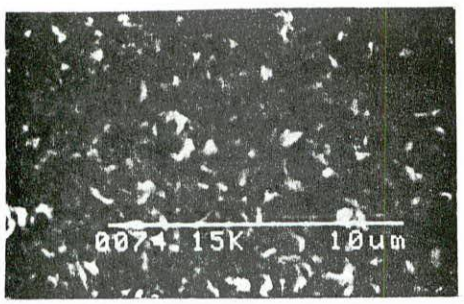


(b) 2,2'-dipyridyl 100 mg/l

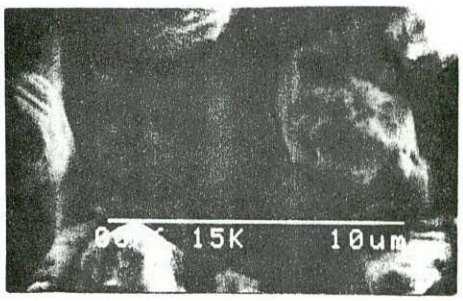


(c) NaCN 10 mg/l

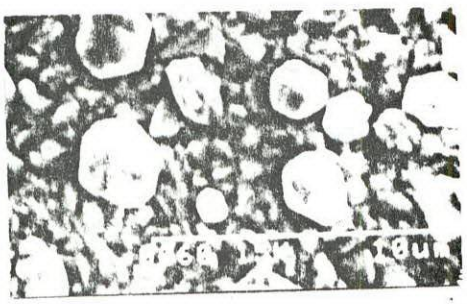

(d) NaCN 100 mg/l

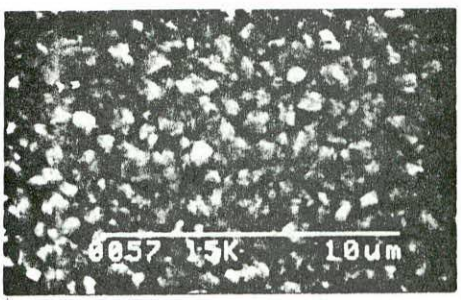


(e) 2,2'-dipyridyl 10 mg/l
Tiodiglycolic acid 5 mg/l

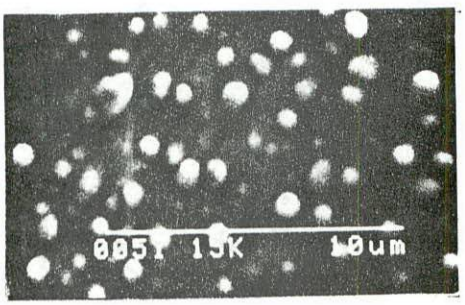


(f) 2,2'-dipyridyl 10 mg/l
EDA 1 g/l

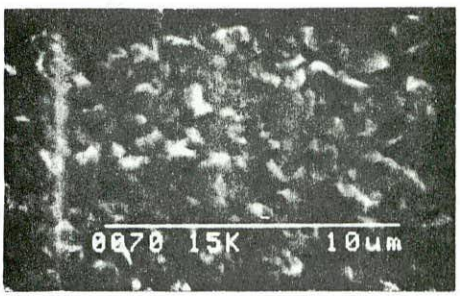


(g) 2,2'-dipyridyl 10 mg/l
$K_2Ni(CN)_4$ 10 mg/l

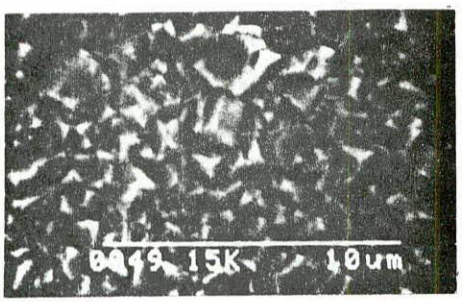


(h) 2,2'-dipyridyl 10 mg/l
PEG #1540 1 g/l

Fig. 7 The crystal form of deposits

I-5

# Electroless Deposition I
# Session I

## Some Physical Properties of Electroless Ni-P Alloy Deposited from Pyrophosphate Bath

Masao Matsuoka, Shinji Imanishi
and Tadao Hayashi
Department of Applied Chemistry
University of Osaka Prefecture
4-804 Mozu-Umemachi, Sakai
Osaka, 591, Japan

# Some Physical Properties of Electroless Ni-P Alloy Deposited from Pyrophosphate Bath

Masao Matsuoka, Shinji Imanishi, Tadao Hayashi

Department of Applied Chemistry, University of Osaka Prefecture
4-804 Mozu-Umemachi, Sakai, Osaka, 591, Japan

## Abstract

Some physical properties of the Ni-P alloys prepared from an ammoniacal pyrophosphate bath were examined as a function of P content. The higher P content gave rise to the lower internal stress of Ni-P alloys. The resistivity of Ni-P deposits was found to decrease with decreasing the P content and also by the heat-treatment. The precipitation of $Ni_3P$ induced by the heating remarkably increased the hardness of Ni-P alloys. Changes in physical properties attributable to the alteration of P content and heating were discussed in view of the crystallographic feature of Ni-P alloys.

## 1. Introduction

It is well known that Ni-P alloys with higher phosphorus content are deposited from acid electroless nickel bath by using hypophosphite as a reducing agent. In particular, the Ni-P alloys of which phosphorus content is greater than 10 wt.% show the characteristic properties due to the amorphous structure, i.e., the high performance of corrosion resistance and hardness. As the amorphous Ni-P alloys have non-magnetic properties, they could be applied to the undercoating of aluminum substrates for the fabrication of magnetic memory disks, in addition to the usage of corrosion and wear resistant coatings[1]. However, the higher deposition rate suitable for the practical use could not be obtained unless operating temperature was greater than 90°C. Therefore, the use of acid electroless nickel plating bath seemed to be somewhat restricted. On the other hand, an ammoniacal electroless nickel bath was generally operated at fairly low temperature and used for the metallization of plastic substrates. The physicochemical properties of the Ni-P alloys deposited from an alkaline bath do not seem to be fully elucidated. Therefore, an ammoniacal pyrophosphate bath that could be operated at 50 to 70°C was employed for the further study and the physical properties of the Ni-P deposits, such as internal stress, hardness and resistivity were examined as a function of phosphorus content of the deposits.

## 2. Experimental

### 2.1 Deposition Rate of Ni-P Alloys and Phosphorus Content

The bath composition and operating conditions for the electroless nickel plating are shown in Table 1. Platinum strips (10 $cm^2$ ) used as the substrates were electrodegreased and activated by the solution of $PdCl_2$. The platinum substrates were immersed in the electroless nickel bath with a volume of

250 ml for 30 min, and then the deposition rate of Ni-P alloys was estimated by the weight gain during the plating. The phosphorus content was determined by dissolving a known amount of Ni-P alloys in a solution of 1 M $HNO_3$. Phosphorus was completely oxidized to orthophosphate by the use of potassium permanganate. An adequate amount of ammonium vanadate and ammonium molybdate were added as color indicator and then absorbance of the solution was measured at 460 nm[2].

2.2 Heat-treatment and X-ray Diffraction

Heating of the sample was carried out in vacuum ($5 \times 10^{-4}$) at 400 °C for 1 h. The hardness and crystallographic structure of Ni-P alloys were examined before and after the heat-treatment. CuKα radiation (45kV, 50mA) was used for the X-ray diffraction analysis. The Ni-P alloys deposited on copper substrates with a thickness of 20 μm were tested. Apparent crystallite size of the deposits was estimated by Scherrer's equation ($0.89\ \lambda\ /\ \beta_{\frac{1}{2}} \cos\theta$)[3]. In the case of heat-treated sample, the amount of nickel phosphide was qualitatively evaluated by the intensity of the diffraction line due to $Ni_3P$.

2.3 Physical Properties of Ni-P Alloys

Copper strips (9 x 1 cm) from which strain was eliminated by annealing in vacuum were employed for the measurement of internal stress of Ni-P alloys. One side of the copper strips was covered with thin scotch tape, and then electroless Ni-P alloys were plated on the other side of the substrate until thickness reached to 10 μm. The bowing caused by the internal stress of the deposits was measured by using a micrometer. The values of the stress were calculated by the following equation[4].

$$S = 4\ E\ d^2 Z / (3\ t\ L^2) \quad \text{--- (1)}$$

where, E is Young's modulus of copper substrates, d thickness of substrates, Z bowing created by the stress, t thickness of Ni-P alloys, and L length of substrates.

The hardness of the Ni-P alloys was measured for the sample with a thickness of 20 μm by using a Shimazu micro vickers hardness tester with a load of 50 g.

The resistivity of Ni-P alloys was determined with a portable double-bride device at room temperature. The Ni-P alloys with a thickness of 2 μm were plated on a cylindrical ceramic substrate which was received by the following conventional pre-treatment: degreasing in an alkaline solution - etching (dichromic acid/sulfuric acid) - sensitizing ($SnCl_2$) - activation ($PdCl_2$).

3. Results and Discussion

3.1 Plating Rate and P Content as a Function of pH or Temperature

As can be seen in Fig.1, the deposition rate of nickel strongly increased when bath pH was increased from 10 to 12, but the deposition rate of phosphorus was independent of bath pH. The phosphorus content, therefore, decreased from 7.3 wt.% to 3.0 wt.%. These results indicate that the reduction of nickel is

much more favorable than the co-deposition of phosphorus under the conditions of high pH. The same tendency has already been reported for the acid electroless nickel plating[5].

The deposition rate of nickel and phosphorus increased exponentially with an increase in operating temperature as shown in Fig.2. The apparent activation energy calculated from the temperature dependence of the deposition rate of nickel and phosphorus was found to be 7 kcal/mole in each case. The phosphorus content of Ni-P alloys was, therefore, independent of bath temperature within the range between 50 °C and 70 °C. The apparent activation energy evaluated from the Schartz's data reported for an ammoniacal pyrophosphate bath was 10 kcal/mole[6]. In general, the value of the activation energy for the deposition of Ni-P alloys was fairly smaller in ammoniacal electroless nickel bath than that in acid bath (17.7 kcal/mole). This fact seemed to be one of the reason that the higher deposition rate could be expected in the case of ammoniacal electroless nickel bath[7]. As described above, if the activation energy for the deposition of nickel and phosphorus was identical, the phosphorus content is independent on temperature. However, it has been found that the temperature dependence of phosphorus content was quite different with bath pH employed[8]. It should be noticed that the activation energy for the deposition of nickel and phosphorus was influenced by the plating conditions. The effect of some additives on the deposition rate of phosphorus has been examined by Feldstein[9]. Through the study, a new mechanism for the deposition of phosphorus via $PO_2^-$ has been proposed instead of one electron reduction from hypophosphite, because the slope of the line obtained by plotting the logarithmic value of the deposition rate of phosphorus against the mixed potential indicated the reduction via 3 electrons. However, this postulation is not yet generally accepted.

3.2 Crystallographic Structure of Ni-P Alloys

Typical X-ray diffraction lines of the Ni-P alloys with a composition of 7.3 wt.% P is shown in Fig.3. As-plated Ni-P alloys gave a diffused line at the angle corresponding to Ni(111). It has been confirmed that the broadness increases by an increase in phosphorus content. The apparent crystallite size evaluated from the half-width of the diffraction line by using Scherrer's equation decreased from 119 Å to 14 Å, when phosphorus content increased from 3.0 to 7.3 wt.%. On the other hand, the heating of the Ni-P alloys resulted in produced the re-crystallization of nickel as well as the formation of $Ni_3P$. It has been confirmed that the intensity of diffraction lines corresponding to $Ni_3P$ increase with increasing the phosphorus content. The crystallographic structure of Ni-P alloys was remarkably influenced by the phosphorus content of the deposits. The broadness of the diffraction line as recognized in the case of as-plated Ni-P alloys was due partly to micro-crystalline structure and partly to the amorphous structure of the deposits. On this point, it has been disclosed by Cargill[10] that Ni-P

alloys became complete amorphous structure in the case of the electrodeposited Ni-P alloys. The contribution of amorphous structure seemed to become dominant when the phosphorus content of the electroless Ni-P alloy increased. The amorphous structure was not stable at 400 °C. Therefore, the heating of the Ni-P alloy deposits yielded the re-crystallization of nickel with the formation of nickel phosphide. Changes in crystallographic structure owing to the heating and also changes in phosphorus content of the Ni-P alloy deposits remarkably influenced the properties of the deposits as will be discussed in the following section.

3.3 Internal Stress of Ni-P Alloys

In general, the internal stress of the Ni-P alloys was characterized by the tensile or compressive nature. All the internal stress observed in this study was found to be tensile stress. The high tensile stress of electroless Ni-P alloys deposited from a pyrophosphate bath was pointed out by Parker[8]. In addition, it has been found by Bartlett [11] that the internal stress of Ni-P alloys was reduced by saccharin and ferrous ammonium sulfate in the plating bath[4]. However, the relationship between internal stress and phosphorus content was not yet established. Changes in internal stress of Ni-P alloys was examined as a function of phosphorus content of the deposits. The values of internal stress of Ni-P alloys deposited from the pyrophosphate bath with different pH and temperature are shown in Fig.4. The internal stress of the Ni-P alloy (7.3 wt.%P) deposited from a bath with pH 10 was found to be 13.5 $kg/mm^2$ . The internal stress of the Ni-P alloy deposited from a bath with pH 11 increased to 44.7 $kg/mm^2$, however, the phosphorus content of the deposits decreased to 3.3 wt.% under these conditions. Further increase in bath pH did not yield any appreciable change in the internal stress of the deposits. On the other hand, the internal stress of Ni-P alloys was independent on bath temperature between 50 °C and 70 °C. Changes in phosphorus content of Ni-P alloys was found to be insignificant, therefore, the internal stress of Ni-P alloys took an almost constant value (44.3-47.1 $kg/mm^2$). The phosphorus content and internal stress of Ni-P alloys were remarkably influenced by bath pH, but they were not affected by operating temperature. The values of internal stress of Ni-P alloys are shown in Fig.5 as a function of phosphorus content. It is evident that the internal stress of Ni-P alloys decreased with an increase in phosphorus content of the deposits. The correlation coefficient of the data shown in Fig.5 was found to be 0.89. This result was comparable to the Parker's results obtained from acid electroless nickel bath[11]. Such a change in internal stress of Ni-P alloys was mainly due to the changes in crystarographic structure caused by alteration of phosphorus content. According to Weil[12], one of the origins for causing internal stress was impurity incorporated into the grain boundaries of the deposits. However, a number of grain boundaries attributable to the stress inducing source might be

reduced by the amorphous structure of the deposits with an increase of phosphorus content. Sugita[13] pointed out that nickel phosphite was co-deposited into Ni-P alloys as an impurity under the conditions of low pH and high hypophosphite concentration. Under these conditions, the crystallinity of the deposits decreased. Since the effect of impurity might be neglected under the conditions tested in this study, the excellent correlation between internal stress and phosphorus content was established.

3.4 Hardness and Resistivity of Ni-P Alloys

The hardness of Ni-P alloys before and after the heat-treatment is shown in Fig.6 as a function of phosphorus content. The hardness of as-plated Ni-P alloys was fairly greater than that of electrodeposited nickel. The hardness was found to be 650-685 Hv, and its value slightly increased by an increase in phosphorus content. The hardness of Ni-P alloys increased to 1000-1170 Hv by the heating at 400°C, since the phosphorus existing as supersaturated solid solution in nickel matrix crystallized to $Ni_3P$. The main reason for improvement of the hardness was confirmed to be deposition hardening due to $Ni_3P$ precipitation. It has been confirmed that the harder deposits could be obtained, the higher the phosphorus content of Ni-P alloys.

The high performance of Ni-P alloys as a resistor was also well known[14]. The changes in resistivity of Ni-P alloy before and after the heating are shown in Fig.7. The resistivity of as-plated Ni-P alloys increased from 60 to 110 μΩ cm by increasing the phosphorus content. The free mean path of conducting electron decreased by increasing phosphorus content of Ni-P alloys. Therefore, the resistivity was much greater than that of pure nickel (7.24 μΩ cm). In the case of amorphous alloy, the value of resistivity was found to be 50-350 μΩcm, which is greater than that of crystalline state by a factor of 10 to 100. In addition, the temperature coefficient of resistivity (TCR) took a very small value[15]. However, the values of the resistivity of Ni-P alloys decreased by a factor of 2 to 3 by the heating, since re-crystallization of nickel and formation of $Ni_3P$ might occur under these conditions.

3.5 Crystallite Size and Physical Properties of the Ni-P Alloys

The physical properties of the Ni-P alloys were influenced by the alteration of crystarographic feature induced by heating and also by changes in phosphorus content of the deposits. The apparent crystallite size calculated from equation (1) was taken as a measure of structural change. The resistivity and also internal stress of Ni-P alloys were plotted against apparent crystallite size, as shown in Fig.8. The internal stress was almost constant (40 $kg/mm^2$) when crystallite size was greater than 60 Å. However, the small value of internal stress was obtained at crystallite sizes less than 60 Å. The resistivity of Ni-P alloys measured before and after the heat-treatment decreased exponentially with increasing crystallite size of the Ni-P alloys. These results can be explained by the disorder of

nickel atom due to the codeposition of phosphorus inducing the reduction of mean free path of conducting electron.

## 4. Conclusions

Physical properties of Ni-P alloys prepared from ammoniacal pyrophosphate bath have been discussed as a function of bath pH and operating temperature.

1) The deposition rate of nickel increased with increasing bath pH, but the deposition rate of phosphorus was independent of pH. As the result, the phosphorus content decreased significantly with increasing bath pH.

2) The deposition rate of both nickel and phosphorus increased exponentially with increasing operating temperature. The activation energy for the deposition of both nickel and phosphorus was found to be identical. Therefore, the phosphorus content was not influenced by operating temperature.

3) The internal stress of Ni-P alloys shows tensile nature, and its value decreased with an increase in phosphorus content.

4) The hardness of as-plated Ni-P alloys was found to be 650-685 Hv. However, the heat-treatment of the deposits increased the hardness to 1000-1200 Hv due to the deposition hardening.

5) The resistivity of as-plated Ni-P alloys was found to be 60-110 $\mu\Omega$ cm. The smaller crystallite size of the deposits gave rise to the greater resistivity. The re-crystallization of the $Ni_3P$ alloy deposits induced by the heating reduced the resistivity by a factor of 2 to 3.

## References


1) T. Osaka, I. Koiwa, J. Metal Finishing Soc., Japan, 34, 330 (1983)
2) U. George, H.Merk, A.F.Bogenschutz, Galvanotechnik, 72, 586 (1981)
3) G.O.Mallory, Plating and Surf. Finish., 63, 34 (June 1976)
4) B.C.Bartlett. L.Cann. J.Hayward. Plating, 56, 168 (1969)
5) Ed., F.Lowenheim, "Modern Electroplating", p.710 (John Willey & Sons, Inc.)(1974)
6) M. Schartz, Proc., Am. Electroplat. Soc., 47, 176 (1960)
7) S. Ishibashi, "Mudenkai Mekki", p.69 (Asakura, 1971)
8) K. Parker, H. Shah, Plating, 58, 230 (1971)
9) N. Feldstein, T.S.Lancsek, J. Electrochem. Soc., 118, 869 (1971)
10) G.S.Cargill, J. Appl. Phys. 41, 12 (1970)
11) K. Parker, H.Shah, J. Electrochem. Soc., 117, 1091 (1970)
12) R. Weil, Plating, 58, 137 (1971)
13) K. Sugita, N. Ueno, J. Electrochem. Soc., 131, 111 (1984)
14) M. Fernandez, J. M. Martinez-Duart, J. M. Albella, Electrochim. Acta, 31, 55 (1986)
15) K. Masumoto, K. Fukamichi, " Amorufasu Goukin", p.208 (Agune,1984)

Table 1 Bath composition and operating condition

| | | |
|---|---|---|
| $NiCl_2 \cdot 6H_2O$ | 24 | g/L |
| $Na_4P_2O_7 \cdot 10H_2O$ | 50 | g/L |
| $NaH_2PO_2 \cdot H_2O$ | 20 | g/L |
| pH (with $NH_4OH$) | 11 | |
| Temp. | 60 | °C |

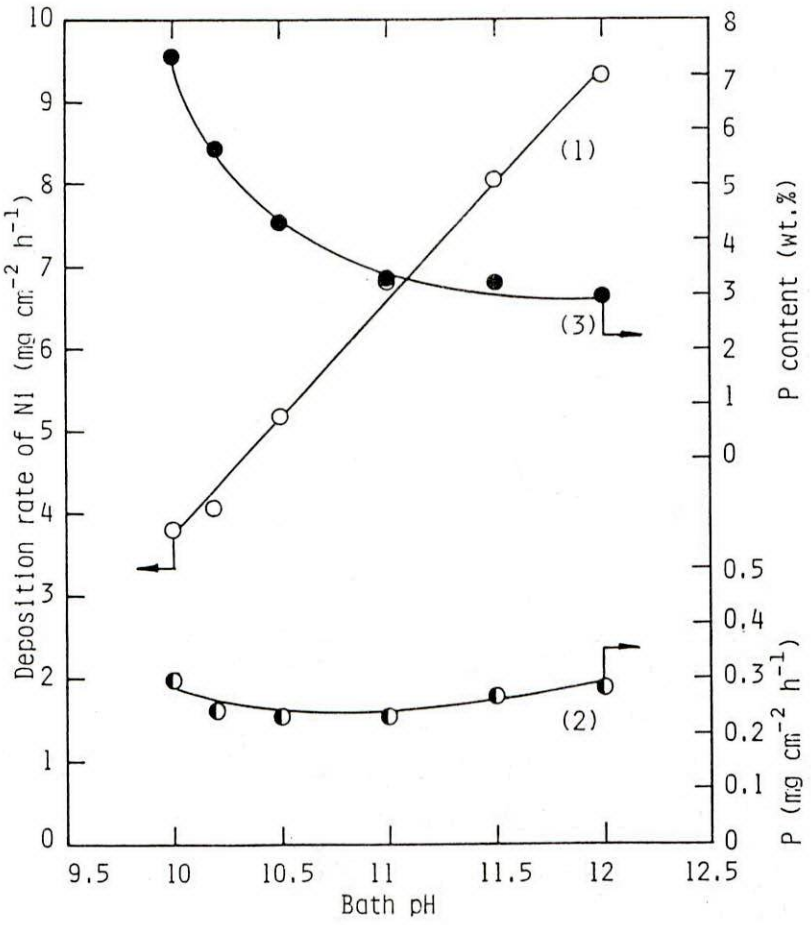


Fig.1 Effect of pH on P content and the deposition rate of Ni and P
(1) Ni, (2) P, (3) P content

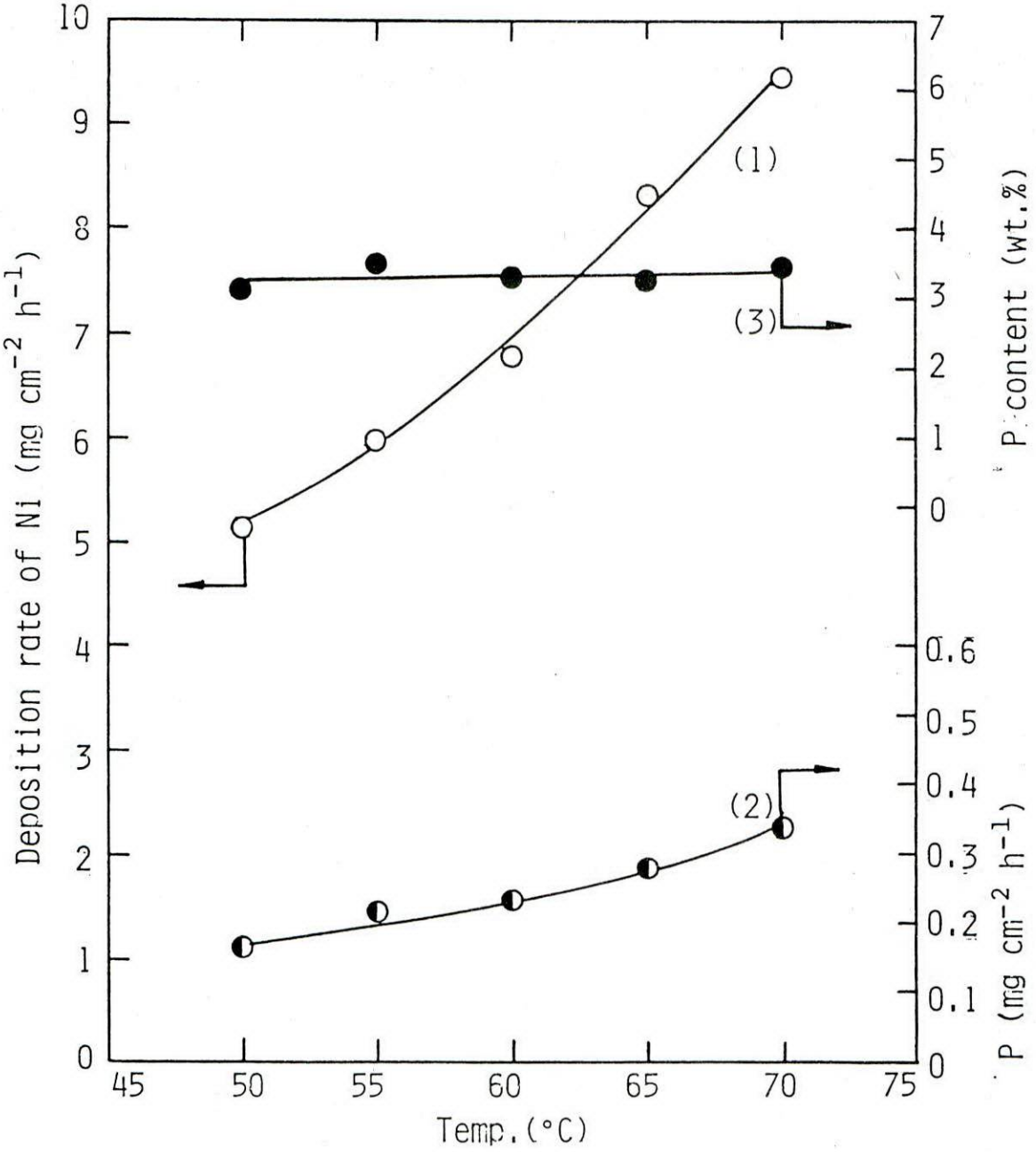


Fig.2 Effect of temperature on P content and the deposition rate of Ni and P
(1) Ni, (2) P, (3) P content

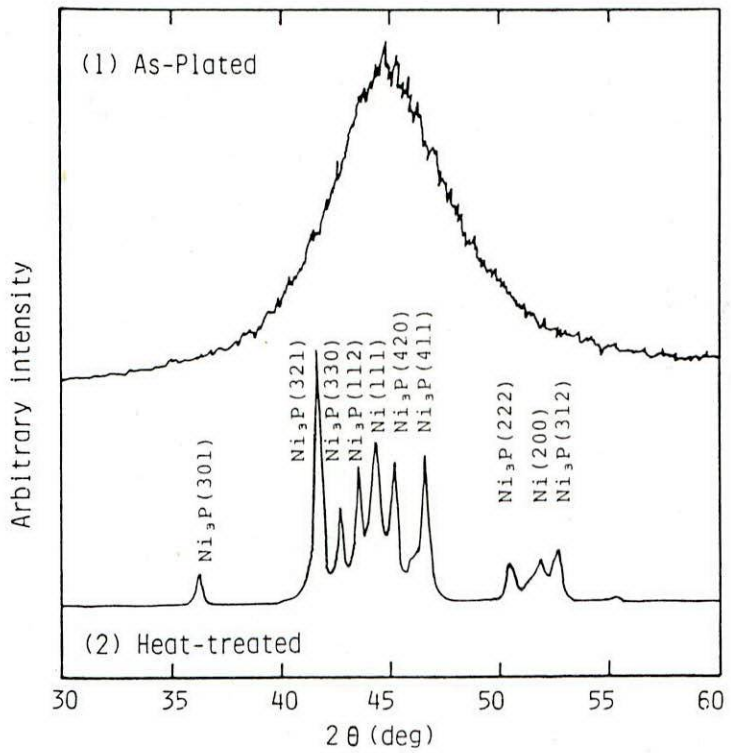


Fig.3 Typical X-ray diffraction patterns of Ni-P deposit (7.3 wt.% P)

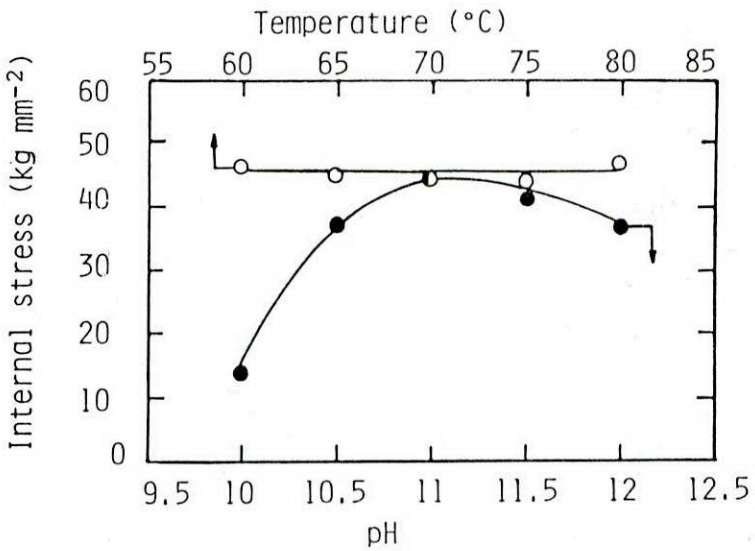


Fig.4 Effects of bath pH and temperature on the internal stress of Ni-P deposits

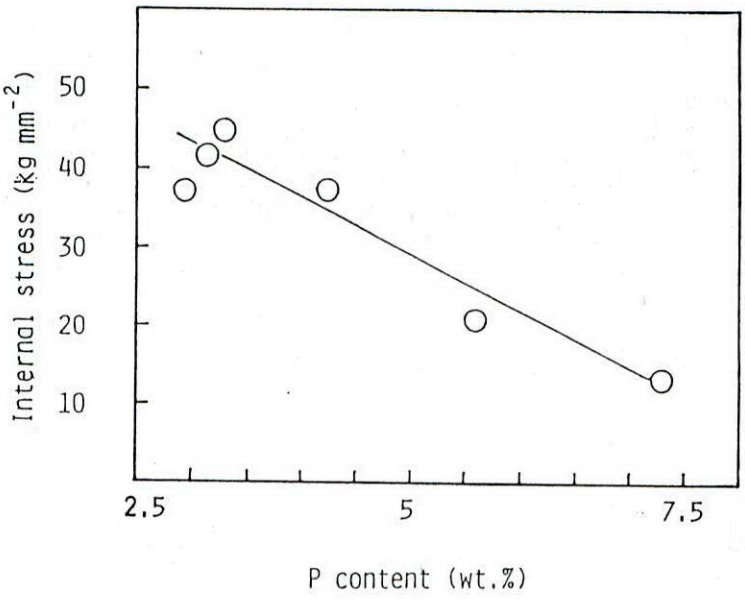


Fig.5 Effect of P content on the internal stress

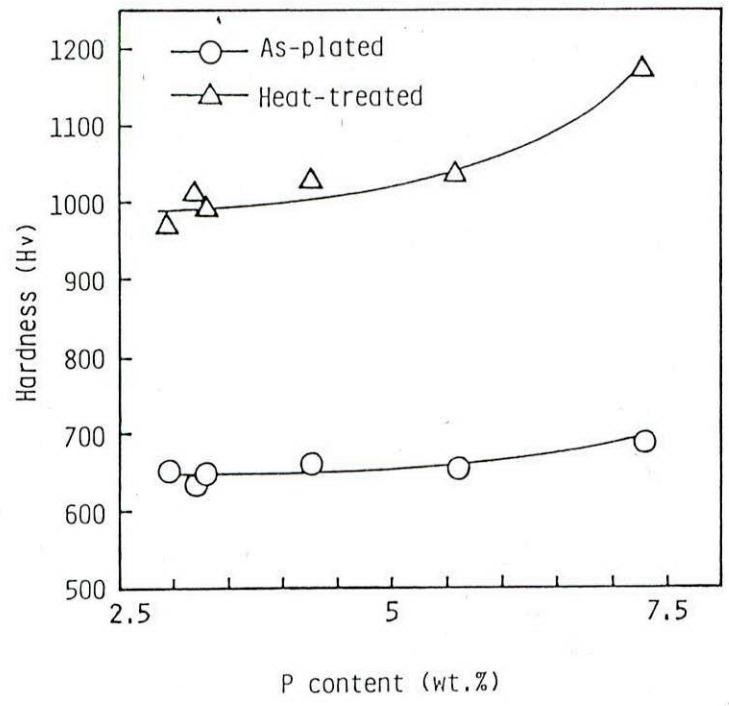


Fig.6 Effect of P content on the hardness of Ni-P alloys

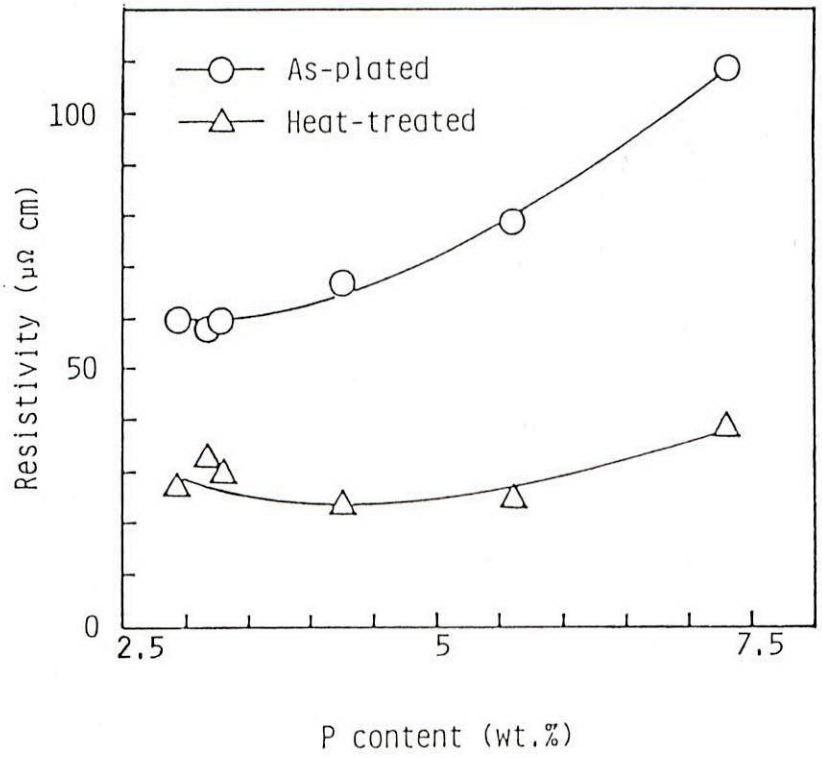


Fig. 7 Effect of P content on the resistivity of Ni-P alloys

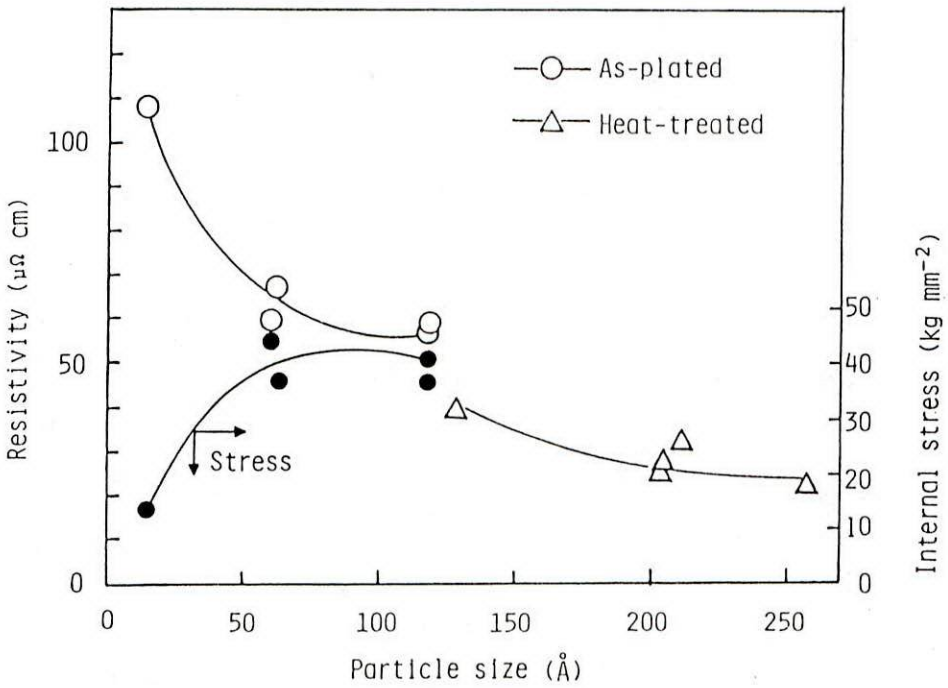


Fig. 8 Effect of particle size on the resistivity and internal stress of Ni-P alloys

I-6

# Electroless Deposition I
# Session I

## Advanced Process Control Methods for Electroless Plating of Plastics

Gary Shawhan, Edwin Bastenbeck
and Richard Bellemare
Enthone, Inc.
350 Frontage Rd.
West Haven, CT 06516

# ADVANCED PROCESS CONTROL METHODS FOR ELECTROLESS PLATING OF PLASTICS

Gary Shawhan, Edwin Bastenbeck, and Richard Bellemare
Enthone, Incorporated
350 Frontage Road
West Haven, Connecticut 06516

## Abstract

The growth in requirements for electroless plating of plastics is focused on a wide range of engineering applications for such industries as computers, business equipment, automotive, aerospace, and military. The purpose of the electroless plating is most often for EMI shielding but may include other reasons such as lightning strike, electromagnetic pulsation protection, wear or abrasion resistance, etc. In all cases, the concern of the user is to provide a high quality product that can last for many years in the environment without loss of performance. Such failures can in fact lead to warrantee problems, and even leave the companies vulnerable to competition due to product failure.

The process for electroless plating of plastics is involved, but when properly operated with good control procedures, consistent and reproducible results with respect to adhesion can be attained. Currently, high volume production of structural foam and molded polycarbonate is being done for purposes of EMI shielding of computer enclosures for example. Industry requirements exist for accelerated temperatures humidity cycling have been established to test the durability of the coating. These requirements are revealing important differences in product quality (related to chemistry and molding) that may indicate where plated plastic parts can perform in service for extended warrantee periods without failure. Unfortunately, this method can take twenty days or more to determine possible failure.

This paper provides information on process control methods which can be employed to improve the consistency of plated plastics. Included among these methods is a new accelerated autoclave test method which allows rapid determination of early failures in temperature humidity and is well suited for on-line confirmation of product quality.

## Introduction

The current use of electroless plating on structural foam and hardwall polycarbonate and polycarbonate blends for business equipment is intended to provide shielding from electromagnetic interference. Clearly from the standpoint of the manufacturer this protection from EMI needs to be capable of maintaining itself over the expectant service life and stated warrantee period of the equipment. Furthermore, during this period, the

integrity of the coating must be retained including its adhesion to the plastic substrate. Test procedures which can be correlated to prolonged service become an important consideration to simulate this longer term environmental period.

## UL-746 Adhesion Testing

One standard used to evaluate the effect of the in-service environment on conductive coatings is UL-746C. This method, summarized in Table I outlines four separate conditions under which adhesion testing is performed according to ASTM Method D3359-83 (measuring adhesion by Tape Test). The criteria for evaluating adhesion of the plating to the plastic is based on a scribed cross-hatch pattern. The amount of plate removed after a specified tape is applied to this cross-hatched surface and then lifted off (in a designated manner) is assigned a rating according to the scale shown in Figure 1.

In the case of plated polycarbonate test results on actual production reveal generally consistent passes per UL-746C in the 4-5 range even with fairly wide swings in plating process chemistry. While this can be somewhat comforting to the design engineer in terms of the width of the operating window, several issues still remain as a concern. First, the correlation to actual service needs to be examined further. Second, the test method does not readily discern differences in process variables which might be expected to influence coating adhesion. In this instance, again, the value of the UL-746C method for determining long term equipment reliability must be questioned. The test matricies for two groups of plated polycarbonate, shown in Figure 2, illustrates this point.

## Accelerated Temperature Humidity Testing

More recently, one equipment manufacturer instituted a test method based on temperature humidity cycling that has proven both more severe and more discerning in its ability to detect variations in coating quality and the related process conditions which produced it. This method, as outlined in Table II is referred to as the "4/4/16 Accelerated Temperature Humidity Test". At the present time, twenty (20) cycles of 4/4/16 testing is required after which a rating of 3B or higher is considered acceptable. Twenty cycles is also an attempt at correlating to five (5) years or more component service life and a better more rigorous means of assuring customer satisfaction beyond the warrantee period. Furthermore, ASTM is presently considering adoption of this test procedure for the purpose of evaluating the integrity of the plated plastic under accelerated aging conditions.

4/4/16 testing was conducted on plated structural foam and hardwall polycarbonate as indicated in a segment of the test results shown in Table III. This testing revealed significant inconsistencies in adhesion of the plated parts. In most cases, results fell far short of the required twenty cycles. Unfortunately, twenty cycles of 4/4/16 take twenty days to run. This does not include the time required to pull parts from the

line, arrange the shipment, plan testing and report the results. Therefore, the actual time involved before results might be available might be one to two months during which a lot of production could be processed and shipped and would require eventual return for reprocessing.

In today's climate of statistical process control, an essential component of process improvement is prevention before the fact, rather than detection of rejects after they are made. That is under "normal" quality control methods where testing is performed after the fact, the principles of SPC are violated. Obviously in this case, the use of the 4/4/16 test falls far short of providing the kind of timely on-line information necessary to insure the process is in control and capable of producing good parts.

## Accelerated Autoclave Test Method

As a consequence of such field experiments, investigations were initiated into test methods which could be used on-line. The intention would be to provide more immediate information on coating adhesion and the control of the process as it related to the quality required by the user. These objectives clearly required careful development of the methodology. Several of the key objectives included:

## General Objectives in Test Method Development

- Simple test method.
  - Low cost.
  - Small, adaptable to most facilities.
- Accelerated test with results available in the shortest time possible.
- Excellent correlation to the long term 4/4/16 temperature humidity test method.
- Suitability for inclusion into an SPC program.

Following several months of experimentation attempting to achieve these objectives, an autoclave procedure was developed that showed significant promise. As shown in Figure 3 adhesion tests performed on production structural foam polycarbonate showed very good correlation between autoclave testing and long term temperature humidity cycling. In fact, continued examination of test results began to establish a correlation between the number of cycles of 4/4/16 temperature humidity testing and single thirty minute autoclave tests. This is graphically represented by the statistical distribution curve in Figure 4.

The accelerated autoclave test method is performed according to the procedure outlined in Table IV. There are several important elements

in the successful implementation of the test method. First, samples need to be removed from the same section of the enclosure to insure that the most critical surfaces are being examined. In this case, the sprew area and gate area are typically the most significant surfaces requiring examination.

## Adhesion Failure Mechanisms

The intention of this test method is to examine adhesion of the plated plastic. The various types of adhesion failures which can occur with plated polycarbonate include the three main mechanisms as illustrated in Figure 5. These include:

| Failure Type | Source of Failure |
|---|---|
| **Cohesive Failure** | Over-etch of plastic resulting in degraded crumbled surface. |
| **External Corrosive Failure** | Moisture attack of the copper/substrate interface through porosity in the nickel. |
| **Internal Corrosion** | Chemicals or moisture left in the polycarbonate substrate plastic attacking the substrate/coating interface. |

## Comparison of 4/4/16 Testing to the Autoclave Method

In general, results from the autoclave temperature humidity test suggested 3-5 cycles could be equated to one thirty minute autoclave test. Furthermore, it was common that if the plated part passed two autoclave cycles (8-10 or more 4/4/16 cycles) it could be expected to pass over twenty cycles of 4/4/16 testing. Thus, one to two hours of on-line testing could be used to supplement (not replace) twenty days or more of extended testing in a full scale accelerated test.

Another important aspect to this type of accelerated testing is its ability to investigate various individual elements of the process. This can help isolate weak points in the process and provide a quantified performance result to identify process improvements. A good example of this approach is illustrated in the data presented in Figure 6. In this instance, we were studying the influence of post plate drying cycles on the adhesion of the plating. The intention was to identify the optimum drying technique and to identify a possible source of premature 4/4/16 adhesion failure on the finished part.

As can be seen by the information presented in Figure 6 air drying over a prolonged period of time clearly produces a poor adhesion result on polycarbonate. The one hour dry cycle followed by accelerated baking

produced the best results in this case. Based on these autoclave results and other tests process changes were implemented on the production line which significantly improved coating adhesion after 4/4/16 testing.

**Process Control for Plated Plastics**

In the broader perspective of today's marketplace process technology, such as that represented by the field of conductive coatings, is undergoing a re-evaluation. The re-evaluation is focused on the fundamental issues of statistical process control (SPC) and statistical quality control (SQC). From the perspective of today's user the selection of conductive coatings must be based on the predictability of its performance, an expectation of consistent quality and the assurance of stable, competitive costs. This cost optimization is achieved primarily from refinements in the process resulting in icreased output and the elimination of scrap. The concept is simple and well known. **Prevention** by process control instead of detection by quality control after the rejects have been made. The advancement of plated plastics particularly for applications such as EMI shielding which services industries heavily involved in SPC programs in essence is predicated on improvements in all of these areas. It is not only desireable for applicators of plated plastics to consider these concepts, it is becoming manditory that established programs be in place. In one sense failure to do so can dictate the selection of one supplier over another. In an even more serious scenario it can dictate a switch to alternate coating technology.

The availability of the accelerated autoclave temperature humidity test is an important tool for plated polycarbonate moldings in helping to meet these objectives. This is especially true in that adjustments in individual elements in the process can be studied with almost immediate feedback on the improvements they might represent in final product quality. This clearly allows tighter control limits to be set on each element of the chemical process and allows the applicator to strive for a defect-free operation.

In an effort to advance plating on plastics technology toward the ultimate goal of defect-free output, statistical process control has been initiated in production. This strategy has followed the basic principles of SPC as outlined in Table V. Our first objective was to try to bring each step of the process in control and eliminate special causes, as graphically illustrated in Figure 7. Second, through the gathering of statistics it was our intention to determine the capability of the process to meet the customer requirements. Then through fine tuning the chemistry we wanted to insure that we could maintain each element of the process within necessary control limits, i.e. establish capability. This concept is illustrated in Figure 8. In most all cases, a control chart format is used as part of establishing a program for controlling the process and improving its capability. An example of this approach is given in Figure 9 whereby you can see the upper and lower control limits, as well as the optimum value (x). Tests are run on each parameter are considered

important to the particular process solution and plotted out an on-going basis. In production, once the proper routine was established for doing the analysis, making timely chemical additions and recording the results, improvements were obvious in product quality and resulting yield.

## Summary

In summary, the accelerated autoclave temperature humidity test offers an important diagnostic tool for studying the plating on plastics product. The fact that this method is under consideration for adoption by ASTM adds to its importance in this regard. Furthermore, its correlation to long term, established industry testing appears very good based on current work with structural foam and hardwall polycarbonate.

Information developed from the accelerated test method has contributed greatly to the cause of studying individual process variables and establishing an SPC program. The ready adaptability of plated plastics to statistical process control methodology should increase the quality of plated product, reduce rejects and ultimately yield an optimal cost per unit.

The validity of this test method for examination of other plastic has not yet been demonstrated in relation to other accelerated tests such as the 4/4/16 method. Further work will be required on each plastic to determine its suitability for use with the accelerated autoclave method.

**TABLE I**

# UL-746C ADHESION TEST METHOD SUMMARY

**CRITERIA: <5% COATING REMOVAL BY TAPE TEST METHOD ASTM D 3359-83**

**TEST CONDITION:**

1) **AS RECEIVED**
2) **AFTER AGING AT 85°C FOR 56 DAYS**
3) **AFTER AGING AT 35°C ± 2°C AND 90 ± 5% RELATIVE HUMIDITY FOR 56 DAYS**
4) **AFTER THERMAL CYCLE TESTING; 1 HOUR AT 85°C; PLUS 1 HOUR AT 23°C; PLUS 1 HOUR AT 23°C**

## TABLE II

# ACCELERATED TEMPERATURE HUMIDITY TEST METHOD (4 / 4 / 16)

CRITERIA: 3B OR HIGHER RATING AFTER 20 CYCLES; EACH CYCLE EQUATES TO 24 HOURS

TEST CONDITION:

a) DWELL 4 HOURS AT 25°C ± 2°C; 47.5% ± 2.5% RELATIVE HUMIDITY

b) RAISE TEMPERATURE OVER 2 HOURS TO + 66°C ± 2°C; RAISE RELATIVE HUMIDITY TO 92.5% ± 2.5%

c) DWELL AT ABOVE CONDITIONS FOR 4 HOURS

d) HOLD TEMPERATURE AT +66°C ± 2°C; COVER RELATIVE HUMIDITY TO 47.5% ± 2.5%

e) DWELL AT ABOVE CONDITIONS FOR 11 HOURS

f) LOWER TEMPERATURE OVER 2 HOUR PERIOD TO 25°C ± 2°C; MAINTAIN RELATIVE HUMIDITY AT 47.5% ± 2.5%

g) RECYCLE

**TABLE III**

# 4/4/16 TEMPERATURE HUMIDITY TESTING OF PLATED POLYCARBONATE

| RUN# | PROCESS CONDITION | 4/4/16 TEST RESULTS 2 CYCLES | 6 CYCLES | 9 CYCLES |
|---|---|---|---|---|
| 1 | STD CYCLE | 2 | - | - |
| 2 | STD CYCLE | 1 | - | - |
| 3 | STD CYCLE | 4 | 1 | - |
| 4 | STD CYCLE | 4 | 1 | - |
| 5 | STD CYCLE | 4 | 1 | - |
| 6 | STD CYCLE | 5 | 4 | 4 |
| 7 | STD CYCLE | 5 | 4 | 4 |
| 8 | STD CYCLE | 5 | 3 | 3 |

TABLE IV

# ENTHONE ACCELERATED TEMPERATURE / HUMIDITY AUTOCLAVE TEST PROCEDURE FOR PLATED POLYCARBONATE

APPARATUS REQUIRED: 1 AUTOCLAVE

1 STEREOCLAVE
ELECTRIC / AUTOCLAVE
VWR CAT. NO. 58617-006

PROCEDURE: * PRIOR TO TESTING, PANELS SHOULD BE AGED FOR MAXIMUM ADHESION BY BAKING AT APPROXIMATELY 170°F FOR 30 MIN. THEN ALLOWED TO AIR COOL TO ROOM TEMPERATURE

1) HEAT AUTOCLAVE TO BOILING
2) PLACE THE PANELS VERTICALLY IN THE AUTOCLAVE ABOVE THE SURFACE OF THE WATER
3) CLOSE THE AUTOCLAVE AND ALLOW TO REACH PRESSURE (12 PSI)
4) HOLD PRESSURE FOR 30 MIN.
5) AFTER 30 MIN., RELIEVE THE PRESSURE, REMOVE THE PANELS AND ALLOW THEM TO EQUILIBRATE TO ROOM TEMPERATURE FOR 1/2 HOUR
6) PERFORM ASTM CROSS HATCH ADHESION TEST AND RATE ACCORDINGLY
7) REPEAT STEPS 2 THRU 6 AS REQUIRED

TABLE V

# PRINCIPLES OF SQC / SPC

- SET QUALITY STANDARDS / REQUIREMENTS
- ESTABLISH PROCESS CAPABILITY
- COMPARE CAPABILITY WITH REQUIREMENTS
- MONITOR THE PROCESS
- MAKE CORRECTIONS TO MAINTAIN PROCESS CONTROL

# FIGURE 1

## ASTM D 3359-83 CLASSIFICATION OF TAPE ADHESION RESULTS

| CLASSIFICATION | SURFACE OF CROSS-CUT AREA FROM WHICH FLAKING HAS OCCURED. (EXAMPLE FOR SIX PARALLED CUTS) |
|---|---|
| 5B | NONE |
| 4B | 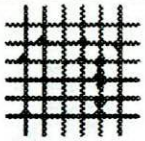 |
| 3B |  |
| 2B |  |
| 1B |  |
| 0B | GREATER THAN 65% |

FIGURE 2

# TYPICAL UL-746C ADHESION TEST RESULTS

| RUN# | CONDITION | UL-746C TEST TEST CONDITION #1 AS RECEIVED | UL-746C TEST TEST CONDITION #3 HUMIDITY CYCLING |
|---|---|---|---|
| 1 | STD CYCLE | 4-5B | 4-5B |
| 2 | STD CYCLE | 4B | 4-5B |
| 3 | STD CYCLE | 4-5B | 4-5B |
| 4 | STD CYCLE | 5B | 5B |
| 5 | STD CYCLE | 4-5B | 4-5B |
| 6 | STD CYCLE | 5B | 5B |
| **RUN#** | | | |
| 1 | DRYING SEQUENCE A | 5B | 5B |
| 2 | DRYING SEQUENCE B | 4-5B | 4-5B |
| 3 | DRYING SEQUENCE C | 4-5B | 5B |
| 4 | DRYING SEQUENCE D | 5B | 5B |
| 5 | DRYING SEQUENCE E | 4-5B | 4-5B |
| 6 | DRYING SEQUENCE F | 4-5B | 4-5B |

# FIGURE 3

## COMPARISON OF 4/4/16 AND AUTOCLAVE TEMPERATURE HUMIDITY TEST RESULTS ON PLATED POLYCARBONATES

| RUN# | 4/4/16 TEST RESULTS | INITIAL RESULTS | 1ST AUTOCLAVE | 2ND AUTOCLAVE | 3RD AUTOCLAVE | 4TH AUTOCLAVE | 5TH AUTOCLAVE |
|---|---|---|---|---|---|---|---|
| FOAMED POLY-CARBONATE | | | | | | | |
| 1 | FAILED BY 3 CYCLES | 3-4B | 2-3B | 2B | 2B | 1-2B | 1-2B |
| 2 | FAILED BY 3 CYCLES | 5B | 2B | 1-2B | 1B | 0B | 0B |
| 3 | FAILED BY 20 CYCLES | 5B | 5B | 3-4B | 3B | 3B | 3B |
| 4 | FAILED BY 20 CYCLES | 5B | 5B | 4-5B | 4B | 3B | 3B |
| 5 | FAILED BY 20 CYCLES | 5B | 5B | 5B | 4-5B | 3-4B | 3B |
| 6 | FAILED BY 20 CYCLES | 5B | 5B | 5B | 5B | 3-4B | 3-4B |
| 7 | FAILED BY 15 CYCLES | 5B | 5B | 4B | 5B | 2B | 3B |
| HARDWALL POLY-CARBONATE | | | | | | | |
| 1 | PASSED 20 CYCLES | 5B | 5B | 5B | 5B | 5B | 5B |
| 2 | PASSED 20 CYCLES | 5B | 5B | 5B | 5B | 5B | 5B |

# FIGURE 4
# RELATIONSHIP BETWEEN ONE-30 MUNUTE AUTOCLAVE TEST AND THE NUMBER OF 4/4/16 TEST CYCLES FOR PLATED POLYCARBONATE

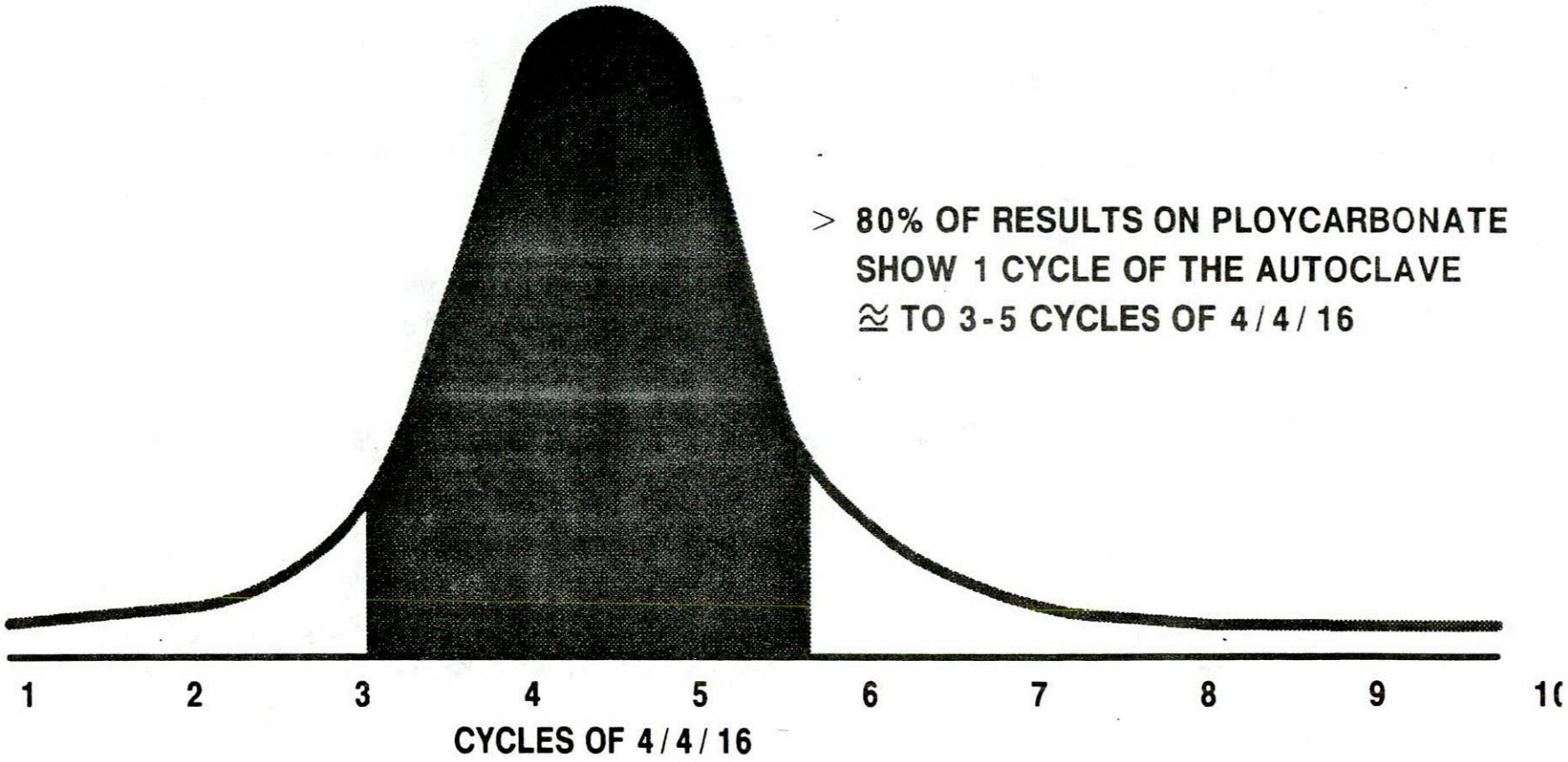

# FIGURE 5 ADHESION FAILURE MECHANISMS

## CORROSION FAILURE MODES

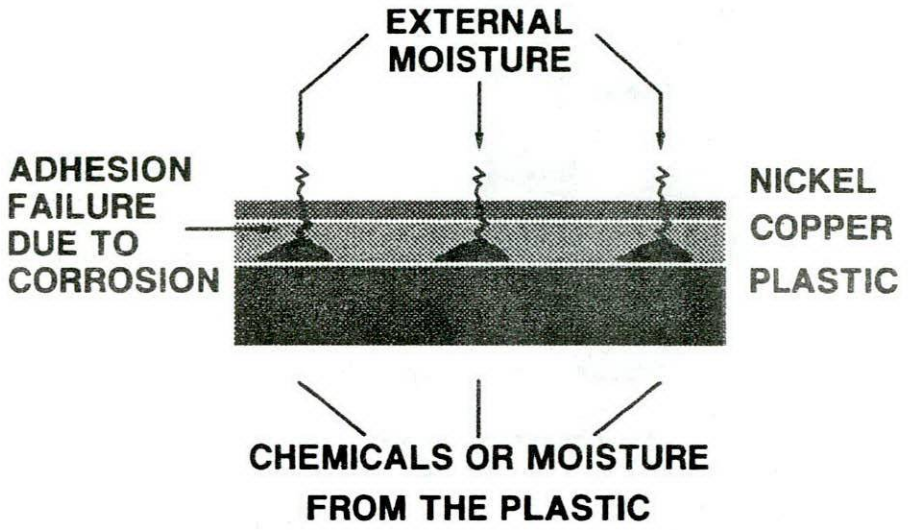


## COHESIVE FAILURE MODE

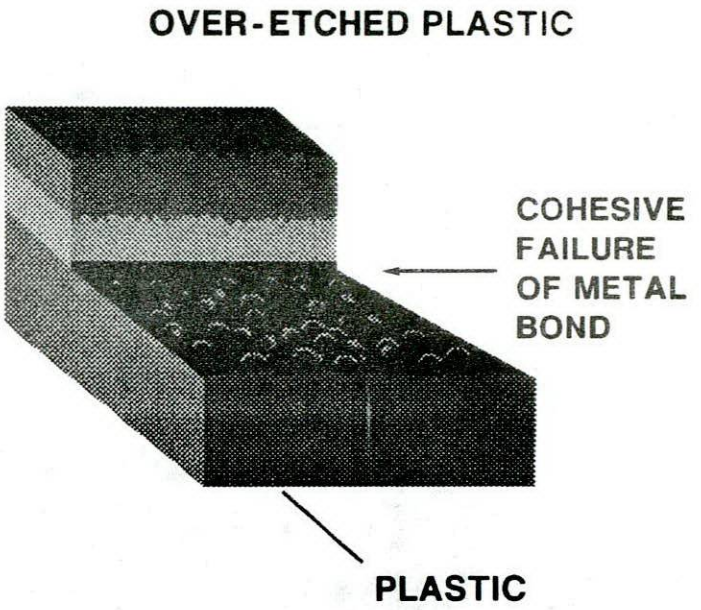

# FIGURE 6

## EXAMINATION OF VARIOUS POST-PLATE DRYING CYCLES USING THE ACCELERATED AUTOCLAVE TEST METHOD

## TAPE TEST

| TEST CONDITION | INITIAL RESULTS | 1ST AUTOCLAVE | 2ND AUTOCLAVE | 3RD AUTOCLAVE | 4TH AUTOCLAVE | |
|---|---|---|---|---|---|---|
| AIR DRY WITH EXTENDED TIME DELAY (NO BAKE) | 4B | ■ | 1B | 0B | 0B | |
| EXTENDED DRY IN AIR EXTRA POST RINSE (BAKE 25 MIN) | 5B | 5B | 5B | ■ | 2B | |
| IMMEDIATE DRYING AFTER RINSE (NO BAKE) | 5B | 5B | 4B | ■ | 2B | |
| **AIR DRY 1 HR, (BAKE 25 MIN)** | **5B** | **5B** | **5B** | **5B** | **4B** | **PASS** |

■ FAILURE POINT (<3B)

FIGURE 7

# PROCESS CONTROL

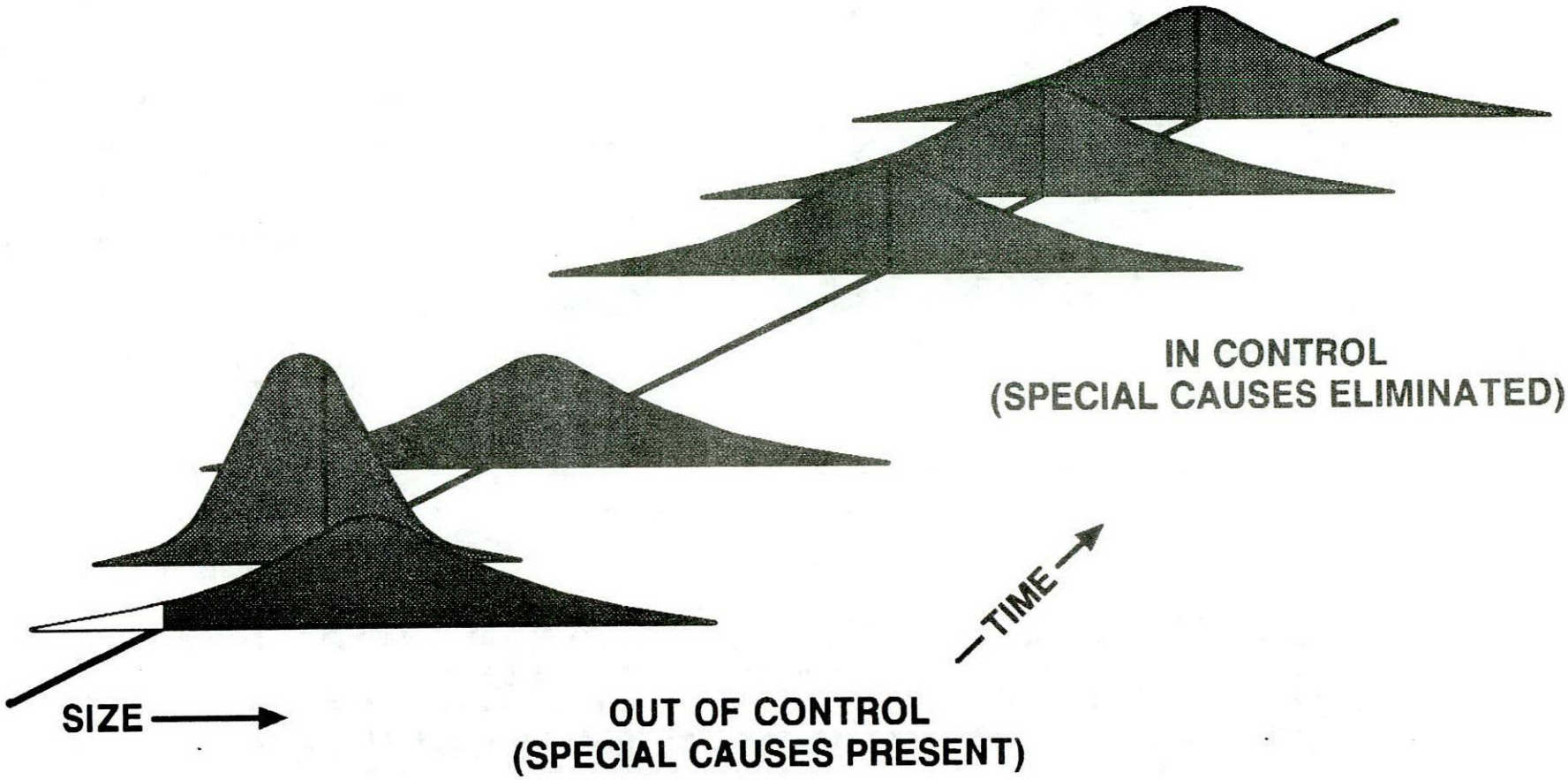

**FIGURE 8**

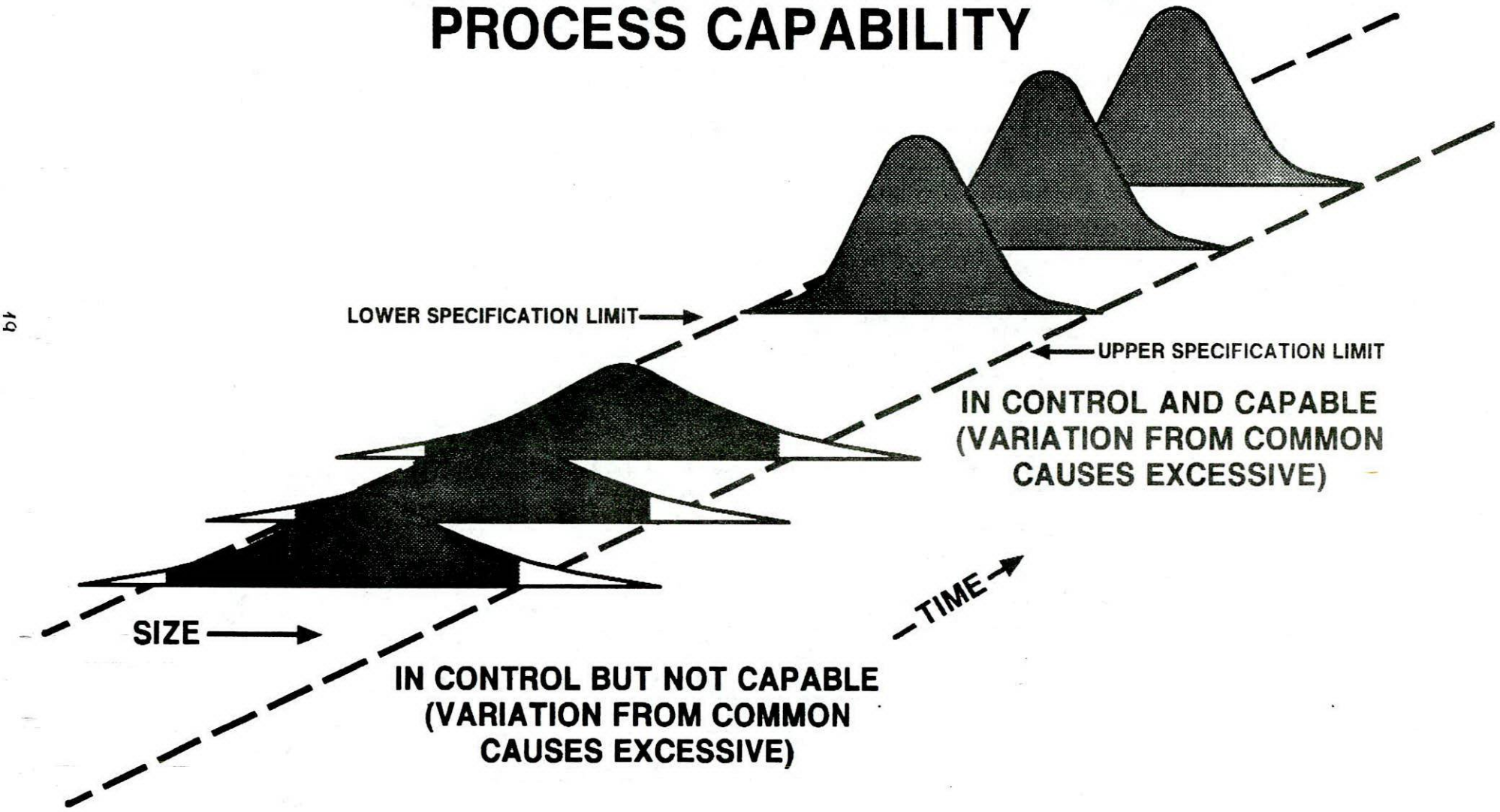
PROCESS CAPABILITY
LOWER SPECIFICATION LIMIT
UPPER SPECIFICATION LIMIT
IN CONTROL AND CAPABLE
(VARIATION FROM COMMON
CAUSES EXCESSIVE)
SIZE
TIME
IN CONTROL BUT NOT CAPABLE
(VARIATION FROM COMMON
CAUSES EXCESSIVE)

# FIGURE 9 SAMPLE CONTROL CHART

| COMPANY | LINE | RACK | PROCESS<br>ELECTROLESS COPPER | TEST FREQUENCY<br>2 HRS. | PART NO. | REPORT NO. |
|---|---|---|---|---|---|---|
| JOB NO. | DATES | | TEST<br>PH OF SOLUTION | | | |

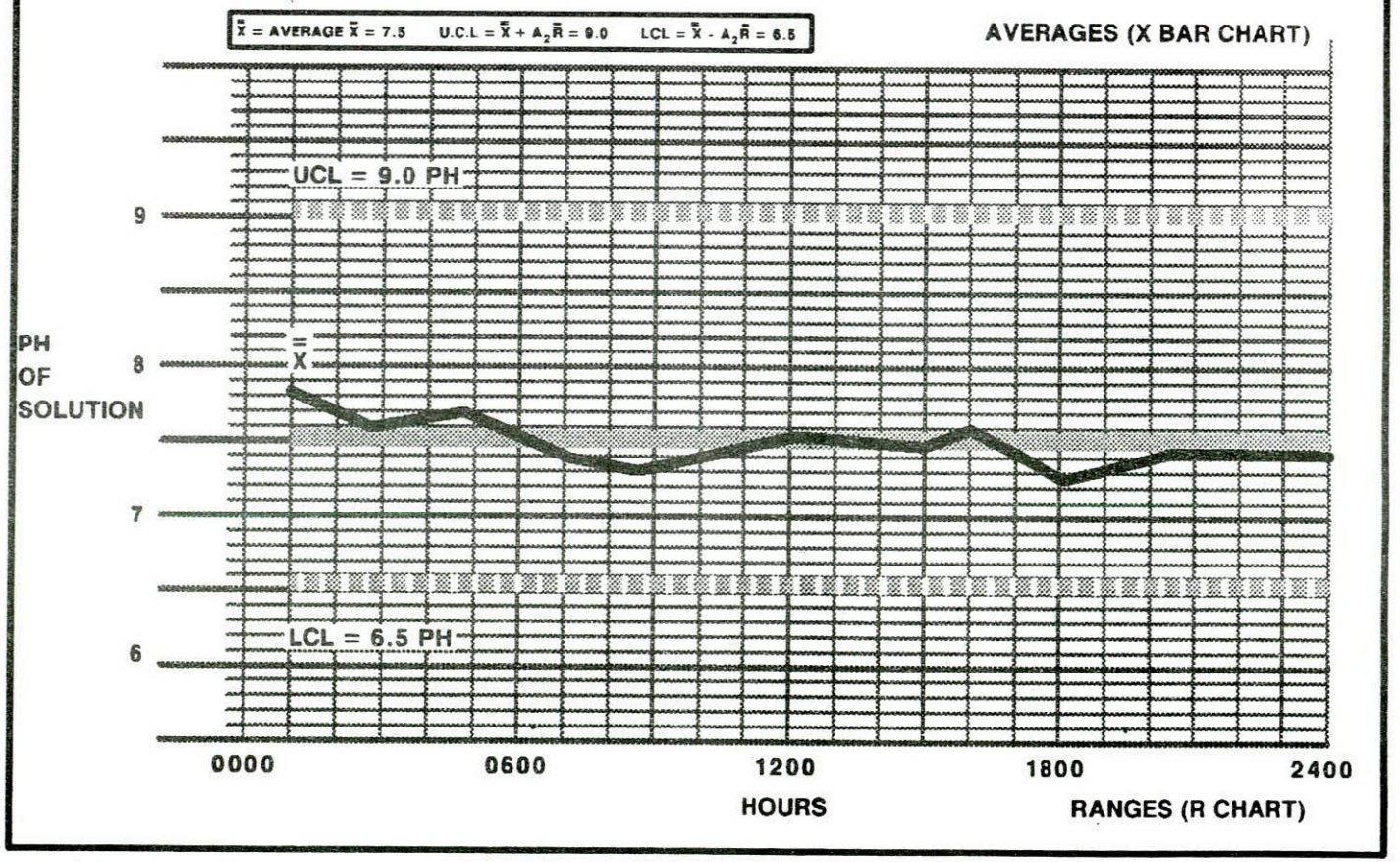

J-1

# Electroless Deposition II
# Session J

## Electroless Nickel Waste Treatment

W. Van Antwerp and T. Yamaguchi
Uyemura International
Los Angeles, CA

T. Otaka, K. Araki and K. Deguchi
C. Uyemura
Osaka, Japan

D. Bailey
Baker Brothers/Systems
Stoughton, MA

**PAPER NOT RECEIVED IN TIME FOR PUBLICATION***

Electroless Nickel Waste Treatment

W. Van Antwerp and T. Yamaguchi, Uyemura International, Los Angeles, Ca; T. Otaka, K. Araki and K. Deguchi, C. Uyemura, Osaka, Japan; and D. Bailey, Baker Brothers/Systems, Stoughton, MA

Chemical waste treatment of spent electroless nickel baths is becoming increasingly important. This paper will investigate some of the common chemical and physical approaches to treatment, including precipitation, thermal destruction, liquid ion exchange, electrowinning, and ozonation. Cost data, chemical and equipment efficiencies, and strategies for reusing the nickel will be discussed.

* For copies of this paper, please contact the author directly

Mr. Bill Van Antwerp
Uyemura International Corporation
5828 Uplander Way
Culver City, Ca 90230
(213) 645-2292

J-2

# Electroless Deposition II
# Session J

## Factors Affecting Quality Electroless Nickel Plating of Thin Film Memory Disks

Michael Aleksinas, Kashmira Parikh
and Phillip Hagberg
Fidelity Chemical Products Corp.
470 Frelinghuysen Avenue
Newark, NJ 07114

# FACTORS AFFECTING QUALITY ELECTROLESS NICKEL PLATING OF THIN FILM MEMORY DISKS

Michael Aleksinas, Kashmira Parikh and Phillip Hagberg
Fidelity Chemical Products Corp.
470 Frelinghuysen Avenue
Newark, New Jersey 07114

## Introduction

Electroless nickel has become the industry accepted standard as a base metal foundation for both plated and sputtered magnetic media on rigid aluminum computer disks. The increased information storage capacity (100 X the capacity of similar "floppy" disks), resistance to wear, increased speed of information capabilities for bulk manufacturing and improved reliability have made this technology ideal for today's booming business computer market.[1] However, due to the low flying heights (<10 micro-inches) of the recording heads and the high speeds used in the Winchester-type disk drives, great care must be taken in providing consistent high quality, low cost plating of aluminum memory disks. This paper will discuss the various factors that can affect the overall yields of high quality plating and finishing which in turn can affect the technological risks each company faces as it enters the making of thin film media for hard disk drives.

## Discussion

Inherent properties of electroless nickel make this coating an obvious choice for rigid aluminum disks. These properties include uniform deposit thickness, diffusion barrier characteristics, corrosion resistance, non-magnetic nature of the deposit, and the ability to be polished to an optical finish.[2] To maintain consistency, certain parameters must be closely monitored in the plating operation. These parameters include smoothness of the as-plated surface, pitting, adhesion of the EN to the substrate, and of course certainly the non-magnetic nature of the deposits.

To control these parameters several factors must be followed closely. These factors, which can influence overall yields individually or in combination, are as follows:

1) Substrate, type and quality
2) Pretreatment
3) Electroless Nickel Bath
4) Polishing

Since the finished product must be essentially defect-free, variations such as the mineral content of the water can cause catastrophic problems. Hence, a complete understanding of every possible factor which can affect the overall quality of plating is essential.

## Substrates

The aluminum substrate plated with the electroless nickel barrier coat has a profound affect on the quality of the final product. Among the important characteristics of the substrate are coefficient of expansion, moment of inertia, stiffness, residual stress and workability. Experience indicates 5000 series aluminum provides the core of plated disks, but other materials are prime candidates for future disk substrates such as glass, ceramics, and plastics.

At present aluminum alloys 5086 and 5586 are used mainly as the disk substrates. A summary of some of the aluminum alloys available from suppliers is found in Table I.

Table I

Aluminum Alloys by Supplier

Chemical Composition Limits/Ranges

| Alloy | Fe | Si | Mn | Cu | Mg | Cr | Ti | Zn | Al |
|---|---|---|---|---|---|---|---|---|---|
| Alum.(5086) Assoc. Std. | 0.40 | 0.50 | .2-.7 | 0.10 | 3.5-4.5 | .05-.25 | .15 | | Balance |
| Kobe | | | | | | | | | |
| KS5086 | 0.5 | 0.4 | .2-.7 | 0.1 | " | " | " | .25 | Balance |
| KS5186 | 0.16 | 0.1 | .05 | 0.03 | 4.3-4.9 | .05-.1 | .03 | .05 | Balance |
| KS5586 | 0.16 | 0.1 | .05 | .05-.4 | " | " | .03 | .05-.4 | Balance |
| NLM | | | | | | | | | |
| 5086 | .08 | .05 | .2-.3 | .03 | 3.4-4.5 | .05-.1 | .03 | -- | Balance |
| T4M | .08 | .05 | -- | .003 | 3.7-4.7 | -- | -- | -- | Balance |
| M4M | .06 | comb. | -- | .02-.1 | 3.7-4.7 | -- | -- | -- | Balance |
| Sumitomo | | | | | | | | | |
| 486S | .5 | .4 | .2-.7 | .1 | 3.5-4.5 | .05-.25 | .15 | .25 | Balance |
| XA334 | .07 | .07 | .02 | .02 | " | .06 | .01 | .01 | Balance |
| ZG50 | .5 | .4 | .3 | 1.0-1.4 | 2.5-3.1 | .13-.17 | .2 | 4.6-5.4 | Balance |
| Stolle | | | | | | | | | |
| 5086 | .4 | .5 | .2-.7 | 0.1 | 3.5-4.5 | .05-.25 | .15 | .25 | Balance |
| CW66 | .08 | .08 | .2-.6 | .02 | 3.5-4.5 | .02-.1 | .15 | .25 | Balance |
| CZ46 | .08 | .08 | 0.1 | 0.2 | 3.7-4.7 | .1 | -- | .45 | Balance |

As seen in Table I, all substrates are predominantly magnesium alloys of aluminum. Hence, pretreatment must be specific for this type of substrate.

Upon further experimental investigation, it has been found that the relationship between intermetallic compound distribution and the grain size of the alloy can profoundly affect the defects of the Ni-P layer. Materials which are free from intermetallic compounds and/or are dense and homogeneous can improve the quality of the EN film (i.e., surface roughness and adhesion).[3] Figures 1 and 2 are photographs which depict the differences between the surface roughness of different alloys in the pretreatment and plating processes.

The differences of the EN film can be attributed to the differences of the zinc precipitates upon each alloy. The homogeneity of the zinc immersion layer has been found to be directly proportioned to the uniformity and grain size of the alloy itself.

Besides the quality of the alloy, there are two types of manufacturing techniques which provide distinct finishes of the substrate that the plater must cope with. These finishes are commonly referred to as diamond turned disks and matte finish or polished disks. Both finishes respond very differently to pretreatment methods and must be understood clearly in order to address the requirements of each.

Diamond turned disks are machined to a very flat, very smooth surface, to a typical finish of 0.0127 micrometers maximum arithmetic average deviation.[4] These disks have been rough cut from a stamped blank using a high carbon steel cutter. Since the first cut usually removes more material than the second cut, the first side can have much greater internal stress. This condition, concomitant with the fact that very high temperatures are produced in the cutting operation, may recrystallize the alloy and provide further differences between one side of the disk and the other. For example, greater levels of nodularity will manifest itself as a result, especially on the stressed side of the disks. Often this is perceived as a plating problem when it is not. Another consequence that can occur will be the difference in domain formation of the cobalt layer on one side of the disk versus the other. Different levels of nickel stress can affect the uniformity of the cobalt layer especially at the thin deposit ranges of 2-4 micro inches commonly used today.

Matte finishes are also constructed from a stamped blank. Unlike the diamond turned disks, these are ground to rough dimensions using large volumes of lubricant. Both sides are processed at the same time, hence surface stresses can be eliminated with this process.[5] Finished surfaces are achieved by proprietary polishing compounds. This method produces very flat disks with smooth surfaces which platers can easily activate, provided proper care is given to complete removal of polishing compounds in the pretreatment cycles.

## Pretreatment

Pretreatment is crucial to developing consistent, reliable results in the production of high quality thin film disks and its importance cannot be overstated. In the past 10 years great strides have been made in the preparation of aluminum which have resulted in consistent plating yields of 99% or higher. A typical process cycle for various disk alloys is found in Table II.

Table II

General Pretreatment Process for Rigid Film Memory Disks

| Process Step | Time | Temperature |
|---|---|---|
| 1. Alkaline Soak Cleaner | 2 - 8 minutes | 130 - 160°F |
| 2. DI Water Rinse | | |
| 3. Acid Etch/Conditioner | 30 sec. - 2 minutes | R.T.- 150°F |
| 4. DI Water Rinse | | |
| 5. 50% Nitric Acid Desmut | 30 - 60 sec. | 65 - 75°F |
| 6. DI Water Rinse | | |
| 7. Dilute Alloy Zincate | 30 - 60 sec. | 65 - 75°F |
| 8. DI Water Rinse | | |
| 9. 50% Nitric Acid | 30 - 60 sec. | 65 - 75°F |
| 10. DI Water Rinse | | |
| 11. Dilute Alloy Zincate | 20 - 30 sec. | 65 - 75°F |
| 12. DI Water Rinse | | |
| 13. EN Plate to Desired Thickness | | |
| 14. Dry | | |

Every step in the cycle is critical in order to obtain excellent performance and yields. Each step works in concert with the preceding and subsequent steps; hence a complete understanding of the mechanism of the pretreatment cycle is essential for successful plating of rigid disks.

### Alkaline Soak Cleaner

The first step in the pretreatment cycle is the alkaline soak cleaner. Its job is simply to remove soils, lubricants and polishing compounds from the disks' surfaces by emulsification or dissolution. Pre-cleaning may be necessary to remove excess lubricants or polishing compounds which can cause dullness, pitting and/or nodularity. Some soak cleaners can actually etch aluminum causing voids which later appear as shallow spots. Careful control of time, temperature, pH, and concentrations of cleaner is essential for excellent yields. Silicated soak cleaners are most commonly used since they tend to be less aggressive towards aluminum and are excellent cleaners at elevated temperatures. However, when silicated cleaners are used, thorough rinsing is necessary following their use. Careless rinsing can lead to the formation of an insoluble silicate film which may lead to increased nodule formation as well as decreased adhesion of the EN to the aluminum substrate.

## Acid Etch/Conditioner

One of the more critical steps in the preplate cycle is the acid/etch conditioner. Its primary function is to deoxidize the surface and remove the various alloying elements and inclusions from the aluminum surface. Most alloying constituents not removed can and will manifest themselves as sources for pits, nodules, blisters or cause poor adhesion for many reasons. Alloying elements such as magnesium, manganese, and copper found in 5086 and 5586 alloys will be removed in the acid etch. However, profilometer studies on acid etches indicate only modest changes of the surface from its original polished condition. Thus, removing the alloying elements at the surface and minimally attacking the aluminum rich surface of the memory disk substrate make acid etches the preferred etch in the process. For some applications acid conditioners have been used in place of acid etches. However, for diamond turned substrates the acid etch is preferred.

## Nitric Desmut

The next step of the process involves the desmutting of the aluminum surface. The purpose of this step is to remove insoluble residues from the previous conditioning steps. Desmutting should leave a uniform, white, thinly oxidized aluminum-rich surface for the application of zincate. If the desmutting is incomplete and excess alloy segregations are left on the surface adhesion failures or nodules will become obvious.

## Zinc Immersion Process

Following the desmutting of the surface comes the immersion process, commonly referred to as "zincating". Zincating continues to be the most reliable way to produce consistent adherent deposits of EN on aluminum. Aluminum has a natural affinity for oxygen, so there is always an oxide film present on the aluminum surface. This ever present oxide film interferes with the formation of metallic bonds of the EN to the aluminum. Consequently, the zincate immersion process was created simply to replace the oxide film with a thin metallic film of zinc which is resistant to oxidation. This process was first described by Hewitson in 1927[6] and modified later by Korpium[7] and Pernier.[8]

Within the last 5-7 years, alloy zincates have been found to be superior to the conventional alkaline zincates for many disks. Lashmore[9] reports that alloy zincates are superior in part to the alloying effects of the other metals. Immersion deposits from alloy zincates have been found to be thinner, more durable and highly uniform, which lead to improved adhesion and greater life of the EN bath. Deposits from these types of zincates leave thin "zinc rich zones" as described by Mallory.[10] These "zones" create excellent reproducible adherent EN deposits. Filtering of these solutions can be advantageous by the removal of zinc oxide which can be created at the air-solution interface. Nodules or poor adhesion will become noticeable by improper maintenance of these solutions.

Immersion times, concentration of the zincate, and temperature can affect the properties of the zincate. Constant attention to these parameters will provide consistent high quality deposits.

Finally, double zincating has been proven to yield more adherent, smoother EN deposits. The first zincate is removed in the dilute nitric acid followed by a second shorter immersion in a similar zincate. The mechanism of improved adhesion using double zincating is based on the fact that the first zincate provides porous incomplete coverage allowing potential sites for bad adhesion to occur. The nitric acid dip after the first zincate is important because it purifies the aluminum disk by removing exposed inclusions brought to the surface by the aggressive first zincate. The second zincate immerses much more densely and uniformly as a result and is noticeably thinner. Profilometer measurements clearly indicate the second zincate application is much more uniform and smoother than the first.[11]

Electroless Nickel Bath

One of the most important factors in providing high quality yields is the selection and control of the electroless nickel solution itself. Many different compositions of EN baths can give various results. For instance, the EN bath itself can directly be responsible for the following results:

1) Smoothness of the as-plated process
2) Non-magnetic nature of the deposit
3) Pitting of the deposit
4) Life on aluminum before blisters occur
5) Maintenance of rate over the life of the bath

All these factors are important to successful plating of rigid film disks and can substantially affect the overall yields.

The smoothness of the deposit is important in order to reduce polish cycles and allow for thinner deposits. Large cost savings can be realized by smoother as-plated deposits. Pits, even after polishing, can become evident if the EN deposit is crystalline in appearance masking over "shallow spots" areas. Figure 3 depicts EN deposits from two different formulations with DEKTAK traces of each.

The non-magnetic nature of the deposit is also a vitally important aspect of the EN bath. This non-magnetic quality is directly related to the amorphous structure of electroless nickels of high phosphorus content. Also, different types of chelation have been shown to affect the magnetic nature of the deposit.[12] It is imperative the EN bath be non-magnetic and amorphous since the coercivity of magnetic film overcoats are affected by the physical character of the surface upon which it is plated. If the crystallites of the magnetic layer should start non-uniformly, the squareness of the loop will suffer as will the noise ratio of the film.

Pitting of the EN deposit can be induced by the bath itself. Improper chelation, buffering, wetting agent selection, and stabilization are factors which can greatly exaggerate the phenomenon of pitting. Varied opinions have been voiced on the mechanism of pitting as it pertains to memory disk plating, but this topic goes beyond the scope of this paper and will be addressed in a future paper. Some of the pits experienced are pictured in Figure 4, 5 and 6.

The average life on aluminum for high phosphorus EN baths is 3-6 regenerations before adhesion failure occurs. Yarkosky and co-workers[13] claim the adhesion failure results from the increase in total acidity of the plating bath. Other investigators indicate that the adhesion of the coating to the substrate is influenced by the nature and magnitude of stress in the EN deposit.[14] Careful control of pH values and alkali used in pH adjustments can significantly prolong the useful life on aluminum disks. Bath formulations designed to prevent zinc contamination can further prolong the EN bath life on aluminum.

Maintaining the rate of the EN bath over the life of the bath can be useful and cost effective. By maintaining a consistent rate, high production volumes can be realized, reducing rejects due to low nickel thickness. Shorter bath times late in the EN bath life keep production time useful and profitable. Increased zinc contamination of the EN bath can suppress overall plating rates, so great care must be taken in rinsing after the last zincate to prolong the bath life of the EN.

## Polishing

Since polishing is a major cost step in the process of thin film manufacturing, its economics of technique, materials, labor and yield have a great effect on the success of the enterprise. The character of polishing pads, laps, abrasives, and cutting fluids must be matched to the character of the EN, the type of machinery used, and the desired finish (Ra≤200 A).[15] These optimums can only be experienced at each facility and are usually kept confidential. However, pits after polishing are a common experience and some of the causes are described in Table III.

Table III

Causes of Pits After Polishing

1) Too much pressure in polishing
2) Too slow speed in polishing, get eddying effect
3) Pads too soft. Follows contours of substrate
4) Slurries too thin
5) Lapping action incorrect, must be perfectly parallel to the substrate

As indicated in Table III, many factors can cause pits after polishing. If too much pressure is present in polishing, nodules can be torn from the

surface and the broken nodule can scratch the data surface later in the polish sequence. These scratches can appear as irregular size pits. A typical case is diagrammed in Figure 7.

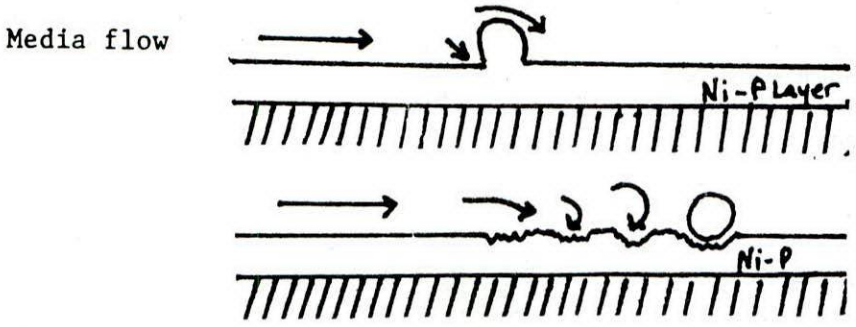


Figure 7

A too-slow speed in polishing can also contribute to pits after polishing. The slower speeds will not break away gross nodules as quickly and an eddying effect may take place immediately after the nodule. Figure 8 depicts this phenomenon.

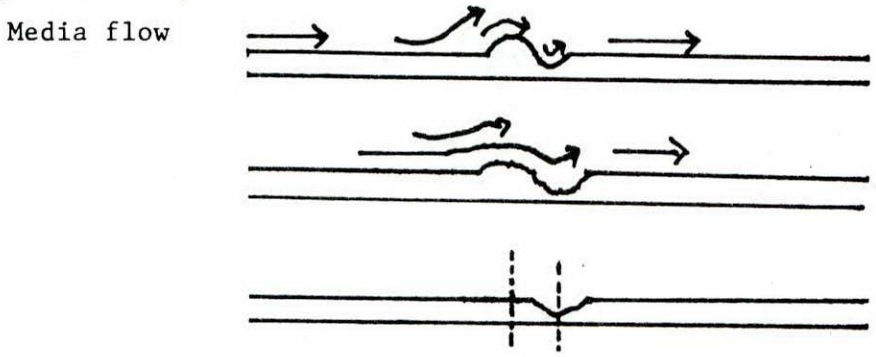


Figure 8

As can be seen, a pit will become evident immediately following the gross nodule. In a similar fashion, soft pads can also create the same phenomenon. Immediately after the gross nodule, soft pads can etch away the nickel more aggressively. The end result is similar to the slow speed polishing.

Slurries too thin can cause aggressive etching to occur. Smooth finishes and high yields will not be attainable if this should occur.

Finally, lapping action must be done very carefully and parallel to the substrate. Any discontinuity here will cause etching of the EN deposit and irregular scratches or pits will be created.

Summary

Herein it has been clearly demonstrated that many complex factors can affect the overall quality and yields of thin film memory disks. Obviously, to trouble-shoot problems in this industry can be difficult, time-consuming, and costly. Companies that have survived up to this point, however, are now attaining yields in the high 90's. This is a substantial increase from the

yields of <70% just a few years ago.

Substrates, pretreatments, EN baths and polishing techniques have significantly improved over the past few years. With continued refinement in all areas this industry will see continued expansion in the future. Further improvements, especially in the EN baths in terms of extended bath life, as-plated smoothness, and faster plating rates, can make EN a more viable choice over the ferric oxide based disks of today.

References


1. Free, J., "The Amazing Winchester - Big Machine Memory for Personal Computers". Popular Science, October, 1982, p. 89-90.

2. Brenner, A., de Minjer C. H., "Studies on Electroless Nickel Plating", Plating, Dec., 1957, pp. 1297-1305.

3. R & D Dept. Kobe Steel Ltd., "New Aluminum Alloy for Electroless Ni-P Plating Disc", Nov., 1983.

4. Baudrand, D., Malik, M., "Autocatalytic Alloy Plating Process for Thin Film Memory Discs", Metal Finishing, March, 1986, p. 15.

5. Lawrence, J., Barnes, L., "The Relaxation of Deformed Si and Al Surfaces". Optical Society of America, April 17, 1984.

6. E. H. Hewitson, U. S. Patent 1,627,900 (1927).

7. J. Korpium, U. S. Patent 2,142,564 (1939).

8. L. Pernier, U. S. Patent 2,297,241 (1942).

9. D. S. Lashmore, "Immersion Coatings on Aluminum", Plating and Surface Finishing, 67, 37 (1980).

10. G. O. Mallory, "The Relationship Between Stress and Adhesion of Electroless Nickel Phosphorus Deposits on Zincated Aluminum", Proc. AES, 70th Annual Technical Conf. (1983).

11. Macary, R. L., "Better Plating of Electroless Nickel on Aluminum", Products Finishing, October, 1987, p. 60-62.

12. W. V. Antwerp, "Some Physical and Magnetic Properties of Electroless Nickel", Proc. AES (1987).

13. E. F. Yarkosky, M. Aleksinas and A. Marzack, "Electroless Nickel Baths as a Factor in Producing Blisters on Aluminum", Proc. AES 66 (1979).

14. G. O. Mallory, pp. 1-16.

15. Garrison, M. C., "Plating Media Manufacturing Methods", Magnetics Materials Seminar, MMS-G, 1983, pp. 10-11.

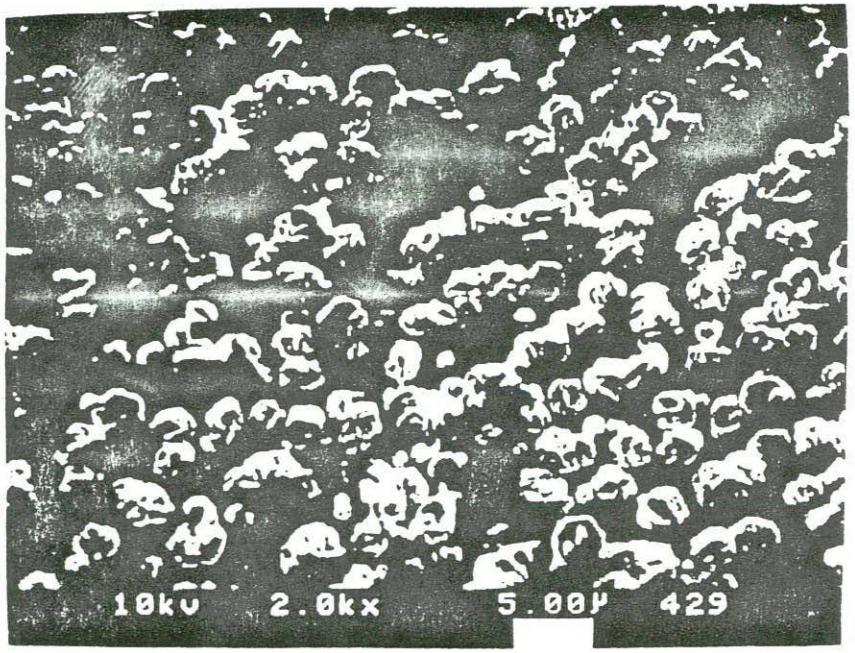


5086 FIRST ZINCATE

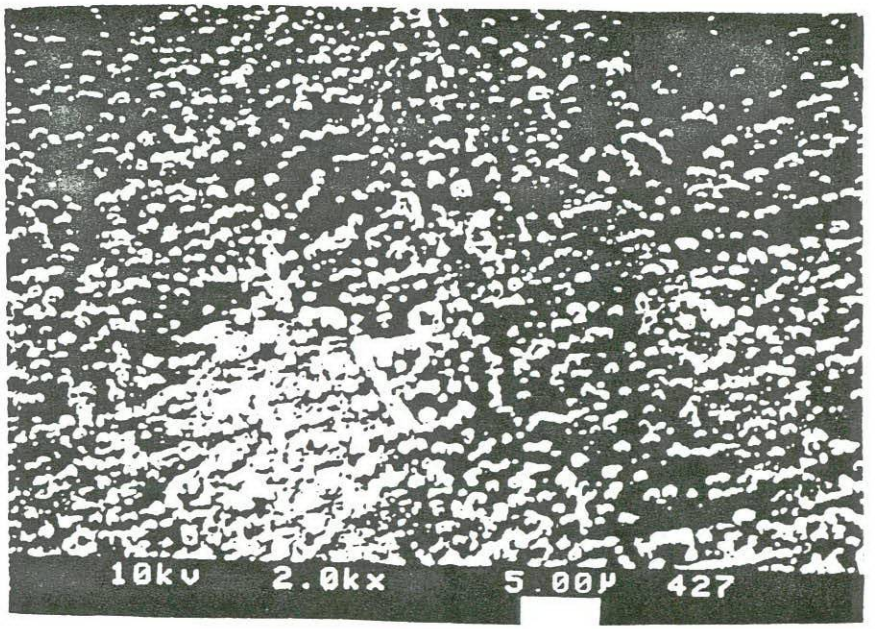


CZ46 FIRST ZINCATE

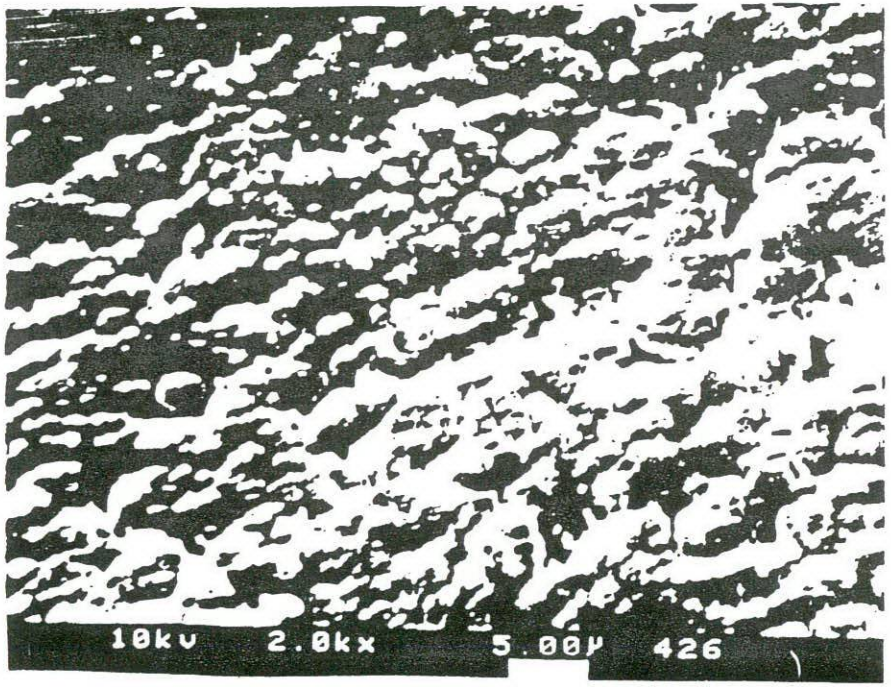


5086 SECOND ZINCATE

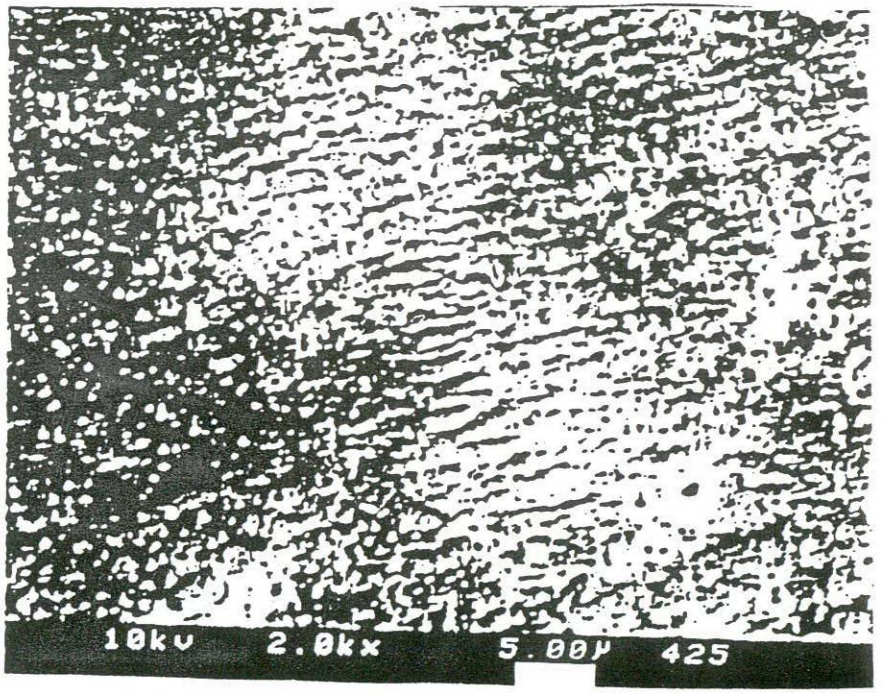


CZ46 SECOND ZINCATE

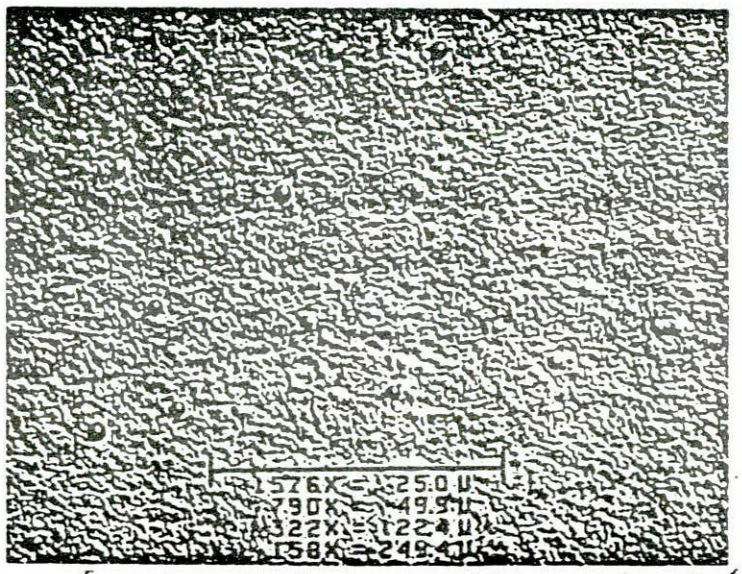


ALLOY 5586 160X

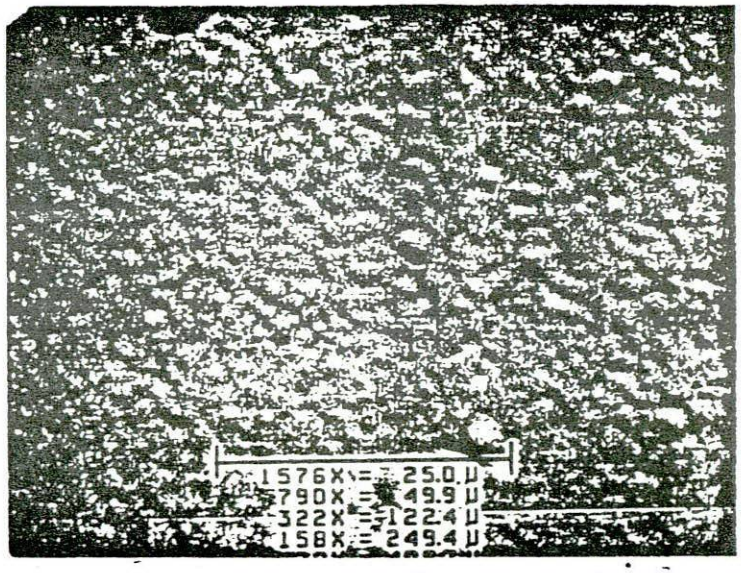


ALLOY 5086 250X

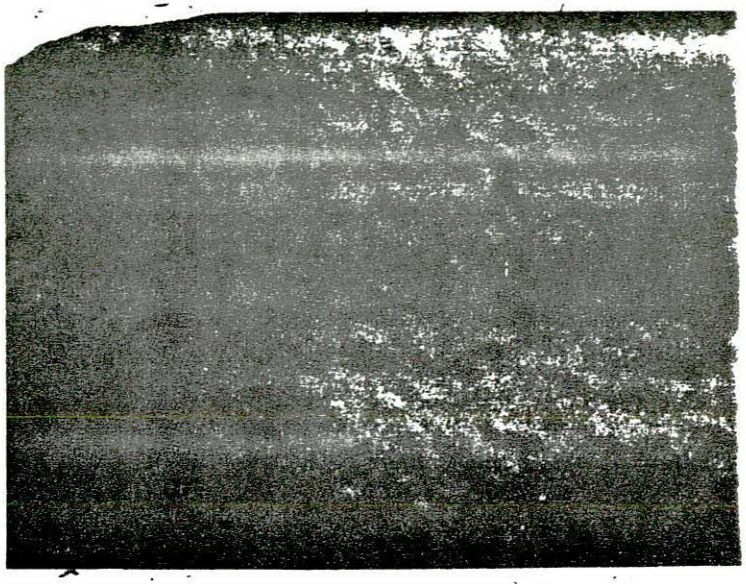

ALLOY CZ46 500X



ALLOY CW66 500X

Figure 2
EN Deposit on Various Alloys

# DEKTAK TRACES

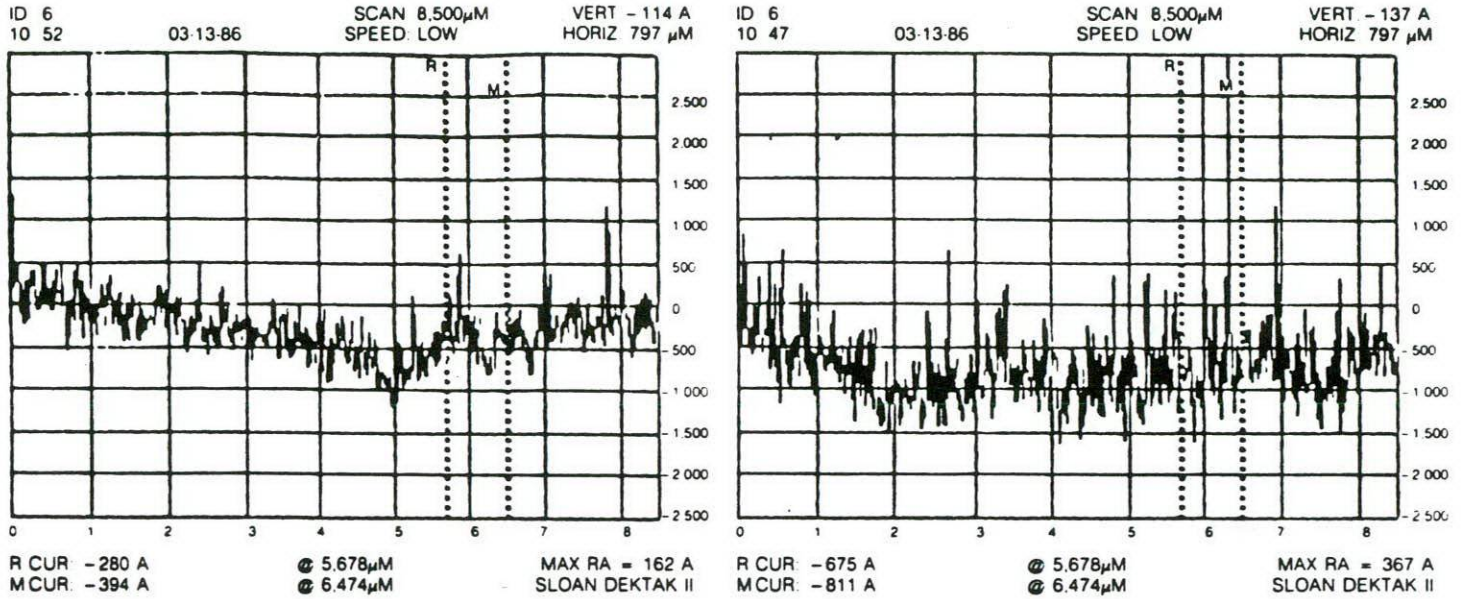


507X AS PLATED

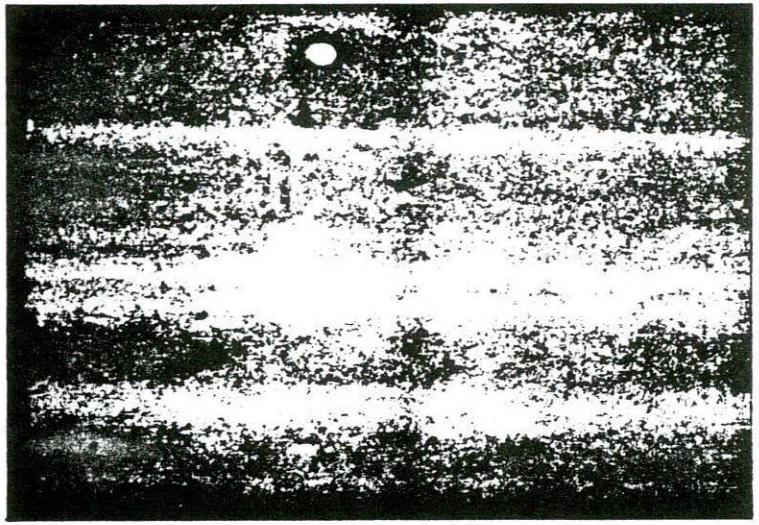

504X AS PLATED

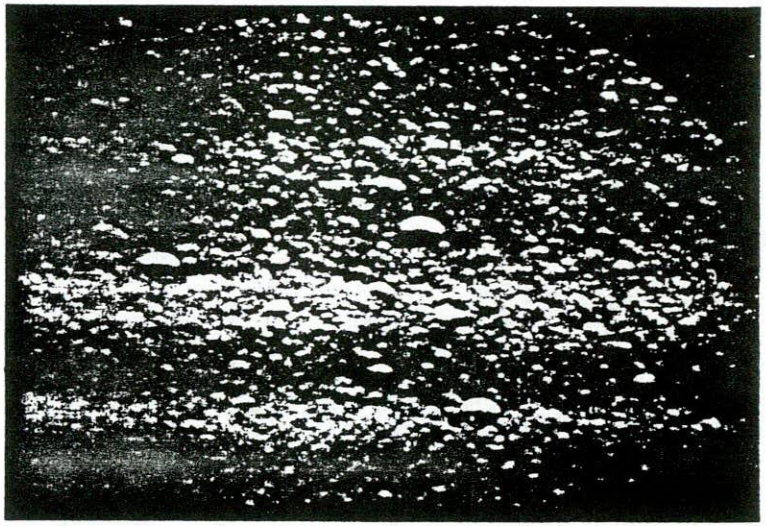

Figure 3

Two Different EN Coatings on 5586 P.T.

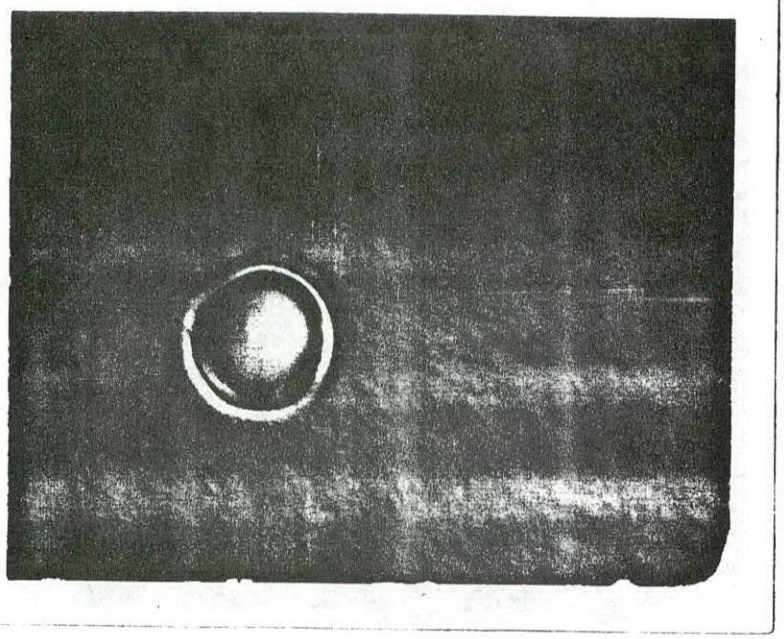

GAS PIT 500X

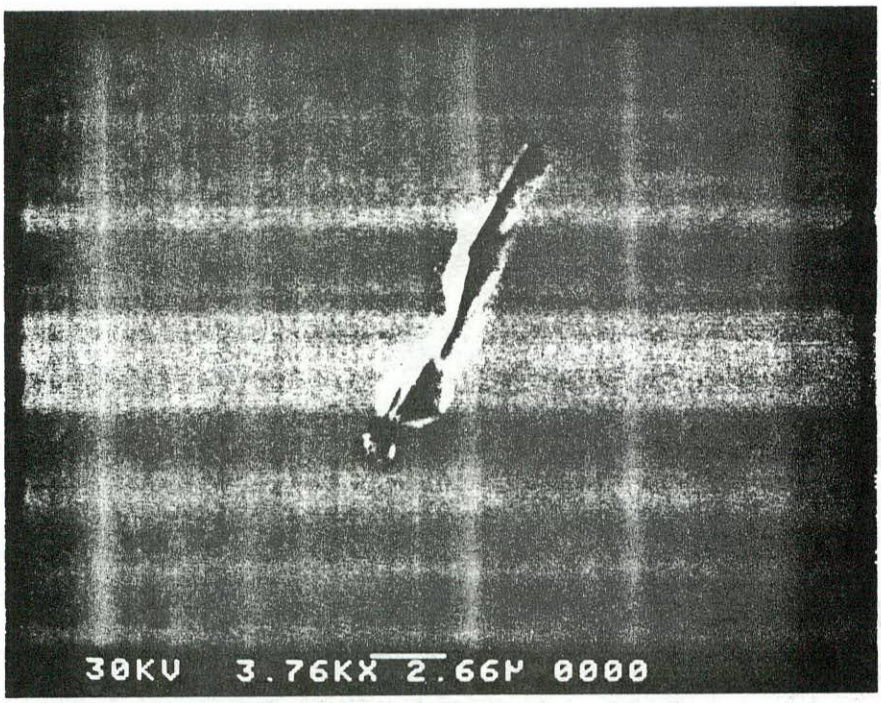


ORGANIC PARTICULATE 3760X

Figure 4

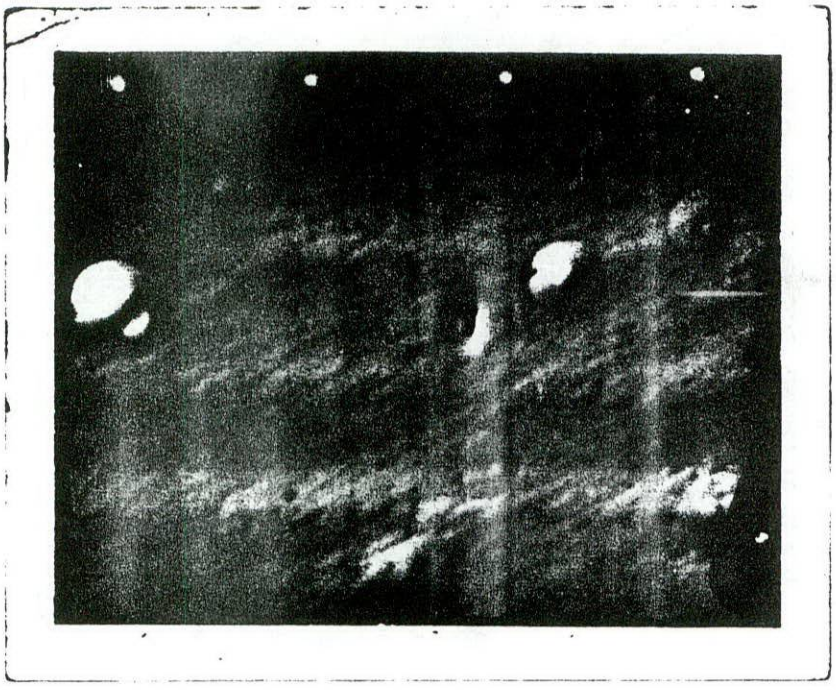

SHALLOW SPOTS 500X

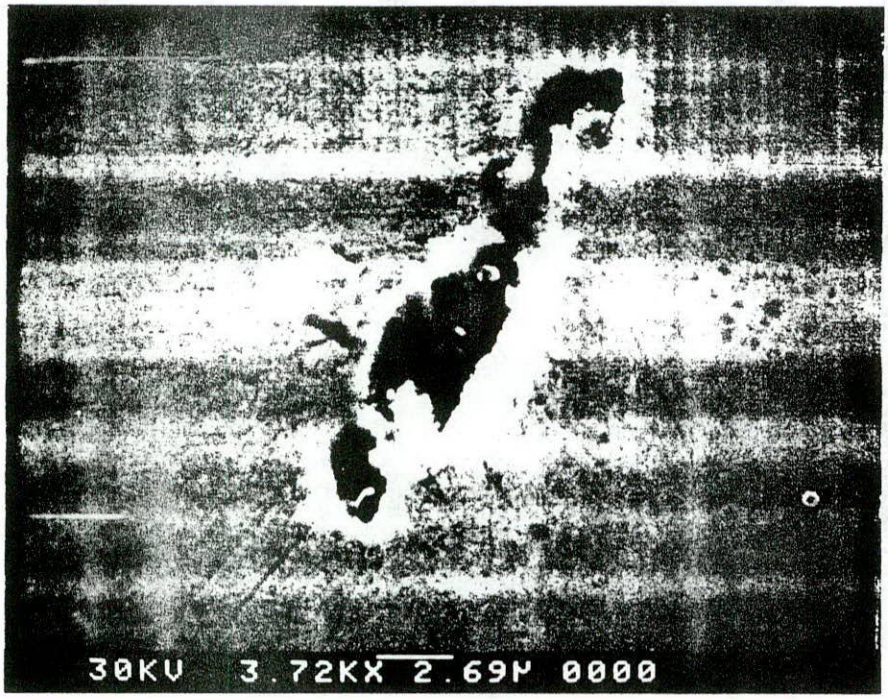


ORGANIC PIT 3720X

Figure 5

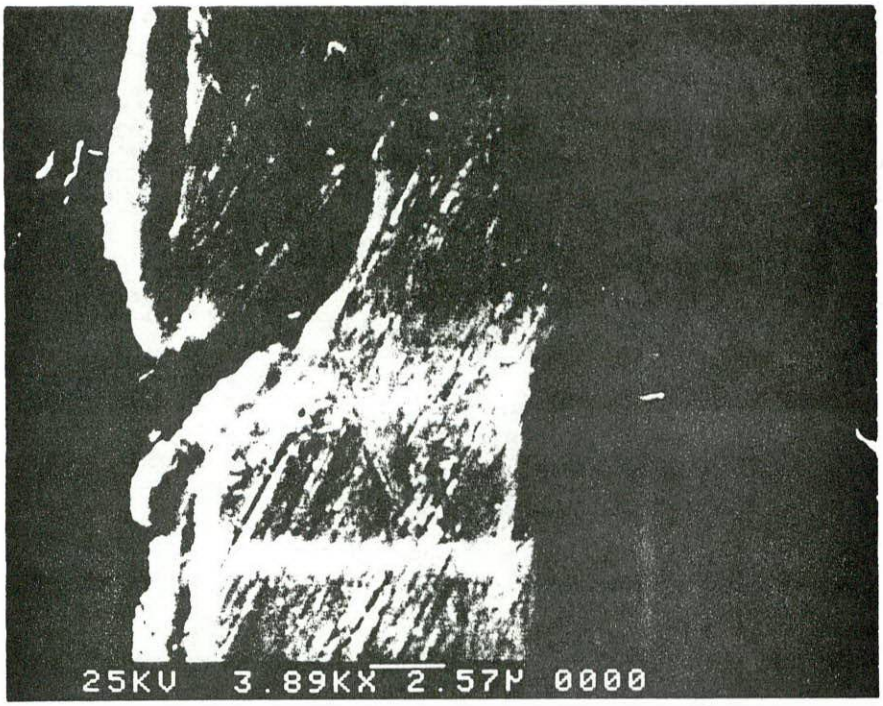


CROSS SECTION ORGANIC PIT 3890X

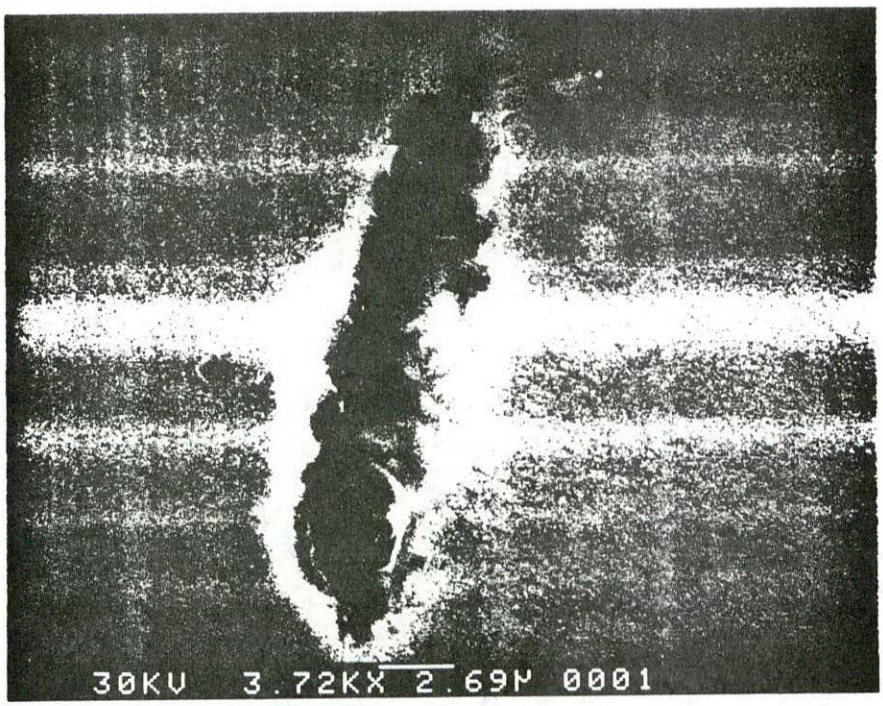


ORGANIC PIT 3720X

Figure 6

J-3

# Electroless Deposition II
# Session J

## Sublayer Processing for Rigid Memory Disks

D. Leibman
Shipley Company Inc.
Newton, MA

# Sublayer Processing for Rigid Memory Disks

**D. Leibman**
**Shipley Company Inc., Newton, MA**

## Introduction

Recently, rigid memory disks for high density magnetic recording have become a reality. After extensive laboratory development, many millions of disks are manufactured each year in modern production facilities throughout the world. The fast growth of thin-film recording media has opened new opportunities and established higher requirements for electroless plating processes.

Rigid memory disks (RMD) employed in high density recording (Winchester-type drives) consist of an aluminum substrate, a non-magnetic sublayer, a magnetic layer, and finally a protective overcoating. As both the magnetic layer and the overcoating are extremely thin films (approx. 500Å thick), properties of the sublayer become crucial to the overall performance of the disk. This layer must provide a hard durable surface with virtually zero defects (pits, nodules, etc.), while providing for adhesion both to the substrate and the magnetic layer. The crystalline structure of the sublayer can influence the properties of the magnetic layer and interfere with recording, so it must be amorphous and non-magnetic. The process described in this paper has been developed to satisfy all of the above requirements for the sublayer.

## Experimental

Aluminum alloy (5086 series) 5.25" diameter (140mm outside diameter with 40mm inside diameter hole) diamond turned disks were used as the substrate in our study. The disks were pretreated and plated using rotating fixtures. Evaluation of each step in the process was done based on measurements of surface roughness (Dektak IID by Sloan Technology), adhesion (180° bend test, conical mandrel bend tester), deposit thickness and uniformity (X-ray Fluorescence Thickness Analyzer SFT-157 by Seiko Instruments and Electronics Ltd.).

Deposit magnetic properties were determined in the as plated condition and after heat treatment at various temperatures and times using a vibrating sample magnetometer (VSM 155, EG&G Princeton Applied Research).

The crystalline structure of the deposit was analyzed by X-ray diffraction and Differential Scanning Calorimetry (DSC) techniques. In order to analyze defects which occurred during sublayer deposition, scanning electron microscopy ( using an ISI-100B SEM ) of the same area at each step of the process was done. The same evaluation was done for substrates prepared using a conventional pretreatment plating line (widely used by disk manufacturers at the present time) and served as the reference point in our study.

Results and Discussion:

Electroless nickel plating is an integral part of the disk manufacturing process. The quality of the electroless nickel deposit depends not only on the substrate material and its surface finish, but the chemical pretreatment process as well. It has a major effect on on subsequent process steps including mechanical polishing of the sublayer and deposition of the magnetic layer. Thus the quality of the electroless nickel deposit has a major impact on the ultimate performance of the memory disk.

Pretreatment process-In order to obtain a smooth, highly adherent nickel deposit on an aluminum alloy disk, several pretreatment steps are required. The disks must be cleaned (degreased but not etched) and then relieved of the tenacious oxide film which forms on aluminum when exposed to the atmosphere. By far the most popular method of removing this oxide film is based on the formation of an "immersion" zinc layer in alkaline solutions of zinc salts. It is commonly known as "zincating" (1). This layer provides a fresh, active surface for electroless nickel plating and assures adhesion of the deposit to the substrate.

We have developed a pretreatment process specifically for plating high density rigid memory disks. This process, combined with a proprietary electroless Ni-Cu-P alloy deposit, provides an extremely smooth, non-magnetic, bright sublayer coating. This proprietary pretreatment line features a very mild, non-etching alkaline cleaner, which is followed by a desmutter-conditioner and a unique acidic zincating solution. Details of process times and temperatures are given in Table 1.

**Pretreatment Process For electroless Ni-Cu-P deposition on 5086 Al-alloy RMD.**

Table 1

| Process Step | | | | Conditions |
|---|---|---|---|---|
| | Proprietory Solutions | Concentration | Time(min.) | Temp.(°F) |
| 1. | Alkaline cleaner | 20% | 5 | 135±5 |
| 2. | DI water rinse | | 2 | 70±2 |
| 3. | Conditioner | 20% | 45 sec. | 70+2 |
| 4. | DI water rinse | | 2 | 70±2 |
| 5. | Acidic zincate | 25% | 2 | 70±2 |
| 6. | DI water rinse | | 2 | 70±2 |
| 7. | Nitric acid strip | 50% | 1 | 70±2 |
| 8. | DI water rinse | | 2 | 70±2 |
| 9. | Acidic zincate | 25% | 2 | 70+2 |
| 10. | DI water rinse | | 2 | 70±2 |
| 11. | Electroless Ni-Cu-P Deposition at pH = 4.6 ± 0.5 T = 195±2°F, to 500 ± 50μ" thickness. | | | |

Disks prepared according to this process demonstrate very high adhesion of electroless nickel to the substrate. They pass 180° bend tests without any sign of deposit flaking on any part of the disk (no annealing was done prior to the test). As shown in Figures 1 and 2, the process provides a very fine , uniform zinc layer with low roughness. This assures rapid initiation of electroless nickel deposition and also results in an extremely smooth sublayer.

Electroless nickel bath- The proprietary electroless solution employed in this study produces an alloy deposit typically containing 86.5% Ni, 1.5% Cu, and12% P. The copper content of the deposit is largely responsible for its high brightness and smoothness. Presence of copper in the plating bath helps to assure stability. The phosphorus content of an electroless nickel deposit determines its crystalline structure and magnetic properties (2). Buildup of orthophosphite in the plating solution slows the rate of deposition and can eventually cause bath decomposition. Therefore, bath performance was evaluated here by measuring the deposition rate under various plating conditions (temperature, pH, number of cycles or bath metal turnovers) and determining the effect of these variables on the P and Cu contents of the deposit.

As with most electroless nickel solutions, the rate of deposition in this bath increased with increasing temperature and pH, while Cu and P content of the deposit decreased (Fig. 3,4) with increasing temperature and pH. Analysis of deposit properties showed that high Cu and low P content result in rough deposits. Such deposits can be slightly magnetic as plated and will recrystallize easily at elevated temperatures to become highly magnetic. In order to avoid degradation of magnetic properties while still maintaining a rather high rate of deposition (0.4 mil/hr.) this bath should be operated at 195°F and a pH of4.6±.5

The performance of this plating solution has been extensively studied by Dr. S. K. Doss (3). His results are in good agreement with this study. If operated at optimum conditions, the bath exhibits a slight decrease in the rate of deposition after 2.5 cycles. The Cu content in the deposit is very consistent, Figure 5. Consistency of performance that is independent of the number of plating cycles separates this bath from many other electroless nickel solutions presently used for rigid memory disks. It also makes possible complete automation of the plating line.

Deposit roughness- As has been demonstrated above, immersion zinc deposits from acidic zincating solutions are very thin, extremely fine, and uniform. Deposition of an electroless Ni-Cu-P alloy over the acidic zinc immersion coating produces a sublayer with an Ra (average surface

roughness) of 80 ± 5Å. This compares very favorably with an Ra of 180± 10Å for the surface finish achieved through conventional pretreatment processes. Such a low roughness of the Ni-Cu-P sublayer can be very beneficial to further disk processing. It allows the manufacturer to reduce sublayer polishing time or in some cases avoid it entirely.

Deposit crystallinity- The crystal structure of the sublayer can affect crystallinity and therefore the magnetic properties of the recording layer (4). In order to avoid such interference, the sublayer must be amorphous. X-ray diffraction and differential scanning calorimetric analysis (Fig. 6) shows that the Ni-Cu-P alloy produced in our process has no definite crystalline structure (i.e. was amorphous) in the as plated condition and after heat treatment at 250°C for one hour. No changes in structure occurred up to 325°C but strong recrystallization took place at that temperature leading to changes in deposit characteristics, especially the magnetic parameters.

Deposit magnetic properties-It is absolutely crucial to disk performance that the sublayer remain non-magnetic during the manufacturing process. A sublayer displaying ferromagnetic behavior can interfere with the read/write process by causing losses in signal amplitude, peak-shifts, and a decrease in resolution. Measurements of magnetic parameters of the deposit (magnetization-$M_S$, retentivity-$B_r$) showed that the deposit did not change the magnetic behavior of the Al-alloy substrate (Fig. 7). It stayed non-magnetic even after heat treatment at 250°C for up to five hours (Figure 8) or at 275°C for one hour (Figure 9).

Sublayer coating defects-Testing of the finished RMD showed a direct correlation between defects in the recording (missing or extra bit, low signal to noise ratio etc.) and the surface condition or defects in the sublayer (pits and nodules). A scanning electron microscope study of the nature of defects in the sublayer (5) showed that nodules and deposit roughness are mainly related to the plating solution formulation. However pitting, the most frequently encountered problem, depends on the substrate material and the pretreatment process. As the substrate contains intermetallic inclusions (Mg, Mn, Si) which can be easily etched out even in mild cleaners, some pits in the aluminum substrate are probably unavoidable. The task of the sublayer coating is to correct substrate defects caused by mechanical handling and chemical processing without introducing defects of its own. According to SEM study (Fig. 10) this can be achieved by using the proper pretreatment solutions which include a mild cleanerand an acidic zinc immersion coating applied under optimum conditions. The high rate of deposition and formulation of the Ni-Cu-P plating solution provides rapid fill-in of substrate defects. This

is practically complete during the first 5 minutes of plating and leads to a bright, uniformly smooth surface.

## Summary

Standards for rigid memory disks used for high density magnetic recording demand that the sublayer meet very stringent requirements for surface finish and non-magnetic behavior. These requirements can be satisfied by the electroless deposition of a Ni-Cu-P alloy, combined with a unique pretreatment process designed specifically for applying the sublayer to RMD aluminum alloys. The sublayers produced in our study are amorphous alloys that are bright, smooth and non-magnetic. This alloy deposit retains all of its non-magnetic behavior even after heating at 250°C for 5 hours. The electroless bath used to apply this alloy deposit maintains a consistent deposit composition and plating rate up to at least 2.5 bath turnovers.

## Acknowledgements

The author would like to thank Anthony J. Marczak and Howard A. MacKay for their help in collecting the data on the Ni-Cu-P plating parameters, deposit composition, and solution formulations. Special thanks to Gabrielle Bene for her expertise and valuable advice in the SEM study of the process. Also thanks to Rolf Krause and Gordon Fisher whose constant interest and participation in discussions made this paper possible.

References


1. S. Wernick, R. Pinner, Finishing of Aluminum, Robert Draper LTD, 1959.

2. Konrad Parker, "Effects of Heat Treatment on the Properties of Electroless Nickel Deposits", Plating and Surface Finishing, Dec. 1981.

3. Saad K. Doss, "Electroless Nickel-Phosphorous-Copper Plating Bath Performance and Its Relation to Deposition Parameters", ECS Meeting, Honolulu, HA, Oct. 1987.

4. B.D. Cullity, Introduction to Magnetic Materials, Addison-Wesley, 1972.

5. Robert W. Dummer, "Magnetic Disk Substrate Overview", IRTC Papers, CDC, 1981.

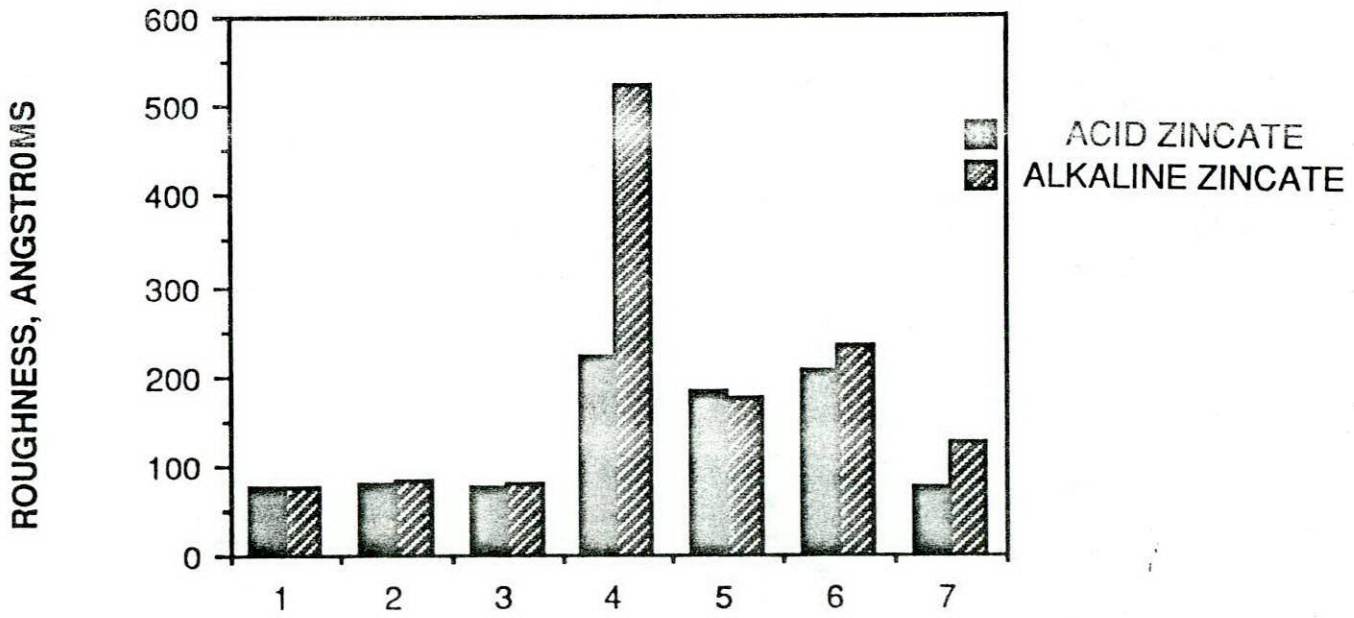


**FIG. 1 COMPARISON OF SURFACE ROUGHNESS AT DIFFERENT STAGES OF SUBLAYER PROCESSING WHEN USING ACIDIC AND ALKALINE ZINCATE**

1 - DIAMOND TURNED 5086-AL SUBSTRATE
2 - SAME SUBSTRATE AFTER CLEANING
3 - CLEANING / CONDITIONING
4 - FIRST ZINCATING
5 - NITRIC ACID STRIP
6 - SECOND ZINCATING
7 - ELECTROLESS NI-CU-P DEPOSIT (400μ")

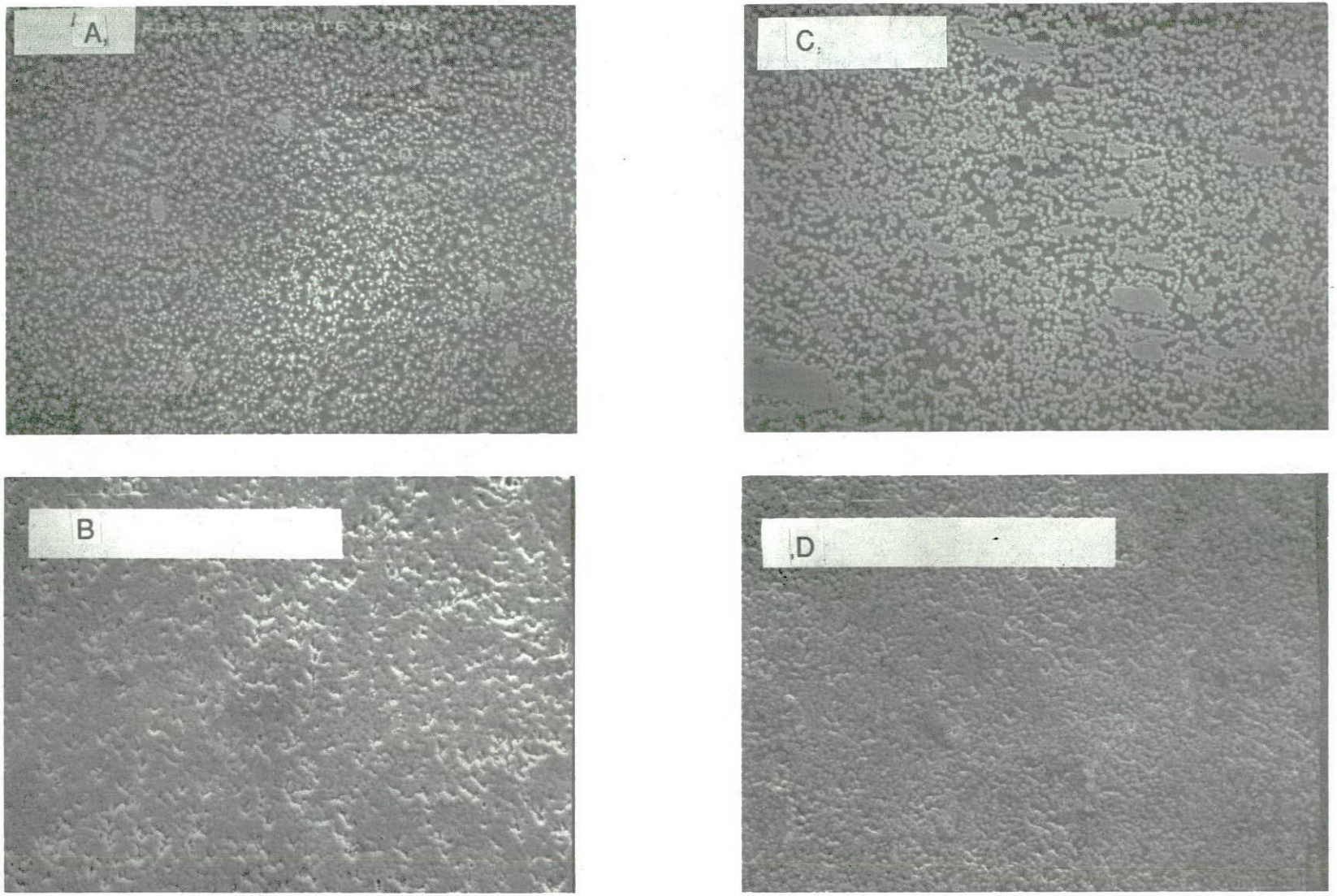


FIG.2 5086 AL-ALLOY DIAMOND TURNED SUBSTRATE AFTER FIRST AND SECOND ZINCATING STEPS CONVENTIONAL ALKALINE (C,D) SOLUTONS. SEM PICTURES, 750X

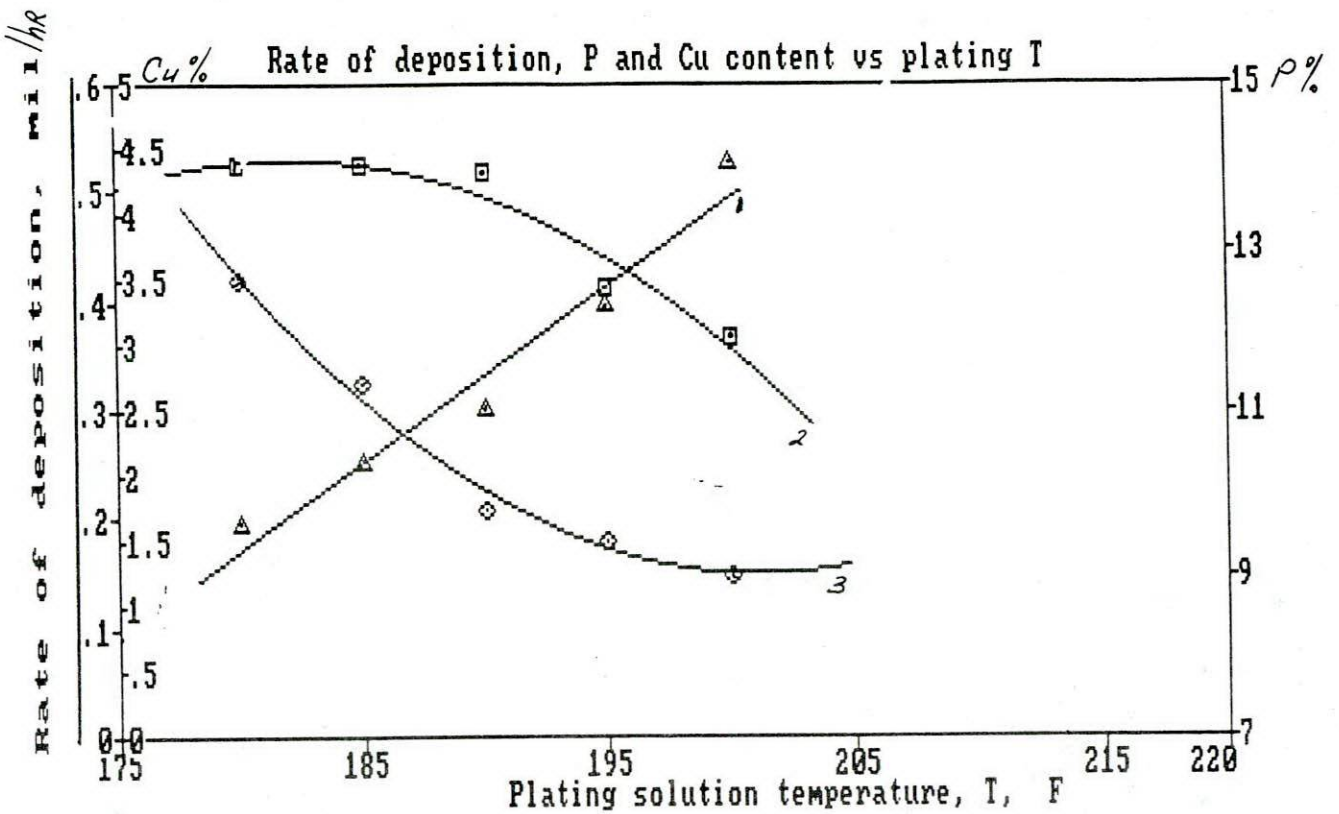


**FIG. 3 EFFECT OF THE PLATING TEMPERATURE (T) ON THE RATE OF NI-CU-P DEPOSITION (R), PHOSPHOROUS (P) AND (CU) CONTENT IN THE DEPOSIT.**

1-RATE OF DEPOSITION

2-P CONTENT IN THE NI-CU-P ALLOY

3-CU CONTENT IN THE NI-CU-P ALLOY

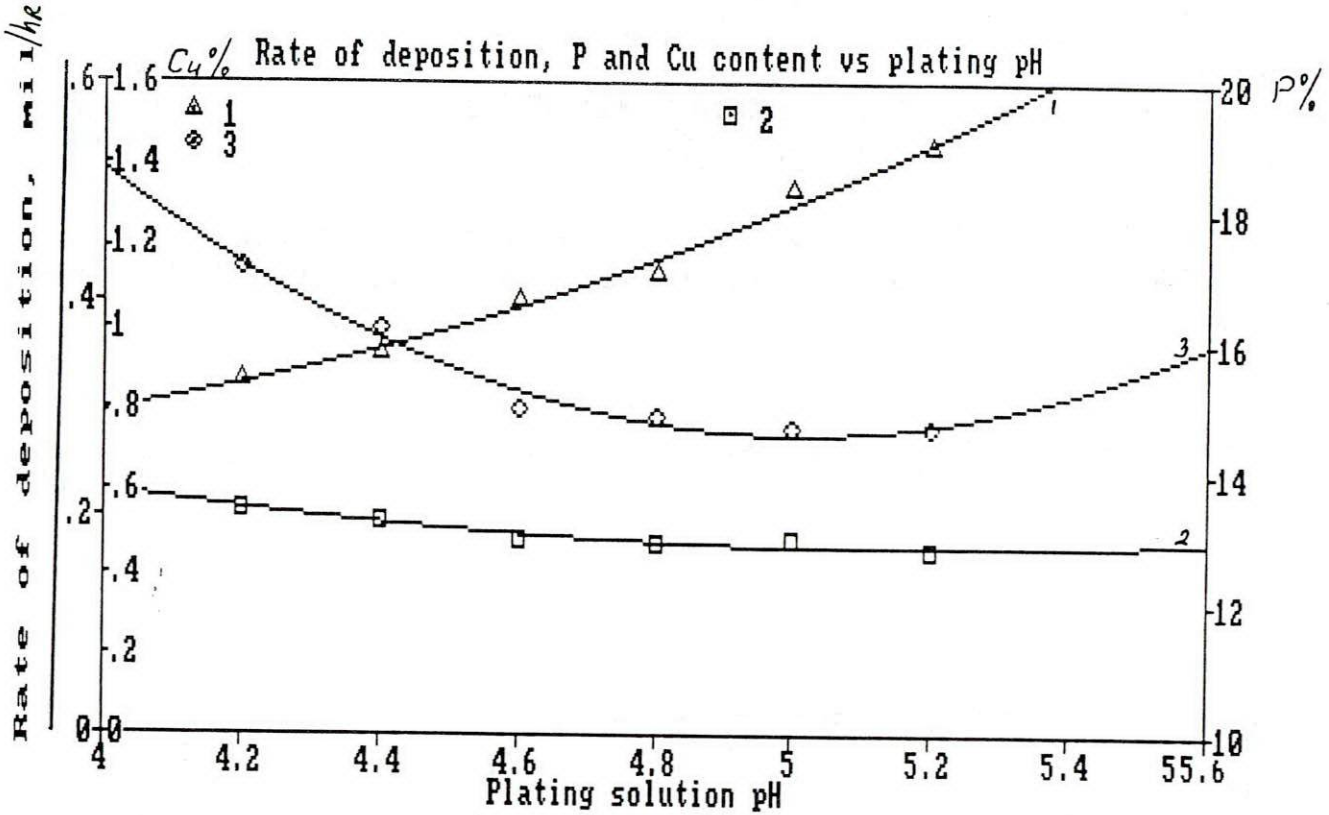


**FIG. 4 EFFECT OF THE PLATING SOLUTION PH ON THE RATE OF NI-CU-P ALLOY DEPOSITION ( $R$ ), PHOSPHOROUS (P) AND COPPER (CU) CONTENT IN THE DEPOSIT**

1-RATE OF DEPOSITION

2-P CONTENT IN THE NI-CU-P ALLOY

3-CU CONTENT IN THE NI-CU-P ALLOY

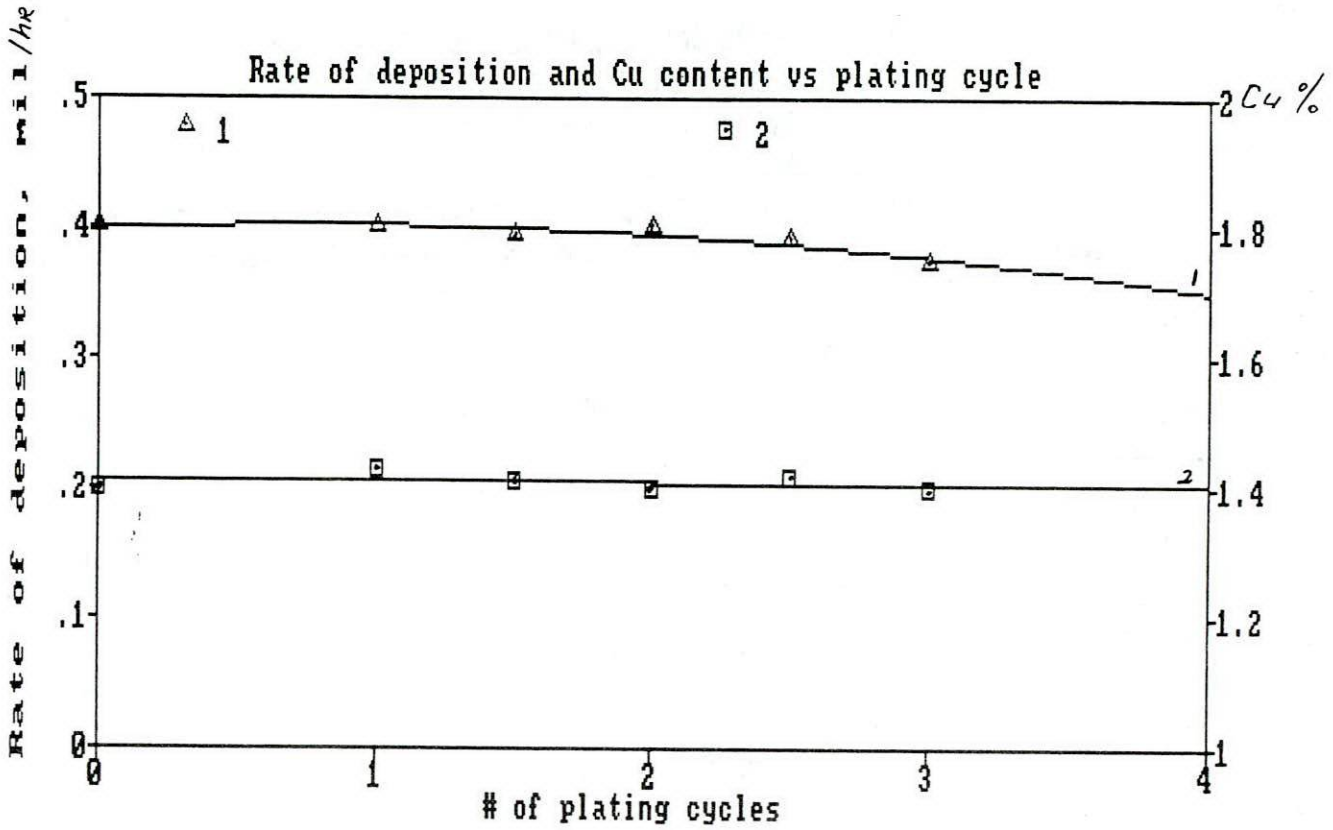


**FIG . 5 DEPENDENCY OF THE RATE OF DEPOSITION ($R$) AND COPPER CONTENT (CU) IN THE DEPOSIT ON THE NUMBER OF THE PLATING CYCLES.**

1- RATE OF DEPOSITION

2- CU CONTENT IN THE DEPOSIT

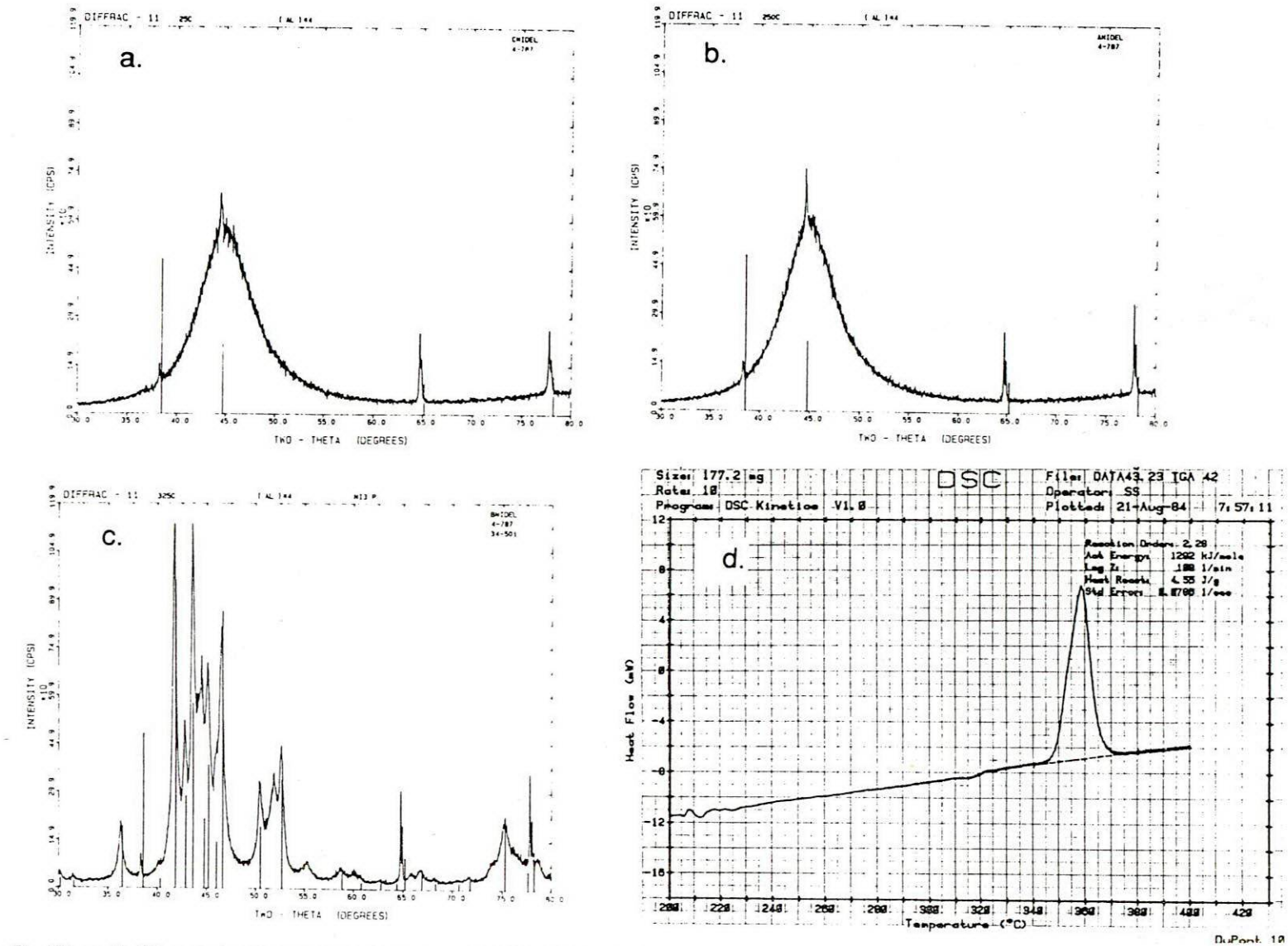


**Fig. 6 Crystalline structure and recrystallization temperature range of electrolessly deposited Ni-Cu-P alloy.**

a. X-ray diffraction of as plated sample b. X-ray diffraction of heat treated sample at 250°C for 1 hour.

c. X-ray diffraction of heat treated sample at 325°C for 1 hour. d. Recrystallization range via DSC analysis.

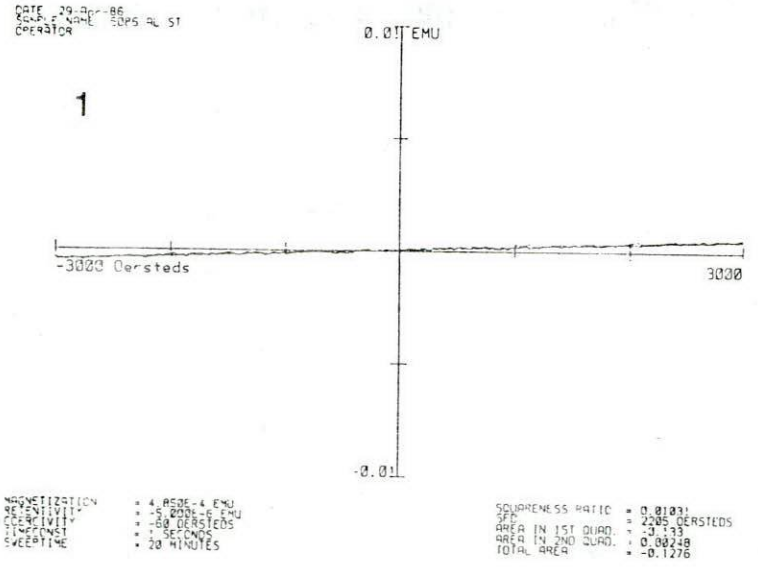


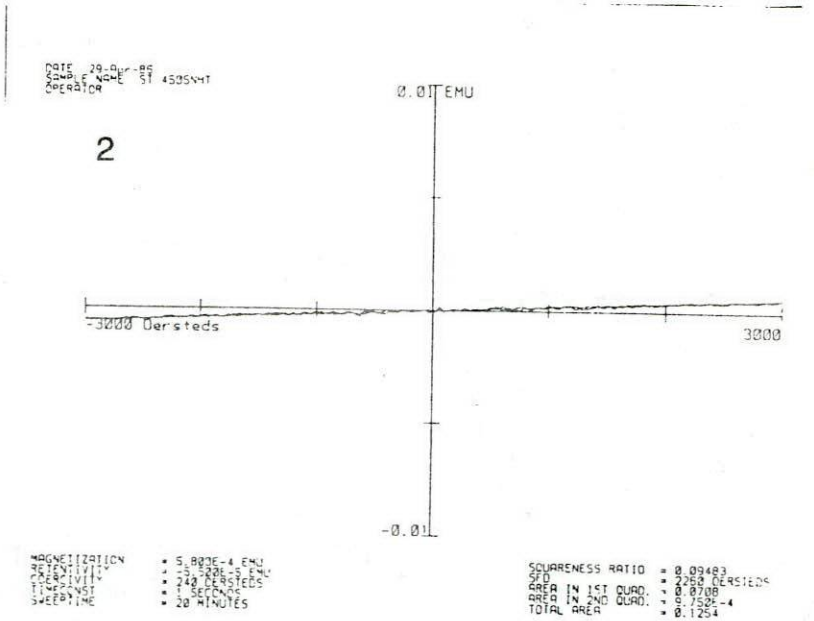


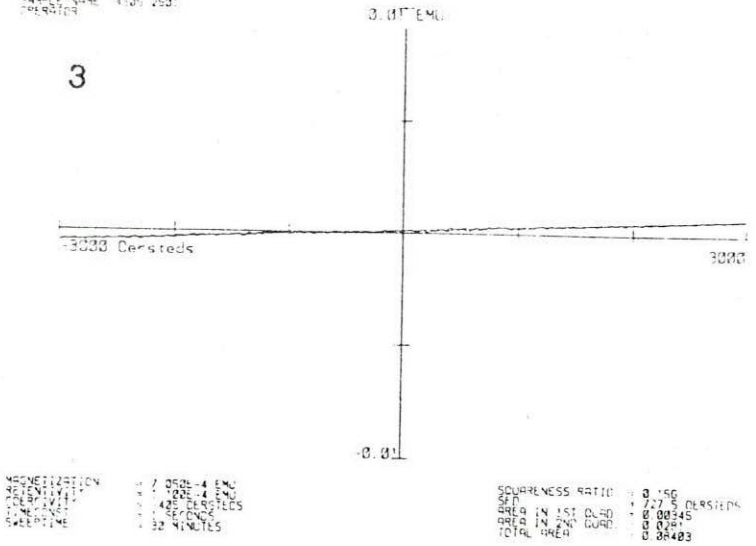


**Fig. 7 Magnetic parameters of the electrolessly deposited Ni-Cu-P alloy (500μ" thick)**

1- VSM chart of 5086 Al-alloy substrate (reference).
2- VSM chart of "as plated" Ni-Cu-P deposit (500μ" thick) over the same substrate.
3- 250° / 1 hr. heat treatment.

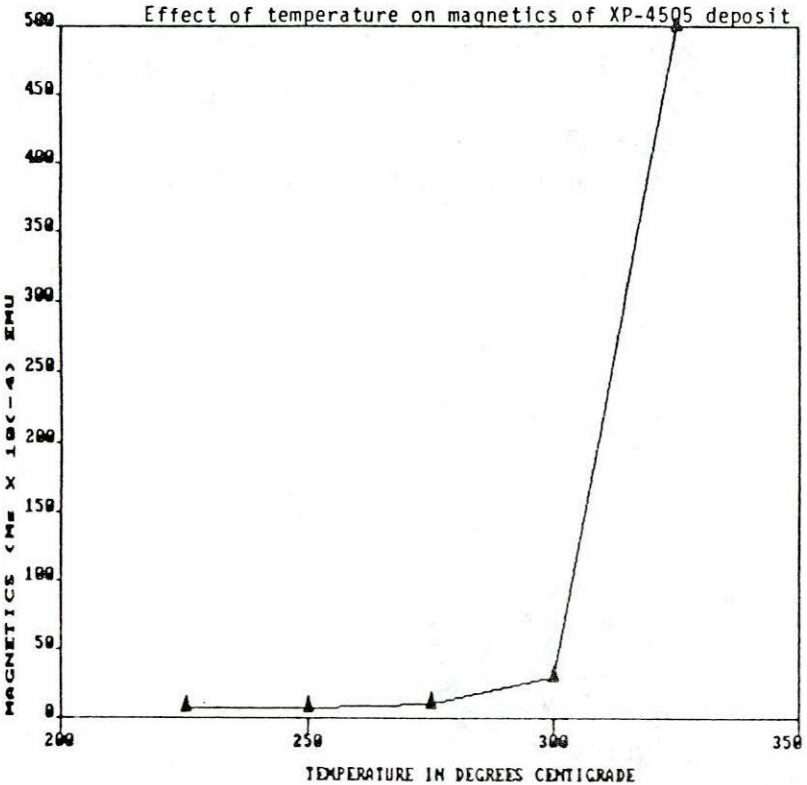


**Fig. 8 Effect of the heat treatment temperature on the Ni-Cu-P deposit's magnetic parameters ($M_S$).**

Magnification ($M_S$) vs. T° applied for 1 hour

Sample size : 0.25x0.25"; 500μ" deposit thickness on each sample side.

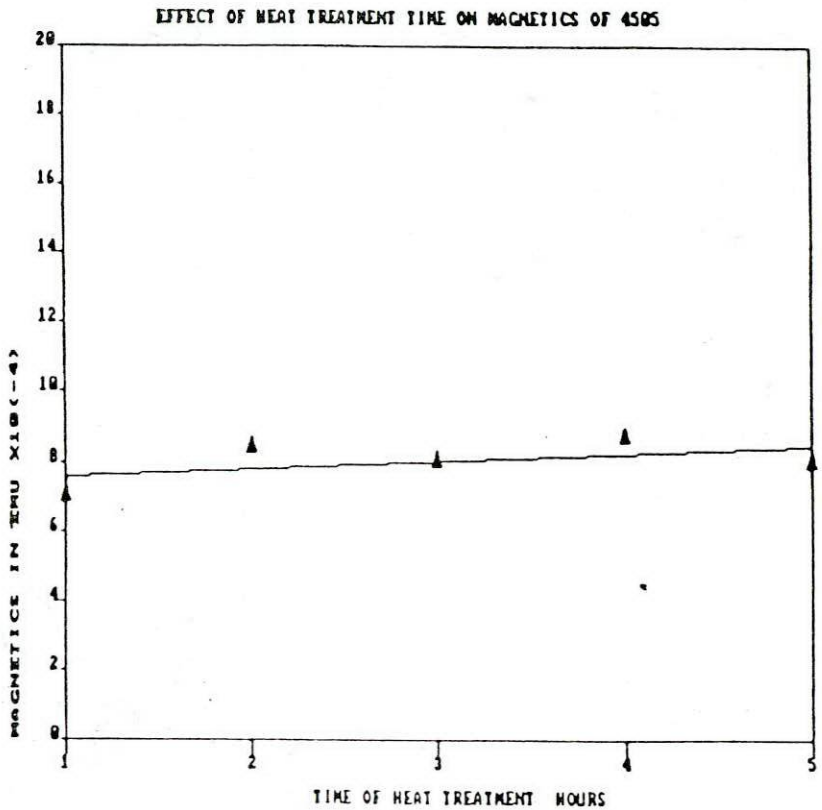


**Fig. 9 Effect of the heat treatment time on the Ni-Cu-P deposit's magnetic parameters ($M_S$)**

Heat treatment was done at 250°C for each period of time. Sample size: 0.25 x 0.25", 500μ" deposit thickness on each sample size.

**SEM study of the defects nature and correction through electroless sublayer deposition.**

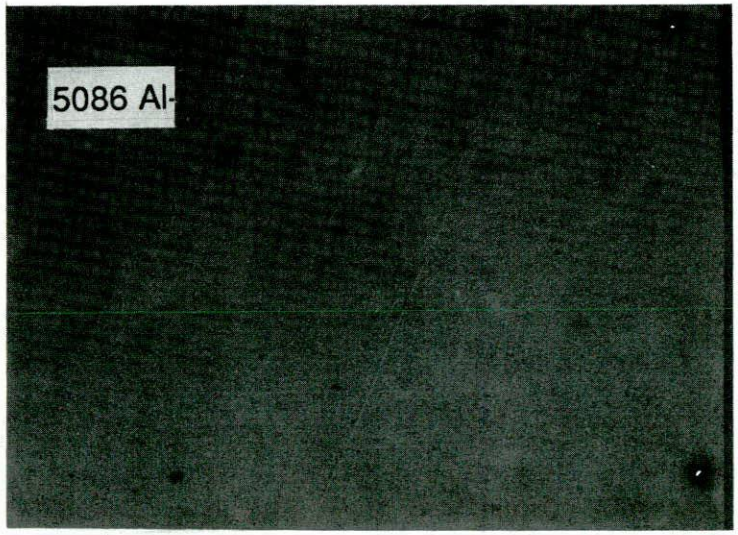


Diamond-turned 5086 Al-alloy substrate prior to processing 1500 X

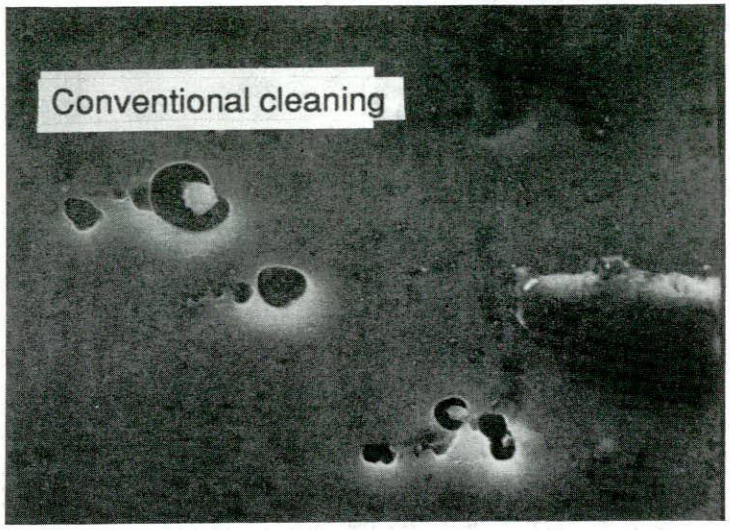


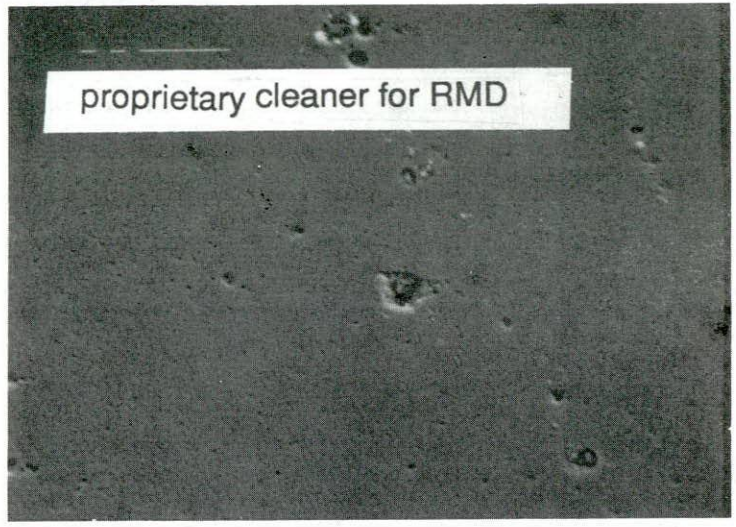


Same substrate after cleaning-degreasing at optimized conditions.

Same substrate after 1st. zincating step at optimum conditions.

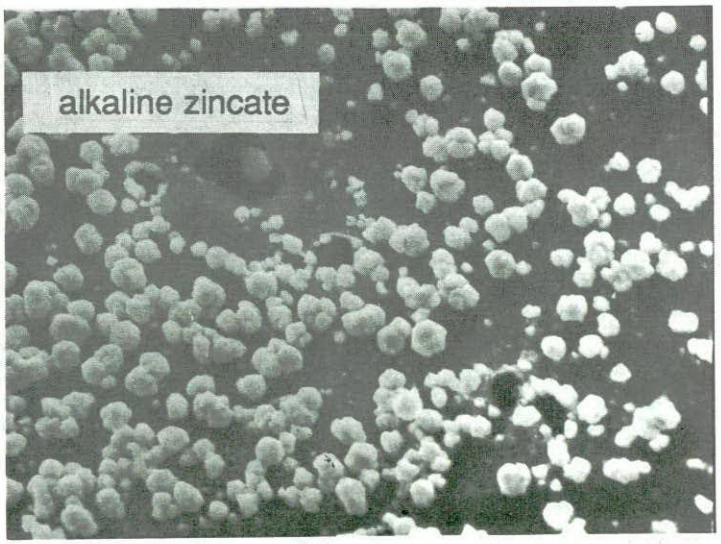


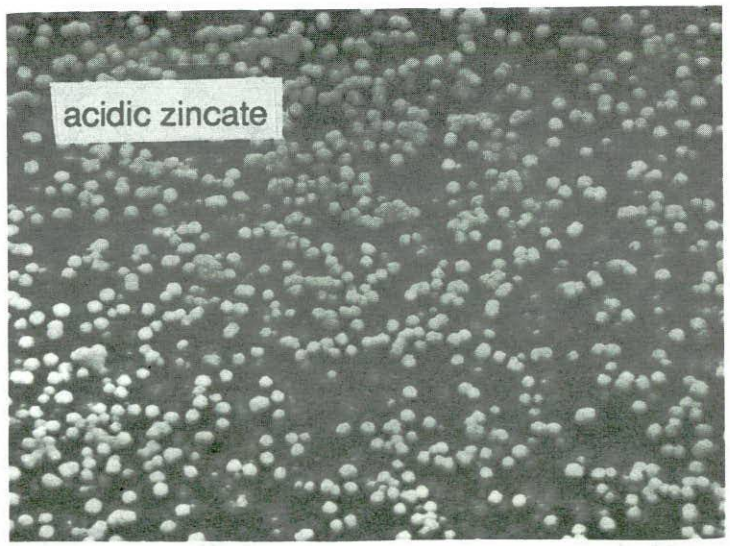


Same substrate after nitric strip following first zincating.

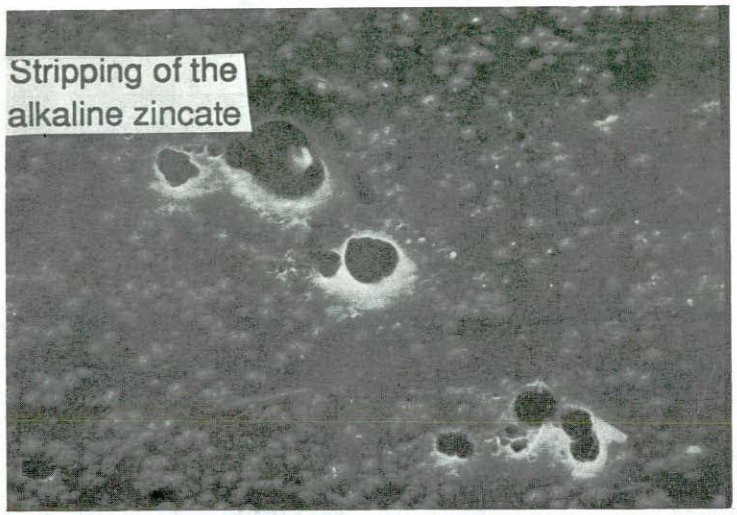


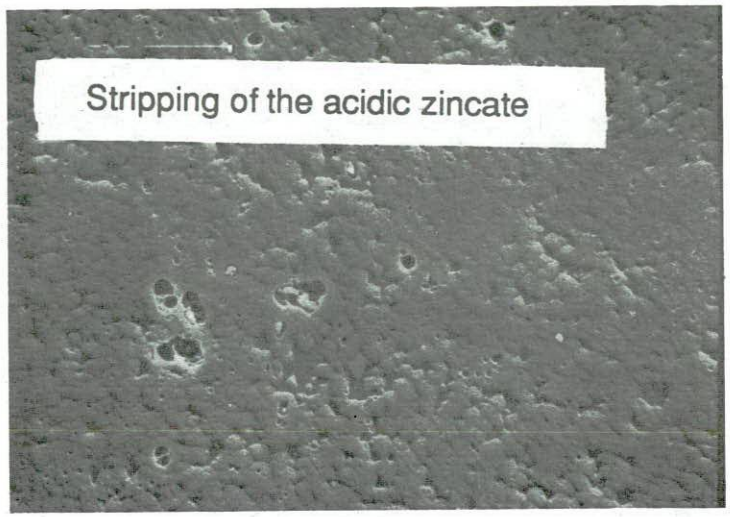

Same substrate after second zincating at optimum conditions

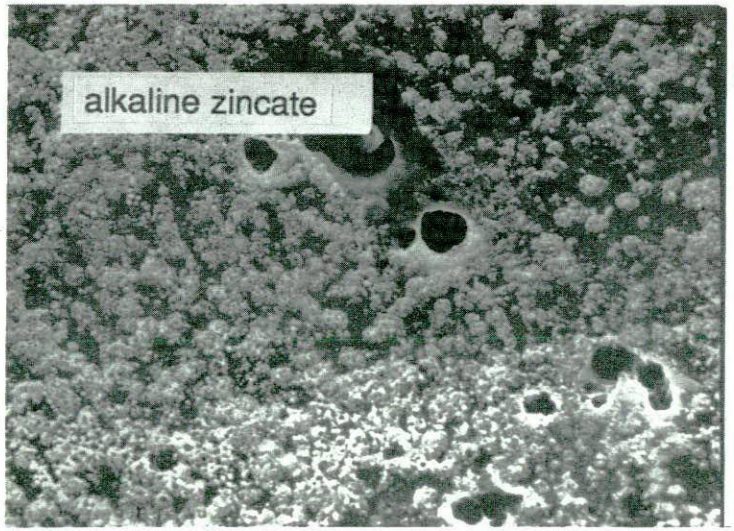


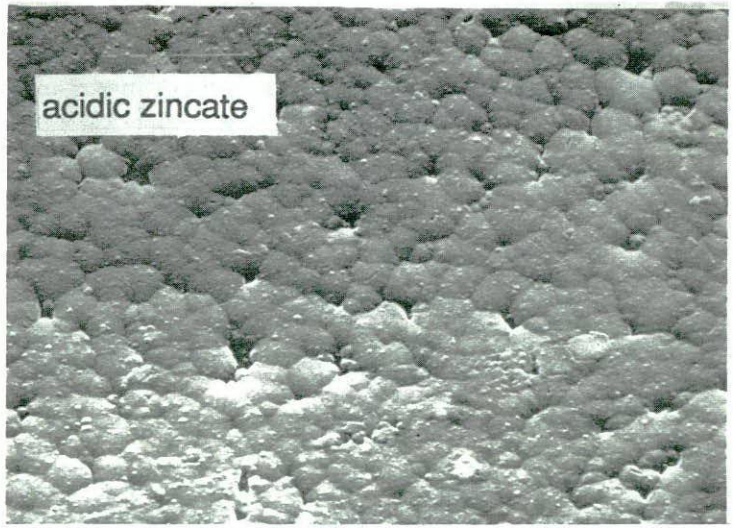


Same substrate during electroless nickel deposition for 20 sec,

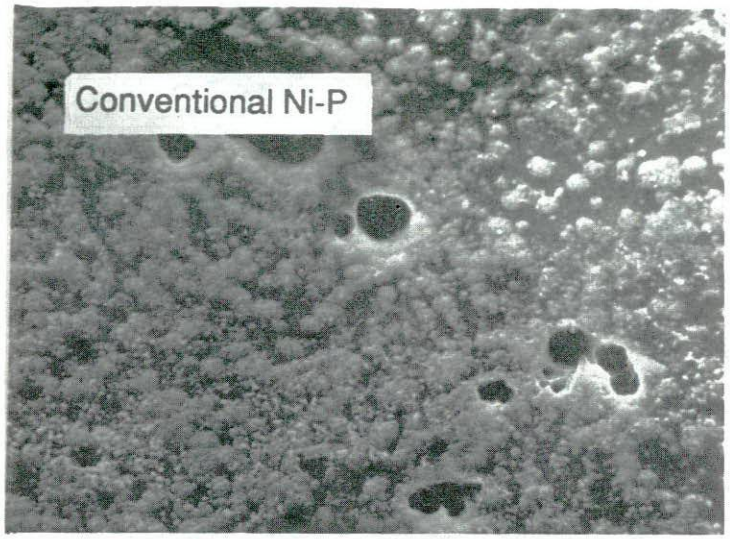


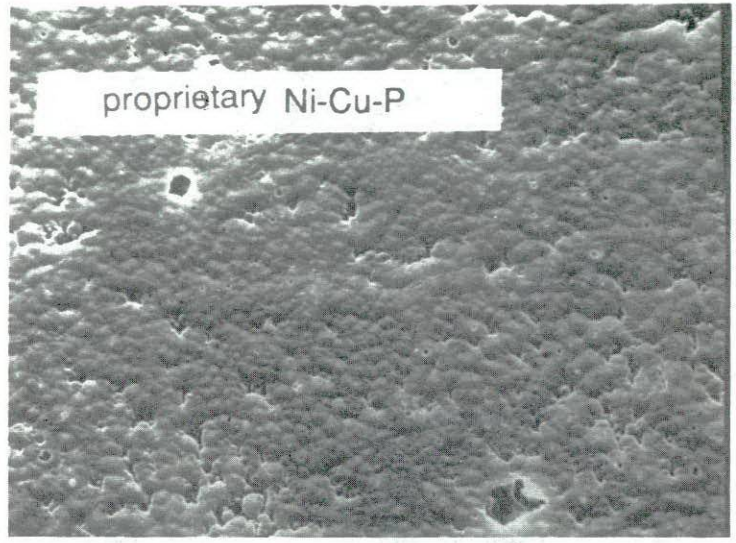

Same substrate during electroless nickel deposition for 1 min.

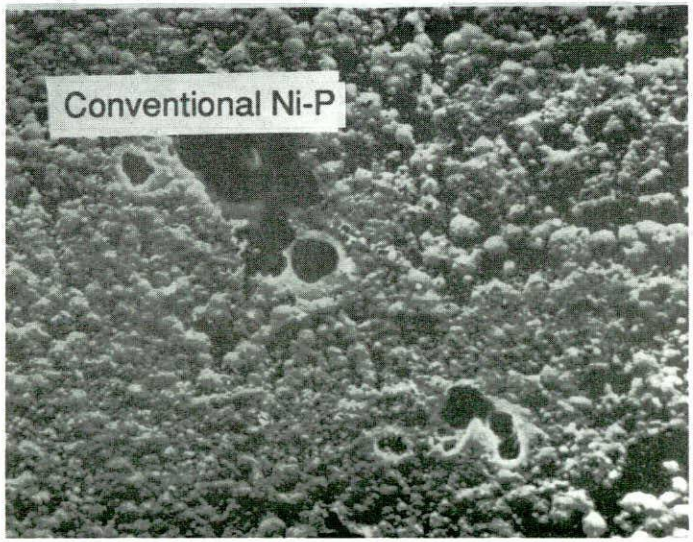


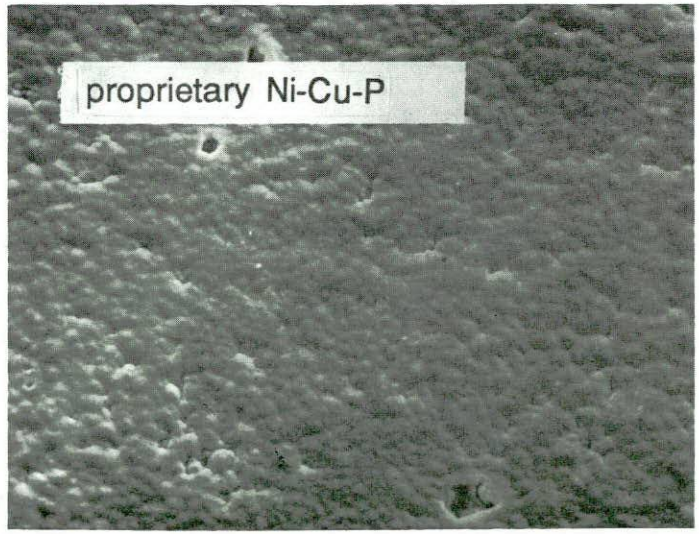


Same substrate during electroless nickel deposition for 5 min.

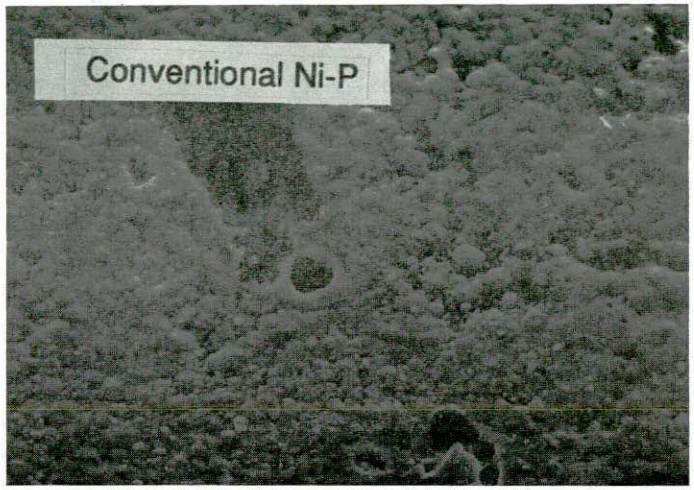


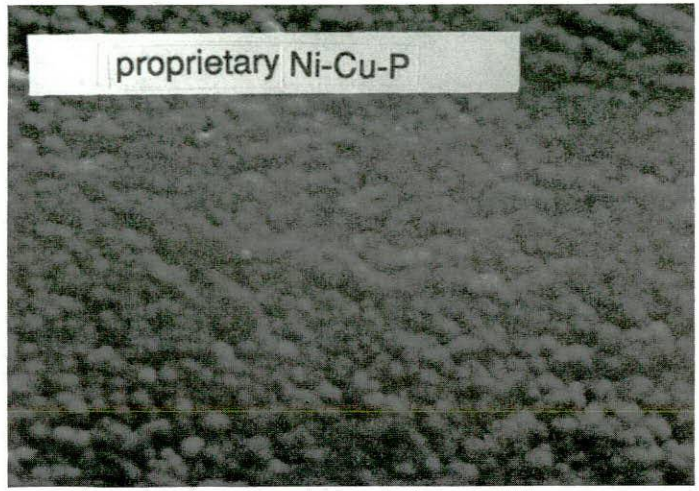

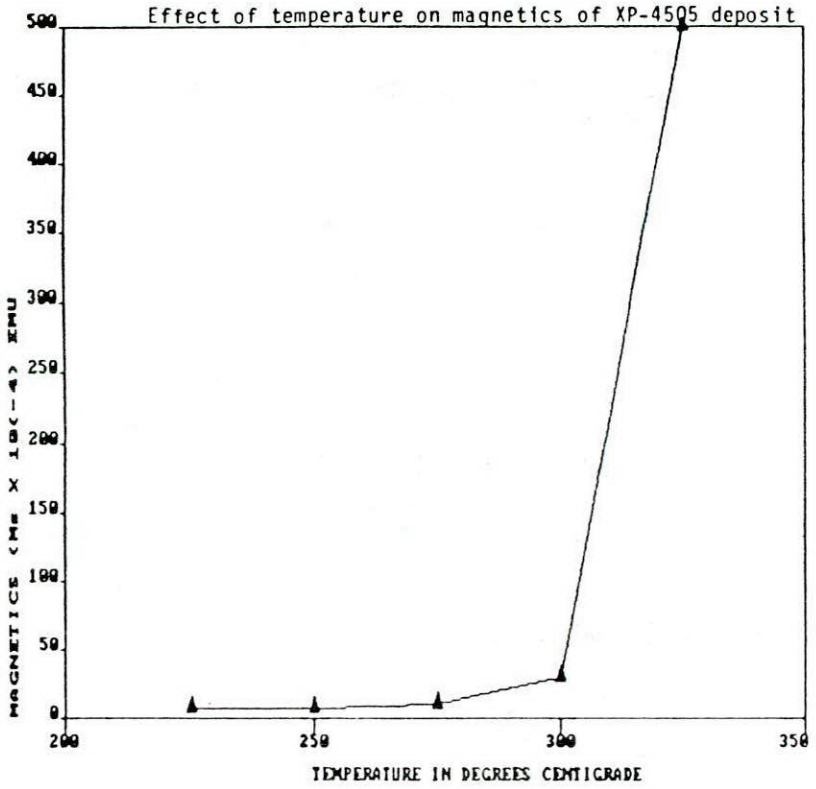


**Fig. 8 Effect of the heat treatment temperature on the Ni-Cu-P deposit's magnetic parameters ($M_S$).**

Magnification ($M_S$) vs. T° applied for 1 hour

Sample size : 0.25x0.25"; 500μ" deposit thickness on each sample side.

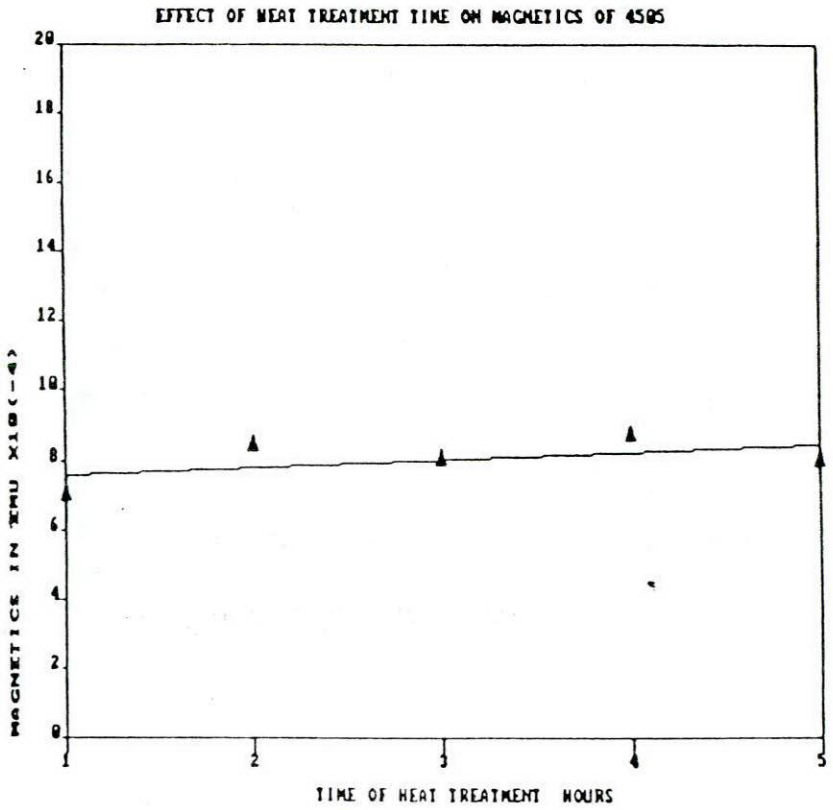


**Fig. 9 Effect of the heat treatment time on the Ni-Cu-P deposit's magnetic parameters ($M_S$)**

Heat treatment was done at 250°C for each period of time. Sample size: 0.25 x 0.25", 500μ" deposit thickness on each sample size.

J-4

# Electroless Deposition II
# Session J

## Mechanism of Electroless Nickel Deposition: A Review

Glenn O. Mallory
Electroless Technologies Corp.
Los Angeles, CA

# MECHANISM OF ELECTROLESS NICKEL DEPOSITION: A REVIEW

**Glenn O. Mallory**

**Electroless Technologies Corporation**
**Los Angeles, California**

## INTRODUCTION

Four reducing agents are used in the chemical reduction of nickel from aqueous solutions:

Sodium Hypophosphite

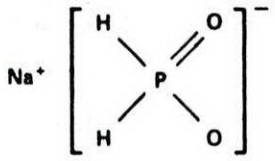

$NaH_2PO_2 \cdot H_2O$

Sodium Borohydride

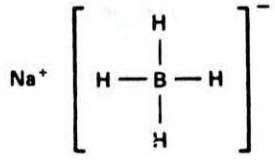

$NaBH_4$

Dimethylamine Borane (DMAB)

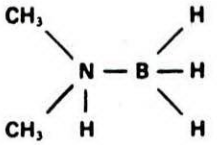

$(CH_3)_2NHBH_3$

Hydrazine

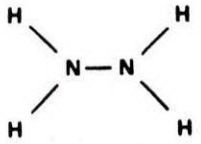

$N_2H_4 \cdot H_2O$

The four reducing agents are structurally similar in that each contains two or more reactive hydrogens, and nickel reduction is said to result from the catalytic dehydrogenation of the reducing agent.

Electroless nickel deposition can be viewed, in a very elementary manner, as the sum of two chemical reactions occurring in an electrochemical cell — an oxidation reaction that liberates electrons, and a reduction reaction that consumes electrons:

Oxidation of reducing agent:

$$Red \longrightarrow Ox + ne$$

Reduction of nickel ion:

$$mNi^{+2} + 2me^{-} \longrightarrow mNi^{0} \quad , 2m = n$$

With the overall or sum reaction:

$$mNi^{+2} + Red \longrightarrow mNi^{0} + Ox$$

The sum equation is a schematic illustration of the type of stoichiometric reactions usually written to describe the chemical reduction of nickel by a reducing agent. However, these overall reactions do not account for all of the phenomena that are observed during plating. Experimentally detected reaction characteristics indicate that the course of the reaction is considerably more complex than described by simple stoichiometric equations. Hence, it is necessary to attempt to ascertain the mechanism of the nickel reduction by the various reducing species.

An explicit understanding of the reaction mechanisms that govern electroless nickel deposition is necessary from both theoretical and practical viewpoints. Knowledge of the mechanisms of the reaction of a reducing agent with nickel ions can lead to the solution of a series of problems; development of methods to increase the plating rate, for enhancing hypophosphite efficiency, and for regulating the phosphorus or boron content of the deposit. It must be emphasized that an understanding of the course of the reaction, especially as it relates to the reduction of phosphorus or boron, is extremely important. It is the inclusion of P or B in the respective nickel alloys (Ni-P and Ni-B) that determines the properties of each alloy.

Before discussing the individual reducing agents, and the proposed mechanisms of their reactions with nickel, it might be informative to recall certain characteristics of the process that the mechanism must explain:

a) The reduction of nickel is always accompanied by the evolution of hydrogen gas;
b) The deposit is not pure nickel but contains either phosphorus or boron depending on the reducing media used;
c) The reduction reaction takes place only on the surface of certain metals;
d) The generation of hydrogen ions is a by-product of the reduction reaction;
e) The utilization of the reducing agent is considerably less than 100 percent; and
f) The molar ratio of nickel deposited to reducing agent consumed is usually equal to or less than 1.

## Hypophosphite, $H_2PO_2$

Nickel deposition by hypophosphite is usually represented by the following equations:

$$Ni^{+2} + H_2PO_2^- + H_2O \longrightarrow Ni^0 + H_2PO_3^- + 2H^+ \quad (1)$$

$$H_2PO_2^- + H_2O \xrightarrow{Cat.} H_3PO_3^- + H_2 \quad (2)$$

overall,

$$Ni^{+2} + 2H_2PO_2^- + 2H_2O \longrightarrow Ni^0 + 2H_3PO_3^- + 2H^+ + H_2 \quad (3)$$

The product of nickel plating with hypophosphite are alloys of nickel and phosphorus; however, equations 1, 2, and 3 completely fail to account for the phosphorus component of the alloy. Further, if the plating reaction took place in accordance with the above equations, the rate of deposition would be proportional to the concentrations of the reactants. Experimental data shows that in acid plating solutions, pH $\geq$ 3.0. The plating rate is dependent on the hypophosphite concentration over a very wide concentration range, and dependent on the nickel concentration over a very small concentration range; the rate is independent of nickel concentration beyond about 0.075M $Ni^{++}$[1]. In alkaline solution, the rate is dependent only on the hypophosphite concentration.

Scholder and Heckel[2] were the first to observe that the products of the homogeneous reduction of nickel salts by hypophosphite was a mixture of metallic nickel and nickel phosphides. According to these researchers, the reduction of nickel salts by hypophosphite in alkaline solutions yields metallic nickel and several nickel phosphides, whereas in acid solutions only a mixture of different nickel phosphides is obtained. Scholder and Heckel explained the formation of metallic nickel and nickel phosphide by the following equations:

$$NiO + H_3PO_2 \longrightarrow Ni^0 + H_3PO_3 \quad (4)$$

$$3H_3PO_2 \longrightarrow H_3PO_3 + 2P + 3H_2O \quad (5)$$

$$2Ni + P \longrightarrow Ni_2P \quad (6)$$

They postulated that reactions 4 and 5 occur simultaneously, followed by the formation of $Ni_2P$ according to reaction 6. They based their assumption on the fact that in nickel-free solutions, the disproportionation reaction (equation 5) yields hydrogen phosphide instead of phosphorus. The authors also assumed that hydrogen gas evolution was a consequence of the formation of metallic nickel, which then catalyzed the decomposition of hypophosphite; they made no connection between nickel reduction and hydrogen gas evolution. It must be remembered that the interest of these investigators was directed mainly to the study of the composition of the powders obtained as the products of nickel and/or cobalt reduction with hypophosphite.

Since the publication in 1946 of the paper by Brenner and Riddell[3], four principal reaction mechanisms have been proposed to explain electroless nickel deposition, which is incompletely represented by the stoichiometric reactions in equations 1,2 and 3. These reaction schemes attempt to explain nickel reduction by hypophosphite in both acid and alkaline media. To account for the phosphorus in the deposit, the proposed mechanisms involve a secondary reaction of hypophosphite to elemental phosphorus.

Appropriately, the first chemical nickel reaction proposed was advanced by Brenner and Riddell[3]. They postulated that the actual nickel reductant is atomic hydrogen, which acts by heterogeneous catalysis at the catalytic surface. The atomic hydrogen, generated by the reaction of water with hypophosphite, is absorbed at the catalytic surface, that is:

$$H_2PO_2^- + H_2O \longrightarrow H_2PO_3^- + 2H_{ad} \quad (7)$$

The absorbed atomic hydrogen reduces nickel ions at the catalytic surface:

$$Ni^{+2} + 2H_{ad} \longrightarrow (Ni^{+2} + 2H^+ + 2e) \longrightarrow Ni^0 + 2H^+ \quad (8)$$

The evolution of hydrogen gas, which always accompanies catalytic nickel reduction, was ascribed to the recombination of two atomic hydrogen atoms:

$$2H_{ad} \longrightarrow (H + H) \longrightarrow H_2 \quad (9)$$

Gutzeit[1] essentially agrees with the Brenner-Riddell atomic hydrogen concept of nickel reduction. However, Gutzeit[1] attributes the formation of atomic hydrogen to the dehydrogenation of the hypophosphite ion during formation of the metaphosphite ion:

$$H_2PO_2^- \xrightarrow{Cat.} PO_2^- + 2H$$

followed by the formation of O-phosphate molecule and a hydrogen ion according to:

$$PO_2^- + H_2O \longrightarrow HPO_3^{-2} + H^+ \quad (10)$$

A secondary reaction between hypophosphite and atomic hydrogen results in the formation of elemental phosphorus:

$$H_2PO_2^- + H \longrightarrow P + OH^- + H_2O \quad (11)$$

Although the atomic hydrogen mechanism, which has received the support of several authors, sustains the observed results, it fails to explain certain other phenomena. The scheme does not account for the simultaneous reduction of nickel and hydrogen, nor does it explain why the utilization of hypophosphite is always less than 50 percent.

The second mechanism, known as the "hydride transfer mechanism," was first suggested by Hersch[4], who claimed that the behavior of hypophosphite is analogous to the reduction of nickel ions by borohydride ions. That is, Hersch assumed that hypophosphite acts as the donor of hydride ions. Hersch's proposed mechanism was later modified by Lukes[5].

In acid solution, the primary step in the mechanism involves the reaction of water with hypophosphite at the catalytic surface, and may be described by the following equation:

$$2H_2PO_2^- + 2H_2O \xrightarrow{Cat.} 2H_2PO_3^- + 2H^+ + 2H^- \quad (12)$$

The corresponding reaction in alkaline solution is given by:

$$2H_2PO_2^- + 6OH^- \xrightarrow{Cat.} 2H_2PO_3^- + 2H_2O + 2H^- \quad (13)$$

The reduction of nickel ion in this mechanism proceeds as follows:

$$Ni^{+2} + 2H^- \longrightarrow (Ni^{+2} + 2e^- + 2H) \longrightarrow Ni^0 + H_2 \quad (14)$$

The hydride ion can also react with water or a hydrogen ion:

$$\text{Acid: } H^+ + H^- \longrightarrow H_2 \quad (15)$$

$$\text{Alkaline: } H_2O + H^- \longrightarrow H_2 + OH^-$$

According to Lukes, the hydrogen that appears as hydride ion was originally bonded to phosphorus in the hypophosphite. If equation 11 is included in this scheme, the co-deposition of phosphorus is also accounted for. The hydride mechanism presents a satisfactory explanation for the coupled reduction of nickel and hydrogen.

The third mechanism is the so-called electrochemical mechanism originally proposed by Brenner and Riddell and later modified by others. This theory can be represented as follows:

(i) An anodic reaction where electrons are formed by the reaction between water and hypophosphite:

$$H_2PO_2^- + H_2O \longrightarrow H_2PO_3^- + 2H^+ + 2e^- \quad (16)$$

(ii) Cathodic reactions that utilize the electrons generated in equation 16:

$$Ni^{+2} + 2e \longrightarrow Ni^0 \quad (17)$$

$$2H^+ + 2e \longrightarrow H_2 \quad (18)$$

$$H_2PO_2^- + 2H^+ + e \longrightarrow P + 2H_2O \quad (19)$$

According to this mechanism, the evolution of hydrogen gas that takes place during nickel deposition is due to the secondary reaction represented in equation 18. The electrochemical mechanism implies that the nickel ion concentration should have a significant effect on the rate of deposition; however, the converse is the case.

The fourth mechanism involves the coordination of hydroxyl ions with hexaquonickel ion. This mechanism was proposed by P. Cavallotti and G. Salvago[6], and later supported by the results of calorimetric studies on electroless nickel plating by J.P. Randin and H.E. Hintermann[7]. The chemical reduction of nickel at a catalytic surface can be represented by the following reactions:

Decomposition of water:

$$2H_2O \longrightarrow 2H^+ + 2OH^- \quad (20)$$

Coordination of hydroxyl ions to solvated nickel ion:

$$Ni(H_2O)_6^{+2} + 2OH^- \left[ \begin{matrix} & OH \\ Ni\ (aq) & \\ & OH \end{matrix} \right] + 2H_2O \quad (21)$$

Reactions of hydrolyzed nickel species with hypophosphite:

$$\left[ \begin{matrix} & OH \\ Ni\ (aq) & \\ & OH \end{matrix} \right] + H_2PO_2^- \longrightarrow NiOH_{ads} + H_2PO_3^- + H \quad (22)$$

$$NiOH_{ads} + H_2PO_2^- \longrightarrow Ni^0 + H_2PO_3^- + H \quad (23)$$

Where $NiOH_{ads}$ represents a hydrolyzed $Ni^{+1}$ species adsorbed at the catalytic surface. The two atoms of atomic hydrogen can react and evolve as hydrogen gas:

$$H + H \longrightarrow H_2 \quad (24)$$

and it can reduce hypophosphite to phosphorus:

$$H_2PO_2^- + H_{ads} \longrightarrow P + H_2O + OH^- \quad (25)$$

The reaction of hypophosphite with water must also be included in the reaction scheme:

$$H_2PO_2^- + H_2O \longrightarrow HPO_3^{-2} + H^+ + H_2 \quad (26)$$

$\left[ \begin{matrix} & OH \\ Ni\ (aq) & \\ & OH \end{matrix} \right]$ is a schematic representation of the reacting species formed by loosely bonded $OH^-$ ion in the coordination sphere of partially solvated $Ni(H_2O)_4^{+2}$ ions, and not nickel hydroxide. Cavallotti and Salvago, in fact, point out that when nickel hydroxide precipitates, inhibition phenomena are evident. If the hydroxyl ions are bonded too tightly to the nickel, they will not react with the hypophosphite ion. The adsorption of the hydrolyzed species on the active surface probably influences the lability of the coordination bonds.

Among the four proposed reaction mechanisms, only the hydride transfer and hydrolyzed nickel mechanisms account for the observed values for the ratio of moles of nickel deposited to the moles of hypophosphite consumed during deposition. The data obtained in the studies of Franke and Moench[8] and later Sutyagina, Gorbunova, and Glazunov[9] concerning the origin of the hydrogen gas evolved from the interaction between water and hypophosphite ion can be explained by either of these two mechanisms.

Each of the heterogeneous reaction mechanisms outlined above requires a catalytic surface on which the reaction sequence will proceed. Hence, electroless nickel plating occurs only on specific surfaces. The reduction reaction begins spontaneously on certain metals; almost all metals of Group VIII of the Periodic Table in active form.

Metals that are more electropositive than nickel, such as iron or aluminum, will displace nickel from a solution of its ions as follows:

$$Fe^{0} + Ni^{+2} \longrightarrow Fe^{+2} + Ni^{0}_{Cat.} \quad (27)$$

or

$$2Al + 3Ni^{+2} \longrightarrow 2Al^{+3} + 3Ni^{0}_{Cat.} \quad (28)$$

forming the catalytic surface. It is ironic to note that when steel or aluminum, the most commonly plated substrates, are electroless nickel plated, the initial phase in the deposition process is the displacement reaction.

If the substrate metal is more electronegative than nickel, it can be made catalytic by electrolytically depositing a thin nickel deposit on its surface. This can also be accomplished by providing contact, in the solution, between the substrate and a more electropositive metal, thereby forming an internal galvanic cell. For example, copper and its alloys are usually plated with either of these techniques.

## The Borohydride Ion, $BH_4$

The only complex hydrides of non-transition elements known at the present time are formed by boron, aluminum, and gallium. They occur as salts of hydride ions, that is, $NaBH_4$, Li ($AlH_4$), etc. The $MX_3$ group behaves as an electron acceptor and the hydride ion as an electron donor:

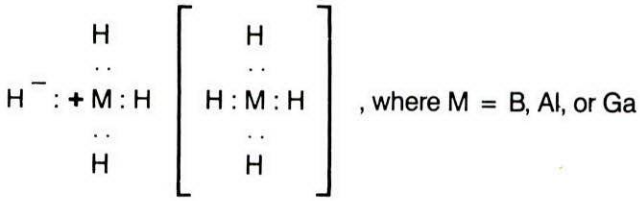


, where M = B, Al, or Ga

The thermal and chemical stabilities of the three anions vary relative to the ability of the $MH_3$ group to act as an electron acceptor, the order being:

$$B > Al > G$$

$BH_4^-$ is stable in water, while $AlH_4^-$ and $GaH_4^-$ are rapidly and sometimes explosively hydrolyzed by water:

$$MH_4^- + 4H_2O \longrightarrow M(OH)_4^- + 4H_2$$

and acid hydrolysis,

$$MH_4^- + H^+ \longrightarrow MH_3 + H_2$$

The alkali metal salts of $MH_4^-$ anion are very powerful reducing agents; however, only the salts of $BH_4^-$, such as $NaBH_4$, can be utilized in aqueous solutions.

In the 40 or so years since the discovery of "electroless" nickel plating by Brenner and Riddell, hundreds of papers describing the process and the resulting deposits have been published. Although other electroless systems are covered, the vast majority of these publications (papers and patents) are concerned with nickel- or cobalt-phosphorus alloys and the plating solutions that produce them.

Attempts to develop alternative reducing agents led several workers to investigate the boron containing reducing agents; in particular, the borohydrides and amine boranes. Subsequently, several patents were issued covering electroless plating processes and the resulting deposits.

The deposits obtained from electroless systems using boron containing reducing agents are nickel-boron alloys. Depending on the solution operating conditions, the composition of the deposit can vary in the range of 90 - 99.9 percent nickel with varying amounts of reaction products. In some cases, the metallic stabilizer will be incorporated in the deposit during the plating reaction.

As is the case with nickel-phosphorus alloys, nickel-boron deposits are characterized by their unique chemical and physical properties.

The borohydride reducing agent may consist of any water soluble borohydride compound. Sodium borohydride is generally preferred because of its availability. Substituted borohydrides in which not more than three of the hydrogen atoms of the borohydride ion have been replaced can also be used; sodium trimethoxyborohydride ($NaB(OCH_3)_3H$) is an example of this type of compound.

The borohydride ion is a powerful reducing agent. The redox potential of $BH_4^-$ is calculated to be $E^0_{ca} = 1.24V$. In basic solutions, the decomposition of the $BH_4^-$ unit yields eight electrons for the reduction reaction:

$$BH_4^- + 8OH^- \longrightarrow B(OH)_4^- + 4H_2O + 8e^- \quad (29)$$

Then, each borohydride ion can theoretically reduce four nickel ions. That is, adding equation 29 to:

$$4NI^{+2} + 8e^- \longrightarrow 4Ni^0 \quad (30)$$

gives the overall reaction,

$$4Ni^{+2} + BH_4^- + 8OH^- \longrightarrow B(OH)_4^- + Ni^0 + 4H_2O \quad (31)$$

However, it has been found experimentally that one mole of borohydride reduces approximately one mole of nickel.

There are only a few published articles that are concerned with the mechanism of nickel deposition with borohydride, and most of the proposed schemes are not supported by experimental data. In spite of the experimental evidence to the contrary, several authors still assume that each borohydride ion reduces four nickel ions, that is:

$$4Ni^{+2} + BH_4^- + 8OH^- \longrightarrow 4Ni^0 + BO_2^- + 6H_2O \quad (32)$$

Although the authors of three separate mechanisms agree that nickel reduction proceeds as expressed in equation 32, the reduction of boron is approached differently in each case.

Case 1[10]. Here the author assumes that only three hydride ions are oxidized to protons; the fourth hydride is oxidized to a hydrogen atom, which leads to the formation of a molecule of evolved hydrogen gas:

$$4Ni^{+2} + 2BH_4 + 6OH^- \longrightarrow 2Ni_2B + 6H_2O + H_2 \quad (33)$$

Case 2[11]. In this instance, it is assumed that all hydride ions are oxidized to protons, so that:

$$5Ni^{+2} + 2BH_4 + 8OH^- \longrightarrow 5Ni^0 + 2B + 8H_2O \quad (34)$$

Case 3[12]. Boron reduction is, as assumed by these authors, the catalytic decomposition of borohydride to elemental boron that takes place independently of nickel reduction:

$$2BH_4^- + 2H_2O \longrightarrow 2B + 2OH^- + 5H_2O$$

K.M. Gorbunova, M.F. Ivanov, and V.P. Moiseev[13] raised an objection to the three above hypotheses. They argue, that based on data relating to the reduction reactions by hypophosphite, it is doubtful that the hydrogen atoms, formed during the oxidation of the hydride ions of $BH_4$, are intermediate products that can take part in either nickel or boron reduction.

Data obtained from mass-spectrometric measurements of the isotope composition of hydrogen gas evolved during electroless Ni-B deposition experiments using heavy water ($D_2O$), led Gorbunova and co-workers to propose a mechanism that more nearly fits the results of their studies. Their experiments were carried out using plating solutions prepared with $D_2O$, and also containing NaOD. It should be noted that calculations based on previously proposed schemes yielded results that deviated by almost 200% from the experimental data obtained in isotope experiments.

The proposed scheme of Gorbunova et al. for the reaction mechanism of nickel-boron plating consists of three main steps:

(1) Reduction of nickel:

$$BH_4^- + 4H_2O \longrightarrow B(OH)_4^- + 4H + 4H^+ + 4e^- \quad (35)$$

$$2Ni^{+2} + 4e^- \longrightarrow 2Ni^0 \quad (36)$$

---

$$(35) + (36) \quad BH_4^- + 2Ni^{+2} + 4H_2O \longrightarrow 2Ni^0 + B(OH)_4^- + 2H_2 + 4H^+ \quad (37)$$

(2) Reduction of boron:

$$BH_4^- + H^+ \longrightarrow BH_3 + H_2 \longrightarrow B + \frac{5}{2} H_2 \quad (38)$$

(3) Hydrolysis of borohydride:

$$BH_4^- + 4H_2O \longrightarrow + B(OH)_4^- + 4H + 4H^+ + 4e^- \longrightarrow B(OH)_4^- + 4H_2 \quad (39)$$

G.O. Mallory has also investigated the reduction of nickel ions by borohydride and amine boranes[14]. On the basis of experimental data, the author suggests that the hydrolyzed nickel mechanism of Cavallotti and Salvago, proposed to explain nickel reduction with hypophosphite, can be adapted to explain nickel reduction with borohydride or amine boranes. The modified hydrolyzed nickel mechanism with borohydride can be represented by the following sequence of reactions:

(1) Decomposition of water:

$$4H_2O \longrightarrow 4H^+ + 4OH^- \quad (40)$$

(2) Coordination of hydroxyl ions to solvated nickel ion:

$$2Ni(H_2O)_6^{+2} + 4OH^- \longrightarrow 2 \left[ \begin{matrix} OH \\ Ni(aq) \\ OH \end{matrix} \right] + 4H_2O \quad (41)$$

(3) Reaction of hydrolyzed nickel species with borohydride ion:

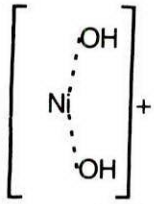

$$+ BH_4^- \longrightarrow NiOH_{ads} + BH_3OH^- + H \quad (42)$$

$$NiOH_{ads} + BH_3OH^- \longrightarrow Ni^0 + BH_2(OH)_2^- + H \quad (43)$$

The $BH_2(OH)_2^-$ species reacts with the second hydrolyzed nickel ion in a similar manner:

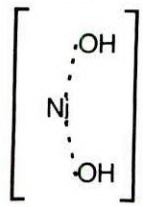

$$+ BH_2(OH)_2^- \longrightarrow NiOH_{ads} + BH(OH)_3^- + H \quad (44)$$

$$NiOH_{ads} + BH(OH)_3^- \longrightarrow Ni^0 + B(OH)_4^- + H \quad (45)$$

(4) The four atoms of atomic hydrogen react to form hydrogen gas:

$$2H + 2H \longrightarrow 2H_2 \quad (46)$$

Thus, equations 40 through 46 can be represented by the overall reaction:

$$2Ni^{+2} + 4H_2O + BH_4^- \longrightarrow 2Ni^0 + B(OH)_4^- + 2H_2 + 4H^+ \quad (47)$$

The reduction of boron is accounted for in the reaction of $BH_4^-$ with a hydrogen ion:

$$BH_4^- + H^+ \longrightarrow BH_3 + H_2 \longrightarrow B + \frac{5}{2}H_2 \quad (48)$$

Equations 47 and 48 can be combined to obtain:

$$2Ni^{+2} + 2BH_4^- + 4H_2O \longrightarrow 2Ni^0 + B + B(OH)_4^- + 3H^+ + \frac{9}{2}H_2 \quad (49)$$

The mechanism proposed by Gorbunova et al. and the modified Cavallotti and Salvago proposal lead to the same overall reaction. Also, in both schemes, the increase in acidity observed in the process is due to hydrogen ions that originate from water molecules only. Finally, the two mechanisms indicate that the mole ratio of nickel reduced to borohydride consumed is 1:1, which is supported by experimental evidence.

## The Amine Boranes

In the $BH_3$ molecule the boron octet is incomplete, that is, boron has a low-lying orbital that it does not use in bonding owing to a shortage of electrons. As a consequence of the incomplete octet, $BH_3$ can behave as an electron acceptor (Lewis acid). Thus, electron pair donors (Lewis bases), such as amines, form 1:1 complexes with $BH_3$ and thereby satisfy the incomplete octet of boron. The linkage between $BH_3$ and dimethylamine is illustrated by the following:

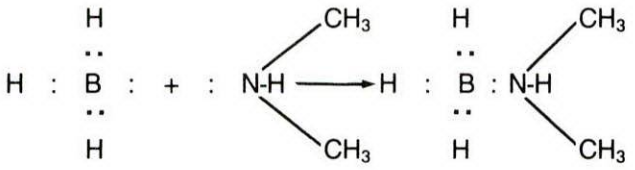

The amine boranes are covalent compounds, whereas borohydrides such as $NaBH_4$ are completely ionic; that is, $NaBH_4 = Na^+ + BH_4^-$. Although the amine boranes do not ionize like other molecules with heteronuclear covalent bonds, one of the atoms will, in general, have a greater affinity for the electrons than the other and the bond will therefore be polar, i.e.:

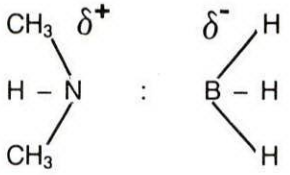

In this case, the electrons are displaced toward the boron atom giving the boron atom excess negative character; whereas, the nitrogen atom displays excess positive charge. The electrical polarity of a molecule, expressed as its dipole moment, plays an important role in the reactions of covalent compounds.

The commercial use of amine boranes in electroless nickel plating has, in general, been limited to dimethylamine borane (DMAB), $(CH_3)NHBH_3$. DMAB has only three active hydrogens bonded to the boron atom and, therefore, should theoretically reduce three nickel ions for each DMAB molecule consumed (each borohydride ion will theoretically reduce four nickel ions). The reduction of nickel ions with DMAB is described by the following equations:

$$3Ni^{+2} + (CH_3)_2NHBH_3 + 3H_2O \longrightarrow Ni^0 + (CH_3)_2NH_2^+ + H_3BO_3 + 5H^+ \quad (50)$$

$$2[(CH_3)_2NHBH_3] + 4Ni^{+2} + 3H_20 \longrightarrow Ni_2B + 2Ni^0 + 2[(CH_3)_2NH_2^+] + H_3BO_3 + \tfrac{1}{2}H_2 + 6H^+ \quad (51)$$

In addition to the above useful reactions, DMAB can be consumed by wasteful hydrolysis:

$$\text{Acid: } (CH_3)_2 + NHBH_3 + 3H_2O + H^+ \longrightarrow (CH_3)_2NH_2^+ + H_3BO_3 + 3H_2 \quad (52)$$

$$\text{Alkaline: } (CH_3)_2NHBH_3 + OH^- \longrightarrow (CH_3)_2NH + BH_3(OH)^- \quad (53)$$

However, the theoretical expressions for nickel reduction are not supported by experimental findings. The results of studies on chemical nickel plating with DMAB indicates that the molar ratio of nickel ions reduced to DMAB molecules consumed is approximately 1:1[14]. A modified hydrolyzed nickel mechanism satisfactorily accomodates the experimental data.

Based on his studies, M. Lelental[15] suggests that nickel deposition with DMAB is dependent on the adsorption of the reducing media on the catalyst surface followed by cleavage of the N-B bond of the adsorbed amine borane. The adsorption step is consistent with the polar nature of the DMAB molecule. The mechanism can be illustrated as follows:

(1) N-B bond cleavage:

$$2R_2NHBH_3 \xrightarrow{\text{Cat.}} 2R_2NH + 2BH_{3ads} \quad (54)$$

(2) Reduction of hydrolyzed nickel with $BH_{3ads}$:

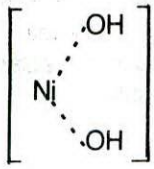


$$+ BH_{3ads} \longrightarrow Ni^0 + BH(OH)_{2ads} + 2H \quad (55)$$

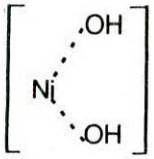


$$+ BH(OH)_{2ads} \longrightarrow NiOH_{ads} + B(OH)_3 + H \quad (56)$$

$$NiOH_{ads} + BH_{3ads} \longrightarrow Ni^0 + BH_2OH + H \quad (57)$$

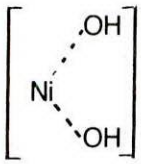


$$+ BH_2OH \longrightarrow Ni^0 + B(OH)_3 + H \quad (58)$$

The sums of the above equations, including the decomposition of water, is given by:

$$3Ni^{+2} + 2R_2NHBH_3 + 6H_2O \longrightarrow 3Ni^0 + 2R_2NH_2^+ + 2B(OH)_3 + 3H_2 + 4H^+ \quad (59)$$

(3) Boron reduction:

$$R_2NHBH_3 \xrightarrow{Cat.} R_2NH + BH_3 + H_2 + H^+ \longrightarrow R_2NH_2^+ + B + \frac{5}{2} H_2 \quad (60)$$

Equations 59 and 60 can be combined to give:

$$3Ni^{+2} + 3R_2NHBH_3 + 6H_2O \longrightarrow 3Ni^0 + B + 3R_2NH_2^+ + 2B(OH)_3 + \frac{9}{2}H_2 + 3H^+ \quad (61)$$

## Hydrazine

Soon after Brenner and Riddell published their findings on nickel reduction with hypophosphite, L. Pessel[16], in 1947, was issued a patent claiming the use of hydrazine as a metal reductant. During the succeeding 16 years many papers and patents were published detailing electroless nickel-phosphorus deposition. However, it was not until 1963, when D.J. Levy[17] reported the results of his investigations, was any information forthcoming on electroless nickel plating with hydrazine. Later, Dini and Coronado described several electroless nickel-hydrazine plating baths and the properties of the deposits obtained form ther solutions.[18]

Hydrazine is a powerful reducing agent in aqueous alkaline solutions:

$$N_2H_4 + 4OH^- \longrightarrow N_2 + 4H_2O + 4e^-, E_B^0 = 1.16V$$

Levy proposed the following reduction reaction for nickel ions with hydrazine in an alkaline solution:

$$2Ni^{+2} + N_2H_4 + 4OH^- \longrightarrow 2Ni^0 + N_2 + 4H_2O \quad (62)$$

## CONCLUSION

Of the four mechanisms proposed to explain the chemical reduction of Ni-P and Ni-B alloys, the so-called hydrolyzed nickel theory of Cavalloti and Salvago is the one that is supported by experimental evidence. The hydrolyzed nickel theory can also be considered a universal mechanism since it can also be used to characterize the reduction processes with borohydride and amineboranes as well as with sodium hypophosphite.

## REFERENCES


1. G. Gutzeit, *Plating,* **46**, 1158, 1275, 1377, (1959); Ibid, **47**, 63 (1960).
2. R. Scholder and H. Heckel, *Z. Anorg. Und Allgem. Chem.,* **198**, 329 (1931).
3. A. Brenner and G. Riddell, *J. Res. Nat. Bur. Std.,* **37**, 31 (1946); ibid, **39**, 385 (1947).
4. P. Hersch, *Trans. Inst. Metal Finishing,* **33**, 417 (1955-56).
5. R.M. Lukes, *Plating,* **51**, 969 (1964).
6. P. Cavallotti and G. Salvago, *Electrochim. Metall.,* **3**, 239 (1968).
7. J.P. Randin and H.E. Hintermann, *J. Electrochem. Soc.,* **117**, 160 (1970).
8. W. Franke and J. Moench, *Liebigs Ann. Chem.,* **64**, 29 (1941).
9. A.A. Sutyagine, K.M. Gorbunova, and P.M. Glazunov, *Dokl. Akad. Nauksssr,* **147**, 1133 (1962).
10. K. Lang, *Galvanotechnik,* **56**, (6), 347 (1965).
11. L.E. Tsupak, *Kandidatskaya dissertatsiya,* Moscow (1969).
12. A. Yu. Prokopchik, Ya. I. Valsyunene, Yu. P. Butkyavichyus, and D.P. Kimtene, *Zashchita Metal.,* **6**, 517 (1970).
13. K.M. Gorbunova, M.V. Ivanov, and V.P. Moiseev, *J. Electrochem. Soc.,* **120**, 613 (1973).
14. G. O. Mallory, *Plating,* **58**, 319 (1971).
15. M. Lelental, *J. Electrochem. Soc.,* **122**, 436 (1975).
16. U.S. Patent 2,430,581 (1947), L. Dessel
17. D.J. Levy, *J. Electrochem.,* **1**, 38 (1963).
18. J.W. Dini and P.R. Coronado, *Plating,* **54**, 385 (1967).

J-5

# Electroless Deposition II
# Session J

## Electronic Applications of Electroless Nickel, New or Unusual

Donald W. Baudrand
Allied-Kelite Div.
Witco Corp.
2701 Lake Street
Melrose Park, IL 60160

# ELECTRONIC APPLICATIONS OF ELECTROLESS NICKEL, NEW OR UNUSUAL

Donald W. Baudrand
Allied-Kelite Division
Witco Corporation
2701 Lake Street
Melrose Park, IL 60160

Electroless nickel deposits provide functional characteristics that are useful for many electronic devices. Deposit characteristics such as electrical conductance/resistance, magnetic properties, hardness, and amorphous/partially crystalline structure can be varied by using different plating solution compositions and operating conditions. Good brazing, soldering, laser welding, and wire and die bonding can be achieved using special bath formulations. This paper discusses some of the specific applications which take advantage of the unique properties of various electroless nickel plating systems.

## Ceramic Microballoons

Electronic circuits often require protection from electromagnetic interference (EMI), particularly at radio frequencies (RF interference). One common method of providing EMI shielding is by depositing a layer of electroless copper followed by a layer of electroless nickel onto the plastic cases that house the electronics. The electroless nickel must exhibit reasonably good conductivity, such as a low-phosphorus nickel or a nickel-boron alloy. Much has been written about this type of shielding.[1,2,3] Electroless nickel can also be applied by other methods to provide EMI and RF shielding. One significant example is a coating of electrically conductive "microballoons" (Figs. 1 and 2)†[4,5]

These microballoons (microspheres) are hollow spheres of fired ceramic with a typical outer diameter of 50 microns and wall thickness of near 10 microns, and are coated with a thin layer of metal to provide a conductive surface. Since RF energy is only conducted on the outer surface (about one microinch thick) of a solid conductor — the "skin effect" — the microballoons provide the same shielding and conductivity as plated metal deposits or paints containing solid metal particles, yet provide significant cost savings and weight reduction due to the lower amount of metal used. They are structurally strong yet lightweight, with a density of about 0.7 and a crush strength of about 4,000 psi isostatic. Their spherical shape is ideal since it has maximum volume per surface area, thus using the least amount of metal to fill any unit volume. Spherical particles spray easily when applied with coating resins, are isotropic to RF energy, and have a dense continuous packing arrangement, filling about 70% of the coating volume.

Spheres can be made slightly magnetic by including magnetite into the ceramic or using a magnetic electroless nickel deposit. Magnetic attraction between the spheres promotes dense packing and uniform properties. It also increases the shield effectiveness due to hysteresis losses. This improves the low impedance EMI shielding effectiveness. Ferrite is added to the ceramic as a strong absorber of RF energy. "With these additions a particle is created with superb conductivity which absorbs strongly any induced fields."[4,5]

Noble metals such as silver, gold, platinum, palladium, iridium, and osmium provide greater long-term conductivity than metals such as copper that oxidize with age, increasing contact resistance. The least expensive of these metals is silver. Coatings containing silver are excellent conductors and shields, and the basic chemistry of silver deposition is well known.

Electroless nickel plated onto the microballoons followed by a very thin silver immersion deposit reduces the amount of silver used, and therefore the cost of production, without sacrificing shielding effectiveness. Highly conductive electroless nickel deposits may eliminate the need for silver in some applications. Deposit conductance is enhanced by using a reducing agent that produces nearly pure nickel, such as a boron agent (boron content of deposit less than 0.3%) or hydrazine (caution — hydrazine is highly toxic and explosive).

Gindrup† discusses the shielding performance of silver coated magnetic ceramic microballoons (SCMCM) on Norel™ plastic:

"A typical coating on NOREL appears as a very smooth light tan paint. It has a dry weight of 0.04 g. to 0.05 g. per square inch. This coating contains one half by weight SCMCM or 0.02 g. to 0.025 g. per inch square. The film gives a conductance between 0.1 and 0.2 ohms per square. The shielding effectiveness will exceed -40 dB from zero to one Gigahertz with very little change due to frequency. Reflection of EMI by a conductive surface is caused by an impedance mismatch. RF currents are induced into the shield and are attenuated as they pass through the shield. RF energy reaching the back of the shield is partially reflected back into the shield and partially radiated into the enclosure. A solid metal shield mainly attentuates the induced currents by only ohmic losses which are small in a solid metal wall, allowing considerable energy to reach the backside. In comparison, the silver coated microballoons cause great attenuation because each microballoon creates six impedance mismatches. This results in large amounts of energy being dissipated by multiple internal reflections and destructive interference. The absorption is enhanced by the multiple conductive paths."

Electroless nickel solutions used for this application are generally more concentrated than for other applications. The surface area-to-solution volume ratio is extremely large compared to normal plating situations. For example, each 100 grams of microballoon material has a surface area of 8-10 square meters, resulting in bath loading of over 100 square feet per gallon. In comparison, typical bath loading is about 0.5 to 1 square foot per gallon when plating ordinary devices. Depending on the particle size being coated, the nickel coating will range from 10% to 20% by weight. The plating temperature is from 25-35 C with a plating time of 30-45 minutes.

Typical preparation consists of a dilute palladium chloride solution rinse and immersion in an alkaline formaldehyde solution to reduce the palladium to the metal. Careful rinsing follows, then electroless nickel plating.

Other applications include ablative laser shields, electrically conductive liquids, radar scattering and absorption, electrostatic capacitors, electrostatic generators, ultra-high speed projectiles, and ultra-light aerospace composites.[4,5,6]

Electroless nickel plated fibers have also been plated for similar applications.

## Via Hole Filling

Integrated circuit (I.C.) designers constantly strive to increase the operating speed and decrease the cost of complex circuits by squeezing more circuit elements onto smaller areas of silicon chip "real estate". Today's very large scale integrated circuits (VLSI) use multilevel circuit interconnections to provide high density and reliability in a compact structure.

During fabrication, a layer of metallization is deposited on the silicon wafer, and conductors are etch-defined. A layer of dielectric is then deposited, and windows ("via holes") are etched through to connection points on the metallization. The next layer of metallized conductors is then applied to form interconnections.

It is important to have a flat (planar) surface topography at all stages of production, or stress, etching irregularities, and serious problems in lithographic patterning can result. However, the upper level of metallization is not completely planar because of the depth of the via holes (Fig. 3)[7]; and this problem is compounded when additional layers are required to complete all interconnections. Therefore, it is essential to fill the via holes with a conductor before metallization to produce high-reliability interconnections (Fig. 4)[7]. Vacuum deposition methods have been studied extensively, but fall short of the results of electroless nickel plating. Electroless processes are simple, low cost, and easy to implement.

Ting, Paunovic and Chiu† [8,9,10] report the following process:
"Substrates with one micron Al-Si layer deposited by a standard sputtering process. The dielectric layer over Al is 1.0-1.5 micron thick undoped oxide deposited by an LTO process. Via holes of 1.5 micron nominal size are formed by the usual photolithography and plasma etching process." The aluminum conductor is first activated by using a light etch to remove surface oxides, a deionized water rinse follows, then immersion in a palladium activation solution ($PdCl_2$, HCl and water) at about 40 C. The wafers are rinsed and immersed in an electroless nickel-boron plating solution, pH about 6, temperature 55 C; the plating rate was slowed to 2.8 microns/hr. (by the lower temperatures) to minimize nodule formation.

For plating onto the silicon surfaces, palladium activation is not necessary. The silicon is first etched lightly in a nitric acid-fluoride salt or hydrofluoric acid-water mixture. The pH of the electroless nickel -boron solution is raised to about pH 8. Plating proceeds when the wafer is immersed in the plating bath at 55 C.

Harada, Fushimi, Madakoro, Sawai and Ushio[11] report via hole filling by electroless nickel onto aluminum conductors patterned on 4 in. silicon substrates with 600 nm thickness of phosphosilicate glass (PSG) films deposited on the Al patterns for interlayer insulation. Via holes of 2,3, and 4 micrometers in diameter were formed using reactive ion etching (RIE), and activated with palladium chloride, followed by electroless nickel-boron plating. Two methods of activation were reported. The "wet" method where the bottom of the hole was activated, and the "lift off" method where palladium is vacuum deposited selectively in the holes coating the walls as well as the bottom. The wet method resulted in a flat, smooth (planar) surface with 100% process yield (Fig. 5)[11].

Ceramic-to-Metal Joining †††

Bonding metals to ceramic substrates to produce high strength joining has long been a problem. Differences in the thermal expansion characteristics of metals and ceramics account for much of the problem. Irregularities including bumps and micro-fissures in the ceramic surface result in stresses which can lead to joint failure. Preparation of the ceramic surface to produce a smooth but sufficiently porous surface to allow adhesion has been difficult.

Methods have been developed which produce joints sufficiently strong for engineering applications such as bearings, seals, turbochargers, gas turbine engines, and diesel engines, as well as electronic applications such as producing circuits directly on ceramic substrates (without metallization by metal pastes such as molybdenum manganese), joining two or more ceramic devices, and producing multilayer ceramic devices. The preparation steps involve machining of the ceramic component to remove surface irregularities which could

lead to stress, and chemical surface preparation in mixed acid/fluoride treatment. "It alters the grain boundry to matrix structure and provides a more regular surface with reduced flaws."[12]

The prepared ceramic is catalyzed and plated in an electroless nickel-boron plating bath. Direct bonding is achieved. Part configuration is not a limiting factor since deposit distribution is uniform over all surfaces to be plated. Joining is accomplished by brazing. Test results show as high as 450 MPa tensile force (ASTM Std. F692) is necessary to separate the metal layer. Nickel-boron plating is chosen because it will withstand thermal excursions without cracking. It does not alter structure due to formation of intermetallic compounds as is the case with nickel-phosphorus. It is also easily soldered and wire and die bonded, making it suitable for a varity of applications.

"Ceramics to which metals have been bonded include alumina, silicon carbide, lithium aluminum silicate, mullite, steatite, sintered silicon nitride and partially stabilized zirconia."[12]

## Additional Applications

Electroless nickel deposits are used in an increasing number of electronic devices too numerous to discuss in detail in the this paper. Additional examples are:

"Air-bridges" used to connect circuit elements on wafers and other substrates for integrated circuits and microhybrid circuits. An air bridge is produced by masking the conductor to be transversed, electroless nickel plating to form a bridge conductor, and then removing the mask.

Medical devices such as pacemakers utilize electroless nickel plating on piezoelectric ceramic which is joined to metal to form a sensor.

Solder bumps are used to join flip chip devices to the electronic package. An electroless nickel layer prior to forming the solder bumps provides high reliability to the device.

Multi-layer flexible circuits utilize electroless nickel layer to promote bonding of copper conductor layer to polyimide substrate material. Copper-clad polyimide sheet is produced by one supplier utilizing a thin electroless nickel-boron bonding layer followed by copper plating. This technique results in an extremely thin laminate since it eliminates the adhesive bonding layers, allowing a larger number of layers in a multilayer circuit.

Electroless nickel baths are readily adaptable to modification by alloying other metals to produce specific properties to suit many electronic device requirements. Some examples are: nickel-iron-boron to produce a highly permiable soft magnetic deposit; nickel-cobalt-phosphorus and cobalt-phosphorus deposits to produce a hard magnetic deposit, nickle-tungsten-boron deposits for good solderability and high temperature resistance; and cobalt-boron and cobalt-nickel-boron alloys which produce special soft magnetic deposits. Many other alloys are possible to achieve specific characteristics, and new applications continue to unfold as technology advances.

Acknowledgements

Additional information was supplied couresty of the following:

† Wayne Gindrup
Carolina Solvents, Inc.
P.O. Box 9206
Hickory, N.C. 28603

†† Dr. Milan Paunovic and George Chiu
Intel Corp., 3601 Juliette Lane,
Santa Clara, CA 95052

†††M. A. DeLuca and J. W. Swain, Jr.
PCK Technology Div., Hollmorgen Corp,
Melville, NY 11747
and J. R. Swank, Ford Motor Co.,
Dearborn, MI 48121

References:

1. EMI Shielding Effectiveness, Walter J. Miller
Metal Finishing, Vol. 83, No. 1, Jan 1985
2. Numerous publications by the American Society of Electroplated Plastics (ASEP), 1133 15th Street N.W., Washington, D.C. 20005
3. "ASEP Presents Some Facts and Information on EMI and Electroless Shielding"
Am. Soc. of Electroplated Plastics
1133 15th Street N.W.
Washington, D.C. 20005
Publications ASTM ES7-83
4. U.S. Patent 4,624,798 Wayne L. Gindrup, Rebecca R. Vinson
5. U.S. Patent 4,624,865 Wayne L. Gindrup, Rebecca R. Vinson
6. Private communication with Wayne Gindrup, Carolina Solvents, Inc.
7. "Application of Electroless Nickel Plating in Semiconductor Microcircuit Industry", Kaiser Wong, Xerox Corp., to be published
8. Electrochemical Society Extended Abstracts, Vol. 87-1, Philadelphia, PA, May 10-15, 1987
No. 239, Ting, Paunovic, and Chiu
9. Electrochemical Society Extended Abstracts, Vol. 87-2, Honolulu, Hawaii, Oct. 18-23, 1987
No. 512, Ting, Paunovic, and Chiu
10. Electrochemical Society Extended Abstracts, Vol. 87-2, Honolulu, Hawaii, Oct. 18-23, 1987
No. 514, Ting, Paunovic, and Chiu
11. "The Characterization of Via-Filling Technology with Electroless Nickel Plating Method"
Harada, Fushimi, Madakora, Sawai, and Ushio
J. Electrochemical Society, 133, Nov. 1986
12. "An advanced Ceramic to Metal Joining Process"
by DeLuca, Swain, and Swank — to be published.

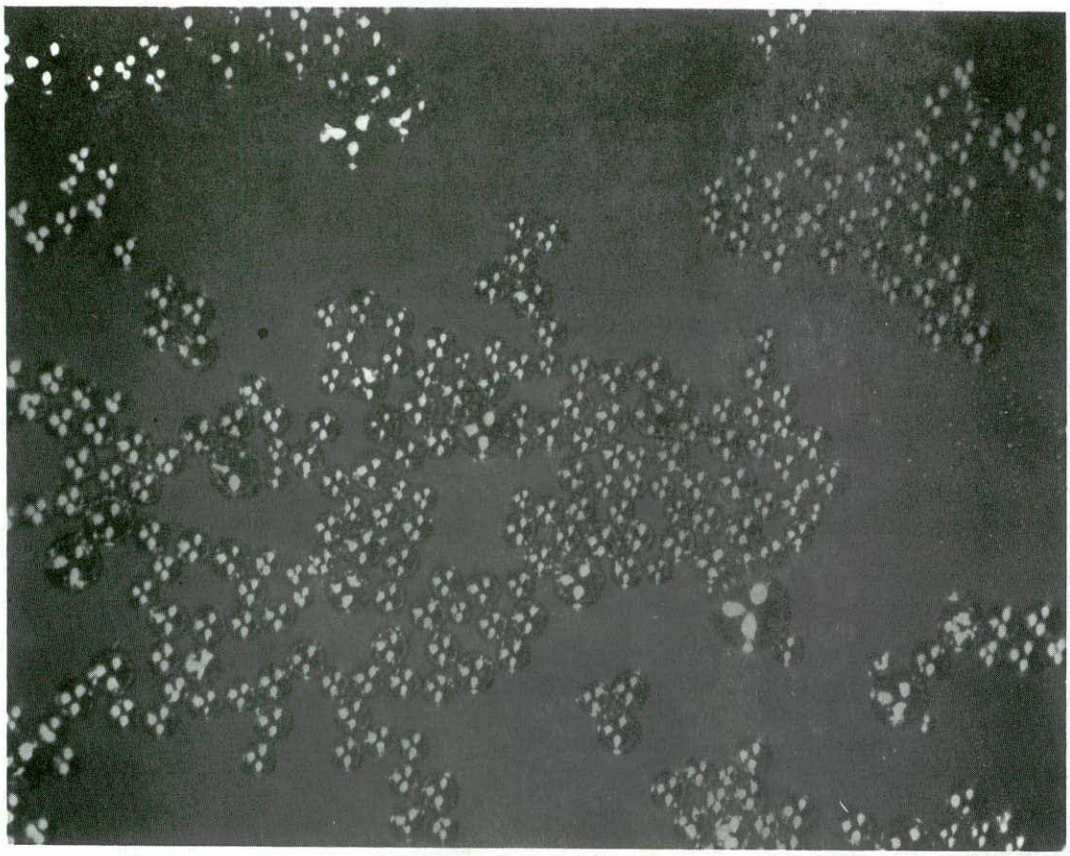

**Figure 1. 100X Photomicrograph of nickel-coated magnetic ceramic microspheres (15% by weight nickel-phosphorus)**

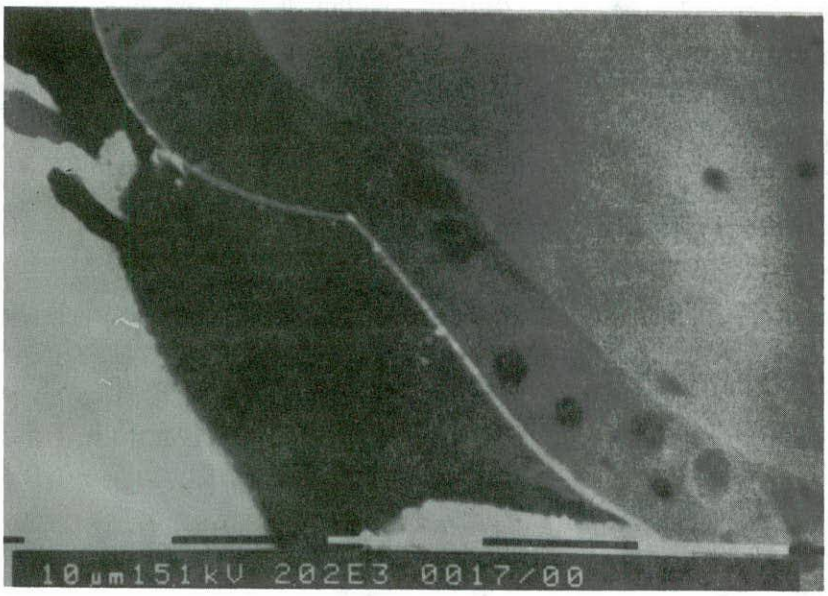


**Figure 2. SEM showing cross-section of broken metal-coated microsphere**

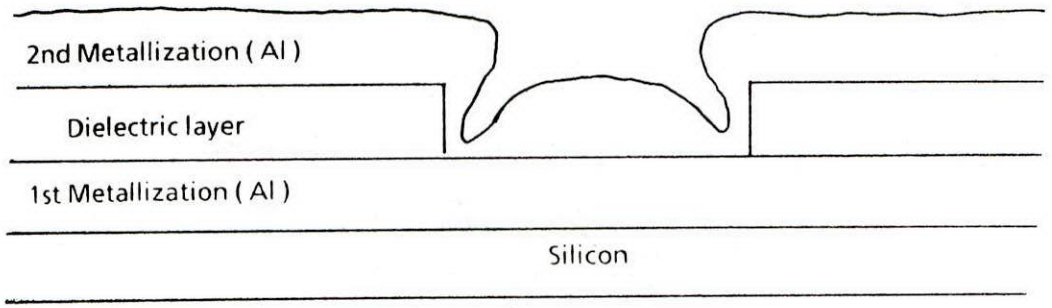


**Figure 3. Poor step coverage on non-planar topological metallization**

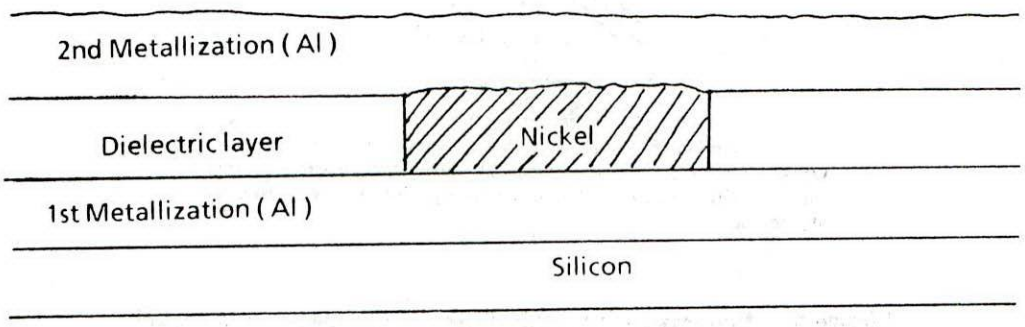


**Figure 4. Planarization of metallization by via hole filling with electroless nickel plate**

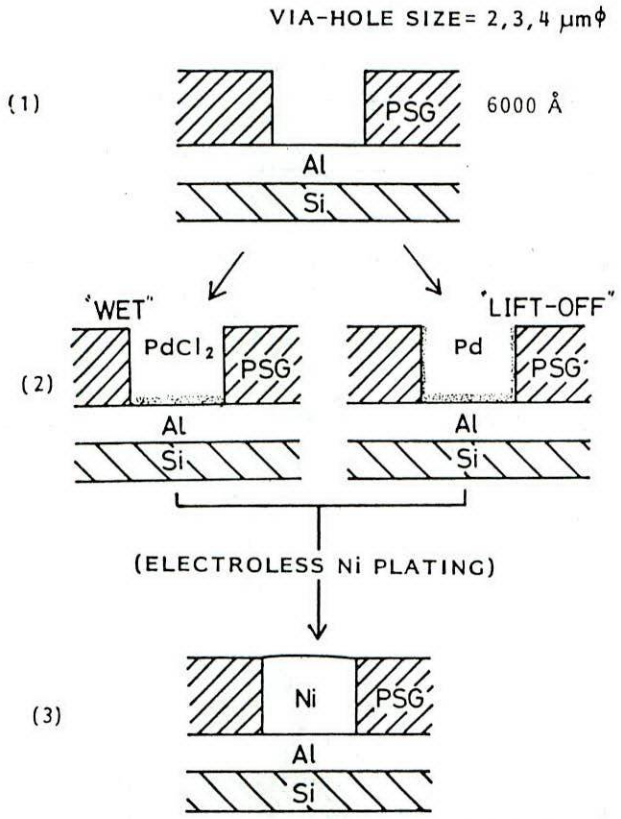


Via-hole filling process flow. (1), After via-holes formation using a reactive ion etching method. (2), After selective activation into via-holes. (3), After completion of via-filling using electroless Ni plating method.

**Figure 5. Process for via hole filling using electroless nickel**

J-6

# Electroless Deposition II
# Session J

## Optimizing the Manufacturing Economics of Electroless Nickel Bath Operation

Louis J. Kosarek
Technical Director
Precision Microelectronics
11550 Pellicano Dr.
El Paso, TX 79936

# OPTIMIZING THE MANUFACTURING ECONOMICS OF ELECTROLESS NICKEL BATH OPERATION

Louis J. Kosarek, Technical Director
Precision Microelectronics, 11550 Pellicano Drive, El Paso, Texas 79936

In the world marketplace, with product quality being equal, the price of manufactured goods dictates acquisition of market share via cost leadership. The goal associated with reducing manufacturing cost is to maintain competitive prices. Various methods of reducing manufacturing cost have been implemented including the use of relatively low cost labor in the Pacific Rim countries and Mexico. Another strategy which has proven to be successful in maintaining competitive prices is to focus attention to manufacturing detail aiming at the reduction of direct materials consumption in the manufacturing process [1]. Electroless nickel (EN) plated surfaces are a direct material cost in numerous industrial sectors. These EN plated products range from valves, drilling machinery and chemical processing equipment to aerospace and electronics/computer components with applications seemingly limited only by the imagination [2,3]. One method of reducing manufacturing cost in the industrial sectors which utilize EN as a direct material is to optimize the manufacturing economics of electroless nickel bath operation.

Various process parameters contribute to the costs associated with the application of EN plated surfaces. A portion of the cost of these process parameters is related to the EN bath composition and the reducing chemistry of the bath. The reducing chemicals in the bath supply the electrochemical energy required to reduce the nickel in solution to metallic nickel. Several different reducing chemicals such as sodium hypophosphite, sodium borohydride, dimethylamine borane and hydrazine have been successfully used in EN plating baths [4]. The majority of commercially available EN bath formulations incorporate either sodium hypophosphite or dimethylamine borane as reducing agents. The EN bath composition formulated with sodium hypophosphite is abbreviated as EN-P and the EN bath composition formulated with dimethylamine borane is abbreviated EN-B. The EN-P formulation selected in this economic analysis is a commercially available product [5]. The EN-B formulation used in this economic analysis is also a commercially available product [5]. The EN plating bath which is chosen by the consumer (either EN-P or EN-B) is selected based upon the amenability of the nickel plate finish to the consumer's application and compliance with specifications.

The process parameters which contribute to EN plating cost can be separated into the general categories of: 1) optimum chemical consumption, 2) minimizing extraneous EN bath plate-out, and 3) maintaining a homogeneous bath. These process parameters are generally independent of the type of EN bath be it EN-P or EN-B. However, a portion of the cost of operating an EN bath is related solely to the reducing chemistry. The scope of this presentation does not include the EN plating cost related to the specific reducing chemistries.

## Optimum Chemical Consumption

Optimum chemical consumption is designated as the minimum quantity of chemical cost required to EN plate a surface in compliance with a

specification or requirement. Compliance of an EN surface to grade, specification or requirement is usually designated in terms of a minimum plating thickness with coverage over all required surfaces[6]. Other parameters include: corrosion resistance, different basis metals, hardness, adhesion, lack of discoloration, appearance of surface finish, solderability, high temperature resistance, uniform thickness, fretting resistance and wire bondability. The economic consideration associated with plating thickness is the unnecessary expenditure for chemicals used in EN plating for excessive thickness and the cost of scrap generated by adhesion defects related to excessive nickel thickness[7,8].

On any given part which is EN plated, there is an average cost which can be calculated empirically for each mil of plating thickness over the surface of one foot of area requiring EN plating. For example, if the actual thickness of EN plate exceeds the specified thickness range for a compliant part by 25%, the average EN plating cost per unit will be 125% of required cost. There is no need to waste the money associated with excessive thickness and the cost of scrap generated by adhesion defects related to excessive nickel thickness. The EN plating thickness can be readily controlled in-process by the use of a thickness measuring device. The thickness of a nickel plated surface can be non-destructively measured using beta-back scatter or x-ray fluorescent spectrometry[9,10,11]. A statistically reliable sample quantity must be used in order for the thickness measurements to be reliable. The parts subjected to non-destructive thickness analysis should be randomly drawn from the group in accordance with MIL-STD 105 or in accordance with MIL-C-26074 C[6].

A comparison of the thickness measuring methods of beta backscatter (BB) and x-ray fluorescence (XRF) within a high volume manufacturing facility designates that XRF retains distinct advantages. The advantages of XRF nickel thickness measuring methods include: accuracy associated with product geometry, time required to complete the analysis, separation of input signals from metals with close atomic numbers[12], non-contact with components and operation without consideration to barometric pressure, temperature, humidity, light, or other environmental influences[13]. Following is a short summary of the operational details associated with nickel thickness measurements by x-ray fluorescent spectrometry.

X-ray fluorescence is an emission of x-ray photons which is resultant of the displacement of a low energy electron within an atom caused by an incident photon of energy. When the incident photon of energy releases a low energy electron within an atom, the higher energy electrons in the outer electron shells move to the lower energy positions and the extra energy is emitted[14]. The fluorescent x-rays which are emitted are characteristic for each element[15]. The thickness measurements are conducted electronically by comparing known fluorescent emission values which are stored in a computer versus the actual emission data. The known values consist of the quantity of x-rays emitted at a specific energy level generated by a known thickness. The thickness measurement includes emissions from both the surface material and the base material. See Figure 1.

The typical XRF thickness gauge contains: an x-ray source with a constant incident beam energy, a

collimator which controls the sample area which is exposed to the incident x-rays, a stage upon which the sample is placed at a constant focal length, a filter which is required on occasion to separate fluorescent x-rays, a proportional counter which amplifies signals and a multichannel analyzer which classifies signals regarding the quantity of signals (counts per minute) and the energy of the signals [14]. See Figure 2. In the case of nickel thickness measurement, the 7.48 KeV energy emission is monitored [15]. The quantity of signals at the 7.48 KeV energy level is proportional to the nickel thickness. The nickel thickness measurements are affected by: variation in alloy composition, counting statistics relative to collimator area, beam-to-part angular alignment, x-ray target plus window specifications and software designed to correct for drift and intensity. The nickel thickness measurements are also affected by: composition (absorption, enhancement, spectral overlap, and phosphorous content in EN-P plus boron content in EN-B) effects, surface smoothness, angular part to beam relationships and sample porosity inclusive of impurities [14]. The standards used to calibrate an XRF thickness instrument should be as close in deposit characteristics to the sample as possible.

Spectral overlap limits the use of beta backscatter when measuring the thickness of nickel over metals which have an atomic number near 28 [12]. The thickness of nickel (atomic #28) over copper (atomic #29) can be measured by XRF instrumentation which incorporates either a cobalt secondary filter or software which is capable of digital filtration[a]. Figure 3 specifies the benefit available when using mechanical filtration with a cobalt filter. Digital filtration is the term which describes the software which conducts a computerized spectral deconvolution of a thickness curve for two overlapping spectra into two component curves. See Figure 4. Digital filtration can also be used to deconvolute overlapping curves from nickel over iron, nickel over alloy 42 and nickel over kovar [15]. The currently available XRF thickness measuring instrumentation also retains the capability to measure: single layer coatings, double layer coatings, triple layer coatings, binary alloy composition, elemental qualifications and metal content analysis of nickel plating solution [16].

Control of Plating Thickness

A short calculation can be made utilizing the data from the XRF thickness gauge measurements to control in-process EN plating thickness. While maintaining the operational parameters of the EN bath (pH, bath activity, temperature, nickel concentration), plating two groups of the same parts for equal periods of time will provide results for nickel thickness within a demonstrated range. The range (R) of nickel thickness can be calculated by subtracting the lowest demonstrated thickness value from the highest demonstrated thickness value. The optimum plating time (t2) can be calculated by multiplying the original plating time (t1) by the ratio of the desired thickness (N2) to the difference of the average demonstrated nickel plated thickness minus one half of the range (R).

(See calculation on following page).

[a] SFT-7000. Seiko Instruments, Torrence, CA.

$$t_2 = \frac{N_2}{N_1 - 0.5R} \times t_1$$

where: $t_1$ = plating time to achieve demonstrated thickness
$t_2$ = projected plating time to obtain desired average thickness
R = range of demonstrated nickel thickness (high-low)
$N_1$ = demonstrated average nickel thickness
$N_2$ = desired average nickel thickness

This calculation is based on empirical data and the actual thickness gauge measurements which are used include R and N1. Since the calculation is based upon empirical data, compensation is made for subtle variations which may be present including: different lots of material, varying lots of parts, slightly different process parameters, and normal in-plant variations. This in-process thickness control calculation can be used numerous times to project the optimum plating time for the next group of parts. By conducting this calculation on each processed group of parts, the actual average plating thickness per group will fluctuate in a range whose average is within R of the desired thickness. It should be noted that only data from the preceding group (R and N1) of the same type of parts should be used to project the plating time for the next group of parts. This calculation to project the plating time of the next group of parts is not necessarily applicable if part quantities change.

Modeling the Cost of EN Bath Operation

In order to optimize the manufacturing economics of EN bath operation, a baseline cost should first be defined. Once this baseline is established, the improvement phase can begin and progress can be monitored in actual dollars by which cost is reduced. A typical EN bath contains: nickel salts, chelating agents, stabilizers, pH regulators, exhaltants, buffering agents and reducing agents[17]. The EN bath constituents which are consumed during plating or plate-out consist primarily of nickel salts, pH regulators, and reducing agents. The cost per unit (CPU) associated with the operation of an EN bath can be calculated by summing the cost of chemicals consumed divided by the total number of parts processed. The cost of EN bath operation includes the cost of make up chemicals (C1), the cost of replenishment chemicals (C2) and the cost of pH controlling chemicals (C3).

$$\text{Cost Per Unit (CPU)} = \frac{C_1 + C_2 + C_3}{\text{Number of Units}}$$

where: $C_1$ = cost of make up chemicals
$C_2$ = cost of replenishment chemicals
$C_3$ = cost of pH control chemicals

The CPU can be calculated to establish baseline cost. The CPU can be calculated after changes have been implemented and the difference in the CPU is equal to the cost improvement or increased cost associated with the change.

Following are models that can be used to calculate the cost of operating an EN bath. Bath make up is the first chemical cost encountered. Per the specification sheet for the EN-P process[5], make up of the alkaline solution includes the use of 15% by volume of the component which contains nickel salts and other required make up chemicals plus the use of 8% by volume of the component

which contains the hypophosphite reducer[b]. The pH adjusting solutions are either 1:1 ammonium hydroxide which raises the pH or 25% sulfuric acid to lower the pH. All solutions are mixed to 100% volume using distilled water. The specification sheet for the EN-B process , designates that 15% by volume of the component which contains nickel salts and other required chemicals be mixed with 5% by volume of the component which contains the borane reducer[c]. The pH adjusting solutions are either concentrated ammonium hydroxide which raises the pH or 50% acetic acid to lower the pH. All solutions are mixed to 100% volume using distilled water. The cost of bath make up can be calculated as follows:

$$C_1 = V_1 M_1 + V_2 M_2 + V_3 M_3$$

where: $C_1$ = cost of make up chemicals
$V_1$ = volume of nickel make up solution
$M_1$ = cost of nickel make up solution per volume
$V_2$ = volume of reducer
$M_2$ = cost of reducer per per volume
$V_3$ = volume of pH adjusting solution
$M_3$ = cost of pH adjusting solution per volume

The calculation for the cost of EN bath make up (C1) will change if more or less components are required in bath make up.

Bath replenishment is the second EN bath cost which is encountered. The replenishment chemicals which are used in the EN-P process[5], are: the solution which is used to maintain nickel concentration, the solution which is used to maintain hypophosphite reducer concentration and the solution which is used to replace materials lost by normal drag-out. The replenishment chemicals which are used in the EN-B process[5], are: the solution which is used to maintain nickel concentration and the solution which is used to maintain borane reducer concentration. The cost of replenishment chemicals can be calculated as follows:

$$C_2 = V_4 M_4 + V_5 M_5 + V_6 M_6$$

Where $C_2$ = cost of replenishment chemicals
$V_4$ = volume of nickel replenishment solution
$M_4$ = cost of nickel replenishment solution per volume
$V_5$ = volume of reducer replenishment
$M_5$ = cost of reducer replenishment per volume
$V_6$ = volume of other solutions
$M_6$ = cost of other solutions per volume

The calculation for the cost of EN bath replenishment (C2) will change if more or less components are required in bath replenishment.

The pH control chemicals for the EN-P bath and the EN-B bath are different as previously mentioned in the discussion of solution make up. Per the specification sheet for the EN-P alkaline solution[5], the pH is adjusted up using 1:1 ammonium hydroxide or the pH is lowered with 25% sulfuric acid. Per the specification sheet for the EN-B solution[5], the pH is raised using concentrated

---

[b] Niklad 776, Allied-Kelite, Melrose Park, Illinois
[c] Niklad 752, Allied-Kelite, Melrose Park, Illinois

ammonium hydroxide and the pH is lowered with 50% acetic acid. The pH of EN plating solution can be adjusted after make up, during replenishment or alone. The cost of pH adjustment chemicals can be calculated as follows:

$$C_3 = V_7 M_7 + V_8 M_8$$

Where: $C_3$ = cost of pH control chemicals
$V_7$ = volume of pH elevating solution
$M_7$ = cost of pH elevating solution per volume
$V_8$ = volume of pH lowering solution
$M_8$ = cost of pH lowering solution per volume

The calculation for the cost of EN bath pH adjustment (C3) will change if more or less components are required in bath pH adjustment.

Minimizing Extraneous Bath Plate-Out

Extraneous bath plate-out is a major economic consideration in EN bath operation within a manufacturing facility. Extraneous bath plate-out is defined here as any nickel deposition and chemical depletion that takes place which is not associated with nickel deposition and chemical depletion on predesigned surfaces and desired locations. Once the baseline CPU for an EN plated product has been established, various avenues can be investigated which have the potential to decrease the CPU by minimizing extraneous bath plate-out. One of the major causes of extraneous bath plate-out is improper bath activation. Substrate metal surfaces such as: aluminum, cobalt, gold, iron, nickel, palladium, rhodium, and steel are catalytically active substrates which initiate electroless nickel deposition[4,17,18]. Whenever products containing these inherently catalytic surfaces are EN plated, the potential exists for metallic fines or dusts to enter the plating bath and cause extraneous plating[17,19]. These catalytic particles serve as nucleation sites for improper activation and increase the cost associated with the CPU. Remedial action which can be taken to minimize this improper activation is to either completely clean the parts of fines and dusts or continuously filter the bath solution to remove this source of improper EN bath activation.

Another major cause of extraneous plating is improper activation of components. Substrate surfaces such as brass, ceramic, copper, molybdenum, molybdenum-manganese, molybdenum-manganese-silica, plastic, tungsten, tungsten-manganese-silica, and silver are noncatalytic for an electroless nickel bath and require activation[4,20,21]. These noncatalytic surfaces can be activated by immersion plating with a catalytically active metal as mentioned above, galvanically plated by contacting an actively plating surface[20], immersed in palladium chloride[4,8,21], or cathodically activated with nickel[4]. Wherever parts are activated, the potential exists for excessive activation on the parts. Although extraneous activation will not always be visible prior to EN plating, extraneous activation is definitely visible after EN plating. Extraneous bath plating in the form of excessively activated parts can be monitored by inspecting and documenting the quantity of parts which retain excessive plating. Once the magnitude of an excessive plating problem has been specified, corrective steps can be taken in the activation cycle to decrease extraneous plating. Remedial action aimed at reducing extraneous

plating and the baseline CPU includes: decreased time for immersion activation, reduced concentration of immersion activation chemistry, reduced contact time for galvanic plating, a modified ratio of parts to galvanic media used in galvanic activation, reduced palladium concentration in palladium activation, reduced activation time in palladium, improved rinsing of palladium after activation and optimization of parameters associated with cathodic activation.

Extraneous bath plating in the form of catalytically activated handling equipment such as racks or barrels can also increase the CPU. Remedial action focussing on the reduction of costs associated with the plating of handling equipment includes: changing of racks or barrels between activation and plating, nickel stripping after the plating cycle or resurfacing of original surfaces with noncatalytic materials.

Extraneous bath plating in the form of plated tank walls, plated heaters, plated racks, plated barrels, plated filters, etc. can be caused by excessive heating or hot spots[17,19]. Excessive heat alone will cause spontaneous deposition of an EN bath resulting in the plating of nonactivated surfaces. Heat induced extraneous plating can be minimized by using derated heaters with a maximum density of 20 watts per square inch, the use of a double boiler system to evenly distribute heat and circulation of plating solution to provide homogeneous bath temperature without hot spots. Reduction of the baseline CPU aiming at heat related extraneous EN bath plating can be accomplished by proper heat design, the use of heater output commensurate with needs wherein heaters are operational in excess of 70% of production time, only heating the bath when production needs exist and controlling bath temperature.

Extraneous bath plating in the form of plated tank walls, plated heaters, plated racks, plated barrels, plated filters, etc. can be caused by extended exposure to EN plating solution. Although a surface is not catalytically activated or subjected to excess heat within an EN bath, the nickel particulate within the solution may activate the surface. Although this particulate is filtered, removal from solution does not eliminate the potential for catalytic activation. Whenever a tank or other equipment is unacceptably plated with nickel, this nickel can be stripped. However the use of liners has been considered as a means to reduce tank wall plate-out[17,22]. Plate-out on tank walls is reduced by periodically changing the liner to present a new, nonactivated surface to the bath solution. Since liners are available in different materials and costs vary, an analysis of the CPU with and without the use of a liner should be conducted to insure that cost savings justify the use of liners.

The presence of palladium in the form of a dissolved ion will cause spontaneous decomposition of an EN bath resulting in greatly reduced bath longevity and an undesirably increased CPU. The drag-in of such contaminating chemicals will cause irreversible bath problems[17]. When a palladium activation cycle is used[4,18,21], extensive control of rinses should be monitored to insure that the parts entering the bath are free from dissolved palladium[23]. The monitoring of rinse water quality after activation can be accomplished by the use of: resistivity meters, pH monitoring of rinse water or maintaining proper rinse flow rate.

Maintaining a Homogeneous Bath

An Electroless nickel bath is composed of a variety of chemicals. An EN bath contains a balance of nickel salts, chelating agents, pH regulators, stabilizers, exhaltants, buffering agents and reducing agents [17]. The chemical parameters which generally required control include: nickel concentration, concentration of reducer and pH control. The cost of operating an EN bath will increase as the quantity of chemicals used in replenishment is increased or as bath longevity is decreased. An imbalance in the chemical control of the bath will cause the excessive generation of one type of by-product while the bath is deficient in other components. An imbalance in the pH control can induce precipitation of compounds in the EN solution and increase replenishment requirements and ultimately the cost of an EN bath. This imbalance can lead to premature catastrophic decomposition of the bath or increased chemical requirements such as reducer. Both of the activities of increased replenishment requirements and catastrophic decomposition lead to increased bath costs. Maintaining a homogeneous bath will minimize the possibility of bath imbalance and reduce the increased cost associated with a bath which is out of control.

The frequency of additions is another criteria which should be evaluated in perspective to the economics of EN bath operation. When the frequency of analysis and additions is such that process controls and limits cannot be maintained without making adjustments within a 20 minute period, then there may be a design problem. A complete EN bath analysis for pH, nickel concentration and concentration of reducer requires approximately 20 minutes. If the parameters which are monitored undergo a change to a concentration outside specification within 20 minutes, actual bath control is non-existent. When the monitored parameters undergo an excursion beyond process controls and limits, this imbalance leads to premature catastrophic decomposition of the bath or increased chemical requirements such as reducer. The proper frequency of additions promotes the maintenance of a homogeneous bath and this control allows operations to decrease chemical costs. The maintenance of a homogeneous bath is further promoted by minimizing the volume of each chemical addition.

The design problem associated with maintaining proper frequency of additions is the proper ratio of tank volume versus product throughput. Each load of parts which enters an EN plating bath will consume a certain quantity of chemicals per minute. If the tank volume is too small, then a replenishment will be required in less than 20 minutes. In order to compensate for insufficient tank volume, the quantity of parts must be reduced or the rate of plating must be reduced to decrease the quantity of chemical consumed per minute. Under limitations of capacity and throughput, the tank should be sized to accommodate requirements or a continuous feed rate of chemicals should be used. A tank which is too small can induce a chemical excursion outside of proper operating limits and cause a solution imbalance increasing the EN operating cost.

The opposite is also true in that an oversized EN plating tank will increase plating costs. When an EN bath is at operating temperature, the reducer is being consumed by thermal decomposition independent of the quantity of parts being plated. When the bath loading (square feet

of plating surface per gallon of solution) is very low, excessive reducer is consumed because the quantity of reducer consumed by thermal decomposition exceeds the quantity of reducer consumed in plating [24]. The presence of an oversized EN plating tank can be compensated for by increasing throughput or lowering plating rate by reducing bath temperature.

## Conclusion

This presentation has focussed on the methods used to reduce the direct material cost associated with EN plating. The methods used to reduce direct material consumption include: 1) optimizing plating thickness using a predictor calculation with an x-ray fluorescent thickness gauge; 2) minimizing extraneous bath plate-out by controlling factors of excessive heating, improper activation, extraneous activation and undesirable drag-in; and 3) maintaining a homogeneous bath by the use of minimally sized chemical additions, operating an EN bath without chemical imbalances, using a properly sized plating tank and setting the correct frequency of replenishment additions. In an effort to facilitate a cost reduction program, models have been presented to calculate optimum plating time for proper thickness and to calculate chemical costs. The chemical cost model can be used to calculate baseline chemical costs and can be used to calculate the changes in bath cost associated with manufacturing improvements.

## References


1. T.R.Pound, Electronic Package & Production, 27, 12, 9 (1987).
2. D.W.Baudrand, Plating & Surface Finishing, 70, 12,14 (1983).
3. R.E.Miller, Ibid, 74, 12, 52 (1987).
4. F.Lowenheim, Modern Electroplating, Wiley & Sons (1976).
5. G.A.Laitinen, Allied-Kelite Div. of Witco Chemical, Melrose Park, IL.
6. MIL-C-26074 C. Requirements for Coatings, Electroless Nickel (1985).
7. V.Jirkovsky et al, Telsa Electronics, 3, 75, (1977).
8. H.Honma and K.Kanemitsu, Plating & Surface Finishing, 74, 11, 62 (1987).
9. Federal Specification QQ-N-290-A, Nickel Plating (Electrodeposited).
10. ANSI/ASTM Method B567-78 Coating Thickness by Beta Backscatter (1978).
11. ASTM Method B568-79, Coating Thickness by X-Ray Spectrometry (1979).
12. R.Asher and E.Ruiz, Plating & Surface Finishing, 73, 7, 30 (1986).
13. Woster, E. Production Environment Quantitative Analysis of Plating Thickness Using X-Ray Fluorescence for Small Parts Manufacturing. Seiko Instruments USA, Torrence, California.
14. Nelson, R. Accuracy and Precision of Measurement By X-Ray Fluorescence of Ni-P Deposits and Solutions. Seiko Instruments, Torrence, California.
15. P.Wright, Electrionics, 29, 7, 61 (1983).
16. J. Bronson, Expandable SFT7000 Series X-Ray Sample Quality Measurement System, Seiko Instruments, Torrence, CA.
17. G.A.Laitinen, Plating & Surface Finishing, 64, 11, 39 (1977).
18. D.W.Baudrand, AES Symposium on Cleaning, Pickling, and Etching (1983).
19. N.Zaki, Plating & Surface Finishing, 73, 7, 33, (1986).
20. D.W.Baudrand, Ibid., 68, 9, 67 (1981).

21. D.W.Baudrand, Metal Finishing, 85, 6, 115 (1987).
22. Roistacher, Ibid., 84, 6, 47 (1986).
23. W.Karaces, Ibid., 83, 1, 15 (1985).
24. D.W.Baudrand, Plating & Surface Finishing, 73, 7, 34 (1986).

# PRINCIPLE OF MEASUREMENT

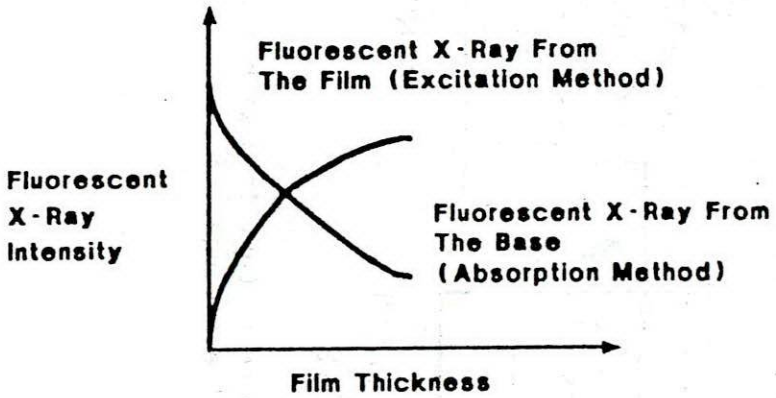


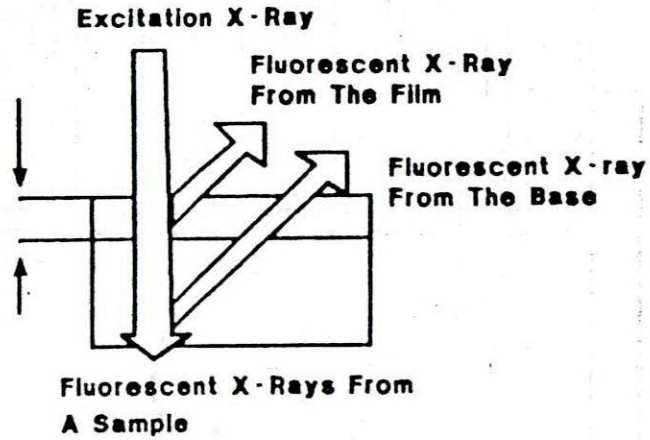


$I = (I_\infty - I_0)(1 - e^{-\mu x}) + I_0$

$\mu$: Absorption Coefficient

I: Fluorescent X-Ray Intensity

$I_0$: Background Intensity

x: Thickness Of The Film

$I_\infty$: Saturation Intensity

Figure 1. Graphic Depiction of the Principle of Thickness Measurement for X-ray Fluorescence Using Fluorescent X-rays from the Surface and the Base.

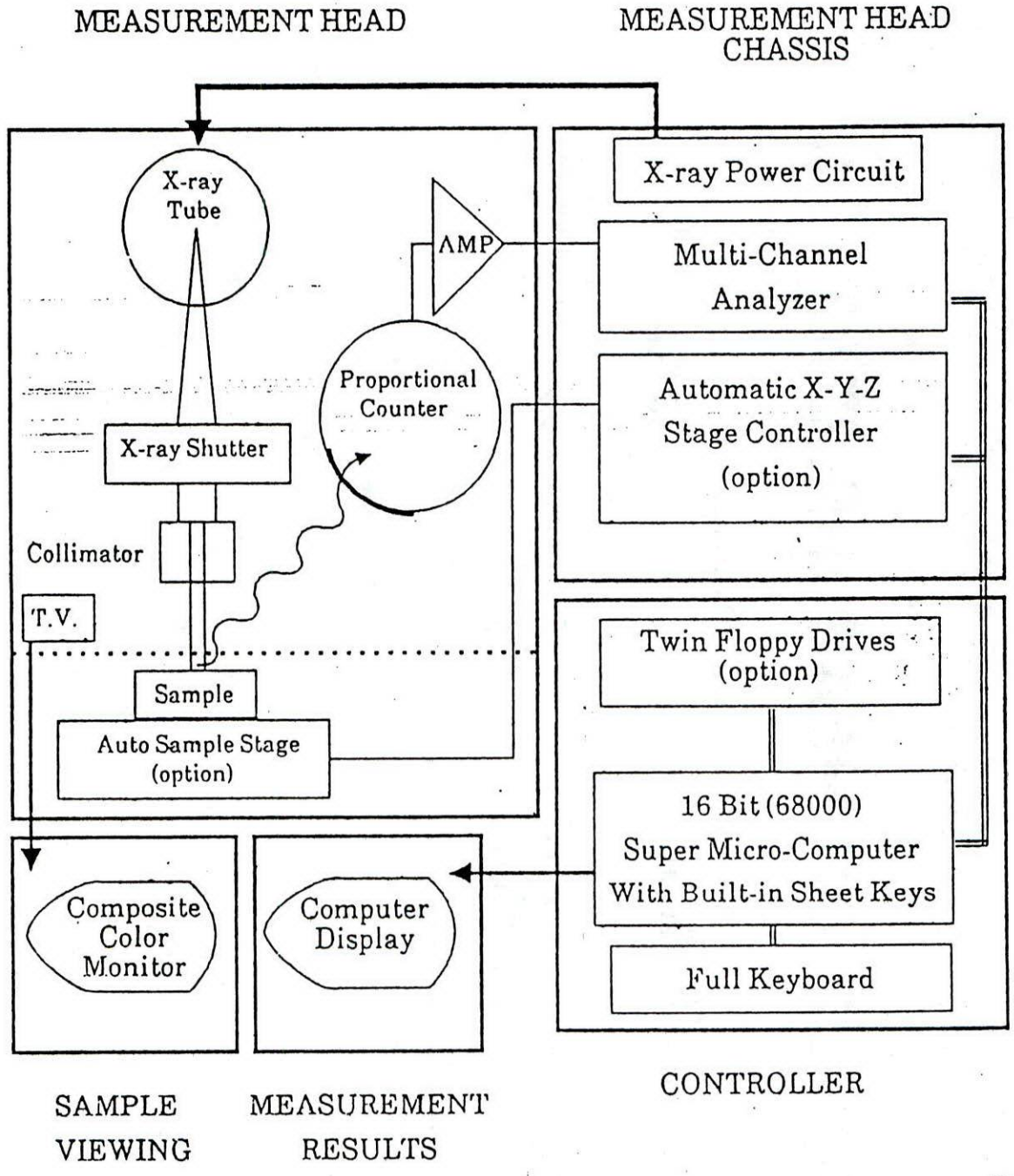


Figure 2. Functional Components Contained within a Typical X-ray Fluorescent Thickness Gauge.

# MECHANICAL FILTRATION SPECTRUMS

Ni / Cu
349 µ" Ni
Co Off
2694 CPS Ni

Ni / Cu
349 µ" Ni
Co On
960 CPS Ni

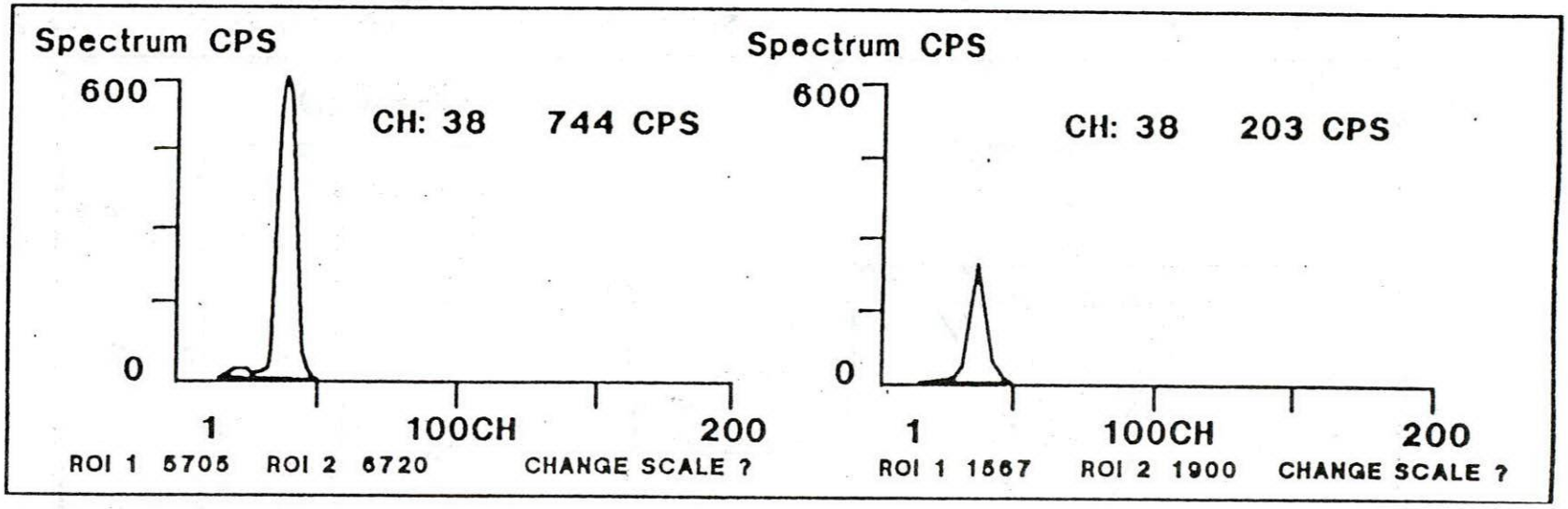


Figure 3. Mechanical Filtration Spectrum of an X-ray Fluorescent Thickness Gauge with and without a Cobalt Filter.

# DIGITAL FILTRATION METHOD

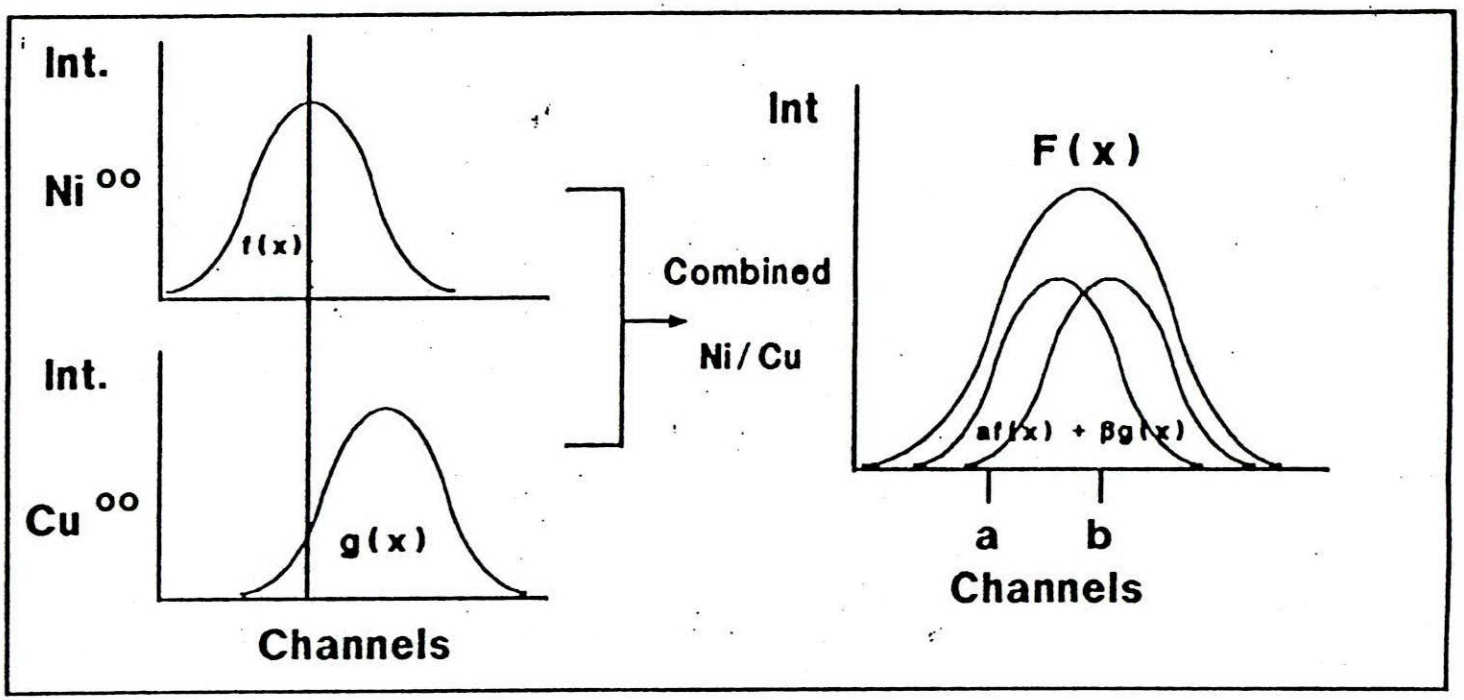


- $F(x) = \alpha f(x) + \beta g(x)$ total coating signal
- a and b are channel limits for signal processing
- $\alpha$ and $\beta$ are the Ni and Cu intensity ratio coefficients derived from a complex least square fitting routine
- Using the ratios $\alpha$ and $\beta$, A calibration curve is derived for each component

Figure 4. Digital Filtration Used in X-ray Fluorescent Thickness Measurements to Deconvolute Two Overlapping Spectra into Two Component Curves.

J-7

# Electroless Deposition II
# Session J

## Hope for the Best But be Prepared for the Worst

David Kunces, CEF
MacDermid Inc.

## ABSTRACT

# HOPE FOR THE BEST
# BUT BE PREPARED FOR THE WORST

By David Kunces CEF
MacDermid Incorporated

Waste treatment regulations are becoming more stringent. Each day the public becomes more concerned over our natural resources and they do have a right to protect them.

Methods to meet today's electroless nickel waste treatment standards, i.e. removal of metal, as well as methods for tomorrow's worst, i.e. all the constituents, will be discussed.

To meet today's regulations for waste treating electroless nickel and to prepare for tomorrow is a constant concern to all users. Regulations affecting the plater varies in different locations. The nickel and any other trace metals associated in the solution is the only common restriction with today's baths. Today's chal-challenge to the electroless nickel plater is to develop an acceptable method of disposal of the metal in an electroless nickel bath. This method encompasses the "cradle to grave responsibility". Specifically, (1) locating a licensed hauler for the solutions and/or sludge, (2) locating a disposal site for above, and (3) making sure that the waste is disposed of in an acceptable manner as the plater will in most cases retain liability.

Tomorrow's regulations most likely will be more stringent due to an increase in public concern over our natural resources. The ability to be able to waste treat all of the constituents in an electroless nickel bath may be necessary, i.e. (1) nickel and heavy metal stabilizer, (2) reducers, (3) complexor/chelator, (4) buffers (i.e. ammonia), and (5) phosphite by products.

To do this, new technologies will either have to be developed or present technologies refined to meet these needs.

Nickel and other heavy metals normally in an EN bath are treated in one of the following ways:

1. Reduction - in which powerful reducing agents such as sodium borohydride, hydrazine, sodium hydrosulfite, DMAB, or even sodium hypophosphite reduce $Ni^{+2}$-$Ni^{0}$. The reduced metals can be made to deposit on metal parts or scrap metal (controlled plateout) or can be made to form a precipitate.

2. Precipitation - of $Ni^{+2}$ with hydroxides, sulfides, carbonates, carbamates and starch xanthate products to produce an insoluble nickel compound that is removed from solution after settling; a (sludge) precipitate is also produced.

3. Separation - of nickel ions. Ion exchange is one example. Nickel ions are absorbed onto cationic resin and replated by $H^{+}$ or $Na^{+}$ ions. Another example is electrodialysis. An electric current induces partial separation of components in an ionic solution. Reverse osmosis is a third possibility, which utilizes a semi-permeable membrane to separate, under pressure, nickel ions (as well as other ions) from the solution.

Of all the above methods, reduction is the most popular. To avoid any precipitation, the control plateout method will meet today's as well as tomorrow's regulations. Control plateout will eliminate the need to haul away solid waste thereby lessening the liability.

**Controlled plateout** is a reduction method which simply continues to plate out the nickel alloy ($Ni^{+2}$ reduced to $Ni^{0}$) until very low levels are obtained. No precipitate or sludge is produced, thereby eliminating the need to haul away solid waste. Control plateout can be performed in one's production EN tank. You operate the spent EN bath at normal plating temperatures with metal (steel or aluminum) scraps in the bath. Addition of reducing agents and stabilizers control the rate and amounts of deposition. The nickel concentration in an EN solution can easily be brought down below 10 ppm using control plateout.

If necessary, any of the remaining amounts of nickel metal not plated out can be reduced further with any of the polishing agents commonly used in waste treatment. The solution is now free of any metals and can be directly dumped down the drain. With regard to any further regulating, local and state ordinances should be contacted.

The solution still contains ammonia (if used), phosphorous and chelators/complexors which usually are organic acids.

**Ammonia** which is used to adjust pH and as a buffer in some electroless nickel baths can be expelled. If ammonia is left in the bath, it may become a hinderance for complete removal of nickel as shown in Table 1 or a hinderance down the waste stream.

TABLE 1

| Bath | w/o $NH_4^+$ | w/10% $NH_4^+$ added |
|---|---|---|
| Med P % Semi Bright 1 | 5.3 ppm Ni | 16 ppm Ni |
| Med P % Bright 2 | <1 | 18.6 |
| High P % w/$NH_4^{++}$ Buffer 3 | 6.2 | 179 |

NOTE: All above baths had 6 metal turnovers. Precipitation method was used.

Baths using the control plateout method were were reduced to <1 ppm of nickel metal even with a 10% $NH_4^+$ added.

Ammonia can be removed from the solution by the following method:

1. Add caustic soda to raise pH above 12.5
2. Agitate solution with air
3. Heat bath to 185°F or higher to hasten the reaction

A spent bath after control plateout with 10% by volume 28% $NH_4OH$ added took 2 hours to expell the ammonia by the above method.

## Phosphorous

Typically, electroless nickel baths are high in phosphorous, all of it coming from the reducing agent hypophosphite ($NaH_2PO_2$) and the breakdown products, sodium phosphite ($Na_2HPO_3$). Where phosphorous is restricted, the following can be performed to oxidize the $PO_2$ ion to $PO_4$ so as to form the insoluble phosphate, calcium phosphate.

1. Raise pH to 10.5 with lime
2. Add peroxide
3. Filter solution

In Table 2, a spent electroless nickel bath with 8 turnovers was treated.

TABLE 2

| | Spent EN Bath | After Treatment |
|---|---|---|
| Nickel* ($Ni^{++}$) | 5 g/l | .2 g/l |
| Hypophosphite ($NaH_2PO_3$) | 4 g/l | 0.0 g/l |
| Phosphate ($PO_4$) | .32 g/l | 0.023 g/l |
| Phosphite ($PO_2$) | 12.2 g/l | 0.0 g/l |
| Total P as $PO_4$ | 12.5 g/l | 0.023 g/l |

*Precipitation method used.

In the above table, the $PO_2$ ion was oxidized by the $H_2O_2$ to $PO_4$ where the excess lime reacted to reduce the phosphorous. In order to reduce the phosphorous to the lowest levels, the $PO_2$ ion must be oxidized to $PO_4$ since calcium phosphite is slightly soluble. A possibility to make the hauling of this sludge non-hazardous is that the insoluble phosphate may have commercial use in the fertilizing industry, thus further eliminating the location of a disposal site.

**Chelators** (organic acids) which could affect phosphorous removal can all to a greater or lesser extent react with $KMNO_4$. The end product formed is dependent on the reaction conditions which include:

1. $KMNO_4$ concentration
2. Concentration of organic acids
3. Temperature
4. pH of reaction
5. Presence of ion, such as Ca or F, which may increase the reaction rate.

To simply illustrate the several reaction paths using citric acid per the following example:

$$H_2C\text{-}COOH \xrightarrow[\text{alkaline}]{+\ 4KMNO_4\ +\ 2OH} 6CO_2 + 5H_2O + 4MNO_2$$

$$HO\text{-}C\text{-}COOH \xrightarrow{+\ 3KMNO_4\ +\ 14H^+} 6CO_2 + 7H_2O + 3MN^{++}$$

$$H_2\text{-}C\text{-}COOH \xrightarrow[\text{slightly acidic } 80°C]{+\ KMNO_4} \begin{array}{l} \qquad\qquad CH_3 \\ \qquad\qquad | \\ COOH + C = O + CO_2 \\ \qquad\qquad | \\ COOH \quad CH_3 \end{array}$$

For waste treatment of citric, lactic and hydroxy acetic acid, the $KMNO_4$ will oxidize their hydroxy groups. For the other organic acids, maleic, succinic and EDTA, the $KMNO_4$ cleaves the double bond. The reaction products $MN^{++}$ or $MNO_2$ may have commercial value for the steel industry in its manufacturing process, thus eliminating the location of a disposal site and associated problems.

## CONCLUSION

The oxidation/reduction and destruction of the constituents of an electroless nickel bath is possible. Such a method would include:

1. Control plateout of the nickel method
2. Removal of $NH_3$
3. Destruction of chelators/complexors
4. Precipitation of phosphorous compounds as calcium phosphate.

The regulations dictating what the plater can introduce into the environment are becoming more stringent. There may come a day when all the constituents of any electroless nickel bath is regulated. The time is now to be prepared with a method. Whether or not the individual uses one or more of these methods will depend on the regulations specific to the area and the economics involved.

## References

1. David Kunces and William Toller, "Waste Treatment of Electroless Nickel to Remove Heavy Metal, Phosphites and Chelators", Product Finishing Electroless Nickel Conference IV, 1985.

2. David Kunces, "Plate-Out Pollution Control", Product Finishing Magazine, December 1987.

3. Jon Bengston, "Meeting Today's Regulations and Preparing for Tomorrow", The Institute of Metal Finishing, Electroless Nickel, 1987.

K-1

# Analytical Methods
# Session K

## CPVS Analysis of Acid Copper Plating Baths Used for Printed Circuit Boards

G.L. Fisher and W. Sonnenberg
Shipley Co.
Newton, MA

# CPVS ANALYSIS OF ACID COPPER PLATING BATHS USED FOR PRINTED CIRCUIT BOARDS

G. L. Fisher and W. Sonnenberg
Shipley Company, Newton, MA

## Abstract

Cyclic Pulse Voltammetric Stripping has been in use for over two years for controlling the additive concentration of acid copper plating baths. This method steps the potential of a rotating disk electrode to plate, strip, and prepare the electrode for subsequent analyses. The reason for the significant increase in sensitivity of the technique by introducing an open circuit delay into the cycle is given. The detectability limit for the brightener component of an acid copper plating additive is estimated and the applicability of CPVS to both dye and non dye additive systems is demonstrated. Hull cell and CPVS analyses of the additive concentration in an acid copper bath are compared.

## Introduction

Pressure on printed circuit manufacturers continues to mount as they build increasingly complex and more expensive boards to greater standards of quality. The acid copper plating step is critical to success in this production operation. The boards reach this point with a high value added incremental cost and with no opportunity to rework defective boards after plating.

Circuit board manufacturers are striving for better control of the plating operation to avoid scrap losses. Of the analytical techniques being used to control bath additive concentration, cyclic pulse voltametric stripping (CPVS) has shown particular utility. It was first described by Tench and White (1) who stepped the potential of a rotating disk electrode immersed in a plating bath to plate, strip, clean and equilibrate it. The CPVS stripping charge was a function of the additive concentration in an acid copper plating bath. The technique was modified by Fisher and Pellegrino (2) who added an open circuit delay to the CPVS analytical cycle to increase its sensitivity.

CPVS, like the Hull Cell, is a functional test. It determines whether the different components of the plating additive are interacting properly to produce the required deposit characteristics. Unlike the Hull cell, CPVS provides a quantitative measure of bath performance.

This work was undertaken to determine the reason for the increased sensitivity of CPVS due to introduction of an open circuit delay into the cycle. We have also further demonstrated the usefulness of the technique for controlling acid copper plating baths used in the production of printed circuit boards.

## Experimental

An ECI Qualiderm Model Q-2000 microprocessor programmed to perform CPVS analyses was employed. Besides the ECI rotator, a Pine Instruments Model MSR rotator and speed control was used in some of the experiments. An ECI platinum rotating disc electrode (RDE) with a 4.0 mm diameter disc was used in all cases. A saturated calomel electrode was used as a reference. The temperature was held at 26°C and an electrode rotation speed of 500 rpm was employed unless otherwise noted. The CPVS cycle used in this study is as follows:

Plate (-0.25V for 2s)
Strip (0.20V )
Clean (1.6V for 5s)
Equilibrate (0.425V for 5s)
Delay at Open Circuit for 30s

For most experiments, a plating solution containing nominally 80g/l $CuSO_4 \cdot 5\ H_2O$, 200 g/l of concentrated $H_2SO_4$ and 50 mg/l chloride was used. It was made up using electrolytic grade copper sulfate, semiconductor grade sulfuric and hydrochloric acids, and deionized water. A commercial non dye additive for acid copper plating (ELECTROPOSIT* 276) was used with these solutions to study the CPVS technique. The suppressor was a medium molecular weight polyalkylene glycol.

Hull cell analyses were done in a 267 ml cell using brass panels and a corrugated phosphorus copper anode. The polished brass panels were cleaned in an acid cleaner, rinsed and then dipped in 10% bv sulfuric acid before plating. Agitation was provided by an air sparger next to the cathode. The panels were plated for 5 minutes at 3 Amps.

## Results

Reason for sensitivity increase from the open circuit delay- It was shown in previous work that the adddition of a delay at open circuit increases the sensitivity of the technique by nearly 50%. It was believed that the delay allowed time for greater quantities of the brightener portion of the additive to move to the vicinity of the rotating disk electrode. This would enhance sensitivity because of the elevated brightener concentration at the electrode.

Further experiments were done to delineate the nature of the sensitivity enhancement. In the first, the effect of the delay on the base plating solution, the base solution with 750 mg/l of suppressor, and the base solution with the entire additive (suppressors and brightener) was determined. The results are given in Table 1.

*registered trademark of Shipley Company, Newton, MA

**TABLE 1. Effect of Open Circuit Delay on CPVS Analysis of the Components of an Acid Copper Plating Additive**

| Solution | CPVS Stripping Charge, mC | |
|---|---|---|
| | Without Delay | With Delay |
| 1. Base Plating Solution | 47.4 | 47.5 |
| 2. Base Solution with Suppressor | 2.9 | 2.9 |
| 3. Base Solution with 5 ml/l Additive | 4.5 | 6.8 |

These results clearly show that the delay at open circuit affects only the analysis of the solution containing the brightener. The lack of response of solution 2 to the delay in the cycle means that the suppressor must completely adsorb on the electrode during the equilibration step (0.425V for 5 seconds).

The nature of the adsorption of the brightener portion of the additive during the open circuit delay was examined next. Figure 1 shows that, for all three solutions, the potential at open circuit (OCP) rises rapidly with time and then levels off to between 750 and 775 mV. There were slight differences in the value of the OCP after 30 seconds; the base solution =767 mV, the base plus suppressor=773 mV, and base plus additive=747 mV. It was felt that these small differences in behavior during the delay could not account for its effect on sensitivity.

Figure 2 shows the effect of mass transport rate on CPVS response. The CPVS stripping charge was measured as a function of delay time at electrode rotation speeds of 500, 1000 and 2000 rpm. If the adsorption of the brightener is mass transport controlled, one would expect the slope of the curve to increase with increasing rotation rate (3). Since this did not happen, another explanation for the increased sensitivity due to the delay was sought.

To determine whether brightener adsorption at the RDE is related to potential, the CPVS analytical cycle was altered by eliminating the delay and raising the equilibration potential to 600 mV. Figure 3 shows an almost linear increase in the stripping charge with time at the equilibration potential. Adsorption of the brightener is clearly potential/time dependent. Thus, the delay at open circuit in the CPVS cycle provides the proper potential range to enable the brightener portion of the additive to adsorb on the electrode.

Response of different plating additives to CPVS analysis-To indicate how broadly CPVS can be applied, three different acid copper plating additives were analyzed using it. The results, in Figure 4, reveal that CPVS works quite well with non dye brightener additive systems. Note

that the two non dye additives give nearly identical CPVS stripping charge versus concentration plots even though they are made up of dissimilar constituents. The additive system employing a dye as the brightener responded poorly to the technique. There was an initial sharp increase in the stripping charge between an additive concentration of 1 and 2.5 ml/l followed by an increase in stripping charge of only 13% between 2.5 ml/l and 10 ml/l. This is probably too small an increase to enable CPVS to be used with this particular additive system.

Detectability limit of CPVS analysis- As found previously, CPVS analyses respond primarily to the brightener portion of copper plating additives. The following experiment was conducted to determine the minimum level of brightener that could be detected by CPVS. A solution containing the base acid copper plating bath plus 750 mg/l of suppressor was first analyzed by CPVS. Then, incremental amounts of a known brightener compound were added to the solution and it was analyzed after each addition. The results are shown in Figure 5. Note that CPVS can detect as little as 5 nanomoles/l of the brightener compound in an acid copper bath.

Correlation of CPVS analyses with the Hull Cell- The Hull Cell has been accepted as the primary method for controlling plating baths since its invention in 1939. It provides a simple method of checking bath operation over a wide current density range. It can be used to determine proper replenishment rates and detect bath contamination.

Any method of instrumental analysis of plating baths must reflect the actual behavior of the bath and results from the Hull Cell. A series of experiments were performed to determine if there is a correlation between Hull Cell and CPVS analyses. A sample of a 700 gallon operating acid copper plating bath used for production of PC boards was allowed to stand for several weeks to allow the brightener to decay to a low level. Then additions of the additive replenishment solution were made to 500 ml aliquots of the sample and CPVS and Hull cell analyses performed on them.

The results are shown in Figures 6 and 7. Figure 7 shows schematic diagrams of Hull Cell panels taken at various additive levels with the CPVS stripping charge measured in the same solution. Note that an addition of 2.5 ml/l of replenishment solution to the depleted bath completely eliminates the region of dullness on the Hull Cell panel. It does leave a rather wide burn region. Further additions of the additive to a total of 7.5 ml/l continue to reduce the region of high current density burn on the panel. These replenishment solution additions to the depleted bath are readily detected by CPVS. The stripping charge increases in a nearly linear fashion with additive concentration, Figure 6.

Further additions of replenishment solution, from 7.5 ml/l to 12.5 ml/l, cause no change in Hull Cell appearance. However, the stripping charge continues to increase, rising by 2 mC over this concentration range. At an additive level of a 15 ml/l, the Hull Cell appearance remains unchanged except for a very slight haze in the low current density region. However, the stripping charge rises by nearly 1 mC when the additive concentration is increased from 12.5 to 15 ml/l. Finally, at an additive concentration of 20 ml/l, the burn region on the Hull Cell panel begins to widen while the low current density haze is still present.

These experiments show that the Hull cell is a very insensitive method for controlling the additive level in acid copper plating baths. A wide range of additive concentrations gave identical Hull cell panels. Thus, a significant rise in bath additive concentration can occur without being detected by the Hull cell. This could result in bath over-replenishment and cause production circuit boards to be rejected for low current density dullness and poor leveling.

The Hull cell is known to be a very poor method for detecting organic contamination or excessive additive levels in acid copper plating baths. These affect the plated deposit at low current densities where, because of very low plating rates, the Hull cell is least sensitive. As shown above, CPVS can easily detect changes in additive concentration of as little as 0.5 ml/l.

## Conclusions

The significant increase in sensitivity of CPVS by the introduction of an open circit delay into its analysis cycle is the result of potential driven adsorption of the additive. During the delay, the potential of the rotating disc electrode rises through a region where strong adsorption of the brightener component of the additive occurs. This enables the technique to detect as little as 5 nanomoles/l of the additive in an acid copper plating bath. CPVS is better suited to non dye rather than dye containing acid copper plating additives. Comparison of Hull cell and CPVS analyses of the additive concentration in acid copper plating baths indicated a deficiency in the former method. The Hull cell was found to be insensitive to large changes in additive concentration that are easily detected by CPVS.

## References


1. D. Tench and J. White, J. Electrochem. Soc., **132**, 831, 1985.

2. G. L. Fisher and P. J. Pellegrino, "The Use of Cyclic Pulse Voltammetric Stripping for Acid Copper Plating Bath Analysis" presented at SUR/FIN 87, Chicago, IL.

3. A. J. Bard and L. R. Faulkner, *Electrochemical Methods, Fundamentals and Applications*, John Wiley & Sons, New York, NY, 1980, pages 518-519.

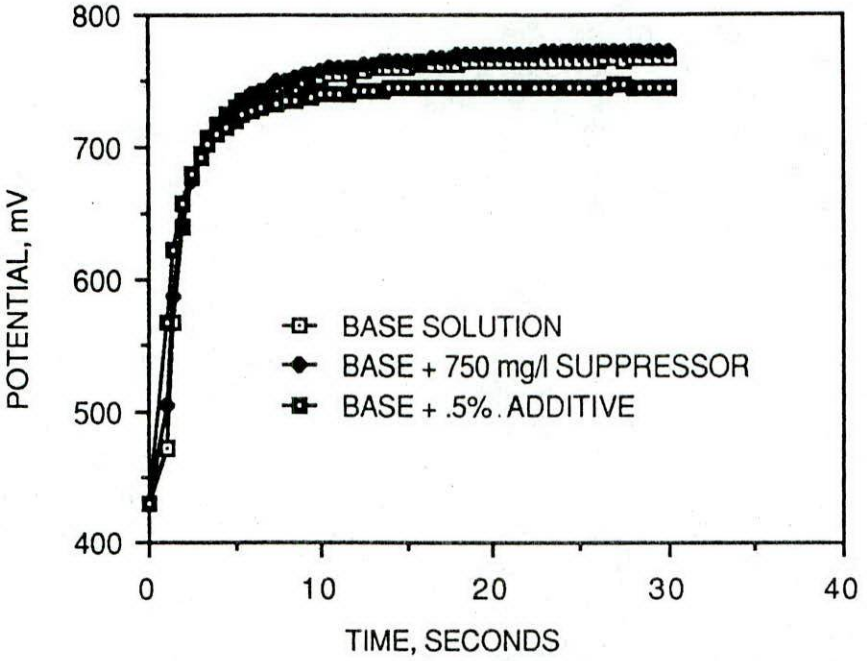


Figure 1. Effect of bath additions on CPVS open circuit potential.

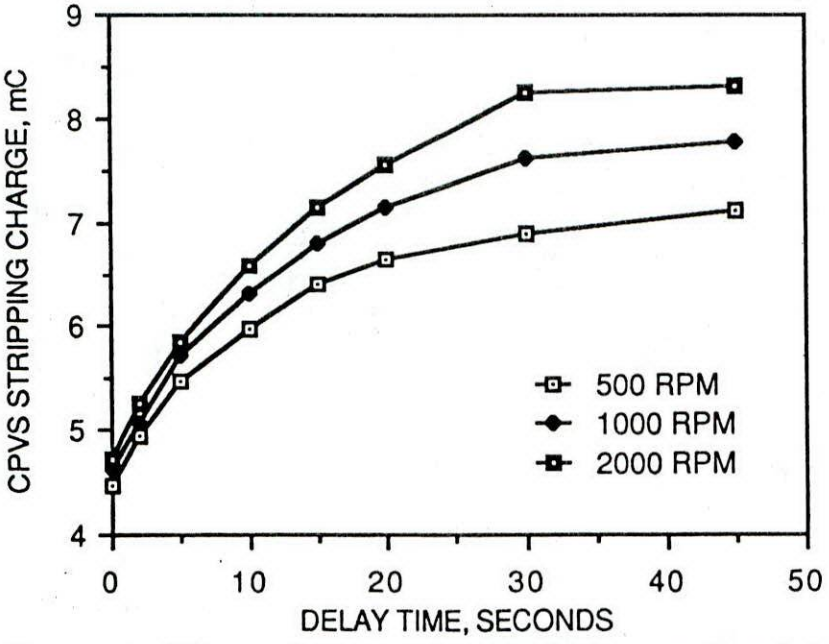


Figure 2. Effect of electrode rotation speed and delay time on CPVS stripping charge.

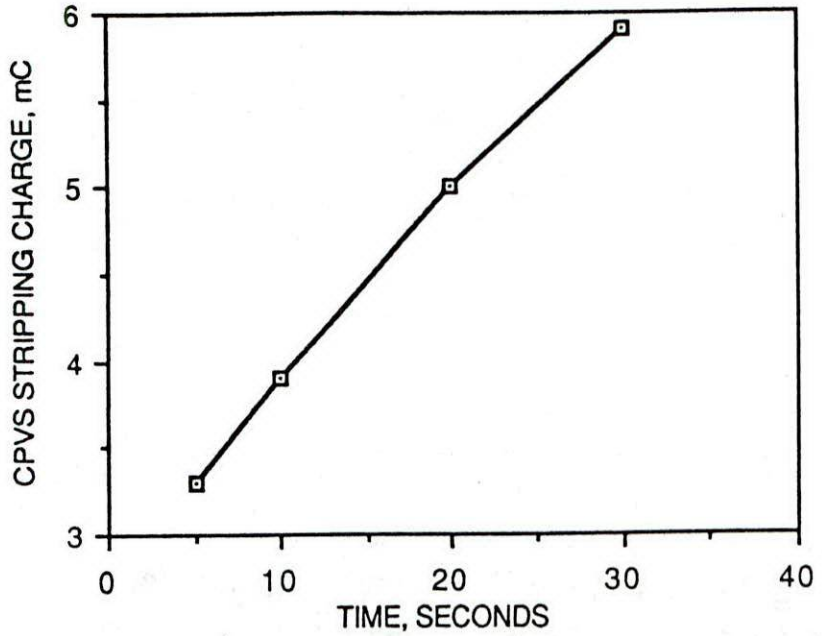


Figure 3. Plot showing increase in stripping charge with time. Equilibration potential = 600 mV.

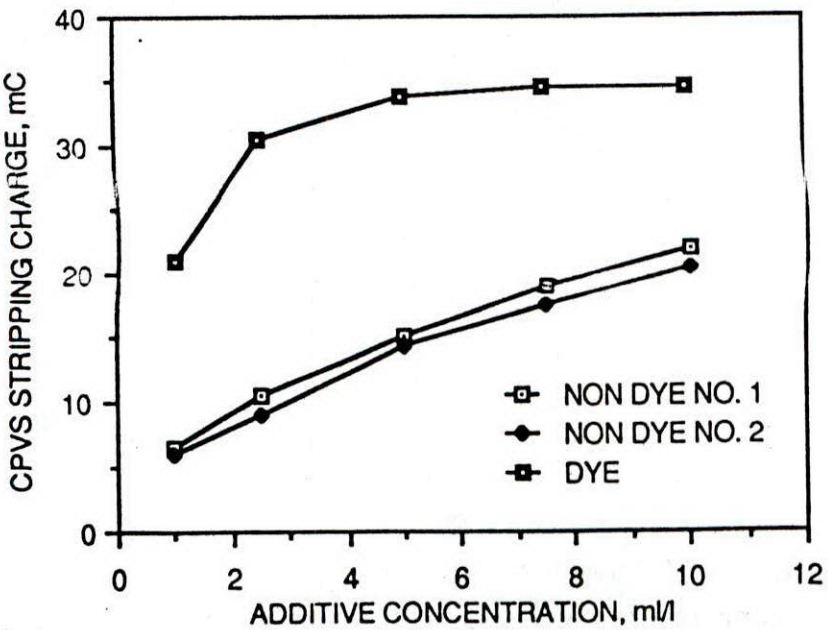


Figure 4. Response of different plating additives to CPVS analysis.

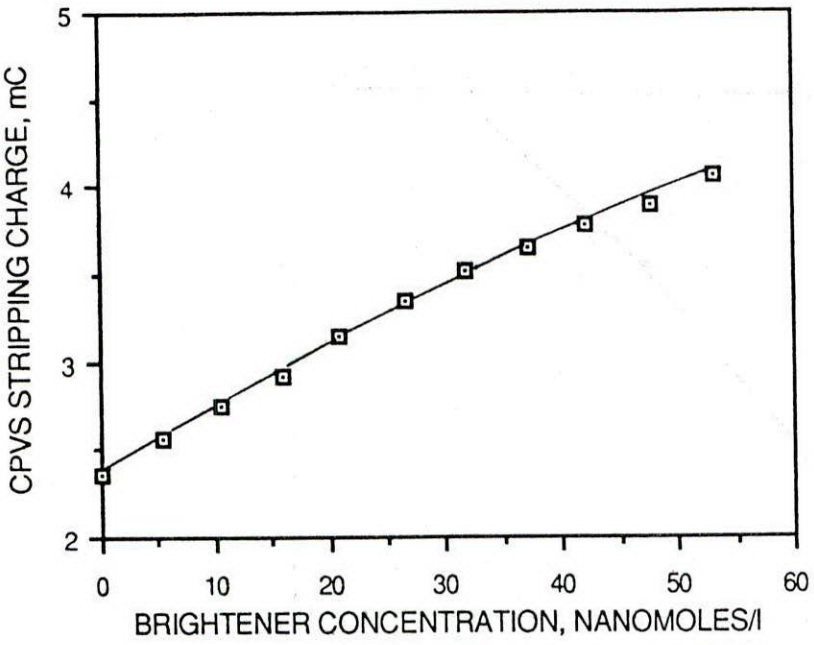


Figure 5. Plot showing detectability limit of CPVS analysis for brightener component of acid copper plating additive.

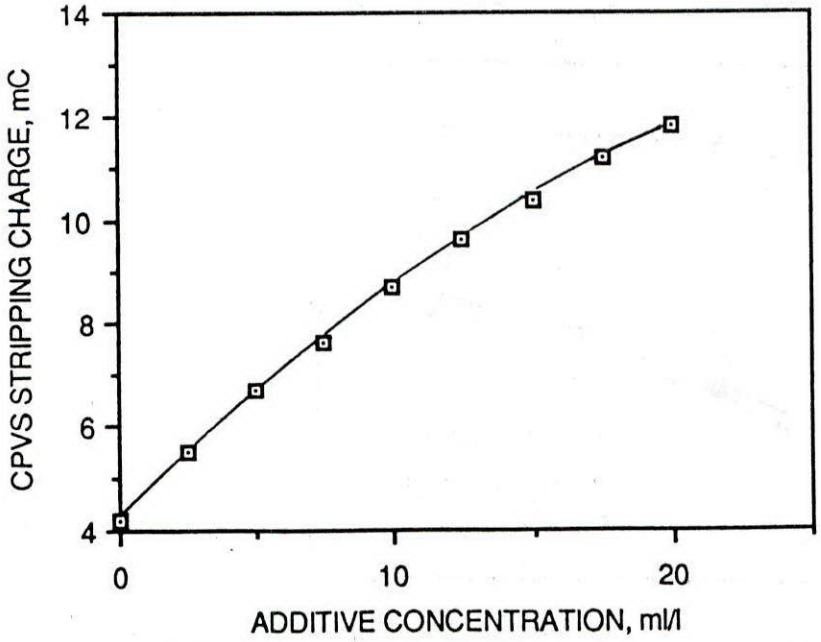


Figure 6. CPVS stripping charge versus concentration of replenishment solution in acid copper bath.

Figure 7. Hull cell panel appearance for an acid copper bath containing various levels of replenishment solution. CPVS stripping charge values are indicated for each level of additive.

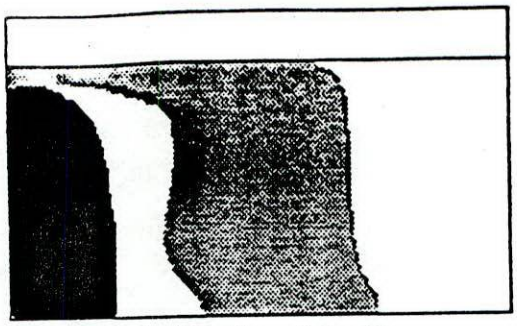

Depleted Bath - 4.2 mC

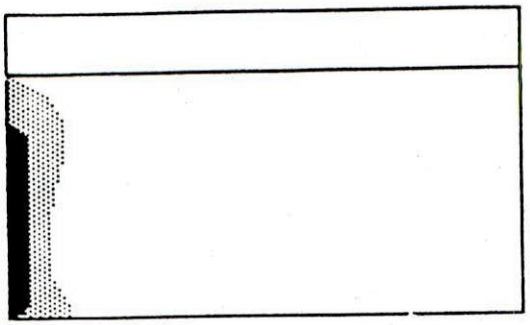

7.5 ml/l additive - 7.6 mC
10 ml/l additive - 8.7 mC
12.5 ml/l additive - 9.6 mC

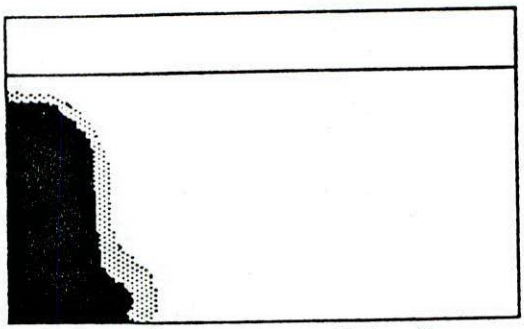

2.5 ml/l additive - 5.5 mC

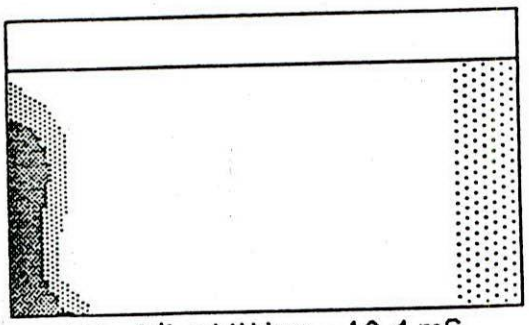

15 ml/l additive - 10.4 mC

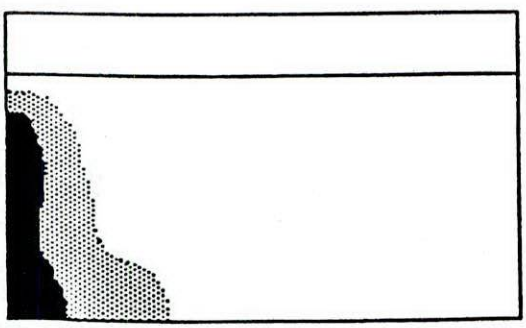

5 ml/l additive - 6.7 mC

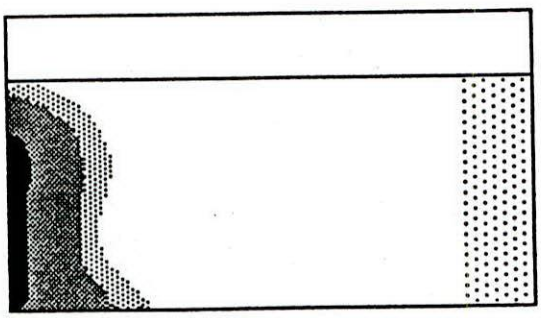

20 ml/l additive 11.8 mC

Heavy Burn

Medium Burn

Light Burn

Light Haze

Bright

K-2

# Analytical Methods
# Session K

## Plating and Micro-Etch Process Control For Printed Circuit Boards

Dr. Trudy Lionel
Hewlett-Packard
Sunnyvale, CA

# PLATING AND MICRO-ETCH PROCESS CONTROL FOR PRINTED CIRCUIT BOARDS

Dr. Trudy Lionel
Hewlett-Packard
Sunnyvale, CA

## Introduction

The Sunnyvale Printed Circuit Facility of Hewlett Packard has been concerned with process control since its startup in 1980. A well equipped and staffed chemical laboratory has provided the resources for developing new analytical methods using diode array spectroscopy (1,2,3). These methods are used to control additive levels in Watts nickel, acid tin and acid gold plating baths, but not acid copper baths. In 1985 Liquid Chromatographic (LC) methods were initiated to quantify the additive components of the copper plating bath (4). In addition Total Organic Carbon (TOC) analysis was set up to improve carbon treatment. More recently LC techniques have been used to separate additives and contaminants in tin and nickel baths, respectively. Improvements have been made in sampling and control of peroxide/sulfuric micro-etch baths. These methods and their effects on process control will be described below.

## Copper Plating

### LC

Acid copper plating baths are usually composed of three types of organic additives: brighteners, carriers and levelers (5,6). At Sunnyvale the first two components are analyzed by LC. Since the brightener is consumed during plating, upon startup the bath was analyzed throughout the day to determine automatic amp-hour feed rates. Daily measurement, lasting 6 minutes per bath, is sufficient to alert technicians to brightener pump or bath conditions. The carrier analysis involves extraction before chromatography and need only be done biweekly. Since it was discovered that this component degrades over time, carrier solution must be added separately based on the extracted weight. Chromatograms indicate the carrier distribution as well as the presence of contaminants such as dry film leachates.

TOC

The buildup of organic compounds is monitored by weekly TOC analysis. The need for carbon treatment of copper baths is determined when TOC levels exceed 600 ppm and/or LC shows interference of the brightener analysis. The batch treatment process at Sunnyvale was optimized using the TOC analyzer. Figure 1 shows the decrease in TOC during treatment. TOC decreases rapidly during the first hour of carbon treatment and a more gradual decrease is observed in the remaining four hours of the first pass on carbon. TOC levels drop significantly during the first hour of the second pass, however, very little change in TOC occurs during the remaining four hours. The same is true for the third pass on carbon. The TOC data resulted in a decision to change filters every two hours instead of every five. Similar experiments on the effects of hydrogen peroxide and heat treatment have led to their elimination from the carbon treat process.

The acquisition of a TOC analyzer capable of corrosive bath measurement is a valuable tool for process control (7). Plating baths, rinses, smear removal, developers, screen wash and other baths may all be examined for quality.

Nickel Plating

The Watts nickel bath is a stable bath, with long lifetimes and few problems. A buildup of foam on the surface was traced to residual acid cleaner, using extraction and chromatography. The standard curve for the contaminant surfactant present in nickel bath samples is presented in Figure 2. The surfactant concentration was reduced by adsorption on granulated carbon. A program of carbon polishing with on-line filter cartridges was implemented for process maintenance.

The routine spectroscopic analysis of the nickel bath indicates that the saccharin component is consumed during plating. The remaining components of the additive build up in the bath and are not completely removed by carbon filtering. Levels may be quantified by comparison with standard spectra, and saccharin additions rebalance the bath.

## Tin Plating

The acid tin plating bath is not found in many shops. However it is becoming more popular because of concern over the environmental hazards of tin-lead baths. The spectroscopic analysis separates the additive into wetter and brightener components. The bath is controlled within ranges of these components, depending on the age of the bath. However the analysis was unable to predict solderability failure. Three new procedures were undertaken:

1) to plate and wave solder a buried trace board containing isolated high current density pads, on a daily basis,
2) to measure the efficiency of the tin plating using copper coulometry (8), and
3) to separate the additive components using an LC gradient method (9).

The first option has been successful for solderability trouble shooting.

The second option of copper coulometry also examines bath performance. A tin plating cell and a copper plating cell are connected in series and the ratio of deposit weight gives the tin efficiency. Results showed that efficiency decreased from 80% to 50% over the bath lifetime. The correlation between the efficiency value and solderability could not be established and the test was discontinued. It is possible that an electrochemical analysis such as CVS may identify activity critical to tin plating uniformity.

The third option was evaluated for 4 months. Results are shown in the Table as a comparison between LC and spectroscopic methods. In both methods, the wetter component increases and the brightener component decreases during the first two weeks, then both hold steady over the 3 month lifetime. Although the LC analysis separated 4 of the 5 additive components, it was more time consuming than the spectroscopic analysis. Because similar information was available from both methods, the LC option was discontinued.

Over the years of controlling the acid tin bath, we have found various factors which are critical to solderability of the plated boards. These include: bath age, presence of brightener crystals, size of brightener add, anode condition, ratio of brightener to wetter, bath temperature, postplate rinse quality, board design, dummy plating, additions of $SnSO_4$ with $H_2SO_4$ followed by filtering, solubility of $SnSO_4$, and tank cleanliness before bath makeup. General improvements planned for plating distribution, will also improve board solderability.

## Micro-etch

The pre-copper-plate micro-etch bath is critical to production of fine line circuitry PC boards. Despite quantification of all components, this peroxide/sulfuric etch was difficult to control. Bath performance is measured by timed immersion of electroless copper "coupons". Etch rates are calculated either 1) by change in thickness measured by resistivity through a hole, or 2) by change in weight of a standard surface area. Etch rate reliability and precision were improved by preparing fresh electroless coupons weekly, Coupons were handled and stored away from skin and dust contact. Figure 3 shows etch rates before and after improving the coupon procedure. A holder was constructed to allow 5 hole coupons to be immersed at one time; the five values and their average are plotted in the figure. As would be expected, the etch rate depends greatly on the quality of the electroless copper plating. An even fine grained deposit will have a lighter etch than an uneven deposit. The latter condition may be produced in coupons from a new or poorly controlled electroless bath, or from uneven catalyst deposition leading to voids.

## Conclusions

The analytical techniques discussed in this paper were developed to improve process control of printed circuit board fabrication.* Through the use of chromatography and spectroscopy, a better understanding of the function of bath components has been achieved. Plans for 1988 are for statistical examination of accumulated data.

* Details of specific methods are available from the author.

References


1. T. R. Mattoon, P. McSwiggen, S. A. George, "Metal Finishing", 83, 83, February 1985,

2. S. A. George, T. R. Mattoon, "Metal Finishing", 83, 23, March 1985.

3. S. A. George, T. R. Mattoon, "Metal Finishing", 83, 50, April 1985.

4. K. E. Heikkila, R. K. Williams, B. Bohnen, J. Flicek, "Electrionics", August and September 1985.

5. K. H. Dietz, "Galvanotechnik" 78 (8) 1987.

6. L. Mirkowa et al. "Surface Technology", 15, 181, 1982.

7. L. C. Whitney, R. K. Williams, K. E. Heikkila, 73rd AESF Annual Conference, Electronics I-5, June 1986.

8. E. F. Duffek, Adion Engineering, Cupertino, CA, personal communication.

9. J. E. McCaskie, Lea Ronal, Freeport, NY, personal communication.

Table

Comparison of Tin Additive Analysis

| Bath Age | Brightener | | Wetter | |
|---|---|---|---|---|
| | LC %of control | UV %vol.of bath | LC %of control | UV %vol.of bath |
| 1 day | 106 | 7.17 | 98 | 8.80 |
| 1 week | 83 | 4.75 | 153 | 9.82 |
| 2 weeks | 64 | 3.56 | 150 | 10.43 |
| 3 weeks | 64 | 3.59 | 157 | 10.67 |
| 4 weeks | 59 | 3.14 | 140 | 10.83 |
| 5 weeks | 59 | 3.15 | 158 | 10.48 |
| 6 weeks | 55 | 2.85 | 163 | 10.11 |
| 8 weeks | 56 | 3.13 | 137 | 10.04 |
| 9 weeks | 60 | 3.24 | 146 | 10.04 |
| 10 weeks | 61 | 4.34 | 95 | 10.21 |
| 11 weeks | 48 | 3.11 | 104 | 10.01 |

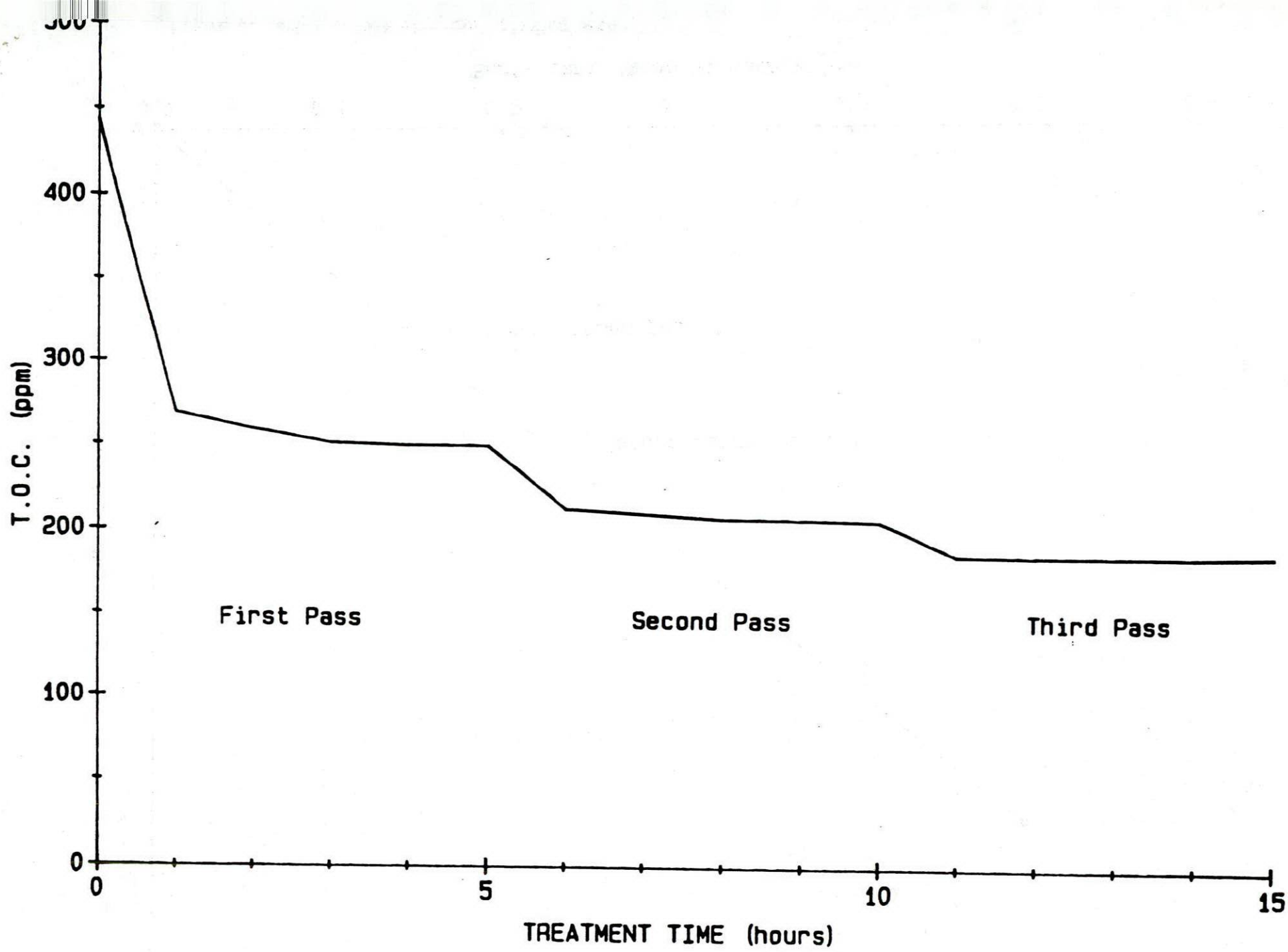


Figure 1. Carbon treatment of copper plating bath.

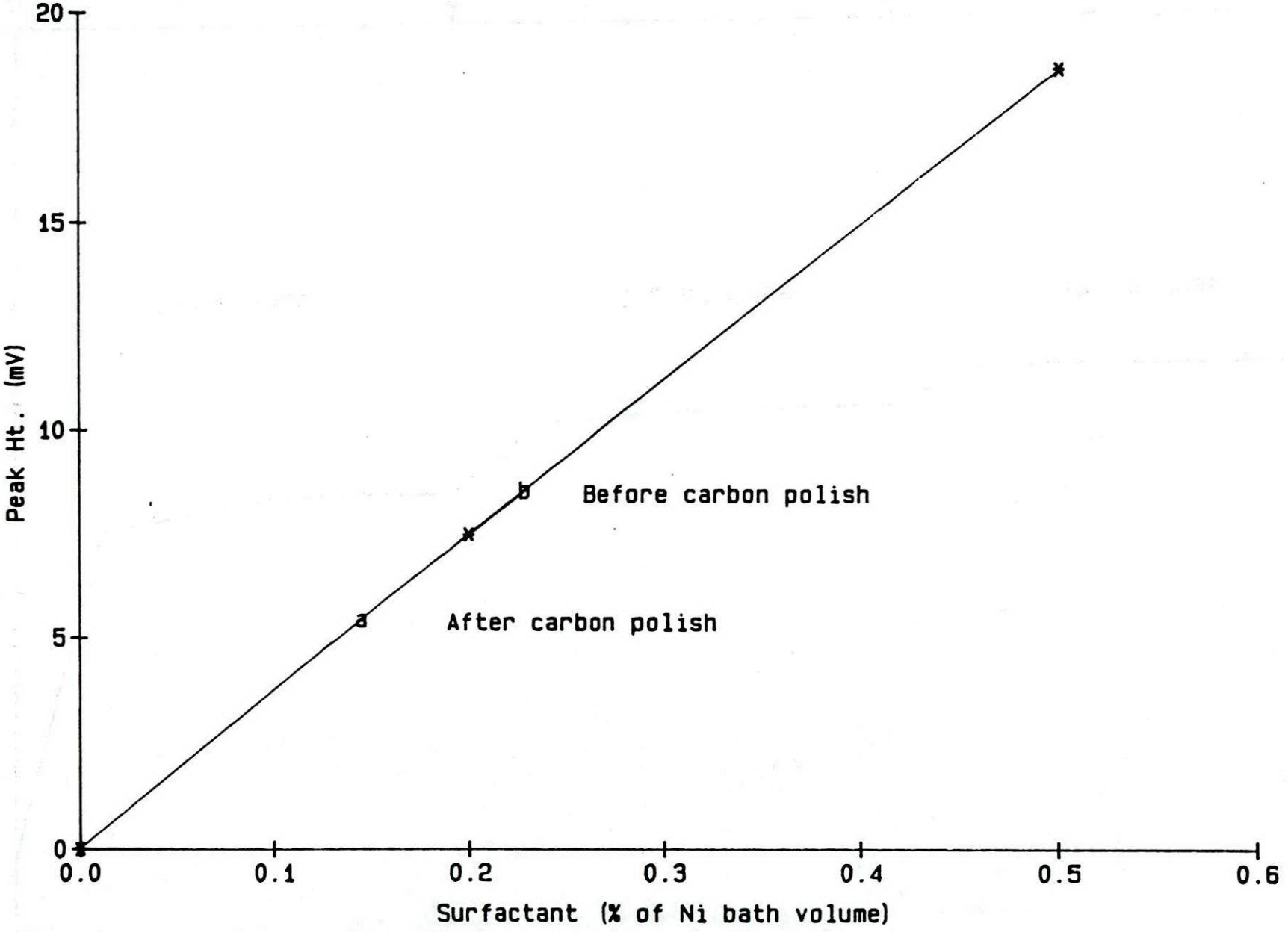


Figure 2. Carbon polish of nickel plating bath.

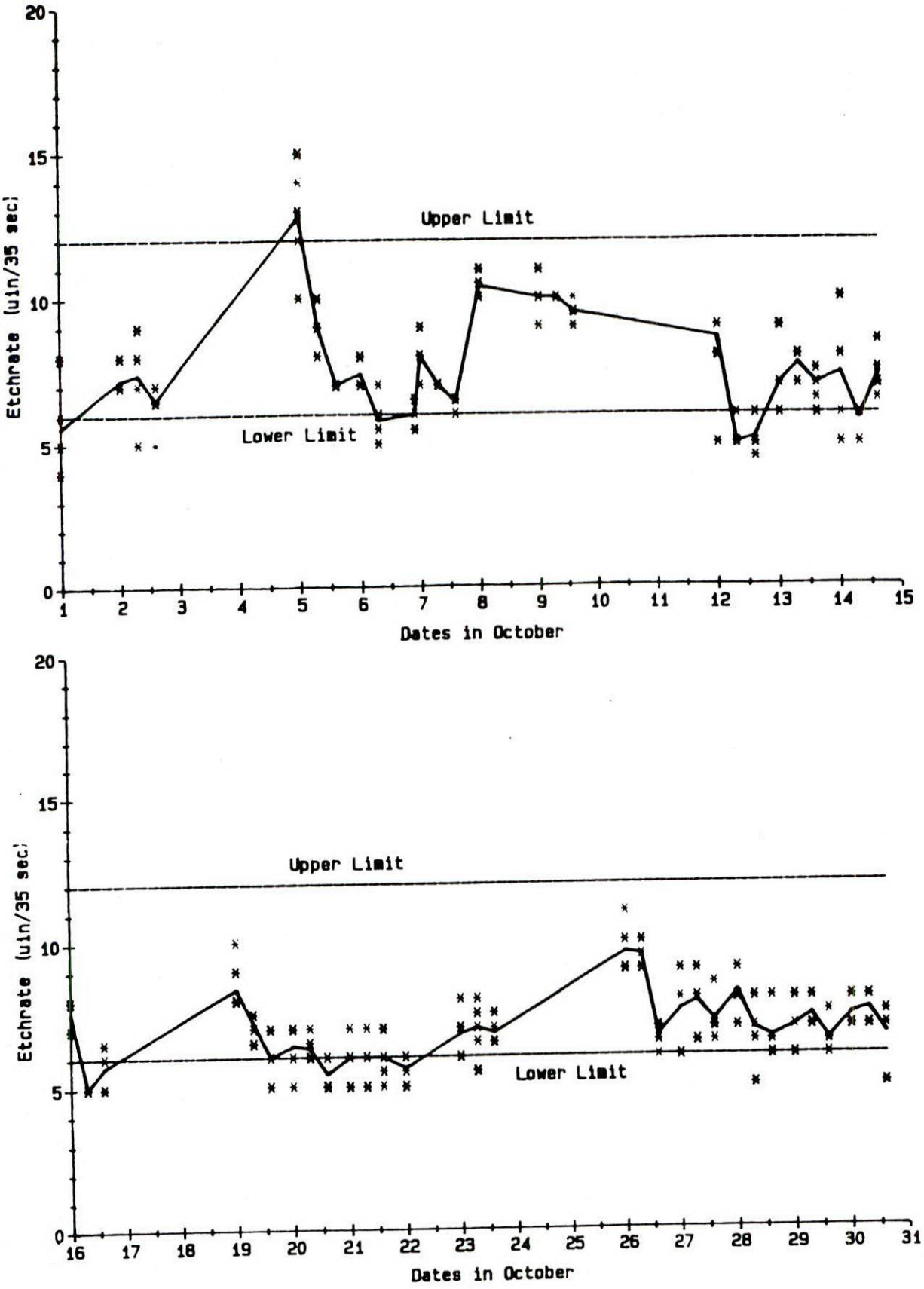


Figure 3. Etch rates before (top) and after (bottom) improving coupons.

K-3

# Analytical Methods
# Session K

## In-Situ Composition and Rate Monitor For Tin-Lead Alloy Electrodeposition

K. Keiji Kanazawa, Alison Sue
and Owen R. Melroy
IBM Research Division
Almaden Research Center
San Jose, CA

**PAPER NOT RECEIVED IN TIME FOR PUBLICATION***

# In-Situ Composition and Rate Monitor for Tin-Lead Alloy Electrodeposition

Mr. K. Keiji Kanazawa, Alison Sue and Owen R. Melroy, IBM Research Division, Almaden Research Center, San Jose, CA

Experimental evidence in support of the theoretical considerations for the use of a quartz microbalance as a composition and rate monitor for Sn-Pb alloy deposition will be presented. Details of the apparatus and potential problems and solutions for commercial implementation will be discussed.

* For copies of this paper, please contact the author directly

Mr. K. Kanazawa
IBM Corporation
Almaden Research Center
650 Harry Road
San Jose, CA 95120
(408) 927-2468

K-4

# Analytical Methods
# Session K

## Data Forecasting and Warning Signal For the Control of the Plating Baths

H.T. Morris, P.R. Scherer
and T.M. Tam
Lockheed Missiles & Space Co., Inc.
P.O. Box 3504
Sunnyvale, CA 94088

# Data Forecasting And Warning Signal For The Control Of The Plating Baths

By

(H. T. Morris*, P. R. Scherer, T. M. Tam)

Lockheed Missiles & Space Company, Inc.

P.O. Box 3504

Sunnyvale, CA 94088-3504

* Speaker

ABSTRACT:

Various data forecasting techniques have been investigated for the control of the printed circuit board plating baths at Lockheed Missiles and Space Company. This paper compares two statistical monitoring techniques , namely the Shewhart and Trigg methods. Applications of these two methods in the control of the plating baths, forecasting the process chemistry, and detecting errors in laboratory analysis are discussed.

INTRODUCTION.

Statistical process control (SPC) has been used at Lockheed Missiles and Space Company (LMSC) to monitor manufacturing processes, detect trends, and out of control conditions. SPC is intended to provide early warning that the process has changed. This will allow the process control engineer to take corrective action in a timely manner to ensure that the process is consistently controlled. To implement SPC effectively, automatic computer procedures are used. This report will show a computerized data processing system that will enable one to:

- o Forecast the chemistry of the process solutions and use this information for preventive maintenace.
- o Detect errors in laboratory analysis.
- o Detect data that are deviating from the predicted norm and produce a warning before the process goes out of control.

THEORY.

1. SHEWART METHOD (k-mod)[1]

This model assumes that each process has its own mean and standard deviation, and that the process fluctuates within the mean and 3 standard deviations( $\sigma$) for 99.7% of the time. The "mean" is the "predictor" what will be used to forecast future value by:

$$\text{forecast value} = \text{mean} + 3\sigma$$

If the latest measured value differs significantly from that of the forecast value in comparision to some set limits (e.g. $>3\sigma$) , it can be assumed that either the chemistry of the process behaves

differently from its norm, or the model itself does not work. Process Control Engineering is using this technique to construct Shewart control charts. The problem with this model is the assumption that the behavior of the process chemistry is constant. This assumption is only true for some processes where the mean of the process always remains constant.

## 2. TRIGG METHOD (g-avg model)[2]

This method is the geometric average technique (g-avg). This technique puts the greatest emphasis on the most recent observations and the emphasis declines geometrically as one goes back in time. The technique assumes that a prediction of the next observation can be made with an exponentially weighted average and is given by:

$$E_t = \alpha x_t + (1-\alpha) E_{t-1}$$

where $x_t$ is the latest measured value

$E_{t-1}$ is the previous exponentially weighted average

$\alpha$ is the smoothing factor which ranges from 0 to

The smoothing factor is equal to $2/(n+1)$ where n is the number of observations in an equivalent moving average.

In Trigg's method, the exponentially smoothed average, $E_t$, is used as the forecast value. The forecast error, $e_t$, is the difference between the actual observation value and the forecast value.

$$e_t = E_t - x_t$$

The smoothed forecast error (SE) becomes:

$$SE_t = \alpha e_t + (1-\alpha) SE_{t-1}$$

If a process is under control then the smoothed forecast error will be around zero. Any increase or decrease in the actual measurements will cause the smoothed forecast error to differ from zero. Thus, a tracking signal as defined by Trigg is:[2,3]

$$\text{Trigg signal} = \frac{SE}{MAD}$$

where MAD is the mean absolute deviation which measures the variation (noise) in a process.

$$MAD_t = \alpha e_t + (1-\alpha) MAD_{t-1}$$

In this study, Trigg's method was modified . A flag signal is calculated as follows:

$$\text{Flag signal} = \frac{e_t}{MAD}$$

The Trigg signal and the flag signal are then compared to see which one is more sensitive to changes in the chemistry of the process.

RESULTS AND DISCUSSION:

A. FORECAST VALUE.

The tin concentrations obtained from the tin-lead bath for three years (1983 - 1985) were used for testing of the models as discussed below. A computer procedure was written to calculate the forecast value, the forecast error, Trigg signal and Flag signal. To initiate the calculation the following values were assumed at the beginning:

Initial forecast value= mean value

Initial forecast error= zero

Initial MAD = standard deviation.

alpha ($\alpha$) = 0.2

The data of the first year (1983) were used to calculate the process mean and standard deviation. These values were then used to calculate the remaining second and third year data. Figure 1 shows the plot of concentration of Sn versus sample number for the last two years (1984 and 1985). Superimposed on this plot are the forecast values calculated by the constant (k-mod) and the geometric average (g-avg) models. Figure 1 clearly shows that the geometric avearage model gives a better forecast than the constant model. The confidence level for the k-mod is 0.0001 as compared to 0.57 for the g-avg. The confidence level for the k-mod forecast value can be improved by adjusting the initial mean value. However, if the mean is adjusted, the k-mod becomes th same as the g-avg. The reason that the g-avg can make better forecast is because this model is capable of re-adjusting th "predictor" based upon the recent trend of the process data. Thus it can be concluded that the g-avg model is more flexible and ca forecast the immmediate observation more accurately.

B. TRIGG & FLAG SIGNAL.

Figure 2 shows the comparison of the Trigg and Flag signals. The following observations can be made:

a) Both the Trigg and Flag signals scattered around zero.

b) Both signals follow the same trends. However, the Flag signal tends to be sharper. The Trigg signal is less sensitive to sudden change in trend of the process chemistry. This is because the data used to calculate the Trigg signal were smoothed, therefore, the abrupt changes are also smoothed.

c) Figures 1 and 2 are compared to determine whether the Flag signal greater than +1.96 will correspond to a significant change in the solution chemistry . (The value of +1.96 is chosen for about 95% statistical significance)[4]. It can be seen that large Flag signals appear at places that are obvious and at places that are not so obvious. Close examition of the data leads us to suggest that the Flag signal will be produced only if there is a step change in trend of the solution chemistry. Figure 3 shows a step change in the downward trend of the tin concentration and Figure 4 shows a step change in the direction opposite to the trend. The Flag signals for both cases are larger than 1.96. On the other hand , if the trend of process chemistry is consistent, no apparent large warning signal is observed, as shown in Figure 5.

C. APPLICATION OF THE FORECASTING SYSTEM.

Based upon the above observations, it can be concluded that in order to set up a computer flag system, two calculations are needed:

1) The g-avg model is used to calculate the forecast value, which will be compared to a set of predetermined upper and lower

control limits. A warning will be produced if these limits are exceeded. This will ensure that the process is kept within the control limits even if the process is drifting towards a given direction with no abrupt changes ( i.e. cases where the flag signal calculation would not produce a warning).

2) The Flag signal calculation can be used to produce a warning if the change in solution chemistry is significant or the trending is reversed. A Flag signal can be used as an initial check for laboratory data. Laboratory analysis should be repeated when a warning Flag signal is posted. The analytical result will be accepted if it can be repeated.

3) After the analytical data is accepted, one can conclude that there is a definite change in the process , and thus the process needs to be adjusted or the cause of the change be investigated.

CONCLUSIONS.

This computer procedure has also been extended to process data from other processing situations with similar success. In all cases, the g-avg method produces a better forecast value than the k-mod method ,and the Flag signal is more sensitive to changes in the process chemistry. This procedure is currently being applied to real time monitoring of the plating bath. Excellent forecast values are obtained. The Flag signal calculation; however, need to be modified to account for the fact that in realtime control, the mean absolute deviation (MAD) is very small ,thus making the Flag-signal too sensitive to small fluctuations in the process.

FIGURE CAPTION

FIGURE 1 Predicted values for Tin concentration in the Tin Lead Bath(1984-86) using the g-avg and k-mod models.

FIGURE 2 Trigg and Flag Signal for Tin concentration in the Tin Lead Bath (1984-86).

FIGURE 3 Comparision between the Tin concentration and the Flag Signal for cases when the tin concentration is decreasing

FIGURE 4 Comparision between the Tin concentration and the Flag Signal for cases when the tin concentration is increasing.

FIGURE 5 Comparision between the Tin concentration and the Flag Signal for cases when the tin concentration fluctuates within the process variability.

ACKNOWLEDGMENT

The authors wish to extend their deepest appreciations to Kevin A Mchugh, Tim W. Rogers, and Dick Taylor for their technical support and discussions.

REFERENCES

1) S. C. Puri, Staistical Process Quality Control, Standard-Quality Management Group , Ottawa and Washington D. C., p 148 , 1984

2) D. W. Trigg, Operational Res. Quart., 15, 271, 1964

3) G. S. Cembrowski, J. O. Westgard, A. A. Eggert and E. C. Toren, Jr., Clinical Chemistry, 21, 1396, 1975

4) L. Blank, Statistical Procedures for Engineering, Management and Science, McGraw-Hill Book Comp., N.Y., p 540, 1980

5) R. G. Brown, Smooth Forecasting and Prediction. Prentice Hall Inc., Englewood Cliffs, N.Y., 1963

6) M. Batty, Operational Res. Quart., 20, 319, 1969

Figure 1

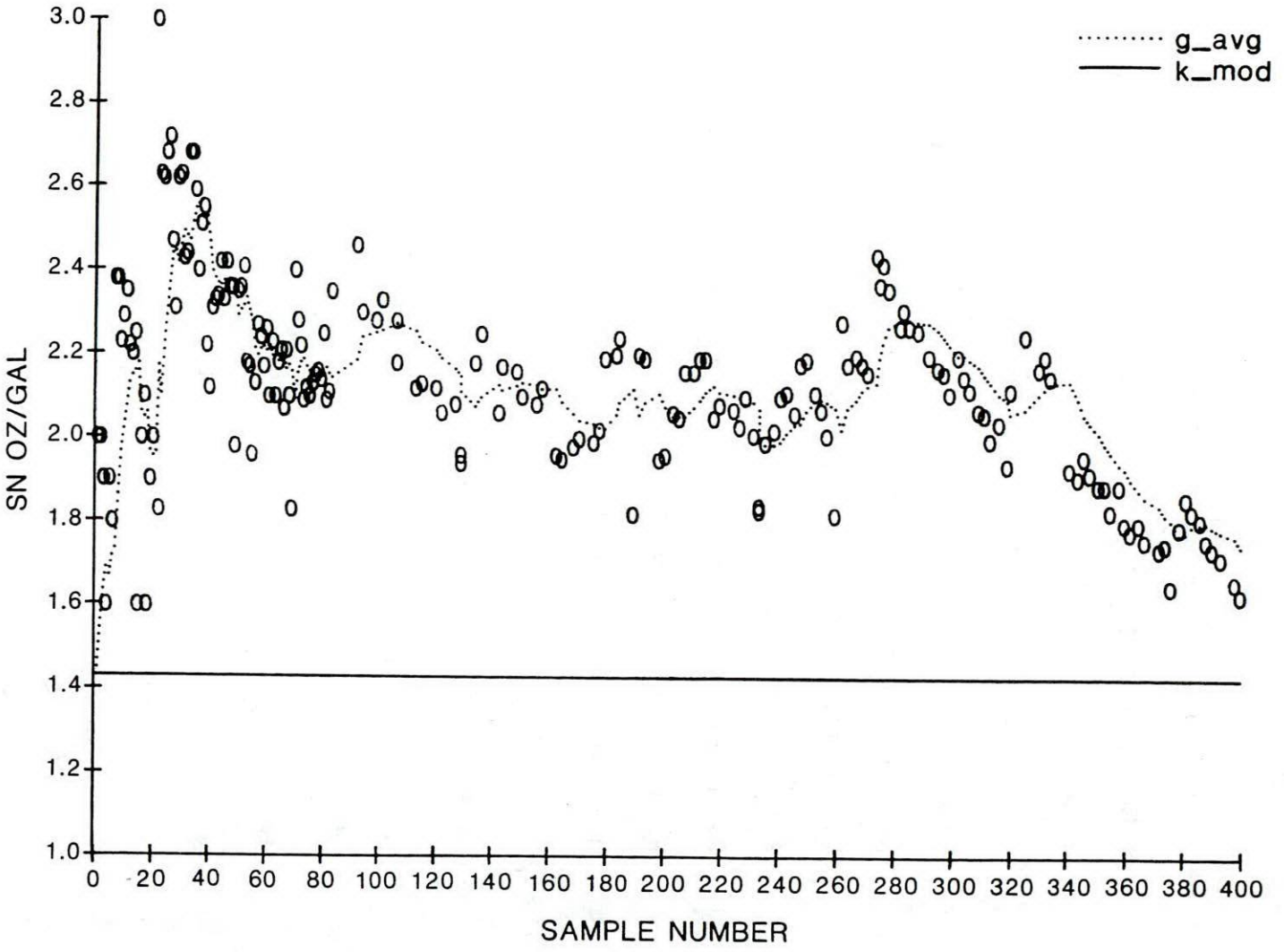
g_avg
k_mod
SN OZ/GAL
3.0
2.8
2.6
2.4
2.2
2.0
1.8
1.6
1.4
1.2
1.0
0
20
40
60
80
100
120
140
160
180
200
220
240
260
280
300
320
340
360
380
400
SAMPLE NUMBER

Figure 2

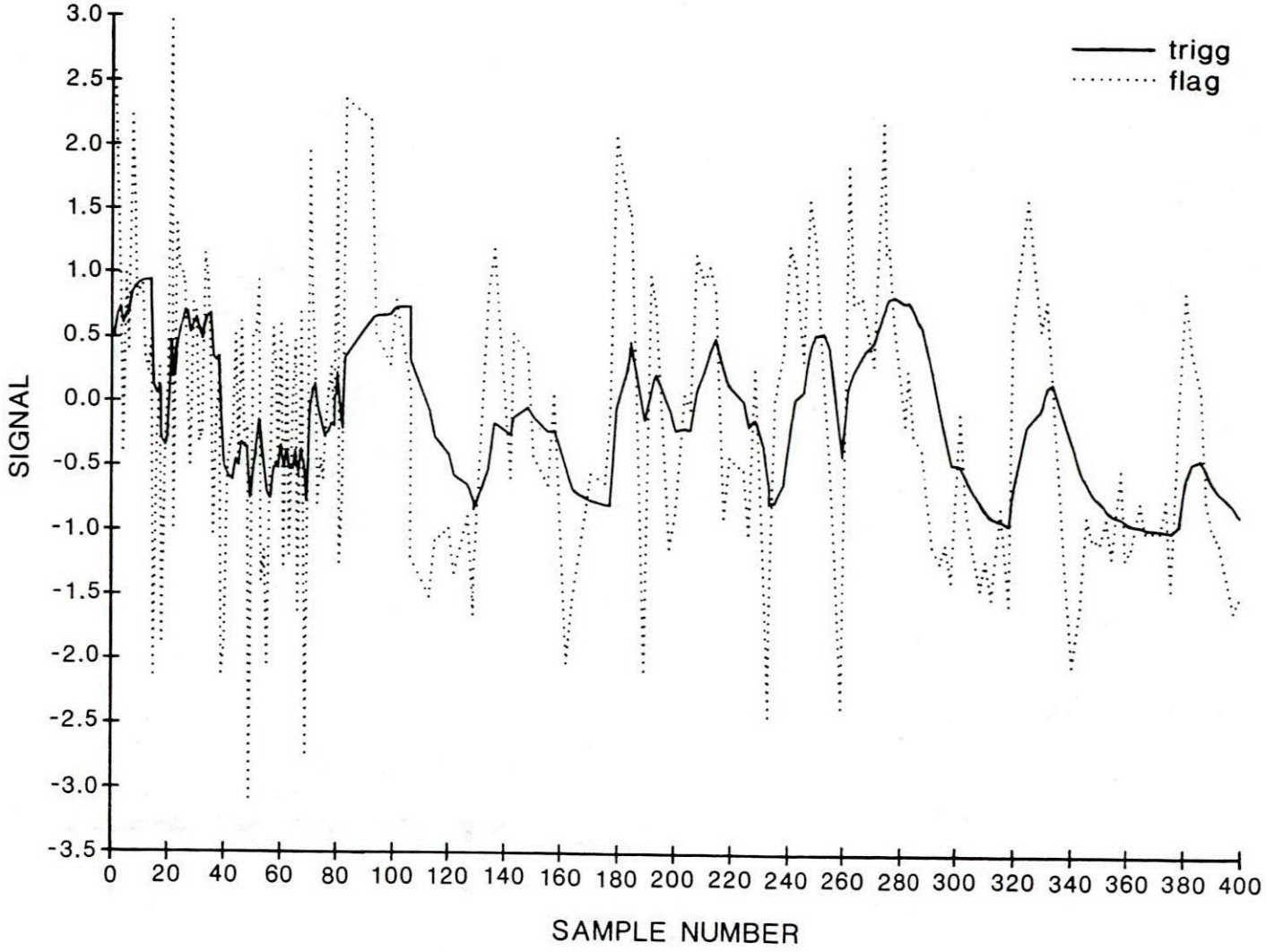
trigg
flag
SIGNAL
3.0
2.5
2.0
1.5
1.0
0.5
0.0
-0.5
-1.0
-1.5
-2.0
-2.5
-3.0
-3.5
0 20 40 60 80 100 120 140 160 180 200 220 240 260 280 300 320 340 360 380 400
SAMPLE NUMBER

Figure 3

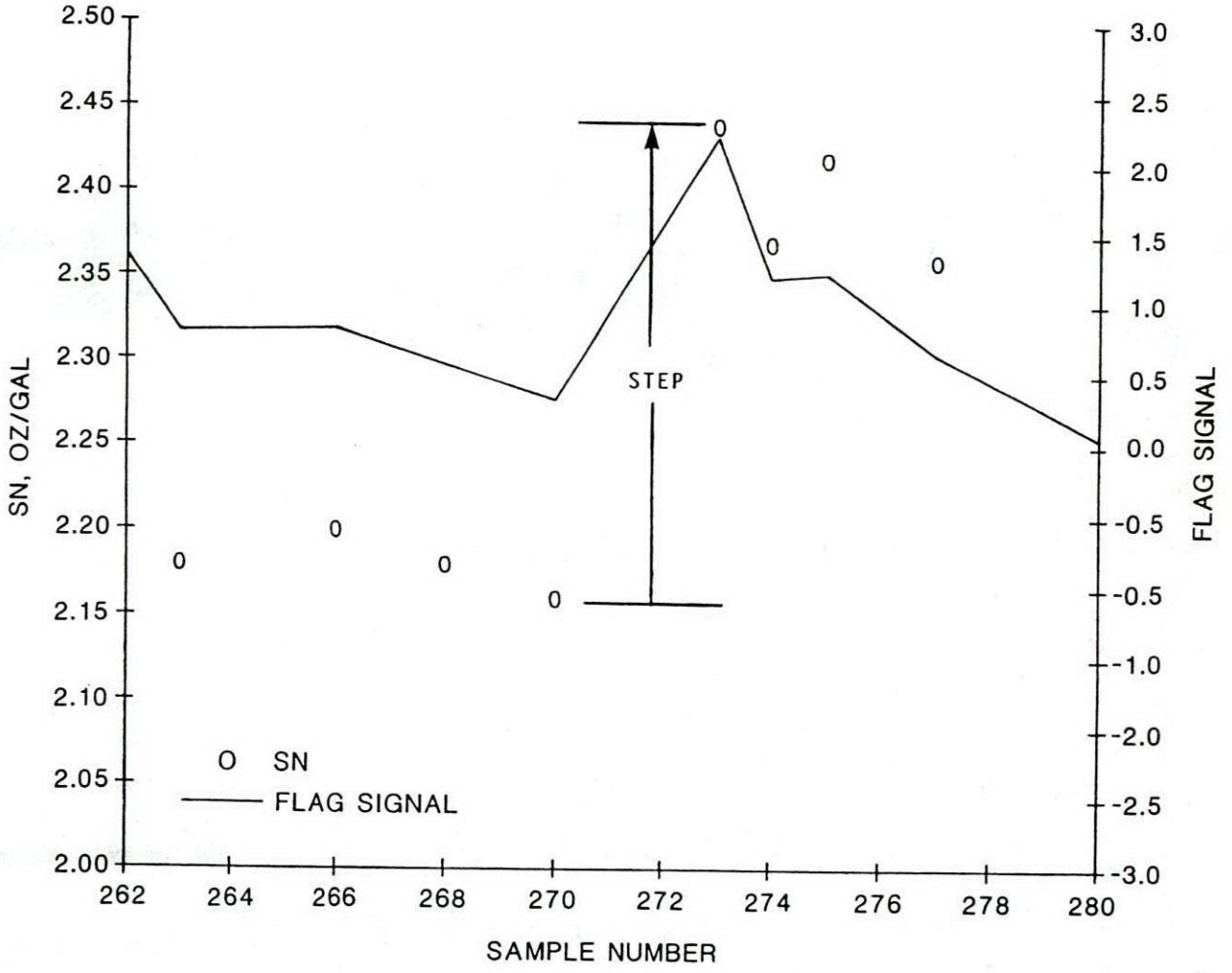
2.50
2.45
2.40
2.35
2.30
2.25
2.20
2.15
2.10
2.05
2.00
SN, OZ/GAL
3.0
2.5
2.0
1.5
1.0
0.5
0.0
-0.5
-0.5
-1.0
-2.0
-2.5
-3.0
FLAG SIGNAL
STEP
O SN
FLAG SIGNAL
262
264
266
268
270
272
274
276
278
280
SAMPLE NUMBER

FIGURE 4

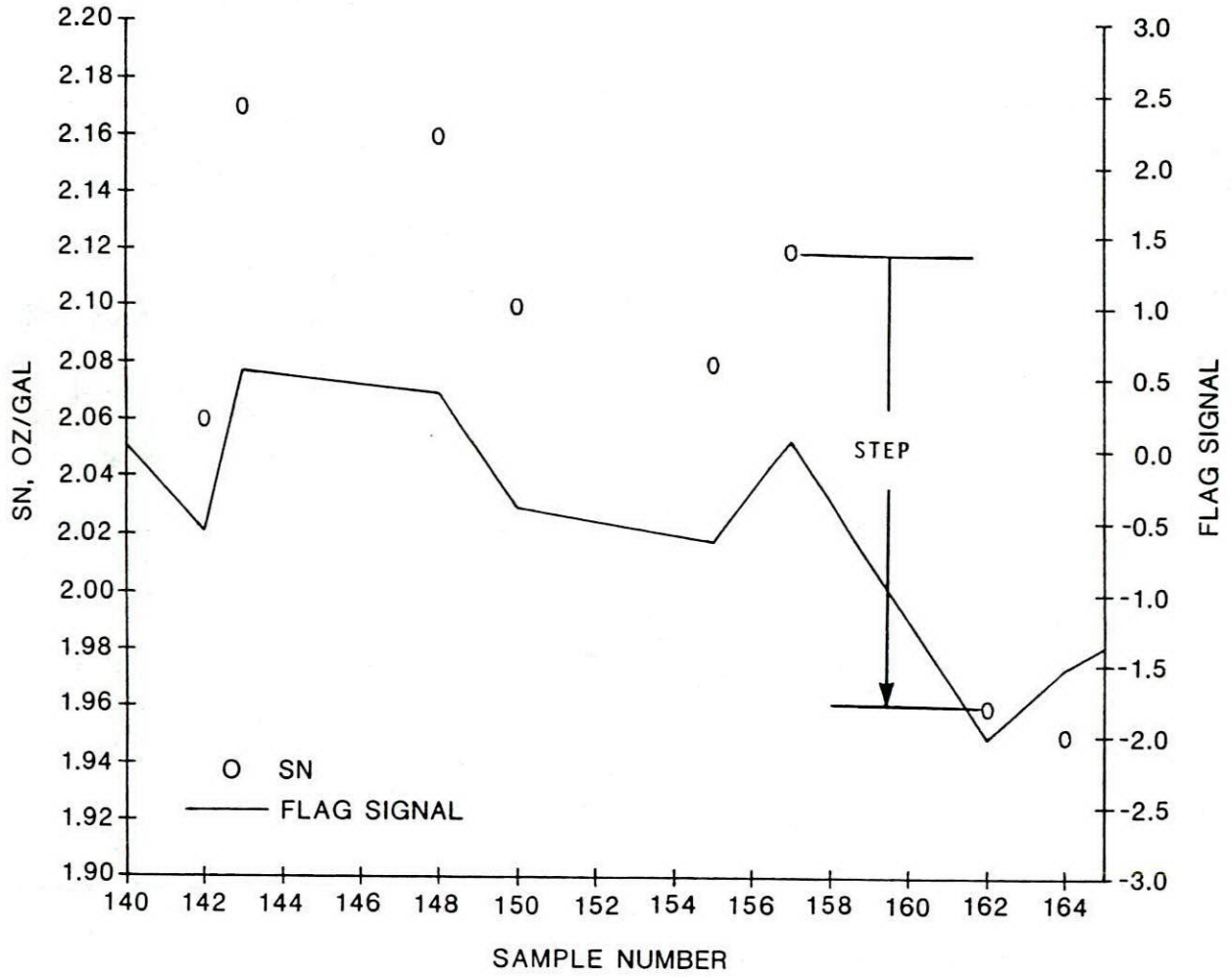
SN, OZ/GAL
FLAG SIGNAL
SAMPLE NUMBER
STEP
O SN
FLAG SIGNAL
2.20
2.18
2.16
2.14
2.12
2.10
2.08
2.06
2.04
2.02
2.00
1.98
1.96
1.94
1.92
1.90
3.0
2.5
2.0
1.5
1.0
0.5
0.0
-0.5
-1.0
-1.5
-2.0
-2.5
-3.0
140
142
144
146
148
150
152
154
156
158
160
162
164

- Figure 5 -

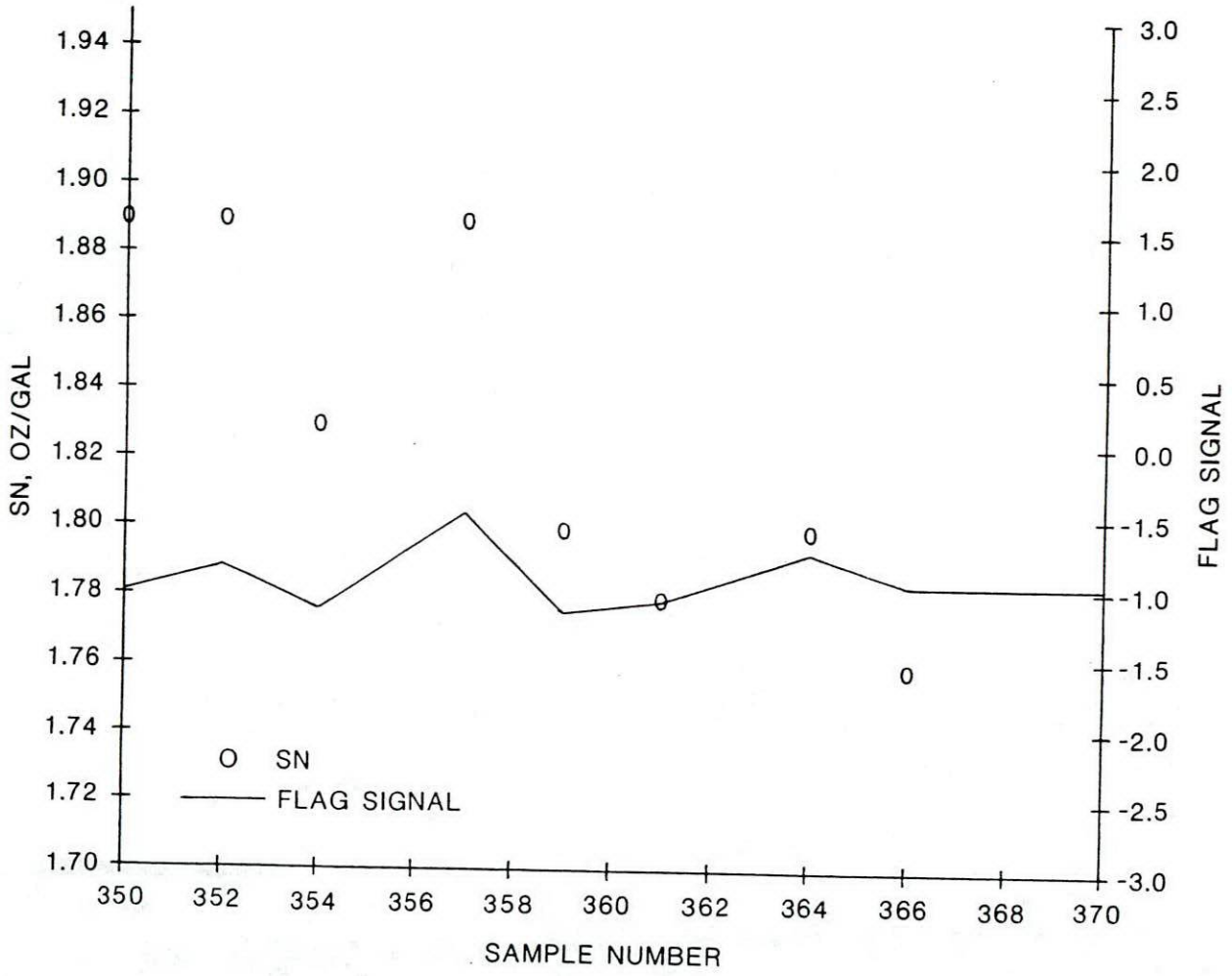
SN, OZ/GAL
1.94
1.92
1.90
1.88
1.86
1.84
1.82
1.80
1.78
1.76
1.74
1.72
1.70
FLAG SIGNAL
3.0
2.5
2.0
1.5
1.0
0.5
0.0
-1.5
-1.0
-1.5
-2.0
-2.5
-3.0
O SN
FLAG SIGNAL
350
352
354
356
358
360
362
364
366
368
370
SAMPLE NUMBER

K-5

# Analytical Methods
# Session K

## A Study of Titanium and Aluminum Etching Solutions by Fluorine-19 Nuclear Magnetic Resonance Spectroscopy

M.N. Cooper and T.W. Rodgers
Lockheed Missiles & Space Co.

# A Study of Titanium and Aluminum Etching Solutions by Fluorine-19 Nuclear Magnetic Resonance Spectroscopy

by M.N. Cooper and T.W. Rodgers
Lockheed Missiles & Space Company.

## Introduction

Fluorine-19 nuclear magnetic resonance (NMR) spectroscopy is well suited to investigate metal-fluoride complexes in aqueous etchant solutions. Aqueous solutions of fluoride ion can easily be detected at 0.005 M concentrations. This sensitivity allows non destructive detection of different fluoride ion chemical environments in etchant solutions and requires only ~0.5 mL sample. Several studies have investigated the kinetics and structural properties of complex fluoroanions in aqueous electrolyte solutions by $^{19}F$ NMR. Tetrafluoroborate ion, $BF_4^-$, has been studied in aqueous solutions of $Cd^{+2}$, $Sb^{+3}$, $Sn^{+2}$, and $Pb^{+2}$. (1) Various studies (2) have reported metal-fluoride complex chemical shifts using $^{19}$ F NMR. Aluminium fluoride complexes (3) have been studied to determine the extent of fluorine exchange between species in equilibrium. Hydrolysis and structural investigations have been performed on titanium fluoride complexes in both aqueous (4) and alcohol (5) solvents. The current work presents a study of titanium and aluminum etchant solutions which were followed as a function of etch rate and metal-fluoride complex growth by $^{19}F$ NMR spectroscopy.

As a fluoride etchant is used, the concentration of metal in the solution increases. This investigation was designed to study the effects of aging on etchant solutions by monitoring the etch rate and chemical composition as a function of dissolved metal. Two simple commercial etchant preparations were chosen for this study. A series of known amounts of either aluminum or titanium metal were allowed to etch in the solutions and the etch rates were

recorded. The etch rate was determined by the weight loss versus time in solution. After etching, the solutions were analysed for titanium or aluminum metal concentration by AA spectroscopy. Fluorine-19 NMR spectroscopy was then used to characterize the fluorinated species in the etched solutions. The aging effects observed in the etchant solutions are discussed below.

## Experimental

Six solutions were prepared for titanium etching and eight solutions were prepared for aluminum etching following the data in table 1. Known panel volumes of titanium and aluminum were then etched in the solutions for known times. Etch rates were calculated for these solutions and metal concentrations were determined by AA spectroscopy. Standard solutions of titanium and aluminum for AA analysis were prepared from Baker Instra-Analyzed atomic spectral standards. AA analysis of the solutions required large dilutions (from 1:10 to 1:1000 v/v) which minimized the matrix effects of the acidic samples. All AA analyses were performed on a Thermo Jarrell-Ash IL 951 atomic absorbtion spectrometer.

The high acid concentration and the presence of hydrofluoric acid in the etchant solutions required special sample handling for NMR analysis. Etchant solutions (~0.5 ml) were placed directly (without dilution) in teflon NMR tube inserts and were run unlocked in the spectrometer. The superconducting magnetic field was sufficiently stable to run unlocked experiments of this nature. The spectra were externally referenced to 0.1M NaF in deuterated water ($D_2O$) at -121.4 ppm. (This assignment was determined experimentally by externally referencing $CFCl_3$ in deuterated benzene at 0 ppm to 0.1M NaF) A 45 degree pulse (5μs) was used with a 4 s delay. The samples were run in a 5mm broad band probe without decoupling. Due to the large chemical shift range of fluorine compounds, a sweep width of 100,000 Hz was used to prevent peak aliasing. Linewidth (at half-height) of the standard 0.1M NaF at this sweep width was measured at 5.1 Hz. Assignments for resonances in the etchant spectra were accomplished by

running model compounds in $D_2O$. All spectra were obtained on a Varian XL-300 superconducting spectrometer operating at 282 MHz.

Sodium hexafluoroaluminate was obtained from Aldrich (gold label: 99.99%). Potassium hexafluorotitanate(IV) (98%) was obtained from Crescent Chemical Company. Both were used unpurified as supplied from the manufacturer. All other chemicals in this study were reagent grade or better unless otherwise stated and were used unpurified from the manufacturer. Deuterated solvents and the teflon NMR inserts were obtained from Wilmad Glass Company; Buena New Jersey.

**Results**

Table 1 presents the panel dimensions and bath conditions used to etch the titanium and aluminum metals. The etchant conditions were used as recommended by the manufacturer. Figure 1 shows the results of the six titanium etch solutions. Plot 1a shows the linear ($r^2$=0.948) *decrease* in etch rate as the concentration of titanium in the etchant *increases* . The ppm titanium was determined by AA spectroscopy. Etch rate was calculated from the mg/minute of weight loss of a known volume of titanium panel. Plot 1b shows the linear ($r^2$=0.979) *increase* in the titanium-fluoride complex (assigned as $TiF_6^{-2}$) with increase in titanium concentration. The $TiF_6^{-2}$ concentration was determined as the mole percent of the total fluorinated species in solution by integration of the $^{19}F$ NMR spectra. Figure 2 presents a typical $^{19}F$ spectrum for the third etchant solution. Two broad peaks are observed which correspond to the HF and $TiF_6^{-2}$ specie. The concentration is given as the mole percent of $TiF_6^{-2}$ as compared to the total moles of HF + $TiF_6^{-2}$. Figure 3 shows the plot of etch rate -vs- $TiF_6^{-2}$ complex growth for the six titanium solutions. The etch rate is shown to *decrease* linearly ($r^2$=0.954) as the concentration of $TiF_6^{-2}$ *increases* .

Figure 4a plots the etch rate of the eight aluminum solutions as a function of aluminum metal concentration. Figure 4b plots the growth of $AlF_2^+$ and $AlF^{+2}$ with increasing aluminum metal concentration. Neither of these appeared as simple linear functions. Figure 5 shows the plot of etch rate -vs- growth in aluminum-fluoride complex formation. Two $^{19}F$ NMR spectra corresponding to etch solutions 6 and 7 are presented in figure 6. The identity of the fluorinated species are labeled. The broad resonance corresponding to HF which is present at ~-161 ppm in etch solution 6 is notably absent in etch solution 7 (similiarly in solution 8). Hence, solutions 7 and 8 were assigned as 100% aluminum-fluoride complex formation.

**Discussion**

Several mechanisms may be responsible for the broad resonances and lack of splitting for fluoride species observed in the $^{19}F$ spectra. Unsymmetrical environments in the complexes [6] and the acidic nature of the solutions [7] have been reported to cause these phenomena. Initially, it was not assumed that the $^{19}F$ NMR spectra would yield quantitative results due to the long $T_1$ (spin-lattice relaxation time) values for metal-fluoride complexes in aqueous solution. It appears from figure 1, however, that the NMR mole percent values obtained are at least proportional to the complex concentration since plots 1a and 1b are both nearly linear as would be expected. The linear relationship between etch rate and $TiF_6^{-2}$ growth suggests that the formation of the metal-fluoride complex may be decreasing the availibility of free $F^-$ or HF needed for etching. Hence, in the titanium case, the etch rate of the solution can be determined directly if either the titanium metal or the $TiF_6^{-2}$ concentration is known.

The aluminum etch case appears to be more complex. Figure 4a indicates that the decrease in etch rate follows the increase in aluminum concentration as an exponential function. There

appears to be an initial rapid change in the etch rate as Al metal increases until ~ 2000 ppm (or ~0.2%) Al metal is present. The etch rate then changes very little although large concentrations of the metal (up to 14000 ppm (or 1.4%) are added. This behavior is comparable to the aluminum-fluoride complex growth plot in figure 4b. This plot shows that at a concentration of 2000ppm aluminum metal, the aluminum-fluoride complex represents ~ 65% of the total fluoride species in the etchant solution. All of available fluoride in the solution was observed as the complex at aluminum metal concentrations above 5000 ppm (or 0.5 %). Since the etch rate falls off so rapidly in this case, the aluminum-metal complex may tie up the free fluoride in aged solutions to such an extent that the etch rate is dramatically effected. This suggests a narrower window of usable etch solution life for the aluminum etchant when compared to the titanium etchant.

Two resonances were observed $^{19}F$ NMR spectra of aluminum etchant solutions. Connick and Poulson [8] have identified these as $AlF^{+2}$ and $AlF_2^+$ from equilibrium studies of aluminum-fluoride complexes. Figure 6 shows the growth of these resonances with respect to the HF peak for two of the aluminum solutions.

**Conclusions**

Two commercial etchant solutions; for titanium and aluminum; were studied. The titanium etchant operated at 140 F with 75% nitric/5% HF and the aluminum etch operated at room temperature with 15% nitric/1%HF. A series of etchant solutions were prepared and known amounts of titanium and aluminum metal were etched for varying lengths of time. The etch rate for each solution was calculated and the concentration of metal in the solution was determined. Fluorine-19 NMR spectra of the etched solutions were obtained and the mole % of metal-fluoride complex ($TiF_6^{-2}$ or $AlF^{+2}/AlF_2^+$) was determined.

The titanium etch rate was observed to lineraly decrease with either increasing titanium metal concentration or increasing $TiF_6^{-2}$ concentration. A non-linear correspondence was observed for the aluminum solutions when plotted against aluminum metal concentration or $ALF^{+2}/AlF_2^{+}$ concentration. The aluminum etch rate was found to decrease rapidly and then level off with ~ 5000ppm (or 0.5%) aluminum metal in solution. These results suggested a dependence of free fluoride (or HF) on the solution etch rate in both the titanium and aluminum cases. This study also showed that the etch rate was inversely proportional to the growth of the metal-fluoride complex for both titanium and aluminum.

*Table 1. Etch Conditions and Results for Titanium and Aluminum Coupons*

**Titanium Coupons** (A16-V4 alloy) 1"x 2" x 0.05"
Etched in 75% nitric + 5% HF at 140 F for 5 minutes

| Solution | ppm Ti | Etch rate in μ inches per min. |
|---|---|---|
| 1 | <12 | 90.5 |
| 2 | 1200 | 75.3 |
| 3 | 4100 | 59.0 |
| 4 | 6800 | 48.0 |
| 5 | 7400 | 29.0 |
| 6 | 11000 | 21.6 |

**Aluminum Coupons** (1100 alloy) 1.25" x 1.5" x 0.064"
Etched in 15% $HNO_3$ + 1% HF at room temperature for 5 minutes

| Solution | ppm Ti | Etch rate in μ inches per min. |
|---|---|---|
| 1 | <6 | 28.1 |
| 2 | 36 | 21.7 |
| 3 | 380 | 14.8 |
| 4 | 540 | 10.8 |
| 5 | 930 | 8.6 |
| 6 | 1500 | 7.2 |
| 7 | 4800 | 2.8 |
| 8 | 14000 | 1.3 |

## References


1. R. Hague and L.W. Reeves. *Can J. Chem.* **214**, 2769 (1966)

2. E.L. Muetterties and W.D. Philips. *J Amer. Chem. Soc.* **81**, 1084, (1959)

3. P.A. Dean and D.F. Evans. *J Chem Soc. (A)*, 689 (1967)

4. R.E. Connick and R.E. Poulson. *J Amer. Chem. Soc.* **79**, 5153 (1957)

5. E.L. Muetterties and W.D. Philips. *op. cit.*, **81**, 1084, (1959)

6. R.O. Ragsdale and B.B. Stewart. *Inorganic Chem.*, Vol 2, No 5, 1002 (1963)

7. E.L. Muetterties and W.D. Philips. *op. cit.*, **81**, 1084, (1959)

8. R. Hauge and L. W. Reeves. *op. cit.*, **214**, 2769 (1966)

9. R.E. Connick and R.E. Poulson. *op.cit.*, **79**, 5153, (1957)

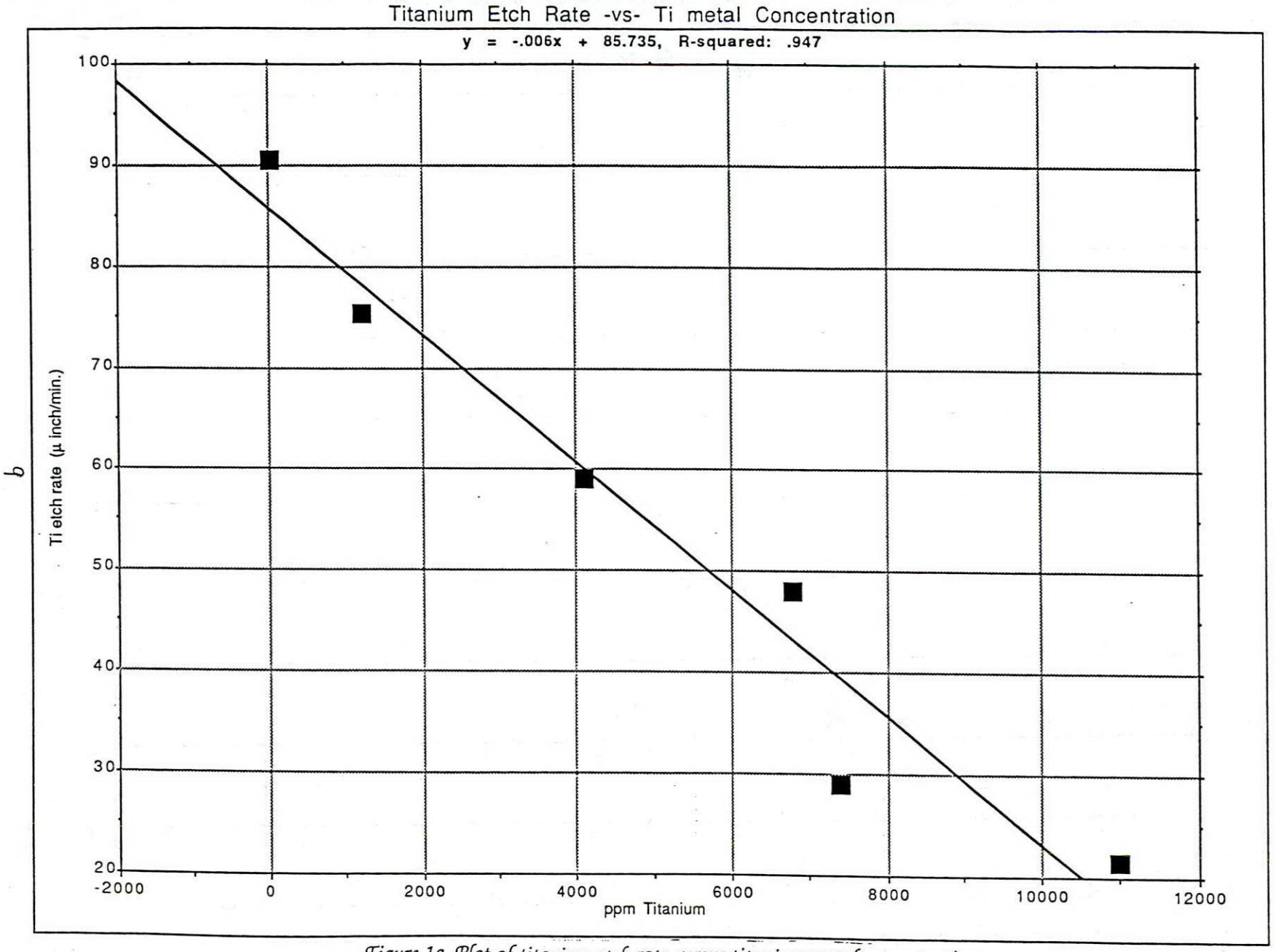


*Figure 1a. Plot of titanium etch rate versus titanium metal concentration*

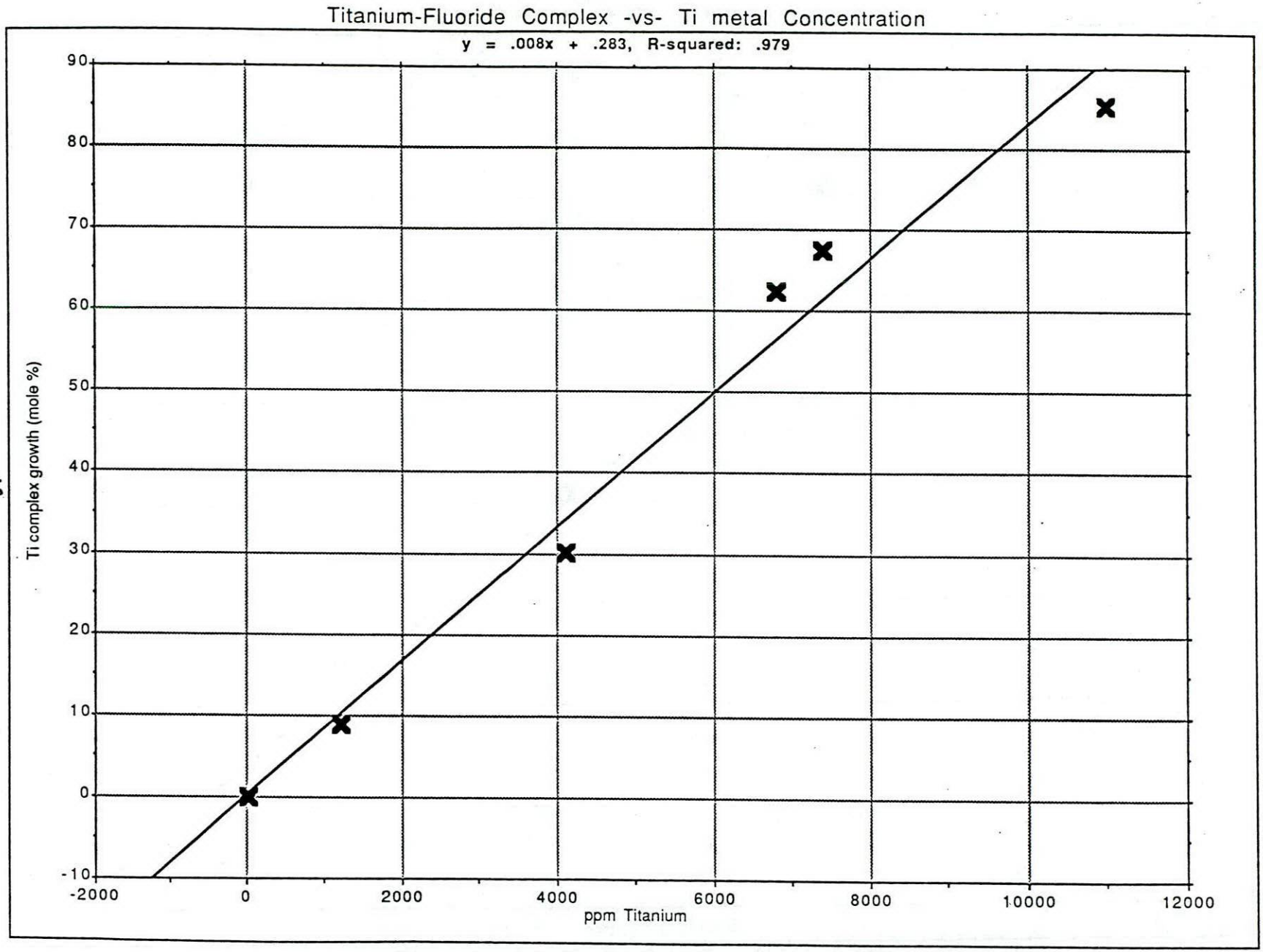


*Figure 16. Plot of titanium- fluoride complex growth versus titanium metal concentration*

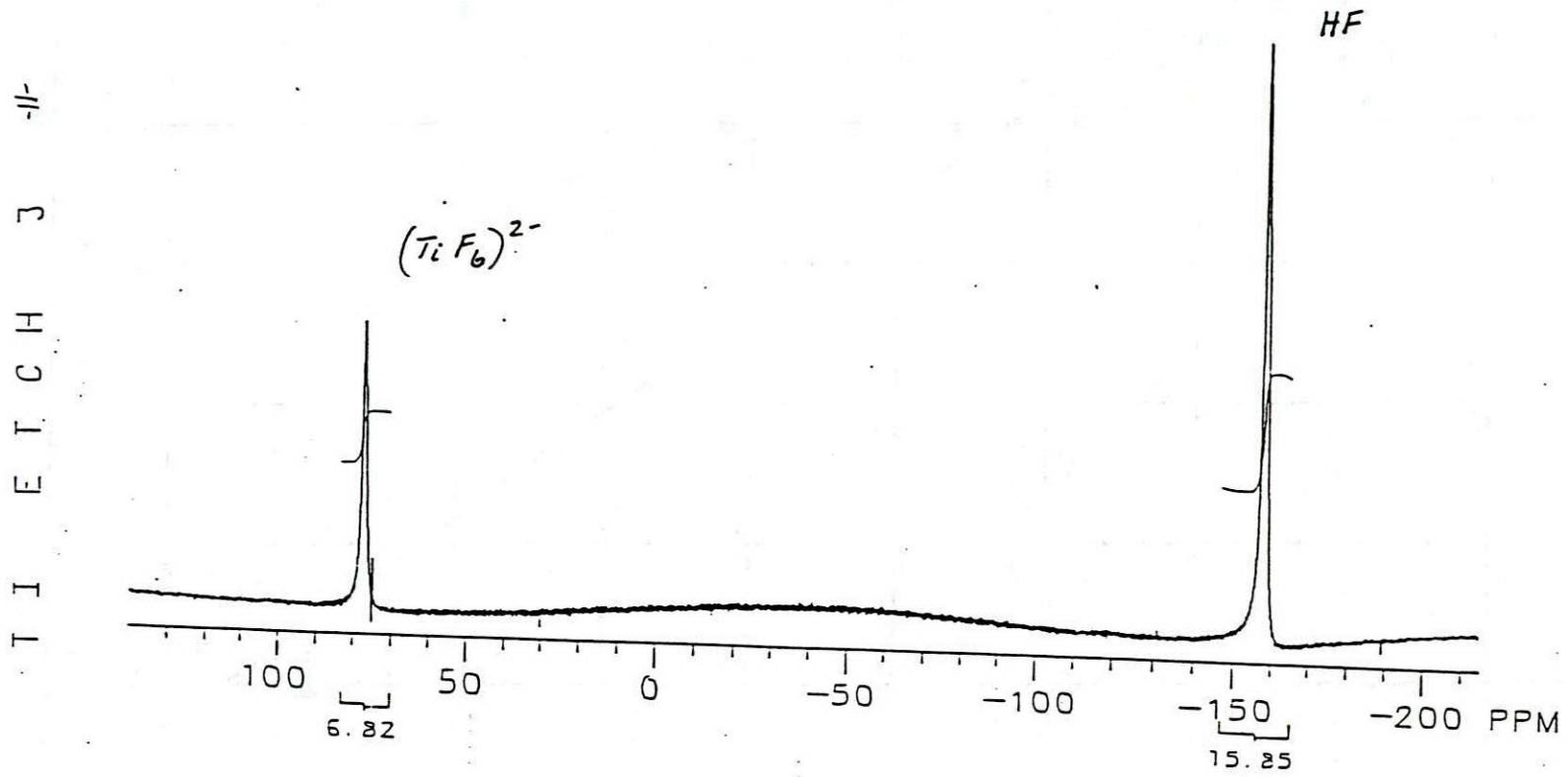


*Figure 2. Fluorine-19 NMR spectrum of titanium etch solution #3*

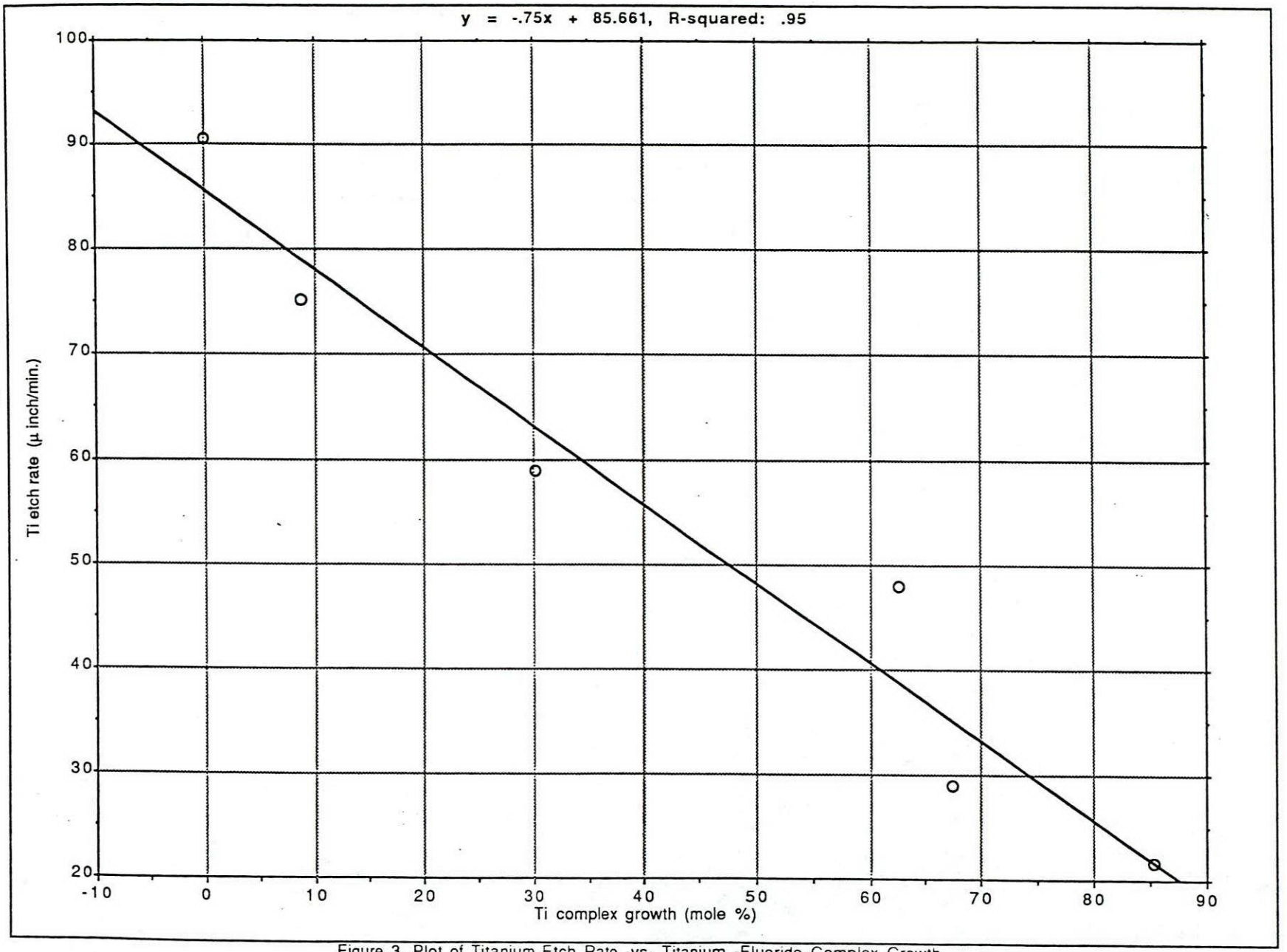


Figure 3. Plot of Titanium Etch Rate -vs- Titanium -Fluoride Complex Growth

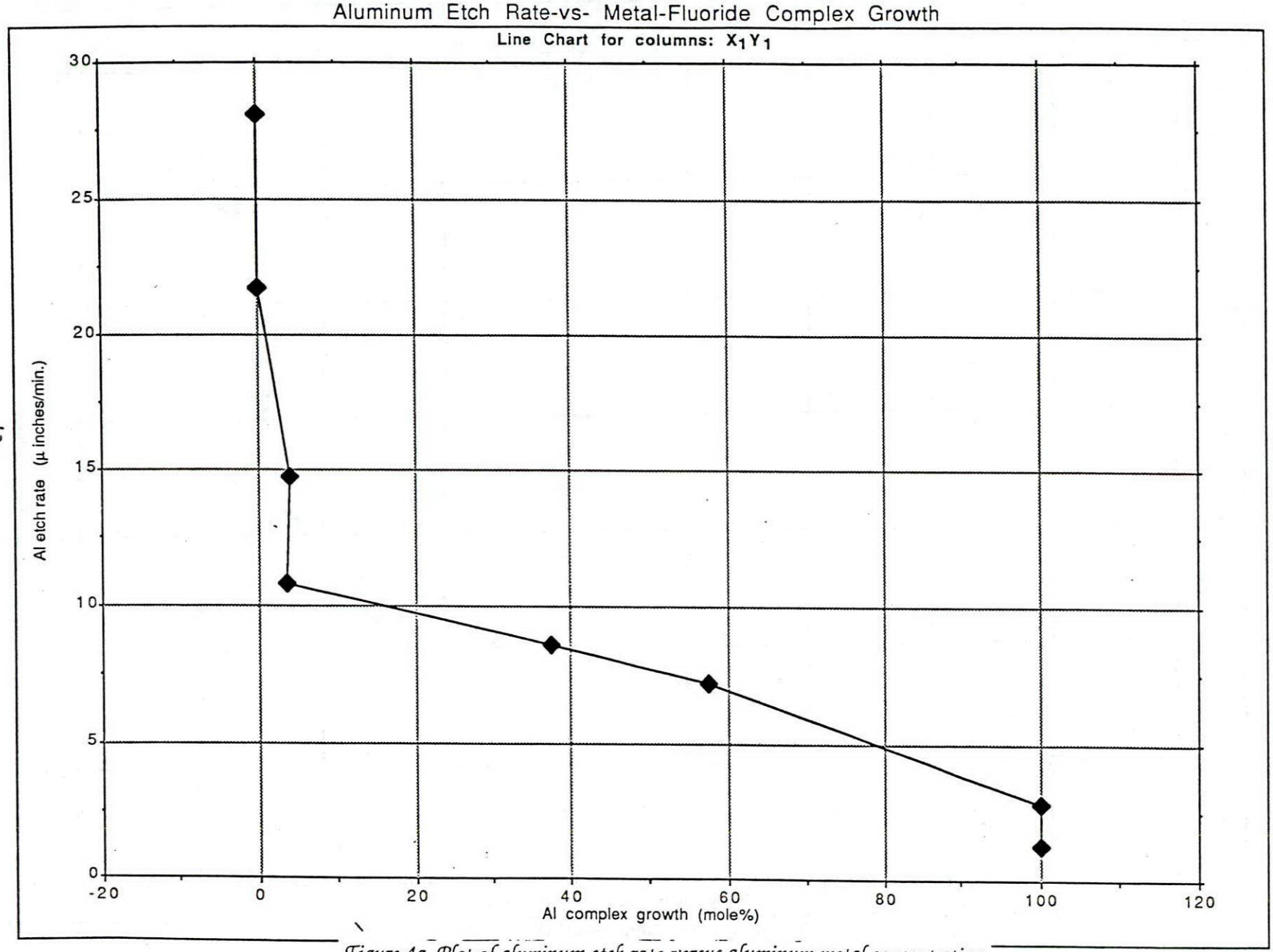


*Figure 4a. Plot of aluminum etch rate versus aluminum metal concentration*

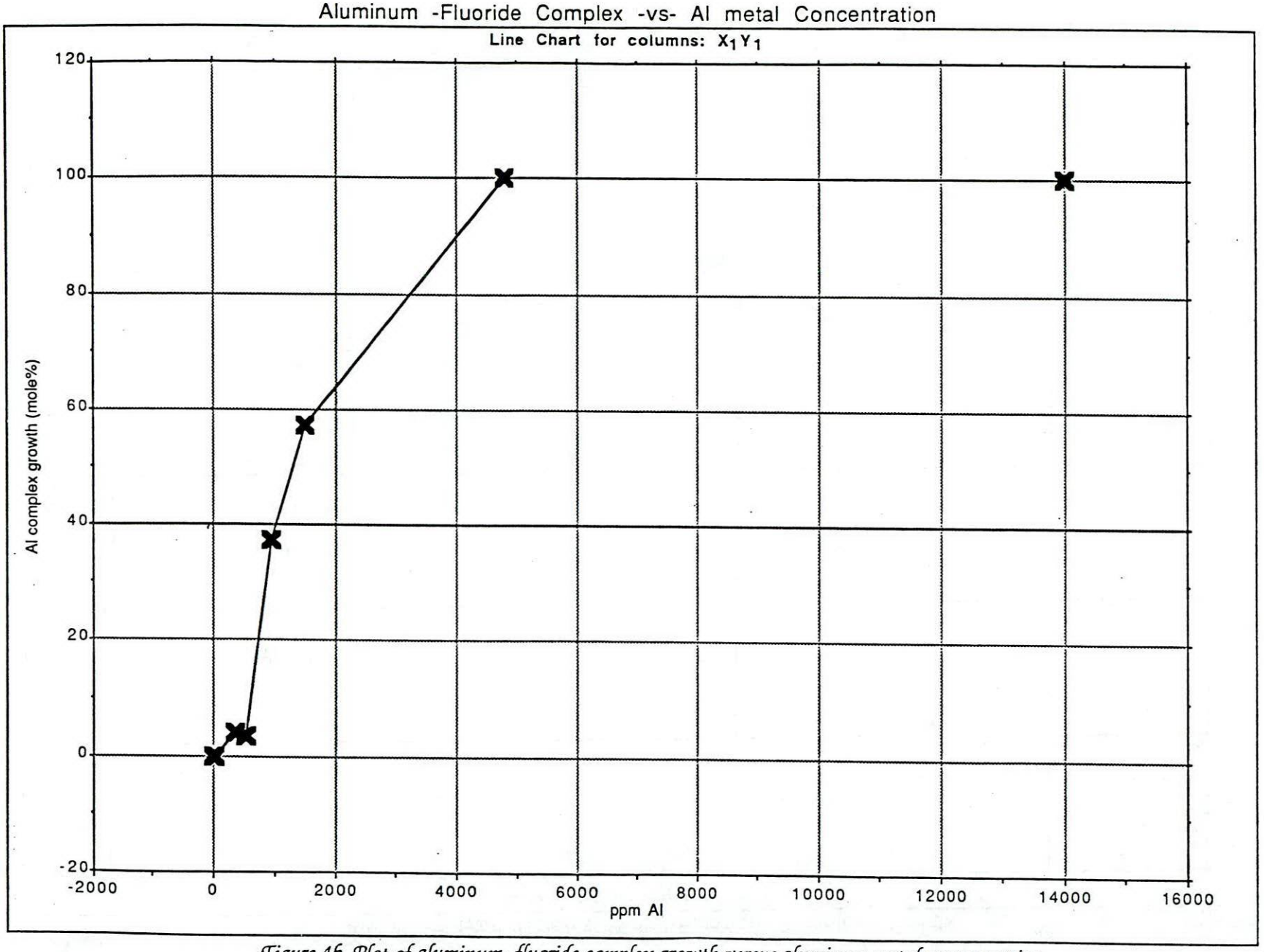


*Figure 4b. Plot of aluminum- fluoride complex growth versus aluminum metal concentration*

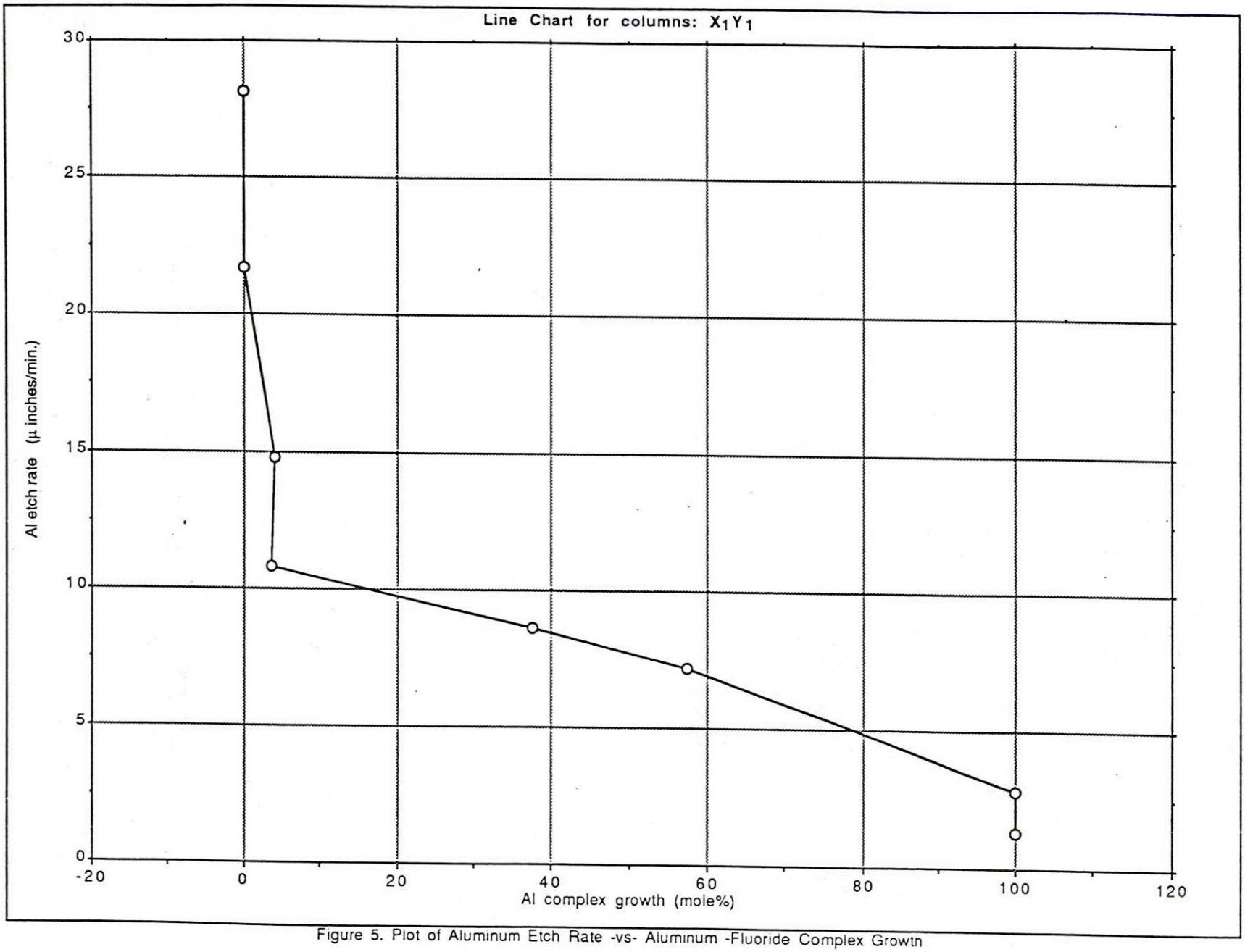


Figure 5. Plot of Aluminum Etch Rate -vs- Aluminum -Fluoride Complex Growth

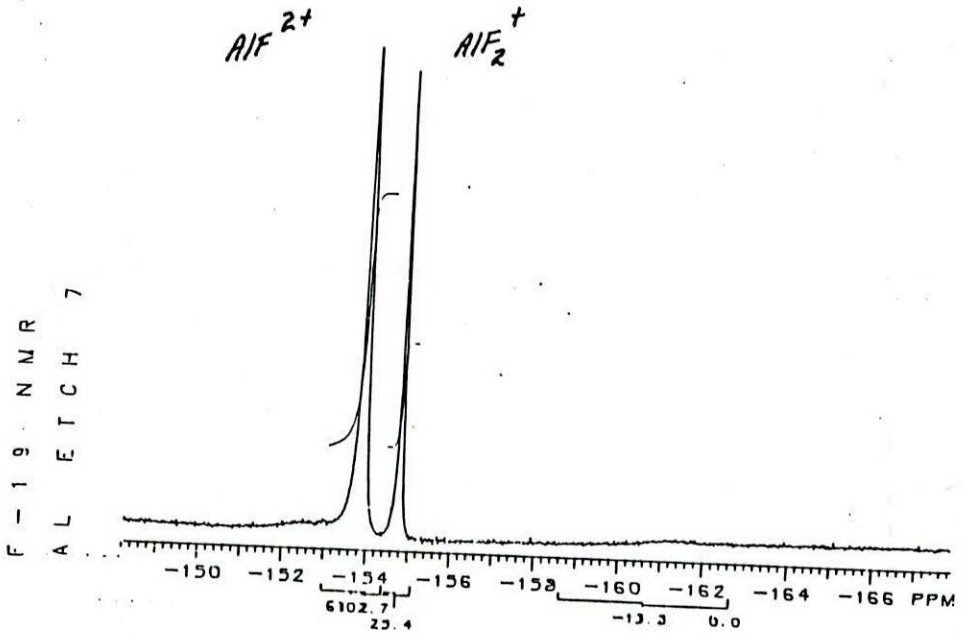


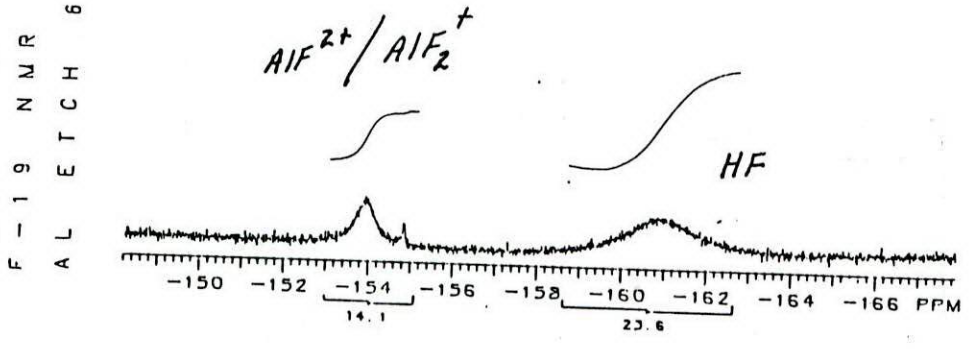


*Figure 6. Fluorine-19 NMR spectrum of aluminum etch solutions # 6 and # 7*

# K-6

# Analytical Methods
# Session K

## Measuring PTH Copper Ductility for Process Control

Donald E. Storjohann
Shipley Company Inc.
Newton, MA

**PAPER NOT RECEIVED IN TIME FOR PUBLICATION***

Measuring PTH Copper Ductility for Process Control

Donald E. Storjohann, Shipley Company Inc., Newton, MA

The integrity of the interconnecting deposited copper is central to the reliable performance of the printed wiring board. This paper discusses the development and use of specialized equipment for measuring both the ductility and tensile strength of copper foils.

* For copies of this paper, please contact the author directly

Mr. Donald E. Storjohann
Senior Engineer
R&D PC/SF
Shipley Company Inc.
2300 Washington Street
Newton, MA 02152-1469
(617) 969-5500

K-7

# Analytical Methods
# Session K

## On-Line Electroplating Thickness Monitor

C.G. Moore, P.E.
and J.P. Cosentino
Rohrback Cosasco Systems
11841 East Smith Avenue
Santa Fe Springs, CA 90670

# ON-LINE ELECTROPLATING THICKNESS MONITOR

C. G. Moore, P. E. and J. P. Cosentino

Rohrback Cosasco Systems
11841 East Smith Avenue
Santa Fe Springs, CA 90670

## Abstract

A new instrumental technique for the on-line measurement of electroplating is described and test results presented.

The technique measures the thickness of an electroplated deposit using electrical resistance data processed with a microprocessor based instrument. The instrument filters and processes the signals and continuously displays the thickness in microinches. Field test results for copper, gold and nickel are accurate and repeatable over the range of 30 to 1500 microinches.

## Introduction

The corrosion resistance of products has frequently been related to the thickness of the electroplated deposit. In typical applications the thickness of the electroplated deposit is critical to performance parameters such as durability, corrosion resistance, conductivity, hardness and lubricity, to name a few. Now, more than ever, the metallurgical properties and the thickness of electrodeposited coatings are integral parts of the engineered design of the product and as a result thickness maxima and minima are frequently specified to a close tolerance. Likewise, the cost effectiveness of a plated part and productivity of a plating process are also critically linked to the precision of the thickness of the plated deposit.

The plating thickness measurement techniques that are available today vary in many respects and they all have limitations which have prevented any single technique from becoming the industry standard. For example, the very popular beta backscatter technique is restricted to combinations of materials that exhibit a difference in atomic numbers between substrate and coating of at least 20% and the accuracy is a function of this difference. X-ray spectrometry has few technical shortcomings but does carry a very expensive price tag. The coulometric approach is considered a destructive test and utilizes wet chemistry. The myriad of thickness measurement devices based on magnetic methods have the shortcoming of only working with a magnetic substrate material, a magnetic coating or both. And, none of the aforementioned techniques generate on-line or real time information.

The measurement technique described in this paper can be used to determine the thickness of a wide selection of plated metals on most commonly used metal substrates. And, most important, the measurement is made in the plating bath as the plating process is taking place. This technique offers the promise of real-time, on-line process control.

## System Operating Principle

The system consists of a wire loop sensor and a microprocessor controlled micro-ohmmeter that provides a digital readout of the plated metal thickness in microinches. Interference from the high plating currents in the solution is eliminated by a patented sensor configuration and multiple stages of analog and digital filtering in the instrument.

The sensor (Figure 1) element is fabricated from a length of 0.040 inch diameter AISI 316 stainless steel wire formed into a loop and mounted in a tubular G-10 epoxy glass body which protects the integral cable connections from attack by the plating and cleaning solutions. The sensor test surface is the 1.00 inch long midsection of the loop which has a centertap lead that is used for connection to the parts rack (cathode power supply). A 0.50 inch length of wire, directly adjacent to the test element, is used as a reference and provides a first order correction for temperature effects. The reference element is protected from chemical attack or plating by a thin, chemical-resistant fluorocarbon coating. Interconnection to the instrument is via a six-conductor cable.

The instrument (Figure 2) is Z-80 microprocessor controlled and consists of a high gain front-end with a synchronous detector feeding a 12-bit analog-to-digital converter. Once coverted to a digital signal, the microprocessor executes additional filtering, converts the sensor signals to microinches of metal thickness, and interfaces with the operator's keypad and digital display.

In operation, the test element of the sensor is connected directly to the rack or part being plated. This serves to minimize sampling error by having the sensor exposed to the same voltage as the parts. The sensor is positioned on the rack so that it is exposed to a current density comparable to the parts being plated. When this condition is achieved, the metal plates out on the test surface at the same rate as it does for all exposed parts resulting in a decrease in the resistance of the test element in the same manner in which the total resistance of two resistors in parallel decreases. In this instance, the stainless steel wire test element is the fixed resistance and the deposited metal is the variable resistance. The resistance of the deposited coating decreases with increasing thickness because the resistance of a conductor is inversely proportional to its average cross sectional area.

The instrument continuously monitors the resistance of the test element and converts this resistance to the thickness of the deposit in microinches.

The conversion factor used to convert the resistance data to microinches of deposited metal is the resistivity of the metal. In most plating applications the resistivity value of a plated metal will be substantially higher than the handbook value for resistivity. Also, the actual resistivity value for a plated metal will vary depending on the plating solution chemistry, use of organic brighteners, temperature, current density and many other factors. For this reason, calibration using empirical data is required in order to achieve optimum measurement accuracy. This is accom-

plished by plating a sensor for several minutes at normal plating currents in the solution to be used while monitoring the thickness using a handbook value of resistivity as the calibration factor. After the plating operation is complete, the sensor is removed and the plating thickness on the test element is precisely determined by thin-sectioning or other accurate means. The corrected calibration factor can be determined by multiplying the initial calibration factor by the actual plated thickness divided by the indicated thickness. The corrected calibration factor is input through the operator's keypad.

Different metals are accomodated by using the appropriate handbook resistivity values and correcting as above. As expected, the measurement span varies in proportion to the resistivity. That is, the larger the resistivity value, the larger the measurement span. Therefore, in order to measure highly conductive metals such as silver, copper and gold in thicknesses greater than a few hundred microinches, a thicker wire (0.080 inch diameter) is used for the sensor and the instrument software is modified to extend its resistance resolving capability.

The error introduced by the thermal coefficient of resistivity is compensated by the reference element which is exposed to the same thermal environment as the test element. However, it must be recognized that the thickness measurement is only valid when the sensor is in the plating solution and at the same temperature as the plating solution. Errors due to shunting of the sensor by the plating solution are negligible beause the resistivity of the plating solution is several orders of magnitude greater than the resistivity of the deposited metal.

Laboratory Testing

Initial laboratory testing was in an acid copper bath without any brighteners. The handbook value of resistivity for pure annealed copper, 1.93 microhm-cm, when corrected for bath temperature of 55°C, was used in the testing. The actual thickness of the copper plating was very repeatable through three test runs. However, the indicated thickness was approximately 35% of the actual thickness. The sensor test elements were removed and the weight of the deposited copper was compared with the coulometric data (product of plating current and time) from the three test runs. The three independent sets of data determined the repeatability to be within ±2%. Based on this data, a new value of resistivity was calculated using a simple proportion of the actual thickness divided by the indicated thickness multiplied by the initial value of resistivity. The value obtained, 6.4 microhm-cm, was used for three subsequent tests. Again the repeatability was good, ±3%, and correlated closely with the coulometric data. The test elements were then removed and thin sectioned. The quality of the plating made the thin section evaluation very difficult but averaged thin section results showed the indicated thickness values were within ±3%.

A new plating bath was prepared using a common organic brightener. A resistivity value of 2.68 microhm-cm was established for coatings plated from this bath. Three tests were run in this bath with carefully controlled location and orientation of the sensor test element. The plating current

was applied until the indicated thickness reached 400 microinches. The coulometric data from the three tests was within ±2%. The plating on the sensors was measured by both beta backscatter and thin section techniques with the following results.

COPPER THICKNESS IN MICROINCHES

| Run No. | Plating Thickness Monitor | Thin Section Average | Beta Backscatter Average |
|---|---|---|---|
| 1 | 400 | 408 | 412 |
| 2 | 400 | 421 | 416 |
| 3 | 400 | 427 | 418 |

Further testing was performed to determine system sensitivity and dynamic range. Repeatable results were achieved at indicated thicknesses of 5 and 10 microinches when compared with coulometric data. Actual thickness measurements were not available for comparison purposes. Testing was also performed at thicknesses in the 1.5 to 2.0 mil range with good results; however, resolution in this range of thickness is not as great as smaller thicknesses.

All laboratory testing was performed at plating currents equivalent to 50 amperes per square foot in order to determine the plating current rejection capabilities of the instrument and sensor.

## Field Testing

Prototype instruments and sensors were provided to three test sites to determine performance in representative production environments. Figure 3 shows the typical installation with the sensor mounted on the parts rack in a location where the sensor should experience the same plating current density as the parts being plated. In all tests the sensor test element centertap was connected directly to the rack so that the sensor is at the same voltage as the parts being plated. And, in all tests, the sensor was exposed to all the same processes as the parts, including "strikes."

FIELD TEST 1
GOLD THICKNESS IN MICROINCHES

| Run No. | Plating Thickness Monitor | Thin Section Average | Beta Backscatter Average |
|---|---|---|---|
| 1 | 110 | 112 | 105 |
| 2 | 110 | 101 | 100 |
| 3 | 110 | 104 | 101 |

In Field Test Number 1, a calibration test run determined the calibration factor for gold to be 4.57 microhm-cm. A single rack of parts was gold plated in each of three test runs, the plated test element was subsequently

removed and the thickness was measured in several locations using the beta backscatter technique. The elements were then measured using thin section techniques. The results are presented in the table above.

Analysis of the thin section data disclosed that in Run 1 the cylinder of plated material was not concentric with the test element, probably as a consequence of differences in current densities. This kind of non-uniformity should have only a minor effect on the measurement since the cross sectional area of the plated coating is not a function of concentricity. More testing is being planned in order to determine the effects of orientation and location on accuracy and repeatability.

In Run 1, the location of the sensor was in a region with high current density gradients and in Run 2 and 3 the sensor was mounted in a region with lower current density gradients. Thin section and beta backscatter data indicated that the plating was most nearly concentric with a cylindrical segment of the test element in Runs 2 and 3.

The results of Runs 2 and 3 suggest a lower value of resistivity than the one used would be more appropriate.

FIELD TEST 2
NICKEL THICKNESS IN MICROINCHES

| Run No. | Plating Thickness Monitor | Thin Section Average |
|---|---|---|
| 1 | 250 | 258 |
| 2 | 278 | 276 |
| 3 | 260 | 262 |

Field Test 2 was performed in a sulfamate nickel bath after establishing a calibration factor of 10.57 microhm-cm. In these tests the location of the sensor was in the center of the plane of the parts. The results are presented in the table above.

Beta backscatter information was not available since the technique is not applicable to combinations of coatings and substrates where the atomic numbers are different by less than 20%.

## Summary

The emphasis thus far has been to develop a sensor and instrument that will demonstrate the technique in a typical electroplating environment.

The results from both laboratory testing and field testing have been very positive with no reportable failures. Correlation of thicknesses measured with this on-line technique has been excellent when compared with the beta backscatter and thin sectioning measurements made on the sensor. The first field tests have demonstrated the sensitivity of plating thickness on an object with respect to its location in the bath. Further development and

testing will be directed toward minimizing these effects and maximizing the correlation between the sensor measurement and the actual deposit thickness on the plated parts.

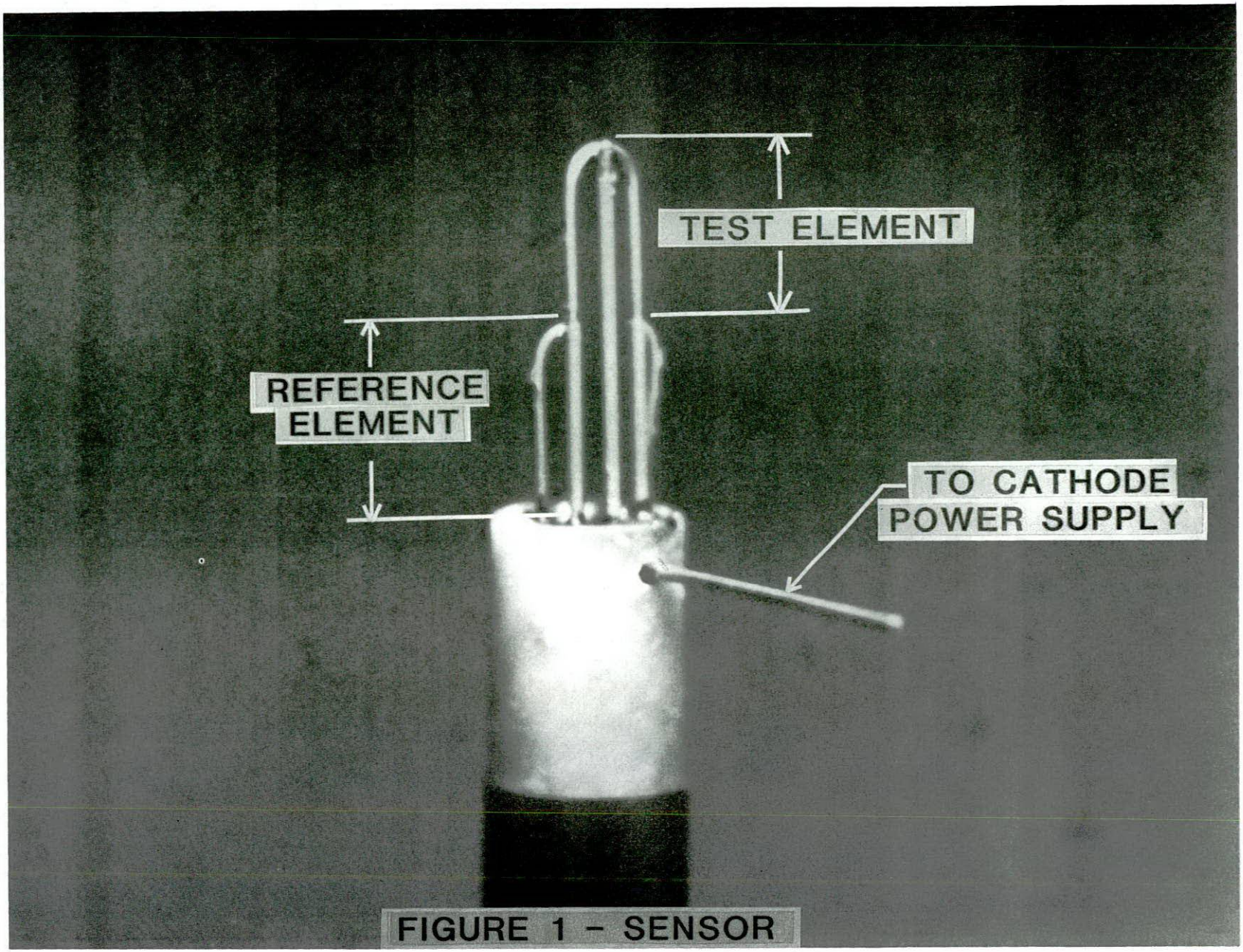


FIGURE 1 - SENSOR

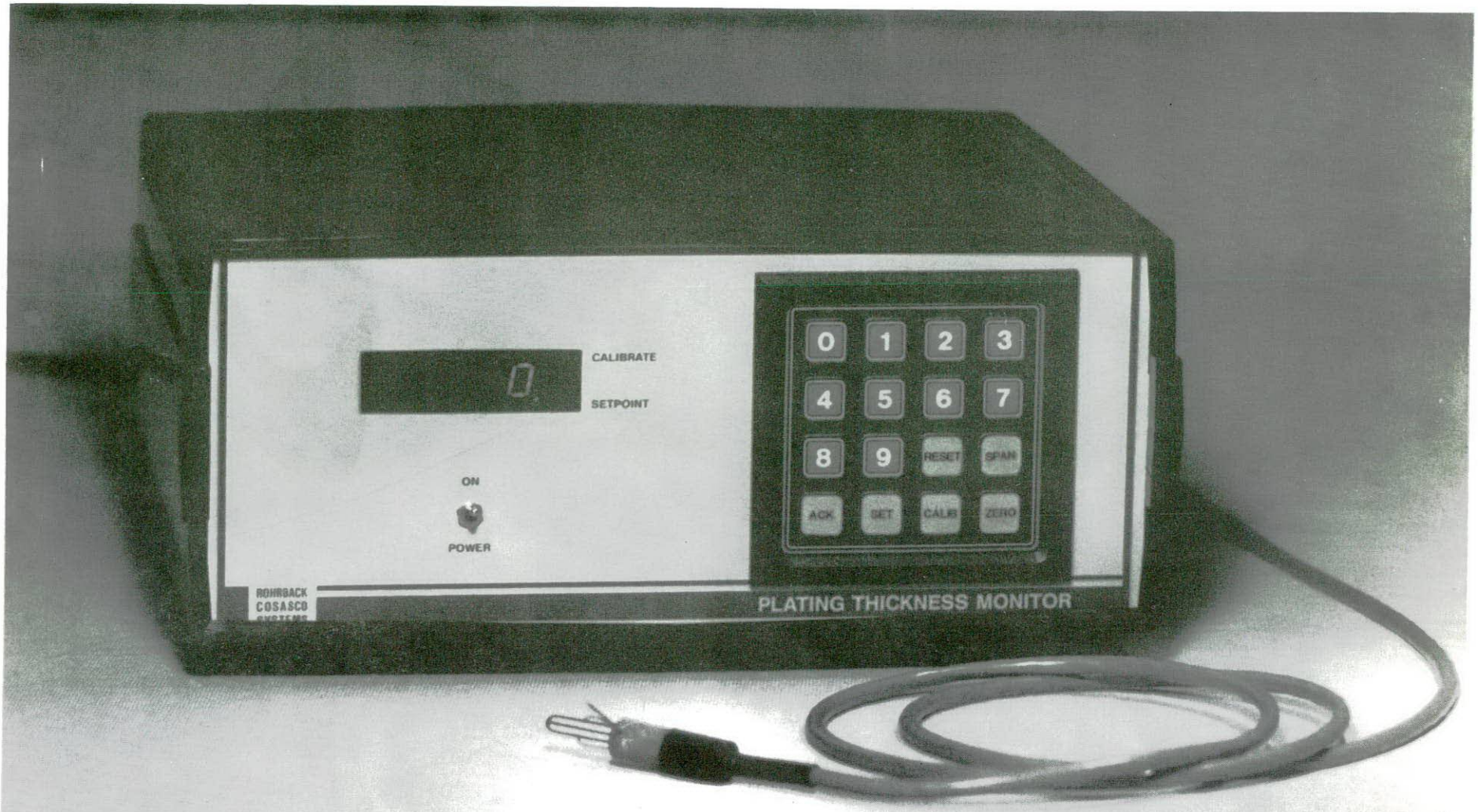


FIGURE 2 - ON-LINE PLATING THICKNESS MONITORING SYSTEM

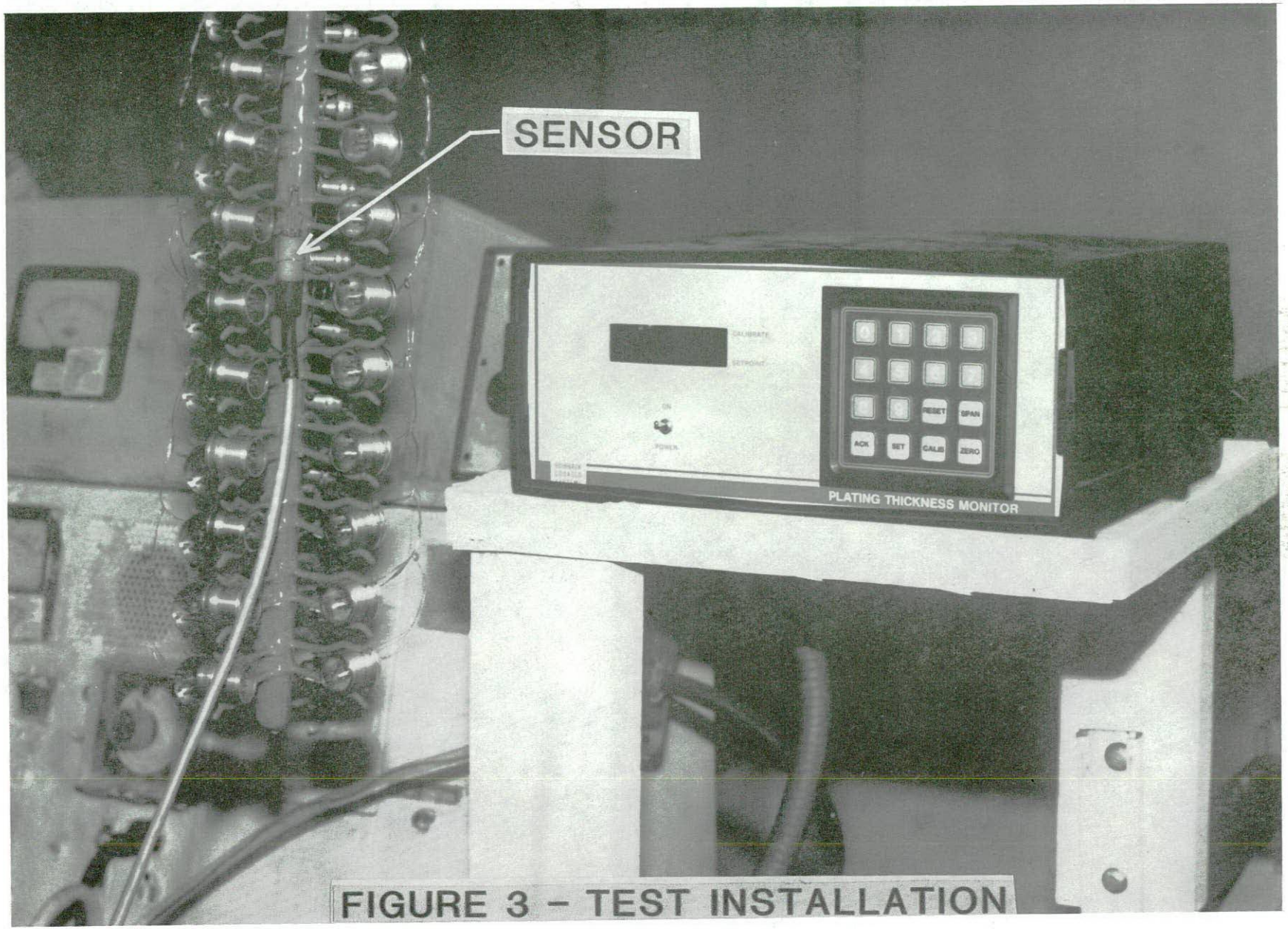


FIGURE 3 – TEST INSTALLATION

L-1

# Advances in Fundamentals And Applications Session L

## Review and Update on Electrocomposites

V.P. Greco
U.S. Army Armament Research,
Development, and Engineering Center
Close Combat Armaments Center
Benet Laboratories
Watervliet, NY 12189

# REVIEW AND UPDATE ON ELECTROCOMPOSITES

V. P. Greco
US Army Armament Research, Development, and Engineering Center
Close Combat Armaments Center
Benet Laboratories
Watervliet, NY 12189-4050

## ABSTRACT

The demand for metal matrix composites (MMC) is reaching a new height in the material community in view of their superior strength at elevated temperatures. Several methods are employed in producing these composites in which high strength inert particles, fibers, or filaments are incorporated in the matrix of a conventional metal. A critical problem in producing metal matrix composites is the handling and damaging of candidate brittle high strength fibers due to high process temperatures and pressures. A process for producing composites, which does not require high temperatures or pressures, is electrodeposition in aqueous solutions which offers a number of other benefits. Electrocomposites are reinforced electrodeposits or electroforms with high strength inert particles, fibers, or continuous filaments.

From a review of the literature, an updated evaluation of electrocomposites will be given, followed by a review of their strengthening mechanisms and the proposed theories of particle encapsulation. The results and properties of electrocomposites previously reported will also be reviewed and the future role that platers will have in producing high performance composites which out-perform superalloys will be assessed.

## A. INTRODUCTION

Composites are often described as polymers or resins which have been reinforced with glass filaments. In reality, any combination of two or more materials with each making a property contribution can be identified as a composite. Some composites are found in nature, such as bamboo and asbestos, and manmade composites date back to the cave man who reinforced mud bricks with straw. The most recent concepts which have been ushered into the arena of high performance materials are metal matrix composites which have high modulus and high strength retention at elevated temperatures.

The types* of metal matrix composites which are being considered in today's material community for high performance application are:

- dispersion-strengthened composites
- particle-reinforced composites
- composites reinforced with fibers, whiskers, or filaments

Fine inert particles or filamentary reinforcements with high temperature strengths combined with soft conventional matrix metals can produce composites which out-perform superalloys.

The use of inert particles to improve mechanical properties of metals at elevated temperatures was first exploited in 1910 by Coolidge[1] in thoriated tungsten to increase creep resistance. The first dispersion-strengthened material designed as a structural load bearing system was sintered aluminum particles (SAP) in aluminum reported in 1952.[2] Another dispersion-strengthened material that received considerable attention in the early 1960's was thoria in nickel,[3] which is more commonly known as TD-nickel.

Whiskers (a major candidate reinforcement) were observed on silver ores as far back as the 19th century and were referred to as hair silver.[4] No attention was given to their growth, which was influenced by temperature and humidity, until they became a problem on tin plated electronic components causing an electrical short during World War II. These whiskers, which were observed as being strong and flexible, were identified as a plating reject and it wasn't until the early 1950's that they were intentionally grown in the laboratory.[5] The testing of tin whiskers (single crystals) was found to have strengths several hundred times that of bulk tin.[6] The latter results stimulated much interest and studies on whisker growth of high modulus-high temperature refractory metals quickly followed.

The achievements in producing high strength whiskers followed by the remarkable development of high modulus-low density boron filaments in 1958 by Talley[7] triggered the composite technology explosion. With the advanced developments that followed, some of the potential whiskers and filaments such as alumina, silicon carbide, boron, and graphite became commercially available on a very limited scale in the late 1960's.

It was during the latter decade that the concept of high performance manmade fiber-reinforced composites became a reality. The strength of conventional engineering materials is only a fraction of their theoretical strength and their usage in high temperature environments is very limited. However, we now have high temperature and low density fibrous or filamentary materials which do approach their theoretical strengths. However, these

*Laminates are also an important type of composite, however, their laminae actually consist of the composites listed above which means a series of thin composites bonded together produces a large composite, and therefore will not be discussed here.

high modulus fibers or filaments, which have anisotropic properties, are unsuitable as a structural material in their monolithic state not only because of their very small diameters, but due to their brittleness, their difficulty to handle in filamentary form, and their tendency to degrade in some atmospheres.

Therefore, by encapsulating these fragile high strength fibers or filaments in a suitable protective matrix metal, we can tailor the composite to our specific needs. Two important requirements in the search for these new materials are a high strength or high modulus/density ratio* and high thermal stability. The strength/density ratios of some of the candidate filamentary materials can be compared to some of the conventional engineering materials by reviewing Table I.

TABLE I. PHYSICAL AND MECHANICAL PROPERTIES OF SOME COMMON FILAMENT AND WHISKER MATERIALS*

| Material | Melting Point (°C) | Modulus of Elasticity x $10^3$ MPa | Modulus of Elasticity x $10^6$ psi | Ultimate Tensile Strength MPa | Ultimate Tensile Strength Ksi | Density g/cm³ | Density lb/in.³ | Max. Modulus to Density Ratio (x $10^4$ in.) |
|---|---|---|---|---|---|---|---|---|
| Copper | 1083 | 100-117 | 14.5-17 | 338-552 | 49-80 | 8.97 | .324 | 52 |
| Tungsten | 3460 | 400 | 58 | 3448-4275 | 500-620 | 19.24 | .695 | 83 |
| Titanium | 1670 | 115 | 16.7 | 1931 | 280 | 4.91 | .282 | 98 |
| Steel | 1605 | 200 | 29 | 3103-4137 | 450-600 | 7.81 | .170 | 103 |
| Aluminum | 660 | 73.1 | 10.6 | 414-621 | 60-90 | 2.69 | .097 | 109 |
| E Glass | 1315 | 73 | 10.5 | 2413-3448 | 350-500 | 2.55 | .092 | 114 |
| S Glass | 1650 | 85.5 | 12.4 | 4317-4827 | 600-700 | 2.49 | .090 | 138 |
| Bamboo | - | 33.4 | 4.9 | 345 | 50 | 0.50 | .018 | 272 |
| Asbestos | 1520 | 172 | 25 | 1379 | 200 | 2.49 | .090 | 278 |
| SiC | 2100 | 483 | 70 | 2068-2758 | 300-400 | 3.46 | .125 | 560 |
| Boron | 2040 | 379-414 | 55-60 | 2068-3448 | 300-500 | 2.55 | .930 | 276 |
| Beryllium | 1285 | 303 | 44 | 1310 | 190 | 1.85 | .067 | 657 |
| Graphite | 3690 | 152-600 | 22-87 | 2758-3896 | 400-565 | 1.50 | .054 | 1000 |
| Alumina Whiskers | 2080 | 414-1034 | 60-150 | 1379-24133 | 200-3500 | 3.96 | .143 | 1049 |
| SiC Whiskers | 2705 | 483-1034 | 70-150 | 13790-41370 | 2000-6000 | 3.18 | .115 | 1304 |
| Graphite Whiskers | 3650 | 1000 | 145 | 20685-24133 | 3000-3500 | 2.10 | .076 | 1908 |

*Averages of various published values.

*It was often quoted in the early years that a bonus of $250 would be paid by the military for every pound that was saved in aerospace structural components.

In spite of these accomplishments in the development of reinforcements in the 1960's, interest in the implementation of MMC floundered in the early years mainly due to the unavailability and high cost of the reinforcements and fabrication of components. In more recent years, the cost of reinforcements has decreased, but it is still considered high. However, they are more available on a commercial scale and their strengths and reproducibility have significantly improved. Also, due to the technological advancements in aerospace structures and high performance engines where conventional materials will not meet the new requirements, the demand for MMC is reaching a new height. These new composites may be regarded as one of the most potential classes of high strength structural materials of all times because of their versatility to be tailored to meet the requirements for severe high temperature environments.

However, some serious obstacles still have to be surmounted. Reproducibility, post-machining, welding, and quality acceptance testing are problem areas which are currently being explored. Because of the anisotropic properties of composites, the measurement of their properties, such as fatigue, fracture toughness, and thermal stability, are much more difficult to perform. Performance testing and property measurements are being given full attention by ASTM groups based on the series of meetings and symposiums focused on composites on an international level. In 1980 the Department of Defense established a Metal Matrix Composite Information Analysis Center (MMCIAC) to promote the advancement of composite materials.

## B. FABRICATION PROCESSES

Composites are being produced by several processes such as castings, powder metallurgy, extrusion, diffusion bonding, vacuum infiltration, etc. A common problem with the fabrication of composites is the handling and damaging of the fragile and reactive candidate filamentary reinforcements due to the high process temperatures and pressures. A process which does not require high temperatures and pressures is electrodeposition in an aqueous electrolyte which offers a number of other benefits.

In spite of the obvious advantages of producing composites by electrodeposition techniques, the plater does not appear to be keeping pace with the ambitious investigators who are exploiting other processes in their attempt to meet the demand for fiber-reinforced composite materials. In constrast to fiber reinforcements, electrocomposites containing particles are being produced by the plater, but the literature indicates that the bulk of the studies are being carried on in foreign countries. A review of the literature also implies that a closer interface is needed between the user and the fabricator of composite materials to produce high quality potential metal systems. In order to achieve this, the fabricator must have a clear understanding of their strengthening mechanisms and composite behavior, which is the intent of this paper.

## C. STRENGTHENING MECHANISMS

The dispersion-strengthening of metals or alloys by inert particles has been treated by a number of investigators.[8-12] The filament reinforcement of metals has been reported by Kelly and his co-workers[12-15] among others.[16] The work by Grant[10] and Kelly and Nicholson[12] is most extensive; however, the proposed theories on strengthening are still incomplete. It should be sufficient for this discussion to briefly state the principal conclusions which have been established on the theory of strengthening. In addition, some of the simple equations are presented to predict the increase in composite strength without entering into the details of stress analysis or the associated dislocation mechanics. Some of these equations have been previously reported in the plating literature,[17,18] but will be repeated here in order to make this summary more comprehensive.

### 1. Characterization of the Three Composite Systems

• Dispersion-strengthened: This composite is characterized by a microstructure consisting of a metal matrix within which fine inert particles are uniformly dispersed. The particle diameter ranges from about 0.01 to 0.1 μm, and the volume percent (v/o) of the particles ranges from 1 to 15 percent.

• Particle-reinforced: This composite is characterized by dispersed inert particles of greater than 1.0 μm diameter with a v/o dispersoid usually in excess of 25 percent.

• Fiber-reinforced: This composite is characterized by the introduction of fibers or filaments aligned unidirectionally or randomly with dimensions and volumes ranging as follows:

| | |
|---|---|
| Diameter: | from submicron to several mils |
| Length: | from mils to continuous lengths |
| Volume: | from a few percent to more than 70 percent |

### 2. Performance of the Different Composite Systems

#### a. Dispersion-strengthening:

The performance of a metal which has been strengthened by a dispersion of a low v/o of small fine encapsulated particles is as follows:

- The matrix metal carries the load.
- The hard, fine inert particles impede the motion of dislocations in the matrix; recrystallization and grain growth are retarded at high temperatures.

The first attempt to relate the particle dispersion with the shear strength of a matrix metal was proposed by Gensamer[8] during his studies with steels in which he showed that the shear strength[5] is directly proportional to the logarithm of the mean free path (λ) between carbide particles:

$$\sigma = -A\lambda + B \tag{1}$$

The theory receiving most attention was that of Orowan[9] who considered only particle spacing:

$$\tau = Gb/D_p \tag{2}$$

where: $\tau$ = shear stress
$G$ = matrix shear modulus
$b$ = Burger's vector
$D_p$ = average spacing between particles

Gensamer[8] showed that the mean free path $\lambda$ and interparticle spacing $D_p$ are related to the volume fraction $V_p$ and mean particle diameter d through the relations:

$$\lambda = (2d/3V_p)(1-V_p) \tag{3}$$

and

$$D_p = (2d^2/3V_p)(1-V_p) \tag{4}$$

Typical ranges for these parameters in dispersion-strengthened composite materials are

$\lambda$ - 0.3 to 0.01 $\mu$m
$D_p$ - 0.3 to 0.01 $\mu$m
$V_p$ - 0.01 to 0.15
d - < 0.1 $\mu$m

Dispersion-strengthened alloys are mainly noted for their high creep resistance and retention of strength at elevated temperatures.

The behavior of two dispersion-hardened alloy systems as a function of temperature can be observed in Figure 1.

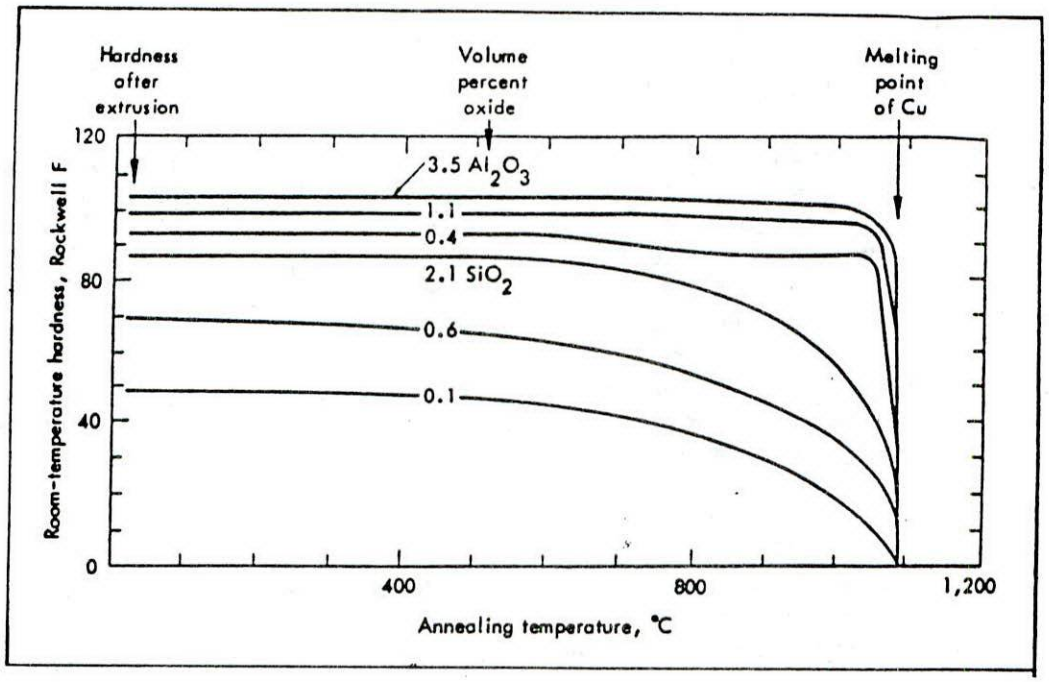


Figure 1. Hardness retention as a function of temperature for various copper-silica and copper-alumina dispersion-strengthened materials.[19]

b. **Particle Reinforcement:**[20]

The performance of a metal which has been strengthened by a dispersion of high v/o of large coarse encapsulated particles is as follows:

- The matrix and dispersed particles share the load.
- Strengthening occurs initially when the dispersed particles restrict the matrix deformation by a mechanical constraint.

Since the elastic moduli of dispersed-particulate composites should follow an isostress modulus, any positive deviation from Eq. (5) which follows signifies matrix constraint. All systems investigated exhibit positive deivation and thus, matrix constraint.

$$E_c = \frac{E_m E_p}{V_m E_p + V_p E_m} \qquad (5)$$

where: E = modulus of composite (c), matrix (m), or particle (p)
V = volume fraction of matrix (m) or particle (p)

- In a ductile metal matrix, the particle increases the local resistance of the matrix to slip and to undergo large plastic deformation.

- In a brittle matrix, the matrix is the primary load-carrying element and the ductile metal particles function by limiting the size of the largest or most severe flaw or crack that can occur in the brittle matrix.

c. **Fiber or Filament Reinforcement:**

The performance of a metal which has been strengthened by high strength-high modulus inert fibers or filaments is as follows:

- The fibers carry the load.
- Soft matrix protects fibers.
- Matrix transfers applied stress to high stress fibers.

(1) **Strength of Fiber Composites** - Studies by McDanels, et al.[21] have shown that the ultimate tensile strength of unidirectional continuous-fiber composites ($\sigma_c$) is expressed by the rule of mixtures:

$$\sigma_c = \sigma_m' V_m + \sigma_f V_f \qquad (6)$$

where: $\sigma_m'$ = stress in matrix at the ultimate tensile strain of the fibers
$V_m$ = volume fraction occupied by matrix
$\sigma_f$ = ultimate tensile strength of fiber
$V_f$ = volume fraction occupied by fiber

The equation assures a strong bond exists between the fiber and matrix metal without any interfacial reactions and neglects the interaction between the constituents due to the differences in their Poisson ratios. The insensitivity of the composite modulus, $E_c$, to the difference in constituent Poisson ratios has been treated in some detail by Tsai, et al.[22]

According to Kelly and Davies,[15] deformation of a composite with uniaxially aligned continuous fibers stressed parallel to the fibers proceeds in four stages as follows:

1. Both the fibers and the matrix deform elastically.
2. The fibers continue to deform elastically, but the matrix now deforms plastically.
3. Both the fibers and the matrix deform plastically (ductile fibers only).
4. The fibers fracture, followed by composite fracture.

In stage 1, the composite modulus, E, can be predicted by Eq. (6).

The linear relationship presented by Eq. (6) has been confirmed by several investigators[23-26] reporting experimental data with the tungsten-copper and steel-silver systems.

(2) **Minimum and Critical Volume Fraction of Fibers** - Equation (6) is valid only when the fibers exceed a certain minimum volume fraction in the composite[27,15] as computed from the following relationship:

$$V_{min} = \frac{\sigma_m - \sigma_m'}{\sigma_f + \sigma_m - \sigma_m'} \qquad (7)$$

where $\sigma_m$ = the ultimate tensile strength of the matrix.

The value of $V_{min}$ increases as the strength of the fibers decreases or as the strength of the matrix approaches that of the fiber. In order for the composite strength to exceed the ultimate strength of the matrix, the volume fraction of the fibers must exceed a critical value, $V_c$, which is shown as follows:

$$V_c = \frac{\sigma_m - \sigma_m'}{\sigma_f - \sigma_m'} \qquad (8)$$

The critical volume increases as the degree of work-hardening in the matrix ($\sigma_m - \sigma_m'$) increases and also as the strength of the matrix approaches that of the fibers. The relative values of $V_{min}$ and $V_c$ are shown in Figure 2.

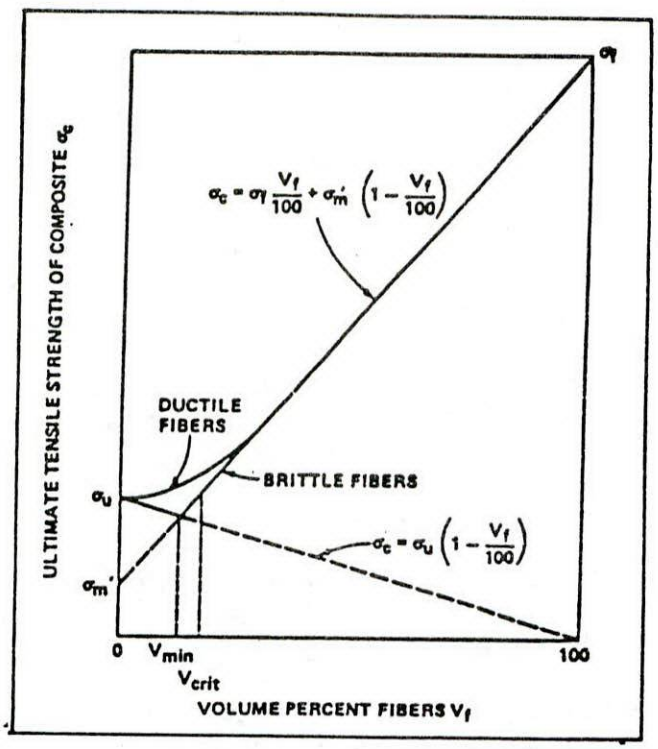


Figure 2. Theoretical values of composite strength $\sigma_c$ with fiber content $V_f$ for reinforcement with continuous fibers.[15]

(3) <u>Critical Fiber Length</u> - When discontinuous fibers are used, the length of the fiber must be greater than a critical length, $L_c$, in order to achieve strengthening of the composite.[25-30] Figure 3 illustrates the stress distribution along a fiber length in relation to the critical length.

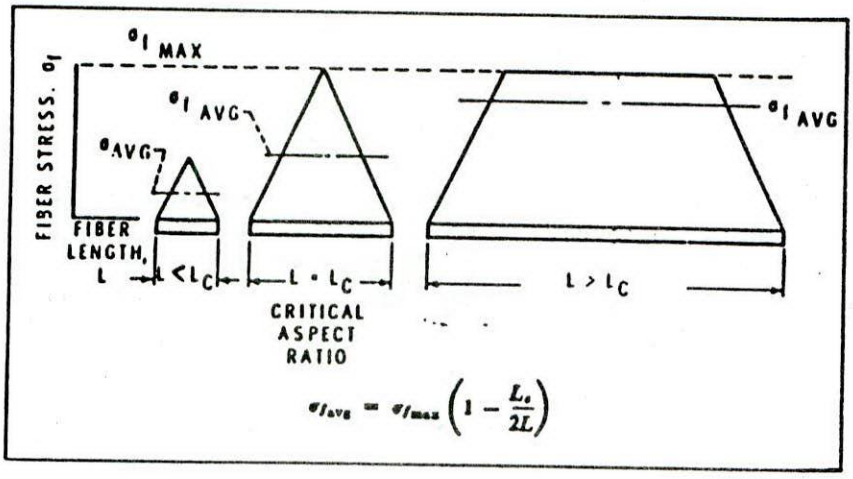


Figure 3. Fiber stress distribution. Tensile stress gradient on fiber versus length.[30]

Different investigators[14,24,31,32] have derived similar equations that relate discontinuous fiber-reinforced composite strength with the length of the fiber in the composite. Kelly and Tyson's equation[14,24] is as follows:

$$\sigma_c = \sigma_m'(1 - V_f + \sigma_f(1 - \frac{\ell_c/D}{2\ell/D})V_f \ldots \tag{9}$$

where: $\ell/D$ = length-to-diameter ratio of fibers in composite
$\ell_c/D$ = critical length-to-diameter ratio of fiber necessary to stress fiber to its ultimate tensile strength

The preceding equation is valid for values of $\ell/D$ equal to or greater than $\ell_c/D$ (critical aspect ratio). An approximate value for $\ell_c/D$ can be obtained from:

$$\ell_c/D = \sigma_f/2\tau \tag{10}$$

where $\tau$ is the shear strength of the matrix or interface.

**d. <u>Strength of Ribbon-Reinforced Composites</u>:**

When stressed parallel to the axis, the tensile stress of ribbon-reinforced composites may be expressed by the usual rule of mixtures formula, Eq. (6). In the direction perpendicular to the ribbon axis,[33,34] the tensile strength is given by

$$\sigma_c = \sigma_m'(1 - V_r) + \sigma_r V_r(1 - \frac{1 - \beta}{W/W_c}) \tag{11}$$

where $V_r$ is the volume fraction of the ribbon; $\beta$ is a constant $\cong 0.5$; $W$ is the ribbon width; and $W_c$ is the critical ribbon width necessary for the transfer of stress to the ribbon from the matrix. The critical width depends on the strength of the ribbon, $\sigma_r$, the shear strength of the matrix

at the interface, $\tau$, and the ribbon thickness, t:

$$W_c/t = \sigma_r/\tau \tag{12}$$

It is possible, by employing wider ribbons, to obtain transverse strengths close to the longitudinal strength. Also, it has been demonstrated[35] both theoretically and experimentally[36] that the elastic modulus in the transverse direction approximates the longitudinal modulus.

e. **Flakes**:[37]

Flake-reinforced composites are perhaps the least known which have been examined for structural applications. There are many applications where the two-dimensional elements of flakes are preferable to the one-dimensional nature of fibers.

Flakes can be highly packed with their planar reinforcement being their major advantage. Metal flakes can be used as electrical or thermal conductors and nonconductive flakes can serve as insulators. The most widely used flakes for the latter application are glass and mica. Some of the other candidate flakes are aluminum diboride, beryllium, and graphite. The rule of mixtures can also be applied on flake-reinforced composites.

f. **Bond Strength Requirements**:

In order to transfer the stress from the matrix to the filament, a specified bond strength, which is measured in shear, must be exceeded. If it is assumed that the filaments are perfectly round with a radius, r, and length, $\ell$, encapsulated in the matrix, the following equation must be satisfied for optimum stress transfer:[38]

$$\pi r^2 \sigma_f = 2\pi r \ell S_b \quad \text{or} \quad S_b = \frac{\sigma_f}{2\ell/r} \tag{13}$$

where $S_b$ is the minimum bond strength required and $\sigma_f$ is the filament strength. For small values of $\ell$ (which may be the case with discontinuous fiber composites or composites with many interfacial voids), $S_b$ may be quite large. Thus, it becomes exceedingly important that the conditions for maximum adhesion be established.

## D. REQUIREMENTS FOR HIGH PERFORMANCE COMPOSITES

Some of the problems which have to be addressed in the production of high performance composites are interfacial reactions, bond strength, and voids. The requirements essential to a satisfactory particle-type composite are usually also applicable to fiber-reinforced composites. Important requirements for a successful reinforced composite are

- The tensile strength and modulus of elasticity of the reinforcement should be higher than those of the matrix metal.

- The bonding of the reinforcement and matrix interface should be sufficient for efficient transfer of shear stress from matrix to reinforcement during loading in a direction parallel to the reinforcement.
- The reinforcement and matrix should be thermally compatible and free of chemical interaction.
- For maximum strength in a given direction, the composite should have a minimum of voids with the reinforcement aligned parallel to the tension axis and uniformly spaced and separated in the matrix.

## E. ELECTROCOMPOSITES

### 1. Theory of Particle or Fiber Encapsulation

Two methods that are commonly known for the encapsulation of particles are conventional electrocodeposition (CECD) and sediment codeposition (SCD). While some of the early investigators proposed or suggested a possible mechanism of particle capture during deposition, little attention was given to the theoretical details. The three proposed mechanisms which have generally been reported in the literature are: mechanical entrapment, electrophoresis, and the adsorption of particles on the cathode surface. The possibility of electrophoretic forces playing a role in capturing the particles was suggested by Withers[39] and Baimakov and Zhurin[40] in the early 1960's. Martin and Williams[41] reported particle capture by entrapment during rapid plating. Brandes and Goldthorpe[42] noted adsorption forces of ions on the particle surface. Tomaszewski and co-workers[43] investigated the effect of monovalent cations and aliphatic amines in influencing codeposition of inorganic particles from an acid copper bath and found that cationic additions such as thallium enhanced particle codeposition. Chen, et al.[44] found that additives do not promote the codeposition of gamma-alumina from the acid copper bath, but oxides of the stable crystalline form such as alpha-alumina and rutile titania are favorably codeposited. Foster and Kariapper[45] investigated the streaming potential and adsorption of nickel and copper ions on aluminum and the improvements with additions of thallium and rubidium ions.

As experimental studies continued on particle codeposition, increasing attention was given to the theory of particle encapsulation. Saifullin and Khalilova[46] presented a formula to calculate the particle concentration in electrocomposites. Bazzard and Boden[47] proposed a mathematical expression for the codeposition of solid conducting particles with metals, but did not consider the effects of pH, temperature, or bath constituents.

In 1972, Guglielmi[48] received considerable attention on his investigation of the kinetics of codeposition of inert particles from an electrolyte in which he considered the combined effect of adsorption and electrophoretic forces. He presented a mathematical model to describe the process based on the interesting similarity of the curves relating v/o of codeposited particles versus suspended particles with the well-known adsorption isotherm.

Figure 4 is a revised schematic of Gugliemi's model to better describe his proposed mechanism which involves two adsorption steps:

1. The loosely adsorbed particles in the outer layer are coated with a thin layer of ions and solvent molecules that may screen any interaction between the particles and the electrons.

2. The second step involves the more rigidly adsorbed particles in the inner layer. The electrical field existing at the interface helps to uncover the particles so that a stronger field-assisted adsorption takes place.

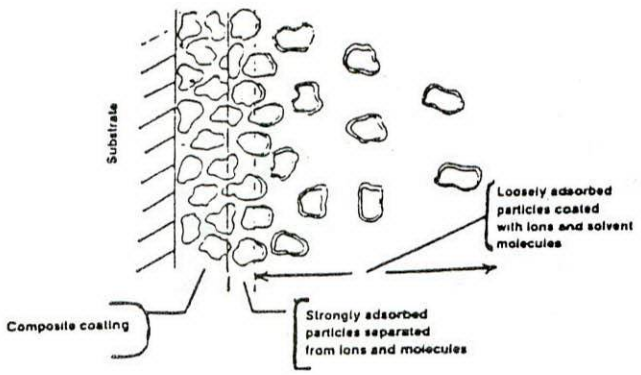


Figure 4. Revised schematic of the two-step deposition process of the Gugliemi model.

A quantitative treatment of the proposed model was presented and subjected to experimental verification. The adsorption of particles in the outer and inner layer described above is analogous to the adsorption of ions in the Hemholtz electric double layer. For the proposed model, the following equation was devised relating volume fraction of embedded particles ($\alpha$) to the suspension concentration of particles (C) and the electrode overpotential ($\eta$):

$$\frac{\alpha}{1 - \alpha} = \frac{nFdv_o}{Wi_o} \cdot e^{(B-a)} \cdot \frac{kC}{1 + kC} \qquad (14)$$

where: F = Faraday constant
n = balence of electrodeposited metal
W = atomic weight of electrodeposited metal
$i_o$ = exchange current density
d = density of the metal

$i_o$ and A are related to metal deposition and are constants in the Tafel equation, which gives a relation between current density (i) and overpotential ($\eta$):

$$i = i_o \cdot e^{A\eta} \tag{15}$$

$v_o$ and B are related to particle deposition and play a symmetrical role with $i_o$ and A. K is derived from the Langmuir adsorption isotherm and depends on the intensity of interaction between particles and cathodes.

In the restricted case of low values of $\alpha$, the factor $(1-\alpha)$ can be dropped and Eq. (14) can be rearranged as follows:

$$\frac{C}{\alpha} = \frac{Wi_o}{nFdv_o} \cdot e^{(B-A)\eta} \cdot \left(\frac{1}{k} + C\right) \tag{16}$$

Since Guglielmi proposed his mechanism for particle encapsulation, a number of investigators have demonstrated its validity with alpha and gamma alumina in copper using the sulphate bath;[49] chromium-graphite system;[50] nickel-tungsten carbide;[51] gold-silicon carbide and gold-tungsten carbide;[52] and more recently with the nickel•tin-silicon carbide system.[53] However, the model did not hold for zinc-phenal resin particles in rigorously agitated electrolytes[54,55] or the chromium-alumina system.[56]

Dunkerly, et al.[57] found that when the concentration of electrolyte exceeded a critical value, the magnitude of the zeta potential decreased drastically and the particles no longer had sufficient charge to repel each other. They also stated that the electrophoretic repulsive forces involved are too small when the suspended particle concentration is large and these are obscured by the higher forces of mechanical stirring and ultrasonic vibration that are employed. In 1966 Hoffman and Mantell[58] observed no electrophoretic effects in the codeposition of alumina in copper in the sulfate bath which is in contrast to other studies.[49] Adsorption of organic additives on silica produced a positive surface charge changing the zeta potential in the formation of the gold-nickel-silica composites.[59] Foster and Kariapper[60] indicated that particle encapsulation is strongly influenced by a surface charge produced by the strong adsorption of metal ions onto the particle surface in their studies with nickel-alumina and copper-alumina. Particle encapsulation in a copper cyanide bath was much greater than the acid baths. Brandes and Goldthorpe[42] made similar observations.

Based on the number of investigators who found Guglielmi's model to be valid when applied to their own experiments, some degree of merit should be given to his mathematical treatment. However, refinement seems justified since the model does not provide for important process parameters such as effect of size, type, and pretreatment of particles,[44,49] effect of bath constituents,[61] bath pH,[62] temperature, and hydrodynamic effects.[63]

Foster and Kariapper[45] proposed a formula which appears to answer the hydrodynamic effects, but the complex interrelationship between some of the associated factors indicates that quantitative treatment of proving its validity may be limited.

In a more recent study, Celis, et al.[64] acknowledged the worthy contributions of Foster and Kariapper[45] and Guglielmi[48] in providing a better understanding of the mechanism of particle deposition. At the same time, however, they critically reviewed the inadequateness of their quantitative treatment and the uncertainties reported in the literature and proposed a more extensive mathematical model.

Up to this date, the latter model appears to be the most comprehensive treatment for attempting to elucidate the mechanism of inert particle codeposition but will undoubtedly also be regarded as too complex for quantitative treatment which includes a number of limitations.

In determining the validity of the model,[64] steady state conditions must exist and the following should be assured:

- A constant voltage, temperature, pressure, and concentration should be maintained during the process.
- The particles should be uniformly suspended in solution.
- The exposure of the cathode surface to the plating solution should be uniform.
- Both the free and adsorbed ionic species are considered equal with respect to transport and reduction processes.

## 2. Evaluation of Mechanism of Particle Encapsulation

From the experimental results reviewed, one may conclude that electrophoresis may or may not play a role in the mechanism of encapsulation of particles or fine fibers in an electrodeposited metal matrix. It should be evident from their results that electrophoretic forces depend on the particular bath suspension and plating conditions employed and the idea of a combined effect taking place may seem very plausible.

In an attempt to form a reasonable concept of the mechanism of particle codeposition, one must also consider the following:

- Plating baths normally include high concentrations of electrolytes in which electrokinetic phenomena would be expected to disappear because the double layer is compressed about the particle and the increase in electrical conductivity would also cause the electrokinetic action to diminish.
- The particle size and shape are also important parameters.
- The actual current density changes with the adsorption and encapsulation of particles on the cathode surface in which the particles may be conductive or nonconductive.

## 3. Preparation, Plating Conditions, and Properties of Electrocomposites

### a. Dispersion-Hardened and Particle-Reinforced Composites

The optimum conditions for preparing particle suspensions and codepositing a designated v/o of uniformly dispersed inert particles in a metal

matrix have not been completely established. Most of the data in the literature has been empirical in nature in which various type particles and electrolytes were employed with a wide variety of conditions. Some of the extreme limits found in the literature are as follows:

- Particle diameter: ranged from 0.02 μm[62] to 100 μm[65]
- Particles in bath: ranged from 5 g/ℓ[63] to 200 g/ℓ[17,57] and in one study for chromium carbide exceeded 500 g/ℓ[66]
- Particles in deposit: up to 57 v/o for nickel-tungsten carbide[51] and exceeding 60 v/o for nickel-molydisulfide[67]
- Current density: exceeded 30 A/dm² for nickel-molydisulfide[67]

Some of the practices and observations reported in the preparation of codeposited particles are:

(1) **Preparation of Suspension** - The cleaning of particles prior to immersion in the electrolyte may have a significant effect on the final size and amount of encapsulation in the matrix metal depending on the grade and purity of the particle.

The acid cleaning of corundum white and gray powders (alumina) resulted in large particle-size reductions and differences in rates of particle capture in nickel.[65] In other studies, boiling copper sulfate electrolyte was used to preclean alumina, silicon carbide, and barium sulfate particles[68] and tungsten carbide particles were immersed in acetone and dilute hydrochloric acid in order to activate the contaminated particle surface for encapsulation in nickel.[51,63]

Two methods which were successfully employed to prepare solution-particle suspensions[17,62] are

- Immersing the particles directly into the electrolyte and mixing with a magnetic stirrer or preferably with a blender.

- Suspending the particles in a small portion of water and mixing with a blender; conventional electrolyte concentrate can then be added to the blended slurry and prepared for plating; the blending time can be determined experimentally.

(2) **Factors Affecting Particle Encapsulation**

- Particle Concentration - Increased particle concentration in the bath is the most effective variable for increasing the v/o of dispersoids in the matrix[17,47,56,60,62] which approached a maximum in some studies.[63,69]

- Additives - Wetting agents or monovalent cations and aliphatic amines produced a surface change when adsorbed on a particle[17,43,58,70] promoting particle encapsulation and improved dispersion. In other studies, organics caused foaming and particle floatation[60] and adverse dispersing,[42] while other investigators found no effects.[44]

- Current Density - The concentration of particles (alumina, silicon carbide, chromium carbide, and molydisulfide) in the deposit generally decreased as the current density increased,[17,53,62,67] however, no effects were observed with graphite in chromium.[50] In one study,[71] particles were only encapsulated in chromium at low current density (2-4 A/dm$^2$).

- Type of Bath - Particle encapsulation is less in a copper sulfate bath than a cyanide bath.[42,43,58] The presence of chloride ions inhibited the codeposition of oxides with copper[72] in the sulfate bath. Particle encapsulation in an electroless bath was also investigated.[73]

- Type of Particle - The encapsulation of rutile titania (0.3 μm) is greater than alpha-alumina (0.05 μm) in nickel;[17] alpha-alumina (0.3-1.0 μm) and rutile titania (0.3 μm) are readily codeposited in copper (acid bath), while gamma-alumina (0.2 μm) and anatase titania are not.[44] Calcining promoted codeposition of alpha-alumina particles in copper.[44]

- Current Mode - The use of pulse or periodic reverse currents have resulted in copper-alumina composites where concentrations of particles increased with increasing current density[74-75] which is in contrast to normal direct current plating reported above. Microstructural changes of the matrix metal, improved particle dispersion, and composite strength retention at high temperatures have also been observed when pulse or periodic currents are employed.[74,76,77]

- Ultrasonics - Ultrasonic agitation was found to reduce agglomeration and improve particle distribution and strength retention of copper-alumina[76] and nickel-alumina.[75]

- Bath Temperature - The influence of temperature on the codeposition of particles is not very well defined. Codeposition decreased with increasing temperatures up to 50°C for graphite powder in chromium[50] and concentrations of silicon carbide and alumina in tin•nickel and nickel, were found to be independent of temperature.[53,62]

- Bath pH - The influence of pH on particle concentration is also not very well defined. No effects were found by increasing pH with the nickel-alumina system,[42,43,58] while one investigator noted an increase in particle codeposition with pH up to 2.0 which remained constant above 2.0.[62] Graphite powder increased in nickel with increasing pH, while molydisulfide powder in nickel decreased.[78]

### (3) Other Particle Dispersions

**(a) Solid lubricants** - The production of electrocomposites has also included particulates with lubricating properties, such as molydisulfide, tungsten disulfide, and graphite particles.[67,78,79,80] High wear resistant properties have been reported with such composites.

**(b) Metal particles** - Studies also included the encapsulation of dispersed metal powders in a matrix for the purpose of achieving alloys by post-heating.[47,81,82] The benefits derived from this practice are the formation of alloys into complex shapes at considerably lower temperatures and costs than are required for casting.

**(c) Electroless composites** - Particle-reinforced composites have also been produced by electroless plating of nickel.[43,83] Particulate matter such as alumina, diamond, silicon carbide, and teflon have been encapsulated in an electroless nickel matrix.

**(4) Properties of Particle-Dispersed Electrocomposites** - The increase in as-plated hardness of submicron particle-dispersed composites is significant, but the strength is marginal. When subjected to high temperatures, their strength retention is fairly significant, however, in order to achieve maximum suspension strengthening, composites must be subjected to a combination of mechanical and thermal treatments.[19,84,85] For example, TD-nickel (a well-known high strength alloy) is hot extruded, stress-relieved, and subjected to a prolonged series of moderate rolling reductions and intermediate anneals. The effects of cold rolling copper-alumina electrocomposites have been reported[77] to produce significant strengthening, but were embrittled.

The following discussion of results refers to as-plated and post-heat treated composites without any subsequent mechanical working. A suitable combination of mechanical and thermal treatments to achieve the maximum properties in an electrocomposite containing submicron-sized particles for the purpose of dispersion-strengthening may have to be devised for each system.

In contrast to the dispersion-strengthening, the strengths of particle-reinforced composites may well be at their maximum level in the as-plated condition or may require a post-heat treatment for optimum performance.

Some of the studies reviewed have shown that codeposition of hard inert particles in a metal:

- increases the hardness and strength, but decreases the ductility of various composite systems;
- increases the creep strength of dispersion-hardened gold-alumina;[87,88]
- increases the electrical resistivity of dispersion-hardened copper-alumina slightly,[77] but aluminum-alumina is not changed;[88]
- increases the corrosion resistance of nickel-alumina;[94] and
- increases the wear resistance of cobalt-chromium carbide,[66] nickel-silicon carbide,[90] cobalt-chromic oxide,[91] and nickel-diamond.[63,92] Increased wear resistance is also obtained with the chromium-silicon carbide and systems using submicron-sized particles.[93]

Figure 5 shows the yield strengths versus post-heating for nickel, nickel-alumina, and nickel-titania alloys which also includes cross sections of the microstructure of two of the alloys in the insets.[17] Note that these

alloys have not been mechanically worked, therefore the plot does not represent their full potential of strength retentions.

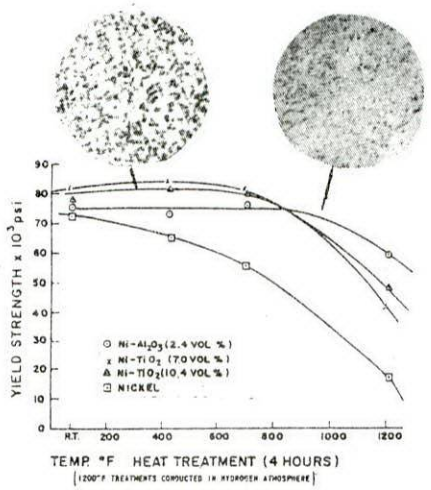


Figure 5. Yield strength versus heat treatment for nickel, nickel-alumina and nickel-titania (insets are cross sections of the alloys (1000X)).

### b. Discontinuous Fiber (Whiskers or Filaments)-Reinforced Electrocomposites

**(1) Preparation of Suspensions** - Since whiskers and most high strength fibers are fragile and easily damaged during handling, great care must be exercised in preparing solution-fiber suspensions. Suggested methods of preparing suspensions are the following:

- Immersing the fibers or whiskers directly into the electrolyte and stirring gently (by air, magnetically, or ultrasonically) during plating.
- Adding the fibers or whiskers gradually into the electrolyte during plating and relying on gradual settlement of the dispersoids onto a horizontal cathode surface.

**(2) Factors Affecting Encapsulation** - The formation of electrocomposites with discontinuous fibers are by far the most difficult to produce. The difficulty of encapsulating freely suspended discontinuous fibers increases with increasing length and diameter of the fiber due to the probable clustering and pileup on a cathode surface before the fibers are completely encapsulated. The problem is more complex if the fibers are electrically conductive or if their surfaces are difficult to wet. However, the optimum plating conditions should be the same as for particles.

Since whiskers are the most potentially high strength candidate materials for fiber reinforcement, techniques for their successful encapsulation should be regarded as a valuable asset.

(3) **Properties of Discontinuous Fiber-Reinforced Electrocomposites** - Nickel composites up to 11 v/o alpha-alumina whiskers (30 μm diameter) have been successfully electroformed in contrast to composites with silicon carbide whiskers (10 μm diameter) which resulted in excessive voids in the nickel matrix due to the semiconductive surfaces of the fibers.[94] The strengths of the nickel-alumina alloys (Figure 6), after annealing in $H_2$ at 650°C for one-half hour, agree with the calculated rule of mixtures. A cross-sectional view of one of the alloys with 11 v/o alumina is shown in the inset.

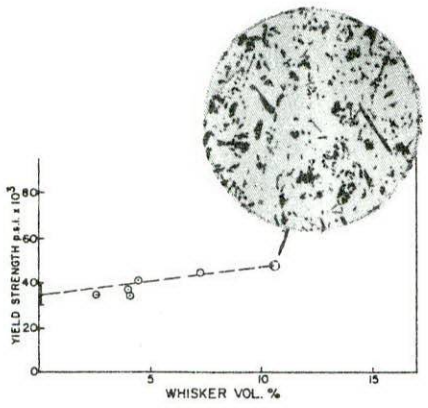


Figure 6. Variations of yield strengths of alpha-alumina whiskers - nickel composites annealed. (Inset is a cross section of the composite).

### c. Continuous Fiber-Reinforced Electrocomposites

An excellent handbook on the preparation, structure, and properties of reinforcing fibers is by Watt and Perov.[95] Continuous filament-reinforced composites are potentially among the highest strength and highest performance structural materials that can be produced by electrodeposition. With cylindrical-shaped cathodes, reinforcements can be easily wound on a rotating cathode and encapsulated in a plated matrix metal with complete control of the spacing and v/o of the filament.

The preparation of such composites will depend on the filament characteristics and cathode geometry. Factors that must be considered are

- monofilament or strand
- filament geometry and size
- conductive or nonconductive filament
- filament reaction at high temperatures
- pretreatment - cleaning, activating, or etching requirements
- cathode design - cylindrical, oval, etc.
- winding apparatus - spacing, guides, tension, filament breaks, etc.
- winding pattern - unidirectional or cross-wrap
- prewinding or simultaneous winding

(1) **Properties and Microstructures of Some Electrocomposites with Continuous Unidirectional Filaments** - A variety of continuous unidirectional filament-reinforced electrocomposites have been produced.[18,94,96-105] Some of the systems are the following:

- Monofilaments:
  Tungsten (1 mil) in copper
  Tungsten (½ mil) in nickel
  Boron (4 mil) in nickel, copper, or aluminum
  Boron (2 mil) in nickel
  Silicon carbide (4 mil) in nickel
  Boron nitrided coated boron (4 mils) in nickel
- Strand:
  Glass in nickel
  Graphite in nickel or aluminum

Tungsten - Strength measurements of continuous filament-reinforced electrocomposites with minimal voids compare favorably with calculated values from the rule of mixtures. The stress-strain plots in Figure 7 show increasing strength with increasing v/o values of 12 μm (½ mil) diameter tungsten filaments in electrodeposited nickel.[94] The inset shows a cross section of one of the composites in which the tungsten filament was simultaneously wound on a cathode drum during plating.

Boron and Silicon Carbide - Candidate low density conductive monofilaments such as boron and silicon carbide are usually supplied in minimum diameters of 100 μm (4 mil) and are not easily encapsulated without voids due to radial crystal growth of the plated metal around the filament. In this case, the filament had to be prewound on the cathode drum prior to nickel plating. View "a" of Figure 8 shows the profiles of plated nickel encapsulating a single conductive boron filament which has a tungsten core. View "b" shows the voids formed between two filaments when they are spaced too close[97] during plating. View "c" shows the increasing interfacial reaction which occurs with temperature between boron and nickel.[18] Fortunately, voids are easily eliminated when the surfaces of boron filaments are nitrided, making it nonconductive which prevents the radial crystal growth around the filament (Figure 9) permitting higher filament loading (i.e., spacing as close as one-half filament diameter).

Furthermore, the nitrided coating prevents interfacial reactions with nickel at 650°C as compared with pure boron (Figure 8). Work by Camahort[106] has shown that surface nitridation protects boron from reacting with aluminum for ten minutes at 800°C (1470°F).

Equation (13) dictates that as the diameter of the filament increases, the bore strength requirements increase. Therefore, the bond strength of 100 μm diameter filaments of boron and silicon carbide in nickel were investigated.[18] Results of filament pull-out studies indicated that etching the filament and post-heating electrocomposites up to 500°C improved the bond strength.

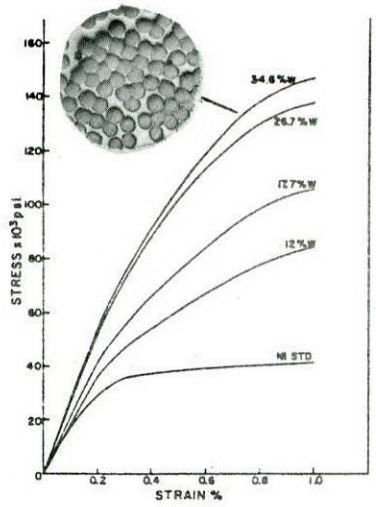


Figure 7. Stress-strain 0.005-inch tungsten filament in nickel composites (annealed).

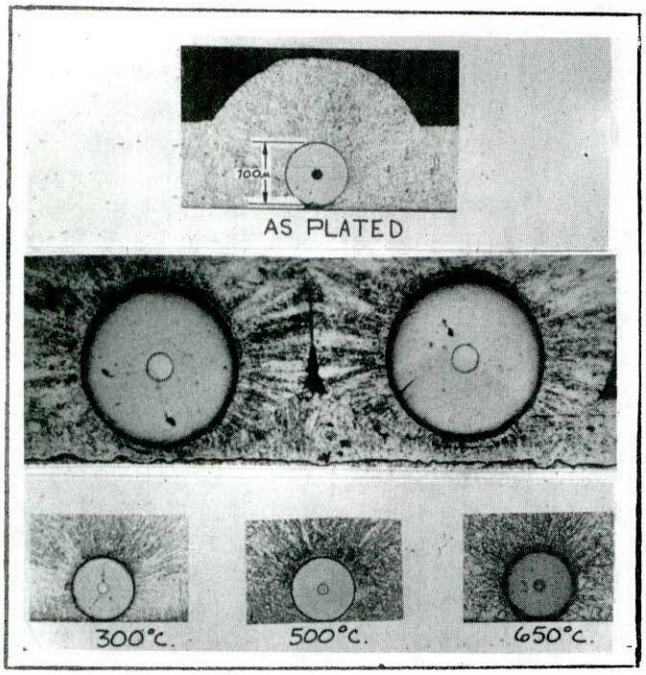


Figure 8. Nickel-boron (4 mil) composites: (a) nickel contour over filament; (b) voids formed between filaments; (c) interfacial reactions with temperature.

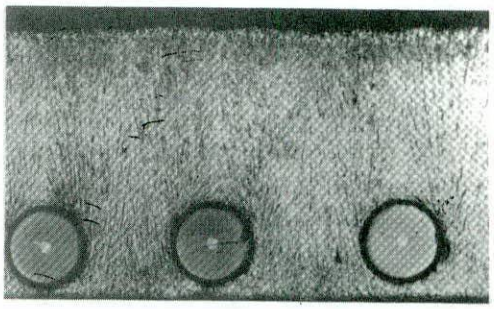

Figure 9. Cross section of nickel-boron (BN-coated) composite with the absence of radial crystal growth of nickel around the filaments and subsequently void-free.

Glass and Graphite - High strength-low density filaments such as glass and graphite do have small diameters (8-12 μm) which are ideal for encapsulation by plating. However, such reinforcements are normally supplied in strands consisting of several filaments which are coated with an organic film for use with an epoxy matrix. For complete encapsulation of the

indivdual filaments in a metal matrix, the strands have to be thoroughly washed to remove the organic film and carefully spread apart and placed on a cathodic surface prior to plating. Figure 10 shows a cross section of glass fibers in a plated nickel matrix.

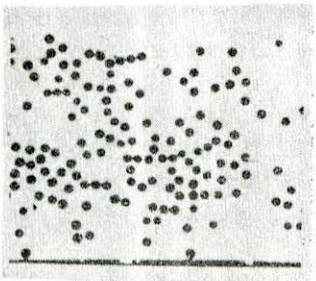

Figure 10. Glass filament-nickel composite by prewound filament technique (200X).

Undoubtedly, graphite has the most potential of all the reinforcements due to its high strength-to-density ratio and thermal stability, but it has poor oxidation resistance. For over the past decade, extensive studies have concentrated on applying various plating coatings on graphite filaments for resistance against reactions with matrix metals such as aluminum.

Table II shows some of the results of different electrocomposite systems reported in the literature.

**TABLE II. MECHANICAL PROPERTIES OF SOME CONTINUOUS FILAMENT ELECTROCOMPOSITE SYSTEMS**

| Composite System | | V/O Fil | kg/mm² | $10^3$psi | kg/mm² | $10^3$psi | kg/mm² | $10^3$psi |
|---|---|---|---|---|---|---|---|---|
| 4 mils B/Ni[98] | | 42 | 285 | 405 | 42 | 61 | 132 | 188 |
| | | 51 | 273 | 388 | 63 | 90 | 132 | 188 |
| 4 mils B/Al[104] | | 15 | 210 | 300 | 10 | 14.3 | 25.4 | 32.6 |
| 4 mils B/Al[105] | | 32 | - | - | 18 | 25.4 | 85 | 121 |
| 2-4 mils W/Ni[105] | | 50 | 352 | 500 | 70 | 100 | 155 | 221 |
| ½ mil W/Ni[94] | as-plated | 34.3 | 352 | 500 | 73 | 104 | 149 | 212 |
| | 650°C ½ hour | 34.6 | - | - | 39 | 55 | 117 | 166 |

## F. SUMMARY OF ELECTROCOMPOSITES

Electrodeposition is a viable process for producing sound and high strength composites. However, improvement in the reproducibility of composites with further advancements in plating techniques and filament making are required. Form the foregoing, we have learned that successful electrocomposites were produced with the following techniques:

- Conductive filaments with a diameter of 25 μm (1 mil) or less were simultaneously wound on a mandrel during plating.
- Nonconductive filaments of 100 μm (4 mils) diameter were unidirectionally wound in single rows with a minimum spacing of one-half filament diameter followed by plating for complete encapsulation. Then, a second row was wound and plated, etc., without removing the mandrel or interrupting electrolysis when the deposit was relatively smooth.
- Conductive filaments of 100 μm (4 mils) diameter were processed as above with two exceptions: minimum spacing was one filament diameter, and the mandrel was removed after each row was plated to remove surface irregularities by machining.

Two of the changes that will significantly improve the quality of electrocomposites are the following:

- The use of finer diameter (< 50 μm) monofilaments with high strength and high modulus-to-density ratios.
- The use of nonconductive filaments when their diameter is greater than 50 μm (2 mils).

Studies are also needed in:

- Determining the benefits of other pretreatments to improve the wetting and bond strength of filaments.
- Expanded use of ultrasonics, periodic reverse, pulse plating, and other aids to determine their influence on voids and properties of the matrix metal.
- The plating of matrix alloys.

**ACKNOWLEDGEMENT**

Gratitude and special thanks are given to Ellen Fogarty for typing and editing the manuscript.

## REFERENCES


1. W.D. Coolidge, in: Proc. Am. Inst. Elec. Eng., AIEE, 1910, p. 961.
2. R. Irmann, Metallurgia, Vol. 46, 1952, p. 125.
3. G.B. Alexander, et al., U.S. Patent No. 2,972,529, February 21, 1961.
4. M.J. Salkind, "Whiskers and Whisker-Strengthened Composite Materials," WVT-RR-6315, Watervliet Arsenal, Watervliet, NY, October 1963.
5. K.G. Compton, A. Mendizza, and S.M. Arnold, Corrosion, Vol. 7, October 1951, p. 327.
6. C. Herring and J.K. Galt, Physical Review, Vol. 85, 1952, p. 1060.
7. C.P. Talley, Boron Synthesis, Structure and Properties, Plenum Press, New York, 1960, pp. 94-105.
8. M. Gensamer, Trans. Am. Soc. Metals, Vol. 36, 1940, p. 30.
9. E. Orowan, in: Symposium on Internal Stresses in Metals and Alloys, Institute of Metals, 1947, p. 451; Rept. Progr. Phys., Vol. 12, 1948-9, p. 214.
10. N.J. Grant, in: The Strengthening of Metals, (D. Peckner, ed.), Reinhold, New York and London, 1964, p. 163.
11. G.S. Ansell, in: Physical Metallurgy, (R. W. Cahn, ed.), North-Holland Publishing Company, Amsterdam, 1965, p. 887.
12. A. Kelly and R.B. Nicholson, eds., Strengthening Methods in Crystals, John Wiley and Sons, Inc., New York, 1972.
13. A. Kelly, Proc. Royal Soc. London, Ser. A, Vol. 282, No. 1388, October 20, 1964, pp. 2-9.
14. A. Kelly and W.R. Tyson, in: High Strength Materials, (V.F. Zackey, ed.), John Wiley and Sons, Inc., New York, 1965, pp. 578-602.
15. A. Kelly and G.J. Davies, Met. Rev., Vol. 10, No. 37, 1965, pp. 1-77.
16. R. Hill, J. Mech. Phys., Vol. 12, 1964, p. 199.
17. V.P. Greco and W. Baldauf, Plating, Vol. 55, No. 3, March 1968, pp. 250-257.
18. V.P. Greco, W.A. Wallace, and J.N.L. Cesaro, Plating, Vol. 56, 1969, pp. 262-270.
19. X.O. Preston and N.J. Grant, Trans. AIME, Vol. 221, 1961, p. 164.
20. L.J. Broutman and R.H. Krock, eds., Modern Composite Materials, Addison-Wesley Publishing Company, Reading, MA, 1967, Chapters 1 and 2.
21. D.L. McDanels, R.W. Jech, and J.W. Weeton, in: Proceedings of the Sixth Sagamore Ordnance Materials Research Conference, Report No. MET-661-601, Syracuse University Research Institute, 1959, p. 116.
22. S.W. Tsai, J.C. Halpin, and N.J. Pagano, Composite Materials Workshop, Technomic Publishing Company, Inc., Stamford, CT, 1968, pp. 1-8.
23. D. Cratchley, Powder Metallurgy, Vol. 11, 1963, p. 59.
24. A. Kelly and W.R. Tyson, J. Mech. Phys. Solids, Vol. 13, 1965, p. 329.
25. D.L. McDanels, R.W. Jech, and J.W. Weeton, Trans. TMS-AIME, Vol. 233, 1965, pp. 636-642.
26. H. Piehler, Trans. TMS-AIME, Vol. 233, 1965, pp. 12-16.
27. W.H. Sutton, in: Modern Composite Materials, (L.J. Broutman and R.H. Krock, eds.), Addison-Wesley, Reading, MA, 1967, pp. 412-441.
28. W.H. Sutton and J. Chorne, in: Fiber Composite Materials, American Society for Metals, Metals Park, OH, 1965.

29. W.R. Tyson and G.J. Davies, British Journal of Applied Physics, Vol. 16, 1965, p. 199.
30. D.W. Petrasek, R.A. Signorelli, and J.W. Weeton, in: Fiber-Strengthened Metallic Composites, ASTM STP 427, Am. Soc. Testing Mats., 1967, pp. 149-175.
31. J.S. Islinger and D.E. Miller, "Mechanism of Reinforcement of Fiber Reinforced Structural Plastics and Composites," WADC TR-59-600, Wright Air Force Development Center, Appendix 1, 1960.
32. A.J.M. Spencer, Int. J. Mech. Sci., Vol. 7, 1965, p. 197.
33. E. Anderson, J. Mater. Sci., Vol. 8, 1973, pp. 676-687.
34. N.S. Stoloff, in: Alloy and Microstructural Design, (J.K. Tren, G.S. Ansell, eds.), Academic Press, New York, 1976, Chapter III.
35. P.J.E. Forsyth, R.W. George, and D.A. Ryder, Appl. Mater. Res., Vol. 3, 1964, pp. 223-228.
36. E. Anderson, B. Lux, and C. Crussard, Mem. Sci. Rev., Vol. 69, 1972, pp. 165-180.
37. M.M. Schwartz, Composite Materials Handbook, McGraw-Hill Book Co., New York, 1984, Chapter 1.
38. S.S. Brenner, J. Metals, Vol. 14, 1962, p. 809.
39. J.C. Withers, Prod. Fin., Vol. 8, 1962.
40. Yu. V. Baimakov and A. I. Zhurin, Metallurgizdat, Vol. 61, 1963 (in Russian).
41. P.W. Martin and R.V. Williams, in: Proc. Interfinish '64, British Iron and Steel Research Association, London, 1964, pp. 182-188.
42. E.A. Brandes and D. Goldthorpe, Metallurgica, Vol. 195, November 1967.
43. T.W. Tomaszewski, L.C. Tomaszewski, and H. Brown, Plating, Vol. 56, 1969, p. 1234.
44. E.S. Chen, G.R. Lakshminarayanan, and F.K. Sautter, Met. Trans., Vol. 2, No. 7, April 1971, p. 937.
45. J. Foster and A.M.J. Kariapper, Trans. Inst. Met. Finish., Vol. 51, No. 1, Spring 1973, p. 27.
46. R.S. Saifullin and R.G. Khalilova, J. Appl. Chem. (USSR), Vol. 43, No. 6, 1970, p. 1266.
47. R. Bazzard and P.J. Boden, Trans. Inst. Met. Finish., Part I, Vol. 50, 1972, p. 63.
48. N. Gugliemi, J. Electrochem. Soc., Vol. 119, 1972, p. 1009.
49. J.P. Celis and J.R. Roos, J. Electrochem. Soc., Vol. 124, No. 10, October 1977, pp. 1508-1511.
50. Raj. Narayan and B.H. Narayana, J. Electrochem. Soc., Vol. 128, No. 8, August 1981, pp. 1704-1708.
51. P.K. Gupta, A.N. Tiwari, and B.K. Agrawal, Trans. Jpn. Inst. Met., Vol. 23, No. 6, June 1982, pp. 320-327.
52. He-tong Guo and Zhao-yong Wang, Journal of Tianjin University, Tianjin, China, Vol. 1, 1985, pp. 13-19 (in Chinese).
53. J. Sadowska-Mazur, M.E. Warwick and R. Walker, Trans. Inst. Met. Finish., Vol. 64, No. 4, November 1986, p. 142.
54. K. Naitoh, J. Met. Finish. Soc. Jpn., Vol. 30, No. 4, April 1979, pp. 185-188 (in Japanese).

55. K. Naitoh, K. Deguchi, M. Kubo, and S. Kurosaki, J. Met. Finish. Soc. Jpn., Vol. 30, No. 11, November 1979, pp. 584-590.
56. R. Narayan and S. Chattopahyay, Surf. Technology, Vol. 16, No. 3, July 1982, pp. 227-234.
57. F.J. Dunkerly, H.W. Leavenworth, and G.E. Eichelman, in: Joint Proceedings of the Metallurgical Society and the American Institute of Mining, Metallurgical and Petroleum Engineers, Second Bolton Landing Conference, Vol. 47, Gordon and Breach Science Publishers, New York, pp. 695-718.
58. J.E. Hoffman and C.L. Mantell, in: Trans. TMS-AIME, Vol. 236, 1966, p. 1015.
59. Shunichi Yoshimura, Eiichi Sato, and Shin Chida, "The Formation of Au-Ni-$SiO_2$ Dispersion Coatings," Department of Industrial Chemistry, Faculty of Engineering, Utsunomiya University, 2753, Ishii-machi, Utsunomiya-shi 321, Japan.
60. J. Foster and A.M.H. Kariapper, Trans. Inst. Met. Finish., Vol. 51, 1973, pp. 27-31.
61. T. Hayashi, N. Maeda, and N. Furukawa, in: Proc. Interfinish '76, Amsterdam, 1976.
62. F.K. Sautter, "Electrodeposition of Dispersion-Hardened Nickel-$Al_2O_3$ Alloys," WVT-RR-6204, Watervliet Arsenal, Watervliet, NY, February 1962; also F.K. Sautter, J. Electrochem. Soc., Vol. 110, 1963, p. 557.
63. J. Zahavi and J. Hazan, Plating, Vol. 70, No. 2, February 1983, pp. 57-61.
64. J.P. Celis, J.R. Roos, and C. Buelens, J. Electrochem. Soc., Vol. 134, No. 6, June 1987, pp. 1402-1408.
65. R.S. Saifullin, Zh. Prikl. Khim., Vol. 39, No. 4, April 1966, pp. 810-814.
66. E.C. Kedward and K.W. Wright, Plating, Vol. 65, No. 8, August 1978, pp. 38-41.
67. E.C. Vest and D. Frank Bazzarre, Met. Finish., Vol. 65, November 1967, p. 52.
68. R.S. Saifullin, R.E. Fomina, and A.R. Saifullen, "Inhibitors and Stimulators of Formation of Composite Electrochemical Coatings." Translated from Zashch. Met., Vol. 22, No. 4, July-August 1986, pp. 611-615.
69. J. Zahavi and H. Kerbel, Proc. Interfinish 1980, 1980, p. 208; Proc. AES An. Conf., Vol. 68, 1981.
70. J.P. Roos, J.P. Celis, and J.A. Helson, in: Trans. Inst. Met. Finish., Vol. 55, 1977, pp. 113-116.
71. Tomoya Minegishi and Shobun Takatani, "Composite Chromium Plate Method," Japan Patent Agency (JP), 1983-107497, 27 June 1983.
72. G.R. Lakshminarayanan, E.S. Chen, and F.K. Sautter, Plating, Vol. 63, No. 4, 1976, p. 38.
73. N. Feldstein, T. Lancsek, D. Lindsey, and L. Selerno, "The State of the Art in Electroless Composite Plating," Surface Technology, Inc, Princeton, NJ.

74. V.V. Grinina and Yu. M. Polukarov, "Effect of Periodic Current on the Incorporation of Foreign Particles in Electrolytic Copper Deposits," Institute of Physical Chemistry, Academy of Sciences of the USSR, Moscow. Translated from Electrokhimiya, Vol. 21, No. 11, November 1985, pp. 1569-1571.
75. M.M. Davliev, G.P. Petrov, I.A. Abdullin, V.A. Golovin, and P.A. Norden, Elektronnaya Obrabotka Materialov, No. 3, 1986, pp. 26-28.
76. E.S. Chen and F.K. Sautter, Plating and Surface Finishing, Vol. 63, No. 9, September 1976, pp. 28-32.
77. G.R. Lakshminarayanan and E.S. Chen, Plating, Vol. 63, No. 5, May 1976, pp. 35-39.
78. M. Visawanathan and M. Ghouse, Met. Finish., Vol. 77, October 1979, p. 67.
79. M. Ghouse, M. Visawanathan, and E.E. Ramachandran, Met. Finish., Vol. 78, No. 8, August 1980, p. 57.
80. M. Ghouse, M. Visawanathan, and E.G. Ramachadran, Met. Finish., Vol. 78, November 1980, pp. 55-60.
81. M.E. Browning, H.W. Leavenworth, Jr., W.H. Webster, and F.J. Dunkerley, "Deposition Forming Processes for Aerospace Structures," MLTDR 64-26, Air Force Materials Laboratory, Wright-Patterson Air Force Base, June 1964, AD No. 433559.
82. R. Bazzard and P.J. Boden, Trans. Inst. Met. Finish., Vol. 50, Part II, 1972, p. 207.
83. F.X. Hassion and J. Szanto, "Occlusion of Various Refractory Materials in Chromium Plate on Steel Substrates," Springfield Armory, U.S. Dept. Comm. 1965, p. 43, AD No. 621-920.
84. B.Z. Wilcox and A.H. Clauer, in: Joint Proceedings of the Metallurgical Society and the American Institute of Mining, Metallurgical, and Petroleum Engineers, Second Bolton Landing Conference, Vol. 47, Gordon and Breach Science Publishers, New York, pp. 323-355.
85. R. Grierson and L.J. Bonis, in: Joint Proceedings of the Metallurgical Society and the American Institute of Mining, Metallurgical, and Petroleum Engineers, Second Bolton Landing Conference, Vol. 47, Gordon and Breach Science Publishers, New York, pp. 357-373.
86. P.D. Gorsuch, "Mechanical Properties of Internally Oxidized Binary Silver Alloys," Doctoral Thesis, Rensselaer Polytechnic Institute, Troy, New York, June 1956.
87. E.S. Chen and F.K. Sautter, "Interfacial Energy and the High Temperature Strength of Dispersion-Strengthened Gold-$Al_2O_3$ Alloys," WVT-7153, Watervliet Arsenal, Watervliet, New York, August 1971.
88. F.K. Sautter, "Electrodeposition of Dispersion-Strengthened Au-$Al_2O_3$ Alloys," WVT-RR-6321, Watervliet Arsenal, Watervliet, New York, December 1963.
89. T.W. Tomaszewski, R.J. Clauss, and H. Brown, in: Proceedings of the 50th Annual Technical Conference of the American Electroplaters' Society, 1963, p. 169.
90. M. Ghouse, "Wear Characteristics of Sediment Codeposited Ni-SiC Composite Coatings," Met. Finish., Vol. 82, No. 3, March 1984, pp. 33-37.

91. M. Thoma, Plating and Surface Finishing, Vol. 71, No. 9, September 1984, pp. 51-53.
92. K. Sato and K. Suzuki, Met. Finish., Vol. 71, No. 21, December 1984, pp. 21-26.
93. M. Takaya, M. Matsunaga, and T. Otaka, Plating and Surface Finishing, Vol. 74, September 1987, pp. 70-72.
94. I. Ahmad, V.P. Greco, and J.M. Barranco, Composite Journal, Vol. 2, No. 2, January 1967, pp. 18-29.
95. W. Watt and B.V. Perov, eds., Handbook of Composites: Strong Fibers, Vol. 1, Elsevier Science Publishers, New York, 1985, p. 752.
96. W.H. Sutton and J. Chrone, "Developments of Composite Structural Materials for High Temperature Applications," W-65-0176C, Space Sciences Laboratory, Missile and Space Division, General Electric Company, February 1965.
97. N.R. Adsit, in: Fiber-Strengthened Metallic Composites, ASTM-STP 427, 1967, pp. 27-33.
98. W.A. Wallace and V.P. Greco, Plating, Vol. 57, 1970, pp. 342-348.
99. J.A. Alexander and W.F. Sturhke, in: Fiber-Strengthened Metallic Composites, ASTM-STP 427, 1967, pp. 34-52.
100. R.G. Shaver and J.C. Withers, "Reinforced Metal Composites," Presented at the Tenth Refractory Composites Working Group Meeting, Atlanta, 1965.
101. J.A. Alexander, K.L. Chuang, and J.C. Withers, Presentation at the Second Metal Matrix Composites Working Group Meeting, Dayton, 1966.
102. J.A. Alexander, AMFL-TR-67-101, Air Force Materials Laboratory, Wright Patterson Air Force Base, June 1967.
103. G.A. Cooper, J. Mater. Sci., Vol. 2, 1967, p. 409.
104. R.N. Hanson, D.G. DuPree, and K. Lui, Plating and Surface Finishing, Vol. 55, 1968, p. 347.
105. J.C. Withers and E.F. Abrams, Plating, Vol. 55, No. 6, 1968, p. 605.
106. J.L. Camahort, J. Composite Materials, Vol. 2, 1968, p. 104.

# L-2

# Advances in Fundamentals And Applications Session L

## Electrodeposition of Amorphous Ni-Cr-P Alloys

Terry R. Guilinger and James E. Voytko
Sandia National Laboratories
Albuquerque, NM 87185

# ELECTRODEPOSITION OF AMORPHOUS Ni-Cr-P ALLOYS

Terry R. Guilinger and James. E. Voytko
Sandia National Laboratories
Albuquerque, New Mexico 87185

## Abstract

We developed a plating bath to deposit adherent, pore-free, amorphous Ni-Cr-P alloys which exhibit excellent corrosion resistance. The bath consists of the chlorides of chromium and nickel with hypophosphite ion or a mixture of phosphorous and phosphoric acids as the phosphorus source. We used citrate ion as a complexing agent to shift the Ni deposition potential to more cathodic values so that Ni and Cr codeposition could occur. Potentiodynamic corrosion testing of amorphous deposits with at least 10 at% Cr showed corrosion resistance in pitting acid chloride environments superior to such engineering alloys as 304 stainless steel and Hastelloy C-276.

## Introduction

Because of the strategic importance of chromium, there is an impetus to use thin coatings of chromium-containing alloys for protecting base materials from corrosive environments. Researchers [1,2] have demonstrated the outstanding corrosion resistance of amorphous nickel-chromium-phosphorus alloys containing greater than 10 at% Cr and 20 at% P produced by rapid quenching techniques. However, these processes produce only thin, narrow foils unsuitable as coatings. These alloys may also be produced by ion implantation. but this technique is unsuitable for large scale coating practice. Electrodeposition is useful for making thin coatings for appearance, corrosion resistance, or surface properties on an industrial scale. With this in mind, we investigated the Ni-Cr-P alloy system to determine the conditions under which it may be electrodeposited.

Because of the large (ca. 500 mV) difference in deposition potentials for nickel and chromium, complexing agents must be added to shift the nickel deposition potential to more cathodic values. This problem was addressed by Lashmore et al. [3] in their study of Ni-Cr alloy deposition. They showed that complexing agents such as citrate, nitrate, and nitrate/boric acid mixtures bring the Ni and Cr deposition potentials within 200 mV. Commonly used sources of chromium in nickel-chromium alloy plating baths include chromium chloride [3] and chromic acid [4,5]. Nickel is usually added as a chloride [6] or sulfate [7]. Citrate ion or glycine [3,7] are the commonly used complexing agents. Iron-nickel-chromium-phosphorus amorphous alloys have been produced [8] by using glycine to shift the nickel and iron deposition potentials.

## Experimental

The bath reported here was a modification of the Ni-Cr bath of Lashmore et al.[3] in that sodium hypophosphite or a mixture of phosphorous and phosphoric acids was added as a source of phosphorus. Table I shows the composition of the plating bath. Deposits were made on 1 $cm^2$ Pt or Cu disks with vigorous agitation. Applied current densities ranged from 200 to 300 $mA/cm^2$. The disks were prepared by polishing through 2400 SiC grit followed by degreasing in acetone, a 10 sec immersion in concentrated nitric acid (only for Cu) and then by soaking in concentrated hydrochloric acid until just before plating.

## Results

We analyzed the electrodeposits by quantitative electron microprobe analysis and X-ray fluorescence (XRF) for elemental concentrations and by X-ray diffraction (XRD) to determine the crystallinity of the deposits. XRD showed that the deposits plated at 250 and 300 $mA/cm^2$ were completely amorphous. The deposits plated at 200 $mA/cm^2$ showed some indications of $Ni_2P$ crystalline phase. Table II shows the composition of the deposits as a function of bath chemistry and deposition current density as measured by XRF. Phosphorus contents were uniform at 24-28 at% over each of the deposits in the hypophosphite bath. In agreement with Brenner et al. [9], who worked with Ni-P binary alloys, increasing current density decreases the P content of the deposit. However, the Ni and Cr contents varied considerably depending on the deposition current density. We observed that high Cr was associated with high current density, as would be expected since high current density favors the inclusion of the less noble element in the deposit [10].

We also investigated another phosphorus source, phosphorous/phosphoric acid, in the plating bath because of a concern over bath stability due to the presence of the strongly reducing hypophosphite ion. Table II shows that alloy P contents were considerably lower in deposits from the phosphorous/phosphoric acid plating bath than in the hypophosphite bath. Total phosphorus content in each bath was 0.1 molar but in the phosphorous/phosphoric acid bath, the electroactive phosphorus concentration (from phosphorous acid) was 0.05 molar. Further, P is in a higher oxidation state in phosphorous acid (+3) than in hypophosphite (+1) which could lead to kinetic or equilibrium constraints in phosphorus codeposition. By increasing the phosphorous acid content in the bath, we have formed electrodeposits from this acid mixture bath which contain sufficient phosphorus (>12 at%) to stabilize an amorphous Ni-Cr-P alloy.

Table II also shows the composition of alloys deposited from a third plating bath which used hypophosphite ion as the P source but did not use KBr, HCOOH, $NH_4Cl$, or $H_3BO_3$ additions.

We tested this bath to determine if deposits could be made using only the sources of Ni, Cr, and P along with the citrate ion complexing agent. As Table II shows, alloys with all three constituents were formed at the two higher deposition current densities. At the lowest current density, no deposit was formed. However, plating rate and plating quality were not as high with this bath as with the other baths tested.

Preliminary deposit adherence tests on deposits from the hypophosphite bath using a 90° bend test showed excellent adherence of amorphous Ni-Cr-P to Cu substrates. We are currently examining adherence using the ring shear test described by Dini and Johnson [11]. We performed porosity testing by plating a 2 $\mu$m deposit of amorphous Ni-Cr-P at 250 mA/cm$^2$ on a copper substrate. After exposing the plate to aqua regia, we found no evidence of corrosion of either the electrodeposit or the underlying substrate. Thus, even for thin deposits, the amorphous Ni-Cr-P deposit appeared pore-free.

Potentiodynamic corrosion testing of Ni-Cr-P deposits with at least 10 at% Cr and 20 at% P showed that these electroplates exhibit a wide passive region (ca. 1 V) with passive current densities less than 10 $\mu$A/cm$^2$ in both pitting (0.2 N hydrochloric acid) and non-pitting (0.2 N sulfuric acid) environments. Comparative tests with 304 stainless steel and Hastelloy C-276 showed that the amorphous Ni-Cr-P performed at least as well in non-pitting environments and was more corrosion resistant in pitting chloride environments. We are currently testing these amorphous deposits under accelerated atmospheric corrosion conditions [12].

## Summary

We developed a plating bath to deposit adherent amorphous Ni-Cr-P alloys which exhibit excellent corrosion resistance in both sulfuric and hydrochloric acids. The plating bath uses either hypophosphite or a mixture of phosphorous and phosphoric acids as a phosphorus source. Bath stability is a concern with the hypophosphite bath because of the presence of strongly reducing hypophosphite ion as the phosphorous source. Future experiments include ring shear adherence testing and deposit stress testing as well as examining the effects of pulse plating on deposit composition and properties.

## Acknowledgments

Thanks are due to J. O. Stevenson and W. G. Yelton for experimental assistance, to H. Levine for X-ray fluorescence analyses, to R. Tissot for X-ray diffraction results, and to P. F. Hlava for electron microprobe analyses. This work was performed at Sandia National Laboratories, supported by the United States Department of Energy under contract number DE-AC04-76DP00789.

References


1. Kawashima, A., K. Asami, and K. Hashimoto, J. Non-Cryst. Solids, 70(1), 69-83, (1985).

2. Kawashima, A., K. Asami, and K. Hashimoto, Corrosion Science, 24(9), 807-23, (1984).

3. Lashmore, D.S., I. Weisshaus, and K. Pratt, Plating and Surface Finishing, 73(3), 48-55, (1986).

4. Wallace, G.L., U.S. Patent 1,948,145, (1934).

5. Chisholm, C.U., Trans. Inst. Met. Finish., 46(4), 147-57, (1968).

6. Quaely, M.F., U.S. Patent 2,739,108, (1956).

7. Shenoi, B.A. and S. Gowri, Met. Finish., 70(5), 96-9, (1972).

8. Feng Li-Qun and Shen Mou-Xian, Metallic Corrosion, Proceedings: Eighth International Congress on Metallic Corrosion, Frankfurt, Ger., 2, 1121-6, (1981).

9. Brenner, A., D.E. Couch, and E.K. Williams, J. Research National Bureau of Standards, 44, 109-22, (1950).

10. Lowenheim, F.A., Ed., Modern Electroplating, 3rd. Ed., Wiley Interscience, New York, pg. 501, (1974).

11. Dini, J.W. and H.R. Johnson, ASTM Special Technical Publication 640, 305-26, (1978).

12. Guilinger, T.R., T.M. Christensen, and R.B. Diegle, to be presented at NACE Research in Progress Symposium, St. Louis, Mar. 21-25, (1988).

Table II. Composition of Electrodeposited Alloys

| Bath* (at%) | Current Density ($mA/cm^2$) | Ni (at%) | Cr (at%) | P |
|---|---|---|---|---|
| $NaH_2PO_2$ | 200 | 65 | 7 | 28 |
| | 250 | 51 | 23 | 26 |
| | 300 | 21 | 55 | 24 |
| $H_3PO_3$ | 200 | 89 | 5 | 6 |
| | 250 | 82 | 12 | 6 |
| | 300 | 44 | 53 | 3 |
| No Add | 200 | -- | -- | -- |
| | 250 | 43 | 39 | 18 |
| | 300 | 10 | 76 | 14 |

* $NaH_2PO_2$ bath uses bath from Table I with hypophosphite; $H_3PO_3$ bath uses bath from Table I with phosphorous and phosphoric acids mixture; No Add bath uses bath from Table I with no HCOOH, KBr, $NH_4Cl$, or $H_3BO_3$ added and a hypophosphite phosphorus source.

Deposits plated at 20-23°C.

Table I. Bath Composition

$NiCl_3.6H_2O$.....30 g/l

$CrCl_3.6H_2O$.....100 g/l

HCOOH.....35 ml/l

KBr.....17.3 g/l

$NH_4Cl$.....50 g/l

$Na_3(Cit).2H_2O$.....80 g/l

$H_3BO_3$.....35 g/l

P Source

$NaH_2PO_2.H_2O$.....30 g/l

or

$H_3PO3$.....14 g/l
+
$H_3PO_4$.....11 g/l

pH.....ca. 3.0

Temperature.....20-30°C

L-3

# Advances in Fundamentals And Applications Session L

## Pulsed Plating for Hard Chrome

Lou Latham and Peter Cambria
Rapid Power Technologies
Brookfield, CT

# Pulsed Plating for Hard Chrome

by **Lou Latham** and **Peter Cambria**
*Rapid Power Technologies, Brookfield, CT*

*Abstract*

A case study on how pulsed power doubled production for a major producer of chrome-plated circular saw blades, while improving the finish, cutting waste, and eliminating robbers. Contrary to conventional wisdom, some characteristics of pulsed power made it particularly suitable for hard-chrome plating on these complex and difficult parts.

## Introduction

Among metal-finishing processes, electroplating depends heavily on electric current and the power supply which provides it. Yet plating news is predominately about solution chemistry or the pre- or post-treatment of the metal itself; except for occasional breakthroughs in control or efficiency, the power supply is more or less taken for granted.

Many chemical, metallurgical and environmental variables affect finish quality, so platers face a lot of hurdles in producing the perfect finish. Some of these have an electrical component; every electrochemical process operates within a variety of electrical constraints for which there are optimal solutions. But the right power supply can also help overcome some less obvious difficulties facing the plater.

### *The Situation*

This is particularly true of chrome, for which power-supply requirements have always been especially stringent. Our customer was a large supplier of circular saw blades, who was looking for better current distribution and productivity. As the following case history will show, conventional wisdom does not always prevail. Chrome platers often stress the undesirability of ripple, yet in this case, reducing the current for ten milliseconds out of every twenty brought substantial benefits to one plater with a particularly tough application.

*The Power Supply*

The power supply the customer chose to meet this demanding application was an 8000-amp, 12-volt SCR-controlled pulsing rectifier with adjustable voltage and current controlled by reference signals fed back from the output. Pulsing was provided by a solid-state timing control which allowed independent adjustment of both on-time and off-time at the front panel. A base level could also be set, as a percentage of the peak (on-time) output.

*Pulse Characteristics*

The basic power supply for any electrochemical process is the dc rectifier. However, straight dc has some drawbacks which can be overcome by using other types of power. Clearly, the ideal power supply should be able to produce dc, but other waveforms may provide added benefits that dc cannot duplicate.

A dc signal can be *modulated* in various ways to produce specific power characteristics. In general, any such modulated waveform is known as *pulsed power.* The most basic form is a simple "chopper" which interrupts the dc output of an ordinary rectifier to create pulses of various widths. It tends to reduce the impedance at the surface of the work, permitting the applied voltage to generate a higher local current density. Generally, the on-time and off-time are individually adjustable, providing a wide range of duty cycles, and some non-zero voltage may be supplied during the "off" period, called the *base level.* If a short on-time is selected with a zero-volt base level, the output is very sharply pulsed, while a long duty cycle or a high base voltage will behave almost like straight dc. A good pulse unit is many power supplies in one.

With this type of unit, "current" becomes a matter of definition, since the measurement is integrated over the total time of the pulse cycle. At a 50% duty cycle (equal on and off times) the average current is one-half of the instantaneous current during the on-time, which is referred to as *peak current.* So the 8000-amp unit actually delivered 16,000 amps during the "on" portion of the cycle. It is the average current which usually identifies the equipment.

**Plating Problems and the Power Supply**

The current from the rectifier has two tasks: it drives the ionized metal particles to the cathode, then it furnishes the missing electrons to reassemble the molecule and plate it on as a metal.

It's important to realize that the power supply is the *most* adjustable item in the tank. Everyone would like to process easy parts all day, but the parts are

as they come. Racking, refrigeration and solution changes consume valuable labor and production time. The power supply can quickly respond to changing conditions with immediate effect, so it's desirable to meet as many challenges with it as possible. To understand better how modulating the power supply can contribute to plating success, let's review some of the variables in the process.

*The Bath*

The acid in the bath dissolves the plating metal and imparts conductivity to the solution. It permits the voltage of the power supply to carry ions to the part, but at a cost to the part, which is soluble in the acid. The price is corrosion of the part itself. The problem is particularly severe with parts that have sharp angular protrusions, such as the teeth on a saw blade, which provide a "hot spot" or preferential current path. Keeping currents low enough to avoid "burning" the teeth underplates other areas, and they become susceptible to corrosion.

*The Workpiece*

The hardness required for saw blades is of course extremely high. In addition, the shape of the piece places severe demands on the process. The teeth are "lightning rods" which attract high currents but are also fragile, due to their high edge area. The disk of the blade develops a gradually increasing impedance approaching the center hole, where the piece is held. To the plater, this is certainly a "problem part."

To illustrate the current distribution on a saw blade, hold a flashlight near the edge and shine it across the blade at a shallow angle. It's very bright on the teeth, but falls off toward the center. On an ordinary saw blade there may be 90 millionths near the teeth, and only 1 or 2 in the center. The chromic acid bath corrodes the metal wherever the plate is too thin, so the bath actually prevents the plate from adhering in the center. That's why most saw blades have a painted area around the hole, to protect the part that didn't plate.

*The Robber*

The high sensitivity of the teeth makes them vulnerable to damage. The *robber* is an alternate current sink which diverts ("robs") current from the fragile area. In this case, it formed a ring around the blade edge, grounded to the rack. Along with the current, it naturally attracts chrome. To our customer, the robbers were a nuisance:

> The teeth are the high-current area. If you plate normally you can ruin the tooth, because the chrome piles up on the edges in little spheres that make it dull. So you have to put a robber on the rack, to protect the blade. A lot of chrome goes to the robber. On a typical saw blade, if you plate 90 millionths on the teeth, you might put two thousandths on the robber, which is going to waste, and down in the center you still have nothing. Sometimes the center becomes passivated and the blade has to be replated.

This affected waste management and pollution control. When the robbers went through the electrocleaning bath, it stripped off the chrome, but they coudn't recover the chrome without a process so long, complex and expensive that it wasn't worth it. The robbers were robbing profits as well as current.

*The Depletion Zone*

The solution itself introduces a barrier as the layer next to the surface loses chromium ions to the oxide and becomes *depleted*. This reduces plate formation by robbing the solution near the coating surface of metal, and uneven plating occurs. The solution near the high-current areas is the first to be depleted. Since there are no more ions in the neighborhood, the local conductivity is lowered. The solution is now a dielectric. Increased agitation does not solve this problem, because the depletion zone is so thin that mechanical agitation cannot replenish the solution so close to the part. However, this depletion zone became a key factor in the pulse solution.

**The Pulse Mechanism**

Under dc conditions, the current cannot spread away from the preferential areas enough to prevent burning, or to ensure adequate coverage of the less attractive zones. Pulsed power, however, makes this redistribution possible. Periods of zero or low voltage suspend the transfer process, allow the metal content of the depleted solution to normalize, and perform a sort of "micro-agitation" which enhances the normal agitation process by removing hydrogen bubbles and contaminants from the surface.

The pulses also add another factor. The conductive ionic solution and the conductive metal part are at opposite polarities, separated by a non-conductive layer. They form a capacitor, which stores energy on each side of the interface as long as the current is on. This capacitance is high, because the insulating layer is extremely thin (perhaps as little as one molecule thick).

Once the pulse turns off, two things occur. First, the depletion of the specie ceases. Second, the capacitance between the piece and the solution discharges,

allowing the ionic balance in the depleted area to normalize while gas bubbles and impurities on the surface diffuse back into the solution. When the current resumes, there is a fresh supply of material ready to plate immediately.

Surprisingly, though, this distributes much more evenly across the surface of the part, including the area around the center hole, which normally plates badly. Where there were 2-3 millionths around the hole with dc, with the pulse system there was as much as 40 millionths, and the hole itself plated through.

The customer discovered that, due to the capacitive current caused by the discharge, certain areas of the piece actually continued to plate *during* the off-time. The capacitive currents generated by the discharge circulate through the tank in complex patterns like the radiation from an antenna, away from the heavily depleted zones and into other, less polarized areas, distributing chrome more evenly across the blade.

By varying the duration of the on and off periods in very fine increments, this plater achieved so much control over the behavior of the depletion zone that he was also able to eliminate another troublesome part of the dc process: the robbers. The current flow was so controllable with the pulsed power supply that they were no longer necessary to protect the fragile teeth. With them went the lost specie and the time and labor required to reclaim them. The customer was happy to get rid of them:

> We used robbers because we had to, but a lot of chrome goes onto the robber. It's nearly impossible to recover the chrome economically, but you can't just throw it away. You have to reduce it to flock, press the flock into cakes, and take it to a toxic landfill which may be miles away. It costs a fortune just to get rid of it.

*Productivity*

With very little history or published literature to go by, the customer adjusted the peak voltage of the pulse empirically, by slowly increasing the voltage until microscopic burning appeared on the edges of the teeth. Even without robbers, he found that he could safely operate at 15 volts with a base (off-time) level of 2 volts, an increase of almost 100% over the normal dc voltage. Current density was nearly 500 amps per square foot, rather than the usual 250-300. This had a dramatic effect on production. The customer explains:

> The plating room is always the bottleneck in a production plant. Without worrying about burning the teeth, we could double the speed of our line by increasing the current density from 2 amps to 4 amps per square inch. Before, we had one man running the tank, loading and removing the parts and monitoring the process. Now we

> needed a man at each end of the tank because the line was moving so fast. We had to install bigger busbars to handle the current.

The temperature requirements for this operation had always been very stringent--no more than one or two degrees on either side of 130 degrees F. However, he discovered that with the pulse unit, he could plate successfully at temperatures as high as 150 degrees F. The tank still required added cooling and ventilation, however, since the increased current density created both more heat and also a larger volume of outgassed hydrogen. However, it was a small price to pay for the improved productivity and coating characteristics.

**Conclusion**

Any power supply will plate exterior surfaces to a greater depth than interior surfaces, but pulse can create more even current distribution around the part through the capacitance-discharge mechanism described above. The pulse system uses the available voltage more effectively, producing a more constant and even current density across the surface of the part. Periods of rest allow the solution to replenish and the barrier capacitance to relax, equalizing the overall surface impedance before the next pulse arrives. How long that takes is determined by many factors. In this case, an on-time of 5 to 10 milliseconds and an off-time of 10 to 20 ms resulted in the most uniform coating and the greatest productivity.

Using a ten-millisecond pulse at up to twice the normal voltage and current density, this plater doubled production with corresponding improvements in finish quality and a dramatic reduction in waste treatment costs. Before installing pulse, the plant consistently experienced uneven plating and had a severely over-burdened waste treatment system. Power usage was 8 to 9 volts at a current density of 250 amps per square foot. With the pulse sustem, they were able to plate uniformly and avoid burning while raising current density to 500 amps per square foot at 15 volts, by controlling current distribution with the pulse waveshape. The system also allowed them to eliminate robbers and reduce chrome losses and waste treatment costs substantially.

Overall, this plater's improvements included finer grain and reduced porosity in the coating, better distribution and adhesion, higher productivity and the elimination of robbers with their attendant cost and waste. He was more than satisfied, he says:

> Until pulse came along, there had always been two methods of ionizing and plating chrome in the handbook. Now there are three. *This is the one that works.*

**Afterword: The Future of Pulse Power**

Pulse plating offers many benefits, but not all processes or circumstances justify it. However, there is no need to purchase two types of power supply. Any pulse unit can deliver dc, and most provide base currents which can be raised to produce almost-flat outputs that approach dc while retaining the benefits of pulse. Pulse is dc, but not the reverse: its strength is flexibility.

In addition to creating square waves of any duty cycle with various base levels at up to 5000 pulses per second, the latest generation of fully programmable power supplies can modify the internal shape of each pulse, including on- and off-time, rise and fall rate (which need not be linear), upper and lower limit, total amplitude and frequency. By independently controlling each portion of the waveform, users can create any number of "custom" outputs such as sine, step, sawtooth and asymmetrical waveforms to meet specific process needs.

Modern rectifiers can be very tightly controlled down to the millisecond level, which makes possible the high-frequency pulses and exotic "custom" waveforms now on the horizon. But this flexibility goes beyond the waveform. Another semiconductor device, the microprocessor, can extend this control to the process cycle and into the manager's office. Being all-electrical devices which respond to signals from the outside, solid-state power controls are very easily *computerized*.

In the future, platers will demand more flexibility from their power, for recording, storing and quickly changing voltage and current levels or timing and ramp functions, or for monitoring and responding to other process events. A programmable power supply can change its behavior to meet new conditions, from second to second or from day to day. Any personal computer can control a large number of power supplies from the process tank or the plant manager's office, and eliminate much of the hardware required in today's systems. Sealed terminals showing up to twenty-five sets of status readings on a single screen can replace huge consoles with dozens of switches, pots, lights and meters. The time and expense of field remote wiring is substantially less. User-friendly software can guide operators through complex procedures simply and quickly. Preset parameters can be stored and selected easily, or quickly modified to reflect process changes or advances in the art. The computer can interface easily to external equipment such as a hoist controller or process monitor to provide overall plant automation, logging and reporting.

The advantage of programmability on the micro-scale of the pulse waveform also applies on the scale of the process cycle, and again on the larger scale of factory management. The tools that make it possible are the tools that brought the modern pulse system: high-speed solid-state controls and the intelligent systems that operate them. As we move into the future, we may find our tools becoming partners in our search for better control of our power.

L-4

# Advances in Fundamentals And Applications Session L

## Comparison of Magnesium Acid Pickling Solutions by Electrochemical Impedance Spectroscopy

Dr. Tim Rodgers, CEF
Lockheed Missiles & Space Co.
Sunnyvale, CA

# COMPARISON OF MAGNESIUM ACID PICKLING SOLUTIONS BY ELECTROCHEMICAL IMPEDANCE SPECTROSCOPY

Dr. Tim Rodgers, CEF
Lockheed Missiles & Space Co.
Sunnyvale, CA

## Abstract

A wide range of acid pickling solutions are commonly used for final cleaning of magnesium alloys prior to surface treatment. The choice of pickle is important to ensure proper adhesion of the coating, whether it is intended as a paint base or to provide additional corrosion protection. An investigation of the surface cleanliness of pickled magnesium alloys has been completed using electrochemical impedance spectroscopy (EIS). The method allows rapid comparison of the effectiveness of pickling solutions on magnesium alloys AZ31B and HM21A. The results suggest additional considerations for process selection.

## Introduction

The search for low density/high strength materials has led the aerospace industry to a growing reliance on parts fabricated from magnesium alloys. Generally, the performance of these materials has lived up to the promise, however the natural alkaline surface film of magnesium has created two problems. First, the bond strength of organic coatings, primers, adhesives or paints on a bare magnesium surface tends to be poor. The second problem is the failure of the native film to adequately protect the underlying metal from corrosion in many service environments. Fortunately, a number of chemical treatments have been developed to solve these problems. Some simply replace the alkaline film with a more acidic surface which presents a better base for organic coatings. Others have been specifically designed to provide short-term corrosion protection during shipment and storage.

Clearly, the choice of specific surface treatment depends on the intended use. Nevertheless, the success of any treatment is greatly influenced by the preliminary surface preparation. Loosely-adherent soils, grease and lubricating oils are easily removed by standard solvent and alkaline cleaners and therefore pose little problem. Many magnesium parts also require an acid pickling step to dissolve such tenacious surface contaminants as mill scale, residual oxides from heat treatment and corrosion products.

In this paper, a relatively new technique, electrochemical impedance spectroscopy (EIS), has been used to evaluate the effectiveness of various acid pickling solutions to clean magnesium surfaces. Two alloys commonly used in the aerospace industry were selected for consideration: AZ31B-H24 and HM21A-T8. EIS has been previously applied to investigations of corrosion processes and organic coatings (1). The theoretical details of this technique are described elsewhere (2), however the analysis is based on the measurement of the impedance at the interface of the test sample and a corrosive medium (in this case a mildly alkaline solution -- 0.05 M sodium borate, pH 9.25). This impedance varies with the frequency of the applied potential. If a model of the sample/solution interface is assumed, the resulting impedance spectrum can provide information about the sample, such as resistance to charge transfer and surface charge density. By comparing the impedance behavior of magnesium samples treated with different acid pickles, the ability of these solutions to provide a chemically "clean" surface can be compared.

Results

Table 1 summarizes the EIS spectra for a number of acid pickles widely-used in industrial magnesium processing. Two features of the spectra are useful for comparison. The low-frequency limit of the impedance (Rlf) is related to the charge-transfer resistance. A low value indicates the absence of protective surface layers or residual, adherent coatings. The surface charge density is a major influence on the value of the psuedocapacitance (C), thus a relatively "clean" metallic surface would be suggested by a high value of C. In order to simulate such a "clean" surface, magnesium samples were mechanically polished using 600 grit silicon carbide.

The data in Table 1 shows that certain pickling treatments approximate a polished surface quite closely. For AZ31B-H24 sheet, which is initially coated with a burned-on graphite lubricant, the phosphoric acid pickle or the acetic/nitrate pickle result in a near-polished surface. These two solutions, as well as the nitric acid pickle, have a similar effect on the HM21A-T8 sheet. Other treatments appear to either incompletely clean the magnesium or chemically modify the surface. Although these pickles may still be adequate for certain applications, the presence of an additional surface layer could be a problem for subsequent chemical processing.

EIS has frequently been considered strictly as a tool for the

evaluation of materials and corrosion resistant coatings. However, as demonstrated in this study, it can also provide important insights that recommend placing it next to other surface analytical techniques.

References:

(1) F. Mansfeld, M.W. Kendig and S. Tsai, Corrosion, 38, 478 (1982).

(2) D.C. Silverman, Electrochemical Techniques for Corrosion Engineering, National Association of Corrosion Engineers, Houston, TX, 1986, p. 73.

TABLE 1

IMPEDANCE DATA FOR MAGNESIUM SURFACE TREATMENTS

AZ31B-H24

| acid pickle | low-frequency limit of the impedance, Rlf (ohms-sq.cm.) | psuedocapacitance, C (uC/sq.cm.) |
|---|---|---|
| original surface | 909 | 23 |
| polished (600 grit) | 260 | 70 |
| phosphoric acid | 210 | 79 |
| acetic/nitrate | 198 | 81 |
| sulfuric acid | 1110 | 30 |
| nitric acid | 3370 | 3.3 |
| chromic acid | 470 | 100 |
| chromic/nitrate | 578 | 138 |
| acid fluoride | 505 | 16 |
| phosphoric acid -> acid fluoride | 574 | 70 |

HM21A-T8

| | | |
|---|---|---|
| original surface | 229 | 113 |
| polished (600 grit) | 184 | 89 |
| phosphoric acid | 168 | 117 |
| acetic/nitrate | 126 | 128 |
| nitric acid | 131 | 115 |
| chromic acid | 391 | 92 |
| chromic/nitrate | 359 | 109 |
| sulfuric acid | 309 | 88 |
| acid fluoride | 752 | 54 |
| phosphoric acid -> acid fluoride | 472 | 59 |

L-5

# Advances in Fundamentals And Applications Session L

## The Fundamentals of Zinc Brightener Design

David E. Crotty, PhD
Allied-Kelite Div.,
Witco Corp.
29111 Milford Rd.
New Hudson, MI 48165

# THE FUNDAMENTALS OF ZINC BRIGHTENER DESIGN

David E. Crotty, Ph.D.
Allied-Kelite Division
Witco Corporation
29111 Milford Road
New Hudson, Michigan 48165

## Abstract

A survey of the patent literature is used to illustrate the components required to prepare working brighteners for zinc plating baths. The chemicals described in the literature will be used, without necessarily revealing the contents of specific commercial products, to demonstrate the roles of the carrier and brightener in the uniform deposition of zinc from the three common electrolyte systems.

## Introduction

The electrodeposition of zinc is an extremely important segment of the plating industry that has largely been taken for granted. Very few publications have appeared discussing the technological aspects of zinc plating since the series of articles by Geduld [1] in 1975-76, Lowenheim's "Modern Electroplating" [2], most recently updated in 1974, and DaFonte's [3] rare discussion of additive chemistry which appeared in 1978.

While zinc plating technology involves a good deal of old art it is by no means stagnant. The zinc brightener market is fiercely competitive, with improvements — sometimes dramatic improvements — in operation, cost, and deposit quality appearing regularly. At the same time, the end users of a plating shop's product are taking a greater interest in quality control standards. The individual plater clearly needs information that can help him or her keep abreast of the market and improve the quality of the shop's work.

The purpose of this paper is to add to the insight provided by Geduld, Lowenheim, and DaFonte by perhaps updating a few items here and there, but mostly by discussing the nature of the components of the brightener systems themselves. A discussion of the chemicals used in the brighteners of the several popular classes of plating processes can lend a considerable amount of understanding to a process that might otherwise remain a mystery. It is difficult to maintain a process that is not understood.

Any open discussion of the components of a zinc brightener system is difficult because brightener systems are proprietary. A supplier guards its formulations from distribution simply because the brightener market is so competitive. However, it is possible to mine the published patent literature for information that will make it possible to piece together skeletal brightener formulations that can be used to illustrate the functional properties of a system.It will also be informative to present the differences between these skeletal brighteners and a few commercial products. This discussion will not knowingly present any supplier's proprietary formulation.

This paper will discuss the functions of the organic components of the three main classes of zinc plating systems: cyanide, alkaline non cyanide, and acid chloride. The basic chemistry was described well by Geduld and these principles still apply for the most part. The paper will also include data to compare some of the deposition characteristics of the three systems.

## The Additives

In zinc plating, the additives used to improve the natural deposit from a particular electrolyte can usually be grouped into three categories. First, the carrier makes the deposit smooth, overcoming a natural tendency to form a black smutty or "burned" deposit, and also prevents the formation of dendrites. Second, the brightener adds clarity to the smoky deposit provided by the carrier, thus forming a truly bright deposit. The third classification is that of purifiers which are used to remove the last traces of smokiness in the deposit that might be caused by the presence of metals that are present in small quantities in zinc anodes and the other chemicals that make up the basic electrolyte.

The discussions that follow of the cyanide, akaline non cyanide, and acid chloride brightener systems will be based on these three additive classifications.

## High Cyanide Processes

Cyanide-based electrolytes were usually the first to be developed for many of the metals that are plated from water solutions. Zinc is no exception. Zinc has been plated in volume from cyanide electrolytes that closely resemble the electrolytes of today ever since the invention of the first practical electrical generators. Before that the plating of zinc was a laboratory curiosity since the only sources of electrical current were rather expensive batteries.

For most of plating history zinc was plated without the use of any additives. It wasn't until the 1930's [4,5] that Hull and Oplinger claimed the use of sulfur compounds for their ability to precipitate metal impurities, most commonly lead, cadmium and copper, that are found in small amounts in the zinc used for anodes. It seems likely, however, that the use of glue (some platers liked LePages best) to cure a high current density burn predates the first reference [6] this author has found to claim it.

Table I lists components that make up the electrolyte for the three general classifications of cyanide baths: high cyanide, mid cyanide, and low cyanide. Typical optimum NaCN/Zn ratios for the three electrolytes are listed in Table I. However, since this optimum tends to vary with temperature, Table II is provided to show how this ratio may be adjusted to suit the temperature of the bath.

The basic carrier for a higher cyanide zinc plating system is the cyanide itself. Figure I is a diagram of Hull cell panels from a mid cyanide electrolyte plated at 2 amps and 0.5 amps for 10 minutes. Panels A1 and A2 were obtained without additives, other than a sulfide purifier. The deposits are fairly nice, and the 2 amp panel is almost bright. The lowest current density areas are dull and this is the major challenge confronting the chemist who might wish to design a cyanide brightener.

Rindt [7] described a typical brightener system for the higher cyanide electrolytes, using polyvinyl alcohol (PVA) that was first claimed by Barret [8] in 1939, glue, anisaldehyde (another very frequently mentioned brightener), and one of a list of some 38 compounds of niacin. Typically the nitrogen of the niacin ring was quaternized with an alkyl or aryl chloride, Equation 1.




(1)

The structures of niacin and one of the preferred niacin derivatives are shown in Figure II. Rushmere [9,10,11] also claimed the use of a number of quaternized niacin compounds. Figure I shows Hull cell panels with some of these materials, including: B) quaternized niacin; C) anisaldehyde; and D) a commercial quality brightener. These skeletal systems do provide an improved deposit over that obtained using the basic electrolyte, but it takes some tinkering to produce a trouble-free commercial quality system.

Low Cyanide

As it became obvious that waste treatment of effluent would be required of electroplaters, an effort was made to provide organic brightener systems that overcame the problems encountered with low and non cyanide electrolytes. The low cyanide electrolyte does not provide enough carrier. The alkaline non cyanide electrolyte has no carrier at all.

The groundwork for low and non cyanide carriers was probably provided by Winters [12] in 1957. This work described the use of epichlorohydrin, a bifunctional polymerization agent, to build polymers of amines. Winters described two step reactions in which ammonia or primary amines such as ethylene diamine were reacted at low temperature (Equation 2).

$$NH_2\text{-}CH_2\text{-}CH_2\text{-}NH_2 + H_2\overset{\overset{O}{\wedge}}{C}\text{-}CH\text{-}CH_2\text{-}Cl \xrightarrow{H_2O} \underset{\text{Intermediate}}{NH_2\text{-}CH_2\text{-}CH_2\text{-}\overset{\overset{H}{|}}{\underset{\underset{H+}{|}}{N}}\text{-}CH_2\text{-}\overset{\overset{H}{O}}{CH}\text{-}CH_2\text{-}CL} + OH^- \qquad (2)$$

The mixture is heated to polymerize the intermediate through the reaction of the chloride end of one molecule with the amine end of another (Equation 3).

$$\underset{\text{Intermediate}}{R\text{-}\overset{\overset{H}{O}}{CH}\text{-}CH_2\text{-}CL + NH_2\text{-}CH_2\text{-}R} \longrightarrow R\text{-}\overset{\overset{H}{O}}{CH}\text{-}CH_2\text{-}\overset{\overset{H}{|}}{\underset{\underset{H+}{|}}{N}}\text{-}CH_2\text{-}R + Cl^- \qquad (3)$$

The temperature of the second step determines the degree of polymerization. The use of water as the solvent limits the temperature of the reaction to an acceptable range. While this reaction product provided a certain amount of carrier activity it was not enough for a true low cyanide bath.

Burnson [14] was granted a patent in 1966 for a reaction product similar to that described by Winters using a tertiary polyamine, hexamethylene tetramine, Figure III. This probably provided the first really useful carrier for low cyanide as well as alkaline non cyanide systems and was sold under the Trubek #1 tradename. Similarly, Greer [15] wrote a chemical patent that described a polymeric amine from the reaction of another tertiary diamine, dimethylaminopropylamine, Figure IV, with epichlorohydrin but did not specify a particular use for the polymer.

During the 1970's a number of patents were issued claiming the use of these types of polyamines in low and non cyanide plating baths. One of these was Nobel and Ostrow [16] who claimed the Greer polyamine specifically.

Figure V is a diagram of Hull cell panels obtained using several brightener systems in a low cyanide electrolyte. These include: A) no brightener; B) a quaternized niacin compound, and the Trubek #1 polyamine; C) anisaldehyde, and the polyamine described by Greer [15]; and D) a commercial brightener system. Again, the panels using skeletal brightener systems are bright but slightly hazy, except for the commercial system which is fully bright over both the 2 amp and the 0.5 amp panel. These examples show that the patented materials do work as advertised, but only after some experimentation to determine optimum conditions.

In summary, we have seen the cyanide based systems evolve. The basic high cyanide electrolyte originally was dull and depended little on additives. With some research bright baths were developed to provide a more decorative appearance. When waste treatment became important, low cyanide baths were made possible with the development of polyamine carriers and better brightener agents.

## Alkaline Non Cyanide Zinc Plating

The development of the polyamine carrier was the key factor in making alkaline non cyanide zinc plating practical. The non cyanide electrolyte as listed in Table III does not provide a usable zinc deposit without considerable help from additives as illustrated in Figure VI, panel A. The deposit is black and powdery.

During the 1970's considerable research was conducted by a number of laboratories resulting in continual improvement. Some of the work was published in the form of patents, a few of which are listed here [16-27]. Most of these described improved preparation techniques for polyamine carriers that were perhaps only slightly different from the method of Winters'. Others claimed improved brighteners.

Kessler [24] provides an example that is typical of the formulations found in the patent literature. This example uses Greer's [15] reaction product of dimethylaminopropylamine and epichlorohydrin for the carrier, with a substituted pyridine brightener. Figure VI shows some Hull cell panels of deposits with: B) Greer's polyamine carrier; and C) the polyamine carrier plus the quaternized niacin brightener. The panels are comparable with those shown in Figures I and III. The carrier eliminates the dark burn, leaving a smoky, smooth deposit. The pyridine brightener provides a clearer deposit. Again, some work is required to make a commercial quality brightener system from these building blocks and Figure VI, panels D illustrate the results of such work.

Much was learned over the years about maintaining a non cyanide zinc bath. Polysulfides were found to be unsuitable as purifiers but other chemicals similar to those described in the 1930's were quite usable. Some early baths contained tartaric acid, gluconate, EDTA or other complexors. It was soon found that complexors allowed the buildup of iron in the plating bath causing serious problems. It is now well known that care must be taken to avoid complexors, even in cleaners if possible.

Most of the early baths could not tolerate more than about 7.5 gm/L of zinc metal. Higher concentrations would cause high current density burning, simply because the carriers were not good enough. Today some baths operate well at 18-22 gm/L zinc, and some recent brightener systems provide improved high current density efficency at the higher zinc concentrations. Today, the properties of some alkaline non cyanide systems match or exceed those of the cyanide systems they were designed to replace.

Non cyanide zinc deposits tend to be less pure than cyanide deposits. The only significant result of this is that some methods used to determine deposit thickness have been found to give erroneous results. Horner [28] recently published a study comparing magnetic, coulometric, and eddy current methods, showing that the magnetic method, when used on demagnetized parts, provides the only reliable results.

## Acid Chloride Zinc Plating

The development of the acid chloride zinc plating processes has run parallel with that of alkaline non cyanide. However, while the cyanide and non cyanide have properties that are similar, the acid system provides a number of advantageous differences. As will be discussed later, while the throwing power of the acid chloride bath is low, the coverage is very good. Another difference is that the acid chloride baths can plate some metals, like high carbon steel, that preferentially form hydrogen gas rather than zinc plate when the alkaline systems are used. Acid baths are also able to provide the brightest deposits, although some non cyanide processes come close to the acid baths in this regard.

It should be noted that the original acid chloride baths contained ammonia. These systems proved to be relatively trouble-free and operated over a very wide range of conditions. However, the ammonia systems have fallen into disfavor in most localities due to waste treatment concerns.

The composition of a typical acid chloride bath is given in Table IV. Like the alkaline non cyanide system, the acid electrolyte without additives plates deposits that are burned and very dull as shown in Figure VII, panel A.

Many useful carriers for acid chloride electrolytes have been selected from a group of compounds known as wetting agents or surfactants. Harbulak [29], for example, identified a class of compounds known as alkyl phenol ethylene oxide polyethers, Figure VIII, to be useful carriers. Numerous other surfactant groups, most of them ethylene oxide polymers, have been found to operate as carriers as well. The Hull cell using this type of wetting agent as a carrier is shown in Figure VII, panel B. The deposit is smooth but dull across the entire panel.

One of the functions of a surfactant is to solublize oily materials that normally would not be soluble in water. It happens that the most commonly used brighteners in acid chloride plating processes are benzylidine acetone [30,31] and o-chlorobenzaldehyde [32,33], Figure IX, which are rather insoluble in concentrated salt solutions. The use of surfactants blended with napthalene-formaldehyde condensates [34] and other materials [35] allows the formulation chemist to prepare a stable brightener concentrate. Figure VII, panel C shows the use of benzylidine acetone to brighten the deposit obtained with the surfactant carrier. The dull band in the center of panel C is a typical problem that is readily resolved with the use of sodium benzoate, which is mentioned very frequently in the patent literature. The effect of sodium benzoate is shown in panel D. The few remaining defects are removed from the deposit by a complete commercial brightener, panel E.

Purification of an acid chloride bath is simplified because most metallic impurities plate out rather readily in acid electrolyte. Copper and cadmium tend to appear occasionally due to poor housekeeping and must be plated out. Iron, however, readily disolves in the electrolyte and remains in solution as the ferrous ion. Concentrations of iron cause darkness in the deposit after chromating, a lowered cloud point temperature, and deposit roughness. Hydrogen peroxide is commonly used, very regularly in very small quanities, to oxidize the ferrous ion to the insoluble ferric ion and the precipitate is removed by filtration. Another impurity is clay that is included with potassium chloride which also must be removed by filtration. The use of less expensive but more pure sodium chloride with some proprietary brightener systems eliminates this impurity.

In early acid chloride systems one of the major problems was the cloud point temperature, where the oil-like brightener becomes insoluble and splits out of the bath, causing the solution to become cloudy and the work to become very dull. Over the years the brightener systems have evolved so that the average cloud point of a working bath exceeds 130-140 F, a temperature range that is well above normal operating temperature.

Efficiency, Throwing Power and Coverage

In the past, a discussion of the differences among the three main classes of zinc plating systems would quickly center on operational problems. These problems have been ironed out through dedicated development efforts. Today the discussion properly focuses on the advantageous differences of the processes. The main differences are really in cathode efficiency, throwing power, and coverage. Several commercial brightener systems will be used to illustrate the differences.

For a quick set of definitions: efficiency is the percentage of current that is used to deposit metal rather than evolve hydrogen. Throwing power is the ability to plate an even thickness of metal over a wide range of current densities. Coverage, on the other hand, is the ability to deposit at least some metal at very low current density, even if it isn't very much, when compared with thicknesses over the rest of the work piece.

For zinc, there really is no quantifiable measure of coverage and this report will not attempt to present one. The plater generally makes a relative judgement on coverage from the rear of a Hull cell panel. There is a need in this area.

Methods for measuring throwing power are well known. Horner [36] used the Haring cell to investigate the effects of a wide range of plating conditions on cyanide copper throwing power. This paper will not attempt to match the scope of that report for zinc although that would be a good topic for another time. Horner also described the standard method of measuring plating efficiency. The use of the Haring cell has been criticized and alternate methods presented recently [37,38,39]. While these new approaches may have merit, a comparison of results is a subject for another time.

For the work presented here, throwing power was measured using the standard Haring cell (6.5 cm by 8 cm deep by 24 cm long). A fresh solution was prepared for each measurement. The anode was a steel panel with numerous ¼ inch holes to permit circulation, and the anodes and cathodes were placed in the cell at a 5:1 distance ratio. The two cathodes were connected with a bus bar which made positive contact with the panels through a steel bolt that was attached through the cell wall. This arrangement avoided any problem with faulty clip connections. Current was measured with an amp.hour meter.

The major problem with throwing power measurements has been the method of reporting results. If throwing power is defined as the percent improvement of distribution over that expected from the distance ratio, then one might write Equation 4:

$$\% \text{ Throwing Power} = \frac{(DR-WR) * 100}{DR} \qquad (4)$$

where the DR is the ratio of the distances of the two cathodes at each end of the cell to the anode in between and WR is the ratio of weight gain for the two cathodes after plating. Using Equation 4, if an "ideal distribution" were achieved, the near and far panel would have the same weight and WR would be 1.0. Thus:

$$\% \text{ Throwing Power} = \frac{(5- 1)*100}{5} = 80\%$$

Some early workers felt that this 80% result was not very satisfying, suggesting that the "ideal distribution" should have a throwing power of 100%. Thus Equation 5 was used:

$$\% \text{ Throwing Power} = \frac{(DR - WR) * 100}{(DR + WR - 2)} \qquad (5)$$

Using Equation 5, a weight ratio of 1.0 would result in:

$$\% \text{ Throwing Power} = \frac{(5 - 1) * 100}{(5 + 1 - 2)} = 100\%$$

The fact is that other equations exist for calculating throwing power that differ substantially from Equations 4 or 5. Some workers avoid this problem by simply reporting the weight ratio itself. Thus, for a distance ratio of 5, a weight ratio of 5 would indicate very poor throw, and a weight ratio of 1 would indicate "ideal" throw. This work will report results both by the weight ratio and Equation 4.

The efficiency measurements reported here were actually obtained in the Haring cell using one cathode and one anode spaced at six inches. The efficiency was calculated using Equations 6:

$$d = \frac{wt * area}{density} \quad \text{deposit thickness} \qquad (6)$$

$$\%Eff = \frac{d * 14.3 * 100}{CD * Time} \quad \text{percent efficiency}$$

where d is the deposit thickness on the cathode calculated from the weight gain, the density is that of zinc, 7.14, CD is the current density, and time is the plating time. The factor, 14.3, is the equivalance factor for zinc [40].

Table V provides efficiency and throwing power results obtained using a representative collection of commercial brighteners. Each was measured in a fresh electrolyte, at concentrations centering on that recommended by the manufacturers. Performance in a well used plating bath can be quite different, depending on addition rates, the concentrations of the basic electrolytes, and presence of impurities.

The results in Table V illustrate that a wide variation in performance is obtainable, but a few general observations may be made:

1. The efficiency must be reported over a range of concentrations and current densities. It is especially important to note the performance over the current density range.
2. A system with high throwing power will tend to have higher than average efficiency at low current density and lower than average efficiency at high current density. This is a natural requirement for throwing power.
3. A system that has low throwing power may show a more steady efficiency over the working current density range. This may be an advantage when uncomplicated work is plated.
4. In general, as more carrier is added to the bath the throwing power will increase.
5. In general, as excessive brightener is added throwing power and coverage will decrease.
6. Acid chloride baths, when compared with alkaline baths, have very low throwing power but very high efficiency over a broad current density range.

The use of efficiency and throwing power measurements, while somewhat tedious to perform, can be an important tool for the control of a plating bath. Systems that are provided in two packages, carrier and brightener, can be used to their best advantage in conjunction with these measurements. The amount of carrier and brightener may be balanced carefully to obtain the best deposit. On the other hand, most alkaline brightener systems are provided as a single additive with carrier and brightener being balanced through experience by the manufacturer. In these cases, the occasional use of efficiency and throwing power measurement may be used to verify that the balance is still correct. Despite the best experience with such systems, occasions do arise where the brightener or carrier has been depleted preferentially, resulting in an unbalanced system.

## Conclusion

The plating process of any metal contains many components that interact in complex ways. Unfortunately, the most complex components, the brighteners, are generally provided with little information concerning their functions. This sometimes leaves the plater without enough information to exercise intelligent control over his or her processes.

This discussion has attempted to illustrate the function of the various components of the alkaline cyanide and non cyanide and the acid chloride zinc brightener systems by using the chemicals disclosed in the published patent literature.These chemicals were used in typical plating electrolytes to show their effects on the plating process, and show how a complete brightener system can be developed.

Finally, this paper discussed two tools, efficiency and throwing power measurement, that are seldom used to full advantage in the maintenance of zinc plating processes.

## Acknowledgements

The author would like to thank Carl Steinecker, Senior Development Chemist, and John Horner, Director of Technical Services, for helpful discussions in preparation of this paper, and the Allied-Kelite Division of the Witco Corporation for the support of this work.

References


1. Geduld, H, Metal Finishing, 73(10),29(1975); IBID, 73(11),50(1975); IBID, 73(12),50(1975); IBID, 74(1),41(1976); IBID, 74(3),27(1976); IBID, 74(4),46(1976).
2. Lowenheim "Modern Electroplating", J. Whiley & Sons, New York, 1974.
3. DaFonte, D., Proc. 65th Ann. AES Tech. Conf. 1978, St. Louis.
4. Hull, R.O., US Patent 2,080,483, 1935.
5. Oplinger F., US Patent 2,146,439, 1939.
6. Hoff, E.F., US Patent 2,080,479 1937.
7. Rindt G., US Patent 3,318,787 1967.
8. Barret, H.J., US Patent 2,146,439 1939.
9. Rushmere, J.D., US Patent 3,296,105, 1967.
10. Rushmere, J.D., Us Patent 3,386,898, 1968.
11. Rushmere, J.D., Us Patent 3,411,996, 1968.
12. Hoyer, P.J., Rushmere, J.D., US Patent 3,734,839, 1973.
13. Winters, J.B., US Patent 2,791,554, 1957.
14. Burnson, R.H, and Rucins, L, US Patent 3,227,683, 1966.
15. Greer, A.H., US Patent 3,642,663, 1972.
16. Nobel, F.I, Ostrow, B.D., US Patent 3,869,358, 1975.
17. Szilagyi, Hajdu, J., US Patent 3,745,099, 1973.
18. Geduld, H., US Patent 3,803,008, 1974.
19. Rosenberg, W., US Patent 3,824,158, 1974.
20. Koch, R., US Patent 3,840,444, 1974.
21. Kampe, M., US Patent 3,849,325, 1974.
22. Creutz, H., US Patent 3,853,718, 1974.
23. Duchene, J., Dechristopher, P., US Patent 3,871,974.
24. Kessler, R.B., US Patent 3,884,774, 1975.
25. Duchene, J. Dechristopher, P., US Patent 3,886,054.
26. Fikentscher, R., US Patent 4,135,992, 1979.
27. Rushmere, J.D., US Patent 4,046,648, 1977.
28. Horner, J., Metal Finishing, 85(10),15 (1987).
29. Harbulak, E.P., US Patent 3,669,854, 1972.
30. Rosenberg, W., US Patent 3,808,110, 1974.
31. Skimin, C.W., US Patent 3,909,374, 1975.
32. Poor, J., US Patent 3,730,855, 1973.
33. Hsu, G.R., US Patent 4.070,256, 1978.
34. Beckwith, M., US Patent 3,729,394, 1973.
35. Anchor, M., US Patent 4,528,075, 1985.
36. Horner, J., Proc. 51st Ann. AES Tech. Conf., 1964.
37. Shawki, S., Hanna, F., Hamid, Z. A., Metal Finishing, 85, (12) 59 (1987)
38. Tan, T. C., Plat. Surf. Fin., 74 (7) 67, 1987
39. Tan, T. C., J. Electrochem Soc., 134 (12) 3011, 1987
40. "Metal Finishing Guidebook and Directory", Metal Finishing, 84(1A), 892 (1986).

Table I
Components of Typical Cyanide Zinc Electrolytes

| Chemicals | High Cyanide | Mid Cyanide | Low Cyanide |
|---|---|---|---|
| Zinc Metal | 105 gm/L | 18 gm/L | 7.5 gm/L |
| Sodium Cyanide | 110 | 45 | 18.5 |
| NaCN/Zn Ratio | 2.0 | 2.3 | 2.6 |
| Sodium Hydroxide | 12 | 12 | 12 |
| Sodium Carbonate | 20-100 | 20-100 | 20-100 |

Table II
Variation of NaCN/ZN Ratio with Temperature [2]

| Temperature | High Cyanide | Mid Cyanide | Low Cyanide |
|---|---|---|---|
| 22 C | 2.6 | 2.2 | 2.0 |
| 26 | 2.7 | 2.3 | 2.1 |
| 30 | 2.8 | 2.4 | 2.2 |
| 34 | 2.9 | 2.5 | 2.3 |
| 38 | 3.0 | 2.6 | 2.4 |
| 42 | 3.2 | 2.7 | 2.5 |
| 46 | 3.3 | 2.7 | 2.5 |

Table III
Typical Alkaline Non Cyanide Electrolyte

| Chemicals | Concentration |
|---|---|
| Zinc Metal | 3.5-20 gm/L |
| Sodium Hydroxide | 90-120 gm/L |
| Sodium Carbonate | 20-40 gm/L |

Table IV
Typical Acid Chloride Electrolyte

| Chemicals | Rack | Barrel |
|---|---|---|
| Zinc Metal | 37 gm/L | 26 |
| Total Chloride | 135 | 120 |
| Boric Acid | 26 | 30 |
| pH | 5.0-5.5 | 4.8-5.5 |
| Agitation | Air or mechanical | Natural with barrel motion |
| Filtration | Continuous | Occasional |

Table V
Efficency and Throwing Power of a Variety of Brighener Systems

| Process | Efficiency At | | | Throwing Power At | |
|---|---|---|---|---|---|
| | 10 ASF | 25 ASF | 55 ASF | 15 ASF, Ratio 5:1 Percent | Ratio |
| NonCyanide 7.5 gm/L Zn 12gm/L NaOH: | | | | | |
| Brightener A | 74 | 69 | 53 | 32 | 3.4 |
| Brightener B | 90 | 55 | 25 | 70 | 1.5 |
| Brightener C | 75 | 54 | 49 | 54 | 2.3 |
| NonCyanide 15 gm/L Zn 20 gm/L NaOH: | | | | | |
| Brightener B | 93 | 56 | 43 | 63 | 1.9 |
| Brightener C | 78 | 77 | 75 | 28 | 3.6 |
| Mid Cyanide: | | | | | |
| Brightener D | 73 | 81 | 66 | 30 | 3.5 |
| Brightener E | 84 | 88 | 63 | 40 | 3.0 |
| Acid Chloride: | | | | | |
| Brightener F | 99 | 99 | 99 | 20 | 4.0 |

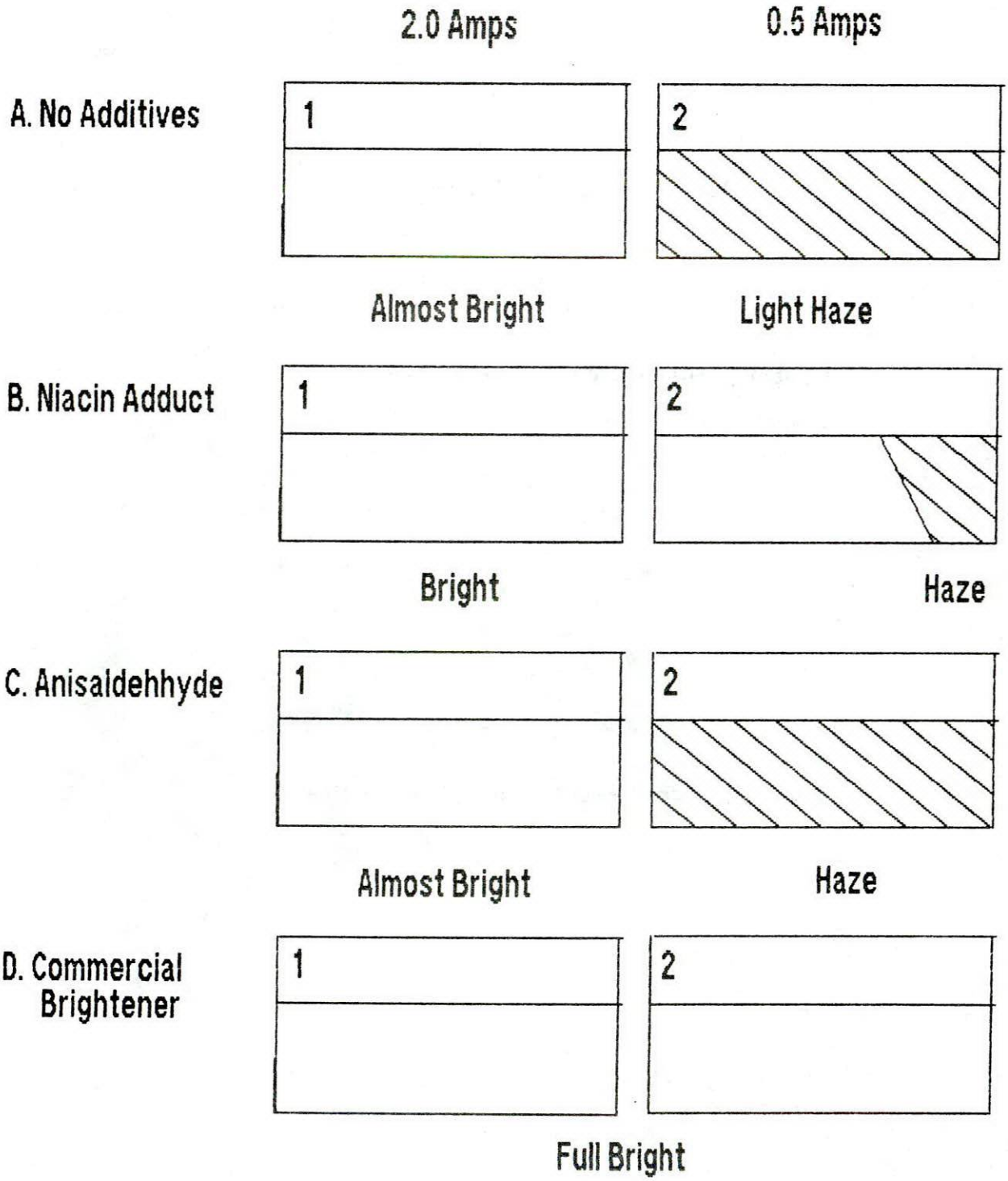


**Figure I. Mid cyanide Hull cell panels plated for 10 minutes at 2.0 and 5.0 amps**

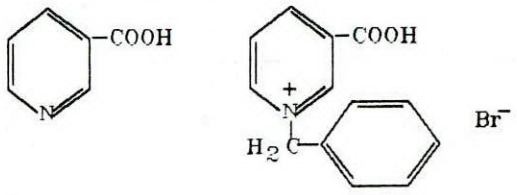


Niacin N-Benzyl-3-Carboxylate Pyridinium Bromide

**Figure II. Structure of niacin and a derivative**

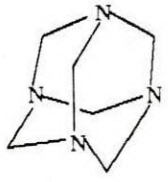


Hexamethylenetetramine

**Figure III. Structure of hexamethylenetetramine**

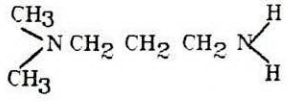


Dimethylamionpropylamine

**Figure IV. Structure of dimethylaminopropylamine**

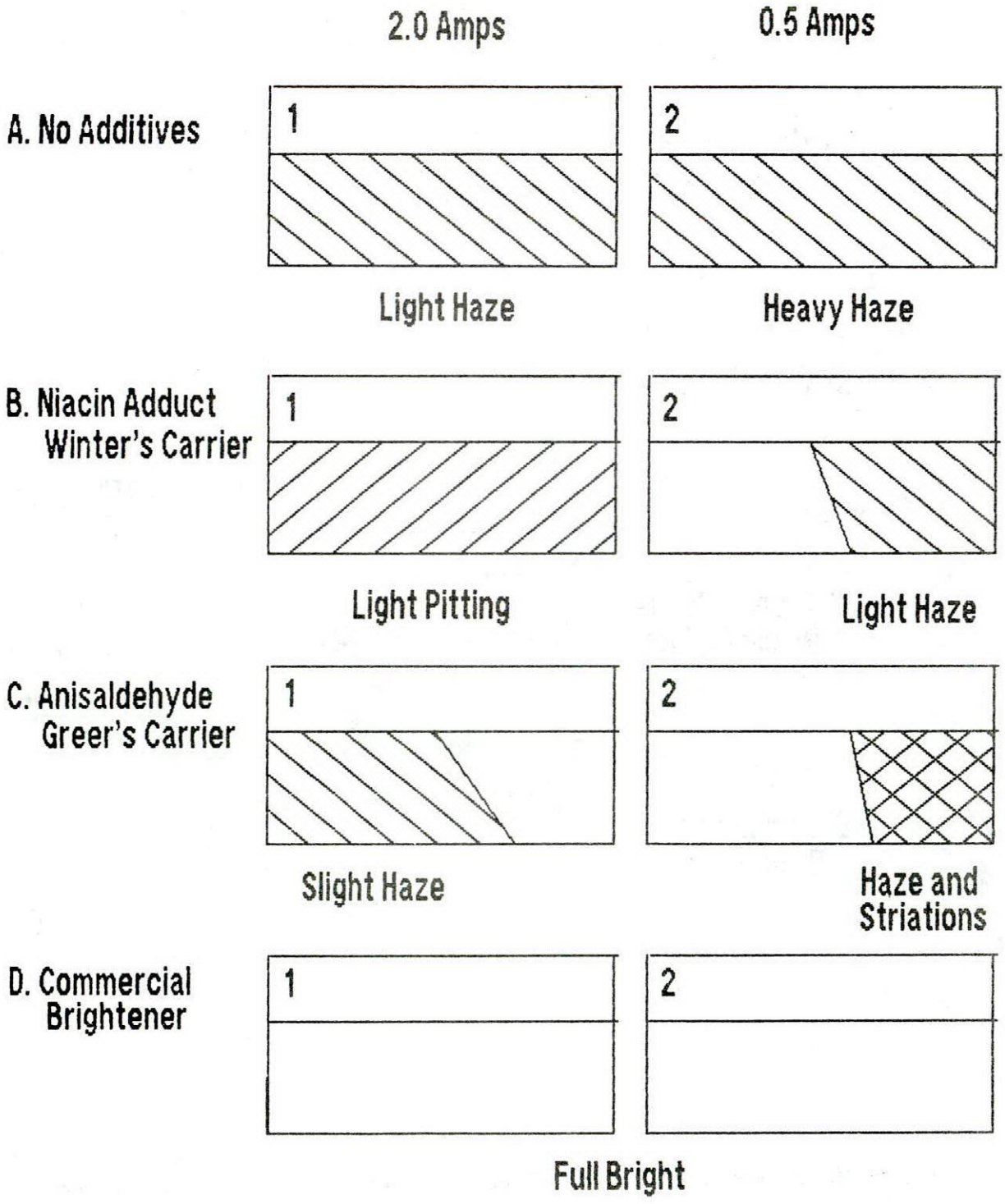


**Figure V. Low cyanide Hull cell panels plated for 10 minutes at 2.0 or 5.0 amps**

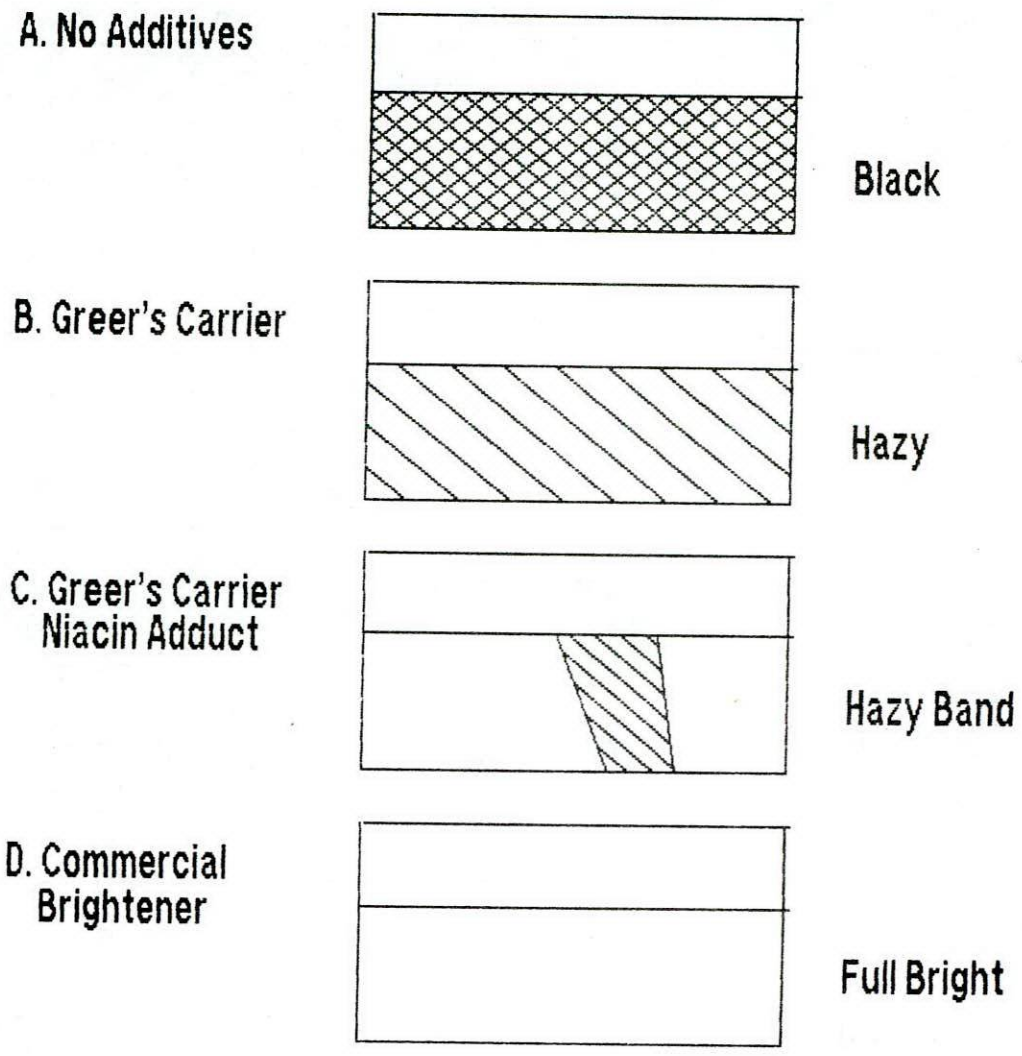


**Figure VI. Alkaline non cyanide Hull cell panels plated for 10 minutes at 2.0 amps**

A. No Additives

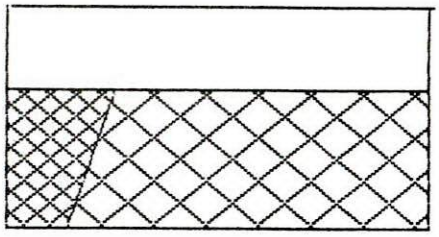

Black Grey

B. Wetting Agent

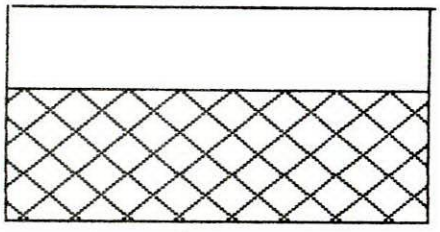

Grey to Haze

C. Wetting Agent
Benzylidene Acetone

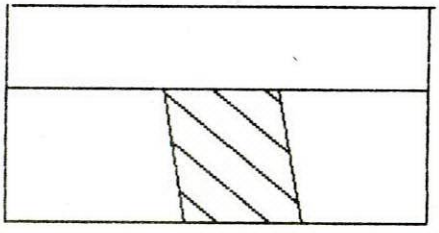

Grey Band

D. Wetting Agent
Benzylidene Acetone
Sodium Benzoate

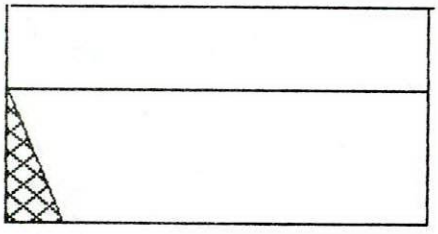

Black Bright

E. Commercial
Brightener

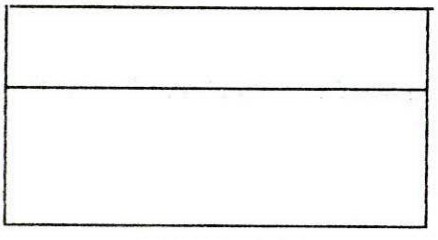

Full Bright

**Figure VII. Acid chloride Hull cell panels plated for 10 minutes at 2.0 amps**

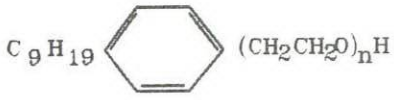


**Figure VIII. Structure of nonylphenol polyethoxylate**

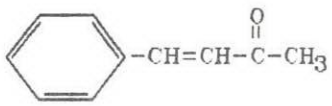


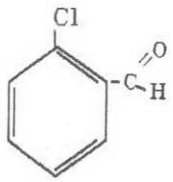


**Figure IX. Structure of benzylidene acetone and o—chlorobenzaldehyde**

# L-6

# Advances in Fundamentals And Applications Session L

## Electroplating: Where it's Going and Why

Earl C. Groshart
The Boeing Co.
P.O. Box 3999
M/S 2E-01
Seattle, WA 98124

# ELECTROPLATING: WHERE ITS GOING AND WHY

Earl C. Groshart
The Boeing Company
P. O. Box 3999 M/S 2E-01
Seattle, Washington 98124-2499

Before looking ahead to where we are going, let's briefly look at where we are as an industry. In surveying the plating shops in Western Washington, you find them plating zinc, cadmium, copper, silver, chromium, nickel, electroless nickel and gold. They also anodize, conversion coat and dye.

What you further find, if you look very closely, is that the zinc solution being used isn't much different than the zinc solution patented by Procter and Werlund in 1922 or the one proposed by Blum in 1921. The baths are dressed up with fancy trappings, but they contain the same cyanide/zincate chemistry. The cadmium baths are not unlike Udy's 1919 bath; the high efficiency copper baths are those introduced in 1938; and the silver baths have essentially the same chemistry as that used at the beginning of the industry (1840) by the Elkingtons.

Chromium is currently plated from Finks 1923-24 patented formula, or a 1949 self-regulating formula, and while the newer sulfamate nickel bath is used, the 1915 watts formulas are still in place.

Grace Riddle's ammonia bath for electroless nickel has disappeared, but hypophosphite is still used as a reducing agent and gold is still shrouded in the ancient mystique. The acid (alloy) golds are perhaps the results of recent chemistry, but then perhaps not, since little was written outlining the work of the Guilds.

This all sounds like the present is the past. What is probably more true, is that it is comfortable to adopt the "if it ain't broke, don't fix it." attitude, and one can certainly not claim that any of the presently used plating baths "is broke." Nor have the needs for the services of the plating shops changed. Iron and steel still rust; aluminum still won't handle a wearing load; stainless steel bolts still gall; and, in spite of the painted automobile bumpers, we still require (demand) bright and shiny, or dull, or verdigris green products to make us happy.

The future of the plating shop, the job shop, and the entire industry, from the point of view of the service provided, does not appear to be vastly different from that which has always been provided. The products may change some, but the big changes will be in the way these products are produced. One of the reasons for these changes, while not the only one, is abbreviated "EPA."

For example, cadmium is disappearing for use in industry. Afew years ago cadmium in the shop effluent nearly caused its demise. Plant treatment of the effluents cured the problem and the use of cadmium continued. Now, with the new regulations,the previous cure, which was to precipitate it, form it into a cake and bury it, cannot be accomplished, so a new solution is necessary. The solution most likely to occur is the elimination of cadmium from design. Most of the military establishments are requiring that cadmium either be eliminated or restricted in use. For example, MIL-Std-186D "Protective Finishing For Army Missile Weapon Systems" states, "4.16 Cadmium plating. Cadmium plating shall be restricted to essential applications only. Use zinc plating, tin plating or aluminum coating instead." Essential applications have been nuts and bolts, an application which is progressively being replaced by Ion vapor deposited aluminum.

This Army quote leads to the immediate conclusion that the use of zinc, tin and aluminum will increase. In the case of zinc and tin, this probably isn't true, but for aluminum it is. At the beginning of 1988, there were 60 ion vapor deposition machines in service. A 15% increase in this number is anticipated for this year, and in the future, this coating will become even more important. Two events should be noted here: Obar Ispen, a company which makes quality vacuum equipment has taken over the sale and distribution of the "Invadizer" equipment; and second, the Air Force is sponsoring research, through the McDonnell Douglas Company (James Reilly), to eliminate cadmium and/or replace it with IVD aluminum. The future of zinc plating lies in its being applied from solutions which are less hazardous than the predominant cyanide solutions. For the automatic lines, the acid zinc solutions can be used. There are also new non-cyanide alkaline processes available. The future use of zinc,the metal, looks very good. There are few other materials better at protecting steel products than zinc; and there are several environmentally safe ways of applying it. The use of galvanizing has been on the increase and should continue. The plasma spraying of pure zinc produces a surprisingly corrosion resistant coating. The purity eliminates the anodic sites which caused corrosion. It is also finding use as a coating for molded, plastic electronic boxes. The greatest increase in zinc, however, will be in its use as a pigment in primers, especially as the $Cr^{+6}$ pigments disappear.

The use of tin shouldn't change in the immediate future. It should figure in alloys, like tin-nickel, as new corrosion resistant coatings with nonhazardous anions are developed. Copper, as an engineering tool, will become less important. Ceramic and organic heat-treat stop-off materials are effective in replacing copper. As an undercoating, it is really not

needed for most operations, and its use becomes less necessary as zinc die castings are replaced by plastic. Electroless copper as a plastic plating process may increase, but ultimately vaccuum techniques should take over. The use of nickel, and especially electroless nickel, can do nothing but increase in the next few years. These processes are relatively clean, and their effluent is controllable. As chromium is removed from the market place, nickel properties will be sorely needed as a replacement in many designs. There are electroless nickel processes available with enough variations, such as brightness, hardness and smoothness, to replace many uses of chromium.

Now, the chromium story: Two years ago, at the Philadelphia meeting of the AES, there was a paper (not published) which stated that hexavalent chromium had been shown to cause mutations by causing problems with DNA. This was fully documented in EPA's Final Report #PB 85-115905, "Health Assessment Document For Chromium." Therefore, chromium, long known as a material which can cause or contribute to dermatitis, breathing problems, and cancer, is also a possible cause of birth defects. Any one of these problems is enough to cause the eventual elimination of chromium as a wet plating process. What then, is to replace chromium with its myriad of engineering and decorative uses? Fortunately, all of the properties are seldom needed at one time, so there should be a substitute for the one property needed in a given design. As already mentioned, electroless nickel can be hardened to give a good wear surface. It can be plated bright (as can electroplated nickel) to produce a reflectant surface. For uses where extreme hardness or heavy build-up are required, the environmentally-safe spray processes are available. These have matured in the past few years, from the old flame-sprayed aluminum wire processes, to modern plasma and detonation spray processes, with sprayable materials lists that are nearly unlimited. Any material, with a reasonable temperature range between melting and boiling, is a candidate, including ceramics and stainless steels. Even without needing them to replace lost chromium processes, their versatility and environmentally-safe operation assure their future use on an increasing basis.

Two relatively new processes will also supplant the chromium processes: Ion implantation and laser surface modifications. By ion implantation, the substrate surface can become harder, brighter, and more corrosion resistant, depending on the metal used for implantation. With laser treatments, new surface alloys, and new forms of surface materials are formed by the laser.

In more conventional electroplating, alloy plating is gaining, and will continue to gain, popularity. While the chromium-nickel alloy announced at the Indianapolis meeting by

Dr. Lashmore, has not been put into commercial practice, it has led the way to other alloys such as nickel /tungsten which has many properties of chromium. The old nickel/zinc alloy (with new additives) is being researched as a replacement, low embrittlement process for corrosion protection on high strength steel. These are only the beginning; many more are following. Most of these new alloys are being planned so that they are either clean, or any effluents are cleanable.

Decorative finishing too is affected not only by the EPA problems, but the economy as well. Titanium carbide applied by vacuum sputtering at any price, is probably less expensive than gold. It is replacing gold in jewelry. Stainless steel replaces silver, and much of today's decorative chromium is already replaced by vacuum deposited aluminum.

## The New Construction Materials

A great number of finishing changes are being brought about because of changes in materials used in manufacture. We are only at the beginning of the "Plastic Age." In the last few years, we have seen more and more pounds of metal replaced with plastic in our automobiles--whole bodies, interior and exterior trim, buttons, head lamp reflectors, etc. are all molded from plastics and are, for the most part, metallized. Airplanes and missile structures are made of the new high, strength, light weight, rigid plastics and composites. These structures are subject to static electricity build-up, lightning strikes, and electromagnetic interference. Adding carbon or graphite to the material makes them stiff and able to carry loads, but it doesn't make them conduct electricity. For this function, metals are still required. Electroless nickel, sprayed metals, vacuum deposited metals, and conducting lacquer-like materials are used for this purpose. The new metal-matrix materials add more metal to the bulk of the material, but even these need complete metal coatings for conductivity, joining (soldering), appearance, etc.

The EMI problem mentioned above becomes acute where plastic enclosures are used for critical electronics. Some of the solid state devices will fire at nanovolts of energy, something easily transmitted across a plastic sheet or an ungrounded joint. To prevent this interference, these enclosures will require additional finishing by some means of metal application. Work in this area can only increase as the use of electronic devices increase.

## Conclusion

The foregoing outlines where I see the metal finishing industry being needed in the not-too-distant future. I haven't said much about automation, which is already recognized and will most certainly continue. We have had automated plating lines for years; we have robotic painters

in-service, and the computer networks to keep them all functional. Now, if we never allow anyone near our hazardous solutions; never allow them to escape to a waste stream; and learn to destroy their wastes safely, all of the agencies would be happy and we could go on unchanged. The facts are that the changes mentioned above are all necessary and our future depends on responding quickly and responsibly to these new production demands.

L-7

# Advances in Fundamentals And Applications Session L

## The Wear Characteristic of Ni-P-SiC Composited Coating

Deng Zongang and Huang Xinmin
Department of Materials and Science
Hefei Polytechnic University
People's Republic of China

# THE WEAR CHARACTERISTICS OF NI-P-SIC COMPOSITED COATING

Deng Zongang & Huang Xinmin
The Department of Materials and Science
Hefei Polytechnic University
People's Republic of China

## ABSTRACT

In this paper, the wear resistance of electroless co-deposited Ni-8.73%P-SiC coating has been studied and the effects of microstructure and properties of the coating on wear have also been researched by comparing it with Ni-8.9%P, Ni-4.5%P-SiC and electroplated chromium coatings. It has been found that the high wear resistance of Ni-8.73%P-SiC coating is a result of the SiC particle fines in the matrix grain, which increases the coating hardness and resists microcut. Also, the Ni-P alloy matrix with high phosphorus content is hard and supports the SiC properly. The Ni-8.73%P-SiC coating is more wear resistant than electroplated chromium coating because the latter exhibits surface network cracking, and its high hardness decreases quickly at high temperature.

## Introduction

Electroless co-deposition is one of the most important techniques for producing composite coatings of metallic and non-metallic constituents. Although the largescale applications for these coatings are yet to be tried, various engineering applications such as resistance to wear, and corrosion resistance have already been reported in the literature.[1-4] The electroless deposited coatings have advantages over electroplated coatings because they deposit a uniform thickness on complex shaped articles without the need for elaborate jigging systems. In addition, some deposits, such as Ni-P and Ni-B alloy, can be heat-treated to give increased hardness. When these properties are allied with the incorporation of hard particles, such as SiC and $Al_2O_3$, materials having good wear resistance characteristics can be produced. However, many papers on the electroless co-deposited coatings report only its applications, a few papers deal with the mechanism of wear, and effects of structure and properties on wear. If we want to enlarge the applications for the electroless co-deposited coatings, it is necessary to study the above problems.

## Experiment

The electroless co-deposited Ni-P-SiC coatings,electroless deposited Ni-P coating and electroplated chromium coatings were prepared on high carbon steel substrates. The bath composition, operating conditions and the coating compositions are shown in Table 1.

| | 1 | 2 | 3 |
|---|---|---|---|
| Composition of bath (g/l) | | | |
| $NiSO_4 7H_2O$ | 10 | 10 | 30 |
| $NaH_2PO_2 H_2O$ | 15 | 15 | 8 |
| $CH_3COONa \cdot 3H_2O$ | 15 | 15 | 15 |
| $H_3BO_3$ | 5 | 5 | 5 |
| SiC (<3um) | 15 | 1 | 15 |
| Operating condition | | | |
| temprature ( C) | 84 | 84 | 84 |
| ph volue | 4.8-5 | 4.8-5 | 5-5.4 |
| Composition of coatings | | | |
| P content (wt%) | 8.73 | 8.9 | 4.5 |
| Ni content (wt%) | 88.43 | 91.04 | 92.5 |
| SiC (wt%) | 2.8 | | 2.95 |

Table 1. The operating conditions, the compositions of the bath and the coatings.

The electroless deposited Ni-P coating and electroplated chromium coating were chosen as the comparison for explaining the wear characteristics of Ni-P-SiC composite coating. High carbon steel was chosen as the substrate because the composite coating is usually applied to tools and dies made of high carbon steel.

The wear test was done with a wear testing machine of MM-200 (block and rotating ring type). The testing load was 60 kg, the speed was 50m/min, and a machine oil lubricant was added to the surfaces at 1-2ml/min. The block samples are made of coating and the ring samples are made from mild steel.

Experimental Results (The Structure and Hardness of Coatings)

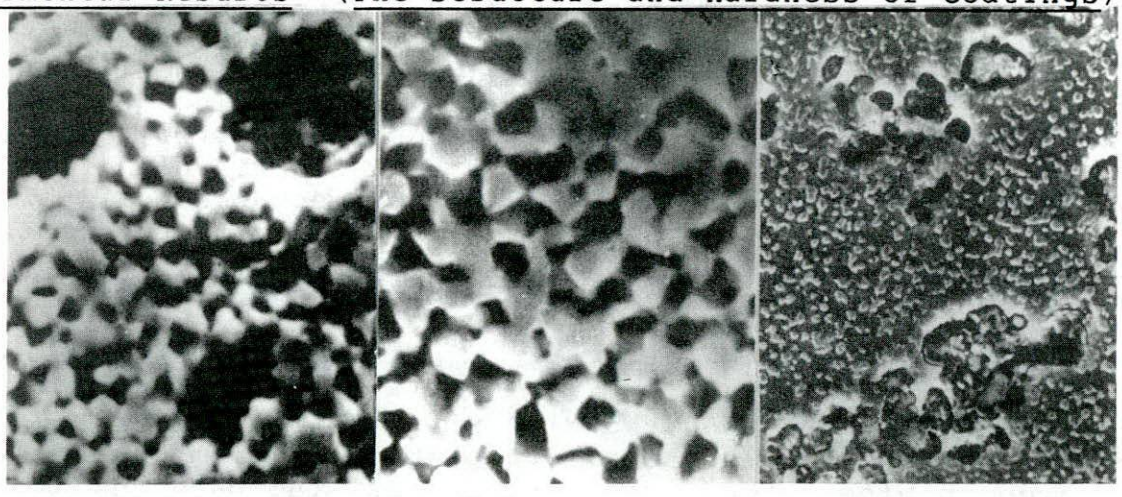

(a) X10000 (b) X10000 (c) X3000

Fig. 1. The structure of (a) Ni-8.73%P-SiC, (b) Ni-8.9%P and (c) Ni-4-5%P-SiC coatings.

Observing these photos, we find that the matrix of Ni-8.73%P-SiC coating is essentially identical to the structure of Ni-8.9%P coating. The $Ni_3P$ phase grains touch each other much more than the Ni solid solution, which fill up the clearance between the $Ni_3P$ grains. While on the matrix of the Ni-4.5%P-SiC coating, a few $Ni_3P$ grains are scattered.

The microstructure of electroplated chromium is known to all as the multicrystal of bcc solid solution with much surface network cracking, as Fig. 2.

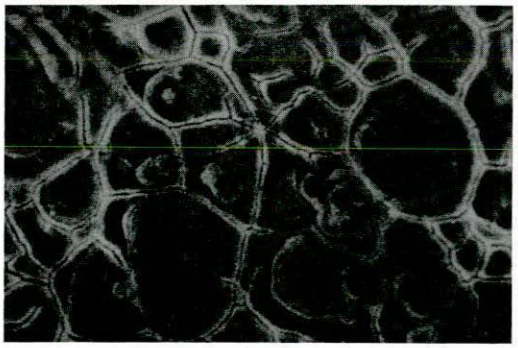

Fig. 2. The surface network cracking of electroplated chromium coating.
x1000

The hardness of all the coatings is shown in Fig. 3. The hardness of chromium coating is very high as-plated and decreases rapidly when the coating is heated. However, the hardness of all electroless deposited coatings are relatively low at first, increasing gradually with the heating, reaching a maximum at about 400°C. The hardness is different for the individual coatings. Among three electroless deposited coatings, the hardness of Ni-8.73%P-SiC coating is the highest and it decreases very slowly when heated above 400°C.

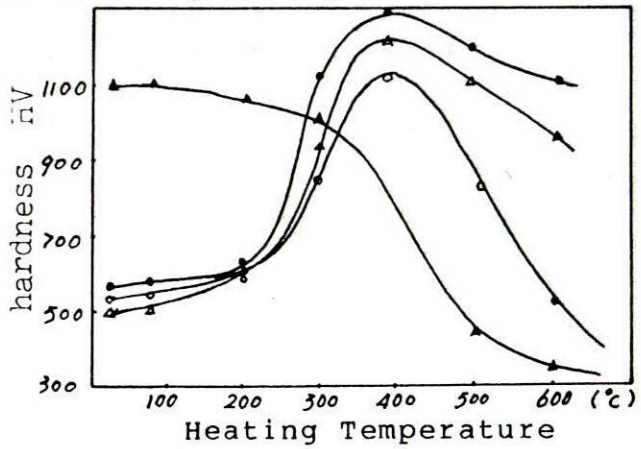


Fig. 3. Effect of heating temperature on hardness of coatings.
-•- Ni-8.73%P-SiC
-△- Ni-8.9%P
-○- Ni-4.5%P-SiC
-▲- Chromium coating

## The Results of Wear Test

The wear curves of all coatings are shown in Fig. 4. The wear volume of Ni-8.73%P-SiC coating is the least of all coatings and it rises very slowly. Comparing the four curves, the wear volume of the electroless deposited Ni-P-SiC and Ni-P coatings

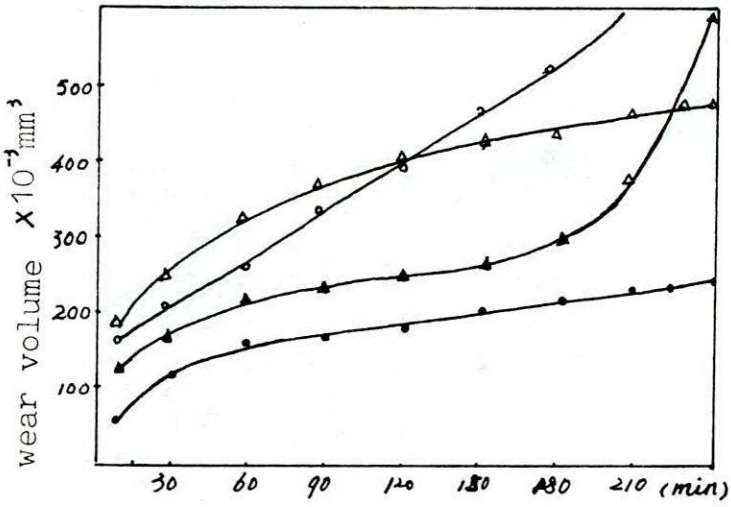


Fig. 4. The variation of wear volume with testing time for coating

-•- Ni-8.73%P-SiC
-▲- Chromium coating
-△- Ni-8.9%P
-○- Ni-4.5%P-SiC

with high phosphorus content rise very slowly, but the electroplated chromium and electroless co-deposited Ni-4.5%P-SiC coatings wear more quickly.

The wear scars of coatings are shown in Fig. 5. The wear scar of Ni-8.73%P-SiC coating shows only plowing grooves. However, many peeling and adhesion traces, besides microcut, are incorporated in the wear scars of other coatings.

The results of adhesive junction test are shown in Fig. 6. When the frictional moment rises abruptly during increasing test load, the adhesive junction is produced. According to these curves, the load of resistance to adhesive junction for Ni8.73%P-SiC coating is the highest.

The adhesive junction scars of electroless Ni-P and Ni-P-SiC are similar, but these are different from that of the electroplated chromium coating which is shown in Fig. 7.

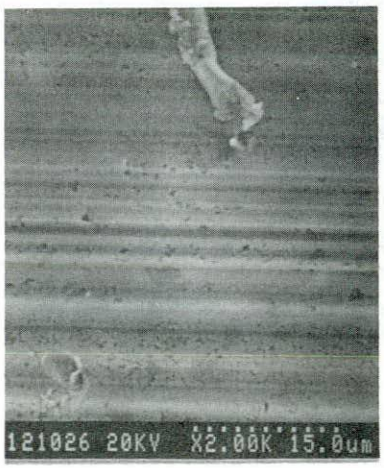


(a) Ni-8.73%P-SiC




(b) Ni-8.9%P




(c) Ni-4.5%P-SiC




(d) chromium

Fig. 5. The wear scar of all coatings which are tested for four hours at the same conditions.

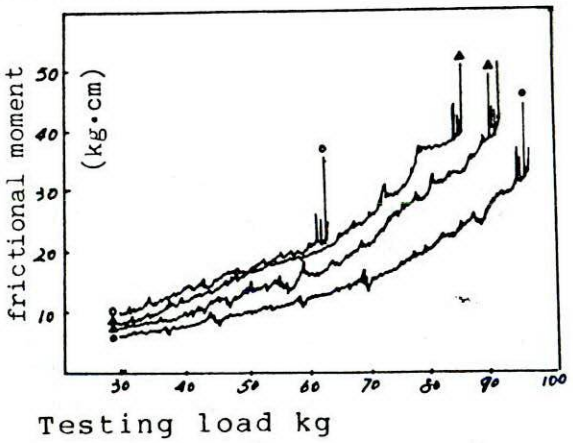


Fig. 6. The variation of frictional moment of all coatings at adhesive junction test.

-●- Ni-8.73%P-SiC
-▲- Chromium coating
-△- Ni-8.9%P
-o- Ni-4.5%P-SiC

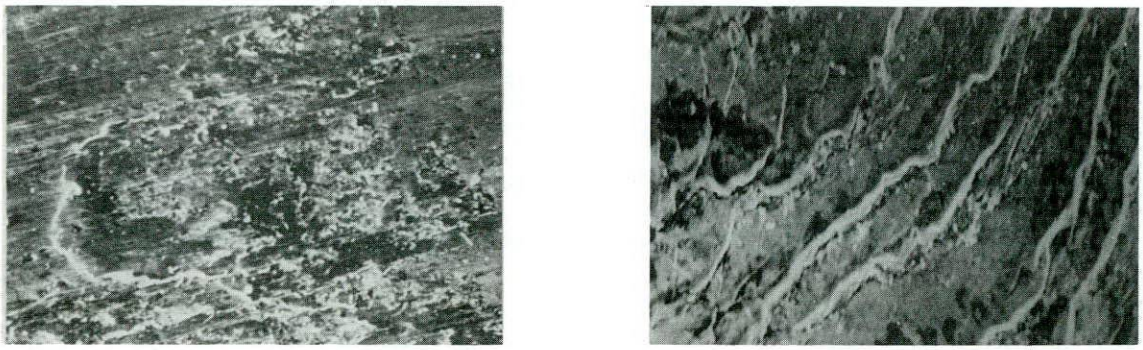

(a) x100 (b) x100

Fig. 7. The scar of adhesive junction test for (a) Ni-8.73%P-SiC and (b) chromium coatings.

## Discussion

### The effects of the structure and hardness on wear

Analyzing the above results of wear, we find that the behavior of each coating is different. Since all test conditions are the same, the different results must be caused by the structures and properties of the individual coatings.

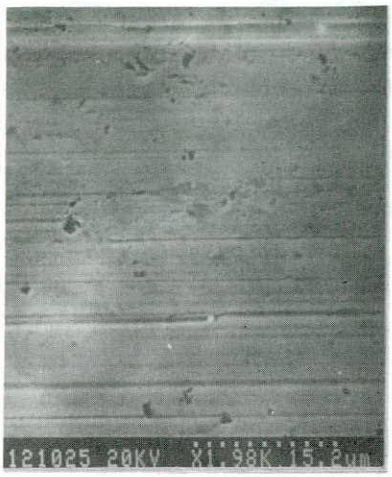


Fig. 8. The scar of the SiC particle resisting microcut.

Comparing the Ni-8.73%P-SiC coating with the Ni-8.9%P coating, the difference is that the composite coating has more SiC particles. As the SiC particles are dispersed in the composite coating, the coating hardness is increased greatly, the matrix grain is finer (comparing Fig. 1a with b) which will increase the coating strength and toughness, the probability of adhesion to mild steel is reduced as a result of the changing of the surface component and the SiC particles resist microcut (see Fig. 8). All these factors take an important part in resistance to wear. In addition, it can be found that the matrix alloy of

Ni-8.73%P-SiC coating is very resistant to wear by comparing Ni-8.73%p-SiC coating with Ni-4.5%P-SiC coating. This is because the Ni-P alloy with high phosphorus content (>7%P) is harder than that with low phosphorus owing to the $Ni_3P$ phase being more than 50% and the hard matrix not only resists wear, but supports the SiC particles to exert resistance to wear. This can be demonstrated by analyzing curve 1 and 2 in Fig. 3. At first, the SiC provides the resistance to wear, so the wear volume of Ni-4.5%P-SiC coating is less than Ni-8.9%P coating. Later, when the SiC is pushed into the soft matrix, the wear volume of Ni-4.5%P-SiC coating increased severely and exceeds that of Ni-8.9%P coating.

According to the above analysis, the high wear resistance of Ni-8.73%P-SiC results from a combination of SiC particles and Ni-P alloy matrix with high phosphorus content; i.e., the wear resistance of composite coating is dependent on the hard particle and good matrix.

The comparison of Ni-8.73%P-SiC coating with electroplated chromium coating

The electroplated chromium coating has been used extensively in industry for resistance to wear. Although some good results are required for its applications, the failure often appears as its hardness is decreased by frictional heat during wear testing. Since the good wear resistance of chromium coating is dependent on its high hardness, if the high hardness loses, the wear resistance will go bad suddenly, which can be found from Fig. 4., the curve 3 shows that the wear volume of chromium coating increases abruptly after wearing some time later. On the other hand, the surface network cracking is very harmful to wear resistance; it causes the coating to crack and peel as Fig. 9. Further, low adhesion strength is the third cause for decreasing wear resistance of chromium coating; it results in the coating becoming striped as Fig. 7b.

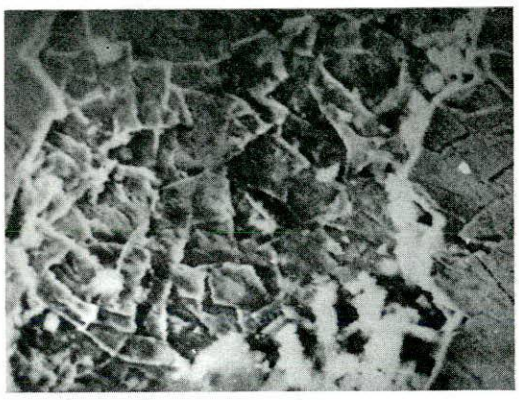

Fig. 9. The crack at the surface of chromium coating.

However, the hardness of electroless co-deposited coating can be chosen by means of heat treatment, and it is less influenced by frictional heat after heat treated at relatively high temperature, so that its wear curve (in Fig. 4) is stable. The wear resistance is contributed by SiC and Ni-8.73%P alloy. As the composited coating, there is no surface crack and it adheres to the substrate very strongly; the adhesive junction scar at Fig. 7 displays only small local adhesion, even though the load is very high.

All the above discussions show that the Ni-8.73%P-SiC composite coating has more advantages than electroplated chromium coating.

## Conclusion

1. Electroless co-deposition is a good method of surface finishing for resistance to wear. The high wear resistance of Ni-8.73%P-SiC composite coating is supplied by hard particles and good matrix.

2. The particles can increase the hardness of composite coating and the resistance to abrasion, but it must be supported by hard and stable matrix.

3. The hardness of coating plays an important part in resistance to wear. If the high hardness of a coating is influenced less by heat from friction, circumstances or other things, and there is no network cracking on the coating surface, the coating will show a good wear resistance. Because of these factors, the electroless co-deposited coating is often more resistant to wear than electroplated chromium.

## References

1. Nobuhiko Takeuchi and Nobuo Hatanaka, The Journal of the Metal Finishing Society of Japan, Vol. 36, No. 10, 1985, p. 409.

2. D. Buchkov, G. Garrilov, Metall, Vol. 34, No. 3, 1980.

3. N. Feldstein and T. Lancsek, Metal Finishing, Vol. 81, No. 8, 1983.

4. J. K. Dennis, S. T. Sheikh and E. C. S. Silverstone, Trans. Inst. Met. Finish, Vol. 59, 1981, pp. 118 - 122.

M-1

# Organic Coatings
# Session M

## Measurement Systems Evaluation for Organic Coatings Surface Finishers Using Statistical Methods

Gordon G. Perrin Jr.
Ford Motor Co.
Livonia, MI

**PAPER NOT RECEIVED IN TIME FOR PUBLICATION***

# Measurement Systems Evaluation for Organic Coatings Surface Finishers Using Statistical Methods

Gordon G. Perrin Jr., Ford Motor Company, Livonia, MI

The current approach in dealing with measurement systems in North America fails to take advantage of the considerable opportunities afforded by statistical methods. Specifically, areas not carefully and properly considered and addressed include measurement certification, calibration, and systems stability. This paper will provide insight on and methods to aid in the assessment of these measurement systems using readily available and easily understood statistical methods.

* For copies of this paper, please contact the author directly

Mr. Gordon G. Perrin Jr.
Quality Office
Parts & Service Division Center
29500 Plymouth Road
Livonia, MI 48150
(313) 523-5618

M-2

# Organic Coatings
# Session M

## Advanced Solid Lubrication for Tribological Control at Elevated Temperatures

Dr. Robert M. Gresham
E/M Corp.
P.O. Box 2400
West Lafayette, IN 47906

# ADVANCED SOLID LUBRICATION FOR TRIBOLOGICAL CONTROL AT ELEVATED TEMPERATURES

Dr. Robert M. Gresham
E/M Corporation
P.O.Box 2400, West Lafayette, IN 47906

In 1980 the energy conversion and utilization technologies division of the U. S. Department of Energy sponsored a study which was released in late 1985[1]. This program identified over four quadrillion BTU's of energy loss in the United States due to simple friction and wear. As such, the DOE/ECUT program was initiated to assess market needs and later to study friction and wear as a science itself. Until this study was issued, tribology research emphasized component development, fluid film and elastohydrodynamic lubrication. Since the report was issued the emphasis has shifted dramatically. Research efforts now concentrate on lubricants, materials, coatings and friction and wear mechanisms. Most current tribology research is related to Dept. of Defense objectives of longer life, low maintenance/failure free machinery and the basic understanding of friction, wear, materials and coatings.

High temperature lubrication continues to be a major objective in tribology research. The effects of new materials and solid lubricants on current temperature limitations are also being studied. Coatings are receiving considerable attention in general materials development (see Figure 1). The study concluded that the U.S.Government high temperature lubrication work is the most applicable to energy conservation goals. Specific projects in this area include developing new tribological materials, and research to determine physical and chemical interactions and processes in tribological systems. Liquid and solid lubricants, tribological coatings and surface modifications, and ceramic and cermet materials are specific topics under consideration[1].

At one time solid lubricants were used almost entirely in aerospace applications. Today there is a pronounced trend to use them over a much wider range of applications. New directions for solid lubricant technology growth have been identified. In recent years solid lubricants have been used extensively in the automotive, metal working, computer/office machine industries and throughout industry in general.

Three basic solid lubricant materials have been used historically: Molybdenum Disulfide, Graphite, and Polytetrafluoroethylene. However, the variety of coating and composite formulations in which these three basic materials are used is very large and indeed can be confusing. The trend in advanced technology is to use solid lubrication for high temperature applications. The driving force for these applications comes from the Dept. of Defense particularly in engine systems currently under development (e.g., the adiabatic diesel engine, small gas turbine engine, and the upgraded rotary engine). These advanced solid lubricants are required in the high temperature areas of these engines which preclude the use of conventional grease and oils. It is anticipated that the temperatures encountered in the adiabatic diesel and the ceramic gas turbine are so high that conventional solid lubricant materials will likely not be suitable. Temperatures well in excess of 1,000°F may be encountered. Metallic structural and bearing materials will be replaced with ceramics. These ceramics must be either self lubricating or coated with a solid lubricant.

Thus the trend of future solid lubricant use can be summarized as follows: 1) continued use of molybdenum disulfide, graphite and PTFE lubricants throughout general industry; 2) the expanding use of self lubricating composites; 3) emphasis on multi-functional coatings which provide corrosion protection as well as lubrication and 4) creation of high temperature solid lubricants for advanced technology engines, especially those with ceramic hot section structural and bearing materials[2]. The balance of this paper will describe examples of solid lubricating materials which are being developed to meet the needs of this expanding elevated temperature oriented market.

Bonded solid film lubricants contain proprietary mixtures of solid lubricating materials bound to the surface of the part by some kind of "binder" material. High temperature failure of bonded solid film lubricants results from lack of oxidative or thermal stability of either the solid lubricating materials or the "binder" material. Some environments cause failure of both. The most common solid lubricating materials, as mentioned earlier, are graphite, molybdenum disulfide and PTFE. Graphite is stable to >1500°F. Molybdenum disulfide is stable to 1200°F in vacuum or non-oxidative environments and to 750°F in oxidative atmospheres. PTFE begins to soften at >500°F.

There are other solid lubricating materials which are used for high temperature applications such as indium, silver, graphite fluoride, niobium selenide, antimony trioxide and lead oxide. These materials are often blended into proprietary mixtures which exhibit synergy for exceeding the properties of the individual components.

The binder materials and the method of application have a dramatic effect on the high temperature performance of bonded solid film lubricants. While bonded solid film lubricants contain proprietary mixtures of solid lubricants, they are often classified into types by the binder chemistry or mechanism used to adhere the solid lubricants to the bearing surface.

The first major class of solid lubricant coating binder types are described loosely as high temperature organic and inorganic bonded lubricants (see Table I). For high temperature use there are two major types of organic binders used: the silicones and the polyamide-imides. The silicone coatings provide protection from corrosion, abrasion and high temperature up to 850°F while exhibiting outstanding wear life. Their weakness is primarily in the area of solvent resistance. Typical physical properties of a silicone-based bonded lubricant are shown in Figure 2. Polyamide-imide chemistry provides coatings with excellent abrasion resistance, good solvent resistance, high temperature use up to 750°F and outstanding wear life. A typical polyamide-imide solid film lubricant is described in Figure 3.

Inorganically bonded solid film lubricants are the next class of high temperature bonded solid film lubricants. These materials are usable for temperatures as high as 1200°F. They have outstanding oxidation resistance, radiation resistance and compatibility to materials such as dimethylhydrazine and liquid oxygen (LOX). However, these materials exhibit less effective wear life and durability and are more difficult to apply. Typical physical properties of inorganically bonded solid lubricants are shown in Figure 4. Additionally, in the area of inorganic bonded solid lubricants, a new class of coating has been developed to provide resistance to high frequency fatigue in the root section of rotor vanes in jet engines. This material is not designed to have typical lubricating capability but is resistant to thermal shock and oxidation, and is it extremely stable to very high temperatures as shown in Figures 5, 6, and 7.

Table 2 shows additional classes, by binder type, of high performance, high temperature coatings. The first of these are coatings applied by impingement processes while utilizing a proprietary ceramic binder. In this case, graphite, molybdenum disulfide or tungsten disulfide is applied by a proprietary impingement process to provide a very thin, dimensionally stable film with outstanding solvent resistance, vacuum outgassing resistance and compatibility with liquid oxygen. Typical performance properties of impingement applied solid lubricants are shown in Figure 8. There is currently a military specification being written around these processes (MIL-L-85645).

Ceramics and cermets make up the next class of solid lubricant materials designed for high temperature application. These materials are applied either as a spray coating, which is subsequently fired in a high temperature oven, or as a plasma spray. These coatings exhibit extreme hardness, corrosion resistance, solvent resistance, vacuum outgassing stability and temperature application at least as high as 1200°F. Their weaknesses are impact resistance, machinability, lubricity and difficulty of application. Performance properties of typical ceramic/cermet-based bonded products are shown in Figure 9.

One of the emerging technologies for high temperature coating processes involves physical vapor deposition of extremely thin films of very hard, wear-resistant materials such as titanium nitride, halfnium nitride, tungsten carbide, etc. These coatings, in addition to their thinness, provide outstanding solvent resistance, wear resistance, vacuum resistance and temperature stability as high as 2000°F. Additionally, these materials are extremely resistant to oxidation; however, they are expensive to apply and have certain part conformation limitations.

These PVD-applied coatings have now been used in conjuntion with impingement processes to provide lubricity. The result is a new generation of coatings synergistically combining these advanced technologies to provide the properties required for this emerging market. Typical physical properties of such coatings are shown in Figure 9.

In summary, there are a variety of technologies being advanced for use in high temperature applications (see figure 10). The lubricant systems, while still based on molybdenum disulfide and graphite, involve new proprietary systems, or in some cases the actual coefficient of friction requirements have been minimized in lieu of wear resistance and temperature stability. In the earlier solid film lubricant products, the low coefficient of friction was a means of reducing overall temperature allowing for use of materials with less temperature stability. In high temperature applications, incremental increases in temperature due to frictional forces is of reduced significance. However, friction at whatever temperature must be overcome by energy, and for that reason there will always be a need for solid materials which can impart a lower coefficient of friction in a given environment.

No single technology has emerged. We believe that ceramic components, coated with the appropriate coating for lubricity, will result in one major material classification. The other will likely be high temperature corrosion resistant alloys coated with thin, physical vapor deposited films for lubricity and wear resistance.

* * *

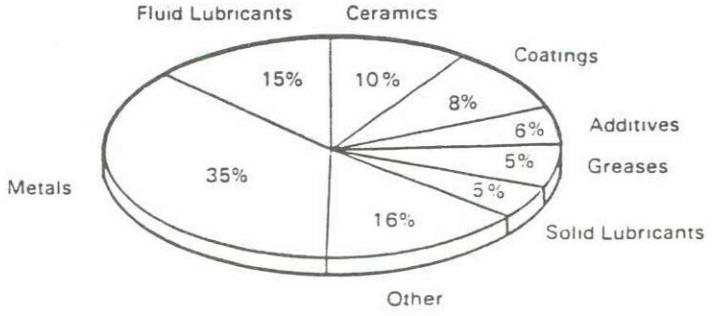


Figure 1: Materials Under Consideration in the 215 Current Government-Sponsored Tribology Projects

Table I

COMPARISON TABLE

HIGH TEMP. ORGANIC BONDED LUBRICANTS

| | STRENGTHS | WEAKNESSES |
|---|---|---|
| Silicones | Corrosion Resistance<br>Abrasion Resistance<br>Thermal Stability<br>Wear Life<br>Ease of Application | Solvent Resistance |
| Polyamide-Imide | Abrasion Resistance<br>Solvent Resistance<br>Thermal Stability<br>Wear Life | Corrosion Resistance<br>Ease of Application |

HIGH TEMP. INORGANIC BONDED LUBRICANTS

| | STRENGTHS | WEAKNESSES |
|---|---|---|
| Silicates/<br>Phosphates | Oxidation Resistance<br>Radiation Resistance<br>LOX Compatibility<br>Thermal Stability<br>High Vacuum | Wear Life<br>Ease of Application |

Figure 2

TYPICAL PHYSICAL PROPERTIES
OF A
SILICONE BASED BONDED LUBRICANT

| | |
|---|---|
| Usable Temperature Range | -65°F - 750°F |
| Pencil Hardness (ASTM D-3363) | 4H |
| Taber Abraser (ASTM D-4060)<br>1Kg Load, CS-10 Calibrase Wheel | 6.4 mg/1,000 cycles |
| LFW-1 Endurance (ASTM D-2714)<br>630 lbf. Load | 257,000 cycles |
| Coefficient of Friction<br>(ASTM D-2714) 630 lbf. Load at 5,000 cycles | 0.05 |
| Thermal Shock Stability (ASTM D-2511) | Pass |
| Fluid Resistance (ASTM D-2510, Method C) | |
| TT-S-735 Test Fluid | Pass |
| MIL-L-2104 Lube Oil | Pass |
| MIL-L-23699 Turbine Lube Oil | Pass |
| MIL-T-5624A, JP-4 Jet Fuel | Pass |
| MIL-H-8446, Non-Petroleum Hydraulic Oil | Pass |
| O-T-634, Trichloroethane | Pass |
| 1,1,1-Trichloroethylene | Pass |
| Methyl Ethyl Ketone | Pass |
| Toluene | Pass |

Figure 3

TYPICAL PHYSICAL PROPERTIES
OF A
POLYAMIDE-IMIDE BASED BONDED LUBRICANT

| | |
|---|---|
| Usable Temperature Range | -300°F - 750°F |
| Pencil Hardness (ASTM D-3363) | 6H |
| Taber Abraser (ASTM D-4060)<br>1Kg Load, CS-10 Calibrase Wheel | 2.3 mg/1,000 cycles |
| LFW-1 Endurance Life (ASTM D-2714)<br>630 lbf. Load | 416,000 |
| Coefficient of Friction (ASTM D-2714)<br>630 lbf. Load, @ 5,000 Cycles | 0.06 |
| Thermal Shock Stability (ASTM D-2511) | Pass |
| Fluid Resistance (ASTM D-2510, Method C) | |
| TT-S-735 Test Fluid | Pass |
| MIL-L-2104 Lube Oil | Pass |
| MIL-L-23699 Turbine Lube Oil | Pass |
| MIL-T-5624A, JP-4 Jet Fuel | Pass |
| MIL-H-8446, Non-Petroleum Hydraulic Oil | Pass |
| O-T-634, Trichloroethane | Pass |
| 1,1,1-Trichloroethylene | Pass |
| Methyl Ethyl Ketone | Pass |
| Toluene | Pass |

Figure 4

TYPICAL PHYSICAL PROPERTIES
OF
INORGANICALLY BONDED LUBRICANT

| | |
|---|---|
| Usable Temperature Range | -360°F - 1200°F |
| Pencil Hardness (ASTM D-3363) | HB |
| Taber Abraser (ASTM D-4060)<br>1Kg Load, CS-10 Calibrase Wheel | 67 mg/1000 cycles |
| Falex Endurance (ASTM D-2625, Method A) | 80 Minutes |
| Coefficient of Friction (ASTM D-2625) | 0.06 |
| Thermal Shock Stability (ASTM D-2511) | Pass |
| Fluid Resistance (ASTM D-2510C) | |
| TT-S-735 Test Fluid | Pass |
| MIL-L-2104 Lube Oil | Pass |
| MIL-L-23699 Turbine Lube Oil | Pass |
| MIL-T-5624A, JP-4 Jet Fuel | Pass |
| MIL-H-8446, Non-Petroleum Hydraulic Oil | Pass |
| O-T-634, Trichloroethane | Pass |
| 1,1,1-Trichloroethylene | Pass |
| Methyl Ethyl Ketone | Pass |
| Toluene | Pass |
| Nitrogen Tetroxide ($N_2O_2$) | Pass |
| Dimethyl Hydrazine | Pass |
| Liquid Oxygen | Pass |

Figure 5

TYPICAL PHYSICAL PROPERTIES
OF
MICROSEAL 100-2A

| | |
|---|---|
| Color and Appearance | Smooth White Film |
| Gouge Hardness, Pencil Method (ASTM D-3363) | > 9H |
| Mar Hardness, Pencil Method (ASTM D-3363) | > 9H |
| Coefficient of Friction (dynamic) | .2 |
| Abrasion Resistance, Taber Abraser Method (ASTM D-4060), CS-10 Wheel, 1KG Load | < .1 mg per 1000 cycles |
| Flexibility, 1/2" Mandrel | Pass |
| Fluid Resistance (ASTM D-2510, Method C) | |
| Distilled Water | Pass |
| MIL-H-5606, Hydraulic Fluid | Pass |
| DC-200 Silicone Fluid | Pass |
| Rockwell Nordstrom 147 Grease | Pass |
| Skydrol 500A Hydraulic Oil | Pass |
| Nitrogen Tetroxide ($N_2O_4$) | Pass |
| Dimethyl-Hydrazine, Rocket Fuel | Pass |
| Liquid Nitrogen | Pass |
| Liquid Oxygen | Pass |

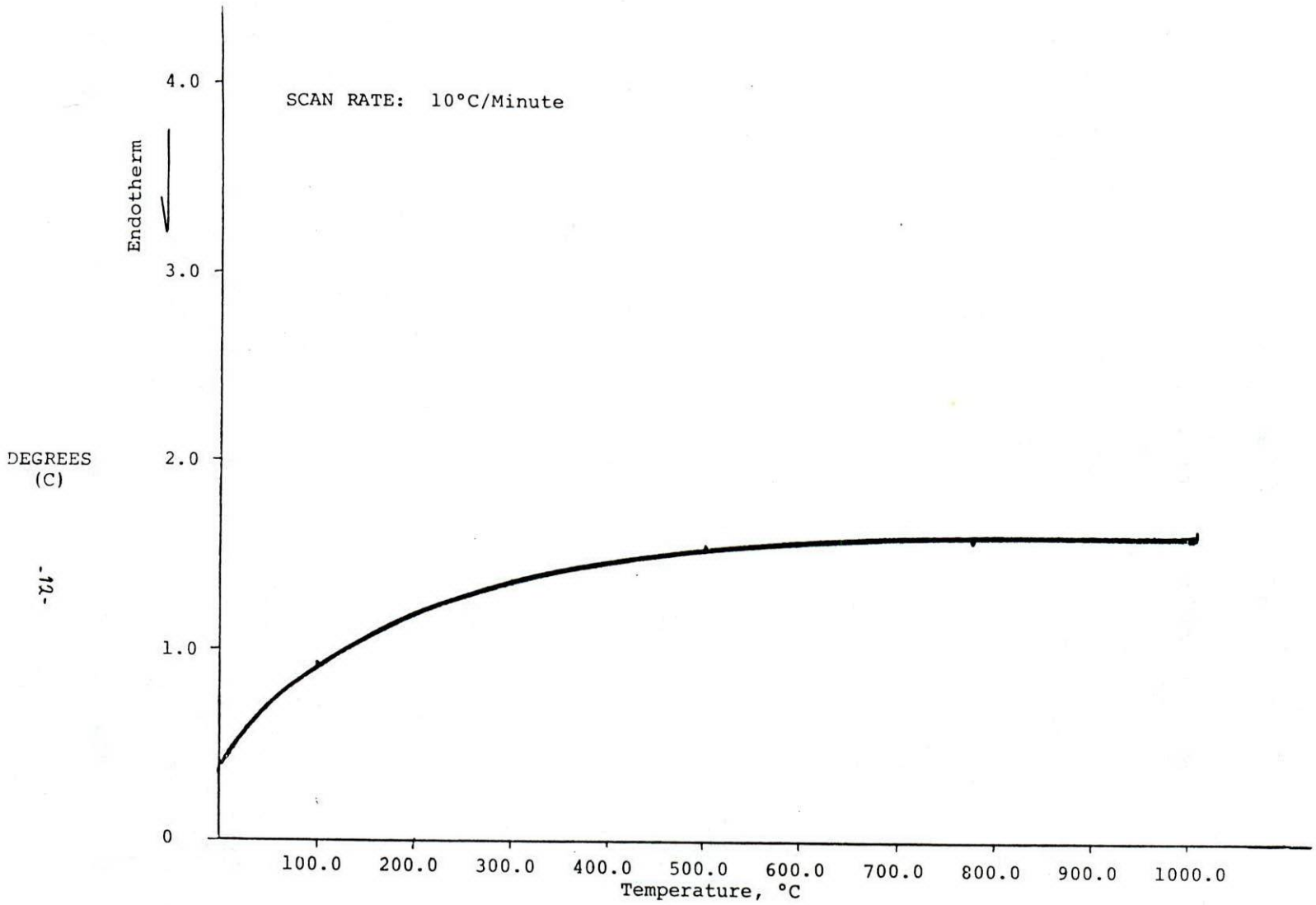


Figure 6: Differential Thermal Analysis of Microseal 100-2A Film

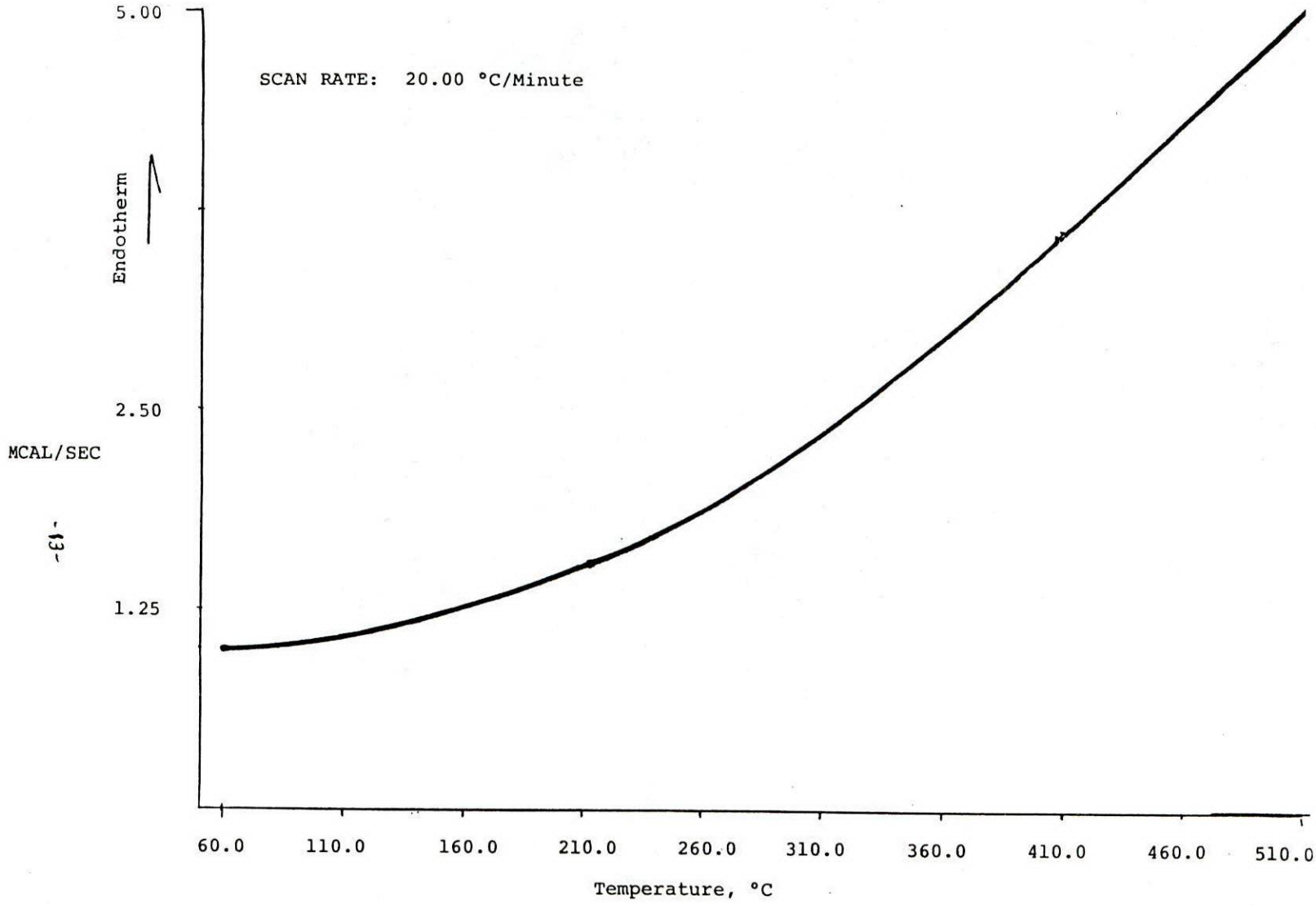


Figure 7: Differential Scanning Calorimeter Plot of Microseal 100-2A Film

Table II

BONDED SOLID LUBRICANTS

BINDER SELECTION

PERFORMANCE CHARACTERISTICS

| BINDER TYPE | STRENGTHS | WEAKNESSES |
|---|---|---|
| Impingement | Thin Film ( < .0001")<br>Dimensional Stability<br>Solvent Resistance<br>Radiation Resistance<br>Vacuum Outgassing<br>High Temperature Use<br>LOX Compatibility | Corrosion Resistance<br>Durability<br>Load Carrying<br>Ease of Application |
| Ceramics/Cermets | Extreme Hardness<br>Corrosion Resistance<br>Solvent Resistance<br>Vacuum Outgassing<br>High Temperature Use | Impact Resistance<br>Machinability<br>Lubricity<br>Ease of Application |
| Physical Vapor Deposition (PVD) | Thin Films ( < .0001")<br>Dimensional Stability<br>Solvent Resistance<br>Vacuum Outgassing<br>High Temperature Use<br>Corrosion Resistance | Load Carrying<br>Ease of Application |

Figure 8

COMPARISON OF IMPINGEMENT LUBRICANT PROPERTIES

| Lubricant Employed | Maximum Dimensional Surface Build-Up | Thermal Stability in Air | | Thermal Stability in Vacuum | Compatibility |
|---|---|---|---|---|---|
| | | Low | High | ($10^{-9}$ Torr) | |
| High purity electric furnace graphite | <.0001" (.00025 mm) | −423°F (−253°C) | +2000°F (1093°C) | +2700°F (1482°C) | Distilled water, MIL-H-5606 hydraulic fluid, DC200 silicone fluid, Rockwell Nordstrom 147 grease, UDMH compatibile grease, IRFNA compatible grease, solid propellents, Skydrol 500 A hydraulic oil or $N_2O_4$. |
| MOLYBDENUM DISULFIDE | <.0001" (.00025 mm) | −325°F (−198°C) | +750°F (399°C) | +1400°F (760°C) | Distilled water, MIL-H-5606 hydraulic fluid, DC200 silicone fluid, Rockwell Nordstrom 147 grease, UDMH compatible grease and IRFNA compatible grease. |
| TUNGSTEN DISULFIDE | <.0001 (.00025 mm) | −325°F (−198°C) | +850°F (454°C) | +1400°F (760°C) | Distilled water, MIL-H-5606 hydraulic fluid, DC200 silicone fluid, Rockwell Nordstrom 147 grease, UDMH compatible grease, and IRFNA compatible grease. |

Figure 9

TYPICAL PHYSICAL PROPERTIES
OF A
CERAMIC/CERMET BASED BONDED LUBRICANTS

| | |
|---|---|
| Usable Temperature Range | -60° - 1200°F |
| Pencil Hardness (ASTM D-3363) | > 9H |
| Taber Abraser (ASTM D-4060)<br>1Kg Load, CS-10 Calibrase Wheel | > .1mg/1000 Cycles |
| Thermal Shock Stability (ASTM D-2511) | Pass |
| Fluid Resistance (ASTM D-2510, Method C) | |
| TT-S-735 Test Fluid | Pass |
| MIL-L-2104 Lube Oil | Pass |
| MIL-L-23699 Turbine Lube Oil | Pass |
| MIL-T-5624A, JP-4 Jet Fuel | Pass |
| MIL-H-8446, Non-Petroleum Hydraulic Oil | Pass |
| O-T-634, Trichloroethane | Pass |
| 1,1,1-Trichloroethylene | Pass |
| Methyl Ethyl Ketone | Pass |
| Toluene | Pass |

Figure 10

Physical Vapor Deposition/Impingement

Microseal® TN Series Coatings

| Properties | TN | TN-100 | TN-200 |
|---|---|---|---|
| Vickers Hardness | >2,000 | >2,000 | >2,000 |
| Thickness | 2-3 microns | 4-6 microns | 4-6 microns |
| Lubricant | - | Graphite | Molybdenum Disulfide |
| Coefficient of Friction | .49 | .09 | .07 |
| Melting Point (°C) | 2950 | 2950 | 2950 |
| Humidity Resistance (D-2247) | >336 Hrs | >336 Hrs | >336 Hrs |

Figure 11

SUMMARY OF HIGH TEMPERATURE

TRIBOLOGICAL FINISHES

---

ORGANIC BASED BONDED LUBRICANTS

INORGANIC BASED BONDED LUBRICANTS

CERAMIC/CERMET BASED LUBRICANTS

IMPINGEMENT LUBRICANTS

PHYSICAL VAPOR DEPOSITION (PVD) FILMS

FOOTNOTES

1. "Energy Conservation Potential of Surface Modification Technologies", PNL-5538, Pacific Northwest Laboratories, Richmond, WA, Sept. 1985.

2. Tribology in the 80's, Volume II, NASA Conference Publication 2300, dated April 1983, pg 665-666.

M-3

# Organic Coatings Session M

## From Plating to Powder: How to Get Started in Powder Coating

Donald S. Tyler
Volstatic, Inc.
Florence, KY

**PAPER NOT RECEIVED IN TIME FOR PUBLICATION***

From Plating to Powder: How to Get Started in Powder Coating

Donald S. Tyler, Volstatic, Inc., Florence, KY

Environmental regulations, including those for handling effluent and complying with cradle-to-grave responsibilities for hazardous-waste disposal, have encouraged some electroplaters and allied finishers to branch into organic systems via the rapidly growing technology of powder coating. This presentation will highlight the benefits of these attractive, rugged, colorful, environmentally compatible organic finishes and itemize the elements of a modern powder coating line. Economic models will be emphasized.

* For copies of this paper, please contact the author directly

Mr. Donald S. Tyler
Volstatic, Inc.
P. O. Box 6150
Florence, KY 41042
(606) 371-2557

M-4

# Organic Coatings
# Session M

## The Power & Free Conveyor and Its Potential for Productivity Improvement

Theodore A. Tylman
Unibilt Division
Jervis B. Webb Co.
Farmington Hills, MI

# THE POWER & FREE CONVEYOR AND ITS POTENTIAL FOR PRODUCTIVITY IMPROVEMENT

Theodore A. Tylman
Unibilt Division, Jervis B. Webb Company
Farmington Hills, Michigan

The demand for higher quality, reduction in inventory, the many types of coatings that must be applied,- these and many other factors are driving surface coatings facilities planners to find and install manufacturing systems of higher levels of productivity than ever before. As they work to solve these problems they are finding that a key element in the solution is an improved material handling system. The material handling concept that is most often found to be the centerpiece of these systems is the power and free conveyor. This paper will describe this time-tested concept, show how it can improve product flow, help achieve better quality, lower inventory and reduce handling. It will examine several systems installations using power and free conveyors and indicate how creative design of layout and the use of automated control techniques have raised the levels of productivity for their users.

What are some of the current production practices in many surface coating facilities today? Here are a few that you may recognize.

1. Workers manually moving product from manufacturing areas into and out of the paint booth and/or dip tank for coating.

2. Product is manually loaded on an Overhead Monorail or floor conveyor to be pushed or pulled to and then through and from the coating application.

3. The transport of product from the manufacturing area on a continuous overhead or floor conveyor to and through the paint process. This type of powered system reduces manual handling of the product it's true, but it lacks the sophistication of design that will provide needed flexibility and speed.

These are a few concepts that have been and are presently being used in surface coating facilities. They contrast sharply with the material handling technology found in modern industry today and they must be replaced if these plants are to remain competitive in the marketplace.

The use of the power and free conveyor as the principal means of product handling in the surface coating facility allows greatly increased flexibility in the types of product

that can be handled, more flexibility of choice in the coating materials used and in the methods of their application. With power and free the variations in processing time required by differing coating methods can be accommodated without interruption of product flow. Improved handling reduces production costs through labor reduction, fewer rejects, higher quality and lower inventory requirements. The power and free conveyor can use overhead space for transportation paths and storage of work-in-process, as well as the empty racks and/or carriers when not in use. It is one of the most versatile and flexible of all conveying methods.

This type of conveyor is characterized by its two-track cross section in contrast to the more familiar straight overhead chain monorail conveyor.

The Monorail Conveyor Reviewed

First a brief review of the straight overhead system. In this type of conveyor only a power track is used. The carrier and their loads are suspended directly from the continuously moving power chain and are captive to it. The carriers must follow the path formed by the track and cannot be switched on to another path. Product must be unloaded and reloaded on to another overhead conveyor if travel to a different processing area is required. The carriers also must travel at a constant speed and cannot be halted, individually or in groups, without halting all carriers suspended from the chain. Although this type of conveyor has applications in the field of product painting or finishing the limitations of the design restrict its use to only the simplest of applications.

The Power & Free Conveyor

In the power and free conveyor carriers are not captive to the moving chain. They are suspended from trolleys that run in a second or free track usually mounted immediately below the power track. They are propelled along the free track by pusher dogs that extend from the power chain. These dogs can be disengaged from the free trolleys allowing the carriers and their loads to be halted individually or in groups without interrupting the movement of other loads on the conveyor.

Because the free trolleys carriers and loads are not captive to the power chain, they can be diverted through a track switch onto another spur, propelled by another powered chain, perhaps at a slower speed or into another type of process. As with the straight overhead or monorail conveyor, power and free systems can include vertical curves that allow loaded carriers to ascend to upper levels of the plant work space while on their way to other area.

The means of control of product movement in power and free systems is most often the programmable logic controller. Although the PLC is not a computer in the technical sense, it directs conveyor operation in a computer-like manner. The PLC will receive information regarding product flow from various

types of devices long the conveyor path and at work stations throughout the system. The PLC will respond to these signals by controlling the conveyor in accordance with a preset program installed in the PLC's solid state circuitry. In this manner, certain carrier loads will be switched into designated work stations or segregated by type, color or any other variable called for by the product mix. To facilitate this control, carriers are able to identify themselves or their loads by means of steel code cards mounted on each carrier.

As you can readily see the power and free conveyor is much more flexible in its application and is more suited to the more complex coating processes of today.

Case Study #1

A manufacturer of floor care and cleaning machines built a new facility to house its painting system. It needed a conveyor system flexible enough to transport metal parts through various paint operations. The choice was a 3" power and free conveyor. By using this conveyor the manufacturer has been able to route parts ranging from castings to sheet metal through approximately 30 different paths.

There are three (3) basic groups of parts: Castings, Metal Parts and Metal Parts with multiple colors. In this system all carriers carry a permanent code card identifying the carrier by number When a part is loaded on an empty carrier, the part number is keyed into a control panel and married to that particular carrier. Whenever the carrier code card is "read", the control system is able to identify the part being carried and will respond by automatically routing the part through the system so that the product will be coated with the proper finish.

Castings and Metal Parts

The pass through the paint system for both castings and metal parts is basically the same. After being loaded on to the carriers and their identity keyed into the central controller at the control panel, the parts are transported through a five (5) stage iron phosphate washer, dry off and preheat oven, one of three powder coat paint booth (white, black or multiple colors), and sent through a bake oven. After the bake oven the carriers are transferred to a cool down spur. Once the part has cooled sufficiently, the carriers are transported to an unload area. An average of 80 carriers an hour can be routed through the casting paint path.

Multiple Color Paint Parts

Metal parts with multiple colors follow a different path through the paint system. After the parts are loaded on to the carrier and identified to the central controller they are sent through the washer and dry off cycle; the carriers are next sent to a cool down loop where the parts are masked. The carriers then proceed through the powder paint booth where a

base coat is applied and then on to the bake oven. Before the carriers reach the bake oven, however, excess paint is vacuumed off in areas to be left unpainted. Upon leaving the bake oven the carriers are switched to a second masking loop before entering the wet paint booth for liquid stripping.

After the wet paint booth and demasking, the carriers once again are transported through a separate liquid bake oven and on to a cooling loop spur before being sent to an unload area.

Some features of this installation made possible by the use of power and free conveyors are carriers being stopped at load/unload and masking unload areas, and the rotation of the parts in liquid booths. Another feature is the conservation of carrier storage space by utilizing diagonal banking on 8" centers for the storage of 80 4' long carriers. The switching is mechanical, which allows fully automatic control into and out of the diagonal bank.

Case Study #2.

A manufacturer of very high quality brass products required a conveyor to handle a variety of rack designs carrying multiple products through protective coating process. This required the storage of 800 empty carriers that could be loaded and sent through the finishing system as required. As with the installation described above, power and free conveyors were chosen for this facility.

The systems begins with the diagonal bank storage of carriers holding empty racks 4' long in six separate lanes on 8" centers, thereby conserving much valuable plant space. Each storage lane is dedicated to a single rack style. The empty racks can be called out of storage in batches of six or less to one of eight load station spurs.

Seven of the eight load stations automatically send out six loaded racks to the paint system. The eight load stations can be set to handle batches from one to six as required. If racks are not required at loading, they can be sent back to empty rack storage. Loaded racks are conveyed at transportation speed to a stop just prior to transferring to the paint line conveyor.

The paint conveyor moves the rack through the process at a controlled speed and spacing. The speed is approximately 12' per minute with racks spaced at 5'-4" centers. The spacing is opened up when a different width rack is fed into the line, this allows enough time to adjust the spray gun setting in the booths to handle the narrow or wider width. The paint line conveyor goes through a hot degreaser, cool down chamber, two (2) automatic paint booths, a manual paint booth, flash off area, bake oven and cool down chamber. The carriers are held in tight bite throughout the paint line. If the degreaser does not meet the required quality the racks can be rerouted on a

recirculating loop back through the degreaser. Additional racks arriving at the paint area from loading are held back at the stop just prior to the transfer to the paint conveyor until the degreaser is brought back to acceptable operation.

Finished product is moved at transportation speed and switched into one of four unload station spurs. A stop at each of the unload stations disengages the carrier from the moving chain, allowing the manual unloading of the product. After each rack is unloaded, it is released from the stop by the unload station operator and is conveyed up a vertical curve to the mezzanine level for storage in one of the six (6) empty rack storage lanes.

For rack stripping, the last of the eight unload station is used for rack removal. With the system operation placed in special strip mode, carriers with empty racks are called out of one storage lane and transported directly to the unload station #8. Once the empty rack has been removed for stripping, the carrier - empty or with a clean rack - is released and transported back to the same storage lane on the mezzanine.

Case Study #4

The facility described in this Case Study paints front and rear plastic RIM facias for General Motors new GM-10 front-wheel-drive cars. The painted parts are delivered on a just-in-time basis to the assembly plant 12 miles from the paint facility. Here all of the production demands mentioned in the first paragraph of this paper are brought into play. High levels of quality and a reliable flow of product through the system made power and free a necessity in this recently completed plant.

In this instance the recently developed inverted power and free conveyor was chosen. With the inverted design the track cross section is reversed - that is, the free track is now above the power track and the product to be painted is carried above both of them. With this design the conveyor can become floor-mounted as well as travel overhead. Because the moving chain and all other conveyor components are below the product to be finished, surface contamination from overhead is virtually eliminated. Because there is no carrier arm holding the product from above, access by automated spray guns is unlimited. This inverted version retains all other power and free characteristics such as switching capability, halting at load stations, accumulation of empty carriers in a storage area, etc.

The facias are transported through the system on individual "bucks". The facility has two paint lines; a line for solid colors and a two-tone line, with crossover capabilities. Each line has two automatic basecoat booths and two automatic clear coat booths. The booths are separated by flash-off tunnels and are preceded by a vestibule containing an ionized air blow-off system to remove dust particles prior to painting.

The conveyor system is too complex to lend itself to a detailed description, however some of its features include:

* an empty buck storage area consisting of seven storage lines (50 carriers per line) with each line dedicated to a certain fascia style.
* air operated indexing conveyors that use cylinders to move the fascias through the paint booths.
* strip-out capability that allows carriers to be released from the paint booths and accumulated on-line without shutting down the entire system.
* a crossover feature that allows unpainted fascias to cross over to the second line for painting in the event that one of the lines becomes inoperative thus preventing interruption of production flow.

Summary

As can be seen from the case studies above, today's painting and surface coating facilities require automated material handling systems with routing flexibility, and controls at levels of sophistication previously not considered necessary. The power and free conveyor, in either of the configurations described, because of its two-track design, and because it lends itself so well to automated control, is an ideal choice for those facilities where high productivity levels must be attained and maintained.

M-5

# Organic Coatings
# Session M

## Thermal Insulation and Related Properties Of Organic Coatings

J.S. Chen, C.C. Chang
and T.S. Lee
Chung-Shan Institute of Science & Technology
P.O. Box 1-2-26 Lung Tan, Taiwan 32526
Republic of China

# Thermal Insulation and Related Properties of Organic Coatings

*J. S. Chen, C. C. Chang & T. S. Lee**

*Chung-Shan Institute of Science & Technology*

*P. O. Box 1-2-26 Lung Tan, Taiwan 32526*

*Republic of China*

**Scientific Resources, Inc.*

*1058 Whytecliff, Palatine, IL 60067*

*Abstract*

*Thermal insulation of organic coatings, epoxy resins and silicone rubbers, & its adhesions on aluminum and stainless steel are examined. Related properties such as thermoconductivity, specific heat, enthalpy change, weight loss upon heating etc. are also determined with the aid of DSC, TGA, TMA, and other instruments.*

## I. Introduction

*The purpose for applying thermal insulation coatings to a metallic surface is to minimize damage to the surface structure and internal parts caused by heat from flame, sun, friction and radiation. There are two types of polymers that are used as thermal insulation coatings. One is the organic-inorganic copolymer which has a silane structure and usually is the silicone rubber type of polymer. The other is organic polymer which is mainly epoxy type thermosetting plastics. The physical and chemical stability on heat resistance of these polymers depend on the inorganic structure and filler in them.*[1][2] *Thus, for thermal insulation coatings the heat resistance of silicone rubber is better than that of epoxy thermosetting plastics because the former contains silicon. Howerer, there is no direct or quantative comparison of the thermal resistance between these two types of polymers in the literature. The purpose of this paper is to compare the heat resistance and other related properties of these two types of polymers on a few selected coatings in the heat resistance*

temperature range referred to JIS K-5400*. Because adhesion is an important physical property of the coatings. The other purpose of this paper is to compare the adhesion of these coatings on aluminum and stainless steel substrate after various pretreatment and its relationship between the physical property and the thermal properties (thermal insulation and heat resistance).

## II. Experimental

The materials of thermal insulation coatings selected for this study on both silicone rubber and epoxy type polymers and its manufacturers are listed below:

(1) Silicone rubber (SR), GE RTV 630.

(2) Silicone rubber (SV), Dow Corning ERTV.

(3) Silicone rubber, talc filled (TR), a mixture of 40 phr talc, 325 mesh E-Thim Co. of Korea, in silicone rubber SR.

(4) Polysulfide epoxy resin (SE), FMI Flexfram 605 TH.

(5) Polyaminoamide epoxy resin (AE), home made by the Institute E-22 and E-23.

(6) Ablative coating (AC): Desoto 790-005.

The experimental procedures for the study is outlined in a flow chart as shown in Fig.1. The Fig.1-a is for the adhesion test and Fig.1-b is for the thermal analyses. Other experimental details that are not shown in the flow chart are described under the following headings.

### 1. Adhesion Test (Fig.1-a)

Both aluminum (2024-F) and stainless (304) are used as the substrate, 152 x 76 x 0.5 mm; and one of the following pertreatments is applied to one of the substrates at random: anodic, chromate conversion, chemical passivation, and glass or emery blasting. The primers applied to the substrate after pretreatments is epoxy resin or zinc chromate filled polyvinyl-butyral resin. The film thicknesses of the thermal insulating coatings under tests are: SE, 350-464 u ; AE, 120-142 u ; AC, 170-238 u and SR, 103- 121 u.

*JIS K-5400, Japan Industrial Standard K-5400, heat resistance temperature is the temperature when thermal insulation coatings loss its practical heat-resistance function.

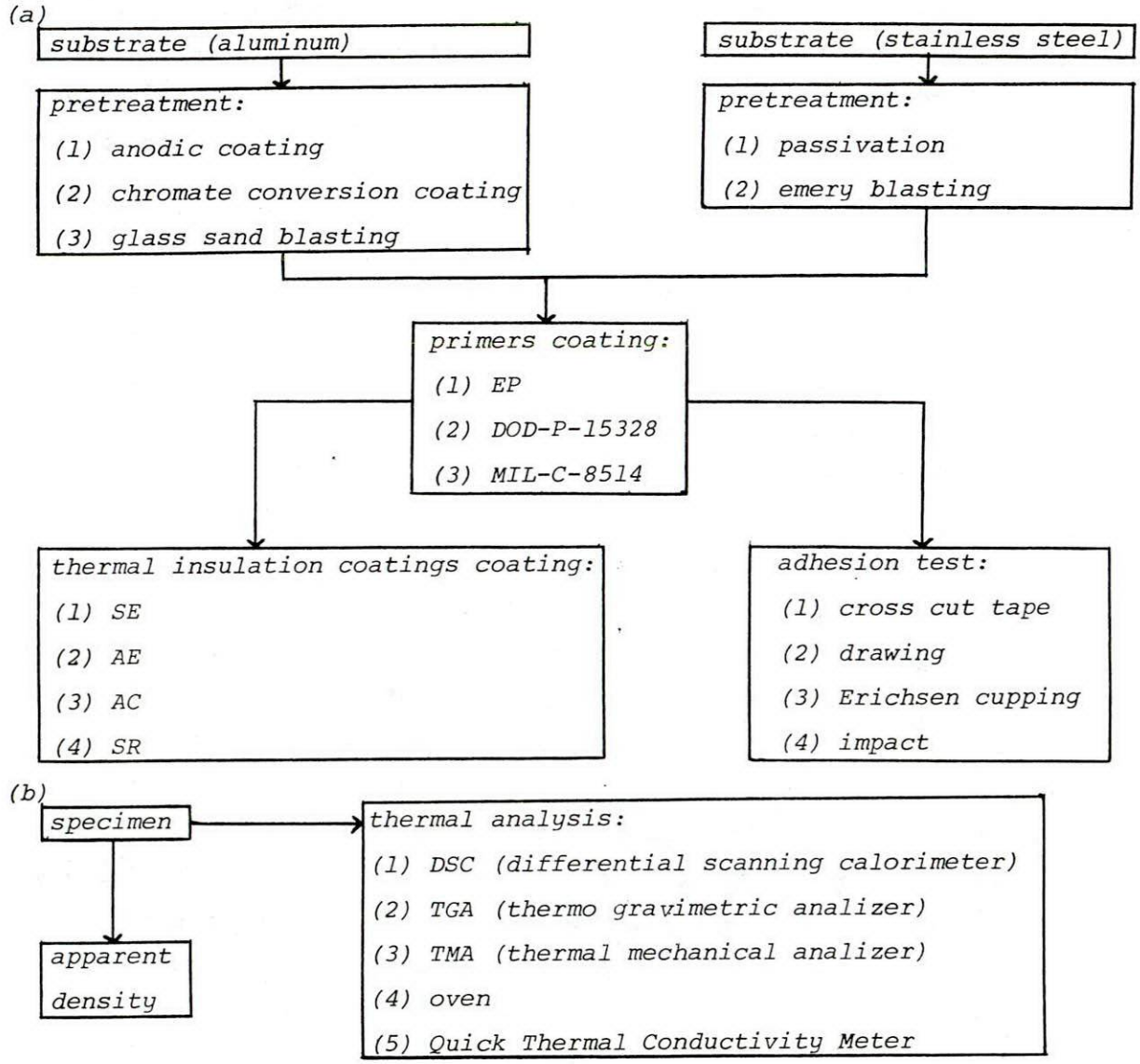


*Figure 1. Experimental flow chart*

*(a) adhesion test*

*(b) thermal analysis test (thermal insulation and heat resistance).*

*The tests described below are applied to each of the coatings on the aluminum as well as the stainless substrate. (a) Cross Cut Tape Test, following the procedure given in CNS 10756 and K6800[3], brittleness and adhesion of the film is determined by cut squares as described in ASTM D3359-83.[4] (b) Drawing Test, following the procedure given in*

JIS K-6894[5] and using 1200g loaded needle, hardness and adhesion of the film is determined. (c) Erichsen Cupping Test, following the procedure given in ISO 1520[6], elasticity and adhesive quality is determined. (d) Impact Test, following the procedure given in JIS K-5640[7] and CNS 10756 and K6800[3], toughness and adhesion of the film is determined.

2. Thermal Analyses (Fig. 1-b)

For thermal analysis, the tested materials are coated on a glass plate, 150 x 70 x 2 mm, without primer in the following thickness.

(a) for heat resistance test: SE, 450-514 u ; AE, 320-410 u ; AC, 210-250u ; SR, SV and TR, 500-1300 u.

(b) for thermoconductivity test: a minimum of 6 mm thickness is made for all coatings.

(c) for instrumental analysis: cut out about 1 gr. of the coatings ftom the specimen mentioned in (a) or (b).

The apparent density is determined by using Archimede's principle to immerse the specimen into D.I. water or n-heptane.

The DSC tests are determined by using a Perkin-Elmer DSC-2C instrument applying a heating rate of 10°C/min. The TGA tests are determined by using a Perkin-Elmer TGS-2 instrument on a heating rate of 10°C/min. The TMA test is done under a 10g load at different temperatures by applying a heating rate of 10°C/min employing Perkin-Elmer TMS-2 instrument. The last test will give the softness of the materials and its response to the heat applied. The heat resistance test is done by following the procedure given in JIS K-5400[8]. The tested materials are coated on a glass plate, then put into a constant temperature oven. After in the oven for a certain period of time and taking out staying in the air for one hour, observe the change on the specimens' surface and compare it with the standard. The thermoconductivity of the specimen is measured by using a Shotherm QTM-D2 thermal conductivity meter made in Japan following the procedure described in ASTM C 177[9].

III. Results and Discussion

Since the adhesion tests of the thermal insulation coatings are not done on the bare metal surfaces, a layer of primer is applied to the metal surface first before applying the coatings. Three different commercially

available primers are used for this purpose. One is a U.S. product and two are domestic products made in Taiwan. The absorption, wettability and mechanical adhesion of these primers to the metal surfaces are very good and conform to the Adhesion Theory[10][11].

The detailed adhesion test data of the coatings will not be given here. Only a summary of the test result is described. In general, the adhesion of silicone rubber on a non-silane primered surface is not as good as the epoxy resin on the same primered surface. However, the situation can be improved by using a silane primer when the silicone rubber is applied.

From the four adhesion tests, cross cut tape, drawing, Erichsen cupping and impact, the related physical properties of the coatings can be arranged in a decreasing order as follows. For the elasticity as well as the toughness the order is SR, AE, SE, AC. For the hardness, the order is AC, AE, SE, SR. This is due to different chemical structures of the coatings. Silicone rubber (SR) possesses the quality of an elastomer, therefore, it is the most elastic and the most tough but the least hard materials in this series of coatings. Polysulfide epoxy resin (SE) has a long chain of polysulfide which similar to that of vulcanlized rubber, thus, it has the property of toughness as the rubber. Polyaminoamide epoxy resin (AE) also has a long chain structure but it differs from that of the vulcanlized rubber, hence, it is relatively more tough. Ablative epoxy resin (AC) is the hardest and the most brittle material in this series of coatings because the base resin or the curing agent belongs to the group of short-chain or aromatic compound.

The physical properties of these coatings can be changed by adding filler to them. As an example, the mechanical strength of polysulfide epoxy resin is increased about 30% while its strain is decreased about 150% by adding 20% carbon fiber[12]. In our experiments, we found that the relatively soft and elastic polyaminoamide epoxy resin can become harder and more brittle after adding $ZrO_2$ or $TiO_2$ into it.

In addition to the four materials used for the adhesion test that stated above two more materials, a silicon rubber (SV) from a different manufacturer and a mixture of 40 phr talc and the rubber SR (TR), are

added to the group to perform heat resistance test and instrumental analysis in order to determine their thermal properties and apparent density. All the six materials are subjected to instrumental analyses by using DSC, TGA, TMA and thermal conductivity meter. The results are shown in Table 1. The results of heat-resistance of all the materials, which based upon the procedure of JIS K-5400, are shown in Table 2. All the graphs produced by DSC, TGA and TMA will not be shown here. Only selected few are given to illustrate how the data were obtained. The Fig.2 is the enthalpy change against temperature for the ablative epoxy resin obtained by DSC at a scan rate of 10°C per minute. From the figure one can see that below 364°K as well above 385°K the slope of the curve is not steep which represents only heat transfer between the heat source and the tested material. The peak between this two temperatures is an indication that the tested materials undergo some kind of chemical change which absorbs heat (endo) at an average value 4.21 cal/gm. Begining at the temperature of 690°K the slope of the curve increases very rapidly that indicates decomposition of the tested material by absorbing a relatively large quantity of heat. The Fig.3 is also plotted by DSC for talc-filled silcone rubber to obtain specific heat of that material. The dotted line in this figure stands for culmulative endothermal quantity per gram from which the average specific heat of that material can be obtained. The average specific heat for the material is obtained at a temperature range that no or very little chemical reaction takes place. The Fig.4 is a plot by TGA for polyaminoamide epoxy resin. The solid line represents the percentage of the material remained at a particular temperature. One can see that at 301°C the remaining weight is about 95% of the original. between 301° and 485°C there is a big weight loss occured which represents cheminal decomposition. The dotted line is a derivative of the solid line from which the percentage change of the weight loss cam be easily obtained. The Fig.5 shows the dimension change of polysulfide epoxy resin at different temperature obtained by TMA. From the figure one can get some idea on dimension change, softness, expansion and penetration of the material at certain temperature. At the temperature when the 10g loading needle of the instrument penetrates the coating, it is called penetration temperature. In Fig.5 it is at 291°C. Just before the point of abrupt

change of slope, the temperature is called heat-tolerance temperature. It is 285°C in Fig.5.

From Table 2, the heat-resistance properties determined by following the procedure of JIS K-5400, one can see that the property of the material AE, AC and SE are below 200°C while those of SR, SV and TR are up to 300°C. This is because the former group of material are organic polymers which are easily carbonized by applying relatively small amount of heat to them. The latter group are inorganic-organic silane polymers which usually have better thermal stability[1]. In practical applications, nevertheless, the heat-resistance temperature of these materials can be shifted to a higher value without jeopardizing its thermal insulation function if one can tolerate a little color change and dilation. If so, the heat-resistance temperature of the materials AE, AC and SE can be lift from below 200°C to about 300°C and that of SR, SV & TR can be lift from 300°C to around 400°C. From the heat-resistance data listed in Table 2, in combination with the thermal properties of these coating materials listed in Table 1, one can arrange an overall heat resistance comparsion. In a decreasing order, it is TR, SR, SV, AE, SE, AC. This order, in comparsion with that in the adhesion test on the elasticity and the toughness, is consistent. There is a correlation between the adhesion tests as well as heat resistance test, which is done under a practical application condition using relatively a large amount of material, and instrumental thermal analyses, to which only a small amount of material is needed. In the adhesion test, the ablative epoxy resin (AC) is the hardest and most brittle material. In the heat-resistance test and instrumental thermal analysis, it has the lowest heat tolerance temperature, the lowest peneteration temperature and the most weight loss and is one of the worst heat-resistant materials. On the other hand, the mixture of silicone rubber & talc (TR) has the highest heat tolerance temperature, the highest penetration temperature and the least weight loss and is one of the best heat-resistant material. Even though there is no data shown on the adhesion test for this material (TR) in this study, it is known that this kind of material is a strong composite against heat[2] and could not be easily crushed and producing cracking[13], a good heat-resistance

material.

As to the thermal insulation is concerned, it is a general knowledge that a material which has a high specific heat and low thermoconductivity is a good thermal insulating material. With reference to the Table 1, one can see that this is the case. The ablative resin (AC), which has the highest value of specific heat 0.614 and the lowest value of thermoconductivity, 0.120 at 100°C, is the best thermal insulating material among those material listed. In addition to that, it has a low value of apparent density and heat tolerance temperature. From this it appears to be that the values of apparent density[14] and heat tolerance temperature could be used to correlate and evaluate the thermal insulating materials. If one separates these six materials listed in Table 1 into two groups according to their heat-resistance property listed in Table 2. One group is these materials its heat resistance temperature is practically below 300°C, i.e. AC, AE, & SE. The other group is those materials its heat resistance temperature is practically around 400°C (SV, SR & TR). One can see that, among the higher heat resistance temperature group, the talc filled silicone rubber (TR) has a high value of apparent density, 1.412, and a high value of heat tolerance temperature, 411, it is not a good thermal insulating material even it is the hardest material in this group. In the low heat resistance temperature group, AC, AE and SE, the same is true. The ablative resin (AC) is the good insulating material in this group because it has a low value of both apparent density and low heat tolerance temperature. The possible reason for this correlation is that a low value of apparent density indicats that it has a high volume in a unit weight. When heat flows through this material, since a good thermal insulating material has a low thermoconductivity, the heat energy will stay on the outer layer of this material. A good thermal insulating material also has a low heat tolerance temperature, when the heat stay on the outer layer for certain length of time it will soften the outer layer. When time goes on, this layer may even be deterioated by absorbing more heat and produce some product that may have a lower value of thermoconductivity, hence, become a good thermal insulating material. A case in point is the ablative resin (AC), its delaminating nature of the

outer surface when subjected to the heat is a good example of this explanation.

## IV. Summary

1. There is a direct correlation between the overall heat resistance and the elasticity as well as the toughness of the thermal insulating coatings in different chemical structures and compositions.

2. Besides the effect of thermoconductivity and specific heat, heat tolerance temperature, apparent density, and the hardness of a thermal insulating coating is inversely proportion to the quality of its thermal insulation function. The lower the heat tolerance temperature, the lower apparent density, and the harder of the material, the higher the thermal insulating function is.

## V. Reference


1. D. C. Miles and J. H. Briston, "Polymer Technology", Chemical Publishing Co., Inc., N.Y. (1979).
2. L. Mascia, "The Role of Additives in Plastics", Edward Arnold LTD, London (1974).
3. Chinese National Standard 10756, K6800.
4. ASTM D3359-83.
5. Japanese Industrial Standard K-6894.
6. International Organization for Standardization 1520.
7. Japanese Industrial Standard K-5640.
8. Japanese Industrial Standard K-5400.
9. ASTM C 177.
10. Derek Hull, "An Introduction to Composite Materials", Cambridge University Press, Cambridge (1981).
11. D. M. Brewis, "Surface Analysis and Pretreatment of Plastics and Metals", Applied Sci. Pub. LTD, London (1982).
12. B. D. Agarwal and L. J. Broutman, "Analysis and Performance of Fiber Composite", John Wilky and Sons, Inc., New York (1980).
13. Oil and Colour Chemist's Association, Australia, "Surface Coatings", Chapman and Hall, N. Y. (1983).
14. W. L. McCabe & J. C. Smith, "Unit Operations of Chemical Engineering", McGraw-Hill Book Co., N. Y. (1976).

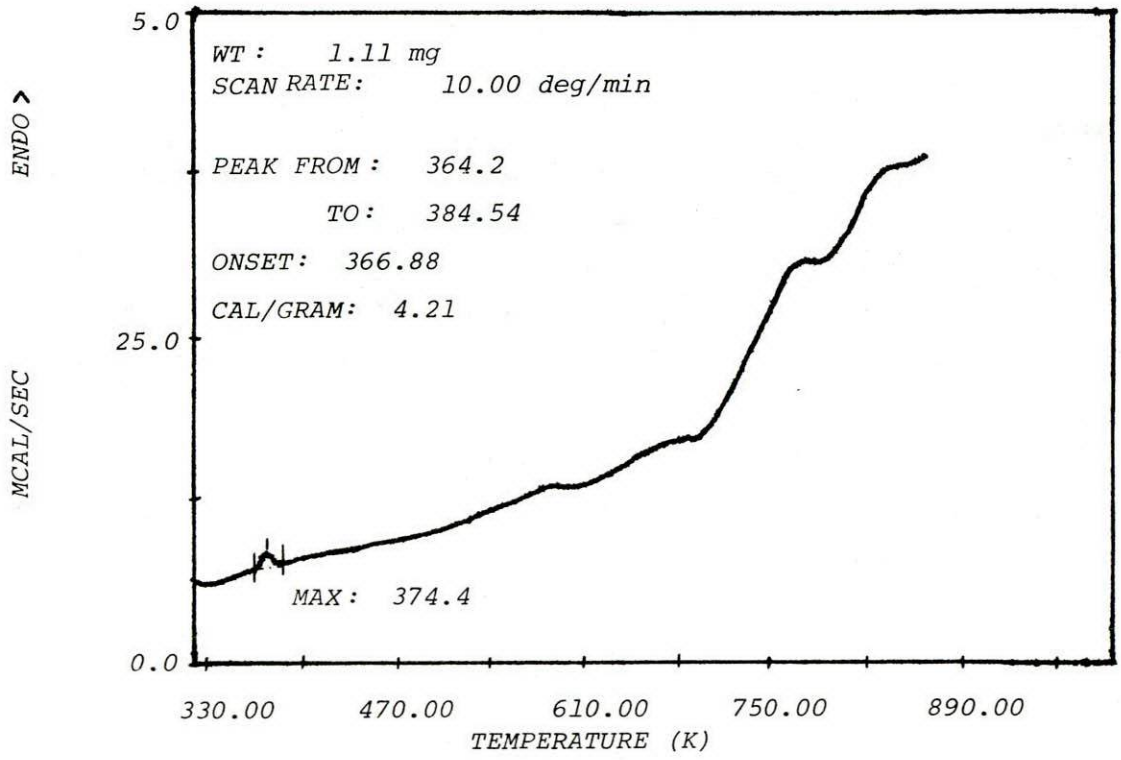


*Figure 2. Enthalpy change vs. temperature curve for ablative epoxy resin by DSC*

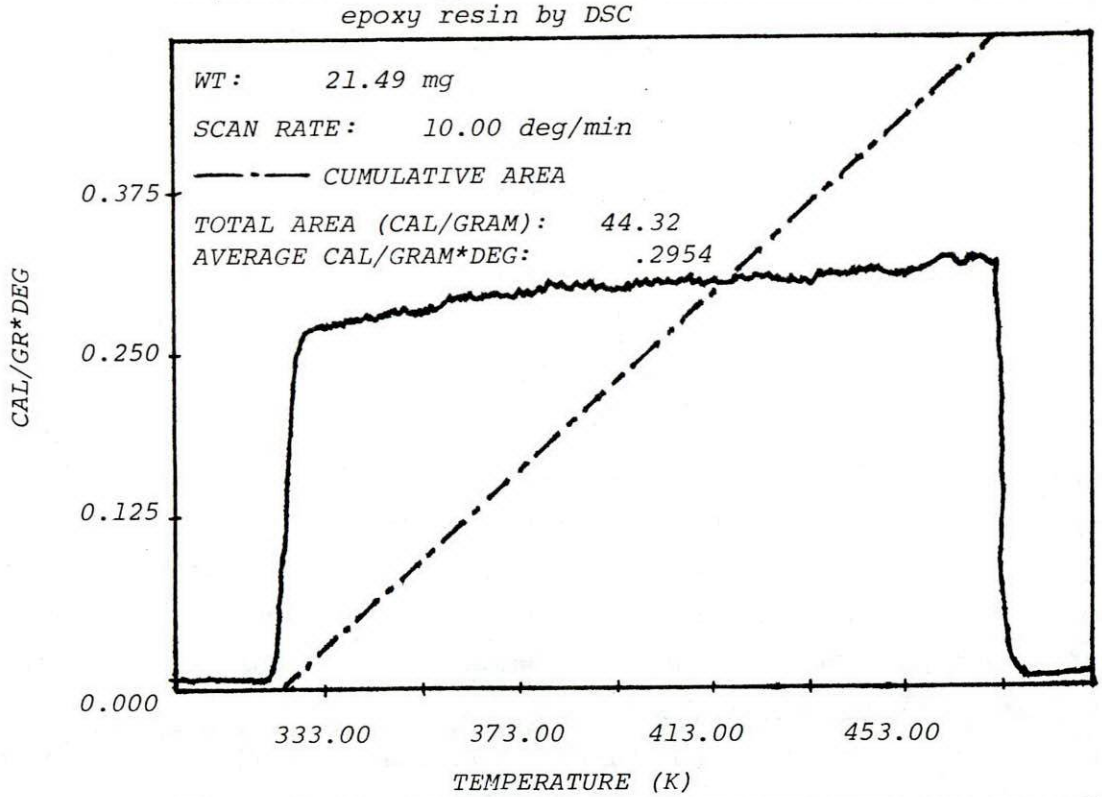


*Figure 3. Specific heat vs. temperature curve for talc-filled silicone rubber by DSC*

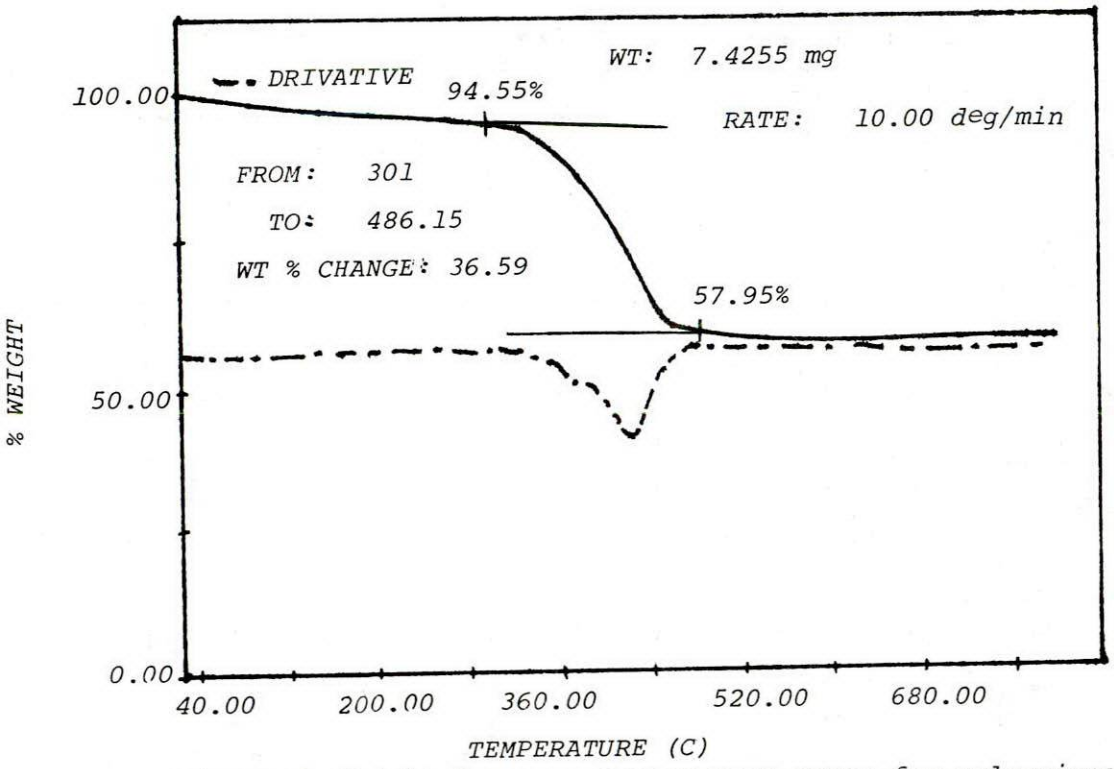


Figure 4. Weight loss vs. temperature curve for polyaminoamide epoxy resin by TGA

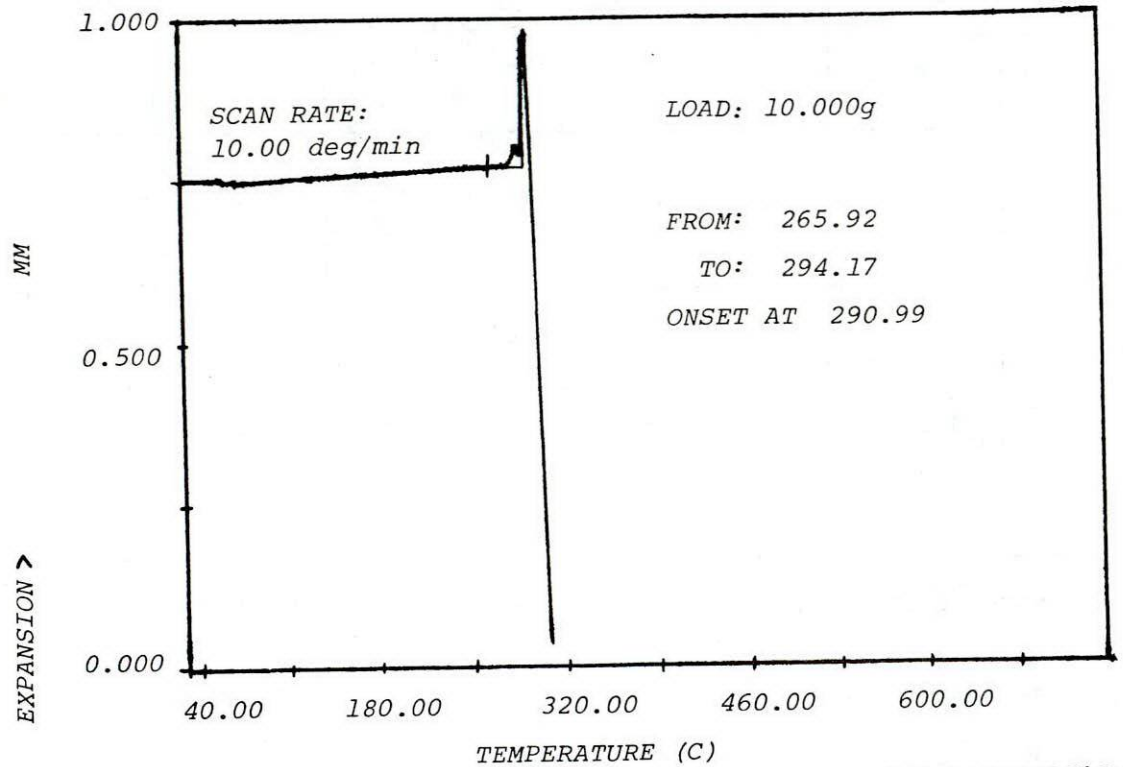


Figure 5. Dimension vs. temperature curve for polysulfide epoxy resin by TMA

Table 1. Apparent density and related thermal properties of thermal insulation coatings

| coatings* / properties | AE | AC | SE | TR | SR | SV |
|---|---|---|---|---|---|---|
| apparent density (g/ml) | 1.751 | 0.745 | 1.289 | 1.412 | 1.252 | 1.115 |
| specific heat (cal/g.°C) | 0.317 | 0.614 | 0.486 | 0.295 | 0.234 | 0.241 |
| weight loss(%) | 36.6 | 86.2 | 50.1 | 15.4 | 21.9 | 39.6 |
| @start temperature(°C) | 301 | 210 | 224 | 51 | 253 | 186 |
| @end temperature(°C) | 486 | 515 | 563 | 789 | 797 | 797 |
| heat-tolerance temperature(°C) | 318 | 270 | 285 | 411 | 360 | 371 |
| pentration temperature(°C) | 349 | 286 | 291 | 476 | 428 | 415 |
| thermocon-ductivity (Kcal/m.h.°C)at | | | | | | |
| 25°C | 0.789 | 0.127 | 0.240 | 0.414 | 0.241 | 0.176 |
| 100°C | 0.691 | 0.120 | 0.221 | 0.378 | 0.226 | 0.168 |
| 180°C | 0.612 | — | 0.180 | 0.366 | 0.176 | 0.162 |

*AE: polyaminoamide epoxy resin.
AC: ablative epoxy resin.
SE: polysulfide epoxy resin.
TR: talc-filled silicone rubber.
SR: silicone rubber.
SV: silicone rubber.

Table 2. Heat-resistant properties of thermal insulation coatings (based on JIS K-5400)

| Temperature (°C) | time (min) / phenomina* / coatings** | AE | AC | SE | TR | SR | SV |
|---|---|---|---|---|---|---|---|
| 200 | 2 | E,Y | E,Y | E,Y | 0 | 0 | 0 |
| | 10 | E,Y | E,Y | E,Y | 0 | 0 | 0 |
| 300 | 1 | Bl,Y | Bl,Y | Bl,Y | 0 | 0 | 0 |
| | 10 | Bl,Y | Bl,Y | Bl,Y | Y | Y | Y |
| | 15 | B | B,R,Bl | B,Y,E | Y | Y | Y |
| | 20 | B | B,R,Bl | B,E | Y | Y | Y |
| 400 | 1 | Y,D | Y,E | Y,E,D, | Y | Y | Y |
| | 2 | $ | $ | $ | Y | Y | Y |
| | 5 | — | — | — | Y,E | Y,E | Y,E |
| | 10 | — | — | — | C | C | C,D |
| | 15 | — | — | — | C | C | D,P |
| 500 | 1 | — | — | — | Y | Y | Y |
| | 2 | — | — | — | Y | Y | Y,D |
| | 5 | — | — | — | C,Bl | C,Bl | C,D |
| | 10 | — | — | — | C | $ | $ |
| | 15 | — | — | — | $ | — | — |

**AE: polyaminoamide epoxy resin.
AC: ablative epoxy resin.
SE. polysulfide epoxy resin.
TR: talc-filled silicone rubber.
SR: silicone rubber.
SV: silicone rubber.

*0: without any change.
Y: becoming yellow.
B: becoming black.
R: becoming red.
Bl: blistering.

E: blustering.
C: crazing.
D: delamination.
P: crushing.
$: burning.

# M-6

# Organic Coatings
# Session M

## A Novel Alternative to Decorative Brass Electroplate

Michael P. D'Angelo
Market Manager, Metal Finishing
MacDermid Inc.
245 Freight Street
Waterbury, CT 06702

# A Novel Alternative to Decorative Brass Electroplate

Michael P. D'Angelo
Market Manager, Metal Finishing
MacDermid Incorporated
245 Freight Street, Waterbury, CT, 06702

David Hurwitz
National Sales Manager
DeSoto Incorporated
1700 South Mount Prospect Road, Des Plaines, IL 60017

Electrocoating, the electroless deposition of paint, is similar to electroplating but differs in that organic resins are deposited instead of metal ions. In industrial applications, electrocoating continues to thrive as a method of applying an organic finish, and smaller volume finishing operations are converting to electrocoating because of productivity, performance and environmental compliance. A new automated E-coat system costing about $300,000 can often be justified for a production level of less than 5,000,000 sq ft/year. This fact has opened new markets for E-coat finishes. One application that is gaining much attention is the potential replacement of brass plating with an electrocoated finish.

## Background

Metallic coatings are used to provide functional or aesthetic qualities not achievable with the base metal alone. Once plated, the base metal provides physical or load bearing properties at a reasonable cost. The plated metal coating imparts corrosion, wear resistance or aesthetic qualities to the composite structure. In recent years, the plating industry has come under strict government scrutiny for environmental, safety and health problems. New plating chemistries and processes will address some of the demands being placed upon the plating industry, but other finishing processes will replace electroplating for certain applications.

## The Environment

Looking first at environmental and safety issues, metal finishers are subject to EPA compliance regulations for water pollution reduction under the metal finishing section of the Code of Federal Regulations (CFR) (40CFR433) promulgated in 1983 and the electroplating section (40CFR413). They are further controlled by local requirements for wastewater treatment facilities.

The Clean Air Act of 1970, Section 112, allows the EPA to propose national emission standards for hazardous air pollutants. The EPA places importance on state regulation of toxic air pollutants, and metal finishers must consult with their own local authorities.

Hazardous waste is a third area of concern to the metal finisher, even if he is below the 100 to 1000 kilograms per month level fully regulated under the Resource Conservation and Recovery Act of September 1986.

Small quantity generators are required to determine if their waste is hazardous and dispose of it properly per regulation 40CFR262.44. This includes obtaining an EPA generator identification number, certifying on a uniform hazardous waste manifest that a waste minimization program has been implemented and assuring that waste is being shipped only to a permitted or "interim status" facility.

In summary, metal finishers are coming under close scrutiny and will have to incur the increased costs of proper disposal of process wastes unless they find ways to produce their finished goods via other processes.

One last area of government regulation is the implementation on May 25, 1986, of the OSHA "Hazardous Communication Standard" under Title 29, Code of Federal Regulations Part 1910.1200. These regulations preempt state and local right-to-know laws affecting industries listed under SIC Codes 20-39, and require an employer to teach employees about the hazards inherent in the use of materials found in their facility.

This review of applicable government regulations is not intended to be a definitive report. It is presented as an overview of the problems facing electroplaters that will provide the impetus to evaluate alternative manufacturing processes.

The brass plater is confronted with all of the above mentioned regulations: air pollution control, water pollution control, hazardous waste treatment and disposal, and training under right-to-know laws. Of particular concern to the brass plater is the handling and disposal of cyanide chemicals and the elimination of volatile organic compounds (VOCs) associated with the lacquering of solid brass and brass plated articles.

## Brass Plating Review

Most brass plating is done for decorative purposes. Brass is plated over zinc and aluminum castings, steel stampings and tubing, with these combinations often replacing solid brass for cost and weight reduction. Most brass plating systems in use today deposit a very thin layer which will not level the basis metal. Relatively thicker deposits are used where brushing, tumbling, coloring or antiquing operations will be performed after plating for aesthetic reasons. Because today's brass coatings are very thin, the appearance of a "flash" brass finished item depends upon the surface condition of the basis metal. Production of most decorative parts involves the deposition of a bright nickel layer which levels the surface before flash brassing to produce a bright brass appearance. Subsequently, the parts are coated with either a solvent or waterborne organic lacquer by spray or dip coating methods to protect the brass layer from tarnishing. This process is widely used to finish wire goods, household items such as lamp parts, furniture, locks, and hardware.

## Market Overview

The replacement of a decorative flash brass coating and lacquer topcoat with a single electrocoat finish is proposed as a commercially viable and desirable new use for electrocoating technology.

Attempts to replace lacquers with clear anodic electrocoat finishes over brass in the lighting fixture industry were unsuccessful because of electrolyte attack on the brass surface. The effect was a loss of the bright brass appearance due to hazy films. More recently, both a European and an American manufacturer of plating materials have marketed a clear anodic electrocoat system for application over bright nickel with a subsequent dip dye step to achieve a brass appearance finish. Custom plating operations employing this process are reported to produce an aesthetically pleasing and durable finish. The fresh electrocoat layer may be colored in a variety of dip-dye baths before baking, enabling the custom plater to provide a wide range of custom color finishes.

The application of a transparent tinted electrocoat finish over a bright nickel surface achieves the same aesthetic qualities as the above mentioned process, and for the brass plater eliminates the various conditioning and dyeing steps that follow the actual electrocoating procedure.

The electrocoating process provides many benefits for the decorative metal finisher. First, the cyanide plating process is eliminated. Second, the dip or spray application of lacquers is eliminated. If solvent-borne lacquers have been used, a VOC reduction is achieved, and improved performance can be achieved versus most of the current commercial water-borne topcoats. The lacquering process is also characterized by nonuniform film build, pin holes, tear drops, and runs and sags. The application of a finish by electrocoating techniques produces a very uniform, pin-hole free film that is devoid of runs and sags. The thermoset nature of an electrocoat finish gives it better abrasion resistance and chemical resistance when compared to most dip or spray coatings currently in use. The elimination of the flash brass layer means that any scratch down to the metal will expose a bright "white" substrate which will not tarnish to produce an unsightly black mark. Last, the corrosion resistance of an electrocoat finish over bright nickel will be far superior to that provided by a flash brass plus lacquer combination. More information on this topic will be presented in the discussion of laboratory test results.

## Understanding Electrocoating

### How are Electrocoat Paints Formulated?

Electropaints contain a basic resin system, a cross-linker, pigments, solvents and additives. In addition, electrocoating paints must contain a solubilizing agent to render them either water soluble or water dispersible. In anodic electrocoat systems, the solubilizer is a base; the cathodic process requires an acid.

The vehicle or resin portion must provide performance properties both during the coating process and after baking, such as hardness, flexibility and corrosion resistance. Typical generic vehicles are epoxies and acrylics. The vehicle must be chosen carefully for resistance to hydrolysis and degradation.

The solvents used in electrocoat formulations are usually water-miscible alcohols and glycol ethers. Besides controlling the viscosity of the feed material, solvents also play a role in how the film builds. The more water-insoluble the solvent, the higher the film build capability.

Pigments contribute to the electrocoat properties, to the stability of the bath, and must also be free of ionic impurities. Any ionic contamination of the bath will cause severe coating problems.

The solubilizing agent for the vehicle is chosen on the basis of two factors: 1) its ability to disperse the system and produce a stable product in water, and 2) its effect on the electrocoated film. In anodic systems, amines are usually chosen as solubilizers. In the cathodic process, organic acids are most often used as solubilizers.

Electrocoating is both electrolytic and electrophoretic, since the bath contains species of both ions and colloidal particles. When a DC voltage is applied to a bath, the particles migrate toward the electrode of opposite charge. In the anodic system, the solubilizer migrates to the cathode, and the vehicle migrates to the anode.

The cathodic electrocoat process is the opposite. The cathode becomes the workpiece or the coated object.

During electrocoating, the insoluble material is deposited on the workpiece at the areas of highest current density. Since the film is electrically resistive, it forms a barrier to further deposition and the coating proceeds into recesses and around to the back of the workpiece. This ability to penetrate recesses and deposit uniformly is called throwing power. This property is the single greatest reason for the popularity of electrocoating.

Deposition occurs in a very short time period, with the majority of the coating deposited in the first few seconds. Typical coating times are in the 60- to 90-second range. This allows water deposited with the coating to migrate out of the film, giving a high-solids (90+ pct) coating that is less prone to film defects during baking.

The deposited electrocoated film has a special property not normally encountered in other application methods. This is the flat appearance of the coating immediately after deposition. This low gloss is caused by a very porous film, a result of gas bubbles formed during deposition becoming trapped in the film. Baking is usually necessary to eliminate these pores and produce a continuous film with high gloss.

Upon removal from the bath, parts that have been electrocoated contain a water-insoluble electrodeposited film and a water-soluble bath drag-out. In order to obtain perfectly smooth films, it is necessary to remove this dragged-out paint. In the early days of electrocoating, this was accomplished by rinsing the part with D.I. water. The rinse water was either flushed to drain, creating a water pollution problem, or the paint was flocculated, floated and skimmed, then put in drums for disposal. In either case, a loss of valuable paint solids resulted. Losses of up to 40% were observed on some parts, depending on their configuration.

The development and introduction of ultrafiltration (UF) to the electrocoat system not only solved the waste problem, but also gave users a means of controlling the tank for excess conductivity, water-soluble contaminants and solvent levels.

The UF process utilizes a semi-permeable membrane, which is affixed to a porous backer. The membrane readily allows small molecules such as water, solvent, solubilizer and ionic salts to pass through while retaining the larger molecules and micelles. The liquid passing through is called permeate.

Typical permeate composition is 95% water, 4% solvent, 1% solubilizer, and traces of ionic contaminants. By discarding the permeate to drain, it is possible to control the water-soluble constituents in the bath. The most attractive and economical feature of UF, however, is its use in closed-loop rinsing.

The amount of permeate required to effectively clean the parts depends on a variety of factors, including line speed, surface area of work coated, part configuration, and number of rinse stages. However, a rule of thumb is two gpm of permeate for each 100 sq ft of work.

Equipment Considerations

Electrocoat tanks are normally constructed of mild steel or black iron. The interior of the tank is coated with chemical-resistant and electrical-resistive coating. The use of copper, brass, aluminum or galvanized metal is not recommended since these metals react with the paint. Tank size is based on having a 90-second immersion time at top conveyor speed. Molded polypropylene tanks will work in small sizes.

Typical E-coat systems are designed to filter tank contents by diverting some circulating bath through a cartridge or bag filter. Filter media should be a water-insensitive material such as polypropylene sized at 50 to 100 microns.

Both the anodic and cathodic systems operate in a bath temperature range of 75 to 90°F. The cooling unit must be capable of holding this temperature under full load. Due to the acidic nature of cathodic systems, stainless steel is recommended for use in the heat exchanger.

Stainless steel electrodes are recommended for use in both anodic and cathodic systems. A 1:4 ratio of electrode-to-work surface area is suitable.

A rectifier giving 0 to 50 volts should be sufficient for most coating needs. Amperage requirements will vary with production, temperature, film thickness requirements and voltage. Most electrocoat products require 2.0 to 2.5 asf to deposit 1.0 mil/min.

The purpose of bath replenishment is to replace components lost through deposition and drag-out. Replenishment materials are either one-component formulations or two-component systems consisting of resin and a pigment-rich portion. One-component replenishment is fully formulated by the supplier.

One-component replenishment is usually pumped directly into the intake with a low pumping rate to match solids usage or it is automated with an amp-hour meter.

E-coat operation is not complex, but requires a trained operator. Most coating manufacturers provide a list of QC equipment and supplies needed to operate the tank. Training is typically provided to ensure smooth, trouble-free operation.

## Bath Controls and Contamination

Paint bath solids must be controlled. Too-high solids result in excessive drag-out; too-low solids result in poor film properties. Bath solids should be kept within a narrow range specified by the paint supplier. Other parameters such as pH, conductivity and amine concentrations are important, but do not vary as readily as bath solids.

In addition to regularly checking the solids, pH, conductivity and MEQ concentrations, one should check periodically for the pigment/binder ratio, the resin ratio (if more than one resin is present) and the organic solvent content. These are usually done by the paint supplier.

Contaminants may be water-soluble or water-insoluble. As mentioned earlier, the most frequent water-soluble contaminants are salts carried into the tank from the pretreatment and cleaning stages. Thorough rinsing with deionized water reduces this carry-in. Ultrafiltration may be used to remove dissolved contaminants from the electrocoat tank.

Water-insoluble contaminants may enter the tank via improperly cleaned metal or drippings from the conveyor. This type of material may cause cratering or other problems in the paint film. Usually, when such a source of contamination is removed, the corresponding problem also disappears.

Electrocoating, like any other painting process, is not without its share of problems. However, it does offer excellent coating efficiencies and a quality product. It may be said that when electrocoating operates trouble-free, no other process can match it.

Electrocoating will not replace flash brass plus lacquer finishes in all applications. This discussion is presented to generate interest in the concept and to expand the evaluation of its benefits in the variety of commercial decorative brass plating applications.

The electrocoating process does require a separate finishing system, as described above, from the nickel plating line, whereas the flash brass plus lacquer process is usually placed in-line with the nickel on a continuous plating system. Separation of the electrocoating system from the plating line is an important step in minimizing the potential contamination of the electrocoating bath with ionic drag-out from the plating system.

Also, the vinyl coated racks typical of many plating systems may become pitted, with the pits acting as containers for plating solutions which may not get properly cleaned out during the rinsing steps. The racks also limit the baking temperature for the electrocoat to about 325°F. Above this temperature, the thermal degradation of the vinyl coating becomes excessive and diminishes rack life. When maximum solvent resistance, pencil hardness and abrasion resistance are required, the electrocoated parts may have to be post-baked after being removed from the plating racks. Alternatively, the nickel plated parts will have to be reracked before electrocoating.

Demands for consistent color control will require closer monitoring of the electrocoat bath than with pigmented electrocoat finishes and automated replenishment feed is strongly suggested. Color control is crucial for decorative applications which will therefore require consistent bake temperatures and regular oven maintenance. Color can be controlled through tint strength of the electrocoat bath and to a limited degree through adjustment of film build. Control of the plated substrate is also important for consistent appearance. On balance, the use of a single electrocoated finish over a bright plated substrate to replace brass plating offers performance, productivity, safety and environmental pluses for the metal finisher. On the other side of the equation, the metal finisher must cover the additional capital cost of an expanded system ($100m to $400m) and he must retrain personnel to operate a new and unfamiliar process.

Equipment used in the electrocoating process is well known and is presented in some detail in several reports. In large operations, the plated items could be transferred to a continuous conveyor operation typical of most electrocoat systems in existence today. In smaller throughput applications, the plated parts can be electrocoated on a modified push bar system typical of many plating lines. A typical flow chart is shown below for the tinted electrocoat process starting after the last stage of bright metal plating:

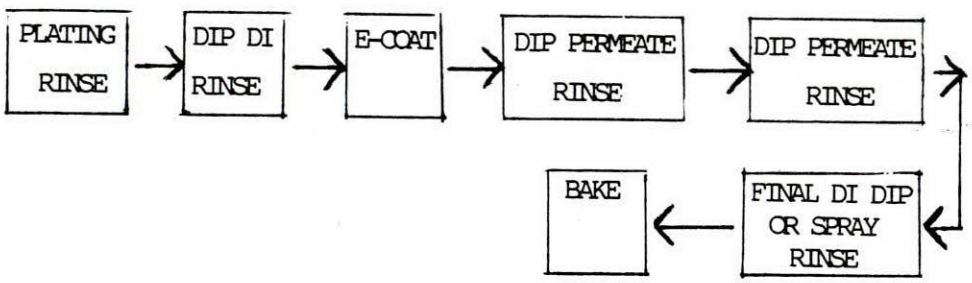

The reference to bright metal plating rather than nickel plating is intentional because substrates tested for this report include both nickel and zinc plating. The failure of clear electrocoat over brass (mentioned earlier) was caused by the attack of the anodic coating bath on the brass surface. If suitable clear cathodic finishes had been available, this process might have been commercially successful. The nickel plated surface is sufficiently inert, i.e., will not react with the anodic process, and clear films are achieved on the finished product. Substrates such as aluminum, brass or zinc require cathodic systems because they are attacked during the anodic coating process. "Lacquering" of brass using cathodic electrocoat is commercially attractive because of the uniform, pin-hole free films produced by electrocoat, because the finish is superior to most dip or spray coatings currently used and because the electrocoat finish meets current VOC regulations.

The creation of a "brass" decorative finish using bright zinc plating is commercially attactive in some applications because zinc is about one-fourth (1/4) the cost of nickel. Top quality furniture and houseware applications will most likely continue to use nickel because of superior brightness, uniformity and corrosion resistance. Applications such as hardware, however, are ideal end-uses for zinc.

The current Builders Hardware Manufacturers Association (BHMA) specifications list salt spray standards for various grades of hardware. The target range for brass plated and lacquered items is 16 to 24 hours in salt spray with less than 5% red rust under ASTM B117. The nickel plate plus "brass" electrocoat system passes several hundred hours in salt spray without failure as defined in the specifications. Cathodic electrocoat finishes over zinc easily surpass the standards for current brass plated systems but can show the typical white rust blisters exhibited in the lab salt spray testing of any organic coating over zinc substrate. The economic advantages for zinc plating plus cathodic electrocoating are significant, and where applicable will enable this combination to achieve a greater level of substitution versus flash brass plating.

Technical Results

The data generated for this report is intended to indicate the potential value of the process in replacing decorative brass plating in many applications.

The applicable tests and desired performance goals were drawn from several specifications including:

1. Sears Laboratory Specifications on Industrial Applied Organic, Composite, and Inorganic Finishes

2. American National Standard for Butts and Hinges dated 12/7/81

3. B.H.M.A. Product Standards - Section F - Locks and Lock Trim, 11. Performance Requirements for Coatings

Additional tests such as solvent resistance were added because they are typically used to evaluate organic finishes. The panels tested were prepared at commercial plating facilities and at DeSoto's electrocoat laboratory. Panels coated with the "brass" electrocoat included aluminum, nickel plated steel, and bright zinc plated steel, and a cathodic finish was applied over the aluminum and zinc plated steel panels. Controls consisted of nickel plated steel panels that were flash brassed and lacquered in actual commercial processes. The comparative test results are summarized in the following table.

## TABLE I

## PERFORMANCE SPECIFICATION

| *TEST* | *SPECIFICATION* | *CATHODIC OVER:* *ALUMINUM* | *ZINC* | *NICKEL* | *ANODIC OVER: NICKEL* | *CONTROL: BRASS PLATING* |
|---|---|---|---|---|---|---|
| Water fog | Lock & lock trim & Sears 500 hours | Pass | Pass | Pass | Pass | 60% corrosion |
| | Sears 48 hours | Pass | Pass | Pass | Pass | 20% corrosion |
| Salt spray | Butts & hinges & Sears 24 hours | Pass | Pass | Pass | Pass | Pass |
| | Butts & hinges 72 hours | Pass | 5% corrosion | Pass | 2% corrosion | 30% corrosion |
| Weather-ometer | Sears 100 hours | Definite fade/chalk | Definite fade/chalk | Definite fade/chalk | Fading & chalking | Complete errosion of film |
| Fadeometer | Sears 75 hours | Definite fade | Moderate fade | Light fade | Slight fade | Slight fade |
| Impact | Sears 30 in-lb | 7 in-lb | 40 in-lb | 30 in-lb | >160 in-lb | >160 in-lb |
| Hoffman scratch adhesion | Sears 500 gr-cm | 175 gr-cm | 175 gr-cm | 175 gr-cm | 225 gr-cm | 50gr-cm |

| TEST | SPECIFICATION | CATHODIC OVER: ALUMINUM | CATHODIC OVER: ZINC | CATHODIC OVER: NICKEL | ANODIC OVER: NICKEL | CONTROL: BRASS PLATING |
|---|---|---|---|---|---|---|
| Tabor adhesion | Sears: till breakthrough | 90 cycles | 155 cycles | 130 cycles | 50 cycles | 40 cycles |
| Pencil hardness | Sears Lock & 4H lock trim | H | 2-3H | 2-3H | H | H |
| Falling sand | Sears: 20 liters | 6 liters | 14 liters | 14 liters | 12 liters | 2 liters |
| Methyl ethyl ketone resist | DeSoto 50 double rubs | >100 | >100 | >100 | >100 | 4 |
| 3/4" bar Mandrel | DeSoto | No Striations | No Striations | 3/4" Striations | 1/2" Striations | 1/2" Striations |
| Crosshatch adhesion | Sears: as is | Pass | Pass | Pass | Pass | Pass |
| | Water fog 500 hours | Pass | Pass | Pass | Pass | Pass |
| | Salt spray 72 hours | Fail | Pass | Pass | Pass | Pass |
| | Weatherometer 100 hrs | Pass | Fail | Pass | Pass | Pass |
| | Fadeometer 300 hours | Pass | Pass | Pass | Pass | Pass |
| Chemical cleaners | Sears: | | | | | |
| | Abrasive | Fail | Fail | Fail | Fail | Fail |
| | Non-abrasive | Pass | Pass | Pass | Pass | Pass |
| Perspiration | Locks & lock trim & Sears | Fail | Fail | Fail | Pass | Pass |
| Staining | See Table II | | | | | |

## TABLE II

## STAIN TEST
## PERFORMANCE VERSUS SPECIFICATION

| *SPECIFICATION* | *CATHODIC OVER: NICKEL* | *ANODIC OVER: NICKEL* | *CONTROL: BRASS PLATING* |
|---|---|---|---|
| DeSoto & Sears 18 hours | | | |
| Food | | | |
| Cake | No effect | No effect | No effect |
| Coffee | No effect | No effect | *Gloss loss |
| Wesson Oil | No effect | No effect | No effect |
| White vinegar | *Loss of film | Blistering & discoloring | Total lifting |
| Tomato catsup | No effect | Stain | No effect |
| Mustard | *Blistering #9D | *Blistering #9D | Stain |
| Grease | No effect | No effect | No effect |
| Cleaners | | | |
| Windex | No effect | No effect | Blue stain |
| Fantastik | No effect | No effect | Yellow staining |
| Pine Sol | No effect | Total lifting | Discoloring |
| Clorox | *Slight lightening | Total lifting | Partial lifting |
| Ammonia | No effect | No effect | Total lifting w/bluing |
| Hygiene | | | |
| Suave Shampoo | No effect | No effect | Film swells |
| Suave Styling Spray | No effect | No effect | Staining |
| Lipstick | No effect | No effect | *Stain |
| Old Spice Cologne | No effect | No effect | Film removal with streaking |

* No effect seen with two hour test

## Summary

The commercial use of electrocoating as a replacement for brass plating is a reality today. The multi-step electrocoat plus dip-dye process is currently being used over nickel in several countries. The single step tinted electrocoat process evaluated for this report is currently being used commercially in both the anodic form over nickel and the cathodic form over bright zinc. The continued monitoring of these installations will provide valuable data needed to attain acceptance and expansion of the electrocoating process within the decorative metal finishing market.

## References

1. Geissman, W. C. and Bennett, D. J.: "Brass", MODERN ELECTROPLATING, Chapter 19, John Wiley & Sons, Inc., 1974

2. The Staff of Mabbett, Capaccio & Associates, Inc.: "Environmental/OSHA Update for Metal Finishers", METAL FINISHING, p. 13-16, November, 1986

3. "EPA Sets New Water Pollution Rules", AUTOMOTIVE NEWS, p. 23, August, 1983

4. H. Stow: "Brass Plating", PRODUCTS FINISHING DIRECTORY, p. 80-83, 1986

5. Special New Product Report: "New Competition for Brass Plating", PRODUCTS FINISHING, p. 88-91, August, 1987

6. Litten, H. L. and Skimm, C.: "A Substitute For Brass Plating", PLATING AND SURFACE FINISHING, p. 24-27, October, 1987